University of Novi Sad
Faculty of Technical Sciences
DEPARTMENT OF GRAPHIC ENGINEERING AND DESIGN

GRID 2026

13. INTERNATIONAL SYMPOSIUM ON GRAPHIC ENGINEERING AND DESIGN

https://www.grid.uns.ac.rs/symposium/enzbornik2026.html

PUBLISHED BY

University of Novi Sad
Faculty of Technical Sciences
DEPARTMENT OF GRAPHIC ENGINEERING AND DESIGN

Address:
Faculty of Technical Sciences,
Department of Graphic
Engineering and Design,

Trg Dositeja Obradovića 6

Email:
grid_info@uns.ac.rs

Web address:
https://www.grid.uns.ac.rs/symposium/enzbornik2026.html

Frequency: 1 issue in 2 year
Printing: Faculty of Technical Sciences,
Department of Graphic Engineering and Design

Electronic version of journal available on:
https://www.grid.uns.ac.rs/symposium/enpocetna.html

E-ISSN 2620-1429

The Proceedings is abstracted/indexed
in the Scopus and Directory of Open Access Journals

Scopus®

Proceedings - The Thirteenth International Symposium GRID 2024
12-14. November 2026, Novi Sad

EDITION:
INTERNATIONAL SYMPOSIUM ON GRAPHIC ENGINEERING AND DESIGN

PUBLISHER:
University of Novi Sad
Faculty of technical sciences
Department of graphic engineering and design
21000 Novi Sad, Trg Dositeja Obradovića 6

EDITORIAL COMMITTEE:
PhD Nemanja Kašiković
PhD Živko Pavlović
PhD Sandra Dedijer
PhD Gojko Vladić

TECHNICAL SECRETARY:
Gala Golubović

EDITOR:
PhD Ivan Pinćjer

LAYOUT AND PRODUCTION:
GRID team

PRINT:
Grafički centar GRID, Trg Dositeja Obradovića 6, Novi Sad

CIRCULATION:
150 copies

13. INTERNATIONAL SYMPOSIUM ON GRAPHIC ENGINEERING AND DESIGN

12-14. November 2026.

SCIENTIFIC COMMITTEE

Nemanja Kašiković, University of Novi Sad, Faculty of Technical Sciences, Novi Sad, (president) (SRB)
Thomas Hoffman-Walbeck, Stuttgart Media University, Stutgart (DEU)
Lidija Mandić, University of Zagreb, Faculty of Graphic Arts, Zagreb (HRV)
Igor Majnarić, University of Zagreb, Faculty of Graphic Arts, Zagreb (HRV)
Tomislav Cigula, University of Zagreb, Zagreb (HRV)
Diana Gregor-Svetec, University of Ljubljana, Ljubljana (SVN)
Aleš Hladnik, University of Ljubljana, Ljubljana (SVN)
Deja Muck, University of Ljubljana, Ljubljana (SVN)
Raša Urbas, University of Ljubljana, Ljubljana (SVN)
Urška Stankovič Elesini, University of Ljubljana, Ljubljana (SVN)
Tomáš Syrový, University of Pardubice, Pardubice (CZE)
Michal Veselý, Brno University of technology, Brno (CZE)
Petr Nemec, University of Pardubice, Pardubice (CZE)
Michal Čeppan, Slovak University of Technology in Bratislava, Bratislava (SVK)
Joanna Ewa Izdebska-Podsiadły, Warsaw University of Technology, Warsaw (POL)
Sabu Thomas, Mahatma Gandhi University, Kottayam (IND)
Ákos Borbély, Obuda University, Budapest (HUN)
László Koltai, Obuda University, Budapest (HUN)
Rafael Huertas, University of Granada, Granada (ESP)
Anastasios Politis, University of West Attica, Athens (GRC)
Panagiotis Kyratsis, University of Western Macedonia, Kozani (GRC)
Iskren Spiridonov, University of Chemical Technology and Metallurgy, Sofia (BGR)
Borislav Malinović, University of Banja Luka, Banja Luka (BIH)
Mladen Stančić, University of Banja Luka, Banja Luka (BIH)
Miljana Prica, University of Novi Sad, Novi Sad (SRB)
Sandra Dedijer, University of Novi Sad, Novi Sad (SRB)
Gojko Vladić, Faculty of Technical Sciences, Novi Sad (SRB)
Ivan Pinćjer, University of Novi Sad, Novi Sad (SRB)
Živko Pavlović, University of Novi Sad, Novi Sad (SRB)
Magdolna Pál, University of Novi Sad, Novi Sad (SRB)
Jonas Malinauskas, Vilnius College of Technologies and Design, Vilnius (LTU)
Roberto Pašić, St. Clement of Ohrid University of Bitola, Bitola (MKD)
Vladan Končar, Ecole Nationale Supérieure des Arts et Industries Textiles, Roubaix (FRA)
Arif Özcan, Marmara University, Istanbul (TUR)
Catarina Silva, Polytechnic Institute of Cávado and Ave, Barcelos (POR)
Tim C. Claypole, Swansea University, Swansea (GBR)
Alexandra Pekarovicova, Western Michigen University, Kalamazoo (USA)
Irma Puškarević, Wichita State University, Wichita (USA)

ORGANIZATIONAL COMMITTEE

Nemanja Kašiković, University of Novi Sad, Faculty of Technical Sciences, Novi Sad (SRB)
Sandra Dedijer, University of Novi Sad, Faculty of Technical Sciences, Novi Sad (SRB)
Živko Pavlović, University of Novi Sad, Faculty of Technical Sciences, Novi Sad (SRB)
Miljana Prica, University of Novi Sad, Faculty of Technical Sciences, Novi Sad (SRB)
Gojko Vladić, University of Novi Sad, Faculty of Technical Sciences, Novi Sad (SRB)
Magdolna Pál, University of Novi Sad, Faculty of Technical Sciences, Novi Sad (SRB)
Uroš Nedeljković, University of Novi Sad, Faculty of Technical Sciences, Novi Sad (SRB)
Željko Zeljković, University of Novi Sad, Faculty of Technical Sciences, Novi Sad (SRB)
Ivan Pinćjer, University of Novi Sad, Faculty of Technical Sciences, Novi Sad (SRB)
Neda Milić Keresteš, University of Novi Sad, Faculty of Technical Sciences, Novi Sad (SRB)
Ivana Tomić, University of Novi Sad, Faculty of Technical Sciences, Novi Sad (SRB)
Ivana Jurič, University of Novi Sad, Faculty of Technical Sciences, Novi Sad (SRB)
Bojan Banjanin, University of Novi Sad, Faculty of Technical Sciences, Novi Sad (SRB)
Rastko Milošević, University of Novi Sad, Faculty of Technical Sciences, Novi Sad (SRB)
Stefan Đurđević, University of Novi Sad, Faculty of Technical Sciences, Novi Sad (SRB)
Jelena Vladušić, University of Novi Sad, Faculty of Technical Sciences, Novi Sad (SRB)
Savka Adamović, University of Novi Sad, Faculty of Technical Sciences, Novi Sad (SRB)
Vladimir Zorić, University of Novi Sad, Faculty of Technical Sciences, Novi Sad (SRB)
Jelena Novaković, University of Novi Sad, Faculty of Technical Sciences, Novi Sad (SRB)
Vesna Gvoić, University of Novi Sad, Faculty of Technical Sciences, Novi Sad (SRB)
Saša Petrović, University of Novi Sad, Faculty of Technical Sciences, Novi Sad (SRB)
Gordana Bošnjaković, University of Novi Sad, Faculty of Technical Sciences, Novi Sad (SRB)
Predrag Ubović, University of Novi Sad, Faculty of Technical Sciences, Novi Sad (SRB)
Nada Miketić, University of Novi Sad, Faculty of Technical Sciences, Novi Sad (SRB)
Petar Vasilić, University of Novi Sad, Faculty of Technical Sciences, Novi Sad (SRB)
Katarina Maričić Picajkić, University of Novi Sad, Faculty of Technical Sciences, Novi Sad (SRB)
Gala Golubović, University of Novi Sad, Faculty of Technical Sciences, Novi Sad (SRB)
Iva Juretić, University of Novi Sad, Faculty of Technical Sciences, Novi Sad (SRB)
Teodora Gvoka, University of Novi Sad, Faculty of Technical Sciences, Novi Sad (SRB)
Tamara Ilić, University of Novi Sad, Faculty of Technical Sciences, Novi Sad (SRB)
Sanja Cvetojević, University of Novi Sad, Faculty of Technical Sciences, Novi Sad (SRB)
Milena Ristić, University of Novi Sad, Faculty of Technical Sciences, Novi Sad (SRB)

CHAIR OF ORGANIZATIONAL COMMITTEE

Ivan Pinćjer, University of Novi Sad, Faculty of Technical Sciences, Novi Sad (SRB)

TECHNICAL SECRETARY

Gala Golubović, University of Novi Sad, Faculty of Technical Sciences, Novi Sad (SRB)

REVIEWING COMMITTEE

Tomislav Cigula, University of Zagreb, Zagreb (HRV)
Tomislav Hudika, University of Zagreb, Zagreb (HRV)
Igor Majnarić, University of Zagreb, Zagreb (HRV)
Sanja Mahović Poljaček, University of Zagreb, Zagreb (HRV)
László Koltai, Obuda University, Budapest (HUN)
Raša Urbas, University of Ljubljana, Ljubljana (SVN)
Klementina Možina, University of Ljubljana, Ljubljana (SVN)
Iskren Spiridonov, University of Chemical Technology and Metallurgy, Sofia (BGR)
Rafael Huertas, University of Granada, Faculty of Science, Granada (ESP)
Markéta Držková, University of Pardubice, Pardubice (CZE)
Bohumil Jašúrek, University of Pardubice, Pardubice (CZE)
Petr Dzik, Brno University of Technology, Brno (CZE)
Viera Jančovičová, Slovak University of Technology in Bratislava, Bratislava (SVK)
Pavol Gemeiner, Slovak University of Technology in Bratislava, Bratislava (SVK)
Miljana Prica, University of Novi Sad, Novi Sad (SRB)
Sandra Dedijer, University of Novi Sad, Novi Sad (SRB)
Živko Pavlović, University of Novi Sad, Novi Sad (SRB)
Nemanja Kašiković, University of Novi Sad, Novi Sad (SRB)
Magdolna Pál, University of Novi Sad, Novi Sad (SRB)
Gojko Vladić, University of Novi Sad, Novi Sad (SRB)
Uroš Nedeljković, University of Novi Sad, Novi Sad (SRB)
Ivan Pinćjer, University of Novi Sad, Novi Sad (SRB)
Mladen Stančić, University of Banja Luka, Banja Luka (BIH)
Thomas Hoffman-Walbeck, Stuttgart Media University, Stutgart (DEU)
Joanna Ewa Izdebska-Podsiadły, Warsaw University of Technology, Warsaw (POL)
Zuzanna Żołek-Tryznowska, Warsaw University of Technology, Warsaw (POL)
Anastasios Politis, University of West Attica, Athens (GRC)
Panagiotis Kyratsis, University of Western Macedonia, Kozani (GRC)
Thomas Sabu, Mahatma Gandhi University, Kottayam (IND)
Jonas Malinauskas, Vilnius College of Technologies and Design, Vilnius (LTU)
Roberto Pašić, St. Clement of Ohrid University of Bitola, Bitola (MKD)
Vladan Končar, Ecole Nationale Supérieure des Arts et Industries Textiles, Roubaix (FRA)
Arif Özcan, Marmara University, Istanbul (TUR)
Catarina Silva, Polytechnic Institute of Cávado and Ave, Barcelos (POR)
Tim C. Claypole, Swansea University, Swansea (GBR)
Alexandra Pekarovicova, Western Michigen University, Kalamazoo (USA)

WITH SUPPORT OF:

Ministry of Science, Technological Development and Innovation, Republic of Serbia
Vojvodina, Republic of Serbia
Faculty of Technical Sciences, Novi Sad, Republic of Serbia
CEEPUS III RS-0704-13-2425
CEEPUS III-RS-1311-07-2425

CO - ORGANISERS:

University of Zagreb, Faculty of Graphic Arts,
Zagreb, Republic of Croatia
Obuda University, Faculty of Light Industry and Environmental Engineering,
Budapest, Hungary
University of Ljubljana, Faculty of Natural Sciences and Engineering,
Ljubljana, Republic of Slovenia

EQUIPMENT AND MATERIAL DONORS:

Contents

INVITED LECTURES

Ingrid Calvo Ivanovic:
MORE THAN A VISUAL ELEMENT: COLOUR AS A TRANSDISCIPLINARY KNOWLEDGE AND COMPETENCE FRAMEWORK FOR DESIGN 19

Sam Anvari, Gabriella M. Hancock:
BRIDGING THE GAP: A SITUATED PEDAGOGICAL FRAMEWORK FOR INTERDISCIPLINARY GRAPHIC DESIGN AND HUMAN FACTORS RESEARCH 33

Dimitris Mylonas:
BRIDGING COLOUR COMMUNICATION ACROSS LANGUAGES 39

Igor Karlovits:
TOWARDS A TOTAL PACKAGING SYSTEM: INTEGRATING MATERIAL PERFORMANCE, SAFETY, AND CIRCULAR SUSTAINABILITY 43

PRINTING TECHNOLOGIES AND QUALITY

Vyacheslav Repeta, Pavlo Ryvak, Yurii Petriv:
COMPARATIVE ASSESSMENT OF TONE AND LINE REPRODUCTION ON FABRIC USING DTF AND SUBLIMATION TRANSFER PRINTING 57

Vladimir Oličkov, Nemanja Kašiković, Sandra Dedijer, Miljana Prica:
THE ROLE OF WASHER SYSTEMS IN ALUMINUM CAN MANUFACTURING: IMPACT ON PRODUCT QUALITY AND PROCESS SUSTAINABILITY 63

Pavlo Valovyi, Svitlana Havenko, Marta Labetska:
INFLUENCE OF HALFTONE DOT GEOMETRY ON DOT GAIN AND TONE REPRODUCTION IN FLEXOGRAPHIC PRINTING ON ALUMINIUM FOIL 73

Igor Majnarić, Ivana Bolanča Mirković, Meri Huljev, Stanko Bauk:
POSSIBILITY OF REALISATION WHITE ELECTROINK ON A METALLISED PRINTING SUBSTRATE 79

Maja Strižić Jakovljević, Jana Špiranec, Sanja Mahović Poljaček:
OPTIMIZATION OF THERMOCHROMIC PRINTING INKS FOR FUNCTIONAL TEMPERATURE INDICATORS 87

Spomenko Kešina, Irma Horvat, Dean Valdec, Petar Miljković:
COMPREHENSIVE REVIEW OF TECHNICAL AND MATERIAL FACTORS INFLUENCING OFFSET PRINT QUALITY 95

Tetyana Holubnyk, Olha Borysenko:
BENCHMARKING COLOR REPRODUCTION QUALITY: A COMPARATIVE STUDY OF DIGITAL PRINTING SYSTEMS 107

Khloud Khaled Nasr:
THE POWER OF PACKAGING DESIGN IN SUPPORTING GLOBAL AND LOCAL EVENTS 115

Georgij Petriaszwili, Serhii Komarov, Piotr Janicki, Leszek Markowski:
POSSIBILITIES OF INCREASING THE TOOL LIFE OF AN ECCENTRIC CIRCULAR KNIFE IN VIBRATION-ASSISTED CUTTING OF BOOK BLOCKS 125

Vitalii Semeniv, Natalia Zanko, Mariia Semeniv, Bohdan Kovalskyi:
A METHODOLOGICAL FRAMEWORK FOR THE PREPRESS PREPARATION OF COLOUR IMAGES BASED ON NEW APPROACHES TO OPTIMISING THE COLOUR REPRODUCTION PROCESS. 133

Branka Ružičić, Dragana Grujić, Blanka Škipina, Biljana Pećanin, Sandra Dedijer:
COLOUR CHARACTERISTICS OF ALGINATE-BASED SCREEN PRINTS INCORPORATING ARONIA POMACE EXTRACT AND ZnO. 145

Jan Vališ, Tereza Vrbová, Bohumil Jašúrek:
CREATING PROOFS FOR INDIGO.....151

Iskren Spiridonov, Kremena Karchakova, Rumyana Boeva:
INVESTIGATION OF THE INFLUENCE OF OPAQUE WHITE INK ADDITION ON COLOUR CHARACTERISTICS OF SOME PROCESS AND PANTONE COLOURS PRINTED WITH WATER-BASED FLEXO INKS ON KRAFT PAPERS. 157

Nikola Petrović, Zoran Gazibarić:
AI IN ELECTROPHOTOGRAPHIC PRINTING:
QUALITY EVALUATION AND DECISION MAKING 169

Ivana Jurič, Aleksandra Nešić, Branka Pilić, Nemanja Kašiković,
Magdolna Pál, Živko Pavlović:
PRINTING POSSIBILITY ON BIOPOLYMER BASED FILMS.....179

Diana Bratić, Denis Jurečić, Suzana Pasanec Preprotić, Gorana Petković:
LATENT REFERENCE PATTERNS FOR GEOMETRIC
DRIFT DETECTION IN THE PRINTING PROCESS 189

Magdolna Pál, Nada Miketić, Ivana Jurič, Neda Milić Keresteš, Ivan Pinćjer
PRELIMINARY ANALYSIS OF IMAGE-BASED QUALITY
ASSESSMENT OF LASER-ENGRAVED GRAPHICS 199

Tomislav Cigula, Rene Hoblaj, Katarina Itrić Ivanda, Rahela Kulčar, Iva Šarčević:
INFLUENCE OF SCREEN PRINTING MESH COUNT ON DEPOSITION OF GRAPHITE-STARCH CONDUCTIVE INK ONTO CARDBOARDS.....209

Žanko Sremac, Nemanja Petrović, Uroš Mančić:
MOTTLING IN PRODUCTION OF CARDBOARD AND IN OFFSET PRINTING.....215

August Eriksson, Oisik Das:
FIRE SAFETY IN THE PRINTING INDUSTRY:
THE CURIOUS CASE OF THE MISSING LITERATURE 223

COLOR SCIENCE AND MANAGEMENT

Barbara Blaznik, Evelin Pipan, Sabina Bračko:
ANALYSIS OF MEMORY COLOUR
USING SELECTED FOODS AS AN EXAMPLE 231

Jože Guna, Raša Urbas:
INFLUENCE OF BLENDER RENDERING ENGINES AND VIEW TRANSFORMS ON COLOUR REPRODUCTION IN 3D VISUALISATION 237

Ingrid Calvo Ivanovic, Francesca Mattioli:
MORE THAN HUE—A METHODOLOGICAL APPROACH TO COLOUR DESIGN FOR VISUAL IDENTITY AND BRANDING..... 243

Rafael Huertas, Luis Gómez Robledo, Miguel Ángel Martínez-Domingo, Eva M. Valero, Javier Hernández-Andrés, Neda Milić Keresteš, Ivana Tomić:
EVALUATION OF PASSIVE AND ACTIVE AIDS FOR COLOR VISION DEFICIENCY: A COMPARATIVE ANALYSIS OF PERCEPTUAL EFFICACY..... 255

Bojana Narić, Mladen Stančić, Igor Majnarić, Miroslav Dragić:
COLORIMETRIC AND LIGHTFASTNESS ASSESSMENT OF WATER-BASED MAGENTA INKJET PRINTS ON WOOD-FREE OFFSET SUBSTRATE..... 265

PACKAGING DESIGN AND ADDED VALUE

Ayorinde S. Oluyemi, Oluwafemi S. Adelabu, E. Bankole Oladumiye:
PERCEPTUAL AND KANSEI RESPONSES TO ALPHANUMERIC ONOMASTICS IN EMOTIONAL PACKAGING DESIGN ACROSS AGE GROUPS 275

Alan Nikolić-Šipek, Katarina Itrić Ivanda, Marina Vukoje Bezjak, Rahela Kulčar:
INTERACTIVE PACKAGING ENABLED BY NFC TECHNOLOGY..... 285

Ioanna Kalamakidou, Vasileios Kyratsis, Giorgos Lychridas, Thomas Liokos, Athanasios Manavis, Nikolaos Efkolidis:
TEA PACKAGING THOUGH DESIGN THINKING: A HOLISTIC METHODOLOGY TO PRODUCT IDENTITY 291

Nada Miketić, Ivan Pinćjer, Magdolna Pál, Milena Ristić:
INFLUENCE OF PACKAGING FINISHING TECHNIQUES ON CONSUMER PERCEPTION.....297

Daria Mustić
THE ACCESSIBILITY PARADOX OF PACKAGING AS A COMMUNICATION CHANNEL.....303

Gordana Bošnjaković, Gojko Vladić, Katarina Maričić Picajkić, Teodora Gvoka:
CONSUMER EXPERIENCES WITH SCREW-CLOSURE PACKAGING: ERGONOMIC CHALLENGES AND USER DIFFICULTIES..... 311

Jesenka Pibernik, Mila Mihaljević, Marija Magdalena Mendeš:
HOW ARCHETYPE-BASED PACKAGING DESIGN SHAPES VISUAL ATTENTION AND EASE OF USE 315

R. Ragavaraja:
THE INVISIBLE PROTOTYPE: AI-POWERED DIGITAL TWINS FOR RESILIENT GRAPHIC PACKAGING DESIGN 321

Gregor Franken, Urška Klenovšek, Urška Vrabič-Brodnjak:
REDESIGNING HAIR CARE PACKAGING FOR GENERATION Z THROUGH A STUDENT-LED CASE STUDY OF A SLOVENIAN COSMETIC BRAND 333

David Pinćjer, Gojko Vladić, Teodora Gvoka, Gordana Bošnjaković, Stefan Đurđević:
DIFFERENCES IN THE PERCEPTION OF WINE PACKAGING ATTRIBUTES
BASED ON TACTILE-VISUAL AND VISUAL-ONLY TEXTURE EVALUATION 339

Chris Trochoutsos, Gerasimos Vonitsanos, Marios Tsigonias:
INTEGRATING ARTIFICIAL INTELLIGENCE IN THE DESIGN
OF SUSTAINABLE AND SMART PACKAGING: CHALLENGES
AND PERSPECTIVES IN GRAPHIC ENGINEERING 347

GRAPHIC DESIGN AND VISUAL COMMUNICATION

Ana Stevanovski, Tanja Medved, Klementina Možina:
PROMOTION OF THE DIXI VARIABLE TYPEFACE FAMILY
FOR READERS WITH DYSLEXIA 359

Eva Jankulovska, Klementina Možina:
THE IMPACT OF TYPOGRAPHY
ON LEGIBILITY FOR PEOPLE WITH DYSLEXIA 371

Boris Beja:
PARTISAN GRAPHIC ART AND THE
CONTEMPORARY CONSTRUCTION OF COLLECTIVE MEMORY 379

Tinkara Stanonik, Boris Beja:
ARTISTIC AND MATERIAL ANALYSIS OF DINAR, TOLAR AND EURO 387

Laila Mušić:
FROM SIGNAGE TO CIVIC IDENTITY:. A THEORETICAL FRAMEWORK FOR
VISUAL COMMUNICATION IN POST-CONFLICT URBAN SPACE 395

Hana Muck, Raša Urbas:
REINTERPRETATION OF THE ARTWORK ATELJE BY GABRIJEL
STUPICA INTO DIDACTIC AND TACTILE PRODUCTS 403

Charles T. Weiss:
HUMAN BY DESIGN: GRAPHIC DESIGN AND DESIGN THINKING
IN THE AGE OF AI 413

Gábor Tóth, Kornél Remete, Csaba Horváth, László Koltai:
THE ROLE AND FUTURE POTENTIAL OF BOOKS AND BOOK
PRINTING IN THE EUROPEAN KNOWLEDGE ECONOMY 419

Raša Urbas, Žiga Ceglar, Boris Beja:
ADAPTATION OF MUSEUM EXHIBITS
FOR BLIND AND VISUALLY IMPAIRED VISITORS 427

Ewa Kołodziejuk, Joanna Izdebska-Podsiadły:
POP-UP MECHANISMS AS A MEANS OF
VISUAL EXPRESSION IN CARD DESIGN 435

DIGITAL MEDIA AND USER EXPERIENCE

Andrej Iskra, Helena Gabrijelčič Tomc:
HEATMAP-BASED AREA ANALYSIS OF FRONTAL FACE IMAGES
USING AN EYE-TRACKING SYSTEM 445

Josip Bota, Nina Hasukić, Rea Franković:
COMPREHENSION OF MEDICATION DOSAGE INSTRUCTIONS:
A COMPARISON OF FOUR INSTRUCTION FORMATS 451

Júlio Silva, Paulo Coelho, Ana do Carmo:
DISTRIBUTED AUDIOVISUAL PRODUCTION AND THE EVOLUTION OF
COMMUNICATION METHODOLOGIES FOR LARGE-SCALE CULTURAL
EVENTS: A CASE STUDY OF THE FESTA DOS TABULEIROS 459

Klara Manca Čanžek, Jure Ahtik:
EVALUATING THE IMPACT OF GENERATIVE ARTIFICIAL
INTELLIGENCE ON PHOTOGRAPHIC WORKFLOW 473

Gala Golubović, Saša Petrović, Sanja Cvetojević, Iva Juretić, Stefan Đurđević:
DESIGNING MENTAL WELL-BEING MOBILE APPLICATIONS:
INSIGHTS INTO USER PREFERENCES FOR USER INTERFACE DESIGN..... 481

Leszek Markowski:
A STUDY OF THE IMPACT OF JPEG COMPRESSION ON
VISUAL AND DIGITAL IMAGE DEGRADATION..... 489

Rina Petričević, Jure Ahtik:
EVALUATION OF VISUAL AESTHETICS AND
COMMUNICATION EFFECTIVENESS IN DIGITAL ADVERTISING 495

Patricija Nakić, Aleš Hladnik:
COMPARISON OF VARIOUS LEAST SIGNIFICANT BIT
MODIFYING METHODS USED FOR IMAGE DATA HIDING 501

Jelena Kerac, Tamara Ilić, Neda Milić Keresteš, Sandra Dedijer, Bojan Banjanin:
THE EFFECT OF AVATAR REALISM ON CHARACTER
RESEMBLANCE, ENJOYMENT, AND DATA-SAFETY
CONCERN IN SELF-AVATAR VIDEO GAMES..... 507

Brita Mandelj, Tanja Nuša Kočevar, Andrej Iskra:
ANIMATED PRESENTATION OF THE STORY OF THE NEVLJE MAMMOTH 515

Stefan Đurđević, Gala Golubović, Dragana Žilić:
USER-CENTERED UX/UI DESIGN OF
A MOBILE FLIGHT SEARCH APPLICATION..... 525

Jelena Spajić, Ksenija Mićić, Bojana Milić:
DECODING BRAND EXPERIENCE IN AR VS. WEB
INTERFACES VIA GAUSSIAN GRAPHICAL MODELS. 531

Iva Juretić, Ivana Jurič, Saša Petrović, Sanja Cvetojević:
ARTIFICIAL INTELLIGENCE FOR ENHANCEMENT OF
LOW-LIGHT PHOTOGRAPHS..... 537

Rastko Milošević, Selena Nikolić, Savka Adamović, Ivana Tomić:
PERSONAL VS. PROMOTIONAL INFLUENCER CONTENT ON INSTAGRAM
AND TIKTOK: ENGAGEMENT AND DISCLOSURE PRACTICES..... 549

ECOLOGY AND SUSTAINABLE MATERIALS

Vesna Gvoić, Aleksandra Tubić, Maja Vujić, Jasmina Agbaba, Dejan Krčmar, Živko Pavlović, Miljana Prica:
OPTIMIZATION OF FENTON-LIKE OXIDATION FOR CYAN PRINTING DYE REMOVAL IN THE PRESENCE OF POLYETHYLENE TEREPHTHALATE MICROPLASTICS 557

Betul Eymur Donmez, Aslı Beyler Cigil:
DEVELOPMENT AND CHARACTERIZATION OF A FUNCTIONAL UV-PHOTOPOLYMERIZED PEGDA/PETMP/BMEP HYDROGEL ADSORBENT FOR METHYLENE BLUE REMOVAL FROM AQUEOUS MEDIA 565

Savka Adamović, Rastko Milošević, Aleksandra Mihailović, Selena Samardžić Cvijanović, Robert Lakatoš:
ADSORPTION OF POLLUTANTS FROM COMPLEX OFFSET PRINTING WASTEWATERS: MECHANISMS, MASS TRANSPORT AND KINETIC MODELS..... 573

Iskren Spiridonov, Katya Pashova, Rumyana Boeva, Nevena Lazarova-Zdravkova:
PHOTO-ASSISTED GREEN SYNTHESIS WITH LED(590nm) OF SILVER NANOPARTICLES AND EVALUATION OF THEIR ANTIBACTERIAL ACTIVITY IN SPECIFIC WATER BASED COATINGS..... 579

Milena Ristić, Vesna Gvoić, Živko Pavlović, Miljana Prica:
BIO-BASED, BIODEGRADABLE AND HYBRID COATINGS FOR PAPER-BASED PACKAGING: FUNCTIONAL PERFORMANCE AND END-OF-LIFE CONSIDERATIONS 585

Hatice Birtane:
DEVELOPMENT AND CHARACTERIZATION OF PLA/PBAT/CHITOSAN-BASED BIODEGRADABLE FILMS FOR ACTIVE STRAWBERRY PACKAGING APPLICATIONS 599

Teodora Gvoka, Savka Adamović, Gojko Vladić, Katarina Maričić Picajkić, Gordana Bošnjaković, Gala Golubović:
ECOLOGICAL ASPECTS OF THE PRODUCTION OF MOLDED PAPER PULP PACKAGING: GENERATION AND TREATMENT OF INDUSTRIAL WASTEWATER..... 611

Marina Vukoje Bezjak, Nika Krajačić, Rahela Kulčar, Katarina Itrić Ivanda:
RECYCLABILITY ASSESSMENT OF PRESSURE-SENSITIVE LABELS MADE FROM AGRO-INDUSTRIAL BY-PRODUCTS..... 621

Tamara Ilić, Bojan Banjanin, Jelena Kerac:
THE ROLE OF THE GRAPHIC INDUSTRY IN EXTENDING GARMENT LIFESPAN..... 629

Filiz Kara
DEVELOPMENT OF GREEN-SYNTHESIZED SILVER NANOPARTICLE-CONTAINING PCL COATINGS FOR PAPER PACKAGING MATERIALS..... 639

Aslı Beyler Çiğil, Berat Çınar Acar, Zehranur Yüksekdağ, Hatice Birtane:
IMPROVING THE PRINTABILITY OF PLA-BASED ACTIVE
PACKAGING FILMS USING EXOPOLYSACCHARIDE
OBTAINED BY LIGILACTOBACILLUS SALIVARIUS KC66L 649

GRAPHIC MATERIALS AND SUBSTRATES

Emine Arman Kandirmaz, Arif Ozcan:
BIO-BASED ANTIBACTERIAL PAPER COATINGS ENABLED
BY SURFACE-MODIFIED SILVER NANOPARTICLES 663

Sanja Mahović Poljaček, Tamara Tomašegović, Davor Donevski:
pH-RESPONSIVE STARCH FILMS INCORPORATING PURPLE
SWEET POTATO ANTHOCYANINS AND BACTERIAL NANOCELLULOSE 673

Bohumil Jašúrek, Veronika Holeňová, Jan Vališ:
SURFACE FREE ENERGY OF POLYETHYLENE AFTER CORONA TREATMENT
AND ITS STABILITY AT DIFFERENT STORAGE TEMPERATURES 683

Urška Kavčič, Patricija Pevec:
THE INFLUENCE OF PAPER SUBSTRATE AND COATING FORMULATION
ON BARRIER PROPERTIES OF PACKAGING PAPERS 687

Nevena Vukić, Darko Manjenčić, Marijana Vasić, Milica Ivanović:
SILICONE ELASTOMERS AS ADDITIVES IN THE
PAPER MANUFACTURING PROCESS.....693

Arkadiusz Jeznach, Łucja Dybowska-Sarapuk, Zuzanna Żołek-Tryznowska:
EFFECT OF GLYCEROL AND HYDROPHOBIC SILICA ON THE MECHANICAL
AND SURFACE PROPERTIES OF STARCH-BASED FILMS:
A RESPONSE SURFACE METHODOLOGY APPROACH 699

Urška Klenovšek, Urška Vrabič-Brodnjak:
FORMULATION-DEPENDENT PROPERTIES OF RICE STARCH-BASED
ADHESIVES FOR WET-STRENGTH PAPER LABELS 705

EDUCATION AND LEARNING INNOVATION

Ivan Pinćjer, Nada Miketić, Vladimir Dimovski, Jelica Čupić:
STUDENT PREFERENCES IN SHAPING THE LEARNING SPACE
AND THEIR IMPACT ON THE EDUCATIONAL PROCESS 713

Patricija Nakić, Nuša Ceglar, Lara Koštomaj, Jan Simončič, Urška Stanković Elesini:
ANALYSIS OF THE USE OF AND ATTITUDES TOWARDS GENERATIVE
ARTIFICIAL INTELIGENCE AMONG GRAPHIC ART STUDENTS.....717

Nemanja Kašiković, Dragana Glušac, Velibor Premčevski,
Aleksandar S. Anđelković, Nemanja Tasić:
ARTIFICIAL INTELLIGENCE AS A LEARNING ASSISTANT:
DESIGN AND EVALUATION OF THE ASKING AI+
PLATFORM FOR GRAPHIC ENGINEERING EDUCATION.....731

Miguel Sanches, Ana do Carmo, Júlio Silva:
INDUSTRIAL HERITAGE AS A LEARNING ENVIRONMENT: AN EXPLORATORY CASE STUDY IN GRAPHIC TECHNOLOGIES AND DESIGN EDUCATION 739

Asja Komadina:
KIS MAGYARÓRA: LEARNING A LANGUAGE THROUGH APPLIED ART 753

Petra Merhy:
FROM STUDIO TO SHELF: INTEGRATING RETAIL CONTEXTS INTO PACKAGING DESIGN EDUCATION 761

Bojan Banjanin, Tamara Ilić, Jelena Kerac, Rastko Milošević:
CROSSING THE BOUNDARIES OF CONVENTIONAL: EXAMINING VARIOUS APPROACHES IN TEACHING VIDEO GAME DEVELOPMENT 769

EMERGING TECHNOLOGIES

George-Robert Reynik, Panagiotis Kyratsis:
RAPID PROTOTYPING AND FABRICATION OF UNMANNED SURFACE VESSELS: A 3D PRINTING CASE STUDY 779

Panagiota Ligka, Athina Tziarou, Renata Gudaitiene, Panagiotis Kyratsis:
A CASE STUDY IN FUNCTIONALLY GRADED LATTICE DESIGN FOR A SURFSKATE DECK: WORKFLOW AND REDUCED-SCALE PROTOTYPE 785

Athina Tziarou, Panagiota Ligka, Nikolla Vesho, Panagiotis Kyratsis:
A CASE STUDY IN AUXETIC STRUCTURE DESIGN FOR AN ADAPTIVE 3D-PRINTED HANDBAG 791

Alan Divjak, Mile Matijević, Krunoslav Hajdek, Marko Morić:
FDM 3D PRINTING OF LOW-DENSITY LATTICE STRUCTURES USING MODIFIED INFILL PATTERNS 799

Jure Jarc, Nataša Nemeček, Gašper Oitzl, Andrej Učakar, Deja Muck:
NON-CONTACT 3D ACQUISITION OF CHALLENGING MUSEUM OBJECTS FOR CULTURAL HERITAGE DIGITALIZATION 805

Primož Weingerl, Larisa Kosi, Brina Stankovič Elesini, Svit Bartolj,
Urška Stanković Elesini, Sašo Stefanovski:
WORKFLOW FOR EXTRACTING AND STRUCTURING GEOLINGUISTIC DATA FROM TESNIÈRE'S ATLAS 813

Foreword

Dear readers,

It is my great pleasure to present the proceedings of the Thirteenth International Symposium on Graphic Engineering and Design – GRID 2026. Continuing a tradition established in 2002, this biennial symposium has served as an important platform for exchanging scientific knowledge, research findings, and professional experience for more than two decades.

We are pleased that GRID 2026 has once again brought together researchers, academics, and professionals from various countries, strengthening the international character and significance of this event.

The papers presented in these proceedings reflect recent research achievements and developments in graphic engineering, graphic technology, graphic design, and related scientific disciplines. Over the years, the GRID Symposium has helped establish and maintain valuable cooperation with educational and research institutions worldwide, encouraging the exchange of ideas and the development of new approaches and solutions.

I would like to express my sincere gratitude to all authors and participants for their valuable contributions to GRID 2026. Their dedication and research efforts play an essential role in the continued success and development of the Symposium.

I believe that the scientific findings and professional insights presented in these proceedings will provide a valuable resource for the academic and professional community and inspire further research and collaboration.

Editor

Invited lectures

https://doi.org/10.24867/GRID-2026-p1

More Than a Visual Element: Colour as a Transdisciplinary Knowledge and Competence Framework for Design

ABSTRACT

Colour is everywhere in design, and yet design education has not kept pace with what colour does in contemporary practice. Across the discipline, colour continues to be framed primarily as a visual element: something applied to a design, concerning aesthetics and composition, addressed once the more consequential decisions have been made. This paper argues that this framing is too narrow, and that its narrowness carries consequences for practice, for education, and for the capacity of design to respond to the challenges it now faces. Colour decisions in contemporary design extend well beyond the palette, into ecological impact, cultural specificity, accessibility and inclusion, and AI-assisted production, among others. In each of these domains, design is already making colour decisions of consequence without necessarily recognising them as colour decisions. The paper presents a framework for colour competence in design, developed across seventeen years of doctoral and post-doctoral research and teaching, and organised into four knowledge domains: Colour Context and Strategic Framing; Colour, Human Experience and Inclusion; Colour Decision and Materialisation; and Colour Performance and Impact. Aligned with the Double Diamond model of the design process, and structured across two dimensions, stable knowledge domains and the five capacities of colour literacy that operate across them, the framework functions as a map of the territory colour actually occupies in design practice. The paper argues that accountability, one of those five capacities, is the competence the framework makes operable: a designer can account for a colour decision only by knowing which domains of colour knowledge it draws upon, and by which ways of knowing.

Ingrid Calvo Ivanovic

Design Department,
Universidad de Chile,
Santiago, Chile
AIC+ISCC Colour Literacy
Project- www.colourliteracy.org

KEY WORDS
Colour literacy, colour competence, design knowledge, colour decision-making, ways of knowing colour

1. Introduction

Every designed object, environment, and communication has colour. It is physically inescapable, the result of how light interacts with every material surface a designer specifies, every screen a designer composes for, every space a designer shapes. And yet colour is one of the design domains that operates with the least disciplinary accountability, the least explicit knowledge, and the least sustained preparation (Bantom, 2006; Csillag, Lupinacci & Hirschler, 2018; Mottram, 2018; Calvo Ivanovic, 2022).

Colour is everywhere in design, and in design it is largely unexamined. This paper takes that paradox as its point of departure and proposes a framework for addressing it.

The paradox has a structural cause. Across the design discipline, colour has been classified as a visual element: a compositional unit, alongside form, line, and texture, that is applied to a design and that concerns aesthetics. This classification is so deeply embedded in design education and practice that it operates as common sense rather than as a choice that could be otherwise.

Its consequences are visible in the curriculum. In most design programmes, colour is encountered early and briefly, concentrated in a first-year foundational course, most often through exercises in perceptual relationality inherited from Albers's (1963) Interaction of Color . These exercises are valuable: they train the eye to see that colour is relational and context-dependent. But they were never designed to constitute a complete colour education for a designer, and in most curricula they are followed by little or nothing. The designer then meets colour again in professional practice as a finishing tool, a decision made once the form, the function, the material, and the user have already been settled. Several scholars have documented the marginal position of colour in design and architecture education over the past three decades (Calvo Ivanovic, 2024).

The problem, however, is not simply that colour is taught too little. It is that the discipline has misclassified what colour is. Recent work in colour and design education has proposed that colour is more accurately understood not as a visual element that design contains, but as a form of infrastructure within which design operates (Calvo Ivanovic, 2026). The reframing draws on Susan Leigh Star's analysis of infrastructure, which identifies properties characteristic of infrastructural systems: they are embedded in everything they make possible; they recede from notice while functioning; they are learned as part of membership in a community of practice; and they become visible only when they break down (Star, 1999). Colour exhibits each of these. It is embedded in every designed artefact; it is invisible when it works, so that a user experiences the product, the space, or the message rather than "the colour of" it; it is acquired through membership in particular communities of practice, so that a textile dyer, a colour scientist, and a film colourist each know a different colour; and it becomes conspicuous precisely when a colour decision fails.

Contemporary design practice is producing such failures with increasing frequency and visibility. Consider four brief instances, each of which this paper will return to. First, the ecological: textile dyeing alone accounts for approximately 20% of global water pollution, and up to 80% of a product's environmental impact is determined by decisions made at the design stage, among them the choice of colourants and their material behaviour (European Parliament, 2020; Murzyn-Kupisz & Hołuj, 2021). Second, the cultural: colour decisions that presuppose universal meaning misfire when deployed across cultural contexts, as when a global beverage brand's colour choice communicates celebration in one market and mourning in another (Madden, Hewett & Roth, 2000). Third, the accessibility of colour-coded systems: wayfinding schemes that rely on colour alone fail the approximately 8% of men and 0.5% of women with colour vision deficiency, and fail further under the lighting conditions and among the ageing populations of the environments in which they are actually used (Mollon, 2003). Fourth, the algorithmic: generative AI image systems reproduce systematic colour biases, with one 2025 study finding that widely-used models generated dermatological images featuring light skin tones in nearly 90% of cases (Joerg et al., 2025).

These are not isolated failures of individual judgement. They are the visible surface of a structural condition: colour decisions of real consequence are being made across the full arc of contemporary design practice, by practitioners who have not been prepared to recognise them as colour decisions, and who therefore make them without the knowledge those decisions require. The remedy cannot be simply more colour content added to an already crowded first-year course. What the discipline needs is a map of the territory colour actually occupies, one that can orient educators and practitioners to the domains in which colour competence is required, and that can locate where in the design process each domain is called upon. This paper presents such a map. It sets out a four-area framework for colour competence in design, describes the developmental history and epistemological commitments that underpin it, introduces the cross-cutting capacities that operate across its four domains, and argues that accountability, one of those capacities, is what the framework finally makes operable.

2. A framework for colour competence in design

2.1. Origin, development and epistemological grounding

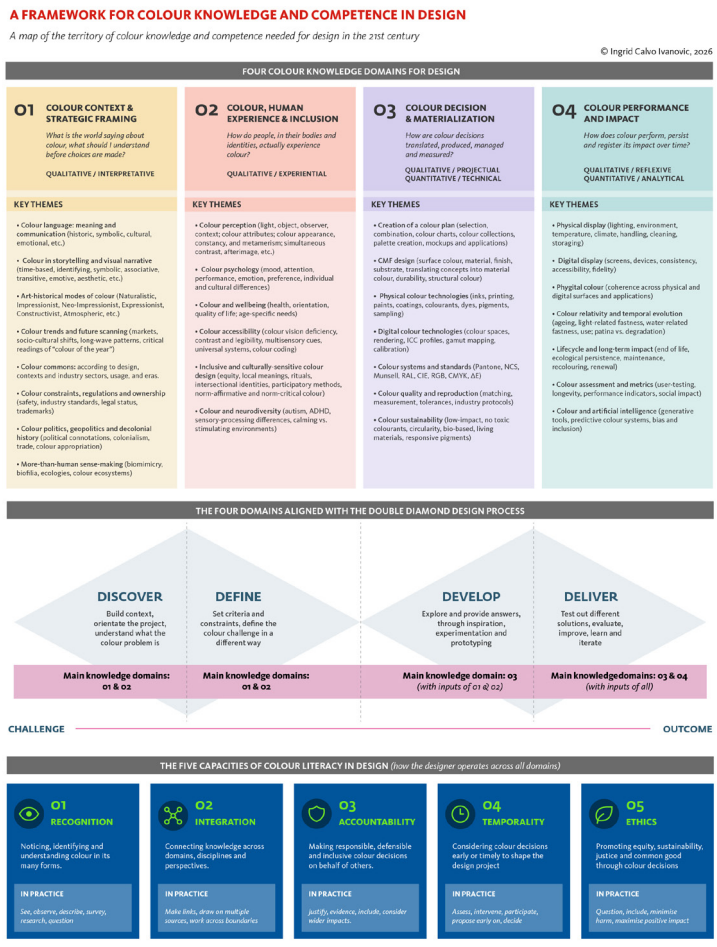
The framework presented here (Figure 1) did not arrive fully formed. It is the product of seventeen years of research and teaching in colour for design, and it has evolved substantially. Its first articulation appeared in the author's doctoral thesis (Calvo Ivanovic, 2022), which, on the basis of a literature review of where and when colour decisions occur in the design process, identified four phases of colour decision-making: a Conceptual phase, concerned with colour meaning, association, and selection; a Human Factors phase, concerned with perception, psychology, and the human response to colour; a Manufacture phase, concerned with the material and technical realisation of colour; and an Exhibition phase, concerned with how colour is displayed and perceived in its final context. This first version, grounded in the literature, mapped colour decisions onto the temporal sequence of a design project and demonstrated that colour is not confined to a single moment but recurs throughout.

As the author socialised this version through international presentations, workshops, and teaching, and developed it through practice, two limitations became

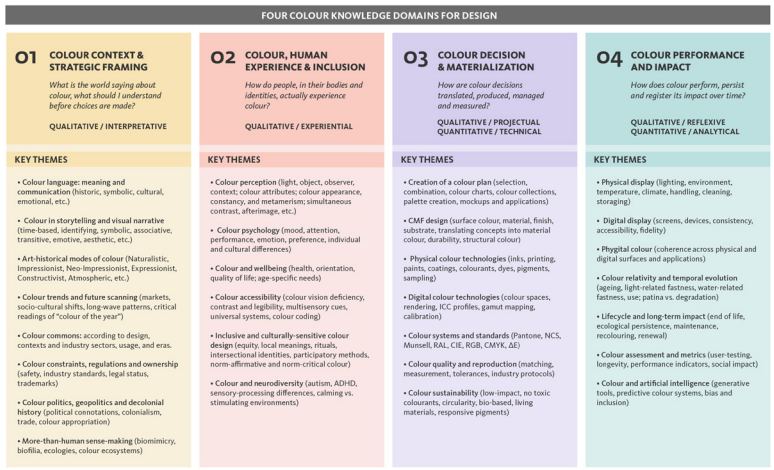
evident. The first was conceptual. The phase-based labels described when colour decisions occur rather than what kind of knowledge they require. A phase is a moment in a sequence; but the difficulty designers face with colour is not primarily one of timing, it is one of knowledge. What a designer needs is not to be told that colour decisions happen at the conceptual stage, but to understand what body of knowledge a colour decision at that stage draws upon, and what it would mean to make it well. The second limitation was one of completeness: as the author's understanding developed through further research and practice, the original four phases proved too narrow to accommodate the full range of contemporary colour concerns, from sustainability and cultural specificity to algorithmic mediation and neurodiversity.

The current version responds to both. It reconceives the four phases as four domains of colour knowledge and competence, renamed to foreground the domain of knowing rather than the stage of the process: Colour Context and Strategic Framing; Colour, Human Experience and Inclusion; Colour Decision and Materialisation; and Colour Performance and Impact (Figure 2). This shift, from phases to domains, is the framework's central conceptual move. It transforms the framework from a description of a sequence into a map of a territory. A phase is something a project passes through and leaves behind; a domain of competence is something a designer inhabits and returns to. The re-conception also allows each domain to expand well beyond its original phase content, to encompass the strategic, cultural, ecological, ethical, and inclusive dimensions contemporary colour decisions require. In its development beyond the doctoral version, the framework is author-derived, grounded in research, teaching, and professional practice rather than in a single systematic study; its validation through teaching and application is ongoing work. The framework models colour as an accountable decision made by a designer, on behalf of others, within a design process, which is also the boundary of its scope: artistic colour practice, answering to no brief and no external accountability, and colour as a primary product in its own right, as in a colour-forecasting house or a paint manufacturer's range, draw on the same bodies of knowledge but lie outside the decision model the framework describes.

Two structural properties govern how the framework should be read. The first concerns ways of knowing. The four domains do not all rest on the same kind of knowledge, and they do not divide evenly between



» **Figure 1:** *Overview of the Framework for Colour Knowledge and Competence in Design*

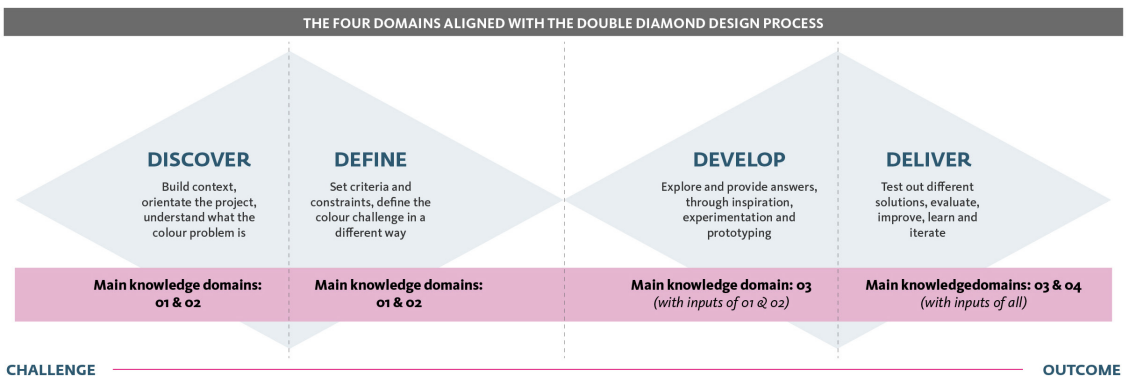


» **Figure 2:** *The four colour knowledge domains for design. Each domain names the question it addresses, the ways of knowing it draws upon and presents its main themes*

kinds. The first two domains are predominantly qualitative, but in distinct registers: Area 01 knows colour interpretatively, through cultural reading, historical understanding, and strategic analysis, while Area 02 knows it experientially, through perceptual, psychological, and participatory inquiry into how colour is lived in the body and in communities. The second two domains are each dual. Area 03, where a colour is decided and made, joins a projectual way of knowing — the designerly act of composing a palette and conceiving a colour-material-finish — to a technical, quantitative one: colorimetry, standardised colour systems, measurable tolerance. Area 04, where colour performs and registers its impact, joins an analytical way of knowing — the measurement of display, durability, and change — to an evaluative one: the qualitative assessment of how colour is received, and whether it does what it was intended to do, once real people live with it.

This division is not incidental, and it maps onto the structure of the design process itself. The four domains are aligned with the Double Diamond model of the design process (Design Council, 2021), a widely-used articulation of design as a movement through Discover, Define, Develop, and Deliver (Figure 3). The alignment is deliberate but loose. It does not claim that colour decisions must follow a fixed order; it indicates where in the design process each domain is most actively called upon, while recognising that any domain may be relevant at any point. The alignment makes the framework legible to designers who already use the Double Diamond, and situates colour competence within the process of design rather than alongside it.

The challenge space of the first diamond, Discover and Define, is navigated qualitatively, by interpretation and lived experience; the outcome space of the second, Develop and Deliver, demands the qualitative and the quantitative together, because making a colour real, and accounting for its life in the world, cannot be done in either register alone. This is not a hierarchy, and it is not an admission that some domains are better evidenced than others. It reflects a genuine plurality in how colour is known, one the colour research community has increasingly come to recognise, moving from an earlier period in which quantitative measurement was treated as the only fully legitimate form of colour knowledge, toward a contemporary understanding in which experiential, practice-based, and situated ways of knowing are acknowledged as equally valid and equally necessary (Calvo



» **Figure 3:** *The four-domain framework for colour competence in design, aligned with the Double Diamond model*



» **Figure 4:** *The five capacities of colour literacy operate across all four, with accountability foregrounded*

Ivanovic, 2026). Colour literacy, on this account, is not competence in one way of knowing but the capacity to move appropriately between several of them. A designer who can measure the difference of two colour samples to a ΔE tolerance but cannot interpret its cultural meaning, or a designer who can interpret its cultural meaning but cannot specify it for production, are each colour-literate in one register and illiterate in another. The framework holds both, and insists that both are required.

The second structural property is that the framework operates across two dimensions. The four domains are one dimension: they describe what a colour decision touches, and, as argued below, they are structurally stable. The other dimension consists of the five capacities of colour literacy that operate across all four domains (Figure 4): recognition, integration, accountability, temporality, and ethics (Calvo Ivanovic, 2026). These describe how a designer operates within the territory the domains define, and, unlike the domains, they are historically contingent in their emphasis. This two-dimensional structure is developed in Section 2.7; it is noted here because it shapes everything between. Accountability, the capacity this paper foregrounds, belongs to this second dimension: it is not a domain but a way of operating across all of them.

The four knowledge domains are described in turn below. Each represents a distinct territory of colour knowledge, with its own body of evidence, its own methods, its own vocabulary, and its own standards of accountability. A designer is unlikely to hold equal depth across all four; a printing specialist will dominate the third domain more than the first, just as a brand strategist will command the first more fully than the third. But a colour-literate designer is one who is aware that all four domains exist, who can recognise when a decision draws upon a domain outside their depth, and who knows how to seek the knowledge that decision requires.

2.2. Colour context and strategic framing

The first domain concerns the strategic and cultural foundations of colour decisions. It is most active during the Discover phase, when the designer builds context, orients the project, and establishes the intellectual and cultural territory within which colour decisions will be made. It asks: what is the world saying about colour, and what should I understand before any choice is made? Its characteristic way of knowing is qualitative and interpretive, drawing on the humanities and social sciences rather than on measurement. Crucially, this domain treats culture as external context to be researched, knowledge about the world that informs a decision, a framing that distinguishes it from the second domain, where culture appears as lived human difference to be included.

At its core is colour language: meaning and communication: how colour carries meaning across symbolic, cultural, and emotional registers, and how those meanings shift across geographies, communities, and histories. Here a designer learns that colour associations are not universal facts but cultural conventions, and develops the interpretive capacity to establish what a colour communicates in a given context rather than assuming a shared meaning. Closely related is colour in storytelling and visual narrative, the ways colour operates as a narrative device: performing distinct functions that include the time-based (marking periods, flashbacks, or the passage of time), the identifying (distinguishing characters, brands, or elements), the symbolic and associative (carrying thematic meaning), the transitive (guiding the eye and signalling change), the emotive and aesthetic (setting mood and tone), and the audio-visual and communicative (operating alongside sound and motion). It also encompasses the major art-historical modes of colour in image-making, each offering a distinct logic that contemporary visual designers continue to draw upon, often without naming it: the Naturalistic (colour as the faithful description of the observed world, the local colour of things as they are), the Impressionist (colour as the record of perceived light, dissolving local colour into the atmosphere that falls on it), the Neo-Impressionist (colour as optical mixture, the divided, systematic juxtaposition of pure tones that fuse in the eye and exploit simultaneous contrast deliberately), the Expressionist (colour as the vehicle of emotion and subjectivity, released from description altogether), the Constructivist (colour as structural and functional element, assigned a job rather than a mood), and the Atmospheric (colour as the carrier of depth and distance, the

cooling and desaturation of receding planes). These are not historical curiosities. Each survives as a living logic in contemporary design: the Naturalistic and Atmospheric wherever colour renders a world and situates the eye within it, in cinematography, environmental and spatial design, and photographic grading; the Impressionist and Neo-Impressionist wherever colour is treated as light and optical event, in screen-based and generative image-making; the Expressionist in any deliberately heightened palette chosen for emotional charge, in branding, title sequences, and editorial illustration; and the Constructivist wherever colour is given a structural task, coding information, organising a layout, distinguishing zones in an interface, a building or a transit map. A designer who can name which logic a project calls for is making a more deliberate and more defensible colour decision than one working by untheorised preference.

Adjacent to these is colour trend and future scanning: tracking colour change over time and anticipating its directions, and, critically, distinguishing the genuine cultural and social signals in colour movements — through market cycles, socio-cultural shifts, and long-wave historical patterns — from their commercial orchestration. The annual "colour of the year" phenomenon is frequently received as cultural insight when it is more accurately understood as a commercial product; a designer competent in this domain reads such phenomena critically rather than simply following them (Calvo Ivanovic, 2025). This attention to the collective movement of colour leads directly to a further concern of the domain: colour decisions do not stay singular. They aggregate, through shared tools, trends, and markets, into the colour commons — the collective colour languages of a sector, an industry, or an era. A strategically and ethically literate designer is aware of the contribution each decision makes to this shared resource, and not only to the individual artefact, and reads the commons of their field as part of understanding what the world is already saying about colour. The domain also sets out what the world requires of a colour decision before it is free to be made. Many colour decisions are not open at all but prescribed, through colour constraints, regulation, and ownership: mandated safety colours, industry and regulatory standards, and the legal status of colour itself, including trademarked and protected colours a designer may not use and may wish to establish. The competence is to research and surface these early, in the Discover phase, rather than to discover them after a decision has been made. The domain includes colour, geopolitics, and decolonial history, which recovers the ways colour history has been shaped by colonialism, trade in dyes and pigments, and cultural appropriation — an aspect of colour knowledge that design education has largely omitted and that a responsible practice increasingly requires. And it extends, at its outer edge, to more-than-human sense-making, which asks how colour functions beyond human perception, drawing on biomimicry and the study of ecological colour signalling, the pigment and pattern strategies of other species, and the chromatic logic of habitats and ecosystems, as sources of design knowledge and inspiration. Treated as applied inquiry rather than speculation, it offers designers a repertoire of colour strategies refined over evolutionary time.

2.3. Colour, human experience and inclusion

The second domain concerns colour as a dimension of human experience: the perceptual, psychological, physiological, and social registers through which colour is received and responded to. It is most active at the transition from Discover to Define, as the designer deepens understanding of the people for whom they are designing and translates it into criteria and constraints. It asks: how do people, in their bodies and identities, actually experience colour? Its characteristic way of knowing is qualitative and experiential, though it draws also on the empirical evidence of perceptual and health science. Where the first domain treats culture as external context to be researched, this domain treats culture as lived human difference to be included, the situated experience of specific people who must be designed with rather than for. The first is epistemic; the second is ethical and participatory. A study of how the red hue family communicates across cultures belongs to the first domain; designing a colour system with and for a particular community belongs to the second.

The domain begins with colour perception: how colour is physically and cognitively processed, including the interdependence of light, object, observer, and context, the phenomena of colour constancy and metamerism, and the relational instability of colour in interaction, where adjacent colours alter one another through simultaneous contrast and afterimage. It extends to colour psychology in its empirically grounded form, distinguished sharply from the universal hue-based symbolism that circulates through popular discourse: the evidence shows that colour's effects on mood, attention, performance, and emotion are real but are strongly mediated by lightness and saturation as well as hue, by context, and by individual preference and cultural difference. It includes colour and wellbeing: how colour in built environments affects health, orientation, and quality of life, with particular attention to age-specific needs and to supportive environments in healthcare and care settings. It encompasses colour accessibility: colour vision deficiency and its design implications, legibility and contrast, multisensory colour cues, universal and safety-colour systems, and the principle of redundant coding, in which colour information is usually paired with a second channel so that no user depends on colour discrimination alone. Two phenomena from this domain deserve emphasis because they are routinely underestimated in practice. The first is the sheer

prevalence of colour vision deficiency, which affects roughly one in twelve men: a colour decision that relies on distinguishing red from green is, in effect, a decision that a significant fraction of the audience will misread, which is why redundant coding, adding a pattern, a label, a shape, or a position to carry the same information, is not an optional accommodation but a baseline of competent colour design. The second is metamerism, the phenomenon by which two colours that match perfectly under one light source diverge visibly under another. A pair of materials specified to match in the studio may fail to match in the showroom, the street, or the hospital corridor, with real consequences for products assembled from differently-sourced components. Both phenomena reward the same disposition: treating the perceiving human, in the actual conditions of use, as the final arbiter of a colour decision, rather than the designer's eye in the controlled conditions of the studio.

It contains inclusive and culturally-sensitive colour design: the practice of designing colour for equity and participation, centring marginalised and underserved communities, attending to local colour meanings and regional palettes, to rituals and customs, and to intersectional and hybrid identities, and working through participatory decision-making rather than imposing a dominant colour standard. It admits both norm-affirmative approaches, which work within a community's existing colour conventions, and norm-critical ones, which challenge inherited defaults, and it draws on affective-measurement methods to understand subjective and emotional responses to colour across diverse groups. And it now includes colour and neurodiversity: the design of colour for autistic people, people with ADHD, and those with sensory-processing differences, attending to sensory overload, to neurodivergent colour preference, and to the difference between calming and stimulating colour environments, a significant and underserved territory in both practice and education.

2.4. Colour decision and materialisation

The third domain concerns the transformation of a colour decision into realised form — physical, digital, or a hybrid of the two. It is most active during the Develop phase, the period of decision, prototyping, specification, and technical resolution in which colour moves from intention to outcome. It asks: how are colour decisions translated, produced, managed and measured? This is the domain where the two ways of knowing the framework insists upon are not merely both present but inseparable. It joins a projectual way of knowing — the designerly act of composing palettes and conceiving how colour will meet material and surface — to a quantitative, technical one: the colour science, measurement, and standardisation through which a decision either survives the journey to the finished artefact or is lost in translation. It is where the designer's responsibility for a colour decision meets the material and technological reality of what can actually be produced. Precisely because it holds both registers at once, it is the clearest demonstration in the framework that a decision made well and a decision made real are two faces of a single competence.

At the point of decision is the colour plan: the concrete, specified set of colour choices the designer commits to and will hand over, expressed through colour selection, colour charts and collections, palette creation, and application of colours across the designed artefact and its mock-ups. Central to the colour plan is colour combination: the relational craft of deciding which colours sit together, in what proportion and arrangement, to form a working palette. This paper deliberately declines the traditional vocabulary of "harmony" and "contrast" to name this craft, because those terms carry — and have carried into generations of design teaching — the misconception that colour combination is governed by the attribute of hue only, and fixed rules of correct and incorrect pairing (Colour Literacy Project, n.d.; Calvo Ivanovic, 2026). Combination is better understood as a situated, intentional act of composition, answerable to the project rather than to a rulebook. Its perceptual basis — how adjacent colours alter one another through simultaneous contrast, vibration, and the relational instability demonstrated by Albers (1963) — is knowledge held in Area 02; what belongs here, in the colour plan, is the designer's act of deciding and specifying the combination itself. The colour plan is where the designer's reasoning across all four domains becomes a tangible, defensible artefact; it is, in a precise sense, accountability made material — the palette as the justification rendered concrete and ready to go into the world.

The decision becomes material through CMF design — Colour, Material, and Finish — the practice in which colour specification is inseparable from material selection and surface treatment. The appearance and behaviour of a colour depend on the substrate that carries it, on its finish and texture, and on its performance against fade, wear, humidity, UV exposure, and ageing. This theme includes the systematic study of surface behaviour, sometimes approached through frameworks such as CESIA, and the phenomenon of structural colour — colour produced by physical microstructure rather than pigment, as in iridescence and certain structural blues. It is given material existence through the physical colour technologies — inks and printing, paints, coatings, colourants, dyes, and pigments, and the practice of colour sampling — and through the digital colour technologies — colour spaces, rendering, ICC profiles, gamut mapping, calibration, and colour management — which determine whether a colour decision is reproduced faithfully from screen to output and across the devices and production chains that carry it.

These technologies are governed by shared colour systems and standards — the Pantone Matching System, NCS, Munsell, RAL, the CIE colour spaces, the RGB and CMYK models, and the ΔE colour-difference metric — the languages through which colour is specified and communicated across the production chain, varying by region and industry. And they are held to account through colour quality and reproduction: colour matching, instrumental and visual assessment, colorimetric measurement, and ΔE tolerance management, through which fidelity is verified and each industry defines the limits of acceptable difference. It is worth making this concrete, because it is the bridge from which the framework extends. The ΔE metric expresses the perceived difference between two colours as a single number: a ΔE of roughly one marks the threshold of a just-noticeable difference under controlled conditions, a ΔE below one is generally imperceptible, and the number grows as two colours diverge. Different industries set their acceptable tolerance accordingly, and the choice is an economic and perceptual judgement as much as a technical one: a premium automotive finish, where a visible mismatch between a body panel and a bumper would read as a defect, may demand a tolerance near ΔE one; whereas a printed textile, where the eye is more forgiving and the production process less controllable, may accept a ΔE of several units. The colour-literate designer understands not only how to read such a number but why the tolerance differs between a car door and a cotton shirt, and can therefore specify colour in a way the production chain can actually deliver. This is quantitative colour knowledge in its most developed form; and it sits, in this domain, alongside the projectual judgement of the colour plan, so that Area 03 holds the two ways of knowing in a single working relationship. The rigour designer, in collaboration with other professionals, brings to ΔE, is precisely the standard the framework asks the other domains to match in their own registers.

Finally, the domain carries colour sustainability at the point of production: low-impact colourants, circular approaches to colour, durability and repairability, and the emerging fields of bio-based and living colour materials, and of active or responsive pigments — thermochromic, photochromic, UV-reactive, time-based or photodegradable, and electrochromic — that change with temperature, light, or time. Sustainability is not a separate concern bolted onto production but a dimension of every material and technological choice the domain makes, and it is where the ecological consequences of a colour decision are first determined, before they are later observed in use.

2.5. Colour performance and impact

The fourth domain concerns what colour does after it enters the world: how it performs over time, in real environments, for real people, and with consequences the designer must anticipate before they can be observed. It is most active during the Deliver phase, and its subject matter extends well beyond it, into the in-use life of the artefact — which means the domain is often drawn upon anticipatorily: at the moment of delivery the designer is already reasoning about a performance that will only unfold over the months and years after the project closes. It asks: how does colour perform, persist, and register its impact over time? Its ways of knowing are dual — an analytical, quantitative measurement of display, durability, and change, and an evaluative, qualitative assessment of how colour is received and whether it achieves what it was designed to achieve. The intended emotional impact of a colour, and its influence on behaviour, are not decided here; they are formed in the first and second domains, on the basis of cultural framing and human understanding, and the colour that carries them is decided and specified in the third. What this domain does is test those intentions against reality: it is the site of evaluation, not of origination.

It encompasses physical display: how a colour is perceived under the specific lighting, spatial relationships, and surrounding colours of its actual environment, which may differ markedly from the studio, and how it responds to natural and artificial light, temperature and seasonal shifts, storage, handling, cleaning, and climate. It includes digital display: the performance of colour across screen technologies and devices, cross-device consistency, colour accessibility in user interfaces, and the constraints of gamut. And it now includes phygital colour: the coherence of colour across physical and digital surfaces experienced together, as in a product and its companion application, or a printed artefact and its augmented overlay, highly relevant today for e-commerce and online purchasing. Phygital coherence belongs here, rather than with the production technologies that achieve it, because it is ultimately a question of performance in experience — whether the colour reads as one and the same across the surfaces a person encounters in use — and it is verified, like everything else in this domain, against the world rather than in the studio.

It contains colour relativity and temporal evolution: how colour evolves as materials age and are exposed to light and use; how designed colour change may be valued as a quality, as in materials designed to patina, or mismanaged as a failure; and how designing for colour evolution requires competences distinct from designing for stability. This temporal dimension is one the discipline is least trained to consider, because design education and design representation both favour the fixed, finished image — the render, the mock-up, the swatch — over the artefact as it will actually look after a year, a decade, a lifetime of weather and use. Yet almost every physical colour decision is in truth a decision about a trajectory: a façade colour is a decision about how a building will look as its coating chalks and fades; a naturally dyed

textile is a decision about how a garment will soften with washing; a patinating metal is a decision to let the material write its own colour over time. A designer competent in this domain decides not only the colour of the thing at the moment of delivery but the colour of its whole life, and can tell the difference between an evolution that enriches an artefact and a degradation that ruins it. It encompasses the lifecycle and long-term impact of colour decisions in use: the fate of coloured materials at end of life, the ecological persistence of dyes and pigments, the legibility of visible recycled colour, strategies of maintenance, recolouring, and renewal that reward care over replacement, and the reception of colour over time within the communities that inhabit it.

It contains, too, colour assessment and metrics, the under-developed but essential question of how the success of a colour decision is actually measured: user-testing protocols for colour, longevity benchmarking, colour performance indicators in brand strategy, and social-impact assessment, including the evaluation of whether the emotional and behavioural effects a colour was designed to produce are in fact produced once it is experienced by real people. Without this evaluative competence, colour decisions cannot be judged against evidence, and the discipline cannot accumulate knowledge about which colour decisions succeed and why.

Finally, and most recently, the domain has come to include colour and artificial intelligence, placed here because the most consequential questions AI raises about colour are questions of impact. Generative tools that produce palettes and images, and predictive systems that anticipate colour directions, are increasingly the instruments through which colour is delivered; but their most far-reaching effect is systemic. The datasets on which these tools are trained encode cultural and racial biases, and because the tools operate at scale, they reproduce those exclusions across countless outputs at once, registering an impact on the colour landscape far larger than any single decision. Treating colour and AI as a matter of performance and impact, rather than of production technique alone, keeps the designer's attention on the right question: not only what the tool can make, but what — cumulatively, and across whole populations of users — it brings into the world.

2.6. Two dimensions: stable domains and the capacities that operate across them

The four domains are only one dimension of the framework. Operating across all of them is a second dimension: the five capacities of disciplinary colour literacy (shown in Figure 4), recognition, integration, accountability, temporality, and ethics (Calvo Ivanovic, 2026). These are not themselves domains of knowledge but ways in which the designer operates within the territory the domains define. Recognition is the capacity to see when a design decision is also a colour decision. Integration is the capacity to draw on the relevant knowledge domains, and on the contributing disciplines and research methods behind them, without being expert in all of them. Accountability is the capacity to justify a colour decision, which includes being able to name, document, and communicate it, since a decision that cannot be articulated cannot be justified. Temporality is the capacity to make colour decisions early enough to shape the design rather than merely finish it. And ethics is the recognition that colour decisions are made on behalf of others who must live with their consequences. Colour research methods and colour communication, sometimes treated as separate competences, are better understood as integral to these capacities: research is how integration and accountability reach their fullest expression, the production of colour knowledge rather than its mere application, and communication is accountability made external.

The distinction between the two dimensions is not merely organisational; it is a claim about how the framework relates to time. The four knowledge domains are proposed as structurally stable, and are an attempt to exhaust the dimensions of a colour decision in design. They are defined by what a colour decision necessarily touches: the world it enters, the people it is for, the matter it is made of, and the consequences it produces over time. The five capacities, by contrast, are historically contingent in their emphasis. They are exercised differently, and weighted differently, as the needs of design change. Accountability is foregrounded now because the present moment, with its ecological, cultural, inclusive, and algorithmic pressures, makes the justification of colour decisions unusually urgent; a different moment may foreground a different capacity.

The relationship between the two dimensions is dynamic, and it is worth stating as the framework's central hypothesis about its own evolution. When a new design condition arises, it registers first as a new demand on the capacities, a new way the designer must operate, which practice suddenly requires. The arrival of generative AI in mainstream design is a clear instance: it created, almost overnight, an intensified demand on accountability, the need to verbalise colour precisely, and on integration, the need to understand how models handle colour and encode bias. That demand is cross-cutting; it operates across every domain. But to meet it, designers need knowledge that did not previously sit clearly in any domain — how diffusion models process colour, how corpora encode chromatic bias — and that knowledge is then absorbed into the existing domains: the systemic, cultural, and racial bias these tools reproduce settles into Area 04, as a question of colour's impact at scale, informed by the human and cultural understanding of Areas 01 and 02, while the demand to verbalise colour precisely settles into the practice of decision and speci-

fication in Area 03, where the colour plan is composed and made. The capacities, in other words, are the framework's leading edge, where new needs first register; the domains are its slower-moving structure, which absorbs the new knowledge those needs demand. This is how the framework has already grown: sustainability, neurodiversity, decolonial history, and algorithmic colour all entered as new demands and were absorbed into the four domains without requiring a fifth. The hypothesis on which the framework rests is that this absorption will continue: that emerging demands will enrich the domains, including by bringing new ways of knowing into them, rather than requiring the domains themselves to multiply. This is offered as a design hypothesis rather than a law; should future research reveal a colour concern no existing domain can absorb, the framework would need revision. But its structure is deliberately built to make such revision rare, by carving the domains at the joints of what a colour decision fundamentally is. For instance, one specific body of practice — colour in service and experience design, the sustaining of colour coherence across the many touchpoints of a designed service — is best understood not as a domain or a capacity but as a context in which all four domains and all five capacities are exercised together.

3. Accountability: the capacity the framework makes operable

Of the five capacities, one has a special relationship to the framework, and it is the focus of the remainder of this paper: accountability. A recent account defines disciplinary colour literacy as the full set of five, and situates accountability among them as the capacity to answer the question why this colour? with reasoning grounded in evidence and context, to the standard the discipline routinely applies elsewhere (Calvo Ivanovic, 2026). It is worth dwelling on how unusual the absence of this standard is. In design education and practice, decisions the discipline takes seriously are decisions it expects to see justified. A student who selects a material, specifies an ergonomic feature, or chooses a typeface is expected to explain the choice: what informed it, what alternatives were weighed, why this one. The justification standard signals that a decision is consequential, and it is how design knowledge accumulates.

Colour decisions are, almost universally, exempted from this standard. The question why this colour? is seldom asked in design critique, and when it is asked, answers such as "it felt right," "it suits the brand," or "it works with the other elements" are commonly accepted as sufficient, in a way the equivalent answers would not be accepted for a structural or material decision. This exemption is so normalised that it is rarely experienced as a problem. But it is the clearest expression of colour's misclassification: a domain treated, in practice, as falling below the threshold of serious accountability.

Here the framework and the capacity meet, and this is the central argument of the paper. Accountability for colour decisions is not possible without the framework, because one cannot justify a colour decision without knowing which domains of colour knowledge it draws upon, and by which ways of knowing. To answer why this colour? responsibly is to answer with reference to the relevant domains: to the cultural and strategic context that informed the decision (Area 01), to the perceptual and inclusive requirements of the people it serves (Area 02), to the material and technical constraints that shaped it (Area 03), and to the environmental and temporal conditions under which it will perform (Area 04). The four domains are, in this sense, the very structure of a colour justification. They are what a well-reasoned answer to why this colour? is made of. Without the map of the territory, accountability has no content; it can only gesture at intuition. With it, accountability becomes a concrete practice: the designer locates the decision within the relevant domains, marshals the knowledge each requires in the way of knowing appropriate to it, and justifies the choice accordingly. The other four capacities support this: recognition identifies the decision as a colour decision in the first place; integration gathers the knowledge across domains; temporality ensures the decision is made early enough to be shaped by that knowledge rather than retrofitted to it; and ethics orients the whole toward the people who will live with the result.

This argument has a specific and timely implication for AI-assisted design. Generative image systems will not accept an intuitive colour decision; they require it to be verbalised before it can be executed. A designer working with a generative tool must specify the hue, the saturation, the finish, the relationship between tones, in language, before the system can act. The tool imposes, by technical necessity, precisely the accountability design culture has never required voluntarily: the demand that a colour decision be put into words. The verbalisation demand of the generative tool and the justification demand of the framework are, at bottom, the same demand. The designer who cannot say why this colour cannot direct the tool, just as they cannot defend the decision in critique. Design's long tolerance of colour intuition, sustained because intuition was never required to explain itself, is being ended not by pedagogy but by the operating conditions of the discipline's newest tools.

4. The framework in practice: colour decisions across the domains

The framework's value is clearest when a single colour decision is traced across the domains it touches. In practice, consequential colour decisions rarely belong to one domain alone; they move through several, and accountability requires the designer to answer for the decision in each. Five worked examples follow, drawn from different fields of design practice, each reading a colour decision as a movement across the framework.

A global brand colour for a new market. Consider a designer adapting a global brand's colour identity for a culturally distinct market, the situation behind the beverage-industry noted earlier. The decision begins in Area 01: it requires cultural research into what the proposed colours communicate in the specific market, historical understanding of local associations, and strategic reasoning about the relationship between colour and brand equity. This is where the beverage company failed, deploying a light blue associated regionally with mourning without the cultural research the domain demands. But the decision does not stay in Area 01. It moves into Area 02, where the designer must consider how the colours will be perceived by the actual population, including those with colour vision deficiency, and whether the palette carries inclusive or exclusionary associations for the communities it addresses. It moves into Area 03, where the brand colours are composed into a colour plan and specified to production standards, held within tolerance across every manufactured touchpoint. And it resolves in Area 04, where the colours are evaluated in situ on real signage under real light and on real screens, and tracked over time. A designer accountable for this decision must answer for it in all four domains; a failure in any one — unresearched culture, excluded users, unmatched production, unevaluated performance — is a failure of the whole.

A hospital wayfinding system. A colour-coded wayfinding scheme for a hospital begins, unusually, in Area 02, because its governing consideration is human: the perceptual and cognitive experience of navigating a stressful environment, including the substantial minority of users with colour vision deficiency and the age-related changes in colour perception common among patients. Competence here yields the principle of redundant coding, pairing each colour with a distinct pattern so that no user depends on colour alone. But the decision also draws on Area 01, in understanding the cultural colour associations of the medical sector across its usage; on Area 03, where the colours are composed into a colour plan and specified so they reproduce consistently across painted surfaces, printed signs, and digital displays, and hold under the building's actual lighting; and on Area 04, where the system is evaluated once installed, to confirm it reduces disorientation and continues to perform as signage ages. The wayfinding decision that fails is almost always one made in a single domain; an aesthetically pleasing palette selected without the Area 02 knowledge that renders it navigable.

A bio-based colour for a product. A designer choosing a bacterial or algae-derived colourant for a textile or product, following bio-pigment projects such as Living Colour (Luchtman & Siebenhaar, 2017), makes a decision anchored in Area 03: the material and biological behaviour of the colourant, its fastness, its production process, its place within the emerging science of living colour. But the decision is legible as a colour decision only across the full framework. It draws on Area 01 in its strategic and ethical framing, the state of the art of ecological responsibility made visible through colour; on Area 02 in ensuring the palette remains perceptually effective and inclusive; and, crucially, on Area 04, where the colour's defining characteristic — that it may shift and fade over time as a living material — must be anticipated and later evaluated not as a failure of stability but as an intended quality of colour evolution. That intention is recorded in the colour plan when the colourant is chosen (Area 03); whether the evolution is in fact experienced and valued as intended is what Area 04 assesses. A designer who specifies a bio-colour with only the material knowledge of Area 03, and who has formed no Area 04 account of how its temporal change will be received, has made an incomplete decision.

A data-visualisation colour system. A designer building the colour scheme for a dashboard, an information graphic, or a data-heavy interface, makes a decision that is easy to mistake for pure aesthetics and is in fact one of the most constrained colour problems in design. It is anchored in Area 02, because its first obligation is perceptual and inclusive: a categorical palette must remain distinguishable for the substantial minority of users with colour vision deficiency, which rules out the red-green pairings still common in financial and medical charting, and a sequential or diverging scale must preserve a perceptually uniform progression so that equal steps in the data read as equal steps in colour, a property that naive rainbow scales notoriously violate. The decision then draws on Area 03, where the chosen colours must survive the quantitative realities of digital reproduction — the gamut limits of different screens, the shifts introduced by varying calibration, and the need for sufficient measured contrast against background and between adjacent categories — and where the colour plan, the documented set of categorical hues, scale endpoints, and contrast ratios, becomes the specification handed to developers. It extends into Area 04, where the palette must be evaluated across the actual devices and lighting conditions in which the data will be read, from a calibrated desktop monitor

to a phone in sunlight. Area 01 is present too, more quietly, in the conventions a given field attaches to colour, the expectation that red marks loss or danger, green gain or safety, which the designer must either honour or deliberately subvert. A data-visualisation palette chosen for visual appeal alone, without the Area 02 knowledge that governs its legibility, is among the most common and most consequential colour failures in contemporary practice, because it silently excludes readers and distorts the data it was meant to clarify.

An architectural colour scheme for a public building. A designer or architect developing the colour scheme for a building, a façade in an urban streetscape, or the interior of a civic or healthcare space, makes a colour decision that unfolds across all four domains over a timescale measured in years. It begins in Area 01, with the cultural and contextual intelligence the setting demands: the local colour identity of the place, the heritage and material palette of its surroundings, the regional and historical colour conventions a new intervention will either continue or disrupt. It moves deeply into Area 02, because a building is inhabited: the colours must support wellbeing and orientation for the people who will use the space, account for how colour is perceived under the specific daylight and artificial lighting of the site across seasons, and serve diverse and sometimes vulnerable populations, patients, children, older adults, whose perceptual and psychological responses to colour differ. It is realised through Area 03, where architectural colour meets the hard constraints of materials: the coatings, renders, cladding, and finishes available; their fade resistance, weathering, and maintenance behaviour; and the CMF decisions that determine how a specified colour will actually appear on a given surface at architectural scale; it is here that the scheme is composed into an architectural colour plan. And it is tested and sustained in Area 04, the domain where architectural colour is most exposed, because a building's colour performs in public, under changing light, through weather and ageing, for decades: the scheme must be evaluated for how it reads at different distances and times of day, how it will weather and patina, how it integrates with and affects its surrounding environment, and how it can be maintained or renewed. Architectural colour is perhaps the clearest demonstration that a colour decision is not a moment but a trajectory, and that accountability for it requires reasoning across the full territory the framework maps.

In each case the framework performs the same work. It converts a diffuse sense that "colour matters here" into a specific account of which domains of knowledge the decision engages, which ways of knowing each requires, where in the design process each is called upon, and how the resulting decision can be justified. This is what it means to make colour accountable: not to eliminate judgement, but to give it structure, evidence, and a language in which it can be defended.

5. Implications for design education and practice

The framework asks of design not a reorganisation of the curriculum but a reorientation of attention. Its central claim for education is that colour decisions are already present throughout the work designers do and teach, in material specification, in brand strategy, in wayfinding, in data visualisation, in healthcare communication, in AI-assisted production, and that these decisions can be taught as the colour decisions they are, wherever in the curriculum and the process they appear.

The foundational colour course is not the problem, and this paper does not propose abolishing it. Perceptual training in colour relationality is valuable and should be retained. The problem is the assumption that it is sufficient, that colour, having been addressed in the first year, has been dealt with. When the foundational course is followed by no colour content in materials or production courses, no colour criteria in project briefs, no colour accountability in design critique, and no colour research in professional practice, the discipline signals that foundational colour is all a designer requires. The framework challenges that signal, and offers educators a map of where colour knowledge can be integrated into existing courses without creating new ones. Colour management and quality control, which already live in production and prepress teaching, can be framed explicitly as colour competence, the quantitative core of Area 03. Colour, accessibility, and wellbeing belong in briefs for environmental and communication design (Area 02). Cultural and narrative colour research belongs in any brief addressing diverse audiences, global markets, or visual storytelling (Area 01). The colour plan, lifecycle, and evaluation belong within delivery and sustainability teaching (Area 04). What the framework adds, in each case, is the recognition that these are colour decisions, subject to colour accountability, drawing on distinct but equally valid ways of knowing.

For practitioners, the framework functions as an instrument of self-assessment. The question it prompts is which domains of colour knowledge do I navigate with confidence, and in which do I default to intuition because I have never been equipped with the evidence? A materials specialist who commands the knowledge of Area 03 but has never engaged the qualitative cultural research of Area 01 can now name the gap precisely. A brand strategist strong in Area 01 but unschooled in the perceptual research of Area 02 can locate what is missing. The framework does not demand expertise across all four domains; it demands awareness of all four, and the capacity, precisely the capacity of integration, to recognise when a decision requires knowledge one does not yet hold, and to seek it. And it fosters practising colour accountability across the full framework,

holding together the quantitative and qualitative ways of knowing that colour literacy, fully understood, requires.

6. Conclusions

Colour is an infrastructure of consequential decision-making, distributed across the full arc of design practice, that the discipline has not yet claimed with the seriousness those decisions require. This paper has argued that the remedy is not more colour content in a single course, but a map of the territory colour occupies, and it has offered one: a framework for colour competence in design, developed across seventeen years of research and teaching, evolved from a literature-grounded description of the phases of colour decision-making into an author-derived account of the domains of colour knowledge, and aligned with the design process through the Double Diamond model.

The framework's four domains, Colour Context and Strategic Framing; Colour, Human Experience and Inclusion; Colour Decision and Materialisation; and Colour Performance and Impact, describe not a sequence but a landscape: four stable territories of colour knowledge, each with its own characteristic ways of knowing, that any practitioner making serious colour decisions must navigate. Operating across them are the five capacities of colour literacy, recognition, integration, accountability, temporality, and ethics, foremost among them, at this moment, accountability. The paper has argued that accountability is the competence the framework makes operable, because a colour decision can be justified only by reference to the domains of knowledge it draws upon and the ways of knowing they require. The four domains are the structure of a colour justification; they are what a reasoned answer to the question why this colour? is made of.

The contemporary challenges that intersect with colour, sustainability, inclusion, algorithmic mediation, cultural responsibility, are intensifying, not receding, and each brings new demands the framework expects to absorb as the emphasis among its capacities shifts. The design discipline will continue to be present at the colour decisions these challenges demand. Whether it is present with the knowledge and the accountability those decisions deserve is the question the framework sets out to answer. Colour literacy is not a specialist credential, nor competence in a single way of knowing; it is a basic condition of responsible design practice, and it requires the capacity to move between the many ways colour is known. The work of building it is overdue, and it is entirely possible.

7. References

Albers, J. (1963) Interaction of Color. Yale University Press.

Bantom, J. (2006) *Color Education in the Interior Design Curriculum. Master's thesis*. Marymount University. Universal Publishers Repository.

Calvo Ivanovic, I. (2022) *Colour Design Training Itinerary: A Framework for the Teaching and Learning of Colour in the Design Discipline*. Doctoral dissertation. Politecnico di Milano. POLITesi Digital Archive.

Calvo Ivanovic, I. (2024) 'Analysing color training in design education: A review of 2010–2022', *Color Research & Application*, 49(5), pp. 498–514. DOI: 10.1002/col.22930

Calvo Ivanovic, I. (2025) 'Sustainable colour design strategies: A framework for action', *Coloration Technology*, 141(6), pp. 776–800. DOI: 10.1111/cote.70018

Calvo Ivanovic, I. (2026) 'Colour literacy as design infrastructure: Reclassifying colour for contemporary design practice'. In Calvo Ivanovic, I. (ed.) *Advances in Colour Literacy*, vol. 1, pp. 241–264. Colour Literacy Project.

Colour Literacy Project (n.d.) *Misconceptions: No Rules for Harmony*. Available from: https://colourliteracy.org/no-rules-for-harmony

Csillag, P., Lupinacci, A.L. and Hirschler, R. (2018) 'Overview of colour education in Brazilian universities: A focus on design courses in the state of São Paulo', *Journal of the International Colour Association*, 22, pp. 4–14.

Design Council (2021) *The Double Diamond: A Universally Accepted Depiction of the Design Process*. Available from: https://www.designcouncil.org.uk/resources/the-double-diamond/

European Parliament (2020) *Fast Fashion: EU Laws for Sustainable Textile Consumption*. Available from: https://www.europarl.europa.eu/topics/en/article/20201208STO93327/fast-fashion-eu-laws-for-sustainable-textileconsumption

Joerg, L., Kabakova, M., Wang, J.Y., Austin, E., Cohen, M., Kurtti, A. and Jagdeo, J. (2025) 'AI-generated dermatologic images show deficient skin tone diversity and poor diagnostic accuracy: An experimental study', *Journal of the European Academy of Dermatology and Venereology*, 39(12), pp. 2134–2141. DOI: 10.1111/jdv.20849

Luchtman, L. and Siebenhaar, I. (2017) *Living Colour*. Kukka Studio. Available from: https://www.livingcolour.eu/

Madden, T.J., Hewett, K. and Roth, M.S. (2000) 'Managing images in different cultures: A cross-national study of color meanings and preferences', *Journal of International Marketing*, 8(4), pp. 90–107.

Mollon, J.D. (2003) 'The origins of modern color science'. In Shevell, S.K. (ed.) *The Science of Color*, 2nd ed., pp. 1–39. Elsevier.

Mottram, J. (2018) 'Identifying colour use and knowledge in textile design practice'. In MacDonald, L.W., Biggam, C.P. and Paramei, G.V. (eds.) *Progress in Colour Studies*, pp. 371–389. John Benjamins Publishing Company.

Murzyn-Kupisz, M. and Hołuj, D. (2021) 'Fashion design education and sustainability: Towards an equilibrium between craftsmanship and artistic and business skills?', *Education Sciences*, 11(9), Article 531. DOI: 10.3390/educsci11090531

Star, S.L. (1999) 'The ethnography of infrastructure', *American Behavioral Scientist*, 43(3), pp. 377–391. DOI: 10.1177/00027649921955326

© 2026 Authors. Published by the University of Novi Sad, Faculty of Technical Sciences, Department of Graphic Engineering and Design. This article is an open access article distributed under the terms and conditions of the Creative Commons Attribution license 4.0 Serbia (http://creativecommons.org/licenses/by/4.0/rs/).

https://doi.org/10.24867/GRID-2026-p2

Bridging the Gap: A Situated Pedagogical Framework for Interdisciplinary Graphic Design and Human Factors Research

ABSTRACT

As graphical user interfaces (GUI) evolve beyond static screens into dynamic, high-stakes interfaces—such as autonomous vehicles and healthcare control units—the traditional silos separating visual communication from human factors psychology and broader human-computer interaction (HCI) present a critical barrier to effective education. This paper outlines a seven-year pedagogical framework developed at California State University, Long Beach (CSULB) that structurally bridges the School of Art Graphic Design Program and the Master of Science in Human Factors (MSHF) Psychology program. Informed by Activity Theory (Kaptelinin & Nardi, 2006), this interdisciplinary model evolved from ad hoc usability testing of Environmental Control Units (ECUs) at the VA Hospital into a formalized "Design-as-Research" infrastructure. By establishing a shared laboratory environment equipped with a BeamNG.drive physics simulator, graphic design students shifted from designing static visual aesthetics to engineering "XUI in Motion"—interfaces shaped by the temporal, physical, and cognitive constraints of driving. This framework shows that pairing graphic design students with rigorous human-factors testing produces joint peer-reviewed publications, advances human-factors capstone research, and prepares graphic design students for successful placement across leading technology and automotive sectors.

Sam Anvari [1]
Gabriella M. Hancock [2]

[1] Graphic Design Program, School of Art, California State University, Long Beach (CSULB), California, USA
[2] Department of Psychology, California State University, Long Beach (CSULB), California, USA

KEY WORDS
Interdisciplinary design education, human factors psychology, Human-Computer Interaction (HCI), XUI in motion, Right-to-Left (RTL) localization, simulation

1. Introduction

Traditional graphic design pedagogy is rooted in visual communication, typography, and aesthetics, often teaching students to design static displays. However, professional engagements in the automotive and technology sectors show that interfaces are situated systems that require effective human-computer interaction strategies (Shneiderman, 1986). Direct exposure to cutting-edge automotive interface projects—facilitated through independent design consulting with agencies—highlighted a severe pedagogical gap: traditional design tools do not account for temporal constraints, divided attention, and physical motion.

Meanwhile, human factors and ergonomics (HF/E) focuses on human cognitive load and user safety yet often lacks the rapid prototyping capabilities needed to build the interfaces it tests. To address this friction, an applied pedagogical incubator was established at CSULB, combining the aesthetic and structural expertise of the Graphic Design program with the behavioral-science rigor of the Psychology Department's Stress & Technology Applied Research (STAR) Laboratory.

This framework treats graphic design and human factors research as two sides of the same coin for GUI design projects: one shapes how an interface communicates, the other empirically measures how people actually use it and/or how effective the design is in achieving user goals. Bringing them together in the classroom is a practical response to interfaces that now operate in dynamic, high-stakes environments, producing graduates with hands-on training in this collaborative process: graphic designers who understand how their work will be tested, and researchers who understand how interfaces get built.

2. The beginning of the collaboration: the VA hospital project

This interdisciplinary workflow began in 2019 with a project focused on optimizing usability for the autonoME Hospital Environmental Control Unit (ECU; Accessibility Services, Inc., Homosassa, FL). The objective was to redesign an interface for paralyzed veteran users with spinal cord injuries and disorders (SCI/D), enabling them to complete daily tasks autonomously.

Inspired by professional design agency workflows, the team created a design and evaluation process. Seven trained human factors students, together with Hancock and Anvari, conducted an on-site heuristic evaluation of the ECU's touchscreen interface at the VA hospital, applying established usability frameworks (Nielsen, 1994; Shneiderman, 1986). The evaluation identified specific usability issues—including a missing back button and inconsistent placement of functions across screens—and was published as the team's first paper on the project (Hancock et al., 2020a), directly informing an enhanced redesign of the interface. When the COVID-19 pandemic suspended physical access to the VA facility in 2020, the team built an interactive prototype based on the original screens and planned for four representative tasks—placing a phone call, adjusting the bed, watching a video, and composing an email—to A/B test the enhanced design against the original (Figure 1).

This shift reflected more than a change of tools. Within an Activity Theory framework (Kaptelinin & Nardi, 2006), the pandemic functioned as a contradiction that disrupted the established activity system—physical access to the ECU—forcing the team to reconstruct its mediating artifact as a digital prototype without abandoning the underlying objective of the work: improving usability for SCI/D users. The same pattern recurred when the driving simulator later replaced the physical vehicle cabin as the mediating artifact for testing in-vehicle interfaces.



» **Figure 1:** *Digital replica of the ECU interface, developed in Figma for remote A/B usability testing*

The team pivoted to remote testing over Zoom with 60 student participants serving as a neurotypical comparison group, replacing the original veteran users. During this testing, Hancock administered the NASA Task Load Index (NASA-TLX; Hart & Staveland, 1988) to assess perceived workload and the System Usability Scale (SUS; Brooke, 1996) to assess perceived usability, generating over 90 hours of processed video data.

The collaboration continued after the pandemic with a separate heuristic evaluation of the ECU's eye-tracking control modality—this time conducted by Anvari alongside Hancock's human factors students and published (Hancock et al., 2020b). The collaboration formalized into an interdisciplinary research program—bridging graphic design and human factors methodologies to support veterans with SCI/D—presented at the 21st Congress of the International Ergonomics Association (Anvari et al., 2021).

The team grew accordingly, from seven students at its 2019 launch to nearly nineteen by its later years, coordinating through Slack and Microsoft Teams in a semi-realistic professional environment that encouraged cross-pollination across disciplines. Graphic design students were also recruited as test participants for the human-factors students' research, gaining firsthand experience of the user-research process from the participant's perspective, with extra credit and co-authorship used as incentives.

3. Situated simulations and XUI in motion

Building on the ECU project's success, the methodology was formalized and applied to the highly dynamic domain of in-vehicle information systems. The upper-division graphic design curriculum was restructured around the concept of XUI in Motion—teaching how interfaces, the human body, and the environment interact sequentially over time in physical space (Anvari, 2026).

To execute this vision, the team engineered a fixed-base partial-cab simulator using the BeamNG.drive physics engine (BeamNG GmbH, Bremen, Germany), which provides a controlled environment for testing cyber-physical systems and driving scenarios. Equipped with an Xbox gaming steering wheel and pedals, a short-throw projector for environmental display, and an iPad Pro center console (Figure 2), the car simulator was integrated into the Art-419 (5D) course. This integration allowed undergraduate graphic design students to physically experience their own user interface prototypes under the cognitive and visual demands of simulated Level 3 automated driving.

The surrounding hardware, including the iPad, steering wheel, Xbox pedals and panel controls, and chair, was funded by the CSULB Undergraduate Research Opportunities Program (UROP) and the College of the Arts (COTA). It was later equipped with a 45-inch monitor with just a slight curve—chosen over more curved options to sit closer to a flat cluster-panel display—mounted on a height-adjustable actuator to replicate cluster-panel and dashboard layouts. This combination of static and interactive screens supported a wide range of user testing, using Figma as the prototyping tool. A free BeamNG.drive license, obtained as the project progressed, extended the platform's capabilities to replicate both manual and autonomous driving conditions.



» **Figure 2:** *A student is preparing the fixed-base, partial-cab simulator for a capstone research project's user testing and data collection*

4. Case studies in interdisciplinary capstone research

This shared simulator infrastructure made it possible to progress from subjective aesthetic grading to empirical validation of design usability. It was also used for advanced interdisciplinary capstone projects for human factors master's students, several of which have participated in the CSULB Student Research Competition, an annual event hosted by the Office of Undergraduate Research Services (OURS) at CSULB that showcases excellence in scholarly research and creative activity through oral presentations to a jury of distinguished faculty (California State University, Long Beach, 2026):

4.1. Visual Impairments and Contrast Polarity

This capstone project investigated how varying levels of visual distortion and interface contrast (light vs. dark mode) affect driving performance and readability in a simulated environment. Preliminary results were presented as a poster at the 20th Annual HFES Student Research Chapter at California State University Long Beach, and the full findings are being prepared for a separate publication. The work also won first prize in the Creative Arts and Design category at the 2025 CSULB Student Research Competition.

4.2. Multimodal Takeover Requests in Semi-Autonomous Vehicles

This capstone project used the car simulator to study takeover requests in self-driving mode: while the simulated car drove itself, drivers performed non-driving-related tasks (NDRTs) such as playing video games or watching videos. The study compared the effectiveness of audio-visual alerts with combined audio-visual-haptic alerts in returning drivers to manual control. Preliminary results were presented as a poster at the 21st Annual HFES Student Research Chapter at California State University Long Beach, with full findings to be reported in a forthcoming publication. This work also won second prize in the Creative Arts and Design category at the 2026 CSULB Student Research Competition.

4.3. Adverse Weather and Interface Usability

A third capstone project examined how weather (clear, rain, fog) and interface contrast (light vs. dark mode) affect driving performance in the simulator. Perceived usability was measured separately, using instruments including the System Usability Scale (SUS; Brooke, 1996). Findings were presented as a poster at the 21st Annual HFES Student Research Chapter conference at California

State University Long Beach, and the student is preparing the work for a forthcoming publication. This project also won third prize in the Creative Arts and Design category at the 2026 CSULB Student Research Competition.

5. Industry integration and localization

Parallel to the academic research incubator, Anvari's independent industry consulting for the automotive sector—including a peer-reviewed study on localizing interfaces for Right-to-Left (RTL) languages such as Arabic and Hebrew (Anvari & Woods, 2024)—provided firsthand exposure to situated, high-stakes interface design described in the Introduction, reinforcing the practical need for the pedagogical framework outlined in this paper.

Separately, Edenspiekermann—a design agency headquartered in Berlin with a Los Angeles branch office—has worked with the Art-419 (5D) course since 2018, helping draft project briefs, guest lecturing, and running student workshops; several Bachelor of Fine Arts (BFA) graphic design students have since interned there.

6. Structured educational outcomes

This multidisciplinary approach fundamentally shifts how students frame cognitive problems. Consistent with Activity Theory's emphasis on analyzing an activity before designing a tool to mediate it (Kaptelinin & Nardi, 2006), the curriculum now guides graphic design students to analyze the user's context before designing an interface. Paired with the human factors testing described above, this approach shifts students from open-ended aesthetic exploration toward structured, evidence-based problem-solving.

This growth was also reinforced through direct cross-enrollment: human factors students were encouraged to take Art-419 (5D)class, and BFA graphic design undergraduates were encouraged to take PSY 327 Introduction to Human Factors as an elective course. Human factors students who completed Art-419 (5D) gained hands-on experience in user-centered design, presentation, documentation, and iterative design, skills central to graphic design practice.

Anvari's engineering background further enabled participation as a mentor in the university's Undergraduate Research Opportunity Program (UROP), which funded research assistants—recruited from engineering, health science, and art—to support the simulator's setup, maintenance, and data collection and analysis. Both the UROP assistants and the human factors students recruited for the capstone projects in Section 4 completed CITI (Collaborative Institutional Training Initiative) certification as a prerequisite for CSULB Institutional Review Board (IRB) approval, then conducted user testing and processed the resulting data. In the process, they gained a working understanding of graphic design, user interface prototyping, human factors, and user-centered design testing, turning the lab into a small-scale model for further cross-disciplinary exchange.

This program shows that an accessible, modestly funded infrastructure can still produce meaningful design-in-industry outcomes, from internships to full-time jobs. Students have landed roles at BMW Designworks, Edenspiekermann, various automotive companies, Google, Activision, and the broader gaming industry.

7. Conclusion

Digital interfaces have moved well beyond the desktop screen, shaping how people interact across healthcare, transportation, smart devices, entertainment, and daily life. Design education must keep pace with this shift to address the communication challenges these new contexts create. The interdisciplinary partnership at CSULB shows that a shared, localized infrastructure enables graphic designers and human factors psychologists to integrate their methodologies effectively. The ECU interface redesign and the BeamNG-based driving simulator documented here are not isolated case studies; each began as a single course-embedded project and matured into peer-reviewed research, industry consulting, and direct student placement in the field.

To enable similar interdisciplinary research pipelines, institutions should focus on three actionable strategies. First, with thoughtful replication and creativity, accessible consumer-grade simulation tools—such as gaming engines, steering wheels, and tablet displays—can recreate authentic industry conditions in any studio setting, enabling rigorous testing regardless of institutional resources. Second, programs must support co-teaching models and joint studio critiques, in which design and engineering psychology students co-evaluate prototypes using standardized rubrics. Finally, academia must reframe design metrics by integrating quantitative human factors benchmarks, such as task completion time, cognitive load, and contrast legibility, directly into design rubrics alongside traditional aesthetic criteria. By bridging this gap, graphic design education can approximate the collaborative rigor of industry practice and produce practitioners capable of navigating emergent technological landscapes.

8. References

Anvari, S. (2026) 'XUI in Motion- Teaching Temporal Interface Design through a Portable AV Simulator', *Twentieth International Conference on Design Principles & Practices*. Sapienza University of Rome, Italy, 25–27 February, p. 154.

Anvari, S.S., Hancock, G.M., Mok, N.B., Ayvazyan, A., Machado, C.L., Chompff, R.M.E., McCoy, K.M., Nare, M.T., Shiraiwa, Y., Mizushima, Y., Morales, N. and Alcharbaji, L. (2021) 'Interface Design for Users with Spi-nal Cord Injuries and Disorders: An Interdisciplinary Research Program with the US Department of Veterans Affairs'. In: Black, N.L., Neumann, W.P. and Noy, I. (eds.) *Proceedings of the 21st Congress of the Internatio-nal Ergonomics Association (IEA 2021) Volume IV: Healthcare and Healthy Work*. Cham: Springer, pp. 232–238.

Anvari, S.S. and Woods, P. (2024) 'Localizing Graphical User Interfaces for Right-to-Left Languages: A Practi-cal Study', *The Human Side of Service Engineering*, 143, pp. 231–234. DOI: 10.54941/ahfe1005102

Brooke, J. (1996) 'SUS: A quick and dirty usability scale'. In: Jordan, P.W., Thomas, B., Weerdmeester, B.A. and McClelland, A.L. (eds.) *Usability Evaluation in Industry*. London: Taylor & Francis, pp. 189–194.

California State University, Long Beach. (2026) *Student Research Competition*. Available from: https://www.csulb.edu/student-research-competition [Accessed 21 September 2026].

Hancock, G.M., Anvari, S., Nare, M.T., Mok, N.B., Ayvazyan, A., McCoy, K.M., Bai, X., Mather, G.P., McBride, A.S. and Morales, N. (2020a) 'Environmental Control Units for Inpatient Care at Veterans Affairs Spinal Cord Injury Centers: Heuristic Evaluation and Design Recommendations'. In: Yamamoto, S. and Mori, H. (eds.) *Human Interface and the Management of Information. Designing Information. HIMI 2020. Lecture Notes in Computer Science*, vol. 12184. Cham: Springer, pp. 23–38.

Hancock, G.M., Anvari, S.S., Mok, N.B., Ayvazyan, A., Bai, X., McCoy, K.M., Nare, M.T., Mather, G.P., Macha-do, C.L., Chompff, R.M.E., McBride, A.S. and Morales, N. (2020b) 'A Heuristic Evaluation of Usability for Environmental Control Units' Eye-Tracking Interfaces at Veterans Affairs Spinal Cord Injuries and Disorders Centers'. *Proceedings of the 2020 HFES 64th International Annual Meeting*. Human Factors and Ergono-mics Society.

Hart, S.G. and Staveland, L.E. (1988) 'Development of NASA-TLX (Task Load Index): Results of empirical and theoretical research', *Advances in Psychology*, 52, pp. 139–183. DOI: 10.1016/S0166-4115(08)62386-9

Kaptelinin, V. and Nardi, B.A. (2006) *Acting with Technology: Activity Theory and Interaction Design*. Cambridge, MA: MIT Press.

Nielsen, J. (1994) 'Enhancing the explanatory power of usability heuristics'. *Proceedings of the SIGCHI Con-ference on Human Factors in Computing Systems*, pp. 152–158.

Shneiderman, B. (1986) *Designing the User Interface: Strategies for Effective Human-Computer Interaction*. Addison-Wesley.



© 2026 Authors. Published by the University of Novi Sad, Faculty of Technical Sciences, Department of Graphic Engineering and Design. This article is an open access article distributed under the terms and conditions of the Creative Commons Attribution license 4.0 Serbia (http://creativecommons.org/licenses/by/4.0/rs/).

https://doi.org/10.24867/GRID-2026-p3

Bridging Colour Communication Across Languages

ABSTRACT

Colour naming bridges vision and language. We group colours into categories that we refer to by names such as yellow, turquoise, or periwinkle blue. The number of colour names in languages is often large, as finer distinctions allow colour to be communicated with greater precision (Gage, 1995). For brand owners, designers and colour technologists, this diversity has real consequences: a colour name that communicates clearly within one linguistic community may mislead, or fail to translate at all, in another — with direct effects for the intended audience across branding and visual communication design.

Dimitris Mylonas

Computing, Northeastern University London, London, United Kingdom

KEY WORDS

Colour naming, cross-linguistic communication, Serbian, colour translation

Since 2009, we have led an international collaborative project to collect unconstrained colour names with their corresponding colour ranges in different languages and viewing conditions through crowdsourcing, laboratory, and field experimental methodologies (Mylonas & MacDonald, 2010; Mylonas, Griffin & Stockman, 2019; Mylonas, Caparos & Davidoff, 2022). We developed robust computational tools, trained on these multilingual datasets, that automate the colour naming task across the full colour gamut at different degrees of granularity, highlighting both the consistency and the development of colour languages (Mylonas et al., 2026). Our findings suggest that learned, linguistic processes, rather than innate perceptual mechanisms, are the driving force behind how colour lexicons expand (Mylonas, Caparos & Davidoff, 2022). This keynote reviews our colour naming research and its computational tools, before turning to its newest bridge — Serbian — and its connections to the other colour languages we studied.

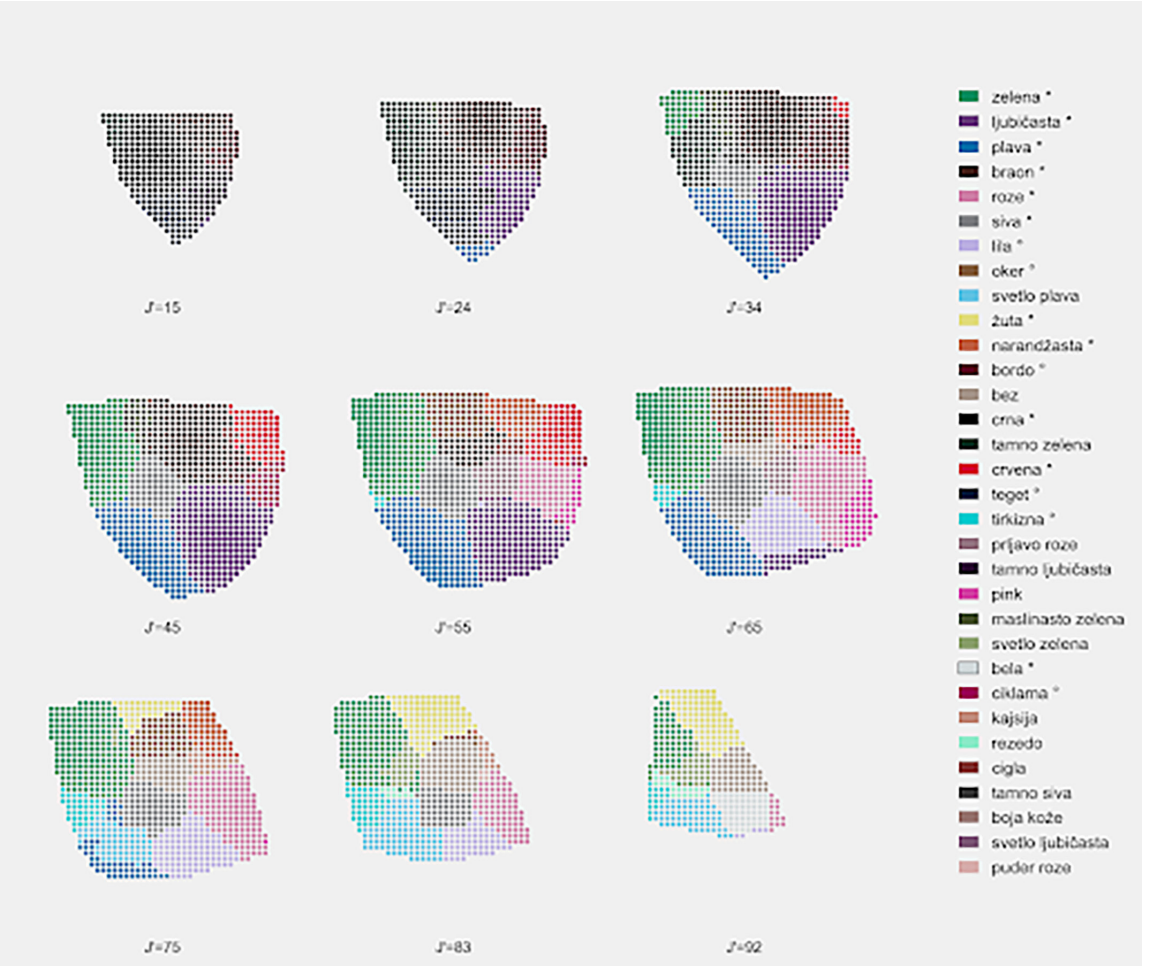
The core experimental methodology behind this research programme has stayed largely consistent across settings: observers view a sequence of colour patches, drawn from an approximately uniform sampling of the Munsell system spanning the full gamut, presented one at a time against neutral or chromatic backgrounds, and type an unconstrained colour name for each, with response time recorded. Standard controls include colour-vision screening, brightness calibration, and a background questionnaire (Mylonas & MacDonald, 2010). The same protocol carries over to laboratory settings and to fieldwork in unwritten languages, with calibrated monitors and verbal responses recorded (Mylonas, Griffin & Stockman, 2019; Mylonas, Caparos & Davidoff, 2022).

This lineage underpins two related recent outputs: a modelling paper establishing Spin Colour Forest (SCF) — a novel ensemble colour naming method that applies partial orthogonal transformations to perceptual colour space to capture complex category boundaries — and a colour translation benchmark across five languages (Mylonas et al., 2026); and Colour Spinner, a deployed visualisation tool making these naming distributions explorable through six linked views — Picker, Namer, Thesaurus, Translator, Mapper, and Profiler — spanning six languages, with Spanish added as the sixth (Sinkeviciute et al., 2026) just before the current Serbian extension. Together this work has shown that the minimal set of terms necessary to name all colours in a display gamut — what we call indispensable colour terms — ranges from just 7 in OtjiHimba, a remote society in Namibia, to 47 in American English. For the written, well-resourced languages, large language models translate colour names fluently while mapping them onto near-invariant focal colours — the single 'best example' of a colour category — regardless of target language, producing very large mean perceptual errors. For OtjiHimba, the failure is more basic still — as an unwritten language, it could not be translated at all, with AI unable to produce any usable output. Serbian sits at neither

extreme: unlike OtjiHimba, it is a written language with a substantial web presence, yet until this study empirical unconstrained colour-naming datasets were limited.

For bridging the gap with the Serbian colour language, we used the same unconstrained naming paradigm, and we collaborated with Serbian native-speaking colour researchers (Jakovljev & Zdravković, 2018; Martinovic, 2024) to collect and analyse a large dataset from 1,049 speakers, producing 34,781 clean responses across 454 unique terms. We replicate earlier results (Jakovljev & Zdravković, 2018) of the 11-term Serbian basic colour term (BCT; Berlin & Kay, 1969/1991) inventory (bela, crna, crvena, žuta, zelena, plava, braon, ljubičasta, roze, narandžasta, siva). We extend it with 21 further terms identified by SCF grid-coverage modelling, together forming a 32-term indispensable vocabulary (Figure 1). This count of indispensable colour terms matches British English, Greek and Spanish (32 each) — though the actual categories across languages differ — is richer than French (27) and OtjiHimba (7), and considerably smaller than American English (47). Six of these non-basic 21 terms form a converging near-basic tier (teget, bordo, tirkizna, oker, lila, ciklama): the first four independently corroborate the candidate categories flagged by our own composite behavioural scoring — a ranking that combines naming frequency, consensus, and response time — while lila and ciklama emerge from the model alone. Two of the six, teget (dark blue) and bordo (dark red), correspond directly to the categories Jakovljev and Zdravković identified through colour-term elicitation (2018); our grid-coverage evidence offers a complementary, model-based confirmation that these occupy separate, irreducible regions of colour space. A full statistical analysis is in preparation as a separate journal article, and in parallel we are now extending Colour Spinner to Serbian, including corpus data (Kostić, 1999), so that users can explore the Serbian colour vocabulary directly alongside the other six.

Effective colour communication draws on principles of visual perception (MacDonald, 1999) and can be further enhanced by knowledge of the addressed speakers' language (Schirillo, 2001). Across the languages, speakers divide the same perceptual colour space with vocabularies of different size and with category boundaries



» **Figure 1:** *Serbian indispensable colour names across nine CAM16-UCS lightness slices (J' = 15–92), from the darkest (left) to the lightest (right) colours. Terms marked with asterisks are the 11 BCTs; degree-marked terms are the converging near-basic tier. Legend entries are ordered by size in colour space*

that do not necessarily align. The practical consequence is straightforward: effective colour communication cannot be assumed to perfectly translate across languages simply because the words do. Our translation benchmark reinforces this distinction, showing that lexical fluency in current AI systems does not guarantee perceptual correspondence between the colour categories used by different linguistic communities.

For graphic engineering and design in an international context, this shifts the problem from asking what is the translation of this colour name? to asking how will this colour be recognised, understood, and named by the people for whom we are designing? Serbian's near-basic tier is a clear case in point: these distinctions would be obscured by a universal eleven-category account, whereas Colour Spinner makes them directly inspectable rather than reducing colour translation to a one-to-one correspondence between words.

Our broader direction is therefore towards language-aware colour tools grounded in human naming behaviour (Mylonas & MacDonald, 2012). For designers working across markets and languages — in marketing, graphic communications, image processing and quality control — our tools can expose where a colour choice is robust across linguistic communities and where communication becomes uncertain. Colour management gives us increasingly precise ways to reproduce a stimulus while colour-naming research complements it by asking whether that reproduced colour carries the same communicative distinction for its intended audience. Together, these two forms of precision — the colour we reproduce and the colour we intend to communicate — define the bridge this symposium is helping us build.

1. Acknowledgments

We thank Ivana Jakovljev, Jasna Martinovic and Sunčica Zdravković for their contribution to the Serbian data collection and analysis and the more than a thousand Serbian speakers who gave their colour names. This work was supported by the Leverhulme Trust (Cones to Words, RPG-2024-096).

2. References

Berlin, B. and Kay, P. (1969) *Basic Color Terms: Their Universality and Evolution*. Berkeley, CA: University of California Press.

Gage, J. (1995) *Colour and Culture: Practice and Meaning from Antiquity to Abstraction*. London: Thames and Hudson.

Jakovljev, I. and Zdravković, S. (2018) 'The colour lexicon of the Serbian language – a study of dark blue and dark red colour categories Part 1: Colour-term elicitation task', *Psihologija*, 51(2), pp. 197–213. DOI: 10.2298/PSI160521002J

Kostić, Đ. (1999) *Frekvencijski rečnik savremenog srpskog jezika*. Vols. I–VII. Belgrade: Institute for Experimental Phonetics and Speech Pathology and Laboratory for Experimental Psychology, Faculty of Philosophy, University of Belgrade.

MacDonald, L. W. (1999) 'Using color effectively in computer graphics', *IEEE Computer Graphics and Applications*, 19(4), pp. 20–35. DOI: 10.1109/38.773961

Martinovic, J. (2024) 'Acquisition of colour categories through learning: Differences between hue and lightness', *Cognition*, 242, 105657. DOI: 10.1016/j.cognition.2023.105657

Mylonas, D. S. and MacDonald, L. (2010) 'Online Colour Naming Experiment Using Munsell Colour Samples'. In: *Proceedings of the 5th European Conference on Colour in Graphics, Imaging, and Vision (CGIV)*, 14–17 June 2010, Joensuu, Finland. Springfield, IS&T, pp. 27–32.

Mylonas, D. and MacDonald, L. (2012) 'Colour naming for colour communication'. In: Best, J. (ed.) *Colour Design: Theories and Applications. Cambridge*, Woodhead Publishing, pp. 254–270. DOI: 10.1533/9780857095534.2.254

Mylonas, D., Ahmed, R., Sinkeviciute, A. and Koliousis, A. (2026) 'Colour in Translation: Data, Models, and Benchmarking for Cross-Linguistic Colour Naming'. In: *Proceedings of the 2026 CHI Conference on Human Factors in Computing Systems (CHI '26)*, 13–17 April 2026, Barcelona, Spain. New York, ACM, pp. 1–21. DOI: 10.1145/3772318.3791626

Mylonas, D., Caparos, S. and Davidoff, J. (2022) 'Augmenting a colour lexicon', *Humanities and Social Sciences Communications*, 9, 29. DOI: 10.1057/s41599-022-01045-3

Mylonas, D., Griffin, L. D. and Stockman, A. (2019) 'Mapping colour names in cone excitation space'. In: *25th Symposium of the International Colour Vision Society (ICVS)*, 5–9 July 2019, Riga, Latvia. p. 52.

Schirillo, J. A. (2001) 'Tutorial on the importance of color in language and culture', *Color Research & Application*, 26(3), pp. 179–192. DOI: 10.1002/col.1016

Sinkeviciute, A., Ahmed, R., Stutters, J., Koliousis, A. and Mylonas, D. (2026) 'Colour Spinner: Making Cross-Linguistic Colour Naming Diversity Visible'. Manuscript under review, *IEEE Transactions on Visualization and Computer Graphics.*



© 2026 Authors. Published by the University of Novi Sad, Faculty of Technical Sciences, Department of Graphic Engineering and Design. This article is an open access article distributed under the terms and conditions of the Creative Commons Attribution license 4.0 Serbia (https://creativecommons.org/licenses/by/4.0/deed.en).

https://doi.org/10.24867/GRID-2026-p4

Towards a Total Packaging System: Integrating Material Performance, Safety, and Circular Sustainability

ABSTRACT

The discipline of packaging development has historically evolved not as a unified science, but as a fragmented collection of independent sub-disciplines. Academic and industry packaging development frameworks mimic this fragmentation where packaging design, material science, logistics, and end-of-life recovery are treated as isolated domains rather than a single, integrated system .Recent changes where sustainability requirements through more system thinking approach (life cycle analysis) and different economic instruments like plastic taxes, extended producer responsibility fees and new directives regarding toxicology requirements require a paradigm shift. Driven by escalating climate pressures, stringent European Union regulatory mandates, and the imperative of the circular economy, packaging is no longer evaluated merely as a single-use vessel. Instead, we must conceptualize it as a Total Packaging System (TPS). While similar to Total Quality concepts (reduce waste, continuous improvement, data driven) this review outlines a new comprehensive framework which goes beyond as tries to go outside just the rigid fragmented techno sphere domain. This new framework harmonizes structural material performance (permeability, mechanical integrity) with advanced chemical safety standards—specifically the complex convergence of REACH, Food Contact Material (FCM) regulations, and the newly active Packaging and Packaging Waste Regulation (PPWR, Regulation (EU) 2025/40) together with sustainability requirements done through new material development approaches like Sustainable and Safe by Design (SSbD) tools, life cycle analysis (LCA) and multifactorial optimization.

Igor Karlovits

Pulp and Paper Institute, Ljubljana, Slovenia

KEY WORDS
Packaging development, material performance, sustainability, system thinking

1. The roots of fragmentation in packaging development: a systems-thinking introduction

The discipline of packaging development has historically evolved not as a unified science, but as a fragmented collection of independent sub-disciplines. While modern scholarship advocates for integrated paradigms like "Sustainable Packaging Logistics" (SPL) (García-Arca, Garrido & Prado-Prado, 2017) or "Packaging Logistics" (Hellström, 2007; García-Arca, Comesaña-Benavides & Prado-Prado, 2021), both industrial practice and academic literature remain stubbornly siloed. Traditionally, packaging development frameworks are bifurcated into three distinct, non-communicating functional spheres: the commercial/marketing function (graphics, haptics, and brand building), the logistics/manufacturing function (containment, protection, and automation), and the environmental/end-of-life function (circularity, collection, and degradation) (Bramklev, 2009b; de Koeijer, de Lange & Wever, 2017). At a fundamental level, the separation of packaging frameworks is an artifact of Cartesian reductionism—the belief that

a complex system can be understood by breaking it down into its individual parts and optimizing each one. Both in academia and industry this manifests as:

Disciplinary Silos: Universities and research institutions train professionals in highly specialized, non-communicating verticals. A structural engineer is trained to optimize for mechanical strength; a graphic designer for visual brand cues; a chemical engineer for barrier properties; and a waste-management specialist for sorting throughput.

Sequential "Over-the-Wall" Development: Because of this training, frameworks traditionally follow a linear, sequential pipeline. Marketing designs the concept and "throws it over the wall" to engineering; engineering sources the materials and throws it to manufacturing; manufacturing struggles to run it on existing machinery and throws it to logistics. By the time the package is produced, it is too late to retroactively design it for systemic circularity or optimal shipping cubage.

These manifestations are deeply rooted in three structural dimensions: cognitive and social human traits, economic path-dependencies, and institutional reductionism. At the individual and social scale, human evolutionary biology actively works against the integration required for systems thinking. Systems thinking requires an engineer or designer to hold a massive array of interconnected variables in their mind simultaneously—balancing chemical barrier requirements, structural compressive strength, high-speed machine tolerances, shipping cubage, consumer ergonomics, and localized municipal recycling capabilities. However, human cognition is bound by Working Memory Capacity (Miller, 1956). According to Cognitive Load Theory, when an individual is tasked with managing highly complex, open-ended systems, their intrinsic cognitive load (the inherent difficulty of the task) and extraneous load (the mental effort of processing poorly structured data) quickly overwhelm their limited working memory capacity (Sweller, Ayres & Kalyuga, 2011). To prevent cognitive overload, human designers revert to bounded rationality (Simon, 1957). Another cognitive challenge pointed out by several anthropologists but synthetized by Bateson (1972) where the Western civilization is dominated by: linear causality, reductionism and control-oriented thinking while natural system work by feedback loops, circular causality and self-organization. Donella Meadows (2008) repeatedly argued that many policy failures occur because humans intuitively think linearly while complex systems behave cyclically. To ease the cognitive load people split the complex system into simpler, isolated sub-problems— here focusing on packaging example: optimizing the packaging's weight first, then its aesthetics, then its recyclability. This reductionist approach reduces the immediate cognitive load on the designer but completely fractures the integrity of the broader product-packaging-logistics system. As packaging development moves from a single designer to an organizational level, a different cognitive constraint emerges: social scaling limits. Anthropological and organizational research demonstrates that humans have a natural cognitive limit—historically termed Dunbar's Number—constraining the size of a cohesive, trusting social network to roughly 150 individuals (Dunbar, 1993; Clegg, 2022). Beyond this boundary of ~150 people, human groups naturally fragment into subgroups to reduce the social and cognitive transaction costs of maintaining relationships. In large corporations, these subgroups manifest as highly protective functional silos (e.g., procurement, marketing, supply chain). As Clegg (2022) highlights, these silos construct distinct, insular "thought worlds" and proprietary lexicons. A procurement professional's "thought world" is governed by cost-per-unit, whereas an environmental specialist's world is governed by carbon-equivalent metrics. Because of human social-scaling limits, cross-functional collaboration over 150-person boundaries breaks down, and communication is replaced by sequential, formal "over-the-wall" handoffs. The organizational fragmentation created by human cognitive limitations is further cemented by corporate cost-accounting structures and macro-economic models. Within corporate settings, financial performance is tracked through localized, department-specific Key Performance Indicators (KPIs). Procurement is evaluated on raw material purchase costs; plant managers are evaluated on packaging line speeds; logistics managers are evaluated on transport cubage and pallet utilization (Hellström, 2007). Standard financial frameworks struggle to quantify cross-functional trade-offs. For example, procurement may hit their localized KPI by sourcing a cheaper, thinner corrugated box, but this decision risks systemic failure if the box buckles under humidity, causing product damage during transport and costing the logistics department far more than the procurement savings (García-Arca & Prado-Prado, 2008). Traditional management accounting systems fail to attribute downstream logistics or waste costs back to early-stage design decisions, reinforcing siloed optimization. For decades, global markets allowed companies to treat the end-of-life disposal of packaging as an economic externality. Because the financial burden of managing, landfilling, or recycling packaging waste fell on municipal tax bases or the natural environment rather than the brand owners, corporate development frameworks had zero economic incentive to include circularity variables in their initial designs. Only with the modern rise of legislated Extended Producer Responsibility (EPR) and circular-economy mandates (such as the EU's Packaging and Packaging Waste Regulation) are these external costs beginning to be internalized, forcing a painful, retrospective pivot toward systemic design (de Koeijer, de Lange & Wever, 2017). A recent comprehensive overlook of the miscommunication problems due to these factors and how directly influences the packaging can be found in an online book Unpacked (Rogerson, 2025) and claims that

the answer lies in communication—or more precisely, the misalignment in the packaging development process is the failure to communicate clearly, accurately, and persuasively between different siloed in stakeholder group.

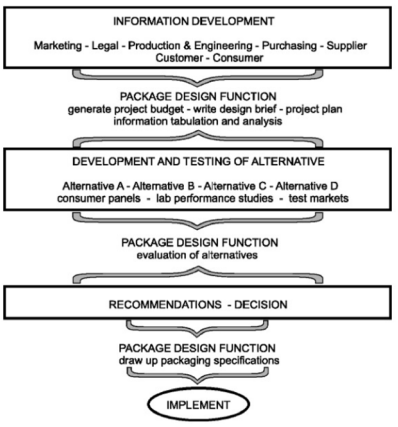
2. Overview of existing packaging development models

In the early stages of formalized packaging science, models focused strictly on the immediate physical relationship between the package, the product, and its environment. Developed by Hugh Lockhart at Michigan State University (Lockhart, 1997), this framework established packaging as a formal "Socio-Scientific Discipline." It organized design criteria into a static 3x3 grid mapping the three core functions of packaging (Protection, Utility, Communication) against the three primary environments it encounters:

- The Physical Environment: Mitigating shock, vibration, drops, and compression
- The Ambient (Biospheric) Environment: Controlling moisture, oxygen, UV light, and temperature.
- The Human (Social) Environment: Ensuring ease of opening, portion control, tamper-evidence, and branding.

It shifted packaging design away from purely trial-and-error physical testing toward a systematic, multi-variable engineering matrix (Bix et al., 2009). But it also has some downsides: the Lockhart matrix was entirely static. It treated these vectors as isolated grid cells, offering no mathematical models to resolve functional trade-offs (e.g., maximizing barrier protection vs. maintaining ease of opening) and entirely omitted lifecycle, carbon footprint, or chemical safety metrics. Saghir (2002) expanded packaging theory by introducing the concept of Packaging Logistics, emphasizing the alignment of packaging decisions with supply chain operational efficiency. His framework operated with the tri-level structure of primary (consumer), secondary (transport/groupage), and tertiary (pallet/unit load) packaging systems. He also integrated functional tradeoffs by balancing conflicting requirements between marketing (appeal, volume, branding) and logistics (cube utilization, stack ability, handling efficiency). And all this is synchronized through the supply chain where one can evaluate how packaging parameters directly impact fill rates, transport costs, material handling, and inventory management across the entire network (Saghir, 2004).

The next phase tried to more integrate product and packaging development models in the period between 2007 and 2009 by the works of Bramklev (2009a), who advocated for concurrent engineering, where product design and packaging design occur simultaneously rather than sequentially. Traditional approaches design the product first and package it later, often leading to sub-optimal shipping volumes or fragile product designs. IPPD treats product and packaging as a co-dependent, unified system. It also Incorporates requirements from raw material selection, manufacturing constraints, retail displays, and end-of-life recovery into the early conceptual phases of product development (Bramklev, 2009b). A similar approach was promoted also by (Bix et al., 2009) who, building on Lockhart Matrix and concurrent engineering, proposed that truly optimal designs consider all viewpoints, a combination of PCD (Product Centric Design) and UCD (User Centric Design) processes. During the entire process the design team must attempt to balance requirements of the three environments (physical, ecospheric, and human) and the three functions (protection, utility, and communication) described earlier from varying stakeholder perspectives. Their system is also a linear six step approach with the steps: Planning, Concept Design, System Design, Specification, Refinement and Production. In a similar fashion to classic packaging textbooks (Larkin & Burcham, 2022) you can find also a linear based model focusing on the technical operations and flows of information (Figure 1).



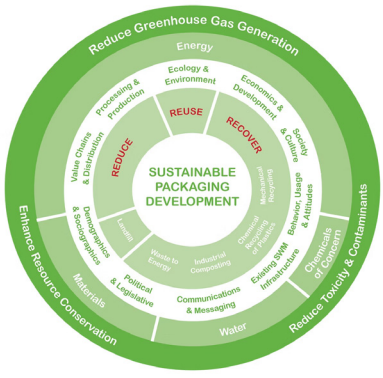
» **Figure 1:** *General package design process (Larkin & Burcham, 2022)*

This model goes into specifications and data needed to support every stage of the packaging design process (including some of the legislation, technical and other data) but does not draws conclusion about the interconnection of different design decisions, but uses more of a to do list lacking overall comprehension of systems outside the focused packaging process. These approaches do not contain more detailed environmental and toxicological methods, which are addressed in the next models. In response to growing environmental awareness, design frameworks evolved to prioritize resource efficiency, waste reduction, and end-of-life (EoL) recoverability. The Sustainable Packaging Coalition (SPC) moved the industry away from vague "eco-friendly" buzzwords by introducing the SMART design methodol-

ogy (Pålsson, Finnsgård & Wänström, 2011).: S | Systems Approach: Designing with the entire distribution and recovery infrastructure in mind. M | Material Health: Restricting toxic additives and prioritizing safe chemical inputs. A | Accessibility: Ensuring packaging remains functional and safe for all consumers. R | Reduction & Elimination: Minimizing excess headspace, wall thickness, and unnecessary components. T | Life-Cycle Thinking: Using Life Cycle Assessments (LCA) to guide material selection. Grounding sustainable design in the Circular Economy, the Ellen MacArthur Foundation (2021) (introduced the "Eliminate, Innovate, circulate" framework, separating packaging flows into two distinct thermodynamic loops (the "Butterfly Diagram"):

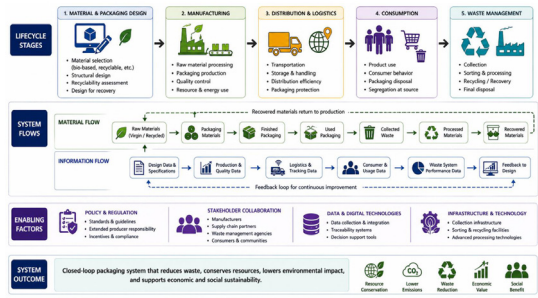
- The Technical Cycle: Keeping synthetic materials (like polymers and metals) in high-value, closed-loop mechanical or chemical recycling systems, avoiding downcycling.
- The Biological Cycle: Utilizing non-toxic, bio-based materials that can safely return to the earth via biodegradation or composting without leaving hazardous residues.

The SPRING Sustainability Roadmap and the sustainable packaging development wheel (Figure 2.) formulated by the Sustainable Packaging Research, Information, and Networking Group (SPRING emphasizes a holistic decision-making framework focused on three overarching goals: reducing greenhouse gas generation, enhancing resource conservation, and eliminating toxicity/contaminants. It replaces the traditional "Reduce, Reuse, Recycle" triad with four core strategies—Energy & Water Conservation, Material Optimization, Elimination of Substances of Concern, and Recovery as the "New Third R" (including industrial composting and chemical recovery where traditional recycling falls short) (Lilienfeld, 2021). It is inspired (most probably by the famous Donut Economics) diagram developed by Kate Raworth (2012).



» **Figure 2:** *SPRING sustainable packaging development wheel (2021 SPRING and Robert M. Lillienfield)*

One more recent model was introduced by Ali (2026) in a form of a system-level framework that connects packaging design with waste management processes across the full lifecycle. The method combines system modeling, lifecycle mapping, and performance evaluation to capture interactions among design, production, distribution, consumption, and disposal stages. It also introduces several new System Performance Evaluation Metrics (mainly focusing on the end-of-life stages (recovery, recycling and Environmental Index Metrics). The framework is presented in Figure 3. While encompassing new parameters and metrics, it omits some established tools like LCA (life cycle analysis) and ISO defined impact categories on the environment and also does not establish dynamic interconnection between system elements but rather offers an extended and more detailed linear packaging development model.



» **Figure 3:** *System-Level Packaging Lifecycle Framework (Ali, 2026)*

3. Recent methodological developments and regulatory requirements

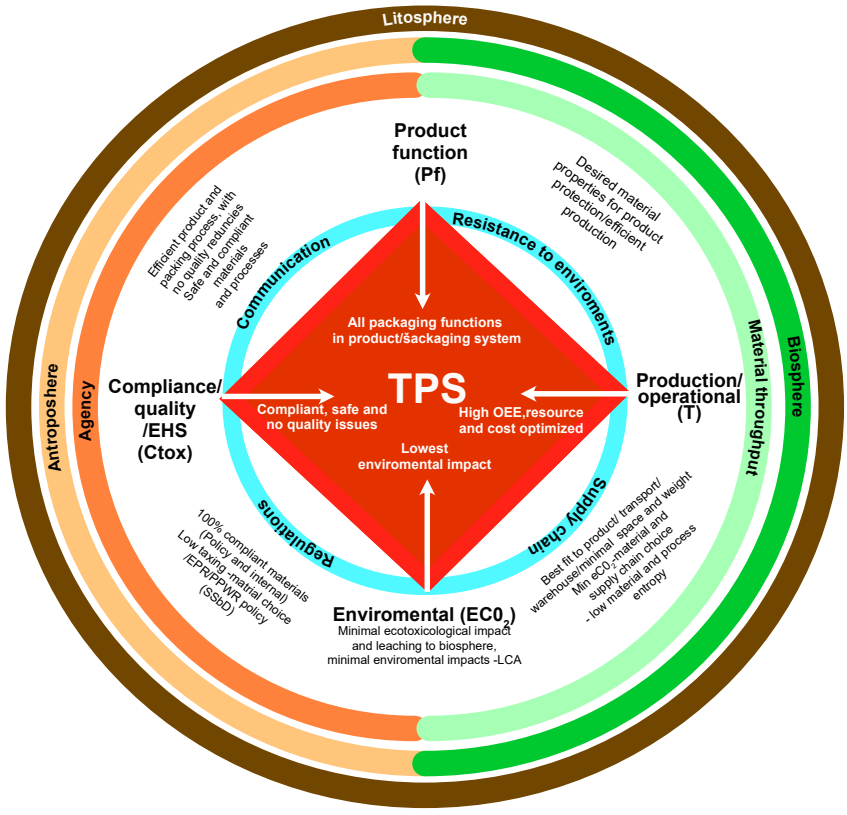
European packaging policy has traditionally been guided by Directive 94/62/EC on Packaging and Packaging Waste (European Parliament and Council, 1994), which established essential requirements for packaging recovery, recycling, and waste minimization. Although the Directive played a pivotal role in harmonizing packaging legislation across the European Union, its emphasis remained largely focused on waste management after packaging had already entered the market. Over time, rising packaging volumes, increasing environmental concerns, and the strategic objectives of the European Green Deall highlighted the need for a more comprehensive framework. This transition is particularly visible in the European Union, where legislation increasingly addresses the entire life cycle of packaging rather than focusing solely on waste management. The Packaging and Packaging Waste Regulation (PPWR) , Extended Producer Responsibility (EPR) schemes, and restrictions on synthetic polymer microparticles are among the most influential legislative drivers shaping packaging development and innovation today (European Parliament and Council, 2025; European Commission, 2025).

The regulation covers the entire packaging life cycle, from design and manufacture through use, collection, recycling and disposal and has several key implications for the packaging design: material selection and design, recycled content ratios and reusing quotas. One of the most significant and not yet fully comprehended emerging regulatory developments affecting packaging graphics and printing is also the Commission Regulation (EU) 2023/2055 concerning intentionally added microplastics. The regulation restricts synthetic polymer microparticles smaller than 5 mm that are insoluble and non-biodegradable, aiming to reduce environmental releases of microplastics (European Commission, 2023; ECHA, 2025). Many modern printing inks and varnishes contain polymer dispersions, polyethylene waxes, synthetic resin additives and functional coatings. Some of these materials may fall within the regulatory definition of synthetic polymer microparticles (EuPIA, 2025). Although printing inks and varnishes used in industrial applications are currently exempt from the direct sales prohibition because they are used in controlled industrial environments, the legislation introduces important obligations regarding material identification and documentation requirements together with the reporting of emissions and end of life management (European Commission, 2023; EuPIA, 2025). To support all these additional requirements also new tools are needed. For a modern packaging system, Safe and Sustainable by Design (SSbD) and Life Cycle Assessment (LCA) are complementary tools that help companies move from simple regulatory compliance toward optimized circular packaging design. Developed by the European Commission's Joint Research Centre (JRC) to align the Green Deal with chemical safety, the SSbD framework is a transformative methodology for designing packaging materials from the molecular level up. SSbD mandates that packaging materials be pre-screened for chemical safety (toxicology, migration) concurrently with Environmental Life Cycle Assessments (LCA) from the earliest Technology Readiness Levels (TRLs) (European Commission, 2022).

4. Total (unified) packaging system

In this section a newly developed packaging framework is presented. Previous iterations were presented in (Karlovits, 2025). The aim of this framework and the newest iteration is to break the fragmentation of the current mental development process by applying a systemic approach and unifying the multiple aspects a packaging or a packaging product system must encompass. Also, it tries in a visually easy model to represent the connection between underlying natural and energy systems beyond current economic models which funnel the previous models into the fragmented linear approaches.

The framework is visually presented in Figure 4.



» **Figure 4:** *The Total Packaging System framework*

In the model and framework, we start with the outer ring which is governed by the three laws of thermodynamics and the innate geosphere (solid, inanimate parts of the world). Inside that we make a blended circle with two distinctive spheres the anthroposphere and biosphere, or some others called it the techno sphere but it is an artificial extension where without energy depletion from the biosphere the techno sphere cannot exist on its own. One the left side is the half ring of the anthroposphere with an additional subring of agency which delegates power from the anthroposphere. Which institutions, legal entities, persons, states, unions wield power to shape the legislation and market side of the packaging development process. On the right side the half ring of the biosphere is extended to material throughput which is directly connecting the influences of humans with the biosphere in form or extraction, transformation and output phase (the breakdown when earth is absorbing back the materials). In the middle is a diamond shape which easily shows the four main pillars of a packaging material: material properties /resistance to different environments, performance during packaging production and supply chain operations, sustainability and compliance and safety (for anthroposphere and biosphere – humans and all biological life on the geosphere. The angles are interconnected through several human induced material throughput pathways. The effects and influences of these interactions are measurable with a few high-level key process indicators, and supported by several tools and methodologies like SSbD and LCA.

Product functions (Pf) are the inherent material properties engineered or natural properties of packaging materials in terms of resistance to different environments. These functions include the physical biological environmental (biosphere) in terms of resistance to heat, moisture, UV light and human environments (production lines on terms of friction, shocks, drops) or human intervention (opening up the protective packaging). These are sometimes known as the protection/containment properties where oxygen, moisture barriers provide the right protection from the biosphere for a prolonged shelf life for food packaging or rust prevention on machine parts for example.

Production/operational (T) performance can be defined on high level of overall equipment effectiveness (OEE), scrap/reject rate, throughput/output rate, first pass yield (FPY)/rejection rate where the packaging machinery or packaging line does not stop with downtime due to poorly designed or materials with non-adequate properties. These properties can be connected with tensile strength, stiffness, coefficient of friction, a wide category of material properties ensuring smooth machine runnability. Also, the ability to shape it, pool it and transport in a manner with the most optimized space, weight ratios during which the entropy of the transport and materials process is low is the key for low impact supply chains.

The third corner or pillar is sustainability or environmental functions where the elements taken from the biosphere to make the packaging (and of course the product itself) use a minimal amount of energy and does now impact the biosphere long term and enables regenerating the biosphere source. Based on the sustainability roadmap by Lilienfeld/Spring (2021) these can be defined as minimizing the environmental impacts of sourcing raw materials and converting them into packaging. Further minimizing the environmental impact of both package and product disposal, including unanticipated release into both land and marine environments. Minimize the production of greenhouse gases and the potential to exacerbate AGW (anthropogenic global warming). This applies to both the package and the product(s) it contains. All this with efficient transport and logistics and designing use scenarios which minimize the influence of this stage (single use or reusable). On a high level this can be calculated through eCO_2 kg of GWP of the chosen raw materials and transportation and use phase environmental impacts, with scalable end of life options (recycling, composting).

Moving towards the next step for safety is the minimization of contaminants and toxicity associated with the production, use, and disposal of packaging. Here one important notice is the second law of thermodynamics - specifically entropy generation ($\Delta S > 0$) during mechanical re-processing with entropic constraints exposes the physics-based boundaries of circular economy models, proving that "closed-loop" mechanical recycling cannot operate perpetually without continuous virgin material inputs and high energy expenditures. Thermal-mechanical shear during re-extrusion breaks covalent bonds in polymer backbones. This irreversible chain scission reduces average molecular weight, severely compromising tensile strength, impact resistance, and barrier properties. Separating complex, multi-material waste streams (such as multi-layer PE/EVOH film structures) back into pure polymer phases requires work Reprocessing cycles continuously concentrate Non-Intentionally Added Substances (NIAS), legacy additives (e.g., phthalates, heavy metal catalysts), and volatile degradation products. This causes recycled packaging to routinely exceed regulatory toxicity limits (C_{tox}) under REACH and EU PPWR. Decontaminating, washing, and re-polymerizing highly entropy-dense waste streams consumes massive quantities of useful energy (exergy). When the energy input needed to purify post-consumer, resin exceeds the energy required to synthesize pristine virgin polymer, recycling transitions from an environmental savings mechanism into a net-positive thermodynamic burden. Connecting with the previous parts it means to preserve minimum operational line speeds (OEE) and prevent packaging failures on high-speed filling lines, reprocesses must continuously blend degraded recycled content with pristine virgin polymer.

The forth corner is safety/health and compliance which are mix of physical, chemical properties which influence the anthroposphere and biosphere through complying with national and international laws defining these chemicals and their present limits where chemicals of concern must be minimized, removed, isolated or immobilized within a package and its contents. These limits and laws are defined through agencies like governments, international bodies or different organizations with social power. For example, the physical safety is that during the handling of the packaged units also no harm is done to the users or operators which includes the scope of the Operational Health and Safety Aspects (EU-OSHA, 2021) of the packaging product system. Here pallet unit deformation (collapsed rate) together with the Ergonomics & Manual Handling Risks (Directive 90/269/EEC) (European Council, 1990) can monitor handle/grip failure rate. The chemical and toxicology compliance through definition of micro leakages and chemical safety limits are defined as for example: the concentrations of Substances of Very High Concern (SVHC) on the ECHA REACH Candidate List. The target threshold is strictly < 0.1% weight by weight (w/w), Heavy Metal Cap Compliance: which tracks concentration of Lead (Pb), Cadmium (Cd), Mercury (Hg), and Hexavalent Chromium (Cr). PPWR Article 5 mandates this KPI must be below 100 mg/kg (100 ppm). Additionally, PFAS content (ppb/ppm) can be included to monitor the presence of restricted per- and polyfluoroalkyl substances, which is critical for food-contact packaging. Standard limits dictate < 25 ppb for individual non-polymeric PFAS and < 50 ppm for Total Fluorine, where a high level KPI can be the Hazard Classification Score Which Evaluates the number of materials classified under CLP Regulation hazard categories (e.g., carcinogenicity, mutagenicity, or aquatic toxicity), with an SSbD target of zero high-tier hazards. All this data can part of the EU Digital Product Passports (DPP) under the "Agency/Anthroposphere" sub-ring which is a critical regulatory vector for data transparency and is digital container for products, components, and materials, which will store relevant information to support products' sustainability, promote their circularity and strengthen and facilitate legal compliance. Currently it is aimed to be introduced for batteries, but in future this format could be a viable data structure for all types of products, including packaging.

By taking account into all these necessary data we can reduce the uncertainty to decrease the hidden impacts of our packaging or packaging/product system choices.

So, one important question will most probably come in the reflection of this proposed framework – how to integrate (current) economics in this one? Where is the cost of packaging in this framework? Is not that the most important parameter? What about the total cost ownership of the packaging (raw material cost, transportation, labor, etc…). Here it is again a question of the level of thinking. In microeconomics where packaging companies operate, they are bound by direct materials costs like expenses for raw materials (plastics, paper, glass, metals), inks, adhesives, and coatings, manufacturing and conversion costs like machinery depreciation, tooling, labor, line speeds, and throughput efficiency during assembly/filling. Further there are logistics & warehousing costs which are driven by packaging weight and volume (cube utilization), freight/shipping fees, pallet layout, and warehouse storage costs. Recently more and more end-of-Life & compliance costs are introduced through Extended Producer Responsibility (EPR) fees, recycling levies, waste handling fees, and regulatory compliance. And finally, the indirect & risk costs like product damage during transit, brand perception, consumer convenience, and shelf differentiation add to the total cost ownership of packaging. These are the so called microeconomic "household" accounting costs in which currently the society is organized and is bounding the survival or elimination of the economic entities. Here also we need to think in systems and take a step above to look at the foundations. Currently mainstream ("neoclassical") economic models treat the economy like a closed loop of money, entirely separate from nature. In these equations, energy is minimized to a minor footnote. Because energy costs only make up about 5% to 10% of total production expenses, the math assumes energy only drives 5% to 10% of economic growth (Ayres, 2001; Kümmel, Ayres & Lindenberger, 2010). The rest is credited to human cleverness and technological progress—a mathematical placeholder known as the "Solow Residual" (Stern, 2011). This viewpoint ignores a fundamental law of physics: the economy is not a perpetual motion machine. It is an open system that physically feeds on the biosphere. Every single product made requires material throughput—a continuous, one-way flow of energy and raw matter extracted from the earth, which is eventually spit back out as waste and pollution (Kümmel & Lindenberger, 2020). Whether we are burning fossil fuels (which are just ancient, deeply concentrated biomass) or utilizing active wood and crops, we are constantly draining the living biosphere to power our industries. Standard economics assumes that if energy runs out, we can simply "substitute" it with more human labor or high-tech machinery. In reality, machines and workers are just transformers of energy; they cannot do any work without a physical power source (Lindenberger & Kümmel, 2011). By treating energy as a minor financial expense rather than the lifeblood of physical work, standard models ignore the hard-environmental limits of consuming the planet's finite resources (Režný & Bureš, 2019). So, to integrate the real cost of the product packaging system a new type of economic system is needed which accounts for energy depletion and degradation from the biosphere to a much realistic scale. We can start with an extended total cost ownership type of formula where the environmental and health and safety factors are also accounted for:

$$\text{TPS} = \frac{T * P_f}{OE + \beta * E_{CO_2} + \gamma * C_{tox} + \delta * \Delta S} \quad (1)$$

Subject to $E_{CO2} \leq E_{max}$, $C_{tox} \leq C_{treshold}$, $\Delta S \leq \Delta S_{max}$

Where:

T: Net Production Throughput (good units passing First Pass Yield per hour or OEE).

P_f: Functional barrier (mechanical, oxygen, gas, etc…) and structural performance factor (0≤ Pf≤ 1).

OE: Direct Operational Expense (raw materials, processing energy, conversion, and logistics).

ECO_2: Lifecycle Greenhouse Gas Intensity (kg CO_2 eq) per functional packaging unit delivered).

C_{tox}: Chemical hazard index (migration risk, SVHC concentration, heavy metals).

ΔS: Entropic degradation score across circular reprocessing loops (chain scission, contamination).

B, δ, γ Conversion weight factors translating environmental carbon (EC02), chemical toxicity, and entropic degradation into system penalty values (e.g., carbon taxes, EPR penalties, internal shadow carbon pricing).

E_{max}: Maximum allowable lifecycle carbon footprint per unit under regulatory or corporate Science Based Targets.

This approach captures trade-offs across material transitions which are currently popular like the paperization or completely switching materials. For instance, swapping a polymer pouch for glass reduces entropic degradation (ΔS = 0) and chemical migration ($C_{tox} \approx 0$), but drastically increases transport E_{CO2} and OE for energy used/cost for remelting the glass. The expanded denominator penalizes this swap unless transport distances are near zero.

As an example we can take the case of currently popular paperization (switching polymer composites to paper composites) the TPS value would be:

$$\text{TPS}_{\text{paperization}} = \frac{\overbrace{(T\downarrow)}^{\text{Lower line speed}} * \overbrace{(P_f\downarrow)}^{\text{Weaker barrier}}}{\underbrace{OE\uparrow}_{\text{Higher basis mass}} + \beta * \underbrace{(E_{CO2}\uparrow)}_{\text{Pulp Energy and transport}} + \gamma * \underbrace{(C_{tox}\uparrow)}_{\text{PFAS/MOSH /adhesives}} + \delta * \underbrace{(\Delta S\uparrow)}_{\text{Composite entropic trap}}} \quad (2)$$

Here we would have several different angles to solve:

Mechanical & Throughput Penalties ($P_f \downarrow$, $T \downarrow$) Raw paper lacks intrinsic moisture, grease, and gas barrier properties. On high-speed converting and packaging lines, paper's lower tear resistance and stiffness lead to higher line downtime and reduced throughput (T). A lower P_f also increases product spoilage rates, creating indirect lifecycle carbon spikes.

Mass & Carbon Transport Burden ($E_{CO2} \uparrow$) To match the structural integrity of a thin polymer film, paper packaging requires significantly higher mass per functional unit (basis weight). This added weight drives up transportation emissions (E_{CO2}), while pulp production remains highly water- and energy-intensive compared to standard resin extrusion.

The Composite Entropic Trap (ΔS↑): To fix paper's barrier limitations, manufacturers laminate the fiber substrate with thin plastic coatings (e.g., PE or EVOH layers). This creates a multi-material composite structure that dramatically increases mixing entropy (ΔS_{mix}). The resulting hybrid material is difficult for standard paper mills to hydropulp, turning an ostensibly recyclable paper product into an unrecyclable entropic waste stream.

Chemical Hazard Migration ($C_{tox} \uparrow$): Paperization often introduces toxicological risks. Recycled paper pulps frequently carry mineral oil hydrocarbons (MOSH/MOAH) from inks, while grease-resistant paper variants historically relied on per- and polyfluoroalkyl substances (PFAS) or specialized functional adhesives, elevating the chemical hazard score (C_{tox}). Of course, this needs to be cross evaluated with the similar risk from polymeric recycling. The TPS-TOC model demonstrates that unless a paperization strategy uses mono-material, bio-based barrier coatings that preserve fiber pulping efficiency, it penalizes the system's net value denominator by trading lightweight polymer efficiency for heavy, chemically complex composite packaging.

So, to implement this approach first one has to identify the constraints and pinpointing whether system capacity is bottlenecked by line runnability (P_f), toxicity limits (C_{tox}) under PPWR/REACH), or thermodynamic degradation (ΔS). After that the next step is maximizing line output and shelf-life protection without exceeding toxicologic, environmental impact thresholds or triggering higher EPR penalty tiers. Through this approach all processes need to be subordinated from aligning upstream resin selection and downstream sorting strictly to support the identified constraint and excluding siloed in KPIs (like procurement lowest cost with no regards to other systems). Deploying Safe-and-Sustainable-by-Design (SSbD) innovations—such as bio-based mono-polymer coatings—to shift the physical performance and reducing toxicological, environmental and line production break impacts and at the end comes the mitigation of entropic inertia: re-evaluating system dynamics as shifts in PPWR compliance or material fatigue alter the primary constraint.

5. Conclusion

Modern packaging science is undergoing a fundamental paradigm shift. Driven by escalating climate pressures, stringent European Union regulatory mandates, and the imperative of the circular economy, packaging is no longer evaluated merely as a single-use vessel abstracted from the environment. Instead, we must conceptualize it as a Total (unified) Packaging System (TPS) where all subsystems where packaging and packaging /product are a part of the material world flow. While packaging is never an item itself but developed for a specific product, at its core, a packaging system must successfully execute several fundamental functions across physical, chemical, and human environments. These developments must surpass the fragmented siloed in and over the wall approach which perpetuates the status quo. By fully integrating all aspects with the available tools and key process indicators (and having consciousness about the interconnection of the decision to the biosphere) is a first step to start thinking and designing product packaging systems. The presented packaging development framework is a starting point on connecting all the dots to include and truly account for all upstream and downstream safety, toxicology and environmental impact with the most optimal choices available. They are either bound by material throughput of the production and transportation system or by agencies of governments which prescribe rules and policies. While the material performance, sustainability and safety have many newly developed tools and assessment frameworks like LCA, SSbD, which can be already today fully integrated the main challenge remains the current economic models which due to the downplayed energy cost and environmental costs (and its implication to biosphere and of course anthroposphere) are the main obstacles for full integration of these types of frameworks. The full accounting of all these downplayed factors would change the packaging and distribution of goods dramatically in some sectors demanding complete overhaul of the packaging concepts. While that is not likely in the near future due to the excess amount of energy needed to change the current systems and concepts, this proposal is a brick on paving the future road for a long journey many anthropogenic systems will need to go through to mitigate the climate risks we all are facing.

6. References

Ali, A. (2026) 'A system-level framework for sustainable packaging design and waste management integration', *Saudi Journal of Engineering and Technology*, 11(5), pp. 429–437. DOI: 10.36348/sjet.2026.v11i05.006

Ayres, R.U. (2001) 'The minimum complexity of endogenous growth models: the role of physical resource flows', *Energy*, 26(9), pp. 817–838. DOI: 10.1016/S0360-5442(01)00031-7

Bateson, G. (1972) *Steps to an Ecology of Mind*. Chicago: University of Chicago Press.

Bix, L., de la Fuente, J., Sundar, R. and Lockhart, H. (2009) 'Packaging design and development'. In: Yam, K.L. (ed.) *Encyclopedia of Packaging Technology*. 3rd edn. Hoboken: John Wiley & Sons, pp. 851–862.

Bramklev, C. (2009a) 'Towards integrated product and packaging development – exploring the missing link', *Packaging Technology and Science*, 22(3), pp. 129–145.

Bramklev, C. (2009b) *Towards a framework for packaging design in new product development*. PhD thesis. Lund University.

Clegg, S. (2022) *Elgar Introduction to Designing Organizations*. Cheltenham: Edward Elgar Publishing.

de Koeijer, B., de Lange, J. and Wever, R. (2017) 'Desired, perceived, and achieved sustainability: trade-offs in strategic and operational packaging development', *Sustainability*, 9(10), 1923. DOI: 10.3390/su9101923

Dunbar, R.I. (1993) 'Coevolution of neocortical size, group size and language in humans', *Behavioral and Brain Sciences*, 16(4), pp. 681–694. DOI: 10.1017/S0140525X00032325.

ECHA (2025) *Microplastics*. European Chemicals Agency. Available from: https://echa.europa.eu/hot-topics/microplastics [Accessed 12 September 2026].

Ellen MacArthur Foundation (2021) *The butterfly diagram: visualising the circular economy*. Available from: https://www.ellenmacarthurfoundation.org/circular-economy-diagram [Accessed 16 September 2026].

EU-OSHA (2021) *Directive 90/269/EEC – manual handling of loads: minimum health and safety requirements*. Bilbao: European Agency for Safety and Health at Work. Available from: https://osha.europa.eu/en/legislation/directives/6 [Accessed 17 September 2026].

EuPIA (2025) *Customer information note on microplastics in printing inks and printed products*. Brussels: European Printing Ink Association. Available from: https://www.eupia.org/wp-content/uploads/2025/06/202506_EuPIAstatement_microplastics_FINAL.pdf [Accessed 1 October 2026].

European Commission (2022) *European framework for Safe and Sustainable by Design (SSbD) chemicals and materials: assessment framework for new chemicals and materials*. JRC Science for Policy Report. Luxembourg: Publications Office of the European Union. DOI: 10.2760/487955

European Commission (2023) 'Commission Regulation (EU) 2023/2055 of 25 September 2023 amending Annex XVII to Regulation (EC) No 1907/2006 as regards synthetic polymer microparticles', *Official Journal of the European Union*, L 238, pp. 67–88. Available from: https://eur-lex.europa.eu/legal-content/EN/TXT/?uri=celex%3A32023R2055 [Accessed 1 October 2026].

European Commission (2025) *Packaging & Packaging Waste Regulation (PPWR)*. Brussels: European Commission. Available from: https://environment.ec.europa.eu/topics/waste-and-recycling/packaging-waste/packaging-packaging-waste-regulation_en [Accessed 16 September 2026].

European Council (1990) 'Council Directive 90/269/EEC of 29 May 1990 on the minimum health and safety requirements for the manual handling of loads where there is a risk particularly of back injury to workers', *Official Journal of the European Communities*, L 156, pp. 9–13.

European Parliament and Council (1994) 'Directive 94/62/EC of 20 December 1994 on packaging and packaging waste', *Official Journal of the European Communities*, L 365, pp. 10–23.

European Parliament and Council (2025) 'Regulation (EU) 2025/40 of 19 December 2024 on packaging and packaging waste, amending Regulation (EU) 2019/1020 and Directive (EU) 2019/904, and repealing Directive 94/62/EC', *Official Journal of the European Union*, L 2025/40.

European Union (2025) *Packaging and Packaging Waste (from 2026): Summary of Regulation (EU) 2025/40*. EUR-Lex. Available from: https://eur-lex.europa.eu/EN/legal-content/summary/packaging-and-packaging-waste-from-2026.html [Accessed 16 September 2026].

García-Arca, J. and Prado-Prado, J.C. (2008) 'Packaging design as a strategic tool for business competitiveness', *International Journal of Logistics Research and Applications*, 11(5), pp. 377–393. DOI: 10.1080/13675560802141680

García-Arca, J., Garrido, A.T. and Prado-Prado, J.C. (2017) 'Sustainable Packaging Logistics: the link between sustainability and competitiveness in supply chains', *Sustainability*, 9(7), 1098. DOI: 10.3390/su9071098

García-Arca, J., Comesaña-Benavides, J.A. and Prado-Prado, J.C. (2021) 'Methodology for selecting packaging alternatives: an action research application in the industrial sector', *Central European Journal of Operations Research*, 29(4), pp. 1427–1446. DOI: 10.1007/s10100-020-00724-3

Hellström, D. (2007) *On interactions between packaging and logistics – exploring implications of technological developments*. PhD thesis. Lund University.

Karlovits, I. (2025) 'Extended Producer Responsibility for packaging – industry perspective from a global company'. In: Kavčič, U. and Lavrič, G. (eds.) *Proceedings of the 4th International Circular Packaging Conference (4CPC 2025), 16–17 October 2025, Ljubljana, Slovenia*. Ljubljana: Pulp and Paper Institute and Faculty of Polymer Technology, pp. 116–122. DOI: 10.5281/zenodo.17295166

Kümmel, R., Ayres, R.U. and Lindenberger, D. (2010) 'Thermodynamic laws, economic methods and the productive power of energy', *Journal of Non-Equilibrium Thermodynamics*, 35(2), pp. 145–179. DOI: 10.1515/jnetdy.2010.009

Kümmel, R. and Lindenberger, D. (2020) 'Energy, entropy, constraints, and creativity in economic growth and crises', *Entropy*, 22(10), 1156. DOI: 10.3390/e22101156

Larkin, R. and Burcham, D. (2022) 'The package development process'. In: *Fundamentals of Packaging Technology*. 6th edn. Herndon: Institute of Packaging Professionals, pp. 676–704.

Lilienfeld, R.M. (2021) *Sustainable Packaging Roadmap and the Sustainable Packaging Wheel*. Sustainable Packaging Research, Information, and Networking Group (SPRING). Available from: https://www.springpack.net/roadmap [Accessed 17 September 2026].

Lindenberger, D. and Kümmel, R. (2011) 'Energy and the state of nations', *Energy*, 36(10), pp. 6010–6018. DOI: 10.1016/j.energy.2011.08.014

Lockhart, H.E. (1997) 'A paradigm for packaging', *Packaging Technology and Science*, 10(5), pp. 237–252. DOI: 10.1002/(SICI)1099-1522(199709/10)10:5<237::AID-PTS395>3.0.CO;2-#

Meadows, D.H. (2008) *Thinking in Systems: A Primer*. London: Earthscan.

Miller, G.A. (1956) 'The magical number seven, plus or minus two: some limits on our capacity for processing information', *Psychological Review*, 63(2), pp. 81–97. DOI: 10.1037/h0043158

Pålsson, H., Finnsgård, C. and Wänström, C. (2011) 'An evaluation model for sustainable packaging systems in supply chains'. In: *Proceedings of the 23rd Annual NOFOMA Conference, 9–10 June 2011, Harstad, Norway*. Harstad: Harstad University College, pp. 1023–1040.

Raworth, K. (2012) 'A safe and just space for humanity: can we live within the doughnut?', *Oxfam Discussion Papers*. Oxford: Oxfam. Available from: https://policy-practice.oxfam.org/resources/a-safe-and-just-space-for-humanity-can-we-live-within-the-doughnut-210490/ [Accessed 17 September 2026].

Režný, L. and Bureš, V. (2019) 'Energy transition scenarios and their economic impacts in the extended neoclassical model of economic growth', *Sustainability*, 11(13), 3644. DOI: 10.3390/su11133644

Rogerson, M.W. (2025) *Unpacked: the Science, the Strategy, and Psychology Behind Modern Packaging*. Independently published.

Saghir, M. (2002) 'Packaging logistics: evaluation method of packaging in supply chain', *Packaging Technology and Science*, 15(1), pp. 41–49.

Saghir, M. (2004) *A platform for packaging logistics development: a systems approach*. PhD thesis. Lund University.

Simon, H.A. (1957) *Models of Man, Social and Rational: Mathematical Essays on Rational Human Behavior in a Social Setting*. New York: John Wiley & Sons.

Stern, D.I. (2011) 'The role of energy in economic growth', *Annals of the New York Academy of Sciences*, 1219(1), pp. 26–51. DOI: 10.1111/j.1749-6632.2010.05921.x

Sweller, J., Ayres, P. and Kalyuga, S. (2011) *Cognitive Load Theory*. New York: Springer. DOI: 10.1007/978-1-4419-8126-4



© 2026 Authors. Published by the University of Novi Sad, Faculty of Technical Sciences, Department of Graphic Engineering and Design. This article is an open access article distributed under the terms and conditions of the Creative Commons Attribution license 4.0 Serbia (https://creativecommons.org/licenses/by/4.0/deed.en).

Printing technologies and quality

01

Original Scientific Paper https://doi.org/10.24867/GRID-2026-p5

Comparative Assessment of Tone and Line Reproduction on Fabric Using DTF and Sublimation Transfer Printing

Vyacheslav Repeta
Pavlo Ryvak
Yurii Petriv

Institute of Printing Art and Media Technologies of Lviv Polytechnic National University, Lviv, Ukraine

ABSTRACT

Digital transfer printing technologies such as Direct-to-Film (DTF) and dye-sublimation printing are increasingly used for personalized textile production; however, the influence of textile surface structure and fibre orientation on the stability of tone and line reproduction remains insufficiently investigated. In this study, a comparative assessment of the reproduction of halftone and fine line elements on gabardine fabric using DTF printing with a white underbase, DTF printing without a white underbase, and dye-sublimation transfer printing is presented. A digital test scale containing cyan and magenta halftone areas and black line elements with different orientations was printed under identical resolution conditions (720 × 1440 dpi). Optical density measurements and relative information capacity loss were used as quantitative indicators of tonal and line reproduction. The obtained results showed that all investigated technologies provide stable reproduction in highlight tonal regions, whereas DTF printing with a white underbase provides improved colour field saturation in midtones and shadows compared to the other variants. Analysis of line reproduction demonstrated a significant influence of textile surface anisotropy, with relative spatial information capacity losses exceeding the reference threshold level of 15% in all investigated cases and reaching maximum values in prints produced without a white underbase. The results confirm the effectiveness of the white intermediate layer in improving the stability of reproduction of fine image elements on structured textile substrates and provide experimental data for the optimisation of digital transfer printing workflows.

KEY WORDS
DTF printing, dye-sublimation printing, textile printing, halftone reproduction, line reproduction, optical density, quality, information capacity loss

1. Introduction

The global market for digital heat-transfer textile printing technologies is demonstrating steady growth driven by the expansion of personalized apparel production, the rapid development of e-commerce platforms, and the transition of the textile industry toward short-run on-demand manufacturing models. Within this segment, dye-sublimation printing remains one of the leading technologies due to its high capability for continuous-tone image reproduction and its extensive application in sportswear, promotional textiles, and interior fabric products. According to estimates by Mordor Intelligence (2025), the global dye-sublimation printing market reached approximately USD 15.22 billion in 2025 and is projected to grow to about USD 28.05 billion by 2031 (CAGR ≈ 10.7 %). At the same time, Direct-to-Film (DTF) technology is rapidly expanding its application in the personalized textile production sector due to its capability to transfer images onto natural and blended fabrics without preliminary substrate preparation, which significantly simplifies short-run production workflows. According to Grand View Research (2025) the global DTF printing market was valued at approximately USD

2.72 billion in 2024, with projections indicating growth to around USD 3.92 billion by 2030 (CAGR ≈ 6 %). As a result, dye-sublimation and DTF printing technologies are increasingly considered complementary digital heat-transfer solutions for textile image reproduction, particularly in applications requiring flexibility in substrate selection and rapid production adaptation.

Textile materials represent anisotropic substrates with direction-dependent mechanical and surface properties. Therefore, the orientation of fibres relative to printed image elements may affect spatial reproduction stability, edge sharpness, and tonal uniformity. Despite the rapid industrial adoption of transfer technologies, the influence of fibre orientation on reproduction characteristics of printed elements remains insufficiently investigated.

Previous studies in the field of dye-sublimation textile printing have mainly focused on the influence of technological process parameters on image quality indicators such as colour strength, colour difference (ΔE), and print uniformity. For example, Toshikj et al. (2019) investigated the effect of total ink limiting levels and transfer paper properties on the colour strength and visual uniformity of sublimation prints on polyester fabrics, demonstrating that transfer media significantly affect final image quality characteristics. In paper (Özomay & Özomay, 2020) analysed the influence of temperature and pressing time on colour reproduction and fastness properties in sublimation transfer printing on polyester and nylon fabrics and confirmed that thermotransfer conditions directly determine the stability of colour coordinates and wash resistance. Other studies have addressed optimisation of thermotransfer regimes and material absorbency effects on optical density formation in sublimation printing processes, indicating that substrate properties play a critical role in determining the final reproduction quality of textile prints Repeta, Petriv & Kukura, 2025).

Printing technologies such as screen transfer and digital inkjet printing are widely applied for image reproduction on textile substrates (Lilić, Kašiković & Miketić, 2018: Stančić et al, 2020); however, most existing studies have focused primarily on colour fastness, adhesion behaviour and durability properties of printed layers rather than on spatial reproduction accuracy of fine image elements. At the same time, the rapidly emerging Direct-to-Film printing technology has been primarily investigated from the perspective of workflow efficiency, substrate compatibility, and production flexibility, whereas systematic studies addressing the reproduction stability of halftone areas and fine line elements on structured textile surfaces remain limited.

In particular, the combined influence of textile fibre orientation and transfer technology type on spatial reproduction characteristics has not yet been sufficiently analysed in comparative experimental studies.

Therefore, the present study aims to investigate the reproduction characteristics of halftone areas and fine line elements produced using dye-sublimation and DTF transfer technologies on gabardine fabric, taking into account the influence of textile surface structure and fibre orientation on optical density variation and line fidelity. The obtained results are expected to contribute to a deeper understanding of image formation mechanisms in digital heat-transfer textile printing and to support the optimisation of reproduction quality in personalised textile production workflows.

2. Methods

Printing of the test scale for evaluating the reproduction quality of tonal and line elements on textile material was performed using two digital transfer printing technologies: Direct-to-Film (DTF) and dye-sublimation printing. Both methods were implemented using the same image formation resolution of 720 × 1440 dpi (6 Pass mode), ensuring comparability of the experimental results with respect to halftone structure formation parameters.

Printing of the test scale using the DTF technology was carried out on an AINKJET DTF A-620 SUPER digital printer with DTK Ink pigment inks. Image formation was performed on an intermediate carrier – a polyethylene terephthalate (PET) film with a thickness of 95 µm, which ensures dimensional stability of raster elements during printing. After forming the color layer, a thermoplastic polyurethane (TPU) adhesive powder with a particle size of 80-200 µm was applied to the surface of the print, corresponding to standard DTF transfer conditions. The melting temperature of the adhesive powder was approximately 95-115 °C, providing effective thermal activation of the adhesive layer prior to image transfer onto the textile substrate. Image transfer onto the fabric was performed by heat pressing at a temperature of 165 °C for 15 s, ensuring sufficient adhesion of the polymer layer to the textile surface without significant deformation of raster elements.

Dye-sublimation printing of the test scale was carried out using a SureColor SC-F7200 digital printer with Epson Ultra Chrome® DS disperse inks. Image formation was performed on an intermediate carrier – Jasper sublimation paper with a grammage of 65 g/m², which ensures uniform transfer of the dye into the polymer structure of textile fibres during thermal diffusion. Image transfer onto the textile substrate was performed by heat transfer at a temperature of 215 °C for 30 s, corresponding to standard sublimation printing conditions and ensuring complete dye migration into the fiber structure of the material.

The use of identical printing resolution and standardized transfer conditions ensured the reliability of comparative

analysis of raster and line element reproduction when applying different digital textile printing technologies.

The print quality control test scale (Ryvak et al., 2014) consists of 44 functional blocks containing line and halftone elements intended for evaluating the accuracy of raster structure formation and the stability of tonal gradation reproduction in digital printing on textile substrates. The appearance of the test scale printed on the fabric is shown in Fig. 1.

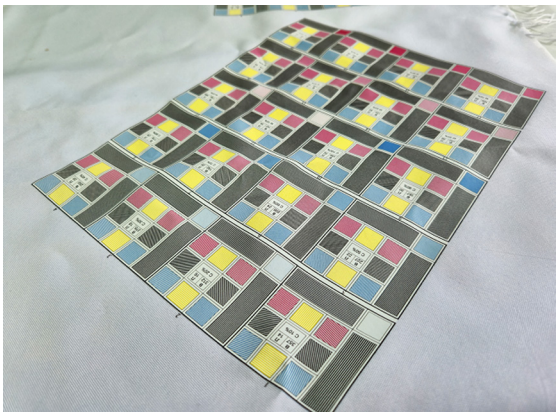
The scale includes line elements with screen rulings ranging from 14 to 100 lines/cm, arranged at standard screen angles commonly used in multicolor printing: 75° for magenta, 15° for cyan, 45° or 135° for black (Fig. 2).

Additionally, variants of element orientation are provided taking into account a possible 90° rotation of the substrate, allowing evaluation of anisotropic effects in line reproduction depending on the direction of the textile structure.

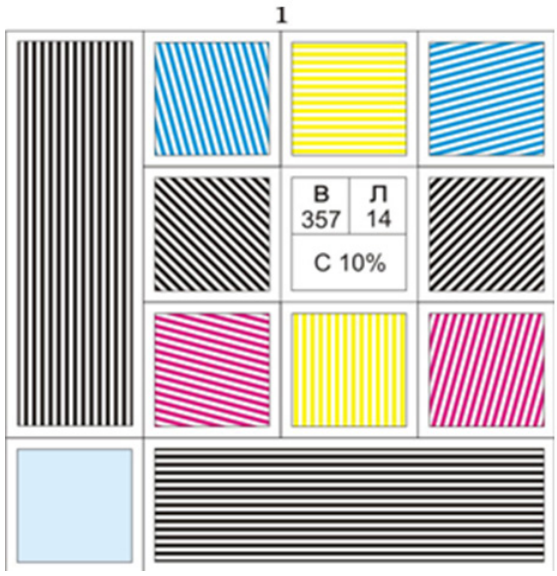
Besides line elements, the test scale includes halftone patches for each process color, corresponding to tonal coverage values of: 10, 20, 30, 40, 50, 60, 70, 80, 90, and 100 %.

The use of the test scale provides comprehensive control of multicolor image reproduction quality in DTF and dye-sublimation printing technologies, since arranging raster elements at appropriate screen angles minimizes moiré formation and ensures reliable assessment of geometric raster structure parameters on textile substrates.

To compare reproduction capabilities of transfer printing technologies on gabardine fabric, a digital test scale containing cyan and magenta halftone patches and black line elements with decreasing widths and different orientations was printed using three variants: DTF transfer with white underbase, DTF transfer without white underbase, and sublimation transfer printing. Optical densities of halftone fields and minimum reproducible line widths



» **Figure 1:** *Appearance of the test scale*



» **Figure 2:** *First block of the test scale elements (screen ruling 14 lines/cm, line element size 357 µm, cyan tonal value 10 %)*

were measured to evaluate tonal and spatial reproduction performance. The theoretical tonal capacity of an amplitude-modulated halftone cell depends on the relationship between device resolution and screen ruling and can be estimated as:

$$N = \left(\frac{R}{L}\right)^2 + 1 \tag{1}$$

where R is device resolution (dpi) and L is screen ruling (lpi). This relationship describes the number of distinguishable tone levels within a halftone cell and is widely used in digital halftoning theory (Ulichney, 1987; Kipphan, 2001).

Based on this relationship, the equivalent information capacity per unit area of the reproduced halftone structure was estimated as (Ryvak et al, 2018):

$$I_e = L^2 \log_2 \left[\left(\frac{R}{L}\right)^2 + 1\right] \tag{2}$$

This parameter was used as an analytical indicator for comparative evaluation of reproduction performance of DTF and sublimation transfer printing technologies on gabardine fabric. The relative amount of loss of information capacity of prints can be determined by the formula:

$$\Delta I = \frac{I_e - I}{I_e} \cdot 100\% \tag{3}$$

I_e – theoretical information capacity;

I – actual information capacity.

Additionally, the influence of textile surface structure

was assessed by analysing the minimum reproducible line width at different orientations relative to the rib structure of the fabric.

3. Results and Discussion

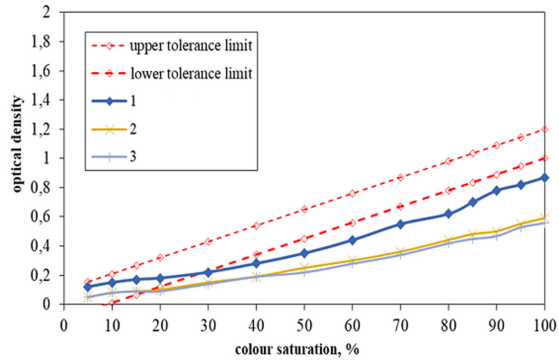
Since standardized reference values of solid ink optical density are not defined for textile transfer printing technologies such as DTF and dye-sublimation printing, the obtained density values were compared with typical pressroom control targets for offset printing on wood-free uncoated paper. According to common process control practice in compliance with ISO 12647-2 (2013) printing conditions, the recommended solid ink density ranges are approximately 1.00-1.20 for cyan, 1.05-1.25 for magenta, 0.85-1.05 for yellow, and 1.30-1.55 for black (Brotherhood Paper, 2026). Since ISO 12647-2 defines process control targets for offset lithographic printing on paper substrates, these density ranges were applied in the present study only as auxiliary comparative reference levels and not as normative quality criteria for textile transfer printing technologies such as DTF and dye-sublimation printing. The optical density of cyan and magenta imprints was measured using an X-Rite SpectroEye spectrodensitometer.

The results of optical density measurements for cyan and magenta halftone patches reproduced using sublimation transfer printing and DTF printing with and without white underbase are presented in Figures 3 and 4.

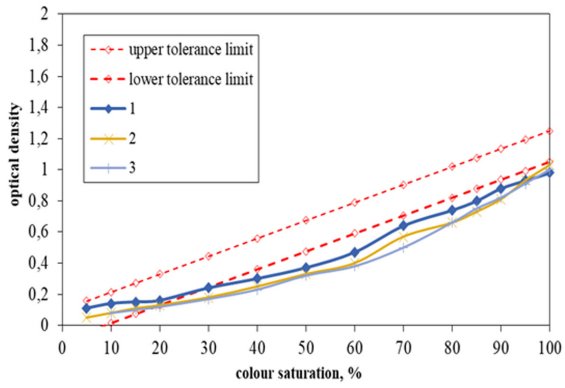
Analysis of the obtained data shows that in highlight tonal regions all three printing variants demonstrate optical density values within the reference interval typical for offset printing on uncoated paper. This indicates sufficient stability of tone reproduction at low coverage values regardless of the transfer technology used.

However, in midtone and shadow regions a noticeable divergence between the investigated technologies can be observed. In the case of cyan reproduction, density values obtained by sublimation printing remain closer to the lower boundary of the reference interval, while DTF printing with white underbase provides slightly higher optical density values due to additional reflection from the supporting white layer. At the same time, DTF printing without white underbase demonstrates reduced density values in darker tonal regions, which can be explained by partial penetration of the colour layer into the textile structure and increased influence of substrate anisotropy.

For magenta reproduction a similar tendency is observed. In highlight regions all printing variants demonstrate comparable behaviour, whereas in midtones and shadows density values decrease relative to the reference offset interval, especially in the case of DTF printing without white underbase. This behaviour



» **Figure 3:** *Optical density of cyan reproduction on prints: 1 – sublimation printing; 2 – DTF printing with white underbase; 3 – DTF printing without white underbase*



» **Figure 4:** *Optical density of magenta reproduction on prints: 1 – sublimation printing; 2 – DTF printing with white underbase; 3 – DTF printing without white underbase*

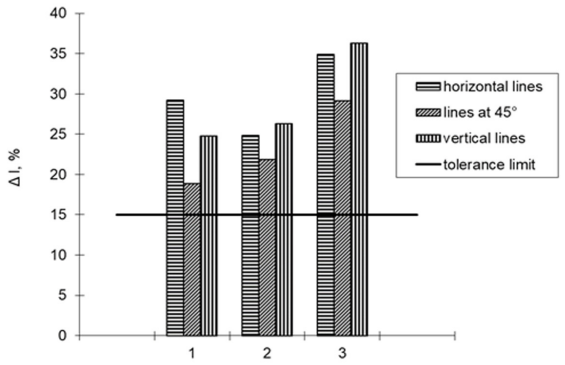
confirms that the presence of a white intermediate layer significantly improves colour field saturation stability during transfer printing on structured textile substrates.

Further analysis was performed for reproduction of line elements with different orientations relative to the textile rib structure in order to estimate the relative loss of image information capacity. The obtained results are presented in Fig. 5.

The largest loss of information capacity is observed for DTF printing without white underbase in horizontal and vertical line elements. At the same time, line elements oriented at 45° demonstrate improved reproduction stability, which confirms the anisotropic influence of gabardine fabric structure on spatial reproduction accuracy.

Both sublimation printing and DTF printing with white underbase demonstrate improved stability of line reproduction compared to the variant without white underbase. Nevertheless, in all investigated cases the relative loss of information capacity exceeds the reference threshold level of 15%, indicating the significant influence

of textile surface structure on spatial reproduction limitations in transfer printing technologies.



» **Figure 5:** *Relative loss of image information capacity in prints: 1 – sublimation printing; 2 – DTF printing with white underbase; 3 – DTF printing without white underbase*

4. Conclusions

A comparative experimental assessment of tone and fine-line reproduction on gabardine fabric using dye-sublimation transfer printing and Direct-to-Film (DTF) printing with and without a white underbase demonstrated that all investigated technologies provide stable tone reproduction in highlight regions under identical image formation resolution conditions.

The presence of a white intermediate layer in DTF printing improves the stability of fine-line reproduction compared with DTF printing without a white underbase, confirming its compensating role in reducing the influence of substrate structure on spatial image formation. At the same time, dye-sublimation printing demonstrated comparable or lower information capacity losses for certain line orientations, indicating that reproduction stability depends not only on the transfer technology but also on the orientation of structural textile elements relative to image features.
The analysis of line element reproduction showed that the relative loss of image information capacity reached 29.23% for horizontal lines, 18.8% for lines oriented at 45°, and 24.8% for vertical lines in the case of dye-sublimation printing. For DTF printing with a white underbase, the corresponding values were 24.9%, 21.8%, and 26.3%, respectively. The highest losses were observed for DTF printing without a white underbase, reaching 34.9%, 29.2%, and 36.3%.

Quantitative analysis of spatial reproduction accuracy showed that the relative loss of image information capacity exceeded the reference threshold level of 15% in all investigated cases and reached maximum values for DTF printing without a white underbase. This confirms the significant influence of the anisotropic rib structure of gabardine fabric on the reproduction of fine graphic elements in digital transfer printing technologies.

The obtained results provide experimental evidence of the importance of considering textile surface anisotropy and intermediate layer structure when selecting digital transfer printing workflows for personalised textile production requiring stable reproduction of halftone gradients and fine line elements.

5. References

Brotherhood Paper. (n.d.) *CMYK values reference chart*. Available from: https://brotherhoodpaper.com/cmyk-values [Accessed 1 April 2026].

Direct to Film Printing Market (2025–2030). (n.d.) Available from: https://www.grandviewresearch.com/industry-analysis/direct-film-printing-market-report [Accessed 3 April 2026].

International Organization for Standardization. (2013) ISO 12647-2:2013. *Graphic technology – Process control for the production of half-tone colour separations, proof and production prints – Part 2: Offset lithographic processes*. Geneva: International Organization for Standardization.

Kipphan, H. (2001) *Handbook of Print Media*. Berlin, Heidelberg: Springer. DOI: 10.1007/978-3-540-29900-4_8

Lilić, A., Kašiković, N. and Miketić, N. (2018) 'Rubbing fastness of green ink printed on textile using screen printing transfer technique'. In: *Proceedings of the 9th International Symposium on Graphic Engineering and Design (GRID 2018)*. Novi Sad, Serbia. DOI: 10.24867/GRID-2018-p41

Mordor Intelligence. (2025) *Dye-Sublimation Printing Market Analysis*. Available from: https://www.mordorintelligence.com [Accessed 12 April 2026].

Özomay, M. and Özomay, Z. (2020) 'Effect of transfer temperature and time on colour properties of sublimation printing on polyester and nylon fabrics', *Journal of Engineered Fibers and Fabrics*, 15, pp. 1–10. DOI: 10.1177/1558925020913737

Ryvak, P.M., Shabliy, I.V. and Repeta, V.B. (2014) *Quality control scale for printing on digital machines and devices*. Ukraine Patent UA 104837. Published 11 March 2014.

Ryvak, P.M., Shabliy, I.V., Bernatsek, V.V., Kamyanska-Hasyuk, L.I. and Hlova, A.P. (2018) 'Influence of paper structure on information capacity loss of offset prints', *Science Notes, Ukrainian Academy of Printing*, 1(56), pp. 71–81.

Repeta, V., Petriv, Y. and Kukura, Y. (2025) 'Optimization and forecasting models of the sublimation printing process on textile materials', *Journal of Print and Media Technology Research*, 13(4), pp. 189–197.

Stančić, M., Ružičić, B., Vujčić, Đ., Grujić, D., Dragić, M. and Janković, B. (2020) 'Influence of inkjet print parameters on thermal resistance of printed knitwears'. In: *Proceedings of the 10th International Symposium on Graphic Engineering and Design (GRID 2020)*, pp. 437–442. DOI: 10.24867/GRID-2020-p49

Toshikj, E., Dimovski, V., Pavlovska, G. and Trajkovska, J. (2019) 'Influence of transfer paper characteristics and ink limiting on colour strength and print uniformity in dye-sublimation printing', *Tekstil ve Konfeksiyon*, 29(3), pp. 243–251.
Ulichney, R. (1987) Digital Halftoning. United States: MIT Press.



© 2026 Authors. Published by the University of Novi Sad, Faculty of Technical Sciences, Department of Graphic Engineering and Design. This article is an open access article distributed under the terms and conditions of the Creative Commons Attribution license 4.0 Serbia (https://creativecommons.org/licenses/by/4.0/deed.en).

Professional Paper https://doi.org/10.24867/GRID-2026-p6

The Role of Washer Systems in Aluminum Can Manufacturing: Impact on Product Quality and Process Sustainability

ABSTRACT

The aluminum beverage can manufacturing process is a highly automated and tightly controlled industrial system where surface preparation plays a critical role in ensuring product quality and long-term performance. Within this production chain, the Washer system represents one of the most important stages, as it is responsible for removing process contaminants, preparing the aluminum surface, and enabling proper adhesion of subsequent coating and printing layers. This paper analyzes the role of Washer systems in aluminum can manufacturing, with a specific focus on their impact on product quality, process stability, and overall production sustainability. The study combines a literature review, analysis of industrial practice, and operational process data from production environments. Key process parameters such as pH, conductivity, fluoride concentration, and FA/TA ratio are discussed in relation to their influence on surface treatment efficiency and defect prevention. An experimental Etching Rate Test was conducted to quantitatively evaluate the intensity of aluminum surface etching as an indicator of accelerator activity within the Washer system. The results showed an average material loss of 8.6 mg per can (114 mg/m²), which falls within the established industrial reference range, confirming stable and controlled process conditions. The findings highlight the Washer system as a critical interface between mechanical forming and final surface finishing operations, directly influencing coating adhesion, defect formation, and downstream process efficiency. In addition, the study emphasizes the dual role of the Washer in ensuring both product quality and environmental sustainability through optimized chemical consumption, water recirculation, and process control strategies.

Vladimir Oličkov [1]
Nemanja Kašiković [2]
Sandra Dedijer [2]
Miljana Prica [2]

[1] Ball Packaging Europe d.o.o., Belgrade, Serbia
[2] University of Novi Sad, Faculty of Technical Sciences, Department of Graphic Engineering and Design, Novi Sad, Serbia

KEY WORDS
Aluminum can manufacturing, washer system, aluminum surface preparation, chemical process control, etching rate, quality control, sustainability

1. Introduction

1.1. Industry context

The aluminum beverage can industry represents one of the most technologically advanced sectors of modern packaging production, with an annual global output exceeding 400 billion cans (Green, 2007). The widespread use of aluminum cans is primarily driven by their low weight, high recyclability, mechanical stability, and suitability for high-speed industrial filling and distribution systems. In addition to their functional advantages, aluminum cans are recognized as an important example of circular economy principles, since the average recycling cycle from a used can to a newly produced can, can be completed in approximately 60 days (European Aluminium Association, 2020a).

The manufacturing process of aluminum cans is highly automated and consists of multiple interconnected production stages, including material forming, surface preparation, coating, printing, curing, inspection, and palletizing. Modern production lines are capable of producing more than 2,000 cans per minute, requiring extremely stable process conditions and continuous quality monitoring throughout the entire manufacturing chain (Campbell, 2006). The quality demands of dry offset can printing require precise control of ink deposition, coating uniformity, and color variation, particularly in high-volume manufacturing environments (Oličkov et al., 2026). These requirements place significant importance on the Washer process, whose role is to create a clean and chemically stable substrate that enables consistent performance in subsequent coating and printing operations. Due to such production speeds and technical complexity, even minor deviations in one phase may negatively affect downstream operations and final product performance.

In parallel with quality requirements, sustainability has become a major priority in the packaging industry. Manufacturers are increasingly focused on reducing water consumption, chemical usage, energy demand, and environmental emissions while maintaining high production efficiency and consistent product quality (Ball Corporation, 2023).

Previous studies in graphic and printing processes have demonstrated that process variables such as pH and conductivity can significantly influence final product quality, highlighting the importance of systematic monitoring and control of chemical parameters in industrial production systems (Kiurski & Oros, 2012; Dharavath, 2021; Gurgal et al., 2013).

1.2. Washer systems and process challenges

Among all production stages, the Washer system represents one of the most critical processes in aluminum can manufacturing. Positioned between the forming and decorating operations, the Washer is responsible for removing lubricants, metal particles, aluminum oxides, and other contaminants generated during the drawing and ironing process. At the same time, it chemically prepares the aluminum surface for subsequent coating and printing operations by creating conditions necessary for proper adhesion and corrosion resistance.

Washer systems directly influence product quality, process stability, and operational efficiency. Inadequate Washer performance may lead to defects such as poor lacquer adhesion, surface staining, corrosion, mobility problems, or printing inconsistencies, ultimately increasing waste generation and production costs. Because Washer systems consume significant quantities of water, chemicals, and thermal energy, their optimization is also closely connected with sustainability objectives and resource efficiency (European Aluminium Association, 2020b).

Modern Washer technologies therefore require continuous monitoring and precise control of chemical and mechanical process parameters, including pH, conductivity, fluoride concentration, acid balance, spray performance, filtration efficiency, and drying conditions. Maintaining stable operating conditions is essential for minimizing defects and ensuring consistent production quality in high-speed manufacturing environments.

1.3. Aim of the paper

This paper analyzes the role of Washer systems in aluminum can manufacturing, with particular emphasis on their influence on product quality, process stability, and sustainability. The study combines literature review, industrial process analysis, and experimental evaluation through a quantitative Etching Rate Test used to assess aluminum surface treatment efficiency. Special attention is given to the relationship between chemical process control, surface preparation quality, and defect prevention in downstream production stages. In addition, the paper discusses sustainability-related aspects of Washer operation, including water recirculation, chemical optimization, and reduction of environmental impact within modern aluminum can manufacturing systems.

2. Methodology

2.1. Approach

The methodology applied in this study combines literature review, industrial process analysis, and experimental evaluation in order to provide a comprehensive assessment of Washer systems in aluminum can manufacturing. The research approach was designed to examine Washer operation from both technical and sustainability perspectives, while simultaneously linking theoretical principles with practical industrial application.

Particular attention was given to the interaction between Washer performance, process stability, and final product quality. The study therefore integrates qualitative analysis of process design and operational practices with quantitative assessment of selected process indicators related to surface treatment performance.

2.2. Data sources

The research was based on multiple complementary sources of information. A review of available technical and scientific literature related to aluminum can manufacturing, metal surface treatment, and industrial qual-

ity control was performed to establish the theoretical background of the study (Ball Corporation, 2010). In addition to literature sources, industrial documentation and operational information from Washer systems and associated quality control procedures were analyzed. These sources provided insight into process design, chemical treatment principles, machine components, control systems, and sustainability-related practices used in contemporary can manufacturing environments (European Aluminium Association, 2020b).

Operational and laboratory data obtained through routine process monitoring and quality control procedures were also considered. Parameters such as pH, conductivity, fluoride concentration, and acid balance were reviewed as representative indicators of Washer process stability and chemical control.

2.3. Experimental method - Etching rate test

As part of the experimental methodology, a quantitative Etching Rate Test was conducted to evaluate the intensity of aluminum surface etching as an indicator of accelerator activity within the Washer process. The method is based on measuring the mass loss of individual aluminum cans before and after exposure to the etching stage, where the difference in mass represents the quantity of removed aluminum and provides a direct indication of chemical attack.

The experiment was performed using individually identified can samples measured on a calibrated analytical balance under controlled drying conditions. The obtained values were expressed both as average mass loss per can (mg/can) and normalized surface loss (mg/m²), allowing comparison with established industrial reference values. A detailed description of the experimental procedure, calculations, and results is presented in the dedicated experimental section of this paper.

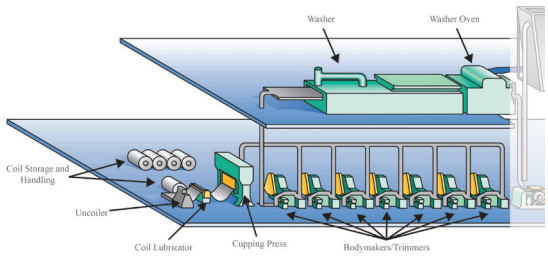
3. Overview of end-to-end can manufacturing process

The production of aluminum beverage cans is a highly standardized and technologically advanced manufacturing process characterized by high production speeds, automation, and strict quality requirements. Modern production lines are designed to ensure continuous material flow with minimal process interruptions and high operational efficiency, while simultaneously meeting sustainability and product quality standard The manufacturing process generally consists of two main technological segments: the front-end and the back-end production phase (Ball Corporation, 2010). Each phase includes several interconnected operations that must function in a synchronized manner to maintain process stability and product consistency.

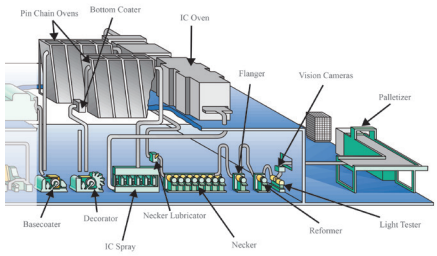
The front-end phase includes the primary forming operations of the aluminum can body. The process begins with coil handling, where rolled aluminum sheets are prepared and fed into the production line. In the cupper unit, circular aluminum blanks are formed into shallow cups, which are then transferred to the bodymaker machine. During the drawing and ironing process, the cup is elongated and thinned to achieve the final can body geometry. Afterward, the trimmer cuts the can body to the required height and dimensional specification. The formed cans then enter the Washer system and Washer Oven, where cleaning, chemical surface preparation, rinsing, and drying operations are performed prior to decoration and coating processes.

The back-end phase includes all subsequent coating, decoration, curing, forming, and inspection operations. A base coating layer is first applied to the can surface using a basecoater unit, after which the graphic design is transferred through dry offset printing in the decorator machine. The printed cans are then cured in the decorator oven (Pin Oven). Internal protective coatings are applied through internal coating spray systems, followed by thermal curing inside the Internal Bake Oven (IBO).

In the final production stages, the cans pass through necking, flanging, and dome reforming operations, where the final can geometry is achieved. Quality control systems such as light testers, vision inspection systems, and label verification units are used to identify defective products and ensure compliance with technical and visual quality requirements. Finished cans are then automatically palletized and prepared for transport and distribution. Among all production stages, the Washer system represents a critical interface between mechanical forming and final surface finishing processes. Its performance directly affects coating adhesion, print quality, corrosion resistance, and overall process stability, making it one of the most important quality-control stages in aluminum can manufacturing. Figure 1 presents the main operations of the front-end production phase, while Figure 2 illustrates the back-end manufacturing process.



» **Figure 1:** *Front-end phase of the technological process of making aluminum cans (Ball Corporation, 2022)*



» **Figure 2:** *Back-end phase of the technological process of making aluminum cans (Ball Corporation, 2022)*

4. Washer system – function and role in aluminum can manufacturing

The Washer system represents one of the most important process stages in aluminum can manufacturing, as it performs both cleaning and chemical surface preparation functions prior to coating and decoration operations. Positioned between the body forming and printing stages, the Washer is responsible for removing lubricants, metal particles, aluminum oxides, and other contaminants generated during the drawing and ironing process. At the same time, it prepares the aluminum surface for the application of protective coatings, base coats, inks, and overvarnish layers.

The importance of the Washer system can be observed from three closely connected perspectives: product quality, process efficiency, and production sustainability. From a quality standpoint, the Washer ensures a clean and chemically stable surface required for proper adhesion of coatings and printing layers. Inadequate cleaning or unstable chemical treatment may lead to defects such as poor lacquer adhesion, corrosion, staining, discoloration, or printing inconsistencies. From a process-efficiency perspective, Washer performance directly affects the stability of downstream manufacturing operations, including base coating, decoration, curing, and internal coating processes. Properly cleaned and dried cans reduce the probability of production interruptions, defect generation, and product rejection, thereby improving overall line efficiency and reducing operational costs.

In addition to quality and efficiency requirements, the Washer system also plays an important role in sustainable manufacturing. Since the process involves intensive use of water, chemicals, compressed air, and thermal energy, optimization of Washer parameters is essential for reducing environmental impact and resource consumption (European Aluminium Association, 2020b). Modern Washer systems therefore incorporate technologies such as water recirculation, filtration systems, automated chemical dosing, process monitoring sensors, and optimized drying systems in order to improve sustainability and operational stability.

The Washer process itself consists of multiple sequential cleaning, rinsing, chemical treatment, and drying stages designed to progressively prepare the aluminum surface for subsequent manufacturing operations. Typical process stages include pre-rinsing, pre-washing, surface preparation, rinsing phases, conversion coating treatment, deionized water rinsing, mobility enhancement treatment, and thermal drying. Each stage performs a specific function and requires precise control of process parameters such as temperature, pH, conductivity, spray pressure, chemical concentration, and flow conditions.

Modern Washer systems are additionally integrated with automated control platforms and SCADA-based monitoring systems that enable real-time process supervision and optimization. These systems continuously monitor critical process parameters, allowing rapid correction of deviations and improved consistency in product quality and process performance (Astles Control Systems Ltd., 2022).

Due to its direct influence on surface preparation quality, downstream coating adhesion, defect prevention, and sustainability performance, the Washer system represents one of the key technological stages in modern aluminum can manufacturing.

5. Washer process description

The Washer process consists of multiple sequential cleaning, chemical treatment, rinsing, and drying stages designed to progressively prepare the aluminum surface for subsequent coating and decoration operations. Each phase performs a specific function within the overall surface treatment process and must operate under carefully controlled conditions in order to ensure consistent product quality and process stability.

Modern Washer systems are typically designed as multi-stage modular units through which cans are transported continuously at high production speeds. In addition to cleaning and surface preparation, Washer systems are optimized to minimize water and chemical consumption through recirculation and backflow principles (Ball Corporation, 2025b). A typical Washer configuration includes several rinsing and active chemical stages, combined with air blow-off and thermal drying systems.

The process generally begins with the pre-rinse stage, where loose oils, aluminum particles, and contaminants generated during body forming operations are removed from the can surface. This is followed by the pre-wash stage, where acidic solutions are used to eliminate the

majority of lubricants and prepare the surface for more intensive chemical treatment. The surface preparation stage represents the main chemical cleaning phase of the Washer system. During this process, a combination of sulfuric acid, surfactants, and fluoride-based accelerators is used to remove remaining contaminants, dissolve aluminum oxides, and create a clean and chemically active aluminum surface suitable for conversion coating treatment. Proper control of chemical concentration, temperature, and acidity is essential for achieving uniform surface quality and preventing excessive or insufficient aluminum etching. After chemical surface preparation, the cans pass through the first rinse stage, where process water is used to remove residual chemicals and stabilize the surface before conversion coating treatment. The conversion coating stage is particularly important because it forms a protective chemical layer on the aluminum surface that improves coating adhesion, corrosion resistance, and resistance to discoloration during pasteurization processes. In modern aluminum can manufacturing, zirconium-phosphate-based conversion systems are commonly used due to their improved environmental performance and process stability.

Following conversion coating, the cans enter additional rinsing stages designed to remove remaining treatment residues and minimize contamination transfer between process zones. Final rinsing is typically performed using reverse osmosis (RO) or deionized (DI) water with very low conductivity in order to prevent salt residues and ensure optimal surface cleanliness before coating operations. The final chemical stage of the Washer process commonly includes a mobility enhancer treatment, where specialized surfactants are applied to improve can mobility during downstream transportation and decoration processes. These additives also improve water drainage and reduce the probability of scratches and surface damage during high-speed production (Crown Holdings, 2020).

After completion of all chemical and rinsing stages, the cans enter the Washer Oven, where thermal drying removes residual moisture from the surface. Effective drying is essential because any remaining water may negatively affect coating adhesion, print quality, and curing performance in subsequent production stages. A typical example of Washer process stages is illustrated in Figure 3.

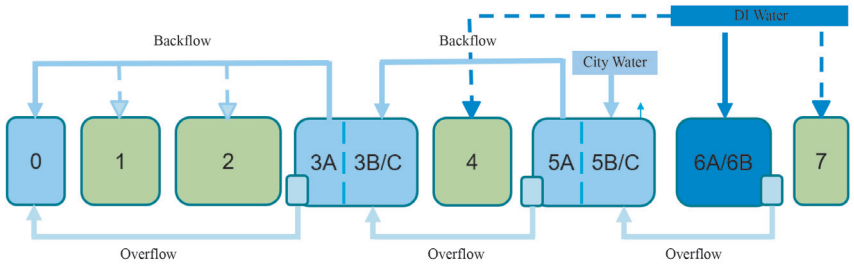
6. Washer equipment and process control systems

In addition to chemical treatment efficiency, the overall performance of a Washer system strongly depends on its mechanical components, transport systems, filtration units, spray technologies, and automated process control systems. Proper integration and maintenance of these elements are essential for ensuring stable operating conditions, minimizing contamination, reducing resource consumption, and maintaining consistent product quality throughout high-speed aluminum can production.

One of the key mechanical elements of the Washer system is the transport section, including infeed and outfeed conveyor systems. These systems ensure continuous and synchronized movement of cans through all Washer stages while minimizing the risk of jamming, instability, or mechanical damage (Yam, 2010). In industrial applications, air table systems are commonly used to improve can mobility and reduce surface contact between cans and transport components. Sensors installed within the transport system continuously monitor can flow conditions and help prevent accumulation or transport interruptions (Henry, 2012).

Spray systems and nozzle design also play a critical role in Washer performance. Each process stage contains dedicated spray bars equipped with specially designed nozzles that distribute water or chemical solutions across the entire can surface. V-jet nozzles are commonly used for wide and uniform surface coverage, while full-cone nozzles provide more intensive rinsing and improved contaminant removal efficiency (Spraying Systems Co., 2020). Proper nozzle alignment, spray pressure, and flow conditions are necessary to achieve consistent cleaning and minimize chemical consumption.

To reduce liquid carryover and contamination between Washer stages, blow-off systems are positioned between process zones. These systems use high-velocity air



» **Figure 3:** *Washer phases (Ball Corporation, 2025)*

streams to remove residual liquids from can surfaces and conveyor sections before the cans enter the next stage. Additional brush systems located beneath the conveyor help remove accumulated liquids and improve drainage conditions. Proper adjustment of blow-off units is particularly important in high-speed production environments because insufficient liquid removal may negatively affect downstream chemical stability and rinsing efficiency.

Filtration and separation systems further contribute to process stability and sustainability. Screen filters installed inside Washer tanks prevent large particles and debris from entering pumps and spray nozzles, while inline filters provide additional removal of smaller particles and contaminants. In addition, coalescer systems are commonly used in pre-wash and surface preparation stages to separate oils and emulsified lubricants from process liquids. By reducing oil concentration inside the tanks, coalescers help maintain chemical efficiency, reduce contamination levels, and extend bath lifetime At the exit of the Washer system, vacuum transfer units are used to transport cans from the Washer conveyor to the drying oven conveyor. These systems also help remove overturned or damaged cans that could otherwise cause contamination, transport instability, or mechanical interruptions in downstream operations.

Modern Washer systems are highly automated and integrated with chemical dosing and process monitoring platforms such as Astles and VisCan systems (Astles Control Systems Ltd., 2025). These systems continuously monitor critical process parameters including pH, conductivity, fluoride concentration, free acid (FA), total acid (TA), and chemical dosing conditions. Data collected from sensors installed throughout the Washer are transferred to centralized software platforms that enable real-time monitoring, automatic dosing correction, alarm management, and process optimization.

The implementation of automated monitoring and control systems provides several important advantages, including improved process consistency, reduced chemical consumption, increased operational safety, faster detection of process deviations, and enhanced sustainability performance. As a result, modern Washer systems represent a combination of chemical engineering, mechanical design, automation, and digital process control technologies integrated into a single high-performance production system.

7. Quality control in washer process

Quality control in the washer process is a critical factor in ensuring consistent surface preparation of aluminum cans, minimizing process variability, reducing waste, and supporting overall production sustainability. Within the washer system, quality assurance is achieved through a combination of chemical monitoring, laboratory verification, and functional testing of treated cans. The objective of these procedures is to ensure that all chemical stages (pre-washing, surface preparation, treatment, and rinsing) are correctly executed, that the can surface is properly cleaned and prepared for coating and printing, and that no defects are present which could compromise final product quality or downstream performance. Quality control in the washer process includes:

- chemical analysis of process baths,
- laboratory testing in dedicated CPO facilities,
- functional quality tests on cans,
- defect detection and corrective actions.

This multi-level approach ensures continuous process monitoring and timely correction of deviations, reducing quality risks and production losses.

7.1. Chemical analysis

Chemical analysis represents the primary control layer of the washer process, providing real-time information on bath composition and process stability. Key monitored parameters include pH, conductivity, fluorides, FA/TA ratio, and metal content (ME).

- pH indicates bath acidity/alkalinity and is critical for controlling cleaning and rinsing stages (Henkel, 2025).
- Conductivity reflects the concentration of dissolved ions and contamination levels (ASTM International, 2023).
- Fluorides influence etching rate and uniformity of aluminum surface treatment (Henkel Technologies, 2025).
- FA/TA (Free Acid/Total Acid) provides insight into bath activity and chemical balance (ASTM International, 2025).
- ME (Metal content) indicates dissolved aluminum concentration and bath saturation level (Ball Corporation, 2025a).

Continuous monitoring of these parameters enables timely chemical dosing adjustments and ensures process stability while minimizing resource consumption.

7.2. Laboratory (CPO)

Laboratory control in the CPO (Can Plant Operator) laboratory provides verification of chemical and process stability through standardized analytical methods. These include titration (FA/TA), ion-selective electrodes (fluorides), conductivity measurements, and spectrometric or gravimetric analysis for metal content. The laboratory serves as a reference system for validating in-line measurements and ensuring process compliance

with specifications. Its role is not only analytical but also operational, as CPO operators directly interpret results and initiate corrective actions when needed.

Table-based monitoring distinguishes between rinsing and chemical phases, where key parameters include pH, conductivity, chlorine content, FA, TA, RP, fluorides, and mobility enhancer concentration. Conductivity is a key indicator of water quality and contamination, while fluoride control is essential for consistent etching and conversion layer formation. FA/TA analysis provides insight into chemical balance, while derived indicators such as RP (TA–FA) and AR (TA/FA) are used to assess contamination and bath efficiency. Mobility enhancer (ME) concentration is determined by titration and ensures stable surface treatment in final rinsing stages.

7.3. Quality tests

Functional quality tests verify the effectiveness of the washer process on the treated aluminum surface and provide direct feedback on surface cleanliness, treatment uniformity, and coating readiness.

Water Break Test - Evaluates surface cleanliness by observing water film continuity. Immediate film break indicates contamination, while uniform film formation confirms proper cleaning.

Finger Wipe Test- Assesses residual particles or aluminum dust on the surface. It is a simple visual/physical inspection method dependent on operator experience.

Muffle Test - Evaluates conversion layer formation by thermal treatment at 538 °C. Color change intensity (golden tone) indicates treatment level.

Dome Stain Test- Assesses corrosion and staining resistance of the can dome area after immersion in borax solution at elevated temperature.

Pasteur Test- Simulates thermal processing conditions (95 °C, 30 min) to evaluate coating adhesion and resistance to delamination.

UV BRC Test - Checks UV coating coverage on the base rim area using UV inspection and chemical exposure (copper sulfate solution).

7.4. Product defects and corrective actions

Defects in the washer process are categorized into mechanical, chemical, and coating-related (oPRP) defects.

Mechanical defects result from transport and handling issues, leading to dents, scratches, moisture, or deformation. Corrective actions include adjustment of transport systems, vacuum transfer, blow-off units, and dryer settings.

Chemical defects arise from improper bath parameters (pH, fluorides, flow rates) and include overtreated or undertreated surfaces, stains, and abnormal test results. Corrective measures involve chemical balancing, nozzle replacement, and process optimization.

Coating/oPRP defects relate to final coating and include undercured lacquer, missing spray, foreign bodies, and neck peeling issues. These are controlled through coating system adjustments and equipment maintenance.

8. Experimental study – Etching rate test

8.1. Aim of the experiment

The objective of the experiment was to quantify the intensity of chemical etching of aluminum cans (etching rate) as a direct indicator of accelerator activity in the Washer etching stage. The result is expressed as the mass of removed aluminum per can (mg/can) and per unit surface area (mg/m^2).

8.2. Materials and equipment

The experiment was conducted using standardized conditions and the following materials and equipment:

- Aluminum can type: STD 500 ml (total surface area 755 cm^2)
- Calibrated analytical balance (accuracy ±0.001 g)
- Demineralized (DI) water for rinsing
- Drying equipment (ventilated oven) for consistent moisture removal
- Identification markings for samples
- Personal protective equipment (PPE)

8.3. Experimental procedure

The Etching Rate Test was performed according to established industrial methodology (Henkel, 2023), following these steps:

1. Five identical aluminum cans (STD 500 ml) were selected and individually marked.
2. After the first rinsing stage, cans were thoroughly dried and weighed to obtain the initial mass (m_1).
3. The same cans were reintroduced into the Washer system and passed once more through the etching stage.
4. After treatment, cans were dried again and weighed to obtain the final mass (m_2).

5. Mass loss per can (etching rate) was calculated: Attack (mg) = (Total Mass Before (g) – Total Mass After (g)) × 1000 (conversion from grams to milligrams).
6. The average value was calculated for all tested samples.

$$\text{Average Etching Rate} = \frac{(\text{Total Mass Before} - \text{Total Mass After})}{\text{Number of Tested Cans}} \times 1000 \quad (1)$$

7. Results were normalized per surface area:

$$\text{mg/m}^2 = \frac{\text{mg/can}}{0.0755\ \text{m}^2} \quad (2)$$

8.4. Reference values

According to industrial data and Henkel guidelines (Henkel, 2023), acceptable etching values for 500 ml cans are presented in Table 1.

Table 1
Reference values for STD 500 ml cans

Surface (cm²)	Min (mg)	Avg (mg)	Max (mg)	Min (mg/m²)	Avg (mg/m²)	Max (mg/m²)
755	7.2	9.0	11.0	95	119	146

8.5. Experimental results

Measured values for five samples are given in Table 2.

Table 2
Experimental results of five can samples

Can	Mass before (g)	Mass after (g)	Loss (mg)
Sample 1	11.994	11.985	9
Sample 2	11.997	11.989	8
Sample 3	11.986	11.978	8
Sample 4	11.933	11.925	8
Sample 5	11.950	11.940	10
Total	59.860	59.817	43
Average: mg/can	/	/	8.6

Average values:

- Total loss: 43 mg
- Average mass loss per can = 43 mg / 5 = 8.6 mg/can.
- Total surface area (both sides) = 755 cm² = 755 / 10,000 = 0.0755 m².
- Etching rate = 8.6 mg / 0.0755 m² = 113.9 mg/m² ≈ 114 mg/m².

The average result of 8.6 mg/can (114 mg/m²) falls within the Henkel reference range (7.2–11.0 mg/can) and is very close to the industrial target average of 9.0 mg/can (119 mg/m²). Therefore, the measured etching attack can be considered normal and acceptable when compared with the reference values. Although slightly below the target average, it remains well within the specified tolerance limits.

9. Discussion

9.1. Relationship between Washer performance and final can quality

The efficiency of the Washer process directly influences the final quality of aluminum cans. Each stage-pre-washing, surface preparation, conversion coating, rinsing, and drying-contributes to contaminant removal, preservation of surface properties, and preparation for coating and printing.

The Etching Rate Test showed an average mass loss of 8.6 mg/can (114 mg/m²), which lies within the reference range (95–146 mg/m²). This confirms stable and controlled etching conditions. Controlled etching is essential for forming a uniform conversion coating, which directly reduces defects such as dome stain and neck peeling, ensuring reliable coating adhesion and corrosion resistance.

9.2. Impact on downstream process efficiency

Washer performance significantly affects subsequent production stages. Properly cleaned and dried cans enable better coating adhesion, improved print quality, reduced drying time, and higher packaging efficiency.

The experimental results indicate that the balance between fluoride concentration and FA/TA ratio provides optimal etching intensity. Excessive etching may weaken the conversion layer, while insufficient etching can lead to poor adhesion and increased defect rates. The obtained values confirm that chemical process control was well optimized, supporting efficient downstream operations.

9.3. Process risks and critical control points (oPRP)

Washer process risks, defined as oPRP (Operational Pre-requisite Programs), include mechanical damage, improper chemical treatment, transport instability, and cross-contamination between stages.

The experiment confirms that fluoride concentration and FA/TA ratio are critical for etching stability. Devi-

ations in these parameters may result in defects such as dome stain, neck peeling, and failures in functional tests (muffle and pasteur). Continuous monitoring and rapid corrective actions are therefore essential to maintain process stability and reduce scrap rates.

9.4. Future development and innovation

Future development of Washer systems focuses on improving resource efficiency and process control. Advanced chemical dosing systems, water recirculation, improved blow-off technologies, and sensor integration enable more precise operation.

Digitalization and real-time monitoring support predictive control, improving process stability, reducing chemical consumption, and minimizing environmental impact while maintaining product quality.

9.5. Quality vs. sustainability balance

Optimization of Washer processes must balance product quality and sustainability. Reduced consumption of water and chemicals should not compromise surface preparation quality. A well-controlled process, combining precise chemical management and efficient resource use, enables high product quality, minimal defect rates, and sustainable production. Achieving this balance remains a key objective for future technological development.

10. Conclusion

10.1. Summary of key findings

The analysis of the Washer process confirms that the quality and stability of all stages-pre-washing, surface preparation, conversion coating, rinsing, and drying-are essential for achieving high-quality aluminum cans. Continuous control of key parameters such as pH, conductivity, FA/TA ratio, fluoride concentration, and mobility additives ensures the formation of a uniform protective layer.

The experimental results (Etching Rate Test) confirmed stable and controlled etching conditions, supporting proper surface preparation and reducing the occurrence of defects such as dome stain, neck peeling, and transport-related issues. This demonstrates the strong link between chemical process control and consistent product quality.

10.2. Importance of the Washer in quality and sustainability

The Washer system represents a critical stage in aluminum can manufacturing, directly influencing surface quality and preparation for coating, printing, and packaging. Proper process control reduces defect rates, improves operational efficiency, and optimizes the consumption of chemicals, water, and energy. As such, the Washer plays a dual role-ensuring high product quality while supporting sustainable manufacturing. Balancing these aspects is essential in modern industrial production.

10.3. Recommendations for process improvement

To further enhance Washer performance, the following measures are recommended:

- Implementation of advanced monitoring and automated chemical control systems
- Regular maintenance and calibration of sensors and measurement instruments
- Optimization of water recirculation and consumption
- Continuous training of personnel regarding oPRP control points and quality testing procedures
- Introduction of digital and predictive process control systems

For future research, it is recommended to perform the Etching Rate Test on a larger sample size (≥10 cans) to improve statistical reliability and more precisely define the relationship between etching intensity, chemical control, and product quality.

11. Acknowledgment

This research has been supported by the Ministry of Science, Technological Development and Innovation (Contract No. 451-03-34/2026-03/200156) and the Faculty of Technical Sciences, University of Novi Sad through project “Scientific and Artistic Research Work of Researchers in Teaching and Associate Positions at the Faculty of Technical Sciences, University of Novi Sad 2026” (No. 01-3609/1). This research did not receive any specific grant from funding agencies in the public, commercial, or not-for-profit sectors.

12. References

Astles Control Systems Ltd. (2022) *Process Control Solutions for the Metal Packaging Industry*. Astles Control Systems Ltd.

Astles Control Systems Ltd. (2025) *Chemical Dosing and Control Systems for Can Washers*. Available from: https://www.astles.co.uk/ [Accessed 25 September 2026].

ASTM International. (2023) ASTM D1125-23. *Standard Test Methods for Electrical Conductivity and Resistivity of Water.* West Conshohocken, PA: ASTM International.

ASTM International. (2025) ASTM D513. *Standard Test Methods for Total and Free Acidity of Alkaline and Acidic Substances*. West Conshohocken, PA: ASTM International.
Ball Corporation. (2010) *Aluminum Can Manufacturing*. Internal documentation.
Ball Corporation. (2022) *Aluminum Can Manufacturing*. Internal documentation.
Ball Corporation. (2023) *Sustainability Report*. Internal documentation.
Ball Corporation. (2025a) *Metal Extraction and Bath Contamination Monitoring in Can Washer Systems*. Internal documentation.
Ball Corporation. (2025b) *Washer Machine*. Internal documentation.
Campbell, F.C. (2006) *Manufacturing Technology for Aerospace Structural Materials*. Amsterdam: Elsevier.
Crown Holdings. (2020) *Canmaking Technology Manual*. Crown Holdings.
Dharavath, H.N. (2021) 'Statistical evaluation of a Color Managed Digital Printing Workflow (CMDPW) consistency [4th C of CMW]', *Journal of Graphic Engineering and Design*, 12(4), pp. 17–31. DOI: 10.24867/JGED-2021-4-017
European Aluminium Association. (2020a) *Recycling Aluminium: A Pathway to Sustainability*. European Aluminium Association.
European Aluminium Association. (2020b) *Sustainability of Aluminium in Packaging*. European Aluminium Association.
Green, J.A.S. (2007) *Aluminum Recycling and Processing for Energy Conservation and Sustainability*. Materials Park, OH: ASM International.
Gurgal, N., Repeta, V., Senkivsky, V. and Shybanov, V. (2013) 'Definition of quality criteria of the technological process of narrow web UV-printing', *Journal of Graphic Engineering and Design*, 4(2), pp. 7–11. DOI: 10.24867/JGED-2013-2-007
Henkel. (2023) *Etching Process in Beverage Can Washers*. Henkel MP Technical Bulletin.
Henkel. (2025) *Aluminum Can Pretreatment: Process Control Guidelines*. Surface Treatment Manual.
Henkel Technologies. (2025) *Aluminum Surface Treatment: Fluoride Control in Acid Cleaning and Conversion Coatings*. Henkel Technologies.
Henry, J.R. (2012) *Packaging Machinery Handbook: The Complete Guide to Automated Packaging Machinery Including Packaging Line Design*. [S.l.]: CreateSpace Independent Publishing Platform.
Kiurski, J. and Oros, I. (2012) 'The influence of pH/conductivity of fountain solution on dot circularity, line and text raggedness', *Journal of Graphic Engineering and Design*, 3(2), pp. 1–7. DOI: 10.24867/JGED-2012-2-001
Oličkov, V., Kašiković, N., Prica, M., Dedijer, S. and Zeljković, Ž. (2026) 'Color management in can printing proofing: A colorimetric comparison of conventional and digital technologies', *Color Research & Application*, 51(4), e70100. DOI: 10.1002/col.70100
Spraying Systems Co. (2020) *Spray Nozzle Technology for Industrial Applications*. Spraying Systems Co.
Yam, K.L. (ed.) (2010) *The Wiley Encyclopedia of Packaging Technology*. 3rd ed. Hoboken, NJ: John Wiley & Sons.

© 2026 Authors. Published by the University of Novi Sad, Faculty of Technical Sciences, Department of Graphic Engineering and Design. This article is an open access article distributed under the terms and conditions of the Creative Commons Attribution license 4.0 Serbia (http://creativecommons.org/licenses/by/4.0/rs/).

Original Scientific Paper https://doi.org/10.24867/GRID-2026-p7

Influence of Halftone Dot Geometry on Dot Gain and Tone Reproduction in Flexographic Printing on Aluminium Foil

ABSTRACT

This study investigates the influence of halftone dot geometry on dot gain and tone reproduction in UV flexographic printing on non-absorbent aluminium foil 20 µm thick. Two screening technologies were compared — conventional regular round dots (AM) and a fractal structure. The microstructure of the imprints was examined by optical microscopy (150× magnification), followed by analysis of dot perimeter and area in the DinoCapture 2.0 software environment; the effective dot area was determined densitometrically for nominal tone values from 1 to 99%. The fractal screen was found to exhibit substantially higher dot gain in the midtone region (a maximum of ΔA = +23.8% at the 50% tint, compared with +6.1% for the round screen), whereas in the highlight region (1–5%) the fractal structure provided better isolation of individual dots and lower dot gain. Regression models of the dot-gain curves were developed; the best fit to the experimental data (R^2 = 0.93–0.99) was achieved by a third-degree polynomial and a smoothing spline. The results confirm the perimeter-driven ink-squeeze mechanism as the dominant factor in dot gain on metallised non-absorbent substrates and indicate the need to construct separate dot-gain compensation curves (DGC) for fractal screening in foil flexography.

Pavlo Valovyi
Svitlana Havenko
Marta Labetska

Lviv Polytechnic National University, Lviv, Ukraine

KEY WORDS
Flexographic printing, aluminium foil, screening, dot gain, tone reproduction, fractal geometry, optical density, regression modelling

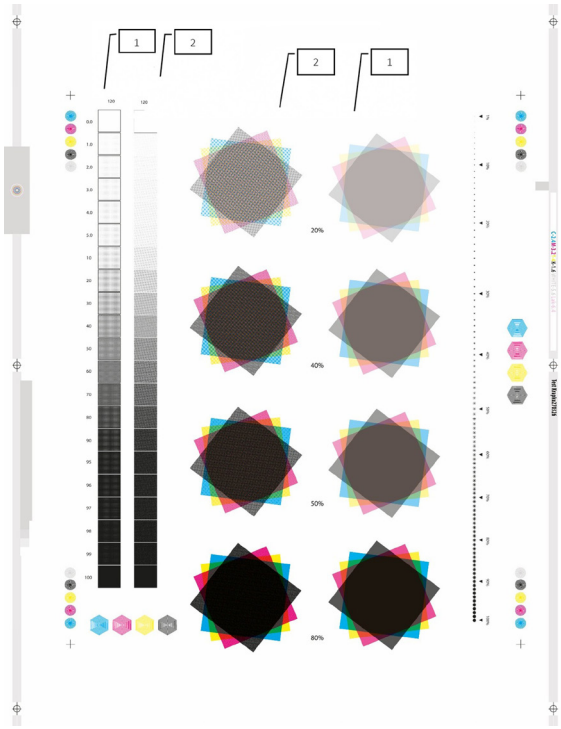
1. Introduction

Flexographic printing is being increasingly used to apply images to non-absorbent and metallised substrates, in particular aluminium foil, which is widely used in the manufacture of flexible food and pharmaceutical packaging, as well as in advanced metallisation processes such as photovoltaic front-side contact printing (Lorenz et al., 2016). A distinctive feature of printing on such materials is the absence of ink absorption into the substrate, as a result of which the entire excess volume of the ink layer is squeezed onto the surface and spreads along the edges of the halftone dot, causing pronounced mechanical dot gain. Ink formulations developed specifically for printing on non-absorbent flexible foil substrates have also been the subject of recent research (Várza, Joóbné Preklet & Horváth, 2021).

The quality of flexographic imprints on metallised and polymer films has repeatedly been addressed in the literature: the influence of printing-process parameters on optical density and tonal value increase on printed films has been studied (Żołek-Tryznowska et al., 2020), as has the deformation of halftone dots in flexography in general (Valdec et al., 2021). It has been shown that ISO-defined substrate properties substantially determine colour reproduction in the flexographic process (Valdec, Miljković & Augustštin, 2017), and that a geometric dot-gain model allows AM and FM screening technologies to be compared quantitatively (Valdec et al., 2026).

A separate direction in screening improvement is the use of irregular and fractal structures, which, unlike the classical regular (AM) screen, make it possible to reduce visual moiré and increase the subjective smoothness of tonal transitions. At the same time, the fractal geometry of the dot contour is characterised by a considerably greater total perimeter for the same nominal area, which potentially reinforces the perimeter-driven ink-squeeze mechanism and, correspondingly, dot gain. Studies of flexographic imprints by optical and electron microscopy confirm the value of microstructural analysis of halftone dots for establishing the physical causes of tonal distortions (Havenko, Labetska & Telehina, 2024), while the influence of printing speed on the occurrence of the 'bouncing effect' further demonstrates the sensitivity of the flexographic process to the mechanical parameters of plate-to-substrate contact (Havenko, Telegina & Labetska, 2026).

Despite the considerable number of studies devoted separately to dot gain on films and to the moiré-suppression advantages of fractal screening, a quantitative comparison of round and fractal screens specifically for aluminium foil, together with the construction of mathematical models of tonal shift for both technologies, has to date been practically absent from the literature. This defines the aim of the present study.



» **Figure 1:** *Digital layout of the test form for flexographic printing on aluminium foil with control elements (a Siemens-star-type target, a microelement scale, and round (1) and fractal (2) screening fields)*

2. Materials and Methods

To reduce moiré interference effects and improve tone reproduction in critical tonal ranges, a new type of halftone dot with a multi-ray, star-like geometry was proposed. As the basic geometric prototype, a dot analogous to a snowflake-like structure with four main rays positioned at angles of 0°, 45°, 90° and 135° was chosen.

The general appearance of the digital layout of the test form with the control scale elements is shown in Figure 1. In the round (AM) screening zone, a regular structure of ink overlap and a periodic grid are clearly visible at the 40–50% tints, whereas for fractal screening the boundaries of the tonal zones appear more diffuse and the transition smoother, which is consistent with the well-known ability of irregular structures to suppress moiré.

The experimental samples were printed on a Varyflex V2 670 flexographic printing press equipped with a web-tension control system and UV curing. Aluminium foil 20 µm thick was used as the substrate. Printing was carried out with UV flexographic inks at a speed of 80 m/min, using corona treatment before printing and instant UV curing after each ink station, in line with the general process-control requirements for flexographic printing (International Organization for Standardization, 2020). Microstructural analysis of the imprints of the test scales was performed by reflected-light optical microscopy using a Dino-Lite Edge AM7915MZTL digital microscope with a built-in polarising filter that minimises specular reflection from the foil surface. The geometry of the round and fractal halftone dots was studied at 150× optical magnification; the perimeter, dot area and the zone of edge ink squeeze-out (halo) were determined in the DinoCapture 2.0 software environment. The optical density of the imprints was measured spectrodensitometrically in accordance with the ISO 13656 procedure (International Organization for Standardization, 2021) for nominal tone values from 1 to 99%.

The effective halftone dot area was determined from the optical density of the imprint on the basis of a modified Yule–Nielsen equation:

$$A_{eff} = \frac{1-10^{-D_t/n}}{1-10^{-D_s/n}} \quad (1)$$

where Dt is the optical density of the halftone field; Ds is the density of the solid (full-tone) element; and n is the light-scattering coefficient at the ink–foil interface, which for the specular metallic surface was determined by residual-minimisation separately for the round and fractal screens.

The absolute and relative dot gain were calculated as:

$$\Delta A = A_{eff} - A_{nom}, \quad DG = \frac{A_{eff}-A_{nom}}{A_{nom}} \times 100\% \quad (2)$$

where Anom is the nominal halftone dot area.

To quantify the contribution of the dot contour to dot gain, a perimeter-influence coefficient was used:

$$PI = \frac{P}{\sqrt{A}} \quad (3)$$

where P is the perimeter of the halftone dot and A is its area; an increase in PI corresponds to an increase in the relative length of the contour along which ink squeeze-out occurs.

The dot-gain curves were approximated by a third-degree polynomial:

$$\Delta A(x) = a \cdot x^3 + b \cdot x^2 + c \cdot x + d \quad (4)$$

and the quality of the fit was assessed using the coefficient of determination R^2 and the root-mean-square error:

$$RMSE = \sqrt{\frac{1}{n}\sum_{i=1}^{n}(y_i - \hat{y}_i)} \quad (5)$$

For each nominal tone value, the mean, standard deviation and coefficient of variation of the measured dot area were calculated, and the 95% confidence interval was used to assess the reliability of the differences between the screens. The significance of the differences in mean ΔA values between the round and fractal screens within each tonal zone was tested using Student's t-test; the coefficient of determination R^2 and RMSE were used to compare the quality of the linear, polynomial and spline models.

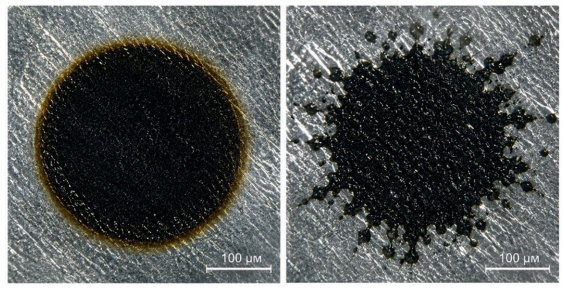
3. Results

In the course of the experiment, a comparative analysis of halftone dot gain in flexographic printing on aluminium foil was carried out for round (conventional) and fractal screening. Measurements were performed for nominal tone levels from 1 to 99%; the results are summarised graphically and in a table of raw data, and a physical interpretation is provided on the basis of microstructural analysis of the imprints.

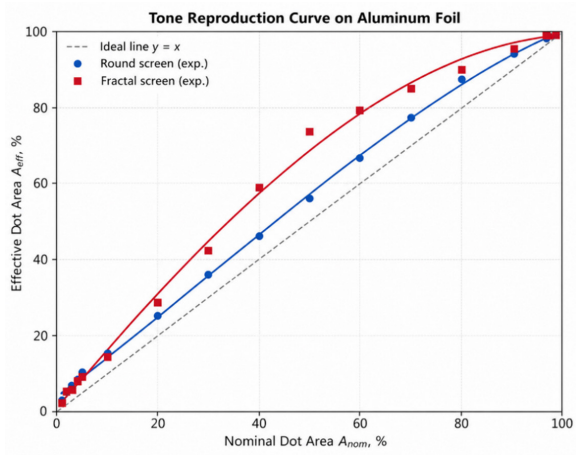
Micrographs of the halftone dots at the 50% tint (Figure 2) demonstrate a fundamental difference in the contour of the two screening technologies. The classical round dot has a clear Euclidean shape with a slight elliptical deformation caused by pressure in the printing-contact zone; a characteristic narrow dark halo forms along its perimeter, caused by ink squeeze-out on the non-absorbent foil. The fractal dot, in contrast, is characterised by a branched contour of fractional dimension: the disproportionately large perimeter length causes the excess ink to be distributed along numerous micro-branches, resulting in a diffuse edge-spreading zone forming around each micro-vertex.

On the basis of the experimental values obtained for the effective area and dot gain of both screening technologies across the entire tonal range, a tone-reproduction curve was plotted (Figure 3). The data analysis shows that both screening technologies provide relatively stable reproduction in the highlights and shadows, while the most pronounced differences are observed in the midtone zone (20–70%). For round screening, the measured area increases almost linearly with nominal coverage, indicating moderate and uniform mechanical dot gain (ΔA within +5...+8%). Fractal screening, by contrast, shows a considerably greater increase in effective area in the midtone zone: the maximum deviation was recorded at the 50% tint, where the measured area reached 73.8% (ΔA = +23.8% versus +6.1% for the round screen — a difference of more than 17 percentage points).

At the same time, in the critical-highlight zone (1–3% tints), the fractal screen shows somewhat lower effective-area values than the round screen (for example,



» **Figure 2:** *Micrographs of halftone dots on aluminium foil (nominal area 50%, magnification 150×): left — regular round screen; right — fractal screen*



» **Figure 3:** *Tone-reproduction curve on aluminium foil: measured (effective) halftone dot area as a function of nominal area for round and fractal screening (the dashed line shows the ideal line y = x)*

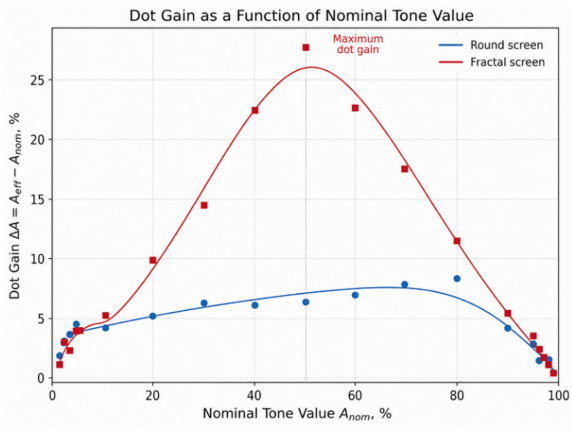
2.4% versus 3.2% at the 1% tint), indicating better isolation of individual microelements and the absence of premature dot 'closing-up' in this region.

The tone-reproduction curve clearly illustrates that for round screening the deviation from the ideal line y = x is smooth and almost symmetrical about the midpoint of the scale, whereas for fractal screening the curve deviates sharply upward as early as after 20% nominal coverage, reaching a maximum at approximately 50–55%, after which the deviation gradually decreases in the shadow region.

The dot-gain diagram (Figure 4) confirms the fundamentally different behaviour of the two screening technologies. For the round screen, the dot-gain value remains relatively stable, within approximately 5–8%, over most of the scale, which is characteristic of a mechanically predictable flexographic process. The fractal screen, in contrast, shows a pronounced non-linear, near-parabolic dependence with a clear maximum in the 50–55% zone and a subsequent decline towards the shadows, consistent with the dominance of the perimeter-driven ink-squeeze mechanism for dots of complex geometry.

Particular attention should be paid to the local inversion of values for the round screen at the 95–96% tints (98.3% → 97.8%), which should be interpreted not as a measurement error but as a manifestation of a mechanical artefact — micro-creases and local folds of the thin 20 µm foil in the printing-contact zone, causing a short-term redistribution of pressure. The fractal screen in this same zone shows a monotonic increase (98.7% → 98.8%), indicating its greater resistance to such mechanical defects owing to its more diffuse contact geometry.

Since aluminium foil scatters practically no light within the substrate (unlike paper), the effective scattering coefficient n in the Yule–Nielsen equation for the round screen was found to be close to 1.0, whereas for the fractal screen it increases statistically significantly owing to additional light scattering at the developed microrelief of the ink–air interface along the numerous micro-branches of the contour.



» **Figure 4:** *Dot gain ΔA as a function of nominal tone value for round and fractal screening*

For a quantitative comparison of approximation models for the dot-gain curve ΔA(Anom), linear, polynomial (2nd- and 3rd-degree) and spline regressions were constructed separately for each screen type (Table 1).

Table 1

Goodness of fit of experimental dot-gain curves by different regression models

Model	Round R^2	Round RMSE	Fractal R^2	Fractal RMSE
Linear	0.060	1.96	0.000	6.85
2nd-degree polynomial	0.742	1.03	0.921	1.92
3rd-degree polynomial	0.828	0.84	0.929	1.83
Smoothing spline	0.878	0.71	0.989	0.71

The linear model proved unsuitable for describing dot gain of the fractal screen ($R^2 \approx 0$) owing to the pronounced non-linearity of the curve with an extremum in the midtones, while for the round screen it also gives an unsatisfactory result ($R^2 = 0.06$). The third-degree polynomial substantially improves the fit for both screens ($R^2 = 0.83$ and 0.93, respectively), and the best fit to the experimental points is provided by the smoothing spline ($R^2 = 0.88$ for the round screen and $R^2 = 0.99$ for the fractal screen), which is recommended as the basis for constructing dot-gain compensation curves (DGC) during pre-press calibration.

4. Discussion

4.1. Physical mechanism of dot gain

The results obtained confirm that the decisive factor behind the differences in dot gain between round and fractal screens on aluminium foil is the perimeter-driven ink-squeeze mechanism. The round dot has the minimum possible perimeter for a given area, so the zone of edge ink spreading is limited, and dot gain remains moderate and stable over a wide tonal range. The fractal dot has a substantially greater length of contact boundary, as a result of which the ink spreads more intensively along the numerous micro-branches of the contour. Since aluminium foil is a practically non-absorbent substrate, the entire excess volume of ink remains on the surface and is redistributed precisely along the perimeter, which explains the sharp increase in the effective area of the fractal screen in

the midtones, where the density of dot placement and the total length of their contours are at a maximum.

4.2. Mathematical interpretation

In general form, dot gain can be regarded as a multifactor function of geometric and technological parameters:

$$\Delta A = f(P/A, \eta, v, p, \gamma) \quad (6)$$

where P/A is the perimeter-to-area ratio of the dot (the PI coefficient), η is the ink viscosity, v is the printing speed, p is the process pressure, and γ is the surface tension of the ink at the interface with the metal. The experimental data obtained are consistent with this representation: for fixed technological parameters (η, v, p, γ), it is precisely the increase in the P/A ratio for the fractal screen that determines its systematically higher dot gain compared with a round screen of the same nominal area. This confirms that dot gain on a non-absorbent metal substrate is not a purely geometric characteristic of screening, but the result of the interaction of contour geometry with the hydrodynamics of the thin ink layer.

4.3. Technological implications

- fractal screening is advisable for applications where the priority is maximum optical density, saturation and contrast in the midtones, as well as moiré suppression
- round screening remains the better choice where precise and predictable differentiation of highlight gradations and ease of process calibration are critical
- for fractal screening on aluminium foil, the application of separate dot-gain compensation curves (DGC), constructed on the basis of a spline or third-degree polynomial model, is mandatory
- a further reduction in dot gain can be achieved by optimising UV ink viscosity, process pressure and anilox roll line screen, taking into account the increased P/A value for fractal dots (Xue et al., 2026)

5. Conclusions

The geometry of the halftone dot substantially affects dot gain and tone reproduction in flexographic printing on non-absorbent aluminium foil: the dominant physical factor is the perimeter-to-area ratio of the dot (the PI coefficient).

The fractal screen shows substantially higher dot gain in the midtone zone (a maximum of ΔA = +23.8% at the 50% tint) compared with the round screen (ΔA = +6.1% at the same tint), which is attributable to the considerably greater perimeter length of the fractal dots.

The round screen provides more stable and almost linear dot-gain behaviour (5–8%) over a wide tonal range, which simplifies its calibration, whereas in the critical-highlight region (1–3%) the fractal screen shows better dot isolation and lower dot gain.

The experimental dot-gain curves are well described by non-linear models: the third-degree polynomial and the smoothing spline provide R^2 values of 0.83–0.99, making it possible to use them for constructing compensation curves.

For the practical implementation of fractal screening in flexographic printing on aluminium foil, technological compensation of dot gain (DGC) in the midtone zone is required, together with optimisation of ink viscosity and printing pressure.

6. References

Havenko, S., Labetska, M. and Telehina, T. (2024) 'Study of flexographic imprints using the methods of optical and electron microscopy', *Sixteenth International Conference on Correlation Optics. Proceedings of SPIE*, 12938, 129380W. DOI: 10.1117/12.3012269

Havenko, S., Telegina, T. and Labetska, M. (2026) 'Detection of the influence of flexographic printing speed on the occurrence of the bouncing effect on imprints', *Eastern-European Journal of Enterprise Technologies*, 2(1/140), pp. 115–124. DOI: 10.15587/1729-4061.2026.359494

International Organization for Standardization. (2020) *ISO 12647-6: Graphic technology — Process control for the production of half-tone colour separations, proof and production prints — Part 6: Flexographic printing*. Geneva: ISO.

International Organization for Standardization. (2021) *ISO 13656: Graphic technology — Application of reflection densitometry and colorimetry to process control or evaluation of prints and proofs*. Geneva: ISO.

Lorenz, A., Gredy, C., Beyer, S., Yao, Y., Papet, P. and Ufheil, J. (2016) 'Flexographic printing — towards an advanced front side metallization approach with high throughput and low silver consumption', *Solar Energy Materials and Solar Cells*, 157, pp. 550–557.

Valdec, D., Hajdek, K., Vragović, L. and Geček, R. (2021) 'Determining the print quality due to deformation of the halftone dots in flexography', *Applied Sciences*, 11(22), p. 10601.

Valdec, D., Miljković, P. and Augustštin, B. (2017) 'The influence of printing substrate properties on color characterization in flexography according to the ISO specifications', *Tehnički glasnik*, 11(3), pp. 73–77.

Valdec, D., Štumerger, M., Majnarić, I. and Valdec, L. (2026) 'Analytical modeling of geometrical dot gain relationship between AM and FM halftone screening technologies', *Applied Sciences*, 16(7), p. 3413.

Várza, F., Joóbné Preklet, E. and Horváth, C. (2021) Application analysis of white flexographic printing inks on biodegradable flexible foils. In: *Proceedings of the 2nd International Conference on Circular Packaging CPC*, pp. 311–320.

Xue, B., Liu, X., Liu, Y., Xu, Q., Ke, J. and Jiang, M. (2026) 'Mussel-inspired multi-functional adhesive for metal flexographic printing plates: superior metal and polymer adhesion, strength, toughness, and long-lasting durability', *Progress in Organic Coatings*, 212, p. 109913.

Żołek-Tryznowska, Z., Rombel, M., Petriaszwili, G., Dedijer, S. and Kašiković, N. (2020) 'Influence of some flexographic printing process conditions on the optical density and tonal value increase of overprinted plastic films', *Coatings*, 10(9), p. 816.



© 2026 Authors. Published by the University of Novi Sad, Faculty of Technical Sciences, Department of Graphic Engineering and Design. This article is an open access article distributed under the terms and conditions of the Creative Commons Attribution license 4.0 Serbia (https://creativecommons.org/licenses/by/4.0/deed.en).

Original Scientific Paper https://doi.org/10.24867/GRID-2026-p8

Possibility of Realisation White Electroink on a Metallised Printing Substrate

ABSTRACT

White printing is a general trend necessary for the production of printed media on highly saturated substrates and transparent surfaces. Such industrial printing is achieved primarily via classical technologies. However, electrophotography with liquid white ElectroInk is now increasingly common. A new trend is printing ElectroInk white on metallised substrates, where it serves as a base layer (mask) for subsequent in-line CMYK colour reproduction. Applying white ElectroInk in thicker layers is challenging. Achieving higher TiO2 pigment concentration requires more white layers. In this work, the reproduction of standard white ElectroInk is investigated on an HP Indigo WS 6800 machine, using one, two, and three machine prints repetitions. To enhance the white ink effect, experimental embossing of the metallised substrate (Vacuum metal silver lux ultra ws label material) will be performed with the Pantek Rhino S510 unit. This process forms a rough surface layer using two embossing plates. Printing white ElectroInk and overprinting on such a surface introduces a new challenge. It creates visual effects with better white acceptance on the metallised surface. Experiments show the best sample is the one printed on an HP Indigo machine with two coats of white ElectroInk. It was also found that changing the surface structure with embossing causes greater changes at higher white tone coverage. White halftone patches achieve rapid tone change (1 layer: ΔE_{00}=1.95; 2 layers: ΔE_{00}=2.34; 3 layers: ΔE_{00}=1.55), while solid tones change slightly (1 layer: ΔE_{00}=1.55; 2 layers: ΔE_{00}=0.70; 3 layers ΔE_{00}=0.32).

Igor Majnarić
Ivana Bolanča Mirković
Meri Huljev
Stanko Bauk

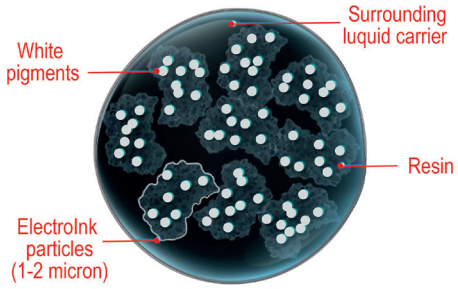
University of Zagreb,
Faculty of Graphic Arts,
Zagreb, Croatia

KEY WORDS
Digital colour offset, embossing, white electroInk, metallised substrate

1. Introduction

Special printing effects are often achieved through the use of white ink. In modern printing houses, electrophotographic (EP) and inkjet machines are increasingly equipped to apply specialized white inks and toners (Majnarić, 2015). The ability to produce high-quality personalized prints and manage small, frequently repeated print runs is one of the main advantages associated with white ink (Kipphan, 2001). Depending on the type of printed product, spot white ink can be applied to substrates with intense colors or used as masks on completely transparent substrates. This allows for the subsequent printing of process inks, which prevents the transparency of the substrate and enhances the contrast of the final color print (Gorski, 2026). Electrophotographic HP Indigo machines are utilized with a specialized liquid printing ink known as ElectroInk. This ink is designed for Digital Colour Offset technology and is characterized by its low viscosity. During the printing process, a solid state is achieved by the ink through polymerization and the temperature-driven evaporation of the volatile Isopar solvent, resulting in a pasty adhesive substance (Landa et al., 1988). ElectroInk is

categorized as an EP ink and is composed of several key components. Pigments in the form of a thermal polymer (24-29%) are dispersed in a non-polar volatile oil (70-75%). Additionally, additives to enhance conductivity (approximately 10%) and charged pigmented toner particles suspended in a liquid carrier are included in the formulation. To attain maximum opacity in the printed image, the proportion of white ElectroInk pigment particles (paste) is required to be optimized (Forgacs & Teishev, 2013; Morić, Majnarić & Modrić, 2020).



» **Figure 1:** *Schematic representation of white ElectroInk for HP Indigo machines*

2. Theoretical part

white printing inks are expertly crafted using white pigments and fillers that reflect nearly 100% of visible light, resulting in a brilliantly bright white appearance. the most notable chemical compounds that contribute to this exceptional whiteness include titanium dioxide (tio2), zinc oxide (zno), calcium carbonate (caco3), aluminum oxide (al2o3), silicon dioxide (sio2), magnesium oxide (mgo), and barium sulfate (baso4). in the market of printing inks, ten key white pigments and fillers stand out, each selected for their optimal concentration and particle size. these include zinc white, lithopone white, zinc sulfide, bleached calcium carbonate, china clay, blanc fixe, aluminum hydrate, talc, and silica.

2.1. Zinc white - chinese white

Zinc white pigments are bright white with medium opacity, providing reliable coverage for industrial applications. Finely ground, they meet FDA approval, exhibit strong UV absorption, and resist fungal growth. Their alkaline nature neutralizes oxidation products and makes them suitable for acidic resins. Color changes occur with copper compounds, showing yellow in warm conditions and white in cold. Used as fillers in can printing and other inks, these pigments enhance flow and application. Cl White 4 (Cl No. 77947; CAS No. 1314-13-2) consists of 99% to 99.7% zinc oxide (ZnO) and 0.3% to 1.0% volatile solvents (Leach & Pierce, 1999).

2.2. Lithopone white

Lithopone white pigment is chemically inert, making it compatible with formulations that include TiO2. Available in micro-sized particles, it acts as a white, transparent filler that is acid-degradable. It is made from calcined copper pyrite, zinc sulfide, and barium sulfate, and is increasingly used as a filler in TiO2 systems. Cl Pigment White 5 (Cl No. 77115; CAS No. 1345-05-7) consists of approximately 60% to 72% barium sulfate (BaSO4) and 28% to 40% zinc sulfide (ZnS) (Leach & Pierce, 1999).

2.3. Titanium dioxide - anatase and rutile structure

Titanium dioxide is the most widely used white pigment due to its high refractive index and excellent opacity. It has largely replaced other pigments due to its resistance to various pH levels and stability under light and heat. Unlike zinc, aluminium, zirconium, or silicon oxides, titanium dioxide can be coated in multiple ways. Understanding its safety profile and environmental impact is crucial for industry professionals, as these factors influence regulatory compliance and sustainability. There are two primary crystal forms: rutile, which is harder and more durable with a higher refractive index (2.71), and anatase, which is softer and has a lower refractive index (2.55) and lower hiding power. Rutile is suitable for long-lasting coatings, while anatase is preferred for applications requiring a bluer tone and increased translucency.

Titanium dioxide pigment is widely used in various ink systems. Pure, uncoated pigment is often used in water-based flexographic and screen printing inks, while surface-treated pigments enhance print quality and gloss but are less transparent. These coated pigments require specific dispersion techniques and are primarily used in lithographic offset and letterset printing, where high-whiteness substrates are preferred for tone tinting (Tomerlin et al., 2023).

Ilmenite ($FeTiO_3$) is processed to produce titanium dioxide (TiO_2) pigments by treatment with sulphuric acid, followed by hydrolysis, calcination at around 1000 °C, wet-milling, and finishing steps such as washing and drying. Alternatively, in the chloride process, titanium-rich feedstock is chlorinated to form titanium tetrachloride ($TiCl_4$), which is subsequently oxidised to form TiO_2. Both processes are used for the production of pigment-grade TiO_2. Newer methods produce easier-to-disperse particles with high opacity and gloss, with crystal sizes around 0.2 µm, which helps optimise visible-light scattering. C.I. Pigment White 6 (C.I. No. 77891; CAS No. 13463-67-7) typically consists of 80% to 99.9% TiO_2, with up to 20% additional oxides and a small organic coating (Leach & Pierce, 1999).

2.4. Zinc sulphide

Zinc sulphide is an opaque white pigment known for excellent abrasion resistance and higher UV reflectance than titanium dioxide (TiO_2). It resists most liquids except acids and offers good heat and ageing resistance. While not as opaque as TiO_2, it effectively serves as a filler for TiO_2 in various formulations. This pigment can be used in all printing techniques, except with acidic resins or in metal decoration applications, which require a clear enamel after baking. C.I. Pigment White 7 (C.I. No. 77975; CAS No. 1314-98-3) has the following composition: ZnS (97%), ZnO (less than 0.3%), solubles (less than 0.4%), moisture (less than 0.2%), and residue (3%) (Leach & Pierce, 1999).

2.5. Bleached calcium carbonate

Bleached calcium carbonate ($CaCO_3$) is a cost-effective white filler used in printing inks, enhancing quality while reducing costs. It often contains up to 3% stearate or resin, and both coated and uncoated forms are available with larger particle sizes, which contribute to good workability and a glossy finish. The opacity of the pigment varies from opaque to translucent, depending on grinding intensity. This pigment is used in various inks, including letterpress, offset lithography, and gravure, achieving a matte finish. When added to copper plate pigments, it improves adhesion to substrates. However, it should not be mixed with acidic binders due to reactivity with moisture and potential reactions with certain pigments.

Calcium carbonate also serves as a dusting powder to prevent smudging. Higher-quality ground mineral versions, particularly from Japan, offer high gloss and transparency but come at a higher cost. Calcium carbonate ($CaCO_3$) occurs naturally in forms such as chalk and limestone. It can be obtained by grinding natural mineral sources or synthesised by slaking quicklime and subsequently reacting it with carbon dioxide. It is also a by-product of water purification. The composition of Natural C.I. Pigment White 18 (C.I. No. 77220; CAS No. 471-34-1) varies based on its source: it typically contains 95% to 98% $CaCO_3$, 1% to 3% $MgCO_3$, and trace amounts of other compounds. The synthetic version is purer, with 98% to 99% $CaCO_3$ and lower levels of impurities (Leach & Pierce, 1999).

2.6. China clay (kaolin)

China clay is a white to pale grey, chemically inert powder with a high absorption capacity for printing oils. It is commonly used to produce inexpensive, moisture-resistant white inks and also acts as a thickening agent. China clay is also approved by the FDA for certain applications.

China clay is primarily composed of naturally occurring hydrated aluminium silicate and often contains impurities such as calcium, magnesium, iron, quartz, and mica. Purification is achieved through levigation and settling tanks. The composition of C.I. Pigment White 19 (C.I. No. 77005; CAS No. 8047-76-5) varies by medium and calcium content. For instance, the aqueous version typically contains 37–45% Al_2O_3 and 44–53% SiO_2, while the calcined version contains 42–45% Al_2O_3 and 51–53% SiO_2, with minimal impurities (Leach & Pierce, 1999).

2.7. Blanc fixe, process white

Blanc fixe is a high-quality white filler known for its resistance to all pH levels, good light fastness, and thermal stability. It has high diffuse light reflectance, maintaining gloss and tone when mixed with other colors. Primarily used in inks for pastel colors, its high density allows for significant weight additions without affecting print yield. Its safety is confirmed by FDA approval and low solubility. Cl Pigment White 21 (CI No. 77120; CAS No. 7727-43-7) has the following composition: BaSO4 (97% to 99%), SiO2 (0% to 2%) Residues (0% to 1%) (Leach & Pierce, 1999).

2.8. Aluminum hydrate, lake white, transparent white

Aluminium hydrate ($Al_2O_3 \cdot H_2O$) is a versatile white filler known for its soft texture and transparency. It is resistant to most chemicals, except for dilute hydrochloric acid (HCl), ensuring reliable performance in various applications. This filler offers thermal stability and lightfastness and improves the flowability of lithographic offset inks and varnishes. Available in formulations with different viscosities, ranging from pastes to liquids, it is a cost-effective and easily dispersible option that is FDA-approved. C.I. Pigment White 24 (C.I. No. 77002; CAS No. 1332-73-6) (Leach & Pierce, 1999).

2.9. Talc, french chalk

Pure talc has a hardness of 1 on the Mohs scale, while diamond has a hardness of 10 (International Gem Society , 2025). It appears as a shiny, very fine white powder that is chemically inert, light-resistant, and can withstand temperatures up to 850 °C. Talc is commonly used as an inexpensive filler in high-quality lithographic offset inks, where it helps reduce tack and improve rub resistance. Composed mainly of magnesium silicate, talc occurs naturally in mineral deposits and is commonly associated with soapstone. For C.I. Pigment White 26 (C.I. No. 77718; CAS No. 8005-37-6), the typical composition includes 25% to 30% magnesium oxide, 52% to 56% silicon dioxide, and smaller amounts of calcium oxide, iron(III) oxide, and aluminium oxide. In the pure pigment variant, the magnesium oxide content increases to 31% to 32%, and the silicon dioxide content to 60% to 64%, with reduced levels of other components (Leach & Pierce, 1999).

2.10. Silica

Silica is a lightweight, transparent white filler with a matting effect, high oil absorption, and chemical inertness, making it stable in various applications. It is used as a filler in inks, preventing the settling of other particles and reducing tack and gloss. It can also form gels when dispersed in non-polar solvents. C.I. Pigment White 27 (C.I. No. 77811; CAS No. 7631-86-9) consists of 98% SiO_2 and 0.1% other oxides, with a loss on ignition of 2.0% (Leach & Pierce, 1999).

3. Experimental part

For this study, an SRA3+ test motif featuring multiple white halftone wedges ranging from 0% to 100% tone value (TV), in 10% increments, was created. The test motif was designed in Adobe Illustrator 2022, saved in PDF/X-4 format, and loaded into the RIP (ESCO, HPE ProLiant ML350) using the standard LUT 0.5 calibration curve (Majnarić et al., 2025). White ElectroInk was used for printing on the HP Indigo WS6800, with a varying number of ink layers. The printing substrate used in this experiment was the metallised foil Vacuum Metal Silver Lux Ultra WS/SH6020 Plus/WG80, which was printed using two different methods (Fedrigoni Group, 2026).

In the first part of the experiment, direct white printing was performed on the metallised foil layer using the HP Indigo WS6800. In the second part, the metallised foil was embossed using the Pantec Rhino S 510, resulting in a relief structure on the foil (Rhino, 2026). Following embossing, white ink was printed on the structured metallised aluminium self-adhesive foil using the HP Indigo WS6800 (HP Indigo, 2026). A total of two sets comprising six samples were created using the HP Indigo WS6800 printer. The first set was printed with one, two, and three layers of white ElectroInk. The second set was printed with one, two, and three layers of white ElectroInk on embossed metallised foil. All samples with white imprints were adhered to a 4 mm-thick glass surface after removal of the liner. This setup was designed to simulate realistic measurement conditions corresponding to the application of the printed foil to a glass bottle. A 1 kg FINAT roller with a hardness of 70° Shore was used to apply the printed foil (FINAT, 2019).

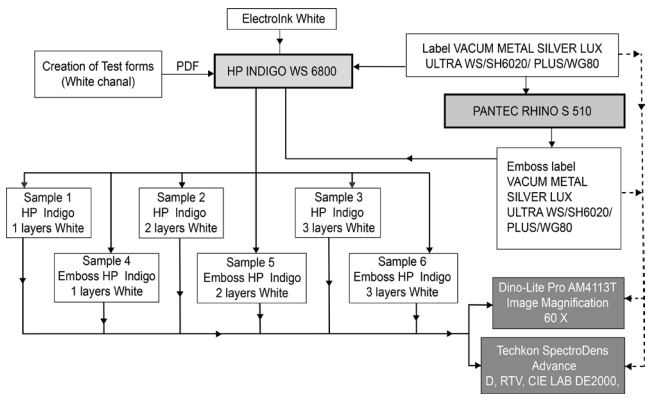
All generated white samples (S1, S2, S3, S4, S5, and S6) were subjected to optical measurements using a Techkon SpectroDens spectrophotometer/densitometer. CIE Lab* values, optical density (D) of the various white ink coatings, colour differences (CIEDE2000, ΔE_{00}), and tone values (TV) were obtained from the measurements (Techkon, 2026). The final results were processed and presented using OriginPro 8.5, while enlarged images were examined using a Dino-Lite AM4113T microscope. Additionally, all images were processed in Adobe Photoshop 2022. The chronological flow of the experiment is illustrated in Figure 2.

4. Results and discussion

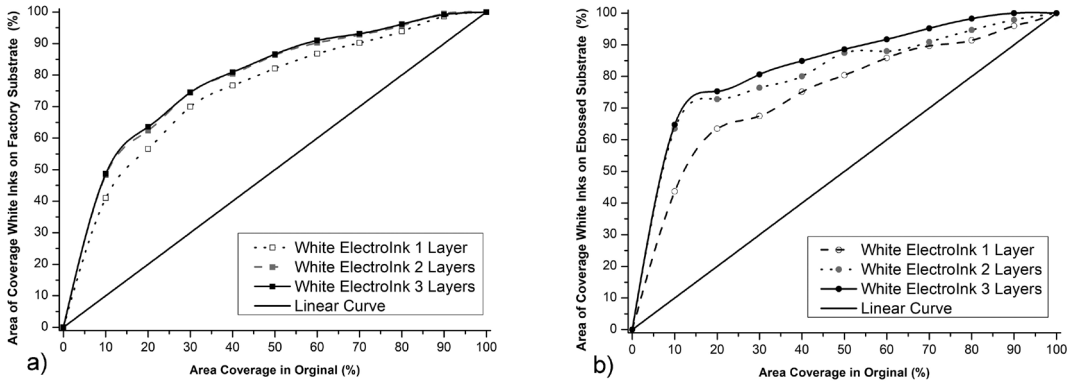
4.1. Densitometry

A modified densitometric method was utilised to evaluate white ElectroInk deposits. With increasing whiteness, the densitometric values of the reproduction curve decrease; therefore, the corresponding deviations are represented in the negative coordinate space. In the analysis of print reproduction, reproduction curves are commonly generated by plotting the tone value specified in the digital file against the measured tone value of the printed reproduction, covering the range from 10% to 100% TV in increments of 10%. Figure 3 shows the reproduction curves for the HP Indigo WS6800.

The largest deviations in white tone reproduction occur within the medium-to-high halftone range, particularly between 40% and 60% TV, while notable differences are also observed between 10% and 20% TV. As the number of white ElectroInk layers increases,



» **Figure 2:** *Schematic representation and chronology of the performed experiment with the application of measuring equipment and materials*



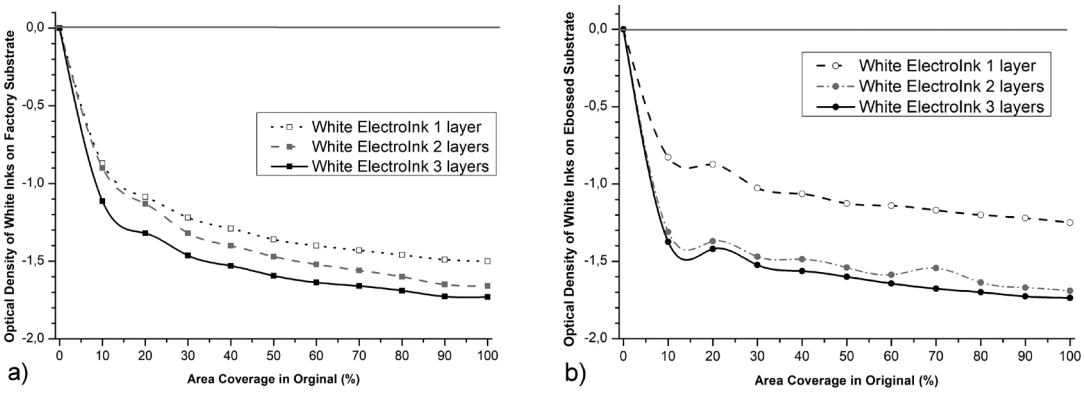
» **Figure 3:** *ElectroInk white reproduction curves printed on the HP Indigo WS6800: a) original (factory) metallised substrate; b) embossed metallised substrate*

TV gain also increases. There are no substantial differences between two and three layers of white, with consistent average gain values, such as ΔTV_W1layer_W2layer = 7.9% at 10% TV. For prints with two and three layers of white, the average gain remains at 4.28%, with ΔTV_(2layer_3layer) also at 7.9%.

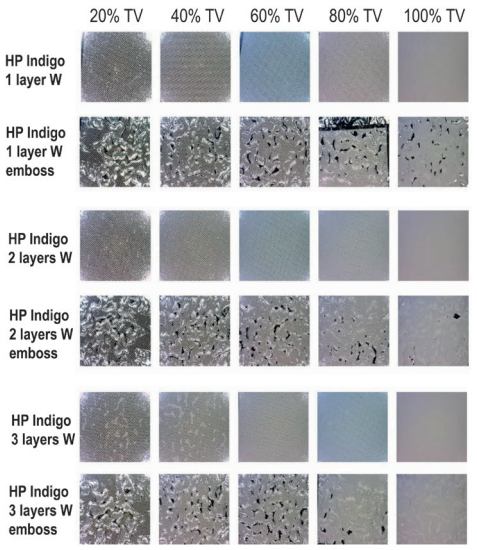
Patterns on embossed metallised substrates exhibit visible differences depending on the number of white ElectroInk layers, with smoother tonal gradations on roughened surfaces compared with smooth surfaces. Light-tone reproduction shows pronounced deviations, with ΔTV_W10% = 20.93% for both one and two layers of white. For medium halftone values, the difference between the first and second layers is ΔTV_W1layer_W2layer = 7.46%, while the addition of a third layer results in a further difference of 3.44%. In darker TV areas, minor tone-value differences occur between layers, with ΔTV_W60%–W90% = 2.23% for one versus two layers and 3.51% for two versus three layers. Accurate reproduction of white tones depends on the optical density of the solid white ink layer, which also affects the optical densities of the halftone areas. Figure 4 shows the relationship between the optical density of the white fields and tone value.

When using the HP Indigo, a double layer of white ink produces an average optical density (D_avg) of 0.15. Adding a third layer results in an additional optical density increase of ΔD_avg = 0.07. The difference in optical density between one and two layers increases, with an average difference from 20% TV to 90% TV of ΔD_W20%–W90% = 0.12. For the third layer, this value is ΔD_W20%–W90% = 0.11.

Figure 4b shows the tone-range curve for white ElectroInk on an embossed metallised substrate. With one and two layers, a deviation of ΔD_W100% = 0.44 occurs at the solid area (100% TV), while adding a third layer results in a minor deviation of ΔD_W100% = 0.05. The average optical density difference between 10% TV and 90% TV is ΔD_W1layer_W2layer = 0.45. The addition of a third layer does not substantially change the optical density, with ΔD_W2layer_W3layer = 0.07. Ultimately, a third layer of white ElectroInk is mainly beneficial for achieving solid areas, as illustrated in Figure 5 by enlarged microscopic images (60×) obtained using a Dino-Lite microscope.



» **Figure 4:** *Densitometric curves of ElectroInk white ink printed with the HP Indigo WS6800: a) original (factory) metallised substrate; b) embossed metallised substrate*



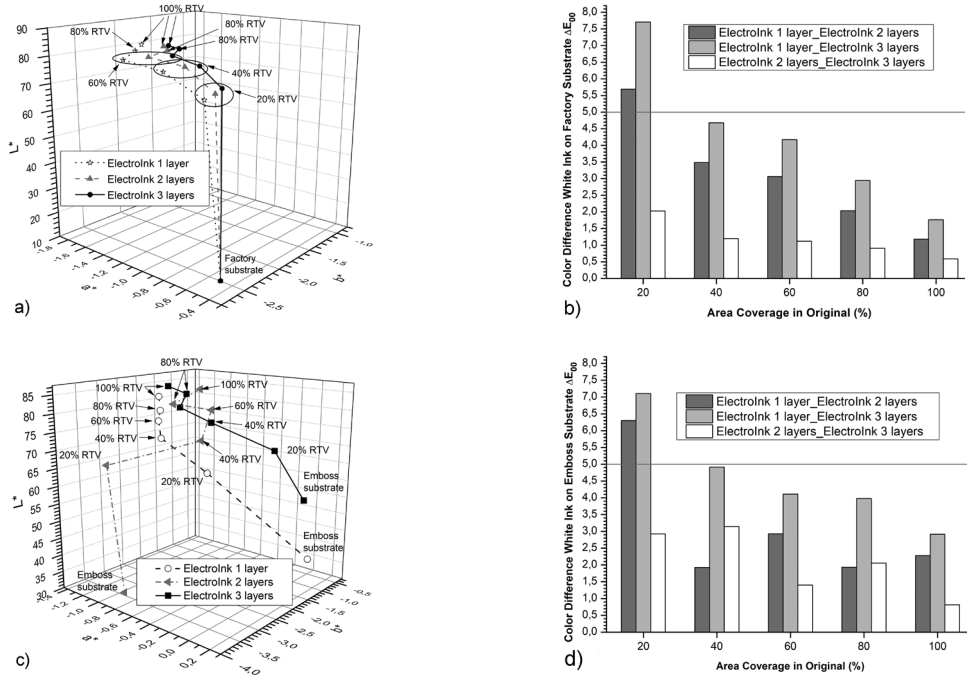
» **Figure 5:** *Microscopic images of imprints on five characteristic patches on embossed and original metallised surfaces printed using the HP Indigo WS6800*

4.2. Colourimetric analysis of white prints

The modified densitometric method used in this study is less suitable for assessing white surfaces, as the measurement is influenced by the optical properties of the white colourant and the aluminium metallisation of the self-adhesive foil. This makes comparisons across different experimental settings challenging, especially for materials with different surface structures. In contrast, colourimetry provides a more appropriate basis for evaluating and comparing colour differences in relation to human visual perception. Figure 6 illustrates the colour variations resulting from printing with different numbers of white ElectroInk layers.

Figure 6a illustrates a three-dimensional representation of different applications of white ink on an original metallised surface printed using the HP Indigo. Applying white ink markedly increases lightness (L*) at 20% tone value (TV). As surface coverage increases, more noticeable changes in chromaticity occur, while changes in lightness become smaller. Increasing TV shifts chromaticity along the negative b* axis of the CIE Lab* colour space, giving the white a more bluish hue. Up to 60% TV, all layers of white ElectroInk display similar changes. Beyond this point, there is a noticeable shift along the positive a* axis, resulting in a warmer shade of white.

Figure 6b displays the colour differences between different layers of white ink printed using the HP Indigo. The bar graph shows that as the tone value increases, the colour difference between white ElectroInk imprints decreases. Notably, prints with two layers exhibit greater colour differences than those with three layers. The largest colour difference occurs at 20% TV, where the differences exceed the defined quality threshold of $\Delta E_{00} = 5$. The recorded colour difference between one and two layers is ΔE_W1layer_W2layer = 5.7, and that between two and three layers is ΔE_W2layer_W3layer = 7.7, the largest value recorded in the study. As the coverage of white ElectroInk increases, the colour differences decrease,



» **Figure 6:** *Colourimetric changes of white ElectroInk on the HP Indigo WS6800: a) 3D CIE Lab representation of prints on an original metallised surface; b) ΔE_{00} colour differences on an original substrate; c) 3D CIE Lab* representation of prints on an embossed metallised surface; d) ΔE_{00} colour differences on an embossed substrate*

reaching the lowest values at the solid tone (100% TV), with ΔE_W1layer_W2layer = 1.2, ΔE_W1layer_W3layer = 1.8, and ΔE_W2layer_W3layer = 0.6. Differences of $\Delta E_{00} < 1$ are typically imperceptible to the human eye.

After embossing, the roughness of the metallised surface markedly affects the applied white ink layer. The three-dimensional graph in Figure 6c shows the variations in these layers on an embossed metallised substrate printed using the HP Indigo. When one layer of white ElectroInk is applied at 40% TV, noticeable changes in lightness and chromaticity occur, with additional layers primarily affecting lightness.

The largest chromaticity changes occur along the positive b* axis, leading to yellowing. With two layers of white ink, changes in lightness are stable up to 20% TV, while only minor changes are subsequently observed along the positive a* axis. For white tones above 60% TV, fluctuations in lightness and chromaticity are minimal. Three layers show pronounced changes in lightness from 20% to 60% TV, accompanied by chromaticity changes along the a* axis, while darker tones shift towards a bluer appearance.

Figure 6d shows the colour differences (ΔE_{00}) among prints with one, two, and three layers of white ElectroInk on an embossed metallised substrate printed using the HP Indigo. The embossed samples exhibit more pronounced variations in white tones than samples printed on the original smooth substrate. The largest colour difference, ΔE_W1layer_W3layer = 7.20, is observed at 20% toner coverage between one and three layers of white. As white coverage increases, the average colour difference between one and two layers is ΔE_W1layer_W2layer = 2.20 for 40% to 100% TV. When comparing one and three layers, the mean difference increases to ΔE_W1layer_W3layer = 3.90. The smallest mean difference, ΔE_W2layer_W3layer = 1.90, is found between the second and third layers, with a minimum difference of ΔE_W2layer_W3layer = 0.80 at 100% TV.

5. Conclusions

Densitometric measurements on a metallised substrate showed that the smallest average tone-value gain was obtained with a single layer of white ink printed using the HP Indigo, with ΔTV = 77.32. No substantial differences in tone-value gain were observed in the white midtones when comparing two and three layers of white ink, both showing a tone-value gain of approximately 4% compared with one layer.

For embossed prints with one layer of white ink, the quality of intermediate white tones was comparable to that obtained on smooth surfaces. Additional layers of white ink led to increased tone-value gain, reaching 2.38% for two layers and 5.74% for three layers. Variations in optical density were also observed, with Dmax changing from –1.29 for one layer of white to –1.73 for three layers. On an embossed substrate, the tone value decreased only with one layer; however, two and three layers maintained the tone value in the solid area, indicating effective ink filling.

Colourimetric measurements revealed that the largest fluctuations in white tones occurred with three layers of white ink on the original substrate printed using the HP Indigo, resulting in an average colour difference of ΔE_avg = 4.88 and a colour difference of ΔE_W100% = 1.76 at 100% TV. On the embossed substrate, similar variations were observed, with ΔE_W100% = 2.91.

For a solid white field, the colour difference with one layer of ElectroInk was ΔE_W100%_1layer = 1.54, decreasing to ΔE_W100%_2layer = 0.70 with two layers and further to ΔE_W100%_3layer = 0.35 with three layers. In halftone patches, the colour differences were $\Delta E_{00} = 1.95$ for one layer, $\Delta E_{00} = 2.34$ for two layers, and $\Delta E_{00} = 1.55$ for three layers. Overall, increasing the number of white ElectroInk layers improved solid-white reproduction, while the effect of additional layers was more pronounced on embossed metallised substrates.

6. References

Landa, B., Ben-Auraham, P., Hall, J. and Gibson, G. A. (1988) Toner for Use in Compositions for Developing Latent Electrostatic Images, Method of Making the Same, and Liquid Composition Using the Improved Toner. United States Patent and Trademark Office, US4794651 (Patent).

Fedrigoni Group. (2026) Datasheet Vacuum Metal Silver LUX Ultra WS. Available from: http://en.arconvert.it/products/WNE0368-es/print/?tipus%5B0%5D= [Accessed 8 February 2026].

Forgacs, P. and Teishev, A. (2013) 'Electro-Rheological Model of HP Indigo ElectroInk', *Journal of Imaging Science and Technology*, 57(3), pp. 1–7. DOI: 10.2352/J.ImagingSci.Technol.2013.57.3.030403

Gorski, J. (2026) White Ink as a Color-Management Variable. Available from: https://www.printing.org/content/2026/07/21/white-ink-as-a-color-management-variable [Accessed 25 July 2026].

HP Indigo. (2026) HP Indigo WS6800 Digital Press. Available from: https://h20195.www2.hp.com/v2/GetPDF.aspx/4AA7-9277ENW.pdf [Accessed 25 July 2026].

International Gem Society. (2025) The Mohs Hardness Scale and Chart for Select Gems. Available from: https://www.gemsociety.org/article/select-gems-ordered-mohs-hardness/ [Accessed 25 July 2026].

Kipphan, H. (ed.) (2001) Handbook of Print Media: Technologies and Production Methods. Berlin: Springer.

FINAT (2019) FINAT Technical Handbook: Test Methods. 10th edn. The Hague: FINAT.

Leach, R. H. and Pierce, R. J. (eds.) (1993) The Printing Ink Manual. 5th edn. Dordrecht: Kluwer Academic Publishers.

Majnarić, I., Huljev, M., Bauk, S. and Macan, F. (2025) 'The influence of the metallic substrate's embossing process and the possibility of printing white ElectroInk'. In: Gorjanc, M., Tomšič, B. and Gabrijelčič Tomc, H. (eds.) Crossing boundaries: 50th International Symposium on Novelties in Textiles, *10th Conference on Information and Graphic Arts Technology: proceedings*, 29–30 May 2025, Ljubljana, Slovenia. Ljubljana, Faculty of Natural Sciences and Engineering, University of Ljubljana, pp. 559–569.

Majnarić, I. (2015) Osnove digitalnog tiska. Zagreb: Grafički fakultet Sveučilišta u Zagrebu.

Morić, M., Majnarić, I. and Modrić, D. (2020) 'The Possibility of Increasing the Achromatic Tone Values of FOGRA 51 Standards Achieved by the Modification of in Line Pre-Treatment of the Printing Substrate', *Tehnički vjesnik*, 27(3), pp. 732–736. DOI: 10.17559/TV-20190329095201

Rhino. (2026) Data sheet Rhino S510. Available from: https://graval.cl/wp-content/uploads/2019/09/RHINO_System-description_EN_10.05.pdf [Accessed 25 July 2026].

Techkon. (2026) Techkon SpectroDens. Available from: https://www.techkon.com/files/downloads/prospekte/SpectroDens%20Brochure%20Web.pdf [Accessed 25 June 2026].

Tomerlin, R., Valdec, D., Tomiša, M. and Vusić, D. (2023) 'The Impact of Underlying Opaque White Coating Parameters on Flexographic Print Quality', *Applied Sciences*, 13(15), 8575. DOI: 10.3390/app13158575



© 2026 Authors. Published by the University of Novi Sad, Faculty of Technical Sciences, Department of Graphic Engineering and Design. This article is an open access article distributed under the terms and conditions of the Creative Commons Attribution license 4.0 Serbia (http://creativecommons.org/licenses/by/4.0/rs/).

Original Scientific Paper https://doi.org/10.24867/GRID-2026-p9

Optimization of Thermochromic Printing Inks for Functional Temperature Indicators

ABSTRACT

Thermochromic printing inks are functional graphic materials widely used in various applications, including the development of temperature indicators. For such systems, material compatibility and the optimization of thermochromic ink properties are essential to ensure reliable temperature indication. In this research, a functional printed indicator was developed for monitoring the temperature conditions of insulin therapy during storage and use. The multilayer indicator consists of a pictogram printed in full tone using thermochromic ink on a self-adhesive label. In its inactive state, a single-coloured graphic indicator signifies the insulin has been stored within the recommended temperature range. Upon activation, the thermochromic ink undergoes a reversible transition from coloured to transparent state, revealing an underlying warning pictogram. This colour change provides an immediate visual alert that the insulin should be stored to a lower-temperature environment to preserve its efficacy. The study was conducted using two thermochromic printing inks formulated with pigment concentrations of 8%, 10%, and 12% in the binder. Each formulation was printed in one, two, and three ink layers to determine printing conditions for achieving optimal opacity and colorimetric properties. The results could provide recommendations for optimizing ink formulation and printing parameters in the production of functional thermochromic temperature indicators for specific purposes.

Maja Strižić Jakovljević
Jana Špiranec
Sanja Mahović Poljaček

University of Zagreb,
Faculty of Graphic Arts,
Zagreb, Croatia

KEY WORDS
Thermochromic ink, temperature indicators, functional printing, colorimetric properties

1. Introduction

Thermochromic printing inks are functional graphic materials that undergo a visible and, in many systems, reversible colour change in response to temperature. Their ability to provide an immediate visual indication without electronic components makes them suitable for the development of temperature indicators and other functional printed products (Lozo, 2012; Kulčar et al., 2010). Thermochromic elements can also provide added functional value in packaging and labelling by communicating information about temperature conditions to the user (Lozo, 2012; Vukoje et al., 2023). A widely used type of thermochromic printing ink is based on leuco-dye systems. These systems typically consist of colour-forming components that are incorporated into microcapsules, enabling their application in printing inks and producing a temperature-dependent transition between coloured and colourless or transparent states (Kulčar et al., 2010; Pu & Fang, 2022). The colour transition can be characterized using colorimetric parameters, while the optical properties of the printed layer are important for applications in which the thermochromic print has to conceal and subsequently reveal information printed underneath (Zhao & Li, 2019; Kavčič et al., 2019). The stability of thermochromic printing inks is also an important consideration for functional applications, particularly with respect to their behaviour under light and elevated temperatures (Friškovec et al., 2013). For a functional temperature indicator based on a multilayer

printed structure, the compatibility of the materials and the properties of the thermochromic ink are essential for achieving the required visual response. In the inactive state, the thermochromic layer should provide sufficient opacity to conceal an underlying graphic element. Upon activation, the thermochromic layer should become sufficiently transparent or decolorized to reveal the underlying information and provide an immediate visual signal. Such a principle can be applied to temperature-sensitive labels in which a visible warning pictogram is revealed when a predefined temperature condition is exceeded. Recent developments in thermochromic sensing also demonstrate the potential of printed thermochromic systems for temperature monitoring and visual temperature indication (Hakola et al., 2021; Jaszczak-Kuligowska et al., 2026). The functional behaviour of thermochromic prints depends on several printing and material parameters, including pigment concentration, number of printed layers and resulting ink-layer thickness. These parameters can influence the colorimetric and optical properties of the printed layer and consequently its suitability for a particular indicator application (Kulčar et al., 2010; Kavčič et al., 2019). Pigment concentration can affect the colour characteristics of the thermochromic layer, whereas the number of applied layers influences the amount and thickness of deposited ink and may consequently affect its opacity and ability to conceal the underlying graphic element (Zhao & Li, 2019; Kavčič et al., 2019; Tomašegović et al., 2021). These properties are particularly relevant for temperature indicators intended for applications where a clear distinction between normal and undesirable temperature conditions is required.

In this study, a functional printed temperature indicator was developed for monitoring the temperature conditions of insulin therapy during storage and use. Maintaining appropriate storage and handling temperatures is important for preserving the quality and efficacy of insulin therapy. A printed thermochromic indicator can provide a simple visual means of communicating changes in temperature conditions by revealing a warning pictogram after activation. The proposed multilayer indicator consists of a pictogram printed in full tone using leuco-dye-based thermochromic printing ink on a self-adhesive label. Two thermochromic printing inks were investigated using pigment concentrations of 8, 10 and 12% in the binder, with each formulation applied in one, two and three ink layers. The influence of pigment concentration and number of layers was evaluated in terms of colorimetric properties, optical density, and thickness of the printed ink layers. Particular attention was given to the functional response of the indicator, specifically the reversible transition of the thermochromic layer from the coloured to the transparent state and the subsequent visibility of the underlying warning pictogram. The investigated combinations of ink formulation and printing parameters were compared to identify suitable conditions for the development of the proposed functional temperature indicator.

2. Materials and methods

2.1. Materials and sample preparation

Blue and red leuco-dye-based thermochromic pigments (CHAOS TRADE, Poland) were used, with activation temperature ranges of 24–30 °C (blue) and 26–31 °C (red), respectively. The pigments were manually mixed with a transparent SEBASTAR binder (SEBEK INKS, Belgium) according to the manufacturer's instructions to obtain printable thermochromic inks while minimizing potential damage to the microcapsules. For each pigment, 100 g of thermochromic ink was prepared, with the pigment concentration in the binder set at 8%, 10%, and 12%. These concentrations were selected for investigation of their influence on the optical and colorimetric properties and functional performance of the temperature indicator. Both the pigments and the binder were water-based, ensuring their compatibility.

A polyester screen with a mesh count of 43 threads/cm, a mesh tension of 13.6 N, and a plain weave (PW) was used for screen printing. The screen was coated with AZOCOL Z 133 UV emulsion containing DIAZO NR.23 powdered stabilizer (KIWO, Germany), prepared according to the manufacturer's instructions. The prepared emulsion was applied to both sides of the screen and subsequently dried. A graphic film featuring a square motif was prepared for the production of the screen-printing plates. During exposure, the photosensitive emulsion polymerized in the exposed areas. The unexposed areas corresponding to the motif remained soluble and were removed during rinsing, forming the open stencil areas. After drying, the plates were ready for printing.

Recycled paper labels with a water-based adhesive were used as the printing substrate (HERMA, Germany). The labels carry the Blauer Engel environmental certification (Herma Sustainable Labels, 2026) and were supplied in A4 sheets (210 × 297 mm), arranged in seven columns with 27 labels per column. Each label measured 25.4 × 10 mm. The substrate was pre-printed using a laser printer with the indicator design. Three pictogram variations were developed in three colours (black, red, and blue) using Adobe Illustrator and Adobe InDesign (Figure 1). The pictograms were original designs based on symbols commonly used in pharmaceutical and safety signage. The thermochromic layer was subsequently intended to conceal the underlying pictogram in the inactive state and reveal it upon activation, forming the multilayer temperature indicator structure.



» **Figure 1:** *Design of the pictograms for the multilayer temperature indicator*

The TC inks were printed onto the pre-printed substrates using a semi-automatic screen-printing process. Each TC ink was printed at three pigment concentrations (8%, 10%, and 12% in the binder) and applied in one, two, and three ink layers, resulting in a total of 18 samples (Table 1).

Table 1

List of thermochromic ink samples prepared in the study

Sample	TC ink	Pigment concentration in binder	Number of TC ink layers
P8.1	blue	8%	1
P8.2	blue	8%	2
P8.3	blue	8%	3
P10.1	blue	10%	1
P10.2	blue	10%	2
P10.3	blue	10%	3
P12.1	blue	12%	1
P12.2	blue	12%	2
P12.3	blue	12%	3
C8.1	red	8%	1
C8.2	red	8%	2
C8.3	red	8%	3
C10.1	red	10%	1
C10.2	red	10%	2
C10.3	red	10%	3
C12.1	red	12%	1
C12.2	red	12%	2
C12.3	red	12%	3

2.2. Measurement methods

The thickness of the TC ink layer was measured for all 18 samples using a SaluTron D4-Fe thickness gauge. Ten measurements were taken at different locations on each sample. Densitometric measurements were performed using a Techkon Dens densitometer to determine the optical density of the TC ink layers. Ten measurements were taken for each sample at 23°C and 28% relative humidity. Spectrophotometric measurements were conducted to determine the L*, a*, and b* colorimetric values of the thermochromic prints at different temperatures. Samples printed with blue thermochromic ink were measured from 24 to 30°C and additionally at 32, 35, and 43°C, while samples printed with red thermochromic ink were measured from 26 to 31°C and additionally at 33, 36, and 42°C. Samples were heated using a Julabo heating system, while measurements were performed using an Ocean Optics 2000+ spectrophotometer equipped with an Ocean SR integrating sphere (ISP-30-6-R, 30 mm). Measurements were conducted under D50 illumination using a 2° standard observer and OceanView software. At each specified temperature, one sample of each TC ink, pigment concentration, and number of printed layers was measured.

3. Results and discussion

The densitometric measurements presented in Tables 2 and 3 show that the optical density of the TC prints was strongly influenced by the number of ink layers. For both blue (P8.1–P12.3) and red (C8.1–C12.3) TC inks, optical density increased consistently from one to three ink layers. The effect of pigment concentration was less uniform. For three-layer prints, optical density increased with increasing pigment concentration for both thermochromic inks. For the blue ink, the values increased from 1.369 at 8% to 1.486 at 10% and 1.506 at 12%, while for the red ink they increased from 1.476 to 1.479 and 1.572, respectively. In one and two-layer prints, some deviations from this trend were observed, particularly at 10% pigment concentration. Under the same printing conditions, the red thermochromic ink generally exhibited higher optical density than the blue ink, although a small difference in the opposite direction was observed for the 10% three-layer samples. This indicates that optical density depends on both the ink formulation and the number of ink layers (Viková & Vik, 2023). The standard deviations of ink-layer thickness and optical density were generally low. Most values were below 3% of the corresponding mean, with a few higher deviations in optical density. The observed variability may be related to the semi-automatic screen-printing process and the measurement procedure. These results confirm that the number of ink layers has a pronounced effect on optical density, while the effect of pigment concentration is less uniform and depends on the number of layers and TC ink formulation.

Spectrophotometric measurements were used to generate CIE a*/ b* chromaticity diagrams for the blue TC ink samples. The diagrams show the change in colour coordinates as a function of temperature. The a* axis represents the green–red component, whereas the b* axis represents the blue–yellow component. The negative b* values indicate the blue colour of the samples at the lower measurement temperatures. With increasing temperature, the a* and b* values progressively approach zero, indicating a decrease in chromaticity and a transition towards a colourless state. For the 8% pigment concentration (Figure 2a), this behaviour is observed for P8.1,

Table 2
Ink layer thickness and optical density of the blue TC samples

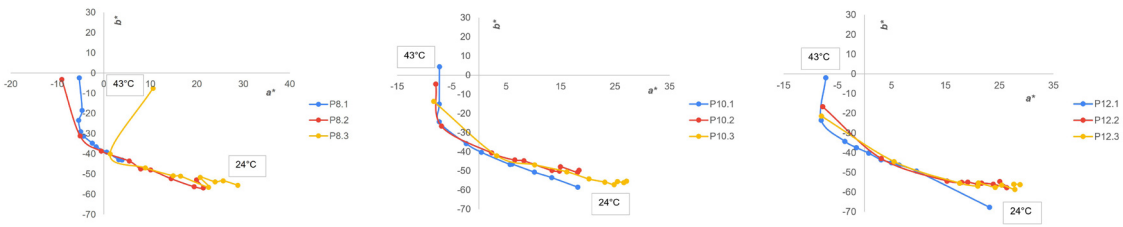
Blue TC samples	Ink layer thickness (µm)	SD	Optical density	SD
P8.1	183,6	3,27 (1,74%)	0,803	0,02 (2,49%)
P8.2	205	3,74 (1,82%)	1,324	0,02 (1,51%)
P8.3	241,6	4,17 (1,72%)	1,369	0,01 (1,09%)
P10.1	181,7	3,13 (1,72%)	1,01	0,03 (2,4%)
P10.2	221,2	3,19 (1,44%)	1,259	0,03 (2,4%)
P10.3	234,1	2,23 (0,95%)	1,486	0,01 (0,67%)
P12.1	193,7	4,55 (2,35%)	1,038	0,05 (4,81%)
P12.2	232,9	3,66 (1,13%)	1,335	0,001 (0,07%)
P12.3	245,4	3,44 (1,4%)	1,506	0,01 (0,66%)

Table 3
Ink layer thickness and optical density of the red TC samples

Red TC samples	Ink layer thickness (µm)	SD	Optical density	SD
C8.1	183	2,75 (1,5%)	1,074	0,01 (0,93%)
C8.2	199,8	4,71 (2,36%)	1,353	0,02 (1,48%)
C8.3	233,3	3,02 (1,29%)	1,476	0,02 (1,35%)
C10.1	191,7	1,95 (1,02%)	1,064	0,02 (1,88%)
C10.2	216,5	3,27 (1,51%)	1,286	0,02 (1,55%)
C10.3	235	3,65 (1,55%)	1,479	0,03 (2,03%)
C12.1	195,6	2,37 (1,21%)	1,199	0,01 (0,83%)
C12.2	229,6	4,4 (1,92%)	1,406	0,02 (1,42%)
C12.3	248	2,58 (1,04%)	1,572	0,02 (1,27%)

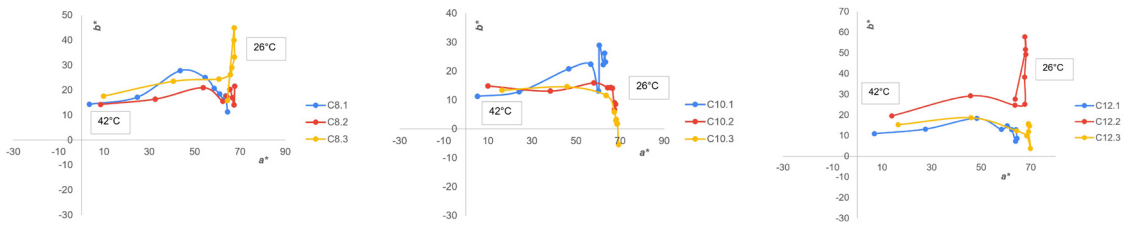
P8.2 and P8.3. The largest shift towards the achromatic region was observed for P8.1, whereas P8.2 and P8.3 retained more negative b* values at higher temperatures, indicating a lower degree of decolorization with increasing number of ink layers. A similar trend was observed for the 10% pigment concentration (Figure 2b), where P10.1 showed the greatest shift towards the achromatic region, while P10.2 and P10.3 retained higher colour saturation. For the 12% pigment concentration (Figure 2c), P12.1 again showed the most pronounced change in the a*/b* coordinates, whereas P12.2 and P12.3 retained more negative b* values at higher temperatures. Overall, the CIE a*/ b* chromaticity diagrams confirm the reversible thermochromic response of the blue thermochromic ink. The extent of decolorization was generally greater for samples printed with fewer ink layers, while samples with two and three ink layers retained a higher degree of chromaticity at elevated temperatures. These differences were particularly evident at the lower and upper ends of the investigated temperature range.

The a*/b* diagrams in Figure 3 show the temperature dependent changes in the colour coordinates of samples containing 8%, 10%, and 12% pigment at different numbers of ink layers for the red TC ink. At the initial temperatures, all samples exhibited positive b* values, indicating a colour position toward the yellow region. With increasing temperature, the colour coordinates changed considerably, with the a* values generally increasing and the b* values showing different trends depending on pigment concentration and number of ink layers. For the 8% pigment concentration (Figure 3a), C8.1 showed a moderate increase in b* followed by a decrease at higher temperatures, while C8.2 exhibited a relatively stable trend with smaller changes in b*. C8.3 showed a more pronounced variation, with a marked



(a) (b) (c)

» **Figure 2:** *CIE a*/b* diagrams of the blue TC ink containing 8% (a), 10% (b), and 12% (c) pigment in the binder, printed in 1, 2, and 3 ink layers*



(a) (b) (c)

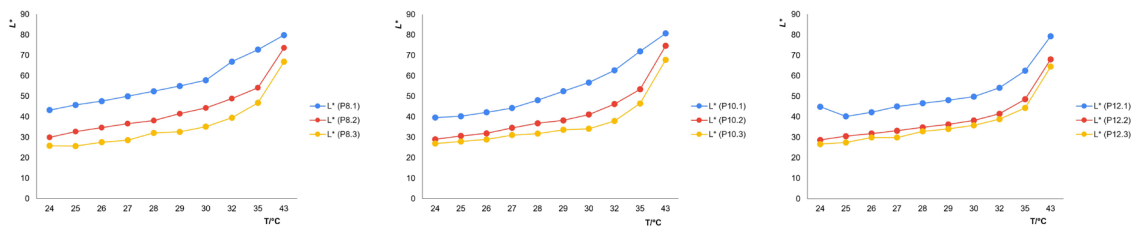
» **Figure 3:** *CIE a*/b* diagrams of the red TC ink containing 8% (a), 10% (b), and 12% (c) pigment in the binder, printed in 1, 2, and 3 ink layers*

increase in b* at higher temperatures. For the 10% pigment concentration (Figure 3b), C10.1 exhibited the most pronounced variation in both a* and b* values, including an increase in b* at intermediate temperatures followed by a decrease at higher temperatures. C10.2 showed a more gradual decrease in b*, whereas C10.3 exhibited a pronounced decrease in b* towards and below zero at higher temperatures. Among the 12% pigment samples (Figure 3c), C12.1 showed a gradual decrease in b* at higher temperatures, while C12.2 exhibited a pronounced increase in b*, reaching the highest values among the investigated samples. C12.3 showed a comparatively smaller variation, with b* remaining within a narrower positive range before decreasing at the highest temperatures. The results demonstrate that the temperature-dependent changes in a* and b* coordinates vary with both pigment concentration and number of ink layers. The differences are particularly evident at higher temperatures, where some samples show a decrease in chromaticity, while others retain or temporarily increase their b* values. This indicates that the thermochromic colour response of the red ink is influenced by the combination of pigment concentration and number of ink layers.

The L/T diagrams of the blue TC ink shown in Figure 4 indicate that the samples printed with one ink layer exhibited the highest lightness, regardless of pigment concentration in the binder. For all three pigment concentrations, the lightness of the two-layer samples was lower than that of the one-layer samples. At 8% and 10% pigment concentrations, the two-layer samples exhibited higher lightness than the corresponding three-layer samples. For the 12% pigment concentration, the lightness values of P12.2 and P12.3 are almost identical, indicating that the additional ink layer had little effect on the lightness of the printed sample. Each sample showed an increase in lightness with increasing temperature. This behaviour corresponds to the decolorization of the TC ink, during which the substrate beneath the thermochromic ink layer becomes increasingly visible. The increase in lightness therefore reflects the temperature-dependent transition of the thermochromic ink towards a more transparent state.

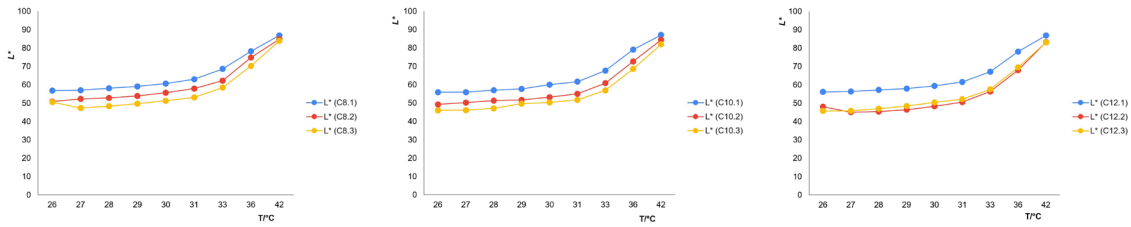
The temperature dependence of lightness of the red TC ink at all three pigment concentrations and number of ink layers is shown in Figure 5. The lightness values of the red TC ink samples were generally higher than those of the blue TC ink, while the differences between samples printed with different number of ink layers were relatively small. The most pronounced difference was observed among the samples containing 12% pigment concentration, where C12.1 exhibited the highest lightness, whereas C12.2 and C12.3 showed lower and nearly identical lightness values. For all red TC samples, increasing temperature resulted in increased lightness, with the change becoming more pronounced at higher temperatures. At lower temperatures, the lightness values were more stable and uniform. This behaviour is consistent with the thermochromic transition and increasing transparency of the thermochromic ink layer at elevated temperatures.

The temperature dependent properties of thermochromic inks enable their application in systems designed to



(a) (b) (c)

» **Figure 4:** *L/T diagrams of the blue TC ink containing 8% (a), 10% (b), and 12% (c) pigment in the binder, printed in 1, 2, and 3 ink layers*



(a) (b) (c)

» **Figure 5:** *L/T diagrams of the red TC ink containing 8% (a), 10% (b), and 12% (c) pigment in the binder, printed in 1, 2, and 3 ink layers*

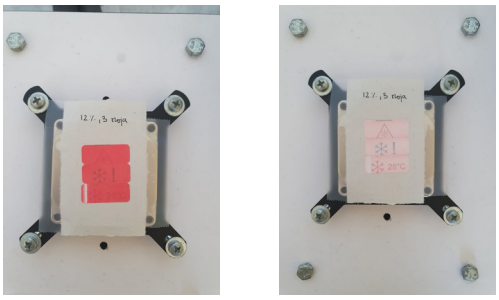
indicate predefined temperature conditions. Examples of the functional temperature indicators developed in this study are shown in Figures 6 and 7. The multilayer indicator printed on a self-adhesive label shown in Figure 6a demonstrates that the red thermochromic ink did not completely conceal the warning pictograms printed underneath the thermochromic ink layer. Consequently, the pictograms remained partially visible in the inactive state, which is not consistent with the intended function of the indicator. This effect was particularly evident for the pictograms printed in blue, whereas the red-line pictograms were less noticeable. With increasing temperature, the red thermochromic ink transitioned to a transparent state, resulting in clear visibility of all three warning pictograms in the activated state (Figure 6b). The appearance of a warning pictogram on packaging, for example for insulin therapy, could provide a visual indication that the product has been exposed to an elevated temperature and should be transferred to a lower-temperature environment.

In practical application, the blue thermochromic ink provided a more effective visual response. In the inactive state (Figure 7a), the blue thermochromic ink almost completely concealed all three warning pictograms, although their outlines remained slightly visible depending on the design and colour of the underlying printed elements. With increasing temperature, the thermochromic ink transitioned to a transparent state, revealing the pre-printed warning pictograms (Figure 7b).

These results demonstrate the feasibility of combining thermochromic ink layers with pre-printed graphic elements to develop a functional multilayer temperature indicator. With appropriate adjustment of the design and printing parameters of the underlying elements, the system could potentially be further developed for repeated thermochromic temperature indication.

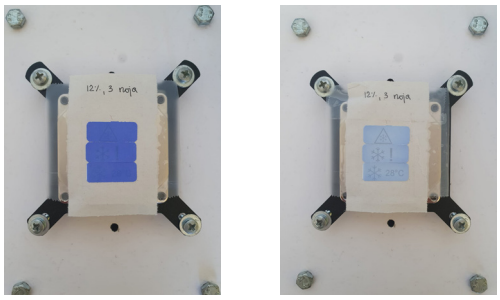
4. Conclusions

This study demonstrated the feasibility of developing a functional multilayer temperature indicator based on leuco-dye thermochromic printing inks. Two thermochromic inks, blue and red, were investigated at pigment concentrations of 8%, 10%, and 12% in the binder, with one, two, and three ink layers applied by screen printing. The results showed that the number of ink layers had a pronounced influence on ink-layer thickness and optical density, while the effect of pigment concentration was less uniform and depended on the number of layers and ink formulation. Spectrophotometric measurements confirmed the temperature dependent colour response of both thermochromic inks. Changes in L*, a*, and b* values demonstrated a transition towards a less chromatic and more transparent state with increasing temperature, although the extent of the change varied with pigment concentration and number of ink layers. The L/T diagrams further confirmed an increase in lightness at elevated temperatures, corresponding



(a) (b)

» **Figure 6:** *Thermochromic indicator printed with 3 layers of red TC ink with 12% of pigment in the binder, recorded at 26°C and 42°C*



(a) (b)

» **Figure 7:** *Thermochromic indicator printed with 3 layers of blue TC ink with 12% of pigment in the binder, recorded at 24°C and 35°C*

to the decolorization of the thermochromic ink layer and increased visibility of the underlying substrate. The practical evaluation showed that the blue thermochromic ink provided more suitable visual concealment of the underlying warning pictograms in the inactive state, while both inks enabled their clear visualization after activation. The developed multilayer structure therefore provides a simple visual means of indicating exposure to elevated temperature conditions. With further optimization of the graphic elements, pigment concentration, and number of ink layers, the proposed concept has potential for application in temperature-sensitive packaging and labelling, including applications related to insulin therapy.

5. Acknowledgments

This research was supported by the NextGenerationEU project NPOO MAHOVIĆ POLJAČEK 2025/2029 2025106.

6. References

Friškovec, M., Kulčar, R. and Klanjšek Gunde, M. (2013) 'Light fastness and high-temperature stability of thermochromic printing inks', *Coloration Technology*, 129(3), pp. 214–222. DOI: 10.1111/cote.12020

Hakola, L., Vehmas, K. and Smolander, M. (2021) 'Functional inks and indicators for Smart Tag based intelligent packaging applications', *Journal of Applied Packaging Research*, 13(2), pp. 1–3. Available from: https://scholarworks.rit.edu/japr/vol13/iss2/3 [Accessed 27 September 2026].

Herma Sustainable Labels (2026) 'Labels made from recycled paper'. Available from: https://www.herma.com/label/products/sustainable-labels/labels-made-from-recycled-paper/ [Accessed 27 July 2026].

Jaszczak-Kuligowska, M., Sąsiadek-Andrzejczak, E., Safandowska, M., Kozicki, M., Florentino Madiedo, L., Barburski, M., Ranz, D. and Mallada, R. (2026) 'Thermochromic textile sensors for temperature measurements', *Measurement*, 257, 118698. DOI: 10.1016/j.measurement.2025.118698

Kavčič, U., Mraović, M., Bračko, S. and Muck, D. (2019) 'Printed thermochromic displays', *Coloration Technology*, 135(1), pp. 60–66. DOI: 10.1111/cote.12372

Kulčar, R., Friškovec, M., Hauptman, N., Vesel, A. and Klanjšek Gunde, M. (2010) 'Colorimetric properties of reversible thermochromic printing inks', *Dyes and Pigments*, 86(3), pp. 271–277. DOI: 10.1016/j.dyepig.2010.01.014

Lozo, B. (2012) 'Chromogenic indicators on packages'. In: *Innovative Packaging*. München: PTS, pp. 107–114.

Pu, Y. and Fang, J. (2022) 'Preparation and thermochromic behavior of low-temperature thermochromic microcapsule temperature indicators', *Colloids and Surfaces A: Physicochemical and Engineering Aspects*, 653, 129889. DOI: 10.1016/j.colsurfa.2022.129889

Tomašegović, T., Mahović Poljaček, S., Strižić Jakovljević, M. and Marošević Dolovski, A. (2021) 'Properties and Colorimetric Performance of Screen-Printed Thermochromic/UV-Visible Fluorescent Hybrid Ink Systems', *Applied Sciences*, 11(23), 11414. DOI: 10.3390/app112311414

Viková, M. and Vik, M. (2023) 'Transition Temperature of Color Change in Thermochromic Systems and Its Description Using Sigmoidal Models', *Materials*, 16, 7478. DOI: 10.3390/ma16237478

Vukoje, M., Krajnović, I., Kulčar, R., Cigula, T., Itrić Ivanda, K. and Jamnicki Hanzer, S. (2023) 'PCL Nanomodified Coating for the Protection of Thermochromic Prints on Packaging', *Materials Proceedings*, 14(1), 51. DOI: https://doi.org/10.3390/IOCN2023-14497

Zhao, Y. and Li, L. (2019) 'Colorimetric properties and application of temperature indicator thermochromic pigment for thermal woven textile', *Textile Research Journal*, 89(15), pp. 3098–3111. DOI: 10.1177/0040517518805390

© 2026 Authors. Published by the University of Novi Sad, Faculty of Technical Sciences, Department of Graphic Engineering and Design. This article is an open access article distributed under the terms and conditions of the Creative Commons Attribution license 4.0 Serbia (http://creativecommons.org/licenses/by/4.0/rs/).

Review Paper https://doi.org/10.24867/GRID-2026-p10

Comprehensive Review of Technical and Material Factors Influencing Offset Print Quality

ABSTRACT

Offset print quality emerges from coupled interactions among standardized process control, substrate structure and surface chemistry, ink formulation and rheology, and post-print finishing. Although these factors are frequently investigated separately, their combined influence on ink transfer, film formation, tone value increase, gloss, colour stability, and final visual appearance remains insufficiently synthesized. This critical review evaluates the technical and material factors governing offset print quality through an integrated process-material perspective. It examines the role of ISO 12647-2-based process control and objective measurement, then compares evidence concerning paper grammage, roughness, porosity, coating composition, surface wettability, ink formulation, ink sequence, varnishing, and drying or curing methods. Particular attention is given to the mechanisms that connect substrate properties and ink behaviour, including wetting, capillary penetration, pigment retention, ink setting, film levelling, and optical changes caused by transparent finishing layers. The review shows that individual indicators such as grammage, roughness, or water contact angle cannot independently predict printability because their effects depend on coating structure, surface-energy components, ink-vehicle polarity, dampening conditions, and ink rheology. It further identifies limitations in the current literature, including inconsistent characterization methods, insufficient separation of aqueous and non-aqueous wetting behaviour, and limited integration of sustainability and end-of-life criteria. The review concludes that high quality and sustainable offset printing requires both standards based measurement and a mechanism oriented understanding of material–process interactions.

Spomenko Kešina
Irma Horvat
Dean Valdec
Petar Miljković

University North,
Varaždin, Croatia

KEY WORDS
Critical review, ink formulation, ISO 12647-2, offset printing, paper properties, print quality, surface coatings, surface wettability

1. Introduction

Achieving consistent and high quality results in offset printing is a persistent challenge because print quality emerges from the interaction of press conditions, colour management procedures, substrates, inks, fountain solution, and finishing processes (Özakhun, Zelzele & Özcan, 2012). Parameters such as colour difference, solid ink density, tone value increase, trapping, gloss, print contrast, and grey balance are therefore not independent quality attributes. Instead, they are observable outcomes of coupled material-process interactions.

ISO 12647-2 provides an important basis for controlling offset lithographic production through defined targets, tolerances, substrates, screening conditions, and measurement procedures. However, standards-based control alone does not explain why identical nominal settings can produce different results on different paper grades, coating structures, ink systems, or finishing combinations. For this reason, reliable process control must be sup-

ported by an understanding of the physical and chemical mechanisms governing ink transfer, ink setting, pigment retention, film levelling, and optical light scattering.

Despite the extensive body of research on individual aspects of offset printability, the literature remains fragmented across process standardization, substrate engineering, ink formulation, and post print finishing. Studies often report changes in optical density, tone value increase, gloss, or colour difference under specific experimental conditions, but the mechanisms connecting these outcomes are not always evaluated consistently. In particular, the effects of surface topography, pore structure, surface free energy, ink rheology, setting behaviour, and transparent finishing layers are frequently treated as separate variables, although they jointly govern ink transfer, film formation, light scattering, and final colour appearance.

Therefore, this review critically examines the technical and material factors governing offset print quality through an integrated process-material framework. Rather than only compiling reported results, the review compares the conditions under which findings converge or diverge, identifies the physical mechanisms proposed to explain these effects, and highlights limitations in the current evidence. The review focuses on four interdependent domains: (i) standards-based process control and colour measurement, (ii) paper and coating properties, (iii) ink formulation, rheology, and ink sequence, and (iv) varnishing, coating, and drying processes.

The objectives are to: (1) identify the dominant material and process variables affecting colour reproduction, tone value increase, gloss, and print uniformity; (2) explain the mechanisms through which those variables interact; (3) evaluate where findings are substrate or process specific and cannot be generalized directly; and (4) define research gaps relevant to sustainable, high fidelity offset printing. By linking standards based control with material-process interactions, the review aims to provide a more coherent basis for future experimental work and industrial process optimization.

The literature was identified through searches of scholarly databases and publisher platforms using combinations of the terms “offset printing,” “print quality,” “ink transfer,” “paper coating,” “surface energy,” “tone value increase,” “colour management,” “varnishing,” and “UV curing.” Priority was given to peer-reviewed publications, international standards, and recent studies addressing mechanisms or measurement based evaluation. Earlier foundational studies were retained where they introduced methods or concepts still used in contemporary research. The review is narrative and critical rather than meta-analytical; consequently, differences in experimental design, substrate class, ink system, measurement geometry, and finishing conditions are explicitly considered when interpreting findings.

2. Quality standards and assurance in offset and digital printing

Achieving consistent and high-quality print production requires the systematic application of international standards, measurement protocols, and quality assurance frameworks. In offset lithography, ISO 12647-2 provides a central framework for process control by specifying target values, tolerances, substrates, screening conditions, proofing requirements, and measurement procedures for colour reproduction. This standard defines target values and tolerances for essential quality indicators such as CIE Lab* color values, solid ink densities, tone value increase (dot gain), print contrast, trapping, and gray balance, as well as requirements for substrates, screening, and measurement methods (International Organization for Standardization, 2013). By following these guidelines, print results are visually and metrically consistent across different runs and facilities, with Table 1 in ISO 12647-2 2013 providing CIELAB coordinates and gloss values for typical paper types as a key reference for substrate selection and process control.

Table 1

Print substrate specifications according to ISO 12647-2:2013 (International Organization for Standardization, 2013)

Characteristics	Paper type and surface											
	PS1			PS2			PS3			PS4		
Type of surface	Premium coated			Improved coated			Standard glossy coated			Standard matte coated		
Mass-per-area[a] g/m²	80 to 250 (115)			51 to 80 (70)			48 to 70 (51)			51 to 65 (54)		
CIE Whiteness[b]	105 to 135			90 to 105			60 to 90			75 to 90		
Gloss[c]	10 to 80			25 to 65			60 to 80			7 to 35		
Colour[d]	Coordinates			Coordinates			Coordinates			Coordinates		
	L*	a*	b*	L*	a*	b*	L*	a*	b*	L*	a*	b*
White backing	95	1	-4	93	0	-1	90	0	1	91	0	1
Black backing	93	1	-5	90	0	-2	87	0	0	88	0	-1
Tolerance	±3	±2	±4	±3	±2	±2	±3	±2	±2	±3	±2	±2
Fluorescence[e]	moderate			low			low			low		

Characteristics	Paper type and surface											
	PS5			PS6			PS7			PS8		
Type of surface	Premium coated			Improved coated			Standard glossy coated			Standard matte coated		
Mass-per-area[a] g/m²	70 to 250 (120)			38 to 60 (56)			40 to 56 (49)			40 to 52 (45)		
CIE Whiteness[b]	140 to 175			45 to 85			40 to 80			35 to 60		
Gloss[c]	5 to 15			30 to 55			10 to 35			5 to 10		
Colour[d]	Coordinates			Coordinates			Coordinates			Coordinates		
	L*	a*	b*	L*	a*	b*	L*	a*	b*	L*	a*	b*
White backing	95	1	-4	90	0	3	89	0	3	85	1	5
Black backing	92	1	-5	87	0	2	86	-1	2	82	0	3
Tolerance	±3	±2	±2	±3	±2	±2	±3	±2	±2	±3	±2	±2
Fluorescence[e]	high			low			faint			faint		

Visual inspection remains useful for identifying gross defects, but it is insufficient as the sole basis for process control because visual judgement is influenced by illumination, observer adaptation, viewing geometry, and the absence of numerical tolerances. Objective measurement of CIE L*a*b* values, solid ink densi-

ty, tone value increase, trapping, grey balance, and print contrast enables deviations to be quantified and corrected systematically. The study conducted in an Egyptian printing house demonstrated that an offline quality control procedure based on ISO 12647-2 improved conformance without replacing existing equipment or materials (Mostafa, 2016).

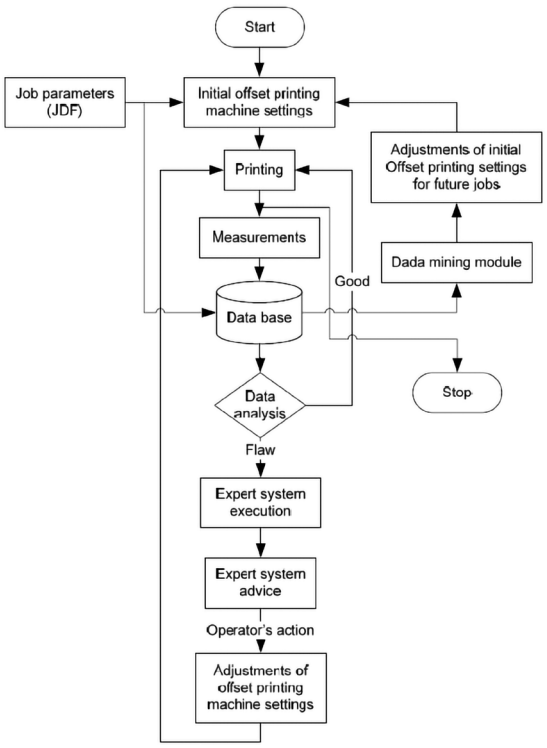
The reported improvement should be interpreted in relation to the specific press, substrate, RIP configuration, operator practice, and measurement protocol used in that study. It demonstrates the value of measurement based feedback, but it should not be generalized as a universal performance gain for all offset printing environments. More broadly, the evidence indicates that the greatest benefit of ISO based control arises when prepress linearization, characterization, press calibration, and production verification are treated as a continuous feedback loop rather than as isolated quality checks (Mostafa, 2016).

Table 2

Tone value inputs for RIP calibration and adjustment of reproduction curves to minimize tone value increase (Mostafa, 2016)

Dot %	Target Black %	Target Cyan %	Target Magenta %	Target Yellow %
0	0	0	0	0
2	1.5	1.5	1.5	1.5
5	3.8	3.5	3.8	3.5
10	7.5	7.7	7.7	7
20	14.7	14.5	14.7	14.2
25	18.3	18.2	18.7	18
30	22	22	22.8	22
40	29.5	30.5	32	30.5
50	37.5	40.8	42.5	40.3
60	46	50	53.2	50.5
70	55.2	60	63.8	60
75	59.8	65.2	68.8	64.5
80	64.5	70.8	74	69
90	75.5	82.8	86.5	79
95	82.9	91	93.5	86.3
100	0	0	0	0

Quality assurance frameworks can extend measurement based control by storing job parameters, press settings, measurement results, and corrective actions in a traceable database (Korytkowski, Olejnik-Krugły & Zaikin, 2009). Such systems allow deviations to be linked to recurring combinations of substrate, ink, press settings, and production conditions. In the framework (Figure 1) proposed by Korytkowski, Olejnik-Krugły and Zaikin (2009), measured data is analysed to identify a quality flaw, after which an expert system proposes corrective action and the resulting outcome is fed back into the database. The scientific value of this approach lies not only in automation, but in its potential to reveal causal patterns that are difficult to identify through isolated measurements. However, expert system recommendations are only as reliable as the quality, completeness, and representativeness of the recorded data. A system trained on one press, paper family, or ink set may not transfer directly to another production environment. Future work should therefore validate data-driven quality-control systems across multiple presses, substrates, and operating conditions.



» **Figure 1:** *Quality assurance framework algorithm (Korytkowski, Olejnik-Krugły & Zaikin, 2009)*

As demonstrated in a Croatian study, systematically measuring essential parameters, including density, dot gain, gray balance, and trapping with standardized control strips and devices is fundamental to optimizing and standardizing print reproduction. Through iterative adjustment of RIP curves and press settings, deviations from ISO targets are minimized (Valdec, Ivančić & Vusić, 2009). Emphasis is placed on starting quality control in prepress, not just during print production, resulting in a reproducible, high-quality process that aligns with international standards regardless of operator or machine variability. Taken together, the reviewed studies support a common conclusion: quality control should begin before production and continue throughout the printing workflow. Calibration curves and press adjustments are not universally transferable because they are influenced by the interaction of the RIP, screening method, plate,

ink set, fountain solution, press condition, substrate, and measurement instrument. Thus, standardization does not eliminate material variability; rather, it provides a controlled framework within which material specific behaviour can be measured, documented, and compensated (International Organization for Standardization, 2013; Korytkowski, Olejnik-Krugły & Zaikin, 2009; Mostafa, 2016; Valdec, Ivančić & Vusić, 2009).

3. Paper and surface effects on offset print quality

Paper affects offset print quality through a combination of bulk structure, surface topography, coating chemistry, pore geometry, compressibility, and liquid-uptake behaviour. Consequently, properties such as grammage, thickness, density, air permeability, and roughness should not be interpreted as independent causes of print-quality changes. In practical paper grades, these parameters are often correlated with one another and with unmeasured variables such as coating weight, pore-size distribution, binder distribution, and calendering intensity.

Tutuş, Yılmaz and Çiçekler (2017) reported that increasing grammage, thickness, and air permeability was associated with higher tone value increase, print contrast, and trapping, while print density could decrease. These outcomes should not be interpreted as evidence that grammage or thickness alone determines printability. A more open and compressible substrate structure can alter pressure distribution and ink-vehicle penetration, while the surface can retain or lose pigment differently depending on coating coverage and porosity. Thus, the relationships observed in the study are best understood as combined structural effects of the tested paper grades rather than universal causal effects of individual physical parameters (Havlínová et al., 2000; Sonmez et al., 2022).

Table 3 presents the measured grammage, thickness, and roughness values for the paper grades evaluated by Tutuş, Yılmaz and Çiçekler (2017); it also demonstrates that the compared papers differ in several physical characteristics simultaneously.

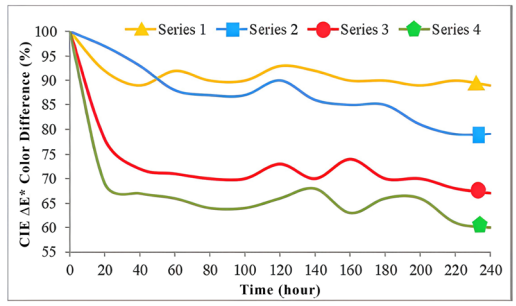
Surface roughness is an important but incomplete indicator of substrate suitability for offset printing. Smoother surfaces can improve the uniformity of ink transfer, promote more continuous ink film formation, and reduce diffuse scattering, thereby increasing apparent gloss and optical density. However, roughness measurements alone do not describe pore geometry, coating heterogeneity, or the chemical affinity between the ink vehicle and the substrate. These additional factors can determine whether ink remains near the surface, penetrates into the coating, or forms a non-uniform film.

Table 3

Physical properties of each tested paper (Tutuş, Yılmaz & Çiçekler, 2017)

Physical properties	Grammage (g/m^2)	Thickness (Micron)	Roughness (ml/min)
American Bristol 230gsm	224	300	2.4
American Bristol 350gsm	342	475	170
Coated Matt	115	90	0-3
Coated Gloss	115	110	5
I. High Grade 70gsm	70	85	302
I. High Grade 80gsm	78	100	366
II. Med Grade 48gsm	49	75	75
II. Med Grade 54gsm	54	83	104
III. Low Grade 70gsm	71	120	103
III. Low Grade 80gsm	81	85	339

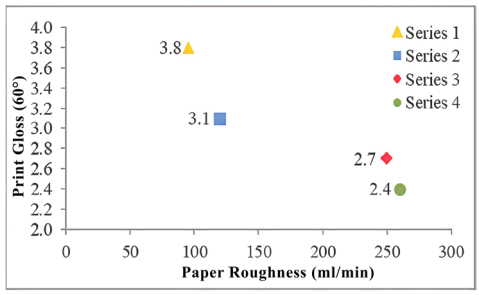
Aydemir et al. (2021) reported that the smoother uncoated papers examined in their study had lower water contact angles, higher measured surface energies, higher print gloss, and better colour stability. The finding is consistent with improved surface uniformity and aqueous wettability, but it should be interpreted carefully. Because the contact angle was measured using water, it primarily characterizes interaction with an aqueous liquid, not necessarily with the predominantly hydrophobic vehicle of conventional offset inks. The relationship between water wettability and offset ink setting therefore depends on the polar and dispersive components of surface energy, coating or fibre chemistry, pore structure, fountain-solution behaviour, and ink formulation (Hubbe, Gardner & Shen, 2015; Özakhun, Zelzele & Özcan, 2012). Figure 2 shows the time dependent colour difference behaviour of the tested paper samples and indicates that the observed colour stability was associated with their measured surface characteristics.



» **Figure 2:** *Impact of surface characteristics on ink color change (Aydemir et al., 2021)*

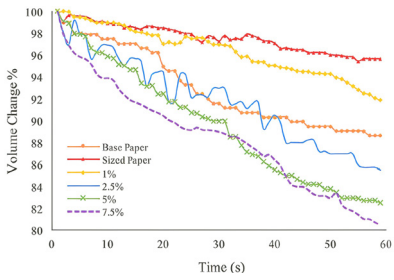
The combined evidence nevertheless suggests that a uniform, smooth, and well controlled substrate surface

is generally advantageous for gloss and colour stability (Aydemir et al., 2021). Future studies should pair roughness data with measurements of coating porosity, surface energy components, liquid penetration kinetics, and direct ink setting behaviour so that the mechanisms behind observed print quality differences can be separated more reliably. Figure 3 visualizes the association between paper roughness and print gloss for the investigated samples, supporting the view that a smoother surface can facilitate a more uniform reflective ink film.



» **Figure 3:** *Relationship between paper roughness and print gloss (Aydemir et al., 2021)*

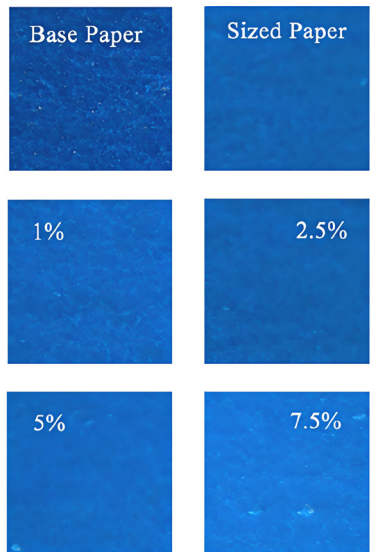
Surface coatings containing calcium carbonate ($CaCO_3$) pigment and cationic starch are used to tailor coating porosity, smoothness, liquid uptake, gloss, and printability (Kandirmaz et al., 2020). Their effect cannot be reduced to a single "absorbency" variable, because the coating controls both the chemical affinity of the surface and the capillary structure through which liquids penetrate. In the study of Kandirmaz et al. (2020), surface sizing increased the measured surface energy and reduced the water contact angle, indicating enhanced wettability toward water. This result should be interpreted primarily in relation to aqueous liquids and fountain solution interactions; it does not, on its own, demonstrate increased absorption of conventional oil based offset inks (Özakhun, Zelzele & Özcan, 2012). The changes in water drop volume observed for the differently treated paper surfaces are illustrated in Figure 4 and should likewise be interpreted as water related liquid uptake behaviour rather than as a direct measure of conventional offset-ink absorption.



» **Figure 4:** *Variation of water drop volume on papers with distinct surface treatments (Kandirmaz et al., 2020)*

A lower water contact angle may indicate a more hydrophilic surface, which can facilitate water uptake or interaction with the dampening solution (Aydemir et al., 2021; Kandirmaz et al., 2020). However, for solvent or oil based ink vehicles, the relevant variables include the dispersive and polar components of surface free energy and the contact angle of representative non polar liquids or the ink vehicle itself. A hydrophilic surface may not necessarily favour penetration of a hydrophobic vehicle; indeed, incompatibility can reduce wetting and retard ink setting. Therefore, conclusions about offset ink absorption should be supported by ink or oil specific contact angle measurements, liquid penetration tests, ink setting measurements, or direct printability measurements rather than water contact angle alone (Hubbe, Gardner & Shen, 2015).

In the study of Kandirmaz et al. (2020) as the $CaCO_3$ content increased, the reported surface energy decreased and the water contact angle increased. In a coating formulation, this trend may reflect changes in pigment packing, accessible binder at the surface, pore structure, and surface heterogeneity. At high pigment concentrations, inadequate dispersion or insufficient binder can promote agglomeration of $CaCO_3$ pigment particles. These agglomerates may increase roughness and create a non-uniform coating topography, potentially impairing ink-film levelling and lowering print gloss. However, the effect is formulation specific: $CaCO_3$ particle size, morphology, dispersant, latex or starch binder level, coating weight, drying conditions, and calendering all influence the final surface (Kandirmaz et al., 2020). Microscopic images of cyan solid tone prints produced on surfaces containing different $CaCO_3$ amounts are presented in Figure 5, illustrating how changes in coating formulation can be reflected in the local uniformity and visual appearance of the printed ink film.



» **Figure 5:** *Cyan solid tone print on different surfaces under 90x magnification (Kandirmaz et al., 2020)*

The practical implication is that water contact angle should not be used as a stand-alone indicator of offset printability. A rigorous evaluation should combine water and non polar liquid wetting measurements with porosity or liquid uptake tests, surface-topography characterization, ink setting assessment, optical density, gloss, tone value increase, and colour-difference measurements. Such a multi parameter approach would distinguish whether a change in print quality is driven primarily by interfacial wetting, capillary penetration, pigment retention at the surface, or ink-film levelling.

The optimum coating formulation must balance surface smoothness, porosity, chemical affinity, mechanical integrity, and ink setting behaviour. Cationic starch can contribute to surface consolidation and smoothness, but the resulting printability depends on the amount of starch, its interaction with pigments and binders, the final pore structure, and the polarity of the liquid contacting the surface (Kandirmaz et al., 2020). Therefore, neither greater hydrophobicity nor greater hydrophilicity should be considered intrinsically favourable without reference to the specific ink vehicle and fountain solution system.

Print gloss is a perceptual and optical indicator strongly influenced by the smoothness and continuity of the printed ink film. Coating composition, coating weight, solids content, pigment packing, supercalendering conditions, and internal or surface sizing can all influence gloss because they modify surface topography and the extent to which the ink film can level before setting.

Elsayad et al. (2001) reported that higher supercalendering pressure and temperature, increased coating solids, and thicker coating films enhanced print gloss. These findings are consistent with the mechanism that a smoother and more uniform coating permits more regular ink transfer and ink film leveling, reducing micro scale surface irregularities that scatter light diffusely. Conversely, high mechanical pulp content or excessive internal sizing can increase roughness or modify liquid uptake, thereby reducing gloss. The reported benefit of plastic pigment in calcium carbonate based coatings further illustrates that gloss depends not simply on pigment chemistry, but on the packing, deformability, and surface forming behaviour of the complete coating formulation (Kandirmaz et al., 2020; Sonmez et al., 2022).

4. Ink formulation, sequence, and interaction with substrates in offset printing

Ink formulation and substrate properties must be considered as an interacting system rather than as separate determinants of offset print quality. During printing, the ink splits between rollers, plate, blanket, and substrate. The ink vehicle may penetrate the coating or paper structure while pigment and binder components remain at or near the surface. The balance between transfer, setting, penetration, and film levelling is influenced by ink viscosity, tack, thixotropy, pigment concentration, vehicle polarity, substrate roughness, porosity, coating chemistry, and press conditions.

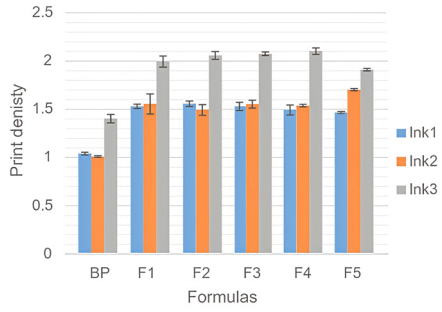
Studies of kaolin and precipitated calcium carbonate (PCC) coatings show that a greater proportion of kaolin can improve surface smoothness, print gloss, and print density (Sonmez et al., 2022). However, the outcome should not be attributed to pigment identity alone. Kaolin and PCC differ in morphology, packing behaviour, pore structure, and interactions with the latex binder. These characteristics influence the distribution of the ink vehicle and the extent to which pigment remains close to the surface, both of which affect optical density and gloss (Sonmez et al., 2022). Table 4 presents the kaolin-PCC formulation gradient used in the cited study, with latex content held constant, and therefore provides the material basis for comparing the resulting print density and gloss behaviour.

Table 4

Coating formulations of coated cardboard samples (Sonmez et al., 2022)

Coatings	F1	F2	F3	F4	F5
Kaolin	-	30	50	70	100
PCC	100	70	50	30	-
Latex	10	10	10	10	10

The finding that UV inks produced the highest density and gloss in the reviewed coating study is also mechanistically plausible because rapid curing can preserve a continuous, high solids ink film at the surface (Sonmez et al., 2022). Nevertheless, comparisons between UV, mineral oil based, and vegetable oil based inks must account for differences in curing mechanism, ink film thickness, substrate compatibility, colourant formulation, and measurement time. Plant derived inks may offer environmental advantages, but their performance should be evaluated using the full set of relevant criteria: colour reproduction, gloss, rub resistance, drying or curing energy, VOC emissions, migration requirements where applicable, deinkability, and recyclability. Figure 6 compares the print density measurements obtained for the different coating formulations and ink systems, showing that the observed optical response reflects the combined effects of pigment composition and ink type rather than a single coating variable.

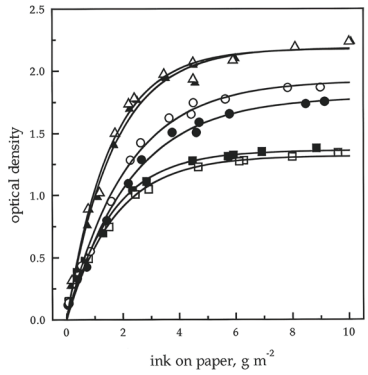


» **Figure 6:** *Print density measurements of coated cardboard samples with various formulations (Sonmez et al., 2022)*

Offset inks are viscoelastic, pseudoplastic, and thixotropic materials, and these rheological properties influence both transfer and film formation (Havlínová et al., 2000; Jasurek et al., 2018). High enough tack is needed for stable transfer through the inking train, but excessive tack can increase picking risk or undesirable ink splitting on weak or porous substrates (Jasurek et al., 2018). Viscosity and thixotropy determine how the ink responds under the high shear conditions of printing and how it levels after transfer. Therefore, a reported print-density or gloss difference cannot be attributed to substrate properties alone when ink rheology differs.

The ink mileage models applied by Havlínová et al. (2000) showed that smoother, brighter, and less absorbent papers reached higher saturation densities with more efficient ink transfer. This result supports the view that substrates capable of retaining pigment near the surface tend to produce higher optical density. However, reduced absorbency is not universally advantageous. If ink setting is too slow, it can create problems with set off, trapping, drying, or production speed. Optimal substrate behaviour therefore requires a balance between sufficient surface retention for optical performance and sufficient vehicle uptake or curing for stable production. The substrate dependent ink mileage curves and their different saturation density plateaus are illustrated in Figure 7, based on IGT black offset-ink tests modelled using the Tollenaar-Ernst equation (Havlínová et al., 2000).

The vehicle composition of offset inks influences wetting, penetration, setting, gloss, lightfastness, cleaning behaviour, VOC emissions, and suitability for specific applications. Aydemir et al. (2018) reported that linseed soybean based ink produced the highest gloss in their experiment, whereas mineral oil based ink showed greater resistance to fading on coated paper. In the same study, soy-based ink produced lower gloss values. These findings demonstrate that oil source can affect visual performance, but they should not be generalized as universal rankings because the outcome also depends on pigment composition, resin system, drying additives, substrate coating, ink-film thickness, and measurement conditions.



» **Figure 7:** *Ink mileage curves for several paper types, calculated via the Tollenaar-Ernst equation from IGT black offset ink tests. The symbols denote specific sides of each substrate: OC (■ top, □ bottom), SP (● top, ○ bottom), and SA 2:M (▲top, △ bottom) (Havlínová et al., 2000)*

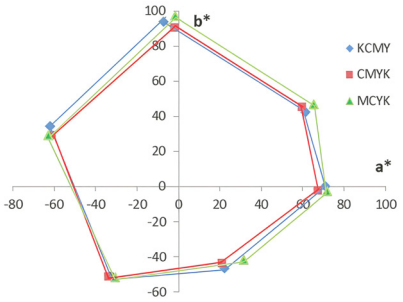
Vegetable oil based inks can reduce dependence on petroleum derived vehicles and may offer lower VOC emissions or easier cleaning in certain formulations (Aydemir et al., 2018). However, “bio based” does not automatically mean superior environmental performance or universal suitability for food packaging. A robust comparison should consider the complete formulation, drying mechanism, migration behaviour where relevant, emissions, energy use, recyclability, deinkability, and end-of-life effects alongside print quality metrics.

Ink sequence can influence colour gamut, density, contrast, and trapping because each subsequently printed ink interacts with an underlying ink film whose tack, setting state, and surface condition are changing during the press run. The magnitude of this effect depends on whether printing occurs under predominantly wet-on-wet or wet-on-dry conditions, as well as on the tack sequence of the ink set, ink film thickness, substrate absorption, and press speed (Nguye, 2024; Solanki, Jangra & Garg, 2016).

On Maplitho paper, YMCK and MYCK sequences produced higher red and orange density values than CMYK and KCMY in the reviewed experiment (Solanki, Jangra & Garg, 2016). However, the effect was smaller for green and brown. This pattern suggests that ink order does not affect all overprint colours equally; its influence is strongest where the relevant colour is sensitive to trapping efficiency and the optical contribution of the underlying ink layers.

The comparison between coated and uncoated papers further illustrates the importance of substrate dependent setting behaviour. On coated paper, MCYK sequences

produced a more extensive colour gamut, particularly in the red region, whereas uncoated paper showed smaller differences among sequences because rapid absorption reduced the duration of wet-on-wet interaction (Nguye, 2024). Thus, sequence optimization is most likely to be beneficial on less absorbent coated substrates, where ink trapping and interlayer interaction remain significant. It should not be assumed that a single preferred sequence applies to all papers, inks, or image contents. The colour gamut differences among the tested ink sequences on coated paper are illustrated in Figure 8, supporting the conclusion that sequence effects become more apparent when wet-on-wet trapping and interlayer interactions remain significant.

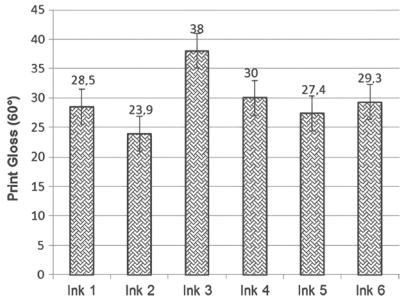


» **Figure 8:** *Color gamuts at different color sequences on coated papers (Nguye, 2024)*

Colour mixing components such as transparent and opaque white modify the rheology, optical opacity, and film forming behaviour of process inks. Transparent white can increase viscosity and tack, while also allowing greater optical contribution from the underlying substrate or ink layer. Opaque white introduces stronger light scattering and can reduce apparent chroma or gloss depending on the formulation and substrate (Aydemir et al., 2017).

In the reviewed study, mixtures containing a higher proportion of transparent white produced higher gloss and colour density than mixtures containing more opaque white (Aydemir et al., 2017). This result is consistent with improved ink film continuity and lower optical scattering, but the optimum mixture remains application specific. A formulation selected for high gloss may not be optimal for opacity, colour matching, surface uniformity, or print stability. The variation in print gloss among the tested ink mixtures on matt-coated paper is shown in Figure 9, illustrating that changes in colour mixing components can alter the optical appearance of the printed surface.

Ink consumption is a critical technical, economic, and environmental variable. Increasing ink quantity beyond the level required for target colour reproduction can prolong drying, increase set off risk, raise energy use, and increase material consumption without producing a proportional visual benefit. In the experiment reported by Aydemir, Yenidoğan and Özsoy (2020), an ink amount of 0.752 g/m² corresponded to a print density of 1.40 and the lowest reported ΔE*ab value of 3.13.



» **Figure 9:** *Print gloss values of inks on matt coated papers (Aydemir et al., 2017)*

This numerical optimum should be understood as specific to the ink, substrate, press conditions, and measurement setup used in that study. It should not be transferred directly to other printing systems. The broader conclusion is that ink-film thickness should be optimized against defined colour targets and production constraints rather than increased indiscriminately. Future research should combine ink-consumption measurements with drying kinetics, rub resistance, set-off, VOC emissions, and recyclability indicators in order to identify genuinely sustainable operating windows.

5. Coating, varnishing, and surface treatments

Coatings, varnishes, and laminating films can protect the printed surface and modify its gloss, abrasion resistance, barrier properties, and tactile appearance. At the same time, a transparent finishing layer changes the optical path of incident and reflected light and can therefore alter colour coordinates, tone value increase, contrast, and the visual appearance of halftone structures. The resulting effect depends on varnish chemistry, refractive index, layer thickness, coverage, curing or drying conditions, substrate gloss, ink-film topography, and viewing geometry (Hébert, Dailliez & Simonot, 2021; Hoffstadt, 2004).

Hudika, Majnarić and Cigula (2020) reported that changing UV LED varnish coverage altered the b* coordinate, especially on light samples, and affected the optical appearance of the prints. The effect was more visually pronounced with gloss varnish because specular reflection contributed more strongly to the observed appearance. However, the reported overall colour differences remained within the ISO tolerances for the tested conditions, whereas the optimum print gloss was obtained at 100% varnish surface coverage. Rather than treating varnishing as a purely protective

operation, these findings show that finishing must be included in colour management and proofing decisions whenever colour critical reproduction is required.

Clear coatings and laminating layers can produce an optical "halo effect," in which light propagation through the transparent layer changes the apparent reflectance of halftone structures. The coating can smooth sharp optical transitions at dot edges and alter internal reflection, making halftones appear darker or producing an apparent increase in tone value. The magnitude of the effect depends on the halftone geometry, dot profile, coating thickness, refractive properties of the finishing layer, and the initial roughness of the printed surface (Hébert, Dailliez & Simonot, 2021).

This mechanism explains why finishing-induced changes are not uniform across all images. Prints with sharp halftone profiles and low initial tone value increase can be more sensitive to additional optical spreading, whereas prints already affected by substantial substrate related tone value increase may show a smaller relative change (Hébert, Dailliez & Simonot, 2021). Consequently, colour critical halftone work should be evaluated after the final finishing operation rather than only before varnishing or lamination.

In packaging applications, finishing decisions must balance colour fidelity, protection, ink coverage, production efficiency, and environmental requirements. Cigula, Hudika & Donevski (2022) showed that reducing ink coverage through grey component replacement did not necessarily compromise colour reproduction on varnished cardboard. Their results also indicated that UV varnish could produce greater tone value increase and higher colour differences in some tertiary colours than water-based or conventional offset varnishes.

The difference between varnish systems is consistent with their different film forming and optical properties. UV varnishes form rapidly cured layers that can substantially alter surface reflectance and apparent dot structure, whereas water based and conventional offset varnishes may produce smaller changes under comparable conditions (Cigula, Hudika & Donevski, 2022; Galić, Ljevak & Zjakić, 2015). However, the final effect remains dependent on coating weight, coverage, substrate roughness, ink formulation, curing conditions, and the colour being evaluated.

Spot colours require particular caution because their spectral reflectance is determined by the specific pigment mixture rather than by standard CMYK overprinting. UV varnishing, other varnish systems, and thermal lamination can alter gloss, saturation, metameric behaviour, and measured colour coordinates (Galić, Ljevak & Zjakić, 2015; Galić, 2017). Therefore, a spot colour specification should define not only the ink formulation and substrate, but also the intended finishing process, measurement geometry, backing condition, and viewing conditions.

Comparative simulations by Hoffstadt (2004) indicated that film coatings can cause stronger apparent tone value increase than varnishes, particularly at low nominal dot values. In the reported results, UV varnish caused an additional tone value increase of approximately 3–6%, dispersion varnish remained below 3%, and OPP film coatings produced substantially larger values, exceeding 12% at dot areas around 20%.

Although these values are useful for illustrating the relative optical influence of finishing systems, they should not be used as fixed compensation values in other workflows. The magnitude of finishing-induced tone value increase depends on the imaging structure, ink film topography, substrate, coating thickness, measurement condition, and film or varnish formulation. Nevertheless, the evidence supports a practical requirement: finishing-related compensation should be determined experimentally for each colour critical production combination (Hébert, Dailliez & Simonot, 2021; Hoffstadt, 2004).

The mechanisms behind finishing-related colour changes are closely connected to the condition of the underlying ink and coating layers. Coating porosity and topography influence ink setting and the uniformity of the printed film; ink viscosity and surface tension influence film levelling; and a transparent finish changes the way light interacts with the resulting microstructure. Non uniform coatings can create uneven ink setting and mottling, while an irregular ink film can produce spatial variations in gloss and colour. For this reason, finishing quality cannot be fully controlled at the finishing stage alone. It begins with the compatibility of the substrate, ink, press conditions, and pre-finish print surface (Hébert, Dailliez & Simonot, 2021; Sonmez et al., 2022).

Drying conditions during surface sizing and coating can alter the final substrate structure and thereby influence subsequent print behaviour. Yenidoğan et al. (2019) reported that oven drying produced more pronounced colour changes and lower gloss than air drying in their tested materials, whereas air drying increased surface wettability and print gloss. These results may be related to drying induced changes in binder migration, pore structure, surface chemistry, or coating stress, but the available evidence does not establish a universal ranking of drying methods.

The most appropriate drying method therefore depends on the required balance between liquid resistance, coating integrity, surface smoothness, ink setting, and final optical appearance. Because increased water wettability does not necessarily mean improved wetting by hydrophobic offset-ink vehicles, future drying studies

should distinguish water-related behaviour from ink vehicle penetration and should evaluate the complete printing system rather than the paper surface alone Hubbe, Gardner & Shen, 2015; Yenidoğan et al., 2019).

UV-curable inks and lacquers offer rapid curing, high surface gloss, and potential reductions in conventional solvent emissions (Oguz, Ozcan & Oktav, 2012). However, their performance and environmental value depend on formulation, photoinitiator chemistry, curing dose, substrate compatibility, residual-monomer or migration requirements where relevant, deinkability, and energy use. The rapid formation of a cured surface film can be advantageous for productivity and gloss, but it can also increase sensitivity to layer thickness and optical effects in colour-critical work (Hébert, Dailliez & Simonot, 2021; Oguz, Ozcan & Oktav, 2012).

Coatings and varnishes should be treated as active components of the print system rather than as post print additions. Their selection must be based on measured effects on colour, gloss, tone value increase, mechanical protection, substrate compatibility, production efficiency, and end-of-life requirements.

6. Research gaps and future directions

Although the reviewed literature confirms the importance of substrate, ink, and finishing variables, several limitations restrict direct comparison and generalization across studies.

Many investigations isolate one variable, such as roughness, coating pigment, or ink-oil type, while the practical offset process involves strongly coupled interactions among substrate porosity, surface chemistry, dampening conditions, ink rheology, printing pressure, and drying or curing. Future research should employ multifactorial experimental designs and report process variables in sufficient detail to support comparison (Aydemir et al., 2021).

Water contact angle is frequently used as a proxy for printability. Although it is useful for characterizing aqueous wettability, it is not sufficient to predict the setting or penetration of hydrophobic offset-ink vehicles. Future work should distinguish aqueous and non-aqueous interfacial behaviour through component-resolved surface-free-energy analysis, contact-angle measurements with liquids of different polarity, and direct ink-setting or penetration measurements (Aydemir et al., 2021).

The relationship between coating structure and visual appearance requires more standardized characterization. Surface roughness values alone cannot capture pore geometry, coating heterogeneity, pigment packing, or binder distribution (Elsayad et al., 2001; Kandirmaz et al., 2020; Sonmez et al., 2022). Combining profilometry or atomic-force microscopy with porosimetry, optical microscopy, and spectrophotometric print evaluation would provide a more complete explanation of mottle, gloss, density, and tone value increase.

Sustainable ink and coating systems require evaluation beyond their immediate optical performance. Vegetable-oil-based inks, water-based and UV/LED-curable varnishes, low-migration formulations, and recyclable or deinkable coating systems should be assessed simultaneously for colour stability, mechanical resistance, migration safety where relevant, VOC emissions, energy demand, recyclability, and compatibility with substrate recovery processes (Aydemir et al., 2018).

Digitalization of print quality control creates opportunities for more predictive process control. The combination of inline spectral measurement, job data archiving, colour management data, and machine learning models could enable early detection of deviations in ink density, tone value increase, trapping, or colour difference. However, such systems require transparent validation across press types, substrates, and environmental conditions before their industrial adoption can be generalized.

7. Conclusion

Offset print quality is not determined by any isolated material or process parameter. It emerges from coupled interactions between standardized process control, substrate topography and pore structure, surface chemistry, ink rheology and setting behaviour, ink sequence, and post-print finishing. ISO 12647-2 remains a central framework for reproducible colour control, but conformance requires measurement based calibration combined with a material specific understanding of the print system (International Organization for Standardization 2013; Korytkowski, Olejnik-Krugły & Zaikin, 2009; Mostafa 2016).

The available evidence supports the general advantages of smooth, well controlled coating surfaces for ink transfer, pigment retention, gloss, and colour stability (Aydemir et al., 2021; Havlínová et al., 2000; Sonmez et al., 2022). However, common indicators such as grammage, air permeability, roughness, or water contact angle should not be interpreted independently. Their relationship with print quality depends on pore structure, coating formulation, surface energy components, fountain solution interactions, ink vehicle polarity, and ink film formation (Kandirmaz et al., 2020; Tutuş, Yılmaz & Çiçekler, 2017). In particular, low water contact angle indicates improved aqueous wettability, but does not automatically

predict favourable setting or absorption of hydrophobic offset inks (Aydemir et al., 2021; Kandirmaz et al., 2020).

Ink formulation and ink sequence can influence density, gloss, trapping, and achievable colour gamut, but their effects are conditional on the substrate and press environment (Aydemir et al., 2018; Nguye, 2024; Solanki, Jangra & Garg, 2016). Similarly, varnishes, laminations, and UV-curable systems must be recognized as optical as well as protective layers because they can alter colour coordinates, tone value increase, and halftone appearance (Cigula, Hudika & Donevski, 2022; Hébert, Dailliez & Simonot, 2021; Hudika, Majnarić & Cigula, 2020). Therefore, colour critical quality assessment should be performed on the final, finished print whenever finishing is part of the intended product.

The review further indicates that environmentally preferable printing materials cannot be assessed only by immediate density or gloss (Aydemir et al., 2018; Cigula, Hudika & Donevski, 2022; Oguz, Ozcan & Oktav, 2012). Future research and industrial evaluation should integrate optical performance, mechanical resistance, drying or curing energy, VOC emissions, migration safety where relevant, recyclability, deinkability, and end-of-life effects. More recent, mechanism oriented, and statistically robust studies are needed to connect laboratory surface characterization with full-scale press performance. A future research agenda should therefore prioritize standardized multi-parameter methods, multifactorial experiments, and validated data-driven quality-control systems capable of predicting print performance across substrate and ink classes.

8. Acknowledgement

This research was supported by the European Union through the project “Strategic Partnership for Research and Development of Smart Products and Services to Increase the Efficiency of Production, Work, and Use of Resources Using Advanced Digital Technologies-GrafIT” grant number IP.1.1.03.0065.

9. References

Aydemir, C., Kašiković, N., Horvath, C. and Durdevic, S. (2021) 'Effect of paper surface properties on ink color change, print gloss and light fastness resistance', *Cellulose Chemistry and Technology*, 55(1–2), pp. 133–139. DOI: 10.35812/CelluloseChemTechnol.2021.55.14

Aydemir, C., Yenidoğan, S., Karademir, A. and Arman Kandirmaz, E. (2017) 'Effects of color mixing components on offset ink and printing process', *Materials and Manufacturing Processes*, 32(11), pp. 1310–1315. DOI: 10.1080/10426914.2017.1279323

Aydemir, C., Yenidoğan, S., Karademir, A. and Arman Kandirmaz, E. (2018) 'The examination of vegetable- and mineral oil-based inks’ effects on print quality: Green printing effects with different oils', *Journal of Applied Biomaterials & Functional Materials*, 16(3), pp. 137–143. DOI: 10.1177/2280800018764761

Aydemir, C., Yenidoğan, S. and Özsoy, S. A. (2020) 'Effects of ink consumption on print quality on coated cellulose-based paper surfaces', *Cellulose Chemistry and Technology*, 54(1–2), pp. 89–94. DOI: 10.35812/CelluloseChemTechnol.2020.54.10

Cigula, T., Hudika, T. and Donevski, D. (2022) 'Color reproduction on varnished cardboard packaging by using lower ink coverages due to the gray component replacement image processing', *Color Research & Application*, 47(1), pp. 172–181. DOI: 10.1002/col.22704

Elsayad, S., El-Sherbiny, S., Morsy, F., Wiseman, N. and El-Saied, H. (2001) 'Effect of some paper coating parameters on print gloss of offset prints', *Surface Coatings International Part A*, 84(3), pp. 1–6.

Galić, E. (2017) *Kolorimetrija spotnih boja kod različitih postupaka lakiranja*. PhD thesis. University of Zagreb, Faculty of Graphic Arts.

Galić, E., Ljevak, I. and Zjakić, I. (2015) 'The Influence of UV Varnish on Colorimetric Properties of Spot Colors'. In: Katalinic, B. (ed.) *Procedia Engineering, 25th DAAAM International Symposium on Intelligent Manufacturing and Automation*, DAAAM 2014, 26–29 November 2014, Vienna, Austria. Amsterdam, Elsevier Ltd., pp. 1532–1538. DOI: 10.1016/j.proeng.2015.01.525

Havlínová, B., Hornáková, L., Brezová, V., Liptáková, Z., Kindernay, J. and Jančovičová, V. (2000) 'Ink receptivity on paper- characterization of paper materials', *Colloids and Surfaces A: Physicochemical and Engineering Aspects*, 168, pp. 251–259. DOI: 10.1016/S0927-7757(00)00489-1

Hébert, M., Dailliez, F. and Simonot, L. (2021) 'Why a clear coating modifies halftone color prints'. In: Hébert, M., Simonot, L., Sole, A. S. and Tastl, I. (eds.) *Material Appearance 2021*, 11–28 January 2021, online. Springfield, Society for Imaging Science and Technology, pp. 131-1–131-8. DOI: 10.2352/ISSN.2470-1173.2021.5.MAAP-131

Hoffstadt, J. (2004) 'Simulating color changes due to coating of offset prints'. In: *Conference on Colour in Graphics, Imaging, and Vision: CGIV 2004 Proceedings*, 5–8 April 2004, Aachen, Germany. Springfield, VA, USA, Society for Imaging Science and Technology, pp. 489–493. DOI: 10.2352/CGIV.2004.2.1.art00098

Hubbe, M. A., Gardner, D. J. and Shen, W. (2015) 'Contact angles and wettability of cellulosic surfaces: A review of proposed mechanisms and test strategies', *BioResources*, 10(4), pp. 8657–8749.

Hudika, T., Majnarić, I. and Cigula, T. (2020) 'Influence of the varnishing "surface" coverage on optical print characteristics', *Technical Journal*, 14(4), pp. 428–433. DOI: 10.31803/tg-20191129104559

International Organization for Standardization. (2013) ISO 12647-2:2013. Graphic technology – Process control for the production of half-tone colour separations, proof and production prints – Part 2: Offset lithographic processes. Geneva, Switzerland, International Organization for Standardization.

Jasurek, L., Vališ, M., Syrový, T. and Jablonovský, J. (2018) 'Study of rheological properties and tack of offset printing inks', *International Circular of Graphic Education and Research*, 11, pp. 37–43.

Kandirmaz, E. A., Yenidoğan, S., Aydemir, C. and Karademir, A. (2020) 'Effect of using calcium carbonate (CaCO3) in surface coating on liquid absorption of paper and some printability parameters', *Cellulose Chemistry and Technology*, 54(5–6), pp. 485–493. DOI: 10.35812/CelluloseChemTechnol.2020.54.49

Korytkowski, P., Olejnik-Krugły, A. and Zaikin, O. (2009) 'A framework for a quality assurance in offset printing'. In: Bakhtadze, N. and Dolgui, A. (eds.) *13th IFAC Symposium on Information Control Problems in Manufacturing*, 3–5 June 2009, Moscow, Russia. Amsterdam, Elsevier Ltd., pp. 1875–1880. DOI: 10.3182/20090603-3-RU-2001.0451

Mostafa, N. M. M. (2016) 'Printing Quality Enhancement According to ISO 12647-2 (Applying in One of Egyptian Printing-Houses)', *International Design Journal*, pp. 2–13.

Nguye, H. T. K. (2024) 'Ink sequence effects on color gamut in multicolor lithographic printing', *International Journal of Scientific Research in Science and Technology*, 11(3), pp. 602–606. DOI: 10.32628/IJSRST2411334

Oguz, M., Ozcan, A. and Oktav, M. (2012) 'Examination of the optimum use of UV lacquers and inks in the offset printing', *Asian Journal of Chemistry*, 24(11), pp. 5133–5136.

Özakhun, Ş. C., Zelzele, Ö. B. and Özcan, A. (2012) 'Analysis of the fountain solution in offset printing in terms of printability', *Asian Journal of Chemistry*, 24(2), pp. 641–645.

Solanki, V., Jangra, V. and Garg, S. K. (2016) 'Effect of ink sequence on print quality in offset printing', *International Journal of Innovative Trends in Engineering (IJITE)*, 15(1), pp. 29–36.

Sonmez, S., Gong, R., Fleming, P. D. III, Wu, Q. and Pekarovicova, A. (2022) 'The effects of the interaction of pigment coating with ink on the offset print quality', *Journal of Coatings Technology and Research*, 19(6), pp. 1851–1858. DOI: 10.1007/s11998-022-00656-4

Tutuş, A., Yılmaz, U. and Çiçekler, M. (2017) 'Effects of physical properties of some papers on offset printing quality'. In: *IV. International Multidisciplinary Eurasian Congress (IMCOFE)*, 23–25 August 2017, Rome, Italy. pp. 209–215.

Valdec, D., Ivančić, S. and Vusić, D. (2009) 'Kalibracija i karakterizacija reprodukcijskog procesa tiska na temelju ISO specifikacija', *Tehnički glasnik*, 3(1–2), pp. 20–24.

Yenidoğan, S., Aydemir, C., Karademir, A. and Kandirmaz, E. A. (2019) 'Examination of the impact of drying techniques in surface sizing-coating operations on the quality of paper and printing', *Cellulose Chemistry and Technology*, 53(3–4), pp. 325–331. DOI: 10.35812/CelluloseChemTechnol.2019.53.32



© 2026 Authors. Published by the University of Novi Sad, Faculty of Technical Sciences, Department of Graphic Engineering and Design. This article is an open access article distributed under the terms and conditions of the Creative Commons Attribution license 4.0 Serbia (http://creativecommons.org/licenses/by/4.0/rs/).

Original Scientific Paper https://doi.org/10.24867/GRID-2026-p11

Benchmarking Color Reproduction Quality: A Comparative Study of Digital Printing Systems

ABSTRACT

The article investigates one of the key challenges of modern reproduction technology—the quality of color reproduction, the overall efficiency of printing production largely depending on its accuracy and predictability. The study employs a comprehensive empirical and theoretical approach based on the instrumental measurement of colorimetric parameters and chromatic coordinates of experimental prints produced on different output systems. These measurements were used for mathematical modeling and for determining the actual limits of the color gamut of the equipment. The obtained results demonstrate that the Indigo digital printing press provides the widest and most stable color gamut among the analyzed systems. To ensure a comprehensive technical and economic evaluation of the technologies, the article also presents experimental data on production time for different print-run volumes and graphical representations of printing efficiency. The analysis proves that, according to time-related criteria, digital printing systems are superior for short print runs, whereas conventional offset equipment remains the most appropriate and technologically justified solution for large-volume production.

Tetyana Holubnyk
Olha Borysenko

Lviv Polytechnic National University, Lviv, Ukraine

KEY WORDS
Quality of color reproduction, digital systems, color gamut

1. Introduction

The current stage of color science development is characterized by a transition from classical three-dimensional colorimetry to multi-channel spectral analysis and the prediction of print parameters using artificial intelligence techniques. Direct analysis of printing limits and ink synthesis stability requires studying the influence of the physicochemical properties of substrates and expanding conventional color reproduction models.

One of the fundamental problems of modern printing remains ensuring highly accurate and reliable color reproduction at the stage of transition from the screen original to the physical print. The complexity of solving this problem is due to the fundamental difference between additive color synthesis in monitors (RGB system) and subtractive synthesis in printing processes (CMYK system). To achieve the expected quality of the finished product, the end-to-end technological process requires a clear definition of the limiting colorimetric capabilities of specific printing equipment within the "print–substrate–ink" system. Even under conditions of precise production standardization, the actual technological process is always accompanied by random and systematic fluctuations, which necessitates the establishment, control, and quantitative assessment of technological tolerance values for color deviations.

In order for printing results to be predictable, the designer must clearly understand which colors a printing house is capable of reproducing and take this into account during the design process. It is important to realize that even with the highest quality of the finished product, certain tolerances always exist, and their magnitude must be considered.

In this context, print quality is understood as the accuracy of reproducing a specified color, as well as the possible variations between prints at different stages of the process, i.e., the stability and predictability of the result. High quality implies minimal tolerances; however, they will always be present, and it is impossible to eliminate them completely, as this is an objective reality. This determines the feasibility, relevance and scientific novelty of the presented work.

2. Literature review

The study by Blahová et al. (2025) focuses on the analysis of color reproduction variations in high-speed industrial inkjet printing systems using papers with different coating types. The authors demonstrate that the structure of the coated layer significantly affects the geometry of the color gamut. To extend these limits in modern packaging production, expanded multi-color printing technologies are increasingly employed, as described in detail by Green et al. (2024). Their research presents an extended colorimetric analysis of Expanded Color Gamut (ECG) printing and highlights the specific features of color profile generation beyond the standard CMYK process.

When complex secondary substrates such as recycled cardboard are used, where color stability is often limited, (Zhu et al., 2024) justify the application of machine-learning models for the real-time prediction of color deviations. This approach emphasizes the growing importance of automated quality control in contemporary pressroom environments.

The development of precise spectral prediction models is addressed in the study by Fan et al. (2025), which proposes a multi-channel prediction model for printed products based on HMSSA-BP neural networks. The authors demonstrate that intelligent optimization of weighting coefficients significantly reduces colorimetric errors in the CIELAB color space. This approach is consistent with the concept of preserving the color structure of high-resolution images proposed by Pan et al. (2022) through residual dense neural networks.

An important contribution to objective quality assessment is the metric introduced by Urban et al. (2023), which is based on the simulation of the Human Visual System (HVS) for spectral color reproduction analysis. This method enables consideration of the nonlinear nature of human color perception. Consequently, the standardization of quality parameters requires a comprehensive approach to the preparation of both traditional printed and modern electronic products.

In the works of Ukrainian scientific schools, in particular Senkivskyy et al. (2023), information technologies for producing high-quality visual content for newspaper publications have been developed, where color stability is limited by the properties of microporous substrates with low whiteness. In contrast, the conceptual foundations of multimedia content evaluation are addressed in Havenko et al. (2025), where a conceptual information technology model for the comprehensive assessment of electronic book publication quality is proposed. The transformation of color parameters in modern display systems is studied by Kao et al. (2025) using color electronic paper with front illumination (Color Electronic Paper) as an example, while algorithms for the mathematical restoration and correction of color characteristics on liquid crystal displays are investigated by Jia et al. (2018).

The issue of tonal reproduction of high dynamic range images using cone response functions of the human visual system based on the CAM16 color appearance model is addressed in Choi et al. (2019), which is essential for accurate cross-media visualization. A classification and comparative analysis of modern mathematical color models for efficient search and encoding of graphical content is provided in Shamoi et al. (2022). Digital compensation of geometric distortions and enhancement of color field resolution using generative adversarial networks (GANs) is presented in Kawabata et al. (2023). Multispectral analysis of microstructures using high-resolution 4K cameras for precise capture of color characteristics is demonstrated in (Kobayashi et al., 2023). Adaptive filtering and color balance correction in distorted environments are effectively addressed using two-domain fusion modules proposed in Cao et al. (2026). The visual reproduction of symbolic sign systems in media technologies is investigated in Li et al. (2019).

In the article (Mika et al., 2025), an in-depth comparative study between modern sheet-fed offset printing and premium digital presses (including HP Indigo liquid toner technology) is conducted. The authors focus on the analysis of color deviations using metric-based approaches and demonstrate that modern digital electrophotography is not only comparable to offset printing in plate reproduction accuracy but also provides a wider color gamut in the high-cyan and magenta regions due to the unique physicochemical properties of liquid toners.

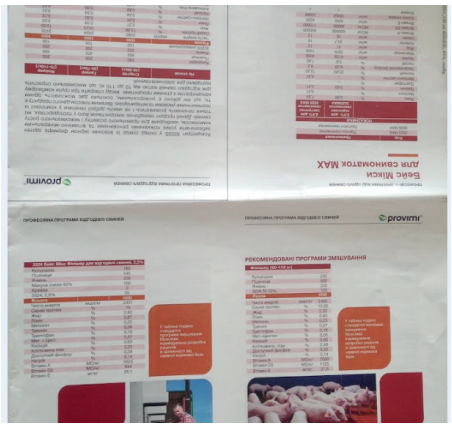
The work by García-Manrique et al. (2024) is directly related to the calculation and modeling of color volumes. The authors propose optimized algorithms for the rapid construction of ICC profiles of output devices by analyzing three-dimensional data arrays in the CIELAB space. They demonstrate that the combination of spectrophotometric control and mathematical approximation of print boundaries enables printing houses to dynamically reconfigure workflows (color workflows) in response to varying print run requirements without loss of colorimetric accuracy.

The study by Rovira et al. (2024) and Chen et al. (2024) addresses a topic that is critically important for this paper — technical and economic analysis and time-to-market. The researchers develop a mathematical model of production time that clearly differentiates efficiency zones of digital printing (where flexibility, fast setup, and the absence of plate-making processes dominate) and large-format offset systems (where high throughput compensates for prepress time). The authors determine the dynamic break-even point of print runs, which fully supports the analytical conclusions of this study and underlines its feasibility, relevance, and scientific novelty.

3. Research into the quality of color reproduction of digital and offset systems

At present, analog and offset color proofs in the printing industry have been almost completely replaced by digital color proofs, as the latter demonstrate excellent color reproduction while having significantly lower costs. Different monitors possess different color gamuts, and the same applies to printing on various types of substrates. For example, a color that can be reproduced on one type of paper may be impossible to reproduce on another. Even with a properly calibrated system and a correctly configured ICC profile, a color that lies outside the printer's gamut will be replaced by the closest reproducible color.

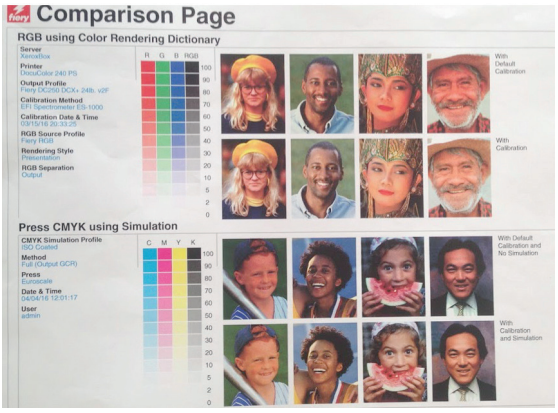
For the research, images output in various output systems were used as model images, namely: prints printed using the Heildenberg MOV offset printing method, digital machine HP Indigo press ws6800p, digital laser multifunction device Xerox DocuColor240PS and digital Konica Minolta bizhub C224.



» **Figure 1.** *Offset machine Heildenberg MOV*



» **Figure 2.** *Digital HP Indigo press ws6800p*



» **Figure 3.** *Digital Laser Multifunction Device*



» **Figure 4.** *Digital Konica Minolta bizhub C224*

To assess the color reproduction of different output systems during the study, Lab and xyY color coordinates were measured on experimental prints using Vip Spectra 2000. Measurement conditions D50, observation angle 2º, without polarizing filter, zeroing by paper color, substrate color white.

The empirical-theoretical method of studying color reproduction is based on the instrumental measurement

of print coordinates and their subsequent mathematical formalization in the form of spatial geometric models.

The advantage of the two-dimensional representation according to the CIE system is that, instead of describing color using three standard color values, X, Y, and Z, it can be represented by only two chromaticity coordinates, x and y, which characterize hue and saturation. Brightness is represented separately. The disadvantage of this representation is that it is valid only for a specific level of spectral brightness. If the spectral brightness changes, the standard color value Y must also be changed, resulting in a new diagram corresponding to that particular Y value.

To analyze the color reproduction capabilities of various printing systems and digital image preparation technologies, it is necessary to construct color gamuts on the CIE 1931 xyY chromaticity diagram. In this study, the color gamuts of the printing systems are compared with the color gamut of the Adobe RGB (1998) working color space.

3.1. Input data: xy chromaticity coordinates of experimental prints obtained from each printing system

The CIE 1931 xy chromaticity diagram was used to visualize and compare the color gamut boundaries of the evaluated printing systems against the reference Adobe RGB (1998) color space. Gamut boundaries were constructed using a 6-point chromatic vertex model comprising primary and secondary color patches (C, M, Y, R, G, B).

Spectrophotometrically measured XYZ tristimulus values for the printing systems and theoretical reference values for Adobe RGB (1998) were converted into CIE 1931 xy chromaticity coordinates using the Bruce Lindbloom Color Calculator under CIE D65 illuminant and 2º standard observer conditions, according to Eq. (1):

$$X = \frac{X}{X+Y+Z}, Y = \frac{Y}{X+Y+Z} \quad (1)$$

where X, Y, Z represent the tristimulus values, and x, y denote the calculated chromaticity coordinates.

The calculated chromaticity coordinates are summarized in Table 1. All data processing and 2D polygon constructions were carried out using Origin software (OriginLab Corp.).

Superimposing the reference Adobe RGB (1998) gamut onto the printed systems' polygons enables direct identification of color clipping, saturation limits, and hue shifts across specific color sectors during the printing process. Although the CIE xy space is perceptually non-uniform—particularly due to the visually extended green region—it provides a standardized, robust, and sufficient basis for the comparative evaluation of the investigated printing technologies.

Adobe RGB (1998) is used as the working space because it is the most commonly used monitor working space in Intel-based desktop publishing systems. Adobe RGB (1998) is a radical option for prepress. Its color coverage area almost completely includes the entire CMYK color range- pure cyan corresponds to approximately 98 percent cyan, 2 percent magenta and yellow, and the gamma of Table provides visual uniformity (Table 1).

Table 1

Adobe RGB (1998) has the following chromaticity coordinates

	X	Y
Red	0.6400	0.3300
Green	0.2100	0.7100
Blue	0.1500	0.0600
White	0.3127	0.3290

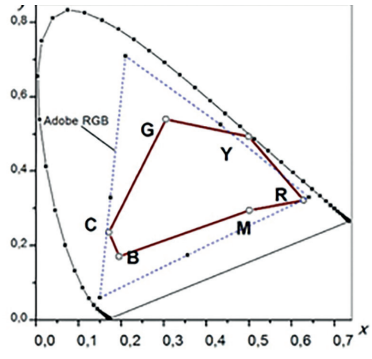
The calculated chromaticity coordinates for the 7 primary and secondary color vertices (C, M, Y, R, G, B) are summarized in Tables 2-5. All coordinate data were imported into Origin software (OriginLab Corp.) to generate 2D chromaticity polygons and perform comparative visual.

Table 2

Digital printing on the machine Konika Minolia Bizhub C 224

	X	Y
Cyan	0,171	0,235
Blue	0,195	0,171
Magenta	0,501	0,295
Red	0,628	0,322
Yellow	0,499	0,493
Green	0,305	0,54

We construct color coverings based on color coordinates.

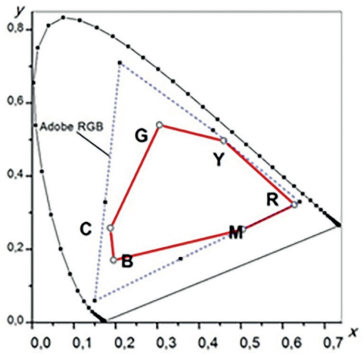


» **Figure 5:** *Color gamut on the machine Konika Minolia Bizhub c224*

Table 3

HP Indigo press ws6800p

	X	Y
Cyan	0,187	0,258
Blue	0,195	0,171
Magenta	0,504	0,254
Red	0,628	0,322
Yellow	0,459	0,497
Green	0,305	0,54
Green	0,305	0,54

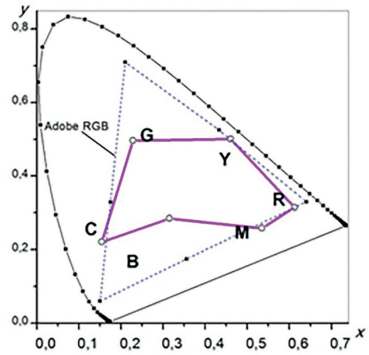


» **Figure 6:** *Color gamut HP Indigo press ws6800p*

Table 4

Laser digital multifunction copier DocuColor240PS

	X	Y
Cyan	0,154	0,221
Blue	0,315	0,285
Magenta	0,535	0,258
Red	0,612	0,315
Yellow	0,461	0,501
Green	0,228	0,497

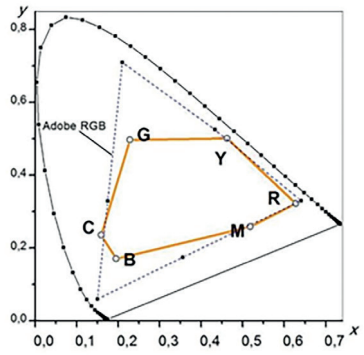


» **Figure 7:** *Color gamut of laser digital multifunction device DocuColor240PS*

Table 5

Offset press Heildenberg MOV

	X	Y
Cyan	0,154	0,221
Blue	0,315	0,285
Magenta	0,535	0,258
Red	0,612	0,315
Yellow	0,461	0,501
Green	0,228	0,497



» **Figure 8:** *Color gamut an offset press Heildenberg MOV*

Based on the constructed color gamuts, the digital printing machine HP Indigo Press WS6800P demonstrated the widest color coverage and the closest approximation to the reference color gamut.

3.2. Production time of products by different output systems

The speed of production is the main advantage of digital machines. There are cases when the customer is ready to pay twice the price for urgent production of products. It is known that color copies are not expensive. It is clear that the preparation and printing time on a printing machine is longer than on a digital one.

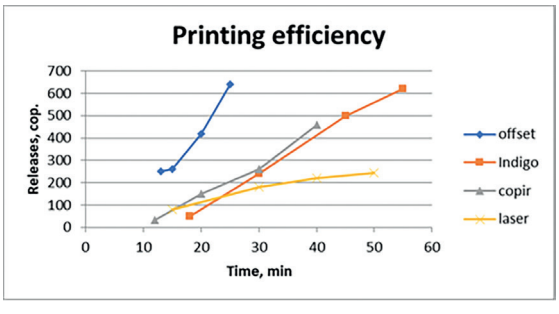
For further analysis, the next stage involved preparing data obtained from various output devices. The actual production time was determined and is presented in minutes for different print run volumes (Table 6).

Table 6

Time to print a contribution on different output systems

	Time, min	Realeses, cop.
Offset	13	250
	15	260
	20	420
	25	640
Indigo	18	50
	30	240
	45	500
	55	620
Copir	12	34
	20	150
	30	260
	40	460
Laser	15	80
	30	180
	40	220
	50	245

Based on production data (Table 6), a dependence was built



» **Figure 9:** *Efficiency of product manufacturing on various equipment*

The dependence shown in Fig. 9 illustrates the number of prints that can be produced on different types of equipment over a specified period of time. For print runs of up to 300 copies, the highest productivity is achieved by the Konica Minolta Bizhub C224 and the Xerox DocuColor 240 multifunctional printing system, whereas large print runs are most efficiently produced using offset printing equipment. The simple linear nature of the dependence is explained by the fact that only two characteristics of each printing device were used for its construction: the time required for preparatory operations and the maximum production speed.

4. Discussion

The geometric reconstruction of the 3D color gamuts in the CIELAB space confirmed that the digital liquid toner technology utilized in the HP Indigo system achieves a more comprehensive and stable color volume compared to conventional offset lithography. This phenomenon can be scientifically interpreted through the lens of print macrostructure and ink-substrate chemistry.

Conventional offset printing is inherently bound by the mechanics of ink film splitting and a relatively thick ink layer (often leading to a higher variance in dot gain), which can restrict the boundary saturation of chromatic primaries, particularly on standard substrates, as observed by Blahová et al. (2025). On the contrary, the liquid electrophotographic toner (ElectroInk) forms an extremely thin, uniform polymeric film that completely transfers to the substrate without absorbing deep into the fibers. This minimizes optical dot gain and preserves the chromatic purity of the primary (CMY) and secondary (RGB) clusters.

Our findings closely align with the benchmarking criteria established by Mika et al. (2025), who demonstrated that digital liquid toners provide superior color accuracy in high-saturated blue and magenta zones. When mapped using the modern human visual system simulations advocated by (Urban et al., 2023), the expanded volume of the Indigo's gamut represents not just a mathematical abstraction, but a noticeable improvement in visual fidelity, making it highly suitable for high-fidelity Expanded Color Gamut (ECG) applications (Malik et al., 2024).

The interpretation of the temporal data provides a clear techno-economic demarcation between digital and conventional systems. The generated operational efficiency curves illustrate a classic trade-off between setup time and run speed.

For low-volume production (small print runs), the digital platform demonstrates overwhelming operational dominance. This is directly attributed to the complete elimination of prepress workflows, such as computer-to-plate (CTP) manufacturing, plate mounting, and physical press ink-key calibration. As digital press workflows feed data directly to the imaging cylinder, the "time-to-market" for the first print is virtually instantaneous. This operational flexibility supports the contemporary shift toward short-run, localized print demands documented by Keypoint Intelligence and Senkivskyy et al. (2023).

However, as the run length increases, a definitive crossover point is reached. The high mechanical speed of modern offset presses rapidly dilutes the fixed initial time investment required for prepress preparation. Once the press is calibrated and running, the marginal

time per individual print in offset lithography drops significantly below that of high-volume digital systems.

This dynamic is perfectly synchronized with the hybrid production models evaluated by Rovira et al. (2024), confirming that the operational curves are governed by predictable time-efficiency laws. The choice of equipment cannot be based solely on colorimetric capacity; it must balance the volumetric color space requirement against the volume of the print run to optimize both quality and time-efficiency.

5. Conclusions

The study employed an empirical-theoretical method for investigating color reproduction, based on the instrumental measurement of print color coordinates and their subsequent mathematical formalization in the form of spatial geometric models. The research was carried out using prints produced by various output systems. Based on the measured color coordinates, color gamuts of multicolor prints were constructed on the CIE chromaticity diagram.

Analysis of the constructed color gamuts showed that the HP Indigo Press WS6800P digital printing machine provides the widest color coverage, indicating superior color reproduction capabilities compared to the other investigated systems.

It was also demonstrated that digital printing machines are optimal for small print runs due to their high production speed and operational efficiency. In contrast, offset printing machines are more suitable for large print runs, where reducing the unit cost of production becomes a decisive factor.

Therefore, when selecting a printing technology, it is important to consider both the print run volume and the required production time. Digital printing is advantageous for urgent and small-volume orders, whereas offset printing is more efficient for large-volume production.

6. Acknowledgments

The authors express their gratitude to the students of the Ukrainian Academy of Printing.

7. References

Blahová, M. and Samek, O. (2025) 'Analyzing color reproduction variance on high-speed inkjet devices across varied substrate coatings', Journal of Graphic Engineering and Design, 16(1), pp. 12–19. DOI: 10.24867/JGED-2025-1-012

Cao, L., Cao, Z., Jin, K., Wang, X., Pu, Y. and Wang, X. (2026) 'D2AFM: Dual-domain adaptive fusion module for underwater image enhancement'. In: *ICASSP 2026 - 2026 IEEE International Conference on Acoustics, Speech and Signal Processing (ICASSP)*, pp. 4156–4160. IEEE. DOI: 10.1109/ICASSP55912.2026.11464931

Choi, H.-H., Kim, E.-S. and Yun, B.-J. (2019) 'Tone mapping High Dynamic Range Image using cone response function based on CAM16'. In: *2019 Eleventh International Conference on Ubiquitous and Future Networks (ICUFN)*, pp. 639–641. IEEE. DOI: 10.1109/ICUFN.2019.8806090

Fan, D., Zhan, H., Xu, F., Zou, Y. and Zhang, Y. (2025) 'Research on multi-channel spectral prediction model for printed matter based on HMS-SA-BP neural network', *IEEE Access*, 13, pp. 2340–2359. DOI: 10.1109/ACCESS.2024.3523471

García-Manrique, J., López-Sánchez, A. and Martínez, L. (2024) 'Operational profiling and 3D color gamut volume rendering for advanced digital press systems', *Color Research & Application*, 49(5), pp. 712–725. DOI: 10.1002/col.22915

Green, P. and Field, R. (2024) 'Advanced colorimetric analysis of Expanded Color Gamut (ECG) printing in packaging production', *Color Research & Application*, 49(3), pp. 344–356. DOI: 10.1002/col.22891

Havenko, M., Havenko, S., Labetska, M. and Kadyliak, M. (2025) 'Conceptual model of information technology for assessing the quality of electronic book publications'. In: *Proceedings of SPIE - The International Society for Optical Engineering*, 12308. DOI: 10.1117/12.3087736

Jia, W. (2018) 'Research on image color restoration and its application in LCD display'. In: *2018 International Conference on Information Systems and Computer Aided Education (ICISCAE)*, pp. 189–192. IEEE. DOI: 10.1109/ICISCAE.2018.8666846

Kao, W.-C., Hsu, Y.-C., Hong, K.-D., Chen, H., Lin, C.-M. and Yin, R.-X. (2025) 'Color electronic paper with front light', *IEEE Consumer Electronics Magazine*, 14(3), pp. 94–104. DOI: 10.1109/MCE.2024.3508096

Kawabata, N. and Nakaguchi, T. (2023) 'Optimal design of color laparoscopic super-resolution image quality based on generative adversarial networks'. In: *2023 International Conference on Computer Graphics and Image Processing (CGIP)*, pp. 1–7. IEEE. DOI: 10.1109/CGIP58526.2023.00009

Kobayashi, N., Chiba, T., Togashi, K., Shrestha, P., Murata, M., Obi, T. and Yamaguchi, M. (2020) 'Telepathology support system with gross specimen image using high resolution 4K multispectral camera'. In: *2020 42nd Annual International Conference of the IEEE Engineering in Medicine & Biology Society (EMBC)*, pp. 1388–1391. IEEE. DOI: 10.1109/EMBC44109.2020.9175398

Li, L. and Cong, H. (2019) 'Research on visual reproduction and communication of Dongba character symbols in animation technology production'. In: *2019 International Conference on Robots & Intelligent System (ICRIS)*, pp. 102–105. IEEE. DOI: 10.1109/ICRIS.2019.00034

Lindbloom. (2017) *XYZ to xyz*. Available from: http://www.brucelindbloom.com/index.html?Eqn_XYZ_to_xyY.html

Malik, S. and Ganotra, D. (2024) 'Enhancing color accuracy in virtual reality: Process control of DCI display using spectral sensor and active 3D glasses'. In: *2023 Second IEEE International Conference on Measurement, Instrumentation, Control and Automation (ICMICA)*, pp. 1–5. IEEE. DOI: 10.1109/ICMICA61068.2024.10732105

Mika, J., Horváth, P. and Novotný, M. (2025) 'Benchmarking color gamut accuracy and print quality stability: Digital liquid toner versus conventional offset lithography', *Journal of Media and Printing Technologies*, 18(2), pp. 85–94. DOI: 10.1016/j.jmpt.2024.10.012

Pan, B., Qu, Q., Xu, X. and Shi, Z. (2022) 'Structure–color preserving network for hyperspectral image super-resolution', *IEEE Transactions on Geoscience and Remote Sensing*, 60, 5520512, pp. 1–12. DOI: 10.1109/TGRS.2021.3135028

Rovira, M. and Chen, Y. (2024) 'Production efficiency curves and crossover point analysis in hybrid printing environments: Offset vs. High-volume digital platforms', *International Journal of Production Economics*, 268, 109110. DOI: 10.1016/j.ijpe.2024.109110

Senkivskyy, V., Holubnyk, T., Havrysh, B. and Snihur, N. (2023) 'The information technology for the formation of high-quality visual content of newspaper publications', *CEUR Workshop Proceedings*, 3373, pp. 302–319. Available from: https://ceur-ws.org/Vol-3675/paper5.pdf

Shamoi, P., Sansyzbayev, D. and Abiley, N. (2022) 'Comparative overview of color models for content-based image retrieval'. In: *2022 International Conference on Smart Information Systems and Technologies (SIST)*, pp. 1–6. IEEE. DOI: 10.1109/SIST54437.2022.9945709

Urban, P. and Deshpande, A. (2023) 'Spectral color reproduction quality metric based on human visual system simulation', *IEEE Transactions on Image Processing*, 32, pp. 1420–1432. DOI: 10.1109/TIP.2023.3241105

Xu, X., Wang, Y., Zhang, J., Sun, X. and Wang, Z. (2022) 'ColorPolarNet: Residual dense network-based chromatic intensity-polarization imaging in low-light environment', *IEEE Transactions on Instrumentation and Measurement*, 71, 5025210, pp. 1–10. DOI: 10.1109/TIM.2022.3216391

Zhu, Y. and Liu, X. (2024) 'Application of machine learning models for predicting color reproduction quality on recycled paperboard', *Nordic Pulp & Paper Research Journal*, 39(2), pp. 211–223. DOI: 10.1515/npprj-2023-0089



© 2026 Authors. Published by the University of Novi Sad, Faculty of Technical Sciences, Department of Graphic Engineering and Design. This article is an open access article distributed under the terms and conditions of the Creative Commons Attribution license 4.0 Serbia (https://creativecommons.org/licenses/by/4.0/deed.en).

Original Scientific Paper https://doi.org/10.24867/GRID-2026-p12

The Power of Packaging Design in Supporting Global and Local Events

ABSTRACT

Packaging design has evolved beyond its traditional role of protecting products to become a strategic communication tool that supports branding, cultural identity, and consumer engagement during global and local events. This research investigates the role of packaging design in enhancing the visual identity and promotional impact of major international and local events through the development of event-inspired packaging concepts. The study aims to identify the design elements and visual strategies that strengthen the relationship between products and event branding while increasing consumer attraction and emotional engagement. A mixed-methods approach was employed, combining a literature review, analytical study of selected local and international product packages associated with major events, a questionnaire targeting consumers and design specialists to evaluate public perceptions of event-oriented packaging, and experimental design applications developed by the researcher. The experimental designs explored the integration of event visual identity, color schemes, typography, illustrations, structural packaging, and interactive features into commercial packaging to create memorable consumer experiences. The findings demonstrate that packaging inspired by global and local events significantly enhances product visibility, reinforces brand recognition, increases purchase intention, and strengthens consumers' emotional connection with both the product and the event. The analytical and experimental results further indicate that integrating cultural and event-specific visual elements into packaging contributes to effective marketing communication and product differentiation in competitive markets. The study concludes that event-oriented packaging design represents an innovative marketing and communication strategy capable of creating added value for brands while promoting cultural and sporting events. Accordingly, the research recommends encouraging collaboration between packaging designers, manufacturers, and event organizers to develop limited-edition packaging that celebrates local and global events, enhances consumer experience, and supports economic and cultural sustainability.

Khloud Khaled Nasr

Egyptian Russian University, Faculty of Applied Arts, Department of Printing and Packaging, Cairo, Egypt

KEY WORDS

Packaging design, limited-edition packaging, consumer engagement, visual communication, event marketing

1. Introduction

Packaging design has sophisticated significantly from its traditional role as a means of containing, protecting, and transporting products to become an influential medium of visual communication, branding, and consumer engagement. Contemporary packaging integrates structural, graphic, material, and informational elements to communicate product values and establish meaningful connections between brands and consumers. Recent literature demonstrates that packaging design can influence consumer perception, brand associations, attention, emotions, and purchase-related behavior, confirming its importance as a strategic component of brand communication rather than merely a functional container (Rodriguez, Antonovica & Martín, 2023).

An example of this communicative role can be observed in Heinz packaging-related visual communication, where the familiar visual characteristics of the brand are transformed into engaging and recognizable forms (The Kraft Heinz Company, 2026).

The examples demonstrate how packaging-related design can extend beyond product identification to create visual associations, attract attention, and strengthen brand recognition through distinctive colors, forms, and symbolic references, as shown in figure 1.



» **Figure 1:** *Heinz packaging inspired by football's red and yellow cards during the 2026 FIFA World Cup*

The communicative power of packaging becomes particularly significant in the context of global and local events, where visual communication plays a central role in creating recognition, expressing the character of an event, and connecting audiences with its cultural and social context.

Major international events such as the Olympic Games demonstrate how a coherent visual identity can be extended across numerous communication and design applications. The Olympic visual identity system, for example, integrates elements such as logos, pictograms, merchandise, posters, uniforms, and other visual applications to establish a consistent and recognizable representation of the host city and event. The design of such events often combines international visual trends with national and cultural characteristics, creating a visual language capable of communicating simultaneously with local and international audiences (Osterwalder, 2020).

Within this context, packaging can function as an extension of event identity, transforming products into tangible representations of a specific occasion, destination, culture, or celebration. Event-related packaging, including limited-edition packages, commemorative packages, promotional packaging, and souvenir packaging, provides opportunities for designers to integrate event themes, symbols, colors, typography, imagery, and cultural references into a physical product.

Packaging therefore has the potential to extend the visual experience of an event beyond its physical location and duration, allowing audiences to retain a tangible reminder of the event. Research on packaging and brand image supports this perspective, demonstrating that consumers interpret both practical and symbolic packaging characteristics and incorporate these perceptions into their broader associations with brands (Ghorbani & Westermann, 2024).

The relationship between packaging and cultural identity is particularly important for local events and destinations. Packaging can communicate elements of local heritage through visual narratives, traditional patterns, symbols, materials, colors, and culturally significant imagery. Such approaches can transform packaging into a form of cultural storytelling that communicates the identity of a place while supporting tourism, local products, and cultural visibility.

Recent research describes packaging as a potential "cultural ambassador," emphasizing its ability to communicate regional identity, preserve cultural narratives, and contribute to tourism and local economic vitality (Aleshaiwi, 2025).

This cultural dimension is especially relevant when local heritage is incorporated into contemporary packaging design. Traditional cultural expressions may include designs, signs, symbols, handicrafts, narratives, patterns, and other artistic forms that are connected to the identity and heritage of local communities. Therefore, incorporating cultural elements into event packaging requires not only aesthetic consideration but also sensitivity to cultural authenticity, representation, and the appropriate use of traditional visual expressions.

The World Intellectual Property Organization (WIPO) emphasizes that traditional cultural expressions form part of the identity and heritage of traditional and local communities and can contribute to cultural diversity and heritage preservation when appropriately managed (WIPO, n.d.).

At the same time, the contemporary role of packaging extends beyond visual identity toward consumer experience and interaction. Packaging can attract attention, communicate information, evoke emotions, and encourage consumers to interact with the product. Recent research has increasingly examined packaging through experiential and consumer-centered perspectives, while emerging forms of interactive and smart packaging provide additional opportunities for connecting physical packaging with digital experiences. For example, the FIFA World Cup 2026 experience demonstrates how physical product packaging can be connected with digital engagement through scannable Coca-Cola labels and the FIFA Panini digital collection, creating an interaction between the physical package and a digital event-related experience (FIFA, 2026). Another critical dimension is sustainability.

The increasing scale of events and promotional activities raises questions concerning the environmental impact of temporary and commemorative packaging. Packaging for events should therefore balance visual impact, functionality, cultural communication, and environmental responsibility. The United Nations Environment Programme and the Ellen MacArthur Foundation have emphasized the need to reduce unnecessary single-use packaging, increase reuse, and move toward circular approaches to packaging (UNEP, 2022).

Accordingly, packaging design can be viewed as a strategic visual communication tool capable of supporting both global and local events by translating event concepts into tangible visual and physical experiences. Its effectiveness may depend on the ability to establish a recognizable event identity while simultaneously reflecting cultural context, attracting audiences, communicating meaningful messages, encouraging engagement, and considering sustainability. Therefore, investigating the power of packaging design in supporting global and local events can provide valuable insights into how packaging can move beyond its conventional commercial function to become an active component of event branding, cultural representation, audience engagement, and destination promotion.

2. Methods

This study adopts a mixed-methods research approach to investigate the role and potential of packaging design in supporting global and local events. The mixed-methods approach combines qualitative and quantitative methods to provide a comprehensive understanding of how event-related packaging communicates visual identity, represents cultural values, enhances audience engagement, and influences consumer perception.

The study consists of four complementary stages: literature review, visual case study analysis, questionnaire survey, and applied design. Integrating these methods enables the research to examine packaging design from both a theoretical and design perspective, as well as from a consumer-perception perspective.

1. The first stage focuses on reviewing relevant academic literature addressing packaging design, visual communication, event branding, cultural identity, consumer engagement, interactive packaging, and sustainable packaging. The literature review establishes the theoretical framework of the study and identifies the key dimensions through which the effectiveness of event-related packaging can be examined.

2. The second stage focuses on the visual analysis of selected global and local event-related packaging examples. The cases are evaluated using predefined criteria to examine how packaging communicates event identity, represents cultural values, engages consumers, and creates memorable experiences (Krishna, Cian & Aydınoğlu, 2017; Yao, 2026).

The analysis considers visual identity and consistency, event recognition, graphic and structural design, cultural representation, emotional appeal, consumer interaction, innovation, sustainability, and memorability and souvenir value, as shown in figure 2.

3. The third stage consisted of a structured questionnaire designed to investigate consumers' perceptions of the role and perceived power of packaging design in supporting global and local events. The questionnaire was developed based on the variables and key themes identified through the literature review and visual case study analysis. It comprised 15 questions directly addressing the research objectives and focused on five key dimensions: packaging design, event identity, cultural representation, consumer engagement, and event promotion, shown in table 1.

A comparative dimension was also included to examine participants' perceptions of packaging associated with global and local events. The questionnaire was distributed to 130 participants from diverse backgrounds.

Participants were asked to evaluate the main statements using a five-point Likert scale, ranging from 1 = Strongly Disagree to 5 = Strongly Agree. The questionnaire was administered electronically using Google Forms.



» **Figure 2:** *Selected event packaging analyzed based on visual, cultural, functional, and sustainability criteria*

Table 1

Questionnaire Statements and Research Dimensions

(The following table presents the 15 statements developed to investigate the role of packaging design in supporting global and local events. The statements were structured according to the principal dimensions identified in the research framework)

No.	Questionnaire Statement	Research Dimension
1.	Event-related packaging can enhance the visual recognition of an event.	Event Recognition
2.	Packaging design can effectively communicate the identity and character of an event.	Event Identity
3.	A well-designed package can strengthen the visual connection between a product and the event it represents.	Product–Event Connection
4.	Packaging can extend an event's visual identity beyond the event venue and duration.	Event Promotion
5.	Distinctive event-related packaging can attract audience attention more effectively than conventional packaging.	Visual Attraction
6.	The use of event-related colors, typography, symbols, and imagery can strengthen event recognition.	Visual Communication
7.	Packaging design can effectively communicate the cultural identity of a local event.	Cultural Identity
8.	The appropriate incorporation of local patterns, symbols, and traditional visual elements can strengthen the connection between packaging, cultural heritage, and the event.	Cultural Representation
9.	Cultural elements incorporated into packaging can increase its appeal to tourists and international audiences.	Tourism and Cultural Promotion
10.	Packaging can communicate cultural stories and values associated with local events.	Cultural Storytelling
11.	Event-related packaging can create an emotional connection between consumers and the event.	Emotional Engagement
12.	Interactive packaging features, such as QR codes and digital content, can enhance the audience's experience of an event.	Interactive Experience
13.	Innovative packaging can increase the memorability of event-related products and experiences.	Innovation and Memorability
14.	Sustainable and reusable packaging can increase the long-term value of event-related products.	Sustainability
15.	Event-related packaging can contribute to promoting an event and maintaining audience awareness after the event has ended.	Long-Term Event Promotion

Data were collected during the International Exhibition for Paper, Board, Carton, Tissue, Printing, and Packaging Industries in Egypt (Paper Middle East Exhibition 2026), providing an appropriate context for reaching participants with diverse backgrounds and interests related to packaging, printing, and product communication.

Participation was voluntary, and respondents were invited to complete the questionnaire through a digital link or QR code. A total of 130 valid responses were collected and included in the analysis.

4. The fourth stage involved an applied design study that translated the findings of the literature review, visual case study analysis, and questionnaire survey into a practical packaging design solution. The study was developed to examine how the identified design principles could be applied to event related packaging and to demonstrate the potential of packaging as a strategic communication and promotional medium for global and local events.

The applied design process focused on integrating the key dimensions identified through the previous research stages, including event identity, cultural representation, visual communication, consumer engagement, innovation, and sustainability. The design solution aimed to establish a clear relationship between the product, the event, and its target audience while extending the event experience beyond its temporary physical context.

The resulting packaging prototype was developed based on the findings and design principles derived from the preceding research stages. The design development and resulting prototype are presented and discussed in the Results section.

3. Results

Based on the findings of the questionnaire survey and visual case study analysis, the applied study identified key design and symbolic elements that can effectively communicate the identity, cultural character, and legacy of global and local events. These findings informed the selection and development of the packaging concept. The main design challenge was to translate the identified elements into a contemporary packaging solution that establishes a meaningful connection between the event, the product, and its target audience.

3.1. Questionnaire Results

The questionnaire was completed by 130 participants and consisted of 15 statements developed to investigate the role of packaging design in supporting global and local events. The responses were analyzed using frequencies and percentages. The findings are presented according to the main research dimensions.

3.1.1. Event Recognition and Identity

The results indicate a high level of acceptance regarding the role of packaging in communicating event identity. 106 participants (81.5%) strongly agreed that event-related packaging can enhance visual recognition of an event. Similarly, 109 participants (83.8%) supported its ability to communicate the identity and character of an event, while 106 participants (81.5%) recognized its role in strengthening the connection between the product and the event. Furthermore, 102 participants (78.5%) agreed that packaging can extend an event's visual identity beyond its venue and duration.

3.1.2. Visual Communication and Audience Attention

A strong level of agreement was also observed regarding visual communication. 112 participants (86.2%) agreed that distinctive event-related packaging can attract audience attention more effectively than conventional packaging. The same proportion, 112 participants (86.2%), agreed that event-related colors, typography, symbols, and imagery can strengthen event recognition. These findings emphasize the importance of visual design elements in communicating and reinforcing event identity.

3.1.3. Cultural Representation and Local Identity

The cultural dimension received particularly strong support. 108 participants (83.1%) strongly agreed that packaging can communicate the cultural identity of a local event. Moreover, 112 participants (86.2%) supported the use of local patterns, symbols, and traditional visual elements to strengthen the connection between packaging, cultural heritage, and the event.

In addition, 106 participants (81.5%) agreed that cultural elements can increase the appeal of packaging to tourists and international audiences, while the same number recognized its ability to communicate cultural stories and values.

3.1.4. Emotional Engagement and Event Experience

The findings show that packaging can also contribute to audience engagement. 101 participants (77.7%) agreed that event-related packaging can create an emotional connection between consumers and the event. This indicates that packaging has the potential to contribute to a more memorable relationship between the audience, the product, and the event.

3.1.5. Interactive and Innovative Packaging

The results demonstrated positive acceptance of interactive and innovative approaches. 103 participants (79.2%) agreed that interactive features, such as QR codes and digital content, can enhance the audience's event experience. Furthermore, 110 participants (84.6%) agreed that innovative packaging can increase the memorability of event-related products and experiences.

3.1.6. Sustainability and Long-Term Event Promotion

Sustainability and long-term promotional value were also strongly supported. 108 participants (83.1%) strongly agreed that sustainable and reusable packaging can increase the long-term value of event-related products. The strongest response in this dimension was recorded for the promotional role of packaging, with 112 participants (86.2%) agreeing that event-related packaging can promote an event and maintain audience awareness after the event has ended.

Overall, the findings reveal a high level of positive acceptance, with the proportion of participants who selected Agree or Strongly Agree ranging from 77.7% to 86.2% across the 15 statements. The strongest levels of acceptance were associated with visual communication, cultural representation, and long-term event promotion, each reaching 86.2%. These findings support the central premise of the study that packaging design can function beyond its conventional product-related role to become a strategic medium for event recognition, cultural representation, audience engagement, and event promotion.

3.2. Applied Study

Based on the findings of the questionnaire survey and visual case study analysis, the applied study translated the identified design principles into practical packaging solutions associated with four selected events.
Two local Egyptian events and two global events

were selected to examine how packaging design can communicate different forms of event identity, cultural representation, and audience engagement across local and international contexts.

The selected events were the International Date Palm Festival of Egypt and the Cairo International Film Festival as local events, and the FIFA World Cup 2030 and World Packaging Day 2026 as global events. The selection provided diverse contexts for exploring the ability of packaging to reflect cultural identity, event characteristics, visual identity, promotional objectives, and audience expectations.

For each event, the applied design process followed a consistent framework. The process began with identifying the event's distinctive visual and symbolic characteristics, followed by selecting and interpreting relevant cultural or thematic elements. These elements were then translated into contemporary packaging through graphic composition, color, typography, imagery, pattern, structural design, and, where appropriate, interactive, innovative, or sustainable features.

The application aimed to establish a meaningful relationship between the event, the product, and its target audience while demonstrating how packaging can extend event communication beyond the physical event itself. The four design applications are presented below, with each case examined in terms of its conceptual development, visual language, cultural or thematic representation, and packaging outcome.

3.2.1. Local Event Packaging

The applied study explored the potential of packaging design to support the identity and communication of selected Egyptian local events through contemporary and culturally relevant design solutions. Two local events were selected: the International Date Palm Festival of Egypt and the Cairo International Film Festival. The selection provided two distinct contexts for examining how packaging can communicate cultural heritage, event identity, and thematic characteristics while creating a tangible connection between the event, the product, and its audience. For each event, the design process focused on identifying its distinctive visual and symbolic elements and translating them into contemporary packaging solutions that support event recognition, cultural representation, promotion, and audience engagement.

3.2.1.1. International Date Palm Festival of Egypt

The International Date Palm Festival of Egypt, was selected as a local application due to its strong association with Egyptian date cultivation, agricultural heritage, and oasis culture (International Date Palm Festival of Egypt, n.d.), as shown in Figure 3. The date palm was identified as the primary symbolic element for translating the festival's identity into a contemporary packaging solution.



» **Figure 3:** *Event context and visual identity of the International Date Palm Festival of Egypt*

The design analysis focused on extracting the palm's recognizable characteristics including its silhouette, leaves, trunk, and organic forms and reinterpreting them through contemporary graphic elements, patterns, color, and typography. Visual references from the oasis environment and Egyptian cultural heritage were selectively incorporated to strengthen the sense of place while avoiding literal reproduction of traditional motifs, as shown in figure 4.



» **Figure 4:** *Cultural and visual references of the Egyptian oasis environment*

The resulting packaging concept positions the product as an extension of the event identity, integrating cultural storytelling with product communication. Through the relationship between symbol, visual identity, product, and packaging structure, the application demonstrates how event-related packaging can transform a culturally significant product into a tangible medium for event recognition, promotion, and audience experience. The applied design presents an event-related date packaging concept inspired by the cultural and environmental identity of Siwa Oasis. Date palms, traditional geometric patterns, Siwan architecture, and desert landscapes create a distinctive visual narrative that connects the product with local heritage.

A clear die-cut window shaped as a date palm leaf provides direct product visibility while enhancing consumer engagement and reinforcing the packaging's cultural and structural concept. A clear visual hierarchy further strengthens event communication and promotional value, transforming the package into a tangible representation of the event and its local identity, as shown in Figure 5.



» **Figure 5:** *Proposed event related packaging design for the International Date Palm Festival of Egypt*

3.2.1.2. Cairo International Film Festival (CIFF)

The Cairo International Film Festival (CIFF), established in 1976, is a major Egyptian cultural event with a strong international presence. It brings together filmmakers, film professionals, and audiences from around the world, contributing to Egypt's cultural and cinematic visibility.

From a packaging design perspective, CIFF provides a relevant local case study for exploring how event identity can be extended to product packaging. Event related packaging can integrate cinematic visual language, Egyptian cultural references, typography, colors, symbols, and festival graphics to strengthen event recognition and create a connection between the product and the audience.

As an applied example, a proposed limited edition Corona chocolate package can be developed specifically for the Cairo International Film Festival, as shown Figures 6 and 7. The concept integrates the festival's cinematic identity with the visual identity of the chocolate brand, transforming the conventional package into an event related product. The limited edition approach enhances the package's exclusivity and collectible value while supporting visual identity, cultural representation, audience engagement, brand recognition, and memorability.



» **Figure 6:** *Limited Edition Corona Chocolate Packaging Inspired by the Cairo International Film Festival (First Proposal)*



» **Figure 7:** *Limited Edition Corona Chocolate Packaging Inspired by the Cairo International Film Festival (Second Proposal)*

3.2.2. Global Event Packaging

Global event packaging refers to the adaptation of product packaging to reflect the identity, themes, and visual language of major international events. By integrating event-related symbols, cultural references, and communication elements, packaging can extend the event experience while maintaining the product's brand identity and functional requirements.

In this study, global event packaging is explored through two selected global events: World Packaging Day 2026 and the FIFA World Cup 2030.The proposed designs examine how packaging can communicate event identity, cultural representation, audience engagement, innovation, and sustainability through limited-edition and event specific visual solutions.

This approach demonstrates the potential of packaging to function not only as a product container but also as a visual communication medium that connects brands with major global events.

3.2.2.1. World Packaging Day 2026

World Packaging Day 2026 was selected as a global event context to explore how packaging design can visually communicate the role and value of packaging in contemporary society. Officially celebrated on 6 September 2026, the initiative is led by the World Packaging Organization (WPO) and focuses on four main pillars: Packaging for Progress, Packaging Against Food Waste, Packaging and Economic Growth, and Packaging and Sustainability.

For the applied study, these themes were translated into a limited-edition packaging concept that combines the visual identity of the event with the identity of the selected product. The design incorporates visual elements representing innovation, sustainability, food protection, economic development, and the wider social role of packaging.

The proposed packaging demonstrates how an existing product package can be transformed into an event related communication tool, while maintaining its functional purpose and recognizable brand identity.

The design therefore connects the product, packaging industry, event identity, and audience within one visual solution, as shown Figures 8 and 9.



» **Figure 8:** *Proposed KitKat packaging for World Packaging Day 2026*



» **Figure 9:** *Proposed Nature Valley Granola packaging for World Packaging Day 2026*

3.2.2.2. FIFA World Cup 2030.

The FIFA World Cup 2030 will be a major global sporting event and a special centenary edition, celebrating 100 years since the first World Cup in Uruguay in 1930.

For the applied study, the event provides an opportunity to develop limited-edition packaging inspired by football, the centenary celebration, and the cultural identities of the host countries. This approach demonstrates how packaging design can support event identity, cultural representation, audience engagement, brand recognition, and memorability.

The applied study explores two approaches to packaging development:

1. Modifying the graphic design while maintaining the original structural form of the package, as shown in Figure (10).
2. Modifying both the graphic and structural design to create a new packaging form, as shown in Figure (11). These two approaches demonstrate how event-inspired packaging can be developed through either visual transformation alone or through an integrated graphic and structural redesign.



» **Figure 10:** *Graphic redesign of adidas packaging inspired by FIFA World Cup 2030.*



» **Figure 11:** *Graphic and structural redesign of the Adidas shoe packaging inspired by the FIFA World Cup 2030.*

4. Discussion

The findings highlight the significant role of packaging design in enhancing the relationship between products, brands, events, and audiences. The high level of participant agreement across the five investigated dimensions packaging design, event identity, cultural representation, consumer engagement, and event promotion suggests that event related packaging can extend beyond its traditional functional role to become an effective visual communication medium.

The applied design studies support these findings by demonstrating how integrating event identity with brand identity can transform conventional packaging into a

distinctive event-related experience. The incorporation of event specific visual elements, cultural references, storytelling, and limited-edition concepts provides opportunities to increase visual appeal, strengthen product event association, and encourage audience interaction.

The study also indicates that the effectiveness of event-related packaging depends on its ability to achieve a balance between recognizable brand identity and relevant event representation. In global events, this requires a visual language that can communicate across diverse audiences, whereas local events allow packaging to incorporate distinctive cultural and place-based elements that strengthen local identity and emotional connection.

Overall, the results indicate that packaging can serve as a strategic extension of event communication, allowing event identity and values to be experienced through a tangible product. Thus, event related packaging represents an opportunity to connect visual communication, cultural identity, brand engagement, and event promotion within a single design solution.

5. Conclusions

This study concludes that packaging design has the potential to play a significant role in supporting and communicating the identity of both global and local events. By integrating event identity, brand identity, cultural representation, and functional packaging requirements, packaging can extend beyond its conventional role as a product container to become an effective medium of visual communication.

The findings from the visual analysis and questionnaire indicate that event-related packaging can contribute to strengthening event recognition, enhancing consumer engagement, communicating cultural values, and promoting the associated event. The high level of participant agreement across the five investigated dimensions packaging design, event identity, cultural representation, consumer engagement, and event promotion supports the relevance of these dimensions in developing event-related packaging solutions.

The applied design studies further demonstrate that adapting conventional packaging to specific event contexts can create distinctive and meaningful visual experiences. The integration of limited-edition concepts, event specific visual elements, cultural symbols, storytelling, and interactive features provides opportunities to connect the product with the identity and values of the event while maintaining its brand recognition and functional requirements.

The study also highlights the importance of adapting packaging strategies according to the nature of the event. Global events require visual solutions that communicate effectively across diverse audiences, while local events provide opportunities to emphasize cultural heritage, local identity, and place-based narratives. This demonstrates the flexibility of packaging design as a tool for communicating different levels of event identity.

Overall, the research establishes that event-related packaging can serve as a tangible extension of event communication, creating a connection between the event, brand, product, culture, and audience. Therefore, incorporating event identity into packaging design represents a valuable design strategy for enhancing communication, engagement, and the overall visual experience of both global and local events.

6. Acknowledgments

I would like to express my sincere gratitude to all the participants who took part in the questionnaire and shared their valuable opinions and insights, which greatly contributed to this study.

7. References

Aleshaiwi, W. (2025) *Packaging design as a cultural ambassador: Promoting local identity through visual narratives*. Available from: https://www.dpublication.com/abstract-of-6th-ictmh/13-2889/ [Accessed 5 September 2026].

FIFA. (2026) *FIFA Panini Collection App: Connecting physical and digital fan experiences*. Available from: https://www.fifa.com/en/tournaments/mens/worldcup/canadamexicousa2026/articles/fifa-panini-collection-app [Accessed 3 August 2026].

Ghorbani, M. and Westermann, A. (2024) 'Exploring the role of packaging in the formation of brand images: A mixed methods investigation of consumer perspectives', *Journal of Product & Brand Management*, 34(2), pp. 186–202. DOI: 10.1108/JPBM-09-2023-4738

International Date Palm Festival of Egypt. (n.d.) *International Date Palm Festival of Egypt*. Available from: https://www.siwafestival.com [Accessed 5 August 2026].

Krishna, A., Cian, L. and Aydınoğlu, N.Z. (2017) 'Sensory aspects of package design', *Journal of Retailing*, 93(1), pp. 43–54. DOI: 10.1016/j.jretai.2016.12.002

Osterwalder, M. (2020) *Olympic Games: The Design: From Athens 1896 to Tokyo 2020*. Salenstein: Niggli.

Rodriguez, V., Antonovica, A. and Martín, D.L.S. (2023) 'Consumer neuroscience on branding and packaging: A review and future research agenda', *International Journal of Consumer Studies*, 47(6), pp. 2790–2815. DOI: 10.1111/ijcs.12936

The Kraft Heinz Company. (2026) *How Kraft Heinz turned soccer's biggest tournament into a global moment*. Available from: https://news.kraftheinzcompany.com/stories-details/2026/How-Kraft-Heinz-Turned-Soccers-Biggest-Tournament-into-a-Global-Moment--2026-fMdq6RW4ft/default.aspx [Accessed 5 August 2026].

United Nations Environment Programme (UNEP) and Ellen MacArthur Foundation. (2022) *The Global Commitment 2022*. Available from: https://www.unep.org/resources/report/global-commitment-2022 [Accessed 22 August 2026].

World Intellectual Property Organization (WIPO). (n.d.) *Traditional Cultural Expressions*. Available from: https://www.wipo.int/en/web/traditional-knowledge/traditional-cultural-expressions/index [Accessed 10 August 2026].

Yao, T.Y. (2026) 'How packaging design and cultural identity influence consumers' willingness to pay a premium—an empirical study based on China's premium teas', *Frontiers in Sustainable Food Systems*, 10, 1841738. DOI: 10.3389/fsufs.2026.1841738



© 2026 Authors. Published by the University of Novi Sad, Faculty of Technical Sciences, Department of Graphic Engineering and Design. This article is an open access article distributed under the terms and conditions of the Creative Commons Attribution license 4.0 Serbia (http://creativecommons.org/licenses/by/4.0/rs/).

Original Scientific Paper https://doi.org/10.24867/GRID-2026-p13

Possibilities of Increasing the Tool Life of an Eccentric Circular Knife in Vibration-Assisted Cutting of Book Blocks

ABSTRACT

The present study investigates the wear process of the cutting edge of an eccentrically positioned circular knife when cutting book blocks. The study further explores methodologies for prolonging the operational longevity of vibrating circular knives within high-speed book production environments. A new method for monitoring circular knife blade wear is proposed. The experimental part of the study involves a comparative analysis of the operational lifespans of traditional and vibrating circular knives (from sharpening to dulling). Computer-aided simulations of cutting processes using eccentric and non-eccentric circular knives have revealed that the vibrating knife blade's trajectory is significantly influenced by its vibration parameters during the cutting process. This reduces the cutting path and consequently minimizes blade wear. The conducted analysis suggests a way to optimize tool wear in bookbinding processes utilizing eccentric circular knives.

Georgij Petriaszwili [1]
Serhii Komarov [3]
Piotr Janicki [2]
Leszek Markowski [1]

[1] Warsaw University of Technology, Institute of Mechanics and Printing, Warsaw Poland
[2] Drukarnia Wydawnicza im. W.L. Anczyca S.A., Kraków, Poland
[3] Lviv Polytechnic National University, Lviv, Ukraine

KEY WORDS
Vibration cutting, tool life, eccentric circular knife, book-edge trimming

1. Introduction

1.1. Preface

Some of the fundamental technological operations in the printing industry include paper cutting operations, which are widely applied throughout the entire printing production cycle: before printing – when cutting stacks of unprinted sheets on single-knife guillotine cutters, as well as in the final processing of book blocks – using three-knife trimmers. Three-knife trimmers are a staple tool in printing houses. The mechanical speed of three-knife trimmers has already reached its peak due to significant cutting forces, which creates a bottleneck in the implementation of technological processes in high-speed, automatic book production lines. The search for new book cutting methods is ongoing. As demonstrated in earlier studies, the vibratory cutting of book blocks using eccentrically positioned circular knives has the potential to significantly reduce the cutting force (Petriaszwili, Janicki & Komarov, 2020). Further research into vibratory cutting processes will facilitate the creation of a new technology for non-stop three-sided book cutting. This will result in a substantial increase in the productivity of the book production process.

1.2. Background

Studies on the new vibration-assisted method of cutting with circular knives were previously conducted by Janicki, Petriaszwili and Komarov (2016, 2017) and Petriaszwili, Janicki and Komarov (2019, 2020, 2021). These studies analyzed the influence of the kinematics of the vibration-assisted cutting process using an eccentric circular knife on the variation of the actual cutting angle of the book block, which affects the magnitude of the cutting force. The analysis of the transformation of the circular knife's cutting angle was carried out for two possible directions of rotation: co-directional – when the direction of rotation matches the feed direction of the processed block, and counter-direc-

tional – when the direction of the knife's rotation is opposite to the feed direction of the book block.

During counter-directional cutting, the actual cutting angle is smaller than in the case of co-directional cutting. This means that when counter-directional cutting is applied, the cutting forces for book blocks are lower. It was established that the oscillating rotary motions of the circular knife lead to cyclic changes in the magnitude of the knife's cutting angles during processing. This, in turn, causes a dynamic impact of the cutting tool's edge on the processed material (Komarov, Petriaszwili & Janicki, 2025; Petriaszwili, 2024; Komarov, Petriaszwili & Janicki, 2024). The research also revealed that cutting with a vibration-assisted circular knife can occur in two different modes: intermittent (pulse) cutting, where the knife edge loses contact with the book block during a certain phase of the knife's rotation, and continuous (constant) cutting, where the edge of the rotating knife remains in constant contact with the book block throughout the knife's rotation cycle.

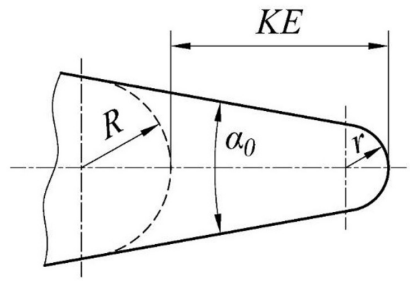
As a result of the analytical studies, it was concluded that the most optimal regime for effectively reducing the cutting force is the application of intermittent cutting. The results of the experimental tests showed a significant, 1.8 to 2-fold reduction in the cutting force (Petriaszwili et al., 2025; Petriaszwili, Komarov & Janicki, 2025). Furthermore, these studies indicated the possibility of increasing the tool life of circular knives through the application of vibrations. Industrial experience shows that the condition of the cutting edge of the knives has a significant impact on the productivity and quality of book trimming. Cutting with knives that have excessively worn edges causes a substantial increase in the dynamic loads on the machine drive components, as well as higher energy consumption. To date, there is no universally applicable and practical method for assessing the condition of the blades of paper-cutting knives. The development of this method will facilitate continuous monitoring of the condition of the cutting edges of three-knife trimmers during production, thereby contributing to the monitoring of the quality of the manufactured books.

The objective of this study is to conduct research on the wear of the cutting edge of an eccentrically mounted circular blade during the cutting of book blocks and to analyze the potential for extending the service life of a vibration-assisted circular blade.

2. Experimental research

Research on the cutting processes of various materials (Daurski & Machihin, 1980; Ginzburg, 1957; Gruszewski, 1963; Reznik, 1975; Krabisch, 1962; Mordowin, 1962; Staniszewski & Porankiewicz, 1997) indicates that the cutting edge radius can be one of the parameters characterising the blunting of a cutting tool's edge. Studies on the processes of cutting books and paper piles have shown that the radius of the cutting edge of trimmer knives immediately after sharpening ranges from 2 to 6 µm, whereas for a blunted knife, the magnitude of the cutting edge radius reaches 25 to 36 µm (Mordowin, 1962).

Fig. 1 presents a simplified diagram of the microgeometry of a circular knife's edge blunting used for cutting book blocks. Increasing the edge radius r as the blade wears causes a reduction in the blade tip height (due to, among others, normal wear) of the cutting edge by the value of KE, which reflects the radial wear (along the bisector of the knife's sharpening angle).



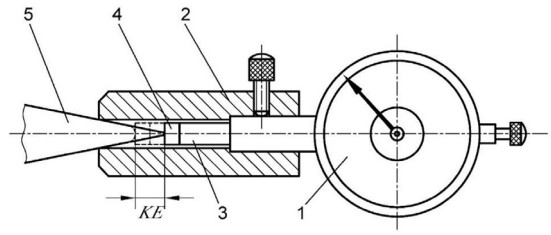
» **Figure 1:** *Simplified diagram of the microgeometry of circular knife edge blunting*

The magnitude of the knife blade wear (KE) can be calculated using the following formula (Petriaszwili, 2002).

$$KE = (R - r)\left[\frac{1}{\sin(\alpha_o/2)} - 1\right], \quad (1)$$

where: r – the edge radius of the sharpened knife blade, R – the radius of the blunted knife edge, α_0 – the knife sharpening angle.

Research indicates that the KE of circular knives can be measured using a special device designed and manufactured for this purpose. The diagram of this device is shown in Fig. 2.



» **Figure 2:** *Diagram of the device for measuring knife wear (Petriaszwili, 2002) 1 – dial gauge, 2 – measuring jaws, 3 – indicator spindle, 4 – hardened steel tip, 5 – circular knife edge*

For the measurement, a dial indicator (1) is used, the body of which is mounted in specially manufactured measuring jaws (2). A hardened, ground cylindrical steel tip (4) is attached to the indicator spindle (3). In order to eliminate scratches on the thrust surface of the ground tip upon contact with the knife edge during measurements, the tip (4) was hardened to a hardness of 68-70 HRC, i.e., above the hardness of the circular knives (5) used in the tests.

The measurement method involves positioning the device's jaws against a sharpened circular knife on a test rig, then oscillating it to establish a zero reading and subsequent wear values based on maximum pointer deflection. This method allows for easy, accurate measurement of blade wear (KE) without removing the knife from the trimmer.

Fig. 3 shows a view of the device manufactured according to Fig. 2, which was used during tests.

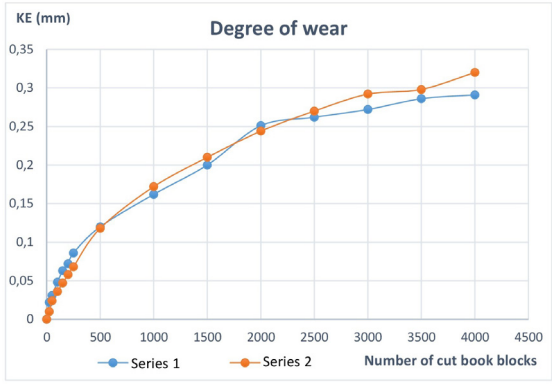


» **Figure 3:** *View of the device for measuring knife blade wear during the measurement process*

Steel circular knives (200 mm diameter, 5 mm thickness, 26° sharpening angle, 55-58 HRC) were tested for wear in traditional and vibration-assisted (0.5 mm eccentricity) setups using 10 mm thick offset paper (80 g/m²) book blocks, with 3 mm strips removed per cut.

Comparative tests were conducted at a 0.5 m/s feed rate and 1500 rpm rotational speed. Tool wear (KE) was measured at three points to plot wear curves against the number of cuts.

Fig. 4 shows the typical wear curves of the knife blades KE for the eccentric knife (series 1) and the traditional knife (series 2) as a function of the number of cuts n. As shown in Fig. 4, knife blade wear is more intense during the initial running-in phase (200–500 cuts) compared to the subsequent steady-state wear stage. Comparative studies revealed that the eccentric knife (series 1) experienced 8-10% less wear than the traditional circular knife (series 2) after 4000 cuts, despite showing a similar wear pattern.



» **Figure 4:** *The following curves illustrate the changes in the degree of wear (KE, mm) of the tested circular knife blades as a function of the number of cut book blocks (n). Series 1 – vibration-assisted circular knife (0.5 mm eccentricity), series 2 – traditional circular knife (without eccentricity)*

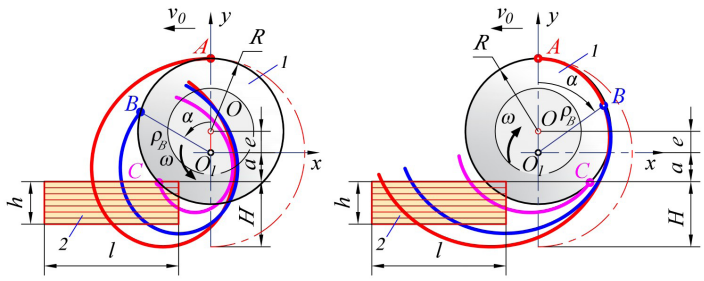
Following the analysis (Janicki, Petriaszwili & Komarov, 2017), it was determined that the trajectory of the vibration-assisted knife blade during cutting is significantly influenced by the knife's vibration parameters. The investigation and analysis of how the knife's vibration parameters affect the contact path between the cutting edge and the paper for an eccentrically positioned circular knife will enable the determination of optimal cutting regimes for vibration-assisted knives and the extension of their tool life, through the appropriate selection of the knife's rotational speed and eccentricity value.

3. Theoretical calculation of increasing the tool life of an eccentric circular knife

During cutting with a rotating circular knife, the points on the knife's cutting edge cover a significantly longer distance in the paper during processing than when cutting with a guillotine (straight) knife. This can lead to accelerated blade wear under certain conditions.

In contrast to a knife mounted without eccentricity (Janicki, Petriaszwili & Komarov, 2017), the motion trajectories of different points on the edge of an eccentric circular knife vary depending on the rotation radius the eccentricity value e, and the ratio of the knife blade's linear velocity to the feed rate of the book block.

A detailed analysis of the motion trajectory of the cutting edge of an eccentrically positioned circular knife during the book block cutting process will be conducted. This analysis will determine the influence of the process parameters on reducing the knife's path in the paper.



» **Figure 5:** *The motion trajectories of points A, B, and C on the edge of an eccentrically mounted knife a – co-directional cutting, b – counter-directional cutting; 1 – knife, 2 – book block*

As illustrated in Figure 5, the trajectories of three distinct points, labelled A, B, and C, are demonstrated on an eccentrically mounted knife. The trajectory of point B, for instance, which lies on the knife edge, can be described by the following parametric equations as a function of time t (assuming that the knife's rotational and feed speeds are constant):

for co-directional cutting –

$$x_B = -v_0 t - \rho_B \cdot \sin(\omega t + \alpha);\ \ y_B = \rho_B \cdot \cos(\omega t + \alpha) \qquad (2)$$

for counter-directional cutting –

$$x_B(t) = -v_0 t + \rho_B \cdot \sin(\omega t + \alpha);\quad y_B(t) = \rho_B \cdot \cos(\omega t + \alpha)\ , \qquad (3)$$

where the distance ρ from point B to the axis of rotation is determined as a function of the angle α in the direction of rotation:

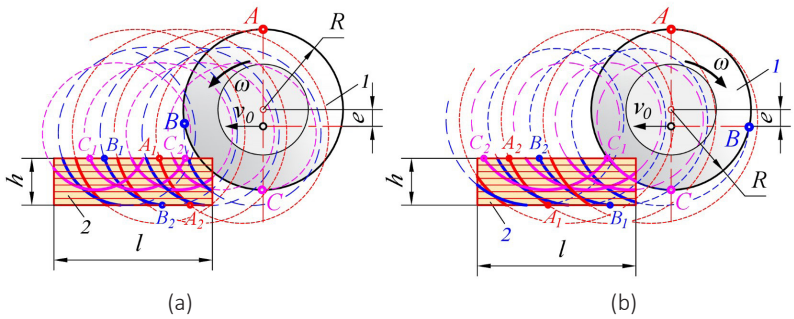
$$\rho_B = e \cdot \cos(\alpha) + \sqrt{e^2 \cos^2(\alpha) + R^2 - e^2} \qquad (4)$$

During the cutting process, each point on the knife edge leaves behind a conventional cutting trace on the surface of the cut block – an elongated cycloid described by equations (1 and 2). Let us examine the marks made on the block surface by the knife edge. When cutting a block, each point on the knife edge will enter into contact with the cut section of the block several times, leaving behind a series of „traces" – cuts arranged at equal distances from one another within each full rotation of the knife (Fig. 6).

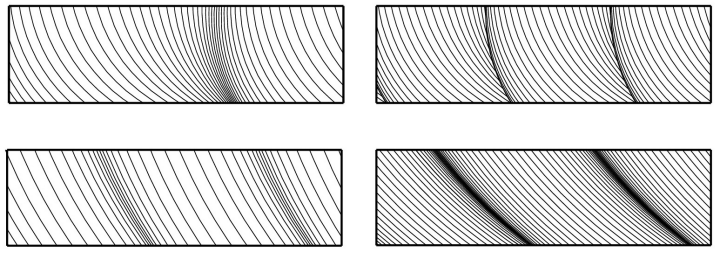
In the case of a knife mounted without eccentricity, the shape and length of the cutting traces on the block surface are consistent for every point on the edge. In the case of an eccentrically mounted knife, the shape and length of the cutting traces for different points (A, B, and C) differ significantly. For instance, point C of the knife edge does not cut completely through the block (see Fig. 6).

Studies (Petriaszwili, Janicki & Komarov, 2019) have shown that, with appropriately selected geometric and kinematic parameters of the machining process, two different modes of intermittent cutting can exist – one with complete separation of the knife blade from the block during the cutting process, and another where a part of the knife blade, during rotation, alternately cuts a partial height of the block and then the full height of the block.

The shape of the cutting trace trajectories is dependent on several factors. These include the position of the point, the direction of the knife's rotation, the knife radius R, the eccentricity value e, the distance from the block to the axis of rotation a, the block thickness b, the knife's rotational speed ω and the block feed rate v_0. During continuous cutting, the trajectories of the knife



» **Figure 6:** *Traces in the block of the cutting trajectories generated by points A, B, and C of an eccentrically mounted knife edge, a – co-directional cutting, b – counter-directional cutting; A1, B1, C1 – blade entry points into the block; A2, B2, C2 – blade exit points from the block; 1 – knife, 2 – book block*



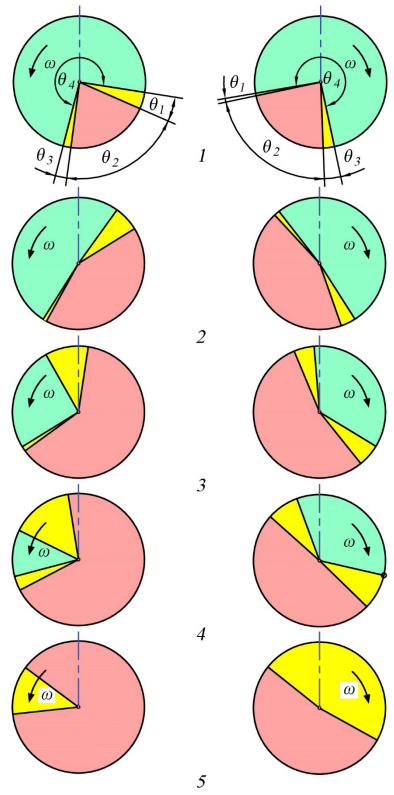
» **Figure 7:** *The diagrams illustrate the trajectories of the knife blade points' motion during the cutting of book blocks at different setup distances a of the block from the knife's axis of rotation a – continuous cutting, b – intermittent cutting*

edge points' motion do not intersect during cutting, but the density of the traces (the distances between them) varies (Fig. 7a). In contrast, during intermittent cutting, the cutting is periodically interrupted during the reverse motion of the knife blade, and the trajectories of the traces of adjacent edge points intersect (Fig. 7b).

Studies conducted using Mathcad software have demonstrated that, under specific machining process parameters, characteristic sectors can exist along the circumference of the eccentric circular knife edge. These include a knife blade sector where the full height of the paper stack in the block is cut, partial cutting sectors (during the cutting of a partial stack height), and a blade sector where the knife does not participate in the cutting process. The size and positioning of these characteristic cutting sectors on the knife are determined by the geometric and kinematic parameters of the cutting process.

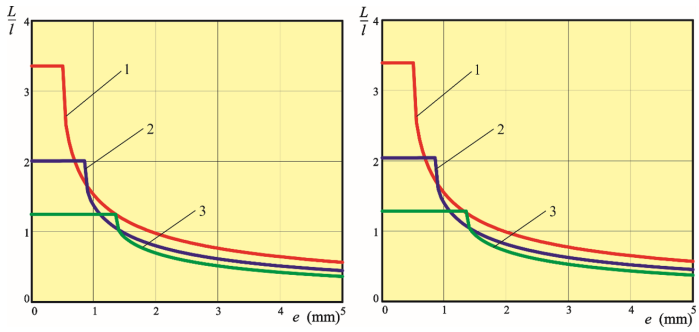
As illustrated in Figure 8, the simulation of potential cutting sector distributions on a circular knife edge under varying co-directional and counter-directional feed rates highlights changes in full cutting, partial cutting, and non-cutting sectors. The full cutting sector is defined as $\theta_2 = \varphi_3 - \varphi_2$; the sector of the blade entering the block (partial cutting) – $\theta_1 = \varphi_2 - \varphi_1$; the sector of the blade exiting the block (partial cutting) – $\theta_3 = \varphi_4 - \varphi_3$; the non-cutting sector – $\theta_4 = \varphi_1 - \varphi_4$.

As illustrated in Figure 8, increasing the block feed rate results in intermittent cutting, leading to an expansion in both the size of the full cutting sector and the partial cutting sectors. Concurrently, the knife edge sector, which does not participate in the cutting process, experiences a reduction. As the feed rate increases, the sector not involved in cutting decreases until, at high speeds (over 680 mm/s co-directional and 717 mm/s counter-directional), the process becomes continuous over the entire material height.



» **Figure 8:** *Simulations of the cutting sector distributions on the eccentric circular knife edge at different values of the book block feed rate a – co-directional cutting, b – counter-directional cutting Parameters: v0 = 1 – 100 mm/s; 2 – 300 mm/s; 3 – 500 mm/s; 4 – 560 mm/s; 5 – 660 mm/s; D = 200 mm, e = 2 mm, h = 10 mm, a = 70 mm, n = 2000 rpm. In the knife edge sectors marked with red, cutting of the full block height occurs; yellow – cutting of a partial height; green – the knife edge sector does not participate in the cutting process.*

In accordance with Petriaszwili, Janicki and Komarov (2019), calculations were performed to determine the path covered by a knife edge point when cutting a block with a circular knife mounted without eccentricity. The process parameters affecting the reduction of this path, and consequently blade wear, were also identified.



» **Figure 9:** *Influence of eccentricity e on the dimensionless cutting length L/l for varying book block feed rates v_0 a – co-directional cutting, b – counter-directional cutting. The analysis, based on the parameters: 1 – v_0 = 150 mm/s, 2 – v_0 = 250 mm/s, 3 – v_0 = 400 mm/s, a = 70 mm, b = 10 mm, R = 100 mm, n = 2000 rpm*

The path covered by point B of the eccentric knife edge during cutting was calculated. The path L of a single trace of the knife edge point B during cutting (Fig. 6) can be found using the expression:

$$L_B = \int_{t_{B1}}^{t_{B2}} \sqrt{v_0^2 + \omega^2 \rho_B^2 \pm 2 v_0 \omega \rho_B \cos(\omega t + \alpha_B)}\, dt \qquad (5)$$

where tB1 and tB2 are the entry and exit times of point B of the blade into and out of the block, respectively (Fig. 2, points B1 and B2). In equation (4), the „plus" sign corresponds to co-directional cutting, and the „minus" sign corresponds to counter-directional cutting.

The blade's entry time into the block and exit time from the block can be calculated based on the trajectory equations of the blade point B (1) – (2). The total number of cutting traces (the path in the paper) left by point B in a book block of length l is: $z = \frac{\omega \cdot l}{2\pi v_0}$. The length of a single trace of the blade point during cutting depends on its distance from the knife's axis of rotation, that is, on its position on the knife edge.

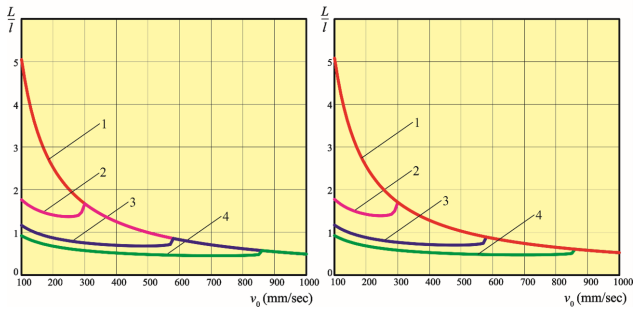
A specialized algorithm using Mathcad software simulations was developed to determine the total cutting path length of an eccentric knife for book block processing.

Figures 9 and 10 compare the relative blade path within the block for an eccentric knife versus a standard, non-eccentric circular knife across various process parameters.

Simulations of eccentric and non-eccentric circular knife cutting show that intermittent cutting results in a shorter cut length, which is heavily influenced by eccentricity. Selecting the correct parameters enables 180° of the knife edge to cut the book block, allowing for rotation and extending the tool's lifespan by utilizing the unblunted side. This analysis suggests optimizing tool wear in bookbinding processes.

4. Conclusions

Vibratory cutting of book blocks using eccentrically positioned circular knives has demonstrated the potential for significantly reducing cutting forces. A new measuring tool that measures the shortening of the circular knife blade tip enables the condition of the cutting edge of these knives to be monitored during book production. The experimental part of the work involved a comparative analysis of the operating times of traditional



» **Figure 10:** *Influence of the block feed rate v0 on the dimensionless cutting length L/l depending on the eccentricity value e; a – co-directional cutting, b – counter-directional cutting. The analysis, based on the parameters: 1 – e = 0 mm, 2 – e = 1 mm, 3 – e = 2 mm, 4 – e = 3 mm, a = 70 mm, b = 10 mm, R = 100 mm, n = 2000 rpm. The changes in curves 2, 3, and 4 indicate the transition from intermittent to continuous cutting mode.*

circular knives and vibrating knives (from sharpening to dulling). This revealed that vibrating circular knives have a tool life that is approximately 10% longer. The study also found that the trajectory of the vibrating knife blade during cutting is significantly influenced by its vibration parameters. Computer simulations of cutting processes using eccentric and non-eccentric circular knives showed that the cutting length is shorter in intermittent mode than in continuous mode and is significantly affected by the degree of eccentricity. During intermittent cutting, not all sectors of the blade are involved in cutting the book block. When the total cutting sector size is appropriately selected – specifically, when it is approximately 180° – only the half of the circular knife blade that comes into contact with the book block paper during cutting will wear. Once this portion of the blade becomes dull, the circular knife can be rotated by approximately 180° to resume cutting using the sharp, unused portion of the blade. This significantly extends the life of vibrating circular knives.

5. References

Daurski, A.N. and Machihin, U.A. (1980) *Rezanie pishchevych materialov: teoria protsessa, mashiny, intensifikatsiya*. Moscow: Pishchevaya Promyshlennost. (in Russian).

Ginzburg, V. (1957) Issledovanie protsessa rezaniya na odnonozhevyh bumagorezalnyh mashinah. In: Sbornik WNIIPM, 3. Moscow, USSR, pp. 15–21. (in Russian).

Gruszewski, V. (1963) Technologiczeskije parametry rezanija broszur diskowymi nożami. In: *Trudy WNIIPM*, 23. Moscow, USSR, pp. 37–48. (in Russian).

Janicki, P., Petriaszwili, G. and Komarov, S. (2016) 'Charakterystyka kinematyki procesu krojenia papieru nożem krążkowym ustawionym mimośrodowo', *Opakowanie*, 10, pp. 57–59. (in Polish).

Janicki, P., Petriaszwili, G. and Komarov, S. (2017) 'Badanie trajektorii ruchu krawędzi tnącej noża krążkowego podczas krojenia wkładów książkowych', *Opakowanie*, 62(9), pp. 76–79. (in Polish).

Komarov, S., Petriaszwili, G. and Janicki, P. (2024) 'Vibrational trimming of book-edge with an eccentrically installed disk knife', *Vibroengineering Procedia*, 57, pp. 8–15. DOI: 10.21595/vp.2024.24503

Komarov, S., Petriaszwili, G. and Janicki, P. (2025) Analytical investigations of cutting force in book block trimming using an eccentrically mounted disc knife. In: *Innovations in Publishing, Printing and Multimedia Technologies: Book of Abstracts*. Kaunas: Kauno Kolegija, pp. 27–28. ISBN 978-9955-27-662-3.

Krabisch, K. (1962) *Schneiden mit rotierenden Messern*. Leipzig: IPM.

Mordowin, B. (1962) *Buchbindereimaschinen.* Berlin: VEB Verlag Technik.

Petriaszwili, G. (2002) 'Diagnostyka stanu ostrzy krajarek jedno- i trójnożowych', *Przegląd Papierniczy*, 56(2), pp. 70–72. (in Polish).

Petriaszwili, G. (2024) 'Badania analityczne i eksperymentalne wibracyjnego krojenia bloków książkowych', *Przemysł Chemiczny,* 103(11), pp. 1331–1333. DOI: 10.15199/62.2024.11.22 (in Polish).

Petriaszwili, G., Janicki, P. and Komarov, S. (2019) 'Influence of the work parameters of the eccentrically set circular knife on the reducing during cutting the trajectory of contact of the blade with a book block', *Przegląd Papierniczy*, 75(4), pp. 253–257. DOI: 10.15199/54.2019.4.1

Petriaszwili, G., Janicki, P. and Komarov, S. (2020) Investigations on book cutting by circular knife with eccentric blade movement. In: Kašiković, N., Novaković, D., Pavlović, Ž. and Dedijer, S. (eds.) *Proceedings of the 10th International Symposium on Graphic Engineering and Design GRID 2020*, 12–14 November 2020, Novi Sad, Serbia. Novi Sad: Grafički centar GRID, pp. 230–233. DOI: 10.24867/GRID-2020-p24

Petriaszwili, G., Janicki, P. and Komarov, S. (2021) Experimental research on book-edge trimming by circular knife with eccentric blade movement. In: Gatsou, C. and Tsigonias, M. (eds.) *Proceedings of the 52nd Annual Conference of the International Circle, IC-2021*, 20–23 September 2021, Athens, Greece. HELGRAMED – The Hellenic Union of Graphic Arts and Media Technology Engineers, pp. 41–51.

Petriaszwili, G., Khadzhynova, S., Komarov, S. and Janicki, P. (2025) Badania nowego sposobu krojenia bloków książkowych nożem krążkowym ustawionym z mimośrodem. In: *X International Scientific-Technical Conference 'Print, Multimedia & Web', PMW-2025*, Vol. 1. Kharkiv, pp. 58–59. (in Polish).

Petriaszwili, G., Komarov, S. and Janicki, P. (2025) 'Development and evaluation of a vibratory book-block cutting method using eccentric disk knives', *Advances in Science and Technology Research Journal*, 19(9), pp. 469–480. DOI: 10.12913/22998624/207552

Reznik, N.E. (1975) *Teoriya rezaniya lezviyem i osnovy rascheta rezhushchikh apparatov*. Moscow: Mashinostroyeniye. (in Russian).

Staniszewski, J. and Porankiewicz, B. (1997) *Kryteria i metody oceny stopnia stępienia ostrzy narzędzi skrawających do obróbki drewna*. Poznań: Wydawnictwo Akademii Rolniczej. (in Polish).



© 2026 Authors. Published by the University of Novi Sad, Faculty of Technical Sciences, Department of Graphic Engineering and Design. This article is an open access article distributed under the terms and conditions of the Creative Commons Attribution license 4.0 Serbia (http://creativecommons.org/licenses/by/4.0/rs/).

Original Scientific Paper https://doi.org/10.24867/GRID-2026-p14

A Methodological Framework for the Prepress Preparation of Colour Images Based on New Approaches to Optimising the Colour Reproduction Process

Vitalii Semeniv
Nataliia Zanko
Mariia Semeniv
Bohdan Kovalskyi

Lviv Polytechnic National University, Lviv, Ukraine

ABSTRACT

Modern colour image reproduction technologies in the printing industry require coordinated integration of colour separation, halftoning, colour synthesis, and ink consumption management while accounting for the nonlinear behaviour of printing processes. Traditional approaches do not always provide both accurate colour reproduction and efficient ink use. This study aims to establish methodological foundations for prepress preparation of colour images and to develop the conceptual model of the IT Color Print information technology for controlled colour reproduction and optimised ink consumption. The proposed methodology integrates mathematical modelling of colour synthesis, colour coordinate transformations, geometric clustering of the colour gamut, nonlinear transformation analysis, and experimental printing. A set of algorithms was developed for four-colour and multicolour prepress processing. The nonlinear transformation index of the printing process and the colorimetric characteristics of printing inks were incorporated into the colour transformation model. A relationship was established between the nonlinear transformation index and the optical densities of printed patches, indicating that minimisation of this index can be used as a criterion for identifying favourable colour reproduction conditions. Based on these relationships, a gamma-correction method for CMY and K components was developed to preserve neutral grey balance and maintain tonal and colour stability. Analysis of colour separations showed that CMY inks are used primarily to reproduce chromatic image components, whereas black ink mainly forms image structure, tonal gradation, and achromatic content. This redistribution reduced CMY ink consumption by approximately 60% while increasing the contribution of black ink. Experimental validation was performed by printing fine-art photographs on an HP Indigo 5500 press. The results confirmed agreement between theoretical predictions and experimental data and demonstrated substantial CMY ink savings without significant deterioration in colour reproduction accuracy. The IT Color Print model integrates colour separation, synthesis, halftoning, and ink-component correction into a unified framework for controlled and resource-efficient colour printing.

KEY WORDS

Colour image prepress preparation, ink consumption optimisation, colour space, colour synthesis, colour reproduction, optical density, gamma correction.

1. Introduction

The reproduction of colour images by printing technologies is a complex multistage process involving the digital representation, processing, and transformation of colour information throughout all stages of prepress preparation and print production. Accuracy and stability of colour reproduction are among the key quality indicators of printed products. Since printing processes are inherently nonlinear, while colour formation is strongly influenced by the properties of printing inks, printing substrates, and technological printing conditions, achieving predictable colour reproduction requires improved methods for processing colour information at the prepress stage.

To compensate for the influence of these factors, researchers widely employ colorimetric measurements of printed samples, as they enable an objective assessment of the final colour reproduction result and facilitate the identification of relationships between the parameters of the digital original, the characteristics of the printing process, and the colour coordinates of the resulting print (Tjandra, Heywood & Chandrawati, 2023).

Numerous colour management methods have been developed on the basis of colorimetric measurements, among which ICC profiling, colour separation techniques, and DeviceLink transformations are the most widely used (Sharma, 2018; International Color Consortium, 2024).

The relevance of this approach is supported by the current ISO 12647 series of standards, particularly ISO 12647-2, in which print quality control is based on colorimetric measurements, printing process characterisation data, and CIELAB colour coordinates (International Organization for Standardization, 2013).

These standards specify target colorimetric characteristics of prints and permissible tolerances. However, they do not define a universal methodology for achieving these characteristics under specific production conditions, nor do they provide tools for determining optimal colour printing conditions that simultaneously ensure stable colour reproduction, resource efficiency, and rational use of printing inks.

In parallel, research continues into universal colour representation systems that could serve as an intermediate framework for coordinating colour information during conversion from the three-component RGB colour space to the four-colour Cyan, Magenta, Yellow, and Black system in the colour separation process (Fraser et al., 2005). The CIELAB system has certain limitations in tasks requiring a geometrically consistent representation of the colour gamut (Kynash & Semeniv, 2025), the evaluation of colour differences, and analytical transformation of colour coordinates, because its perceptual uniformity is not consistent throughout all regions of the colour space (Li et al., 2017; Luo et al., 2023).

Another significant challenge is the reproduction of colours in a digital original that fall outside the colour gamut of the printing process and therefore cannot be reproduced accurately in print (Sikudova et al., 2016; Yuan et al., 2021). An additional factor affecting colour reproduction accuracy is the colour balance of the digital original, which is influenced by lighting conditions, digitisation parameters, and image-processing algorithms (Kovalskyi et al., 2022).

To address these issues, approaches are being investigated that account for the nonlinearity of the printing process, the colorimetric characteristics of printing inks, and the properties of printing substrates, as well as methods for replacing non-reproducible colours based on the Munsell system using the ICaS colour space (Shovheniuk et al., 2019; Kovalskyi et al., 2024).

In this context, the authors have been conducting research aimed at developing a methodology for the prepress preparation of colour images to ensure predictable colour reproduction and optimise printing ink consumption. The approach is based on colorimetric measurements of printed samples, statistical processing of experimental data, and characterisation data provided by Fogra (Fogra, n.d.).

The aim of this study is to develop methodological principles for the prepress preparation of colour images based on mathematical modelling of colour formation and reproduction processes, taking into account the nonlinearity of the printing process and the optimisation of ink consumption.

The objectives of the study are to:

- describe a mathematical model of colour synthesis on the print;
- determine the regularities governing the formation of colour components;
- investigate the nonlinearity of the printing process;
- develop principles for optimised CMYK colour separation;
- experimentally evaluate ink consumption and colour reproduction accuracy;
- develop a conceptual model of IT Color Print.

2. Materials and methods

2.1. Development of the theory of colour synthesis in printing

Colour formation on a printed sample is determined by the spatial interaction of halftone dots from individual ink layers and their overprints on the paper surface. The ambiguity inherent in converting colour from the three-dimensional RGB colour space to the four-component CMYK system necessitates the use of additional colour separation criteria. In conventional colour management systems, this ambiguity is addressed through ICC profiles generated from experimental characterisation of a specific printing process and a predefined colour separation strategy. At the same time, the inverse determination of CMYK components required to reproduce a specified colour remains a non-unique problem. Consequently, obtaining a unique analytical solution requires the introduction of additional parameters and a mathematical framework capable of simultaneously describing colour synthesis on the print and accounting for the nonlinearity of the actual printing process.

The theoretical basis of the proposed framework is formed by the ICaS colour space developed by the authors and the nonlinear transformation index γ. The properties of the ICaS colour space make it possible to integrate, within a unified mathematical description, the RGB space of the digital original, CIE colorimetric spaces used for experimental characterisation of the printing process, and the colour space of the printed output. The nonlinear transformation index γ characterises the deviation of the actual printing process from a linear model and enables the calculations to be adapted to specific printing conditions (Kovalskyi et al., 2024). Accordingly, the ICaS colour space and the nonlinear transformation index γ form a unified mathematical basis for analytical modelling and controlled colour separation.

Within this approach, four-ink colour synthesis is described by a vector equation in the ICaS colour space (1), which accounts for the relative dot areas of the CMYK components, the colour vectors of the paper and solid inks, and the vectors corresponding to their pairwise and three-ink overprints. Transformation of equation (1) makes it possible to treat one of the chromatic inks as a parameter and to describe the limiting cases of synthesis using two chromatic inks and black ink (5), or three chromatic inks and black ink (6).

where $\mathbf{F}_{ICaS}^{CMYK}$ is the colour vector in the ICaS colour space; σ_n, σ_m, σ_j, σ_k are the relative dot areas of the CMYK inks, denoted by the indices n, m, j, and K; $\hat{\mathbf{F}}_W, \hat{\mathbf{F}}_n, \hat{\mathbf{F}}_m, \hat{\mathbf{F}}_j$ are the colour vectors of the paper anwd solid chromatic inks; and $\hat{\mathbf{F}}_{j,n}, \hat{\mathbf{F}}_{j,m}, \hat{\mathbf{F}}_{n,m}, \hat{\mathbf{F}}_{j,n,m}$ are the vectors of pairwise and three-ink overprints of the chromatic inks.

In equation (1), the relative dot area of one of the chromatic inks σ_j is factored out. The amount of the third chromatic ink can be represented by the following quantity:

$$\Delta\sigma_j = (1-\sigma_j) \tag{2}$$

Equation (3) consists of two components.

At σ_j =0, equation (4) takes the following form and describes colour synthesis using two chromatic inks and black ink (Equation 5).

$$\mathbf{F}_{ICaS}^{CMYK} = (1-\sigma_K)\left(\mathbf{F}_{ICaS}^{(2)} + \Delta\sigma_j \mathbf{F}_{ICaS}^{(3)}\right) \tag{4}$$

At σ_j =1, it describes colour synthesis using three chromatic inks and black ink (Equation 6).

The validity of this mathematical representation was verified using experimental data. The CaS diagrams constructed for colours synthesised by two chromatic inks and their combinations with black ink confirmed the relationships predicted by the model (Figure 1). In particular, the introduction of black ink results in a systematic reduction of the corresponding colour surface, while the extent of this transformation is determined by the proportion of black ink and the nonlinear transformation index γ. These results confirm the appli-

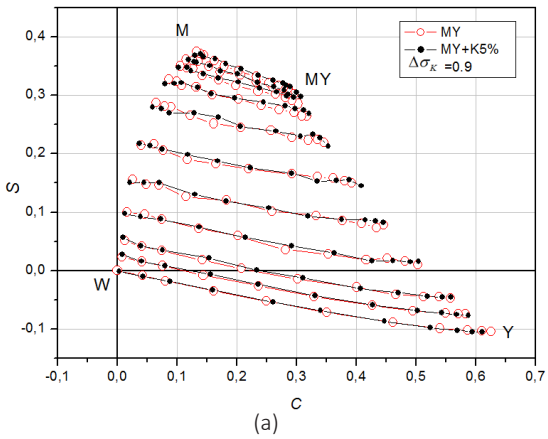
$$\begin{aligned}\mathbf{F}_{ICaS}^{CMYK} = (1-\sigma_K)\{&\hat{\mathbf{F}}_W(1-\sigma_n)(1-\sigma_m)(1-\sigma_j) + \hat{\mathbf{F}}_j\sigma_j(1-\sigma_n)(1-\sigma_m) + \\ &+ \hat{\mathbf{F}}_n\sigma_n(1-\sigma_j)(1-\sigma_m) + \hat{\mathbf{F}}_m\sigma_m(1-\sigma_j)(1-\sigma_n) + \hat{\mathbf{F}}_{j,n}\sigma_j\sigma_n(1-\sigma_m) + \\ &+ \hat{\mathbf{F}}_{j,m}\sigma_j\sigma_m(1-\sigma_n) + \hat{\mathbf{F}}_{n,m}\sigma_n\sigma_m(1-\sigma_j) + \hat{\mathbf{F}}_{j,n,m}\sigma_j\sigma_n\sigma_m\}\end{aligned} \tag{1}$$

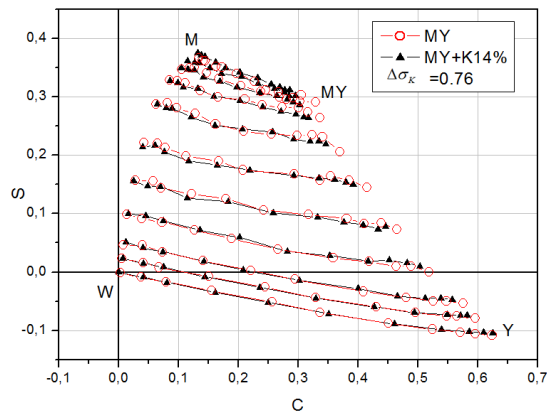
$$\begin{aligned}\mathbf{F}_{ICaS}^{CMYK} = (1-\sigma_K)\{&\hat{\mathbf{F}}_j(1-\sigma_n)(1-\sigma_m) + \hat{\mathbf{F}}_{n,j}\sigma_n(1-\sigma_m) + \hat{\mathbf{F}}_{m,j}\sigma_m(1-\sigma_n) + \hat{\mathbf{F}}_{n,m,j}\sigma_n\sigma_m + \\ &+ \Delta\sigma_j\left[\hat{\mathbf{F}}_W(1-\sigma_n)(1-\sigma_m) + \hat{\mathbf{F}}_n\sigma_n(1-\sigma_m) + \hat{\mathbf{F}}_m\sigma_m(1-\sigma_n) + \hat{\mathbf{F}}_{n,m}\sigma_n\sigma_m - \right. \\ &\left. - \hat{\mathbf{F}}_{n,j}\sigma_n(1-\sigma_m) - \hat{\mathbf{F}}_{m,j}\sigma_m(1-\sigma_n) - \hat{\mathbf{F}}_j(1-\sigma_n)(1-\sigma_m) - \hat{\mathbf{F}}_{j,n,m}\sigma_n\sigma_m\right]\}\end{aligned} \tag{3}$$

$$\mathbf{F}_{ICaS}^{CMYK} = (1-\sigma_K)\left(\hat{\mathbf{F}}_W(1-\sigma_n)(1-\sigma_m) + \hat{\mathbf{F}}_n\sigma_n(1-\sigma_m) + \hat{\mathbf{F}}_m\sigma_m(1-\sigma_n) + \hat{\mathbf{F}}_{n,m}\sigma_n\sigma_m\right) \tag{5}$$

$$\mathbf{F}_{ICaS}^{CMYK} = (1-\sigma_K)[\hat{\mathbf{F}}_W(1-\sigma_n)(1-\sigma_m) + \hat{\mathbf{F}}_{n,j}\sigma_n(1-\sigma_m) + \hat{\mathbf{F}}_{m,j}\sigma_m(1-\sigma_n) + \hat{\mathbf{F}}_{n,m,j}\sigma_n\sigma_m] \tag{6}$$

cability of the proposed mathematical description to colour modelling under actual printing conditions.





» **Figure 1:** *CaS diagrams of colours formed by pairwise overprinting of magenta and yellow inks with the addition of 5% (a) and 14% (b) of Black ink, based on experimental data*

To solve the system of equations derived from the vector equation (7), one of the chromatic inks was treated as a parameter with a fixed relative dot area. Under this formulation, the system is reduced to three unknowns.

The solution was obtained by successive elimination of variables: one unknown was first expressed in terms of the others, and the resulting expression was then successively substituted into the subsequent equations, thereby progressively reducing the number of unknowns.

As a result, the system was reduced to a second-order equation (8) for one of the chromatic inks.

$$a + b\sigma_n + c\sigma_n^2 = 0. \tag{8}$$

Equation (8) yields the solution for one of the chromatic inks:

$$\sigma_n = \frac{1}{2a}\left(b \pm \sqrt{b^2 - 4ac}\right) \tag{9}$$

Where the coefficients of equation (8) and its solution (9) are expressed as determinants of 3 × 3 matrices (Equation 10).

After determining one of the ink components from equation (9), the values of the second chromatic ink and the black ink were obtained by back-substitution. Consequently, for each specified value of the parametric ink, an analytical solution was obtained for the remaining components, while variation of the parameter makes it possible to determine the range of admissible CMYK ratios capable of reproducing the same colour.

The development of four-ink colour synthesis theory is therefore represented by the derived colour synthesis equation (7), in which one of the chromatic inks is assigned a fixed value. This formulation enables analytical solutions to be applied to conventional image colour separation and makes it possible to determine a range of relative dot areas of the printing inks for reproducing each colour of the original image.

$$\begin{aligned}\mathbf{F}_{ICaS}^{CMYK} = \sigma_K\Big\{&\hat{\mathbf{F}}_W(1-\sigma_n)(1-\sigma_m)+\hat{\mathbf{F}}_n\sigma_n(1-\sigma_m)+\hat{\mathbf{F}}_m\sigma_m(1-\sigma_n)+\hat{\mathbf{F}}_{n,m}\sigma_n\sigma_m+\\&+\Big[-\hat{\mathbf{F}}_W(1-\sigma_n)(1-\sigma_m)-\hat{\mathbf{F}}_m\sigma_m(1-\sigma_n)-\hat{\mathbf{F}}_n\sigma_n(1-\sigma_m)-\hat{\mathbf{F}}_{n,m}\sigma_n\sigma_m+\\&+\hat{\mathbf{F}}_j(1-\sigma_n)(1-\sigma_m)+\hat{\mathbf{F}}_{j,n}\sigma_n(1-\sigma_m)+\hat{\mathbf{F}}_{j,m}\sigma_m(1-\sigma_n)+\hat{\mathbf{F}}_{j,n,m}\sigma_n\sigma_m\Big]\sigma_j\Big\}\end{aligned} \tag{7}$$

$$a=\begin{bmatrix} I_{AU}^{(4)} & I_m - I_{n,m} + \Delta\sigma_j\left(I_{n,m} + I_{m,j} - I_m - I_{n,m,j}\right) & I_n - I_W + \Delta\sigma_j\left(I_W + I_{n,j} - I_n - I_j\right) \\ C_{AU}^{(4)} & C_m - C_{n,m} + \Delta\sigma_j\left(C_{n,m} + C_{m,j} - C_m - C_{n,m,j}\right) & C_n - C_W + \Delta\sigma_j\left(C_W + C_{n,j} - C_n - C_j\right) \\ S_{AU}^{(4)} & S_m - S_{n,m} + \Delta\sigma_j\left(S_{n,m} + S_{m,j} - S_m - S_{n,m,j}\right) & S_n - S_W + \Delta\sigma_j\left(S_W + S_{n,j} - S_n - S_j\right)\end{bmatrix};$$

$$b=\begin{bmatrix} I_{AU}^{(4)} & I_{n,m} + \Delta\sigma_j\left(I_{n,m,j} - I_{n,m}\right) & I_n + I_m - I_W + \Delta\sigma_j\left(I_W + I_{n,j} + I_{m,j} - I_n - I_m - I_j\right) \\ C_{AU}^{(4)} & C_{n,m} + \Delta\sigma_j\left(C_{n,m,j} - C_{n,m}\right) & C_n + C_m - C_W + \Delta\sigma_j\left(C_W + C_{n,j} + C_{m,j} - C_n - C_m - C_j\right) \\ S_{AU}^{(4)} & S_{n,m} + \Delta\sigma_j\left(S_{n,m,j} - S_{n,m}\right) & S_n + S_m - S_W + \Delta\sigma_j\left(S_W + S_{n,j} + S_{m,j} - S_n - S_m - S_j\right)\end{bmatrix}; \tag{10}$$

$$c=\begin{bmatrix} I_{AU}^{(4)} & I_n + \Delta\sigma_j\left(I_{n,j} - I_n\right) & I_{n,m} + \Delta\sigma_j\left(I_{n,m,j} - I_{n,m}\right) \\ C_{AU}^{(4)} & C_n + \Delta\sigma_j\left(C_{n,j} - C_n\right) & C_{n,m} + \Delta\sigma_j\left(C_{n,m,j} - C_{n,m}\right) \\ S_{AU}^{(4)} & S_n + \Delta\sigma_j\left(S_{n,j} - S_n\right) & S_{n,m} + \Delta\sigma_j\left(S_{n,m,j} - S_{n,m}\right)\end{bmatrix}.$$

2.2. Extension of mathematical colour separation capabilities

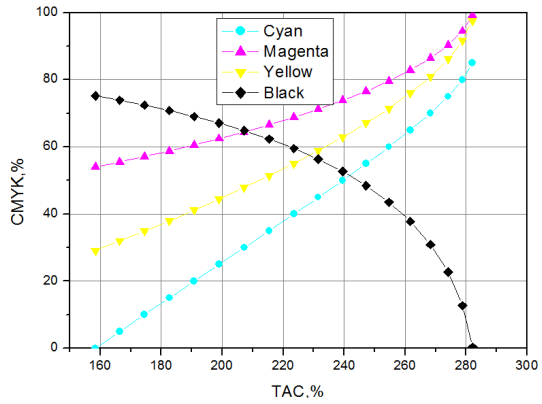
To validate the analytical relationships, modelling was performed using the colour vectors of the printing inks and paper derived from Fogra51 characterisation data for offset printing on coated paper (Table 1).

The modelling yielded a set of admissible combinations of relative dot areas capable of reproducing a specified colour. The modelling results for two colours are presented in Figure 2. For colour 1, as the Cyan component increased from 0 to 85 %, the black (K) component decreased from 75 to 0 %, while the Total Area Coverage (TAC) increased from 158 to 282 %. The limiting synthesis configurations were (M), (Y), (K) and (C), (M), (Y). For colour 2, variation of the Magenta component within the range of 57–98 % was accompanied by a decrease in black (K) from 72 to 0 % and an increase in TAC from 153 to 264 %. The corresponding limiting configurations were (C), (M), (K) and (C), (M), (Y).

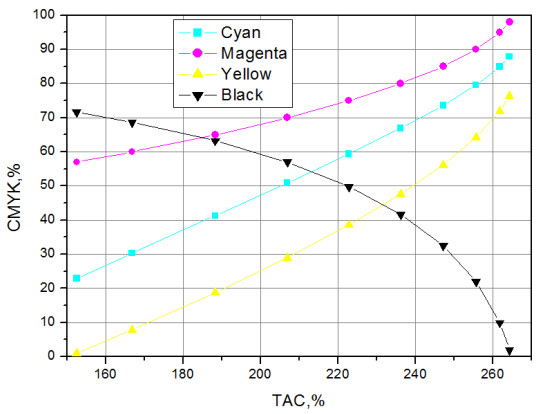
The results indicate that the minimum Total Area Coverage is achieved at the maximum contribution of black ink and the exclusion of one chromatic component. A common relationship was observed for the analysed colours: as the proportion of the parametric chromatic ink increases, the contribution of black ink decreases, while the Total Area Coverage changes accordingly. Hence, the same colour can be reproduced using different C, M, Y, and K ratios, each associated with a different level of Total Area Coverage.

2.3. Geometric clustering of the colour gamut in the icas space

Further analysis showed that the chromatic part of the colour gamut in the ICaS colour space can be represented as a set of geometrically defined regions whose boundaries are determined by the colour vectors of the chromatic printing inks (Figure 3). For CMYK, the C, M, and Y vectors form three principal clusters in the CaS plane, each corresponding to a region of colours reproducible by a specific pair of chromatic inks. The C and S coordinates determine the assignment of a colour to the corresponding cluster and, consequently, the selection of chromatic inks, whereas the I coordinate is associated with formation of the achromatic component. Once a colour has been assigned to a particular cluster, the relative dot areas of the corresponding inks can be determined from the analytical solutions of the colour synthesis equations for the printed sample.



(a)



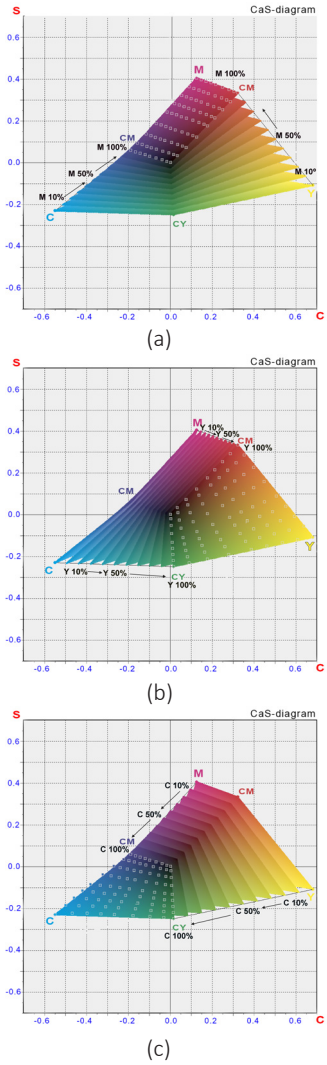
(b)

» **Figure 2:** *Modelling of colour synthesis: (a) colour 1, RGB (83, 56, 57); (b) colour 2, RGB (77, 56, 74)*

Table 1

Colour vectors of the printing inks and different paper types

	Colour coordinates in Adobe RGB (1998)			Colour coordinates in the ICaS colour space		
	r	g	b	I	C	S
C-Cyan	0.000000	0.596527	0.872391	0.8480798	–0.561970	–0.286110
M-Magenta	0.729509	0.028887	0.482240	0.7162811	0.046958	0.500307
Y-Yellow	0.947079	0.872560	0.136045	1.1291141	0.623891	–0.112620
K-Black	0.172533	0.172632	0.174278	0.2999004	–0.001360	0.000291
W-paper	0.937619	0.939018	0.986731	1.6531655	–0.038440	0.009275
CM	0.207390	0.206646	0.504935	0.5305679	–0.234820	0.063464
MY	0.736664	0.134682	0.179107	0.6064790	0.312518	0.356942
CY	0.164517	0.551749	0.305113	0.5896931	–0.029050	–0.275690



» **Figure 3:** *Modelling of colour synthesis on the print using two chromatic inks with (a) Cyan, (b) Magenta, and (c) Yellow as the parametric ink; points represent Fogra51 experimental data*

The proposed mathematical framework is not restricted to the CMYK system and can be extended to multicolour printing. Increasing the number of chromatic inks results in additional clusters in the CaS plane, while the principle of selecting inks for reproducing an individual colour remains unchanged. This establishes a mathematical basis for scalable, controlled colour separation that accounts for the characteristics of a specific printing process.

2.4. Method for determining the nonlinear transformation index of the printing process

The nonlinear transformation index γ, identified in our previous studies (Kovalskyi et al., 2024) as one of the key parameters of the proposed mathematical framework, accounts for the technological conditions of colour reproduction. Unlike parameters specified for a standardised printing process, γ is determined experimentally for a particular printing system and characterises its nonlinearity.

The method for determining the nonlinear transformation index γ was improved, and an algorithm for its calculation was developed. The input data comprise measured CIELAB colour coordinates of the gradation patches of individual printing inks and the corresponding relative dot areas. Following colour conversion to the working RGB colour space, a designated RGB component is used for each ink: R for Cyan, G for Magenta, and B for Yellow. The nonlinear relationship between the input gradation and the colour characteristic of the print was described by a power-law function:

$$F_i = C_0 + K_C(1-\sigma_i)^{\gamma}, \tag{11}$$

Where F_i is the colour characteristic of the *i*- th gradation patch, C_0 is the coordinate of the ink colour vector, K_C is the contrast coefficient, and σ_i is the relative dot area of the printing ink.

The sequence of computational procedures in the improved method was formalised as pseudocode (Algorithm 1).

Algorithm 1. Determination of the nonlinear transformation index

Input: experimental dot areas σ_i measured colour coordinates of gradation patches

1. Convert measured colour coordinates to the working RGB space.
2. Select the highlighting RGB component for the analysed ink: Cyan → R Magenta → G Yellow → B
3. Form and sort the experimental data pairs (σi, F_i).
4. Determine the colour coordinate C_0.
5. Estimate initial values γ_0 and KC using the least-squares method.
6. Set $\gamma = \gamma_0$.
7. Calculate theoretical values Fcalc using the nonlinear model.
8. Calculate the mean deviation between Fcalc and Fexp.
9. Change γ by a predefined increment Δγ.
10. Repeat steps 7–9 while the mean deviation decreases.
11. Select the γ value corresponding to the minimum deviation.

Output: optimal nonlinear transformation index γopt fitted nonlinear gradation characteristic

Initial estimates of γ and KC were determined using the least-squares method. Since this estimate is approximate, particularly when the number of exper-

imental gradation patches is limited, γ was further refined iteratively. At each iteration, the theoretical tone reproduction curve was calculated for a specified γ value together with its mean deviation from the experimental data. The γ value corresponding to the minimum deviation was considered optimal. The resulting γopt is used as a quantitative characteristic of the nonlinearity of a specific printing process.

3. Results and discussions

3.1. Influence of printing conditions on the nonlinear transformation index

Experimental studies were conducted to determine the influence of technological printing conditions on the nonlinear transformation index γ. For this purpose, gradation scales of process inks were reproduced by offset printing on coated and uncoated paper using conventional amplitude-modulated and stochastic screening. The investigated combinations of paper type and screening method corresponded to the conditions represented by Fogra characterisation data.

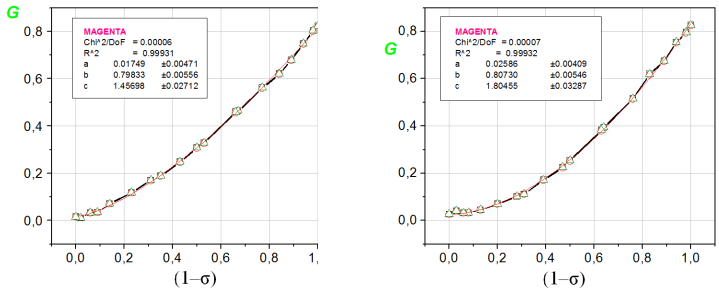
Following printing, colorimetric measurements of the gradation patches were performed. Based on the resulting experimental data (ED), the nonlinear transformation index γ was determined using the improved method for each process ink and each investigated printing condition corresponding to Fogra51, Fogra52, Fogra43, and Fogra44, respectively.

Figure 4 presents an example of γ determination for Magenta prints on coated paper using conventional and stochastic screening. The calculated nonlinear transformation index values for the other inks and technological conditions are presented in Table 2. For comparative analysis, the table also includes γ values determined by the same method from standardised Fogra characterisation data.

The results confirmed that the nonlinear transformation index is characteristic of specific reproduction conditions and depends on the technological parameters of the printing process. Analysis of the tone reproduction characteristics demonstrated the influence of both the printing substrate and the screening method. Higher γ values were obtained for uncoated paper than for coated paper, which is consistent with more pronounced dot gain and the specific interaction between the ink and the paper surface. Stochastic screening was also characterised by higher γ values than conventional amplitude-modulated screening.

The nonlinear transformation index was additionally investigated for digital printing technologies. The analysis was based on colorimetric data from prints produced under production conditions using Konica Minolta bizhub PRESS, Xerox 700 DCP, and HP Indigo 5000 sheet-fed digital presses, as well as Canon Pixma and Epson Stylus Pro inkjet printers.

The resulting values confirmed that the nonlinearity of digital reproduction depends substantially on the image-forming principle and the characteristics of the specific printing system. The mean γ values for the CMY components were 1.51 for Konica Minolta,



» **Figure 4:** *Nonlinear characteristics of Magenta prints: (a) AM screening and (b) FM screening, coated paper*

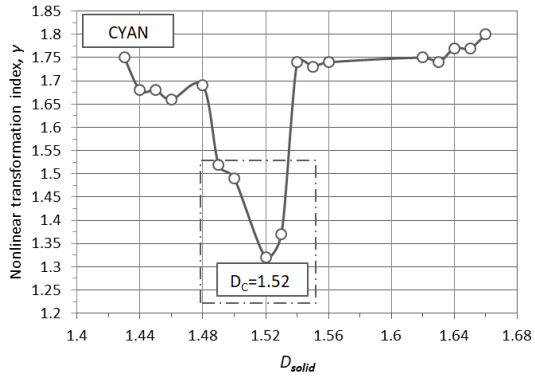
Table 2

Nonlinear Transformation Index for Offset Printing under Different Paper and Screening Conditions

	Fogra 51	ED*	Fogra 52	ED*	Fogra 43	ED*	Fogra 44	ED*
C-Cyan	1.59	1.66	1.98	1.71	2.29	1.82	2.34	1.87
M-Magenta	1.61	1.46	1.99	1.54	2.41	1.80	2.44	1.97
Y-Yellow	1.59	1.54	1.97	1.65	2.25	1.82	2.28	1.91
K-Black	1.57	1.72	2.05	1.80	2.32	1.70	2.32	1.81

1.28 for Xerox 700 DCP, 1.51 for HP Indigo 5000, 1.23 for Canon Pixma MG5240, and 1.29 for Epson Stylus Pro. The investigated digital systems therefore exhibit different degrees of nonlinearity, confirming the need to determine γ experimentally for the specific printing method and operating conditions.

The effect of ink film thickness on the nonlinear transformation index γ was also investigated. Prints were produced on a sheet-fed offset press using Vega Gloss 115 g/m² glossy paper and Huber Group Perfection offset inks. The ink film thickness was varied during printing, while the optical density of the 100 % solid patches was monitored using a densitometer. The colorimetric characteristics of the gradation scales were measured spectrophotometrically in CIELAB coordinates.



» **Figure 5:** *Dependence of the nonlinear transformation index on the optical density of Cyan solid patches*

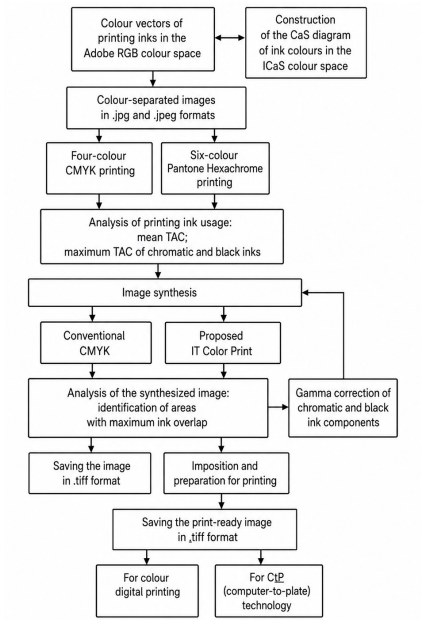
To establish the relationship between the nonlinear transformation index γ and ink film thickness, γ was plotted against the optical density of Cyan, Magenta, and Yellow solid patches. Figure 5 presents the corresponding relationship for Cyan ink. Local minima of the nonlinear transformation index were identified at optical densities of D=1.52 for Cyan, D=1.59 for Magenta, and D=1.46 for Yellow. These results indicate that the minimum γ value can be used as a criterion for selecting a rational ink film thickness and optimising colour reproduction conditions.

Standardised characteristics can therefore serve as a reference basis, although they do not fully represent the nonlinearity of a specific production process. To improve colour reproduction accuracy, prepress preparation should account for the nonlinear transformation index determined experimentally under the actual printing conditions. Such an approach accounts for deviations of the real process from standardised conditions and improves the predictability of tonal and colour reproduction.

3.2. Software implementation of the proposed prepress framework

For the practical implementation of the proposed mathematical framework, the IT Color Print software was developed for prepress preparation of colour images. Its functional structure integrates colour gamut construction for specified printing conditions, analytical colour separation, modelling of image synthesis using printing inks, Total Area Coverage (TAC) analysis, correction of ink components, and generation of colour-separated images for subsequent printing. The software supports both four-colour CMYK and extended multicolour configurations.

The model inputs comprise the colorimetric characteristics of the paper, printing inks, and their overprints, together with the nonlinear transformation index γ determined for the specific printing conditions. The software therefore establishes a direct relationship between the mathematical model of colour synthesis and the actual characteristics of the printing system. The functional scheme of the proposed approach to colour image prepress processing is shown in Figure 6.

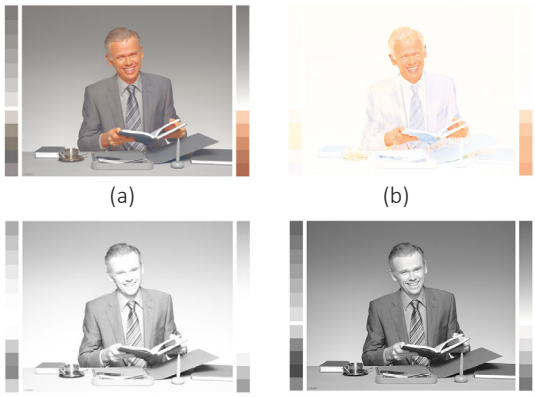


» **Figure 6:** *Functional scheme of colour image prepress processing*

For comparative evaluation of the colour separation results, roman16 bvdm reference test images (Bundesverband Druck und Medien, n.d.) were used. These images were specifically developed for analysing colour reproduction and detail rendering in prepress and printing workflows. The set includes images with different colour, tonal, and subject characteristics and is intended, among other purposes, for evaluating RGB→CMYK transformations and comparing colour separation strategies. The RGB originals from the roman16 set were processed using the conventional

approach with the PSO Coated v3 ICC profile and the proposed IT Color Print method, after which the resulting colour separations were comparatively analysed.

The modelling revealed fundamentally different patterns in the formation of the chromatic and achromatic image components. The C, M, and Y components predominantly form the chromatic content of the image, whereas K plays a greater role in reproducing tonal structure, detail, and achromatic regions. Such redistribution of the inks creates the potential to reduce the use of CMY chromatic inks while preserving the specified colour characteristics of the image.



» **Figure 7:** *Comparison of colour separation results obtained using an icc profile and the proposed method: (a) cmy image synthesis using the icc profile; (b) cmy image synthesis using it color print; (c) black (k) channel obtained using the icc profile; (d) black (k) channel obtained using it color print*

Figure 7 presents the results of simulated synthesis of the test image using only the chromatic C, M, and Y components: conventional colour separation using the ICC profile (Figure 7a) and the proposed method based on analytical solutions of the colour synthesis equations in the ICaS colour space (Figure 7b). The comparison demonstrates a fundamental difference in the formation of the achromatic component. With conventional colour separation, overprinting of C, M, and Y contributes to the reproduction of grey and low-chroma regions, whereas in the proposed method the chromatic inks predominantly form the chromatic component and the achromatic information is transferred to the K channel. The corresponding black ink channels for the two colour separation methods are shown in Figure 7c and 7d.

In terms of CMY and K redistribution, the resulting separation may visually resemble colour separation with a high degree of grey-component replacement by black ink. The fundamental distinction of the proposed approach is that the colour transformation is not based on precomputed tabular relationships and their interpolation; instead, it is determined analytically from the colour synthesis equations in the ICaS colour space while accounting for the characteristics of the specific printing process.

3.3. TAC analysis and gamma correction of ink components

For technological control of colour-separated images, the software incorporates Total Area Coverage (TAC) analysis. Rather than determining only the global maximum TAC value, the proposed approach identifies pixels and image regions in which the total ink coverage exceeds a specified threshold. Potentially critical regions can therefore be detected during prepress preparation.



» **Figure 8:** *Identification of local critical regions with maximum ink overlap (b) in the test image (a)*

A separate module implements gradation gamma correction of the colour-separated components. Correction can be applied individually to C, M, Y, and K while accounting for the nonlinear transformation index of the specific printing process. Modification of one or more ink channels is accompanied by recalculation of the remaining components according to the colour synthesis conditions.



» **Figure 9:** *Result of gamma correction of a two-ink colour-separated image*

A specific feature of the developed method is the preservation of the neutral balance of the image during correction of the ink components. Their tone reproduction characteristics and ink consumption can consequently

be modified without disturbing the component ratios required to reproduce achromatic tones. Gamma correction is therefore used not only to compensate for process nonlinearity but also as an element of controlled ink redistribution during prepress preparation.

3.4. Experimental validation and ink consumption reduction

The effectiveness of the proposed approach was evaluated using a set of reference test images. For each original, a control colour separation was generated using an ICC profile and an experimental colour separation using the IT Color Print method. The comparison was based on the maximum CMYK Total Area Coverage (TAC) and the mean use of the chromatic C, M, and Y components over the image area.

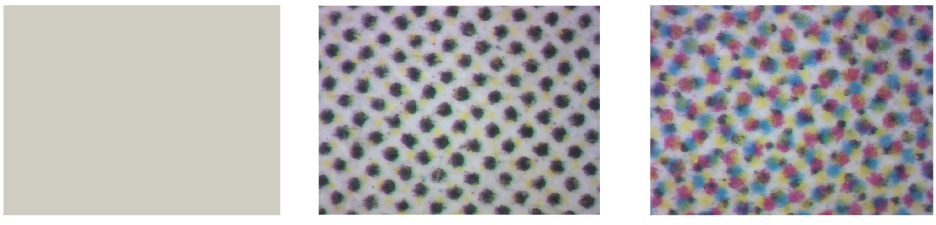
The comparison results are presented in Figure 10. With conventional ICC-based colour separation, the maximum TAC for most test images was approximately 300 %, whereas for the same originals processed using IT Color Print, the maximum TAC did not exceed 250 %. This indicates a reduction in local ink loading in the most highly saturated regions of the images.

More pronounced differences were observed in the analysis of mean chromatic ink usage. The reduction in C, M, and Y depended on the tonal and colour composition of the individual image. For some test originals, the differences were relatively small, whereas the greatest reduction in chromatic components was observed for images dominated by midtones and dark tones, as well as dark olive and brown hues. On average, across the investigated image set, the combined use of C, M, and Y decreased by approximately 60 % compared with ICC-based colour separation, accompanied by an increased contribution of black ink K. These results confirm that the effectiveness of the proposed redistribution of ink components depends on the colour and tonal structure of the image.

For experimental validation, the images were printed on an HP Indigo 5500 digital press. The resulting prints were evaluated spectrophotometrically by comparing the colorimetric characteristics of the control and experimental samples, and the microscopic structure of the halftone dots was also examined. Grey gradation control patches were particularly informative: with IT Color Print, the grey tone was formed predominantly by black and yellow halftone dots, whereas conventional colour separation employed halftone dots of all CMYK components. Micrographs of the prints are presented in Figure 11. The experimental results confirmed the feasibility of implementing the proposed colour separation technology on digital printing equipment, the agreement between the theoretical modelling and the actual structure of the print, and the possibility of



» **Figure 10:** *Comparison of maximum CMYK total area coverage and average CMY ink coverage for ICC-based and IT Color Print colour separation*



(a) (b) (c)

» **Figure 11:** *Grey colour: (a) digital original; (b) colour separation using IT Color Print; (c) colour separation using the conventional approach*

substantially reducing chromatic ink usage without significant deterioration in colour reproduction accuracy.

The theoretical and experimental results were consolidated into the conceptual model of IT Color Print, which integrates printing process characterisation, analytical colour separation, colour synthesis, screening, TAC control, and correction of ink components within a unified system for prepress preparation of colour images.

A key feature of the model is the direct incorporation of parameters of the specific printing process into the mathematical description of colour separation. The colorimetric characteristics of the inks and paper determine the geometry of the available colour gamut, the nonlinear transformation index γ characterises tonal reproduction, and the analytical solutions of the colour synthesis equations determine the admissible ratios of the ink components. Together, these elements form an integrated sequence — characterisation → colour separation → correction → synthesis → printing — in which prepress preparation is adapted to the actual conditions of colour reproduction.

4. Conclusions

The proposed approach to colour image prepress preparation is based on solutions to the colour synthesis equations derived in the ICaS colour space. For practical implementation, a limiting solution is used in which one of the three chromatic components, C, M, or Y, is equal to zero. The component to be excluded is determined by the position of the colour in the chromatic CaS diagram: assignment of the corresponding point to a geometric cluster defines the pair of chromatic inks used for reproduction. Analytical determination of the ink components requires the colour vectors of the process inks, their pairwise overprints, and the paper, together with the nonlinear transformation index γ. The combined use of these parameters enables the proposed mathematical framework to be adapted to a specific printing system.

The proposed approach was implemented in the IT Color Print system, which integrates colour separation based on the developed mathematical model, TAC control, colour synthesis modelling, and correction of ink components. Experimental studies confirmed the dependence of the nonlinear transformation index γ on the printing technology and operating conditions, as well as its applicability as a parameter for prepress preparation. For the investigated images, the proposed colour separation method reduced the total use of CMY by approximately 60% and decreased the maximum TAC from 300 to 210%. Spectrophotometric and microscopic analyses confirmed the practical feasibility of the proposed method, the agreement between the actual distribution of ink components and the theoretical model, and the preservation of acceptable colour reproduction accuracy.

Further research should focus on extending the experimental validation of the method to different printing technologies, substrates, and reproduction conditions; refining the criteria for selecting the optimal ratio of ink components; and investigating the applicability of the proposed mathematical framework to multicolour printing systems.

5. References

Bundesverband Druck und Medien. (2007) roman16 bvdm Reference Images (English). 1st ed. Available from: https://fachliteratur.bvdm-online.de/?article=35 [Accessed 15 August 2026].

Fogra. (n.d.) Characterisation data for standardised printing. Available from: https://fogra.org/en/downloads/work-tools/characterisation-data [Accessed 15 August 2026].

Fraser, B., Murphy, C. and Bunting, F. (2005) Real World Color Management: Industrial-Strength Production Techniques. 2nd ed. Berkeley, CA: Peachpit Press.

International Color Consortium. (2024) Introduction to the ICC profile format. Available from: https://www.color.org/getting-started/ [Accessed 15 August 2026].

International Organization for Standardization. (2013) ISO 12647-2:2013. Graphic technology — Process control for the production of half-tone colour separations, proof and production prints — Part 2: Offset lithographic processes. Geneva: International Organization for Standardization.

Kovalskyi, B., Dubnevych, M., Holubnyk, T., Skarga-Bandurova, I., Maik, L. and Selmenska, Z. (2022) 'Analysis of the effectiveness of means to achieve optimal color balancing in obtaining a digital photographic image'. In: Proceedings of the 3rd International Workshop on Intelligent Information Technologies & Systems of Information Security (IntelITSIS-2022), 23–25 March 2022, Khmelnytskyi, Ukraine. CEUR Workshop Proceedings, 3156, pp. 520–538. Available from: https://ceur-ws.org/Vol-3156/paper40.pdf [Accessed 15 August 2026].

Kovalskyi, B., Semeniv, M., Zanko, N. and Semeniv, V. (2024) 'Application of digital images processing for expanded gamut printing with effect of saving material resources'. In: Proceedings of the Seventh International Workshop on Computer Modeling and Intelligent Systems (CMIS-2024), 3 May 2024, Zaporizhzhia, Ukraine. CEUR Workshop Proceedings, 3702, pp. 226–238. Available from: https://ceur-ws.org/Vol-3702/paper19.pdf [Accessed 15 August 2026].

Kynash, Y. and Semeniv, M. (2025) 'New approach to dominant and prominent color extraction in images with a wide range of hues', Technologies, 13(6), 230. DOI: 10.3390/technologies13060230

Li, C., Li, Z., Wang, Z., Xu, Y., Luo, M. R., Cui, G., Melgosa, M., Brill, M. H. and Pointer, M. (2017) 'Comprehensive color solutions: CAM16, CAT16, and CAM16-UCS', Color Research & Application, 42(6), pp. 703–718. DOI: 10.1002/col.22131

Luo, M. R., Xu, Q., Pointer, M., Melgosa, M., Cui, G., Li, C., Xiao, K. and Huang, M. (2023) 'A comprehensive test of colour-difference formulae and uniform colour spaces using available visual datasets', Color Research & Application, 48(3), pp. 267–282. DOI: 10.1002/col.22844

Sharma, A. (2018) Understanding Color Management. New York: John Wiley & Sons.

Shikudova, E., Kronander, J., Mantiuk, R., Pedersen, M. and Unger, J. (2016) 'A gamut-mapping framework for color-accurate reproduction of HDR images', IEEE Computer Graphics and Applications, 36(4), pp. 78–90. DOI: 10.1109/MCG.2015.116

Shovheniuk, M., Kovalskiy, B., Semeniv, M., Semeniv, V. and Zanko, N. (2019) 'Information technology of digital images processing with saving of material resources'. In: Proceedings of the 15th International Conference on ICT in Education, Research and Industrial Applications: Integration, Harmonization and Knowledge Transfer (ICTERI 2019), 12–15 June 2019, Kherson, Ukraine. CEUR Workshop Proceedings, 2387, pp. 414–419. Available from: http://ceur-ws.org/Vol-2387/20190414.pdf [Accessed 15 August 2026].

Tjandra, A. D., Heywood, T. and Chandrawati, R. (2023) 'Trigit: A free web application for rapid colorimetric analysis of images', Biosensors and Bioelectronics: X, 14, 100361. DOI: 10.1016/j.biosx.2023.100361.

Yuan, J., Chen, G., Li, H., Prautzsch, H. and Xiao, K. (2021) 'Accurate and computational: A review of color reproduction in full-color 3D printing', Materials & Design, 209, 109943. DOI: 10.1016/j.biosx.2023.100361

© 2026 Authors. Published by the University of Novi Sad, Faculty of Technical Sciences, Department of Graphic Engineering and Design. This article is an open access article distributed under the terms and conditions of the Creative Commons Attribution license 4.0 Serbia (https://creativecommons.org/licenses/by/4.0/deed.en).

Original Scientific Paper https://doi.org/10.24867/GRID-2026-p15

Colour Characteristics of Alginate-Based Screen Prints Incorporating Aronia Pomace Extract and ZnO

ABSTRACT

*The incorporation of zinc oxide (ZnO) into bio-based printing formulations offers the potential to introduce additional functionality, while its presence may also influence the optical properties and colour development of the resulting prints. This study examined the colour development of halftone and solid screen prints produced on cotton fabric using a sodium alginate-based printing paste containing aronia pomace extract and ZnO. Printing was performed using a screen with a mesh count of 32 threads cm^{-1}. Prints with a nominal tonal value of 50% and solid prints were produced using one to five successive passes. The prints were evaluated using CIE L*a*b* colour coordinates, while colour differences relative to the unprinted cotton substrate were calculated using the CIEDE2000 formula. K/S values were calculated according to the Kubelka-Munk equation. For the halftone prints, increasing the number of passes resulted in a gradual decrease in L*, while ΔE_{00} increased from 3.97 to 9.60 and the hue angle shifted towards red. The K/S value generally increased from 2.22 to 2.55. In solid print areas, the most pronounced reduction in lightness occurred between the first and second pass, after which the hue angle remained relatively stable. The lowest L* value (59.87), the highest ΔE_{00} (19.40) and the highest K/S value (3.90) were obtained after four passes. Applying a fifth pass did not improve the optical response of the solid print. These findings indicate that the number of successive passes influences both colour strength and hue development, with four passes providing the strongest colour response in solid print areas under the investigated printing conditions.*

Branka Ružičić [1]
Dragana Grujić [1,2]
Blanka Škipina [1]
Biljana Pećanin [1]
Sandra Dedijer [3]

[1] University of Banja Luka, Faculty of Technology, Banja Luka, Bosnia and Herzegovina
[2] Institute of Natural and Technical Sciences, Academy of Sciences and Arts of the Republic of Srpska, Banja Luka, Bosnia and Herzegovina
[3] University of Novi Sad, Faculty of Technical Sciences, Department of Graphic Engineering and Design, Novi Sad, Serbia

KEY WORDS
Aronia pomace, zinc oxide, screen printing, colour strength, halftone printing

1. Introduction

The growing interest in more sustainable textile coloration has encouraged the investigation of natural colourants obtained from renewable resources and agro-industrial by-products. Fruit pomace generated during juice production represents a potentially valuable secondary raw material because considerable amounts of coloured and biologically active compounds may remain in the solid residue after processing (Cucuiet et al., 2026). Recovering these compounds can contribute to waste valorisation while providing alternative colour sources for textile applications (Ružičić et al., 2025).

Black chokeberry (aronia) (*Aronia melanocarpa*) is characterised by a high content of polyphenolic compounds, particularly anthocyanins responsible for its intense red-purple colour. A considerable proportion of these compounds may remain in the pomace after juice extraction, making this by-product a suitable source of natural colourants (Ren et al., 2022). Previous studies have demonstrated the recovery of anthocy-

anins from aronia pomace and its potential application in coloured films and textile materials. However, anthocyanin-based colour systems are sensitive to formulation and processing conditions, which can affect their final hue, lightness and colour strength (Wathon et al., 2019; Hong, 2024; Ugrinović et al., 2025).

Zinc oxide (ZnO) is widely used in textile treatments as a functional inorganic additive due to its potential to provide UV-protective and antimicrobial properties (Li et al., 2012; Kumar et al., 2014). When incorporated into a printing formulation, ZnO may also contribute to the optical response of the resulting print (Lima Lorusso Sampaio et al., 2026). Combining ZnO with a natural colourant obtained from aronia pomace therefore provides a basis for developing coloured textile prints with potential additional functionality. In the present study, the colour characteristics of this formulation were investigated in relation to the number of successive printing passes and the nominal tonal value.

In screen printing, the amount and distribution of paste transferred to the substrate influence the appearance and performance of the resulting print. Ink or paste deposition is affected by the printing formulation, screen characteristics and process parameters, while the deposited amount is directly related to colour strength in conventional printing (Ali et al., 2019). Repeated printing passes can increase the amount of transferred paste, but their effect may differ between halftone and solid areas because these areas differ in nominal surface coverage and interaction with the textile structure. Furthermore, additional passes may not produce proportional colour development once the printed area has received a sufficient deposit.

Accordingly, the aim of this study was to investigate the effect of one to five successive printing passes on the colour characteristics of 50% halftone and solid screen prints produced on cotton fabric using a sodium alginate-based paste incorporating aronia pomace extract and ZnO.

2. Materials and methods

2.1. Materials

A plain-weave cotton fabric with a surface mass of 123.36 g m^{-2} and thread densities of 23 threads cm^{-1} in the warp direction and 21 threads cm^{-1} in the weft direction was used as the printing substrate. Modified sodium alginate (CHT-NV, CHT Germany GmbH) was used as the thickening agent, while zinc oxide (ZnO, Sigma Aldrich, USA) and aronia pomace extract were used to prepare the printing paste.

Aronia pomace was extracted with 80% methanol by maceration for 24 h, followed by ultrasonication for 18 min and filtration. The pomace was subsequently re-extracted with fresh 80% methanol by repeating the same maceration, ultrasonication and filtration procedure. The combined filtrates were concentrated under reduced pressure using a rotary evaporator at 40 °C, transferred to Petri dishes and dried to constant mass at 50 °C. The dried extract was then redissolved in 60% methanol to obtain a concentration of 200 mg mL^{-1}.

The sodium alginate-based printing paste was prepared by dispersing 6 g of modified alginate in 69 mL of distilled water at room temperature under continuous stirring until homogeneous. Subsequently, 25 mL of the aronia pomace extract and 0.3 g of ZnO were incorporated into the alginate paste and mixed until a homogeneous formulation was obtained.

Printing was performed using a semi-automatic Screenprinter S-300 at a speed of 0.08 m s^{-1} and a constant squeegee pressure. A screen with a mesh count of 32 threads cm^{-1} was used, and the printing form contained a halftone area with a nominal tonal value of 50% and a solid area. Both areas were printed using one to five successive passes without intermediate drying. After printing, the samples were dried in an oven at 45 °C. The samples were designated H1-H5 for the halftone prints with a nominal tonal value of 50% and S1-S5 for the solid prints, where the numbers indicate the number of successive printing passes.

2.2. Colour measurement

The colour characteristics of the unprinted cotton substrate and the printed samples were measured using a Konica Minolta CM-2600d spectrophotometer. Measurements were performed using illuminant D65, a 10° standard observer, d/8 measurement geometry, an 11 mm measurement aperture and the specular component included (SCI) mode. Spectral reflectance was recorded over the wavelength range from 360 to 740 nm at 10 nm intervals. Each sample was measured five times, and the mean values were used for further analysis. Colour was expressed using the CIE L*a*b* coordinates, chroma (C*) and hue angle (h°).

Colour differences between the printed samples and the unprinted cotton substrate were calculated using the CIEDE2000 formula (Luo, Cui & Rigg, 2001). Parametric factors of kL = 2 and kC = kH = 1 were applied to account for the textured surface of the textile substrate (Mirjalili et al., 2019). Colour strength was calculated from the measured reflectance according to the Kubelka-Munk equation (1):

$$K/S = \frac{(1-R)^2}{2R} \quad (1)$$

where R is the decimal reflectance, K is the absorption coefficient and S is the scattering coefficient. The K/S values were determined at 360 nm, corresponding to the lowest reflectance within the measured spectral range (Kašiković, 2012).

3. Results and discussion

The colour characteristics of the printed samples were evaluated to determine how the number of successive printing passes affected colour development in the halftone and solid areas. The visual appearance of the samples and the corresponding CIE L*a*b* coordinates, chroma (C*), hue angle (h°), colour difference relative to the unprinted cotton substrate (ΔE_{00}) and colour strength (K/S) are presented in Table 1. The results show that the optical response depended on both the number of printing passes and the nominal tonal value of the printed area.

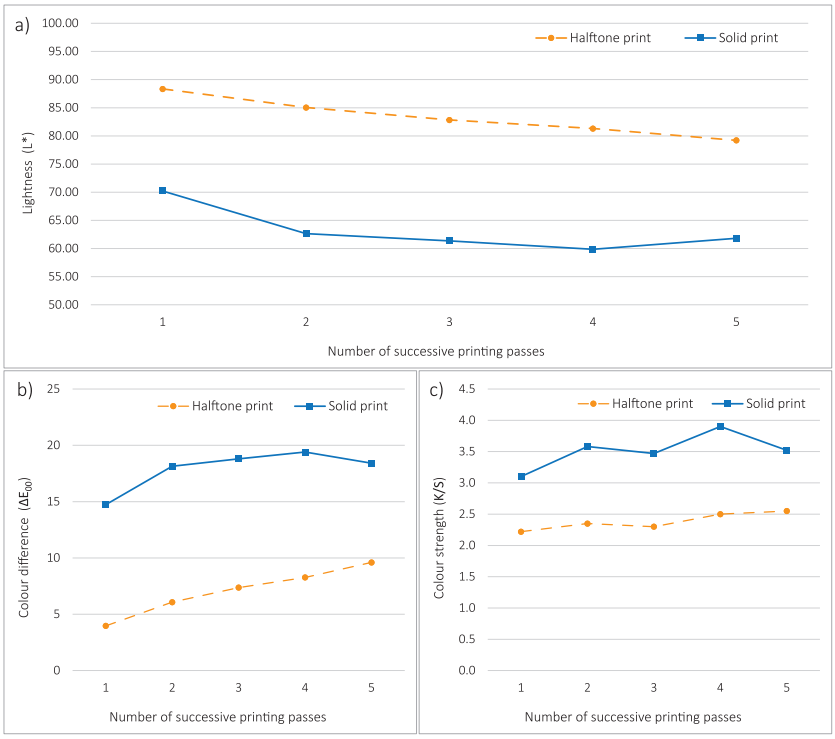
All printed samples were positioned in the positive a* and negative b* regions of the CIE L*a*b* colour space, confirming the presence of combined red and blue colour components. Accordingly, the prints exhibited purple to red-purple shades rather than a purely red colour. The halftone prints had hue angles ranging from 293.76° to 309.55°, indicating a transition from a more bluish-purple shade towards a redder purple shade as the number of passes increased. The solid prints showed higher hue angles, ranging from 321.67° to 331.62°, and therefore exhibited a more pronounced red-purple

Table 1

Colourimetric characteristics and colour strength of halftone and solid screen prints produced using one to five successive printing passes

	Sample images	L*	a*	b*	C*	h°	ΔE_{00} reference unprinted	K/S 360 nm
Unprinted cotton		93.77	2.50	-12.09	12.35	281.68	-	-
H1		88.34	5.39	-12.25	13.39	293.76	3.97	2.22
H2		85.04	6.99	-12.28	14.13	299.66	6.07	2.35
H3		82.83	7.89	-11.78	14.18	303.81	7.37	2.30
H4		81.31	8.67	-11.96	14.77	305.95	8.27	2.50
H5		79.21	9.82	-11.89	15.42	309.55	9.60	2.55
S1		70.22	14.66	-11.59	18.69	321.67	14.73	3.10
S2		62.64	17.26	-10.21	20.05	329.39	18.14	3.58
S3		61.37	17.82	-9.81	20.35	331.16	18.80	3.47
S4		59.87	18.31	-9.89	20.81	331.62	19.40	3.90
S5		61.83	17.13	-9.59	19.63	330.76	18.41	3.52

Note: H – 50% halftone print; S – solid print; numbers 1–5 indicate the number of successive printing passes.



» **Figure 1:** Effect of the number of successive printing passes on: (a) lightness (L*), (b) colour difference relative to the unprinted cotton substrate (ΔE_{00}), and (c) colour strength (K/S) of the halftone and solid prints

character. After the second pass, only minor variations in the hue angle of the solid prints were observed, indicating that subsequent passes primarily affected colour intensity rather than the general colour tone.

In the halftone areas with a nominal tonal value of 50%, increasing the number of passes produced a progressive reduction in lightness. The L* value decreased from 88.34 after one pass to 79.21 after five passes, indicating a gradual darkening of the print. At the same time, the a* coordinate increased from 5.39 to 9.82, whereas the b* coordinate remained comparatively stable. This shows that the increase in the number of passes primarily strengthened the red component of the printed colour, rather than producing a comparable change along the blue-yellow axis. This development was also reflected in the increase in chroma from 13.39 to 15.42 and the shift in hue angle from 293.76° to 309.55°, corresponding to a transition from a more bluish-violet appearance towards a redder purple shade.

The colour difference between the halftone prints and the unprinted cotton substrate increased consistently with each successive pass. The ΔE_{00} value increased from 3.97 after one pass to 9.60 after five passes, demonstrating that each additional pass increased the visual distinction between the print and the substrate. The K/S value showed a generally similar tendency, increasing from 2.22 to 2.55, although a slight decrease was observed after the third pass. The relatively small variation in K/S compared with the more pronounced change in L* and ΔE_{00} suggests that the optical development of the halftone areas was influenced not only by increased absorption but also by the changing contribution of the exposed cotton substrate and the progressive deposition of paste within the screened area.

Solid print areas exhibited a more pronounced colour response than the corresponding halftone areas. After only one pass, the solid print had an L* value of 70.22 and a ΔE_{00} value of 14.73. The greatest change in lightness occurred between the first and second passes, when L* decreased to 62.64 and ΔE_{00} increased to 18.14. Further passes produced smaller and non-linear changes. The lowest lightness, highest chroma, highest colour difference and highest K/S value were obtained after four passes. These concurrent values indicate that the four-pass solid print produced the strongest overall colour response under the investigated printing conditions.

Applying a fifth pass did not further enhance the solid print. Instead, L* increased, while a*, C*, ΔE_{00} and K/S decreased. Because the passes were applied successively without intermediate drying, the additional wet-on-wet application may have altered the distribution or penetration of the printing paste rather than simply increasing the deposited colourant. However, without direct measurements of paste add-on or penetration, this explanation should be regarded as a possible mechanism rather than a confirmed cause. The result nevertheless shows that a greater number of printing passes did not necessarily produce a stronger colour

response and that four passes were more effective than five for the solid print under the applied conditions.

The hue angle of the solid prints increased from 321.67° after the first pass to 329.39° after the second pass and subsequently remained within a narrow range of approximately 329-332°. This indicates that the principal hue development occurred during the first two passes, whereas subsequent applications mainly affected lightness, chroma and colour strength. Overall, the results demonstrate that successive printing altered both the intensity and hue of the prints, but the magnitude and pattern of these changes differed between the halftone and solid areas.

A direct comparison of the two printed areas shows that the solid prints consistently exhibited lower L* and higher C*, ΔE00 and K/S values than the corresponding halftone prints. This difference reflects the greater proportion of the substrate covered by the printing paste in the solid areas. However, while the colour response of the halftone prints continued to develop up to the fifth pass, the solid prints reached their strongest response after four passes. Under the investigated conditions, the fifth pass therefore increased the processing effort without producing an additional improvement in the colour characteristics of the solid print.

The visual appearance of the samples was consistent with the measured colour parameters, showing progressive colour development in the halftone areas and smaller differences among the solid prints produced with three to five passes.

4. Conclusions

This study demonstrated that the number of successive printing passes influenced the colour characteristics of both halftone and solid screen prints produced on cotton fabric using a sodium alginate-based paste incorporating aronia pomace extract and ZnO. In the 50% halftone areas, successive passes produced gradual colour development and shifted the obtained purple shade towards a more pronounced red-purple tone. In the solid areas, the most pronounced colour development occurred during the initial passes, while the strongest overall optical response was obtained after four passes. This sample exhibited the lowest L* value and the highest C*, ΔE_{00} and K/S values.

Applying a fifth pass did not further improve the colour characteristics of the solid print, indicating that increasing the number of passes beyond a certain point does not necessarily enhance colour development. Under the investigated printing conditions, four successive passes provided the most effective colour response in the solid area, whereas the halftone area continued to develop gradually up to the fifth pass. These findings confirm that the number of printing passes should be considered in relation to the nominal tonal value when controlling the appearance of bio-based textile screen prints.

Further research should examine the relationship between the number of passes, actual surface coverage and paste deposition, as well as the functional properties and durability of the resulting prints.

5. Acknowledgments

This work was supported by the Ministry of Scientific and Technological Development and Higher Education of the Republic of Srpska (Contract No. 19.032/431-1-54/23 and 19.032/966-19/23) and (Contract No. 19.032/431-1-93/23 and 19.032/966-20/23).

6. References

Ali, M., Lin, L., Faisal, S., Sahito, I. A. and Ali, S. I. (2019) 'Optimisation of screen printing process for functional printing', *Pigment & Resin Technology*, 48(5), pp. 456–463. DOI: 10.1108/prt-05-2019-0043

Cucuiet, G.-M., Chiș, M. S., Martău, G.-A., Vodnar, D. C., Török, A. I., Angyus, B. S., Man, S. M., Fărcaș, A. C. and Păucean, A. (2026) 'Fruit pomace from brandy production: Nutritional profile and potential for circular food innovation', *Applied Sciences*, 16(12), 5763. DOI: 10.3390/app16125763

Hong, K. H. (2024) 'Functionalization of cotton textiles via screen printing of *Aronia melanocarpa* berry extract–chitosan mixtures', *Journal of Natural Fibers*, 21(1). DOI: 10.1080/15440478.2024.2424930

Kašiković, N. (2012) *Razvoj modela praćenja procesnih parametara štampe tekstilnih materijala*. PhD thesis. University of Novi Sad.

Kumar, R., Anandan, S., Hembram, K. and Narasinga Rao, T. (2014) 'Efficient ZnO-based visible-light-driven photocatalyst for antibacterial applications', *ACS Applied Materials & Interfaces*, 6(15), pp. 13138–13148. DOI: 10.1021/am502915v

Li, Y., Zhang, W., Niu, J. F. and Chen, Y. (2012) 'Mechanism of photogenerated reactive oxygen species and correlation with the antibacterial properties of engineered metal-oxide nanoparticles', *ACS Nano*, 6(6), pp. 5164–5173. DOI: 10.1021/nn300934k

Lima Lorusso Sampaio, R., Costa, U. O., de Lima Vieira, P. and Elias, C. N. (2026) 'Optical and hardness performance of resin composites modified with Cu and ZnO nanoparticles for orthodontic applications', *Journal of Materials Research and Technology*, 43, pp. 6327–6340. DOI: 10.1016/j.jmrt.2026.07.148

Luo, M. R., Cui, G. and Rigg, B. (2001) 'The development of the CIE 2000 colour-difference formula: CIEDE2000', *Color Research and Application*, 26(4), pp. 340–350. DOI: 10.1002/col.1049

Mirjalili, F., Luo, M. R., Cui, G. and Morovic, J. (2019) 'Color-difference formula for evaluating color pairs with no separation – ΔENS', *Journal of the Optical Society of America A*, 36(5), pp. 789–799. DOI: 10.1364/JOSAA.36.000789

Ren, Z., Fang, H., Zhang, J., Wang, R., Xiao, W., Zheng, K., Yu, H. and Zhao, Y. (2022) 'Dietary *Aronia melanocarpa* pomace supplementation enhances the expression of ZO-1 and Occludin and promotes intestinal development in pigs', *Frontiers in Veterinary Science*, 9, 904667. DOI: 10.3389/fvets.2022.904667

Ružičić, B., Grujić, D., Savić, A., Topalić-Trivunović, L., Velemir, A., Škipina, B., Dedijer, S. and Prica, M. (2025) 'Grape pomace extract as a colorant for textile printing applications', *Chemical Industry and Chemical Engineering Quarterly*, 32(1), pp. 75–85. DOI: 10.2298/CICEQ250113012R

Ugrinović, V., Simović, A., Ćorović, M., Mihajlovski, K., Lađarević, J., Bajat, J. and Ivanovska, A. (2025) 'Valorization of *Aronia melanocarpa* pomace: A sustainable source of bioactive compounds for developing colored healthcare textiles, biomedical hydrogels, and green corrosion inhibitor', *Sustainable Chemistry*, 6(4), 46. DOI: 10.3390/suschem6040046

Wathon, M. H., Beaumont, N., Benohoud, M., Blackburn, R. S. and Rayner, C. M. (2019) 'Extraction of anthocyanins from *Aronia melanocarpa* skin waste as a sustainable source of natural colorants', *Coloration Technology*, 135(1), pp. 5–16. DOI: 10.1111/cote.12385

© 2026 Authors. Published by the University of Novi Sad, Faculty of Technical Sciences, Department of Graphic Engineering and Design. This article is an open access article distributed under the terms and conditions of the Creative Commons Attribution license 4.0 Serbia (https://creativecommons.org/licenses/by/4.0/deed.en).

Professional Paper https://doi.org/10.24867/GRID-2026-p16

Creating Proofs for Indigo

ABSTRACT

Indigo digital printing presses are commonly used today for packaging printing. The packaging industry utilizes a much wider variety of print substrates, which makes standardization in this sector much more challenging than in commercial graphic arts printing. Proofing printers are commonly used in color management systems to visualize the final printed product and for ongoing color monitoring. The main advantage of proofing is obtaining a physical sample of the printed product before the costly and irreversible step of producing a printing plate is done. However, proofs also have their place in digital printing when they simulate the output of a production press. This paper focuses on the preparation of profiles for simulation of output of an HP Indigo 6K Digital Press on 11 different substrates. The proofs were printed on an Epson SureColor P5000 inkjet printer.

Jan Vališ
Tereza Vrbová
Bohumil Jašúrek

University of Pardubice,
Faculty of Chemical Technology,
Depatment of Graphic Arts and
Photophysics, Pardubice,
Czech Republic

KEY WORDS
Proof, profile creation, color management, printed material

1. Introduction

Historically, a proof served to check the prepared printing plate during the printing process. As the preparation of print materials became increasingly digitized, the significance of the proof and its role in the production process shifted. It is worth noting here the so-called chemical proof, used to check film negatives before exposing the printing plates. Once prepress preparation was fully digitized, the proof began to serve as a means of checking the prepared data and became one of the fundamental components of color management. Today, the primary function of a proof is to simulate the production print output as faithfully as possible. For the customer, the proof represents the "promised quality" of the future print, and for the printer, it is therefore a commitment and a benchmark for the quality of the printed product. For the proof to fulfill these roles, color management must function flawlessly.

The final quality of the printed image depends on many factors; the most fundamental of these are the printing technique used, the method of creating the printing plate, the printing inks used, the substrate, and the press settings. Other factors include environmental conditions (temperature, humidity), the technical condition of the equipment used, operator procedures, and so on. If all these parameters can be kept constant, consistent color in the print can be expected.

In practice, of course, it is not possible to ensure that all possible influences remain constant; therefore, standardization is used—maintaining the production process under predetermined and as consistent as possible conditions. If standard conditions can be maintained, standard print outputs can also be expected.

In a standardized printing process, all individual production steps, the equipment used, its settings, the materials used, external conditions, etc., are defined as precisely as possible. An absolutely precise description of all factors influencing printing is unrealistic in practice; often (e.g., in flexographic printing), there are hundreds of variables (Shejbal, 2026). If everything (or rather, the most important factors) can be kept within predefined tolerances, the resulting print will remain consistent or will fall within acceptable tolerances. Simply put, a color profile describes the standard output of a specific printing press. If even a single parameter changes, the resulting output will change. If, in a standardized printing process, a printing press is used to print on various substrates, the result on each substrate is described by a different color profile (Shaw et al., 2003).

Proofing printers must be able to simulate the color characteristics described by the production printer's color profile as accurately as possible; therefore, the gamut (the total range of reproducible colors) of the proofing printer must be larger than that of the production

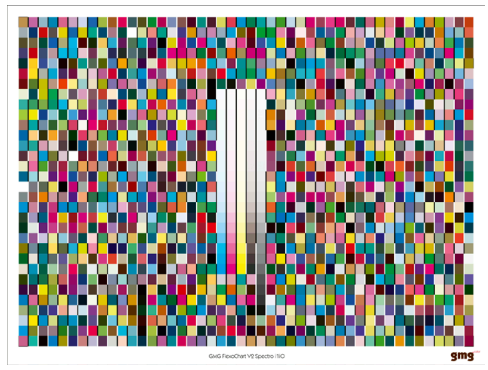
printer (Angerer, 2022). When creating proofs, only one high-quality substrate is typically used, which allows for a wide gamut. To simulate production printing on various substrates, different color profiles are used, each corresponding to the color characteristics (i.e., the limited gamut) of production printing on that specific substrate.

2. Methods

In this study, profiles were created to simulate printing from an HP Indigo 6K Digital Press on an Epson SureColor P5000 proofing printer. HP Indigo printers use a special liquid toner called ElectroInk, which ensures high print quality (Dataline, 2024). The specific machine for which the profiles were created used seven colors (CMYKOVW—in the HP IndiChrome Plus 7-color system (HP Indigo, 2026), green was replaced by opaque white; transparent films are often used when printing stickers) and special Rainbow 196 screening (196 lpi by default, but the line count can be adjusted within the range of 160–300 lpi). To prevent moiré patterns, the individual screens are set at angles of 35° (C), 53° (M), 80° (Y), 27° (K), 72° (O), and 8° (V) (Ruibar, 2026). The use of seven colors expands the achievable color gamut and, of course, places greater demands on the proofing equipment. The Epson SureColor P5000 printer achieves the required gamut by using up to ten inks (C, LC, VM, VLM, Y, LK, LLK, O, G, PK/MK), printheads with a resolution of 360 dpi, and a droplet size of 3.5 pl (Epson, 2017).

Profiles were prepared for 11 different self-adhesive materials: 8 types of paper, transparent and white PE film, and metallic silver PP film; see Table 1. The substrate material and adhesive used are not specified here, this information can be find in Vrbová (2026).

The profiles were created using GMG ColorProof software. The GMG FlexoChart V2 Spectro i1iO test pattern was printed on the production press; see Fig. 1. Three selected prints were measured using an xRite i1 spectrophotometer; the values were averaged, imported into GMG ColorProof software, and smoothed using the Smooth Target Values tool (GMG, 2024). The generated profile was then used to create a proof. The proof was measured again with the spectrophotometer, and the average color values of the print and the proof were compared; the average and maximum color difference (ΔE*00) were evaluated. If the measured values met the required tolerance (average ΔE*00 < 0.5 or maximum ΔE*00 < 2.0), the generated profile was saved. If the tolerances were exceeded, the profile was adjusted and used to create a new proof. This procedure was repeated until appropriate color profiles were prepared for all 11 materials. Subsequently, the color of both the final prints and the test prints was measured manually using an xRite eXact spectrophotometer.



» **Figure 1:** *GMG Flexochart V2*

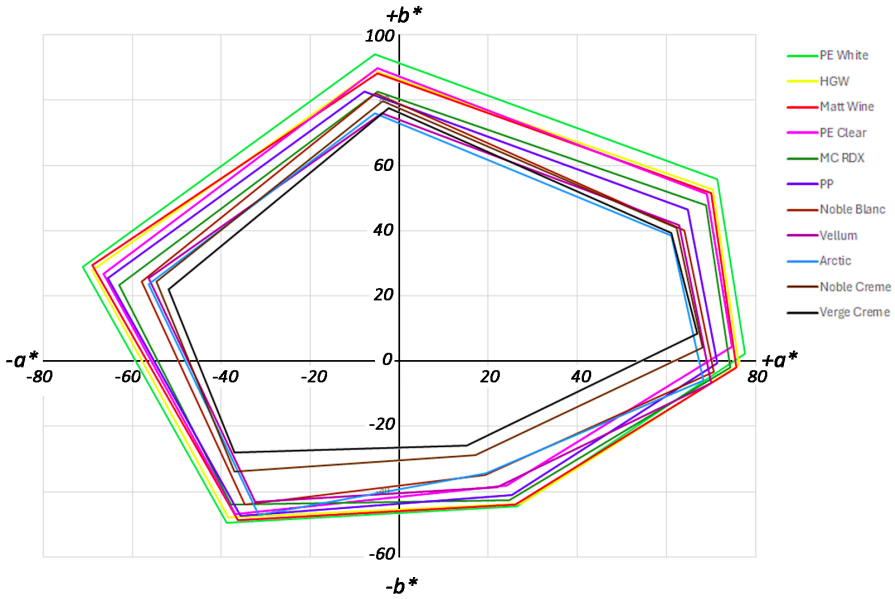
3. Results and discussion

Each of the 11 substrates used has different properties, which affect the resulting color. The graph in Figure 2 shows a simulation of the color gamuts of the individual substrates (CMYRGB colors in the a*b* color space).

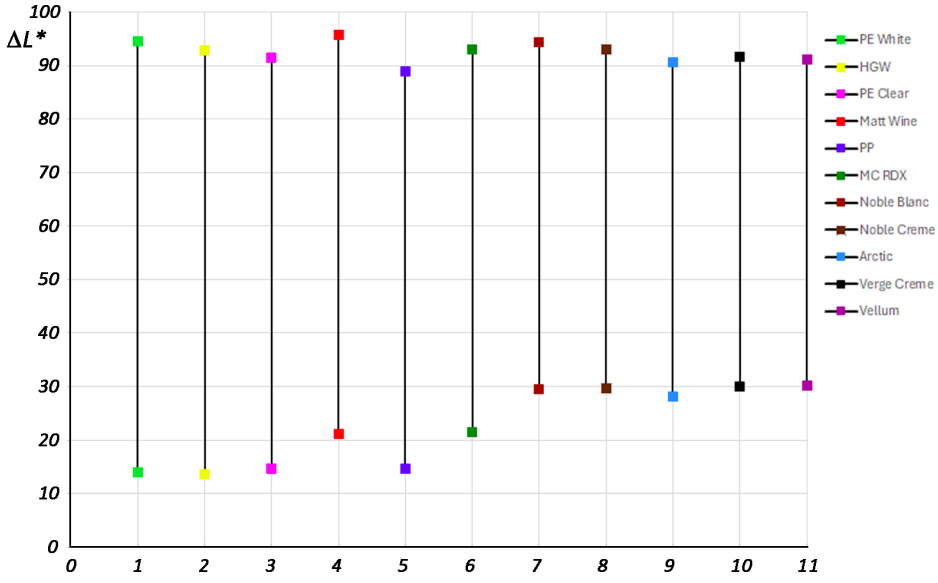
Table 1

Overview of self-adhesive materials for which color profiles have been created

Substrte	Description	L*	a*	b*
Arctic RPlus FSC	matte uncoated paper	90.6	2.4	-9.4
HGW Premium FSC	gloss coated paper	92.8	0.4	-2.7
Matt Wine NG FSC	matte coated paper	95.7	1.8	-3.6
MC RDX FSC	semi-gloss coated paper	93.0	1.5	1.5
Noble Blanc FSC	matte uncoated paper	94.4	0.9	-0.7
Noble Creme RPlus FSC	matte uncoated paper	93.0	0.3	12.2
Vellum Logistics NXT	super-calendered paper	91.2	3.9	-4.6
Verge Creme FSC	matte uncoated paper	91.7	0.8	20.5
PE85 Clear	clear pe film	91.6	0.1	1.1
PE85 White	white pe film	94.6	0.1	1.1
PP light Top Silver	glossy metallized pp film	88.9	-1.1	-2.1



» **Figure 2:** *Comparison of substrates color gamut*



» **Figure 3:** *Comparison of maximum substrates contrast*

It is clear that the largest color gamut is achieved with the white PE film (area in the a*b* color space = 100%) and the smallest with the Verge Crème substrate (59.2%).

The graph in Figure 3 shows a comparison of the contrast (ΔL* = L*paper – L*K100%) for each substrate. Once again, the PE White substrate has the highest contrast, while the Vellum Logistics substrate has the lowest (74.9%).

Table 2 compares the color measurement results for the primary colors C, M, Y, K, R, G, and B on prints from an HP Indigo production press and a proofing press. The results clearly show that the profiles created are of sufficient quality, and that the colors of the proofs match those of the production press prints.

At the end, the color stability of the proofing printer was verified. After 14 months, the GMG Flexochart V2 test pattern was reprinted using these profiles and measurements of color differences was performed. The results confirmed that the colors had not changed significantly; the color differences were within the required tolerance.

Table 2 (part 1)
Comparison of color reproduction between prints and proofs on the tested substrates

Substrate	Color	print HP Indigo			proof Epson			ΔE^*_{76}
		L*	a*	b*	L*	a*	b*	
Arctic RPLUS FSC	C	58.2	-31,5	-47,1	58,5	-32,0	-45,1	2,1
	M	52.8	68,3	-5,9	52,4	68,8	-5,1	1,0
	Y	86.7	-5,5	76,1	85,9	-5,8	75,9	0,9
	K	28.1	0,4	1,1	27,2	1,0	0,1	1,5
	R	52.3	61,1	38,6	52,2	61,3	37,6	1,0
	G	52.9	-56,4	23,5	53,2	-55,9	24,1	0,8
	B	29.7	19,4	-34,5	29,6	20,2	-35,4	1,2
	CMY	30.3	1,6	2,2	30,4	2,3	1,8	0,8
	substrate	90.6	2,4	-9,4	90,9	1,9	-7,5	1,9
HGW Premium FSC	C	55.5	-38,5	-48,0	55,5	-39,8	-47,5	1,4
	M	49.6	76,3	-1,1	49,7	77,1	0,1	1,4
	Y	88.1	-5,8	89,1	88,7	-6,0	90,6	1,6
	K	13.7	-0,3	2,9	13,3	-0,2	2,3	0,8
	R	49.2	70,5	52,7	49,6	70,8	52,9	0,6
	G	49.4	-69,1	27,7	50,0	-70,2	29,3	2,0
	B	19.0	27,4	-43,6	19,6	28,3	-44,3	1,3
	CMY	19.0	3,9	2,0	18,8	4,4	2,2	0,6
	substrate	92.8	0,4	-2,7	93,6	-0,1	-1,5	1,5
Matt Wine NG FSC	C	57.4	-36,4	-48,8	57,9	-37,5	-47,3	2,0
	M	52.8	75,6	-1,9	52,9	75,7	-1,1	0,8
	Y	90.9	-5,0	88,1	90,2	-5,7	89,0	1,4
	K	21.1	-0,1	2,0	21,5	0,3	1,7	0,6
	R	51.6	70.0	51.5	51.8	70.3	51.9	0.6
	G	51.0	-69.1	29.4	51.7	-68.9	31.7	2.4
	B	21.4	26.0	-44.0	21.9	26.9	-45.0	1.4
	CMY	20.8	4.7	2.6	21.1	5.3	2.8	0.6
	substrate	95.7	1.8	-3.6	95.2	0.8	-2.1	1.9
MC RDX FSC	C	57.6	-37.8	-43.9	58.2	-38.5	-42.4	1.7
	M	52.7	74.4	-1.8	52.6	73.8	-2.1	0.7
	Y	89.6	-4.9	82.6	89.4	-5.7	82.7	0.8
	K	21.5	0.0	3.0	21.5	0.2	2.8	0.4
	R	51.9	68.8	47.7	52.0	69.0	47.7	0.2
	G	53.6	-62.9	23.4	54.5	-62.7	25.0	1.8
	B	23.8	24.6	-42.8	24.9	25.2	-43.0	1.3
	CMY	23.4	4.9	-0.4	24.2	5.2	-0.1	0.9
	substrate	93.0	1.5	1.5	93.2	0.9	3.1	1.8
Noble Blanc FSC	C	60.1	-34.8	-44.0	59.8	-35.6	-43.7	0.9
	M	55.0	70.7	-3.3	55.7	70.3	-3.0	0.9
	Y	89.7	-5.4	82.2	89.7	-5.6	81.0	1.2
	K	29.6	0.6	1.2	29.3	0.5	1.4	0.4
	R	54.8	63.9	40.0	55.2	63.6	40.1	0.6
	G	54.4	-57.9	24.3	54.5	-58.0	24.5	0.3
	B	32.1	19.2	-34.9	32.3	19.0	-34.7	0.4
	CMY	30.9	1.3	1.3	30.9	1.0	2.0	0.7
	substrate	94.4	0.9	-0.7	95.0	0.6	-0.8	0.7

Table 2 (part 2)
Comparison of color reproduction between prints and proofs on the tested substrates

Substrate	Color	print HP Indigo			proof Epson			ΔE^*_{76}
		L*	a*	b*	L*	a*	b*	
Noble Creme RPLUS FSC	C	59.7	-37.1	-33.8	59.5	-38.6	-33.9	1.5
	M	55.1	68.0	4.1	55.0	68.1	2.9	1.2
	Y	90.1	-3.8	79.7	89.4	-4.4	79.2	1.0
	K	29.7	0.3	3.2	29.6	-0.3	2.5	0.9
	R	55.0	62.4	41.0	54.9	62.0	40.2	0.9
	G	55.7	-54.6	24.5	55.0	-55.6	24.4	1.2
	B	31.7	17.0	-28.7	31.9	16.8	-30.4	1.7
	CMY	31.8	2.7	2.3	31.8	2.1	1.5	1.0
	substrate	93.0	0.3	12.2	92.6	0.0	12.1	0.6
PE85 Clear	C	54.1	-36.9	-47.0	55.3	-37.4	-45.9	1.6
	M	48.6	74.7	4.5	49.1	75.0	4.5	0.6
	Y	87.3	-5.0	89.9	88.2	-6.1	89.6	1.5
	K	14.6	-0.7	1.3	15.1	-0.5	0.7	0.8
	R	48.4	69.0	51.2	48.9	69.0	51.1	0.5
	G	48.2	-66.5	26.7	49.7	-66.9	28.1	2.1
	B	18.0	24.2	-38.2	19.5	25.0	-39.7	2.4
	CMY	20.3	4.4	3.3	21.3	4.7	3.9	1.2
	substrate	91.6	0.1	1.1	92.8	-0.6	1.7	1.5
PE85 White	C	55.9	-38.8	-49.6	55.9	-39.0	-47.2	2.4
	M	51.3	77.6	2.3	50.6	76.6	2.5	1.2
	Y	90.8	-5.6	94.0	89.6	-6.1	91.7	2.7
	K	13.9	-0.5	3.3	14.8	-0.5	1.6	1.9
	R	51.0	71.5	55.8	49.9	70.1	53.2	3.2
	G	50.1	-71.1	28.9	50.2	-69.2	29.4	2.0
	B	19.1	26.4	-44.6	20.5	25.6	-42.7	2.5
	CMY	19.6	2.0	2.2	20.9	3.3	3.3	2.2
	substrate	94.6	0.1	1.1	95.2	-0.3	1.4	0.8
PP Light Top Silver	C	53.4	-35.7	-47.4	54.4	-36.2	-46.7	1.3
	M	47.2	71.4	-0.7	48.1	71.9	-1.2	1.2
	Y	84.5	-7.8	82.6	84.9	-7.7	81.7	1.0
	K	14.6	-0.9	1.5	15.5	-0.6	0.6	1.3
	R	47.3	64.7	46.5	47.7	64.9	45.5	1.1
	G	48.5	-65.6	25.4	49.8	-64.9	26.9	2.1
	B	19.3	25.3	-41.1	21.1	26.0	-42.4	2.4
	CMY	20.6	3.5	1.1	22.0	3.4	2.0	1.6
	substrate	88.9	-1.1	-2.1	89.2	-0.9	-2.2	0.3
Vellum Logistics NXT	C	59.8	-32.4	-43.1	60.1	-33.5	-41.3	2.1
	M	54.5	70.1	-6.7	54.6	69.6	-6.1	0.8
	Y	88.0	-3.9	75.9	88.0	-4.3	77.0	1.2
	K	30.1	0.6	2.0	30.7	0.5	1.7	0.6
	R	53.4	62.9	41.6	53.9	63.0	41.2	0.6
	G	55.5	-56.4	25.4	56.0	-56.2	27.5	2.2
	B	29.5	22.0	-38.6	30.3	22.2	-38.1	1.0
	CMY	28.8	4.2	1.9	29.0	5.0	1.9	0.8
	substrate	91.2	3.9	-4.6	90.9	2.8	-2.6	2.3

Table 2 (part 3)
Comparison of color reproduction between prints and proofs on the tested substrates

Substrate	Color	print HP Indigo			proof Epson			ΔE^*_{76}
		L*	a*	b*	L*	a*	b*	
Verge Creme FS	C	57.7	-37.0	-28.0	57.8	-37.0	-28.2	0.2
	M	55.2	67.0	8.4	54.7	67.6	6.6	1.9
	Y	89.8	-2.4	77.5	89.0	-2.2	77.1	0.9
	K	30.1	0.5	3.6	29.8	0.6	3.0	0.7
	R	55.5	61.2	39.4	55.3	61.7	38.0	1.5
	G	54.6	-51.9	22.0	54.7	-52.1	23.0	1.0
	B	31.5	15.2	-25.8	31.9	15.4	-26.4	0.8
	CMY	31.9	2.2	1.1	31.7	2.5	0.9	0.4
	substrate	91.7	0.8	20.5	91.5	0.7	20.1	0.4

4. Conclusions

Eleven color profiles were created for the Epson P5000 proofing printer to simulate the output of the HP Indigo 6K Digital Press on the most commonly used label materials. These color profiles have been used in the printer since their creation for all jobs on these materials; they are fully functional, with a small color deviation that falls within the tolerance range for proofing.

5. References

Angerer, S. (2022) Dreaming in Neon: Expanded Gamut and Spot Colours in Digital Printing. Available from: https://www.fespa.com/en/news-media/dreaming-in-neon-expanded-gamut-and-spot-colours-in-digital-printing/ [Accessed 24 September 2026].

Dataline. (2024) HP Indigo 6K. Available from: https://www.dataline.cz/portfolio/hp-indigo-6k/ [Accessed 24 September 2026].

Epson. (2017) Epson SureColor P5000 User's Guide. Available from: https://files.support.epson.com/docid/cpd5/cpd52925.pdf [Accessed 24 September 2026].

GMG. (2024) GMG ColorProof: efficient, accurate, and reliable proofing. Available from: https://gmgcolor.com/products/colorproof [Accessed 24 September 2026].

HP Indigo. (2026) Create a bigger future with HP Indigo technology. Available from: https://www.hp.com/us-en/industrial-printers/indigo-digitalpresses/lep-digital-printing-technology.html [Accessed 24 September 2026].

Ruibar, T. (2026) *Rainbow 196 and angles of the new mesh*. Oral presentation, March 2026, Kuřim.

Shaw, M., Sharma, G., Bala, R. and Dalal, E. N. (2003) 'Color printer characterization adjustment for different substrates', *Color Research & Application*, 28(6), pp. 454–467. DOI: 10.1002/col.10198

Shejbal, M. (2026) *Factors Affecting the Quality of Flexographic Printing*. Oral presentation, September 2026, Pardubice.

Vrbová, T. (2026) *Color Management in Digital Packaging Printing. Bachelor thesis*. University of Pardubice, Faculty of Chemical Technology.

© 2026 Authors. Published by the University of Novi Sad, Faculty of Technical Sciences, Department of Graphic Engineering and Design. This article is an open access article distributed under the terms and conditions of the Creative Commons Attribution license 4.0 Serbia (https://creativecommons.org/licenses/by/4.0/deed.en).

Original Scientific Paper https://doi.org/10.24867/GRID-2026-p17

Investigation of the Influence of Opaque White Ink Addition on Colour Characteristics of Some Process and Pantone Colours Printed with Water-Based Flexo Inks on Kraft Papers

Iskren Spiridonov
Kremena Karchakova
Rumyana Boeva

University of Chemical Technology and Metallurgy, Department of Pulp, Paper and Printing Arts, Sofia, Bulgaria

ABSTRACT

One of the major challenges in flexographic printing on kraft papers is the accurate reproduction of colour, which is strongly affected by the inherent yellow-brown shade of the printing substrate. Due to the limited opacity of most process and spot-colour inks, including CMYK and Pantone water-based flexographic inks, significant deviations in colour appearance occur when they are printed directly on kraft-based materials. The conventional technological solution is the application of one or more opaque white ink underlayers in order to create a sufficiently white printing base. However, this approach is associated with several disadvantages, including increased production costs, additional printing units or passes, the need for extra flexographic printing plates, higher ink consumption, and possible technical problems such as anilox roller clogging caused by the highly pigmented nature of opaque white inks. The present study investigates an alternative approach based on the addition of different quantities of opaque white ink directly into water-based flexographic process inks and Pantone inks. The influence of this modification on the colour characteristics and colour reproduction accuracy was evaluated by measuring the spectral properties and opacity of the white ink, as well as the CIE Lab colour coordinates of the printed samples. Colour differences, expressed as ΔE values, were determined in relation to reference colour characteristics. The inks were printed on brown kraft liner and on white double-coated testliner. Comparative analyses were performed between inks printed on a white substrate and inks printed directly on kraft material with the addition of varying amounts of opaque white ink. The results demonstrate a significant improvement in the colour accuracy characteristics of inks printed on brown kraft paper when opaque white ink is added to the ink formulation. Depending on the investigated ink colour, the colour difference from the reference values was reduced by approximately 30–40%. These findings indicate that controlled addition of opaque white ink may represent an effective technological approach for improving colour reproduction accuracy in flexographic printing on kraft-based substrates. The results are of both scientific and practical importance and are particularly relevant to high-volume printing of corrugated board and packaging production, where kraft papers are widely used and colour consistency remains a critical quality requirement.*

KEY WORDS

Packaging, flexography, water-based flexography inks, opaque white ink, kraft papers, colour reproduction accuracy, colour difference, corrugated board

1. Introduction

Flexographic printing is widely used in packaging production, particularly for corrugated packaging, due to its sustainability for a board range of substrates and high-volume manufacturing. Kraft-based papers are commonly used in this field, however, their inherent brownish colour, resulting from the fibre characteristics and manufacturing process can significantly affect the colour appearance of printed images. Water-based flexographic inks are widely applied in packaging production, but the relatively low opacity of most process and spot-colour inks allows the substrate to contribute substantially to the final optical response. This becomes particularly important when standardized or reference colours must be reproduced accurately.

The colour characteristics of a printed surface depend not only on the optical properties of the ink but also on the substrate. When the ink layer has limited opacity, the colour and reflectance of the substrate influence the amount and spectral distribution of reflected light, resulting in measurable changes in the colorimetric characteristics of the printed image.

Brown kraft liner provides a significantly different optical background compared with the white substrates commonly used for characterizing process and spot colours. In addition, light scattering within the paper structure and ink penetration into the substrate influence the relationship between the physical ink layer and its measured optical response. These effects can be quantified using the CIE L*a*b* colour space, while the deviation from a reference colour can be expressed as a colour difference (ΔE), providing a quantitative measure of colour reproduction accuracy.

A conventional technological solution for reducing the influence of the coloured substrate is the application of an opaque white ink underlayer beneath the process or spot-colour ink. Due to its high pigment concentration and opacity, the white layer provides a lighter and more neutral optical background and reduces the contribution of the kraft substrate to the reflected light. However, the use of a separate white underlayer introduces additional technological and economic requirements, including an additional printing unit or pass, an extra flexographic printing plate, increased ink consumption, and additional requirements for ink handling, equipment cleaning, and anilox roller maintenance. These limitations are particularly relevant in high-volume packaging production, where production efficiency, material consumption, and process stability directly affect manufacturing costs.

An alternative approach involves the controlled addition of opaque white ink directly to the coloured ink formulation, thereby reducing the influence of the kraft substrate without requiring a separate white underlayer. To the authors' knowledge, the application of this approach to Pantone inks printed on kraft substrates, under the conditions investigated in the present study, has not previously been reported. Therefore, the present work represents an innovative experimental investigation aimed at establishing the potential of this method for modifying the colour characteristics of Pantone inks and improving their colour reproduction accuracy on kraft substrates. Different quantities of opaque white ink are incorporated into the Pantone ink formulations, and their effects on the resulting colour characteristics and reproduction accuracy are experimentally evaluated.

The aim of the present study is therefore to investigate the influence of controlled additions of opaque white ink to water-based flexographic process and Pantone inks when printed on kraft-based substrates. The experimental analysis compares the colorimetric characteristics of inks printed on a white double-coated testliner with those obtained when the same inks are printed directly on brown kraft liner with varying amounts of opaque white ink added to the formulation. The influence of the white ink addition is evaluated using spectral characteristics, CIE L*a*b* and LCh° colour coordinates, and colour differences (ΔE) relative to the corresponding reference characteristics. Particular attention is given to the extent to which the addition of opaque white ink modifies the lightness, chroma, and hue of the printed inks, reduces colour deviation, and improves reproduction accuracy. This approach enables a more comprehensive assessment of the colourimetric response of the ink formulations and their potential as a technically viable alternative to a separate opaque white underlayer in flexographic packaging production.

2. Materials and methods

2.1. Printing substrates

Two paper substrates were used in the experimental investigation: brown kraft liner and white double-coated testliner. The selected substrates represent two different optical backgrounds for evaluating the influence of opaque white ink addition on the colour characteristics of water-based flexographic inks.

The brown kraft liner was selected as the primary substrate for the investigation because its characteristic brown coloration provides a strongly coloured background that can influence the colorimetric characteristics of inks printed directly on its surface. The substrate's physical properties were experimentally measured, resulting in a grammage 140 g/m² and a thickness of 160 µm. Its relevant optical characteristics, including brightness, were likewise experimentally determined rather than sourced from manufacturer specification.

A white double-coated testliner with an experimentally measured grammage of 140 g/m² and a thickness of 140 µm was used as the reference substrate. Its bright, coated surface provides a substantially different optical background compared with the brown kraft liner and allows the colour characteristics of the investigated inks to be evaluated under reference-like printing conditions.

Prior to printing, the substrates were conditioned under controlled laboratory conditions of 25 °C and 40 % relative humidity for 24 hours. The samples were stored and handled under the same conditions throughout the experimental procedure in order to minimize the influence of environmental conditions on the measured colour characteristics.

The main characteristics of the printing substrates are summarized in Table 1.

2.2. Printing inks

Water-based flexographic inks from the NAB pigment concentrates series supplied by Druckfarben Group, were used in the experimental investigation. The ink set comprised one process colours – cyan, and one Pantone spot colour – Pantone 300. All investigated inks were formulated for flexographic printing and were used as supplied, except for the controlled addition of opaque white ink described in Section 2.3.

The process ink was selected to represent the principal chromatic components of process-colour printing, while Pantone 300 was selected as representative spot colours with different chromatic characteristics. The inclusion of both process and Pantone inks enabled the influence of opaque white ink addition to be evaluated across different ink formulations and colour characteristics.

Table 1

Characteristics of the printing substrates

Substrate	Grammage [g/m²]	Thickness [µm]	Brightness (ISO R457)	Colour characteristics		
				L*	a*	b*
Brown kraft liner	140	160	0.12	57.54	11.13	26.65
White double-coated testliner	140	140	0.96	93.04	0.50	-2.92

The main physical and optical characteristics of the investigated inks, as provided by the manufacturer and/or determined experimentally, are summarized in Table 2. The measured or specified parameters include viscosity, optical density and CIE Lab colour coordinates. During the experimental procedure, optical density parameters were determined spectrophotometrically. Cyan ink measurements were performed in accordance with ISO 12647-6 and ISO 5-4 (Status T density) (International Organization for Standardization, 2020), whereas Pantone 300 was evaluated at its maximum absorption wavelength, with the dominant spectral density wavelength determined as λ=610.

Particular attention was given to the optical characteristics of the inks because their opacity and interaction with the substrate are directly relevant to the colour reproduction of prints produced on brown kraft liner. The reference colour characteristics of the investigated inks were determined from prints produced on the white double-coated testliner.

These reference samples were subsequently used for comparison with prints produced on the brown kraft liner with different amounts of opaque white ink incorporated into the respective ink formulations.

2.3. Opaque white ink

An opaque white water-based flexographic ink from the NAB pigment concentrates series supplied by Druckfarben was used as the white component in the experimental formulations.

The ink was selected based on its high opacity and hiding power, which are essential for reducing the optical influence of the brown kraft substrate on the colour characteristics of subsequently printed inks. The relevant physical and optical characteristics of the opaque white ink were obtained from the manufacturer's technical documentation and, where necessary, determined experimentally. The investigated parameters included viscosity and density.

Table 2

Characteristics of the investigated water-based flexographic inks

Ink	Ink type	Viscosity ISO 2431 [sec]	Optical density	Colour characteristics		
				L*	a*	b*
Cyan	Process	20	1.35	50.00	-37.00	-50.00
Pantone 300	Spot colour	20	1.56 ($D_{\lambda 610nm}$)	36.45	-8.15	-64.07

Particular attention was given to the optical properties of the white ink, including its spectral characteristics and opacity, as these properties determine its ability to mask the underlying substrate and modify the optical response of the resulting ink layer.

The spectral characteristics of the opaque white ink were determined by spectrophotometric measurements, using X-Rite eXact 2 device. The obtained characteristics were subsequently used to assess the suitability of the white ink for incorporation into the investigated process and Pantone ink formulations.

The investigated ink formulations are summarized in Table 3.

Table 3
Experimental ink formulations

Parameter	Value	Method / Source
Product / Ink series	NAB pigment concentrates	Manufacturer
Colour	White	Manufacturer
Ink type	Water-based flexographic	Manufacturer
Viscosity [sec]	20 (DIN4 cup)	ISO 2431 (International Organization for Standardization, 2019)
Density [g/cm^3]	0.98 – 2.09	ISO 2811-1 (International Organization for Standardization, 2016)

2.4. Ink formulation and white ink addition

To investigate the influence of opaque white ink addition on the colour characteristics of the selected water-based flexographic inks, controlled amounts of opaque white ink were incorporated directly into the original cyan and Pantone 300 ink formulations. For each investigated colour, the original ink without added white ink was used as the control formulation. The opaque white ink was added in predefined proportions of 5, 10, 15, 20, 25, 30, 35, 40, 45, and 50%, respectively. The selected addition levels were identical for all investigated ink colours and were chosen to evaluate the effect of progressively increasing white ink content on the colour characteristics of the resulting formulations. The required amounts of coloured and opaque white inks were accurately weighed to 0.001 g and homogenized for 1 min under controlled laboratory conditions to ensure uniform formulation.

The percentage of opaque white ink addition was calculated based on the ratio between the volume of the added white ink and the initial volume of the coloured ink. Accordingly, an addition level of 5% corresponds to adding extra volume in specific grams of liquid to the initial volume. The formulation procedure and calculation method were kept consistent throughout the experiment to ensure comparability between the different ink colours and white ink concentrations.

A total of 22 modified formulations were prepared in addition to the five unmodified control formulations. The formulations were identified according to the original ink colour and the amount of added opaque white ink. The complete experimental matrix is presented in Table 4.

Table 4
Experimental ink formulations and opaque white ink addition levels

Ink	Ink type	White ink addition [w/w %]	Sample designation
Cyan	Process	0	C-0
Cyan	Process	5	C-5
...	...	...	...
Cyan	Process	45	C-45
Cyan	Process	50	C-50
Pantone 300	Spot colour	0	P300-0
Pantone 300	Spot colour	5	P300-5
...	...	...	...
Pantone 300	Spot colour	45	P300-45
Pantone 300	Spot colour	50	P300-50

2.5. Laboratory printing conditions

The prepared ink formulations were applied to the selected substrates under laboratory conditions using a K Hand Coater (RK PrintCoat Instruments Ltd., UK), a manual wire-wound bar coating system designed for the application of printing inks and other liquid coatings onto various substrates.

For the present investigation, K Bar No. 0 which white handle was used. According to the manufacturer's specifications, this bar has a wire diameter of 0.05 mm and provides a nominal wet film deposit of approximately 4 µm. The same bar was used for all investigated ink formulations in order to maintain a constant nominal ink application thickness throughout the experimental procedure.

Prior to printing, the ink formulations were thoroughly homogenized. A sufficient amount of ink was applied to the starting area of the substrate, after which the K Bar was drawn manually across the substrate in a single continuous movement to form a uniform ink layer. The same application procedure was used for all investigated formulations and substrates.

The unmodified process and Pantone ink were applied both to the white double-coated testliner and to the brown kraft liner. The modified formulations containing different amounts of opaque white ink were applied directly to the brown kraft liner. This experimental arrangement enabled comparison of the colour characteristics of the unmodified inks on the white reference substrate with those of the same ink printed directly on the brown kraft substrate, as well as with the modified formulations containing opaque white ink.

After application, the samples were allowed to dry naturally at room temperature under laboratory conditions. No additional forced drying or thermal treatment was applied. The samples were subsequently stored under the same laboratory conditions until colorimetric measurements were performed. The drying and handling conditions were kept consistent for all samples to minimize variations associated with sample preparation.

2.6. Colour measurement and evaluation

The colorimetric characteristics of the printed samples were evaluated using an eXact 2 portable spectrophotometer (X-Rite, USA). The instrument employs a 45° circumferential ring illumination and 0° viewing geometry (45°:0°).

The measurements were performed using D50 illumination, a 2° standard observer, DIN density standard, and M1 measurement condition (D50-based). The white-base setting was defined as absolute (Abs).

For the investigated cyan and Pantone 300 inks, colour differences were evaluated relative to predefined reference colour coordinates. Target CIELab* reference values for Cyan and Pantone 300 were defined in accordance with ISO 12647-6 (International Organization for Standardization, 2020) and directly from PantoneLIVE, respectively. These reference values served as absolute colorimetric baselines to quantitatively evaluation of colour reproduction accuracy of the printed samples, independently of substrate influence.

Colour differences between the measured samples and the corresponding reference values were calculated using the CIEDE2000 colour-difference formula (ΔE00), in accordance with ISO/CIE 11664-6:2022 (International Organization for Standardization, 2022). For each investigated formulation, the measured L*, a*, and b* values were compared with the corresponding reference values. Particular attention was given to changes in ΔE00 resulting from the addition of opaque white ink to the original ink formulation. The relative reduction in colour difference was subsequently used to evaluate the improvement in colour reproduction accuracy achieved on the brown kraft liner.

In addition to the colorimetric evaluation, the measured spectral data were used to characterize the optical response of the printed samples and to identify changes associated with the incorporation of opaque white ink into the coloured formulations. The resulting colorimetric and spectral data were used for comparative analysis of the unmodified and modified ink formulations under the standardized measurement conditions described above.

2.7. Data analysis

The collected colorimetric and spectral data were analysed to evaluate the quantitative impact of opaque white ink addition on the colour reproduction characteristics of water-based flexographic ink printed on a brown kraft substrate. The analytical framework focused on evaluating changes in lightness (L*), chromaticity coordinates (a* and b*), spectral reflectance curves and total colour differences (ΔE00).

Colour differences between the printed samples and the predefined target reflectance coordinates were quantified using the CIEDE2000 colour-difference formula (ΔE00). The total colour difference ΔE00 was calculated according to Equation 1.

$$\Delta E2000 = \sqrt{\left(\frac{\Delta L'}{k_L S_L}\right)^2 + \left(\frac{\Delta C'}{k_C S_C}\right)^2 + \left(\frac{\Delta H'}{k_H S_H}\right)^2 + R_T\left(\frac{\Delta C'}{k_C S_C}\right)\left(\frac{\Delta H'}{k_H S_H}\right)} \quad (1)$$

where ΔL', ΔC', and ΔH' represent the calculated differences in lightness, chroma and hue, respectively: S_L, S_C, and S_H are weighting functions that compensate for perceptual non-uniformities in the CIEL*a*b* colour space; R_T is the rotation term accounting for hue-chroma interaction in the blue region; and k_L, k_C and k_H are parametric factors set to unity ($k_L = k_C = k_H = 1$) under reference measurement conditions.

To evaluate the technological efficacy of direct white ink addition in migrating substrate interference, and relative percentage reduction in colour difference (ΔE_{red}) was calculated for each modified formulation using Equation 2.

$$\Delta E_{red} = \left(\frac{\Delta E_{00,unmodified} - \Delta E_{00,modified}}{\Delta E_{00,unmodified}}\right) * 100 \quad (2)$$

where $\Delta E_{00,unmodified}$ represents the colour difference of the baseline ink printed on brown kraft liner without white ink addition (0%) and $\Delta E_{00,modified}$ denotes the colour difference of the corresponding ink formulation containing a specific percentage of added opaque white ink (5-50%).

The influence of the substrate optical background was characterized by comparing the baseline colourimetric values (Lab* and LCh°) of unmodified inks printed on brown kraft liner with those obtained on the white double-coated testliner. Statistical trends and visual representations of lightness shift (ΔL*), chromatic

vector changes (Δa*, Δb*), LCh° variations, and the overall ΔE00 trajectory were mapped as a function of opaque white ink concentration to determine the optimum dosage for process and spot colours.

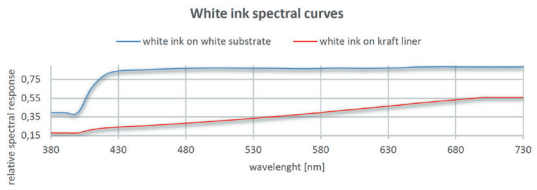
3. Results and discussion

3.1. Optical properties of the opaque white ink

The optical performance of the opaque white flexographic ink determines its capacity to mask the brown kraft substrate and modify the spectral response of the coloured ink formulations. To establish the baseline optical characteristics, the opacity, spectral reflectance and lightness parameters of the pure opaque white ink printed on the brown kraft liner and white double-coated testliner were evaluated.

The opacity of the opaque white ink was evaluated spectrally in accordance with ISO 23498:2022 (International Organization for Standardization, 2022) using the contrast ratio method, defined as the ratio of spectral reflectance measured over a standard black backing (R_b) to that over a standard white backing (R_w). The high concentration of titanium dioxide (TiO_2) pigment within the water-based flexographic vehicle provided opacity value of: 46.98% at a wet film deposit of 4 µm. This high opacity is critical for suppressing the selective light absorption of the underlying brown unbleached kraft fibres, thereby reducing the influence of substrate chromaticity on subsequently applied or blended ink layer.

The spectral reflectance curve of the pure opaque white ink across the visible spectrum (380-730 nm) is presented in Figure 1.



» **Figure 1:** *Spectral reflectance curve of pure opaque white ink*

The spectral profile demonstrates a characteristic high, uniform reflectance across the entire visible spectrum, peaking at approximately 88% reflectance in the 380-730 nm range. A slight decrease in reflectance is observed in the near-ultraviolet/violet region (400-420 nm) which is a typical for TiO2-based pigments due to fundamental band-gap light absorption in the UV spectrum.

When printed on brown kraft substrate, the unmodified white ink yielded CIEDE2000 coordinates of L*=67,56, a*=7,30, and b*=15,97. The height of L* value confirms the significant increase in surface lightness over yellowish-brown background.

These optical properties confirm that the selected opaque white ink possesses the necessary scattering efficiency to serve as an optical modifier in Cyan and Pantone 300 formulations.

3.2. Colour characteristics of process inks printed on white substrate

To establish the baseline printing performance and evaluate colour reproduction under standardized conditions, the unmodified Cyan (process) and Pantone 300 (spot) ink were printed onto the white double-coated testliner. This substrate provides a highly neutral, bright, and smooth optical background minimizing unwanted light absorption and scattering from substrate fibres.

The colorimetric values obtained on the white substrate as the reflectance standard baseline for evaluating colour deviations (ΔE00) when printing directly onto the brown kraft liner. The measures L*, a*, b* coordinates and the calculated total colour difference relative to the digital target standards are summarized in Table 5.

Table 5

Baseline colorimetric characteristics and colour differences (ΔE_{00}) of inks printed on white double-coated testliner

Ink	Ink type	L*	a*	b*	ΔE_{00}
Cyan	Process	52.26	-27.42	-54.18	4.86
Pantone 300	Spot	36.63	-7.03	-54.17	2.65

Analysis of reference prints:

- Cyan ink: Printed on the coated white substrate, the Cyan ink exhibited characteristics high lightness (L*=52.26) and strong negative b* values (b*=-54.18), indicating clear cyan chromaticity with minimal contamination from substrate undertones. The total colour difference relative to the reference standard was ΔE_{00}=4.86, confirming acceptable colour rendering under optimal optical conditions.
- Pantone 300 ink: The spot colour displayed a noticeably deeper cyan-blue tone with lower lightness (L*=36.63) and higher colour saturation compared to process Cyan. The total colour difference on the white substrate reached ΔE_{00}=2.65, establishing the benchmark colour reproduction achievable with the nominal wet film deposit (4 µm) without background interference.

These baseline values demonstrate that both inks achieve predictable colour output on a white optical background. Consequently, any colorimetric shifts observed on the brown kraft liner in subsequent tests can be directly attributed to the optical absorption characteristics of the brown substrate and the modified ink formulations.

3.3. Color characteristics of process ink printed on brown kraft liner

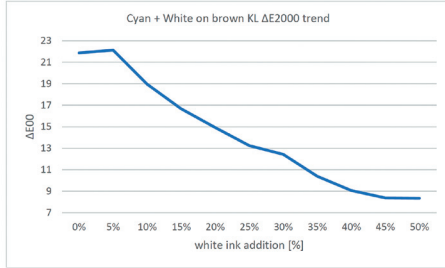
To qualify the optical degradation caused by the unbleached substrate, the baseline unmodified Cyan (C-0) and Pantone 300 (P300-0) inks were printed directly onto both the white double-coated testliner and the brown kraft liner at a constant nominal wet ink film deposit of 4 µm.

Due to selective spectral absorption of unbleached kraft fibres – which act as a strong yellow-red optical filter – the printed baseline inks exhibited a dramatic shift in colorimetric coordinates and spectral reflectance. For Cyan (C-0), reflectance in the blue-green spectral region (400-550 nm) was heavily suppressed, resulting in a lower lightness (L*) and shift toward positive a* and b* coordinates (perceived visually as a dirty, desaturated green-brown tint). Similarly, Pantone 300 (P300-0) lost its characteristic saturated cyan-blue appearance, shifting to a darker slate hue. The total colour difference (ΔE00) relative to the digital target standards reached value exceeding 12.0 for Cyan and 11 for Pantone 300, far above the acceptable industrial packaging tolerance ($\Delta E_{00} \leq 2.0$-3.0).

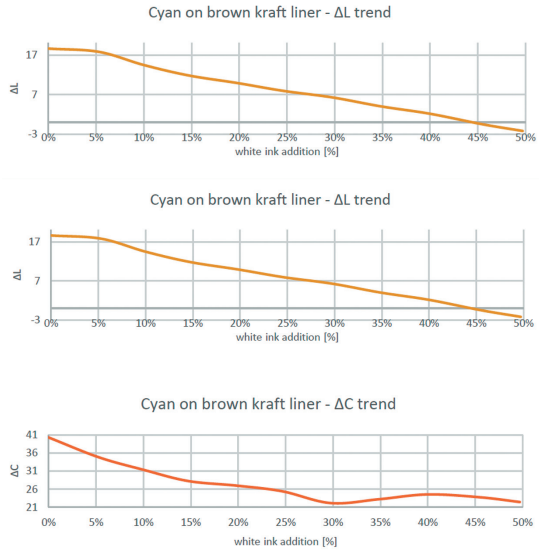
3.4. Influence of opaque white ink addition on process colours

Table 6

Physical parameters and colorimetric values of modified Cyan ink formulations printed on brown kraft liner with 0% to 50% opaque white ink additions – rheological, physical, and colorimetric characteristics

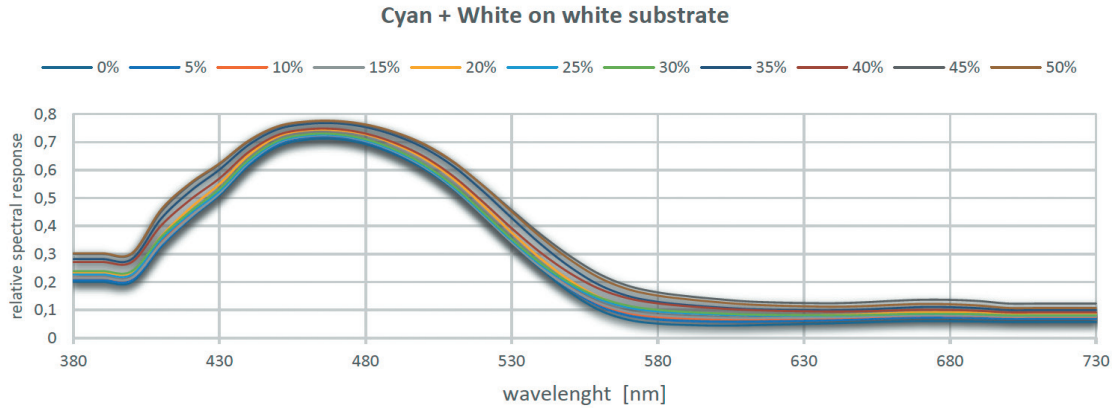


» **Figure 2:** *Colour difference of Cyan formulations as function of opaque white ink addition when printed on the brown kraft liner*

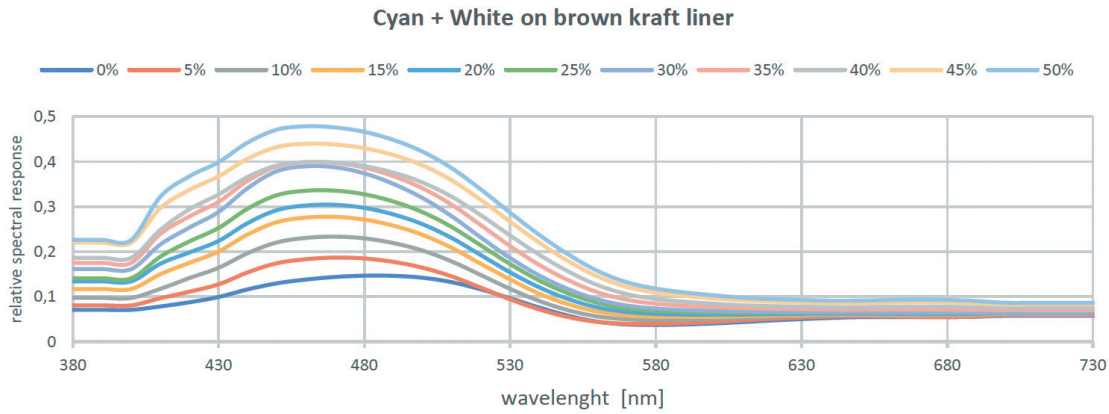


» **Figure 3:** *Variations in CIELCh colour differences (ΔL*, ΔC^*_{ab} and $\Delta h°_{ab}$) of Cyan ink formulations printed on brown kraft liner as a function of opaque white ink dilution percentage (0%-50%). Incremental addition of opaque white ink to the Cyan formulation leads to progressive decrease in both lightness (ΔL*) and chroma (ΔC*), indicating a reduction in overall colour brightness and saturation, while the hue angle difference (Δh) exhibits slight fluctuations across the dilution range*

Sample	White ink content [w/w %]	Viscosity ISO 2431 [sec]	Optical density	L*	a*	b*	C*	h*	ΔE_{00}
Cyan-0	0	20	1,36	31,38	-10,98	-18,96	21,91	239,91	21,87
Cyan-5	5	20	1,32	32,2	-6,92	-26,49	27,38	255,37	22,13
Cyan-10	1	20	1,28	35,54	-9,1	-29,49	30,86	252,85	18,96
Cyan-15	15	20	1,24	38,17	-10,41	-32,32	33,95	252,14	16,67
Cyan-20	20	20	1,22	40,08	-11,79	-33,19	35,22	250,45	14,92
Cyan-25	25	20	1,19	42,06	-12,95	-34,42	36,78	249,38	13,25
Cyan-30	30	20	1,17	43,71	-12,62	-38,01	40,05	251,64	12,43
Cyan-35	35	20	1,12	45,98	-15,01	-35,98	38,99	247,35	10,39
Cyan-40	40	20	1,08	47,85	-17,09	-33,56	37,66	243,01	9,07
Cyan-45	45	20	1,03	50,51	-17,97	-33,99	38,45	242,13	8,38
Cyan-50	50	20	1,00	52,19	-18,34	-35,27	39,76	242,53	8,35



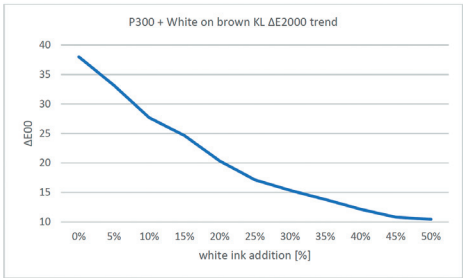
» **Figure 4:** *Spectral reflectance curves of Cyan ink formulations across visible spectrum printed on white substrate*



» **Figure 5:** *Spectral reflectance curves of same Cyan ink formulations printed on the brown kraft liner*

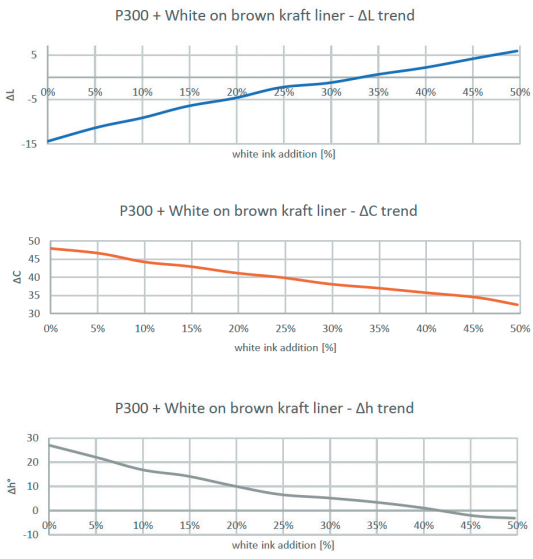
3.5. Influence of opaque white ink addition on Pantone colour

The corresponding physical, rheological and colorimetric parameters for spot colour Pantone 300 across all dilution's levels are presented in Table 7. As shown in Figure 7, the incremental addition of opaque white ink to the Pantone 300 formulation results in a steady increase in lightness (ΔL*), with values shifting from negative to positive, accompanied by a consistent decrease in chroma (ΔC*) and hue-angle difference (Δh).



» **Figure 6:** *Colour difference of Pantone 300 formulations as function of opaque white ink addition when printed on the brown kraft liner*

The ΔL*, ΔC*, and Δh values were calculated relative to the corresponding Pantone 300 reference standard.

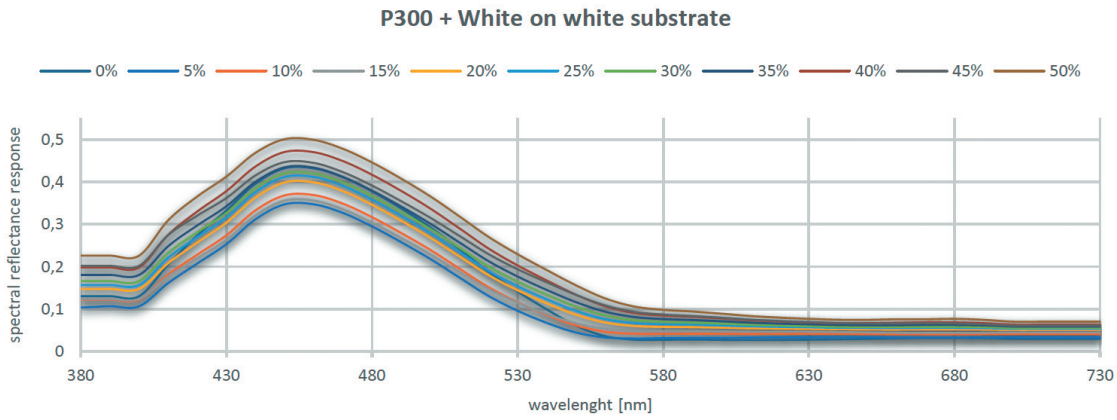


» **Figure 7:** *Variations in CIELCh colour differences (ΔL*, $ΔC^*_{ab}$ and $Δh°_{ab}$) of Pantone 300 (P300) spot ink formulations printed on brown kraft liner as a function of opaque white ink percentage (0%-50%)*

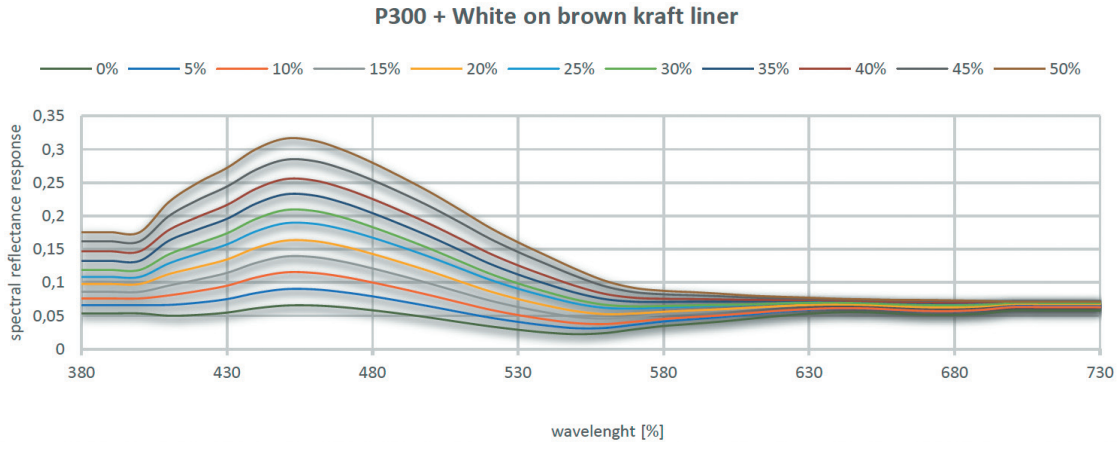
Table 7

Rheological, physical, and colorimetric characteristics of modified Pantone 300 formulations printed on brown kraft liner

Sample	White ink content [%]	Viscosity [DIN 4, sec]	Optical density	L*	a*	b*	C*	h*	ΔE_{00}
P300-0	0	20	1,31	22,09	11,02	-12,49	16,65	311,41	38,01
P300-5	5	20	1,26	25,24	9,00	-15,63	18,04	299,95	33,15
P300-10	10	20	1,24	27,35	6,83	-19,21	20,38	289,58	27,68
P300-15	15	20	1,2	29,92	5,53	-20,85	21,57	284,87	24,65
P300-20	20	20	1,19	31,78	3,15	-23,19	23,41	277,73	20,35
P300-25	25	20	1,17	34,15	1,02	-24,62	24,64	272,37	17,13
P300-30	30	20	1,17	35,19	0,02	-26,44	26,44	270,04	15,35
P300-35	35	20	1,14	37,06	-1,22	-27,52	27,55	267,46	13,81
P300-40	40	20	1,13	38,65	-2,94	-28,68	28,83	264,15	12,15
P300-45	45	20	1,12	40,81	-5,3	-29,71	30,17	259,89	10,81
P300-50	50	20	1,1	42,36	-6,23	-31,52	32,13	258,81	10,45



» **Figure 8:** *Spectral reflectance curves of Pantone 300 ink formulations across visible spectrum printed on white substrate*



» **Figure 9:** *Spectral reflectance curves of same Pantone 300 ink formulations printed on the brown kraft liner*

This trend indicates that increasing white ink dilution enhances the overall lightness of the printed colour while reducing colour saturation and the hue deviation relative to the reference.

3.6. Comparative analysis: Process vs. Spot colour behaviour

A comparative evaluation between process Cyan and spot colour Pantone 300 reveals critical optical and physical behavioural difference when modified with opaque white ink:

Rheological and physical dynamics: Across all addition levels (0-50%), the outflow viscosity remain constant at 20 s (DIN 4 cup). However, wet film density exhibited a linear decrease with increasing white ink concentration – falling from 1.36 to 1.00 for Cyan and from 1.31 to 1.10 for Pantone 300. This drop in density reflects the progressive dilution for the primary colorant pigments by the white formulation vehicle.

Initial substrate shift: Unmodified Pantone 300 printed on both kraft liner (P300-0) suffered significantly higher initial colour distortion (ΔE_{00} = 38.01) compared to Cyan (C-0, ΔE_{00} = 21.87). the brown fibre undertone shifted the chromatic coordinates of Pantone 300 strongly into a positive a* domain (+11.02), severely destroying its blue identity.

Colour difference mitigation (ΔE_{00} trajectory): Both ink sets demonstrated a continuous reduction in total colour difference as opaque white ink concentration increased up to 50%. However, Pantone 300 responded with higher overall error reduction magnitude (ΔE_{red} = 72.5% dropping from 38.01 to 10.45) compared to process Cyan (ΔE_{red} = 61.80% dropping from 21.87 to 8.35).

3.7. Optimal white ink addition

Analysing the trade-off between chromaticity recovery, lightness gain (L*), and colour dilution establishes distinct operational zones for flexographic printing on brown kraft liner:

- Low addition range (5-15%): Insufficient TiO2 light-scattering efficiency. Although lightness increases (L* rises from 31.38 to 38.17 for Cyan, and 22.09 to 29.92 for Pantone 300).
- Effective addition range (20-35%): Provides substantial masking of the brown background. For Cyan, ΔE00 drops below 11.0, while Pantone 300 successfully restores its negative a* coordinate at 35% addition (shifting from +11.02 to-1.22), recovering its true cyan-blue chromatic direction.
- High addition range (40-50%): Yields the lowest overall colour difference relative to reference standards (ΔE00 ≈ 8.35 for Cyan and ΔE00 ≈ 10.45 for Pantone 300). At 50% white ink addition, Cyan lightness (L* = 52.19) perfectly matches the target reference lightness obtained on white double-coated testliner (L* = 52.26). However, additions in this range cause noticeable "pastelisation" and desaturation, which must be balanced against design target specifications.

4. Conclusions

The results demonstrate a significant improvement in the colour accuracy characteristics of inks printed on brown kraft paper when opaque white ink is added to the ink formulation. These findings indicate that controlled addition of opaque white ink may represent an effective technological approach for improving colour reproduction accuracy in printing on kraft-based substrates.

4.1. Main findings

This study demonstrated that the direct incorporation of an opaque white water-based flexographic ink into Cyan process ink and Pantone 300 spot ink provides an effective technical approach to mitigate the strong optical interference caused by brown kraft liner substrates. Without modification, both inks suffer from substantial colorimetric degradation due to selective light absorption by the unbleached kraft fibers, resulting in unacceptably high initial colour deviations (ΔE_{00} = 21.87 for Cyan and ΔE_{00} = 38.01 for Pantone 300) relative to target reference standards.

Progressive addition of TiO2-based opaque white ink systematically increases substrate masking, elevates ΔL* (lightness), and shifts chromatic coordinates towards their true hue directions, successfully eliminating unwanted brown/yellowish undertones.

4.2. Effect magnitude

The addition of opaque white ink yields significant and quantifiable improvements in colour reproduction accuracy across both process and spot ink formulations:

For process Cyan, incremental additions up to 50% reduce the total colour difference from ΔE00 = 21.87 down to 8.35 (a 61.80% overall reduction in colour difference). At 50% white ink concentration, the lightness (ΔL* = 52.19) achieves an exact match with the baseline target printed on white double-coated testliner (ΔL* = 52.26).

For Pantone 300, the modification exhibits a higher magnitude of correction, reducing ΔE00 from an initial 38.01 to 10.45 (a 72.50% reduction of colour difference). Crucially, a 35% addition level is required to recover the negative Δa* coordinate (Δa* =-1.22), effectively restoring the blue-cyan chromatic orientation of the spot colour.

While outflow viscosity remained constant at 20 sec (DIN 4 cup) across all addition levels, wet film optical density decreased linearly (from 1.36 to 1.00 for Cyan, and 1.31 to 1.10 for Pantone 300) due to colorant pigment dilution by the white vehicle.

4.3. Technological implication

From an industrial flexographic perspective, direct modification of process and spot inks offers three primary operational regimes:

- Low addition range (5–15%): Provides insufficient opacity to mask unbleached fibers, resulting in minor lightness shifts without adequate chromatic correction.
- Effective operational range (20–35%): Delivers optimal optical compensation by restoring the true chromatic vector (Δa* and Δb*) while avoiding excessive pigment dilution or target pastelisation.
- High addition range (40–50%): Achieves the lowest absolute ΔE00 values and maximum lightness recovery, but causes noticeable hue desaturation and pastel effects.

This method presents a viable, cost-effective alternative to applying a separate opaque white underlayer in high-volume corrugated board and flexographic packaging production. By eliminating the need for an additional printing unit, additional flexographic plate, and extra printing pass, packaging converters can significantly optimize production efficiency, reduce material consumption, and lower operational overhead while ensuring satisfactory colour consistency on kraft substrates.

This study is funded by the financial support, provided by the Scientific Research Centre at University of Chemical Technology and Metallurgy, Sofia, under Contract No. 59-33.

5. References

Gong, Y., Huang, B.Q. and Wei, X.F. (2013) 'Study on the covering property of white water-based flexo ink', *Applied Mechanics and Materials*, 469, pp. 41–45. DOI: 10.4028/www.scientific.net/AMM.469.41

Horváth, C., Palova, K. and Cziráki, J. (2024) 'Relationships between the surface texture of flexographic printing plates and the printability of kraft paper', *TAGA Technical Abstracts*. Available from: https://www.printing.org/docs/default-source/taga-abstracts-%28member-only%29/t190176.pdf [Accessed 23 August 2026].

International Organization for Standardization (2016) *ISO 2470-1:2016. Paper, board and pulps — Measurement of diffuse blue reflectance factor (ISO brightness) — Part 1: Indoor daylight conditions.* Geneva: International Organization for Standardization.

International Organization for Standardization (2016) *ISO 2811-1:2016. Paints and varnishes — Determination of density — Part 1: Pyknometer method.* Geneva: International Organization for Standardization.

International Organization for Standardization (2017) *ISO 13655:2017. Graphic technology — Spectral measurement and colorimetric computation for graphic arts images.* Geneva: International Organization for Standardization.

International Organization for Standardization (2019) *ISO 2431:2019. Paints and varnishes — Determination of flow time by use of flow cups.* Geneva: International Organization for Standardization.

International Organization for Standardization (2020) *ISO 12647-6:2020. Graphic technology — Process control for the production of half-tone colour separations, proof and production prints — Part 6: Flexographic printing.* Geneva: International Organization for Standardization.

International Organization for Standardization (2022) *ISO 23498:2022. Paper, board and graphic technology — Determination of opacity (paper backing) — Diffuse reflectance method.* Geneva: International Organization for Standardization.

International Organization for Standardization and International Commission on Illumination (2022) *ISO/CIE 11664-6:2022. Colorimetry — Part 6: CIEDE2000 colour-difference formula.* Geneva: International Organization for Standardization.

Ivanova, I., Spiridonov, I.T. and Lasheva, V.G. (2022) 'Spectroscopic technique for studying the characteristics of paper, pigments and inks in the aging process (review)', *Journal of the University of Chemical Technology and Metallurgy*, 57(1), pp. 101–113.

Kumar, S. (2026) 'Comparative evaluation of solvent-based and water-based inks on flexographic print quality using CI Press', *SAJMS*, 10(9). DOI: 10.63665/sajms.v10i09.1

Liu, Y., Huang, B., Wei, X. and Shen, Y. (2017) 'Study on properties of magenta water-based flexo ink used on BOPP film'. In: *Advanced Graphic Communications and Media Technologies.* Lecture Notes in Electrical Engineering, 417, pp. 949–958.

Petrović, S., Kašiković, N., Novaković, D., Bošnjaković, G., Arman Kandırmaz, E. and Özcan, A. (2021) 'Influence of the compressible flexographic sleeve exploitation on print quality', Tehnički vjesnik – *Technical Gazette*, 28(2), pp. 391–400. DOI: 10.17559/TV-20191114164921

Spiridonov, I. and Shopova, M. (2013) 'Determination of the effect of gray component replacement level on colorimetric characteristics of color proof', *Journal of the University of Chemical Technology and Metallurgy*, 48(3), pp. 247–253.

Tomerlin, R., Valdec, D., Tomiša, M. and Vusić, D. (2023) 'The impact of underlying opaque white coating parameters on flexographic print quality', *Applied Sciences*, 13(15), article 8575. DOI: 10.3390/app13158575

Vigneswari, S., Mohammad Idris, M.A.H., Anis, S.N.S., Ramakrishna, S. and Amirul, A.A.A. (2025) 'Characterization and in situ biodegradation analysis of brown kraft paper coated with PHA for potential sustainable packaging', *Food Technology and Biotechnology*, 63(2), pp. 168–176. DOI: 10.17113/ftb.63.02.25.8949



© 2026 Authors. Published by the University of Novi Sad, Faculty of Technical Sciences, Department of Graphic Engineering and Design. This article is an open access article distributed under the terms and conditions of the Creative Commons Attribution license 4.0 Serbia (http://creativecommons.org/licenses/by/4.0/rs/).

https://doi.org/10.24867/GRID-2026-p18

AI in Electrophotographic Printing: Quality Evaluation and Decision Making

ABSTRACT

Print quality evaluation in electrophotographic printing continues to rely predominantly on operator expertise, visual inspection, and conventional quality control procedures, which may limit the consistency and objectivity of decisions made in digital print production. This study investigates whether an AI-assisted recommendation framework, developed from spectrophotometric measurements and experimental colour-difference data, can support the selection of paper substrates and screening conditions for specified CMYK inputs. The purpose is to examine the feasibility of transforming measured print-quality data into practical decision support for the operator. The study introduces Artificial Intelligence-assisted Print Quality Intelligence (AI-PQI), a data-driven recommendation framework that uses spectrophotometric colour measurements and local CMYK-based estimation of CIEDE2000 colour differences. The experimental dataset comprised 400 CMYK patches printed on four paper substrates using six screening conditions on a Xerox electrophotographic printing system. This produced 24 paper–screening combinations and 9,600 measured colour patches. Target CIELAB values, measured CIELAB values and the corresponding ΔE_{00} values were retained as generated within the original experimental and measurement workflow. The results show that the screening condition with the lowest measured colour difference can vary among individual CMYK patches and paper substrates. The proposed framework uses these experimental relationships to estimate the expected ΔE_{00} for the investigated paper–screening combinations and to identify a potentially suitable production condition. Because the reference CIELAB values were defined within the original substrate-specific workflow, the present recommendations should be interpreted as preliminary decision support within the investigated experimental system rather than as a fully standardised comparison against a single substrate-independent colour target. Establishing such a common target and validating predictions for previously unmeasured inputs remain objectives for future research.

Nikola Petrović
Zoran Gazibarić

University of Banja Luka, Faculty of Technology, Department of Graphic Engineering, Banja Luka, Bosnia and Herzegovina

KEY WORDS
Artificial intelligence, electrophotographic printing, print quality evaluation, decision support, digital printing

1. Introduction

Colour reproduction is a critical aspect of print quality in digital and electrophotographic printing, where the reproduced result is influenced by the interaction between digital colour data, the printing process, substrate and colour-management conditions. Objective instrumental measurement therefore provides an important basis for evaluating the quality and consistency of printed output. ISO 13655:2017 specifies procedures for spectral measurement and colorimetric computation for graphic arts images, including those produced by digital printing processes (International Organization for Standardization, 2017). ISO/TS 15311-1:2020 additionally defines print-quality metrics, measurement methods and reporting requirements for printed products, with particular relevance to digital printing systems (International Organization for Standardization, 2020).

Colour difference provides a quantitative basis for comparing a reproduced colour with its reference. The CIEDE2000 colour-difference formula was developed as an improved CIELAB-based colour-difference equation, incorporating weighting and interaction terms to improve the agreement between calculated colour differences and visual colour discrimination (Luo, Cui & Rigg, 2001). Its implementation and mathematical characteristics were subsequently examined in detail, including recommendations for reliable computational implementation (Sharma, Wu & Dalal, 2005). CIEDE2000 (ΔE_{00}) therefore provides a suitable quantitative measure for comparing colour reproduction under different printing conditions.

The resulting colour reproduction is affected not only by the digital colour specification but also by the properties of the printing substrate and the printing conditions. Research on digital printing has demonstrated that paper surface characteristics can influence printing quality and measured print properties (Ataeefard, 2014). In addition, variations in print quality have been associated with paper and printing-process parameters, demonstrating the importance of considering their combined influence on the final printed result (Lundström et al., 2013). These findings indicate that print-quality evaluation should consider both the substrate and the conditions under which a colour is reproduced.

The increasing availability of objective print-quality data also creates opportunities for data-driven assessment and decision support. Machine-learning methods have been investigated for automated print-quality assessment using objectively measured quality attributes and image analysis, demonstrating the potential for replacing or supporting parts of conventional manual evaluation (Lundström & Verikas, 2013). More recently, neural-network-based approaches have been applied to multidimensional digital-print image-quality evaluation, further demonstrating the application of machine learning to quantitative print-quality analysis (Zhong et al., 2024).

However, using experimentally measured colour-difference data to assist the selection of a paper substrate and screening condition for a specific CMYK input represents a more specialised decision-support problem. This study therefore proposes an Artificial Intelligence-assisted Print Quality Intelligence (AI-PQI) approach for electrophotographic printing. The objective is to investigate whether colour-difference relationships contained in an experimental dataset can be used to estimate the behaviour of the tested paper–screening combinations and provide the operator with a preliminary recommendation for a given CMYK input.

The study does not attempt to replace instrumental verification or operator judgement, but to examine how profiling, colour measurement and data analysis can be integrated into a practical decision-support workflow.

The study evaluates four paper substrates and six screening conditions on a Xerox Colour C60/C70 electrophotographic production system. Colour measurements were obtained using an X-Rite i1Pro 2 spectrophotometer, and the resulting experimental dataset was used to examine screening- and substrate-dependent variations and to develop the AI-PQI recommendation procedure.

The central research question was whether experimentally obtained print-quality data could provide a useful basis for estimating colour-difference behaviour and supporting the operator's selection of a paper–screening combination for a specified CMYK input.

2. Methods and materials

The experimental methodology was designed to investigate variations in colour reproduction among paper substrates and screening conditions and to provide a controlled dataset for developing the AI-PQI approach. The study combined controlled printing, instrumental colour measurement and data-driven analysis of the resulting colour-difference values. Four paper substrates and six screening conditions were evaluated using the same 400-patch CMYK chart, resulting in 24 experimental paper–screening combinations and 9,600 measured colour patches. Target CIELAB, measured CIELAB and ΔE_{00} values were retained in the form generated during the original experimental workflow.

No retrospective ICC-based transformation or recalculation of the reported colour values was performed. The measurement approach was based on established principles of instrumental colour measurement and print-quality evaluation in graphic technology (International Organization for Standardization, 2017; International Organization for Standardization, 2020). The use of substrates with different surface characteristics was also intended to account for the known influence of paper properties on digital printing quality (Ataeefard, 2014).

2.1. Materials and experimental setup

The experimental study was conducted using a Xerox Colour C60/C70 electrophotographic production printing system operated through a Fiery colour-management workflow. Four paper substrates with different grammages and surface characteristics were used. Their basic characteristics are presented in Table 1.

The same FOGRA39L_coated.icc colour profile was used throughout the printing experiment, while the paper substrate and screening condition were varied as the principal experimental factors. The profile was part of the applied colour-management workflow; it was not subsequently used to regenerate or replace the Target CIELAB values contained in the original measurement dataset.

Table 1
Paper substrates used in the experimental study

No.	Paper substrate	Commercial name	Grammage (g/m²)	Surface / finish	Paper category
1	Offset paper	Amber Graphic Offset	80	Uncoated, smooth	Uncoated paper
2	Matt-coated paper	Garda Matt Art	135	Matt-coated, smooth	Coated paper
3	Offset paper	Amber Graphic Offset	170	Uncoated, smooth	Uncoated paper
4	Specialty paper	Sirio Pearl – Oyster Shell	300	Pearlescent surface	Specialty paper

2.2. Experimental design and colour measurement

The printed patches were measured using an X-Rite i1Pro 2 spectrophotometer. CIELAB values were determined under D50 illumination using the CIE 1964 10° standard observer, in accordance with the settings applied in the original i1Profiler measurement workflow. For each patch, the dataset contained the input CMYK values, Target CIELAB values, Measured CIELAB values and the corresponding CIEDE2000 colour difference, ΔE_{00}. These values were retained without subsequent conversion or recalculation. The same CMYK patch definitions enabled comparisons between screening conditions within each substrate. However, because the Target CIELAB values were established within the original substrate-specific workflow, direct comparisons of ΔE_{00} between different substrates do not represent deviations from a single substrate-independent colour target.

The screening conditions selected in the experimental configuration were 150 dot, 200 dot, 300 dot and 600 dot (clustered-dot screens), 200 line (rotated-line screen), and stochastic screening. These settings describe the halftoning applied during printing; they are distinct from the system's 2400 × 2400 dpi print resolution. The same FOGRA39L_coated.icc profile and colour chart were used throughout the experiment, while the paper substrate and screening condition were varied.

The printed patches were measured using an X-Rite i1Pro 2 spectrophotometer. CIELAB values were determined under D50 illumination using the 10° standard observer. For each patch, the dataset contained its input CMYK values, reference CIELAB values, measured CIELAB values and the corresponding CIEDE2000 colour difference (ΔE_{00}). The same CMYK inputs enabled comparisons between screening conditions within each substrate. The reference CIELAB values differed between substrates; consequently, cross-substrate comparisons depend on the reference specified for each paper.

2.3. AI-PQI model and recommendation procedure

The AI-PQI model was developed to estimate the expected colour difference for a given CMYK input under each of the investigated paper–screening combinations.

It uses a weighted 12-nearest-neighbour regression procedure based on the experimentally obtained ΔE_{00} dataset. Before calculating distances, the C, M, Y and K values were normalised to the 0–1 range to provide a common numerical scale for all four channels. The procedure models local relationships within the available experimental data and does not independently reconstruct spectral or CIELAB values.

For each paper–screening combination, the 12 experimental patches with the smallest distance from the input CMYK value were identified. Their measured ΔE00 values were combined using distance-based weighting to obtain the predicted colour difference:

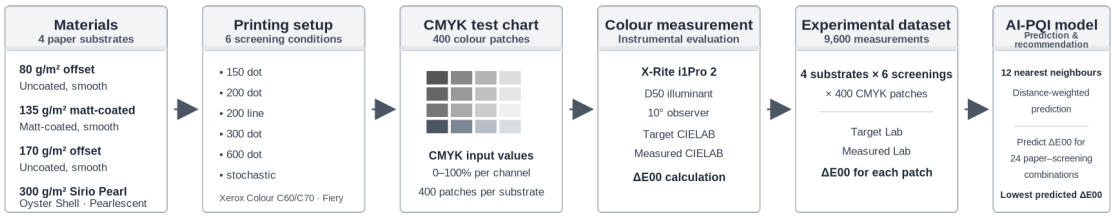
$$\hat{\Delta E}_{00} = \frac{\sum_{i=1}^{12} w_i \Delta E_{00,i}}{\sum_{i=1}^{12} w_i} \quad (1)$$

where $\Delta\hat{E}_{00}$ represents the predicted colour difference, $\Delta E_{00,i}$ is the measured colour difference of the *i*-th nearest experimental patch, and w_i is the corresponding distance-based weight.

The prediction was performed separately for all 24 combinations of the four paper substrates and six screening conditions. The prediction procedure was applied separately to all 24 combinations of four paper substrates and six screening conditions. The combination with the lowest estimated ΔE_{00} was presented as the AI-PQI recommendation. In the present study, this output represents a relative ranking within the original experimental dataset.

Because substrate-specific reference values were used, the recommendation should not yet be interpreted as proof that the selected substrate provides the closest reproduction of one common, substrate-independent target colour.

This approach enables the recommendation procedure to account for local relationships between CMYK composition and experimentally obtained colour difference rather than relying only on the overall mean performance of a screening condition. It therefore represents an initial data-driven decision-support method whose predictive performance for previously unmeasured colours requires separate validation. The overall experimental and AI-PQI workflow is illustrated in Figure 1.



» **Figure 1:** *Workflow of the experimental procedure and AI-PQI recommendation*

3. Results

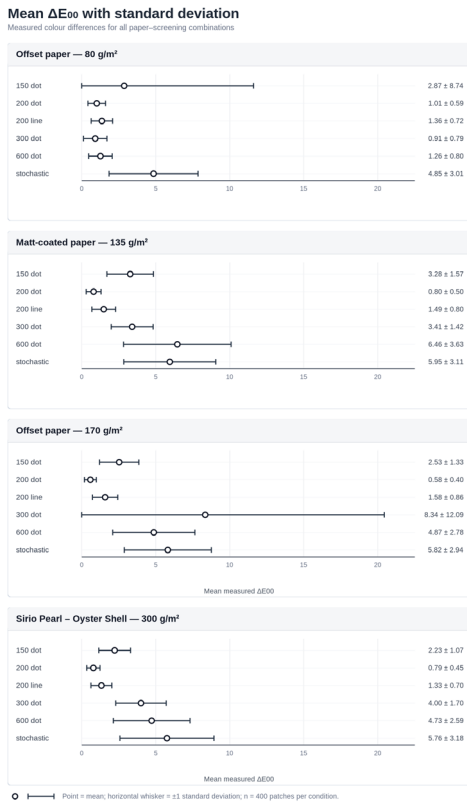
The experimental results were analysed to describe colour-difference behaviour among the investigated paper–screening combinations and to demonstrate how the resulting dataset can be implemented in the AI-PQI decision-support procedure. The results are presented at the overall experimental and individual-patch levels, followed by examples of AI-PQI prediction and recommendation outputs. Descriptive statistics and graphical representations illustrate differences in mean colour difference and variability among the investigated conditions. Predictive accuracy for independent or previously unmeasured inputs was not evaluated in the present study.

3.1. Experimental colour-difference results

The measured colour-difference values for the four paper substrates and six screening conditions are summarized in Table 2 as mean values with their corresponding standard deviations.

The 200 dot screening condition yielded the lowest mean ΔE_{00} on three substrates: 0.80 on the 135 g matt-coated paper, 0.58 on the 170 g offset paper and 0.79 on the 300 g specialty paper. On the 80 g offset paper, 300 dot yielded the lowest mean ΔE_{00} (0.91), followed by 200 dot (1.01). Mean ΔE_{00} values obtained with other screening conditions varied considerably between substrates. These descriptive values refer to the Target and Measured CIELAB data generated within the original measurement workflow. Accordingly, the results describe the colour-difference behaviour recorded for each experimental condition and should not be interpreted as a standardised cross-substrate comparison against one common Target CIELAB dataset.

Differences in variability were also observed between the investigated conditions. The highest standard deviations were recorded for 150 dot on the 80 g offset paper (SD = 8.74) and 300 dot on the 170 g offset paper (SD = 12.09), whereas the 200 dot condition showed comparatively low standard deviations across all four substrates, ranging from 0.40 to 0.59. The mean values and corresponding standard deviations are visualized in Figure 2.



» **Figure 2:** *Comparison of colour-difference behaviour across the investigated paper–screening combinations*

Table 2

Mean measured ΔE00 and standard deviation for the investigated paper–screening combinations

Paper substrate	150 dot	200 dot	200 line	300 dot	600 dot	Stochastic
Offset 80 g	2.87 ± 8.74	1.01 ± 0.59	1.36 ± 0.72	0.91 ± 0.79	1.26 ± 0.80	4.85 ± 3.01
Matt 135 g	3.28 ± 1.57	0.80 ± 0.50	1.49 ± 0.80	3.41 ± 1.42	6.46 ± 3.63	5.95 ± 3.11
Offset 170 g	2.53 ± 1.33	0.58 ± 0.40	1.58 ± 0.86	8.34 ± 12.09	4.87 ± 2.78	5.82 ± 2.94
Specialty 300 g	2.23 ± 1.07	0.79 ± 0.45	1.33 ± 0.70	4.00 ± 1.70	4.73 ± 2.59	5.76 ± 3.18

Table 3

Patch-level comparison of 200 dot with the lowest measured ΔE_{00} on each substrate. The final column is the mean of the lowest measured ΔE_{00} among six screening conditions for each patch; it is not a prediction by the AI-PQI application

Paper substrate	Patches with the lowest ΔE_{00} at 200 dot	Patches with a lower ΔE_{00} at another screen	Mean ΔE_{00} at 200 dot	Mean of the lowest measured ΔE_{00} per patch
Offset 80 g	73 / 400	327 / 400	1.01	0.48
Matt-coated 135 g	310 / 400	90 / 400	0.80	0.71
Offset 170 g	333 / 400	67 / 400	0.58	0.53
Specialty 300 g	266 / 400	134 / 400	0.79	0.65

The 200 dot setting produced the lowest mean ΔE_{00} on three substrates, whereas 300 dot produced the lowest mean on the 80 g offset paper. Nevertheless, the screening condition with the lowest measured ΔE_{00} varied among individual CMYK patches.

The 200 dot setting gave the lowest measured value for 73 of 400 patches on the 80 g offset paper, 310 patches on the 135 g matt-coated paper, 333 patches on the 170 g offset paper and 266 patches on the 300 g specialty paper. Selecting a screen solely from its overall mean therefore does not always identify the condition with the smallest recorded colour difference for a specific input colour.

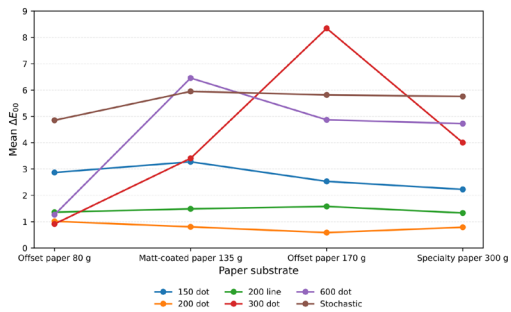
These patch-level results provide the experimental basis for colour-specific screening recommendations within each substrate and demonstrate the potential value of a more comprehensive operator-support system.

3.2. Descriptive relationship between paper substrate and screening performance

The effect of the paper substrate on the colour-difference response of the investigated screening conditions is presented in Figure 3. The results show that the mean ΔE_{00} values of the screening conditions varied differently across the four substrates.

The 200 dot condition maintained relatively low mean ΔE_{00} values across all substrates, ranging from 0.58 to 1.01. In contrast, the response of 300 dot varied substantially, from 0.91 on the 80 g offset paper to 8.34 on the 170 g offset paper.

The 600 dot condition also showed noticeable variation, with mean ΔE_{00} values ranging from 1.26 to 6.46. The 200 line condition exhibited comparatively small changes between substrates, with values ranging from 1.33 to 1.58. Stochastic screening remained within a relatively narrow but higher range, from 4.85 to 5.95.



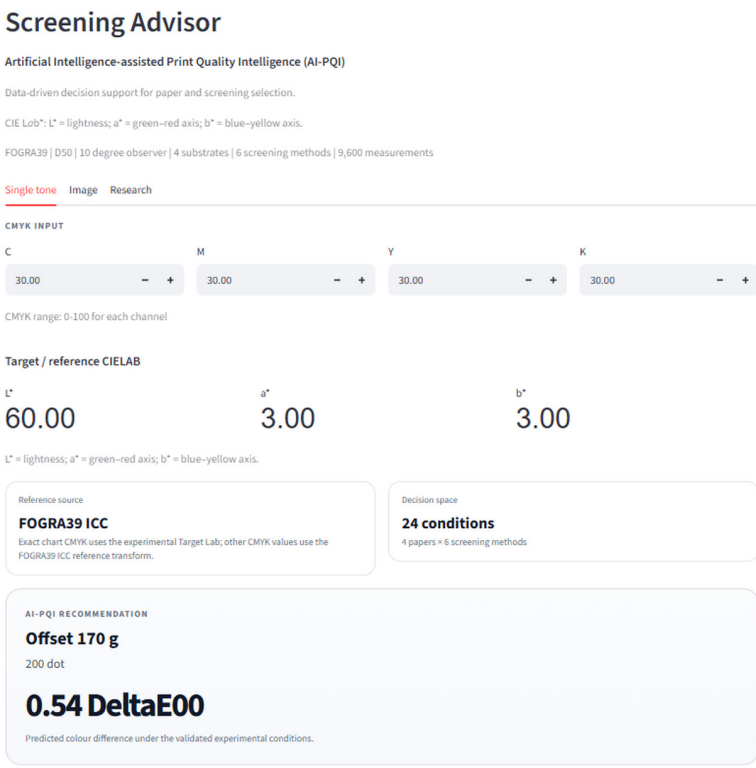
» **Figure 3:** *Descriptive variation in mean ΔE_{00} across paper substrates and screening conditions*

3.3. AI-PQI application and prediction output

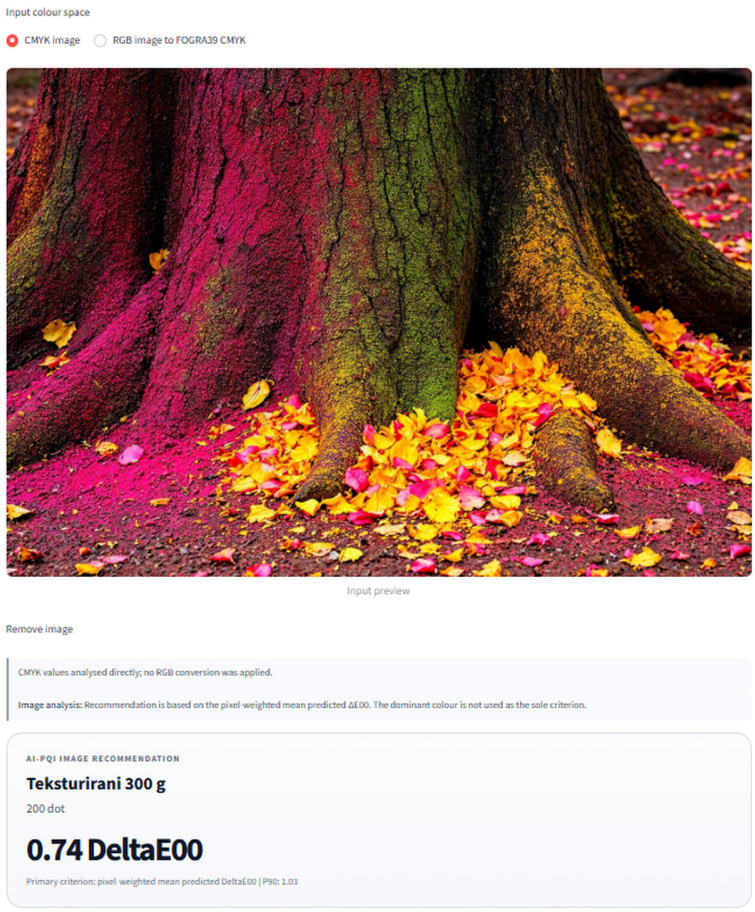
The experimentally obtained colour-difference dataset was implemented in the AI-PQI application to demonstrate prediction for a specified CMYK input across the investigated paper–screening combinations. The application estimates the expected ΔE_{00} for each combination and ranks the available alternatives according to the predicted values, as illustrated in Figure 4. This output demonstrates the operation of the recommendation procedure but does not constitute independent validation of its predictive accuracy.

In addition to single-colour CMYK analysis, the application includes an image-analysis mode in which the input image is evaluated according to its colour content. The image-level estimate is derived from the pixel-weighted contribution of the analysed colours.

This enables the recommendation procedure to consider the overall colour composition of an image rather than only its dominant colour. Figure 5 presents an example of the application output. The current implementation should be regarded as a functional demonstration; its recommendations require validation using independent print samples and complete images. The developed application therefore provides two complementary input modes: prediction for an individual CMYK colour and prediction based on the colour content of a complete image.



» **Figure 4:** *AI-PQI application output for CMYK-based colour-difference prediction and screening recommendation*



» **Figure 5:** *AI-PQI image-analysis mode for substrate and screening recommendation*

4. Discussion

The experimental results show that colour-difference behaviour in electrophotographic printing depends on the combination of paper substrate and screening condition. The 200 dot condition produced consistently low mean ΔE_{00} values on three of the four substrates, whereas the lowest mean value on the 80 g offset paper was obtained with 300 dot screening. We therefore consider screening and substrate to be interdependent production parameters rather than independent choices. This interpretation is consistent with previous research showing that paper surface characteristics affect measured properties and overall print quality in digital printing (Ataeefard, 2014). The pronounced changes observed with 300 dot and 600 dot screening further demonstrate that substrate-dependent variations can remain substantial even when the printing system and colour-management workflow are unchanged.

The dataset also revealed individual colour patches that deviated considerably from the general behaviour of a screening condition. The most pronounced cases occurred with 150 dot screening on the 80 g offset paper and 300 dot screening on the 170 g offset paper, where isolated high ΔE_{00} values increased the overall variability. Because the colour chart, profile and measurement procedure remained consistent, we interpret these deviations as evidence that some paper–screening combinations reproduce different regions of the CMYK space with unequal accuracy. Although the present experiment does not isolate the physical causes of these deviations, it shows why evaluation based on a large set of colour patches is more informative than testing only a few selected colours.

The AI-PQI approach uses this experimentally measured relationship between CMYK composition and ΔE_{00} for each paper–screening combination. Instead of selecting one screening condition for every colour based on its overall average, the model uses neighbouring CMYK samples to estimate the expected colour difference for a specified input. Differences in data uniformity among substrates directly affect these estimates and are therefore relevant to the recommendation procedure. In our view, this colour-specific use of measured data is the main practical contribution of the proposed approach. It is also consistent with earlier research demonstrating the potential of machine-learning methods for print-quality assessment based on objectively measured attributes (Lundström & Verikas, 2013; Lundström et al., 2013).

The difference between the best overall screening condition and the condition producing the lowest measured ΔE_{00} for an individual patch confirms the value of colour-specific decision support. The present application uses these relationships to identify the most promising of the tested conditions for a specified CMYK input and to support the operator's decision before print verification. The current results describe the choices represented in the measured dataset, while evaluation using previously unmeasured CMYK inputs remains an important next stage in the development of the model.

A methodological limitation of the present experiment concerns the definition of the Target CIELAB values. Although the same CMYK patch definitions were used, the reference values were established within the original substrate-specific measurement workflow.

Consequently, the reported ΔE_{00} values provide a valid basis for examining screening behaviour within the corresponding experimental conditions, but direct rankings across papers do not yet represent comparisons against a single paper-independent target. We therefore interpret the current AI-PQI output as preliminary production support based on the original experimental reference structure.

In future research, we intend to establish one traceable Target CIELAB dataset for all paper and screening conditions. The workflow could begin with the original CMYK patch definitions stored in a CGATS text file and transform them into CIELAB coordinates using a documented independent ICC reference profile, such as FOGRA39 or another profile appropriate to the intended reference condition. The resulting Target values could then be incorporated into a compatible CGATS or MXF workflow in i1Profiler. Documenting the ICC profile, rendering intent, black-point compensation and other transformation parameters would allow every printed patch to be evaluated against the same Target CIELAB value.

The colorimetric conditions should also be harmonised before measurements begin. The present study retains the D50 illumination and CIE 1964 10° observer settings used in the original workflow. In the proposed future workflow, both Target and Measured CIELAB values would be generated using D50 illumination and the CIE 1931 2° standard observer. These conditions would be selected directly in i1Profiler before measuring the printed charts. When Target and Measured values are generated under the same D50/2° conditions from the outset, subsequent recalculation of Measured CIELAB values from M1 spectral data is unnecessary.

A common Target dataset and harmonised measurement conditions would enable all paper–screening combinations to be compared on the same colorimetric basis. The resulting system could provide the operator with a ranked list of paper, screening and profile configurations, together with their expected ΔE_{00} values and the need for additional print verification. Validation using CMYK colours excluded from model development, repeated print runs and complete test images would then allow us to evaluate the reliability of these recommendations.

We consider the present study an initial but relevant step towards AI-assisted selection of electrophotographic printing conditions. It demonstrates how profiling, instrumental measurement and local data analysis can be integrated to generate colour-specific recommendations from experimental results.

The objective has been partially achieved: the current model provides structured decision support, while a common Target CIELAB dataset, harmonised D50/2° conditions and independent validation are required to develop it into a standardised instruction system for print operators.

5. Conclusions

The study investigated colour-difference behaviour across four paper substrates and six screening conditions in Xerox Colour C60/C70 electrophotographic printing and examined whether the resulting experimental data could support an AI-assisted recommendation workflow. The original Target, Measured and ΔE_{00} values were retained without retrospective transformation. The findings support the following conclusions:

- The recorded colour-difference response varied among the investigated paper substrates and screening conditions. The 200 dot condition produced the lowest mean ΔE_{00} on the 135 g matt-coated, 170 g offset and 300 g specialty papers, whereas 300 dot produced the lowest mean on the 80 g offset paper. The condition with the lowest measured ΔE_{00} nevertheless varied among individual CMYK patches.
- The experimental data indicate that screening performance should be considered together with substrate characteristics. Particularly pronounced variations were observed for the 300 dot and 600 dot conditions. These results describe the investigated experimental workflow and should not be generalised to other printing systems without additional validation.
- The dataset of 9,600 measured patches provided a basis for developing a local CMYK-based estimation procedure for the investigated paper–screening combinations. The weighted nearest-neighbour approach enables colour-specific estimates rather than recommendations based only on overall screening averages.
- The AI-PQI application demonstrates the feasibility of integrating profiling, instrumental colour measurement and data analysis into an operator-oriented decision-support workflow. Its outputs should currently be interpreted as preliminary recommendations within the investigated dataset, not as independently validated predictions or definitive paper-independent optimisation.
- Future development should establish a common Target CIELAB dataset from the CMYK patch set using a documented independent ICC reference profile. Target and Measured values should be generated directly in i1Profiler under harmonised D50/2° conditions. The resulting method should then be validated using previously unmeasured colours, repeated print runs and additional substrates, screening conditions and colour-management profiles.

The study partially achieved its objective by demonstrating how experimental profiling, colour measurement and AI-assisted data analysis can be combined to support the selection of printing conditions. A fully standardised operator-guidance system will require a common target definition, harmonised colorimetric conditions and independent validation of the resulting recommendations.

6. Acknowledgments

The authors gratefully acknowledge the financial support provided by the Ministry of Scientific and Technological Development, Higher Education and Information Society of the Republic of Srpska under project No. 19.032/961-60/24, titled “Critical Assessment of Color Quality Control in the Printing Industry in Accordance with the Recommendations of ISO 12647, ISO 15311, and ISO 13655 Standards.” and by the Provincial Secretariat for Higher Education and Scientific Research of the Autonomous Province of Vojvodina, Republic of Serbia, through the project "Digital and Ecological Transformation of the Graphic Industry" (No. 004351431 2025 09418 003 000 000 001 04 002).

7. References

Ataeefard, M. (2014) 'Influence of paper surface characteristics on digital printing quality', *Surface Engineering*, 30(7), pp. 529–534. DOI: 10.1179/1743294414Y.0000000264

International Organization for Standardization. (2017) *ISO 13655:2017. Graphic technology — Spectral measurement and colorimetric computation for graphic arts images*. Geneva, Switzerland: International Organization for Standardization.

International Organization for Standardization. (2020) *ISO/TS 15311-1:2020. Graphic technology — Requirements for printed matter for commercial and industrial production — Part 1: Measurement methods and reporting schema*. Geneva, Switzerland: International Organization for Standardization.

Lundström, J. and Verikas, A. (2013) 'Assessing print quality by machine in offset colour printing', *Knowledge-Based Systems*, 37, pp. 70–79. DOI: 10.1016/j.knosys.2012.07.022

Lundström, J., Verikas, A., Tullander, E. and Larsson, B. (2013) 'Assessing, exploring, and monitoring quality of offset colour prints', *Measurement*, 46(4), pp. 1427–1441. DOI: 10.1016/j.measurement.2012.11.037

Luo, M.R., Cui, G. and Rigg, B. (2001) 'The develop-m4ent of the CIE 2000 colour-difference formula: CIEDE2000', *Color Research & Application*, 26(5), pp. 340–350. DOI: 10.1002/col.1049

Sharma, G., Wu, W. and Dalal, E.N. (2005) 'The CIEDE2000 color-difference formula: Implementation notes, supplementary test data, and mathematical observations', *Color Research & Application*, 30(1), pp. 21–30. DOI: 10.1002/col.20070

Zhong, J., Zhan, H., Xu, F. and Zhang, Y. (2024) 'Research on a Multidimensional Digital Printing Image Quality Evaluation Method Based on MLP Neural Network Regression', *Applied Sciences*, 14(14), 5986. DOI: 10.3390/app14145986



© 2026 Authors. Published by the University of Novi Sad, Faculty of Technical Sciences, Department of Graphic Engineering and Design. This article is an open access article distributed under the terms and conditions of the Creative Commons Attribution license 4.0 Serbia (http://creativecommons.org/licenses/by/4.0/rs/).

Original Scientific Paper https://doi.org/10.24867/GRID-2026-p19

Printing Possibility on Biopolymer Based Films

ABSTRACT

The growing demand for sustainable packaging and printed products has increased interest in biodegradable polymeric materials as environmentally friendly alternatives to conventional plastics. However, their printability and color reproduction characteristics remain insufficiently investigated. This study evaluates the suitability of biodegradable polymer films based on poly (lactic acid) (PLA) and its blends with poly (butylene succinate) (PBS), poly (hydroxybutyrate) (PHB), and poly (hydroxybutyrate-co-valerate) (PHBV) for UV inkjet printing applications. Biopolymer films were produced by flat-die extrusion under controlled processing conditions. The printed samples were obtained using a UV inkjet printing system under standardized printing parameters. Print quality was assessed through optical density and CIELAB color measurements using a spectrophotometer, while the chemical structure of the prepared blends was examined by FTIR spectroscopy to verify the absence of chemical reactions during processing. The obtained results indicate that all investigated biopolymer blends provide high optical density values with only minor variations among formulations. Although differences in lightness (L) were observed between individual blends, chromatic coordinates (a* and b*) remained relatively stable, demonstrating consistent color reproduction across the tested materials. FTIR analysis confirmed that no new chemical bonds were formed during extrusion, indicating that the prepared materials represent physical polymer blends. The findings demonstrate that PLA-based biodegradable films and their blends exhibit promising printability for UV inkjet technology while maintaining their chemical integrity after processing. These results contribute to the development of sustainable printed products and provide a basis for further optimization of biodegradable substrates intended for graphic and packaging applications.*

Ivana Jurič [1]
Aleksandra Nešić [2]
Branka Pilić [2]
Nemanja Kašiković [1]
Magdolna Pál [1]
Živko Pavlović [1]

[1] University of Novi Sad, Faculty of Technical Sciences, Department of Graphic Engineering and Design, University of Novi Sad, Novi Sad, Serbia
[2] University of Novi Sad, Faculty of Technology, Novi Sad, Serbia

KEY WORDS
UV inkjet printing, biopolymer films, PLA blends, color reproduction, print quality, FTIR analysis, sustainable packaging

1. Introduction

The excessive use and inadequate disposal of petroleum-derived plastics have led to significant environmental pollution and to the accumulation of plastic waste in terrestrial and aquatic ecosystems (Taib et al., 2024). Conventional polymers such as low-density polyethylene (LDPE) are widely used in flexible packaging because of their low cost and ease of processing; however, they are poorly recycled due to their flexible nature and low residual economic value (Taib et al., 2024). This situation has driven substantial research effort toward biodegradable and bio-based alternatives for packaging applications (Kricheldorf, 2005). Poly(lactic acid) (PLA) has emerged as one of the most commercially attractive biopolymers for sustainable packaging, offering renewability from agricultural feedstocks, good mechanical properties, transparency and biocompatibility (Kricheldorf, 2005). Nevertheless, PLA exhibits limitations that restrict its stand-alone use in flexible packaging, including inherent brittleness, low ductility, limited thermal endurance and weak moisture barrier properties (Kricheldorf, 2005; Ali et al., 2023). To overcome these limitations, PLA is frequently blended with other biodegradable polyesters,

in particular poly(butylene succinate) (PBS), poly(hydroxybutyrate) (PHB) and poly(hydroxybutyrate-co-hydroxyvalerate) (PHBV), the latter two being important members of the polyhydroxyalkanoate family (Chuakhao et al., 2024; Patel et al., 2022; Tubio et al., 2023). PBS is a semicrystalline biodegradable polyester that, when blended with PLA, improves ductility and processability while preserving biodegradability and compostability (Chuakhao et al., 2024). PHB, the principal member of the polyhydroxyalkanoates, exhibits exceptionally high crystallinity (up to 70–75 wt%), which results in a high elastic modulus and tensile strength comparable to conventional petrochemical polymers such as polystyrene (Patel et al., 2022). Blending PLA with PHB improves overall crystallinity and the barrier properties essential for food packaging (Pate Patel). PHBV, a copolymer of hydroxybutyrate and hydroxyvalerate, combines the rigidity of PHB with enhanced flexibility and elasticity (Tubio et al., 2023) PHBV/PLA blends have been reported to yield films with improved mechanical characteristics and increased hydrophilicity compared with neat PHBV (Tubio et al., 2023).

Printability is a critical requirement for packaging materials, yet the surface properties that govern ink anchorage on biopolymer blends remain insufficiently characterized. Surface energy, wettability, roughness and topography together determine ink–substrate interactions and, ultimately, print quality (Mahović Poljaček, Tomašegović & Priselac, 2026). The adhesion of printing inks depends on the reciprocal interaction of the polar and dispersive components of the surface free energy of the film and of the ink; greater similarity between these components results in improved wetting and adhesion (Mahović). Because biopolymer blends generally exhibit phase-separated morphologies, with surface characteristics inherited from each component, their printing behavior may differ appreciably from that of single-polymer systems (Mahović Poljaček, Tomašegović & Priselac, 2026).

A growing body of work has specifically addressed the printability of PLA and its blends. Early flexographic trials on neat PLA film showed that it could reproduce solid tones and half-tone dots to a standard comparable with conventional PET and OPP substrates, although its inherently low surface energy required careful matching of ink formulation, anilox volume and plate screen ruling (Rong & Keif, 2007; Jacobson et al., 2009). Because untreated PLA surfaces are non-polar and offer limited wettability, several studies ; have turned to plasma activation as a pretreatment: oxygen and argon plasma applied to PLA film raised its surface free energy sufficiently to improve flexographic solid-tone density and dot quality (Izdebska-Podsiadły, 2021), while low-pressure plasma applied to PLA/PHB blends plasticized with acetyl tributyl citrate increased surface energy in a way that depended jointly on plasma power, exposure time and blend composition (Omaníková et al., 2020). Closer to the present study, a preliminary investigation of digital printing on biodegradable flexible packaging materials reported that the choice of biodegradable substrate measurably narrows the reproducible colour gamut relative to conventional films (Maňúrová, Preklet & Horváth, 2021). Taken together, these studies establish that PLA and simple PLA blends can be printed to an acceptable standard, but each is limited either to a single polymer, to flexographic rather than inkjet technology, to the effect of an additional surface treatment, or to the reproducible colour gamut rather than the optical density and CIELAB coordinates of a standardized full-tone patch. None examines UV inkjet printing on PLA blended systematically with PBS, PHB and PHBV across a composition range, which is the specific gap addressed here.

UV inkjet technology offers clear advantages for packaging: it is essentially solvent-free, cures by rapid photopolymerisation, and has a reduced environmental footprint compared with conventional solvent-based processes (Kováčik et al., 2024). Modern UV inks are formulated to adhere to a wide range of polymer surfaces, which in principle enables printing on sustainable biopolymer substrates (Kováčik et al., 2024)). However, the compatibility and colour reproduction behavior of UV inks on PLA/PBS, PLA/PHB and PLA/PHBV blend films have not been systematically investigated. It is not known whether variation of the second blend component and its mass fraction — which changes crystallinity, phase morphology and surface topography of the film — translates into measurable differences in optical density or in reproduced colour. A further and largely unaddressed question is methodological: extruded biopolymer films frequently exhibit a pronounced machine-direction line structure and micro-relief, and it is unclear to what extent conventional spectrophotometric evaluation of such surfaces reports genuine colour differences rather than artefacts of measurement geometry.

The objectives of the present study were therefore fourfold: (i) to verify, by ATR-FTIR spectroscopy, that flat-die extrusion of PLA with PBS, PHB and PHBV yields physical blends rather than reactively compatibilized systems; (ii) to quantify the optical density and CIELAB coordinates of full-tone black UV inkjet prints on ten extruded biopolymer films; (iii) to evaluate, through total colour differences in both the CIE 1976 and CIEDE2000 metrics, whether the choice and concentration of the second blend component compromises the consistency of colour reproduction and the machine readability of printed graphic elements; and (iv) to assess the contribution of surface texture to the measured variability and to derive practical recommendations for the colorimetric quality control of printed biodegradable films.

2. Materials and methods

2.1. Materials

Poly(lactide) (PLA) INGEO 2003D (NatureWorks LLC, USA) was used as the main component in all blends. Poly(butylene succinate) (PBS) was supplied by NaturePlast (France). Poly(hydroxybutyrate) (PHB) and poly(hydroxybutyrate-co-hydroxyvalerate) (PHBV) were purchased from Helian Polymers (The Netherlands), grades ENMAT Y3000P and ENMAT Y1000P, respectively. All polymers were dried prior to extrusion in order to prevent hydrolytic degradation of the polyester chains during melt processing.

Prints were produced using the standard CMYK ink set of the press manufacturer. For colorimetric measurement, printed films were backed by a uniform white substrate (Options cool white, 220 g/m²; measured CIELAB values L* = 95.84 ± 0.16, a* = 1.94 ± 0.04, b* = −3.60 ± 0.09; mean of five measurements) so that the semi-transparent films were evaluated against a reproducible and standardized background.

2.2. Film preparation

Films were produced by flat-die extrusion on a custom-built single-screw extruder. Polymer pellets were dry-mixed in the required mass ratio immediately before processing and fed into the extruder hopper without prior compounding, so that blending occurred in the melt during a single extrusion pass. The extruded melt was drawn through a flat die and taken up by a calender. All samples were processed with the calender cooled, with the single exception of sample PLA16, which was produced without calender cooling in order to evaluate the influence of the cooling regime — and hence of the surface topography and degree of crystallinity of the film — on the subsequent print result. The sample designation used throughout this work combines the abbreviation of the second blend component with its nominal mass fraction in the blend: PHB10 denotes a film containing 90 wt% PLA and 10 wt% PHB, PHBV30 a film containing 70 wt% PLA and 30 wt% PHBV, and so forth. Samples PLA15 and PLA16 are neat PLA films and serve as the reference for all blends. The complete list of samples and the corresponding processing parameters is given in Table 1.

2.3. FTIR analysis

Fourier-transform infrared spectroscopy of the prepared films was performed on an IRAffinity-1S spectrometer equipped with an attenuated total reflectance (ATR) accessory (Shimadzu, Japan). Transmittance (T, %) was recorded over the range 400–4000 cm−1 at a spectral resolution of 4 cm−1, accumulating 40 scans per spectrum. Spectra of the neat components were recorded under identical conditions and used as references. The purpose of the analysis was to confirm that no reactive extrusion had taken place and that only physical blends were obtained, which is a prerequisite for interpreting the optical results in terms of blend morphology rather than of newly formed chemical species.

2.4. Printing

Printing was performed on an ArtisJet 3000U flat-bed UV inkjet printer. A dedicated test chart was designed for the study, containing full-tone patches of the process colours, tonal step wedges and QR code elements of graded module size. All samples were printed in a single production run using the standard machine settings in KCMY mode, without an opaque white underprint layer, so that the interaction between the ink and the bare biopolymer surface — rather than between the ink and an interme-

Table 1

List of investigated samples and flat-die extrusion processing parameters

Sample	T zone 1 (°C)	T zone 2 (°C)	T zone 3 (°C)	Screw speed (rpm)	Calender speed (m/min)
PLA15	165	170	175	90	2
PLA16 *	165	170	175	90	2
PHB10	160	165	170	50	1
PHB20	160	165	170	50	1
PHB30	165	170	175	100	2
PBS10	165	170	175	100	2
PBS20	165	170	175	100	2
PHBV10	165	170	175	100	2
PHBV20	165	170	175	100	2
PHBV30	165	170	175	100	2

* Processed without cooling the calender. Sample designation: the numerical suffix denotes the nominal mass fraction (wt%) of the second component in the PLA-based blend; PLA15 and PLA16 are neat PLA films

diate primer — determined the print result. Curing was performed by the integrated UV lamp assembly of the press under nominal settings. Printed films were conditioned for 24h at room temperature before measurement to allow complete dark cure and relaxation of the ink film.

2.5. Optical density and colorimetric measurement

Optical density (D) and CIELAB coordinates (L*, a*, b*) of the full-tone black patches were measured with a Techkon SpectroDens spectrodensitometer. The instrument was calibrated on absolute white before each measurement series. Measurements were carried out using the CIE standard illuminant D50 and the CIE 1931 2° standard observer. Five independent measurements were taken at different positions of each printed patch, giving fifty readings in total, and the results are reported as arithmetic mean ± standard deviation. Measuring at several positions was considered essential, because extruded biopolymer films may exhibit a pronounced micro-relief and machine-direction line structure that can locally modify the measurement geometry; as shown in Section 3.5, this precaution proved decisive for the interpretation of the results.

Surface appearance of the printed films was additionally inspected with a VT300 digital portable microscope. Machine readability of the printed QR codes was verified using two commercially available mobile devices with different camera systems and decoding libraries — an Apple iPhone 15 (iOS) and a Xiaomi Redmi Note 10 Pro (Android) — each code being tested on both devices under diffuse office illumination.

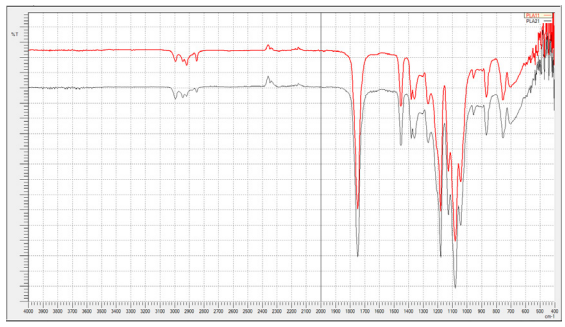
2.6. Evaluation of colour differences and statistical analysis

Total colour differences between printed samples were calculated according to the CIE 1976 colour difference formula. Because the CIE 1976 (ΔE76) metric is known to overstate lightness differences in dark colours, all pairwise differences were additionally recalculated in the CIEDE2000 metric (ΔE00), using the standard parametric weighting factors kL = kC = kH = 1. Chroma and hue angle were derived as $C^*ab = (a^{*2} + b^{*2})1/2$ and hab = arctan(b*/a*). In the interpretation of the results, the conventional perceptibility threshold of ΔE ≈ 1 for a trained observer under optimal viewing conditions and the acceptability threshold of ΔE ≈ 3 for commercial print reproduction were used as reference levels. The statistical significance of differences among the ten samples was assessed by one-way analysis of variance (ANOVA) applied separately to D, L*, a* and b*, followed by Welch's t-test for selected pairwise comparisons. The relationship between optical density and lightness was examined by Pearson correlation, both across sample means and across all fifty individual readings. A significance level of α = 0.05 was adopted throughout. All calculations were performed on the complete set of individual measurements rather than on pre-aggregated values.

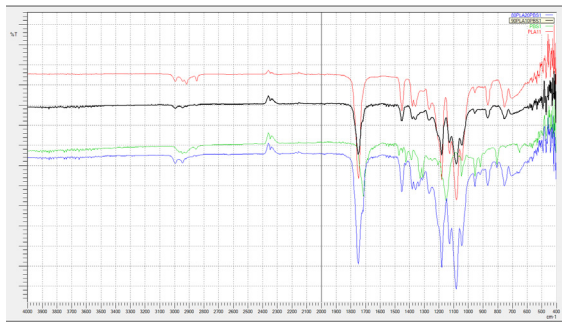
3. Results and discussion

3.1. FTIR analysis — confirmation of physical blending

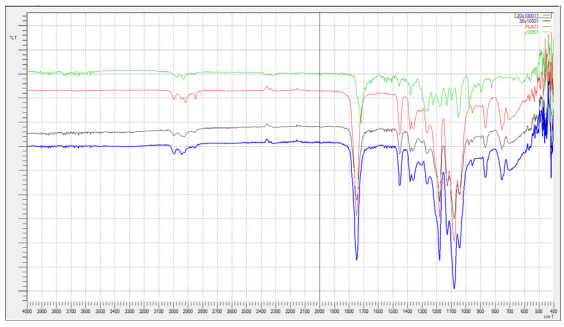
FTIR spectra of all samples showed no chemical reaction between PLA and other biopolymers in the blend, since no new peaks occurred in the spectra. Comparison of the FTIR spectra between pure components and blends is shown in Figure 1.



(a)

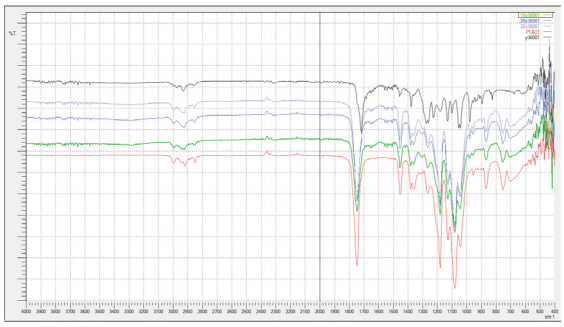


(b)



(c)

» **Figure 1 (part 1):** *FTIR Spectra of pure components and blends (a) PLA1-PLA2, (b) PBS-based series of samples, (c) PHBV-based series of samples and (d) PHB-based series of samples*



(d)

» **Figure 1 (part 2):** *FTIR Spectra of pure components and blends (a) PLA1-PLA2, (b) PBS-based series of samples, (c) PHBV-based series of samples and (d) PHB-based series of samples*

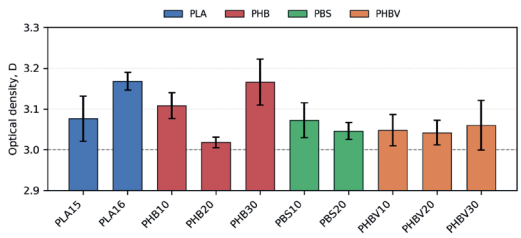
3.2. Optical density of the printed films

The measured optical density and CIELAB coodinates of the full-tone black UV inkjet prints are summarized in Table 2; the corresponding distributions are shown in Figures 2 and 3.

Optical density proved to be uniformly high on every substrate. All fifty individual readings fell between D = 3.00 and D = 3.20, and the sample means occupied the narrow interval 3.018–3.168 with a grand mean of 3.080. An optical density above 3.0 corresponds to transmission of less than 0.1% of the incident light through the printed layer, indicating excellent ink holdout and complete coverage on all ten films. Not a single measurement position on any formulation failed to reach this level.

Within this narrow band the differences between samples are nevertheless statistically significant (ANOVA: $F(9,40) = 8.16$; $p < 0.001$). The highest densities were recorded on PLA16 (3.168 ± 0.022) and PHB30 (3.166 ± 0.056) and the lowest on PHB20 (3.018 ± 0.013). The total spread of 0.15 density units is small in absolute terms, but it is not negligible by the standards of process control in commercial printing, where full-tone density tolerances of ±0.05–0.10 are typical. Substrate selection therefore has a measurable, if modest, influence on solid density and should be considered when a common density target is applied across several film types.

It is notable that the ranking of densities does not follow the mass fraction of the second component in any of the three blend families. Within the PHB series the density falls from 3.108 at 10 wt% to 3.018 at 20 wt% and then rises to 3.166 at 30 wt%; within the PHBV series it varies by only 0.018 units across the whole concentration range. Composition alone therefore does not explain the observed behavior, which points instead to the processing conditions and the resulting surface state of the film — an interpretation developed further in Sections 3.3 and 3.5.



» **Figure 2:** *Optical density (D, mean ± SD, n = 5) of full-tone black UV inkjet prints on the investigated biopolymer films. The dashed line marks D = 3.0*

3.3. Lightness of the printed films

Lightness is by far the most variable of the measured quantities. The sample means span L* = 13.32–24.96, a range of 11.65 units, and the individual readings extend from 12.90 to 26.82. The differences between formulations are highly significant (ANOVA: $F(9,40) = 14.35$; $p < 0.001$). PHB30 produced the visually deepest black of the study (13.32 ± 0.66), followed by PLA16 (15.68 ± 0.44), while PBS20 gave by far the lightest result

Table 2

Optical density and CIELAB coordinates of full-tone black UV inkjet prints on the investigated biopolymer films (mean ± SD, n = 5)

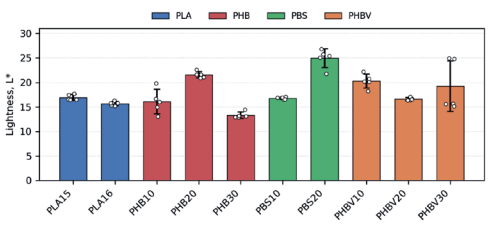
Sample	D	L*	a*	b*
PLA15	3.076 ± 0.055	16.93 ± 0.60	1.65 ± 0.15	−0.47 ± 0.26
PLA16	3.168 ± 0.022	15.68 ± 0.44	1.62 ± 0.10	−0.71 ± 0.14
PHB10	3.108 ± 0.032	16.11 ± 2.50	1.71 ± 0.10	−0.33 ± 0.23
PHB20	3.018 ± 0.013	21.57 ± 0.65	1.97 ± 0.10	−0.32 ± 0.18
PHB30	3.166 ± 0.056	13.32 ± 0.66	1.80 ± 0.47	−0.67 ± 0.61
PBS10	3.072 ± 0.043	16.79 ± 0.25	1.63 ± 0.21	−0.71 ± 0.14
PBS20	3.046 ± 0.021	24.96 ± 1.91	1.84 ± 0.19	−0.77 ± 0.09
PHBV10	3.048 ± 0.038	20.30 ± 1.42	1.82 ± 0.06	−0.53 ± 0.06
PHBV20	3.042 ± 0.030	16.61 ± 0.30	1.76 ± 0.19	−0.49 ± 0.30
PHBV30	3.060 ± 0.061	19.23 ± 5.15	1.75 ± 0.17	−0.58 ± 0.22

(24.96 ± 1.91), with PHB20 (21.57 ± 0.65) and PHBV10 (20.30 ± 1.42) also at the light end of the scale.

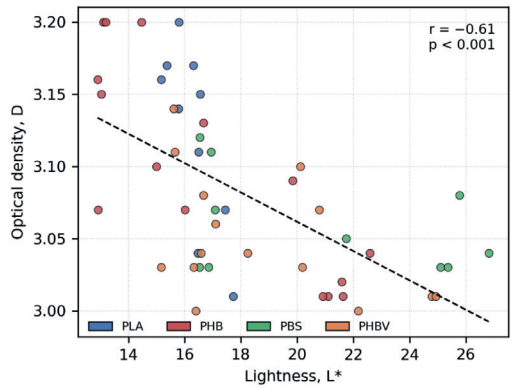
Critically, lightness does not vary monotonically with the concentration of the second blend component in any of the three families. In the PHB series L* rises from 16.11 at 10 wt% to 21.57 at 20 wt% and then falls sharply to 13.32 at 30 wt%, a non-monotonic excursion of more than eight units. In the PHBV series the sequence is 20.30 → 16.61 → 19.23, again with the intermediate concentration as the extreme value. Only the PBS series shows a simple increase, from 16.79 to 24.96. If the mass fraction of the minor phase were the controlling variable, a consistent and preferably monotonic trend would be expected in each family; its absence indicates that composition is not the dominant factor.

Two other observations support this conclusion. First, the two neat PLA films differ significantly from one another (L* = 16.93 ± 0.60 versus 15.68 ± 0.44; Welch's t = 3.74; p = 0.007), even though they are chemically identical and were extruded at the same temperatures and screw speed. The only difference between them is that PLA16 was processed without calender cooling. A change in the cooling regime, which alters the degree of crystallinity, the surface gloss and the micro-topography of the film without altering its chemistry, is therefore sufficient to shift measured lightness by more than one unit and to raise optical density by 0.09. Second, the two samples extruded at the reduced calender speed of 1 m/min (PHB10 and PHB20) behave very differently from one another, which again cannot be attributed to composition alone.

Lightness and optical density are strongly and inversely correlated, as physical consistency requires: r = −0.73 (p = 0.016) across the ten sample means and r = −0.61 (p < 0.001) across all fifty individual readings (Figure 4). Darker prints return higher density readings, and the two quantities respond to the same underlying property of the printed surface. This internal consistency provides useful validation of the measurement series, but it also means that the two parameters should not be treated as independent indicators of print quality.



» **Figure 3:** *Lightness (L*, mean ± SD, n = 5) of full-tone black UV inkjet prints on the investigated biopolymer films. Open circles show the five individual measurement positions per sample; note the two clearly separated populations of readings for PHBV30 and the wide spread for PHB10*



» **Figure 4:** *Relationship between lightness and optical density for all fifty individual measurements. The dashed line is the least-squares fit*

3.4. Chromatic coordinates

In sharp contrast to lightness, the chromatic coordinates are statistically indistinguishable across the entire material set. One-way ANOVA returns no significant effect of formulation either for a* (F(9,40) = 1.42; p = 0.21) or for b* (F(9,40) = 1.81; p = 0.10). The sample means are confined to a* = 1.62–1.97 and b* = −0.77 to −0.32, corresponding to chroma values of only C*ab = 1.71–2.00 and hue angles clustered between 336° and 351°. Every substrate therefore reproduces the full-tone black as an almost achromatic colour with a very slight warm-red cast and a marginal blue bias.

This is the central positive finding of the study for print production. The chemistry of the second blend component and its concentration do not measurably affect the hue or the saturation of the reproduced black. Where a difference appears at all, it is a difference in how light or dark the print is, not in what colour it is. Since colour management systems compensate for lightness far more readily than for hue shifts — a lightness offset can be corrected by a single adjustment of the tone reproduction curve, whereas a hue shift requires re-profiling — this behavior is considerably more favorable than the opposite pattern would be.

Nominally, the PBS-based films display the most negative b* values of the set (−0.71 and −0.77) and the PHB-based films at 10 and 20 wt% the least negative (−0.33 and −0.32), which would correspond to a marginally cooler black on PBS and a marginally warmer one on PHB. However, the within-sample standard deviations of b* are of the same order as these differences, reaching 0.61 for PHB30 and 0.30 for PHBV20, and the effect does not survive the analysis of variance. It should therefore be regarded as a tendency worth confirming in a larger series rather than as an established difference.

3.5. Surface texture and the reliability of the colorimetric data

The within-sample variability differs by more than an order of magnitude between formulations and deserves attention. The standard deviation of L* ranges from 0.25 for PBS10 and 0.30 for PHBV20 — values close to the repeatability of the instrument — to 1.91 for PBS20, 2.50 for PHB10 and 5.15 for PHBV30. Expressed as a coefficient of variation, the spread reaches 26.8% for PHBV30 and 15.5% for PHB10, against 1.5% for PBS10.

The pattern of the individual readings is more revealing than the summary statistics. For PHBV30 the five measurement positions returned L* values of 15.16, 15.61, 15.65, 24.79 and 24.93: two tightly grouped populations separated by more than nine lightness units, with no intermediate values. The arithmetic mean of 19.23 corresponds to no physical location on the sample, and the median of 15.65 differs from it by 3.58 units. A comparable, though less extreme, dispersion is seen for PHB10, where the readings range from 13.03 to 19.84. Such bimodality cannot arise from the colour of a homogeneously printed ink layer; it indicates that the measuring aperture encountered two distinct surface states on the same specimen.

Microscopic inspection of these films showed pronounced machine-direction lines and a distinct micro-relief. Surface structure of this kind alters the local measurement geometry: depending on the orientation of the relief relative to the measuring beam, the aperture may collect an increased specular component or, conversely, fall within a locally shaded region. The instrument registers both cases as a change in lightness. Part of the apparent colour difference between textured samples is therefore of instrumental rather than colorimetric origin, whereas the human visual system, which integrates over a larger field and compensates for surface gradients, does not perceive a comparable difference. This mechanism also explains why the samples with the smoothest measured behavior (PBS10, PHBV20) are those with the lowest dispersion, and why formulation alone fails to account for the lightness ranking discussed in Section 3.3.

Three practical consequences follow. Spectrophotometric data on textured biodegradable films should be acquired at several positions sufficient to reveal multimodality — five is a workable minimum, but more are advisable for visibly structured surfaces — and the individual readings, not only the mean, should be inspected. Where the distribution is clearly bimodal, the median or a mode-resolved analysis is more informative than the arithmetic mean. Finally, instrumental results on such substrates should be corroborated by visual assessment before a batch is rejected on colorimetric grounds.

3.6. Total colour differences

The complete matrix of total colour differences calculated according to Eq. (1) is given in Table 3 and visualized in Figure 5; the corresponding CIEDE2000 values are given in Table 4.

The largest difference in the set, ΔE*ab = 11.65, separates PHB30 from PBS20 — the darkest and the lightest formulation. Nine of the forty-five pairwise comparisons exceed 5 units and would be plainly visible in a side-by-side presentation. At the other extreme, the closest pairs are PLA15–PBS10 (0.28), PBS10–PHBV20 (0.31) and PLA15–PHBV20 (0.34), all well below the perceptibility threshold, showing that films of quite different chemical composition can be colorimetrically interchangeable.

Unlike in a conventional substrate series, the differences do not organize themselves by polymer family. Within the PHB series the three concentrations differ by 2.81 to 8.26 units, and the two PBS films differ by 8.18 units, whereas members of different families may be nearly identical. In every case the difference is dominated by ΔL*: the chromatic contributions Δa* and Δb* never exceed 0.5 units and typically contribute less than 2% to the value of Eq. (1). Expressed differently, Table 3 is essentially a map of lightness differences, and in view

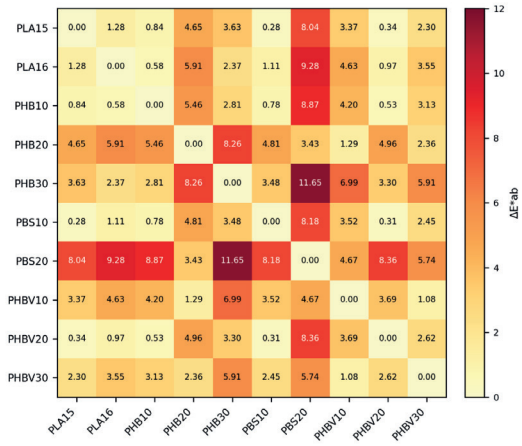
Table 3

Matrix of total colour differences ΔE*ab (CIE 1976) between all pairs of printed biopolymer films

	PLA15	PLA16	PHB10	PHB20	PHB30	PBS10	PBS20	PHBV10	PHBV20	PHBV30
PLA15	0.00	1.28	0.84	4.65	3.63	0.28	8.04	3.37	0.34	2.30
PLA16	1.28	0.00	0.58	5.91	2.37	1.11	9.28	4.63	0.97	3.55
PHB10	0.84	0.58	0.00	5.46	2.81	0.78	8.87	4.20	0.53	3.13
PHB20	4.65	5.91	5.46	0.00	8.26	4.81	3.43	1.29	4.96	2.36
PHB30	3.63	2.37	2.81	8.26	0.00	3.48	11.65	6.99	3.30	5.91
PBS10	0.28	1.11	0.78	4.81	3.48	0.00	8.18	3.52	0.31	2.45
PBS20	8.04	9.28	8.87	3.43	11.65	8.18	0.00	4.67	8.36	5.74
PHBV10	3.37	4.63	4.20	1.29	6.99	3.52	4.67	0.00	3.69	1.08
PHBV20	0.34	0.97	0.53	4.96	3.30	0.31	8.36	3.69	0.00	2.62
PHBV30	2.30	3.55	3.13	2.36	5.91	2.45	5.74	1.08	2.62	0.00

of Section 3.5 a substantial part of those differences reflects surface texture rather than the print itself.

This interpretation is reinforced by the CIEDE2000 recalculation. The CIE 1976 metric is known to exaggerate lightness differences in dark colours, where the lightness weighting function of CIEDE2000 takes values around 1.5. Recalculating in ΔE00 reduces the maximum difference from 11.65 to 7.99, the PHB20–PHB30 difference from 8.26 to 5.57, and the PBS10–PBS20 difference from 8.18 to 5.72 — a systematic reduction of roughly 30% for the lightness-driven pairs, while the already small chromatic differences are essentially unchanged (PLA15–PBS10: 0.28 versus 0.25). The choice of colour difference metric therefore has a material effect on the conclusions, and reporting ΔE*ab alone overstates the magnitude of the substrate effect for dark tones.



» **Figure 5:** *Heat map of the total colour differences ΔE*ab between all pairs of printed biopolymer films.*

3.7. Print–substrate contrast and functional readability

For printed packaging the decisive criterion is frequently not the absolute colour of the ink but the contrast it forms with the unprinted substrate, because this contrast governs the legibility of text and the machine readability of coded graphic elements. Measured against the white backing (L* = 95.84, a* = 1.94, b* = −3.60), the full-tone black prints yield total colour differences of ΔE*ab = 70.9–82.6. The spread of some twelve units across the material set, though it mirrors the lightness differences discussed above, is negligible relative to the absolute contrast achieved: the weakest-contrast substrate, PBS20, still delivers ΔE*ab = 70.9.

Consistent with this, all printed QR codes were decoded successfully on every substrate, using both test devices and both operating systems, and across the full range of module sizes present on the test chart. Neither the choice of the second blend component nor its mass fraction, nor the calender cooling regime, impaired the machine readability of the printed elements. The uniformly high optical density (every reading above D = 3.0) provides the luminance contrast required by the decoding algorithms with a substantial margin, and differences of ten lightness units in a colour whose L* is below 25 are immaterial at this scale.

Taken together with the FTIR results, these findings show that the functional performance of the print is decoupled from the formulation of the film within the composition range studied. Blend composition can therefore be selected based on mechanical, thermal and barrier requirements, or of cost and end-of-life considerations, without a penalty in functional printability.

Table 4

Matrix of total colour differences ΔE00 between all pairs of printed biopolymer films

	PLA15	PLA16	PHB10	PHB20	PHB30	PBS10	PBS20	PHBV10	PHBV20	PHBV30
PLA15	0.00	0.87	0.57	3.21	2.40	0.25	5.63	2.31	0.27	1.57
PLA16	0.87	0.00	0.48	4.06	1.57	0.74	6.45	3.15	0.68	2.40
PHB10	0.57	0.48	0.00	3.75	1.86	0.59	6.18	2.86	0.37	2.12
PHB20	3.21	4.06	3.75	0.00	5.57	3.33	2.48	0.93	3.41	1.67
PHB30	2.40	1.57	1.86	5.57	0.00	2.30	7.99	4.68	2.17	3.94
PBS10	0.25	0.74	0.59	3.33	2.30	0.00	5.72	2.41	0.30	1.67
PBS20	5.63	6.45	6.18	2.48	7.99	5.72	0.00	3.33	5.84	4.06
PHBV10	2.31	3.15	2.86	0.93	4.68	2.41	3.33	0.00	2.51	0.75
PHBV20	0.27	0.68	0.37	3.41	2.17	0.30	5.84	2.51	0.00	1.77
PHBV30	1.57	2.40	2.12	1.67	3.94	1.67	4.06	0.75	1.77	0.00

3.8. Practical implications and limitations

Several recommendations follow production practice. Where the deepest possible black is required — for high-contrast codes or fine reversed-out typography — PHB30 and the uncooled PLA16 are the preferred substrates, combining the lowest lightness with the highest optical density. Where colour consistency across several substrates is the priority, PLA15, PBS10 and PHBV20 form a group that is mutually interchangeable within the perceptibility threshold and can be run to a single colour standard. Where a film with visible surface structure must be used, the quality-control protocol should be adapted as described in Section 3.5 rather than the material being rejected based on a single measurement. In all cases, the chromatic dimensions require no attention: hue and saturation are stable across the entire material set.

Several limitations should be acknowledged. The study evaluated a single UV inkjet system under standard settings and without an opaque white underprint; other ink chemistries, curing configurations or the introduction of a white base layer would be expected to shift the absolute values, although the relative behavior of the substrates should be preserved. Only full-tone black was analyzed in depth, so tonal reproduction, dot gain and the behavior of the chromatic process inks remain to be characterized. Five measurement positions per sample proved sufficient to reveal multimodality but are too few to characterize the underlying distributions quantitatively; a denser sampling grid, ideally combined with profilometric mapping of the same positions, is the obvious next step and would allow the contribution of surface relief to be separated from that of the print. Surface free energy, roughness and ink adhesion were not measured, which limits the mechanistic interpretation of the differences between formulations. Finally, the prints were evaluated shortly after production, so the long-term stability of the ink film on biodegradable substrates — including light fastness, mechanical resistance and behavior during composting — was outside the scope of this work.

4. Conclusions

This study evaluated the UV inkjet printability of ten biodegradable films produced by flat-die extrusion: neat PLA processed with and without calender cooling, and PLA blends containing 10–30 wt% of PHB, PHBV or PBS. The following conclusions can be drawn.

FTIR spectroscopy confirmed that single-pass flat-die extrusion produced physical blends only. No new absorption bands appeared, and no bands of the neat components disappeared, so the optical behavior of the films reflects their phase morphology and surface topography rather than any newly formed chemical structure.

All ten substrates delivered high optical density of the full-tone black print. Every one of the fifty individual readings exceeded D = 3.00, and the sample means occupied the interval 3.018–3.168, indicating excellent ink holdout on all formulations.

Colour reproduction was consistent in the chromatic dimensions. Neither a* ($p = 0.21$) nor b* ($p = 0.10$) differed significantly between formulations; all prints remained confined to a near-neutral region with C*ab = 1.71–2.00 and hue angles between 336° and 351°. The identity and concentration of the second blend component do not affect the hue or saturation of the reproduced black.

Lightness, by contrast, varied significantly between formulations (L* = 13.32–24.96; $p < 0.001$) and was inversely correlated with optical density ($r = -0.61$ across all readings; $p < 0.001$). The variation was not monotonic with the concentration of the second component, and the two chemically identical neat PLA films differed significantly from one another, which shows that processing conditions — in particular the calender cooling regime — and the resulting surface state, rather than blend composition alone, govern this parameter.

Surface texture was shown to contribute substantially to the measured variability. Within-sample standard deviations of L* ranged from 0.25 to 5.15, and PHBV30 returned two clearly separated populations of readings differing by more than nine lightness units. Spectrophotometric evaluation of structured biodegradable films must therefore be based on multiple measurement positions, on inspection of the individual readings rather than the mean alone, and on corroboration by visual assessment.

Total colour differences reached ΔE*ab = 11.65 at most and were dominated almost entirely by lightness, the chromatic contributions never exceeding 0.5 units. Recalculation in the CIEDE2000 metric reduced the lightness-driven differences by approximately 30% (maximum ΔE00 = 7.99), confirming that the CIE 1976 formula overstates the substrate effect for dark tones and that ΔE00 should be preferred when evaluating black prints on such materials.

Print–substrate contrast reached ΔE*ab = 70.9–82.6 on every film, and all printed QR codes were decoded successfully on two independent mobile platforms, confirming that functional graphic elements are reproduced reliably on all the biopolymer films investigated.

Overall, PLA-based biodegradable films and their blends with PBS, PHB and PHBV exhibit promising printability for UV inkjet technology while retaining their chemical integrity after processing. Blend composition can be optimized for mechanical, barrier and end-of-life performance without compromising the chromatic consistency

of the print or the functionality of machine-readable elements, provided that the lightness of the reproduction and the surface texture of the film are controlled at the process level. These results contribute to the development of sustainable printed products and provide a basis for further optimization of biodegradable substrates intended for graphic and packaging applications.

5. Acknowledgments

This research has been supported by the Ministry of Science, Technological Development and Innovation (Contract No. 451-03-34/2026-03/200156) and the Faculty of Technical Sciences, University of Novi Sad through project "Scientific and Artistic Research Work of Researchers in Teaching and Associate Positions at the Faculty of Technical Sciences, University of Novi Sad 2026" (No. 01-3609/1).

6. References

Ali, W., Ali, H., Gillani, S., Zinck, P. and Souissi, S. (2023) 'Polylactic acid synthesis, biodegradability, conversion to microplastics and toxicity: A review', *Environmental Chemistry Letters*, 21(3), pp. 1761–1786. DOI: 10.1007/s10311-023-01564-8

Chuakhao, S., Rodríguez, J.T., Lapnonkawow, S., Kannan, G., Müller, A.J. and Suttiruengwong, S. (2024) 'Formulating PBS/PLA/PBAT blends for biodegradable, compostable packaging: The crucial roles of PBS content and reactive extrusion', *Polymer Testing*, 132, 108383. DOI: 10.1016/j.polymertesting.2024.108383

Izdebska-Podsiadły, J. (2021) 'Effect of plasma surface modification on print quality of biodegradable PLA films', *Applied Sciences*, 11(17), 8245. DOI: 10.3390/app11178245

Jacobson, J., Keif, M., Rong, X., Singh, J. and Vorst, K. (2009) 'Flexography printing performance of PLA film', *Journal of Applied Packaging Research*, 3(2), pp. 91–104.

Kováčik, D., Fleischer, M., Tučeková, Z., Baťková, E. and Kolářová, T. (2024) 'Plasma treatment of large-area polymer substrates for the enhanced adhesion of UV–digital printing', *Nanomaterials*, 14(5), 426. DOI: 10.3390/nano14050426

Kricheldorf, H.R. (2005) 'Polylactic acid'. In: Handbook of Polymer Synthesis. Volume 2. New York, NY: Marcel Dekker, pp. 347–370.

Mahović Poljaček, S., Tomašegović, T. and Priselac, D. (2026) 'Toward sustainable printed packaging: Surface properties and ink adhesion behavior of PLA/PCL/nanosilica biopolymer blends', *Polymers*, 18(3), 422. DOI: 10.3390/polym18030422

Maňúrová, K., Preklet, E. and Horváth, C. (2021) 'Investigation of printable color gamut in digital printing on biodegradable flexible packaging materials'. In: *Proceedings of the 2nd International Conference on Circular Packaging, 9–10 September 2021, Slovenj Gradec, Slovenia*.

Omaníková, L., Bočkaj, J., Černák, M., Plavec, R., Feranc, J. and Jurkovič, P. (2020) 'Influence of composition and plasma power on properties of film from biodegradable polymer blends', *Polymers*, 12(7), 1592. DOI: 10.3390/polym12071592

Patel, M.K., Zaccone, M., De Brauwer, L., Nair, R., Monti, M., Martinez-Nogues, V., Frache, A. and Oksman, K. (2022) 'Improvement of poly(lactic acid)–poly(hydroxy butyrate) blend properties for use in food packaging: Processing, structure relationships', *Polymers*, 14(23), 5104. DOI: 10.3390/polym14235104

Rong, X. and Keif, M. (2007) 'A study of PLA printability with flexography'. In: *TAGA Proceedings, 2007 Technical Association of the Graphic Arts Annual Technical Conference*, pp. 605–613.

Taib, S.M., Taib, N.M., Rahmat, A.R. and Adam, N.M. (2024) 'A review on bio-based polymer polylactic acid potential on sustainable food packaging', *Food Science and Biotechnology*, 33(2), pp. 307–328. DOI: 10.1007/s10068-024-01543-x

Tubio, C.R., Valle, X., Carvalho, E., Moreira, J., Costa, P., Correia, D.M. and Lanceros-Mendez, S. (2023) 'Poly(3-hydroxybutyrate-co-3-hydroxyvalerate) blends with poly(caprolactone) and poly(-lactic acid): A comparative study', *Polymers*, 15(23), 4566. DOI: 10.3390/polym15234566



© 2026 Authors. Published by the University of Novi Sad, Faculty of Technical Sciences, Department of Graphic Engineering and Design. This article is an open access article distributed under the terms and conditions of the Creative Commons Attribution license 4.0 Serbia (http://creativecommons.org/licenses/by/4.0/rs/).

Original Scientific Paper https://doi.org/10.24867/GRID-2026-p20

Latent Reference Patterns for Geometric Drift Detection in the Printing Process

ABSTRACT

Geometric drift in the printing process can alter the position and orientation of graphic elements, degrading print quality and reducing the reliability of print inspection. Timely detection of such deviations is essential for maintaining process stability and ensuring consistent product quality. This study investigates latent reference patterns for detecting translational and rotational drift. The objective was to determine whether a non-periodic spatial arrangement of reference elements can reliably estimate pattern position and orientation and serve as a reference structure for geometric drift detection. Latent reference patterns were generated as binary point structures using Bridson's Poisson disk sampling algorithm. Poisson disk sampling was selected to produce a non-periodic spatial configuration with a controlled minimum separation distance between reference elements, reducing the likelihood of ambiguous geometric correspondences during geometric registration. The centers of the circular reference elements were generated pseudo-randomly subject to a predefined minimum separation distance, while the domain dimensions and generation parameters remained constant, making the spatial arrangement of the reference elements the only variable. Two-dimensional rigid geometric transformations were applied to the generated patterns. Translation was modeled by displacement components Δx and Δy, each varied from −10 px to +10 px in 1 px increments, while rotation was modeled by a rotation matrix about the pattern center over the range from −5° to +5° in 0.5° increments. A transformed latent reference pattern was generated for each translation-rotation combination, forming a dataset of simulated geometric deviations. The original and transformed configurations were compared by estimating the translation and rotation that produce optimal geometric alignment of the corresponding reference elements through minimization of the mean squared coordinate error. The estimated transformation parameters were compared with the prescribed values, and absolute estimation errors were calculated. The results demonstrated that the non-periodic spatial configuration of the latent reference pattern enables reliable estimation of translational and rotational drift within the investigated transformation range. These findings support the use of latent reference patterns as reference structures for developing automated geometric drift detection methods under simulated geometric conditions relevant to the printing process.

Diana Bratić
Denis Jurečić
Suzana Pasanec Preprotić
Gorana Petković

University of Zagreb,
Faculty of Graphic Arts,
Zagreb, Croatia

KEY WORDS

Geometric drift, latent reference patterns, Poisson disk sampling, geometric registration, printing process

1. Introduction

Geometric stability of the printed image is an important factor in maintaining consistent print process quality. Changes in the position and orientation of graphic elements can cause register deviations, alter their relative positions, and affect the reliability of automated quality inspection. Such deviations can occur at different stages of reproduction, and their characteristics depend on the printing technology used. In electrophotographic printing, individual devices have been shown to introduce characteristic geometric distortions during reproduction that can be extracted from the printed image and used as a geometric signature of the device (Bulan, 2009). In continuous roll-to-roll processes, register deviations are also associated with the dynamics of substrate transport and changes in material speed and tension, making their detection and compensation important for process control (Chen, Shan & Zhang, 2025).

The development of machine vision systems has enabled quantitative measurement of geometric deviations based on the positions of elements extracted from captured images. In printed electronics, methods for determining register errors have been developed that combine image processing, edge detection of control marks, and mathematical estimation of their positions. These methods have enabled register deviations to be determined with subpixel accuracy (Zhang et al., 2024). Models have also been developed for roll-to-roll printing systems that relate printing and material transport parameters to the occurrence of register errors (Gafurov et al., 2024). Regardless of the detection method used, determining geometric changes requires a reference structure against which changes in position can be measured.

Geometric drift detection can be considered as a registration problem between two geometric configurations. Registration is the process of spatially aligning different representations of the same structure and is applied in various areas of image processing and computer vision (Cocianu, Uscatu & Stan, 2023). In point set registration, a spatial transformation is determined to align one set of coordinates with another, with point correspondence and transformation parameter estimation representing the main components of the procedure (Pei et al., 2023). In a rigid two-dimensional transformation, the geometric relationships within the configuration remain unchanged, while its position and orientation change. Such a change can be described by horizontal and vertical translation and rotation.

By using a larger number of spatially distributed reference elements, geometric information was not limited to the position of a single registration mark but was contained in the configuration as a whole. Spatial relationships between points have been used in point set registration methods to determine the alignment between different configurations (de Sousa & Kropatsch, 2015; Pei et al., 2023). On this basis, Poisson disk sampling was applied in this study to generate a non-periodic reference structure whose position and orientation could be tracked based on the coordinates of its elements.

Such a structure was considered as a latent geometric reference that differed from a single registration mark. Information about the geometric state was distributed across multiple elements that together formed a non-periodic spatial configuration. Changes in the position and orientation of the structure could therefore be determined by comparing the original and transformed configurations. This enabled the evaluation of a non-periodic pattern as a reference structure for determining rigid geometric drift.

The basic case of this approach was investigated under controlled simulation conditions. The reference pattern was generated as a binary structure of circular elements whose centers were pseudo-randomly distributed using Poisson disk sampling with a defined minimum separation distance. Known horizontal and vertical translations ranging from –10 to +10 pixels were applied to the original configuration in one-pixel increments. Rotation about the pattern center was applied over the range from –5° to +5° in 0.5° increments. For each combination of transformation parameters, translation and rotation were estimated, and the estimated values were then compared with the prescribed values.

The objective of this study was to determine whether a non-periodic latent reference pattern generated using Poisson disk sampling could enable reliable estimation of translational and rotational drift within the defined transformation range. The study was limited to rigid transformations and controlled simulation conditions to investigate the geometric basis of the proposed approach without the influence of additional image degradation and more complex geometric deformations.

The working hypothesis was that a non-periodic spatial configuration of reference elements generated with a controlled minimum separation distance contains sufficient geometric information for reliable estimation of translational and rotational drift within the defined transformation range.

2. Methodology

The study was conducted as a controlled computational experiment to investigate the use of a non-periodic latent reference structure for estimating rigid geometric drift. The use of predefined input parameters enabled systematic evaluation of the simulation model under controlled conditions (Kleijnen, 2008). The procedure included generation of the original reference pattern,

application of known translational and rotational transformations, estimation of the transformation parameters, and comparison of the estimated and prescribed values.

The reference pattern generation parameters were kept constant throughout the experiment, while the rigid transformation parameters were systematically varied. This enabled direct evaluation of the accuracy of translation and rotation estimation under controlled simulation conditions.

2.1. Generation of the latent reference pattern

The latent reference pattern was generated as a two-dimensional non-periodic configuration of circular elements. The positions of their centers were determined using Bridson's Poisson disk sampling algorithm (Bridson, 2007). The pattern was generated within a rectangular domain of defined dimensions, with a predefined minimum distance between the centers of neighboring elements.

The set of image centers of the reference elements was defined as:

$$P = \left\{ \mathbf{p}_i = \begin{bmatrix} x_i \\ y_i \end{bmatrix}, \quad i = 1, \dots, N \right\} \tag{1}$$

where x_i and y_i are the coordinates of the center of the i-th reference element, and N is the total number of elements in the pattern.

The minimum allowed distance between any two different centers was defined by the following condition:

$$\left\| \mathbf{p}_i - \mathbf{p}_j \right\|_2 \geq d_{\min}, \qquad i \neq j \tag{2}$$

where d_{min} is the minimum Euclidean distance between the centers of the reference elements. This constraint prevented local clustering while maintaining a non-periodic spatial distribution.

After the coordinates were determined, a circular element of equal size was placed at each position, resulting in a binary reference pattern. The domain dimensions, minimum distance between centers, size of the circular elements, and other generation parameters were kept constant throughout the experiment.

This ensured that only the parameters of the applied geometric transformation varied between individual test cases.

2.2. Modeling of translational and rotational drift

A two-dimensional rigid transformation consisting of translation and rotation was applied to the original configuration. Translation was defined independently in the horizontal and vertical directions. The translation values Δx and Δy were varied from –10 to +10 pixels in one-pixel increments.

The translation vector was defined as:

$$\mathbf{t} = \begin{bmatrix} \Delta x \\ \Delta y \end{bmatrix} \tag{3}$$

Rotation was performed about the geometric center of the reference pattern domain. The rotation angle θ was varied from –5° to +5° in 0.5° increments. The two-dimensional rotation matrix was defined as:

$$\mathbf{R}(\theta) = \begin{bmatrix} \cos\theta & -\sin\theta \\ \sin\theta & \cos\theta \end{bmatrix} \tag{4}$$

The transformation was performed about the center of the pattern to ensure that the change in orientation did not simultaneously introduce a displacement resulting from rotation about the origin of the coordinate system. The transformed position of the i-th reference element was determined by the following expression:

$$\mathbf{q}_i = \mathbf{R}(\theta)(\mathbf{p}_i - \mathbf{c}) + \mathbf{c} + \mathbf{t} \tag{5}$$

where p_i is the original position of the reference element, q_i is its transformed position, c is the center of the pattern, R(θ) is the rotation matrix, and t is the translation vector.

For each horizontal translation value, all vertical translation and rotation values were applied. For Δx and Δy, 21 values were obtained for each parameter, while 21 values were also obtained for the rotation angle.

The total number of tested combinations of transformation parameters was:

$$N_T = 21 \times 21 \times 21 = 9261 \tag{6}$$

For each of the 9261 combinations, a transformed configuration of reference elements was obtained with known values of horizontal and vertical translation and rotation angle.

2.3. Estimation of rigid transformation parameters

The rigid transformation parameters were estimated by comparing the coordinates of the original and transformed configurations. Since the data were generated synthetically, the identity of individual reference elements was preserved after transformation. The correspondences between the original and transformed points were therefore known, allowing the analysis to focus on the estimation of the rigid transformation parameters.

For a given pair of original and transformed configurations, the transformation that provided the best alignment of the corresponding reference points was determined. The mean squared coordinate error was used as the alignment criterion. For arbitrary values of the rotation angle θ and translation vector t, the error function was defined as:

$$E(\theta, \mathbf{t}) = \frac{1}{N}\sum_{i=1}^{N} \|\mathbf{q}_i - [\mathbf{R}(\theta)(\mathbf{p}_i - \mathbf{c}) + \mathbf{c} + \mathbf{t}]\|_2^2 \quad (7)$$

The value of the function E represented the mean squared deviation between the actual positions of the transformed points and the positions obtained for the considered rigid transformation parameters. The estimated parameters were determined as the values at which this function was minimized:

$$(\hat{\theta}, \hat{\mathbf{t}}) = \arg\min_{\theta, \mathbf{t}} E(\theta, \mathbf{t}) \quad (8)$$

where θ̂ and t̂ are the estimated rotation angle and translation vector.

The minimization was not performed by iterative searching of the transformation parameter space, but by using a closed-form solution to the rigid alignment problem for corresponding point sets (Chen et al., 2024).

After centering the original and transformed configurations, a cross-covariance matrix was formed, and singular value decomposition (SVD) was performed. The optimal rotation matrix was determined from the resulting matrices, and the estimated rotation angle was calculated from this matrix. Translation was then determined from the difference between the centroids, taking the estimated rotation into account. In this way, the estimated values of $(\Delta x)\hat{}$, $(\Delta y)\hat{}$ and $\hat{\theta}$ that minimized the coordinate error between the corresponding reference elements were obtained directly for each transformed configuration.

This formulation enabled direct comparison of the estimated rigid transformation parameters with the parameters previously used to generate the transformed configuration.

2.4. Evaluation of estimation accuracy

Estimation accuracy was evaluated by comparing the estimated parameters with the known values of the applied transformation. For each of the 9261 transformations, the estimation errors for horizontal translation, vertical translation, and rotation angle were determined separately.

The absolute error of horizontal translation was determined as:

$$e_x = \left|\widehat{\Delta x} - \Delta x\right| \quad (9)$$

where $(\Delta x)\hat{}$ is the estimated value and Δx is the prescribed value of horizontal translation.

The absolute error of vertical translation was determined as:

$$e_y = \left|\widehat{\Delta y} - \Delta y\right| \quad (10)$$

where $(\Delta y)\hat{}$ is the estimated value and Δy is the prescribed value of vertical translation.

The absolute error of the rotation angle was determined as:

$$e_\theta = \left|\hat{\theta} - \theta\right| \quad (11)$$

where $\hat{\theta}$ is the estimated rotation angle and θ is the prescribed rotation angle.

In addition to the separate errors of the horizontal and vertical components, the total translation error was determined as the Euclidean distance between the prescribed and estimated translation vectors:

$$e_t = \sqrt{\left(\widehat{\Delta x} - \Delta x\right)^2 + \left(\widehat{\Delta y} - \Delta y\right)^2} \quad (12)$$

The obtained errors were analyzed across the entire set of transformations to determine the estimation accuracy within the investigated translation and rotation ranges. The results were also compared with respect to the magnitude of the prescribed displacement to determine whether the estimation error depended on the position within the investigated transformation space.

2.5. Computational implementation

The generation of the reference pattern, application of rigid transformations, estimation of transformation parameters, and error analysis were performed using Python 3.12.14. NumPy 2.3.5 was used for numerical operations, coordinate processing, and matrix calculations, including singular value decomposition. Pandas 2.2.3 was used to organize and store the results, while Matplotlib 3.10.8 was used for graphical presentation of the results (Dey, 2018).

A fixed random number generator seed (seed = 20261003) was used to generate the pseudo-random spatial configuration, ensuring reproducibility of the generated reference pattern.

For each investigated transformation, the prescribed values of Δx, Δy and θ, their estimated values, and

the corresponding errors were stored. This produced a single dataset that was used for statistical analysis and graphical presentation of the results.

3. Results

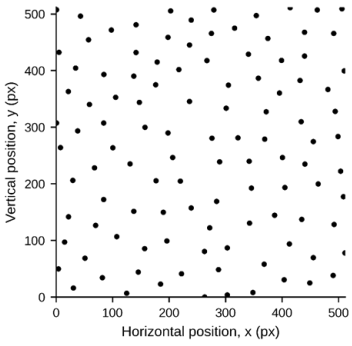
The simulation investigated the possibility of estimating rigid geometric drift parameters using a non-periodic latent reference pattern. The generated spatial arrangement of reference elements was analyzed, and the prescribed and estimated transformation parameters were compared for all defined combinations of horizontal translation, vertical translation, and rotation. Estimation accuracy was evaluated separately for the individual transformation components and for the total translational drift.

A total of 9261 combinations of rigid transformations were analyzed. This covered the entire defined transformation parameter space, including 21 values of horizontal translation, 21 values of vertical translation, and 21 values of the rotation angle. The results were analyzed using all simulated combinations, without subsequent selection or exclusion of individual cases.

3.1. Generated latent reference pattern

Poisson disk sampling was used to generate a non-periodic spatial configuration within a reference domain of 512 × 512 pixels. The minimum allowed distance between the centers of the elements was 40 pixels. With the defined generation parameters, 110 reference elements were obtained.

The spatial arrangement of the elements is shown in Figure 1. The generated configuration did not contain a regularly repeating spatial unit. At the same time, the minimum distance constraint between the centers prevented overlap and pronounced local clustering of the elements.



» **Figure 1:** *Non-periodic latent reference pattern generated using Poisson disk sampling*

Since the same reference pattern was used throughout the experiment, the spatial configuration did not represent an additional variable between individual transformations.

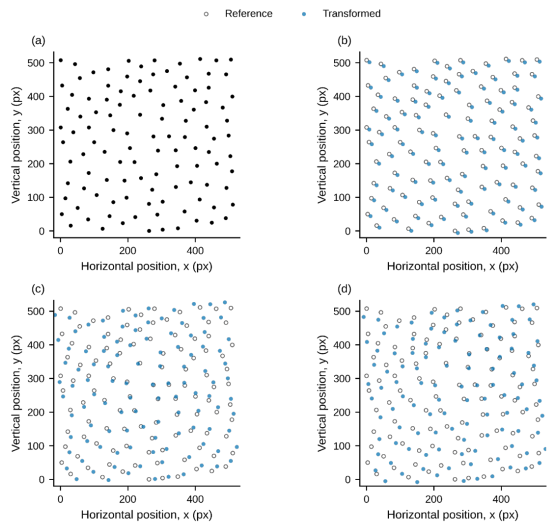
The resulting configuration provided a spatially distributed set of reference elements across the image domain, allowing the geometric state of the pattern to be represented by the configuration as a whole.

3.2. Application of rigid geometric transformations

Horizontal translation Δx, vertical translation Δy, and rotation θ about the center of the reference pattern were applied to the original configuration. Both translation components were varied independently from −10 to +10 pixels in one-pixel increments, while the rotation angle was varied from −5° to +5° in 0.5° increments.

By fully combining the prescribed values, a grid of 21 × 21 × 21, corresponding to 9261 transformations, was obtained. In this way, each horizontal translation value was tested in combination with all vertical translation and rotation values, and the same principle was applied to the remaining parameters.

Figure 2 shows representative examples of the original configuration and the translational, rotational, and combined transformations. The figure was generated from the actual coordinates used in the simulation rather than from a separately created schematic illustration. The geometric relationships between the elements were preserved in the transformed configurations because rigid transformations were applied.



» **Figure 2:** *Representative examples of rigid transformations of the latent reference pattern*

The original configuration (a), translation with $\Delta x = 8$ px and $\Delta y = -6$ px (b), rotation with $\theta = 4°$ (c), and their combination (d) are shown.

The transformed configurations preserved the relative spatial arrangement of the reference elements, while their position and orientation changed according to the prescribed transformation parameters. These examples illustrate the geometric deviations subsequently used to evaluate the estimation of translational and rotational drift.

3.3. Estimation of translational drift

The estimated values of horizontal and vertical translation were compared with the corresponding prescribed values for all 9261 transformations. Across the entire investigated range, the prescribed and estimated translation parameters showed nearly complete agreement.

For horizontal translation, the mean absolute error was 4.917×10^{-15} px, while the RMSE was 6.189×10^{-15} px. The maximum recorded absolute error of the horizontal component was 2.309×10^{-14} px. The median absolute error was 4.219×10^{-15} px.

For vertical translation, the mean absolute error was 5.933×10^{-15} px, and the RMSE was 7.428×10^{-15} px.

The maximum absolute error was 1.954×10^{-14} px, while the median was 5.329×10^{-15} px.

When the horizontal and vertical components were considered together as the total translation vector error, the mean error was 8.542×10^{-15} px. The RMSE was 9.668×10^{-15} px, and the maximum recorded value was 2.474×10^{-14} px. In 95% of the analyzed transformations, the total translation error did not exceed 1.685×10^{-14} px.

The obtained values were several orders of magnitude smaller than one pixel. The horizontal and vertical components showed the same order of error magnitude, indicating comparable estimation accuracy in both translation directions. Considering the simulation procedure, these deviations represented the numerical precision of the calculations rather than a measurable error in determining the position of the reference pattern.

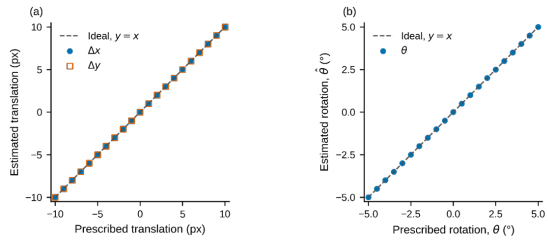
3.4. Estimation of rotational drift

The estimated rotation angle values were also compared with the prescribed values across the entire range from −5° to +5°. As with the translation components, the estimated angles agreed with the prescribed values within the numerical precision of the computational procedure.

The mean absolute error of rotation estimation was $5.973 \times 10^{-15}°$, while the RMSE was $7.329 \times 10^{-15}°$. The median absolute error was $5.773 \times 10^{-15}°$, and the maximum recorded deviation was $1.665 \times 10^{-14}°$. In 95% of the analyzed transformations, the absolute rotation error was less than or equal to $1.332 \times 10^{-14}°$.

No systematic increase in rotation error was observed toward the limits of the rotation range investigated. The estimation accuracy therefore remained comparable across both negative and positive rotation angles within the investigated range.

A comparison of the prescribed and estimated values of the translation components and rotation is shown in Figure 3. Horizontal and vertical translation are shown together, while rotation is shown separately. The estimated values agreed with the ideal relationship y = x, and the numerical deviations were not visually distinguishable at the scale shown.



» **Figure 3:** *Comparison of prescribed and estimated rigid transformation parameters*

Figure 3a shows horizontal and vertical translation, while Figure 3b shows rotation, with the dashed diagonal indicating the ideal relationship between the prescribed and estimated values.

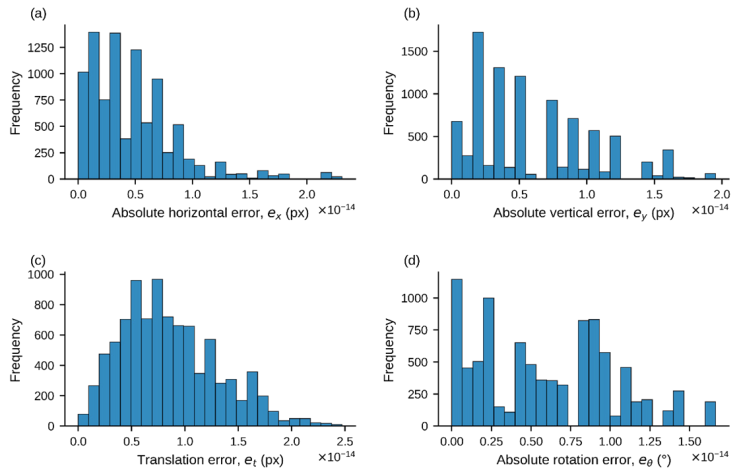
3.5. Analysis of estimation errors

Since the deviations between the prescribed and estimated parameters could not be distinguished in the direct comparison plots, the distribution of absolute errors was additionally analyzed. The results showed that all analyzed errors remained approximately within the range of 10^{-15} to 10^{-14} in the corresponding units.

The magnitude of these errors remained consistent with floating-point numerical precision across the investigated transformation parameter space. No individual transformation produced an error outside the numerical magnitude observed for the complete dataset.

The error distributions for the individual components of the rigid transformation are shown in Figure 4.

For horizontal translation (a), vertical translation (b), and total translational drift (c), the errors remained at approximately 10^{-14} px, while for rotation (d), the



» **Figure 4:** *Distribution of absolute errors in rigid transformation parameter estimation*

maximum deviation remained at approximately 10^{-14}°. Summary error metrics are presented in Table 1.

Table 1
Error metrics for rigid transformation parameter estimation

Parameter	MAE	RMSE	Maximum absolute error	95th percentile
Horizontal translation	4.917 × 10^{-15} px	6.189 × 10^{-15} px	2.309 × 10^{-14} px	1.243 × 10^{-14} px
Vertical translation	5.933 × 10^{-15} px	7.428 × 10^{-15} px	1.954 × 10^{-14} px	1.510 × 10^{-14} px
Total translation	8.542 × 10^{-15} px	9.668 × 10^{-15} px	2.474 × 10^{-14} px	1.685 × 10^{-14} px
Rotation	5.973 × 10^{-15}°	7.329 × 10^{-15}°	1.665 × 10^{-14}°	1.332 × 10^{-14}°

The obtained results showed that, for the non-periodic configuration used, it was possible to reconstruct the prescribed rigid transformation parameters across the entire investigated range of translations and rotations. Under idealized simulation conditions, no practically significant estimation error was observed. The remaining deviations corresponded to the numerical precision of the computational procedure.

4. Discussion

The study investigated the applicability of a non-periodic latent reference pattern for determining rigid geometric drift under controlled simulation conditions. The obtained results showed that the prescribed values of horizontal and vertical translation and rotation could be reconstructed across the entire investigated transformation range. For all 9261 analyzed combinations, the deviations between the prescribed and estimated values remained at the level of the numerical precision of the computational procedure.

This result should be considered in the context of the conditions under which the experiment was conducted. The transformations were applied directly to the coordinates of the reference elements, and the correspondences between the elements of the original and transformed configurations were known.

Therefore, errors on the order of 10^{-14} px for translation and 10^{-14}° for rotation did not represent the estimated accuracy that could be expected in an actual printing process. Instead, they showed that no practically significant error occurred in determining the rigid transformation within the defined mathematical model. A similar principle of evaluating registration methods using known artificially generated transformations has also been applied in previous studies of point set and image registration (Fu, Chen & Wang, 2022; Alba et al., 2015).

The results also showed that the spatial configuration of 110 reference elements contained sufficient geometric information to determine the three investigated rigid transformation parameters. Point set registration is based on determining the spatial transformation between two configurations, with point correspondence and transformation parameter estimation representing the fundamental components of the procedure (Pei et al., 2023). In this study, the latter part of the problem was considered separately from the problem of determining correspondences. Because the identity of the points was known, the results therefore confirm the possibility of estimating transformation parameters from a non-periodic configuration, but do not allow conclusions to be drawn about the effectiveness of automatically establishing correspondences between elements.

The use of Poisson disk sampling enabled the generation of a non-periodic configuration with a controlled minimum distance between elements. This type of spatial distribution has been used in various geometric data processing procedures because it enables control of local density and distances between points (Wei, 2008; Jiao et al., 2024; Comino-Trinidad, Chica & Andújar, 2023). No comparison with periodic or other non-periodic configurations was performed in this study. Therefore, the obtained results do not support the conclusion that the Poisson disk arrangement provided greater registration accuracy than other possible spatial arrangements. They only demonstrate that the investigated Poisson disk configuration enabled unambiguous estimation of the prescribed rigid transformations within the applied simulation model.

The obtained results represented the basic geometric case of drift detection. In actual machine vision systems, the positions of reference elements are determined from captured images, and the estimation may therefore be affected by image resolution, the element detection procedure, and other sources of deviation. Previous studies of registration systems in printing processes have shown that geometric deviations can be determined through image processing and analysis of the positions of control marks (Zhang et al., 2024), while in roll-to-roll processes, registration deviations are also associated with the dynamic parameters of the process and substrate transport (Chen, Shan & Zhang, 2025; Gafurov et al., 2024). These effects were not investigated in this study.

The limitations of the study therefore arose primarily from the idealized simulation model. Image degradation, errors in determining the centers of the reference elements, unknown correspondences, and nonlinear geometric deformations were not included. In addition, only one generated spatial configuration was investigated using constant Poisson disk sampling parameters. Therefore, the results did not represent an assessment of the robustness of the proposed approach under actual printing conditions, but rather a verification of its basic geometric feasibility.

Despite these limitations, the obtained result provided a basis for further investigation of latent reference structures. It was confirmed that the position and orientation of the investigated non-periodic configuration could be determined from the coordinates of its elements without practically significant error under idealized simulation conditions. Future research should progressively incorporate sources of deviation characteristic of the detection procedure and the printing process and investigate the behavior of the reference structure when correspondences between elements are not known in advance.

5. Conclusion

The study investigated the use of a non-periodic latent reference pattern generated using Poisson disk sampling for determining translational and rotational geometric drift. A total of 9261 combinations of horizontal translation, vertical translation, and rotation were applied to the generated configuration of 110 reference elements. Translations were investigated over the range from −10 to +10 px, and rotation over the range from −5° to +5°.

Across the entire investigated transformation parameter space, the estimated values agreed with the prescribed values within the numerical precision of the computational procedure. The maximum total translation error was 2.474×10^{-14} px, while the maximum absolute rotation error was 1.665×10^{-14}°. These results confirmed the working hypothesis that the investigated non-periodic spatial configuration with a controlled minimum distance between reference elements contains sufficient geometric information for estimating translational and rotational drift within the defined transformation range.

The conclusion is limited to idealized simulation conditions and known correspondences between reference elements. The results therefore confirm the basic geometric feasibility of the approach rather than provide an assessment of its accuracy and robustness in an actual printing process. Future research should investigate the effects of the reference element detection procedure, unknown correspondences, and other sources of deviation that arise in the practical application of latent reference structures.

6. Acknowledgments

This paper was supported by the Financial Support of University of Zagreb “Smart systems for technical optimization of KPI indicators in sustainable graphic production”.

7. References

Alba, A., Vigueras-Gomez, J.F., Arce-Santana, E.R. and Aguilar-Ponce, R.M. (2015) 'Phase correlation with sub-pixel accuracy: A comparative study in 1D and 2D', *Computer Vision and Image Understanding*, 137, pp. 76–87. DOI: 10.1016/j.cviu.2015.03.011

Bridson, R. (2007) 'Fast Poisson Disk Sampling in Arbitrary Dimensions'. In: *ACM SIGGRAPH 2007 Sketches*. Article 22. DOI: 10.1145/1278780.1278807

Bulan, O., Mao, J. and Sharma, G. (2009) 'Geometric distortion signatures for printer identification'. In: *Proceedings of the 2009 IEEE International Conference on Acoustics, Speech and Signal Processing*, 19–24 April 2009, Taipei, Taiwan. DOI: 10.1109/ICASSP.2009.4959855

Chen, L., Feng, C., Ma, Y., Zhao, Y. and Wang, C. (2024) 'A review of rigid point cloud registration based on deep learning', *Frontiers in Neurorobotics*, 17, 1281332. DOI: 10.3389/fnbot.2023.1281332

Chen, Z., Shan, L. and Zhang, T. (2025) 'Hybrid modeling and compensation register control for the speed-up phase of roll-to-roll (R2R) gravure printing presses', *ISA Transactions*, 167, pp. 688–696. DOI: 10.1016/j.isatra.2025.08.046

Cocianu, C.-L., Uscatu, C.R. and Stan, A.D. (2023) 'Evolutionary Image Registration: A Review', *Sensors*, 23, 967. DOI: 10.3390/s23020967

Comino-Trinidad, M., Chica, A. and Andújar, C. (2023) 'Revisiting Poisson-disk subsampling for massive point cloud decimation', *arXiv*, arXiv:2311.17604. DOI: 10.48550/arXiv.2311.17604

de Sousa, S. and Kropatsch, W.G. (2015) 'Graph-based point drift: Graph centrality on the registration of point-sets', *Pattern Recognition*, 48, pp. 368–379. DOI: 10.1016/j.patcog.2014.06.011

Dey, S. (2018) Hands-On Image Processing with Python: *Expert Techniques for Advanced Image Analysis and Effective Interpretation of Image Data*. Birmingham, UK: Packt Publishing, pp. 73–92.

Fu, K., Chen, X. and Wang, M. (2022) 'Global optimization point-set registration based on translation/rotation decoupling for image-guided surgery applications', *Medical Physics*, 49, pp. 7303–7315. DOI: 10.1002/mp.15839

Gafurov, A.N., Park, H., Kim, D., Kim, I., Choi, Y., Oh, D. and Lee, T.-M. (2024) 'Machine direction registration modelling in roll-to-roll screen printing by deep learning'. In: *Proceedings of the 2024 IEEE 18th International Conference on Advanced Motion Control (AMC)*, 28 February–1 March 2024, Kyoto, Japan. DOI: 10.1109/AMC58169.2024.10505681

Jiao, X., Lv, C., Zhao, J., Yi, R., Wen, Y.-H., Pan, Z., Wu, Z. and Liu, Y.-J. (2024) 'Weighted Poisson-disk resampling on large-scale point clouds', *arXiv*, arXiv:2412.09177. DOI: 10.48550/arXiv.2412.09177

Kleijnen, J.P.C. (2008) *Design and Analysis of Simulation Experiments*. 1st ed. New York, NY, USA: Springer, pp. 113–123.

Pei, H., Zhou, W., Zhang, P. and Luo, M. (2023) 'A review of point set registration: From fundamental algorithms to geometric quality inspection of aviation complex parts', *Journal of Advanced Manufacturing Science and Technology*, 3, 2023012. DOI: 10.51393/j.jamst.2023012

Wei, L.-Y. (2008) 'Parallel Poisson disk sampling', *ACM Transactions on Graphics,* 27. DOI: 10.1145/1360612.1360619

Zhang, H., Liu, S., Wang, X., Wei, K. and Chen, L. (2024) 'Research on high precision detection method of register error based on machine vision'. In: Song, H., Xu, M., Yang, L., Zhang, L. and Yan, S. (eds.) *Innovative Technologies for Printing, Packaging and Digital Media.* Singapore: Springer, Volume 1144. DOI: 10.1007/978-981-99-9955-2_10

© 2026 Authors. Published by the University of Novi Sad, Faculty of Technical Sciences, Department of Graphic Engineering and Design. This article is an open access article distributed under the terms and conditions of the Creative Commons Attribution license 4.0 Serbia (http://creativecommons.org/licenses/by/4.0/rs/).

https://doi.org/10.24867/GRID-2026-p21

Preliminary Analysis of Image-Based Quality Assessment of Laser-Engraved Graphics

ABSTRACT

This study presents a preliminary image-based method for assessing the quality of laser-engraved graphic elements on colored paperboard. Uncoated, pulp-dyed paperboards in yellow, light blue, and black were engraved with a CO_2 laser at three power settings. The samples were digitized using a flatbed scanner and analyzed in ImageJ with substrate-specific image channels and automatic thresholding. Quality was assessed by measuring the dimensional reproduction of line elements, the area and contour properties of positive and negative geometric shapes, and the uniformity of larger engraved areas. The results showed that engraved lines were consistently wider than their nominal dimensions, with relative deviation rising markedly as nominal line width decreased. The finest lines (0.25 pt) showed the largest dimensional errors and, in several cases, the greatest variability. Positive geometric elements generally increased in area, while lateral expansion of the engraved region could reduce the preserved area of negative elements. Circularity and perimeter measurements revealed contour changes that area measurements alone did not always capture. Surface analysis also showed that the response of normalized non-uniformity to laser power varied by paperboard color. Overall, the findings demonstrate that line-width measurements, shape descriptors, and normalized surface-uniformity parameters provide complementary information and support a multi-parameter approach to objectively evaluating laser-engraving quality on colored paperboard.

Magdolna Pál
Nada Miketić
Ivana Jurič
Neda Milić Keresteš
Ivan Pinćjer

University of Novi Sad, Faculty of Technical Sciences, Department of Graphic Engineering and Design, Novi Sad, Serbia

KEY WORDS
Laser engraving, paperboard, image analysis, dimensional accuracy, contour fidelity, surface uniformity

1. Introduction

Cutting is a fundamental print-finishing operation and an essential step in producing bookbinding and packaging products. Mechanical cutting and die-cutting are well-established methods for separating paper and paperboard, while CO_2 laser cutting has emerged as a digitally controlled alternative. Its non-contact operation, programmable tool path, and ability to reproduce complex contours make it especially suitable for prototypes, customized products, and short production runs (Happonen et al., 2015; Pinćjer, Miketić & Tomić, 2022; Pinćjer et al., 2023; Rosnan & Enomae, 2021).

Laser technology in print finishing extends beyond complete substrate separation. By precisely controlling the laser–material interaction, the surface can be modified locally or material removed to a shallow depth without penetrating the full substrate thickness, enabling both marking and engraving. This allows text, symbols, ornaments, and other visual elements to be created directly on the substrate without applying printing ink (Pinćjer, Miketić & Tomić, 2022; Stepanov et al., 2015; Xie et al., 2020). In graphic products, engraved elements may serve identification, visual or combined functions. For machine-readable symbols, successful detection and decoding provide functional criteria for quality assessment (Matuszczyk and Weichert, 2023). Text, logos, and decorative motifs require broader evaluation, including

shape fidelity, fine-detail reproduction, contrast, and edge definition. Tonal relationships and overall visual fidelity are also relevant when assessing ornamental laser engravings (Lungu, Georgescu & Cosereanu, 2025).

The quality of laser engraving has been evaluated using various approaches, depending on the material and the intended function of the processed surface. Some methods focus on surface topography and roughness (Kažukauskas et al., 2024; Sáenz-Nuño et al., 2025), whereas others characterize laser-induced geometric or colorimetric changes (Nguyen-Thi-Ngoc & Dang, 2023; Stepanov et al., 2010, 2011). Although these measurements objectively describe surface texture, feature dimensions or color change, each captures only one aspect of quality and does not directly indicate whether a graphic element has preserved its intended contour, area, and fine details. Digital image processing has been used to quantify grayscale changes and engraving intensity, distinguish defective from defect-free laser-processed surfaces, and segment visible laser-affected regions on paper (Kasim et al., 2025; Rosnan et al., 2022; Zhang et al., 2021). These applications demonstrate the potential of image-based quality assessment, but they address individual indicators rather than the overall quality of engraved graphic elements. Colored paperboards present an additional challenge because their initial color and texture, together with differences in fiber structure, fillers and coatings can affect both the laser–material interaction and the appearance recorded in the image (Pinćjer, Miketić & Tomić, 2022; Stepanov et al., 2010, 2011, 2015). The aim of this study is therefore to propose and test a methodological approach based on the digital analysis of scanned images in ImageJ for quality control of laser-engraved elements on paperboards of different colors. The approach focuses on contour quality, reproduction of small graphic elements, and uniformity of larger engraved areas. It also examines whether these characteristics can be compared consistently across substrates and laser settings.

2. Methods

2.1. Paperboard samples

For this investigation, an uncoated, pulp-dyed paperboard was selected with a basis weight of 220 g/m² (Fa Colore, Fabriano, Italy). The paperboard was made from 100% ECF pulp and dyed throughout to achieve a solid, homogeneous color with high fade resistance. Because of its natural, uniform surface, this paperboard suits a wide range of graphic products, including invitations, greeting cards, menus, brochures, book covers, leaflets, and similar applications. Three paperboard colors were selected for the present investigation: yellow, light blue and black. Their CIELAB color coordinates were previously measured using a Techkon SpectroDens spectrophotometer with white backing, D50 illuminant and a 2° standard observer. Table 1 presents the measured values.

Table 1

CIELAB values of selected paperboard samples

Colour	Code name	L*	a*	b*
Yellow	Giallo	90.08	4.60	86.26
Light blue	Azzurro	59.86	-27.48	-37.18
Black	Nero	24.35	-0.77	-2.59

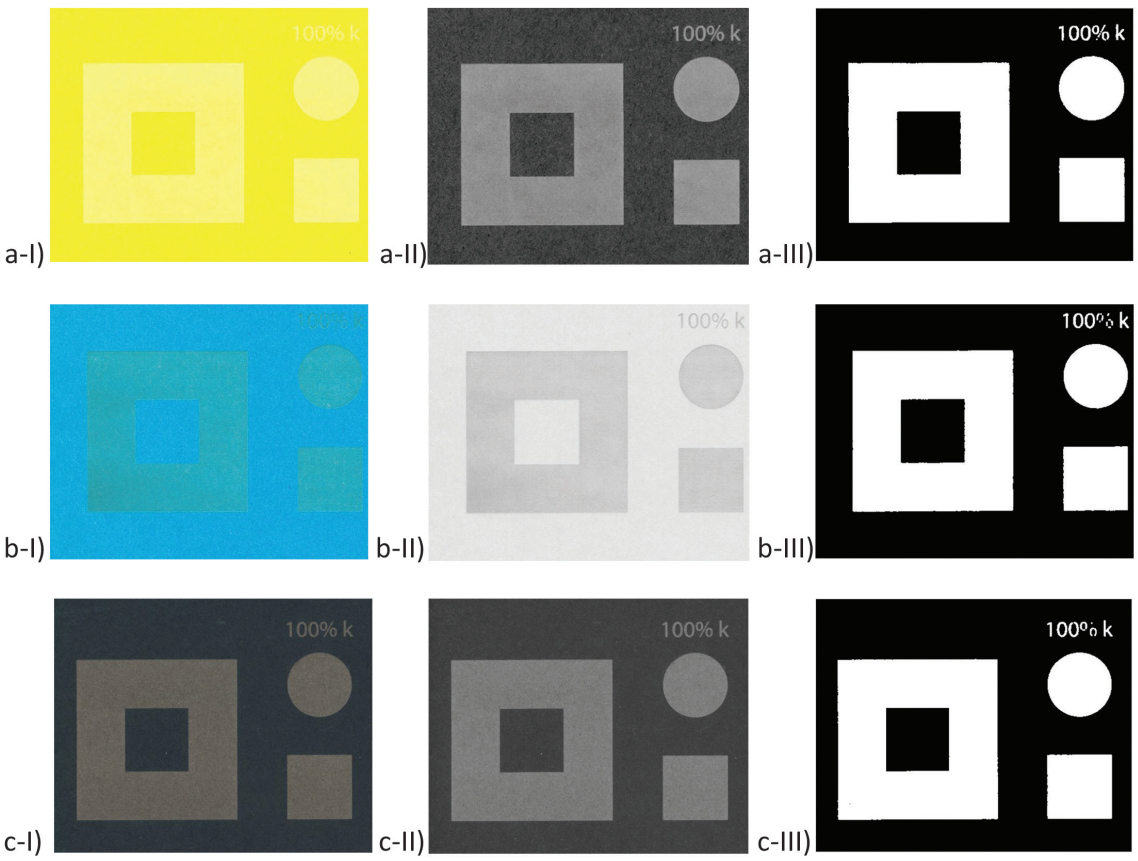
2.2. Laser engraving test elements

The paperboard samples were engraved with a Trotec Speedy 300 CO_2 laser system (Trotec, Marchtrenk, Austria) at three power settings: 55%, 60%, and 65%, designated Laser 1, Laser 2, and Laser 3, respectively. These settings were selected to assess how increasing laser power affects the reproduction of fine graphic elements and the uniformity of larger engraved areas. The laser operated at a wavelength of 10.6 µm, and the engraving speed was set to 30% of the system's maximum speed, as defined in the JobControl software. The laser head's movement in the XY plane was controlled using JobControl software (version 11.1.1).

For this study, a simple test form was designed to include line elements, positive and negative geometric shapes, and a larger solid engraved area. Four nominal line widths were used: 1, 0.75, 0.5, and 0.25 pt, corresponding to approximately 0.353, 0.265, 0.176, and 0.088 mm, respectively. Horizontal and vertical lines were included to assess potential directional effects. The geometric test elements comprised circles with a nominal diameter of 10 mm and squares with a nominal side length of 10 mm, each in positive and negative versions. For the positive elements, the area within the shape was engraved. For the negative elements, the surrounding area was engraved while the shape itself remained untreated. This configuration allowed evaluation of laser-modified boundary displacement on both sides of the nominal contour. The large surrounding engraved area was also used to assess engraving uniformity.

2.3. Image acquisition

To maintain fixed imaging geometry and consistent illumination across samples, the engraved paperboard samples were digitized with a Canon CanoScan 5600F flatbed scanner at 1200 spi. Images were acquired in the sRGB color space (IEC 61966-2-1), with automatic brightness, contrast, sharpening, and other image-enhancement functions disabled. All images were saved in TIFF format without lossy compression.



» **Figure 1:** *Representative image-preprocessing workflow for yellow (a), light-blue (b), and black (c) paperboards: original RGB scans (I), selected analysis channels (II), and binary masks obtained using Huang's automatic thresholding method (III)*

Colored paperboards require substrate-specific preprocessing because their original color, texture, and surface structure affect the recorded intensity distribution (Stepanov et al., 2010, 2011, 2015). Accordingly, the RGB channels of each paperboard were examined separately in ImageJ. The blue channel provided the clearest separation between engraved and untreated regions on the yellow paperboard (Figure 1a-II), whereas the red channel was selected for the light-blue and black paperboards (Figure 1b-II and 1c_II). The selected channel images were saved as grayscale, 8-bit TIFF files, while their copies were segmented using Huang's automatic thresholding method to create binary masks for subsequent geometric measurements. The original grayscale images were retained to assess uniformity within larger engraved areas. Channel selection was intended to improve boundary definition and identify spatial variations within the engraved regions. The resulting grayscale values were used solely as image-analysis data and were not interpreted as colorimetric measures of perceived contrast.

2.4. Digital image analysis

Image analysis was performed using ImageJ (version 1.53). Three groups of characteristics were evaluated: line reproduction, geometrical shape reproduction and engraved-surface uniformity.

2.4.1. Line-width measurements

The width of each engraved line was measured manually using a linear region of interest (ROI) positioned perpendicular to the stroke. Vertical measurement ROIs were used for horizontal lines, and horizontal ROIs for vertical lines. For each nominal line width and laser setting, 40 measurements were taken: 20 from horizontal lines and 20 from vertical lines. After spatial calibration, all measurements were recorded in millimeters. The mean line width (w_{mean}), standard deviation (SD), and coefficient of variation (CV) were calculated for each nominal width, line orientation and laser setting.

The line width deviation (Δw) from the nominal line width ($w_{nominal}$) was calculated as (1):

$$\Delta w = w_{mean} - w_{nominal} \qquad (1)$$

while the relative line-width increase was calculated as (2):

$$\Delta w_{relative} = (w_{mean} - w_{nominal}) / w_{nominal} \times 100 \quad (2)$$

Positive values indicate that the engraved line is wider than its nominal width, while negative values indicate that it is narrower. These parameters capture both systematic dimensional deviations and local variability in the reproduced line width.

2.4.2. Geometrical analysis of circles and squares

Positive and negative geometric elements were segmented from the selected image channels and analyzed using ImageJ shape descriptors. The analysis focused on area and perimeter for both circles and squares, while circularity was additionally evaluated for circular elements as an indicator of contour regularity. Measured areas were compared with the corresponding nominal values. The nominal area was 100 mm² for a square with a side length of 10 mm and 78.54 mm² for a circle with a diameter of 10 mm. Relative area deviation was calculated as (3):

$$\Delta A_{relative} = (A_{measured} - A_{nominal}) / A_{nominal} \times 100 \quad (3)$$

Positive and negative elements were evaluated separately. For positive elements, expanding the laser-modified region increases the measured dimensions and area. For negative elements, expanding the engraved surrounding region reduces the dimensions and area of the preserved, untreated shape.

2.4.3. Evaluation of engraved-surface uniformity

Engraved-surface uniformity was evaluated across the entire solid engraved area. Ten square ROIs measuring 5 × 5 mm were placed at predefined positions within the engraved region. The same ROI arrangement was used for all samples. For each ROI, the mean gray value (MGV_i) and the corresponding standard deviation (SD_i) were calculated. A reference mean gray value ($MGV_{reference}$) was obtained from the untreated area of the same paperboard sample.

Because different image channels were selected for the three paperboard colors, raw grayscale variability was normalized relative to the grayscale change caused by engraving. A normalized local nonuniformity index (NU_i) was calculated for each engraved ROI using (4):

$$NU_i = SD_i / | MGV_i - MGV_{reference} | \times 100 \quad (4)$$

For each laser setting the mean normalized nonuniformity and its standard deviation were calculated from the ten ROI values. A higher (NU) value indicates greater local grayscale variation within the engraved area relative to the grayscale difference between the engraved and untreated regions.

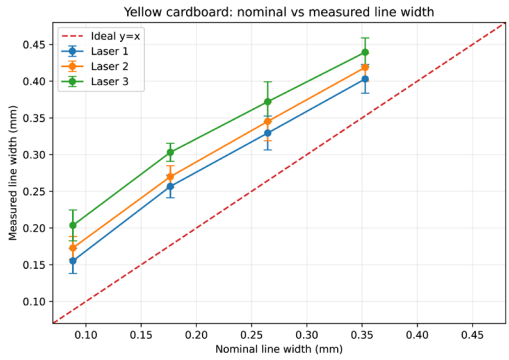
3. Results and discussion

The quality of laser engraving was evaluated through four complementary aspects: dimensional reproduction of line elements, dimensional accuracy of positive and negative geometrical shapes, preservation of shape geometry and uniformity of larger engraved areas. This approach enabled assessment of the influence of laser settings not only on overall dimensional changes, but also on local variability, contour integrity, and surface homogeneity.

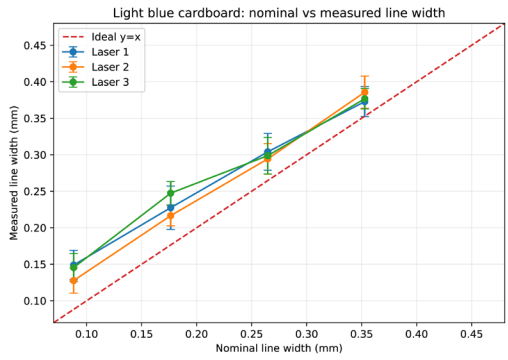
3.1. Reproduction of line elements

The relationship between nominal and measured line width for the three paperboards is presented in Figures 2a–c. In all cases, the measured line width exceeded the nominal value, indicating a systematic widening of the laser-modified region. However, the magnitude of this deviation depended strongly on both the nominal line width and the applied laser setting.

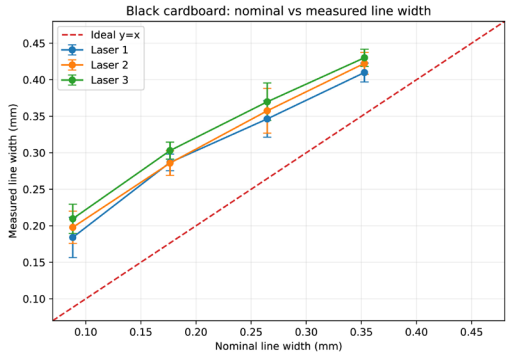
For the yellow paperboard (Figure 2a), line widening increased with laser intensity. The effect was relatively modest for the widest 1 pt (0.353 mm) lines, which measured 14–25% wider than nominal, but became considerably more pronounced as the nominal width decreased. For the finest 0.25 pt (0.088 mm) lines, the relative increase ranged from approximately 76% to more than 130%, depending on the laser setting. A similar relationship between nominal width and relative dimensional error was observed for the black paperboard (Figure 2c). The widest 1 pt (0.353 mm) lines showed a comparatively limited increase, whereas the 0.25 pt (0.088 mm) lines were more than twice as wide as their nominal dimensions under all three laser settings. The increase became progressively greater at higher laser settings, reaching approximately 138% at the highest setting. The light-blue paperboard also exhibited widening of all investigated line elements (Figure 2b). However, unlike the more regular trends observed for the yellow and black samples, the change in measured width with increasing laser setting was not strictly monotonic. Nevertheless, the effect of nominal line width remained evident: the relative dimensional deviation increased substantially as the designed line became thinner. The different response observed for the light-blue paperboard might also be partly affected by its lower grayscale contrast in the selected analysis channel, which could reduce edge visibility and increase uncertainty in the manual positioning of line-width measurements.



(a)



(b)

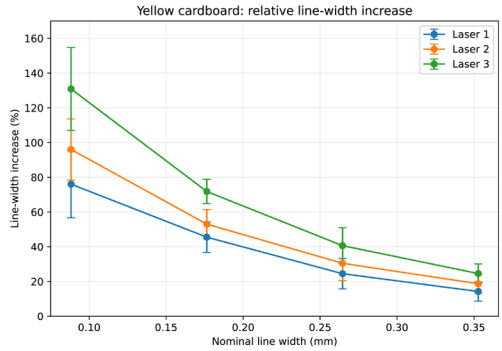


(c)

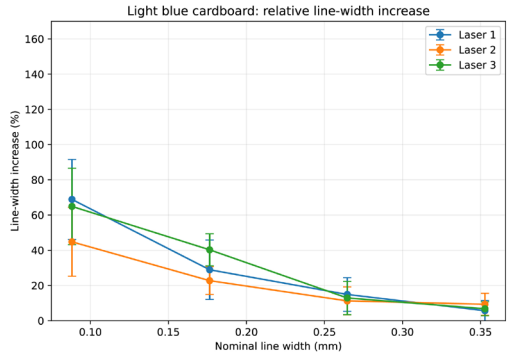
» **Figure 2:** *Line width reproduction - nominal versus measured line width for yellow (a), light-blue (b) and black (c) paperboards, respectively. Error bars represent ±1 SD*

The relative increase in line width for all three paperboards is shown in Figures 3a–c. These results further underscore the engraving process's increasing sensitivity as the nominal line width decreases. Although the relative dimensional change remained relatively small for the widest elements, it increased substantially for the finest lines, particularly at a nominal width of 0.25 pt.

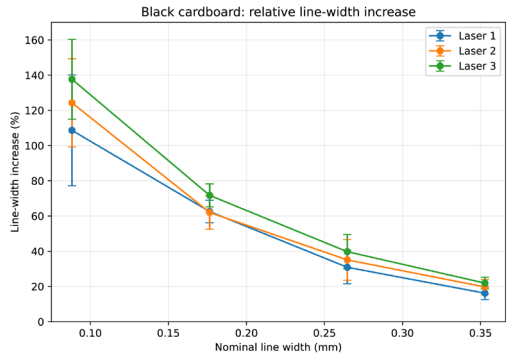
The error bars in Figures 2a–c and 3a–c represent ±1 standard deviation, providing additional information about the local repeatability of line reproduction. For the wider 1 pt lines, coefficients of variation were generally low, indicating relatively consistent reproduction along the measured segments. Relative variability tended to increase as nominal width decreased. This was especially evident for the 0.25 pt elements, where CV values reached approximately 9–15%, depending on the paperboard and laser settings.



(a)



(b)



(c)

» **Figure 3:** *Relative line-width increase for yellow (a), light-blue (b) and black (c) paperboards, respectively. Error bars represent ±1 SD*

Analyzing dimensional deviation alongside CV is important because the two parameters describe different aspects of reproduction quality. A line may show a substantial systematic increase in width while maintaining a relatively low CV, indicating consistent widening along the engraved element. Conversely, a high CV indicates greater local variation in line width and, consequently, lower dimensional uniformity. The pronounced relative error observed for the finest lines can be explained by the lateral extension of the laser-modified zone beyond the nominal graphic boundary. Even a small

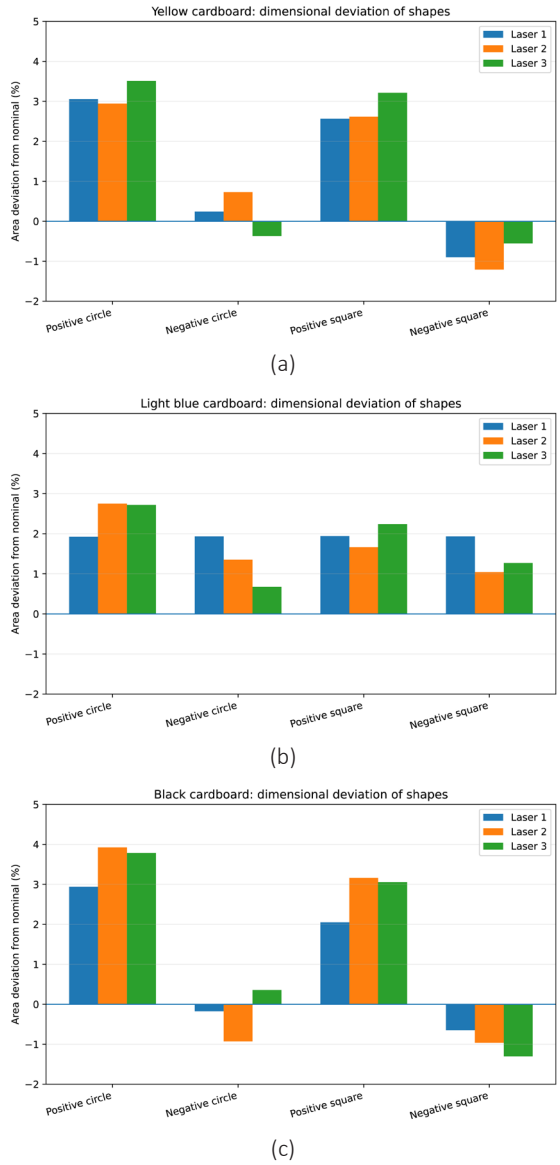
absolute lateral expansion accounts for only a minor fraction of a wide element but becomes a substantial proportion of the nominal dimension when very thin elements are engraved. Therefore, the smallest nominal line widths are inherently more sensitive to the characteristics of the laser–material interaction.

This finding aligns with Lei et al. (2020), who demonstrated that laser engraving quality on paper depends on both laser intensity and the preset width of the engraved marks. A comparable effect of increased energy input on the lateral dimensions of laser-treated zones has also been reported for other lignocellulosic materials, where higher laser power resulted in increased kerf width (Štefančin et al., 2026). The present results therefore confirm that nominal element width should be considered alongside laser parameters when evaluating the reproducibility of fine graphic details.

3.2. Dimensional reproduction of geometrical shapes

The relative area deviation of positive and negative circles and squares for the three paperboards is presented in Figures 4a–c. The results indicate that the dimensional response of each geometric element depended on whether the analyzed shape represented the engraved region itself or an unengraved area enclosed by engraving.

For the yellow paperboard (Figure 4a), positive circles and squares generally exhibited areas larger than their nominal dimensions. The increase was relatively small compared with that observed for the finest line elements, typically remaining within a few percent of the nominal area. Negative elements remained closer to their nominal dimensions, with the negative square showing a slight reduction in area. A similar behavior was observed for the light-blue paperboard (Figure 4b), while positive elements generally exhibited a positive area deviation, whereas the dimensional response of the negative elements was smaller and less regular. In particular, the negative circle showed a tendency toward decreasing area as the laser setting increased. For the black paperboard (Figure 4c), positive circles and squares again showed areas larger than the corresponding nominal values. In contrast, the negative square exhibited a gradual reduction in area with increasing laser treatment, while the negative circle remained comparatively close to its nominal size. Overall, positive circles and squares generally exhibited areas larger than their nominal dimensions. The increase was relatively small compared with that observed for the finest line elements, typically remaining within a few percent of the nominal area. Nevertheless, the direction of the deviation was consistent with the widening observed for the line structures. The behavior of negative elements was different in geometrical terms. Since the region surrounding the shape was engraved, lateral extension of



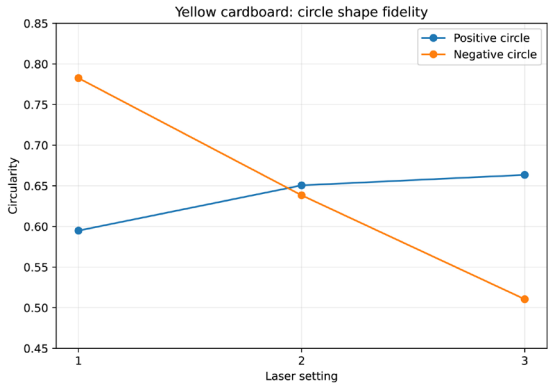
» **Figure 4:** *Relative area deviation of positive and negative circles and squares for yellow (a), light-blue (b), and black (c) paperboards*

the laser-modified area occurred towards the interior of the unengraved element. Consequently, the preserved negative area tended to decrease. This effect was particularly evident for some of the negative square elements, where increasing laser treatment was accompanied by a gradual reduction in measured area. Positive and negative elements should therefore not be interpreted as showing different physical responses to laser treatment. Both behaviors arise from the same lateral expansion of the laser-affected region. The apparent difference results solely from the position of the analyzed contour: outward expansion increases the area of a positive engraving, while inward expansion reduces the remaining area of a negative element. The area measurements further indicate that the dimensional effect observed for isolated lines also extends to more complex closed geometries. However, the relatively small changes in total

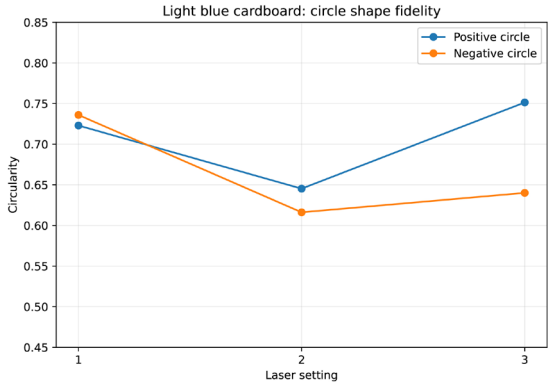
area compared with the more pronounced variations in some contour descriptors demonstrate that area alone is not sufficient to characterize reproduction quality.

3.3. Preservation of shape geometry

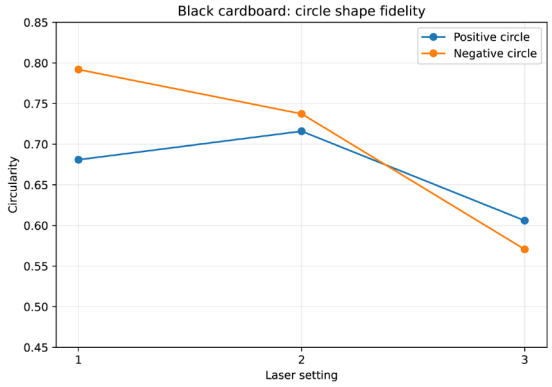
Circularity was used to assess how well the circular geometry was preserved. The results for the yellow, light-blue, and black paperboards are shown in Figures 5a–c, respectively. Unlike area, which mainly reflects an element's overall size, circularity is strongly affected by contour irregularities because it depends on perimeter.



(a)



(b)



(c)

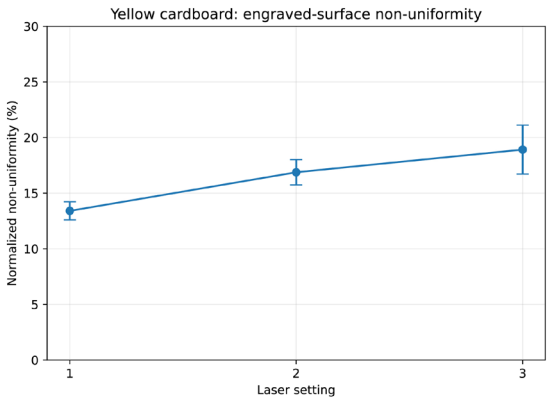
» **Figure 5:** *Circularity of positive and negative circular elements for yellow (a), light-blue (b), and black (c) paperboards*

For the yellow paperboard (Figure 5a), the positive circle's circularity increased slightly with laser setting, whereas the negative circle's circularity decreased markedly. This suggests that the negative element's contour became progressively less regular despite relatively limited changes in its total area. For the light-blue paperboard (Figure 5b), changes in circularity were less monotonic. Both positive and negative circles varied across the three laser settings, indicating that contour response was not governed solely by increasing laser intensity. For the black paperboard (Figure 5c), the positive circle showed its highest circularity at the intermediate laser setting, whereas the negative circle's circularity decreased markedly with increasing laser treatment.

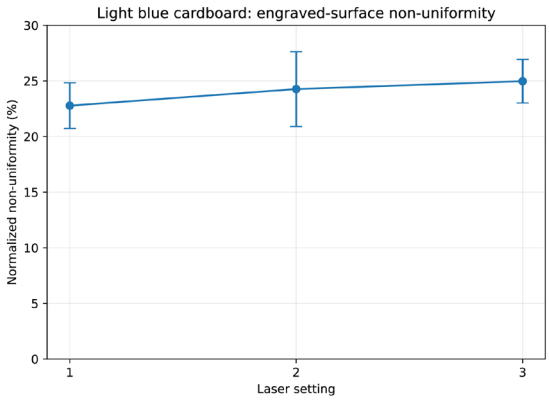
The results show that relatively small changes in measured area can be accompanied by much larger changes in circularity. This was particularly evident for several negative circular elements, where the area remained close to the nominal value while circularity decreased with increasing laser treatment. This behavior indicates that stronger laser treatment may affect the local contour without necessarily producing an equivalent change in total element area. Local protrusions, recesses, fiber removal and boundary irregularities increase the measured perimeter and consequently reduce circularity. For example, the negative circles on both the yellow and black paperboards showed a marked reduction in circularity as the laser setting increased, whereas their total areas changed considerably less. The results therefore demonstrate the importance of separating dimensional accuracy from contour fidelity. The same interpretation is supported by perimeter measurements of the square elements. In some cases, the measured perimeter increased despite only minor changes in total area, suggesting that the contour became geometrically more complex rather than simply larger or smaller. This behavior is consistent with the heterogeneous nature of paper-based materials. Schechtel et al. (2016) demonstrated that laser processing of paper is influenced by both the composition of the paper matrix and the inherent cellulose fibers. Local differences in fiber arrangement and material composition may therefore result in non-uniform material removal along the engraved boundary, contributing to contour irregularity. Accordingly, area, perimeter, and circularity should be viewed as complementary parameters. Area indicates overall changes in size, whereas perimeter and circularity are more sensitive to local changes in boundary quality.

3.4. Uniformity of the engraved surface

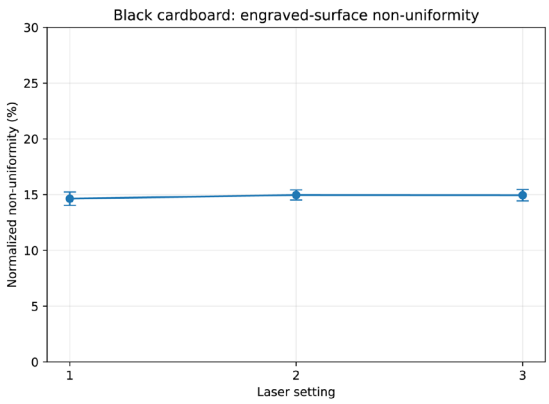
The normalized non-uniformity index was used to characterize local grayscale variation within the larger engraved areas. The results for the three paperboards, expressed as mean normalized non-uniformity ±1 SD, are presented in Figures 6a–c.



(a)



(b)



(c)

» **Figure 6:** *Normalized non-uniformity of engraved surfaces for yellow (a), light-blue (b), and black (c) paperboards. Values represent the mean of ten analyzed ROIs ±1 SD*

For the yellow paperboard (Figure 6a), normalized non-uniformity increased progressively with increasing laser setting, from approximately 13% to 19%. In parallel, the coefficient of variation increased at the highest setting, indicating that the stronger laser treatment was associated not only with greater local tonal variation but also with less consistent surface behavior among the analyzed regions. The light-blue paperboard (Figure 6b) also showed an increase in mean normalized non-uniformity with increasing laser setting, although the magnitude of the change was smaller. The CV varied between the three settings, indicating that spatial variability did not follow a strictly monotonic trend. In contrast, the black paperboard (Figure 6c) exhibited highly similar normalized non-uniformity values under all three laser settings, with mean values close to 15%. The corresponding CV values remained low, approximately 3–4%, indicating relatively stable local surface characteristics throughout the analyzed engraved region. For the light-blue paperboard, the lower grayscale contrast between engraved and untreated regions might also influence the normalized non-uniformity values, since a smaller engraved-to-reference intensity difference increases the sensitivity of the index to local grayscale variations.

These findings demonstrate that surface uniformity does not necessarily respond to laser treatment in the same manner as dimensional reproduction. A laser setting that produces a greater change in line width or contour geometry does not automatically result in a proportionally greater degree of surface non-uniformity. The normalized index is particularly useful in this context because the standard deviation of grayscale values is interpreted relative to the tonal difference between the engraved and unengraved reference areas. Consequently, the parameter describes local variation within the engraved surface rather than its absolute brightness. The use of grayscale variability as an indicator of surface uniformity has methodological parallels in previous image-analysis studies. Kennedy and Niebergall (1997), for example, used standard deviations of optical measurements to assess coating uniformity. The observed variations can also be related to the heterogeneous structure of paperboard. Local differences in fiber distribution, fillers, pigments and surface structure may influence the extent of material removal and thermal modification within the laser-treated area (Schechtel et al., 2016).

4. Conclusions

The results demonstrate that laser engraving quality on colored paperboard cannot be adequately characterized by a single image-analysis parameter. Dimensional accuracy, local repeatability, contour fidelity and surface uniformity describe complementary aspects of engraving quality and may respond differently to changes in laser settings.

Across all investigated paperboards, engraved line widths exceeded their nominal values, indicating consistent lateral expansion of the laser-modified zone. This effect became more pronounced as nominal line width decreased. The largest relative deviations and, in several cases, the highest coefficients of variation occurred in the finest 0.25 pt (0.088 mm) lines, making very thin graphic elements the most critical features for dimensional reproduction. Analysis of positive and

negative geometric elements confirmed that both were affected by the same lateral expansion, although the dimensional impact depended on the location of the analyzed boundary. Positive elements generally increased in area, while expansion of the engraved surroundings could reduce the preserved area of negative elements. Circularity and perimeter offered further insight into contour fidelity, revealing boundary irregularities that were not necessarily evident in total-area changes. The normalized non-uniformity index provided complementary information about spatial variations within larger engraved areas. Its response to increasing laser power varied among the investigated paperboards and did not necessarily align with trends in dimensional reproduction. These findings further underscore the need to assess dimensional and surface-related characteristics separately when evaluating engraving quality.

Overall, combining line-width measurements, shape descriptors, and normalized surface-uniformity analysis offers a useful image-based framework for objectively assessing laser-engraved paperboard. Instead of relying on a single quality indicator, this approach allows different aspects of reproduction quality to be evaluated together and may help define material-specific engraving conditions and minimum reproducible graphic-element dimensions.

Future work should include a broader range of paperboard types and colors, repeat engraving trials independently, and conduct additional analysis of color and visual contrast between engraved and non-engraved areas. In particular, the possible influence of image contrast on edge localization and normalized surface-uniformity measurements should be investigated to distinguish material-related effects from image-analysis sensitivity.

5. Acknowledgments

This research has been supported by the Ministry of Science, Technological Development and Innovation (Contract No. 451-03-34/2026-03/200156) and the Faculty of Technical Sciences, University of Novi Sad through project "Scientific and Artistic Research Work of Researchers in Teaching and Associate Positions at the Faculty of Technical Sciences, University of Novi Sad 2026" (No. 01-3609/1).

6. References

Happonen, A., Stepanov, A., Piili, H. and Salminen, A. (2015) 'Innovation study for laser cutting of complex geometries with paper materials', *Physics Procedia*, 78, pp. 128–137. DOI: 10.1016/j.phpro.2015.11.025

Kasim, M.S., Muhammad, A., Yusof, S.N.A., Awang, R., Mat Rasul, R., Wan Mohamad, W.N.F., Izamshah, R. and Ginting, A. (2025) 'Determining optimal laser engraving conditions for high-contrast and well-defined engraving on Kapur wood (Dryobalanops) using ImageJ', *The International Journal of Advanced Manufacturing Technology*, 141, pp. 397–410. DOI: 10.1007/s00170-025-16670-w

Kažukauskas, E., Butkus, S., Jukna, V. and Paipulas, D. (2024) 'Surface roughness control in deep engraving of fused silica using femtosecond laser ablation', *Surfaces and Interfaces*, 50, 104471. DOI: 10.1016/j.surfin.2024.104471

Kennedy, J.P. and Niebergall, P.J. (1997) 'Preliminary assessment of an image analysis method for the evaluation of pharmaceutical coatings', *Pharmaceutical Development and Technology*, 2(3), pp. 205–212. DOI: 10.3109/10837459709031440

Lei, X., Liu, S., Wu, N., Ge, Y., Hou, H. and Liu, P. (2020) 'Experimental investigation of laser engraving quality on paper', *Applied Optics*, 59(8), pp. 2416–2421. DOI: 10.1364/AO.377221

Lungu, A., Georgescu, S.V. and Cosereanu, C. (2025) 'Color-based laser engraving of heritage textile motifs on wood', *Applied Sciences*, 15(24), 12900. DOI: 10.3390/app152412900

Matuszczyk, D. and Weichert, F. (2023) 'Reading direct-part marking Data Matrix code in the context of polymer-based additive manufacturing', *Sensors*, 23(3), 1619. DOI: 10.3390/s23031619

Nguyen-Thi-Ngoc, H. and Dang, T.-V. (2023) 'Optimization of process parameters for wood laser engraving based on Taguchi method approach', *MM Science Journal*, October 2023, pp. 6723–6729. DOI: 10.17973/MMSJ.2023_10_2023053

Pinćjer, I., Miketić, N. and Tomić, I. (2022) 'Cutting with laser in postpress'. In: Vladić, G. (ed.) *Proceedings of the 11th International Symposium on Graphic Engineering and Design, GRID 2022, 3–5 November 2022, Novi Sad, Serbia*. Novi Sad: Faculty of Technical Sciences, Department of Graphic Engineering and Design, pp. 671–676. DOI: 10.24867/GRID-2022-p73

Pinćjer, I., Miketić, N., Gvoić, V., Maricić, K., Vukelić, D. and Prica, M. (2023) 'Optimization of tensile strength in the paper material cutting process based on CO_2 laser process parameters', *Materials*, 16(7), 2719. DOI: 10.3390/ma16072719

Rosnan, S.M. and Enomae, T. (2021) 'The art of gift-giving: Laser cutting as a value-added technology for fabricating customized biodegradable packaging'. In: *Proceedings of IS&T Printing for Fabrication 2021: International Conference on Digital Printing Technologies (NIP37), 11–12 October 2021, online*. Springfield, VA: Society for Imaging Science and Technology, pp. 69–72. DOI: 10.2352/ISSN.2169-4451.2021.37.69

Rosnan, S.M., Kong, P., Enomae, T. and Nakagawa-Izumi, A. (2022) 'Image analysis of heat-affected zone of laser-cut heat-resistant paper using Otsu thresholding technique', *International Journal of Advanced Computer Science and Applications*, 13(4), pp. 41–48. DOI: 10.14569/IJACSA.2022.0130405

Sáenz-Nuño, M.A., Puente, C. and Rubio, E.M. (2025) 'The characterization of surface texture in laser bamboo engraving: A metrological approach', *Coatings*, 15(6), 624. DOI: 10.3390/coatings15060624.

Schechtel, F., Reg, Y., Zimmermann, M., Stocker, T., Knorr, F., Mann, V., Roth, S. and Schmidt, M. (2016) 'Pulsed laser processing of paper materials', *Physics Procedia*, 83, pp. 46–52. DOI: 10.1016/j.phpro.2016.08.006

Štefančin, L., Igaz, R., Adamčík, L., Ružiak, I., Kubovský, I. and Kminiak, R. (2026) ‹Effects of CO_2 laser cutting parameters on kerf width in native wood species›, *BioResources*, 21(3), pp. 6463–6481. DOI: 10.15376/biores.21.3.6463-6481

Stepanov, A., Piili, H. and Salminen, A. (2010) 'Color change in laser cutting of paper material'. In: *Proceedings of the 29th International Congress on Applications of Lasers and Electro-Optics, ICALEO 2010, 26–30 September 2010, Anaheim, California, USA.* Laser Institute of America, paper P139. DOI: 10.2351/1.5061990

Stepanov, A., Piili, H., Saukkonen, E. and Salminen, A. (2011) 'Effect of linear cutting energy on coloration of paper in laser cutting of paper material'. In: *Proceedings of the 30th International Congress on Applications of Lasers and Electro-Optics, ICALEO 2011, 23–27 October 2011, Orlando, Florida, USA.* Laser Institute of America, pp. 71–79. DOI: 10.2351/1.5062317

Stepanov, A., Saukkonen, E. and Piili, H. (2015) 'Possibilities of laser processing of paper materials', *Physics Procedia*, 78, pp. 138–146. DOI: 10.1016/j.phpro.2015.11.026

Xie, L., Chen, X., Yan, H., Xie, H. and Lin, Z. (2020) 'Experimental research on the technical parameters of laser engraving', *Journal of Physics: Conference Series*, 1646(1), 012091. DOI: 10.1088/1742-6596/1646/1/012091

Zhang, J., Li, Z., Hao, R., Wang, X., Du, X., Yan, B., Ni, G., Liu, J., Liu, L. and Liu, Y. (2021) 'Classification of microscopic laser engraving surface defect images based on transfer learning method', *Electronics*, 10(16), 1993. DOI: 10.3390/electronics10161993



© 2026 Authors. Published by the University of Novi Sad, Faculty of Technical Sciences, Department of Graphic Engineering and Design. This article is an open access article distributed under the terms and conditions of the Creative Commons Attribution license 4.0 Serbia (http://creativecommons.org/licenses/by/4.0/rs/).

Original Scientific Paper https://doi.org/10.24867/GRID-2026-p22

Influence of Screen Printing Mesh Count on Deposition of Graphite-Starch Conductive Ink onto Cardboards

ABSTRACT

Due to the increasing need for flexible and lightweight electronic components, the market for printed electronics is continuously growing and is to reach almost 40 billion USD in 2030. Therefore developing a more sustainable conductive inks is highly important. The aim of this paper is to propose conductive ink with graphite as a conductive component, dispersed in starch paste for the application on cardboard using screen printing technique. For the purpose of this research printed samples were prepared on two types of cardboard (coated and uncoated) by printing with various screen printing mess thread count. The samples were evaluated by measuring optical density, visual inspection and by measuring electrical resistance. The results of the evaluation showed that both cardboard surface finish and screen printing mesh count is significantly influencing ink film formation. Additionally, only samples printed with 32 lpcm screen printing mesh count achieved electrical resistance lower than 2 kΩ. It can be concluded that graphite-starch conductive ink has the potential for use in printed electronics, but due to the high electrical resistance and relatively bad ink film forming on coated cardboard, it should be improved. The future work will be focused on increasing conductivity and improving wetting on smooth, coated surfaces.

Tomislav Cigula
Rene Hoblaj
Katarina Itrić Ivanda
Rahela Kulčar
Iva Šarčević

University of Zagreb Faculty of Graphic Arts, Zagreb, Croatia

KEY WORDS
Screen printing, conductive ink, graphite, starch

1. Introduction

The need for flexible and lightweight electronic components is growing across various industries. That fact is driving the market of the printed electronics with the CAGR of 15.4% from 2025 – 2030, i.e. almost doubling the global market size from 19.46 billion USD in 2025. to 39.85 billion USD in 2030 (Printed Electronics Market Size, Share, Latest Trends & Growth Analysis, 2025-2030, n.d.) . For the successful printed electronics there are two main influencing factors – the functional printing ink and the printing process. Printed electronics include various traditional, master based printing techniques, but inkjet as well (Wiklund et al., 2021) . One of the often used printing processes is screen printing due to the possibility of deploying thick ink layers on the printing substrate. With the growth of environmental concern and a number of electronics applications the research effort was put into development of the sustainable ins for printed electronics. The inks are often composed of metal particles (silver or copper) which are dispersed in some organic solvent (Sanchez-Duenas et al., 2023). In addition, many of the functional inks in printed electronics are solvent based and use thermal energy for curing ("Functional Inks for Printed Electronics- Demystified," 2026).

Graphite offers conductivity and as a relatively cheap material it was investigated as a base for the producing affordable conductive ink with various binders: nail polish (Oliveira & Pereira, 2021) and corn starch (Dey et al., 2025) applied on the substrate by a brush and chitosan (Marchianò et al., 2024) applied by stencil printing. These papers showed that there is high potential in graphite based conductive inks.

Having these results in mind, aim of this paper was to prepare a graphite-starch conductive

ink and apply it on a cardboard substrate using screen printing technique to determine its usability as a screen printing conductive ink.

2. Materials and methods

For the purpose of this paper a conductive printing ink was prepared by mixing graphite powder (particle size 20 µm, Sigma Aldrich) into tapioca starch solution. Composition of the conductive ink can be seen in Table 1.

Table 1
Components of the conductive ink

Component	Amount
Tapioca powder (Nutrigold)	5 g
Graphite powder (Sigma Aldrich)	5 g
Glycerol (pro analysi, Gram.mol d.o.o.)	2.5 g
Distilled water (INA d.d.)	50 ml

The conductive ink preparation was performed by weighing tapioca powder and glycerol using Mettler Toledo XS205DU. The components were put into a glass container and water was added and mixed with the glass stick at room temperature. After achieving even mixture, graphite powder was added to solution and mixed using magnetic stirrer (Tehtnica rotamix). The prepared solution was mixed at 500 rpm and with increasing temperature up to 65 oC by increasing temperature by 2 oC pro minute on average. After achieving defined temperature, printing ink was left to cool down to room temperature.

The procedure was set after a few trials in which increasing temperature to the ones found in literature (Lukavski et al., 2025; Żołek-Tryznowska & Kałuża, 2021) made prepared ink difficult to print. By using the described procedure prepared ink was printable paste.

The printing form used for the purpose of this research was prepared using capillary film with thickness of 25 µm (CDF vision 25, ULANO). Used screen printing meshes were all made of polyester with white threads. The mesh count of the used printing forms is shown in Table 2.

Table 2
Screen printing mesh count used

Screen mesh count	Thread diameter (µm)
32	100
61	64
100	40

The printing substrates were typical cardboards with two surface finishes, one coated with gloss finish (UPM Finesse white gloss) with a grammage of 305 g/m^2 and the other was uncoated (Sappi Tauro) with a grammage of 300 gm^2.

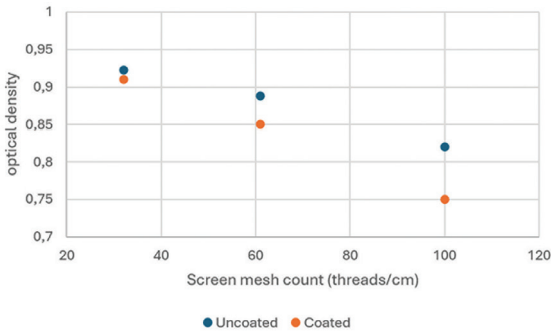
The printing process was performed manually with handheld squeegee and a vacuum table used to hold cardboard fixed during printing.

After printing, prepared prints were dried at room temperature and additionally processed by exposing them to hot air at 100 oC for 20 min by using Memmert UNB400 heating chamber.

The prepared samples were analyzed by measuring optical density of the printed ink film (Techkon SpectroDens), visual inspection of microscopic images obtained using Olympus BX-51 and finally by measuring electrical resistance using Milli-Ohm metar Viei VC480 C+.

3. Results and discussion

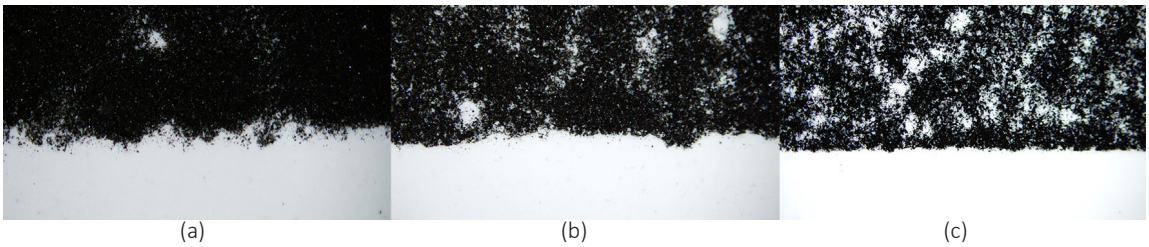
The optical density indicates the ink transfer and indirectly the thickness of the formed ink film on the printing substrate. In Figure 1 one can see the value of achieved optical density printed with different screen printing mesh count. It is visible that higher values of optical density are achieved on the uncoated cardboard compared to the coated cardboard. These results were not expected as prior research like (Cigula et al., 2019; Seymour, 2021) showed that on coated papers optical density is higher than on the uncoated ones.



» **Figure 1:** *Optical density on prepared prints*

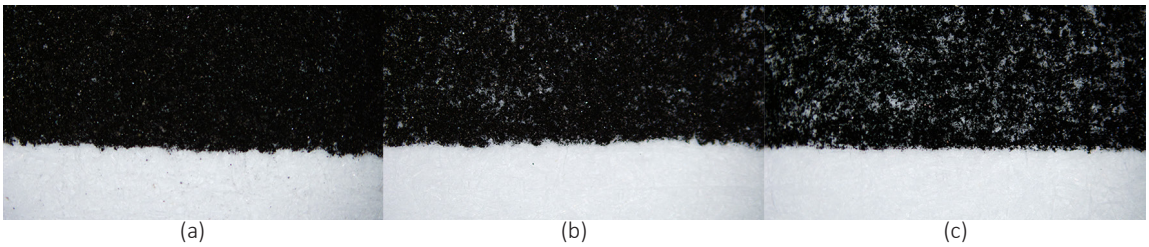
The results of the optical density indicate that the ink film thickness on the coated cardboard is lower than on the uncoated cardboard.

The printed ink is composed of starch and graphite with water as a solvent. Although in the form of paste, it is still a thick liquid and the surface properties of the printing substrate significantly influences the ink transfer. The most paper/cardboard coatings used today are polymer based and therefore have low polar component of the surface free energy leading to lower adsorption of the water based printing ink. On the other hand, uncoated paper/cardboard has rough



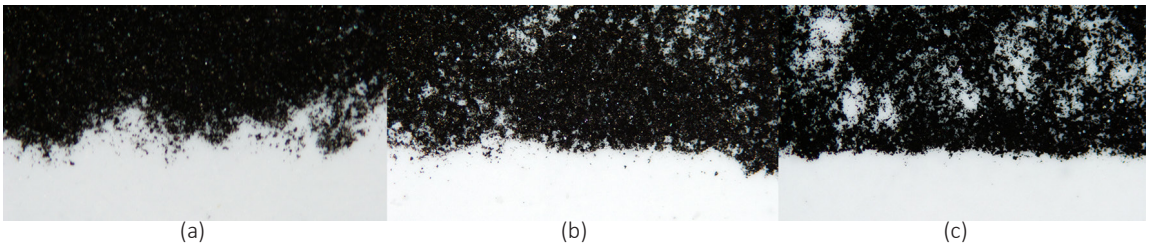
(a) (b) (c)

» **Figure 2:** *Micrographs (50×) of prints on coated cardboard: a) 32 lpcm, b) 61 lpcm, c) 100 lpcm*



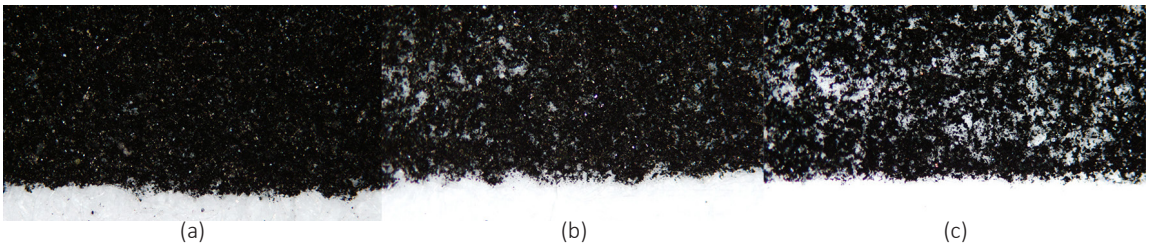
(a) (b) (c)

» **Figure 3:** *Micrographs (50×) of prints on uncoated cardboard: a) 32 lpcm, b) 61 lpcm, c) 100 lpcm*



(a) (b) (c)

» **Figure 4:** *Micrographs (100×) of prints on coated cardboard: a) 32 lpcm, b) 61 lpcm, c) 100 lpcm*



(a) (b) (c)

» **Figure 5:** *Micrographs (100×) of prints on uncoated cardboard: a) 32 lpcm, b) 61 lpcm, c) 100 lpcm*

surface with pores in the structure which enables adsorption of the ink during the printing process. In this case enabled formation of thicker film of ink despite ink's absorption into the paper/cardboard structure.

The above mentioned behaviour of the ink is visible in Figures 2 and 3 where one can observe uneven ink film layer with visible white areas, where ink is not present. These white areas are more present on coated cardboard and when printed with higher screen printing mesh count.

On the other hand, although prints on the coated paper should have sharper edge, observing Figures 4 and 5 one could se the opposite, i.e. the line edge on the uncoated paper is a bit smoother than the prints on coated paper.

In the final step of evaluation, electrical resistance on prepared samples was measured and the results are presented in Table 3. The electrical resistance is very high. The measuring range of the used unit was up to 2 kΩ and the only two samples had electrical resistance lower than the measuring range- samples printed with the screen printing mesh count of 32 lpcm.

The unevenness of the ink film and visible areas where ink is not visible (Figure 2 and Figure 3) are decreasing the conductivity of the printed lines.

Table 3
Electrical resistance on the prepared samples

Screen printing mesh count	Electrical resistance (kΩ)	
	Coated cardboard	Uncoated cardboard
32	1.77	1.51
61	> 2	> 2
100	> 2	> 2

4. Conclusions

The aim of this paper is to propose conductive ink with graphite as a conductive component, dispersed in starch paste for the application on cardboard using screen printing technique. For the purpose of this research printed samples were prepared on two types of cardboard (coated and uncoated) by printing with various screen printing mesh count. The samples were evaluated by measuring optical density, visual inspection and by measuring electrical resistance.

The results of the evaluation showed that both cardboard surface finish and screen printing mesh count is significantly influencing ink film formation. Additionally, only samples printed with 32 lpcm screen printing mesh count achieved electrical resistance lower than 2 kΩ.

To conclude, graphite-starch conductive ink has the potential for use in printed electronics, but due to the high electrical resistance and relatively bad ink film forming on coated cardboard, it should be improved. The future work will be focused on increasing conductivity and improving wetting on smooth, coated surfaces.

5. Acknowledgments

This work was carried out as part of the project IP-2022-10-3864: Improvement of Packaging Products through the Application of Environmentally Friendly Materials and Inclusive Design.

6. References

Cigula, T., Tomašegović, T. and Hudika, T. (2019) 'Effect of the paper surface properties on the ink transfer parameters in offset printing', *Nordic Pulp and Paper Research Journal*, 34(4), pp. 540–549. DOI: 10.1515/npprj-2019-0018

Dey, A., Kalita, A.J., Khatun, H. and Sarma, U. (2025) 'The Development of an Affordable Graphite-Based Conductive Ink for Printed Electronics', *Engineering Proceedings*, 87(1). DOI: 10.3390/engproc2025087017

'Functional inks for printed electronics – demystified' (2026) *Specialist Printing Worldwide*, 17 February. Available from: https://www.specialistprinting.com/articles/functional-inks-for-printed-electronics-demystified/ [Accessed 14 October 2026].

Lukavski, T., Bota, J., Budimir, I., Itrić Ivanda, K., Kulčar, R. and Vukoje Bezjak, M. (2025) 'Functional Starch-Based Biopolymer Coatings for Sustainable Packaging Applications', *Polymers*, 17(24), 3303. DOI: 10.3390/polym17243303

Marchianò, V., Tricase, A., Caputo, M., Farinini, E., Leardi, R., Imbriano, A., Leech, D., Kidayaveettil, R., Gentile, L., Torsi, L., Macchia, E. and Bollella, P. (2024) 'Tailoring Water-Based Graphite Conductive Ink Formulation for Enzyme Stencil-Printing: Experimental Design to Enhance Wearable Biosensor Performance', *Chemistry of Materials*, 36(1), pp. 358–370. DOI: 10.1021/acs.chemmater.3c02229

Oliveira, A.E.F. and Pereira, A.C. (2021) 'Development of a Simple and Cheap Conductive Graphite Ink', *Journal of The Electrochemical Society*, 168(8), 087508. DOI: 10.1149/1945-7111/ac1b02

Printed Electronics Market Size, Share, Latest Trends & Growth Analysis, 2025–2030 (n.d.) Available from: https://www.marketsandmarkets.com/Market-Reports/printed-electronics-market-197.html [Accessed 5 October 2026].

Sanchez-Duenas, L., Gomez, E., Larrañaga, M., Blanco, M., Goitandia, A.M., Aranzabe, E. and Vilas-Vilela, J.L. (2023) 'A Review on Sustainable Inks for Printed Electronics: Materials for Conductive, Dielectric and Piezoelectric Sustainable Inks', *Materials*, 16(11), 3940. DOI: 10.3390/ma16113940

Seymour, J. (2021) 'Coated Versus Uncoated—Why the Difference in Density?', *TAGA 2021 Proceedings*. Available from: https://library.taga.org/2021-proceedings/T20210022 [Accessed 14 October 2026].

Wiklund, J., Karakoç, A., Palko, T., Yigitler, H., Ruttik, K., Jäntti, R. and Paltakari, J. (2021) 'A Review on Printed Electronics: Fabrication Methods, Inks, Substrates, Applications and Environmental Impacts', *Journal of Manufacturing and Materials Processing*, 5(3), 89. DOI: 10.3390/jmmp5030089

Żołek-Tryznowska, Z. and Kałuża, A. (2021) 'The influence of starch origin on the properties of starch films: Packaging performance', *Materials*, 14(5), 1146. DOI: 10.3390/ma14051146



© 2026 Authors. Published by the University of Novi Sad, Faculty of Technical Sciences, Department of Graphic Engineering and Design. This article is an open access article distributed under the terms and conditions of the Creative Commons Attribution license 4.0 Serbia (https://creativecommons.org/licenses/by/4.0/deed.en).

Professional Paper https://doi.org/10.24867/GRID-2026-p23

Mottling in Production of Cardboard and in Offset Printing

ABSTRACT

White Lined Chipboard (WLC), made from wastepaper, is widely used for high-quality packaging applications that require consistent optical density and uniform tonal reproduction. A critical printing defect affecting visual appearance in multicolor offset printing is mottling—characterized by localized variations in ink transfer, uneven ink setting, and cloudy tonal reproduction in solid areas and halftone gradients. This study examines the relationship between wet-end process conditions, middle and print ply formation, baseboard structural uniformity, and offset printability on a 200,000 t/a recycled WLC machine (GD2, GD3 and GT2 grades). Non-uniform fiber distribution creates micro-scale variations in basis weight, porosity, coating holdout, and surface absorbency, which lead to uneven ink absorption during printing—particularly visible in fine screen rulings, light cyan/magenta tones, and smooth gradients. To mitigate mottling, a systematic wet-end optimization program was implemented, focusing on raw material fiber ratio adjustments (OCC and recovered paper blend), shake roll parameters, stock consistency control, and jet-to-wire speed ratio optimization to reduce local basis weight variations prior to blade coating. Process modifications were continuously evaluated in the laboratory using an IGT Amsterdam 2 printability tester to isolate water-interference mottling from back-trapping mottling. Findings were validated through commercial offset press trials operating at 10,000–12,000 sheets/hour. The results confirmed that wet-end formation improvements significantly reduced both laboratory-measured mottling indices and commercial print non-uniformities. The study demonstrates that resolving print mottling requires an integrated, process-oriented methodology connecting board machine wet-end control with laboratory printability simulation and commercial press validation.

Žanko Sremac
Nemanja Petrović
Uroš Mančić

Fabrik kartona Umka,
Umka d.o.o., Umka, Serbia

KEY WORDS
Recycled cardboard, board machine, formation, wet end optimization, mottling, white lined chipboard (WLC), GD2, GD3, offset printing, IGT Amsterdam 2

1. Introduction

Umka D.O.O. Umka is a board mill located close to Belgrade, on the riverbank of the Sava. It is a state-of-the-art facility for the production of WLC (White Line Chipboard). WLC is defined as a multilayer board (three layers – bottom, middle and print ply), characterized by a white colored coated print ply suitable for high-quality printing and converting. It is widely used for folding cartons and other packaging applications (food packaging, pharmaceutical, automotive, cosmetics, etc.).

The main raw material is recovered wastepaper, mostly collected in the Republic of Serbia. Umka is the biggest wastepaper recycling plant in Serbia and surrounding countries. At the moment, yearly production capacity is 200.000t, of finished product, divided into five qualities: Umka Color, Umka Pak, Umka Special, Umka brown back, Umka Liner. Since Umka is exporting more than 85% of its production to countries in the EU, most of the customers are high-end printing houses, with some of the most demanding end users (Lego, Dr Oetker...); expectations regarding the quality of the finished prod-

uct are getting bigger. The aim of this paper is to show the close connectivity of different parameters that are influencing the quality of the finished, printed product with regard to a specific quality characteristic – mottling.

2. Statement of the problem - mottling in WLC board production

WLC (White Lined Chipboard) is a multilayer cardboard that is commonly produced from different types of fibers, originating from recovered paper and cardboard, with individual layers differing in composition, purpose, and properties. For this type of paperboard, the quality of the printing surface depends not only on the final coating but also on the cardboard structure formed during the initial stages of the production process on the board machine. Mottling is a phenomenon characterized by visual non-uniformity in the printed image, manifested as local variations in optical density and color reproduction (Fahlcrantz & Johansson, 2004; Lee et al., 2021). In WLC cardboard production, this issue is particularly significant because the final coating, although it improves surface smoothness and print properties, cannot always fully compensate for irregularities originating in the structure of the baseboard.

Therefore, understanding mottling requires an analysis of the entire production process, starting with stock preparation and layer formation in the wet end of the machine, followed by the press section and drying, and continuing through calendaring, coating, and final printing. Particular attention is paid to the formation of the middle layer (filler ply) and the top layer intended for printing (print ply), as their properties directly affect the uniformity of the cardboard web and the performance of the print ply. The mottling effect in demanding print jobs can occur through several effects:

- **Fine screen ruling**

Mottling can be particularly noticeable when printing low and medium screen rulings, as these conditions require a carefully balanced interaction between the dampening solution and the ink on the printing plate. In halftone areas, the distribution and transfer of ink must remain stable to ensure consistent reproduction. Excessive dampening can disturb the ink–water balance, resulting in irregular ink transfer from the printing plate to the blanket and, consequently, a cloudy or mottled appearance in the printed image. In cardboard printing, non-uniform absorptiveness can further aggravate this problem. Small halftone dots may behave differently depending on the local surface properties of the substrate. In areas with higher or lower absorptiveness, dot deformation and dot gain may vary, resulting in uneven tonal reproduction. For example, a nominal 30% halftone may reach an apparent printed tone value of 40% in areas where ink spreading or other printing-related effects increase dot gain.

- **Smooth tonal gradients**

Smooth tonal gradients (ferlauf) involve a gradual change in tonal value and halftone dot size across the printed area. As with fine screen rulings, uniform substrate properties and stable printing conditions are essential for achieving smooth and consistent tonal transitions. Variations in paperboard absorptiveness may lead to local differences in ink transfer and dot gain, resulting in visible irregularities.

- **Light cyan and magenta tonal values**

Light cyan and magenta tones may be particularly susceptible to back-trapping mottling in multicolour offset printing. Cyan and magenta are often printed in the earlier printing units, depending on the selected ink sequence. Under certain conditions, the ink film transferred to the blanket may be partially disturbed by the subsequent printing unit. This phenomenon can occur when the tack and rheological properties of the inks, together with the condition of the ink film, cause the subsequent printing unit to partially pick off or disrupt the previously transferred ink film on the blanket. The resulting local variations in ink transfer can produce a mottled appearance, particularly in light halftone areas where even small changes in colour density are readily visible. The behaviour of black ink may differ because of differences in pigment characteristics, ink formulation, and its position in the printing sequence. However, the effect cannot be attributed solely to the strength of the black pigment; ink tack, ink sequence, trapping characteristics, and press settings must also be considered.

From the perspective of offset printing, mottling represents one of the most difficult printability defects because it is not visible before printing (multicolour) is finished and usually cannot be eliminated through conventional press adjustments. Increasing ink density, modifying fountain solution balance, changing printing pressure or adjusting blanket packing often produces limited improvements. Consequently, printers experience longer make-ready times, higher waste, and reduced production efficiency.

2.1. Formation – influence on print quality

WLC (White Lined Chipboard) is not a homogeneous material but a multilayer structure whose final properties result from the interaction between its individual layers. Each layer contributes specific mechanical, structural, and surface characteristics to the finished product. Consequently, print quality cannot be assessed solely based on coating properties; the structure of the cardboard beneath the coated surface must also be taken into consideration. The formation of the cardboard

web in the west end of the machine represents one of the key stages in determining print properties of WLC cardboard. During this stage, fibers suspended in water are distributed and bonded to form layers that subsequently acquire their final properties through pressing, drying, calendaring, coating and finishing. Formation quality depends on several interrelated factors, including the preparation and homogeneity of the stock, fiber characteristics, headbox operation, the relationship between jet velocity and machine speed and drainage conditions. Fiber orientation is also an important aspect of the formation process. Fibers may be distributed in different directions, and their degree of orientation influences certain mechanical and structural properties of the material (stiffness MD/CD). Changes in fiber orientation and local fiber distribution can have an effect on possible mottling appearance. The middle layer (filler ply) accounts for the largest proportion of the overall cardboard structure. Its formation influences fiber distribution, local basis weight, porosity, and the compactness of the cardboard web. If local variations in fiber concentration or distribution occur during formation, areas with different densities and different responses to calendaring and drying may develop. These variations can be transferred to the print ply and consequently, to the coating, thereby affecting the final surface structure, i.e. final print quality. The top layer intended for printing (print ply) plays a more direct role in determining surface properties. Its uniformity, fiber distribution and coating acceptance characteristics influence the extent to which a uniform cardboard surface can be achieved. If the print ply is insufficiently homogeneous, the coating may exhibit locally varying penetration into the substrate, uneven distribution and differences in its ability to form a smooth, uniform surface layer. Non-uniformity in the substrate may affect the uniformity of top-layer formation and subsequently contribute to variations in the cardboard surface during pressing, drying, and coating.

One of the key parameters is basis weight, which represents the mass of material per unit area and is expressed in g/m². In addition to the average basis weight, its local distribution is also important. Cardboard may have an acceptable average basis weight while still containing small areas with different local fiber concentrations. Such variations can affect local porosity, thickness and surface absorption. All this can lead to the appearance of mottling.

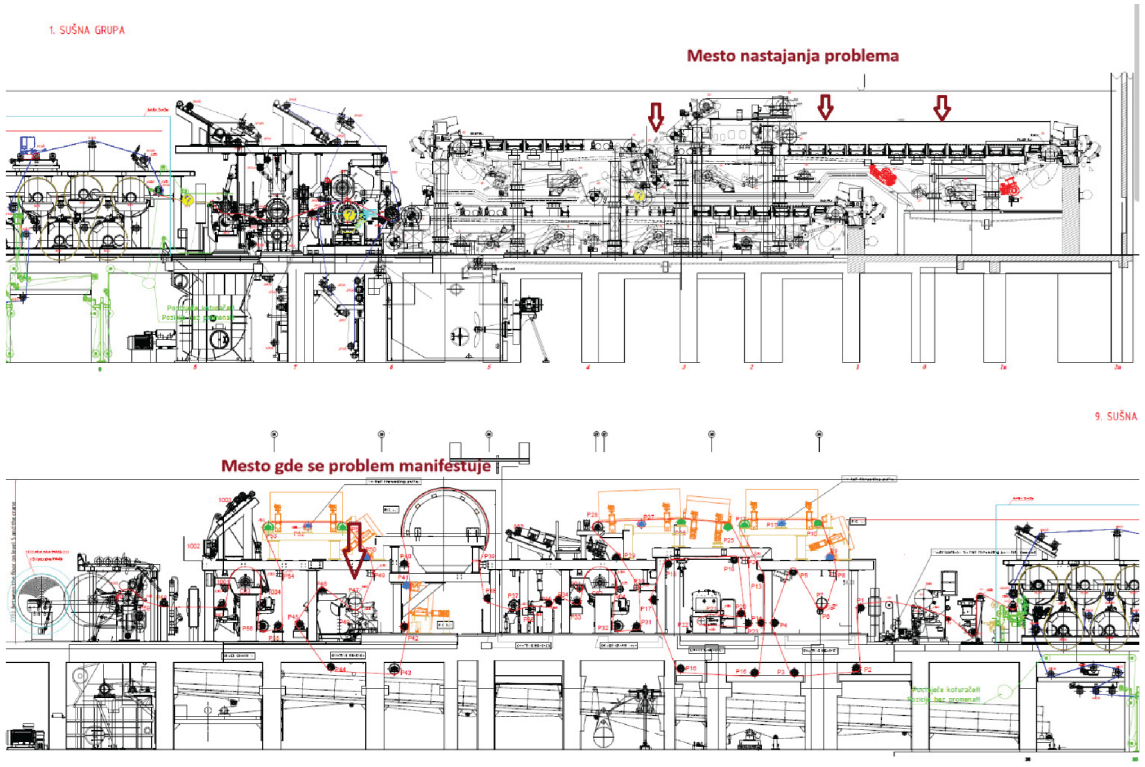
Porosity determines the extent to which the material structure contains interconnected or isolated pores through which, in the case of board production and coating formulations, penetration can occur. Depending on the size, distribution and connectivity of these pores, different areas of the cardboard may exhibit different behaviors during coating application and ink transfer (Karlovits, Lavrič & Nemeš, 2018). Surface absorption is also an important factor, as it influences the rate and extent to which the ink penetrates the material. If absorption varies across the surface, differences may occur in ink transfer, ink setting and the final optical appearance of the printed image.

The purpose of coating is to provide the appropriate smoothness, coverage, and surface properties required for high-quality printing (brightness). However, the coating's ability to form a uniform surface also depends on the properties of the base board, including its smoothness, porosity, absorptiveness and structural homogeneity (Rousu, Gane, Eklund, 2005; Preston, Nutbeem & Chapman, 2011). Consequently, defects in the underlying cardboard structure may be reflected in the final coated surface, even when the coating process parameters remain stable. It is particularly important to emphasize that mottling cannot be regarded solely as a surface defect originating during coating. Coating is one of the final stages in which the printing surface is formed. However, the properties of this surface depend mostly on the characteristics of the underlying substrate. If irregularities develop during the formation stage, subsequent processing operations may mitigate their effects, but they may not be able to eliminate them.

2.2. Wet end optimisation

Wet-end optimisation involves the adjustment of process parameters to achieve the most uniform fiber formation possible. In the context of mottling reduction, optimisation focuses on improving the formation of the middle and top plies, minimising local variations in fiber distribution and ensuring a more uniform substrate prior to coating application. Attention must also be given to the proportions of different recovered paper grades used during stock preparation. One of the fundamental prerequisites for process stability is the consistent dosing and thorough mixing of different raw materials. Recovered old corrugated containers (OCC) are used in the preparation of the middle ply. OCC typically contains relatively long fibers originating from corrugated packaging materials, which contribute to the stiffness and bonding potential of the resulting fiber network. Although these longer fibers promote inter-fiber bonding, their arrangement may leave voids within the fiber structure. These spaces can be partly filled by shorter fibers obtained from recovered coated cardboard, other suitable graphic paper grades and mixed recovered paper.

The purpose of incorporating these materials is not merely to modify the overall furnish composition, but also to achieve a more balanced distribution of long and short fibers. An appropriate combination of fiber lengths can contribute to a more uniform fiber network and improve the structural consistency of the paperboard. The resulting properties depend on the quality and condition of the recovered fibers, their relative proportions and the effectiveness of stock preparation.



» **Figure 1:** *The cardboard production machine setup in Umka board mill*

Following stock preparation, ply formation represents another critical stage in the production process. At this stage, stock consistency and the operating conditions of the shake roll in the middle-ply forming section should be evaluated together, as both may influence fiber distribution, inter-ply bonding, and the uniformity of the paperboard web. Their effects should be assessed in relation to the specific configuration and operating conditions of the board machine. The top ply determines surface smoothness and print quality, whereas the middle plies carry primary bulk. Properties of the middle ply, such as fiber type and density distribution, influence the through-thickness properties and overall stability of the top layer (Nygårds, 2022; Lindberg & Kulachenko, 2022). The relationship between stock consistency and formation quality is influenced by several interacting process variables, including drainage conditions, flow characteristics, and the operating parameters of the forming system.

In particular, lower stock consistency at the point of ply combination may promote more uniform formation of the baseboard and its surface. Under the operating conditions considered in this study, a minimum consistency of 9% is specified as a process constraint and should not be interpreted as a universally applicable threshold. The optimum value must be established according to the design of the forming section, the characteristics of the furnish and the required paperboard properties. From the perspective of print quality, wet-end optimisation should be considered an integral part of a comprehensive strategy for reducing mottling, rather than an isolated measure aimed solely at improving the final coated surface.

3. Materials and methods

Amsterdam 2, an instrument from Dutch company IGT (Figure 2.), is the main testing equipment for top ply, coating and mottling analysis. Tests are done multiple times during a shift – every change of grammage or quality.

The IGT Amsterdam 2 printability tester enables laboratory simulation of offset printing and assessment of the printing performance of cardboard. The instrument can be used to evaluate two types of mottling: water mottling and back-trapping mottling. While there are several other techniques to evaluate mottling from the printing perspective (Jurič et al., 2015), the IGT test methods are mainly used as an industry standard method in the paper and cardboard making industry.

These tests help distinguish between mottling associated with the absorptive properties of the cardboard substrate and mottling that may arise from interactions between successive ink films during multicolour printing.

The water mottling test simulates the interaction between the dampening solution and the cardboard surface during offset printing. In this procedure, water is applied to the paperboard using a dedicated dampening roller, simulating the action of the dampening system and the presence of water on the printing plate in an offset printing press. The purpose of this test is to determine whether the substrate itself contributes to mottling under controlled laboratory conditions.



» **Figure 2:** *IGT Amsterdam 2 lab testing device*

The back-trapping mottling test is particularly relevant when the water mottling test shows no significant mottling, but the customer experiences mottling during production printing. In such cases, the investigation can be extended to assess whether interactions between successive ink films, including their rheological properties and tack, contribute to the observed defect (Lee et al., 2021). The resulting print is evaluated for local variations in colour reproduction and uniformity. If mottling occurs under these conditions despite satisfactory results in the water mottling test, the findings may indicate that ink–ink interactions or other printing-process variables contribute to the defect, rather than substrate absorptiveness alone. However, this interpretation should be confirmed by considering the actual printing conditions, ink properties, and press settings (Ozaki, Bousfield & Shaler, 2008; Kim, Pollock & Wittbrodt, 1997).

The IGT Amsterdam 2 enables multiple cardboard samples to be tested within a short period, with individual tests typically completed within approximately 30 minutes, depending on the test configuration and procedure. This facilitates the comparative assessment of samples produced under different manufacturing conditions or obtained from different production batches. By combining water mottling and back-trapping mottling assessments, the laboratory method provides a practical means of distinguishing between different potential mechanisms responsible for mottling. The results can support root-cause investigations, guide corrective actions in paperboard manufacturing and printing, and contribute to improved print quality in WLC applications.

4. Experimental part – test printing

Laboratory testing and simulation play a key role in quality control; however, their true value can only be established under actual production conditions. Customer trials, conducted under commercial offset printing conditions, provide the final validation of whether laboratory-derived parameters reliably predict the behavior of paperboard on multicolour printing presses. For customer printing trials, paperboard samples are selected from the same production batches previously assessed using the IGT Amsterdam 2 printability tester. The selection includes samples for which testing has confirmed stable printing performance, as well as samples, where available, for which a potential risk of mottling has been identified. Using samples from the same production batches enables a more reliable comparison between laboratory findings and performance under commercial printing conditions. It also helps establish whether the observed differences in print uniformity are associated with paperboard characteristics or with variations in the printing process.

Although laboratory conditions cannot be fully replicated in a commercial printing environment, the customer trial is conducted under controlled and documented press conditions to ensure reliable comparisons.

The main printing parameters to be monitored include:

- Constant printing speed: 10,000–12,000 sheets per hour, where compatible with the press configuration and job requirements.

- Printing pressure: cylinder pressure and impression settings adjusted according to the paperboard's basis weight, calliper and press specifications.
- Dampening solution: controlled dosage and pH, with particular attention to their influence on ink–water balance and their relevance to the laboratory water mottling assessment.
- Ink application and colour density: stable ink supply and monitoring of printed colour density using a densitometer or spectrophotometer on the colour control strip

4.1. Ink sequence and back-trapping assessment

On a multicolour offset press, the standard ink sequence is monitored and documented. Depending on the press configuration and printing requirements, a sequence such as K–C–M–Y (black, cyan, magenta, yellow) may be used. Particular attention is given to the interaction between successive ink films, especially where magenta and yellow are printed over previously deposited cyan. Under certain conditions, differences in ink tack, rheological properties and trapping behaviour may disturb the previously transferred ink film on the blanket. This can result in local variations in colour density and a mottled appearance. The trial therefore assesses whether the back-trapping effects observed during laboratory testing can also be identified under commercial printing conditions.

Once the press has reached stable operating conditions, printed sheets are collected at defined intervals, for example, after every 500 or 1,000 impressions. Sampling intervals should remain consistent throughout the trial and should cover the relevant stages of the production run.

4.2. Instrumental assessment

These results are compared with the quantitative measurements obtained from the IGT Amsterdam 2 system, including high-resolution image-analysis data was supported by the instrument's configuration. Because laboratory and commercial systems may use different measurement principles, the comparison should be based on appropriately defined and validated indicators rather than assuming direct numerical equivalence.

4.3. Visual assessment under standardized illumination

Printing operator and quality-control personnel visually inspect critical printed areas under standardised viewing conditions. Attention is on large solid areas, light cyan and magenta, midtone regions and smooth tonal gradients, where variations in print uniformity may be visible. The visual assessment determines whether mottling observed during laboratory testing is also apparent in the commercial print and whether its location and visual characteristics are consistent with the laboratory findings. By combining instrumental measurements with visual evaluation, the customer trial establishes a practical correlation between laboratory printability results and actual press performance. This approach supports the identification of the dominant mottling mechanism and helps determine whether corrective actions should focus on paperboard manufacture, ink formulation, press settings, or a combination of these factors.

5. Conclusions

Mottling is a print-quality defect that becomes visible during offset printing, but may originate from variations in the structure and surface properties of WLC paperboard. The formation of the middle ply (filler ply) and the top ply (print ply) is particularly important, as it influences substrate uniformity, absorptiveness and the performance of the coated surface. Also, influence on appearance of mottling during offset printing (high-end quality) can be a result of processes on the printing machine. To minimise mottling, a systematic optimisation program was implemented in the mill, on the board machine, i.e. on the wet end. Process adjustments focused primarily on improving middle and print ply formation at the wet end, jet-to-wire ratio and formation uniformity. These measures aimed to reduce local variations in fiber orientation before applying coating. Wet-end optimisation, including control of furnish composition, stock preparation, and ply formation, offers opportunities to minimise structural variations and reduce the risk of mottling.

The successful implementation of process modifications was continuously evaluated using the IGT Amsterdam 2 printability tester, which enabled laboratory simulation of offset printing under controlled conditions. Standardised mottling test prints were produced on samples collected during production, allowing objective comparison of print uniformity. The laboratory results were correlated with commercial offset printing trials and demonstrated that improvements in formation resulted in measurable reductions in mottling intensity and more stable ink transfer. The IGT Amsterdam 2 printability tester enabled controlled laboratory assessment of water and back-trapping mottling, while commercial printing trials establish whether laboratory findings reflect actual press performance. Effective mottling reduction therefore requires an integrated, process-oriented approach, beginning with wet-end optimisation at the board machine and extending through laboratory evaluation to validation under commercial printing conditions. This approach supports more reliable identification of defect mechanisms and helps determine whether corrective measures should focus on cardboard, printing parameters or both.

6. References

Fahlcrantz, C.M. and Johansson, P. (2004) *Print Mottle Evaluation of Flexographic Prints – Using a Scanner-Based Measurement System*. STFI-Packforsk Report No. 42. Stockholm: STFI-Packforsk.

Jurič, I., Karlović, I., Novaković, D. and Tomić, I. (2015) 'Comparative study of different methods for the assessment of print mottle', *Color Research & Application*, 41(5), pp. 493–499. DOI: 10.1002/col.21984

Karlovits, I., Lavrič, G. and Nemeš, T. (2018) 'The influence of micro and macro porosity of paper on wet repellence mottling in offset printing', *Journal of Graphic Engineering and Design*, 9(2), pp. 21–26. DOI: 10.24867/JGED-2018-2-021

Kim, L., Pollock, M. and Wittbrodt, E. (1997) 'Reduction of back-trap mottle through optimisation of the drying process for paper coatings'. In: *TAPPI Coating Conference Proceedings*. Philadelphia, PA: TAPPI Press, pp. 125–136.

Lee, H.L., Youn, H.J., He, M. and Chen, J. (2021) 'Back-trap mottle: A review of mechanisms and possible solutions', *BioResources*, 16(3), pp. 6426–6447. DOI: 10.15376/biores.16.3.Lee

Lindberg, G. and Kulachenko, A. (2022) 'The effect of ply properties in paperboard converting operations: A way to increase formability', *Cellulose*, 29, pp. 6865–6887. DOI: 10.1007/s10570-022-04673-9

Nygårds, M. (2022) 'Relating papermaking process parameters to properties of paperboard with special attention to through-thickness design', *MRS Advances*, 7(33), pp. 789–798. DOI: 10.1557/s43580-022-00282-7

Ozaki, Y., Bousfield, D.W. and Shaler, S.M. (2008) 'Characterisation of coating layer structural and chemical uniformity for samples with backtrap mottle', *Nordic Pulp & Paper Research Journal*, 23(2), pp. 247–253.

Preston, J.S., Nutbeem, C. and Chapman, R. (2011) 'Impact of pigment blend and binder level on the structure and printability of coated papers'. In: *PaperCon 2011*. TAPPI.

Rousu, S., Gane, P. and Eklund, D. (2005) 'Print quality and the distribution of offset ink constituents in paper coatings', *TAPPI Journal*, 4, pp. 9–15.

© 2026 Authors. Published by the University of Novi Sad, Faculty of Technical Sciences, Department of Graphic Engineering and Design. This article is an open access article distributed under the terms and conditions of the Creative Commons Attribution license 4.0 Serbia (http://creativecommons.org/licenses/by/4.0/rs/).

https://doi.org/10.24867/GRID-2026-p24

Fire Safety in the Printing Industry: The Curious Case of the Missing Literature

ABSTRACT

Printing facilities have significant fire and explosion hazards, i.e., combustible paper and toner dust, flammable inks and cleaning solvents, ignition sources from electrical equipment, and static electricity generated during high-speed printing processes. Despite these hazards, the extent of peer-reviewed fire research dedicated to the printing industry remains unclear. This study addresses this gap through a PRISMA-guided systematic review of the academic literature, supplemented by a structured review of key grey literature sources. The academic search was conducted across Scopus, IEEE Xplore, and ScienceDirect for publications in the past 10 years. A total of 314 articles were identified, of which only 4 met the eligibility criteria, and only 1 directly investigated fire or explosion hazards in a printing-adjacent facility. To complement the limited academic evidence, the grey literature review examined widely adopted technical guidance, including FM Global Data Sheets 7-96 (Printing Plants), 3-26 (Fire Protection for Nonstorage Occupancies) and the UK Health and Safety Executive (HSE) guidance on Fire and Explosion Risks in Printing. The findings reveal that the fire-safety knowledge base for the printing industry exists predominantly within technical standards, insurer guidance, and regulatory documents rather than peer-reviewed publications. This work highlights a critical research gap and identifies priorities for future fire research to strengthen the scientific evidence base supporting fire-safety design and risk management in printing facilities.

August Eriksson
Oisik Das

Luleå University of Technology, Luleå, Sweden

KEY WORDS
Fire safety in printing, printing industry, printing plant, fire protection

1. Introduction

Printing industry in many of its forms is at a significant risk when it comes to the fire and explosion hazards. The reason is mainly the fact that the printing plants combine some of the ingredients that the fire safety engineers tend to be wary of the most: large volumes of flammable liquids and large quantities of finely divided combustible solids, often in the same room as heat sources and static-generating machinery.

Pre-press operations, ignitable liquids, printing press operations, drying, storage and waste are where most common major hazards occur. In pre-press, depending on the printing technique there is often a use of paper, film and other photographic chemicals that aid in the process of printing plate creation. Again, depending on the printing technique printing presses are made out of rubber or plastic and coated with different solutions. Volatile organic compounds (VOC) or chemicals responsible for the vapor emission, the use of hydraulic systems, ignition sources that can happen due to the static or other electrical equipment and high combustible loading are some of the hazards during the printing press operations. Liquids such as different inks and dyes, and Ferric Chloride solution for plate making together with different adhesives are the ones commonly pointed out as high-risk substances during the press process. Similar risk can be found during the drying processes due to the high temperatures, lack of residue cleaning in dryer exhausts and vapor release.

Finally, storage facilities that are in relation to the printing facilities pose as a fire hazard as well (Logic, 2021).

In the context of the flammable and combustible liquids solvent-based inks, cleaning solvents (toluene, xylene, hexane, isopropyl alcohol, acetone, methyl ethyl ketone, ethyl acetate, glycol ethers, kerosene), fountain solutions, and blanket washes are used heavily in gravure, flexographic, and offset printing. Many of the printing operations can involve flammable materials, for example: coatings, inks, and cleaning solvents. These materials together with low flashpoint chemicals and suspended paper dust and spray powder can create significant fire and explosion risks. Gravure printing in particular normally uses solvent-based inks classified as Class 1A flammable liquids under NFPA 30 (Logic, 2021; YassamineEbadat, 2023).

Another risk that can be found in printing processes is in relation to the combustible dust. Paper dust, powder coatings, and starch accumulations are a recurring explosion hazard. Dust accumulations in paper and printing operations can lead to increased fire and explosion possibilities. In (Sun et al., 2026) researchers specifically modeled the risk in relation to VOCs and paper dust. In their research, it was pointed out that higher concentrations of paper powder combined with VOCs significantly enhance flame brightness, combustion intensity, heat release rate, and flame duration. The same paper reported two incidents: in 2008, solvent gasoline vapor at a printing factory in Changchun exploded when ignited by a spark, killing two and injuring two, and in 2025 a color printing factory fire in Fuzhou ignited paper and other flammable materials, causing four deaths and significant economic damage. Static-related incidents have also occurred. In 2011 explosion in the Netherlands was traced to a static discharge occurring during the manufacture of a flammable solvent-based ink. Beyond static discharge, conventional ignition sources common to industrial settings such as faulty wiring, overheating equipment, and heat-generating dryers and curing units are also present in printing environments. Drying and UV-curing systems in particular have been linked to solvent vapor accumulation and localized paper ignition (YassamineEbadat, 2023).

Considering the possible fire hazard in the printing processes, this paper aims to conduct the literature review across different scientific data basses and possess two questions:

RQ1: To what extent is the scientific literature in the past ten years dealing with the topic of fire safety in printing industry?

RQ2: Can so-called “gray literature” supplement the scientific literature?

Together with the introduction and conclusion, this paper consists of the following sections: section 2 describes the methodology of the literature review, showcasing it through the PRISMA diagram, section 3 briefly discusses the results, while the discussion with the answers to the research questions is in the section 4.

2. Methods

In order to answer research questions, a two-stage methodology combining a PRISMA-guided systematic review of peer-reviewed academic literature together with a review of grey literature was employed. The systematic review followed the Preferred Reporting Items for Systematic Reviews and Meta-Analyses (PRISMA) (Page et al., 2021). Given the anticipated scarcity of printing-specific academic research, the review was supplemented by a targeted grey literature review of technical standards, insurer loss-prevention guidance, and regulatory documentation, recognized sources of applied fire-safety knowledge in industries where formal research output is limited.

A systematic search of the academic literature was conducted across three databases: Scopus, IEEE Xplore, and ScienceDirect. These databases were selected to capture engineering, fire-safety science, and applied industrial-safety literature across both technical and multidisciplinary indexing platforms. Searches were limited to articles and journal papers published in English within an open-access model over the preceding ten years.

Search terms combined core hazard concepts (e.g., "fire safety," "fire protection," "fire risk," "fire hazard," "combustible dust," "dust explosion," "explosion protection") with industry- and process-specific terms (e.g., "print*," "printing plant," "printing industry," "printing press," "flexograph*," "gravure," "lithograph*," "letterpress," "screen printing") using Boolean operators. Exclusion terms ("3D print*," "additive manufactur*," "rapid prototyping," "printed circuit board*," "PCB") were applied at the search-string level in Scopus and IEEE Xplore to filter out unrelated additive-manufacturing and electronics literature returned by keyword overlap. Because ScienceDirect's advanced search interface could not accommodate the full combined query, three narrower sub-searches were run and their results pooled.

2.1. Eligibility Criteria and Screening

Records identified through the database searches were screened by title and abstract against predefined eligibility criteria. Studies were eligible for inclusion if they:

14. were published as a peer-reviewed journal article in English, in an open-access outlet, within the ten-year search window, and

15. directly addressed fire or explosion hazards, risk factors, or mitigation measures relevant to printing operations, printing-adjacent facilities, or printing materials.

Studies were excluded if the hazard or process described was unrelated to printing (e.g., general electrical fire detection, construction site firefighting equipment, mining, media/broadcast "printing" in the journalistic sense) or if the printing-related term matched only incidentally to an unrelated topic (e.g., "printed circuits" or a stray keyword tag).

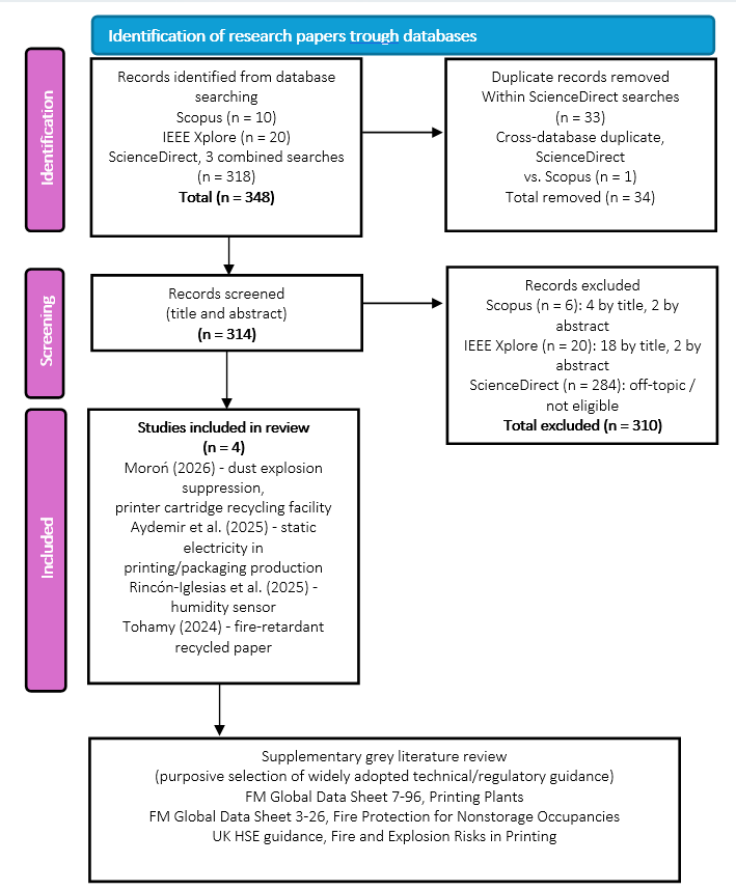
The combined search across the three databases returned 348 raw records (Scopus, n = 10; IEEE Xplore, n = 20; ScienceDirect, n = 318 across three combined sub-searches). Thirty-four duplicate records were removed: 33 internal duplicates arising from the overlap between ScienceDirect's three sub-searches, and one cross-database duplicate in which a ScienceDirect result independently matched a record already retrieved through Scopus. This yielded 314 unique records for title/abstract screening. Of these, 310 were excluded.

1. 6 from Scopus (4 by title, 2 by abstract),
2. 20 from IEEE Xplore (18 by title, 2 by abstract), and
3. 284 from ScienceDirect as off-topic or ineligible

This selection left four studies that met the full eligibility criteria. Of these four, one (Moroń, 2026) directly investigated a fire or explosion hazard within a printing-adjacent facility; the remaining three addressed materials or phenomena relevant to printing (static electricity generation, fire-retardant paper composites, a printed sensor referencing fire-safety applications) without directly studying hazard mechanisms at a printing facility itself. Included papers (Tohamy, 2024; Aydemir et al., 2025; Rincón-Iglesias et al., 2025; Moroń, 2026) together with the gray literature (Fire and Explosion Risks in Printing- HSE, n.d.; FM Global, 2019, 2023, 2026) will be looked over in this paper. This screening process is summarized in a PRISMA flow diagram shown in Figure 1.

2.2. Data Extraction and Synthesis

For each of the four included academic studies, data extracted included the hazard mechanism addressed, the printing process or material system studied, study methodology, and key findings relevant to fire or explosion risk. For grey literature sources, extracted content focused on hazard classifications, prescribed engineering and administrative controls, and occupancy- or process-specific protection recommendations.



» **Figure 1:** *PRISMA with the literature review details*

2.3. Limitations of the Review Approach

The systematic search was limited to three databases and a ten-year window, which may have excluded older foundational studies or literature indexed exclusively elsewhere. ScienceDirect's search interface constraints required splitting the query into three sub-searches, introducing a higher internal duplicate rate (33 of 318 raw records) than the single-query searches used in Scopus and IEEE Xplore; this is a methodological artifact of the platform. The grey literature review was purposive rather than exhaustive, focused on the most widely adopted guidance documents rather than a comprehensive survey of all available industry publications. The marked disparity between the volume of grey literature guidance and the paucity of peer-reviewed academic validation (four included studies, only one directly on-topic) is itself a central finding of this review and is examined further in the Discussion.

3. Results

The systematic search identified 348 raw records across Scopus (n = 10), IEEE Xplore (n = 20), and ScienceDirect (n = 318, pooled from three combined sub-searches). After removing 34 duplicate records, 33 arising from overlap between the ScienceDirect sub-searches and one cross-database duplicate shared between ScienceDirect and Scopus, 314 unique records remained for title/abstract screening. Screening excluded 310 records (Scopus, n = 6; IEEE Xplore, n = 20; ScienceDirect, n = 284), leaving four studies that met the full eligibility criteria, approximately 1.3% of the initial pooled record set. The PRISMA flow diagram (Figure 1) summarizes this process.

Notably, IEEE Xplore contributed zero included studies despite returning 20 records; all were excluded at the title (n = 18) or abstract (n = 2) stage, primarily because the search terms matched unrelated topics such as general electrical fire detection, firefighting equipment inspection, or incidental keyword overlaps (e.g., "printed circuits," a stray "Printing" tag on a forest-fire UAV study). This suggests limited direct engagement with printing-industry fire safety within the venues indexed by IEEE Xplore.

Of the four included studies, only one (Moroń, 2026) directly investigated a fire or explosion hazard within a printing-adjacent facility. This study examined dust explosion risk from toner powder in a laser-printer-cartridge recycling installation, combining hazard-zone identification with laboratory-scale and full-scale on-site testing, and demonstrated that continuous dosing of inert dust achieved greater than 90% explosion suppression.

The remaining three included studies addressed hazards or materials relevant to the printing sector without directly studying a printing facility's fire or explosion risk:

(Aydemir et al., 2025), reviewed the causes, effects, and mitigation of static electricity across printing and packaging production processes, including its role in fire risk, though the study is framed as a broad process and quality-control review rather than a facility-level hazard investigation.

(Tohamy, 2024), developed a fire-retardant composite paper (carbon nanotube/gelatin-enhanced recycled printed paper) and characterized its flame-retardancy properties, addressing material-level fire resistance rather than facility hazard management.

(Rincón-Iglesias et al., 2025), developed an inkjet-printed humidity sensor and noted potential fire-safety monitoring applications, but did not investigate fire or explosion hazards arising from the printing process itself.

3.1. Findings from the Grey Literature Review

In contrast to the sparse academic record, the grey literature review identified substantial, well-established technical guidance addressing fire and explosion hazards in printing facilities.

Printing operations present a distinctive risk profile that spans two normally separate regulatory domains: process fire/explosion safety and occupational chemical exposure.

FM Global's general nonstorage occupancy standard (FM Global, 2019) establishes hazard categories HC-1 to HC-3 based on combustible loading, and explicitly nominates "printing plants" as an HC-3 example under manufacturing occupancies, alongside "coating and printing" operations (FM Global, 2019). This baseline classification is significant because it frames printing as a heavier-than-typical industrial hazard even before ignitable liquids or in-process storage are considered. Indeed, the printing plants data sheet (FM Global, 2023) directly cross-references (FM Global, 2019), recommending that press rooms with little or no in-process storage be protected as HC-3 occupancies under that standard, while rooms with excess ignitable liquid, paste ink, or roll-stock storage escalate to occupancy-specific standards such as ignitable liquid storage or Class 1 to 4 and plastic commodity protection.

Across both FM Global sheets, ignitable liquids emerge as the central fire hazard rather than an incidental one. (FM Global, 2023) catalogues inks, solvents, blanket wash, hydraulic fluid, press lubrication fluid, and heat transfer fluid as ignitable liquids intrinsic to the press itself, and distinguishes low flash point (<200°F/93°C)

from high flash point paste ink liquids (≥200°F/93°C) because this threshold determines whether automatic sprinklers alone are adequate or whether special suppression (typically local-application CO_2) is required. This is reinforced structurally: staging, storage, and mixing of these liquids beyond quantities in (FM Global, 2023) defer to the dedicated ignitable liquid operations standard (FM Global, 2026), which governs containment, drainage, piping, and dispensing-station design.

A recurring theme in (FM Global, 2023) is that printing presses are architecturally resistant to conventional ceiling-level sprinkler protection because catwalks, enclosures, mezzanines, and archways shield the fire source from above (FM Global, 2023). The data sheet's support section states plainly that ceiling sprinklers alone will not adequately protect most printing presses, and that protecting a press is fundamentally a two-part problem: routing water near concealed spaces, and ensuring it is positioned to actually intercept the fire.

4. Discussion

Following the literature review, it became obvious that the scientific literature in the past 10 years is lacking with the field specific empirical and experimental research. It is not to say that this kind of research specific to the printing industry is not being done, rather that it is more often than not tightly tied to the specific printing techniques. Such situation is expected, especially since different printing techniques require completely different approaches in building, electrical power, organization and materials requirement. It does not aid this particular case that the printing industry in itself is immensely multidisciplinary, so it is expected that the researchers from different fields write about different aspects of the printing industry.

RQ 1 set the inquiry “to what extent is the scientific literature in the past ten years dealing with the topic of fire safety in printing industry?” The answer is: very limited, and almost entirely indirect. Across three major databases (Scopus, IEEE Xplore, ScienceDirect) covering engineering, applied science, and multidisciplinary research, a search spanning the full ten-year window returned 348 raw records, reducing to 314 unique records after deduplication. Of these, only four studies (1.3%) met eligibility criteria, and of those four, only one study directly investigated a fire or explosion hazard within a printing or printing-adjacent facility (Moroń, 2026).

RQ 2, on the other hand, has a positive answer. This literature review suggests that the gray literature supplements the academic literature, and even substitutes for it in this domain. It can be concluded following the gray literature review is that it builds upon a wide, multidisciplinary field of printing and fire safety and provides readers with condensed information and guidelines.

5. Conclusions

This paper went through the currently available academic literature with the goal to asses the current state of the research interest in the field. The research query that combined core hazard concepts (e.g., "fire safety," "fire protection," "fire risk," "fire hazard," "combustible dust," "dust explosion," "explosion protection") with industry- and process-specific terms (e.g., "print*," "printing plant," "printing industry," "printing press," "flexograph*," "gravure," "lithograph*," "letterpress," "screen printing") using Boolean operators and exclusion terms ("3D print*," "additive manufactur*," "rapid prototyping," "printed circuit board*," "PCB") showed 348 raw records, reducing to 314 unique records after deduplication. Of these, only four studies (1.3%) met eligibility criteria, and of those four, only one study directly investigated a fire or explosion hazard within a printing or printing-adjacent facility. Those papers were analyzed together with selected gray literature, and it can be concluded that the grey literature search returned substantive, actively maintained, sector-specific guidance, capable of summarizing multidisciplinary finds across multiple scientific fields.

This is not to say that the gray literature is ought to replace the academic one, but rather it should be motivation for stronger cooperation between the researchers across academic disciplines.

6. References

Aydemir, C., Altay, B.N. and Steingraeber, J.K. (2025) 'Static electricity in printing and packaging production processes: Causes, effects, and solutions', *The International Journal of Advanced Manufacturing Technology*, 139(7–8), pp. 4199–4210. DOI: 10.1007/s00170-025-16084-8

Health and Safety Executive. (no date) *Fire and explosion risks in printing*. Available from: https://www.hse.gov.uk/printing/fire-explosion.htm [Accessed 15 September 2026].

FM Global. (2019) Data Sheet 3-26: *Fire Protection for Nonstorage Occupancies. FM Property Loss Prevention Data Sheets*. Available from: https://www.fm.com/FMAApi/data/ApprovalStandardsDownload?isGated=-false&itemId=%7B4881E43C-2D4D-4C8A-AC86-B5D-0DA8A973D%7D [Accessed 10 September 2026].

FM Global. (2023) Data Sheet 7-96: *Printing Plants. FM Property Loss Prevention Data Sheets*. Available from: https://www.fm.com/FMAApi/data/ApprovalStandardsDownload?isGated=true&itemId=%-7B404A9285-8C35-4C14-872B-A0C83ABB-2F1C%7D [Accessed 02 August 2026].

FM Global. (2026) Data Sheet 7-32: *Ignitable Liquid Operations. FM Property Loss Prevention Data Sheets*. Available from: https://www.fm.com/FMAApi/data/ApprovalStandardsDownload?itemId=%7B0E226C82-CA57-47C4-8ECB-E384AA589D34%7D [Accessed 10 September 2026].

Logic, R. (2021) *Fire Protection at Printing Plants*. Risk Logic. Available from: https://risklogic.com/fire-protection-at-printing-plants [Accessed 10 September 2026].

Moroń, W. (2026) 'The explosion suppression effects of added limestone dust on minimizing the risk of dust explosions in the printer cartridge recycling installation', *Journal of Loss Prevention in the Process Industries*, 100, 105875. DOI: 10.1016/j.jlp.2025.105875

Page, M.J., McKenzie, J.E., Bossuyt, P.M., Boutron, I., Hoffmann, T.C., Mulrow, C.D., Shamseer, L., Tetzlaff, J.M., Akl, E.A., Brennan, S.E., Chou, R., Glanville, J., Grimshaw, J.M., Hróbjartsson, A., Lalu, M.M., Li, T., Loder, E.W., Mayo-Wilson, E., McDonald, S., McGuinness, L.A., Stewart, L.A., Thomas, J., Tricco, A.C., Welch, V.A., Whiting, P. and Moher, D. (2021) 'The PRISMA 2020 statement: An updated guideline for reporting systematic reviews', *BMJ*, 372, n71. DOI: 10.1136/bmj.n71

Rincón-Iglesias, M., Krebsbach, P., Correia, D.M., Mendes-Felipe, C., Lanceros-Méndez, S. and Hernandez-Sosa, G. (2025) 'Sustainable Fully Inkjet-Printed Humidity Sensor Based on Ionic Liquid and Hydroxypropyl Cellulose', *ACS Applied Materials & Interfaces*, 17(22), pp. 32680–32690. DOI: 10.1021/acsami.5c00505

Sun, S., Xing, C., Pang, L., Hu, Y., Wang, H. and He, C. (2026) 'Study on the Effects of VOCs Concentration on the Explosion Characteristics of Paper Powder', Fire, 9(1), 34. DOI: 10.3390/fire9010034

Tohamy, H.-A.S. (2024) 'Greener, Safer Packaging: Carbon Nanotubes/Gelatin-Enhanced Recycled Paper for Fire Retardation with DFT Calculations', Journal of Renewable Materials, 12(12), pp. 1963–1983. DOI: 10.32604/jrm.2024.054977

YassamineEbadat. (2023) *Shocking: Printing, Solvents & Thin Films. Stonehouse Process Safety*. Available from: https://stonehousesafety.com/shocking-printing-solvents-thin-films/ [Accessed 03 September 2026].

© 2026 Authors. Published by the University of Novi Sad, Faculty of Technical Sciences, Department of Graphic Engineering and Design. This article is an open access article distributed under the terms and conditions of the Creative Commons Attribution license 4.0 Serbia (http://creativecommons.org/licenses/by/4.0/rs/).

Color science and management

02

Original Scientific Paper https://doi.org/10.24867/GRID-2026-p25

Analysis of Memory Colour Using Selected Foods As an Example

ABSTRACT

In the complex process of recalling a distinct colour, memory plays a crucial role. The accuracy of recall is particularly important in some cases, for example when recognising the colour of food, as it communicates information about its freshness, taste and ripeness. Food manufacturers establish their first contact with consumers through various forms of advertising. To attract attention and encourage purchase, the colour of food must be carefully selected and depicted. This process relies on memory colours for different groups of fruit and vegetables, i.e. the colours of well-known and frequently seen objects. In 2024, a new Preferred Memory Colour (PMC) chart was published, which contains the memory colours of selected objects and foods and enables accurate colour reproduction. The purpose of the present research was to investigate the influence of the mode of colour presentation on the observer's ability to recall a colour sample, namely the colour of fruit or vegetables. In the experiment, three different ways of presenting the colour were used. The experiment took place in a controlled environment under constant observation conditions. The colour vision of the observers was previously checked with the Farnsworth-Munsell 100 Hue test. The test charts were prepared based on the preferred colours of selected foods, and the results were numerically evaluated using the parameters of the CIELAB colour space. The results showed that the accuracy of colour recall is greatly improved with additional directed instruction, due to subconscious associations with a specific object. In addition, it emerged that some food colours are remembered more accurately than others.

Barbara Blaznik
Evelin Pipan
Sabina Bračko

University of Ljubljana, Faculty of Natural Sciences and Engineering, Department of Textiles, Graphic Arts and Design, Ljubljana, Slovenia

KEY WORDS
Colour perception, colour memory, memory colours, food colour, colour recall

1. Introduction

Colour is one of the key attributes of visual communication and influences most of our purchasing decisions (Martinez et al., 2021). It also affects our appetite and food choices, as it is a significant factor in our expectations regarding taste. For most food products, their properties, including colour, change over time through ripening or decay, as well as through processing methods such as baking and cooking (Hutchings, 2010). Every food has an acceptable colour range. If the colour of a particular food does not align with the observer's expectations, it signals that the food is not fresh or ripe, which may deter the consumer from purchasing it (Pathare, Opara & Al-Said, 2013). In everyday life, we often compare colour stimuli separated in time, attempting to match the colour currently being observed with the one held in our memory (Bodrogi & Tarczali, 2001). When buying fruit, for example, we select a product based on the image we hold in our memory. In this process, we must rely on our colour memory.

Food companies establish their first contact with consumers through advertisements, promotional catalogues and attractive packaging. To encourage purchase, the colour of products must be accurately represented, as this reflects their quality. In 2024, the new Preferred Memory Colour (PMC) chart was published, enabling an accurate assessment of colour reproduction quality and including 30 samples of associative colours, i.e. the colours of well-known and frequently seen objects (Luo, 2024). A memory colour is the colour of a well-known

and frequently seen object, a colour that becomes part of the memory representation of an object and constitutes an individual's standard for familiar objects (Granzier & Gegenfurtner, 2012). A specific associative colour, or our mental image of a colour, may influence the objective perception of that colour. The memory colour effect is based on the premise that an object is strongly associated with a typical colour and that the observer is well acquainted with the object (Valenti & Firestone, 2019).

Research on the influence of memory for the colour of familiar objects, primarily food, has shown that preferences for red, yellow, and green shades increase as colour samples approach a specific associative colour, whereas the effect is less pronounced for blue and purple samples (Liao & Yoshizawa, 2024). It has also been found that the accuracy of colour matching for familiar objects in long-term recall can vary among observers due to individual colour preferences and colour memory (Seliger, 2002). The purpose of the present research was to investigate the influence of the mode of colour presentation on observers' ability to recall a colour sample, specifically the colours of fruit and vegetables. The test charts were prepared based on the preferred colours of selected foods and the results were evaluaed using the parameters of the CIELAB colour space.

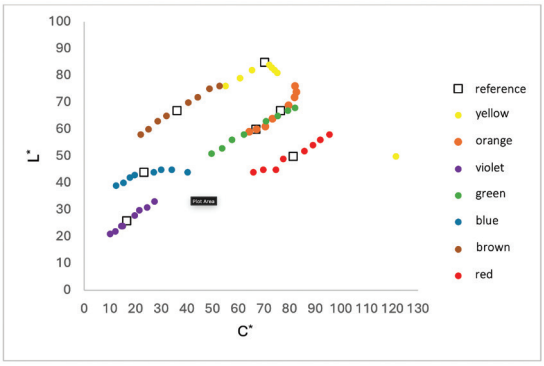
2. Methods

2.1. Preparation of reference colours and samples

Reference colours were obtained from seven food items (banana, pumpkin, aubergine, lime, blueberry, ginger, tomato) selected to cover a wide colour range. Photographs of each item were sourced from Adobe Stock and opened in Photoshop, where colour values (Hue, Saturation, Brightness) were extracted from five random points and used as the final reference colours (Figure 1).

2.2. Selection and adjustment of samples

For each reference colour, eight samples were created by adjusting hue (±2 units), saturation and brightness (±3 units). Additional fine adjustments (1–3 units) were made when samples appeared visually inconsistent with the colour set. In Photoshop, colour-adjusted images for the experiment were produced using masked selections and Solid Colour layers set to Colour blending mode.



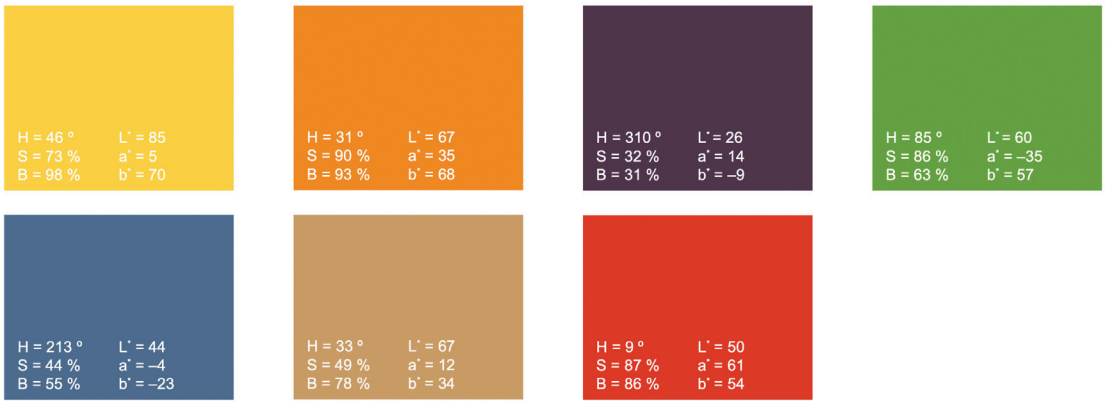
» **Figure 2:** *Selected reference colours and samples in C*L*plane of CIELAB colour space*

2.3. Participants

Seventeen observers (students aged 19–24, 16 female and 1 male) took part in the study. All participants completed the Farnsworth–Munsell 100 Hue Test beforehand. For the experimental part, only those participants with a maximum of four misplacements (0–16 error score) were included. The study was approved by the ethical committee of the University of Ljubljana, Faculty of Natural Sciences and Engineering.

2.4. Viewing conditions

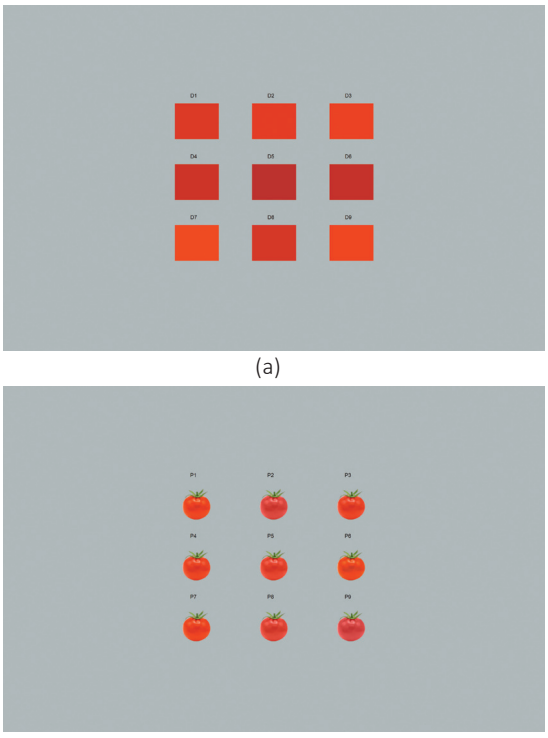
The experiment was conducted in a controlled, as the light source. Observers were seated 77 cm from the screen, positioned perpendicular to it.



» **Figure 1:** *Reference colours with HSB and CIELAB colour values*

2.5. Presentation of Colour Charts

A total of 42 colour charts were prepared, six charts per colour. Each chart included one reference and eight samples, arranged centrally on a neutral grey background (L* = 75, a* = –3, b* = –2). Charts differed in using either rectangular colour patches or colour-adjusted photographs (Figure 3).



(a)

(b)

» **Figure 3:** *Colour charts used in the experimental Part 1, 2 (a) and Part 3 (b)*

2.6. Experimental Procedure

Participants first adapted to a neutral grey screen for 5 s, followed by written instructions. They then viewed a colour chart and selected one sample according to the task. Each trial concluded with a 5-second grey-screen interval.

- Part 1 used non-specific instructions (e.g., “Select the basic red colour”).
- Parts 2 and 3 used directed instructions (e.g., “Select the tomato red colour”).

Each colour was tested in six repeated trials.

3. Results and discussion

3.1. Recall of basic colours

In the first part, observers were asked to select, from nine colour samples, the one they perceived as representing a basic colour. The average colour differences regarding the reference colour are presented in Table 1. The calculated CIELAB (Bračko & Blaznik, 2022) colour difference (ΔE*) showed a relatively high deviation. This result was expected due to the use of non-directed instructions and inherent inter-observer variability, as individuals conceptualise “basic colours” differently.

Yellow showed the highest recall accuracy (ΔE* = 2.19), corresponding to a small colour difference. In contrast, blue exhibited the poorest recall (ΔE* = 8.59), representing a very large deviation. Higher variability was also observed for violet, green, orange, and brown, consistent with their classification as secondary or tertiary colours.

Table 1

Recall of basic colours: colour differences (ΔL*, Δa*, Δb*, ΔC*, ΔE*)

Colour	ΔL*	Δa*	Δb*	ΔC*	ΔE*
Yellow	-1.32	-3.03	1.56	4.20	2.19
Orange	3.50	-2.41	4.91	3.50	5.17
Violet	5.47	8.47	-1.68	8.26	7.65
Green	3.12	-5.32	2.85	5.37	4.92
Blue	0.26	6.47	-13.79	13.60	8.59
Brown	-6.38	-0.59	-10.97	-10.28	7.91
Red	3.15	2.03	5.15	5.08	4.98

Analysis of colour attributes showed systematic shifts. Lightness (L*) varied most for brown (ΔL* = –6.38), which observers consistently recalled as significantly darker, likely due to strong real-world associations (e.g. soil, wood, chocolate). Violet (ΔL* = 5.47) was perceived as lighter, while other colours showed smaller deviations (up to 3 units). Blue showed minimal lightness deviation (ΔL* = 0.26). Hue shifts (Δa*, Δb*) revealed clear perceptual biases:

- Violet, blue and red were recalled as more reddish,
- yellow, orange, green and brown as more greenish.

On the b* axes, warm colours (yellow, orange, green, red) shifted towards more yellow tones, while cool colours (violet, blue, brown) shifted towards more blue tones. Observers generally selected more saturated colours, with two notable exceptions:

- blue was significantly oversaturated (ΔC* = 13.60),
- brown was recalled as less saturated (ΔC* = –10.97).

3.2. Recall of colours with verbal association

In the second part, colour samples were presented with a verbal association to specific food items, introducing a semantic context. Observers again selected the most appropriate colour from nine samples.

The results are presented in Table 2. Overall accuracy improved, with an average colour difference of ΔE* = 4.21, indicating a moderate but reduced deviation compared with the first part. This suggests that verbal association enhances colour recall, although the improvement was smaller than expected, likely because colour perception from flat patches lacks the visual richness of real objects.

Yellow remained the most accurately recalled colour (ΔE* = 2.38). In contrast, blue showed the weakest performance (ΔE* = 5.82). Several observers explicitly reported that none of the samples matched their perception of blueberry colour, highlighting the importance of surface texture and material appearance, which cannot be conveyed by simple colour patches.

Table 2

Recall of colours with verbal association: colour differences (ΔL*, Δa*, Δb*, ΔC*, ΔE*)

Colour	ΔL*	Δa*	Δb*	ΔC*	ΔE*
Yellow	–1.88	–0.09	–1.88	4.40	2.38
Orange	1.76	–1.41	2.41	1.68	4.22
Violet	1.00	2.09	–0.29	1.99	4.26
Green	–1.91	3.38	–3.06	–4.28	4.47
Blue	–1.62	1.03	0.53	–0.21	5.82
Brown	1.79	–1.15	3.29	2.92	4.49
Red	1.47	1.00	1.79	2.07	3.83

Deviations in lightness (L*) were minimal (within ±1 unit), indicating relatively stable brightness perception. However, systematic shifts were still observed:

- Orange, violet, brown and red were recalled as lighter,
- yellow, green and blue as darker.

Hue shifts (Δa*, Δb*) revealed consistent perceptual tendencies:

- Violet, green, blue and red shifted towards more reddish tones,
- yellow, orange and brown towards more greenish tones.
- Along the b* axis, orange, violet, brown and red shifted towards more yellowish tones, while yellow and green shifted towards less yellow (more bluish) tones.

In terms of chroma, most colours were recalled as more saturated, with:

- Yellow showing the highest increase in saturation (ΔC* = 4.40),
- green and blue being recalled as less saturated (ΔC* = –4.28) for green.

3.3. Recall of colours from food images

In Part 3, observers selected the most appropriate colour of a food item based on colour-modified photographs, introducing the highest level of visual realism.

This condition produced the highest overall accuracy, with an average colour difference of ΔE* = 3.77, (Table 3) confirming that realistic visual context significantly improves colour recall. Nevertheless, the deviation remained higher than expected, likely due to individual colour preferences and personal interpretations of food appearance.

Yellow once again demonstrated the highest recall accuracy (ΔE* = 2.17), reinforcing its perceptual stability. In contrast, green showed the poorest performance (ΔE* = 7.33), contrary to expectations.

Table 3

Recall of colour from food images – colour differences (ΔL*, Δa*, Δb*, ΔC*, ΔE*)

Colour	ΔL*	Δa*	Δb*	ΔC*	ΔE*
Yellow	–1.82	1.03	–3.09	4.08	2.17
Orange	–2.5	0.74	–3.47	–2.63	4.04
Violet	–2.29	–2.41	1.06	–2.58	3.51
Green	–6.24	10.06	–8.29	–12.13	7.33
Blue	–1.35	–0.26	2.76	–2.50	3.28
Brown	–0.62	–0.65	–1.38	–1.43	3.45
Red	1.71	1.32	3.00	3.04	2.60

Clear and consistent biases were observed across all colour attributes. Lightness (L*) showed the largest deviation for green (ΔL* = –6.24), which was consistently recalled as significantly darker. This result is notable, as such ambiguity would be more typical in abstract conditions, suggesting that even realistic images do not fully resolve interpretative uncertainty (e.g., lime peel vs. interior). Most other colours were also recalled as darker, with the exception of red, which was perceived as lighter. The smallest deviation was observed for brown (ΔL* = –0.62). Hue (a*, b*) shifts confirmed systematic biases:

- Yellow, orange, green and red shifted towards more reddish (less green) tones.
- Violet, blue and brown shifted towards more greenish tones.

- Along the b* axis, violet, blue and red appeared more yellowish (less blue), while yellow, orange, green and brown shifted towards more bluish tones (less yellowish).

Chroma (C*) revealed a different trend compared with parts 1 and 2:

- Most colours were recalled as less saturated,
- green showed the strongest desaturation (ΔC* = –12.13),
- while yellow (ΔC* = 4.08) and red were remebered as more saturated again.

3.4. Best and Worst Recalled Colours

Across all three experimental conditions, yellow was consistently the most accurately recalled colour, supporting the hypothesis that certain colours are inherently easier to remember. Colour differences remained low throughout the experiment (ΔE* = 2.17–2.38), indicating highly stable colour memory. Although yellow was generally recalled with increased saturation (ΔC* = 4.08–4.40), deviations in hue and lightness remained small, suggesting a robust and consistent memory representation.

The least accurately recalled colours varied between experimental conditions. In Parts 1 and 2, blue showed the largest deviations (ΔE* = 8.59 and 5.82, respectively), primarily due to errors in hue and saturation. Observers tended to recall blue as more saturated and shifted in hue relative to the reference colour. This finding may be related to the complex visual appearance of blueberries, where texture and surface characteristics substantially contribute to colour perception.

In Part 3, when realistic food photographs were presented, green was the least accurately recalled colour (ΔE* = 7.33). The largest contribution to the overall colour difference came from a substantial reduction in saturation (ΔC* = –12.13), accompanied by lower lightness (ΔL* = –6.24) and noticeable hue shifts (ΔH* = 4.77). Observers therefore remembered the green food image as both darker and less saturated than the reference.

4. Conclusions

This study investigated how colour memory influences the recall of food colours under different presentation conditions. The results showed that both the presentation format and the type of instruction significantly affect colour recall accuracy.

Observers achieved more accurate colour recall when given directed instructions. Colour memory therefore benefits from semantic context, enabling observers to associate colours with specific food items rather than relying solely on abstract colour categories.

The most accurate recall occurred when colours were presented within realistic food photographs. Compared with abstract colour samples, photographic representations provided additional visual cues that enhanced memory retrieval and reduced overall colour differences.

The findings also show that some food colours are recalled more accurately than others. Yellow was consistently the best-recognised colour across all three experimental conditions, exhibiting the smallest colour differences and the most stable memory representation. In contrast, blue and green showed the largest deviations, indicating that these colours are more susceptible to memory distortions, particularly in hue and saturation.

Although realistic imagery improved performance, colour recall was not perfectly accurate. Observers tended to remember food colours as darker and less saturated than the reference values, while systematic shifts in hue remained evident. These biases suggest that colour memory is influenced not only by visual information but also by personal experience, colour preferences and learned associations with familiar foods.

Overall, the results demonstrate that food colour memory is highly context-dependent rather than purely perceptual. Providing meaningful visual and semantic cues significantly improves recall accuracy, while the stability of yellow compared with blue and green highlights the unequal memorability of different food colours. These findings contribute to a better understanding of memory colours and may support the evaluation and optimisation of colour reproduction in food packaging, advertising and quality control.

5. References

Bodrogi, P. and Tarczali, T. (2001) 'Colour Memory for Various Sky, Skin, and Plant Colours: Effect of the Image Context', Color Research & Application, 26(4), pp. 278–289. DOI: 10.1002/col.1034

Bračko, S. and Blaznik, B. (2022) *Osnove merjenja barv. Priročnik za vaje*. Ljubljana: Univerza v Ljubljani, Naravoslovnotehniška fakulteta.

Granzier, J. J. M. and Gegenfurtner, K. R. (2012) 'Effects of Memory Colour on Colour Constancy for Unknown Coloured Objects', *i-Perception,* 3(3), pp. 190–215. DOI: 10.1068/i0461

Hutchings, J. (2010) Food, expectations, colour and appearance. In: Caivano, J. L. and Lopez, M. L. (eds.) *Proceedings of the Interim Meeting of the International Color Association*, 12-15 October 2010, *Mar del Plata, Argentina*. pp. 17–22.

Liao, S. and Yoshizawa, T. (2024) 'Memory Colors of Familiar Objects Induce General Color Preference', *Color Research & Application,* 49(1), pp. 79–92. DOI: 10.1002/col.22906

Luo, M. R. (2024) 'The New Preferred Memory Color (PMC) Chart', *Color Research & Application,* 49(6), pp. 564-576.

Martinez, L. M., Rando, B., Agante, L. and Abreu, A. M. (2021) 'True colors: Consumers' packaging choices depend on the color of retail environment', *Journal of Retailing and Consumer Services*, 59, 102372. DOI: 10.1016/j.jretconser.2020.102372

Pathare, P. B., Opara, U. L. and Al-Said F. A. (2013) 'Colour Measurement and Analysis in Fresh and Processed Foods: A Review', *Food and Bioprocess Technology*, 6(1), pp. 36–60. DOI: 10.1007/s11947-012-0867-9

Seliger, H. H. (2002) 'Measurement of Memory of Color', *Color Research & Application*. 27(4), pp. 233–242. DOI: 10.1002/col.10067

Valenti, J. J. and Firestone, C. (2019) 'Finding the "odd one out": Memory color effects and the logic of appearance', *Cognition*, 191, DOI: 10.1016/j.cognition.2019.04.003



© 2026 Authors. Published by the University of Novi Sad, Faculty of Technical Sciences, Department of Graphic Engineering and Design. This article is an open access article distributed under the terms and conditions of the Creative Commons Attribution license 4.0 Serbia (https://creativecommons.org/licenses/by/4.0/deed.en).

Original Scientific Paper https://doi.org/10.24867/GRID-2026-p26

Influence of Blender Rendering Engines and View Transforms on Colour Reproduction in 3D Visualisation

ABSTRACT

*This study examines the consistency of displayed colour between Blender's EEVEE and Cycles rendering engines under the Standard, Filmic and AgX view transforms. A test matrix comprising 36 rendered samples (six primary and secondary colours across six engine-transform combinations) was shown on a profiled Philips 288E2 monitor and measured with an i1PRO 3 spectrophotometer using an Argyll CMS workflow. The virtual scene used frontal illumination with a simulated 6500 K, 1000 W light source. Corresponding EEVEE and Cycles measurements were compared using the CIE 1976 colour difference ΔE*ab (hereafter ΔE76). All inter-engine differences were below 1.0. AgX produced the lowest mean ΔE76 (M = 0.234, SD = 0.085), followed by Filmic (M = 0.438, SD = 0.187) and Standard (M = 0.440, SD = 0.207). The largest individual difference was measured for red under Standard (ΔE76 = 0.803). The results indicate that inter-engine agreement was greatest under AgX, although the experiment does not establish absolute colour accuracy or perceptual equivalence.*

Jože Guna
Raša Urbas

University of Ljubljana, Faculty of Natural Sciences and Engineering, Department of Textiles, Graphic Arts and Design, Chair of Information and Graphic Arts Technology, Ljubljana, Slovenia

KEY WORDS
Colour management, Blender, colour difference, rendering engine, view transform, EEVEE, Cycles, AgX

1. Introduction

Colour management is an important part of 3D design and visualisation because the final appearance of rendered colours is influenced by both the rendering method and the view transform used for display. Blender provides the real-time EEVEE engine and the path-traced Cycles engine. A journal study using both engines reported that Cycles produced more realistic illumination, shadows and material reflections at the cost of longer rendering times, whereas EEVEE reduced computational demand with a possible reduction in realism (Malvido Fresnillo et al., 2024). In a colour managed workflow, this rendering stage must also be distinguished from the subsequent conversion of scene-linear image data for display, as the selected view transform can modify tone scale and chromatic appearance.

The investigated view transforms were Standard, Filmic and AgX. Blender documentation describes Standard as applying no additional transform beyond conversion to the display device, Filmic as a tone-mapping transform for high dynamic range colours, and AgX as its successor with improved handling of saturated and highly exposed colours (Blender Foundation, 2023; Blender Foundation, n.d.). Specifically, AgX applies tone-mapping and desaturates highly exposed colours, whereas Standard does not introduce an additional tone-mapping operation beyond display conversion. These differences make the choice of rendering engine and view transform relevant when colour appearance and consistency are important.

The aim of the study was to compare colour reproduction between EEVEE and Cycles under Standard, Filmic and AgX using controlled colour patches and instrumental measurements. The analysis focused on inter-engine colour differences. Because the primary ΔE76 values compare Cycles directly with

EEVEE, the design evaluates relative agreement between the engines rather than absolute accuracy against an independent reference target.

2. Related work

Research relevant to the present experiment can be organised into two connected strands: the effect of the rendering engine on scene generation and rendering, and the effect of the subsequent display or view transform on reproduced colour. Direct journal comparisons of Blender's real-time and path-traced engines remain limited. In a Blender-based pipeline for generating synthetic cable images, Malvido Fresnillo et al. (2024) allowed either EEVEE or Cycles to be used and reported that Cycles produced more realistic illumination, shadows and material reflections, although with longer rendering times. They also noted that using EEVEE reduced computational demand while slightly compromising image realism. Although their task concerned synthetic data for segmentation rather than colour measurement, the study provides journal-based evidence that engine selection can change visual output before colour management processing is considered.

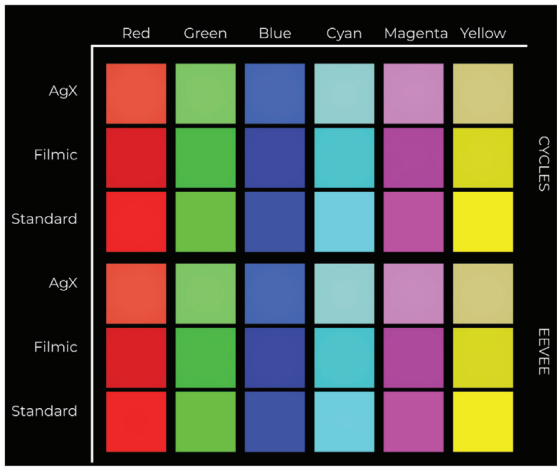
A broader body of work examines the transformation of high dynamic range, or scene referred image data for presentation on displays with a restricted output range. Eilertsen, Mantiuk & Unger (2017) reviewed the reproduction pipeline and categorised a wide range of tone-mapping approaches, emphasising that different operators balance contrast, detail and artefact suppression differently. Their review establishes that a display-ready image is not a neutral representation of the input: the mapping strategy forms a separate processing stage with its own perceptual consequences. This distinction is relevant when Blender outputs are compared across Standard, Filmic and AgX, because a difference in displayed colour may reflect the renderer, the view transform or their interaction. Conventional HDR tone-mapping research therefore provides conceptual context, but it does not directly validate Blender's individual view transforms.

Colour appearance is particularly sensitive at this transformation stage. Mantiuk et al. (2009) demonstrated through subjective appearance-matching experiments that tone-scale manipulation can change perceived colourfulness and that the correction required after contrast compression is nonlinear. Their results show that luminance compression and chromatic appearance cannot be treated as independent variables. More recently, Mehmood et al. (2023) developed a perceptual tone-mapping model based on CIECAM16 correlates of brightness, colourfulness and hue. The model accounts for surround and display conditions and was evaluated using both objective and subjective methods. This work reinforces the importance of evaluating colour management choices in relation to the viewing and display context rather than judging the scene-linear rendering alone.

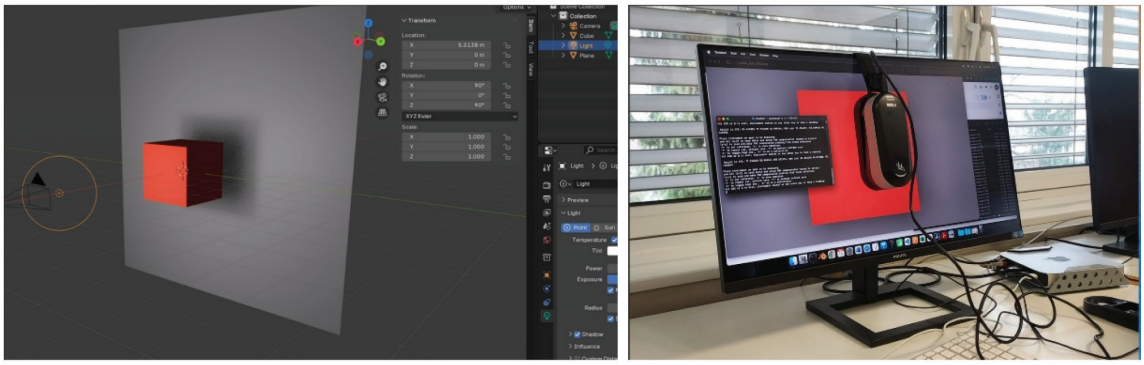
Mehmood, Khan & Luo (2024) extended this line of research with a generic colour correction method for tone-mapping operators. Their approach uses CIECAM16 lightness, chroma and hue, preserves the lightness of the tone-mapped image and the hue of the HDR input, and was validated through objective and subjective assessment. The reported improvement in natural colour reproduction further indicates that transforms designed primarily to compress luminance may also alter chromatic appearance unless colour is explicitly managed. Taken together, the literature supports a methodological separation between rendering and display transformation. However, previous studies have mainly examined rendering realism or tone-mapped natural images; instrumental comparisons of fixed Blender colour patches across both EEVEE and Cycles and multiple view transforms are scarce. The present study addresses this gap by holding the test scene and measurement procedure constant while comparing the two engines under Standard, Filmic and AgX.

3. Methods

The measurement setup comprised an i1PRO 3 spectrophotometer and a Philips 288E2 display. The display was characterised by creating a colour profile, which was then used in the colour measurement workflow. Argyll CMS was used for display characterisation, colour management, measurement acquisition and data processing (Gill, 2026). This distinction is important because display characterisation and profiling describe the behaviour of the physical display, whereas Blender's view transform operates on the rendered scene data before it reaches the display.



» **Figure 1:** *Test colour matrix for Standard, Filmic and AgX in Cycles and EEVEE*



» **Figure 2:** *Blender test scene and physical display measurement setup*

The experiment comprised 36 rendered colour patches: six chromatic colours (red, green, blue, cyan, magenta and yellow), two rendering engines (EEVEE and Cycles) and three view transforms (Standard, Filmic and AgX). The RGB and CMY patches were frontally illuminated by a virtual Blender light source configured to 6500 K, 1000 W. Figure 1 shows the rendered test colour matrix used in the study.

The rendered scene and physical measurement arrangement are shown in Figure 2. Measurements were obtained for corresponding colour samples produced by the two rendering engines. Colour differences between paired Cycles and EEVEE results were expressed as ΔE76 for each tested colour and view transform, following the CIELAB colour difference framework (CIE, 2018). The measured colour coordinates were also plotted on a CIE 1931 x,y chromaticity diagram.

4. Results

4.1. ΔE76 differences between Cycles and EEVEE

The ΔE76 values for the six test colours are shown in Table 1. All measured differences between Cycles and EEVEE were below 1.0. The largest individual difference was 0.803 for red under Standard, while the smallest was 0.147 for yellow under AgX. These values indicate relative differences between engines and are not errors measured against an external colour reference. The mean and sample standard deviation were calculated across the six test colours. The standard deviation represents variation between colours, not measurement uncertainty.

Within AgX, ΔE76 ranged from 0.147 to 0.356; within Filmic, from 0.177 to 0.666; and within Standard, from 0.189 to 0.803. Qualitative inspection of the rendered matrix suggests that Standard and Filmic appeared more similar to each other than to AgX; however, this observation was not assessed in a controlled visual experiment.

Figure 3 visualises the same values without assigning a perceptual threshold to the measured differences.

Table 1

ΔE76 differences between Cycles and EEVEE for the tested colours

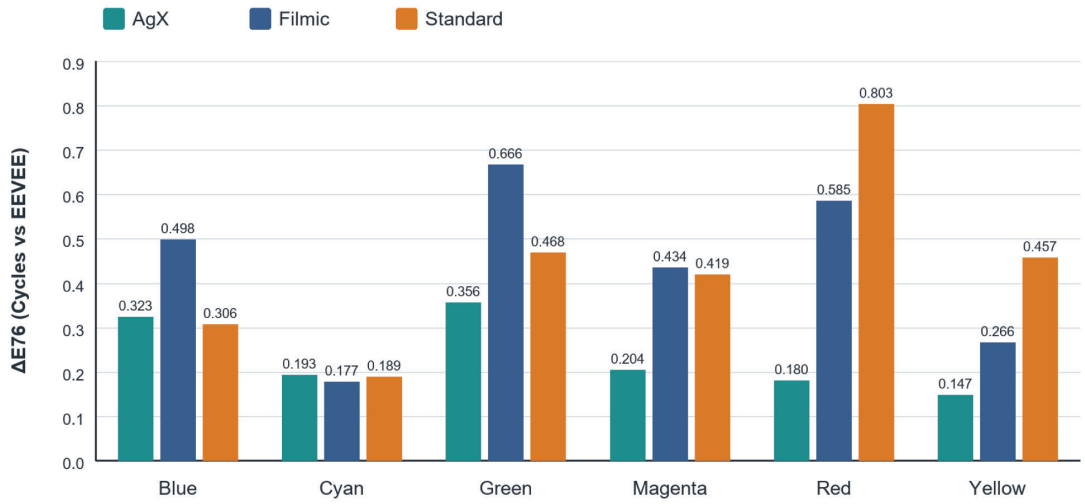
Colour	AgX	Filmic	Standard
Blue	0.323	0.498	0.306
Cyan	0.193	0.177	0.189
Green	0.356	0.666	0.468
Magenta	0.204	0.434	0.419
Red	0.180	0.585	0.803
Yellow	0.147	0.266	0.457
Mean	0.234	0.438	0.440
SD	0.085	0.187	0.207

4.2. Chromaticity distribution

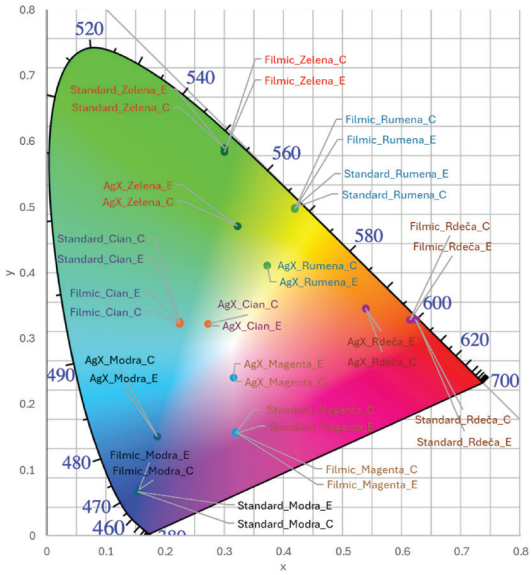
The chromaticity plot for all measurements is shown in Figure 4. The plotted points group the Cycles and EEVEE results for each colour and view transform. Paired points for the two engines remain close within each transform, while AgX points are offset from those associated with Standard and Filmic.

5. Discussion

All 18 paired ΔE76 values between the EEVEE and Cycles measurements were below 1.0. When averaged across the six tested colours, the inter-engine differences were 0.234 for AgX, 0.438 for Filmic, and 0.440 for Standard. AgX had the lowest observed mean inter-engine ΔE76 across the six tested colours, and the lowest ΔE76 value for four of the six colours. The largest individual difference was obtained for red under Standard (ΔE76 = 0.803), whereas the largest differences under Filmic and AgX were obtained for green, at 0.666 and 0.356, respectively. Because ΔE76 is a symmetric distance, these results quantify the dif-



» **Figure 3:** *ΔE76 differences between Cycles and EEVEE by colour and view transform*



» **Figure 4:** *CIE 1931 x,y chromaticity diagram for all measurements*

ference between the two engines but do not indicate which engine was closer to the intended colour target.

The rendered colour matrix also shows that the choice of view transform affects the appearance of the primary and secondary colours. Standard and Filmic appeared more similar to each other, whereas AgX produced a comparatively less saturated and more compressed appearance. This observation is qualitative because no controlled visual assessment was performed. Nevertheless, it is consistent with previous research showing that tone mapping and display transforms can alter saturation, hue, brightness and perceived colourfulness even when applied to the same scene-linear image data (Mantiuk et al., 2009; Eilertsen, Mantiuk & Unger, 2017; Mehmood et al., 2023; Mehmood, Khan & Luo, 2024). It is also consistent with Blender's documented design of AgX, which intentionally desaturates highly exposed colours as part of its tone-mapping behaviour (Blender Foundation, n.d.).

The CIE 1931 x,y chromaticity diagram provides complementary evidence about the relationship between the tested configurations. Corresponding EEVEE and Cycles measurements generally formed closely positioned pairs within each transform, consistent with the relatively small ΔE76 values. The separation between the groups associated with different transforms further indicates that the view transform influenced the resulting chromaticities. However, the diagram represents chromaticity only and does not include luminance information.

The differing computational principles of EEVEE and Cycles offer a plausible explanation for the measured differences between the two engines. Cycles uses a physically based path-tracing approach, whereas EEVEE relies on real-time approximations designed to provide faster rendering. Previous work has similarly shown that rendering pipelines and lighting calculations can influence simulated colour and illumination (Malvido Fresnillo et al., 2024). The present experiment did not isolate individual rendering operations, however, and therefore cannot attribute the observed differences to any particular approximation, sampling procedure or lighting calculation.

Two evaluation criteria must therefore be distinguished. The first is inter-engine consistency: according to the present measurements, agreement between EEVEE and Cycles was greatest with AgX. The second is fidelity to a defined reference colour. Because the reported ΔE76 values compare the engines with each other rather than comparing each configuration with an independently measured target, the experiment does not establish whether AgX, Filmic or Standard provided the most colour-accurate reproduction. Consequently, the lower mean ΔE76 obtained with AgX should be interpreted as greater agreement between the two rendering engines under the tested conditions, not as evidence of greater absolute colour accuracy. Determining absolute colour accuracy would require independently defined or measured reference

CIELAB values and separate target-based colour differences for every engine-transform configuration.

5.1. Limitations

The study was limited to one display, six chromatic colour categories, 36 rendered patches and one measurement workflow. Repeated measurements, uncertainty estimates and observer data were not reported. Because every inter-engine ΔE76 value was below 1.0, instrument and display repeatability should be quantified before the practical significance of the differences is inferred. ΔE76 is useful for a direct metric comparison, but CIELAB is not perfectly perceptually uniform. Consequently, more recent colour difference formulae such as CIEDE2000 can provide a more perceptually refined assessment of small colour differences (Luo, Cui & Rigg, 2001; Sharma, Wu & Dalal, 2005; CIE, 2018). Future work could therefore report repeated measurements with mean values and dispersion, include CIEDE2000 alongside ΔE76, calculate deviations from independently specified reference colours, and evaluate multiple displays.

6. Conclusions

This study identified inter-engine colour differences between corresponding EEVEE and Cycles rendering engines, with all ΔE76 values below 1.0. AgX showed the lowest mean inter-engine ΔE76 across the six tested colours (mean ΔE76 = 0.234), followed by Filmic (0.438) and Standard (0.440). The largest individual difference was measured for red under Standard (ΔE76 = 0.803). These findings demonstrate relative inter-engine consistency but do not establish absolute colour accuracy or perceptual equivalence. Further research should include reference-based comparisons, repeated measurements and controlled observer testing.

7. Acknowledgements

This study is based on seminar work conducted by Neža Mikeln, Špela Polak, Monika Rebec and Laura Rudolf under the mentorship of Professor Raša Urbas and Associate Professor Jože Guna. The authors acknowledge the financial support from the Slovenian Research Agency (research core funding No. P2-0450).

8. References

Blender Foundation (2023) Blender 4.0 release notes: color management. *Blender Developer Documentation*. Available from: https://developer.blender.org/docs/release_notes/4.0/color_management/ [Accessed 13 August 2026].

Blender Foundation (n.d.) *Color management. Blender Manual*. Available from: https://docs.blender.org/manual/de/2.81/render/color_management.html [Accessed 13 August 2026].

CIE (2018) *CIE 015:2018 Colorimetry*. 4th edn. Vienna: Commission Internationale de l'Éclairage. DOI: 10.25039/TR.015.2018

Eilertsen, G., Mantiuk, R.K. and Unger, J. (2017) 'A comparative review of tone-mapping algorithms for high dynamic range video', *Computer Graphics Forum*, 36(2), pp. 565–592. DOI: 10.1111/cgf.13148

Gill, G. (2026) *Argyll Color Management System [Software]*. ArgyllCMS. Available from: https://www.argyllcms.com/ [Accessed 13 August 2026].

Luo, M.R., Cui, G. and Rigg, B. (2001) 'The development of the CIE 2000 colour-difference formula: CIEDE2000', *Color Research & Application*, 26(5), pp. 340–350. DOI: 10.1002/col.1049

Malvido Fresnillo, P., Mohammed, W.M., Vasudevan, S., Perez Garcia, J.A. and Martinez Lastra, J.L. (2024) 'Generation of realistic synthetic cable images to train deep learning segmentation models', *Machine Vision and Applications*, 35(4), 84. DOI: 10.1007/s00138-024-01562-y

Mantiuk, R., Mantiuk, R., Tomaszewska, A. and Heidrich, W. (2009) 'Color correction for tone mapping', *Computer Graphics Forum*, 28(2), pp. 193–202. DOI: 10.1111/j.1467-8659.2009.01358.x

Mehmood, I., Shi, X., Khan, M.U. and Luo, M.R. (2023) 'Perceptual tone mapping model for high dynamic range imaging', IEEE Access, 11, pp. 110272–110288. DOI: 10.1109/ACCESS.2023.3320809

Mehmood, I., Khan, M.U. and Luo, M.R. (2024) 'Generic color correction for tone mapping operators in high dynamic range imaging', *Optics Express*, 32(16), pp. 27849–27866. DOI: 10.1364/OE.527492

Sharma, G., Wu, W. and Dalal, E.N. (2005) 'The CIEDE2000 color-difference formula: implementation notes, supplementary test data, and mathematical observations', *Color Research & Application*, 30(1), pp. 21–30. DOI: 10.1002/col.20070



© 2026 Authors. Published by the University of Novi Sad, Faculty of Technical Sciences, Department of Graphic Engineering and Design. This article is an open access article distributed under the terms and conditions of the Creative Commons Attribution license 4.0 Serbia (http://creativecommons.org/licenses/by/4.0/rs/).

Professional Paper https://doi.org/10.24867/GRID-2026-p27

More Than Hue—A Methodological Approach to Colour Design for Visual Identity and Branding

ABSTRACT

The use of colour in branding has long relied on fixed hue–meaning associations: blue for trust, red for energy, green for sustainability. Treated as rules rather than conventions, these associations limit creativity and differentiation, and in sustainability communication the overuse of green has produced predictable, homogenised visual identities. Through the case of ECODeCK, a research project that supports manufacturing companies in a paradigmatic shift towards sustainable transition, this paper presents a six-step colour design methodology that considers hue, lightness and saturation together: i) researching the project's context and aims; ii) exploring and analysing colour benchmarking; iii) translating concepts into colour attributes; iv) defining a key colour identity palette; v) testing and applying the palette; and vi) scaling it into a chromatic system. The resulting identity departs from the green convention of sustainability communication by distributing meaning across the key palette and the extended chromatic system, rather than relying on a single symbolic hue. The case also shows that the methodology structures, rather than replaces, the designer's judgement. The paper contributes to the beyond-hue approach to colour meaning with a practical methodology for colour design in visual identity, and argues for colour design as a tool for research and knowledge dissemination.

Ingrid Calvo Ivanovic [1]
Francesca Mattioli [2]

[1] Design Department, Universidad de Chile, Santiago, Chile
[2] Department of Design, Politecnico di Milano, Milan, Italy

KEY WORDS
Colour design methodology, colour in branding and visual identity, colour semantics, beyond-hue approach, ECODeCK project

1. Introduction

1.1. The problem

Colour is one of the first elements through which a visual identity is recognised. Branding practice has long relied on shortcut associations between particular hues and particular meanings: blue for trust and reliability, red for energy and urgency, green for nature, health and sustainability. These shortcuts persist because they work at a basic level. They are widely shared, quickly read and easily justified to clients. Their limitation appears when designers treat them not as conventions but as fixed, universal and sufficient explanations of what colour means.

Sustainability communication shows this limitation clearly. Green has become the default visual cue for environmental responsibility, to the point that colour alone can shift judgement. Sundar and Kellaris (2017) found that logos in colours perceived as eco-friendly made ethically ambiguous retail practices appear more ethical. Pancer, McShane and Noseworthy (2017) showed that green used as an isolated environmental cue on packaging can even lower perceived product efficacy, because it activates competing expectations about what the product is. When a colour can confer an ecological image independently of the practice behind it, its communicative value erodes. The code becomes generic, equally available to genuine and superficial commitments, and identities that adopt it converge on a homogeneous visual language. The

problem, then, is not that colour associations exist. It is that they are used as if hue alone carried meaning.

The question designers usually ask, “what does this colour mean?”, assumes that meaning resides in hue. A more productive question is how colour attributes can be systematically explored and configured to communicate a particular identity in a particular context. Research on colour emotion has shown for decades that lightness and saturation carry strong and consistent connotations (Valdez and Mehrabian, 1994; Gao and Xin, 2006). Tools now exist that translate this knowledge into design guidance, such as the Colour Meaning Matrix (Calvo Ivanovic, 2024). However, these tools operate at the level of a single palette. A visual identity is not a single palette. It is a system of colours with different roles, applied across media, that must remain recognisable, legible and coherent. A method that carries a beyond-hue approach through the full development of a chromatic identity system has yet to be articulated.

1.2. Aim and contribution

This paper presents a six-step colour design methodology for visual identity, developed through the colour identity of ECODeCK (Eco-design Circular Knowledge), a design research project at Politecnico di Milano. The methodology was developed in practice and formalised retrospectively. The paper therefore adopts a practice-based case study approach and addresses the following question: *how can a structured colour design methodology move visual identity development beyond stereotypical hue–meaning associations, while producing coherent, distinctive and functional colour systems?*

The paper makes three contributions. First, it describes the six-step methodology that considers hue, lightness and saturation together at every stage, from context research to the scaled chromatic system. Second, it integrates the Colour Meaning Matrix into an identity-design process and extends it from palette selection to system design: semantic dimensions that conflict within a single palette are distributed across the levels of the chromatic system. Third, it argues that colour design can act as a research and knowledge-dissemination tool, not merely an aesthetic layer added to an identity.

Section 2 reviews the shift from hue-based to multidimensional accounts of colour meaning. Section 3 introduces ECODeCK and its colour challenge. Section 4 presents the methodology step by step through the case. Section 5 shows the resulting identity and its applications, and Sections 6 and 7 discuss implications, limitations and conclusions.

2. From hue-based colour meaning to a beyond-hue approach

2.1. Colour meaning and the hue paradigm

Most popular and professional accounts of colour meaning organise associations by hue, an orientation described as the “hue paradigm” (Calvo Ivanovic, 2024; Divers, 2023). This paradigm faces two difficulties. The first is plurality: the same hue carries contradictory meanings. Red has been linked both to danger in achievement contexts and to attraction in relational ones (Elliot & Niesta, 2008). Red has also been matched with both happy and angry faces, and blue with both calm and sad ones (Palmer et al., 2013). The second is cultural variability. Some hue associations differ markedly between cultures, yet studies comparing affective responses across countries report considerable consistency when responses are described in terms of other colour attributes (Adams & Osgood, 1973; Gao & Xin, 2006). Both difficulties point the same way. Hue on its own is an unstable carrier of meaning, and much of what appears to be hue-driven may depend on how light, dark, vivid or muted a colour is.

2.2. Chromatic stereotyping in sustainability communication

In branding, the hue paradigm hardens into sector conventions. Repeated across an industry, these conventions produce homogenisation, weaken differentiation, narrow creative options and privilege one culturally specific reading of colour. Sustainability is an acute case. The palette of saturated, mid-lightness greens that evoke foliage has become so widespread that it signals sustainability in general, independently of the practice it represents. The finding that green and blue can evoke similar perceptions of eco-friendliness (Sundar & Kellaris, 2017) suggests that even this convention is less hue-bound than it appears. If ecological meaning does not depend on green specifically, the convention reflects habit more than necessity. That leaves room for identities that communicate sustainability through other chromatic configurations.

2.3. Beyond hue: lightness and saturation as carriers of meaning

A substantial body of research shows that lightness and saturation shape colour meaning at least as much as hue does. Valdez and Mehrabian (1994) found that saturation consistently affected arousal and lightness affected dominance, while pleasure increased with both. When lightness and saturation were controlled, yellow, conventionally “happy”, was rated among the least pleasant hues. Wright and Rainwater (1962) found that concepts such as happiness and showiness depended mainly on lightness

and saturation rather than hue. Gao and Xin (2006) and Solli and Lenz (2011) likewise concluded that saturation and lightness matter more for colour emotion than hue.

Work using Osgood's semantic differential points in the same direction. Its three core dimensions of meaning are evaluation, potency and activity (Osgood et al., 1957). Across cultures, evaluation is linked mainly to lightness, potency to darkness and saturation, and activity to saturation (Adams & Osgood, 1973). The Colour Meaning Matrix (CMM) operationalises these findings for design (Calvo Ivanovic, 2024, 2025). It asks the designer to assess a concept along the three Osgood dimensions plus a fourth, understanding (simple–complex), and gives orientations for hue, lightness and saturation for each pole. The CMM was developed through palette-construction exercises with more than 300 design students in Chile and Italy, and it is explicitly intended as an orientation rather than a formula.

2.4. From palettes to chromatic systems

Divers (2023) notes that most colour-meaning research studies colours in isolation, whereas designers manage several colours at once, and that generalisations about a hue usually refer to its most saturated form, which designers rarely use. Visual identity sharpens this gap. An identity needs a small set of key colours with clear roles, an extended system for different applications, and functional performance across print and digital media. Established tools linking concepts to colour, such as Kobayashi's (1981) Colour Image Scale and the CMM, guide the choice of colours that match a concept. They do not specify how meaning is maintained when a palette scales into a system, nor what to do when a project's concepts call for incompatible attribute orientations. The methodology presented in Section 4 addresses both questions.

3. The research context and colour challenge

3.1. The project: Eco-Design Circular Knowledge (ECODeCK)

ECODeCK (Eco-design Circular Knowledge) is a design research project of the Department of Design, Politecnico di Milano, developed within the Italian national research initiative MICS – *Made in Italy Circolare e Sostenibile* (Circular and Sustainable Made in Italy) (Bertola et al., 2025). It addresses the sustainable transition of the Italian fashion and furniture industries. These two sectors are central to the Made in Italy identity and face growing environmental and regulatory pressure. Many companies still approach sustainability through compliance and incremental adjustments. It rarely becomes a principle that reshapes how they design and produce (Gaziulusoy & Erdoğan Öztekin, 2019; Davelaar, 2021).

The project starts from the premise that this transition cannot be achieved through technical solutions alone. It also depends on the competences, mindsets and organisational cultures of the people who carry it out (Wiek et al., 2011; Rieckmann, 2012). For this reason, ECODeCK frames its contribution as capacity building, aiming to develop the ability of individuals, organisations and wider ecosystems to understand sustainability challenges and act on them over time (Peiró et al., 2021).

This is where ECODeCK differs from conventional approaches to education for sustainability. Those approaches tend to be transmissive: they deliver standardised knowledge to learners positioned as compliant recipients (Jickling & Wals, 2008). ECODeCK instead adopts a design-based, transformative learning approach (Mezirow, 2003; Sterling, 2011). Participants work on real, open-ended problems from their own organisational contexts. The process encourages them to question established assumptions and to build new ways of acting through iteration, collaboration and reflection.

Table 1
Key dimensions of the ECODeCK project

Dimension	ECODeCK
Project values	Sustainability as a situated, systemic and evolving process, interpreted within each organisational context
Objectives	Building long-term capacity for sustainable transition at the individual, organisational and ecosystemic levels
Stakeholders	Managers and employees of fashion and furniture companies, design researchers, territorial and institutional actors
Sustainability discourse	A transformative, design-based perspective aiming to foster a paradigmatic shift, in which sustainability is enacted through critical reflection, participation and collaborative practice
Communication needs	Making frameworks, training tools and research outcomes accessible to non-designer audiences across media and formats.
Visual identity requirements	A coherent, recognisable identity that is visible, legible and versatile across print and digital applications.

Sustainability is therefore not treated as a fixed set of prescriptions. It is treated as a situated, evolving process that each organisation has to interpret for itself.

The same stance shaped the project's visual communication. A project that questions prescriptive, one-size-fits-all accounts of sustainability could not credibly present itself through the most prescriptive visual code of sustainability.

3.2. The chromatic challenge

Defining ECODeCK's visual identity meant translating the project's defining dimensions into colour. These dimensions are summarised in Table 1: its values, objectives, stakeholders, position in the sustainability discourse, communication needs and visual identity requirements.

Read against these dimensions, the conventional colour code for sustainability is a problem. The ecological-green-grass palette of saturated, mid-lightness greens that evoke foliage and nature is immediately legible, but it has been used so widely that it signals sustainability generically, whatever the practice behind it. Such a code sits uneasily with a project that frames sustainability as situated and evolving, and that aims to foster a paradigmatic shift (Table 1). It also risks reaching the project's stakeholders through the same visual language as the generic messaging many of them already meet with scepticism. This tension defines the design research problem: *how can a project communicating sustainability avoid visually reproducing the very conventions it seeks to challenge, while remaining recognisable, coherent and functional?*

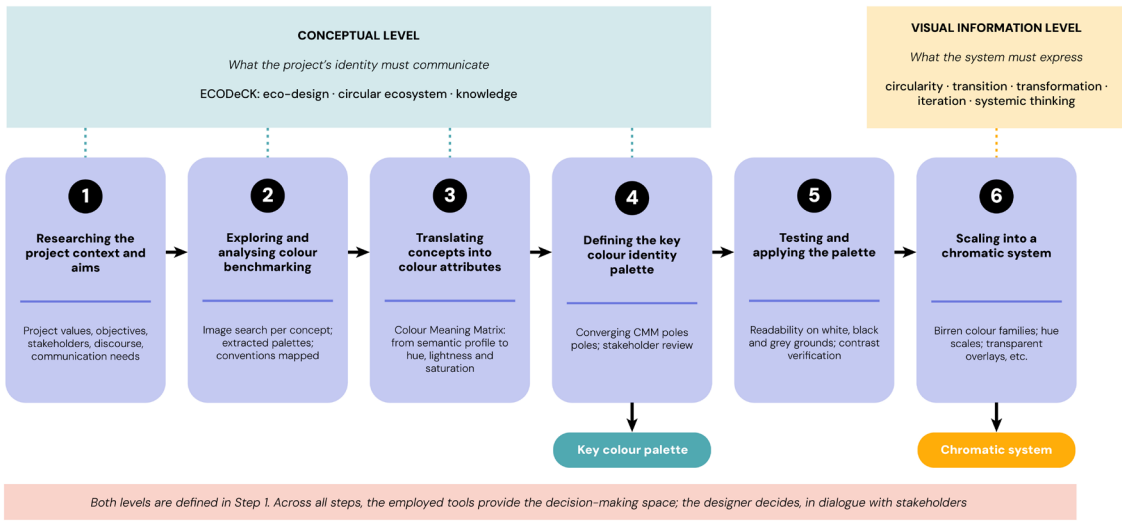
The question has two sides. The first is expressive: the identity has to convey ECODeCK's values and discourse. The second is functional: the identity has to meet the communication needs and visual requirements listed in Table 1. The project therefore decided to move beyond the conventional green-based palette. This did not mean replacing one hue with another. Choosing a different "meaningful" colour would have repeated the logic of fixed hue–meaning associations. Instead, the decision required changing how colour meaning is constructed: through the combined configuration of hue, lightness and saturation, and through the relationships within a chromatic system. Section 4 presents the six-step methodology developed to do this.

4. The six-steps colour design methodology

The following methodology was carried out in practice and formalised afterwards. Each subsection below describes the purpose and procedure of a step, followed by its application in ECODeCK. The methodology is not a formula that outputs colours. Its tools — the CMM orientations, the benchmark, the Birren colour families and the hue scales — structure the decision space and make each decision explicit and traceable. Final choices remain with the designer, and in ECODeCK they were also shaped by dialogue with the project's stakeholders (Section 4.4).

4.1. Step 1 – Researching the project context and aims

Colour selection begins with research rather than preference. The first step establishes what the identity must communicate, to whom, and under what functional constraints. In ECODeCK, this research drew on the project documentation summarised in Table 1: its values, objectives, stakeholders, position in the sustainability discourse, communication needs and visual identity requirements, the review of project documents and several meetings with the research team.



» **Figure 1:** *The six-step colour design methodology and its two levels of meaning*

The six steps are organised around two levels of meaning (Figure 1). The *conceptual* level concerns the ideas the identity must communicate; in ECODeCK, these were the three concepts named in the project's title: eco-design, circular ecosystem and knowledge. This level drives the selection of the key colours (Steps 1–4). The *visual information* level concerns the formal and relational qualities the identity must express as a system; these were taken from the project's key dimensions: circularity, transition, transformation, iteration and systemic thinking. This level drives the expansion of the key colours into a chromatic system (Step 6). Step 5 tests the key palette before it is scaled.

4.2. Step 2 – Exploring and analysing colour benchmarking

The second step maps the visual conventions already attached to each concept. Its aim is not to gather inspiration but to identify which chromatic codes the new identity might reinforce, depart from, or deliberately challenge. For each of the three conceptual-level terms, a Google image search was conducted between October and December 2024, and between 36 and 40 images per concept were compiled into a visual grid. A six-colour palette was then extracted from each grid to summarise its dominant chromatic territory (Figure 2). Because search results vary with location and personalisation, the benchmark should be read as a snapshot of prevailing visual conventions rather than a systematic sample.

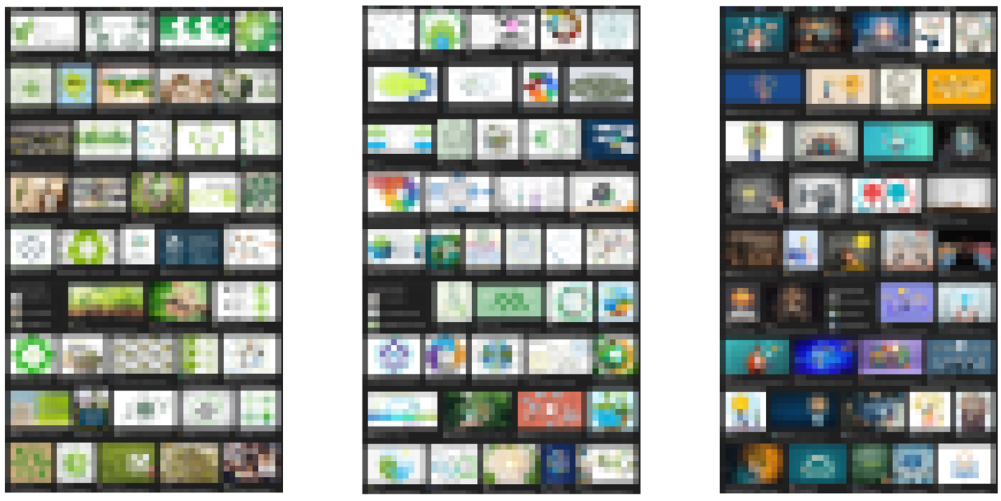
The three benchmarks differed sharply. *Eco-design* was dominated by greens across a range of lightness and saturation, accompanied by earth tones and pale sky blue: the conventional sustainability palette described in Section 2.2. *The circular ecosystem* was more heterogeneous, combining blues, mint and cyan with warm accents and multi-hue diagrams. *Knowledge* clustered around blues and teals, with amber, lavender and greyed tones. The benchmark therefore confirmed that the green convention is specific to the eco-design concept and does not extend to circularity or knowledge, which offered broader chromatic territories. The hues eventually selected all have counterparts within the circular ecosystem and knowledge benchmarks. Differentiation was thus sought specifically from the eco-design convention, and through the configuration of colour attributes rather than through unprecedented hues.

4.3. Step 3 – Translating concepts into colour attributes

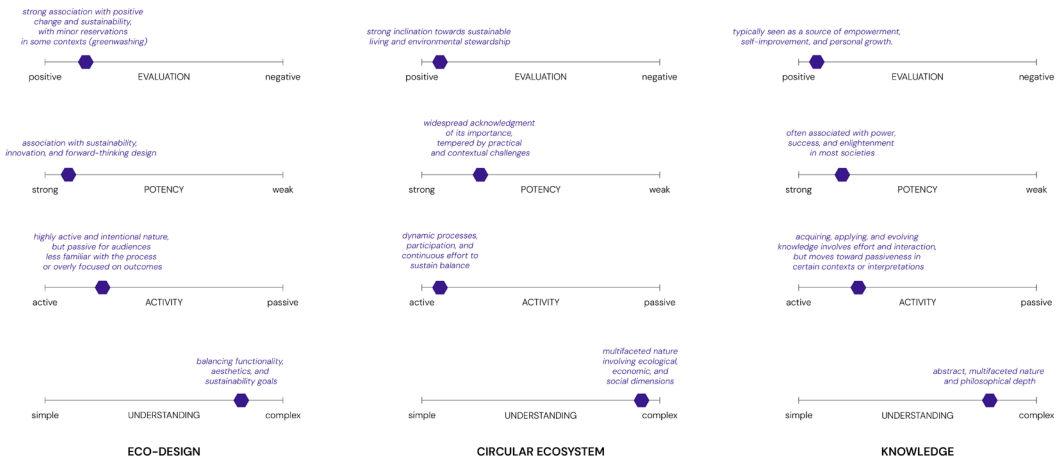
The third step makes the beyond-hue approach operational. Instead of asking which hue represents a concept, it asks which configuration of hue, lightness and saturation corresponds to the way the concept is perceived. ECODeCK used the Colour Meaning Matrix (Calvo Ivanovic, 2024) for this purpose. Following the CMM protocol, each conceptual-level term was assessed on the four bipolar dimensions of evaluation, potency, activity and understanding, with a written rationale for each position (Figure 3).

The three concepts produced closely aligned profiles. All were assessed as positive, strong, active and complex, with minor differences in degree; eco-design, for example, was assessed as active, but less so for audiences unfamiliar with design processes. Table 2 lists the CMM orientations corresponding to these four poles.

Table 2 reveals a conflict that the CMM, as published, does not resolve. Positive, strong and active converge on a shared configuration: basic hues, medium lightness and medium-to-high saturation. Complex calls for the



» **Figure 2:** *Colour benchmarking for the three conceptual-level terms, with Google image search*



» **Figure 3:** *Semantic profiling of the conceptual-level terms with the Colour Meaning Matrix*

opposite on all three attributes. No single set of colours can satisfy all four poles at once. The methodology therefore distributes the semantic dimensions across the levels of the chromatic system. The key palette is weighted towards the converging dimensions (positive, strong and active), while complexity is carried mainly at system level, through relationships between colours rather than individual colours (Step 6). As Step 4 shows, this distribution is a matter of weighting rather than strict separation: one key colour was deliberately configured to bring complexity into the palette itself.

This shift brings the CMM orientation for complexity (low saturation) into the key palette. It adds diversity to the palette's attribute configuration and gives it a quality of sophistication associated in particular with the knowledge concept, whose profile emphasised abstraction and multifaceted depth. The episode shows the conflict identified in Step 3 surfacing in practice: a palette built only on the converging poles was perceived as incomplete, and stakeholder review led to a correction expressed through saturation rather than through a change of hue.

Table 2

CMM orientations for the ECODeCK semantic profile (after Calvo Ivanovic, 2024)

Pole	Hue	Lightness	Saturation
Positive	Basic, easily named hues; also, white and pastels	Medium to high	Medium to high
Strong	Basic, easily named hues; also, black and dark shades	Medium to low	Medium to high
Active	Basic, easily named hues	Medium	High
Complex	Very mixed hues, difficult to name	High or low	Low

4.4. Step 4 – Defining the key colour identity palette

Candidate colours were generated for each converging pole (Figure 4a), and four were selected from the intersection of the active orientation with the positive and strong ones: yellow, cyan, red and violet, complemented by black and white. The first proposal used four highly saturated colours, including a clean, vivid cyan. When this proposal was reviewed with the project leadership, the ECODeCK team observed that the palette appeared uniformly clean and saturated, and asked for a less expected, more sophisticated colour. In response, the cyan was desaturated to #50A8B1 (Table 3, Figure 4-b).

Yellow, red and violet follow the converging orientations closely: they are easily named hues of medium-to-high lightness (L 54–77) *and high chroma* (C 58–82). Cyan departs from this pattern with markedly lower chroma (C* 27). No key colour falls within the green hue range; yellow and cyan come closest to the ecological territory without occupying it. The four chromatic colours have no fixed hierarchy. The logotype and its descriptor rotate across pairs of key colours, while black and white act as neutral grounds and text colours.

4.5. Step 5 – Testing and applying the palette

Before scaling, the key palette was tested against the functional requirements in Table 1. Each key

Table 3

ECODeCK key colours (CIELAB values computed from sRGB, D65)

Colour	Hex	L*	C*	h°
Yellow	#FFAD08	76.8	81.7	76
Cyan	#50A8B1	64.1	26.9	208
Red	#E54B2C	53.9	76.7	41
Violet	#6C78DD	53.9	58.1	294
Black / White	#000000 / #FFFFFF	0 / 100	0	–

colour was shown with white and black text and on white, black and mid-grey grounds, and the logotype was shown in single-colour and two-colour versions on white and black (Figure 5). These tests were assessed visually for readability.

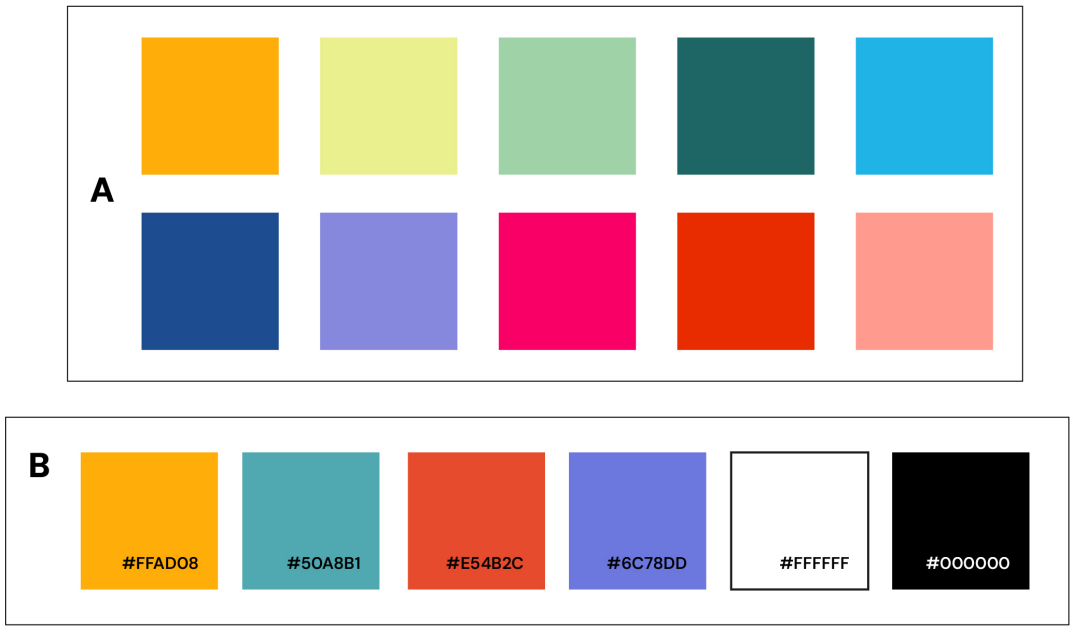
For this paper, a quantitative contrast check was carried out retrospectively using WCAG contrast ratios (W3C, 2023) (Table 4). It supports the main visual finding: all four key colours exceed the 4.5:1 threshold for text against black (5.37–11.23:1), and none reaches it against white (1.87–3.91:1). Black text on colour fields is therefore the functional anchor of the system. The check also exposes limits that visual assessment missed. Contrast between chromatic key colours is low throughout (1.41–2.09:1), and red and violet are isoluminant (1.00:1), so they cannot be told apart in greyscale reproduction and should not be used together to carry information. Methodologically, this suggests that Step 5 should combine visual assessment, which captures overall readability and character, with quantitative contrast verification, which detects isoluminance and sub-threshold text contrast.

4.6. Step 6 – Scaling the key palette into a chromatic system

The final step expands the key palette into a system able to support multiple applications. Here the visual information level takes over: circularity, transition, transformation, iteration and systemic thinking are expressed through three scaling operations.

Hue families. Each key colour was expanded into a colour family using Birren's (1961) colour triangle. Mixing each colour with white, black and grey produced its tints, shades and tones, giving pale, dark, muted and vivid variations of the same hue (Figure 6). The palette is thus structured as four families rather than four colours. Every chromatic colour in the system belongs to one of these families, which keeps applications coherent while extending the identity along the lightness and saturation dimensions.

Hue scales between key colours. Hue scales of thirteen colours were generated in Adobe Illustrator between adjacent key colours (yellow→cyan, cyan→violet, vio-



» **Figure 4:** *From CMM orientations to the ECODeCK key colour palette: (a) preliminary candidate colours palette resulting from the Colour Meaning Matrix analysis; (b) final ECODeCK key colours palette*

Table 4
WCAG contrast ratios between ECODeCK key colours

	Yellow	Cyan	Red	Violet	Black	White
Yellow	–	1.48	2.09	2.09	11.23	1.87
Cyan		–	1.41	1.41	7.58	2.77
Red			–	1.00	5.37	3.91
Violet				–	5.37	3.91

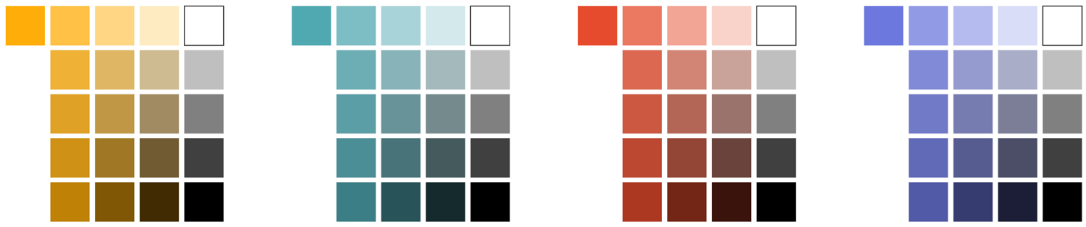
let→red, red→yellow). Two intermediate colours were selected from each scale at equal intervals, producing a twelve-step circular sequence anchored by the four key colours (Table 5, Figure 7). The sequence expresses circularity and transition, and it gives the system room to grow if the project's communication needs become more complex. Generated colours were treated as candidates rather than final values. Where a blend produced colours that were too dull or too close to a key colour, they were adjusted visually; for example, the colour between violet and red was lightened and shifted towards magenta to distinguish it from the red key colour. Such designer adjustments are essential to keep the colours distinguishable and the system harmonious. The yellow→cyan scale passes through a muted sage green: green enters the system as a transitional colour derived from two non-green key colours, not as an identity-defining hue.

Transparent overlays. Shapes in the key colours, derived from the logotype's morphology, are overlaid with transparency, producing intermediate colours where they intersect (Figure 8). These colours are mixed and hard to name, and they are not specified in advance. They therefore realise at system level the complex dimension that the key colours could carry only partially (Step 3). They also express transformation and systemic interdependence: the composite colours exist only through the relationship between key colours.

Taken together, the three operations show the distinction between a palette and a chromatic system. The meaning of the ECODeCK identity does not lie in four hues. It lies in their attribute configuration, their sequence, and the colours they generate in combination.



» **Figure 5:** *Visual readability tests of the key palette*



» **Figure 6:** *The four ECODeCK key hue families using the principles of Birren's triangle*

5. Application: developing the ecodeck colour identity

5.1. The chromatic system

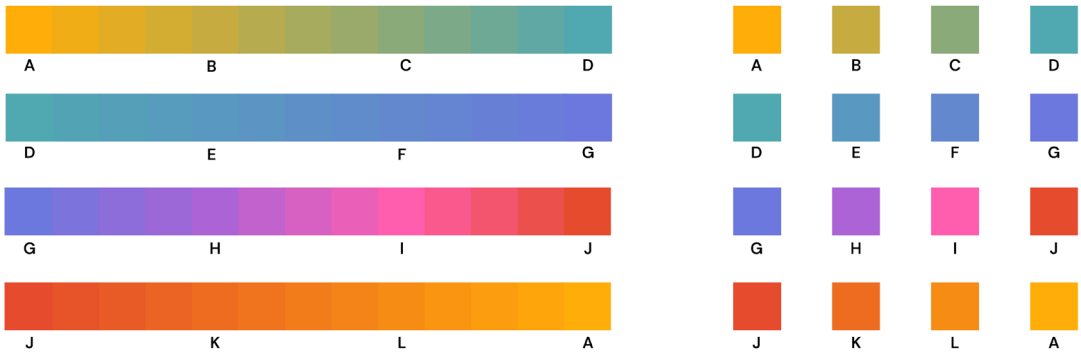
The resulting identity operates on three levels. The key palette of four chromatic colours with black and white carries the converging semantic dimensions – positive, strong and active – with the muted cyan introducing a measure of complexity. The four colour families extend each key colour across lightness and saturation for backgrounds, hierarchies and secondary elements. The twelve-step sequence and the overlay compositions carry circularity, transition and complexity at system level. Meaning is thus distributed rather than concentrated in a single colour or hue.

5.2. Applications

The identity was applied to the ECODeCK logotype in single-colour and two-colour versions on white, black, key-colour and tint grounds, and in overlay versions in which the logotype's ellipses are filled with transparent key colours (Figure 9). The complete colour system was then applied to multiple project resources and substrates, such as training materials, diagrams, reports, visual presentations, website (https://www.ecodeck.polimi.it/en/ecodeck-en/) and several graphic pieces, as shown in Figure 10.

5.3. Assessment against the project requirements

Read against Table 1, the identity meets the expressive side of the challenge. It differentiates ECODeCK from the eco-design convention: no key colour is green, and green appears only as a muted, transitional colour within the sequence. It also renders the project's view of sustainability as situated and systemic through the structure of the colour system rather than through a single symbolic hue. On the functional side, recognisability rests on the consistent use of four key colours in rotating pairs, and versatility on the four colour families. Legibility is robust where black text is set on colour fields, but weaker where chromatic colours are combined with each other or used as text on their own tints. These results are based on design analysis; the identity's reception by ECODeCK's audiences has not been tested.

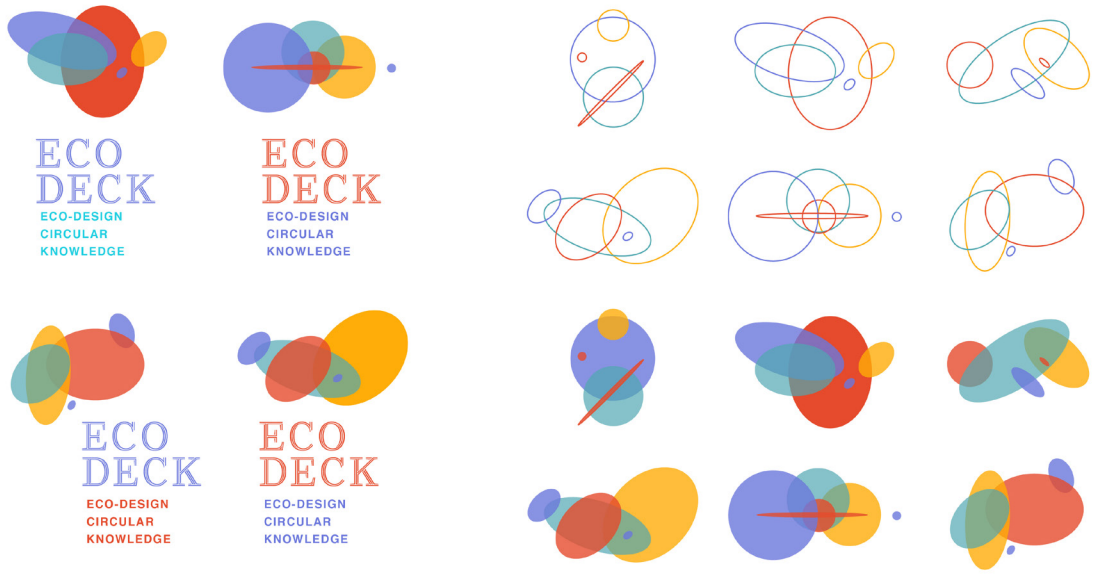


» **Figure 7:** *Hue scales between key colours and the resulting twelve-step circular sequence*

Table 5

ECODeCK twelve-step sequence (key colours in bold)

A #FFAD08	B #C5AB40	C #8AAA79	**D #50A8B1**
E #5998C0	F #6388CE	**G #6C78DD**	H #AC63D6
I #FF5EAE	**J #E54B2C**	K #EE6C20	L #F68C14



» **Figure 8:** *Transparent overlays generating mixed colours at system level*

6. Discussion

6.1. Structuring design judgement

The ECODeCK case shows where structured tools and design judgement meet. The tools generated candidates and exposed conflicts: the CMM showed the incompatibility between “complex” and the other poles, and the blends produced colours that were too dull or too close to the key colours. Judgement resolved these conflicts through the stakeholder-driven desaturation of cyan and through visual adjustments to the hue scales. What the methodology contributes is not the removal of subjectivity but its structuring. Every intervention can be described in terms of hue, lightness and saturation, so it can be justified, discussed and repeated in other projects.

6.2. Beyond hue at the scale of a system

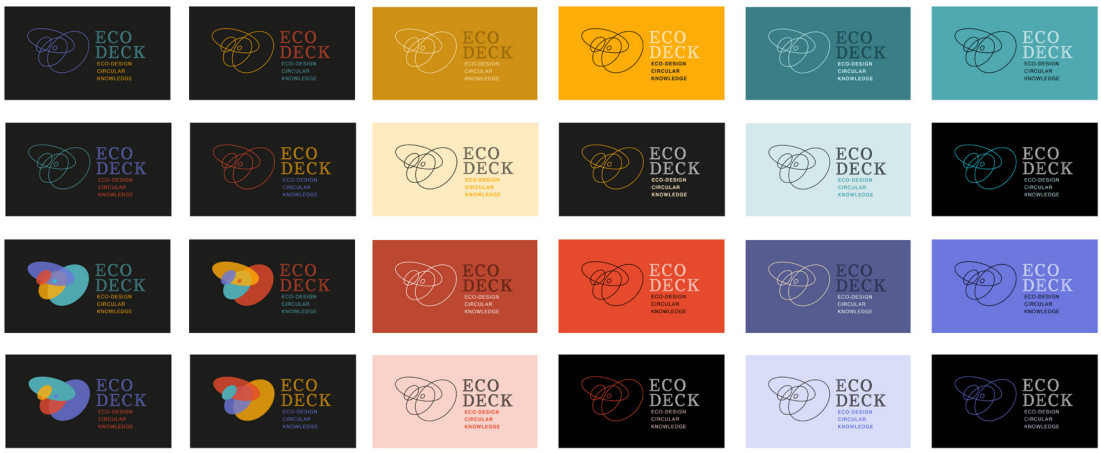
The CMM and similar tools treat colour meaning at the level of a palette. The ECODeCK case shows that when a project’s concepts call for incompatible attribute orientations, the conflict cannot be solved by choosing better colours; it has to be solved structurally, by weighting the semantic dimensions differently across the key palette and the extended system. This extends the beyond-hue approach from the selection of colours to the design of relationships between them, in line with Divers’ (2023) observation that designers work with colours in combination. It also qualifies the role of hue. The ECODeCK identity does not exclude any hue, including green; it changes the role a hue plays and the attributes with which it appears.

6.3. Colour design as research and knowledge dissemination

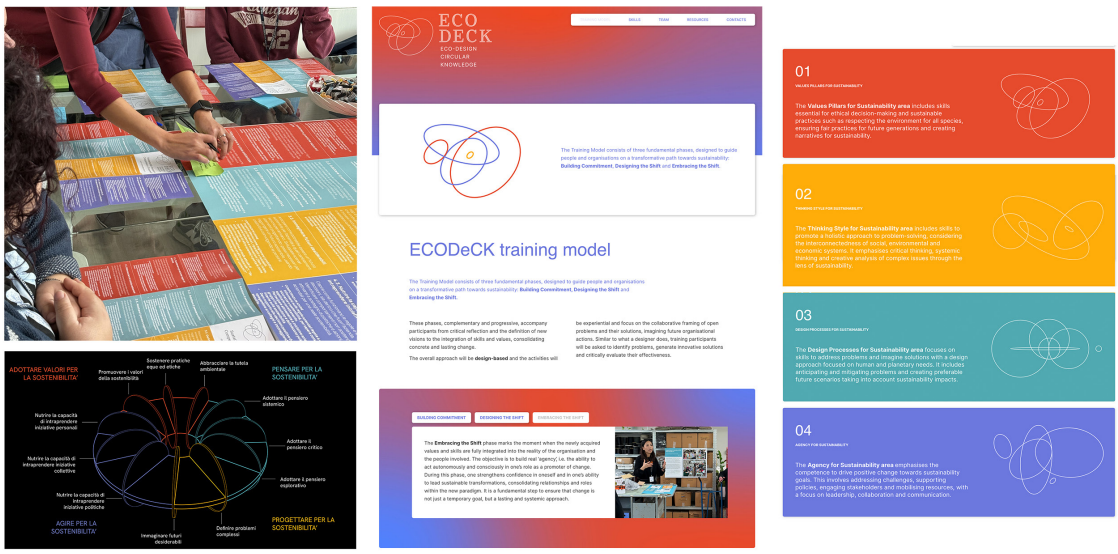
For a research project such as ECODeCK, the visual identity is part of how knowledge reaches its audiences. A project that frames sustainability as situated and evolving, and that seeks to shift established mindsets, gains coherence when its colour identity is developed through a process that is itself researched, documented and open to critique. In this sense, the methodology positions colour design as a research activity: its decisions are grounded in literature and benchmarking, made explicit through a shared vocabulary of colour attributes, and transferable to other projects. The identity communicates the project’s stance not only through what it shows but through how it was made.

6.4. Limitations

Several limitations qualify these findings. The methodology was formalised retrospectively from a single case, and its transferability to other sectors, scales and cultural contexts remains to be tested. The semantic profiles were assessed by the colour designer using the CMM protocol rather than measured with audiences. The benchmark relied on Google image searches, which provide a snapshot rather than a representative sample. Readability was tested visually, with quantitative contrast verification added retrospectively, and the scaled system – families, sequence and overlays – was not tested in the same way; the dark shades of each family could serve as high-contrast text colours on their own tints, which would partly address the legibility issues identified in Step 5. Colour values were specified and analysed in sRGB, so print reproduction was not assessed. Finally, no reception study has evaluated whether ECODeCK’s audiences read the identity as intended.



» **Figure 9:** *The ECODeCK logotype across the chromatic system, on black, key-colour and family variations grounds*



» **Figure 10:** *Applications of the ECODeCK colour identity*

7. Conclusions

This paper has presented a six-step colour design methodology for visual identity and its application to the ECODeCK research project. The case shows that hue-based conventions, such as the green code of sustainability, constrain identity design when treated as fixed meanings, and that a multidimensional approach considering hue, lightness and saturation offers a more flexible and more precise basis for colour decisions. The methodology's main contribution lies in carrying the beyond-hue approach from palette selection to system design. Organising the process around a conceptual level and a visual information level, and distributing semantic dimensions across the key palette and the extended system, made it possible to reconcile meanings that no single palette could carry. At the same time, the case shows that structured tools support rather than replace the designer's judgement, and that stakeholder dialogue can play a decisive role in the process.

Future work should apply the methodology in other projects and sectors, integrate quantitative contrast verification across the whole chromatic system, and test with audiences how identities developed in this way are perceived. Such work would also strengthen the case for colour design as a research and knowledge-dissemination practice in its own right.

8. References

Adams, F.M. and Osgood, C.E. (1973) '*A cross-cultural study of the affective meanings of colour*', *Journal of Cross-Cultural Psychology*, 4(2), pp. 135–156.

Bertola, P., Bruno, C., D'Itria, E., Gramegna, S.M., Mattioli, F., Melazzini, M. and Pei, X. (2025) *Designing the Transition: Seven Design Perspectives to Build Capacities for People, Organisations and Ecosystems*. Milano: FrancoAngeli.

Birren, F. (1987) *Creative Color: A Dynamic Approach for Artists and Designers*. 2nd ed. New York: Reinhold.

Calvo Ivanovic, I. (2024) 'Colour Meaning Matrix: A tool for connecting concepts to hue, value and saturation'. In: Cherubini, F. and Siniscalco, A. (eds.) *Color and Colorimetry. Multidisciplinary Contributions*. Vol. XIX A. Milano: Gruppo del Colore – Associazione Italiana Colore, pp. 214–221. DOI: 10.23738/RCASB.011

Calvo Ivanovic, I. (2025) 'Associare il colore al significato: una guida pratica per i professionisti del design / Associating colour with meaning: a practical guide for design professionals', *Finiture Green*, 25, pp. 10–16.

CIE (2018) *CIE 15:2018 Colorimetry*. 4th ed. Vienna: International Commission on Illumination.

Davelaar, D. (2021) 'Transformation for sustainability: A deep leverage points approach', *Sustainability Science*, 16(3), pp. 727–747.

Divers, E. (2023) 'The compass and the map: colour meaning and the colour design process', *Journal of the International Colour Association*, 32, pp. 44–51.

Elliot, A.J. and Niesta, D. (2008) 'Romantic red: Red enhances men's attraction to women', *Journal of Personality and Social Psychology*, 95(5), pp. 1150–1164.

Gao, X. and Xin, J.H. (2006) 'Investigation of human's emotional responses on colors', *Color Research & Application*, 31(5), pp. 411–417.

Gaziulusoy, İ. and Erdoğan Öztekin, E. (2019) 'Design for sustainability transitions: Origins, attitudes and future directions', *Sustainability*, 11(13), 3601.

Jickling, B. and Wals, A.E.J. (2008) 'Globalization and environmental education: Looking beyond sustainable development', Journal of Curriculum Studies, 40(1), pp. 1–21. DOI: 10.1080/00220270701684667

Kobayashi, S. (1981) 'The aim and method of the color image scale', *Color Research & Application*, 6(2), pp. 93–107.

Mezirow, J. (2003) 'Transformative learning as discourse', *Journal of Transformative Education*, 1(1), pp. 58–63. DOI: 10.1177/1541344603252172

Osgood, C.E., Suci, G.J. and Tannenbaum, P.H. (1957) *The Measurement of Meaning*. Urbana: University of Illinois Press.

Palmer, S.E., Schloss, K.B., Xu, Z. and Prado-León, L.R. (2013) 'Music–color associations are mediated by emotion', *Proceedings of the National Academy of Sciences*, 110(22), pp. 8836–8841.

Pancer, E., McShane, L. and Noseworthy, T.J. (2017) 'Isolated environmental cues and product efficacy penalties: The color green and eco-labels', *Journal of Business Ethics*, 143(1), pp. 159–177. DOI: 10.1007/s10551-015-2764-4

Peiró, J.M., Martínez-Tur, V., Nagorny-Koring, N. and Auch, C. (2021) 'A framework of professional transferable competences for system innovation: Enabling leadership and agency for sustainable development', *Sustainability*, 13(4), 1737.

Rieckmann, M. (2012) 'Future-oriented higher education: Which key competencies should be fostered through university teaching and learning?', *Futures*, 44(2), pp. 127–135.

Solli, M. and Lenz, R. (2011) 'Color emotions for multi-colored images', *Color Research & Application*, 36(3), pp. 210–221.

Sterling, S. (2011) 'Transformative learning and sustainability: Sketching the conceptual ground', *Learning and Teaching in Higher Education*, 5, pp. 17–33.

Sundar, A. and Kellaris, J.J. (2017) 'How logo colors influence shoppers' judgments of retailer ethicality: The mediating role of perceived eco-friendliness', *Journal of Business Ethics*, 146(3), pp. 685–701. DOI: 10.1007/s10551-015-2918-4

Valdez, P. and Mehrabian, A. (1994) 'Effects of color on emotions', *Journal of Experimental Psychology: General*, 123(4), pp. 394–409.

W3C (2023) *Web Content Accessibility Guidelines (WCAG) (WCAG) 2.2.* World Wide Web Consortium.

Wiek, A., Withycombe, L. and Redman, C.L. (2011) 'Key competencies in sustainability: A reference framework for academic program development', *Sustainability Science*, 6(2), pp. 203–218.

Wright, B. and Rainwater, L. (1962) 'The meanings of color', *The Journal of General Psychology*, 67(1), pp. 89–99.



© 2026 Authors. Published by the University of Novi Sad, Faculty of Technical Sciences, Department of Graphic Engineering and Design. This article is an open access article distributed under the terms and conditions of the Creative Commons Attribution license 4.0 Serbia (http://creativecommons.org/licenses/by/4.0/rs/).

Review Paper https://doi.org/10.24867/GRID-2026-p28

Evaluation of Passive and Active Aids for Color Vision Deficiency: A Comparative Analysis of Perceptual Efficacy

ABSTRACT

Congenital red-green Color Vision Deficiency (CVD) affects approximately 8% of Caucasian males and 0.5% of females and can interfere with color-dependent daily and occupational tasks. This review synthesizes psychophysical and computational evidence on passive spectral filters (including EnChroma®, VINO®, and Colorlite®) and active digital recoloration methods. Passive filters alter color appearance but do not restore normal trichromatic vision and do not consistently improve diagnostic chromatic discrimination. Nevertheless, some filters may provide stimulus- and task-dependent enhancement of chromatic contrast or appearance in selected anomalous trichromats. Computational analyses also show that VINO® can reduce the number of discernible colors (NODC) under some simulated conditions. The CVD-MET metric, developed in previous papers, provides complementary measures of efficiency and naturalness for comparing visual aids. In the methods originally evaluated with CVD-MET, active recoloration achieved better efficiency than the tested passive filters, but naturalness did not uniformly favor active methods: EnChroma® showed the lowest total naturalness difference, whereas VINO® showed the highest. Thus, active recoloration offers greater potential for targeted compensation, but not restoration of normal color vision, and its benefit depends on the trade-off between discrimination and naturalness. Current development is moving toward degree-adaptable, real-time, and user-specific recoloration, supporting future evaluation frameworks that combine observer-specific discrimination, task performance, naturalness, and user preference.

Rafael Huertas [1]
Luis Gómez Robledo [1]
Miguel Ángel Martínez-Domingo [1]
Eva M. Valero [1]
Javier Hernández-Andrés [1]
Neda Milić Keresteš [2]
Ivana Tomić [2]

[1] University of Granada, Faculty of Sciences, Department of Optics, Granada, Spain
[2] University of Novi Sad, Faculty of Technical Sciences, Department of Graphic Engineering and Design, Novi Sad, Serbia

KEY WORDS
Color vision deficiency, visual perception, spectral filters, daltonization, CIECAM02

1. Introduction

Normal human color vision is based on a trichromatic system mediated by three types of retinal photoreceptors or cones, sensitive respectively to short-wavelength (S), medium-wavelength (M), and long-wavelength (L) spectral bands. However, approximately 8% of Caucasian males and 0.5% of females present some form of Color Vision Deficiency (CVD) (Birch, 2012; Simunovic, 2010). Congenital red-green deficiencies account for most cases and are classified physiologically according to the type of cone affected and the severity of the defect. When one of the photopigments undergoes a spectral shift in its sensitivity curve without being completely absent, anomalous trichromacy occurs (protanomaly in the case of L cones and deuteranomaly in M cones). In anomalous trichromacy, severity is related to the spectral separation of cone sensitivities. Conversely, the functional absence of one cone class results in dichromacy (protanopia or deuteranopia). Both severe anomalous trichromacy and dichromacy can substantially reduce chromatic discrimination. In daily life, observers with

severe CVD may experience difficulties in tasks such as interpreting maps, charts, signal lights, or food-related color cues, and color-vision standards can restrict eligibility for some safety-critical occupations (Barbur & Rodriguez-Carmona, 2012; Cole, 2004). For common congenital red-green CVD, there is currently no established restorative treatment; therefore, practical assistance has focused primarily on optical and digital compensation.

Faced with the lack of biological solutions, applied research and the optical industry have driven the emergence of various visual assistance systems (Popleteev, Louveton & McCall, 2015). These technologies fall into two main categories: passive aids and active aids (Muñoz-Postigo et al., 2022). Passive aids consist of tinted spectral filters mounted in spectacles or contact lenses (Karepov & Ellenbogen, 2020; Maxwell, 1857; Swarbrick et al., 2001). The idea of interposing optical filters to mitigate color confusion dates back to Seebeck's observations in 1837 and Maxwell's monocular spectacles developed in 1857 (Maxwell, 1857), continued in the 20th century by lenses such as X-Chrom or ChromaGen (ChromaGen, n.d.). In recent years, there has been a notable commercial resurgence led by binocular glasses with notch or multiband filters from brands like EnChroma®, VINO®, Colorlite®, or Pilestone® among others. The commercial claim of these devices is to block specific regions of the visible spectrum to attenuate the overlap between L and M cone responses, aiming to increase perceived chromatic contrast. On the other hand, active aids employ digital image processing techniques on displays or augmented reality devices (such as smart glasses or electronic viewfinders) (Popleteev, Louveton & McCall, 2015). Through recoloration or daltonization algorithms, these systems capture the real scene and dynamically remap confusing hues toward spectral components that are readily distinguishable by the observer's visual system (Milić et al., 2015; Ribeiro & Gomes, 2019).

Despite widespread commercial claims, psychophysical studies do not support the interpretation that passive notch filters restore normal color vision (Almutairi et al., 2017; Badawy et al., 2018; Gómez-Robledo et al., 2018; Martínez-Domingo et al., 2019; Martínez-Domingo et al., 2020; Mastey et al., 2016; Patterson, 2017). EnChroma® testing found changes in perceived color without improvement in standard diagnostic tests or normalization of color vision, while VINO® could improve recognition of some pseudoisochromatic plates while worsening arrangement and color-naming performance (Gómez-Robledo et al., 2018; Martínez-Domingo et al., 2019; Martínez-Domingo et al., 2020). Such gains on screening plates can arise because spectral filtering introduces luminance or brightness cues that were not intended to carry the target information. Computational analyses likewise show that passive filters do not consistently increase the number of discernible colors (NODC), and selected filters may reduce it (Martínez-Domingo et al., 2020). However, the evidence should not be stated as an absolute absence of perceptual benefit: long-term notch-filter use has been associated with increased chromatic contrast response in anomalous trichromats, and recent experiments found task- and stimulus-dependent changes in color appearance with limited effects on threshold discrimination (Somers, Franklin & Bosten, 2024; Werner, Marsh-Armstrong & Knoblauch, 2020). These findings support a distinction between restoration of normal trichromacy, for which evidence is lacking, and selective enhancement of particular chromatic signals or perceptual tasks.

To complement psychophysical testing, computational approaches have used color-appearance modeling and dedicated image metrics. CVD-MET was developed to evaluate two complementary properties of CVD aids using simulated observer vision: efficiency, reflecting how well the transformed image reduces CVD-specific perceptual differences, and naturalness, reflecting preservation of the original scene appearance (Muñoz-Postigo et al., 2022). In the original comparison, the evaluated active recoloration methods (Fidaner, Lin & Ozguven, 2005; Hassan & Paramesran, 2017) achieved lower, and therefore better, CVD-MET efficiency differences than the tested passive filters. Naturalness, however, did not show the same ordering: EnChroma® had the lowest total naturalness difference among the four compared methods, VINO® the highest, and the active methods occupied intermediate positions. The evidence therefore supports an efficiency–naturalness trade-off rather than the broader claim that active recoloration is uniformly both more efficient and more natural.

This review paper presents a comparative synthesis of evidence on the perceptual efficacy of passive and active aids for color vision deficiency. Integrating psychophysical results, hyperspectral simulations, and quantitative image metrics, the objectives are: to analyze the performance of widely used passive optical filters (including EnChroma®, VINO®, and Colorlite®) in standardized color-vision tasks and under adaptation; to compare the efficiency and naturalness dimensions captured by CVD-MET; to distinguish restoration of normal color vision from task-specific perceptual enhancement; and to place the previously evaluated active algorithms in the context of more recent degree-adaptable, real-time, and personalized recoloration approaches.

2. Methods

2.1. Experimental subjects and psychophysical testing protocols

In different studies (Gómez-Robledo et al., 2018; Martínez-Domingo et al., 2019; Gómez-Robledo et al.,

2020; Huertas et al., 2024) the psychophysical evaluation engaged cohorts of human observers diagnosed with congenital red-green CVD (protanomalous, deuteranomalous, protanopes, and deuteranopes) alongside a control panel of color-normal trichromats. Subjects underwent standard diagnostic screening using the Ishihara Pseudoisochromatic Plates (Ishihara, 1977), the FM-100 (X-Rite) and/or an anomaloscope (anomaloscope OCULUS® HMC-Anomaloskop USA) and/or the CAD test (Rodriguez-Carmona et al., 2005).

Chromatic discrimination capacity and error patterns were quantitatively measured using the Farnsworth-Munsell 100 Hue Test. To evaluate color naming accuracy, a dedicated color-naming experiment was conducted utilizing 21 color patches from an X-Rite® GretagMacbeth ColorChecker Chart. Patches were presented in isolated 55 x 55 mm color squares on a dark background on an HP® 2510i 25'' display calibrated with an X-Rite® Eye-One spectrophotometric device. Observers were instructed to categorize each color using the 11 basic color terms established by Berlin and Kay (1991) (white, black, red, green, yellow, blue, brown, purple, pink, orange, grey). Tests were administered under two distinct experimental conditions: without glasses (Glasses OFF) and while wearing commercial passive filters (Glasses ON), including EnChroma® Cx-65, VINO® O2 Amp Oxy-Iso, and Colorlite® spectral lenses.

2.2. Computational simulation and hyperspectral image processing

To model perceptual changes objectively under controlled viewing conditions, the computational work summarized here used hyperspectral scenes drawn from the image sets employed in the original aid-evaluation studies, including hyperspectral measurements of test stimuli and natural-scene data from established spectral-image databases. In the CVD-MET study, the six evaluated scenes were assembled from hyperspectral acquisitions and public spectral-image collections, including the Nascimento/Ferreira/Foster natural-scene database and the Columbia CAVE database (Color Imaging Lab, University of Granada, n.d.; Columbia University CAVE Laboratory, 2008; Foster, Nascimento & Amano, n.d.; Nascimento, Ferreira & Foster, 2002). Scene spectral radiances were transformed into retinal cone responses using standard cone fundamentals, and CVD simulation was then applied at defined severity levels.

Perceptual color coordinates were calculated using the CIECAM02 Color Appearance Model to account for chromatic adaptation effects (Fairchild, 2013). The model parameters reported in the underlying work used a D65 reference white with Xw=97.10, Yw=100.00, and Zw=111.062, an adapting-field luminance La=23 cd/m², background luminance Yb=28, surround factor c=0.59, chromatic induction factor Nc=0.9, and degree of adaptation D=0.84. For every scene element, lightness (J), chroma (C), hue angle (h), and rectangular chromaticity coordinates (ac, bc) were derived.

2.3. Active aid algorithms and the CVD-MET metric

Active digital recoloration algorithms, commonly referred to as daltonization methods, including the Fidaner, Lin and Ozguven (2005) and Hassan and Paramesran (2017) approaches, were evaluated against passive filters. Because conventional image-quality metrics are not designed around CVD-specific confusions, CVD-MET was developed to assess aid performance through separate efficiency and naturalness analyses (Muñoz-Postigo et al., 2022). CVD-MET evaluates two complementary components, efficiency and naturalness. A Fuzzy C-means clustering step in CIELAB color space is used as a preprocessing color-quantization procedure before identifying confused and non-confused color clusters. The two CVD-MET analyses can be summarized as follows:

4. Efficiency (E): Quantifies the degree to which the processed image reduces color confusion, bringing the CVD observer's perception closer to that of a normal trichromat.
5. Naturalness (N): Measures the extent to which the original visual appearance and spatial realism of non-confusing scene elements are preserved.

CVD-MET scores were benchmarked alongside conventional full-reference and no-reference image quality metrics modified for CVD perception, including MS-iCID, cVIF, cVSI, and NIQE difference.

3. Results

3.1. Psychophysical performance with commercial passive filters

Systematic psychophysical testing revealed a major divergence between screening plate recognition and diagnostic chromatic discrimination when observers wore commercial passive filters (Gómez-Robledo et al., 2018; Martínez-Domingo et al., 2019; Martínez-Domingo et al., 2020). Table 1 summarizes the results obtained.

As demonstrated in quantitative psychophysical trials, VINO® glasses produced a notable reduction in error rates on Ishihara pseudoisochromatic plates. However, this improvement in screening plates was accompanied by a severe degradation in chromatic ordering and naming performance.

Table 1

Performance of passive filters (Gómez-Robledo et al., 2018; Martínez-Domingo et al., 2019; Martínez-Domingo et al., 2020)

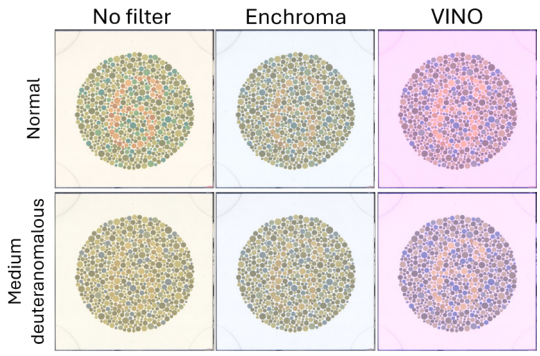
Performance Indicator	Glasses OFF	EnChroma® Cx-65	VINO® O2 Amp	Colorlite®
Ishihara Recognition	High Error Rate	Slight Improvement	Marked Error Reduction	Variable Pass
FM-100 Total Error (SQR)	Baseline (~96.37)	Unchanged (~91.32)	Severe Elevation (~181.32)	Elevated Errors
Color-Naming Fails	Baseline	Unchanged	Increased (+3.05 terms)	Mild Increase
Discernible Colors (NODC)	Baseline Gamut	Slight Drop / Equal	Net Reduction (-22% to-45%)	Net Reduction

In the case of FM-100 Error Scores, while baseline error scores without glasses averaged 96.37 ± 112.43, wearing VINO® glasses elevated mean total error scores to 181.32 ± 106.59, for one of the databases used (Dataset D1). EnChroma® Cx-65 glasses yielded no statistically significant change in FM-100 scores (91.32 ± 100.00) (Martínez-Domingo et al., 2019).

Wearing VINO® filters increased color-naming errors by an average of 3.05 ± 5.39 terms changed relative to the baseline. Observers frequently misidentified neutral and chromatic patches due to the heavy pinkish/reddish tint introduced by the filter.

3.2. Color appearance shifts and chromatic diversity

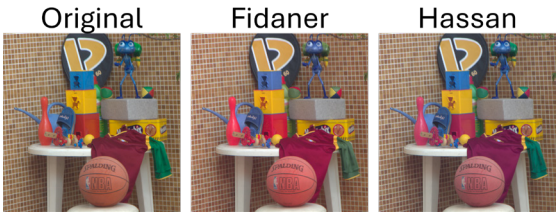
Color vision deficiencies can be modeled by different algorithms, as can the effects of passive filters (Muñoz-Postigo et al., 2022). Chromatic adaptation can also be considered, for example by CIECAM02. Figure 1 shows the simulation result for an Ishihara plate as viewed by a medium-severity deuteranomalous observer.



» **Figure 1:** *Simulation result for a medium deuteranomalous observer viewing an Ishihara plate*

The application of active aids is illustrated in Figure 2 for the Fidaner, Lin and Ozguven (2005) and Hassan and Paramesran (2017) algorithms.

In Muñoz-Postigo et al. (2022), CIECAM02 color appearance simulations illustrated the color shifts caused by passive notch filters. In the CIECAM02 chromaticity plane (ac, bc), unprocessed natural scenes exhibit a continuous distribution of hue angles (h). Interposing VINO® filters forces chromaticity coordinates into a bimodal distribution along a single diagonal line, altering mean angular directions. The angular direction shift depends on the images included in the dataset. This clustering along a single axis reduces overall chromatic diversity, suppressing greens and blues while artificially boosting red-luminance contrast.



» **Figure 2:** *Recoloration results for a mild-deuteranomalous observer*

Calculations of the Number of Discernible Colors (NODC) confirmed that passive filters do not increase the chromatic gamut of CVD observers, and in severe deutan or protan conditions, decrease the total NODC.

3.3. Metric evaluation: passive filters vs. active recoloration

Quantitative assessment using image-difference metrics and CVD-MET demonstrated clear performance differences between passive optical filters and active recoloration algorithms (Muñoz-Postigo et al., 2022). For filtered and recolored images, Tables 2 and 3 show the results of the metrics for naturalness and efficiency, respectively (mean data and standard deviation).

For CVD-MET naturalness (total score), values indicate the perceptual differences, so lower values indicate better naturalness performance. For the CVD-MET efficiency (total score) lower values indicate better efficiency (Muñoz-Postigo et al., 2022).

Table 2

Metrics of naturalness for filtered (EnChroma® and VINO®) and recolored (Fidaner and Hassan recoloration algorithms) images (Muñoz-Postigo et al., 2022)

Metric Category	EnChroma® (Passive)	VINO® (Passive)	Fidaner (Active)	Hassan (Active)
Ms-iCID (Structural)	0.0142±0.0145	0.0700±0.0743	0.0450±0.0462	0.0368±0.0390
cVIF (Information Ratio)	0.2145±0.0613	0.4841±0.1705	0.4285±0.1550	0.2798±0.0842
cVSI (Visual Saliency)	0.0006±0.0007	0.0077±0.0039	0.0103±0.0103	0.0092±0.0090
NIQE Difference (Naturalness)	-0.0346±0.0677	0.0883±0.1281	-0.0040±0.1117	0.0617±0.0859
CVD-MET (Confused Colors)	6.4457±2.2903	22.7177±11.82	10.1310±7.874	8.6198±6.1769
CVD-MET (Non-Confused Colors)	6.8848±0.9950	23.7909±10.34	12.9592±5.867	11.2563±5.239
CVD-MET Total Score	6.8464±1.2035	23.5842±10.67	12.2714±4.908	10.6402±4.147

Table 3

Metrics of efficiency for filtered (EnChroma® and VINO®) and recolored (Fidaner and Hassan recoloration algorithms) images (Muñoz-Postigo et al., 2022)

Metric Category	EnChroma® (Passive)	VINO® (Passive)	Fidaner (Active)	Hassan (Active)
Ms-iCID (Structural)	0.0313±0.0339	0.0706±0.0722	0.0160±0.0169	0.0092±0.0102
cVIF (Information Ratio)	0.3182±0.0497	0.4662±0.1651	0.2785±0.1294	0.0409±0.0548
cVSI (Visual Saliency)	0.0032±0.0022	0.0060±0.0019	0.0031±0.0026	0.0027±0.0023
NIQE Difference (Efficiency)	-0.0783±0.1074	0.0446±0.1239	-0.0476±0.1101	0.0181±0.0342
CVD-MET (Confused Colors)	10.0904±3.9226	23.8317±10.6487	5.2143±3.1246	3.9575±3.0580
CVD-MET (Non-Confused Colors)	11.7277±2.9577	25.1695±8.4239	6.5723±2.3132	5.4546±2.7152
CVD-MET Total Score	11.3425±2.0822	24.7721±8.9941	6.2206±1.7993	5.1430±2.3945

Comparing the values for passive and active aids as shown in Table 3, from the efficiency point of view, the active aids are superior according to all metrics. Regarding the information content (assessed by the cVIF metric), there is also a higher similarity between the original and recolored images, as perceived by the CVD observer, than between the original and filtered images.

From the perspective of naturalness, the EnChroma® filter performs best across all metrics, except for the NIQE difference, as shown in Table 2. However, it provides minimal chromatic differentiation in confusing regions. The VINO® filters exhibited high distortion values, reflecting substantial distortion of scene naturalness without a proportional gain in true chromatic efficiency.

In contrast, active recoloration algorithms (Fidaner and Hassan) achieved a more effective balance: they selectively remapped confusing color clusters to high-efficiency discrimination channels while keeping overall scene distortion within moderate boundaries.

The results suggest that filters that introduce slight changes do so at the expense of effectiveness, while active aids that are more effective produce a less natural appearance in the scenes. The principal result is therefore a method-dependent efficiency–naturalness trade-off, not a general finding that active aids necessarily produce more natural images.

4. Discussion

The primary finding of this literature review is the distinction between restoration of normal chromatic coding and selective enhancement of cues that can improve a particular task. Passive spectral filters alter cone excitations by attenuating selected wavelength bands. In pseudoisochromatic plates, this can introduce luminance or brightness differences that make a hidden target easier to recognize without restoring normal red-green sensitivity. VINO® illustrates this dissociation: improved recognition of some Ishihara plates can coexist with worse FM-100 arrangement and

color-naming performance. At the same time, more recent work indicates that selected anomalous trichromats can experience enhanced chromatic contrast or appearance under some notch-filter conditions (Werner, Marsh-Armstrong & Knoblauch, 2020; Somers, Franklin & Bosten, 2024). Consequently, "does not restore normal trichromacy" is a stronger and better-supported conclusion than "cannot provide any perceptual benefit."

The dimensionality argument should distinguish dichromacy from anomalous trichromacy. In dichromacy, the absence of one cone class creates a missing receptor dimension that a passive spectral filter cannot recreate. In anomalous trichromacy, however, three cone classes remain functional, but their spectral sensitivities are less separated; a notch filter could redistribute relative cone excitations and may enhance selected chromatic contrasts without restoring normal cone fundamentals. This distinction is consistent with evidence of increased chromatic contrast response after two weeks of notch-filter use in anomalous trichromats (Werner, Marsh-Armstrong & Knoblauch, 2020) and with more recent task-dependent effects on color appearance (Somers, Franklin & Bosten, 2024).Such adaptive or contrast-enhancement effects should not be interpreted as reconstruction of the missing or altered photopigment signal, but they do require qualifying the claim that long-term adaptation is entirely unable to modify functional color response.

Active recoloration on digital displays, cameras, and augmented-reality systems offers greater flexibility because the transformation can be content-, task-, and observer-dependent. The Fidaner and Hassan methods evaluated in the original CVD-MET comparison demonstrate the principle, but they no longer represent the full state of the art. Degree-adaptable recoloration has been evaluated with CVD observers while explicitly optimizing contrast enhancement and naturalness (Zhu et al., 2022); real-time daltonization can preserve luminance and temporal stability at interactive frame rates (Ebelin et al., 2023); and recent models such as ColorAdaptNet learn individualized transformations from each user's subjective evaluations rather than relying only on a fixed simulated severity (Chen et al., 2026). These developments strengthen the case for active aids while also shifting the research question from a universal recoloring transform toward personalized and context-dependent compensation.

4.1. Contemporary implementation and personalized active aids

At the implementation level, active color transformations are no longer confined to laboratory prototypes. Windows, Android, iOS, and macOS provide system-level color-filter or color-correction options for common CVD categories (Microsoft, n.d.; Apple, n.d.; Google, n.d.), while Chrome DevTools provides CVD simulation models for developers testing interface accessibility (Google Chrome Developers, n.d.). These functions should not be conflated: developer simulation emulates how content may appear under a CVD condition, whereas end-user compensation intentionally transforms displayed content to improve access. Their widespread availability nevertheless increases the translational relevance of active color-processing research and underscores the importance of evaluating algorithms under realistic screen and interface conditions.

A parallel trend is personalization. Earlier daltonization methods typically assumed a predefined CVD type or severity, whereas newer approaches optimize the transformation for an individual observer or learn directly from user judgments. Personalized evaluation should therefore include not only model-based efficiency, but also discrimination performance on relevant tasks, naturalness, visual comfort, stability over time, and user preference. This is especially important because a transformation that improves one confusing color pair may introduce distortions elsewhere in the image.

These findings have practical implications for clinical diagnostics, occupational standards, and industrial lighting design:

1. Screening Vulnerability: Relying solely on Ishihara plates for occupational screening is insufficient if candidates wear tint-altering filters. Standardized evaluation protocols should incorporate secondary diagnostic tests (such as the FM-100, anomaloscope or CAD) that are resistant to luminance contrast artifacts.
2. Inclusive Lighting Standards: Industrial and architectural lighting metrics must be updated to account for CVD vision. Consequently, a specific colorimetry (including chromatic adaptation models, color difference formulae, etc.) must be developed for CVD observers.

4.2. Limitations and scope

This synthesis combines evidence from heterogeneous studies with different observer samples, tests, filters, illuminants, image sets, CVD models, and severity assumptions. In particular, CVD-MET is simulation-based and therefore inherits the assumptions of the selected CVD simulation, scene set and confused/non-confused color classification; it should complement rather than replace psychophysical testing with CVD observers. The active-aid comparison in the original dataset also includes only two older recoloration algorithms, so conclusions about "active aids" as a class should be restricted to the methods evaluated. Finally, evidence for passive filters differs between dichromacy and anomalous trichromacy, making phenotype-specific interpretation essential.

5. Conclusions

This comparative synthesis leads to the following conclusions regarding passive and active aids for Color Vision Deficiency:

1. Passive spectral filters such as EnChroma®, VINO®, and Colorlite® do not restore normal trichromatic vision. Improvements on pseudoisochromatic plates may be driven by added luminance/brightness cues rather than recovery of normal red-green sensitivity. However, selected anomalous trichromats may show task- and stimulus-dependent enhancement of chromatic contrast or appearance, so restoration and perceptual enhancement should be treated as distinct outcomes.
2. In the studies reviewed in this paper, VINO® produced a clear dissociation between improved recognition of some Ishihara plates and poorer FM-100 and color-naming performance. More broadly, the benefit of passive notch filters depends on CVD phenotype, spectral sensitivities, illuminant, stimulus, and task; therefore, their effects should not be generalized from a single screening test.
3. Within the simulation framework and aid systems evaluated by CVD-MET, active digital recoloration methods achieved better efficiency than the tested passive filters. This advantage does not imply restoration of normal color vision and is accompanied by a naturalness trade-off: EnChroma® was more natural than the two active methods on the total naturalness score, whereas VINO® was substantially worse. Future systems should therefore optimize discrimination and naturalness jointly rather than treating either dimension in isolation.
4. The emerging direction for active CVD assistance is individualized and context-dependent compensation. Recent approaches range from severity-adaptable optimization and real-time temporally stable daltonization to learned models trained from individual perceptual judgments. Future evaluation frameworks should consequently combine observer-specific color-discrimination data, task performance, naturalness, and user preference, and should favor redundant visual cues (e.g., labels, patterns, icons, and luminance structure) whenever color alone is not sufficient.

6. Acknowledgments

This work was supported by research project PID2022-139056NB-I00, funded by MICIU/AEI/10.13039/501100011033 and ERDF/EU, and by the Ministry of Science, Technological Development and Innovation (Contract No. 451-03-34/2026-03/200156) and the Faculty of Technical Sciences, University of Novi Sad through project “Scientific and Artistic Research Work of Researchers in Teaching and Associate Positions at the Faculty of Technical Sciences, University of Novi Sad 2026” (No. 01-3609/1).

7. References

Almutairi, N.M., Kundart, J., Muthuramalingam, N., Hayes, J., Citek, K. and Aljohani, S. (2017) *Assessment of Enchroma filter for correcting color vision deficiency*. MSc thesis. Pacific University, College of Optometry. Available from: https://commons.pacificu.edu/opt/21 [Accessed 21 July 2026].

Apple (n.d.) *Accessibility features for vision: color filters*. Available from: https://www.apple.com/accessibility/features/ [Accessed 1 September 2026].

Badawy, A.-R., Hassan, M.U., Elsherif, M., Ahmed, Z., Yetisen, A.K. and Butt, H. (2018) 'Contact lenses for color blindness', *Advanced Healthcare Materials*, 7(12), e1800152. DOI: 10.1002/adhm.201800152

Barbur, J.L. and Rodriguez-Carmona, M. (2012) 'Variability in normal and defective colour vision: consequences for occupational environments'. In: Best, J. (ed.) *Colour Design: Theories and Applications*. Cambridge: Woodhead Publishing, pp. 24–82. DOI: 10.1533/9780857095534.1.24

Berlin, B. and Kay, P. (1991) *Basic Color Terms: Their Universality and Evolution*. Berkeley: University of California Press.

Birch, J. (2012) 'Worldwide prevalence of red-green color deficiency', *Journal of the Optical Society of America A*, 29(3), pp. 313–320. DOI: 10.1364/JOSAA.29.000313

Chen, L., Zhu, Z., Go, K., Chen, X. and Mao, X. (2026) 'ColorAdaptNet: A novel generative model for personalized color vision deficiency compensation', *IEEE Transactions on Visualization and Computer Graphics*, advance online publication. DOI: 10.1109/TVCG.2026.3728587

ChromaGen (n.d.) *ChromaGen lenses*. Available from: https://www.chromagen.us/ [Accessed 21 July 2026].

Cole, B.L. (2004) 'The handicap of abnormal colour vision', *Clinical and Experimental Optometry*, 87(4–5), pp. 258–275. DOI: 10.1111/j.1444-0938.2004.tb05056.x

Color Imaging Lab, University of Granada (n.d.) *Ishihara spectral database*. Available from: https://colorimaginglab.ugr.es/pages/data [Accessed 1 September 2026].

Columbia University CAVE Laboratory (2008) *CAVE multispectral image database*. Available from: https://cave.cs.columbia.edu/repository/Multispectral [Accessed 1 September 2026].

Ebelin, P., Crassin, C., Denes, G., Oskarsson, M., Åström, K. and Akenine-Möller, T. (2023) 'Luminance-preserving and temporally stable daltonization'. In: Babaei, V. and Skouras, M. (eds.) *Eurographics 2023 – Short Papers*, 8–12 May 2023, Saarbrücken. Goslar: Eurographics Association, pp. 45–49. DOI: 10.2312/egs.20231011

Fairchild, M.D. (2013) *Color Appearance Models*. 3rd ed. Chichester: John Wiley & Sons.

Fidaner, O., Lin, P. and Ozguven, N. (2005) *Analysis of color blindness*. Student project report, Psych 221. Stanford University. Available from: http://acorn.stanford.edu/psych221/projects/2005/ofidaner/project_report.pdf [Accessed 1 September 2026].

Foster, D.H., Nascimento, S.M.C. and Amano, K. (n.d.) *Hyperspectral images of natural scenes (rural and urban)*. Available from: https://personalpages.manchester.ac.uk/staff/david.foster/Hyperspectral_images_of_natural_scenes_02.html [Accessed 1 September 2026].

Gómez-Robledo, L., Hernández-Andrés, J., Huertas, R., Martínez-Domingo, M.A. and Valero, E.M. (2020) 'Effect of Colorlite filters on colorblind observers'. In: *AIC Interim Meeting: Natural Colours – Digital Colours*, 20 and 26–28 November 2020, Avignon. International Colour Association, p. 123.

Gómez-Robledo, L., Valero, E.M., Huertas, R., Martínez-Domingo, M.A. and Hernández-Andrés, J. (2018) 'Do EnChroma glasses improve color vision for colorblind subjects?', *Optics Express*, 26(22), pp. 28693–28703. DOI: 10.1364/OE.26.028693

Google (n.d.) *Color correction and grayscale*. Android Accessibility Help. Available from: https://support.google.com/accessibility/answer/11183305 [Accessed 2 September 2026].

Google Chrome Developers (n.d.) *Simulating color vision deficiencies in the Blink renderer*. Available from: https://developer.chrome.com/docs/chromium/cvd [Accessed 2 September 2026].

Hassan, M.F. and Paramesran, R. (2017) 'Naturalness preserving image recoloring method for people with red–green deficiency', *Signal Processing: Image Communication*, 57, pp. 126–133. DOI: 10.1016/j.image.2017.05.011

Huertas, R., Valero, E.M., Gómez-Robledo, L., Martínez-Domingo, M.A. and Hernández-Andrés, J. (2024) 'Congenital red-green colour deficiency: study of the efficacy of commercial colour filters', *Journal of the International Colour Association*, 35, pp. 24–28. Available from: https://digibug.ugr.es/handle/10481/96450 [Accessed 21 July 2026].

Ishihara, S. (1977) *Tests for Colour-Blindness*. Tokyo: Kanehara Shuppan Co., Ltd.

Karepov, S. and Ellenbogen, T. (2020) 'Metasurface-based contact lenses for color vision deficiency', *Optics Letters*, 45(6), pp. 1379–1382. DOI: 10.1364/OL.384970

Martínez-Domingo, M.A., Gómez-Robledo, L., Valero, E.M., Huertas, R., Hernández-Andrés, J., Ezpeleta, S. and Hita, E. (2019) 'Assessment of VINO filters for correcting red-green Color Vision Deficiency', *Optics Express*, 27(13), pp. 17954–17967. DOI: 10.1364/OE.27.017954

Martínez-Domingo, M.A., Valero, E.M., Gómez-Robledo, L., Huertas, R. and Hernández-Andrés, J. (2020) 'Spectral filter selection for increasing chromatic diversity in CVD subjects', *Sensors*, 20(7), 2023. DOI: 10.3390/s20072023

Mastey, R., Patterson, E.J., Summerfelt, P., Luther, J., Neitz, J., Neitz, M. and Carroll, J. (2016) 'Effect of "color-correcting glasses" on chromatic discrimination in subjects with congenital color vision deficiency', *Investigative Ophthalmology & Visual Science*, 57(12), 192.

Maxwell, J.C. (1857) 'Experiments on colour, as perceived by the eye, with remarks on colour-blindness', *Transactions of the Royal Society of Edinburgh*, 21(2), pp. 275–298.

Microsoft (n.d.) *Use color filters in Windows*. Available from: https://support.microsoft.com/en-us/windows/use-color-filters-in-windows [Accessed 2 September 2026].

Milić, N., Hoffmann, M., Tómács, T., Novaković, D. and Milosavljević, B. (2015) 'A content-dependent naturalness-preserving daltonization method for dichromatic and anomalous trichromatic color vision deficiencies', *Journal of Imaging Science and Technology*, 59(1), pp. 010504-1–010504-10. DOI: 10.2352/J.ImagingSci.Technol.2015.59.1.010504

Muñoz-Postigo, J., Valero, E.M., Martínez-Domingo, M.A., Gómez-Robledo, L., Huertas, R. and Hernández-Andrés, J. (2022) 'CVD-MET: an image difference metric designed for analysis of color vision deficiency aids', *Optics Express*, 30(19), pp. 34665–34683. DOI: 10.1364/OE.456346

Nascimento, S.M.C., Ferreira, F.P. and Foster, D.H. (2002) 'Statistics of spatial cone-excitation ratios in natural scenes', *Journal of the Optical Society of America A*, 19(8), pp. 1484–1490. DOI: 10.1364/JOSAA.19.001484

Patterson, E.J. (2017) 'Glasses for the colorblind: their effect on chromatic discrimination in subjects with congenital red-green color vision deficiency'. In: *International Conference on Computer Vision Systems (ICVS)*, 10–13 July 2017, Shenzhen, China, pp. 18–22.

Popleteev, A., Louveton, N. and McCall, R. (2015) 'Colorizer: smart glasses aid for the colorblind'. In: Ashok, A., Liu, J. and Banerjee, S. (eds.) *Proceedings of the 2015 Workshop on Wearable Systems and Applications (WearSys '15)*, May 2015, Florence. New York: ACM, pp. 7–8. DOI: 10.1145/2753509.2753516

Ribeiro, M. and Gomes, A.J. (2019) 'Recoloring algorithms for colorblind people: a survey', *ACM Computing Surveys*, 52(4), Article 72, pp. 1–37. DOI: 10.1145/3329118

Rodriguez-Carmona, M.L., Harlow, A.J., Walker, G. and Barbur, J.L. (2005) 'The variability of normal trichromatic vision and the establishment of the "normal" range'. In: *Proceedings of the 10th Congress of the International Colour Association (AIC Colour 05)*, 8–13 May 2005, Granada. Granada: International Colour Association, pp. 979–982.

Simunovic, M.P. (2010) 'Colour vision deficiency', *Eye*, 24(5), pp. 747–755. DOI: 10.1038/eye.2009.251

Somers, L.P., Franklin, A. and Bosten, J.M. (2024) 'Empirical tests of the effectiveness of EnChroma multi-notch filters for enhancing color vision in deuteranomaly', *Vision Research*, 218, 108390. DOI: 10.1016/j.visres.2024.108390

Swarbrick, H.A., Nguyen, P., Nguyen, T. and Pham, P. (2001) 'The ChromaGen contact lens system: colour vision test results and subjective responses', *Ophthalmic and Physiological Optics*, 21(3), pp. 182–196. DOI: 10.1046/j.1475-1313.2001.00583.x

Werner, J.S., Marsh-Armstrong, B. and Knoblauch, K. (2020) 'Adaptive changes in color vision from long-term filter usage in anomalous but not normal trichromacy', *Current Biology*, 30(15), pp. 3011–3015.e4. DOI: 10.1016/j.cub.2020.05.054

X-Rite (2006) *FM 100 Hue color vision test: 100 Hue test scoring tool, version 3.0*.

Zhu, Z., Toyoura, M., Go, K., Kashiwagi, K., Fujishiro, I., Wong, T.-T. and Mao, X. (2022) 'Personalized image recoloring for color vision deficiency compensation', *IEEE Transactions on Multimedia*, 24, pp. 1721–1734. DOI: 10.1109/TMM.2021.3070108



© 2026 Authors. Published by the University of Novi Sad, Faculty of Technical Sciences, Department of Graphic Engineering and Design. This article is an open access article distributed under the terms and conditions of the Creative Commons Attribution license 4.0 Serbia (https://creativecommons.org/licenses/by/4.0/deed.en).

Original Scientific Paper https://doi.org/10.24867/GRID-2026-p29

Colorimetric and Lightfastness Assessment of Water-Based Magenta Inkjet Prints on Wood-Free Offset Substrate

ABSTRACT

This study investigates how the surface coverage of water-based magenta inkjet ink printed on uncoated wood-free offset paper influences its lightfastness under long-term exposure to light. The initial hypothesis of the research is that photodegradative changes in the paper substrate directly modify the colorimetric response of printed patches. Furthermore, it is assumed that an increase in surface coverage will result in a smaller total colour difference (ΔE). Over an 18-month period of simulated exposure inside an accelerated ageing chamber, the photodegradation of prints was monitored using CIE ΔE_{00} colorimetric parameters (ΔE_{00}, ΔC_{00}, ΔL_{00}). Obtained results confirmed the initial hypothesis. The unprinted paper substrate exhibited lower lightfastness compared to the printed patches. Due to pronounced photodegradative yellowing, the paper primarily dictates colorimetric deviations in the light tone domain, resulting in light tonal patches undergoing greater colour change compared to middle and dark tones. However, with increasing surface coverage, the higher concentration of magenta pigment reduces the transmission of radiation to the paper fibres. This diminishes the optical contribution of the degraded substrate to the total reflectance, leading to a general decline in the overall colour difference (ΔE_{00}). A notable exception is observed in the 70% TV patch, which achieves higher stability (lower ΔE_{00}) than the full-tone patch (100% TV). Analysis of individual parameters confirmed that chroma variation (ΔC_{00}) represents the primary factor determining the total colour deviation. Conversely, the effect of lightness variation is negligible, with average ΔL_{00} values remaining up to merely 1.26. By considering the synergy between substrate photodegradation and the optical coverage effect of the applied pigment, this work provides deeper insights into ink–substrate interactions and key factors influencing long-term colour reproduction stability in graphic products.

Bojana Narić [1]
Mladen Stančić [1]
Igor Majnarić [2]
Miroslav Dragić [1]

[1] University of Banja Luka, Faculty of Technology, Banja Luka, Bosnia and Herzegovina
[2] University of Zagreb, Faculty of Graphic Arts, Department of printing, Zagreb, Croatia

KEY WORDS
Water-based inkjet, magenta pigment, lightfastness, uncoated offset paper, CIEΔ00, climate chamber

1. Introduction

The digital printing market is experiencing rapid growth, with drop-on-demand inkjet representing one of the most significant and fastest-growing segments of graphic technology. Owing to low operational costs and exceptional adaptability across a wide range of products, inkjet systems hold an increasingly prominent position in the modern graphic arts industry. Although the largest volume continues to stem from continuous web-fed printing (estimated at 500 billion A4 impressions in 2024), sheet-fed inkjet exhibits steady, expansive growth, having reached 60 billion A4 pages. The market for sheet-fed systems in A3, B3,

B2, and B1 formats is currently dominated by smaller-format devices, whereas a drastic increase in installations is projected for larger, more complex systems (B2 and B1) by 2028 (Vujčić et al., 2024; Majnarić et al., 2024a; The Business Research Company, 2024).

In contemporary inkjet production, the implementation of water-based inks is expanding across industrial applications. This market expansion is evidenced by a compound annual growth rate of approximately 5.9%, reflecting a sustained trend towards broader deployment (Narić et al., 2025; The Business Research Company, 2024). The principal advantage of these inks stems from their environmental sustainability, as they contain no volatile organic compounds (VOCs) or residual solvents, reduce odour emissions, and facilitate printhead maintenance by reducing nozzle clogging. Conversely, manufacturers continue to address their primary technological drawbacks, notably slower drying rates, high energy consumption during the fixing process, and reduced adhesion on certain substrates (Jingxiang et al., 2019; Ozcan, Coskun & Arman Kandirmaz, 2024).

In the inkjet printing process, paper—as the most commonly used substrate—substantially impacts both, image formation and the optical durability of the print. Adequate compatibility between the substrate and the ink is governed by the physical and chemical properties of the paper, such as smoothness, surface energy, and absorbency, which directly dictate mechanical dot gain and pigment adhesion (Majnarić et al., 2024b; Narić, 2024; Gazibarić, Stančić & Ružičić, 2024). Beyond physical parameters, the optical properties of the paper (whiteness and brightness) and its chemical composition (the presence of cellulose fibres, lignin, or fluorescent whitening agents) actively participate in degradation reactions under external influences, whereby the substrate directly affects overall colour stability (Kumar, Pathak & Bhardwaj, 2022).

Consequently, evaluating the optical stability of printed material demands a synergistic approach in which the behaviour of the substrate and the ink is considered a unified system exposed to photodegradation, primarily induced by the absorption of ultraviolet photons. In the context of process inks, magenta is particularly susceptible to light-induced chromophore degradation owing to its strong absorption characteristics within the green region of the spectrum. In addition to the pigment itself, the structural components of the paper directly influence the stability of the entire print: while the presence of cellulose with hydrogen bonding and polymer additives containing alkyl groups positively enhances light resistance, polymers incorporated with UV absorbers can destabilise the substrate. Systematic lightfastness analysis is therefore essential for elucidating the mechanisms required to achieve maximum durability in graphic products (Ozcan, Coskun & Arman Kandirmaz, 2024; Lucas, 2001).

Lightfastness testing is conducted under accelerated ageing conditions using chambers basically equipped xenon lights, in compliance with internationally recognised standards, such as ISO 105-B02, ISO 105-B01, ISO 105-B03, ISO 105-B04, ISO 105-B05, ISO 105-B06, ISO 105-B07, ISO 105-B08, and BS ISO 2834 (Boeva et al., 2018; Cofomegra, n.d.; Smithers, n.d.). Objective, reliable evaluation of light-induced changes is attained through spectrophotometric analysis of CIE Lab* parameters and the quantification of total colour difference. To this end, specific colour difference formulae and models are applied, including CMC (l:c), BFD (l:c), CIE 94, LCD, CIE ΔE_{00} and the mathematically refined CIE ΔE_{00} equation (Kašiković, 2015; Aydemir & Yenidoğan, 2018; Milinković et al., 2025).

In accordance with the aforementioned considerations, the objective of this study is to spectrophotometrically assess the impact of accelerated ageing on the lightfastness of prints produced with a water-based magenta inkjet ink, while accounting for the specific characteristics of the applied paper substrate.

2. Methods

To evaluate the printability, tone reproduction stability, and lightfastness performance of water-based inkjet prints on an uncoated paper substrate, a systematic experimental workflow was implemented.

2.1. Materials and printing conditions

Commercial uncoated woodfree offset paper, Mondi Maestro Print 120 g/m² (manufactured from a mixture of dried cellulose, carboxymethyl cellulose, starch, and animal glue), was used as the primary printing substrate. The main technical properties and specifications of the paper substrate are listed in Table 1. Test printing was performed using a water-based inkjet ink formulation designated as IK7125-M magenta, whose technical characteristics and specifications are summarised in Table 2.

A total of 50 samples were produced using the Kyocera TASKalfa Pro 15000c high-speed production inkjet printing machine, integrated with a Fiery PS-50 digital front-end RIP system.

The application of each process colour was carried out by three Kyocera KJ4B-YH piezoelectric printheads (detailed technical specifications of the printing system are outlined in Table 3). Prior to printing the test samples, system calibration and profiling were performed in accordance with the Fogra 52 standard (PSO Uncoated v3 / ISO 12647-2:2013) to ensure tone reproduction accuracy and consistency. For system verification and test printing, the standardised control strip Ugra/Fogra Media Wedge v3.0 was utilized.

Table 1

Mondi Maestro Print 120 g/m² specifications (My Mondi, 2024)

Characteristic	Standard	Value
Basic weight	ISO 536	120 ± 4.5 g/m²
Paper thickness	ISO 536	144 ± 6 µm
Bendtsen roughness	ISO 8791 – 2	225 ± 75 mL/min
Opacity	ISO 2471	96.00 ± 1.6 %
Moisture abs.	ISO 287	6.2 ± 0.7 %
Brightness UV	ISO 2470	135.5 ± 1.5 %
CIE Whiteness	ISO 11 475	145 ± 3.0 %

Table 2

Chemical composition of the Kyocera IK7125-M ink (Kyocera, 2024)

Chemical name	Identifier	Percentage
Water	7732-18-5	40-60%
Polyhydric alcohol	Confidential	20-30%
Triethylene glycol monobutyl	143-22-6	5-10%
Organic pigment	Confidential	5-10%
Glycerol	56-81-5	5-10%
1,2-benzisothiazol-3(2H)-one	2635-33-5	<0.05%
2-methyl-2H-isothiazol-3-one	268-20-4	<0.05%

Table 3

Kyocera TASKalfa Pro 15 000c specifications (Kyocera, n.d.)

Paper size	98 x 148 mm – 330.2 x 488 mm
Print speed	A4: 150 ppm/150 ppm (75 sheets)
	A3: 88 ppm/88 ppm (44 sheets)
	SRA3: 75 ppm/75 ppm (37 sheets)
	A3W: 74 ppm/74 ppm (37 sheets)
Available thickness printing at rated speed	Up to 360 g/m²
Print resolution	600 x 600 dpi, 600 x 1200 dpi

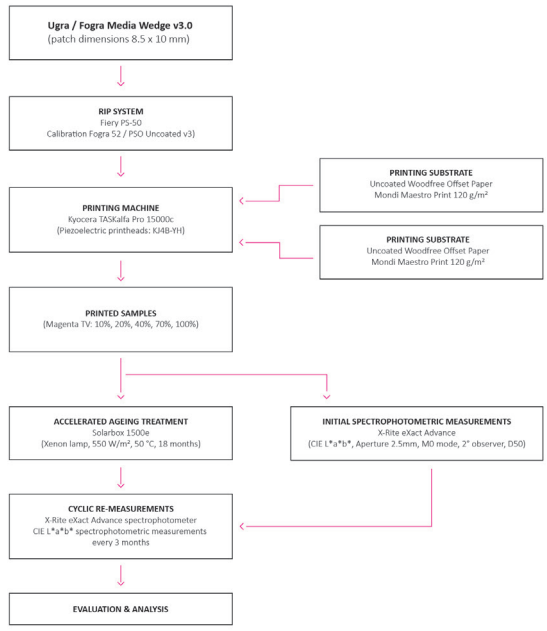
2.2. Spectrophotometric measurements

Evaluation of colour differences were performed by measuring CIE L*a*b* values using an X-Rite eXact Advance spectrophotometer. Although the printed control strip contains a comprehensive set of measurement fields, specific magenta patches were selected for lightfastness testing across the tonal range, representing light tones, midtones, and dark tones at tone value (TV) coverages of 10%, 20%, 40%, 70%, and 100%.Measurements were carried out under standardised geometric and optical conditions: a 2.5 mm measuring aperture, M0 measurement mode (unfiltered standard illumination in accordance with ISO 13655), 2° standard observer, and D50 standard illuminant.

2.3. Lightfastness testing

Lightfastness testing of the prints was performed in a Solarbox 1500e accelerated ageing chamber equipped with a full-spectrum xenon lamp to evaluate pigment stability and substrate degradation under light exposure. The exposure parameters were set to an irradiance of 550 W/m² (without a UV filter), a chamber temperature of 50 °C, and a total exposure duration equivalent to 18 months of natural ageing. To monitor photodegradation's influence, samples were periodically removed from the chamber at 3-month simulated ageing intervals for control CIE L*a*b* spectrophotometric re-measurements of the selected patches.

A schematic representation of the performed experimental methodology is shown in Figure 1.

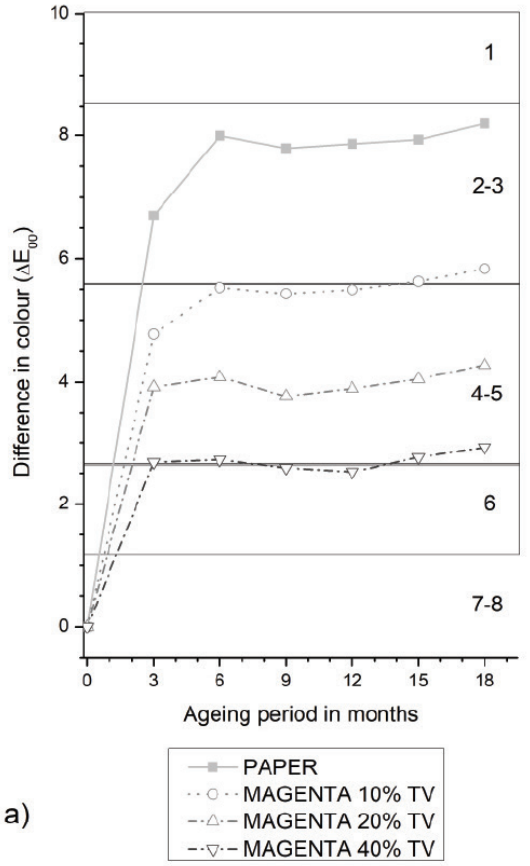


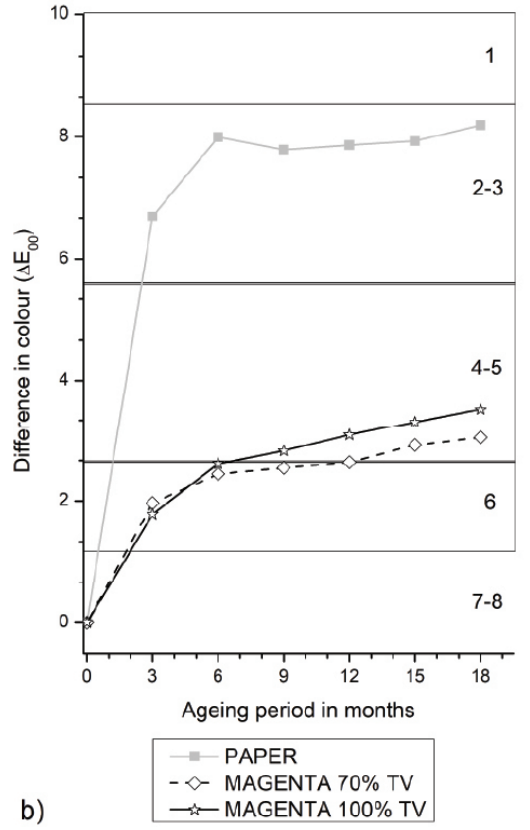
» **Figure 1:** *Schematic representation of the performed experiment*

3. Results

This section presents the spectrophotometric measurement results for the unprinted paper substrate alongside the light tones (10% and 20% TV), midtones (40% TV), and dark tones (70% and 100% TV) of the magenta patches subjected to 18 months of accelerated ageing under controlled conditions (50 °C, 550 W/m²).

The evaluation includes the total colour difference (ΔE_{00}), chroma deviation (ΔC_{00}), and lightness deviation (ΔL_{00}). The total colour difference (ΔE_{00}) for the paper substrate and the magenta printed patches over the 18-month ageing period is illustrated in Figure 2.





» **Figure 2:** *Colour difference diagram of light and midtones (a), Colour difference diagram of dark tones (b)*

The unprinted paper substrate demonstrated the most pronounced increase during the initial 3 months of exposure, reaching a value of ΔE_{3m} = 6.70. After 6 months of treatment, the value increased to ΔE_{6m} = 7.99, following which the total colour difference stabilised at an average value of $\Delta E_{6\text{-}18m}$ = 7.95 for the duration of the testing period.

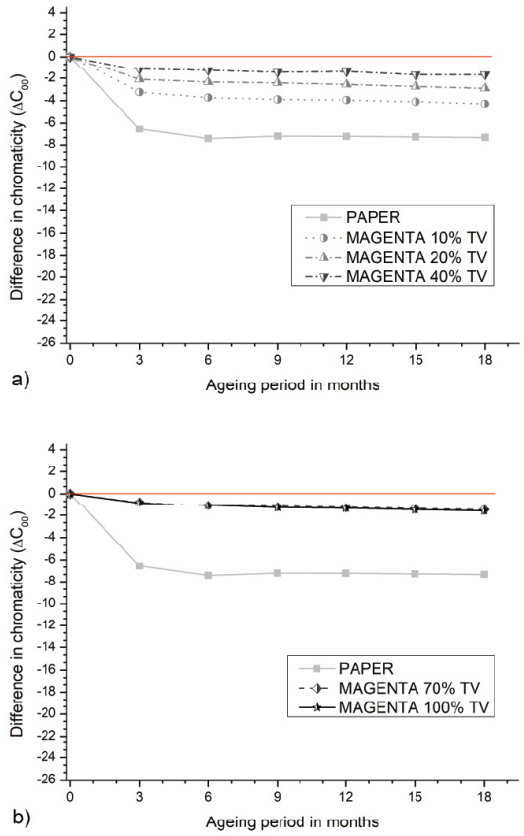
For the magenta printed patches, the 10% TV patch demonstrated a colour difference of ΔE_{6m} = 5.53 after 6 months, maintaining an average value of $\Delta E_{6\text{-}18m}$ = 5.58 through the 6-to-18-month interval. The 20% TV patch displayed a mean total colour difference of $\Delta E_{3\text{-}18m}$ = 4.00 across the 3-to-18-month period, attaining ΔE_{18m} = 4.28 at the 18-month mark. The 40% TV patch maintained an average colour difference of $\Delta E_{3\text{-}18m}$ = 2.70. For the dark tones, measurable changes occurred after 9 months, establishing average values of $\Delta E_{3\text{-}18m}$ = 2.59 for the 70% TV patch and $\Delta E_{3\text{-}18m}$ = 2.85 for the 100% TV patch.

In terms of chroma deviations (ΔC_{00}), shown in Figure 3, the paper substrate displayed an initial decrease of $\Delta C_{0\text{-}3m}$=-6.56 within the first 3 months, stabilising at an average value of $\Delta C_{6\text{-}18m}$ =-7.29 from 6 to 18 months. All printed magenta patches presented strictly negative ΔC_{00} values. For the 10% TV patch, an overall mean chroma deviation of $\Delta C_{3\text{-}18m}$ =-4.17 was attained across the 3-to-18-month interval.

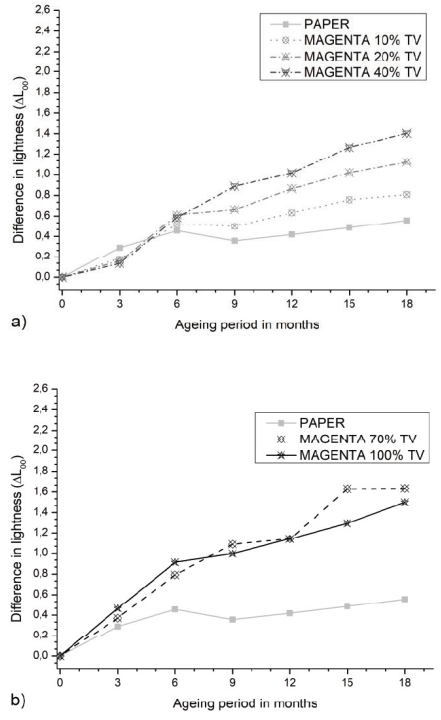
For the 20% TV patch, the chroma deviation progressed from ΔC_{3m} =-2.10 at 3 months to ΔC_{18m} =-2.91 at 18 months, with an overall mean quantified at $\Delta C_{3\text{-}18m}$ = -2.51. The 40% TV patch showed values of ΔC_{3m} =-1.18$ and ΔC_{18m} =-1.69, averaging $\Delta C_{3\text{-}18m}$ =-1.46. The dark tone patches generated initial 3-month deviations of ΔC_{3m}=-0.77 (70% TV) and ΔC_{3m}=-0.82 (100% TV), which expanded to ΔC_{18m}=-1.51 (70% TV) and ΔC_{18m}=-1.61(100% TV) after 18 months, corresponding to period averages of $\Delta C_{3\text{-}18m}$=-1.20 and $\Delta C_{3\text{-}18m}$=-1.28, respectively.

Regarding lightness deviations (ΔL_{00}), presented in Figure 4, the paper substrate registered a mean deviation of $\Delta L_{3\text{-}18m}$= 0.50 across the 3-to-18-month period. For the light tones and midtones (10%, 20%, and 40% TV), the lightness deviation averaged approximately 0.57 during the initial 6 months.

In the subsequent interval (6 to 18 months), the average lightness deviations were determined as $\Delta L_{6\text{-}18m}$= 0.64 for the 10% TV patch, $\Delta L_{6\text{-}18m}$= 0.85 for the 20% TV patch, and $\Delta L_{6\text{-}18m}$ = 1.03 for the 40% TV patch. The dark tone patches displayed 6-month values of ΔL_{6m}= 0.79 (70% TV) and ΔL_{6m}= 0.91 (100% TV). Over the 6-to-18-month timeframe, the 70% TV patch reached a mean value of $\Delta L_{6\text{-}18m}$= 1.26, attaining a maximum deviation at the 15th month prior to stabilisation, whereas the 100% TV full-tone patch manifested an average deviation of $\Delta L_{6\text{-}18m}$= 1.17 with a continuous upward trend.



» **Figure 3:** *Diagram of changes in chromaticity of light and mid-tones (a), Diagram of changes in chromaticity of dark tones (b)*



» **Figure 4:** *Diagram of changes in lightness of light and mid-tones (a), Diagram of changes in lightness of dark tones (b)*

4. Discussion

The spectrophotometric evaluation over 18 months of accelerated ageing reveals distinct degradation behaviours between the unprinted paper substrate and the water-based magenta inkjet prints across varying tone value coverages. The paper substrate demonstrated high sensitivity to light exposure, undergoing its most severe degradation during the initial 3 months. The stabilisation of the total colour difference confirms the presence of clearly visible colour changes on the substrate.

This degradation is primarily associated with an increased influence of chroma, causing a permanent hue variation of the substrate toward a yellow-red region. Conversely, the minimal lightness deviations indicate that lightness changes have a minor contribution to the overall colour difference of the paper substrate compared to the chromaticity variation.

The lightfastness of the magenta prints is directly proportional to surface coverage (TV). In light tones such as the 10% TV patch, colour differences stabilise after 3 months; despite maintaining a classification of very good lightfastness, this coverage demonstrates the highest overall deviation among all printed samples. Increasing coverage to 20% TV brings the print within the threshold of excellent lightfastness (ΔE_{00}= 4.00), exceeding this boundary only slightly at the 18-month mark. Midtones (40% TV) and dark tones (70% and 100% TV) maintain high lightfastness stability, with minor variations appearing only after 9 months. The performance of the 70% TV and 100% TV patches is nearly identical, with the 70% TV patch showing marginally higher stability ($\Delta E_{3\text{-}18m}$ = 2.59).

Analyzing individual colour components—specifically chroma (ΔC_{00}) and lightness (ΔL_{00}) variations—reveals different degradation mechanisms across various tonal coverages. The ΔC_{00} values across all printed patches confirm that changes in chromaticity is the primary cause of total colour difference. Increasing tone value coverage directly reduces this change: transitioning from 10% to 20% TV reduces average chroma variation by 1.35, while advancing to 40% TV provides an additional reduction of 1.05.

In dark tones, changes in chromaticity becomes minimal, confirming that higher pigment density effectively protects the printed layer against saturation loss. In contrast, lightness deviations display an inverse trend during later stages of ageing (6 to 18 months). While light tones (10% TV) preserve relatively stable, full-tone prints (100% TV) experience higher and continually rising lightness values.

This suggests that in full-tone areas, where chroma remains highly stable, lightness alteration becomes an increasingly prominent contributor to ongoing visual colour changes under prolonged exposure.

5. Conclusions

This study provided a comprehensive evaluation of the lightfastness and degradation behaviour of water-based magenta inkjet ink printed on a wood-free offset paper substrate subjected to an 18-month exposure period inside an accelerated ageing chamber. The results confirm that overall print stability is directly determined by tone value coverage, alongside the complex interaction between the pigment layer and the paper substrate. Given that the paper substrate itself undergoes notable colorimetric changes, its influence on the visual degradation of the magenta patches is particularly pronounced in light tonal values (10% and 20% TV), while midtones and dark tones show considerably higher stability.

The unprinted substrate demonstrated high sensitivity to light exposure, achieving a total colour difference of $\Delta E_{6\text{-}18m}$= 7.95 associated with an increased influence of chroma ($\Delta C_{0\text{-}3m}$=-6.56). Increasing surface coverage yielded a clear reduction in total colour difference and chroma change. Increasing surface coverage directly reduces total colour differences and changes in chromaticity, allowing midtones (40% TV) and dark tones (70% and 100% TV) to maintain high stability within the boundaries of excellent lightfastness.

Evaluation of individual colour components demonstrates that chromaticity variation represents the primary cause of total colour difference across all printed patches throughout the entire exposure period. In contrast, lightness alterations exert a minor overall influence; although slightly higher lightness variations appear in dark tones, these values remain low, reaching maximum deviations of ΔL_{18m}= 1.63 for the 70% TV patch at the 18-month mark.

These findings provide valuable insights for evaluating the long-term stability and colour accuracy of water-based inkjet prints on uncoated offset substrates in professional graphic applications. To build upon these insights, future research should expand toward evaluating ink-substrate interaction mechanisms across diverse non-absorbent and coated substrates. Furthermore, investigating the application of protective overprint varnishes, UV-curable coatings, and surface laminates presents a crucial direction for mitigating substrate-induced yellowing and suppressing late-stage lightness alterations in full-tone areas.

6. Acknowledgments

The authors gratefully acknowledge the financial support provided by the Ministry of Scientific and Technological Development, Higher Education and Information Society of the Republic of Srpska under project No. 19.032/961-60/24, titled “Critical Assessment of Color Quality Control in the Printing Industry in Accordance with the Recommendations of ISO 12647, ISO 15311, and ISO 13655 Standards.” and by the Provincial Secretariat for Higher Education and Scientific Research of the Autonomous Province of Vojvodina, Republic of Serbia, through the project "Digital and Ecological Transformation of the Graphic Industry" (No. 004351431 2025 09418 003 000 000 001 04 002).

7. References

Aydemir, C. and Yenidoğan, S. (2018) 'Light fastness of printing inks: A review', *Journal of Graphic Engineering and Design*, 9(1), pp. 37–43. DOI: 10.24867/JGED-2018-1-037

Boeva, R., Spiridonov, I., Yordanov, S., Bozhkova, T. and Ivanov, Z. (2018) 'Investigation of color reproduction accuracy of different ink jet and electrophotographical printing systems'. In Gojo, M., Žiljak Vujić, J. and Nedeljković, U. (eds.) *Proceedings of the 9th International Symposium on Graphic Engineering and Design*, 8–10 November 2018, Novi Sad, Serbia. Novi Sad: University of Novi Sad, Faculty of Technical Sciences, Department of Graphic Engineering and Design, pp. 291–301. DOI: 10.24867/GRID-2018-p36

Cofomegra (n.d.) *Solarbox 1500E–3000E*. Available from: https://cofomegra.it/en/solarbox-1500e-3000e/ [Accessed 9 December 2024].

Gazibarić, Z., Stančić, M. and Ružičić, B. (2024) 'Evaluation of print mottle in textile printing: Impact of printing methods on macro non-uniformities'. In Dedijer, A. (ed.) *Proceedings of the 12th International Symposium on Graphic Engineering and Design*, 7–9 November 2024, Novi Sad, Serbia. Novi Sad: University of Novi Sad, Faculty of Technical Sciences, Department of Graphic Engineering and Design, pp. 69–75. DOI: 10.24867/GRID-2024-p9

Jingxiang, X., Jinyao, L., Haichao, L., Mingming, Z. and Jifei, C. (2019) 'Research progress on water-based ink drying technology', *IOP Conference Series: Materials Science and Engineering*, 565(1), 012017. DOI: 10.1088/1757-899X/565/1/012017

Kašiković, N. (2015) 'Thermovision and spectrophotometric analysis of ink volume and material characteristics influence on colour changes of heat treated printed substrates', *Technical Gazette*, 22(1), pp. 33–41. DOI: 10.17559/TV-20130928115500

Kumar, V., Pathak, P. and Bhardwaj, N.K. (2022) 'Production of advanced fibrillated cellulosic material from wheat straw by refining process to improve paper quality', *Cellulose Chemistry and Technology*, 56(5–6), pp. 625–635. DOI: 10.35812/CelluloseChemTechnol.2022.56.55

Kyocera (n.d.) *TASKalfa Pro 15000c*. Available from: https://www.kyoceradocumentsolutions.eu/en/products/production-printing/TASKALFAPRO15000C.html [Accessed 9 December 2024].

Kyocera (2024) *Safety Data Sheet*. Available from: https://www.kyoceradocumentsolutions.eu/en/support/downloads.name-L2V1L2VuL3Byb2R1Y3Rpb24tcH-JpbnRpbmcvVEFTS0FMRkFQUk8xNTAwMEM=.html#tab=document [Accessed 9 December 2024].

Lucas, J. (2001) 'Keep Your True Colors: Lightfastness and Weatherability Testing', *GATFWorld*, 85, pp. 13–16.

Majnarić, I., Morić, M., Valdec, D. and Milković, K. (2024a) 'The effect of applying UV LED-cured varnish to metalized printing elements during cold foil lamination', *Coatings*, 14(5), 604. DOI: 10.3390/coatings14050604

Majnarić, I., Sabol, S., Stančić, M. and Vujčić, Đ. (2024b) 'The influence of KM1800iSHC inkjet head settings on the colour reproduction quality of the Accurio Jet KM-1 inkjet machine'. In Malinović, B. (ed.) *Proceedings of the XV Conference of Chemists, Technologists and Environmentalists of Republic of Srpska*, 18–19 October 2024, Banja Luka, Bosnia and Herzegovina. Banja Luka: University of Banja Luka, Faculty of Technology, pp. 242–250.

Milinković, B., Stančić, M., Majnarić, I., Blaznik, B. and Urbas, R. (2025) 'Influence of aging process on UV inkjet black printed PVC foil', *Journal of Chemical Technology and Metallurgy*, 60(3), pp. 501–510. DOI: 10.59957/jctm.v60.i3.2025.18

My Mondi (2024) *MAESTRO® PRINT*. Available from: https://www.mymondi.net/ufp/en/brand/maestroprint [Accessed 9 December 2024].

Narić, B. (2024) *Lightfastness of Kyocera Water-Based Inkjet Inks*. Master's thesis. University of Banja Luka, Faculty of Technology.

Narić, B., Stančić, M., Majnarić, I. and Malinović, B. (2025) 'Lightfastness of water-based yellow inkjet imprints', *Cellulose Chemistry and Technology*, 59(3–4), pp. 353–363. DOI: 10.35812/CelluloseChemTechnol.2025.59.31

Ozcan, A., Coskun, S. and Arman Kandirmaz, E. (2024) 'Environmentally friendly water-based inkjet ink production and determining printability'. In Dedijer, A. (ed.) *Proceedings of the 12th International Symposium on Graphic Engineering and Design*, 7–9 November 2024, Novi Sad, Serbia. Novi Sad: University of Novi Sad, Faculty of Technical Sciences, Department of Graphic Engineering and Design, pp. 97–103. DOI: 10.24867/GRID-2024-p12

Smithers (n.d.) *Light Fastness Testing*. Available from: https://www.smithers.com/industries/materials/print/print-quality-durability/light-fastness-testing [Accessed 9 December 2024].

The Business Research Company (2024) *Water-Based Printing Inks Global Market Report*. Available from: https://www.thebusinessresearchcompany.com/report/water-based-printing-inks-global-market-report [Accessed 12 December 2024].

Vujčić, Đ., Kašiković, N., Petrović, S. and Urbas, R. (2024) 'Analysing the reproduction quality of Braille dots on self-adhesive labels produced with UV inkjet printing'. In Dedijer, A. (ed.) *Proceedings of the 12th International Symposium on Graphic Engineering and Design*, 7–9 November 2024, Novi Sad, Serbia. Novi Sad: University of Novi Sad, Faculty of Technical Sciences, Department of Graphic Engineering and Design, pp. 121–128. DOI: 10.24867/GRID-2024-p15

© 2026 Authors. Published by the University of Novi Sad, Faculty of Technical Sciences, Department of Graphic Engineering and Design. This article is an open access article distributed under the terms and conditions of the Creative Commons Attribution license 4.0 Serbia (http://creativecommons.org/licenses/by/4.0/rs/).

Packaging design and added value

03

Original Scientific Paper https://doi.org/10.24867/GRID-2026-p30

Perceptual and Kansei Responses to Alphanumeric Onomastics in Emotional Packaging Design Across Age Groups

ABSTRACT

This study examines perceptual and Kansei responses to alphanumeric onomastics in emotional packaging design across different age groups. Grounded in contemporary perception theory and Kansei Engineering, the research investigates how alphanumeric naming cues on packaging function as affective stimuli that shape emotional meaning and product interpretation. A total of 204 consumers were recruited through convenience sampling and categorized into five age groups, ranging from 12 years to over 41 years. Experimental packaging stimuli featuring alphanumeric names (e.g., H_2O) were designed using Adobe Photoshop. Participants evaluated their affective responses by selecting from 11 emotion-related descriptors, including healthy, desirable, amazing, reliable, and fearful. Word-frequency analysis was used to identify dominant Kansei descriptors, while ANOVA and Kruskal–Wallis tests assessed age-related differences in perceptual responses. Results indicated no significant differences across age groups (ANOVA: $F(4, 50) = 1.27$, $p = .294$; Kruskal–Wallis: $\chi^2(4, N = 204) = 8.43$, $p = .077$), suggesting a consistent perceptual and emotional interpretation of alphanumeric onomastics. Overall, alphanumeric naming elicited moderately positive Kansei responses, with healthy and amazing emerging as the most frequently associated perceptions. These findings suggest that alphanumeric onomastics operate as age-independent perceptual cues, supporting theories of shared cognitive processing and affective perception. The study contributes to Emotional Design of Packaging (EDOP) by demonstrating how alphanumeric naming can function as a universally resonant design strategy, reinforcing Kansei-based approaches to inclusive and emotionally engaging packaging. Also, these findings align with universal design principles, suggesting that alphanumeric onomastics function as inclusive perceptual cues capable of eliciting consistent Kansei responses across age groups. Future research is recommended to explore broader product categories and larger samples to further validate the perceptual robustness of alphanumeric onomastics in packaging design.

Ayorinde S. Oluyemi
Oluwafemi S. Adelabu
E. Bankole Oladumiye

Federal University of Technology (FUTA), Industrial Design, Akure, Nigeria

KEY WORDS
Alphanumeric onomastics, Kansei engineering, emotional design of packaging (EDOP), perceptual and affective processing, consumer emotion, age-related perception, visual naming cues, universal design principle

1. Introduction

TThe landscape of modern packaging research is increasingly multidimensional, as evidenced by the diverse inquiries presented at the 12th International Symposium on Graphic Engineering and Design (Grid 2024). Recent scholarly focus has largely centered on the eco-friendly and material aspects of design, with researchers investigating sustainable alternatives and the technical properties of substrates (Madhan, Nirmala & Kanchana, 2024;

Jamnicki Hanzer, 2024; Nechita, Roman & Năstac, 2024). Concurrently, the integration of Artificial Intelligence (AI) and Smart Packaging technologies (Vladić et al., 2024; Mahović Poljaček et al., 2024) reflects an industry-wide shift toward interactive and data-driven systems. While significant strides have been made in ergonomics (Bošnjaković et al., 2024) and the use of eye-tracking analysis to quantify visual attention (Gvoka et al., 2024), a specialized gap remains regarding the linguistic and affective power of product naming. While recent studies have explored branding broadly (Oluyemi, Adelabu & Oladumiye, 2024; Liokos et al., 2024), there exists a void regarding how alphanumeric nomenclature specifically influences emotional perception—a gap the present study seeks to address through a Kansei-based evaluation.

The growing emphasis on emotional engagement in product communication has significantly transformed contemporary packaging design. Beyond their functional role of protecting and identifying products, packages now serve as emotional interfaces that influence consumer perception, preference, and purchasing behaviour. In increasingly competitive consumer markets, designers and manufacturers seek innovative strategies capable of creating memorable experiences and strengthening emotional attachment between consumers and products. One such strategy is the strategic application of distinctive naming systems, particularly alphanumeric onomastics, in product labeling and packaging design. Although alphanumeric naming conventions have long been established in scientific, technological, and industrial contexts, their predictive emotional influence on consumer perception and behaviour within emotionally driven product categories remains insufficiently examined and has not yet been abundantly established in existing packaging design studies.

Alphanumeric onomastics refers to naming conventions that combine letters and numerical characters within a product name or label. These naming structures have become increasingly visible across several product categories, especially in technology-driven and industrial products where they often communicate technical sophistication, performance differentiation, or product hierarchy. However, despite their growing prevalence, the emotional implications of alphanumeric naming systems in consumer packaging remain insufficiently explored, particularly within non-alcoholic beverage packaging where emotional and sensory associations strongly shape consumer experience.

The increasing scholarly attention to emotional design has reinforced the importance of understanding how visual and verbal design elements stimulate affective responses among users. Emotional engagement in packaging design has attracted considerable academic interest because consumer decisions are often influenced not only by product functionality but also by emotional perception and experiential meaning (Liu, Samsudin & Zou, 2024). This perspective aligns with the principles of Kansei Engineering, a design methodology pioneered by Mitsuo Nagamachi in the 1970s. Kansei Engineering focuses on translating human emotions, impressions, and sensory experiences into design parameters that can improve product appeal and user satisfaction (Suzianti & Aldianto, 2020). According to Nagamachi (2006), Kansei encompasses the subjective psychological impressions individuals develop toward an artifact, environment, or situation through sensory and cognitive interaction.

Within packaging research, emotional responses have been shown to influence product evaluation, consumer attachment, and purchase intention (Donovan et al., 1994; Rook & Gardner, 1993). Previous studies have also demonstrated that packaging elements such as colour, typography, shape, naming, and visual composition contribute significantly to emotional interpretation and consumer behaviour (Pentus, Mehine & Kuusik, 2014; Velasco et al., 2014; Vyas, 2015; Wei et al., 2014). Nevertheless, the emotional role of alphanumeric naming structures within packaging design remains relatively under examined.
Existing research suggests that alphanumeric names are generally perceived as more appropriate for technically complex, utilitarian, or emotionally neutral products (Pavia & Costa, 1993). This observation raises important questions regarding their suitability and emotional effectiveness within non-alcoholic beverage packaging, a category commonly associated with pleasure, refreshment, lifestyle identity, and sensory enjoyment.

Non-alcoholic beverages represent an important context for investigating emotional packaging design because of their widespread consumption across diverse demographic groups and their continued resilience within fluctuating economic conditions (Solange et al., 2014). Packaging in this category plays a central role in attracting attention, shaping expectations, and influencing emotional reactions at the point of purchase. Furthermore, emotional responses to beverage packaging may vary across age groups due to differences in cognitive interpretation, cultural familiarity, visual preference, and generational exposure to alphanumeric communication systems. Understanding these variations is therefore essential for designers seeking to create packaging that effectively resonates with diverse consumer populations.

Against this background, this study investigates the perceptual and Kansei responses to alphanumeric onomastics in emotional packaging design across age groups within the non-alcoholic beverage sector. The study seeks to examine how consumers emotionally perceive and interpret alphanumeric naming systems in beverage packaging and whether such responses differ among age categories. By integrating perceptual evaluation with Kansei-based emotional assessment,

the research contributes to the broader discourse on emotional design, packaging communication, and consumer-product interaction. The findings are expected to provide valuable insights for designers, marketers, and manufacturers interested in developing emotionally engaging packaging strategies that align with contemporary consumer expectations.

1.1. Alphanumeric Onomastics and Visual Naming Cues

The influence of packaging design on consumer emotions has been widely acknowledged, with both verbal and nonverbal elements contributing significantly to perception, interpretation, and purchase behaviour (Pentus, Mehine & Kuusik, 2014). Among these elements, naming systems have become increasingly important in branding and packaging communication(Oluyemi, Adelabu & Oladumiye, 2024). The strategic use of words, symbols, letters, and numerical characters in assigning product identities has attracted scholarly attention within graphic design and consumer studies (Oluyemi, 2018). In this context, alphanumeric onomastics refers to naming conventions that combine alphabetic and numeric characters either in digit or word form to create distinctive product identities.

Alphanumeric brand names have been shown to shape consumer evaluations, perceptions, and associations toward products (Boyd, 1985; Gunasti & Ross, 2010; King & Janiszewski, 2011; Pavia & Costa, 1993). Common examples such as Coke Zero and 5 Alive demonstrate how numerical elements are integrated into commercial branding to enhance uniqueness, memorability, and differentiation. Research suggests that alphanumeric names function as visual and semantic cues capable of influencing overall brand and product assessment (Janiszewski & King, 2010; Van Kerckhove, Slabbinck & Pandelaere, 2011; Kara, 2016; Motoki et al., 2020; Oluyemi, Oladumiye & Adelabu, 2021; Velasco et al., 2014).

The anchoring theory of alphanumeric naming proposes that numbers embedded within brand names can positively signal specific product attributes and guide consumer interpretation (Yan & Duclos, 2013). Certain numbers may therefore be deliberately selected because of their symbolic appeal, familiarity, or semantic associations. Studies by Janiszewski and King (2010) and Van Kerckhove, Slabbinck and Pandelaere (2011) indicate that the success of alphanumeric brand names may partly depend on the perceived attractiveness or likability of the numerical components used. Consequently, alphanumeric names may operate not only as identifiers but also as communicative devices capable of stimulating expectations and emotional associations.

Despite their growing use, previous studies indicate that alphanumeric naming systems are more commonly associated with technical, industrial, and automobile products where numbers often represent specifications, hierarchy, or performance characteristics (Duduciuc & Ivan, 2014). Gunasti and Ross (2010) further argue that alphanumeric names can influence consumer preferences even when consumers do not fully understand the meaning of the attributes represented. Similarly, Gunasti and Ozcan (2016) and Lee (2014) found that semantic associations generated by alphanumeric names can positively influence purchase intention. However, these findings are largely concentrated within technical product categories, leaving limited understanding of their emotional implications in sensory and emotionally oriented products such as non-alcoholic beverages.

Within non-alcoholic beverage packaging, descriptors and naming systems have been found to facilitate product identification and category recognition (Oluyemi, 2021). Nevertheless, the integration of alphanumeric onomastics in beverage packaging may present challenges due to unfamiliarity and weaker semantic associations between numerical elements and the product category (Oluyemi, 2021).
This suggests a possible tension between technical visual naming cues and emotionally driven consumer expectations within beverage markets. The limited empirical evidence surrounding the emotional consequences of alphanumeric naming in beverage packaging therefore reveals an important gap in existing literature.

1.2. Kansei Engineering and Emotional Design of Packaging

The relationship between emotion and design has gained substantial scholarly attention through the development of Kansei Engineering. Originating from the work of Mitsuo Nagamachi in the 1970s, Kansei Engineering seeks to translate human emotional responses, impressions, and sensory experiences into design parameters that can improve product satisfaction and emotional engagement (Suzianti & Aldianto, 2020). Nagamachi (2006) defines Kansei as the psychological feeling or subjective impression experienced by individuals toward an object, environment, or situation through sensory and cognitive interaction.

Within packaging design, Kansei Engineering has contributed to the emergence of Emotional Design of Packaging (EDOP), which emphasizes the ability of packaging elements to evoke affective reactions and emotional attachment among consumers. Emotional design extends beyond functionality and aesthetics by considering how packaging stimulates feelings such as pleasure, excitement, trust, comfort, and curiosity during consumer interaction. Previous studies have shown that packaging elements including typography, colour, shape, material, graphics, and naming systems can influence emotional interpretation and

product preference (Pentus, Mehine & Kuusik, 2014; Velasco et al., 2014; Vyas, 2015; Wei et al., 2014).

The application of Kansei principles to packaging design reflects a broader shift from purely functional communication toward emotionally engaging consumer experiences. In this regard, alphanumeric onomastics may function as emotional design cues capable of shaping affective impressions either positively or negatively depending on consumer interpretation. However, the emotional influence of alphanumeric naming structures within packaging remains insufficiently established, particularly in non-technical consumer goods. This creates the need to examine whether such naming systems can effectively contribute to emotional packaging experiences within non-alcoholic beverage products.

1.3. Perceptual and Affective Processing in Consumer Emotion

Consumer emotional response is a critical aspect of consumer behaviour because it influences evaluation, interpretation, preference formation, and purchasing decisions. Pentus, Mehine and Kuusik (2014) describe emotional response as the reflective emotion associated with an individual's evaluation of a relevant stimulus. Emotional processing within packaging design involves both perceptual and affective dimensions, where consumers cognitively interpret visual information while simultaneously experiencing emotional reactions.

Research indicates that measuring emotional responses remains complex because emotions involve multiple psychological and physiological processes (Pentus, Mehine & Kuusik, 2014). According to Poels and Dewitte (2006), methods of emotion measurement can generally be categorized into self-report techniques and autonomic psychophysiological approaches. Psychophysiological methods include EEG, facial EMG, and fMRI, which measure physiological brain and muscle responses associated with emotional experience. In contrast, self-report methods capture consciously experienced feelings through verbal and visual scales such as PAD (Pleasure-Arousal-Dominance) and SAM (Self-Assessment Manikin).

The present study adopts the self-report approach because it is suitable for examining the conscious and reflective dimensions of emotional experience that consumers can verbally describe (Pentus, Mehine & Kuusik, 2014).
Although self-report methods may not fully capture unconscious emotional reactions, they remain valuable for understanding cognitive-affective interpretation within packaging perception. In the context of alphanumeric onomastics, self-report evaluation can provide insights into how consumers consciously perceive, interpret, and emotionally respond to naming structures integrated into packaging design.

1.4. Age-Related Perception and Universal Design Principles

Consumer interpretation of packaging elements is often influenced by demographic characteristics such as age and gender. Previous studies have shown that demographic variables affect consumer preferences, perception patterns, and emotional interpretation of design cues. Duduciuc and Ivan (2014), for example, found that women tend to respond more positively to feminine verbal expressions than men. Similarly, age differences have been associated with variations in cognitive familiarity, semantic interpretation, and emotional preference in branding and packaging communication.

Research by Oluyemi (2021) emphasizes the importance of considering consumers' age range in the development of product names and branding strategies. The study recommends that companies and advertisers prioritize audience perception when designing brand identities. Age-related differences are particularly relevant in the interpretation of alphanumeric onomastics because familiarity with alphanumeric communication systems may vary across generations due to differences in technological exposure, literacy patterns, and cultural associations.

This perspective aligns with universal design principles, which advocate the creation of products and communication systems that can be understood and appreciated across diverse user groups regardless of age or ability. Within packaging design, universal communication requires that naming systems remain accessible, meaningful, and emotionally engaging to broad consumer populations. Therefore, understanding how different age groups perceive and emotionally respond to alphanumeric onomastics is essential for developing packaging designs capable of achieving inclusive emotional communication.

Building upon these considerations, the present study investigates perceptual and Kansei responses to alphanumeric onomastics in non-alcoholic beverage packaging across age groups. By examining the interaction between visual naming cues, emotional processing, and age-related perception, the study contributes to the growing discourse on emotional packaging design and consumer-centred communication strategies.

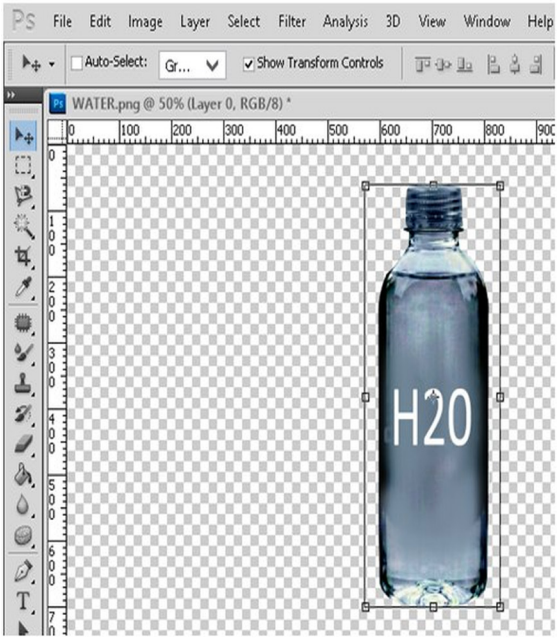
2. Methodology

This study adopted a quantitative survey approach to investigate perceptual and Kansei responses to alphanumeric onomastics in non-alcoholic beverage packaging across age groups. A total of 204 consumers of non-alcoholic beverages participated in the study through convenience sampling.

The sample was divided into five age groups: 12–15 years (n = 14, 6.9%), 16–20 years (n = 40, 19.6%), 21–30 years (n = 85, 41.7%), 31–40 years (n = 31, 15.2%), and 41 years and above (n = 34, 16.7%).Survey design and data collection: Based on the literature review and similar studies, a student survey questionnaire was developed. The survey was conducted anonymously.

2.1. Stimuli Design

The visual stimuli used in this study were designed using Adobe Photoshop. Image adjustment and painting tools were employed to create controlled visual representations of non-alcoholic beverage packaging incorporating alphanumeric onomastics (e.g., “H2O”) (see Figure 1). The designs were developed to maintain visual consistency across stimuli.



» **Figure 1:** *Stimuli Design in Adobe Photoshop*

2.2. Procedure

Participants were shown the designed stimuli and asked to evaluate their emotional responses based on their immediate feelings while viewing the packaging designs. To capture affective reactions, participants were provided with a list of 11 descriptive emotional and perceptual words: healthy, honourable, desirable, nice taste, familiar, amazing, funny, childish, reliable, fearful, and captivating. Participants selected the words that best described their feelings toward each stimulus and recorded their responses on an A4 response sheet.

2.3. Data Collection and Measures

The frequency of each selected descriptor was computed and converted into percentages for each age group, allowing comparison of emotional response patterns across demographic categories. This approach enabled the mapping of perceptual and affective tendencies associated with alphanumeric onomastics in packaging design.

2.4. Data Analysis

A one-way analysis of variance (ANOVA) was conducted to examine differences in emotional response scores across the five age groups. The results indicated no statistically significant difference between groups, $F(4, 50) = 1.27$, $p = .294$, $\eta = .304$, $\eta^2 = .092$, suggesting that approximately 9.2% of the variance in emotional response scores was attributable to age group membership. Overall, the mean differences across groups were relatively small.

Given concerns regarding normality assumptions and the ordinal nature of the response data, a non-parametric Kruskal–Wallis test was also conducted to verify the robustness of the findings. This additional analysis was necessary to further examine differences in emotional responses across multiple age groups without assuming parametric distribution requirements. The Kruskal–Wallis test therefore served as a confirmatory method for assessing whether age significantly influenced emotional perception of alphanumeric packaging stimuli.

3. Results

The results of the analysis are summarized in Tables 1 through 4. Data regarding emotional responses to alphanumeric onomastics in non-alcoholic beverage packaging indicate that a "healthy feeling" was the most prevalent reaction, accounting for 41% of participants (n=84). This sentiment was consistent across all age demographics. Other significant emotional characterizations included an "amazing feeling" (30%, n=63), "childish characteristics" (12%, n=26), "reliable characteristics" (3.9%, n=8), and a "funny feeling" (2.9%, n=6).

When disaggregated by age group, specific emotional patterns emerged:

- Ages 21–30: Peculiar feelings were identified as "Amazing" (18%), "Healthy" (12%), and "Childish" (3.4%).
- Ages 31–40: This group showed a distinct preference for "Healthy" (11%) associations.
- Ages 41 and above: This demographic reported peculiar associations with "Healthy feelings" (9.7%) and a unique "feeling of Familiarity" (1.9%) regarding the alphanumeric onomastics within the package brands.

To determine if these variations were statistically significant across age demographics, a non-paramet-

ric Kruskal–Wallis test was conducted. The results revealed no statistically significant differences between the groups, $\chi^2(4) = 8.43$, $p = .077$, $e^2 = .089$. This indicates that while subtle variations in perception exist among age cohorts, the overall emotional reception of alphanumeric onomastics is relatively uniform, showing only a small-to-moderate effect size.

The results are further elucidated through both parametric and non-parametric analyses, as presented in Tables 2 through 5. The findings from the ANOVA and the Kruskal–Wallis test consistently demonstrate an absence of statistically significant differences across the demographic groups.

While the ANOVA indicated that group membership explained approximately 9.2% of the variance, the lack of statistical significance suggests that this proportion is insufficient to establish meaningful or generalizable group differences. Corroborating this, the Kruskal–Wallis test—utilized for its robustness against deviations in normality and homogeneity—yielded a comparable small-to-moderate effect size ($e^2 = .089$).

Taken together, these statistical outcomes provide strong evidence that the observed variations between groups are likely attributable to random chance rather than systematic, group-level effects.

This suggests that alphanumeric naming conventions in non-alcoholic beverage packaging possess an "age-neutral" quality, exerting a relatively uniform emotional influence across the consumer lifecycle.

3.1. Discussion of Emotional Responses and Demographic Consistency

The empirical data suggests that alphanumeric onomastics in product packaging do not exert significantly divergent effects across age groups, indicating that age is not a primary determining factor in the emotional

Table 1

Percentage Distribution Showing Level of Emotional Response to Alphanumeric Name in the Packaging Design Stimuli in Relation to the Consumers' Age Group (%)

	E1	E2	E3	E4	E5	E6	E7	E8	E9	E10	E11
G1	3.4	0.0	0.0	0.0	0.5	0.0	0.0	2.9	0.0	0.0	0.0
G2	4.9	0.5	0.0	0.0	0.0	8.8	0.5	3.4	0.5	0.0	0.9
G3	12	0.0	0.9	0.5	0.5	18	1.9	3.4	2.9	0.5	0.5
G4	11	0.5	0.0	0.5	0.0	1.9	0.0	0.5	0.0	0.5	0.0
G5	9.7	0.0	0.0	0.0	1.9	1.4	0.5	2.4	0.5	0.0	0.0
Sum%	**41**	**1**	**0.9**	**1**	**2.9**	**30.1**	**2.9**	**12.6**	**3.9**	**1**	**1.4**

E1: healthy, E2: honourable, E3: desirable, E4: nice taste, E5: familiar, E6:amazing, E7: funny, E8: childish, E9: reliable, E10: fearful, E11: captivating; G1: 12-15years, G2: 16-20 years, G3: 21-30 years, G4: 31-40 years, G5: 41 years and above

Table 2

Parametric analysis of variance (ANOVA) for group differences

		Sum of Squares	df	Mean Square	F	Sig.
Between Groups	(Combined)	62.579	4	15.645	1.271	0.294
Within Groups		615.213	50	12.304		
Total		677.792	54			

Table 3

Measure of Association between Emotional Response and Consumers' Age Group

	Eta	Eta Squared
Level of emotional response * Consumers' Age Group	.304	.092

Table 4

Non-parametric Kruskal–Wallis

Test Statistics[a,b]	
	Level of emotional response
Chi-Square	8.432
Df	4
Asymp. Sig.	.077

a. Kruskal Wallis Test
b. Grouping Variable: Consumers' Age Group

Table 5

Hypothesis Test Summary

	Null Hypothesis	Test	Sig.	Decision
1	The distribution of Level of emotional response is the same across categories of Consumers' Age Group.	Independent-Samples Kruskal-Wallis Test	.077	Retain the null hypothesis.

Asymptotic significances are displayed. The significance level is .05.

reception of these naming conventions. Several factors may account for this lack of statistical significance. The moderate effect sizes observed imply that while some variability exists, it was not sufficiently pronounced to achieve statistical significance within the current sample. This suggests a broad consistency in consumer responses, with no single demographic cohort exhibiting disproportionately high or low emotional arousal.

These findings align with the theoretical framework of Yan and Duclos (2013), which suggests that descriptive or suggestive features—as well as anchoring effects—may not always be potent enough to elicit polarized emotional responses. In the context of alphanumeric onomastics, this leads to a "neutralization" of emotional influence across categories. From a practical standpoint, this indicates that alphanumeric identifiers in packaging design may be an effective strategy for reaching a general audience, rather than being limited to a niche age demographic. This is further supported by the work of Gunasti and Ozcan (2016) and Lee (2014), who argue that alphanumeric brand names can positively influence purchase intentions across a wide consumer base.

However, while this "age-neutral" quality can be viewed as an asset for universal marketing, it presents specific challenges regarding the safety of vulnerable populations. Individuals who rely heavily on explicit descriptive cues—such as children, the elderly, or those with lower literacy levels—may experience unfavorable product identification when faced with ambiguous alphanumeric onomastics. While the moderate positive feelings elicited by these names may be universally relatable, the lack of distinct emotional markers could heighten the risk for those who require more concrete visual affordances.

Ultimately, these findings reinforce the assertions of Pavia and Costa (1993) and other scholars who suggest that alphanumeric naming is fitting for products catering to a broad audience, such as non-alcoholic beverages. Rather than prioritizing demographic segmentation, product developers should consider universal design principles that ensure packaging is simultaneously relatable and recognizable for all users. The presence of small-to-moderate effect sizes in this study highlights subtle, non-significant patterns where different age groups emphasize varying emotional nuances, such as "Healthy," "Amazing," or "Childish" associations.

In conclusion, while the statistical analysis did not reveal significant group differences, the results provide critical insights for branding and packaging strategies. Future research involving larger sample sizes, more varied stimuli, and a specific focus on vulnerable populations will be essential to determine if these subtle effects hold greater practical relevance in real-world environments. Furthermore, subsequent studies should explore diverse categories of alphanumeric nomenclature, such as comparing descriptive/suggestive names against chemical-based alphanumeric identifiers, to further refine the safety and appeal of modern packaging design.

4. Conclusion

This research provides a critical evaluation of perceptual and Kansei (affective) responses to alphanumeric onomastics, positioning these linguistic identifiers as central components within the framework of Emotional Design of Packaging (EDOP). By investigating the intersection of alphanumeric naming conventions and consumer age demographics, the study concludes that such onomastic features function as effective emotional triggers, consistently evoking moderate positive affective states—most notably "Healthy" and "Amazing" associations—across the consumer lifecycle.

The lack of statistically significant variance between age cohorts suggests that alphanumeric onomastics possess a unique cross-generational semiotic appeal. This age-neutral quality implies that alphanumeric naming is a viable strategy for achieving universal design, allowing brands to maintain a consistent emotional resonance without the need for fragmented demographic segmentation. These findings reinforce established theories in design semiotics which argue that alphanumeric identifiers can enhance purchase intentions and brand reliability by providing a sophisticated, modern, and universally relatable aesthetic.

However, the transition toward such universal design approaches must be balanced with a commitment to functional safety and cognitive accessibility. While the study identifies a broad emotional consensus, the presence of subtle, non-significant patterns among different age groups suggests that "strangeness" in design prototypicality still requires careful management. To mitigate the risks of misidentification—particularly among vulnerable consumers who rely on clear descriptive affordances—designers and manufacturers must ensure that emotional onomastic appeal does not come at the expense of categorical clarity.

Ultimately, this study contributes a foundational understanding of how Kansei engineering can be applied to packaging nomenclature to harmonize aesthetic attraction with user safety. While the current results validate the effectiveness of alphanumeric onomastics

for general-market non-alcoholic beverages, they also open a new scholarly path for investigating how more specialized or chemical-based alphanumeric naming might influence perception. Moving forward, the integration of these findings into design heuristics will be essential for developing packaging that is not only emotionally engaging but also universally recognizable and safe within the complex modern marketplace.

5. References

Bošnjaković, G., Vladić, G., Maričić, K. and Gvoka, T. (2024) Improving packaging ergonomics through puff-enhanced screen prints. In: Pál, M. (ed.) *Proceedings of the 12th International Symposium on Graphic Engineering and Design GRID 2024, 14–16 November 2024*, Novi Sad, Serbia. Novi Sad: University of Novi Sad, Faculty of Technical Sciences, Department of Graphic Engineering and Design, pp. 491–496. DOI: 10.24867/GRID-2024-p54

Boyd, C.W. (1985) 'Point of view: Alpha-numeric brand names', *Journal of Advertising Research*, 25(5), pp. 48–52. DOI: 10.1080/00218499.1985.12467895

Donovan, R.J., Rossiter, J.R., Marcoolyn, G. and Nesdale, A. (1994) 'Store atmosphere and purchasing behavior', *Journal of Retailing*, 70(3), pp. 283–294. DOI: 10.1016/0022-4359(94)90037-X

Duduciuc, A.C. and Ivan, L. (2014) 'Brand naming: Sound symbolism, brand preference and brand performance', *Studies and Scientific Researches. Economics Edition*, 20, pp. 169–176. DOI: 10.29358/sceco.v0i20.275

Gunasti, K. and Ozcan, T. (2016) 'Consumer reactions to round numbers in brand names', *Marketing Letters*, 27(2), pp. 309–322. DOI: 10.1007/s11002-014-9337-7

Gunasti, K. and Ross, W.T. (2010) 'How and when alphanumeric brand names affect consumer preferences', J*ournal of Marketing Research*, 47(6), pp. 1177–1192. DOI: 10.1509/jmkr.47.6.1177

Gvoka, T., Vladić, G., Bošnjaković, G., Pál, M. and Maričić, K. (2024) Identification of gaze patterns in the observation of font-weight and illustration size on the packaging using eye-tracking analysis. In: Pál, M. (ed.) *Proceedings of the 12th International Symposium on Graphic Engineering and Design GRID 2024*, 14–16 November 2024, Novi Sad, Serbia. Novi Sad: University of Novi Sad, Faculty of Technical Sciences, Department of Graphic Engineering and Design, pp. 515–524. DOI: 10.24867/GRID-2024-p57

Jamnicki Hanzer, S. (2024) Evaluation of the migration potential of colorants and additives in paperboard food packaging materials. In: Pál, M. (ed.) *Proceedings of the 12th International Symposium on Graphic Engineering and Design GRID 2024*, 14–16 November 2024, Novi Sad, Serbia. Novi Sad: University of Novi Sad, Faculty of Technical Sciences, Department of Graphic Engineering and Design, pp. 729–736. DOI: 10.24867/GRID-2024-p78

Janiszewski, C. and King, D. (2010) 'The affective consequences of alpha-numeric branding'. In: *Advances in Consumer Research*, 37, pp. 150–152.

Kara, S. (2016) T*wo Essays on the Effect of Alphanumeric Brand Names on Consumers' Brand Related Decisions*. PhD dissertation. University of Connecticut.

King, D. and Janiszewski, C. (2011) 'The sources and consequences of the fluent processing of numbers', *Journal of Marketing Research*, 48(2), pp. 327–341. DOI: 10.1509/jmkr.48.2.327

Lee, C.T. (2014) *Consumer Linguistics: A Markedness Approach to Numerical Perceptions*. PhD dissertation. University of Oregon.

Liokos, T., Lychridas, G., Kyratsis, V. and Manavis, A. (2024) Champagne packaging design with brand awareness and user-centric criteria: A case study. In: Pál, M. (ed.) *Proceedings of the 12th International Symposium on Graphic Engineering and Design GRID 2024*, 14–16 November 2024, Novi Sad, Serbia. Novi Sad: University of Novi Sad, Faculty of Technical Sciences, Department of Graphic Engineering and Design, pp. 623–630. DOI: 10.24867/GRID-2024-p67

Liu, C., Samsudin, M.R. and Zou, Y. (2024) 'Emotional design of packaging: A bibliometric analysis', *Studies in Media and Communication*, 12(2), pp. 172–188. DOI: 10.11114/smc.v12i2.6698

Madhan, S., Nirmala, J.P. and Kanchana, M. (2024) Preparation of eco-friendly inks for primary & secondary packaging. In: Pál, M. (ed.) *Proceedings of the 12th International Symposium on Graphic Engineering and Design GRID 2024*, 14–16 November 2024, Novi Sad, Serbia. Novi Sad: University of Novi Sad, Faculty of Technical Sciences, Department of Graphic Engineering and Design, pp. 791–800. DOI: 10.24867/GRID-2024-p85

Mahović Poljaček, S., Tomašević, T., Jamnicki Hanzer, S., Strižić Jakovljević, M., Murković Steinberg, I., Žuvić, I., Lavrič, G., Kavčič, U. and Karlovits, I. (2024) Immobilization of anthocyanins by bacterial nanocellulose in production of indicators for pH-controlled smart packaging. In: Pál, M. (ed.) *Proceedings of the 12th International Symposium on Graphic Engineering and Design GRID 2024*, 14–16 November 2024, Novi Sad, Serbia. Novi Sad: University of Novi Sad, Faculty of Technical Sciences, Department of Graphic Engineering and Design, pp. 443–454. DOI: 10.24867/GRID-2024-p48

Motoki, K., Saito, T., Park, J., Velasco, C., Spence, C. and Sugiura, M. (2020) 'Tasting names: Systematic investigations of taste-speech sounds associations', *Food Quality and Preference*, 80, 103801. DOI: 10.1016/j.foodqual.2019.103801

Nagamachi, M. (2006) Kansei engineering and rough sets model. In: Greco, S., Hata, Y., Hirano, S., Inuiguchi, M., Miyamoto, S., Nguyen, H.S. and Slowinski, R. (eds.) *Rough Sets and Current Trends in Computing: 5th International Conference, RSCTC 2006*, 6–8 November 2006, Kobe, Japan. Berlin: Springer, pp. 27–37. DOI: 10.1007/11908029_4

Nechita, P., Roman, M. and Năstac, M.S. (2024) Sustainable food packaging materials based on hemicellulose coated papers. In: Pál, M. (ed.) *Proceedings of the 12th International Symposium on Graphic Engineering and Design GRID 2024, 14–16 November 2024*, Novi Sad, Serbia. Novi Sad: University of Novi Sad, Faculty of Technical Sciences, Department of Graphic Engineering and Design, pp. 711–718. DOI: 10.24867/GRID-2024-p76

Oluyemi, A.S. (2018) *Consumers' Perception of Product Naming and Package Design in Akure*, Nigeria. M.Tech. thesis. Federal University of Technology, Akure.

Oluyemi, A.S. (2021) 'Consumers' age consideration for product naming purposes', *EuroMed Journal of Management*, 4(1), pp. 2–5. DOI: 10.1504/EMJM.2021.117782

Oluyemi, A.S., Adelabu, O.S. and Oladumiye, E.B. (2024) Identification tendencies in the onomastics of non-alcoholic beverage packaging design in Akure, Nigeria. In: Pál, M. (ed.) *Proceedings of the 12th International Symposium on Graphic Engineering and Design GRID 2024*, 14–16 November 2024, Novi Sad, Serbia. Novi Sad: University of Novi Sad, Faculty of Technical Sciences, Department of Graphic Engineering and Design, pp. 537–553. DOI: 10.24867/GRID-2024-p59

Oluyemi, A.S., Oladumiye, E.B. and Adelabu, O.S. (2021) 'Zobo tea package design prototype allied with product onomastics', *Journal of Design Studio*, 3(2), pp. 237–259. DOI: 10.46474/jds.1025264

Pavia, T.M. and Costa, J.A. (1993) 'The winning number: Consumer perceptions of alpha-numeric brand names', *Journal of Marketing*, 57(3), pp. 85–98. DOI: 10.1177/002224299305700306

Pentus, K., Mehine, T. and Kuusik, A. (2014) 'Considering emotions in product package design through combining conjoint analysis with psycho physiological measurements', *Procedia - Social and Behavioral Sciences*, 148, pp. 280–290. DOI: 10.1016/j.sbspro.2014.07.044

Poels, K. and Dewitte, S. (2006) 'How to capture the heart? Reviewing 20 years of emotion measurement in advertising', *Journal of Advertising Research*, 46(1), pp. 18–37. DOI: 10.2501/S0021849906060041

Rook, D.W. and Gardner, M.P. (1993) 'In the mood: Impulse buying's affective antecedents', *Research in Consumer Behavior*, 6, pp. 1–28.

Solange, A.K.A., Georgette, K., Gilbert, F., Marcellin, D.J.K. and Bonfoh, B. (2014) 'Review on African traditional cereal beverages', *American Journal of Research Communication*, 2(5), pp. 103–153.

Suzianti, A. and Aldianto, A. (2020) 'Redesign of product packaging with Kansei engineering: Empirical study on small-medium enterprises in Indonesia', *Makara Journal of Technology*, 24(2), pp. 65–71. DOI: 10.7454/mst.v24i2.2990.

Van Kerckhove, A., Slabbinck, H. and Pandelaere, M. (2011) Alpha-numeric brand names: Is less more or is more better? In: *Society for Consumer Psychology 2011 Winter Conference Proceedings*, pp. 168–170.

Velasco, C., Salgado-Montejo, A., Marmolejo-Ramos, F. and Spence, C. (2014) 'Predictive packaging design: Tasting shapes, typefaces, names, and sounds', *Food Quality and Preference*, 34, pp. 88–95. DOI: 10.1016/j.foodqual.2013.12.005

Vladić, G., Jovanović, D., Bošnjaković, G. and Gvoka, T. (2024) Implementing artificial intelligence in the packaging design for the taste impression. In: Pál, M. (ed.) *Proceedings of the 12th International Symposium on Graphic Engineering and Design GRID 2024*, 14–16 November 2024, Novi Sad, Serbia. Novi Sad: University of Novi Sad, Faculty of Technical Sciences, Department of Graphic Engineering and Design, pp. 507–514. DOI: 10.24867/GRID-2024-p56

Vyas, H. (2015) 'Packaging design elements and users perception: A context in fashion branding and communication', *Journal of Applied Packaging Research*, 7(2), Article 5. DOI: 10.14448/japr.04.0005

Wei, S.T., Ou, L.C., Luo, M.R. and Hutchings, J.B. (2014) 'Package design: Colour harmony and consumer expectations', *International Journal of Design*, 8(1), pp. 109–126.

Yan, D. and Duclos, R. (2013) 'Making sense of numbers: Effects of alphanumeric brands on consumer inference', *International Journal of Research in Marketing*, 30(2), pp. 179–184. DOI: 10.1016/j.ijresmar.2012.09.007

© 2026 Authors. Published by the University of Novi Sad, Faculty of Technical Sciences, Department of Graphic Engineering and Design. This article is an open access article distributed under the terms and conditions of the Creative Commons Attribution license 4.0 Serbia (https://creativecommons.org/licenses/by/4.0/deed.en).

Professional Paper https://doi.org/10.24867/GRID-2026-p31

Interactive Packaging Enabled by NFC Technology

ABSTRACT

The convergence of physical and digital media has created new opportunities for developing interactive packaging that enhances product functionality and user experience. This paper explores the potential of Near Field Communication (NFC) technology to integrate physical packaging with digital content through the development of an interactive music album as a case study. The research is based on a review of the evolution of physical and digital music formats, the role of packaging in shaping user experience, and recent applications of NFC technology in interactive products. Based on these findings, an NFC-enabled CD package was developed, providing seamless access to multimedia content, artist information, and exclusive digital materials via embedded NFC tags. The proposed solution demonstrates how NFC technology transforms conventional packaging into an interactive communication interface that connects physical and digital environments while preserving the aesthetic and collectible value of the product. In addition to improving user engagement, the concept enables product authentication, dynamic content updates, and long-term interaction between creators and users. The presented approach highlights the potential of NFC-enabled packaging as an innovative solution for graphic products and demonstrates its broader applicability in the development of functional, interactive, and user-oriented packaging systems.

Alan Nikolić-Šipek
Katarina Itrić Ivanda
Marina Vukoje Bezjak
Rahela Kulčar

University of Zagreb,
Faculty of Graphic Arts,
Zagreb, Croatia

KEY WORDS
Interactive packaging, NFC technology, smart packaging, user experience, physical–digital integration

1. Introduction

The rapid advancement of digital technologies has significantly transformed the role of packaging, extending its traditional functions of protection, transportation, and information delivery toward interactive communication and enhanced user experience. As interactive technologies become increasingly integrated into graphic products, packaging is expected to provide added value beyond its conventional protective role. Li (2021) argues that interactive packaging design enhances visual communication by establishing a closer relationship between products and users, while Gegeckienė et al. (2022) identify Near Field Communication (NFC) as one of the key technologies driving the development of smart packaging within the graphic industry. Among the available smart technologies, NFC has emerged as a practical solution for connecting physical products with digital content. According to Coskun, Ozdenizci and Ok (2015), NFC enables secure short-range wireless communication that is intuitive for users and compatible with the majority of modern smartphones. The technology has therefore found applications in product authentication, consumer engagement, information exchange, and interactive packaging. Hutson and Hutson (2024) further emphasize the potential of NFC to bridge physical and digital experiences in artistic and cultural contexts, while Tantowibowo and Yau (2024) demonstrate its applicability in authentication systems for physical artworks.

The growing adoption of digital technologies has also influenced the design of music products, where packaging is no longer perceived solely as a protective element but as an important component of the overall user experience. Vad (2021) describes the album cover as an essential medium of visual communication that

contributes to the identity and interpretation of musical works. Likewise, Dorochowicz and Kostek (2019) highlight the close relationship between album cover design and the communication of musical genres, emphasizing the role of graphic design in shaping audience perception. Recent studies further indicate that physical music releases continue to provide experiential value despite the dominance of digital streaming services. Fumihira and Johnston (2025) argue that tangible music products remain relevant when combined with digital interaction, while Scott and Schofield (2025) demonstrate that visual presentation continues to influence user experience even within digital music environments.

Although streaming platforms have become the primary mode of music consumption, physical editions continue to occupy an important niche among collectors and dedicated audiences. This has encouraged artists and publishers to explore new approaches that combine the permanence and collectible value of physical media with the flexibility of digital content. NFC technology provides an opportunity to achieve this integration by enabling immediate access to multimedia materials, artist information, exclusive content, and continuously updated online resources through embedded NFC tags.

Commercial solutions such as NFC-enabled albums, music cards, and collectible vinyl releases demonstrate the practical feasibility of integrating NFC technology into music products (Fumihira & Johnston, 2025). However, these solutions primarily focus on content accessibility, while considerably less attention has been given to packaging as a unified communication interface that simultaneously integrates graphic design, physical interaction, and digital media. This creates an opportunity to develop interactive packaging concepts in which the physical product remains the central element of the user experience while being extended through digital functionality.

Therefore, this paper presents the design and development of an NFC-enabled interactive CD package that integrates physical packaging with digital multimedia content. The proposed concept demonstrates how NFC technology can transform conventional graphic packaging into an interactive communication interface while preserving the visual identity, material qualities, and collectible value of physical music products. Furthermore, the presented solution illustrates the broader potential of NFC-enabled packaging in the development of functional, user-oriented, and digitally connected graphic products.

2. Materials and methods

The research was conducted using a design-oriented approach that combined theoretical analysis with the development of an original interactive packaging concept. The methodological framework consisted of two complementary stages. The first stage involved a review of the historical development of physical and digital music releases, the evolution of album packaging, and the application of NFC technology in contemporary music products. Attention was given to the role of album packaging in shaping user experience (Vad, 2021) and to recent applications of NFC technology in interactive packaging systems (Gegeckienė et al., 2022). The findings of this analysis served as the basis for defining the functional requirements of the proposed interactive packaging concept.

Based on the theoretical findings, an original concept of an interactive music album was developed in the form of a compact disc (CD) package with integrated NFC technology. The project included the design of the visual identity, the structural design of the package, the definition of user interaction scenarios, and the integration of digital content accessible through embedded NFC tags. The concept was designed to establish a seamless connection between the physical product and its digital extension while preserving the aesthetic and collectible characteristics of the music release.

The proposed packaging incorporates multiple NFC interaction points that provide access to different categories of digital content. The embedded NFC tags were programmed using NDEF URI records, allowing users to access predefined online resources simply by bringing an NFC-enabled smartphone close to the designated interaction point. The implementation follows the principles of NFC communication described by Coskun, Ozdenizci and Ok (2015), ensuring compatibility with standard NFC-enabled mobile devices without requiring dedicated applications.

The outcome of the research is a functional design concept demonstrating how NFC technology can be integrated into graphic packaging to create a unified physical–digital user experience. Rather than evaluating user behaviour experimentally, the study focuses on the design process and the implementation of an interactive packaging prototype as a proof of concept.

3. Results and discussion

The outcome of this research is the development of an interactive music album package that combines the tangible qualities of a conventional CD release with the functionality of NFC-enabled digital interaction. Rather than replacing the physical product, the proposed concept extends its communicative role by transforming the package into an interface between physical and digital media. The design preserves the visual identity and collectible value of the album while providing immediate access to additional digital content through embedded NFC tags. The final prototype of the developed NFC-enabled CD



(a) (b) (c)

» **Figure 1:** *Final prototype of the interactive CD package (a) front cover, (b) back cover, and (c) opened package*

package is presented in Figure 1, illustrating the front cover, back cover, and internal layout of the package.

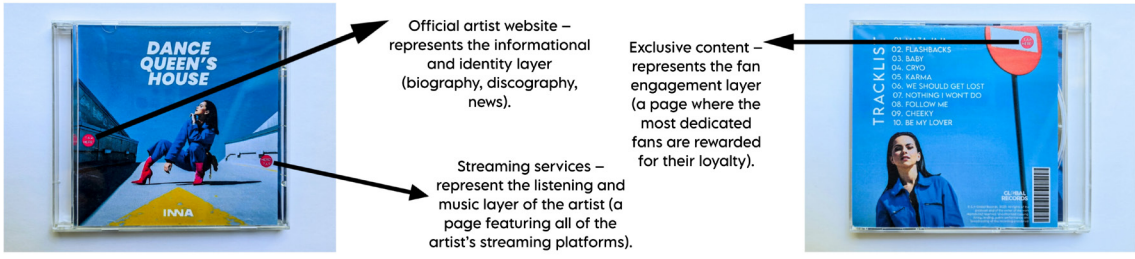
The prototype preserves the visual characteristics of a conventional CD package while incorporating interactive functionality through embedded NFC technology. The developed package was designed around the principle that each NFC interaction should correspond to a clearly defined user intention. Instead of directing all interactions to a single destination, the package incorporates multiple NFC touchpoints, each providing access to a different category of digital content. This interaction model establishes a logical separation between promotional information, music distribution services, and exclusive artist-related content, allowing users to navigate the digital layer intuitively while preserving the simplicity of the physical interface.

The visual design of the package was developed simultaneously with the interaction concept to ensure that the digital functionality remains integrated into the graphic product rather than appearing as an additional technological feature. Attention was paid to the placement of NFC interaction points, which were incorporated into the visual composition using subtle "Tap Here" markers. This approach follows current recommendations for NFC-enabled packaging, where the interaction area should be easily recognizable without compromising the overall aesthetic quality of the product. References to NFC interaction were therefore treated as graphic elements that support usability while maintaining visual consistency. The placement and function of the embedded NFC interaction points are illustrated in Figure 2.

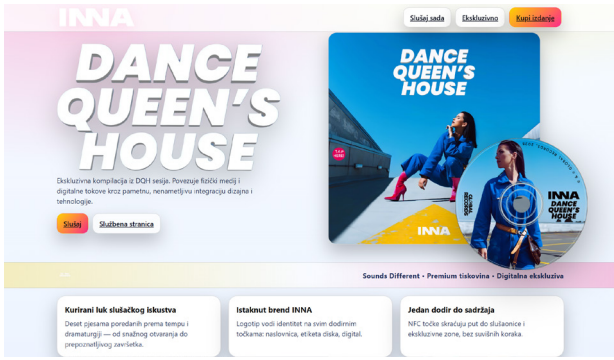
The digital component of the project was implemented through NFC tags programmed with NDEF URI records that redirect users to predefined online resources. Using any NFC-enabled smartphone, users can access the associated content without manually entering web addresses or scanning QR codes. The proposed interaction reduces the number of required user actions and creates a seamless transition from the physical package to the digital environment. This implementation demonstrates how NFC technology can simplify access to multimedia resources while maintaining compatibility with standard mobile devices and NFC communication protocols. Figure 3 presents the landing page that serves as the primary digital interface accessed through the embedded NFC tags.

The use of NFC technology offers several advantages over conventional approaches to linking physical and digital content. Unlike QR codes, which require users to open a camera application and visually scan a printed code, NFC interaction is initiated through a simple tap, resulting in a more intuitive and seamless user experience. Furthermore, NFC tags can be discreetly integrated into the graphic design of the package without affecting its visual appearance, allowing interactive functionality to remain virtually invisible until activated. This approach enhances both the aesthetic quality of the packaging and the overall user experience (Coskun, Ozdenizci & Ok, 2015; Gegeckienė et al., 2022).

Compared with conventional CD packaging, the proposed concept extends the role of the package beyond storage and visual presentation. It becomes an active communication medium capable of delivering con-



» **Figure 2:** *Location of the NFC interaction points integrated into the CD package and their corresponding digital functions*



» **Figure 3:** *Digital content and user interface accessed by interacting with the NFC-enabled CD package*

tinuously accessible digital content while preserving the permanence and material qualities of physical media. Unlike QR-code-based solutions, NFC interaction requires only a simple tap, reducing visual clutter and allowing the interactive functionality to remain discreetly integrated into the package design. These characteristics support a more natural user experience and reinforce the perception of the package as a unified graphic product rather than a printed object supplemented with external digital services.

The proposed concept also demonstrates broader opportunities for applying NFC technology within graphic products. Although developed as a music album, the same design principles can be adapted to other forms of packaging where interaction with digital content adds value to the physical product. Examples include limited-edition publications, exhibition catalogues, promotional packaging, premium product packaging, and collector's editions, where digital content can complement rather than replace the physical experience. Existing commercial implementations, including NFC-enabled albums and music cards, primarily use NFC technology as a gateway to streaming platforms or promotional content. In contrast, the concept presented in this study considers NFC as an integral component of the packaging design process. Rather than functioning solely as a digital shortcut, the embedded NFC tags contribute to a coherent communication system in which graphic design, physical interaction, and digital media are intentionally integrated into a single user experience. This approach extends the communicative role of packaging while preserving the authenticity and collectible value of physical music releases (Fumihira & Johnston, 2025).

From the perspective of graphic product design, the presented prototype illustrates that NFC technology should not be considered merely as an additional technological component but as an integral element of the communication strategy. By integrating visual design, physical interaction, and digital content into a coherent user experience, the developed package demonstrates how traditional graphic products can evolve into interactive communication interfaces while maintaining their aesthetic, cultural, and collectible value.

Overall, the developed prototype demonstrates that NFC technology can be successfully incorporated into graphic packaging without compromising its visual identity or usability. The proposed concept illustrates that interactive functionality can be achieved through careful integration of graphic design, packaging structure, and digital media, creating a unified physical–digital communication environment. Although developed as a music album, the design principles presented in this study are transferable to a wide range of graphic products where interactive communication can enhance product functionality and user engagement.

4. Conclusions

This paper presented the design and development of an interactive music album package that integrates Near Field Communication (NFC) technology with conventional graphic packaging. By combining the physical qualities of a compact disc package with digital content accessible through embedded NFC tags, the proposed concept demonstrates how traditional packaging can be transformed into an interactive communication interface while preserving its aesthetic and collectible value. The proposed concept demonstrates that NFC technology offers a practical solution for connecting physical and digital media in graphic products. Unlike conventional packaging, which primarily serves protective and informational functions, the developed concept extends the role of packaging by enabling immediate access to multimedia content, artist information, and additional digital resources through intuitive user interaction. The integration of NFC technology was achieved without altering the visual identity or usability of the package, illustrating the compatibility of interactive technologies with established principles of graphic design.

Beyond its application in the music industry, the presented concept demonstrates the broader potential of NFC-enabled packaging in the development of innovative

graphic products. The same design approach can be applied to promotional materials, premium packaging, limited-edition publications, museum products, and other applications where physical objects can benefit from an interactive digital extension. In this context, NFC technology represents not only a communication tool but also a means of enhancing user engagement and creating a stronger connection between physical products and digital services. The main contribution of this work lies in the development of a functional design concept that integrates graphic design, packaging design, and NFC technology into a unified user experience. The presented prototype illustrates how interactive packaging can support the ongoing convergence of physical and digital media while opening new possibilities for the design of user-oriented graphic products.

Future research could focus on evaluating user interaction with NFC-enabled packaging through usability studies and user experience assessment, as well as investigating the application of emerging technologies, such as dynamic web content, cloud-based content management, and artificial intelligence, to further expand the functionality and adaptability of interactive packaging systems.

5. Acknowledgments

This work was supported by the Croatian Science Foundation [grant number IP-2022-10-3864].

6. References

Coskun, V., Ozdenizci, B. and Ok, K. (2015) 'The survey on Near Field Communication', *Sensors*, 15(6), pp. 13348–13405. DOI: 10.3390/s150613348

Dorochowicz, A. and Kostek, B. (2019) Relationship between album cover design and music genres. In: *2019 Signal Processing: Algorithms, Architectures, Arrangements, and Applications (SPA 2019), 18–20 September 2019*, Poznań, Poland. Piscataway, NJ: IEEE, pp. 93–98. DOI: 10.23919/SPA.2019.8936738

Fumihira, E. and Johnston, A. (2025) Physical music albums in the digital era: Exploring experiential value through the integration of AR. In: Cavdir, D. and Berthaut, F. (eds.) *Proceedings of the International Conference on New Interfaces for Musical Expression*, 24–27 June 2025, Canberra, Australia. NIME, pp. 582–589. DOI: 10.5281/zenodo.15698968

Gegeckienė, L., Venytė, I., Karpavičė, J., Tambo, T., Vaitasius, K. and Pauliukaitis, D. (2022) Near Field Communication (NFC) technology in the packaging industry. In: Vladić, G. (ed.) *Proceedings of the 11th International Symposium on Graphic Engineering and Design GRID 2022*, 3–5 November 2022, Novi Sad, Serbia. Novi Sad: University of Novi Sad, Faculty of Technical Sciences, Department of Graphic Engineering and Design, pp. 495–501. DOI: 10.24867/GRID-2022-p54

Hutson, P. and Hutson, J. (2024) 'Bridging the digital divide: Innovative uses of QR codes and NFC in the artistic realm', *ISRG Journal of Arts, Humanities and Social Sciences*, 2(2), pp. 338–345. DOI: 10.5281/zenodo.11081838

Li, Y. (2021) 'Analysis of visual communication packaging design based on interactive experience', *Journal of Physics: Conference Series*, 1852(2), 022074. DOI: 10.1088/1742-6596/1852/2/022074

Scott, M. and Schofield, D. (2025) 'The impact of album layout on user experience in smartphone music applications', *International Journal of Multimedia & Its Applications*, 17(1/2), pp. 1–22. DOI: 10.5121/ijma.2025.17201

Tantowibowo, C.H. and Yau, W.-C. (2024) 'ArtProtect: Blockchain and NFC-based anti-counterfeit system for physical art', *IET Blockchain*, 4(4), pp. 423–442. DOI: 10.1049/blc2.12069

Vad, M. (2021) 'The album cover', *Journal of Popular Music Studies*, 33(3), pp. 11–15. DOI: 10.1525/jpms.2021.33.3.11

© 2026 Authors. Published by the University of Novi Sad, Faculty of Technical Sciences, Department of Graphic Engineering and Design. This article is an open access article distributed under the terms and conditions of the Creative Commons Attribution license 4.0 Serbia (http://creativecommons.org/licenses/by/4.0/rs/).

Professional Paper https://doi.org/10.24867/GRID-2026-p32

Tea Packaging Though Design Thinking: A Holistic Methodology to Product Identity

ABSTRACT

Distinctive packaging has a major role in differentiating products within competitive markets by combining visual, structural, material, and communicative characteristics that strengthen the product identity. Through a holistic design approach and based on design thinking, packaging can become a strategic tool that communicates product values, thereby enhancing brand recognition. Therefore, this study focuses on the promotion of local tea products through the application of appropriate design methodologies, tools, and interdisciplinary expertise. Using a case study approach based on design thinking, the study aims to present a product development process that supports brand visibility, addresses the needs of the target group, and enhances the overall functionality.

KEY WORDS
Holistic product design, packaging design, design thinking, product identity, branding, product development, CAD

Ioanna Kalamakidou [1]
Vasileios Kyratsis [2]
Giorgos Lychridas [1]
Thomas Liokos [1]
Athanasios Manavis [2]
Nikolaos Efkolidis [1]

[1] Department of Product and Systems Design Engineering, University of Western Macedonia, Campus Kila Kozani, Kila Kozani, Greece
[2] Department of Interior Architecture, International Hellenic University – IHU Serres, Serres, Greece

1. Introduction

Products play an essential role in everyday life, as they directly affect people's quality of life. People rely on products on a daily basis to satisfy their basic needs, to perform daily tasks and to improve their comfort, productivity, and health. As a result, they have become an important part of daily routines and human dependence in modern society.

Behind every product is a design process that begins with ideation and continues through the phases of development, production, and use. One important area of this process is packaging design, which is divided into three main layers: primary, secondary, and tertiary packaging. These layers serve different purposes, ranging from containing and protecting their content to supporting safe transportation and storage, while also, from communicating information directly and promoting their brand identity to display them more broadly.

2. State of the art

Nowadays, packaging design has evolved from a one-dimensional focus on attractiveness into a multidimensional practice that involves visual communication, functionality, sustainability, and brand strategy. As a result, designers are expected to follow a different kind of workflow that considers all these aspects throughout the design process.

Product concepts that are successfully integrated into the markets are usually supported by a structured digital product life cycle (Elgazzar & Dawood, 2025). Especially in the field of packaging design, where environmental

challenges are critical, Life Cycle Assessment (LCA) can be used to address and optimize sustainability-related decisions (Dobras, Manavis & Kyratsis, 2021), (João, Maceno & Antonelo, 2025). When combined with design thinking tools, this process actively involves end users, thereby increasing design opportunities and improving the likelihood of market success (Almeida et al, 2022). From this perspective, consumer psychology and market analysis are an important part of the aesthetic characteristics of packaging that determine the preferences of the target group (Ding, Yahaya & Abdul Rahman, 2025). Furthermore, packaging design not only interacts as a visual communication tool but also as a physical interaction that supports the needs of the users and interacts at ease with them. Based on the user-centered approach, functionality is the main category turning the concept ideas into practical products (Nemat et al, 2023).

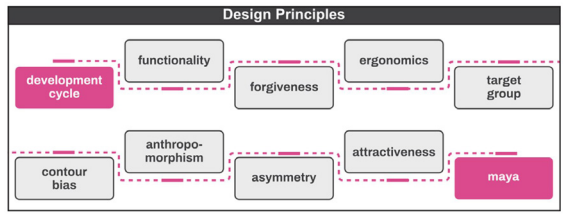
Several case studies demonstrate the importance of research-driven and sustainability-oriented approaches in product and packaging design. Liokos et al. (2024) present a case study about champagne packaging, illustrating the importance of conducting preliminary research methodologically before moving to the design process. In a broader context, Manavis et al. (2019) propose a conceptual product design framework inspired by nature, leading to innovative solutions. Similarly, Malea et al. (2020) focus on improving oral care products such as toothpaste by examining the disadvantages of existing products in the marketplace. Their study follows a sustainability evaluation to reduce material waste in products with a short life cycle.

The proposed paper presents a product design case study that explores innovative approaches beyond conventional packaging. It illustrates how a thematic idea can be gradually developed into practical design opportunities by following a comprehensive design strategy.

3. Design methodology

Design principles are the basic concept guidelines that shape the decisions made during product development. They define the fundamental ideas and considerations behind the design. Namely, the development cycle is the repetitive process of analyzing, designing, developing and testing. This cycle supports the continuous improvement and refinement of the product.

Next is the principle of functionality, which validates that the product must fulfill its intended purpose effectively. Alongside this, the principle of forgiveness includes that the product should help users avoid mistakes and protect them from serious consequences when they occur (Yoruk, Hsu & Lee, 2025). In our case, a possible scenario would be the product falling.



» **Figure 1:** *Design Principles*

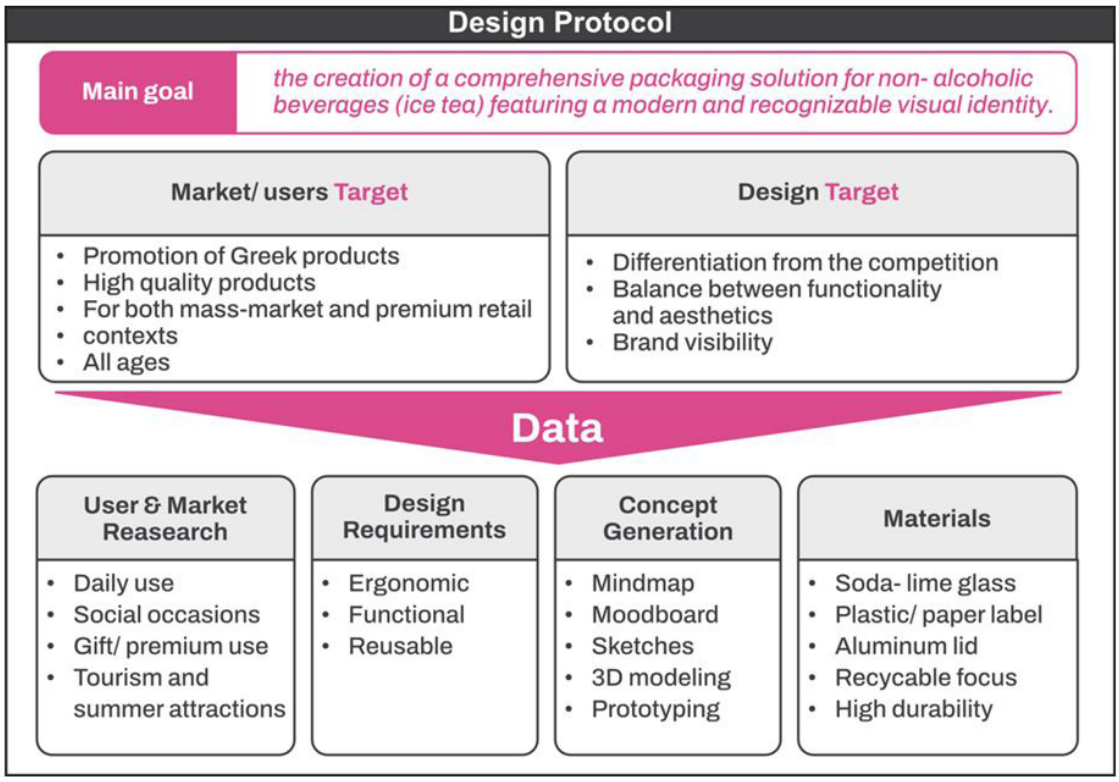
Therefore, the principle of forgiveness would influence the choice of a durable material that is less likely to break when dropped from an alarming height.

Next in line, is the ergonomics principle, which focuses on designing the product according to human needs. This is closely related to the user-centered design where factors such as the comfort during interaction with the product, the amount of effort required from the user and the efficiency of use are included (Bošnjaković & Vladić, 2020). Besides that, the target group is also an important consideration, since the design must correspond to the needs of the specific audience the product is made for (Malik & Ahmed, 2024).

Moving to broader design considerations, the emphasis is placed on aesthetics and psychological design strategies. More specifically, one relevant bias that influences the form of the product is the contour bias, which refers to the human tendency to prefer curved and rounded objects over sharp and angular ones (Tawil, Ascone & Kühn, 2022). Another useful principle related to the visual appeal of the product is anthropomorphism, which involves giving human-like qualities to non-human objects. The combination of rounded forms and subtle human-like characteristics in the design can create a more engaging experience and a stronger connection with the target audience (Chen, Zhang & Ma, 2025). Furthermore, the principles of asymmetry and attractiveness are also considered, as they can boost the dynamic of the design and the visual appeal. Finally, the MAYA (Most Advanced Yet Acceptable) principle focuses on the balance of innovative ideas with familiarity, so that the users are more likely to accept the product (Mulder-Nijkamp et al., 2021).

3.1. Design Protocol

The role of design protocol is to record and organize all the useful information, design requirements and limitations within a structured framework. It is responsible for keeping the project aligned with its goals and supports the translation of design requirements into informed design decisions. More specifically, it acts as a guide for the design process, including important information such as the main goal, the market target, the user target and the design objectives. This information is then organized into thematic fields such as user and market research,



» **Figure 2:** *Design Protocol*

design requirements, concept generation and selected materials. In this way, the design protocol supports a more systematic and informed product development process.

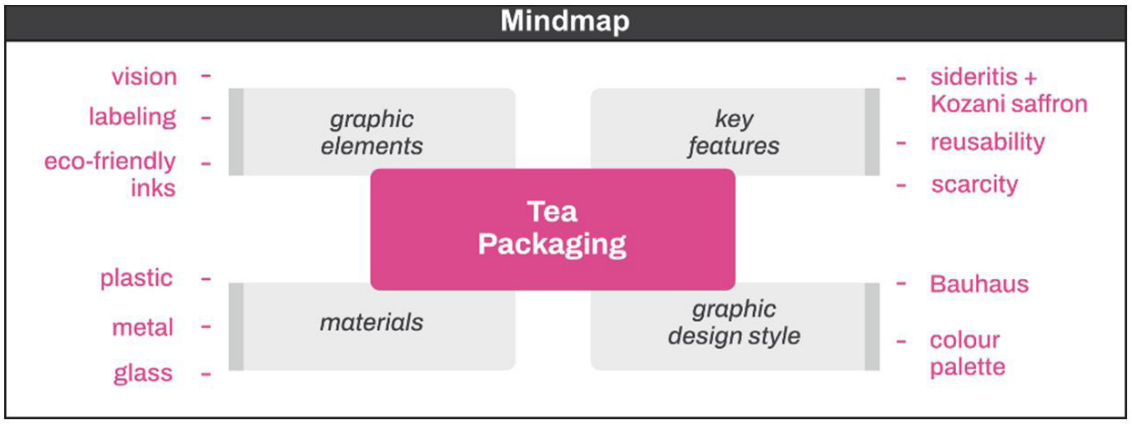
3.2. Concept Exploration

The concept exploration phase consists of two creative tools called mindmap and moodboard. Starting with mindmap, its role is to explore general ideas related to the central topic and decide the final creative direction. Figure 3 presents the initial summary of the mindmap. At the center of the board is the main topic "Tea Packaging" which is further analyzed through four thematic branches: "graphic elements", "key features", "materials" and "graphic design style".

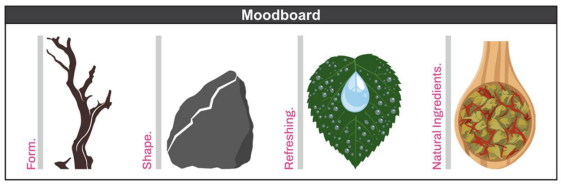
Furthermore, moodboard is the visual tool used to transform verbal ideas into visual content contributing to explore and communicate the direction of the product. As shown in Figure 4, moodboard includes images, shapes and colours that express the design concept.

3.3. Ideation

The ideation phase involves the generation of possible product solutions in the form of sketches. It brings together the previous research findings, design

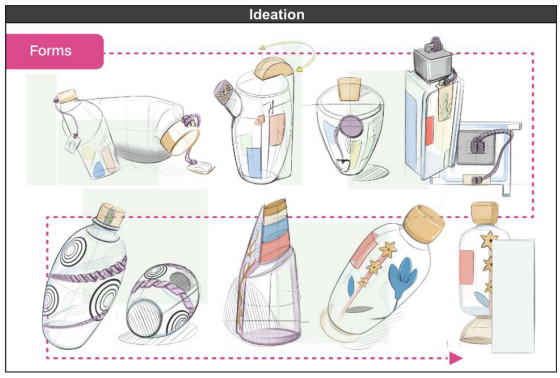


» **Figure 3:** *Mindmap*



» **Figure 4:** *Moodboard*

requirements, and visual references, transforming them into unfiltered and abstract sketched ideas. More specifically, different components, forms, and decorative characteristics are explored while maintaining the design principles of curved forms, the selected colour palette, and labeling graphics that promote the key ingredients: sideritis and saffron. These ideas are then gradually developed into more stable and finalized design concepts, as illustrated in Figure 5.



» **Figure 5:** *Ideation*

3.4. Design Solution

3.4.1. Sideritis and Saffron

The choice of sideritis and saffron as the key ingredients of a complete tea product solution strengthens the Greek identity of the design, while also promoting the cultural value, naturalness, and authenticity. Sideritis, commonly known as “mountain tea”, is a traditional Greek herbal tea strongly connected with nature, wellness, and everyday cultural habits. In combination with saffron, a valuable ingredient known for its distinctive colour, nutritional qualities, and unique cultivation process, the product gains a more premium and sophisticated identity.

3.4.2. Graphic elements

The labeling of the product reflects its ingredients by translating them into abstract geometries, inspired by the Bauhaus art movement. The colors used in the design follow the movement’s principles, namely red, blue, yellow, and black, capturing the user’s attention and interest. Through this approach, the packaging is not limited to a decorative depiction of the ingredients but incorporates them as an organic part of the visual identity.

3.4.3. Packaging design

The shape of the bottle is curved with polished edges, giving a dynamic look and a sense of high quality, standing out from traditional designs. While the asymmetric and organic form cooperates with the unique placement of the label in a more innovative way. At the same time, the form remains simple and ergonomic, following the logic of “less is more”.

Figure 6 depicts the complete production process, beginning with the final sketches and continuing with the creation of the CAD model. Therefore, in the next stage, the textures, the colours, and the labeling graphics were added in the rendered model, allowing the visual identity of the product to be presented digitally. Finally, the design solution is prototyped through additive manufacturing,



» **Figure 6:** *Design Solution*

specifically 3D printing, to evaluate the form, the scale, and the physical characteristics of the final product.

3.5. Early Evaluation

For this section, a 1:1 scale prototype was manufactured to examine and improve the user experience. In the context of an early evaluation, participants were allowed to interact with the final product and assess it using a 0 to 5 rating scale. Across a wide range of ages (25 – 60 years old), 32 users have evaluated attractiveness (4.4), usability (4.3), ergonomics (4.0), awareness (4.3), and purchase intention (4.2). These findings indicate that the prototype was generally well perceived by users, while ergonomics, which received the lowest average score, may require further refinement in the next design iteration.

4. Conclusions

In this article, a structured design methodology was used as a roadmap for product design and development. First, relevant design principles were examined and applied to support proper product development. Information gathered from the market and potential users, as well as

existing limitations, was then collected and organized into a design protocol, ensuring the effective management of design-related requirements. During the design thinking process, mindmap and moodboard tools were used to gather ideas, define restrictions, and guide the creative direction. The development stage involved exploring several concepts and forms through sketching, which gradually led to the final design direction. With the creation of the CAD model of the finalized idea, prototyping and rendering were used as the final stages of the process, providing improved visualization and supporting the early evaluation of the final product. Overall, the methodology enabled a systematic progression from research and ideation to concept development, visualization, and evaluation, resulting in a distinctive packaging solution designed to enhance user interaction and experience.

5. References

Almeida, C., Loubet, P., da Costa, T.P., Quinteiro, P., Laso, J., Baptista de Sousa, D., Cooney, R., Mellett, S., Sonnemann, G., Rodríguez, C.J., Rowan, N., Clifford, E., Ruiz-Salmón, I., Margallo, M., Aldaco, R., Nunes, M.L., Dias, A.C. and Marques, A. (2022) 'Packaging environmental impact on seafood supply chains: a review of life cycle assessment studies', *Journal of Industrial Ecology*, 26(6), pp. 1961–1978. DOI: 10.1111/jiec.13189

Bošnjaković, G. and Vladić, G. (2020) 'Research methodologies for assessing the ergonomics of packaging products- a review'. In: *Proceedings - The Tenth International Symposium on Graphic Engineering and Design, GRID 2020, 12–14 November 2020, Novi Sad, Serbia*. Novi Sad: University of Novi Sad, Faculty of Technical Sciences, Department of Graphic Engineering and Design, pp. 335–345. DOI: 10.24867/grid-2020-p37

Chen, L., Zhang, M. and Ma, K. (2025) 'Adding warmth to packaging! The impact of anthropomorphism in packaging on anticipated consumption enjoyment', *Journal of Retailing and Consumer Services*, 87, 104411. DOI: 10.1016/j.jretconser.2025.10441

Ding, S., Yahaya, M.F. and Abdul Rahman, A.R. (2025) 'Examining the multidimensional impact on soft drink packaging preferences through the unified model of aesthetics', *Scientific Reports*, 15(1), 4782. DOI: 10.1038/s41598-025-87741-x

Dobras, M., Manavis, A. and Kyratsis, P. (2021) 'Innovative packaging design', *International Journal of Manufacturing Economics and Management*, 1(1), pp. 6–12.

Elgazzar, M.A.G. and Dawood, M.E.T. (2025) 'Mastering the phases of design strategy: a comprehensive guide to navigating from conceptualization to launch in the digital product life cycle', *Journal of Art, Design and Music*, 4(2), 1. DOI: 10.55554/2785-9649.1050

João, S., Maceno, M.M.C. and Antonelo, A.K. (2025) 'Proposal for a circular product development model applied to packaging', *Sustainability*, 17(1), 206. DOI: 10.3390/su17010206

Liokos, T., Lychridas, G., Kyratsis, V. and Manavis, A. (2024) 'Champagne packaging design with brand awareness and user-centric criteria: a case study'. In: *Proceedings - The Twelfth International Symposium on Graphic Engineering and Design, GRID 2024, 14–16 November 2024, Novi Sad, Serbia*. Novi Sad: University of Novi Sad, Faculty of Technical Sciences, Department of Graphic Engineering and Design, pp. 623–629. DOI: 10.24867/grid-2024-p67

Malea, A., Tzotzis, A., Manavis, A. and Kyratsis, P. (2020) 'Innovative and sustainable toothpaste packaging design', *Journal of Graphic Engineering and Design*, 11(2), pp. 19–29. DOI: 10.24867/jged-2020-2-019

Malik, H. and Ahmed, Z. (2024) 'The effect of packaging design on consumer preferences', *Journal of Strategic Business Research*, 2(2), pp. 18–34.

Manavis, A., Sourris, T., Dimou, E., Efkolidis, N. and Kyratsis, P. (2019) 'An inspiration from nature design methodology for in-store displays', *Journal of Packaging Technology and Research*, 3(2), pp. 141–148. DOI: 10.1007/s41783-019-00057-w

Mulder-Nijkamp, M., Eggink, W., de Kok, M. and ten Klooster, R. (2021) 'The triangular designers' space: methodical approach to balance brand typicality and novelty'. In: Quartier, K., Petermans, A., Melewar, T.C. and Dennis, C. (eds.) *The Value of Design in Retail and Branding. Bingley*: Emerald, pp. 95–108. DOI: 10.1108/978-1-80071-579-020211008

Nemat, B., Razzaghi, M., Bolton, K. and Rousta, K. (2023) 'Design-based approach to support sorting behavior of food packaging', *Clean Technologies*, 5(1), pp. 297–328. DOI: 10.3390/cleantechno5010017

Tawil, N., Ascone, L. and Kühn, S. (2022) 'The contour effect: differences in the aesthetic preference and stress response to photo-realistic living environments', *Frontiers in Psychology*, 13, 933344. DOI: 10.3389/fpsyg.2022.933344

Yoruk, I., Hsu, J.H. and Lee, Z.W. (2025) 'Consumer forgiveness: a literature review and research agenda', *Psychology & Marketing*, 42(2), pp. 554–578. DOI: 10.1002/mar.22138



© 2026 Authors. Published by the University of Novi Sad, Faculty of Technical Sciences, Department of Graphic Engineering and Design. This article is an open access article distributed under the terms and conditions of the Creative Commons Attribution license 4.0 Serbia (https://creativecommons.org/licenses/by/4.0/deed.en).

Original Scientific Paper https://doi.org/10.24867/GRID-2026-p33

Influence of Packaging Finishing Techniques on Consumer Perception

ABSTRACT

Packaging finishing techniques are widely used to increase the visual appeal and perceived value of products. This study investigates the influence of foil stamping, blind embossing, and window cut-outs on consumer perception of packaging attractiveness. A total of 27 digital packaging prototypes representing three product categories (computer mouse, chocolate, and pharmaceutical products) were evaluated through a questionnaire conducted under controlled laboratory conditions. The results show that packaging enhanced with finishing techniques was consistently preferred over packaging containing only printed graphics. Window cut-outs achieved the highest attractiveness ratings for chocolate and pharmaceutical packaging, while respondents equally preferred window cut-outs and embossed designs for computer mouse packaging. In all product categories, packaging without additional finishing techniques received the lowest preference. The findings indicate that finishing techniques improve the perceived attractiveness of paper packaging and demonstrate that their effectiveness depends on the product category. The study provides practical guidance for selecting finishing techniques that enhance consumer perception and packaging appeal.

Nada Miketić
Ivan Pinćjer
Magdolna Pál
Milena Ristić

University of Novi Sad, Faculty of Technical Sciences, Department of Graphic Engineering and Design, Novi Sad, Serbia

KEY WORDS
Packaging design, packaging finishing, foil stamping, blind embossing, consumer perception, paper packaging

1. Introduction

Packaging has an important role not only in protecting and containing a product but also in communicating product characteristics and attracting consumer attention. In highly competitive retail environments, visual appearance can influence product evaluation before consumers have an opportunity to experience the product itself. Consequently, packaging design has become an important means of differentiating products and communicating perceived quality and value.

Previous studies have demonstrated that visual characteristics such as colour, shape, orientation, prominence and package structure can affect consumer attention and product evaluation (Orquin & Mueller Loose, 2013; Clement, Kristensen & Grønhaug, 2013). Aesthetic package design may also influence product choice and perceived value, indicating that visual appearance can contribute substantially to consumer response (Reimann et al., 2010). Previous research has also indicated that packaging incorporating added-value design elements may be perceived as more attractive by consumers (Malešević & Stančić, 2021).

In addition to printed graphics, packaging can be enhanced using different finishing techniques. Embossing creates a three-dimensional deformation of the substrate and can improve both the visual and tactile characteristics of packaging (Banjanin, 2018). Foil stamping additionally introduces metallic or coloured elements, while blind embossing produces relief without applying foil or ink. Such techniques are frequently used to visually distinguish packaging and enhance its perceived value. Another structural design element is a window cut-out that allows the consumer to see the product inside the package.

Product visibility can affect consumer perception and purchase behaviour, particularly in food packaging (Simmonds & Spence, 2017). However, the effectiveness of transparent elements may depend on the type of product and on other characteristics of the package. However, the effect of product visibility may depend on the product category and packaging context, as transparent packaging has also been associated with lower perceived product quality in some applications (Poslon, Kovačević & Brozović, 2021).

The aim of this study was therefore to investigate the influence of selected packaging finishing techniques and window cut-outs on perceived packaging attractiveness during the design stage. Foil stamping, blind embossing and window cut-outs were evaluated across three different product categories: a computer mouse, chocolate and a pharmaceutical product. Particular attention was given to whether packaging containing additional finishing elements would be preferred over packaging based primarily on printed graphics and whether these preferences differed among product categories.

2. Materials and methods

The study was based on digital packaging prototypes developed to simulate the appearance of selected finishing techniques before physical production. A total of 27 packaging designs were created in Adobe Photoshop and used as visual stimuli in the experiment.

The designs represented three different product categories: a computer mouse as a technology product, chocolate as a food product, and a pharmaceutical product.

For each product category, three basic packaging designs were developed and subsequently presented in three variants, resulting in nine stimuli per product category. The investigated variants included printed graphics without additional finishing, foil stamping, blind embossing and window cut-outs, as well as selected combinations of these elements. Silver foil was simulated for the computer mouse packaging, while gold foil was used for the chocolate and pharmaceutical packaging.

The designs were developed to resemble packaging commonly associated with the corresponding product categories while allowing the influence of finishing and structural elements to be evaluated. Digital prototypes were selected because they represent an important stage in contemporary packaging design and are frequently used to present packaging concepts prior to production.

The study included 53 participants aged between 19 and 36 years, predominantly students in graphic engineering and design, with approximately equal representation of male and female participants.

Given their educational background, the participants were generally familiar with graphic design and the finishing techniques represented in the stimuli.

The evaluation was conducted under controlled laboratory conditions using an EIZO CG241W 24-inch monitor. A questionnaire created in Google Forms was used to collect the responses. Participants evaluated the presented packaging alternatives through questions addressing design preference and attractiveness, as well as perceived quality, price and luxury.

Likert-type scales were used for several evaluation questions. For the purposes of the present study, the analysis primarily focuses on respondents' preference for different packaging designs and finishing variants.

A representative set of digital packaging stimuli developed for the chocolate product category is presented in Figure 1.



» **Figure 1:** *Representative set of digital packaging stimuli developed for the chocolate product category, illustrating the three basic designs and their corresponding finishing and structural variants*

3. Results

The results demonstrated a clear preference for packaging containing additional finishing or structural design elements compared with packaging based primarily on printed graphics.

Across the investigated product categories, designs incorporating window cut-outs or embossed elements were generally preferred, while variants without additional finishing were consistently among the least preferred alternatives.

For computer mouse packaging, both window cut-outs and embossing contributed positively to perceived attractiveness. In the first design group, the window cut-out and blind embossed variants were equally preferred, each being selected by 41.4% of respondents, whereas the printed version was selected by only 17.2%.

When foil stamping was incorporated into the design, the combination of foil stamping and blind embossing was selected by 42.6% of participants, while the combination of foil stamping and a window cut-out was selected by 33.3%.

For chocolate packaging, variants incorporating a window through which the product could be seen were consistently preferred across all three design groups. The window cut-out was selected by 64.8% of respondents in D1, while combinations of a window cut-out with foil stamping (D2) and blind embossing (D3) were preferred by 69.0% and 65.5% of respondents, respectively.

A similar tendency was observed for pharmaceutical packaging. When foil stamping was present, the variant combining foil stamping with a window cut-out was preferred by 58.5% of respondents. When blind embossing was used as the basic finishing treatment, the design combining embossing with a window was preferred by 63.8% of participants.

The evaluation of pharmaceutical packaging differed from the other product categories when broader product perceptions were considered. Participants generally provided more neutral evaluations regarding perceived product quality, price and luxury, although the packaging designs themselves received relatively high evaluations.

Overall, the results show that packaging incorporating finishing or structural design elements was more attractive to respondents than packaging without additional enhancement.

However, the degree of preference for individual techniques varied among the three investigated product categories.

Table 1

Most preferred packaging design variants for each design group across the investigated product categories

Product category	Design group	Most preferred design variant	Preference (%)
Computer mouse	D1	Window cut-out / Blind embossing	41.4 / 41.4
	D2	Foil stamping + blind embossing	42.6
	D3	Blind embossing	43.4
Chocolate	D1	Window cut-out	64.8
	D2	Foil stamping + window cut-out	69.0
	D3	Blind embossing + window cut-out	65.5
Pharmaceutical product	D1	Window cut-out	59.3
	D2	Foil stamping + window cut-out	58.5
	D3	Blind embossing + window cut-out	63.8

4. Discussion

The findings indicate that the influence of packaging finishing techniques and structural elements on consumer perception depends on the type of product being packaged. Although additional finishing generally increased packaging attractiveness, differences between product categories were observed in the relative preference for particular solutions.

The preference for a visible product was particularly pronounced for chocolate packaging. This finding is consistent with previous studies showing that visual exposure to food can affect consumer attention, desire and product evaluation (Wansink, 2004; Piqueras-Fiszman & Spence, 2011; Simmonds & Spence, 2017). The effectiveness of the window therefore appears to be related not only to its structural characteristics but also to the nature of the packaged product. The original study similarly identifies food as a particularly strong visual stimulus and relates the high preference for the chocolate window design to previous findings concerning food visibility.

Product visibility was also positively evaluated for pharmaceutical packaging, although participants were more neutral when evaluating perceived product quality, price and luxury. This may indicate that visual attractiveness alone has a more limited influence on broader judgments concerning pharmaceutical products. This more neutral evaluation may be related to unfamiliarity with the product and brand, as well as to factors such as perceived product effectiveness and brand

trust, which may limit the extent to which product quality is inferred solely from packaging appearance.

For computer mouse packaging, preferences were more evenly distributed between window-based and embossed solutions. In contrast to chocolate and pharmaceutical packaging, no single type of enhancement showed the same pronounced dominance. This suggests that the suitability of a particular finishing technique cannot be considered independently of the product category.

Overall, the comparison between product categories demonstrates that finishing techniques should be selected according to both the visual concept and the characteristics of the packaged product. Window cut-outs appear particularly effective when product visibility contributes directly to the visual evaluation of the contents, whereas embossing and foil stamping can provide an alternative means of increasing visual interest when direct product visibility is less important.

The findings also demonstrate the relevance of evaluating finishing techniques during the digital design stage. Although embossing and foil stamping possess tactile characteristics that cannot be fully represented on a screen, their simulated appearance was sufficient to influence participants' visual preferences. Digital prototypes may therefore provide useful preliminary information when selecting finishing solutions before physical prototypes are produced.

5. Conclusions

The study demonstrated that finishing and structural design techniques can influence the perceived attractiveness of packaging. Across the three investigated product categories, packaging incorporating additional finishing or window cut-outs was preferred to alternatives relying primarily on printed graphics.

Window cut-outs produced the strongest preference for chocolate and pharmaceutical packaging, while both window cut-outs and embossed elements were highly attractive in computer mouse packaging.

The results therefore indicate that the effectiveness of individual finishing techniques depends on the product category and that a single finishing solution cannot necessarily be considered equally effective for all types of packaging.

The findings also demonstrate that digital packaging prototypes can be used to evaluate consumer responses to finishing techniques during the design stage. This may allow designers to identify promising finishing solutions before proceeding to physical production.

A limitation of the study is that finishing techniques were represented through digital simulations and could therefore only be evaluated visually, without the tactile characteristics associated with physically produced packaging. In addition, the participant sample consisted primarily of young respondents with a background in graphic engineering and design. Future research should consequently include physically produced packaging, larger and more diverse consumer samples, and evaluation under actual retail conditions.

6. Acknowledgments

This research has been supported by the Ministry of Science, Technological Development and Innovation (Contract No. 451-03-34/2026-03/200156) and the Faculty of Technical Sciences, University of Novi Sad through project “Scientific and Artistic Research Work of Researchers in Teaching and Associate Positions at the Faculty of Technical Sciences, University of Novi Sad 2026” (No. 01-3609/1).

7. References

Banjanin, B. (2018) *Karakterizacija proizvodnih parametara alata za utiskivanje izrađenih tehnikom 3D štampe.* PhD Thesis. University of Novi Sad, Faculty of Technical Sciences.

Clement, J., Kristensen, T. and Grønhaug, K. (2013) 'Understanding consumers’ in-store visual perception: The influence of package design features on visual attention', *Journal of Retailing and Consumer Services*, 20(2), 234–239. DOI: 10.1016/j.jretconser.2013.01.003

Malešević, M. and Stančić, M. (2021) 'Influence of packaging design parameters on customers’ decision-making process', *Journal of Graphic Engineering and Design*, 12(4), 33–38. DOI: 10.24867/JGED-2021-4-033

Orquin, J. L. and Mueller Loose, S. (2013) 'Attention and choice: A review on eye movements in decision making', *Acta Psychologica*, 144(1), 190–206. DOI: 10.1016/j.actpsy.2013.06.003

Piqueras-Fiszman, B. and Spence, C. (2011) 'Crossmodal correspondences in product packaging: Assessing color-flavor correspondences for potato chips (crisps)', *Appetite*, 57(3), 753–757. DOI: 10.1016/j.appet.2011.07.012

Poslon, S., Kovačević, D. and Brozović, M. (2021) 'Impact of packaging shape and material on consumer expectations', *Journal of Graphic Engineering and Design*, 12(2), 39–44. DOI: 10.24867/JGED-2021-2-039

Reimann, M., Zaichkowsky, J., Neuhaus, C., Bender, T. and Weber, B. (2010) 'Aesthetic package design: A behavioral, neural, and psychological investigation', *Journal of Consumer Psychology*, 20(4), 431–441. DOI: 10.1016/j.jcps.2010.06.009

Simmonds, G. and Spence, C. (2017) 'Thinking inside the box: How seeing products on, or through, the packaging influences consumer perceptions and purchase behaviour', *Food Quality and Preference*, 62, 340–351. DOI: 10.1016/j.foodqual.2016.11.010



© 2026 Authors. Published by the University of Novi Sad, Faculty of Technical Sciences, Department of Graphic Engineering and Design. This article is an open access article distributed under the terms and conditions of the Creative Commons Attribution license 4.0 Serbia (http://creativecommons.org/licenses/by/4.0/rs/).

Original Scientific Paper https://doi.org/10.24867/GRID-2026-p34

The Accessibility Paradox of Packaging as a Communication Channel

ABSTRACT

Packaging is one of the most widespread communication channels in everyday consumer life, carrying the message between sender (manufacturer) and receiver (consumer) at the point of sale and use. Interactive or "smart" packaging like QR codes, NFC tags, embedded video and companion applications extends this channel from a static, printed medium to a mediated, digital one, and is widely promoted as a way to make product information more accessible, including older and visually impaired audiences. This study asks whether that channel actually reaches the audience it is meant to serve. Based on a survey of 404 Zagreb residents aged 18-75 (a probabilistic sample stratified by age and gender), it analyses awareness and use of interactive packaging elements, and the perceived importance of accessing additional product information through apps or video and tests them against age and visual status using chi-square, ANOVA, Pearson's correlation and linear regression. The findings reveal a communication failure rather than a design failure. Reach is weak: 39% of respondents had never encountered interactive packaging and only 9% had ever used it, with awareness collapsing among the oldest group (81% of those over 66 had never heard of it) and among glasses wearers (58% are unaware of it). Perceived value of the channel declines with age ($r = -0.294$, $p < .001$; respondents over 66 rating it lowest, $M = 1.65$), and the products recalled are dominated by beverage and snack brands, indicating that the packaging as a communiction channel functions more often as a marketing tool rather than an accessibility tool. Interpreted through the diffusion-of-innovations framework and the knowledge-gap hypothesis, the results describe an accessibility paradox: a channel introduced to widen access to information instead reproduces an information gap, leaving the audience most in need of accessible communication the least reached by it. The paper argues that the limiting factor is not the technology itself but channel reach, and proposes that the social environment of older consumers - family, caregivers and peers acting as interpersonal intermediaries should be treated as a complementary link in the communication chain, helping to explain the function and use of smart packaging and supporting its capacity to reach and empower the audience it was designed to serve.

Daria Mustić

University of Zagreb,
Faculty of Graphic Arts,
Zagreb, Croatia

KEY WORDS
Packaging communication, channel-audience mismatch, knowledge gap

1. Introduction

Packaging is one of the first things a consumer sees and the last medium a brand controls before a choice is made. It protects the product and it also speaks. On the shelf it delivers a brand's message at the exact moment of purchase (Rundh, 2005).

Its role goes beyond persuasion. Packaging is a communication channel in a more complex sense. It carries identity, meaning and instructions, and it does so through both what the consumer reads on the surface and what the consumer learns by handling and using the product over time (Underwood, 2003). Seen this way, every package is a form of communication between

a sender (the manufacturer) and a receiver (the consumer). For most of its history this channel has been static and printed. Now, that is changed. Interactive or "smart" packaging adds a digital layer to the printed surface through QR codes, Near Field Communication (NFC) tags, embedded video and companion applications, linking the physical product to online content (Liu & Wang, 2024). A shopper can scan a code or tap a tag and reach information that would never fit on a label: fuller instructions, origin and traceability data, allergen detail, or audio and video guidance. In communication terms, the channel has been extended from a one-way printed message to a two-way, mediated exchange.

Much of the positivity around this extension is largely asigned to its potential to enhance accessibility. If a label is too small to read, the argument is, a digital layer can offer magnified text or spoken instructions; if information is too dense, an application can structure and simplify it. This promise is often aimed at older consumers and people with visual impairments. The reasoning is appealing but it also rests on an assumption that is rarely tested: that the intended audience knows the channel exists, understands it, and is willing to use it. Communication theory gives reason to test that assumption. Rogers' (2003) diffusion of innovations describes adoption as a sequence that starts before use - first knowledge of an innovation, then persuasion, then the decision to adopt. People cannot adopt what they have never heard of, and Rogers notes that interpersonal channels, more than mass ones, move people through the persuasion stage. The knowledge-gap hypothesis adds a second caution: as new information flows into a social system, better-resourced groups tend to acquire it faster, so the gap between them and others widens rather than closes (Tichenor, Donohue & Olien, 1970). A digital layer introduced to broaden access can deepen existing divides instead of bridging them. This pattern in research on ageing and technology is called the grey divide. While the digital divide has narrowed for younger cohorts, it persists across generations and is sharpest among older adults, where the use of digital tools falls steeply with advancing age and can leave the oldest groups largely excluded (Friemel, 2016). The divide is not only about access. It reflects differences in confidence, prior exposure and technical interest, and it is shaped by a person's social surroundings. Evidence from the English Longitudinal Study of Ageing suggests that this gap is driven more by generation, or birth cohort, than by age itself. Differences in internet use persist even after income, education, employment and health are taken into account (Gilleard & Higgs, 2008). For older users, technology adoption is frequently shaped by social support, previous experience, facilitating conditions and confidence, while relatives may provide both practical assistance and emotional encouragement (Friemel, 2016; Park & Robinson, 2020). It also runs deeper than access to a device. A Slovenian study of NFC tags on food packaging found low overall awareness, concentrated almost entirely in the younger generations (Žurbi & Gregor-Svetec, 2024). For a channel that depends on a smartphone and the willingness to use it, these are not minor obstacles; they decide whether the message is received at all.

Conventional food packaging frequently presents difficulties for older and visually impaired consumers because essential information is printed in small type, may have insufficient contrast, and is often difficult to locate or read (Plečko, Brozović & Kovačević, 2023; Mustić, Cigula & Kovačević 2025a, 2025b). This becomes more important as Europe's population ages and this group expands (Eurostat, 2025). The importance of accessible packaging is emphasised by Europe’s ageing population. On 1 January 2024, people aged 65 years and over accounted for 21.6% of the EU population, while the corresponding share in Croatia was 23.0%. Croatia was among the EU Member States with the highest proportions of older people. Between 2014 and 2024, the share of people aged 65 and over increased by 4.5 percentage points in Croatia, compared with an increase of 2.9 percentage points at EU level (Eurostat, 2025). In Croatia, the share of people aged 65 and over is projected to reach approximately 30% by 2050 (European Commission, 2024). Population ageing is also evident at the oldest ages: between 2004 and 2024, the share of people aged 80 and over increased in the EU from 3.8% to 6.1% (Eurostat, 2025). The demographic relevance of inclusive packaging is likely to increase further.

This study treats interactive packaging as a communication channel and asks does it reach its intended audience? Using survey data from a general adult population, it measures how far the channel has actually penetrated, how much value people place on it, and how both vary with age and visual status - the two characteristics that define the audience the accessibility argument is meant to serve.

The study has three objectives: to investigate consumer awareness and use of interactive packaging elements; to measure the perceived importance of reaching additional product information through such elements; and to test how awareness, use and perceived importance differ by age and by the use of visual aids. From these objectives, four research questions follow:

- RQ1: How aware are consumers of interactive packaging elements, and how many have used them?
- RQ2: How important do consumers consider access to additional product information through these elements?
- RQ3: How do awareness, use and perceived importance vary by age and visual status?
- RQ4: Does the observed pattern among older consumers and visual-aid users sup-

port the claim that interactive packaging serves their accessibility needs?

In line with diffusion and knowledge-gap reasoning, three hypotheses are proposed:

- H1: Awareness and use are low overall and decline with age.
- H2: The perceived importance of interactive access declines with age.
- H3: Consumers who use visual aids, the group most likely to value accessible information, are no more aware of interactive packaging.

2. Methods

2.1. Data collection method

The study draws on a telephone survey carried out with a structured questionnaire. This mode was chosen deliberately. It lowers the barrier to participation for people who struggle with written or online forms, whether because of age or a sensory limitation, since it removes the need to read or handle survey materials (Dillman, Smyth & Christian, 2014). It also lets the interviewer clarify a question in real time, which matters for scale-based items where a respondent may need an example before answering. The questionnaire combined three formats: closed questions, open questions, and scale-based questions, among them five-point scales measuring degrees of difficulty or importance. It covered socio-demographic indicators together with a broad set of attitudes toward packaging design. The survey underlies two earlier studies, which examined the readability of packaging and its adaptation for older and visually impaired users (Mustić, Cigula & Kovačević, 2025a, 2025b). The present paper analyses the items concerned with interactive packaging- whether respondents were aware of and had used interactive elements such as QR codes and NFC tags, and how important they considered access to additional product information through applications or video. Awareness and use were captured by a question: "Have you ever used products with interactive elements on the packaging, such as QR codes, NFC tags, video content or applications?" Respondents who answered affirmatively were asked to name examples, and from this item two indicators were derived- awareness (whether the respondent had heard of such products) and use (whether they had used them). Perceived importance was measured on a five-point scale (1 = not at all important, 5 = very important) with the question: "How important is it to you that packaging provides access to additional product information through mobile applications or video content?" All 404 respondents answered to both items.

2.2. Population and sample

The target population was residents aged 18 to 75. A probabilistic random sampling method, stratified by age and gender, was used to secure representation across groups. The final sample comprised 404 respondents and the sample size was broadly consistent with the conventional benchmark of a ±5 percentage-point margin of error at the 95% confidence level under simple-random-sampling assumptions. Because the study used stratification and a telephone-survey design, this benchmark should be interpreted as approximate. Respondents were informed of the purpose of the survey and gave verbal consent before participating.

Table 1 summarises the sample by gender, age and use of visual aids. Gender is evenly split, the four age bands are close in size, and just over half of respondents wear glasses or contact lenses. That last distribution matters here, because age and visual status are the two variables against which the interactive-packaging items were tested.

Table 1

Achieved sample by socio-demographic indicators (N = 404)

Indicator	Category	N	%
Gender	Male	202	50.0
	Female	202	50.0
Age	18–35	89	22.0
	36–50	107	26.5
	51–65	111	27.5
	66 and more	97	24.0
Visual aid (glasses or lenses)	Using glasses or lenses	210	52.0
	Not using glasses or lenses	191	47.3
	Without reply	3	0.7
Total		404	100.0

2.3. Data analysis methods

Analysis began with frequency distributions and proportions for each item. Group differences were then examined with appropriate tests. The chi-square (χ^2) test compared frequencies across categories, such as awareness of interactive packaging by age group. The independent-samples t-test and analysis of variance (ANOVA) compared mean scores, and Pearson's correlation coefficient measured the strength and direction of the relationship between variables, in particular between age and the perceived importance of interactive access.

Finally, simple linear regression modelled perceived importance as a function of age, giving an estimate of how much of the variation age alone accounts for.

3. Results

3.1. Awareness and use of interactive packaging

Respondents were first asked whether they had ever used products with interactive elements on the packaging- QR codes, NFC tags, video content or applications and, if so, to name examples. All 404 answered. The overall results show a shallow reach. Across the sample, 39% had never heard of interactive packaging at all. A further 43% had heard of such products but never used them, 9% had used them, and the remaining respondents were unsure. So, four in five people had either never met the channel or knew of it only in passing, and fewer than one in ten had actually engaged with one.

Awareness and use differed sharply by age ($\chi^2 = 129.856$, df = 9, $p < 0.001$). The share of those who had never even heard of interactive packaging was highest among respondents aged 66 and over, at 81%, and fell in the younger groups. Having heard of such products without using them was most common in the 36–50 group (57%), followed closely by the 18–35 (48%) and 51–65 (47%) groups. Actual use sat in the middle of the age range: highest among the 36–50 group (16%) and next among the 18–35 group (12%). The oldest respondents were the least likely to know the channel exists, and use never rose above a small minority in any group.

The divide by visual status was just as clear ($\chi^2 = 67.093$, df = 6, $p < 0.001$). Among respondents who wear glasses or contact lenses, 58% had never heard of interactive packaging, against 19% of those who do not, a gap of nearly forty percentage points. Those without visual aids were far more likely to have heard of such products without using them (59% against 28%). Actual use was low and similar in both groups. Respondents who reported using glasses or contact lenses were less aware that the channel exists.

Of the 37 respondents who had used interactive packaging, 16 named a specific product. Their answers, summarised in Table 2, cluster around a narrow set of categories. Multiple answers were allowed, so the figures sum to more than one hundred percent.

In this sample, the recalled uses of interactive packaging were concentrated in beverage category (Cedevita, Coca-Cola, beer, Pepsi, drinks in general) and snack products (cereals, Nutella, chips, chocolate), suggesting that respondents primarily encountered the technology as a marketing and engagement tool rather than as an accessibility feature. These are consumer goods aimed at a broad, largely younger users, and they are precisely the categories where brands add interactive elements for promotion and engagement.

Table 2

Named examples of interactive packaging (n = 16 respondents who cited an example; multiple answers possible)

Product / category	Count	% of 16
Cedevita	11	69
Coca-Cola	11	69
Beer	7	44
Drinks (general)	7	44
Cereals	4	25
Nutella	2	13
Chips	2	13
Organic products	2	13
Other single mentions*	1	6

* Other single mentions: hygiene products, chocolate, cosmetics, Pepsi, chicken, pasta

3.2. Perceived importance of interactive access

At the end of the section, respondents rated how important it was to them that packaging gives access to additional product information through mobile applications or video, on a five-point scale from 1 (not at all important) to 5 (very important). All 404 participants answered. The result is low and one-sided. More than half the sample, 52%, rated this unimportant- 33% not at all important and a further 19% unimportant. Another 27% were indifferent. Only 20% called it important, and of those just 5% rated it very important. The mean across the whole sample was 2.39, which sits below the midpoint of the scale and matches the skew in the distribution.

Perceived importance fell with age, and the drop was concentrated at the top of the age range. Analysis of variance confirmed a significant difference between groups ($F = 17.663$, $p < 0.001$). As Table 3 shows, the three younger groups gave similar mean ratings, all close to the scale midpoint, while respondents aged 66 and over stood clearly apart at 1.65. Post-hoc tests placed this oldest group significantly below every other. The people for whom the accessibility argument is most often made, then, valued the channel least.

Table 3

Perceived importance of interactive access by age group (1–5 scale)

Age group	Mean	SD
18–35	2.66	1.25
36–50	2.66	1.27
51–65	2.55	1.18
66 and more	1.65	0.87
Total	2.39	

Two further tests examined age as a continuous variable. Pearson's correlation between age and perceived importance was −0.294 ($p < 0.001$), a weak-to-moderate negative relationship: as age rises, the value placed on interactive access tends to fall. This matters because the direction is negative. Across most other packaging attributes in the wider survey, older respondents rated features as more important, not less; here the sign is reversed.

Simple linear regression with age as the predictor confirmed the effect and put its size in context. Age alone explained 8.7% of the variance in perceived importance ($R^2 = 0.087$), and the model was significant overall ($F = 38.162$, $p < 0.001$). Each additional year of age was associated with a drop of about 0.021 points on the five-point scale ($B = −0.021$, $t = −6.178$, $p < 0.001$), with a 95% confidence interval for the slope of −0.028 to −0.015.

Because the interval does not cross zero, age is a genuine predictor of how important a person finds interactive access- but a modest one, accounting for less than a tenth of the variation. The direction is clear and consistent, but the magnitude is small.

4. Discussion

The three hypotheses were confirmed. Awareness and use of interactive packaging were low and declined with age (H1); the perceived importance of interactive access declined with age (H2); and the group most likely to need accessible information, those who use visual aids, were not more aware of the channel but markedly less so (H3). The findings describe a communication failure rather than a design failure. The findings also suggest that the principal limitation may lie less in the technical capacity of the technology than in the reach, visibility and social mediation of the channel.

Rogers (2003) describes adoption as a sequence- knowledge, persuasion, then decision- and an innovation cannot be adopted by people who never reach the first step. Interactive packaging is stuck there. With 39% of the whole sample, and 81% of those aged 66 and over, unaware that such products exist, the channel has not cleared the knowledge stage for the very audience the accessibility argument names. The small group who had used it sat in the middle of the age range and reached mostly for drinks and snacks, which is the profile of early, engagement-driven adopters rather than of users drawn by accessibility.

Rogers also notes that interpersonal channels move people through persuasion more effectively than mass ones; the near-absence of use among older respondents suggests that this interpersonal push has simply not happened for them yet.

Tichenor, Donohue & Olien (1970) observed that when new information enters a social system, better-resourced groups absorb it faster, so the knowledge gap widens rather than closes. A digital layer added to packaging behaves the same way. It is taken up first by younger, connected consumers and passes older ones by, reproducing the very divide it was meant to bridge. This fits the wider evidence on the grey divide, where the use of digital tools falls steeply with age and is shaped by cohort and social context more than by age alone (Gilleard & Higgs, 2008; Friemel, 2016).

Across the survey, older respondents rated packaging attributes as more important than younger ones did- the clarity of information, the adaptation of packaging for older and impaired users, prominent naming on the front of the pack. For interactive access, the correlation with age turned negative ($r = −0.294$). It shows that older consumers do not place a low value on product information as such; they place a high value on it. What they do not value is receiving it through a digital channel. In communication terms, the barrier is the medium, not the message. The same person who wants a larger, clearer printed label does not want to fetch that information by scanning a code or opening an application. Claim that interactive packaging improves accessibility for this group has to reckon with the fact that the group itself does not see it that way. This gap is channel-specific rather than a general unfamiliarity with packaging innovation. Two further findings point the same way. The perceived importance of interactive access was low across the whole sample (mean 2.39), so this is not only about age; the channel is weakly valued in general.

The channel exists; it simply carries a different message, to a different audience, than the accessibility case assumes. This is the accessibility paradox. A channel introduced to widen access to product information reaches the audience that needs it least and misses the audience that needs it most. The failure lies not in the code or the tag but in the match between channel and audience. Seen this way, the problem is not that older and visually impaired consumers reject better information; it is that the route chosen to deliver it does not reach them.

4.1. Limitations

The study has limits. It draws on self-reported awareness and importance rather than observed behaviour, and its design is cross-sectional, so it captures a moment rather than a trend. It measures whether people know and value the channel, not whether they could use it well if shown. Future work should test that directly- through usability studies that pair older users with an intermediary, and through on-pack trials of the kind of clear activation cue recommended here, evaluated with older audiences rather than younger ones.

The use of glasses or contact lenses should not be interpreted as equivalent to visual impairment. It represents a broad self-reported indicator of visual-correction needs and may include respondents without clinically significant visual limitations. A further caution concerns the analysis by visual status. Because the use of glasses or contact lenses rises with age, the two independent variables overlap: older respondents are both more likely to wear visual aids and less likely to be aware of interactive packaging. The lower awareness observed among glasses wearers may therefore partly reflect the age effect rather than visual status as such, since the chi-square comparison by visual status was not controlled for age.

5. Conclusions

This study set out to ask whether interactive packaging, treated as a communication channel, reaches the audience it is meant to serve. Awareness and use are low across the board and lowest among older consumers and those who use visual aids, and the same groups place the least value on receiving product information through a digital channel. A channel promoted as a way to widen access instead reaches the audience that needs it least and misses the audience that needs it most. This is the accessibility paradox, and its cause is a mismatch between channel and audience, not a fault in the technology itself.

If the barrier is the channel, the answer is to change it, or, more precisely, to add one. The results point away from the device and toward the people around the intended user. This is the logic of the two-step flow of communication: messages from a mass channel often reach people only after passing through "opinion leaders" in their immediate circle, who take them up first and relay them onward (Katz & Lazarsfeld, 1955). For interactive packaging, the family member, carer or more confident peer is exactly that intermediary- the person who notices the tag, understands it, and shows the intended user what it does. Diffusion research holds that interpersonal channels, not mass ones, carry people through the persuasion stage of adoption (Rogers, 2003), and work on older adults and digital tools shows that encouragement from family and friends is among the strongest predictors of whether an older person takes up a new technology, with informal help inside trusted relationships working better than formal instruction (Gilleard & Higgs, 2008; Friemel, 2016). The social environment of the older consumer, for example family members, carers, peers, is the interpersonal channel that a printed-plus-digital package cannot supply on its own.

That environment is not hypothetical. The wider survey shows that older respondents and those who use visual aids already rely on exactly such a network for packaging: many older respondents reported needing help from a partner, household member, carer or friend to open packaging or read its information, against almost none of the youngest group. The support structure is already in place. The same person who today helps a parent read a small label or open a jar is well placed to show them how to reach the extra information a package offers. What is missing is not the relationship but a reason and a cue to use it.

This points to recommendations aimed at the environment rather than the device. Awareness efforts for accessible interactive packaging should address families and carers, not only end users, and can draw on intergenerational demonstration, in which a younger or more confident person introduces the feature. On the package itself, interactive elements need a clear, conventional and legible cue- a short, plain invitation to act, set apart by colour and position, so that an intermediary can find and explain it quickly. Above all, a digital layer should complement legible print, not replace it. Interactive access can add value for those who choose it, but it cannot stand in for clear information on the surface, because for much of the intended audience the digital route is still not their first choice. The question is no longer whether the technology can carry accessible information. It can. The question is how to make sure that the message arrives.

6. Funding

The research was funded by
the NextGeneration EU project- EKKA.

7. References

Dillman, D.A., Smyth, J.D. and Christian, L.M. (2014) *Internet, Phone, Mail, and Mixed-Mode Surveys: The Tailored Design Method*. 4th ed. Hoboken, NJ: John Wiley & Sons.

European Commission. (2024) *2024 Ageing Report: Economic and Budgetary Projections for the EU Member States (2022–2070)*. European Economy Institutional Paper 279. Luxembourg: Publications Office of the European Union. DOI: 10.2765/022983

Eurostat. (2025) *Demography of Europe – 2025 Edition*. Luxembourg: Publications Office of the European Union. DOI: 10.2785/5077379

Friemel, T.N. (2016) 'The digital divide has grown old: determinants of a digital divide among seniors', *New Media & Society*, 18(2), pp. 313–331. DOI: 10.1177/1461444814538648

Gilleard, C. and Higgs, P. (2008) 'Internet use and the digital divide in the English Longitudinal Study of Ageing', *European Journal of Ageing*, 5(3), pp. 233–239. DOI: 10.1007/s10433-008-0083-7

Katz, E. and Lazarsfeld, P.F. (1955) *Personal Influence: The Part Played by People in the Flow of Mass Communications*. Glencoe, IL: Free Press.
Liu, Y. and Wang, Z. (2024) 'Intelligent food packaging design based on visual communication and multimedia technology', *Turkish Journal of Agriculture and Forestry*, 48(2), pp. 263–277. DOI: 10.55730/1300-011X.3179
Mustić, D., Cigula, T. and Kovačević, D. (2025a) 'Adaptation of packaging for the elderly population: challenges and opportunities of inclusive design'. In: *Proceedings of the 2nd Global Conference on Aging and Gerontology*, Vilnius, Lithuania. Vilnius: Diamond Scientific Publishing, pp. 11–20. DOI: 10.33422/agconf.v2i1.1025
Mustić, D., Cigula, T. and Kovačević, D. (2025b) 'Impact of packaging design on the independence of older people'. In: *Proceedings of the 2nd Global Conference on Aging and Gerontology*, Vilnius, Lithuania. Vilnius: Diamond Scientific Publishing, pp. 21–30. DOI: 10.33422/agconf.v2i1.1026
Park, G. and Robinson, E. (2020) 'A systematic review of in-home smart technology adoption to improve older adult health and family caregiving', *Innovation in Aging*, 4(Suppl. 1), p. 409. DOI: 10.1093/geroni/igaa057.1318
Plečko, M., Brozović, M. and Kovačević, D. (2023) 'Food product packaging adapted for visually impaired and elderly people', *Journal of Applied Packaging Research*, 15(1), Article 1.
Rogers, E.M. (2003) *Diffusion of Innovations*. 5th ed. New York: Free Press.
Rundh, B. (2005) 'The multi-faceted dimension of packaging: marketing logistic or marketing tool?', *British Food Journal*, 107(9), pp. 670–684. DOI: 10.1108/00070700510615053
Tichenor, P.J., Donohue, G.A. and Olien, C.N. (1970) 'Mass media flow and differential growth in knowledge', *Public Opinion Quarterly*, 34(2), pp. 159–170. DOI: 10.1086/267786
Underwood, R.L. (2003) 'The communicative power of product packaging: creating brand identity via lived and mediated experience', *Journal of Marketing Theory and Practice*, 11(1), pp. 62–76. DOI: 10.1080/10696679.2003.11501933
Žurbi, T. and Gregor-Svetec, D. (2024) 'NFC tag awareness and its visual implementation on food packaging: case study in Slovenia', *Applied Sciences*, 14(21), 9933. DOI: 10.3390/app14219933



© 2026 Authors. Published by the University of Novi Sad, Faculty of Technical Sciences, Department of Graphic Engineering and Design. This article is an open access article distributed under the terms and conditions of the Creative Commons Attribution license 4.0 Serbia (http://creativecommons.org/licenses/by/4.0/rs/).

Original Scientific Paper https://doi.org/10.24867/GRID-2026-p35

Consumer Experiences with Screw-Closure Packaging: Ergonomic Challenges and User Difficulties

ABSTRACT

Understanding consumers' needs and preferences provides a basis for the systematic assessment of the ergonomic quality of packaging solutions. Therefore, this study aimed to investigate consumers' experiences with commercially available bottles and jars with screw closures, with particular emphasis on perceived difficulties during use, problematic packaging characteristics, and strategies adopted to overcome these difficulties. An online questionnaire was conducted using Google Forms and completed by 240 participants aged 19-25 years. The results showed conventional glass jars with metal lids and plastic bottles with plastic caps were frequently identified as problematic packaging types. Participants associated opening difficulties with closure dimensions, surface texture, sharp edges, closure height, and packaging body shape. Participants reported various difficulties when opening packages, including slipping, pain, and difficulty applying sufficient force. Some participants stated that they used improvised tools or asked other people for help. In some cases, difficulties with opening led participants to stop using a product. The findings provide insight into consumer experiences with packaging usability and identify perceived ergonomic challenges that should be considered in the design and development of user-oriented packaging solutions.

Gordana Bošnjaković
Gojko Vladić
Katarina Maričić Picajkić
Teodora Gvoka

University of Novi Sad, Faculty of Technical Sciences, Department of Graphic Engineering and Design, Novi Sad, Serbia

KEY WORDS
Packaging ergonomics, screw closures, consumer experience, opening difficulties

1. Introduction

The opening of packaging represents an important stage of interaction between the consumer and the product. It is often considered a trivial everyday task, as difficulties encountered during opening can sometimes be overcome by using additional aids such as scissors or knives, or by asking another person for assistance (Yoxall et al., 2010). From the consumer perspective, the perceived functionality of packaging, including its ease of opening and handling, may represent an important aspect of the overall user experience (Duizer, Robertson & Han, 2009; Wenk et al., 2016). In particular, the application of excessive force during opening may present a challenge for users with different levels of physical ability or hand function (Theobald & Winder, 2006). Packaging that does not accommodate the diverse abilities of users may negatively affect the consumer experience and may even lead consumers to avoid certain products (Yoxall, Rodriguez-Falcon & Luxmoore, 2013; Bošnjaković & Vladić, 2020). Inclusive design represents an approach aimed at developing products and services that are accessible and easy to use for the widest possible range of users without the need for special adaptation or specialised design (British Standards, 2005). In the context of packaging, this approach focuses on making everyday packaging easier to open and use by a broad range of consumers rather than developing specialised solutions for a particular user group (Clarkson et al., 2003; Keates & Clarkson, 2003; Waller et al., 2015). Consumer feedback can provide valuable information about packaging characteristics perceived as problematic during everyday use and can contribute to the assessment of the ergonomic quality of packaging solutions. Investigating consumers' experiences may therefore help identify difficulties encountered during opening and closing, as

well as the strategies users adopt to overcome them. Therefore, this study aimed to investigate consumers' experiences with commercially available bottles and jars with screw closures, with particular emphasis on perceived difficulties during opening and closing and packaging characteristics associated with these difficulties.

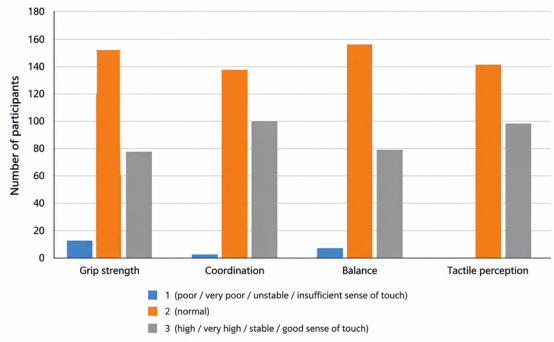
2. Methodology

An online questionnaire was developed using Google Forms to collect subjective data on consumer preferences and experiences related to commercially available packaging. The questionnaire was distributed via a web link and completed electronically by the participants. The questionnaire addressed participants' demographic characteristics, physical activity, previous hand injuries, self-assessed hand abilities, and experiences with opening and closing bottles and jars with screw closures. It also explored participants' subjective evaluations of packaging characteristics, perceived difficulties during use, and strategies adopted to overcome these difficulties. Participants were asked to identify the most and least favourable characteristics of selected packaging examples and to describe their positive and negative experiences during use. A total of 240 participants completed the questionnaire. The collected data were analysed using descriptive statistics. The results are presented as frequencies, showing the number of participants who selected each response option, to describe their experiences with opening and closing packaging and the packaging characteristics associated with opening difficulties.

3. Results and discussion

3.1. Demographic data of the participants

A total of 240 participants aged 19–25 years participated in the study. The mean body weight was 66 kg (range: 43–105 kg), while the mean body height was 173 cm (range: 154–200 cm). Most participants were right-hand dominant (212 participants). Physical activity was reported by 209 participants, with the most frequently reported activities being gym-based exercise (132 participants), volleyball (50 participants), and basketball (35 participants), alongside various other activities. Participants reported different levels of involvement, ranging from recreational to semi-professional and professional activity. Regarding hand-related characteristics, 206 participants reported no previous hand injuries, while 34 reported previous injuries, including sprains, ligament strains, or finger fractures. In addition, 205 participants reported no current problems affecting the skin of the dominant palm, whereas 35 reported issues such as blisters, excessive sweating, or allergic reactions. Participants also provided self-assessments of hand abilities in terms of strength, coordination, balance, and tactile perception. The distribution of these self-assessments is presented in Figure 1. The majority of participants rated their hand abilities as normal or above average across all four assessed categories. This finding indicates that the study sample generally perceived their hand abilities as adequate for everyday activities. Considering the relatively young age of the participants, the predominance of normal or above-average self-assessments provides a relevant context for interpreting the reported difficulties in handling packaging, as these difficulties cannot be predominantly attributed to a generally perceived lack of hand ability within the study sample.

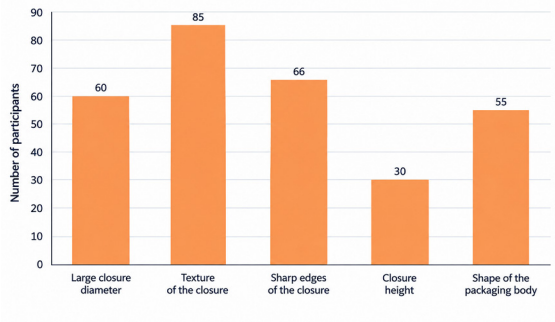


» **Figure 1:** *Participants' self-assessed hand abilities*

3.2. Difficulties in Opening and Closing Packaging

Questions concerning difficulties encountered when opening and closing bottles and jars were included to assess users' experiences during packaging handling. Regarding the frequency of difficulties when opening screw closures, 26 participants reported that they never experienced difficulties, while 108 participants experienced difficulties rarely. A total of 80 participants reported experiencing difficulties sometimes, 23 almost always, and 3 always. Among the packaging types identified as problematic, conventional glass jars with metal lids were most frequently reported, with 160 participants identifying this type of packaging as difficult to open. Plastic water and juice bottles with plastic caps were also identified as problematic by 75 participants. These findings show that difficulties were reported for both glass jars and plastic bottles, suggesting that perceived ergonomic challenges were not limited to a single packaging type. Participants were also asked to identify specific packaging characteristics that contributed to difficulties during use. The characteristics perceived as problematic included closure size, closure texture, sharp closure edges, closure height, and the shape of the packaging body (Figure 2). These findings indicate that difficulties in handling screw closures may be associated with several physical characteristics of both the closure and the packaging itself. In

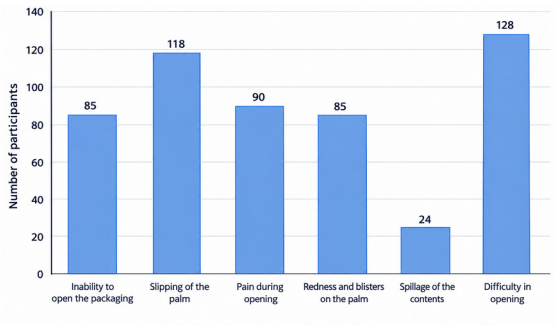
particular, closure dimensions and surface characteristics may affect the user's ability to establish and maintain an adequate grip during opening.



» **Figure 2:** *Packaging characteristics perceived as problematic by participants*

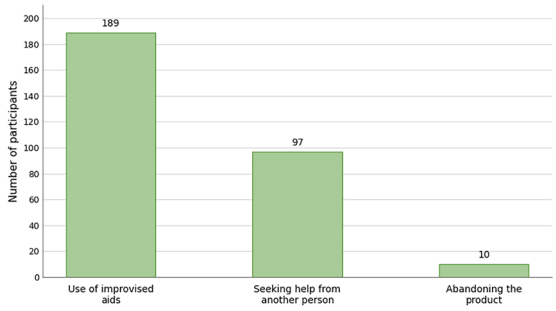
3.3. Problems Experienced and Strategies for Overcoming Difficulties

Participants were also asked to identify the problems they experienced during the initial opening of packaging (Figure 3). The reported problems included inability to open the packaging, palm slipping during opening, pain during opening, the occurrence of redness and blisters on the palm, spillage of the contents during opening, and difficulty in opening the packaging. These responses highlight the range of difficulties encountered during initial opening, including both handling-related problems and physical discomfort.



» **Figure 3:** *Problems reported by participants during initial packaging opening*

When faced with difficulties during packaging opening, participants reported several strategies for overcoming them (Figure 4). The most frequently reported responses included the use of improvised aids, such as cloths to improve grip or a knife to release the vacuum in jars, as well as seeking assistance from another person. In some cases, participants reported abandoning the use of the product when they were unable to overcome the opening difficulty. These responses suggest that difficulties with screw closures may extend beyond temporary inconvenience, leading users to adopt alternative methods, seek external assistance, or discontinue product use. The reported use of improvised aids also highlights potential limitations in the usability of some packaging solutions under everyday conditions.



» **Figure 4:** *Participants' responses to difficulties encountered when opening packaging closures*

In contrast to the difficulties reported during opening, problems during the closing of bottles and jars were considerably less frequent. The majority of participants, 221 in total, reported that they never or rarely experienced difficulties when closing the packaging. Furthermore, subsequent opening and closing of the same packaging was generally perceived as easier than the initial opening. This may be related to the need to overcome the original closure resistance and, in some cases, an initial vacuum seal.

Overall, the findings highlight several aspects of packaging usability that may affect the user experience during opening. The reported difficulties, problematic packaging characteristics, and strategies used to overcome them indicate that some users may rely on improvised aids or assistance from others when handling screw-closure packaging. These findings provide a basis for further consideration of ergonomic requirements in the design and evaluation of screw-closure packaging.

4. Conclusion

This study provided insight into consumers' experiences with commercially available bottles and jars with screw closures, with particular emphasis on difficulties encountered during opening and closing. The findings showed that opening was a more challenging stage of packaging handling than closing. Conventional glass jars with metal lids and plastic bottles with plastic caps were among the packaging types most frequently identified as problematic. Participants identified several packaging characteristics as problematic, including closure size, texture, sharp edges, closure height, and packaging body shape. Participants reported various difficulties during initial opening. To overcome these difficulties,

they often used improvised aids or asked other people for help, while some abandoned the use of the product. Difficulties during closing were less frequent, and subsequent opening and closing were generally perceived as easier. Overall, the findings highlight the importance of considering users' experiences when evaluating the ergonomic quality of screw-closure packaging. The identified difficulties show that closure dimensions, surface texture, edge design, closure height, and packaging body shape are important aspects to consider in packaging design and evaluation. Considering these characteristics together with users' experiences may contribute to the development of packaging that is easier to use and better accommodates users' needs.

5. Acknowledgments

This research has been supported by the Ministry of Science, Technological Development and Innovation (Contract No. 451-03-34/2026-03/200156) and the Faculty of Technical Sciences, University of Novi Sad through project "Scientific and Artistic Research Work of Researchers in Teaching and Associate Positions at the Faculty of Technical Sciences, University of Novi Sad 2026" (No. 01-3609/1).

6. References

British Standards. (2005) BS 7000-6:2005. Design management systems – Part 6: Managing inclusive design. London: British Standards.

Bošnjaković, G. and Vladić, G. (2020) 'Research methodologies for assessing the ergonomics of packaging products – a review'. In: 10. *International Symposium on Graphic Engineering and Design GRID*, Novi Sad: Faculty of Technical Sciences, Department of Graphic Engineering and Design, 12–14 November 2020, pp. 335–345. ISBN 978-86-6022-303-8.

Clarkson, J., Coleman, R., Keates, S. and Lebbon, C. (2003) *Inclusive Design: Design for the Whole Population*. London: Springer-Verlag.

Duizer, L.M., Robertson, T. and Han, J. (2009) 'Requirements for packaging from an ageing consumer's perspective', *Packaging Technology and Science*, 22(4), pp. 187–197. DOI: 10.1002/pts.834

Keates, S. and Clarkson, J. (2003) Countering Design Exclusion – An Introduction to Inclusive Design. London: Springer.

Theobald, N. and Winder, B. (2006) *Packaging Closures and Sealing Systems*. Oxford: Blackwell Publishing Ltd.

Waller, S., Bradley, M., Hosking, I. and Clarkson, P.J. (2015) 'Making the case for inclusive design', *Applied Ergonomics*, 46(Part B), pp. 297–303. DOI: 10.1016/j.apergo.2013.03.012

Wenk, S., Brombach, C., Artigas, G., Jarvenpaa, E., Steinemann, N., Ziesemer, K. and Yildirim, S. (2016) 'Evaluation of the accessibility of selected packaging by comparison of quantitative measurements of the opening forces and qualitative surveys through focus group studies', *Packaging Technology and Science*, 29(11), pp. 559–570. DOI: 10.1002/pts.2237

Yoxall, A., Langley, J., Janson, R., Lewis, R., Wearn, J., Hayes, S.A. and Bix, L. (2010) 'How wide do you want the jar?: The effect on diameter for ease of opening for widemouth closures', *Packaging Technology and Science*, 23(1), pp. 11–18. DOI: 10.1002/pts.874

Yoxall, A., Rodriguez-Falcon, E.M. and Luxmoore, J. (2013) 'Carpe diem, Carpe ampulla: A numerical model as an aid to the design of child-resistant closures', *Applied Ergonomics*, 44, pp. 18–26. DOI: 10.1016/j.apergo.2012.04.006



© 2026 Authors. Published by the University of Novi Sad, Faculty of Technical Sciences, Department of Graphic Engineering and Design. This article is an open access article distributed under the terms and conditions of the Creative Commons Attribution license 4.0 Serbia (http://creativecommons.org/licenses/by/4.0/rs/).

Original Scientific Paper https://doi.org/10.24867/GRID-2026-p36

How Archetype-Based Packaging Design Shapes Visual Attention and Ease of Use

ABSTRACT

Brand archetypes are established tools for differentiating visual identities, but their effects on physical packaging remain underexplored. This study combined a self-report survey and eye-tracking to examine how two coffee-package designs—Fikaféa (Everyman archetype) and Kaffari (Explorer archetype), each with a tear-notch and a standard opening—shape attention to product information and perceived ease of opening. A brand-level survey first confirmed that both identities communicated their intended values: the familiar Everyman identity was rated more aesthetically appealing, whereas the Explorer identity was perceived as more innovative. At the package level, a 2 × 2 repeated-measures design showed that the tear notch improved perceived ease of opening and attracted more fixations to the opening area. Brand design also shaped attention: the high-contrast Everyman layout was rated clearer for product information and drew longer fixations on informational AOIs, whereas the Explorer layout directed relatively more attention to brand-related elements. Because the survey and eye-tracking datasets could not be linked at the participant level, convergence was assessed only at the condition level. At that level, self-report ratings, fixation measures, and qualitative heat maps showed a consistent pattern: opening cues supported ease-of-use perception, while brand design redistributed attention between functional and brand-related package content.

KEY WORDS
Packaging design, eye-tracking, brand archetypes, visual attention, consumer perception

Jesenka Pibernik
Mila Mihaljević
Marija Magdalena Mendeš

Faculty of Graphic Arts,
University of Zagreb,
Zagreb, Croatia

1. Introduction

Brands increasingly compete by building emotional connections with consumers, not only through price or function. Brand personality is central to this process (Aaker, 1997), and Jungian archetype theory adds a layer of widely recognisable symbolic meaning (Jung, 1981). Mark and Pearson systematised this approach into twelve archetypes that help brands construct coherent narratives and values (Mark & Pearson, 2001). Recent work likewise emphasises the role of archetypal meaning in customer–brand relationships (Merlo et al., 2023; Friebe, 2026). Visual identity carries this personality through logotype, typography, colour and imagery (Van den Bosch, De Jong & Elving, 2005; Childers & Jass, 2002). On a coffee package, however, the same surface must both express the brand and communicate mandatory product information. Whether an archetype-driven aesthetic supports or obstructs this functional task remains open. Self-report alone is insufficient, because what consumers say they notice often differs from what they actually look at (Gunaratne et al., 2019; Clement, Kristensen & Grønhaug, 2013). Eye-tracking addresses this gap by recording fixation count, fixation duration and time to first fixation on defined areas of interest (AOIs). These measures are commonly used as indicators of attention and interest (Guo, Kim & Lee, 2024; Lacoste-Badie & Droulers 2020).

This paper therefore focuses on the package as the central object of study. After a preliminary survey estab-

lished what each identity communicated at the brand level, the package-level study examined how these identities direct attention to functional information and how the opening mechanism shapes perceived ease of use.

2. Theoretical background

2.1. Archetypes and visual identity

Mark and Pearson group the twelve archetypes by core human motivation. The Everyman belongs to the "belonging" cluster and communicates equality, accessibility and everyday warmth; the Explorer belongs to the "freedom" cluster and communicates autonomy, discovery and novelty (Mark & Pearson, 2001). These two archetypes were selected as a deliberate contrast between a familiar identity typical of the Croatian instant-coffee market (e.g. Franck, an Everyman brand) and a less common Explorer identity. Visual identity translates such values into colour, typography and imagery (Van den Bosch, De Jong, & Elving, 2005; Childers & Jass, 2002), while recent Jungian-branding scholarship continues to frame brands as symbolic systems built from archetypal meanings (Friebe, 2026).

2.2. Eye-tracking in packaging research

Eye-tracking is widely used in packaging research because it captures visual behaviour that recall-based methods may miss (Gunaratne et al., 2019; Clement, Kristensen, & Grønhaug, 2013). Fixation duration and fixation count are standard indicators of attention to package elements [10]. An elemental AOI approach further allows attention to be assigned to specific components, such as brand name, information label or imagery. Attention and liking, however, do not always coincide. Gunaratne et al. found that fixation on familiar chocolate packaging correlated with positive emotion, whereas novel designs showed no such link. Prior work also shows that low contrast can make relevant information harder to locate. These findings motivate the present combination of brand-level evaluation, gaze metrics and self-report.

3. Brand identity context

Two instant-coffee identities were developed for the contrasting archetypes. Fikaféa (Everyman) refers to Swedish fika, the shared coffee-break ritual (Blom, 2024), and uses beige-brown tones, a handwritten logotype and a stylised cup motif to communicate warmth, simplicity and belonging. Kaffari (Explorer) combines associations of coffee and safari, using a bold sans-serif logotype, a coffee-bean mark and plantation imagery in earth-and-green tones to communicate discovery and adventure (Figure 1.).



» **Figure 1:** *Fikaféa and Kaffari coffee packaging, standard and tear-notch opening*

A brand-level survey (N = 43, predominantly aged 18–25) confirmed that both identities conveyed their intended values. It also revealed an instructive asymmetry (Table 1): Fikaféa was rated more aesthetically appealing and elicited higher purchase intention, whereas Kaffari was chosen as more innovative in direct comparison. In this context, aesthetic appeal appeared to derive from familiarity and simplicity rather than novelty, consistent with the attention–liking dissociation reported for packaging [11]. This brand-level pattern frames the package-level analysis.

Table 1

Brand-level perception of the two identities — Wilcoxon signed-rank test (N = 43)

Attribute	M Kaffari	M Fikaféa	Z	p	r
Aesthetic appeal	4.00	4.51	-2.68	.007	0.51
Innovativeness	3.84	3.81	-0.45	.655	0.09
Purchase intention	3.81	4.26	-2.16	.031	0.42

Note. Five-point scale. Z = standardised test statistic; r = effect size. Innovativeness did not differ on absolute ratings, but Kaffari was chosen as the more innovative brand in direct comparison (binomial test, p = .014).

4. Aims and hypotheses

The study examines how the two identities perform on the physical package. Six hypotheses were specified. Directional hypotheses were used where the pilot data supported a clear expectation, while H2 expressed the expectation that opening mechanism would not substantially affect perceived information clarity or overall affective impression.

H1. The tear-notch opening is rated easier to open than the standard packaging, irrespective of brand design. **H2.** The opening mechanism is not expected to substantially affect perceived information clarity or the overall affec-

tive impression. **H3.** Brand design influences perceived information clarity; the high-contrast Everyman layout (Fikaféa) is rated higher than the illustration-dense Explorer layout (Kaffari). **H4.** The tear-notch mechanism attracts more fixations to the opening area than the standard packaging. **H5.** Brand design governs attention allocation: the high-contrast layout elicits longer fixation on informational AOIs, whereas the illustration-dense layout elicits longer fixation on brand AOIs, producing a design-level dissociative pattern. **H6.** Self-reported ease of opening and information clarity converge with the corresponding eye-tracking metrics at the condition level.

5. Methodology

5.1. Design and stimuli

A 2 × 2 within-subjects design crossed packaging Design (Kaffari vs. Fikaféa) with Opening mechanism (tear notch vs. standard closure), yielding four conditions. Stimuli were photorealistic 3-D renderings of each pouch, shown from the front and back so that brand and informational elements could be assessed separately. All participants saw all conditions, and presentation order was recorded.

5.2. Participants

The packaging questionnaire was completed by 26 participants, and the eye-tracking sub-sample comprised 21 participants. The sample was predominantly female and aged 18–23, limiting generalisability. Because the questionnaire included no identifier matching the eye-tracking records, the two sources were linked only at the condition level.

5.3. Subjective measure

For each condition, participants completed an 11-item five-point-scale block: four information items (quantity, ingredients, expiry date, recycling), a six-item semantic differential for overall impression (e.g. dull–interesting, unappealing–appealing, clumsy–functional), and one ease-of-opening item. The semantic-differential items formed a composite impression score (Cronbach's α = .70–.85 across conditions), and the four information items formed a composite information score.

5.4. Objective measure

Gaze was recorded during stimulus inspection with a Tobii Pro Fusion at 120 Hz. Participants were seated approximately 65 cm from a 1920x1080 px display. A 9-point calibration was performed before the task and accepted when average error was below 0.7°.

Each stimulus was shown for fixed 3-6-second exposure. Participants were instructed to inspect the package freely, as if evaluating it before purchase. Fixations were extracted using Tobii Pro Lab. For the opening region, fixation count and time to first fixation (TTFF) were extracted.

For brand and information processing, total fixation duration was computed per AOI across both faces. AOIs were then aggregated into a brand group (brand name, brand story) and an information group (expiry date, quantity, contents, preparation, recycling, barcode, strength). Individual AOIs present in both designs were also analysed separately.

5.5. Qualitative support

Aggregated heat maps were generated for every condition and both package faces. They were used qualitatively to visualise the spatial distribution of attention and support interpretation of the statistical findings; no inferential test was applied to them.

5.6. Statistical analysis

Each dependent measure was analysed with a 2 × 2 repeated-measures ANOVA (Design × Opening), using generalised eta-squared (η^2G) as the effect-size estimate. Because normality was violated in some conditions, principal effects were additionally checked with the Wilcoxon signed-rank test, with concordant results. The threshold was $\alpha = .05$. Repeated-measures models required complete data across all four conditions. For opening-area metrics, two of the 21 participants did not fixate the opening AOI in at least one condition and were excluded, leaving 19 complete cases (error df = 18). The brand and information AOI models retained all 21 participants.

6. Results

6.1. Ease of opening

H1 was supported. The tear notch was rated easier to open than the standard closure (M = 4.90 vs. 4.21), $F(1, 25) = 14.81$, $p < .001$, $\eta^2G = .20$, with no effect of brand design ($p = 1.000$; Tables 2–3). The gaze data supported H4: the tear notch attracted more fixations to the opening area (M = 5.21 vs. 3.18), $F(1, 18) = 16.97$, $p < .001$, $\eta^2G = .22$ (Table 4). Heat maps showed clustered attention on the labelled tear-notch zone and more dispersed attention along the top edge of standard packs. The higher variability of ease ratings for the standard closure (SD ≈ 0.92 vs. 0.20–0.37) suggests that the opening was located more reliably when an explicit cue was present.

Table 2

Descriptive statistics of the packaging survey by condition (five-point scale; N = 26)

Measure	Kaffari Tear notch	Kaffari Standard	Fikaféa Tear notch	Fikaféa Standard
Information clarity	4.38 (0.58)	4.50 (0.61)	4.59 (0.54)	4.63 (0.51)
Overall impression (SD)	3.99 (0.57)	4.07 (0.56)	4.12 (0.57)	4.12 (0.63)
Ease of opening	4.85 (0.37)	4.27 (0.96)	4.96 (0.20)	4.15 (0.92)

Note. Means with standard deviations in parentheses. SD = semantic differential composite.

Table 3

Packaging survey: 2 × 2 repeated-measures ANOVA (N = 26)

Measure	Effect	F	df	p	η^2G
Ease of opening	Opening	14.81	1, 25	< .001	.203
	Design	0.00	1, 25	1.000	.000
	Design × Opening	2.74	1, 25	.110	.007
Information clarity	Design	6.62	1, 25	.016	.023
	Opening	4.22	1, 25	.051	.006
	Design × Opening	0.38	1, 25	.542	.001
Overall impression	Design	0.51	1, 25	.483	.007
	Opening	0.98	1, 25	.333	.001
	Design × Opening	1.21	1, 25	.282	.001

Note. η^2G = generalised eta-squared. Significant effects ($p < .05$) in bold.

6.2. Information and brand attention

H3 was supported. Fikaféa was rated clearer for information (M = 4.61 vs. 4.44), $F(1, 25) = 6.62$, $p = .016$, and drew longer fixation on informational AOIs (M = 5.02 s vs. 4.06 s), $F(1, 20) = 11.20$, $p = .003$, $\eta^2G = .11$ (Table 5). Conversely, Kaffari drew longer fixation on brand AOIs (M = 3.04 s vs. 2.56 s), $F(1, 20) = 5.22$, $p = .033$. This dissociative attentional pattern supports H5: the designs differed not in total attention, but in its allocation between functional and brand-related content. Exploratory per-element comparisons with Holm correction (Table 6) showed greater attention to the expiry date and preparation instructions for Fikaféa, and greater attention to the brand name and quantity block for Kaffari.

Table 4

Eye-tracking metrics for the opening area by condition: descriptive statistics based on available cases

Metric	Kaffari Tear notch	Kaffari Standard	Fikaféa Tear notch	Fikaféa Standard
Fixation count	4.71 (2.26)	2.80 (1.64)	5.57 (2.16)	3.47 (1.68)
TTFF (s)	0.71 (0.46)	1.00 (0.84)	0.55 (0.35)	0.71 (0.45)

Note. Means with standard deviations in parentheses, computed on all available cases per cell (n = 19–21); the ANOVA was estimated on the 19 participants with complete data across all conditions. TTFF = time to first fixation (lower = faster).

Table 5

Eye-tracking total fixation duration: 2 × 2 repeated-measures ANOVA for brand and information AOIs (N = 21)

Measure	Effect	F	df	p	η^2G
Information AOIs	Design	11.20	1, 20	.003	.111
	Opening	0.91	1, 20	.352	.010
	Design × Opening	0.31	1, 20	.586	.003
Brand AOIs	Design	5.22	1, 20	.033	.039
	Opening	0.10	1, 20	.753	.001
	Design × Opening	2.52	1, 20	.128	.020

Note. η^2G = generalised eta-squared. Significant effects ($p < .05$) in bold.

Table 6

Total fixation duration per AOI element by design (main effect of design; N = 21)

Element (AOI)	Kaffari M (s)	Fikaféa M (s)	F	η^2G	p	p (Holm)
Expiry date	0.02	0.20	10.84	.135	.004	.015
Quantity	0.79	0.53	7.38	.069	.013	.040
Preparation	0.52	1.41	33.23	.228	< .001	.001
Contents	0.40	0.66	3.84	.053	.064	.128
Brand story	0.71	0.93	1.33	.015	.263	.263
Brand name	2.33	1.63	11.43	.149	.003	.015

Note. Means in seconds, summed across opening mechanism; main effect of design from a 2 × 2 repeated-measures ANOVA, df = (1, 20) for each test. η^2G = generalised eta-squared. These per-element analyses are exploratory; the p (Holm) column gives p-values adjusted for the six tests with the Holm correction, and significance (in bold) refers to the adjusted value ($p < .05$).

6.3. Independence of factors

H2 was largely consistent with the data, with one borderline exception. The opening mechanism had no significant effect on overall affective impression in the survey ($p = .333$) or on either gaze AOI group (information AOIs, $p = .352$; brand AOIs, $p = .753$). For survey-rated information clarity, the opening effect approached conventional significance ($p = .051$), so H2 is qualified on that measure. No interaction reached significance, indicating that design and opening operated largely independently.

6.4. Condition-level convergence of self-report and gaze

H6 was supported at the condition level only. Because the survey and eye-tracking records shared no participant identifier, self-report and gaze could be compared between conditions but not within individuals. The aggregated means agreed in direction: tear-notch conditions were rated easier to open and received more fixations on the opening area, while Fikaféa was rated clearer for information and drew longer fixation on informational AOIs. This does not establish that individuals who looked longer at a zone also rated it more highly.

7. Discussion

The study makes two connected contributions. Methodologically, self-report, gaze metrics and qualitative heat maps point in the same direction, although only at the condition level because the two datasets could not be linked by participant (H6, Section 6.4). Conceptually, the study connects archetype-based branding with the functional readability of packaging. It shows that the same surface carrying the brand identity also governs whether mandatory information is seen. Within this scope, the triangulation is informative: an explicit opening cue improves both perceived ease of opening and attention to the opening area, consistent with evidence that low-contrast packaging can hinder information search [10, 12].

The two study levels show a parallel pattern. At the brand level, Fikaféa was more appealing and generated higher purchase intention, whereas Kaffari was perceived as more innovative [11]. At the package level, Fikaféa directed gaze toward functional information, whereas Kaffari directed gaze toward brand identity. This finding should be read cautiously. The observed effect is tied to the concrete visual properties through which each archetype was realised—contrast, illustration density and information-panel organisation. Because only one design represented each archetype, the results demonstrate differences between two concrete identities rather than effects of the archetypes in general.

Practically, a high-contrast layout that separates mandatory information into dedicated panels can improve both attention to information and perceived clarity. A brand-forward, illustration-dense design can strengthen brand attention, but may do so at the cost of functional information. In markets where familiar, warmth-oriented coffee identities are common, an Explorer-oriented identity may therefore support differentiation, provided that its brand-first profile remains aligned with the communicative goals of the package.

8. Conclusion and limitations

Using a multi-method design, this study showed that two concrete archetype-driven packaging identities differed in how they directed attention to brand and product-information elements. The tear-notch mechanism improved perceived ease of opening and attracted more attention to the opening area. The high-contrast Everyman layout supported attention to product information, whereas the illustration-dense Explorer layout concentrated attention on the brand. The central result is the condition-level convergence of survey, eye-tracking and heat-map evidence.

Several limitations temper these conclusions. The samples were small and demographically homogeneous, limiting generalisability and statistical power. Because only one design instantiated each archetype, archetype and visual execution are confounded; stronger future designs should test several executions per archetype. The AOI sets also differed across designs and package faces, so aggregate information comparisons combine non-identical elements, while per-element tests remain exploratory. Finally, survey and eye-tracking data were linked only at the group level. A preregistered study with a larger, balanced sample and a shared participant key is therefore recommended to test individual-level correlations between attention and ratings, ideally including price, taste and shelf context.

9. References

Aaker, J.L. (1997) 'Dimensions of brand personality', *Journal of Marketing Research*, 34(3), pp. 347–356.

Blom, T. (2024) 'The Swedish fika culture as a touristic experience and value-creating resource', *Interna-*

tional Journal of Gastronomy and Food Science, 37, 101008. DOI: 10.1016/j.ijgfs.2024.101008

Childers, T.L. and Jass, J. (2002) 'All dressed up with something to say: Effects of typeface semantic associations on brand perceptions and consumer memory', *Journal of Consumer Psychology*, 12(2), pp. 93–106.

Clement, J., Kristensen, T. and Grønhaug, K. (2013) 'Understanding consumers' in-store visual perception: The influence of package design features on visual attention', *Journal of Retailing and Consumer Services*, 20(2), pp. 234–239. DOI: 10.1016/j.jretconser.2013.01.003

Dominici, G., Tullio, V., Siino, G. and Tani, M. (2016) 'Marketing archetypes: Applying Jungian psychology to marketing research', *Journal of Organisational Transformation & Social Change*, 13(2), pp. 109–122.

Friebe, R.M. (2026) 'Conscious branding, archetypes, and consumer identity: A Jungian framework for symbolic meaning, cultural individuation, and ethical marketing', *Journal of Higher Education Theory and Practice*, 26(1). DOI: 10.33423/56r52t42

Gunaratne, N.M., Fuentes, S., Gunaratne, T.M., Torrico, D.D., Francis, C., Ashman, H., Gonzalez Viejo, C. and Dunshea, F.R. (2019) 'Consumer acceptability, eye fixation, and physiological responses: A study of novel and familiar chocolate packaging designs using eye-tracking devices', *Foods*, 8(7), 253. DOI: 10.3390/foods8070253

Guo, R., Kim, N. and Lee, J. (2024) 'Empirical insights into eye-tracking for design evaluation: Applications in visual communication and new media design', *Behavioral Sciences*, 14(12), 1231. DOI: 10.3390/bs14121231

Jafarnejad Shahri, M., Golbazi Mahdipour, A., Bonyadi Naeini, A., Koleini Mamaghani, N., Broumandi, N., Rahmani, A. and Sadeghi Naeini, H. (2025) 'Eye-tracking study reveals the impact of packaging design on consumer behaviour: A case study of liquid soap bottles', *Journal of Sensory Studies*, 40(4), e70041. DOI: 10.1111/joss.70041

Jung, C.G. (1981) *The Archetypes and the Collective Unconscious*. Princeton, NJ: Princeton University Press.

Lacoste-Badie, S., Yu, J. and Droulers, O. (2020) 'Small change, big change – Increasing attention with product package variations', *Food Quality and Preference,* 86, 104007. DOI: 10.1016/j.foodqual.2020.104007

Mark, M. and Pearson, C.S. (2001) *The Hero and the Outlaw: Building Extraordinary Brands Through the Power of Archetypes*. New York: McGraw-Hill.

Merlo, O., Eisingerich, A.B., Gillingwater, R. and Cao, J.J. (2023) 'Exploring the changing role of brand archetypes in customer-brand relationships: Why try to be a hero when your brand can be more?', *Business Horizons*, 66(5), pp. 615–629. DOI: 10.1016/j.bushor.2022.11.001

Van den Bosch, A.L.M., De Jong, M.D.T. and Elving, W.J.L. (2005) 'How corporate visual identity supports reputation', *Corporate Communications: An International Journal*, 10(2), pp. 108–116.



© 2026 Authors. Published by the University of Novi Sad, Faculty of Technical Sciences, Department of Graphic Engineering and Design. This article is an open access article distributed under the terms and conditions of the Creative Commons Attribution license 4.0 Serbia (http://creativecommons.org/licenses/by/4.0/rs/).

Review Paper https://doi.org/10.24867/GRID-2026-p37

The Invisible Prototype: Ai-Powered Digital Twins for Resilient Graphic Packaging Design

ABSTRACT

Packaging is the first point of visual communication between a brand and its consumers, where graphic design and product security converge. Throughout transit, packaging endures drops, stacking compression, and vibrations that threaten its structural integrity, printed graphics, brand identity, and tamper-evident features. This paper explores how AI-powered digital twins - dynamic virtual replicas - can transform graphic packaging design by realistically simulating logistics conditions before physical production. By integrating AI, designers can predict deformation, print distortion, color degradation, and label damage under handling scenarios - enhancing prepress accuracy and digital image processing - while simultaneously optimizing package geometry, material selection, and visual layouts. The framework enables virtual evaluation of branding elements, authentication graphics, QR codes, and security seals, as well as protective performance, including functional security printing, to ensure packaging remains visually compelling and functionally reliable throughout the supply chain. Acting as an "invisible prototype," the digital twin offers a collaborative platform where graphic designers, prepress operators, engineers, and logistics specialists co-design solutions that drastically reduce physical prototyping and material waste. Rather than replacing creativity, AI augments design decision-making with data-driven insights. This approach effectively bridges graphic aesthetics with engineering performance, positioning intelligent simulation as a key enabler for secure, resilient, and visually impactful packaging systems.

R. Ragavaraja

Department of Printing and Packaging Technology,
College of Engineering Guindy,
Anna University,
Chennai, India

KEY WORDS
Graphic design, packaging design, digital twin, artificial intelligence, visual perception

1. Introduction

Packaging is the first physical encounter between a brand and a consumer. Color, typography, imagery, and form communicate expectations of quality before the contents are ever used. The package is, at the same time, a protective system that contains, preserves, and informs, and is therefore both a marketing tool and a logistics device (Fernandez et al., 2021). In practice, these two roles are engineered separately and in sequence. Structural designers fix the board, geometry, and closure to satisfy stacking and drop requirements, and graphic designers and prepress teams then decorate the result. The hand-off hides a coupling that is rarely examined. A shipper printed with a saturated brand red and a dense QR code can pass every structural test and still arrive with a bulged, scuffed, color-shifted panel and an unreadable authentication code, because none of those outcomes appear in a flat proof or on a press sheet. The designer who approved the artwork never saw the package that the consumer receives.

The consequences extend beyond appearance. Life-cycle studies increasingly count the food lost through inadequate packaging alongside the burden of the packaging itself, although many still rely on rough estimates of

the losses avoided (Williams & Wikström, 2011; Molina-Besch, Wikström & Williams, 2019; Zhang et al., 2026). Right-sizing protection is therefore a sustainability objective in its own right, and a pack that is lighter than it should be may be the more wasteful option once damage is counted. Plastic is the material most frequently assessed in such studies (Hemachandra, Hadjikakou & Pettigrew, 2024). As brand owners move toward fiber-based solutions, a further difficulty arises: fiber-based boards are highly sensitive to humidity and temperature, with stiffness changes of up to roughly 40 percent reported in realistic scenarios (Mann et al., 2026), so their printed surfaces behave differently under load and moisture. Replacing physical iteration with virtual evaluation addresses both pressures at once: fewer sample cartons, inks, and test runs are consumed, and the final design is better matched to the hazards it will meet. This holds only if the virtual evaluation can be trusted.

The digital twin is the natural vehicle for such evaluation. It is now a mainstream concept in manufacturing and engineering, with reviews covering its modeling, twinning, uncertainty quantification, and optimization technologies across many disciplines (Thelen et al., 2022). Surveys distinguish a digital model, a digital shadow, and a digital twin by the direction of data flow between the physical and virtual objects: manual in the first, one-way automatic in the second, and two-way automatic in the third (Yu et al., 2025). In packaging, however, twins have been mostly structural. The printed surface, with its color, image, code, and security layers, has been treated as an afterthought, and the authors' earlier review of augmented and virtual reality in graphic design concluded that immersive prototyping and AR-based authentication are promising but largely qualitative Nirmala, Raja & Kanchana, 2024). Immersive tools show a design; they do not predict how it will age in a truck.

This article, therefore, critically reviews across disciplines what is known about building AI-powered digital twins that predict how structure, print, and security features behave together under logistics loads. It is organized around four review questions (Figure 1). The first asks which logistics stressors damage the printed surface, and through which physical mechanisms. The second asks which twin architectures and AI methods can predict those effects, and how well they are validated. The third asks how security printing and authentication can be evaluated virtually, and the fourth asks what trade-offs with sustainability arise and what evidence is still missing.

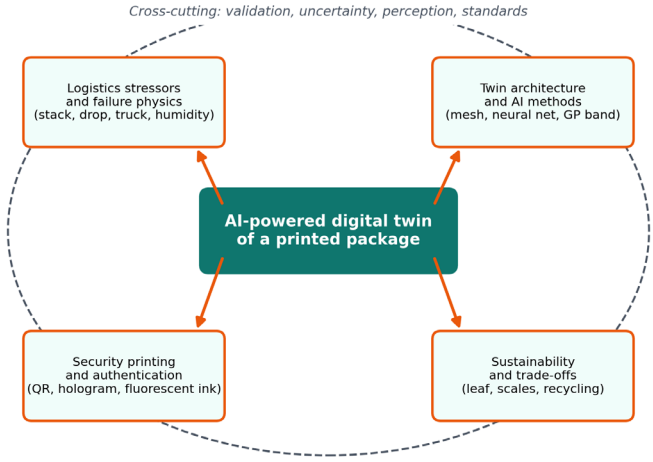
2. Methods

2.1. Scope and review design

This is a structured narrative review. Its scope is the prediction, before physical production, of how a printed package behaves in distribution. A narrative design was chosen over a systematic one because the question sits at the intersection of fields that do not share vocabulary, databases, or evaluation practices. Sources therefore span packaging science, printing and graphic technology, materials chemistry, solid mechanics, computer vision, scientific machine learning, and digital-twin engineering, since no single field covers the coupling. Peer-reviewed journals, conference proceedings, books, and international standards were considered. Items were retained when they (i) addressed structure, print, color, codes, security features, uncertainty, or validation relevant to a coupled prediction, (ii) described their methods transparently, and (iii) where applicable, validated predictions against physical experiments. Standards bodies were treated as primary sources for test conditions and measurement definitions (ASTM International, 2022; ISO, 2024).

2.2. Appraisal criteria

Each body of work was appraised qualitatively against four criteria drawn from verification and validation



» **Figure 1:** *Conceptual map – four questions around the AI-powered digital twin of a printed package*

practice (Jakeman et al., 2026): physical validation, quantification of uncertainty, evidence of generalization beyond the training conditions, and availability of data and documentation sufficient for others to reproduce the result. Physical validation asks whether predictions were compared with measurements of the real artifact. Uncertainty quantification asks whether the prediction carries an honest statement of confidence. Generalization asks whether performance was demonstrated outside the conditions used to build or train the model, and documentation asks whether another group could repeat the work. These four criteria structure the comparative reasoning in Section 3 and the research agenda in Section 4. Because the underlying literature is heterogeneous, no quantitative meta-analysis is attempted.

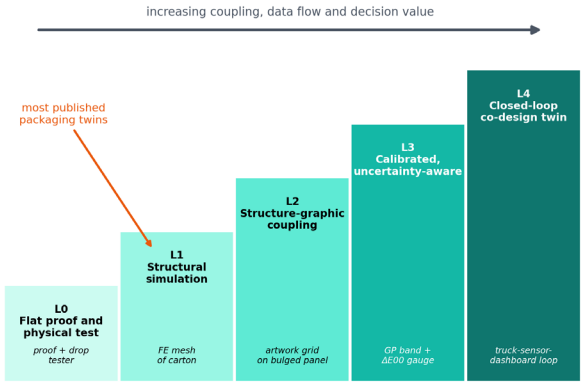
2.3. Coupling taxonomy and maturity ladder

The review uses a taxonomy in which a twin holds three coupled states: a structural state (geometry, material fields, deformation), a graphic state (artwork, ink film, color, code integrity, security features), and a logistics state (loads and climate). The structural state is driven by the logistics state; the graphic state is driven by the structural state and, independently, by the logistics state, for example, through abrasion and light. A twin that holds only the first two states is a conventional structural simulation. A twin that holds all three and propagates changes between them is what this article means by a coupled twin.

By analogy with the data-flow classification of Kritzinger et al. (2018), Table 1 proposes five maturity levels, from conventional practice to a closed-loop twin (Figure 2). The ladder lets readers locate any published system and see what is missing for the next level. Level L1 is where most published packaging twins sit: they predict compression or drop behavior well, but the printed layer is absent from the model.

2.4. Benchmark lens and metrics

To compare case studies on a common basis, a Brand-Integrity Index (BII) aggregates K normalized sub-scores (s_k) in [0, 1] with weights (w_k) set by the brand owner (Equation 1). Typical sub-scores are the color, where (ΔE_{00}) is the CIEDE2000 colour difference (Sharma, Wu & Dalal, 2005) and ΔE_tol is the brand owner's tolerance for that colour; image structure, measured



» **Figure 2:** *Maturity ladder for digital twins of printed packaging, from L0 (flat proof and physical test) to L4 (closed-loop co-design twin)*

Table 1

Proposed maturity ladder for digital twins of printed packaging

Level	Name	Characteristics	Typical evidence
L0	Flat proof and physical test	Artwork approved on a flat proof; structure tested on physical prototypes	ASTM International, 2022
L1	Structural simulation	Offline finite-element or analytical prediction of compression and drop; graphics ignored	Ge, 2022
L2	Structure–graphic coupling	Structural fields warp artwork; color and code change modeled analytically	ISO, 2024; Sharma, Wu & Dalal, 2005
L3	Calibrated, uncertainty-aware twin	AI surrogates, Bayesian calibration, perceptual metrics, and validation envelope	Kapteyn, Pretorius & Willcox, 2021
L4	Closed-loop co-design twin	Field data updates the model; multi-objective search with sustainability and security metrics	Liu et al., 2026

by the structural similarity index or a learned structure-and-texture distance (Wang et al., 2004; Ding et al., 2022); and code readability, graded under ISO (2024). Structural fidelity is expressed as the relative L2 error between predicted and measured fields (Equation 2).

$$\mathrm{BII} = 100 \sum_{k=1}^{K} w_k s_k , \qquad \sum_{k=1}^{K} w_k = 1 \tag{1}$$

$$\varepsilon_u = \frac{|\hat{u}-u|_2}{|u|_2} \tag{2}$$

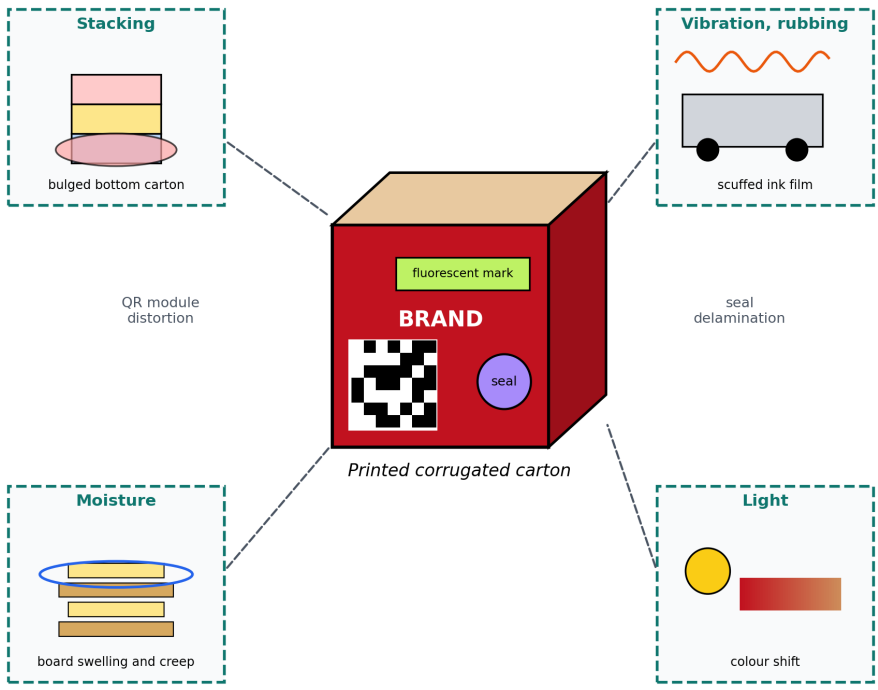
The weights are intentionally left to the brand owner. A luxury cosmetics carton and a bulk industrial shipper will not tolerate the same level of color drift, and a pharmaceutical pack will prioritize weight-code readability above all else. The index is therefore a bookkeeping device that makes assumptions explicit, not a universal quality score.

Six scenarios define what a twin must predict: S1 sustained stacking under humidity, S2 drop and impact, S3 vibration and abrasion, S4 light and climatic aging, S5 security-feature survival, and S6 the composite distribution cycle. Scenarios S1 to S3 are anchored in the shipping-test practice codified by ASTM International (2022); S4 and S5 are added because they act specifically on the printed layer; S6 combines all of them in the order a real shipment would experience. Comparison across methods should follow accepted validation practice (Kersken, Rojas & Strachan, 2025): fixed problems, simple baselines, declared validation envelopes, and reported uncertainty.

3. Results

3.1. Logistics stressors and failure physics of printed packaging

Distribution environments are codified in performance-testing standards that assemble handling shocks, vibration, and compression into representative cycles (ASTM International, 2022). Drops depend on height, orientation, and the fragility of contents, and they concentrate damage in crush zones, corners, and score lines; the shock-absorbing behavior of corrugated board has been studied through drop testing and impact loading (Ge, 2022). Transport vibration energy is typically concentrated at low frequencies, which matters for the printed layer because the same low-frequency motion that fatigues the structure also drives rubbing between adjacent cartons. Compression from stacking often governs corrugated shippers; strength is related to board edge crush, stiffness, and box geometry (Fitas, Schaffrath & Schabel, 2023), and later work has extended prediction to boxes with shifted creases on the flaps (Mrówczyński, Garbowski & Knitter-Piątkowska, 2021), to the optimal design of double-walled packaging (Mrówczyński, Knitter-Piątkowska & Garbowski, 2022), and to ventilated packaging and corrugated medium in the cold chain (Berry et al., 2022; Su et al., 2023). Homogenization of the flute-liner sandwich provides equivalent plate properties for finite-element analysis (Garbowski



» **Figure 3:** *Coupled failure pathways of a printed corrugated carton in distribution*

& Gajewski, 2021; Suarez et al., 2021), and analytical and numerical studies of panel stiffness continue to refine these properties (Suarez et al., 2021). Taken together, these sources show that the structural half of the problem is mature, quantitative, and well standardized.

The printed layer fails differently from the underlying structure (Figure 3). Four pathways dominate. First, panel bulging and score-line rotation distort images and two-dimensional codes. A QR symbology tolerates a degree of damage through built-in error correction, but not unlimited distortion, and print-quality grading penalizes loss of contrast, modulation, and decodability (ISO, 2024). Second, rub and scuff remove pigment and change gloss, so that a saturated solid loses its depth and a fine microtext line loses its edge. Third, color shifts occur through light-induced fading, binder yellowing, and changes in surface optics, all of which can be expressed as a perceptual color difference (Sharma, Wu & Dalal, 2005). Fourth, seals and tamper-evident features are loaded in peel and shear every time a carton is opened, restacked, or re-taped, and they can delaminate or lose their visual response.

Moisture couples all of these pathways. It changes the stiffness that carries the load: numerical homogenization shows that humidity and temperature changes in individual paper layers shift the effective stiffness of 3-ply and 5-ply corrugated board by up to roughly 40 percent (Cornaggia et al., 2023), and failure of the corrugated medium has been examined under simulated cold-chain logistics (Su et al., 2023). A stack that is stable in a dry laboratory can therefore bulge slowly in a humid warehouse; the bulge, in turn, strains the artwork. Moisture, temperature, and coating also change the mechanical properties of coated fiber-based substrates (Nienke, Kwade & Eggerath, 2022), which suggests that ink and coating adhesion, and hence the scuff resistance of the same print, will change as well. The failure of a printed carton is thus a chain, not a single event: climate weakens the structure, the structure deforms the graphics, and handling abrades what the deformation has already stressed. This chain is invisible to a flat proof and to a structural model that ignores the printed layer, and it is exactly what a coupled twin must reproduce.

3.2. Twin architecture and foundations

Digital-twin architectures commonly separate a physical layer, a data and sensing layer, a modeling layer, an intelligence layer, and a service or collaboration layer. This layering follows from the data-flow view of Kritzinger et al. (2018): a twin is distinguished from a mere model by the fact that information moves automatically in both directions between the physical object and its virtual counterpart. For printed packaging, the modeling layer must support structural, graphic, and logistics states, and the sensing layer must align heterogeneous data, such as load histories, spectrophotometric readings, high-resolution scans, and environmental logs, into a common frame. That alignment is more demanding than it sounds, because a bulge measured in millimeters on the board, a color difference measured in ΔE units on the ink, and a decoding grade measured on a letter scale are three different kinds of quantity.

Calibration is central. Bayesian calibration treats the discrepancy between the model and the measurement as an explicit term rather than hiding it within tuned parameters, and predictive twins have been formulated as probabilistic graphical models that update their state as new data arrive (Kapteyn, Pretorius & Willcox, 2021). Credibility also requires separating numerical error, input uncertainty, and model-form error, and stating the range of conditions over which the twin has been validated. In packaging, this means that a twin calibrated on one corrugated grade at moderate humidity must not be silently applied to a different grade at tropical humidity. The validation envelope is a first-class output of the twin, not a footnote.

Immersive augmented and virtual reality interfaces are useful in the collaboration layer, enabling distributed teams to inspect and annotate virtual packages (Nirmala, Raja & Kanchana, 2024), but they present predictions rather than create them. A visually convincing virtual carton is not evidence that the underlying prediction is right. For this reason, the review treats immersive interfaces as a service layer on top of a validated model, not as a substitute for it.

3.3. AI methods for prediction, inspection, rendering, and design search

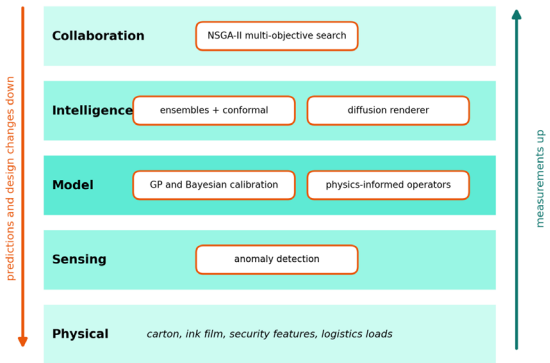
AI methods enter the twin at four points (Figure 4). First, surrogates accelerate expensive simulations. Physics-informed learning embeds governing equations and data together in one model (Würth et al., 2023), and neural operators learn mappings between function spaces, so that one trained network can return a full solution field for a new geometry or load while being orders of magnitude faster than conventional PDE solvers (Kovachki et al., 2023). For packaging, this means that a finite-element run that takes hours could be replaced by a surrogate model evaluated in milliseconds, which makes thousands of virtual design variants affordable. A known caution is that such networks can be difficult to train on stiff or multi-scale problems, and corrugated board, with its thin-layered walls, is exactly that kind of structure; surrogates should therefore be tested against held-out finite-element or experimental fields before being trusted.

Second, uncertainty methods make predictions trustworthy (Abdullah, Hassan & Mustafa, 2024),

and conformal prediction offers distribution-free coverage guarantees on top of any trained model (Zhou et al., 2025). Without such statements, a twin that predicts "ΔE = 2.1" gives a designer no way to know whether the true value could be 1 or 6.

Third, perception models inspect and render. Unsupervised anomaly detection learns what a good print looks like from defect-free examples and flags deviations without requiring a large library of labeled faults, which suits prepress and post-test inspection where defects are rare and varied; unsupervised approaches dominate industrial image anomaly detection because anomalous samples are costly to collect (Liu et al., 2024). Generative models, particularly latent diffusion models, can synthesize highly realistic images (Rombach et al., 2022). Conditioned on contact-pressure and strain fields, they are candidate renderers of scuffing, fading, and distortion, provided every output is labeled as a prediction and not mistaken for a photograph. Fourth, optimization methods search the design space. Bayesian optimization suits costly evaluations such as full finite-element runs (Garnett, 2023), and evolutionary multi-objective algorithms such as NSGA-II return a Pareto front of non-dominated designs, making the trade-offs among protection, graphic fidelity, security, and material use visible rather than collapsing them into a single score.

Taken together, these methods form a pipeline: surrogates predict fields quickly, uncertainty methods bound them, perception models turn them into what a viewer would see, and optimization uses all three to propose better designs. None of the individual components is new. What is new is placing them in a single loop around a printed package and validating the loop through physical distribution trials.



» **Figure 4:** *AI methods mapped onto the layers of the packaging digital twin*

3.4. Graphic fidelity and visual perception

The designer's question is whether a viewer would notice or care. Perceptually uniform color difference, specifically CIEDE2000 (Sharma, Wu & Dalal, 2005), and the structural similarity index (Wang et al., 2004) quantify color and structure, while learned measures that combine structure and texture similarity track human ratings better on textured content and tolerate texture resampling (Ding et al., 2022). Each metric answers a different question. CIEDE2000 tells the prepress operator whether a brand color has drifted outside tolerance; structural similarity tells whether edges, fine lines, and typography have been preserved; a learned perceptual distance tells whether a textured or photographic panel still looks the same to a person even when a pixel-wise error is large.

A spectral measurement alone does not capture what a consumer sees, because color appearance also depends on illuminant, surround, and observer. A red that matches under the proofing lamp can look different under warehouse lighting or on a retail shelf. Metrics must therefore be treated as proxies and checked against human judgment for the specific viewing condition that matters.

Because a viewer judges a package as a whole rather than as isolated pixels, tolerances should be weighted spatially and semantically: a tight tolerance on the primary brand color and logotype, a looser one on background texture. A global average error would let a small but conspicuous scuff across the logotype pass unnoticed because the rest of the panel is perfect. This is why the Brand-Integrity Index is built from separate sub-scores with brand-owner weights, rather than a single image-difference value. Evidence that links such thresholds to purchase behavior remains thin, and the index leaves weights and tolerances to the brand owner for exactly that reason.

3.5. Security printing and authentication

Security features range from overt devices, microtext, and tamper-evident seals to covert luminescent inks and intrinsic, unclonable randomness. Physical unclonable functions (PUFs) are the most prominent route to the latter: a PUF is a physical object whose random, fingerprint-like structure is hard to replicate, and deep learning models are now used to authenticate it. Sun et al. (2023) built random Au-network PUFs by a fractal-guided film annealing strategy and paired them with a dynamic deep-learning authentication system with an expandable database, reporting no false positives and smartphone readout. Digital layers offer additional possibilities, such as AR-triggered authentication via printed codes, as discussed in the authors' earlier review (Nirmala et al., 2024).

The shared gap is survival. The example above demonstrates feasibility and high verification accuracy under the conditions tested by its authors, but the literature

rarely quantifies how abrasion, moisture, and handling over a distribution cycle degrade signal retention or verification accuracy. A security feature that reads perfectly on a fresh sample but fails after a pallet journey has no commercial value, and a verification model trained only on pristine labels may reject genuine, scuffed packs. A coupled twin can evaluate this through scenario S5, by degrading the security layer with the same strain, abrasion, and moisture fields that act on the visible print and passing the degraded signal through the verification model. This also exposes a design trade-off: stronger, more complex security features may be harder to print robustly, and the twin is the place where security strength and robustness can be balanced.

3.6. Sustainability and trade-offs

Life-cycle assessment frames the trade-off, and recent reviews stress that the indirect benefit of packaging, the food loss it prevents, must be counted beside its direct burden (Espinoza-Orias & Lundquist, 2025; Hemachandra, Hadjikakou & Pettigrew, 2024). A heavier pack that prevents damage may therefore be environmentally preferable to a lighter pack that fails, whereas excess coating or laminate adds burden and can impair recycling. The answer is not “use less material” but “use the right material for the real hazard”, and the real hazard is exactly what a validated twin predicts. Barrier coatings are central to this discussion: coatings have been evaluated for improving the durability and water-barrier properties of corrugated cardboard (Marinelli et al., 2022). They protect against moisture and so preserve both structure and print, but they can alter surface energy, adhesion, and gloss, and may compromise recyclability. The twin must therefore carry the printed-surface consequences of a coating choice, not only its barrier benefit.

A twin that carries life-cycle indicators beside structural and graphic metrics lets teams see these trade-offs on a Pareto front before committing to production. A designer can see, for instance, that reducing board grade saves material but moves the stacking-bulge distortion of the brand panel beyond tolerance, or that a protective varnish lowers scuff damage while adding a recycling penalty. The twin also removes much of the board, ink, and energy that would otherwise be spent on physical samples. The missing evidence here is quantitative: few studies assign a measured environmental cost to graphic-quality loss, so the exchange rate between a unit of color error and a unit of material burden remains unknown.

3.7. Case studies

Three published bodies of work are analyzed through the maturity ladder and the benchmark scenarios. They are literature-based; no proprietary data were used, and details are given only to the level reported in the sources.

Case study 1: homogenization-based structural modeling of corrugated board under climatic loads. Cornaggia et al. (2023) used numerical homogenization and global sensitivity analysis to map how changes in humidity and temperature within individual paper layers alter the bending, compression, and shear stiffness of 3-ply and 5-ply corrugated board, and reported stiffness changes of up to approximately 40 percent in realistic scenarios. The work builds on homogenization approaches (Garbowski & Gajewski, 2021) and on classical strength theory (Fitas, Schaffrath & Schabel, 2023). This is a representative L1 twin: it addresses a real hazard, humidity, with a quantitative structural model. The printed surface, however, is outside the model, and the relations between climate and material constants are taken from the literature rather than calibrated against new physical tests reported in the study. Under the benchmark, the study would address structural-field error in S1 but provides no evidence for color, code, or security outcomes. Lesson: Structural modeling of climatic effects is a necessary foundation, and the missing step is the strain-to-graphic mapping, which is conceptually small but unvalidated.

Case study 2: AI-authenticated physical unclonable security features. Sun et al. (2023) realized random Au-network PUFs through a fractal-guided film annealing strategy and authenticated them with a dynamic deep-learning system that can expand its database, reporting no false positives and smartphone-based readout. The work shows that a security feature can be verified by a computational model with high accuracy. Under the benchmark, it establishes feasibility and verification accuracy under laboratory conditions (an L2–L3 characteristic for the verification model), but the scenario most relevant to packaging, S5, requires evidence on retention after abrasion, moisture, and handling over a distribution cycle, which the study, framed around tag stability and authentication accuracy, does not address as a packaging scenario. Lesson: the verification model should be inside the twin, so that the trade-off between security strength and robustness can be quantified.

Case study 3: predictive digital twins with calibration and decision-making. Kapteyn, Pretorius and Willcox (2021) formulated predictive digital twins as probabilistic graphical models that assimilate sensor data, update the twin’s state, and support decisions, and demonstrated the approach on an unmanned aerial vehicle. It sits within the digital-twin concept being reviewed across many disciplines (Thelen et al., 2022) and exemplifies L3–L4 behavior: calibrated, uncertainty-aware, and data-driven. Packaging has no comparable exemplar, so the study is a design template rather than a packaging result. The transferable ideas are explicit uncertainty, scalable updating from field data, and decision rules tied to risk. Lesson: a packaging twin should report a validation envelope and propagate uncertainty to graphic consequences, not only to structural ones.

Read side by side, the three cases mark out the territory. The first covers structure but ignores graphics, the second covers security verification but ignores distribution, and the third covers calibration and decisions but ignores packaging. No case covers more than one of the dimensions that a coupled twin needs, and none reaches L3 or L4 for a printed package. The three studies are complementary, which is encouraging: each supplies a component that the others lack. They are also the reason the maturity ladder is useful: it makes the missing step in each case visible at a glance.

4. Discussion

Cross-cutting findings. Four patterns emerge from the synthesis. First, the field is structurally mature but graphically thin: mature structural and homogenization models exist (Cornaggia et al., 2023), yet almost nothing links strain, abrasion, and moisture fields to color, code, and security outcomes. Second, the AI methods needed for the missing link already exist, from physics-informed and operator-learning surrogates to uncertainty-aware prediction and diffusion-based rendering (Liu et al., 2024; Rombach et al., 2022; Zhou et al., 2025), but they have not been benchmarked on packaging problems. Third, security features are evaluated at the laboratory level rather than through a distribution cycle (Sun et al., 2023). Fourth, sustainability is rarely coupled with the performance model, even though packaging burdens and avoided losses offset each other (Hemachandra, Hadjikakou & Pettigrew, 2024).

Why benchmarking matters. Adjacent fields progressed quickly once shared yardsticks existed: industrial anomaly detection is now organized around shared datasets, metrics, and settings (Mao et al., 2025), and scientific machine learning followed with shared benchmark suites for PDE problems (Takamoto et al., 2022). The scenarios, maturity ladder, and Brand-Integrity Index proposed here are a starting point for the same step in packaging. Credibility depends on declared validation envelopes (Kapteyn, Pretorius & Willcox, 2021) and on open, documented data (Gebru et al., 2021), without which two groups cannot tell whether they disagree about the physics or only about the test conditions.

Research agenda. Five priorities follow from the gaps, ranked by how much they unblock the others. The first is open data: there are no public datasets linking logistics histories to graphic outcomes, and a round-robin study across laboratories on a small set of reference artifacts, released with documentation, would give every later method a common test. The second is validated strain-to-graphic mapping: bulge, color, and code grade should be measured together in scenarios S1 and S6 and compared with predictions through the relative (L_2) error, (ΔE _{00}) , and the ISO (2024). The third is security survival: abrasion, moisture, and handling tests with verification models in the loop should quantify signal retention and verification accuracy. The fourth is calibrated generative rendering: diffusion renderers should be compared with real scans, with outputs labeled by confidence, and interval coverage checked. The fifth is to embed life-cycle indicators in the Pareto search, so that graphic quality, protection, security, and environmental burden are optimized together. These priorities emphasize open data, validated coupling, security survival, and calibrated rendering because they decide whether L3–L4 twins can be trusted in industry.

Implications for practice. Converters and brand owners can adopt twins incrementally: digitize material and test data (L0 to L1), couple structure to artwork (L2), introduce calibration and uncertainty (L3), and finally close the loop with field data (L4). Each step delivers value on its own. Even an L2 twin can warn that a particular panel layout puts the QR code over a high-strain zone, and that single warning can save a reprint. Immersive interfaces help teams collaborate but do not replace predictive validity (Nirmala et al., 2024). The organizational implication is equally important: the twin gives graphic designers, prepress operators, packaging engineers, and logistics specialists a shared object to argue over, thereby moving graphic and structural decisions from a sequence of handoffs to a single conversation.

Limitations of this review. The review is narrative, not a meta-analysis, and so each cited work represents a wider family of studies. The literature on coupled packaging twins is sparse, so two of the three case studies are adjacent-domain exemplars rather than packaging twins. Maturity levels and qualitative appraisals are the authors' judgment and should be tested by independent assessors.

5. Conclusions

AI-powered digital twins can turn graphic packaging design from a sequence of hand-offs into an integrated predictive loop in which structure, print, security, and sustainability are evaluated together before production. This review has shown that the necessary foundations already exist: structural models of corrugated packages, homogenized board properties, drop and vibration characterization, Bayesian calibration, physics-informed and operator-learning surrogates, uncertainty quantification, machine-vision inspection, generative rendering, and multi-objective optimization. Security printing has advanced through covert luminescent inks, unclonable physical features, and computational verification. What remains missing is coupling. Few studies connect strain, moisture, and abrasion fields to color shift, code readability, brand-color fidelity, and tamper-evident signal retention across a full distribution cycle. Consequently, the

field remains structurally mature but graphically thin, and security evaluation remains largely laboratory-bound.

The maturity ladder proposed here locates existing work from L0 flat proofing to L4 closed-loop co-design, while the Brand-Integrity Index and six benchmark scenarios provide a shared basis for comparison. Together, they expose the evidence needed for industrial trust: open datasets linking logistics histories to graphic outcomes, validated strain-to-graphic mapping, security-survival testing with verification models in the loop, calibrated generative rendering, and sustainability indicators embedded in Pareto search. The three case studies illustrate both the promise and the gap: structural simulation, AI-authenticated security features, and predictive twins with calibration exist separately, but no packaging exemplar yet couples them.

For practice, the implication is incremental adoption. Converters and brand owners can digitize material and test data, couple structure to artwork, introduce uncertainty-aware calibration, and close the loop with field data. Immersive interfaces can support collaboration, but predictive validity remains the decisive requirement. If the research agenda is pursued openly, the invisible prototype can become a practical decision-support environment in which designers explore bold visual and material solutions while knowing in advance how they will survive stacking, drop, vibration, humidity, and light. The result would be packaging that is more resilient, more secure, less wasteful, and more visually effective, benefiting brands, consumers, and the supply chain. Future work should therefore prioritize transparent benchmarks, independent validation, and cross-disciplinary collaboration between graphic design, prepress, packaging engineering, AI, security printing, and logistics.

6. References

Abdullah, A.A., Hassan, M.M. and Mustafa, Y.T. (2024) 'Leveraging Bayesian deep learning and ensemble methods for uncertainty quantification in image classification: A ranking-based approach', *Heliyon*, 10(2). DOI: 10.1016/j.heliyon.2024.e24188

ASTM International (2022) *ASTM D4169-22: Standard Practice for Performance Testing of Shipping Containers and Systems*. West Conshohocken, PA: ASTM International. DOI: 10.1520/D4169-22

Berry, T.M., Defraeye, T., Shrivastava, C., Ambaw, A., Coetzee, C. and Opara, U.L. (2022) 'Designing ventilated packaging for the fresh produce cold chain', *Food and Bioproducts Processing*, 134, pp. 121–149. DOI: 10.1016/j.fbp.2022.04.005

Cornaggia, A., Gajewski, T., Knitter-Piątkowska, A. and Garbowski, T. (2023) 'Influence of humidity and temperature on mechanical properties of corrugated board – numerical investigation', *BioResources*, 18(4), pp. 7490–7509. DOI: 10.15376/BIORES.18.4.7490-7509

Ding, K., Ma, K., Wang, S. and Simoncelli, E.P. (2022) 'Image quality assessment: Unifying structure and texture similarity', *IEEE Transactions on Pattern Analysis and Machine Intelligence*, 44(5), pp. 2567–2581. DOI: 10.1109/TPAMI.2020.3045810

Espinoza-Orias, N. and Lundquist, L. (2025) 'Life cycle assessment of reusable food and beverage packaging systems: A proposal of good practice', *Journal of Cleaner Production*, 499, 145207. DOI: 10.1016/j.jclepro.2025.145207

Fernandez, C.M., Alves, J., Gaspar, P.D. and Lima, T.M. (2021) 'Fostering awareness on environmentally sustainable technological solutions for the post-harvest food supply chain', *Processes*, 9(9), 1611. DOI: 10.3390/PR9091611

Fitas, R., Schaffrath, H.J. and Schabel, S. (2023) 'A review of optimization for corrugated boards', *Sustainability*, 15(21), 15588. DOI: 10.3390/SU152115588

Garbowski, T. and Gajewski, T. (2021) 'Determination of transverse shear stiffness of sandwich panels with a corrugated core by numerical homogenization', *Materials*, 14(8), 1976. DOI: 10.3390/MA14081976

Garnett, R. (2023) *Bayesian Optimization*. Cambridge: Cambridge University Press. DOI: 10.1017/9781108348973

Ge, C. (2022) 'A review and update of the corrugated fibreboard cushioning', *Packaging Technology and Science*, 35(9), pp. 701–715. DOI: 10.1002/PTS.2657

Gebru, T., Morgenstern, J., Vecchione, B., Vaughan, J.W., Wallach, H., Daumé III, H. and Crawford, K. (2021) 'Datasheets for datasets', *Communications of the ACM*, 64(12), pp. 86–92. DOI: 10.1145/3458723

Hemachandra, S., Hadjikakou, M. and Pettigrew, S. (2024) 'A scoping review of food packaging life cycle assessments that account for packaging-related food waste', *The International Journal of Life Cycle Assessment*, 29(10), pp. 1899–1915. DOI: 10.1007/S11367-024-02349-Z

ISO (2024) *ISO/IEC 15415:2024: Automatic identification and data capture techniques — Bar code symbol print quality test specification — Two-dimensional symbols*. Geneva: International Organization for Standardization. Available from: https://www.iso.org/standard/76876.html [Accessed 11 October 2026].

Jakeman, J.D., Barba, L.A., Martins, J.R.R.A. and O'Leary-Roseberry, T. (2026) 'Verification and validation for trustworthy scientific machine learning', *Machine Learning: Science and Technology*, 7(2), 025055. DOI: 10.1088/2632-2153/AE59EC

Kapteyn, M.G., Pretorius, J.V.R. and Willcox, K.E. (2021) 'A probabilistic graphical model foundation for enabling predictive digital twins at scale', *Nature Computational Science*, 1(5), pp. 337–347. DOI: 10.1038/s43588-021-00069-0

Kersken, M., Rojas, G. and Strachan, P. (2025) 'Uncertainty of the predictions of different programs and modelling teams based on a detailed empirical validation dataset', *Journal of Building Performance Simulation*, 18(5–6), pp. 631–647. DOI: 10.1080/19401493.2024.2343883

Kovachki, N., Li, Z., Liu, B., Azizzadenesheli, K., Bhattacharya, K., Stuart, A. and Anandkumar, A. (2023) 'Neural operator: Learning maps between function spaces with applications to PDEs', *Journal of Machine Learning Research*, 24(89), pp. 1–97.

Kritzinger, W., Karner, M., Traar, G., Henjes, J. and Sihn, W. (2018) 'Digital Twin in manufacturing: A categorical literature review and classification', *IFAC-PapersOnLine*, 51(11), pp. 1016–1022. DOI: 10.1016/J.IFACOL.2018.08.474

Liu, J., Xie, G., Wang, J., Li, S., Wang, C., Zheng, F., Jin, Y. et al. (2024) 'Deep industrial image anomaly detection: A survey', *Machine Intelligence Research*, 21(1), pp. 104–135. DOI: 10.1007/S11633-023-1459-Z

Liu, X., Wang, H., Han, X., Zan, Y., Zhang, J. and Liu, G. (2026) 'A closed-loop design approach based on the combination of knowledge graph and digital twin: a high-speed train bogie case study', *Advanced Engineering Informatics*, 69. DOI: 10.1016/j.aei.2025.103912

Mann, G.S., Singh, B., Alzahrani, K.A., Khan, A., Kumar, R., Patil, A.Y. and Keshta, B.E. (2026) 'AI-powered innovations in natural fiber packaging for sustainability', *Journal of Natural Fibers*, 23(1). DOI: 10.1080/15440478.2026.2640280

Mao, Y., Chen, Z., Liu, Y., Dong, C. and Song, K. (2025) 'A survey on industrial image anomaly detection: methods, benchmarks and rethinks', *Measurement*, 256, 118377. DOI: 10.1016/J.MEASUREMENT.2025.118377

Marinelli, A., Diamanti, M.V., Lucotti, A., Pedeferri, M.P. and Del Curto, B. (2022) 'Evaluation of coatings to improve the durability and water-barrier properties of corrugated cardboard', *Coatings*, 12(1), 10. DOI: 10.3390/COATINGS12010010

Molina-Besch, K., Wikström, F. and Williams, H. (2019) 'The environmental impact of packaging in food supply chains—does life cycle assessment of food provide the full picture?', *The International Journal of Life Cycle Assessment*, 24(1), pp. 37–50. DOI: 10.1007/s11367-018-1500-6

Mrówczyński, D., Garbowski, T. and Knitter-Piątkowska, A. (2021) 'Estimation of the compressive strength of corrugated board boxes with shifted creases on the flaps', *Materials*, 14(18), 5181. DOI: 10.3390/MA14185181

Mrówczyński, D., Knitter-Piątkowska, A. and Garbowski, T. (2022) 'Optimal design of double-walled corrugated board packaging', *Materials*, 15(6), 2149. DOI: 10.3390/MA15062149

Nienke, T., Kwade, A. and Eggerath, D. (2022) 'Influence of moisture, temperature and bleaching on the mechanical properties of coated fiber-based substrates', *Coatings*, 12(9), 1287. DOI: 10.3390/COATINGS12091287

Nirmala, J.P., Raja, R.R. and Kanchana, M. (2024) 'Transforming graphic design – the impact of augmented and virtual reality on user interaction, security and product packaging optimization'. In: *Proceedings of the International Symposium on Graphic Engineering and Design (GRID 2024)*. Novi Sad: University of Novi Sad, Faculty of Technical Sciences, Department of Graphic Engineering and Design. DOI: 10.24867/GRID-2024-P19

Rombach, R., Blattmann, A., Lorenz, D., Esser, P. and Ommer, B. (2022) 'High-resolution image synthesis with latent diffusion models'. In: *Proceedings of the IEEE/CVF Conference on Computer Vision and Pattern Recognition (CVPR)*, pp. 10674–10685. DOI: 10.1109/CVPR52688.2022.01042

Sharma, G., Wu, W. and Dalal, E.N. (2005) 'The CIEDE2000 color-difference formula: Implementation notes, supplementary test data, and mathematical observations', *Color Research and Application*, 30(1), pp. 21–30. DOI: 10.1002/COL.20070

Su, H., Huang, C., Li, C., Zhao, Y., Zheng, D. and Duan, Q. (2023) 'Failure mechanism of the corrugated medium under simulated cold chain logistics', *ACS Omega*, 8(26), pp. 23673–23682. DOI: 10.1021/ACSOMEGA.3C01668

Suarez, B., Muneta, M.L.M., Sanz-Bobi, J.D. and Romero, G. (2021) 'Application of homogenization approaches to the numerical analysis of seating made of multiwall corrugated cardboard', *Composite Structures*, 262, 113642. DOI: 10.1016/j.compstruct.2021.113642

Sun, N., Chen, Z., Wang, Y., Wang, S., Xie, Y. and Liu, Q. (2023) 'Random fractal-enabled physical unclonable functions with dynamic AI authentication', *Nature Communications*, 14(1), 2185. DOI: 10.1038/s41467-023-37588-5

Takamoto, M., Praditia, T., Leiteritz, R., MacKinlay, D., Alesiani, F., Pflüger, D. and Niepert, M. (2022) 'PDEBench: An extensive benchmark for scientific machine learning', *Advances in Neural Information Processing Systems*, 35, pp. 1596–1611. DOI: 10.52202/068431-0117

Thelen, A., Zhang, X., Fink, O., Lu, Y., Ghosh, S., Youn, B.D., Todd, M.D., Mahadevan, S., Hu, C. and Hu, Z. (2022) 'A comprehensive review of digital twin — part 1: modeling and twinning enabling technologies', *Structural and Multidisciplinary Optimization*, 65(12), 354. DOI: 10.1007/S00158-022-03425-4

Wang, Z., Bovik, A.C., Sheikh, H.R. and Simoncelli, E.P. (2004) 'Image quality assessment: From error visibility to structural similarity', *IEEE Transactions on Image Processing*, 13(4), pp. 600–612. DOI: 10.1109/TIP.2003.819861

Williams, H. and Wikström, F. (2011) 'Environmental impact of packaging and food losses in a life cycle perspective: A comparative analysis of five food items', *Journal of Cleaner Production*, 19(1), pp. 43–48. DOI: 10.1016/j.jclepro.2010.08.008

Würth, T., Krauß, C., Zimmerling, C. and Kärger, L. (2023) 'Physics-informed neural networks for data-free surrogate modelling and engineering optimization – An example from composite manufacturing', *Materials and Design*, 231, 112034. DOI: 10.1016/j.matdes.2023.112034

Yu, W., Liu, G., Zhu, L. and Yu, W. (2025) 'Digital Twin: A literature review of concepts, technologies, and applications', *IEEE Access*, 13, pp. 183075–183095. DOI: 10.1109/ACCESS.2025.3624583

Zhang, L., Zhang, J., Cui, M., Qi, W., Huang, R., Su, R. and Zhang, K. (2026) 'Multifunctional bio-based packaging for perishable foods: Structural design, scalable fabrication, and versatile applications', *Advanced Materials*, 38(33). DOI: 10.1002/ADMA.202521880

Zhou, X., Chen, B., Gui, Y. and Cheng, L. (2025) 'Conformal prediction: A data perspective', *ACM Computing Surveys*, 58(2). DOI: 10.1145/3736575



© 2026 Authors. Published by the University of Novi Sad, Faculty of Technical Sciences, Department of Graphic Engineering and Design. This article is an open access article distributed under the terms and conditions of the Creative Commons Attribution license 4.0 Serbia (https://creativecommons.org/licenses/by/4.0/deed.en).

Original Scientific Paper https://doi.org/10.24867/GRID-2026-p38

Redesigning Hair Care Packaging for Generation Z Through a Student-Led Case Study of a Slovenian Cosmetic Brand

ABSTRACT

The cosmetic packaging market is increasingly influenced by Generation Z, whose purchasing decisions are shaped by visual identity, functionality, environmental responsibility, and brand authenticity. This study investigates the redesign of packaging for hair-care products produced by a Slovenian cosmetic brand, with a particular focus on the preferences and expectations of Generation Z consumers. The research combined an analysis of the Slovenian hair-care packaging market with a student-led design process. Existing products were evaluated according to packaging format, materials, visual communication, functionality, sustainability claims, and differentiation at the point of sale. Based on the market analysis and the defined characteristics of the target group, students developed alternative packaging concepts for selected hair-care products. The proposed solutions were subsequently analysed and compared in terms of visual identity, usability, material selection, environmental considerations, and suitability for the existing brand. The results showed that the student concepts introduced greater visual differentiation and stronger alignment with Generation Z preferences than many existing products identified on the Slovenian market. Recurring design directions included contemporary and simplified graphics, clearer product information, more distinctive colour systems, improved ease of use, and greater emphasis on recyclable, reusable, or refillable packaging solutions. The analysis also revealed that sustainability communication must be clear, credible, and integrated into the overall packaging design rather than presented only as an additional marketing claim. The study demonstrates the value of involving students as representatives of the target generation in packaging development. Their concepts provide relevant insights for cosmetic brands seeking to modernise their packaging, strengthen consumer engagement, and respond to changing environmental and communication expectations.

Gregor Franken
Urška Klenovšek
Urška Vrabič-Brodnjak

University of Ljubljana,
Faculty of Natural Sciences and Engineering,
Department of Textiles, Graphic Arts and Design,
Ljubljana, Slovenia

KEY WORDS
Generation Z, cosmetic packaging, hair care, packaging redesign, sustainability, student-led design, visual communication

1. Introduction

Packaging is one of the most immediate interfaces between a cosmetic brand and the consumer. In crowded retail and digital environments, it must attract attention, communicate product purpose, distinguish variants within a product family, and support the practical use and disposal of the product. Visual features such as colour, shape and contrast can influence early-stage visual attention during product search (Clement, Kristensen & Grønhaug, 2013), while packaging colours and textual claims can also shape young consumers' perceptions of

sustainability and product qualities (Hallez et al., 2023). In cosmetics, these functions are particularly important because the package frequently carries symbolic meanings associated with identity, lifestyle, quality and trust. Generation Z is an especially relevant audience for contemporary cosmetic brands. This group has grown up with visually intensive digital communication, rapid trend cycles and continuous comparison between products and brands. At the same time, environmental concern, eco-labelling, social media content and perceived authenticity can influence green purchase intentions among Generation Z consumers (Panopoulos et al., 2023). Research on green cosmetics similarly indicates that product knowledge, attitudes and social influences are associated with purchase intention among younger consumers (Limbu, Pham & Nguyen, 2022). Consequently, packaging for this audience cannot rely only on aesthetic novelty; it must also provide understandable information and credible sustainability cues. The beauty-care sector is under increasing pressure to reduce packaging impacts while maintaining the visual and tactile characteristics that support brand recognition and premium perception. A recent systematic review of eco-friendly beauty packaging emphasizes that consumer perceptions, expectations and barriers must be considered alongside technical sustainability improvements (Del Greco et al., 2024; Vrabič-Brodnjak & Jestratijević, 2024). Likewise, research on cosmetic packaging attractiveness shows that visual and tactile elements, materials and reusability can contribute to the perceived value of cosmetic packaging among younger consumers (Wang et al., 2024). These findings support a design approach in which sustainability, usability and visual identity are treated as interconnected rather than separate objectives.

This paper presents a practice-based case study in which university students developed redesign proposals for an existing line of hair-care products produced by a Slovenian cosmetic company. The aim was to examine how a student-led design process can reveal design directions that are relevant to Generation Z while remaining compatible with an established product family. The study focused on three questions: (1) which characteristics of existing hair-care packaging limit differentiation and communication at the point of sale; (2) which visual and structural directions recur across student redesign proposals; and (3) how can sustainability be integrated into packaging communication without becoming a detached marketing claim.

2. Materials and methods

2.1. Case-study framework

The study used a qualitative case-study approach combining market observation, design development and comparative analysis. The case concerned a hair-care line from a Slovenian cosmetic manufacturer. The educational design brief asked students to reconsider the visual communication and packaging system of products such as shampoo, conditioner, hair oil and hair-care cream while preserving sufficient continuity for recognition as a coherent product family. The work was developed as a student project under academic mentorship and was used as the empirical material for the present analysis.

Three completed student design directions were selected because they represented clearly different visual strategies and included sufficiently developed applications across several products. The first concept used a saturated pink colour field and bold contemporary typography; the second used a restrained light background with colour-coded organic graphic forms; and the third applied a high-contrast brown-and-white system with expressive illustration and large typographic elements. The attached project documentation includes ideation, label development, dielines and rendered product applications.

2.2. Market analysis and design criteria

Before redesign, students reviewed hair-care packaging available on the Slovenian market. The observation was qualitative rather than a statistically representative audit. Products were compared according to packaging format, dominant materials, colour and typography, hierarchy of product information, differentiation between variants, perceived ease of use, sustainability-related cues and expected shelf visibility.

The market material indicated a broad use of plastic bottles, tubes and smaller bottles, together with highly variable colour systems and information density. This visual diversity provided the reference context for identifying opportunities for stronger brand coherence and more immediate product differentiation.



» **Figure 1:** *Example of the student market-analysis material used to benchmark hair-care packaging formats and visual approaches in the Slovenian market*

2.3. Student-led redesign process

The redesign process followed an iterative sequence: market observation, definition of the communication problem, target-group interpretation, inspiration and mood-board development, initial sketches, label layout, refinement of the graphic system, and application to a family of products. Students (9 students) considered front-panel hierarchy, product naming, colour, typography, graphic motifs, label coverage, secondary packaging and the relationship between product variants. The process was not constrained to one predefined visual style, which allowed different interpretations of a Generation Z-oriented hair-care brand to emerge.

The target-group perspective was embedded through the direct involvement of students as designers who are close in age and media habits to the intended consumer group. This does not replace formal consumer research, but it provides a form of participatory insight: students simultaneously interpreted the market as users, design students and potential purchasers. In the project materials, target-group definitions varied slightly between teams; this variation was retained rather than retrospectively standardized.

2.4. Comparative evaluation

The final concepts were compared using five categories derived from the design brief and the literature: visual identity, product differentiation, information clarity, functional suitability, and sustainability communication. Evaluation was interpretive and based on the submitted design documentation rather than on consumer preference scores. The analysis therefore identifies design tendencies and strengths, not statistically significant differences between concepts.

3. Results and discussion

3.1. Market-level observations

The market review suggested that hair-care packaging competes in a visually saturated environment in which colour, claims, imagery and product-specific terminology frequently overlap. Many products rely on familiar bottle and tube formats, meaning that differentiation is largely achieved through surface graphics and label systems. This is consistent with the importance of contrast and other physical design cues in guiding early visual attention (Clement, Kristensen & Grønhaug, 2013). For an established brand, redesign therefore needs to balance recognizability with sufficiently distinctive cues to interrupt routine shelf scanning.

A second observation concerned information density. Hair-care products typically communicate function, hair type, ingredients, marketing claims, use instructions and regulatory information within a limited surface area. The student work repeatedly responded by simplifying the front panel and strengthening the hierarchy between product family, product type and benefit. This direction is relevant to younger consumers who often encounter the same packaging both in-store and as small digital images, where legibility and rapid recognition are particularly important.

3.2. Student redesign concepts

Figure 2 presents the three principal redesign directions. Concept A developed a playful pink identity centered on large, condensed product lettering and a youthful visual tone. The strong colour field creates immediate family recognition, while the enlarged 'coconut' wording functions as the dominant recognition element. The proposal is visually assertive and likely to perform well in digital communication, although extensive use of a single saturated colour may require careful coding of individual product variants.

Concept B adopted a more restrained, premium-oriented approach. A white base and relatively fine typography were combined with large organic motifs that change colour between product types. This concept directly addressed the problem of weak differentiation within visually similar hair-care families: the graphic language remains consistent, while colour acts as a clear variant code. The submitted work explicitly identified difficulty distinguishing shampoo, conditioner and related coconut-based products as a problem and proposed a common graphic element combined with different colours as the solution.

Concept C used the strongest contrast of the three concepts. Brown and white areas, oversized typography and stylized facial elements produce a recognizable editorial aesthetic. The student documentation described the objective as modernization, stronger consumer connection, shelf stand-out and a natural, minimalist, professional appearance. The concept also retained the existing plastic packaging format and specified matte, soft-touch labels, demonstrating a pragmatic approach in which the visual redesign could be implemented without immediately changing all primary packaging components.



» **Figure 2:** *Student-generated redesign directions: (a) Concept A: bold pink typographic concept; (b) Concept B: light, colour-coded organic-form concept; and (c) Concept C: high-contrast illustrated concept*

3.3. Cross-concept comparison

Despite their visual differences, the three concepts converged on several principles. First, each concept reduced reliance on complex decorative information and instead established a stronger dominant visual cue. Second, all three created clearer relationships between the individual product and the product family. Third, the proposals treated colour as a strategic communication tool: as an overall brand field, as a product-variant code, or as a high-contrast identity system. This finding aligns with experimental evidence that packaging colour and claims can shape perceptions among young consumers (Hallez et al., 2023).

The concepts also demonstrate that Generation Z-oriented design does not correspond to a single aesthetic. One solution is bright and playful, another restrained and premium, and another bold and illustrative. What they share is not a specific style but stronger intentionality: clearer hierarchy, more immediately recognizable systems and a visual language designed for both physical and digital exposure. This is important for brands seeking to modernise without simply imitating short-lived trends.

Table 1

Qualitative comparison of the three redesign concepts based on the project documentation and the evaluation criteria used in the case study

Criterion	Concept A	Concept B	Concept C
Visual identity	Bold pink typography	Minimal white base; colour-coded organic forms	High contrast brown/white illustration face motif
Product differentiation	Strong colour unity; product name hierarchy	Distinct colour coding by product type	Distinctive form/graphics; strong shelf contrast
Information clarity	Simplified front panel	Clear hierarchy; more restrained layout	Large product naming; compact information zones
Brand fit	Youthful, playful	Premium, contemporary	Editorial, expressive
Sustainability direction	Potential for simplified labels and material communication	Supports clear separation of material and product information	Retains existing plastic format; matte/soft-touch label noted

3.4. Sustainability and credibility of communication

Sustainability emerged as both a material and a communication issue. The student proposals and the subsequent comparison considered recyclable, reusable and refillable directions, but the case also shows the limitations of treating sustainability as a decorative claim. A visual signal such as a green colour, a natural illustration or a short environmental statement can shape perception, yet it does not by itself demonstrate lower environmental impact. The systematic review by Del Greco et al. (2024) similarly highlights the need to understand consumer expectations and barriers when developing eco-friendly beauty packaging.

For future development, sustainability information should be linked to verifiable packaging attributes, for example the type and share of recyclable material, mono-material construction where technically possible, refill availability, instructions for separation, or quantified packaging reduction. Clear eco-labelling can influence Generation Z green purchase intention (Panopoulos et al., 2023), but credibility depends on the relationship between the claim and the actual packaging system. The implication for the case brand is that visual redesign and packaging engineering should proceed in parallel.

3.5. Value of student-led co-creation

The student-led process generated a broader range of ideas than would be expected from a narrowly prescribed redesign exercise. Students challenged the existing visual hierarchy, proposed new colour systems, experimented with premium and playful positioning, and considered how the product family would appear across bottles, tubes and cartons. Their proximity to the target generation was particularly useful for identifying visual conventions that feel contemporary in social and digital contexts.

However, student participation should be viewed as an exploratory co-creation method rather than as direct evidence of market acceptance. The strongest application of this approach is as an early-stage innovation tool: student concepts can expand the design space and help a company formulate hypotheses that can subsequently be tested with consumers, production specialists and sustainability experts. In this sense, the project creates a bridge between design education and industrial packaging development.

4. Limitations

The study is qualitative and based on one brand case. The market review was exploratory and did not use a fixed, statistically representative sample of all hair-care products sold in Slovenia. Consumer testing, eye-tracking, shelf simulation and willingness-to-pay measurements were not performed. In addition, the student teams interpreted the target audience with some flexibility, and not every proposal developed material and end-of-life aspects to the same level of technical detail. The findings should therefore be interpreted as design insights and hypotheses for further validation rather than as population-level evidence about Generation Z preferences.

Future research should test selected redesigns with Generation Z consumers using structured preference studies, visual-attention methods and usability tasks. Environmental evaluation should also compare alternative packaging scenarios through measurable indicators such as packaging mass, recycled content, recyclability, refill performance and, where appropriate, life-cycle assessment. Such validation would allow the visual, functional and environmental dimensions identified in this case study to be converted into evidence-based design requirements.

5. Conclusions

The case study demonstrates that involving students in the redesign of hair-care packaging can provide relevant, contemporary directions for brands seeking stronger engagement with Generation Z. Across three distinct concepts, the most consistent improvements were clearer information hierarchy, stronger product-family coherence, more deliberate use of colour, greater shelf differentiation and visual systems suitable for digital communication. The results also show that there is no single 'Generation Z style'; effective solutions can range from playful and saturated to minimal and premium, provided that the design communicates quickly and coherently.

Sustainability should be integrated into this redesign process as a design and packaging-system requirement rather than added as a final claim. For cosmetic brands, the most promising route is therefore to combine student-led or user-near co-creation with technical packaging development and subsequent consumer validation. This approach can support packaging that is visually current, usable, credible and better aligned with changing environmental expectations.

6. Acknowledgements

The authors acknowledge the student design work of Naja Ražem; Anika Kocman and Klara Blatnik; and Ian Vedernjak and Tjaša Guštin, whose project documentation and packaging concepts formed the visual case material analysed in this paper. The project materials identify the case client as Ilirija d.o.o. and list Urška Brodnjak and Gregor Franken as academic mentors.

7. References

Clement, J., Kristensen, T. and Grønhaug, K. (2013) 'Understanding consumers' in-store visual perception: The influence of package design features on visual attention', *Journal of Retailing and Consumer Services*, 20(2), pp. 234–239. DOI: 10.1016/j.jretconser.2013.01.003

Del Greco, A., Bani, M., Rampoldi, G., Ardenghi, S., Galli, P., Strepparava, M.G. and Russo, S. (2024) 'Re-evaluating beauty: Attitudes and perceptions of eco-friendly packaging in beauty care products – A systematic review', *Sustainable Production and Consumption*, 52, pp. 458–468. DOI: 10.1016/j.spc.2024.11.011

Hallez, L., Vansteenbeeck, H., Boen, F. and Smits, T. (2023) 'Persuasive packaging? The impact of packaging color and claims on young consumers' perceptions of product healthiness, sustainability and tastiness', *Appetite*, 182, 106433. DOI: 10.1016/j.appet.2022.106433

Limbu, Y.B., Pham, L. and Nguyen, T.T.T. (2022) 'Predictors of Green Cosmetics Purchase Intentions among Young Female Consumers in Vietnam', *Sustainability*, 14(19), 12599. DOI: 10.3390/su141912599

Panopoulos, A., Poulis, A., Theodoridis, P. and Kalampakas, A. (2023) 'Influencing Green Purchase Intention through Eco Labels and User-Generated Content', *Sustainability*, 15(1), 764. DOI: 10.3390/su15010764

Vrabič-Brodnjak, U. and Jestratijević, I. (2024) 'The future of baby cosmetics packaging and sustainable development: A look at sustainable materials and packaging innovations – A systematic review', *Sustainable Development*, 32(3), pp. 2208–2222. DOI: 10.1002/sd.2775

Wang, I.-C., Jiang, Y.-R., Wang, Y.-W. and Li, C.-Y. (2024) 'Exploring the Multisensory Attractiveness of Cosmetic Packaging: A Study of Visual and Tactile Design Elements and Attractiveness Factors', *Sustainability*, 16(13), 5716. DOI: 10.3390/su16135716



© 2026 Authors. Published by the University of Novi Sad, Faculty of Technical Sciences, Department of Graphic Engineering and Design. This article is an open access article distributed under the terms and conditions of the Creative Commons Attribution license 4.0 Serbia (http://creativecommons.org/licenses/by/4.0/rs/).

Original Scientific Paper https://doi.org/10.24867/GRID-2026-p39

Differences in the Perception of Wine Packaging Attributes Based on Tactile-Visual and Visual-Only Texture Evaluation

ABSTRACT

Texture represents an important element of multisensory packaging design, which can be experienced not only through visual perception but also through tactile interaction with the packaging. Through touching and observing the packaging, texture can convey certain expectations, as well as aesthetic, emotional, and functional values to consumers. However, with the development of online sales, the formation of these expectations and values during purchasing is largely limited to the visual perception of the texture of packaging and products. For this reason, a study was conducted with the aim of identifying differences in perception that arise solely from the visual perception of texture and from texture that, in addition to visual perception, can also be touched. A total of 237 participants aged between 20 and 27 years took part in the study. The participants were divided into two groups depending on the conditions of interaction with the packaging. For the purposes of the study, physical wine packaging stimuli were created, on the surfaces of which texture was formed using glass, wax, paper, textile, twine, and stone. The results of the study showed that tactile interaction with the texture of wine packaging was generally associated with higher ratings of perceived packaging attributes. However, it was also observed that visual perception of certain textures and examined attributes may result in higher ratings compared with interaction that also includes tactile perception.

KEY WORDS

Packaging design, surface texture, tactile perception, visual perception, consumer perception

David Pinćjer
Gojko Vladić
Teodora Gvoka
Gordana Bošnjaković
Stefan Đurđević

University of Novi Sad,
Faculty of Technical Sciences,
Department of Graphic Engineering and Design,
Novi Sad

1. Introduction

Packaging represents a formed or unformed material into which a product is placed, that is, packaged, in order to ensure its safe protection and transportation. It represents a complex technical and commercial system aimed at protecting the packaged contents from the final stage of production until use by end consumers, while at the same time facilitating transportation, handling, recognition, promotion, and marketing of the product (Đurđević, 2023; Sastre, de Paula & Echeveste, 2022). Over time, the functions of packaging, in addition to its primary role of protecting the packaged contents, have become numerous and important for the success of a product. Nowadays, packaging has become an integral part of the marketing mix, with the success of a product in a competitive market largely depending on its functional and aesthetic attributes.

The perception of these attributes is influenced by packaging elements that can be perceived visually, such as color, as well as elements that can be perceived through both sight and touch, such as the shape and texture of packaging (Spence, 2016). Although shape and texture can be experienced through touch, the mechanisms involved in obtaining information about

their characteristics through the sense of touch differ. To obtain information about shape, people use more active touch, which involves the participation of skin receptors, kinesthetic mechanisms, and mechanisms responsible for sensing the position and movement of the body. Such free exploration of a surface is referred to as haptic perception, whereas obtaining information about texture involves the activation of skin receptors resulting from changes in the skin, which is associated with passive touch (Fernandes & Albuquerque, 2012; Simões-Franklin, Whitaker & Newell, 2011).

Texture can be described as a set of visual and tactile characteristics of a surface, for describing and experiencing which people use a rich vocabulary. Visual texture can evoke associations in people that connect it with tactile experiences of that texture, while tactile experience can evoke memories of its visual appearance. These two modes of perception complement each other in forming a clear representation of the surface properties of a particular surface (Alerby & Opstad, 2022). In the context of packaging, texture largely depends on the packaging material used for its production.

Packaging texture represents a means of communication through which designers and companies seek to evoke certain emotions and sensations in consumers, while its experience as pleasant or unpleasant to the touch depends on previous experiences and associations related to that experience (Tangeland, Schulte & Boks, 2008; Alerby & Opstad, 2022). Considering the importance of sight and touch in the perception of packaging texture, a study was conducted with the aim of determining differences in the perception of packaging attributes under conditions of tactile and visual perception of texture on the surface of wine packaging and under conditions of exclusively visual perception of texture.

The examined packaging attributes included the suitability of the texture for wine packaging, as well as the influence of texture on the perception of innovativeness, authenticity, and luxury of wine packaging.

2. Methods

The experimental part of the study was conducted with the aim of examining differences in the perception of wine packaging attributes depending on the conditions of interaction with its texture. A total of 237 participants took part in the study, including 177 women and 60 men. All participants were students of the Graphic Engineering and Design study program, aged between 20 and 27 years.

Depending on the conditions of interaction with the packaging, the participants were divided into two groups. The first group consisted of 137 participants who evaluated the influence of texture on the examined wine packaging attributes based on tactile and visual perception of the texture. The second group consisted of 100 participants who evaluated the influence of texture on the examined attributes exclusively based on photographs presented as part of the data collection instrument, with one representative stimulus shown for each material used in the study.

2.1. Experimental stimuli

A total of 16 physical wine packaging stimuli were used for the purposes of the study. Fifteen stimuli were covered with different materials: wax, paper, textile, twine, and stone, while one stimulus represented uncoated glass wine packaging. Each material used to cover the wine packaging was represented through three variations of the texture of the applied material, achieved through different application techniques, degrees of crumpling, weave structures, thicknesses, or grain sizes of the material (Figure 1).

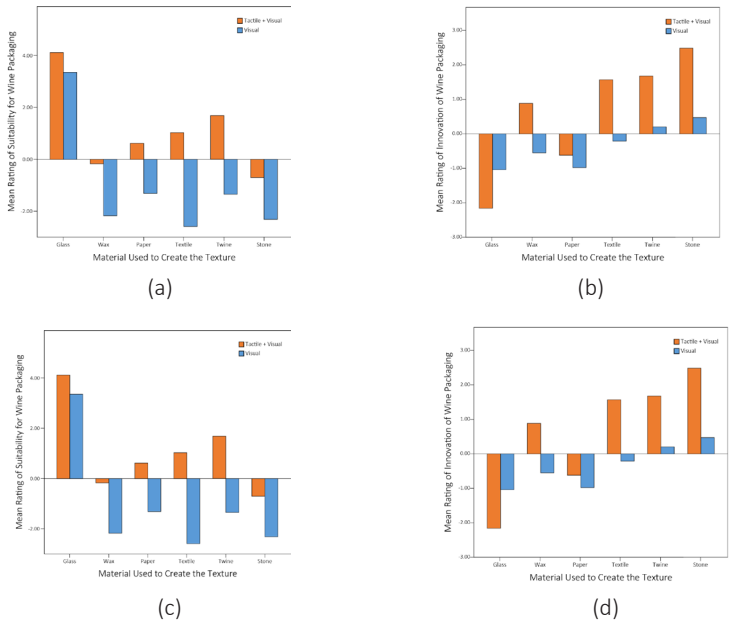


» **Figure 1:** *Overview of the stimuli used in the study: a) uncoated glass packaging, b) wax-covered packaging, c) paper-covered packaging, d) textile-covered packaging, e) twine-covered packaging, and f) stone-covered packaging*

Wax was applied using three different techniques: dipping the bottle in wax, applying wax with a brush, and allowing wax to drip onto the surface of the packaging. Paper was applied in three degrees of crumpling: smooth, moderately crumpled, and heavily crumpled. Textile was applied in three weave structures: fine, medium, and coarse. Twine was applied in three thicknesses: 1 mm, 2 mm, and 4 mm. Stone was applied in three grain sizes: fine sand, medium-grained stone particles, and coarse-grained stone particles with a diameter of approximately 5 mm.

2.2. Experimental procedure and survey instrument

The participants in the first group were presented with physical wine packaging stimuli that enabled them



» **Figure 2:** *Graphical presentation of the results: a) perceived suitability of the texture for wine packaging, b) perceived innovativeness, c) perceived authenticity, and d) perceived luxury*

to interact with the textures through the senses of touch and sight. This group was able to interact with each of the materials used in the study, as well as with different texture variations within each material. Before the evaluation began, the participants were introduced to the materials and texture variations used to create the stimuli. No additional information was provided about the properties of the materials that could potentially influence their perception.

The materials were presented to the participants in a random order, with all three texture variations of one material being evaluated before moving on to the next material. The second group evaluated the packaging attributes exclusively based on the visual perception of the textures, which is why photographs of the stimuli were presented to them. The order of presentation of the stimuli was the same for each examined attribute. For each material used in the study, one representative texture variation of the stimulus was selected and presented to this group.

No additional information about the materials or the textures of the wine packaging was provided to the participants. After evaluating the stimuli, the participants recorded their responses in the data collection instrument, which was created using the Google Forms platform. Both groups evaluated the same wine packaging attributes: suitability, innovativeness, authenticity, and luxury. A Likert-type scale ranging from −5 to +5 was used in the instrument. A rating of 5 represented the highest level of the examined attribute, while a rating of −5 represented the lowest level. The collected data were analyzed using appropriate statistical methods with IBM SPSS Statistics 22.

3. Results

The results of the study were analyzed using independent-samples t-tests to determine whether there were statistically significant differences in the ratings of the influence of texture on the perception of the examined wine packaging attributes depending on the conditions of interaction. Results with p-values lower than .05 were considered statistically significant.

For each examined packaging attribute, the mean ratings are graphically presented in Figure 2, while a detailed overview of the descriptive statistics and t-test results is provided in the following subsections.

3.1. Differences in the influence of texture on the perception of suitability for wine packaging

Table 1 presents the descriptive statistics of the ratings of the perceived suitability of textures for wine packaging for different materials and experimental conditions. The highest mean rating was recorded for glass in the tactile-visual group (M = 4.12, SD = 1.79). In contrast, the lowest mean rating was recorded for textile in the visual group (M = −2.60, SD = 2.47). The largest difference between the groups was observed for textile, with the tactile-visual group giving a significantly higher mean rating of the perceived suitability of the texture for wine packaging (M = 1.03) compared with the visual group (M = −2.60).

Table 1

Descriptive statistics of perceived suitability of texture for wine packaging for both groups

Stimulus	Condition	N	Mean	SD	Std. Error Mean
Glass	Visual + Tactile	137	4.12	1.79	0.15
	Visual	100	3.37	2.96	0.29
Wax	Visual + Tactile	137	-0.17	2.95	0.25
	Visual	100	-2.12	2.94	0.29
Paper	Visual + Tactile	137	0.62	2.48	0.21
	Visual	100	-1.28	3.22	0.32
Textile	Visual + Tactile	137	1.03	2.29	0.19
	Visual	100	-2.60	2.47	0.25
Twine	Visual + Tactile	137	1.69	2.53	0.22
	Visual	100	-1.35	2.91	0.29
Stone	Visual + Tactile	137	-0.70	3.04	0.26
	Visual	100	-2.33	2.73	0.27

Independent t-tests revealed statistically significant differences in the mean ratings of the suitability of the textures for wine packaging between the tactile-visual and visual groups for textures formed using glass, $t(151.12) = 2.24$, $p < .05$; wax, $t(235) = 5.04$, $p < .05$; paper, $t(178.76) = 4.93$, $p < .05$; textile, $t(203.64) = 11.50$, $p < .05$; twine, $t(195.18) = 8.37$, $p < .05$; and stone, $t(235) = 4.25$, $p < .05$. The tactile-visual group gave higher mean ratings of the suitability of the textures for wine packaging for all examined materials compared with the visual group.

3.2. Differences in the influence of texture on the perception of innovativeness of wine packaging

Table 2 presents the descriptive statistics of the ratings of the perceived innovativeness of wine packaging for different materials and experimental conditions. The highest mean rating was recorded for stone in the tactile-visual group (M = 2.48, SD = 2.65). In contrast, the lowest mean rating was recorded for glass in the tactile-visual group (M = −2.16, SD = 2.77). The largest difference between the groups was observed for stone, with the tactile-visual group giving a significantly higher mean rating of the perceived innovativeness of wine packaging (M = 2.48) compared with the visual group (M = 0.47).

Independent t-tests revealed statistically significant differences in the mean ratings of innovativeness between the tactile-visual and visual groups for textures formed using glass, $t(171.76) = -2.51$, $p < .05$; wax, $t(195.46) = 4.00$, $p < .05$; textile, $t(183.25) = 5.14$, $p < .05$; twine, $t(188.08) = 3.93$, $p < .05$; and stone, $t(187.22) = 5.10$, $p < .05$. No statistically significant differences in the mean ratings between the groups were observed for the texture formed using paper. The tactile-visual group gave higher mean ratings of innovativeness for wine packaging covered with wax, textile, twine, and stone,

Table 2

Descriptive statistics of perceived innovativeness for both groups

Stimulus	Condition	N	Mean	SD	Std. Error Mean
Glass	Visual + Tactile	137	-2.16	2.77	0.24
	Visual	100	-1.04	3.80	0.38
Wax	Visual + Tactile	137	0.88	2.51	0.21
	Visual	100	-0.55	2.88	0.29
Paper	Visual + Tactile	137	-0.62	2.18	0.19
	Visual	100	-0.98	2.71	0.27
Textile	Visual + Tactile	137	1.57	2.28	0.19
	Visual	100	-0.21	2.86	0.29
Twine	Visual + Tactile	137	1.68	2.54	0.22
	Visual	100	0.20	3.07	0.31
Stone	Visual + Tactile	137	2.48	2.65	0.23
	Visual	100	0.47	3.23	0.32

Table 3

Descriptive statistics of perceived authenticity for both groups

Stimulus	Condition	N	Mean	SD	Std. Error Mean
Glass	Visual + Tactile	137	0.03	2.60	0.22
	Visual	100	0.92	3.13	0.31
Wax	Visual + Tactile	137	1.31	2.54	0.22
	Visual	100	0.78	2.76	0.28
Paper	Visual + Tactile	137	-0.09	2.37	0.20
	Visual	100	-0.04	2.88	0.29
Textile	Visual + Tactile	137	1.15	2.53	0.22
	Visual	100	0.07	2.88	0.29
Twine	Visual + Tactile	137	2.42	2.33	0.20
	Visual	100	1.04	2.78	0.28
Stone	Visual + Tactile	137	1.61	3.10	0.26
	Visual	100	1.04	3.37	0.34

while the visual group gave a higher mean rating of innovativeness for uncoated glass wine packaging.

3.3. Differences in the influence of texture on the perception of authenticity of wine packaging

Table 3 presents the descriptive statistics of the ratings of the perceived authenticity of wine packaging for different materials and experimental conditions. The highest mean rating was recorded for twine in the tactile-visual group (M = 2.42, SD = 2.33). In contrast, the lowest mean rating was recorded for paper in the tactile-visual group (M = −0.09, SD = 2.37). The largest difference between the groups was observed for twine, with the tactile-visual group giving a significantly higher mean rating of the perceived authenticity of wine packaging (M = 2.42) compared with the visual group (M = 1.04).

Independent t-tests revealed statistically significant differences in the mean ratings of authenticity between the tactile-visual and visual groups for textures formed using glass, $t(189.02) = -2.32$, $p < .05$; textile, $t(235) = 3.05$, $p < .05$; and twine, $t(235) = 4.13$, $p < .05$. No statistically significant differences in the mean ratings between the groups were observed for the textures formed using wax, paper, and stone. The tactile-visual group gave higher mean ratings of authenticity for wine packaging covered with textile and twine, while the visual group gave a higher mean rating of authenticity for uncoated glass wine packaging.

3.4. Differences in the influence of texture on the perception of luxury of wine packaging

Table 4 presents the descriptive statistics of the ratings of the perceived luxury of wine packaging for

Table 4

Descriptive statistics of perceived luxury for both groups

Stimulus	Condition	N	Mean	SD	Std. Error Mean
Glass	Visual + Tactile	137	1.44	2.56	0.22
	Visual	100	2.38	2.62	0.26
Wax	Visual + Tactile	137	0.02	2.90	0.25
	Visual	100	-0.94	3.33	0.33
Paper	Visual + Tactile	137	-0.47	2.42	0.21
	Visual	100	-1.54	2.71	0.27
Textile	Visual + Tactile	137	1.18	2.55	0.22
	Visual	100	-0.98	2.94	0.29
Twine	Visual + Tactile	137	1.31	2.57	0.22
	Visual	100	-0.36	3.05	0.30
Stone	Visual + Tactile	137	1.02	3.25	0.28
	Visual	100	-0.07	3.27	0.33

different materials and experimental conditions. The highest mean rating was recorded for glass in the visual group (M = 2.38, SD = 2.62). In contrast, the lowest mean rating was recorded for paper in the visual group (M = –1.54, SD = 2.71). The largest difference between the groups was observed for textile, with the tactile-visual group giving a significantly higher mean rating of the perceived luxury of wine packaging (M = 1.18) compared with the visual group (M = –0.98).

Independent t-tests revealed statistically significant differences in the mean ratings of luxury between the tactile-visual and visual groups for textures formed using glass, $t(235) = -2.77$, $p < .05$; wax, $t(235) = 2.37$, $p < .05$; paper, $t(198.93) = 3.13$, $p < .05$; textile, $t(194.65) = 5.91$, $p < .05$; twine, $t(190.94) = 4.43$, $p < .05$; and stone, $t(235) = 2.55$, $p < .05$. The tactile-visual group gave higher mean ratings of luxury for wine packaging covered with wax, paper, textile, twine, and stone, while the visual group gave a higher mean rating of luxury for uncoated glass wine packaging.

4. Discussion

The results presented in the previous chapter indicate that tactile interaction with the texture of wine packaging was generally associated with a more positive perception of innovativeness, authenticity, and luxury, and particularly with the perception of the suitability of the texture for making packaging. Participants who had the opportunity to touch the stimuli made from each material included in the study consistently rated the texture as more suitable compared with evaluations based exclusively on the visual perception of texture. The difference between the groups was also significant for glass, which, as a material, is recognizable due to its properties and suitable for packaging products in this category.

Regarding innovativeness, the tactile group generally gave higher mean ratings of the innovativeness of wine packaging, but not as consistently as was the case with the suitability of the texture for making wine packaging. Regarding glass, which is traditionally used for this purpose, participants who made their evaluations solely on the basis of visual texture could have obtained less information about the texture and its surface characteristics compared with the tactile group. The recognizable cold and smooth surface of glass may have influenced participants to recognize with greater certainty that it is a traditional and commonly used material for this purpose, which may have contributed to them perceiving the texture of this material as less innovative compared with the visual group.

The least consistent pattern of higher ratings by the tactile group was observed in the perception of the authenticity of wine packaging, with ratings being statistically significantly higher only for textile and twine compared with the visual group. These results may be explained by the fact that participants who had the opportunity to touch the textures formed using these materials received additional information that could have triggered memories and associations with some traditional ways of decorating wine packaging, as well as with products from the broader cultural context.

Regarding the influence of wine packaging texture on the perception of luxury, the tactile group gave higher ratings of luxury for wax, paper, textile, twine, and stone, possibly due to the rich tactile experience that the textures formed using these materials could provide. On the other hand, the visual group gave a higher mean rating for glass, which can be associated with the gloss of the glass surface. Since glass was the only material whose gloss was clearly visible in the photographs presented, this visual characteristic may have contributed to the formation of a more pronounced perception of luxury among the visual group.

5. Conclusion

The results of this study indicated the importance of consumers' tactile interaction with packaging texture when evaluating the attributes of wine packaging. The possibility of touching the texture of wine packaging was generally associated with higher ratings of the suitability of the texture for making wine packaging, as well as the innovativeness, authenticity, and luxury of wine packaging. The significance of this study lies in highlighting the importance of enabling consumers to engage in tactile interaction with packaging during the purchasing process. When such an opportunity exists and consumers are sufficiently motivated to further examine the packaging texture through the sense of touch, such interaction should be enabled because it can positively influence their evaluations of packaging attributes. Considering that consumers often cannot separate what they think and feel while handling packaging from what they think and feel about the product, such interaction can also influence their perception of product attributes. Future research could examine how different textures, during tactile interaction with the surface of wine packaging, contribute to the formation of perceptions of different wine packaging attributes. The limitations of this study relate to the relatively narrow age range of the participants, with the majority of the sample consisting of students between 20 and 27 years of age. Therefore, future research could include participants from a broader age range.

6. Acknowledgments

This research has been supported by the Ministry of Science, Technological Development and Inno-

vation (Contract No. 451-03-34/2026-03/200156) and the Faculty of Technical Sciences, University of Novi Sad through project “Scientific and Artistic Research Work of Researchers in Teaching and Associate Positions at the Faculty of Technical Sciences, University of Novi Sad 2026” (No. 01-3609/1).

7. References

Alerby, E. and Opstad, K.D. (2022) 'Texture and (Arts) Education: Encouraging Attention, Awareness and Sensitivity', *European Journal of Philosophy in Arts Education*, 7(1). DOI: 10.5281/zenodo.6536166

Đurđević, S. (2023) Grafička ambalaža. Materijal sa predavanja. GRID, Fakultet tehničkih nauka, Novi Sad.

Fernandes, A.M. and Albuquerque, P.B. (2012) 'Tactual perception: a review of experimental variables and procedures', *Cognitive Processing*, 13(4), pp. 285–301. DOI: 10.1007/s10339-012-0443-2

Sastre, R.M., de Paula, I.C. and Echeveste, M.E.S. (2022) 'A Systematic Literature Review on Packaging Sustainability: Contents, Opportunities, and Guidelines', *Sustainability*, 14(11), 6727. DOI: 10.3390/su14116727

Simões-Franklin, C., Whitaker, T.A. and Newell, F.N. (2011) 'Active and passive touch differentially activate somatosensory cortex in texture perception', *Human Brain Mapping*, 32(7), pp. 1067–1080. DOI: 10.1002/hbm.21091

Spence, C. (2016) 'Multisensory Packaging Design: Color, Shape, Texture, Sound, and Smell'. In: Burgess, P. (ed.) *Integrating the Packaging and Product Experience in Food and Beverages: A Road-Map to Consumer Satisfaction*. Woodhead Publishing, pp. 1–22. DOI: 10.1016/B978-0-08-100356-5.00001-2

Tangeland, L., Schulte, K.Ø. and Boks, C. (2008) 'Tactile Qualities of Materials in Consumer Product Packaging'. In: Roosimölder, L. (ed.) *DS 50: Proceedings of NordDesign 2008 Conference, 21–23 August 2008, Tallinn, Estonia. Tallinn*, pp. 89–98.



© 2026 Authors. Published by the University of Novi Sad, Faculty of Technical Sciences, Department of Graphic Engineering and Design. This article is an open access article distributed under the terms and conditions of the Creative Commons Attribution license 4.0 Serbia (http://creativecommons.org/licenses/by/4.0/rs/).

https://doi.org/10.24867/GRID-2026-p40

Integrating Artificial Intelligence in the Design of Sustainable and Smart Packaging: Challenges and Perspectives in Graphic Engineering

ABSTRACT

Sustainability has become a central requirement in graphic engineering and packaging design, driven by environmental regulation and the shift towards a circular economy. At the same time, machine learning and other Artificial Intelligence (AI) methods are being applied across production workflows, material selection and quality control in the printing industry. This paper examines how these methods can support the design and production of environmentally conscious, interactive packaging, treating sustainability and consumer experience as related rather than separate problems. The first part deals with graphic materials: recycled paper substrates and eco-friendly inks are discussed in terms of colour stability and ink penetration during printing, and a machine-learning-based approach is proposed for selecting ink–substrate combinations at the prepress stage. The second part addresses the design process itself: Design Thinking, AI-assisted colour management, and Augmented Reality (AR) are discussed as complementary tools for turning packaging into a channel that also carries traceability and product information. This paper draws on published evidence from graphic engineering, printing science, and consumer research to assess which parts of the proposed framework are already supported by experimental results and which still need testing. The paper ends with a concrete plan to validate the framework on a defined set of substrates, inks, and AR content.

Chris Trochoutsos [1,2,3]
Gerasimos Vonitsanos [1,2]
Marios Tsigonias [1,2]

[1] University of West Attica, Hellenic Graphic-Media Research Lab – GRAPHMEDLAB, Greece
[2] Hellenic Open University, School of Applied Arts and Sustainable Design, Greece
[3] Pressious Arvanitidis, printing company, Greece

KEY WORDS
Packaging design, artificial intelligence, sustainability, graphic materials, smart packaging, colour management

1. Introduction

Packaging is a multidisciplinary field that combines graphic engineering, materials science, manufacturing technologies, and consumer communication (Davidescu et al., 2025). Beyond protecting products and supporting brand identity, modern packaging is increasingly expected to meet sustainability requirements linked to circular economy principles and environmental regulations (International Organization for Standardization, 2013).

Within the European Union, this context is now shaped by the Packaging and Packaging Waste Regulation (PPWR), Regulation (EU) 2025/40, which applies from 12 August 2026. It establishes life-cycle requirements for packaging and packaging waste, including provisions related to prevention, recyclability, labelling, reuse, and resource efficiency, with several technical obligations phased in on later dates (European Union, 2025).

Adopting recycled substrates, renewable materials, and eco-friendly inks has become an important strategy for reducing packaging's environmental impact (Strižić et al., 2024). However, these materials often show greater

variability in surface properties, absorbency, and colour reproduction than conventional alternatives, creating challenges for maintaining print quality and production efficiency (Tomašegović et al., 2021; Svanes et al., 2010).

Recent developments in AI have created new opportunities to address these challenges. Machine learning techniques can support material selection, predict print-quality characteristics, optimise production parameters, and reduce waste throughout the printing workflow (Basak et al., 2025; Abusaq et al., 2023). At the same time, AI applications are increasingly used in packaging design to support decision-making and more sustainable, user-centred solutions (Jin et al., 2024).

In parallel, Design Thinking methodologies have emerged as effective frameworks for developing packaging concepts that integrate technical requirements with consumer needs (Bijitkar & Moule, 2024). Furthermore, Augmented Reality (AR) technologies are transforming packaging into an interactive communication medium by providing access to digital content such as product information, traceability data, and sustainability guidance. Previous studies have demonstrated that AR can enhance consumer engagement and perceived value (Accardi et al., 2025; Gu et al., 2023).

While advances in sustainable substrates, machine learning, and interactive design are well documented, the literature often treats them as distinct disciplines. Consequently, a clear need remains for a workflow that connects AI-driven prepress decisions directly to physical production and digital consumer interfaces.

Building on these complementary approaches, this study proposes a conceptual framework that integrates predictive modelling of ink-substrate interactions, AI-assisted colour management, Design Thinking methodologies, and AR technologies. The objective is to show how these complementary approaches can simultaneously contribute to sustainability, production efficiency, improved print quality, and consumer engagement.

The remainder of the paper is organised as follows. Section 2 reviews the relevant literature, Section 3 presents the proposed framework and its experimental validation plan, Section 4 discusses its feasibility, potential benefits, and limitations, and Section 5 concludes the study and outlines future research directions.

2. Related work

The literature review followed a structured narrative approach. Scopus, Web of Science, and Google Scholar were searched for English-language publications from 2010 to September 2026 using combinations of the terms “sustainable packaging”, “recycled paper”, “eco-friendly inks”, “flexographic printing”, “print quality”, “machine learning”, “colour management”, “Design Thinking”, “augmented reality”, and “smart packaging”. Priority was given to peer-reviewed studies directly addressing packaging engineering, printing processes, colour measurement, resource efficiency, or AR-enabled packaging. We included standards and official regulatory sources where necessary, while excluding sources without a clear methodological or technological connection to the proposed framework.

The packaging industry has evolved from a system focused primarily on product protection and marketing into a multidisciplinary field that integrates sustainability, technological innovation, and digital communication (Bolanča et al., 2018). Sustainable packaging design has become increasingly important because of growing environmental concerns and the transition toward circular economy principles.

Svanes et al. (2010) proposed a holistic approach to sustainable packaging design that considers material reduction, transportation efficiency, product protection, and end-of-life recovery as interconnected parameters. This perspective aligns with circular economy objectives and is further supported by standards such as ISO 18604, which define requirements for material recycling and recovery (International Organisation for Standardisation, 2013).

At the production level, research has highlighted the challenges associated with recycled and environmentally friendly substrates, whose physical properties can significantly influence print quality. Tomašegović et al. (2021) demonstrated that substrate roughness and absorbency affect key flexographic printing characteristics, including dot gain and colour consistency. These findings emphasise the need to predict and optimise material-process interactions accurately.

Recent advances in Artificial Intelligence (AI) have provided effective solutions to address these challenges. Basak et al. (2025) compared several machine-learning techniques for predicting dot gain in flexographic printing and reported prediction accuracies of up to 98% using artificial neural networks. Similarly, Abusaq et al. (2023) demonstrated the potential of AI-assisted analysis to improve energy efficiency and reduce waste in printing production. These studies indicate that machine learning can significantly support process optimisation and sustainable manufacturing.

AI applications have also expanded into packaging design and colour management. Jin et al. (2024) used deep-learning techniques to support sustainable and user-centred packaging development, while Azarenkov and Deineko (2025) investigated neural-network-based approaches to generate colour profiles directly from measurement data. Such meth-

ods are particularly relevant for packaging printed on recycled substrates, where colour behaviour may vary considerably between production batches.

Beyond production processes, research has increasingly focused on human-centred design and digital interaction. Design Thinking provides a structured framework for developing packaging solutions that balance technical requirements with consumer needs through iterative design and evaluation processes (Bijitkar & Moule, 2024). At the same time, Augmented Reality (AR) technologies enable packaging to become an interactive communication medium, delivering product information, traceability data, and immersive consumer experiences. Studies by Accardi et al. (2025) and Gu et al. (2023) demonstrated that AR-enhanced packaging can improve consumer engagement, perceived interactivity, and overall product evaluation.

Although individual technologies like machine learning and AR have proven their value in printing science, they are rarely integrated into a single production pipeline. The intersection of material sustainability, AI-based process control, and digital consumer interaction currently lacks a cohesive methodological structure.

Consequently, the proposed framework integrates AI-driven print-quality prediction, colour management, Design Thinking methodologies, and AR technologies to support the development of sustainable and smart packaging solutions that enhance production efficiency, environmental performance, and consumer engagement.

3. Proposed Framework and Experimental Validation Plan

3.1. Graphic materials: recycled substrates and eco-friendly inks

The proposed framework focuses on recycled paper substrates and environmentally friendly inks as key components of sustainable packaging production. Recycled fibre-based materials, water-based inks, and low-migration UV-curable inks can reduce environmental impact and VOC emissions and support recycling processes. However, recycled substrates often exhibit greater surface roughness, porosity, and variability than virgin-fibre materials, affecting ink transfer, absorption, colour reproduction, and overall print quality (Tomašegović et al., 2021). Colour stability and ink penetration are therefore critical prepress parameters, as they directly influence optical density, colour saturation, and tonal reproduction. These properties depend on interactions among substrate characteristics, ink composition, and printing conditions, including ink viscosity, anilox line screen/cell density and volume, halftone screen ruling, dot percentage, and drying conditions. Because conventional trial-and-error evaluation is time-consuming and resource-intensive, data-driven methods offer a more efficient approach to material selection, process optimisation, and waste reduction.

3.2. Predictive model for ink–substrate interaction

To address the complexity of material-process interactions, the proposed framework incorporates a machine-learning-based predictive model designed to support prepress decision-making. The objective of the model is to estimate the expected performance of different ink-substrate combinations before physical printing takes place, enabling more informed and sustainable production choices.

The model will use material and process parameters as input variables, including substrate properties, ink formulation, anilox line screen/cell density, anilox volume, halftone screen ruling, dot percentage, ageing condition, and selected production settings. Based on these inputs, it will predict print-quality responses, resource-consumption indicators, and waste-related indicators. Resource consumption and waste generation will be treated as bounded sustainability-related proxies within the printing process, rather than as comprehensive measures of environmental sustainability.

Drawing upon previous studies in machine learning for print-quality prediction, several supervised learning techniques can be considered, including linear regression, random forests, gradient boosting algorithms, and artificial neural networks (Basak et al., 2025). These methods offer different capabilities in modelling non-linear relationships between printing variables and production outcomes.

Because ΔE_{00}, resource consumption, and waste generation have different units and numerical ranges, the weighted objective will use normalised values:

$$F(x) = w_1 \cdot \widehat{\Delta E}_{00}(x) + w_2 \cdot \hat{R}(x) + w_3 \cdot \hat{W}(x), \quad \text{with} \quad w_1 + w_2 + w_3 = 1 \tag{1}$$

where each objective is scaled to [0,1], for example $\hat{z}(x) = [z(x) - z_{min}]/[z_{max} - z_{min}]$, using limits defined by the experimental design or an agreed production baseline:

- x represents the vector of material and process parameters;
- $\widehat{\Delta E}_{00}(x)$ is the normalised predicted colour difference;
- $\hat{R}(x)$ is the normalised resource-consumption indicator;
- $\hat{W}(x)$ is the normalised waste-generation indicator;

- w_1, w_2, and w_3 are non-negative weighting coefficients representing the agreed relative priorities.

R(x) will comprise ink, substrate, and energy consumption per accepted production unit. W(x) will comprise makeready waste, rejected sheets or packages, and other process waste generated within the stated system boundary. The coefficients w_1, w_2, and w_3 will be selected transparently through stakeholder-defined priorities, sensitivity analysis, or an analytic decision procedure, and the effect of alternative weight sets will be reported. Pareto-based multi-objective optimisation may also be used to identify non-dominated solutions without imposing a single fixed weighting scheme. The recommendations will be interpreted as decision support for balancing print quality, resource efficiency, and waste reduction.

Table 1

AI and complementary technologies/methodologies integrated into the proposed packaging workflow

Production stage	Technology / methodology	Primary target	Expected contribution to resource efficiency / waste reduction
Material & ink selection (prepress)	Supervised machine learning (regression, ensemble methods, neural networks)	Colour stability, ink penetration	Reduced trial prints, lower resource and ink consumption
Design ideation	Design Thinking supported, where appropriate, by AI-assisted tools	User-centred, iterative prototyping	Fewer design iterations, material-aware concepts
Colour management	AI-assisted spectral / colour prediction and profiling	Cross-substrate colour consistency	Fewer reprints, waste reduction
Consumer interface	Augmented Reality (complementary digital technology)	Traceability, engagement	Extended product lifecycle information, reduced need for extra printed inserts.

3.3. Proposed experimental validation plan

A structured experimental framework is proposed to evaluate the predictive model's effectiveness and investigate relationships between material properties, printing parameters, and print-quality outcomes. The primary objective of this validation process is to generate a representative dataset for training and evaluating machine-learning algorithms while also examining the suitability of sustainable materials for smart packaging applications.

The experimental design focuses on recycled paper substrates and environmentally friendly ink systems commonly used in the packaging industry. Multiple combinations of material and process parameters are considered to ensure that the collected data adequately capture the variability encountered under real production conditions. This approach enables the investigation of both individual parameter effects and interactions among variables that may significantly influence colour reproduction, print quality, resource consumption, and sustainability performance.

To evaluate the proposed framework comprehensively, the proposed validation study will adopt a hierarchical (split-plot/mixed) experimental design. In this design, substrate, ink system, anilox line screen/cell density, anilox volume, halftone screen ruling, and other press settings are assigned at production-run level; dot percentage is evaluated as a within-form test-patch factor, because the different tonal values are patches of the same printed form rather than separate production runs; and ageing condition (or ageing time) is treated as a post-print repeated-measurement factor applied to the same or corresponding printed samples, not as a new production condition. Print run/batch is used as a blocking and grouping variable. Consequently, the full combination of factor levels does not correspond to a comparable number of fully independent production conditions: only the production-level factors define independent press setups. Actual anilox specifications will be selected from commercially/experimentally available roller configurations; line screen and volume combinations will therefore be constrained to physically available engravings. Nominal anilox volume is a characteristic of the cell geometry and engraving, whereas actual ink transfer is additionally influenced by ink rheology and viscosity, surface tension, doctoring, and dynamic printing conditions, effects that become particularly important in high-line-screen engravings where the cells are very small (Savickas et al., 2020). Ink transfer will therefore be treated as a measured response (for example, ink film weight) rather than being inferred from nominal volume alone. Measured response variables will include colour difference (ΔE00), dot gain, print density, tonal reproduction, ink absorption, drying behaviour, AR recognition performance, resource consumption, and waste generation. The experimental unit is a printed test sample produced under a given experimental condition within a given print

run/batch; repeated measurements taken from the same sample are not treated as independent observations. Multiple independent print runs will be performed, with their number selected to permit grouped cross-validation during model development and a genuinely independent run-level test set (at least five runs are planned: four for model development and one held out for final testing). Each independent print run constitutes an independent production replicate. Within each run, each experimental condition will be produced in three within-run production replicates, which assess repeatability and are not regarded as independent replicates. Experimental and measurement order will be randomised, while print run/batch will be treated as a blocking and grouping variable. This structure will permit estimation of main effects and relevant interactions while separating systematic run-to-run variability. Table 2 presents the proposed factors, levels, responses, replication, and blocking structure.

As shown in Table 2, the proposed design separates controllable factors and levels from measured responses. Print quality will be assessed through spectrophotometric and microscopic measurements. Colour performance will be evaluated using CIE L*a*b* coordinates and ΔE00, while ink penetration, print density, dot gain, and tonal reproduction will be measured to assess reproduction accuracy and consistency (Yılmaz et al., 2022). Resource consumption will be recorded as ink, substrate, and energy used per accepted production unit, whereas waste will include makeready material, rejected sheets, and other process waste within the defined printing boundary. The dataset generated during validation will first be separated, at print-run level, into a model-development set and an independent test set. Within the development set only, models will be trained and compared through grouped k-fold cross-validation, with print run/batch as the grouping variable, and hyperparameter selection. The final test set will consist of one or more genuinely independent print runs that have been used neither for training nor for model selection; only after model selection will final performance be estimated on it. All observations from the same print run/batch, including within-run replicates, will remain within the same fold or partition and will never be allocated simultaneously

Table 2

Experimental factors, proposed levels, responses, replication, and blocking for validation of the predictive model

Experimental factor	Proposed levels	Measured response variable(s)	Role in design
Substrate	FSC-certified recycled kraftliner (250 g/m²); recycled coated duplex board (300 g/m²)	Surface roughness, baseline colour, ink absorption	Production-level factor
Ink system	Water-based ink; low-migration UV-curable ink	Drying/curing behaviour, print density, ΔE00	Production-level factor
Anilox line screen / cell density	800 lpi; 1000 lpi	Ink transfer, print density, dot gain	Production-level factor
Nominal anilox volume / volumetric capacity	2.5 cm³/m²; 3.5 cm³/m²	Ink film weight, print density, resource consumption	Production-level factor
Halftone screen ruling	133 lpi; 150 lpi	Dot gain, tonal reproduction, print contrast	Production-level factor
Dot percentage	10% to 100%, in 10% steps	Tonal reproduction curve, dot gain	Within-form test-patch factor
Ageing condition	Standard indoor storage; accelerated ageing	Change in ΔE00 and AR recognition performance	Post-print repeated-measurement factor
Print run / batch	Multiple independent runs (at least five planned)	Run-to-run variability	Blocking/grouping variable
Within-run production replicates	Three per condition within each run	Repeatability and uncertainty	Replication
AR recognition	Controlled illumination, distance, and viewing-angle conditions	Recognition success rate, acquisition time, maximum distance, robustness	Response assessment

to training and test partitions, to prevent data leakage. Model performance will be reported using RMSE, MAE, R^2, and uncertainty intervals where appropriate.

3.4. Design Thinking applied to packaging concept development

While material optimisation is fundamental for sustainable packaging, successful solutions must also address consumer needs and market expectations. To support this objective, the proposed framework integrates Design Thinking as a human-centred methodology for packaging concept development.

The Design Thinking process follows the established sequence of empathise, define, ideate, prototype, and test. In the initial stages, the team collects information on consumer expectations, sustainability concerns, usability requirements, and information accessibility, then translates it into design criteria. This approach keeps technical decisions aligned with user needs throughout development.

During ideation and prototyping, designers generate and evaluate multiple packaging concepts. At this stage, the AI model's predictions can help designers identify material and printing configurations that meet both sustainability targets and visual requirements before producing physical prototypes. This integration shortens development cycles and supports evidence-based decision-making.

The testing phase combines visual evaluation, functional assessment, and the verification of digital features incorporated within the package. Through iterative refinement, Design Thinking facilitates the development of packaging solutions that balance environmental performance, production feasibility, and user experience.

3.5. AI-assisted colour management

Colour consistency remains one of the most critical quality requirements in packaging production. However, maintaining stable colour reproduction across production batches is particularly challenging with recycled substrates because of variations in fibre composition, surface characteristics, and absorption behaviour.

Established colour-management workflows rely on device characterisation targets, spectrophotometric measurements, ICC or spectral profile generation, profile validation, process control, and recalibration when substrate or production conditions change. These procedures remain essential, but their measurement and maintenance burden increases when recycled substrates exhibit substantial batch-to-batch variability.

Within the proposed framework, AI/ML is not intended to replace established ICC-based or spectral colour-management workflows. Instead, machine-learning models will operate as a complementary decision-support layer that learns from characterisation and production measurement data, predicts substrate-specific colour behaviour, and indicates when additional characterisation or recalibration may be required.

This complementary approach may support faster substrate-specific adjustments, identify drift between print runs, and reduce corrective print iterations while preserving compatibility with established colour standards and validation practices. Its effectiveness will be evaluated against the baseline ICC/spectral workflow rather than against an assumed absence of colour management.

3.6. Augmented Reality integration

The final component of the framework concerns integrating AR technologies into sustainable packaging systems. As consumer expectations increasingly shift towards personalised and interactive experiences, packaging is evolving from a static physical medium into a dynamic communication platform.

In the proposed approach, printed visual elements such as markers, logos, QR codes, or image-recognition features serve as triggers that connect physical packaging with digital content accessible through mobile devices. The resulting AR experience may provide product traceability information, sustainability instructions, recycling guidelines, usage recommendations, or interactive brand communication elements.

Beyond marketing applications, AR may reduce the need for some additional printed information by providing digital access to traceability, recycling, and usage guidance (Rani & Ramlie, 2023). This potential contribution is treated as a resource-efficiency opportunity rather than as evidence of comprehensive environmental sustainability.

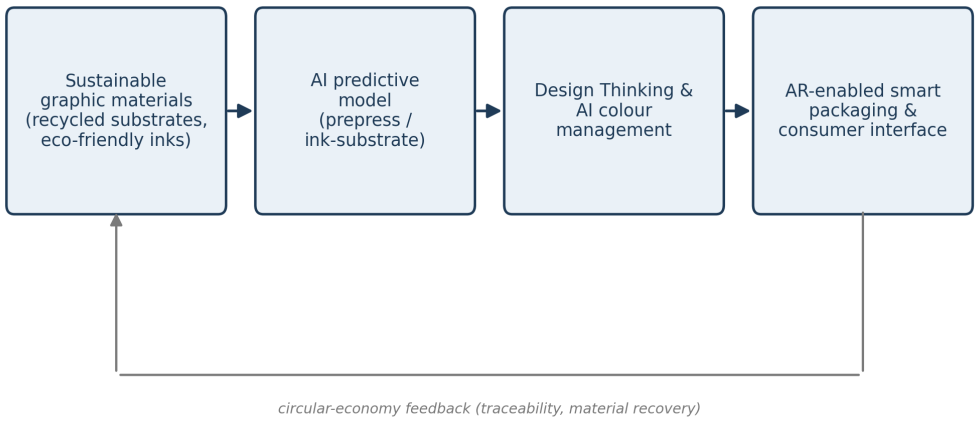
From a graphic engineering perspective, successful AR functionality depends strongly on the printed trigger and its interaction with the substrate. During validation, AR performance will be quantified through recognition success rate, acquisition time, maximum recognition distance, and robustness under controlled changes in illumination and viewing angle. These outcomes will be analysed in relation to ΔE00, print contrast, dot gain, substrate roughness and colour, and ageing-induced degradation. This analysis will connect AR reliability directly with print-quality and process variables, strengthening the graphic-engineering dimension of the framework.

4. Discussion

Figure 1 illustrates the workflow connecting the components described in Section 3: material selection feeds the

predictive model, the predictive model supports Design-Thinking-based concept development and AI-assisted colour management, and the resulting package carries AR content that returns traceability and material-recovery information to the consumer, which in turn can influence the material choices made in the next design cycle.

that its accuracy depends on how the network is configured; this is consistent with the proposal in Section 3.5, though it also means that the colour-management step needs its own, separate tuning and is not simply inherited from the predictive model in Section 3.2.



» **Figure 1:** *Proposed framework connecting AI-based material selection, colour management and AR-enabled interaction in sustainable packaging design*

4.1. Feasibility of the material and predictive-model components

The material and predictive-model components rest on the most direct evidence of the four. Basak et al. (2025) reported prediction accuracies of 95–98% for a neural-network model of flexographic dot gain trained on a comparable set of variables to those proposed in Table 2. Tomašegović et al. (2021) showed that ecologically favourable substrates can reach acceptable print quality once their absorption and roughness are accounted for at the prepress stage. Both results support the assumption in Section 3.2 that colour deviation and dot gain can be predicted from substrate, ink and process parameters with a useful degree of accuracy; what has not yet been shown, and is left for the experimental plan in Section 3.3, is whether the same accuracy holds once resource consumption and waste are added as joint objectives rather than treated as a single response variable.

4.2. Feasibility of Design Thinking and AI-assisted colour management

Bijitkar and Moule (2024) reported that a Design-Thinking-based process produces more technically grounded and better-received packaging concepts than a purely theoretical design process, supporting its use as the organising structure for Section 3.4 rather than treating AI-based screening as a stand-alone step. For colour management, Azarenkov and Deineko (2025) demonstrated that a neural-network-based profile can be built directly from measured colour-target data and

4.3. Feasibility of the AR-enabled consumer interface

The consumer-facing component is supported mainly by marketing and consumer-behaviour research rather than by graphic engineering studies. Accardi et al. (2025) found, using physiological measurements rather than self-report alone, that immersive AR content produces stronger engagement than static AR content; Gu et al. (2023) found, with a much larger sample, that AR reduced negative evaluations of take-away food packaging. Neither study addressed how print quality on the physical marker affects AR recognition rates, which is the specific graphic-engineering question raised in Section 3.6 and is not answered by the consumer-research literature reviewed here.

4.4. Limitations

Several limitations follow from assembling the framework from separate strands of published work rather than testing it as a whole. The predictive model must be trained on data specific to the substrates, inks, anilox specifications, screening conditions, and press technology used by a given converter, and its accuracy outside that domain is unknown. The Design Thinking and colour-management steps require skills in data handling, colour science, and interaction design that are not yet standard across all graphic-engineering settings. The AR component depends on print quality in ways the literature reviewed here has not yet quantified, and its printed trigger must remain compatible with the package's material and recycling

constraints. The framework does not perform a complete Life Cycle Assessment (LCA). Resource consumption and waste generation are therefore sustainability-related indicators or proxies within a defined production boundary, not comprehensive measures of environmental sustainability. Finally, none of the components has yet been tested together on the same samples; Section 3.3 defines the validation plan required to address this limitation.

5. Conclusions and Future Work

This paper proposes an integrated framework for applying Artificial Intelligence and complementary methodologies to resource-efficient and smart packaging development. At the production level, machine learning is proposed to support prediction of ink-substrate interactions and prepress decision-making. At the design and communication levels, Design Thinking, AI-assisted colour management, and Augmented Reality are combined to support packaging concepts that integrate print-quality requirements, traceability, and access to digital information. The principal contribution is a unified workflow and an explicit validation plan rather than a completed experimental demonstration or a comprehensive environmental assessment.

Future work will validate the framework through controlled printing trials using recycled substrates, environmentally preferable ink systems, and clearly separated anilox and halftone-screen parameters. The resulting measurements will support grouped model development, cross-validation, model selection, and independent testing, while a functional AR prototype will be evaluated using measurable recognition metrics. The validation will determine whether the workflow can improve material selection, colour consistency, production efficiency, and waste-related indicators without overstating these outcomes as a full LCA or comprehensive sustainability assessment.

6. Acknowledgments

7. References

Abusaq, Z., Zahoor, S., Habib, M. S., Rehman, M., Mahmood, J., Kanan, M. and Mushtaq, R. T. (2023) 'Improving energy performance in flexographic printing process through lean and AI techniques: a case study', *Energies*, 16(4), 1972. DOI: https://doi.org/10.3390/en16041972

Accardi, S., Campo, C., Bilucaglia, M., Zito, M., Caccamo, M. and Russo, V. (2025) 'Static vs. immersive: a neuromarketing exploratory study of augmented reality on packaging labels', *Behavioral Sciences*, 15(9), 1241. DOI: 10.3390/bs15091241

Azarenkov, V. I. and Deineko, Zh. V. (2025) 'A study on the use of artificial intelligence for building digital profiles of printing equipment'. In: *Printing, multimedia and web technologies: Modern trends.* Vol. 2. Printing House Madrid, pp. 5–26. DOI: 10.30837/PMW.2025.T2.005

Basak, S., Saritha, P. C., Maity, A. and Paul, K. C. (2025) 'Prediction of dot gain in flexographic color printing using machine learning', *Journal of Graphic Engineering and Design*, 16(4), pp. 37–49. DOI: 10.24867/JGED-2025-4-037

Bijitkar, S. and Moule, A. (2024) 'Design thinking: A tool for creative package design', *IIFT International Business and Management Review Journal*, 2(1), pp. 8–18. DOI: 10.1177/jiift.241273716

Bolanča, S., Mrvac, N. and Hajdek, M. (2018) 'Packaging through time', *Acta Graphica: Znanstveni časopis za tiskarstvo i grafičke komunikacije*, 29(4), pp. 29–38. DOI: https://doi.org/10.25027/agj2017.28.v29i4.159

Davidescu, M. A., Pânzaru, C., Mădescu, B. M., Poroșnicu, I., Simeanu, C., Usturoi, A., Matei, M. and Doliș, M. G. (2025) 'Advances and challenges in smart packaging technologies for the food industry: Trends, applications, and sustainability considerations', *Foods*, 14(24), 4347. DOI: 10.3390/foods14244347

European Union (2025) 'Regulation (EU) 2025/40 of the European Parliament and of the Council of 19 December 2024 on packaging and packaging waste, amending Regulation (EU) 2019/1020 and Directive (EU) 2019/904, and repealing Directive 94/62/EC', *Official Journal of the European Union*, L 2025/40, 22 January 2025.

Gu, C., Huang, T., Wei, W., Yang, C., Chen, J., Miao, W., Lin, S., Sun, H. and Sun, J. (2023) 'The effect of using augmented reality technology in takeaway food packaging to improve young consumers' negative evaluations', *Agriculture*, 13(2), 335. DOI: 10.3390/agriculture13020335

International Organization for Standardization (2013) *ISO 18604:2013. Packaging and the environment — Material recycling*. Geneva: International Organization for Standardization.

Jin, W., Chen, W. and Ma, K. (2024) 'Sustainable packaging user-centered design employing CycleGAN and deep learning', *BioResources*, 19(4), pp. 7824–7841. DOI: 10.15376/biores.19.4.7824-7841

Rani, M. N. H. A. and Ramlie, M. K. (2023) 'The utilization of augmented reality (AR) applications as packaging design enhancement', *International Journal of Academic Research in Business and Social Sciences*, 13(7), pp. 251–274. DOI: 10.6007/IJARBSS/v13-i7/17332

Savickas, A., Stonkus, R. and Jurkonis, E. (2020) 'Investigation of anilox roller cell clogging', *Journal of Graphic Engineering and Design*, 11(2), pp. 61–67. DOI: 10.24867/JGED-2020-2-061

Strižić Jakovljević, M., Mahović Poljaček, S., Jamnicki Hanzer, S., Donevski, D. and Tomašegović, T. (2024) 'Towards expanding the use of paper made from recycled and non-woody plants: enhancing the print quality through the application of nano-modified offset inks', *Sustainability*, 16(11), 4785. DOI: https://doi.org/10.3390/su16114785

Svanes, E., Vold, M., Møller, H., Pettersen, M. K., Larsen, H. and Hanssen, O. J. (2010) 'Sustainable packaging design: a holistic methodology for packaging design', *Packaging Technology and Science: An International Journal*, 23(3), pp. 161–175. DOI: https://doi.org/10.1002/pts.887

Tomašegović, T., Pibernik, J., Mahović Poljaček, S. and Madžar, A. (2021) 'Optimization of flexographic print properties on ecologically favorable paper substrates', *Journal of Graphic Engineering and Design*, 12(1), pp. 37–44. DOI: 10.24867/JGED-2021-1-037

Yılmaz, U., Tutus, A. and Sönmez, S. (2022) 'Effects of using recycled paper in inkjet printing system on colour difference', *Pigment & Resin Technology*, 51(3), pp. 336–343. DOI: https://doi.org/10.1108/PRT-03-2021-0032



© 2026 Authors. Published by the University of Novi Sad, Faculty of Technical Sciences, Department of Graphic Engineering and Design. This article is an open access article distributed under the terms and conditions of the Creative Commons Attribution license 4.0 Serbia (http://creativecommons.org/licenses/by/4.0/rs/).

Graphic design and visual communication

04

Professional Paper https://doi.org/10.24867/GRID-2026-p41

Promotion of the Dixi Variable Typeface Family for Readers with Dyslexia

Ana Stevanovski
Tanja Medved
Klementina Možina

University of Ljubljana, Faculty of Natural Sciences and Engineering, Department of Textiles, Graphic Arts and Design, Ljubljana, Slovenia

ABSTRACT

This study presents the development of Dixi, a variable typeface designed to improve legibility for individuals with dyslexia while remaining suitable for everyday use by a wider audience. Based on a review of typographic recommendations and existing dyslexia-oriented typefaces, several key design principles were identified: increased letter spacing, a larger x-height, simplified sans-serif letterforms, and enhanced differentiation between visually similar characters. These principles guided the creation of four typeface variants: Dixi Regular, Dixi Round, Dixi Regular Contrast, and Dixi Round Contrast. To address the highly individual nature of dyslexia, the typeface was developed as a variable typeface, allowing continuous adjustment of visual characteristics through interpolation axes. The effectiveness of the different variants was evaluated with a group of adult readers with dyslexia. The results demonstrate the potential of variable typography to support individual reading preferences while maintaining aesthetic quality and functional legibility. To further communicate the benefits of the typeface, a promotional presentation was developed. The promotion highlights the functionality and adaptability of the variable typeface system, showing how users can customise typographic characteristics according to their individual reading needs and preferences. The Dixi typeface demonstrates how legibility, aesthetics, and personalisation can be successfully integrated within a contemporary variable typeface system.

KEY WORDS
Dixi, dyslexia, legibility, promotion material, typeface design, typography, variable typeface

1. Introduction

Dyslexia affects more than 5% of the population and is one of the most common reading disorders (Lyon, Shaywitz & Shaywitz, 2003). It is a neurodevelopmental condition characterised by difficulties in linking written letters with sounds, often accompanied by challenges in reading, spelling and speech. These difficulties are unrelated to intelligence or educational level (Lyon, Shaywitz & Shaywitz, 2003; Snowling, 2003). Current research views dyslexia as a combination of phonological and orthographic deficits that vary between individuals, suggesting that no single typographic solution can suit all dyslexic readers (Moura, 2020; Snowling, 2003; Stein, 2023).

Typography plays an important role in reading, particularly for people with dyslexia. Research shows that typeface design, character differentiation and text variables such as size and spacing can influence legibility (Beier & Larson, 2010; Krivec et al., 2020; Rello & Baeza-Yates, 2013). These findings underpin dyslexia-friendly guidelines, including the British Dyslexia Association's (BDA) style guide, which recommends clear sans-serif letterforms, larger x-heights and increased spacing (British Dyslexia Association, 2003; Yoliando, 2020). These principles informed the development of the Dixi typeface and were considered alongside broader typographic theory (Chang, 2020; Možina, 2023).

Several typefaces, including OpenDyslexic and Dyslexie, have been developed specifically for dyslexic readers. Their designers claim that features such as bottom-weighted strokes and pronounced differentiation of mirror-image letters prevent letter reversal and loss of place (Gonzalez, 2026). However, studies have not consistently demonstrated better reading performance than with conventional typefaces (Leeuw, 2010; Rello & Baeza-Yates, 2013; Somai, Peiris & Tigwell, 2025; Wery & Diliberto, 2017). This reinforces the need for adaptable rather than universal design solutions.

To address this challenge, Dixi was developed as a variable typeface. By combining four design masters across two interpolation axes, it enables users to adjust typographic characteristics to their individual reading preferences (Luthfiasari, Fadillah & Gunawan, 2023). The design process and user evaluation of Dixi are presented in detail elsewhere (Stevanovski, Medved & Možina, 2026).

Communicating a dyslexia-friendly typeface also presents a branding challenge. Positioning it solely as an assistive tool may reinforce associations with disability and reduce broader acceptance. Dixi was therefore designed and promoted as a typeface for everyone, combining dyslexia-friendly features with a contemporary visual identity.

This paper presents the design rationale behind the Dixi variable typeface family and its promotional strategy, demonstrating how legibility, personalisation and visual appeal can be integrated within a single typographic system.

2. Experimental part

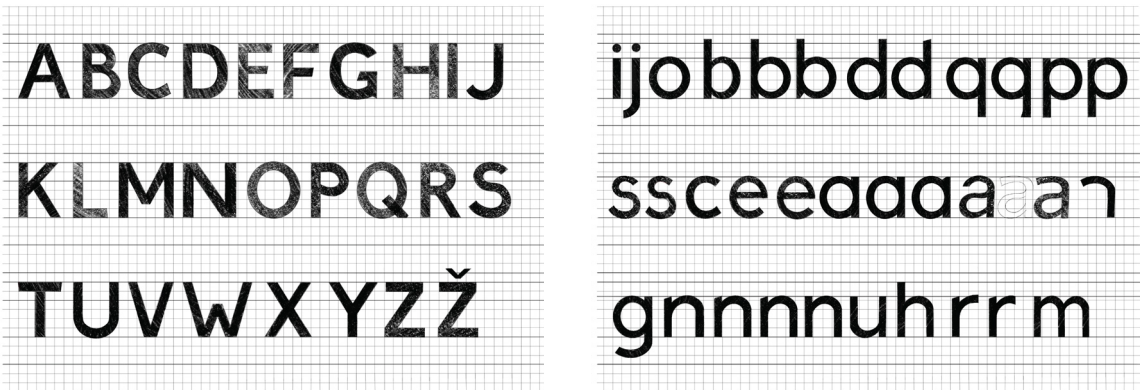
We designed the Dixi typeface in FontLab (https://www.fontlab.com), which enabled us to work with different masters. These gave us the option to create different instances of the Dixi typeface and define the variable axes. For the design of promotional graphics, we used Adobe Illustrator (https://www.adobe.com/products/illustrator.html). Additionally, vectorised graphics were imported into Adobe After Effects (https://www.adobe.com/products/aftereffects.html), which allowed us to create letter animations showcasing the typeface and its variability (Stevanovski, Medved & Možina, 2026).

2.1. Planning and design of the Dixi typeface family

The design process began with a visual analysis of seven reference typefaces (Arial, Helvetica, Verdana, Lexend, Comic Sans, Dyslexie, and OpenDyslexic), selected on the basis of legibility research and BDA recommendations (Beier & Larson, 2010; British Dyslexia Association, 2003; Rello & Baeza-Yates, 2013; Yoliando, 2020). Each typeface was visually analysed for its letterform characteristics, such as stroke width, x-height proportion, aperture size, letter spacing, and the differences between stroke shapes. Based on the analysis, objectives for the design of the Dixi typeface family were established. The objectives were as follows (Stevanovski, Medved & Možina, 2026):

- a clear sans serif typeface intended for general digital use,
- optimal typeface legibility,
- clear differentiation between characters,
- enlarged x-height,
- increased space between characters,
- multiple typeface variations with dyslexia-friendly features and
- variability between typefaces, allowing individual adjustments to user needs.

Based on the reference typeface analysis and the established objectives, sketches of individual letter and non-letter characters were made. These key design steps enabled us to define character parameters. Drawing and experimenting with different letterform stroke shapes led to the definition of the final proportions and variant characteristics (Figure 1). Through the sketching process, four versions of the typeface



» **Figure 1:** *Base sketches for Dixi typeface*

were defined. Three additional instances were based on the first basic sans-serif typeface, Dixi Regular. With the aim of emphasising distinctions between similar letterforms and introducing more circular, softer strokes, the Dixi Round typeface was planned. Subsequently, to test dyslexia-friendly letter proportions, contrasted versions of both typefaces (Dixi Regular Contrast and Dixi Round Contrast) were also sketched.

2.1.1. Designing the base typeface Dixi Regular and establishing proportions

The design process continued in FontLab, a software application for typeface design. At this stage, the sketches were digitally converted into vector glyphs. Before vectorizing the sketches, the vertical typeface proportions were defined. The typeface was developed at 1000 units per em (UPM). The overall type size was set to 910 units, with the x-height occupying 475 units. This configuration results in the x-height representing 52% of the total body height, which is significantly higher than in many standard typefaces (Stevanovski, Medved & Možina, 2026). The decision to use a higher x-height was made in accordance with BDA guidelines, which identify an enlarged x-height as a key factor in improving legibility for dyslexic readers (British Dyslexia Association, 2003), and with research confirming that increasing the size of the middle zone improves character recognition (Beier & Larson, 2010).

Assembly of the Dixi Regular vector glyphs began with the capital letter O, which served as the primary reference for establishing the width proportions of the remaining glyphs. To define the stroke thickness and contrast, the capital letter H was subsequently developed, providing the reference for the stroke widths used throughout the typeface. Bézier curves were used to construct both letterforms, allowing the relationship between the main strokes and the thinner strokes to be carefully defined. These proportions were then applied across the entire uppercase character set. In the capital letters, the thick stroke width is set at 100 units, while the thinnest stroke area measures 90 units, resulting in a difference of only 10 units. Stroke contrast in Dixi Regular is intentionally minimal. Special consideration was given to the overall width of the glyphs and the design of their counters.

After the uppercase character set had been completed, the design process continued with the lowercase characters. At this stage, the same principles were applied, focusing on the balance between character width, counter form structure, and the relationship between thicker and thinner strokes. In lowercase characters, the thickest stroke widths measure 88 units and the thinnest strokes 82 units. This uniform stroke width supports an even typographic tonal value across the page.

When all 118 characters, including numbers, punctuation, and special characters, had been designed, letter spacing was defined. Spacing was adjusted based on character shape according to the principles outlined in Chang (2020), followed by additional visual refinement to align with the typeface design goals. These were set slightly above standard values throughout, consistent with BDA recommendations for increased character spacing (British Dyslexia Association, 2003; Zorzi et al., 2012).

2.1.2. From single Dixi Regular typeface to the Dixi type family

A core design decision in the development of Dixi was to treat the project not as a single typeface but as a typeface family, with each variant serving a distinct typographic function while remaining visually coherent with the others. Four instances were developed: Dixi Regular, Dixi Round, Dixi Regular Contrast, and Dixi Round Contrast.Each instances began with the duplication of Dixi Regular into a new master. Masters are a FontLab feature that enabled us to duplicate all the characters into a new instance and adjust them, functioning similarly to layers in graphic design software. In addition, the use of masters allowed us to develop variability between typeface instances.

Dixi Round was developed through the careful introduction of curved, slightly inclined strokes intended to evoke characteristics of handwriting. These features produced a softer, more rounded appearance.

The contrasted variants (Dixi Regular Contrast and Dixi Round Contrast) introduce bottom-weighted stroke variation into both previously designed styles. By adding weight to the lower parts of the character strokes, we aimed to adopt the purported dyslexia-friendly features used in OpenDyslexic (Gonzalez, 2011) and Dyslexie (Boer, 2008) to improve reading performance for dyslexic readers.

In Dixi Regular Contrast, the thick stroke of capital letters increases from 100 to 130 units in the lower portion of each character, and the thin stroke from 90 to 115 units. In lowercase letters, the wide stroke increases from 88 to 108 units, and the narrow stroke from 82 to 100 units.

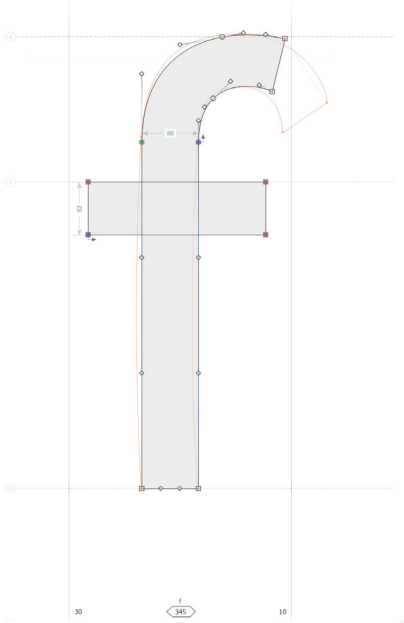
In Dixi Round Contrast, the bottom stroke contrast is more pronounced. The thick stroke in capital letters increases from 100 to 135 units, and the thin stroke from 90 to 125 units. The greater contrast in this variant reflects the design intention that this instance should represent the furthest point from standard sans-serif conventions, while Regular Contrast occupies a middle ground. Increased letter spacing was applied in both contrast variants to compensate for the additional stroke weight.

The key distinction between designing a single typeface and designing a family lies in this systematic relationship between variants. Each variant in Dixi shares the same vertical proportions, spacing system, and base letterform architecture, differing only in the specific parameters that define its typographic instances. This coherence is what allows the family to function as a variable typeface system and as a sound basis for comparing the performance of instances (Beier & Larson, 2010).

2.1.3. Implementation of variable axes between instances

The four instances of Dixi were connected through two interpolation axes defined in FontLab, enabling the typeface to be exported and used as a variable typeface in OTF variable format. This was possible because each instance was designed in its own master. For the interpolation to work, each corresponding letter across the masters had to share the same contour, with the same number of anchor points of the same type (on-curve or off-curve). Only under these conditions did each anchor point have a single unambiguous counterpart in every other master, allowing FontLab to map the outlines onto one another and generate continuous intermediate forms.

Maintaining this correspondence was difficult, as the instances differ in stroke form. The Dixi Round variant introduces curved strokes and additional terminals, which created a challenge in aligning it with the Regular instances. To keep the masters compatible after Dixi Round was designed, additional anchor points were added to the Dixi Regular instance to ensure the two matched. Figure 2 shows the letter outline with the anchor points of the glyph f



» **Figure 2:** *Outline of character f (orange outline Dixi Round and black Dixi Contrast)*

overlaid across the Regular and Round instances. FontLab's master-compatibility check was used throughout to resolve mismatches before export.

With all the elements in place, the two axes were defined. The x-axis, named Custom, operates along the horizontal dimension with values from 0 to 1000. It controls the interpolation between the Regular and Round variants. A value of 0 corresponds to the Regular letterform structure; a value of 1000 corresponds to the Round structure with its curved strokes, inclined terminals, and differentiated confusable letters (d, b, p, q I, l, …).

The second y-axis, named Contrast, operates along the vertical dimension with values from 0 to 100. It controls the interpolation between the Regular and Regular Contrast variants, and simultaneously between the Round and its Contrast variants. A value of 0 corresponds to a uniform stroke width throughout the letterform; a value of 100 corresponds to maximum bottom-weight contrast, while intermediate values produce letterforms with a continuously adjustable degree of stroke contrast (Figure 3).

2.2. Designing promotional material for the Dixi typeface family

Promoting a typeface designed for dyslexic readers presents a particular communication challenge because the typeface must be perceived as both functionally supportive and visually appealing. Typefaces positioned solely as assistive tools for dyslexia may risk reinforcing associations with disability, which can influence user acceptance. Research has also shown that specialised dyslexia typefaces such as Dyslexie and OpenDyslexic are not consistently preferred by readers with dyslexia when compared with conventional typefaces, despite their intended accessibility benefits (Kuster et al., 2017; Leeuw, 2010; Wery & Diliberto, 2017). Dixi was therefore designed and promoted as a typeface for everyone, incorporating dyslexia-friendly characteristics within a contemporary and broadly appealing visual language. This positioning informed the overall promotional strategy.

For the Dixi typeface family, a logo was first developed in Adobe Illustrator. In Adobe After Effects, the logo was then animated into a loop.

For the promotion of the typeface, a specimen poster, social media posts and short promotional animations were created. All materials showcase the range of the Dixi typeface family and its purpose through purely typographic compositions. The specimen poster was produced in A3 format in three monochrome colourways (blue, black and white). Animations and social media posts were created on a 1350 by 10180 px canvas to suit a variety of social media platforms.



» **Figure 3:** *Display of the master list (3a) and the graph display of interpolation axes (3b)*

To enhance the versatility of the typeface and encourage its use, the slogan "Črkovna vrsta, tako za dislektike, kot tudi za vse ostale" (Slovenian for "A typeface for dyslexics, as well as everyone else") was used.

3. Results and Discussion

Dixi was designed to enhance legibility and help minimise dyslexic symptoms. All Dixi instances contain 118 characters needed for Slovenian and English (Stevanovski, Medved & Možina, 2026).

3.1. Planning and design of the Dixi typeface family

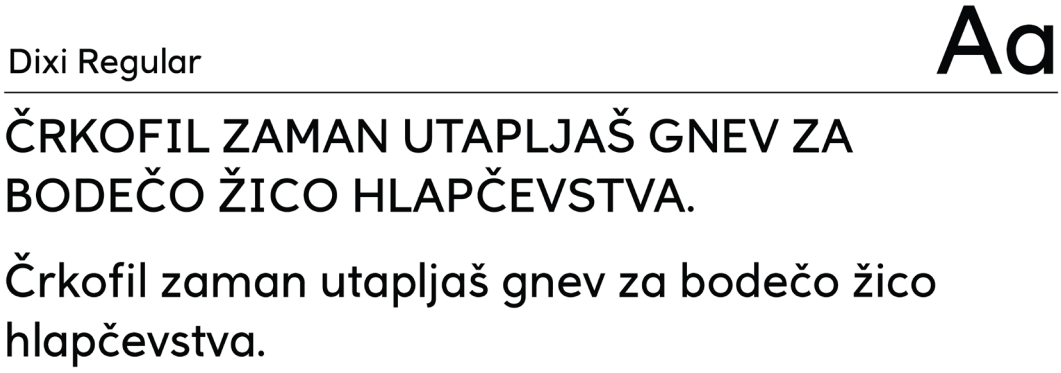
Analysis of reference typefaces for Dixi revealed several shared characteristics. All are sans-serif typefaces. Except for Arial, they exhibit increased apertures at stroke terminals. Typefaces designed for or recommended for dyslexic readers (Lexend, Comic Sans, OpenDyslexic, and Dyslexie) are characterised by a higher x-height, increased letter spacing, and bifurcated forms in characters such as a and g.

3.1.1. Designing the base typeface Dixi Regular and establishing proportions

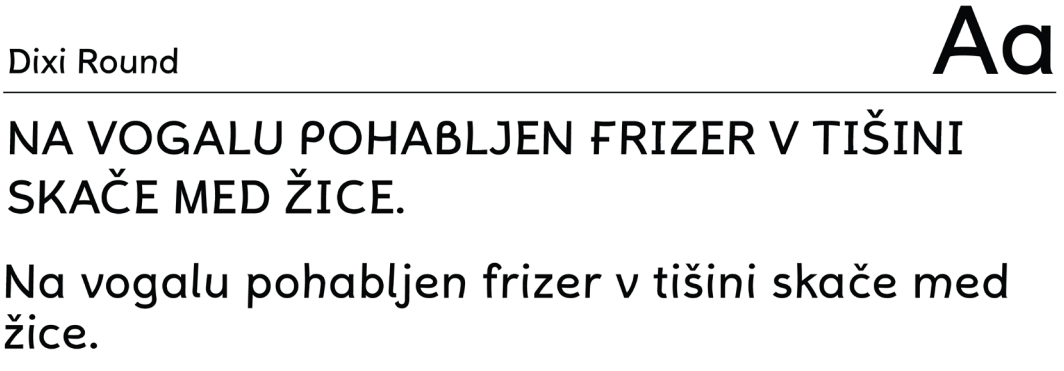
Dixi Regular (Figure 4) serves as the foundational style within the Dixi typeface family. It was designed as a sans-serif typeface with a strong emphasis on legibility. The typeface is intended for use by readers with and without dyslexia (Stevanovski, Medved & Možina, 2026).

To support faster recognition of sentence boundaries, punctuation marks in this typeface were designed with heavier weights than the main strokes. This decision was based on the idea that they would allow faster recognition of sentences, as discussed in Dislexi and OpenDyslexic research on reducing errors caused by losing track while reading (Leeuw, 2010; Stevanovski, Medved & Možina, 2026; Wery & Diliberto, 2017).

Additional specific letterform decisions were made to improve legibility and speed up differentiation between characters. The letters I, l, and numeral 1 were differentiated through the addition of serifs to I and J, and a distinct form for the 1. The lowercase t received a rounded terminal to distinguish it from l and f.



» **Figure 4:** *Pangrams set in Dixi Regular*



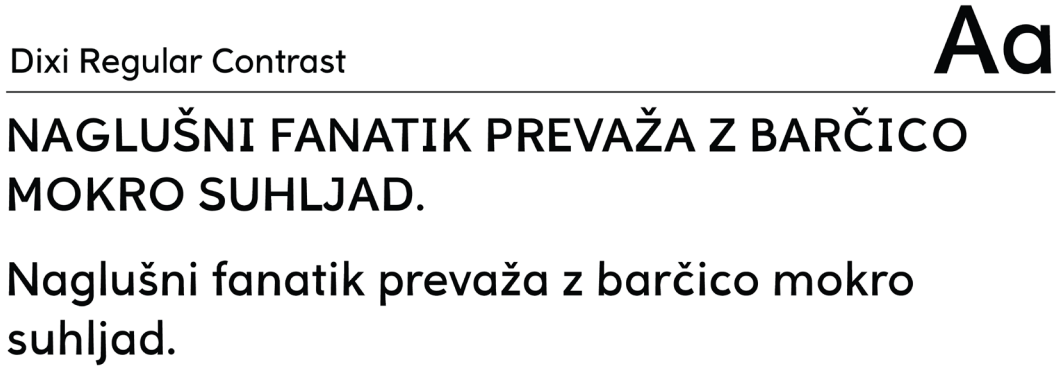
» **Figure 5:** *Pangrams set in Dixi Round*

The apertures of c, č, e, and g were enlarged to prevent confusion with o and with each other. The lowercase a and g were designed in their monocular forms to reduce visual complexity, which is also consistent with the approach taken by the reference typeface Lexend and several BDA-recommended typefaces (British Dyslexia Association, 2003). When designing additional variants, further dyslexia-friendly characteristics were added.

3.1.2. From single Dixi Regular typeface to the Dixi type family

In Dixi Round (Figure 5), the letters b, d, p, and q were redesigned so that no two are mirror images of one another. Each has a distinct combination of stroke-terminal form, internal counter shape, and baseline ending. The letters C, c, Č, and č received further enlarged apertures. The eye of the lowercase e was made conspicuously round. The descending strokes of g and j were enlarged to emphasise the visual weight of the character. Diacritical marks were redrawn with additional stroke contrast. Punctuation was further enlarged and drawn in a uniform shape for an even clearer distinction of sentences. All Dixi Round characteristics include subtly oblique, softened strokes intended to evoke a handwritten appearance. Many strokes are gently curved to reinforce this effect, including crossbars in A, F, H, J, T, 2, 5, and 7, as well as modified stroke weight in the lower parts of D, E, g, h, I, i, L, l, q, and 1, and diagonals in N, v, w, W, y, Z, z, Ž, and ž. Several glyphs are slightly slanted, including D, d, F, J, K, l, m, n, p, R, t, U, u, 4, and 6. Lowercase a, d, q, and l feature serifed terminals, while the lowercase t has an enlarged terminal. Diagonals in v, w, and y follow a calligraphic curvature. Rounded glyphs such as O, Q, G, C, and 0 vary in character width, with a lengthened and curved tail in capital Q and an emphasised foot in capital G. The lowercase e maintains a distinctly round counter, while the loops of g and j are enlarged. Numerals are further differentiated, including a serifless numeral 1, an open numeral 4, enlarged lower curves in 3, 5, 6, and 8, and a crossbar in 7. Special characters such as @, #, &, €, $, %, and the slash were also redesigned to maintain stylistic consistency (Stevanovski, Medved & Možina, 2026).

These modifications collectively increase the visual distinctiveness of potentially confusable letterforms, addressing the orthographic deficit symptoms most commonly associated with reading errors in dyslexia (Rawson, 1986; Snowling, 2003). Most of the changes introduced from the Regular variant to the Round variant



» **Figure 6:** *Pangrams set in Dixi Regular Contrast*

Dixi Round Contrast **Aa**

UŽALJEN FANT SE HRABRO PODI SKOZI GOŠČAVO MACESNOV.

Užaljen fant se hrabro podi skozi goščavo macesnov.

» **Figure 7:** *Pangrams set in Dixi Round Contrast*

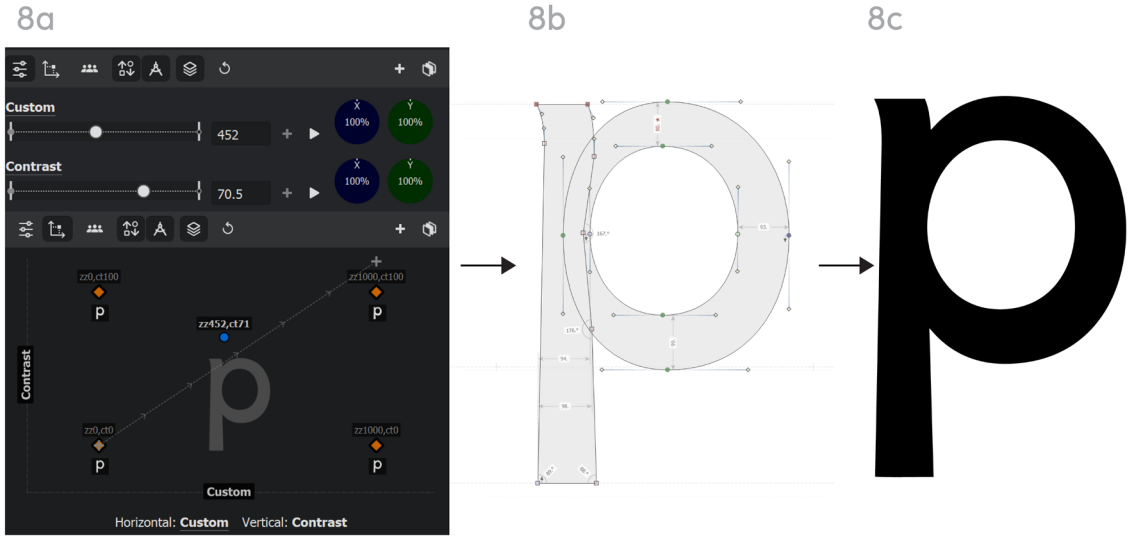
were intended to minimise the symptoms of dyslexia. Clearer differentiation between similar letterforms may help prevent or reduce letter transposition and loss of place during reading, while the slightly slanted, handwritten characteristics may promote more coherent word shapes and facilitate visual word recognition (Beier & Larson, 2010; Rello & Baeza-Yates, 2013). These factors may assist dyslexic readers in reading more effectively.

The final design variants were the contrasted versions of the previously described ones. Dixi Regular Contrast and Dixi Round Contrast retain the core characteristics of their original variants. Dixi Regular Contrast (Figure 6) features slightly reinforced strokes in the lower parts of the letterforms, balanced with increased character spacing. This ensures that the adjustments neither exaggerate nor disrupt the overall typographic tonal density, maintaining a visually balanced text appearance. In Dixi Round Contrast (Figure 7), the emphasised strokes are more pronounced, yet remain balanced in relation to the overall form and character spacing.

3.1.3. Implementation of variable axes between instances

The interpolation produces a continuous spectrum of letterforms rather than four fixed instances. Along the Custom axis, the form transitions from the Regular structure (0) to the Round (1000), with the strokes acquiring curvature and the terminals inclining. The second progression governs the Contrast axis, from uniform weight (0) to maximal bottom-weight contrast (100). At each stage, the contour structure remains consistent while the character form shifts. Variability was one of the key objectives of this work.

As shown in Figure 8, new letterforms can be created, unconstrained by predefined styles; the reader may traverse either axis until the letterforms suit their requirements. Figure 8a shows an interpolated point of the character p between the two axes marked in blue, Figure 8b shows the resulting contour, and Figure 8c shows a final outline of the interpolated character.



» **Figure 8:** *Interpolation of typeface variability in lowercase letter p – graph and slider controls for interpolation (8a) interpolated p (contour outline, 8b, and full character, 8c)*



» **Figure 9:** *Design of the Dixi logo from the word Dixi (9a), with the movement of letters (9b) to the final logo (9c)*

3.2. Designing promotional material for the Dixi typeface family

3.2.1. Logo design

We began the promotional material by designing a basic logo for the typeface, derived from the word “Dixi” itself. The design emerged from the observation that, by rotating the letter “i” by 90 degrees and placing it above the letters “xi”, the two dots of the “i” align into a single horizontal element, with the rotated “D” positioned above, as shown in Figure 9. Together, these elements create an abstract monogram that functions both as a typographic specimen and as a symbol. The primary logo is set in Dixi Regular; in addition, secondary variants were created for all styles.

The animations show how the word “Dixi” transforms into the logotype and back into text. The animation can be viewed by scanning the QR code in Figure 10.

» **Figure 10:** *QR code for the logotype animation*

3.2.2. Typeface specimen poster

The typeface specimen poster shown in Figure 11 sets white typography on a black background. The variants are distinguished by form rather than colour. The composition is built from the diagonal repetition of the word “Spremenljiva” (Slovenian for “variable”), shown in both outline and solid renderings. The outlined instances overlay the contours of all four variants (Regular, Round, Regular Contrast, and Round Contrast) so that their shared structure and points of difference become visible at once, while each solid instance shows a single variant. The alternation between overlapping outlines and filled forms demonstrates how one letterform shifts into another across masters, and thus emphasises the typeface’s variability. Below each solid text, a full set of characters is presented. The typeface logo sits in the upper-left corner with a QR code beneath it. The code (Figure 12) links to a short animation showing the typeface’s variability.



» **Figure 11:** *Dixi specimen poster*

» **Figure 12:** *QR code from the poster – representation of the typeface variability*

3.2.3. Promotional material for social media

The design of additional social media posts and animations extends the promotion of the typeface to a wider digital audience. We based the promotion on animations, as a large proportion of social media content is currently viewed in video format. The material presents the typeface variants and visually represents the family's capabilities. First, a promotional animation shows the letters D, i, x, and i in close-up as they change between variants, after which the characters draw back to assemble the Dixi wordmark. The animation closes with the slogan "Črkovna vrsta, tako za dislektike, kot tudi za vse ostale" (Slovenian for "A typeface for dyslexics, as well as everyone else") written beneath it. Set in the typeface itself, the slogan states the "for everyone" positioning directly, presenting accessibility as one feature of a broadly usable family rather than its defining limitation. The animation can be viewed by scanning the QR code in Figure 13.

» **Figure 13:** *QR code for the promotional animation*

A set of three short animations was then made, each isolating individual letters and presenting them across the variants. The first shows the uppercase and lowercase d set against typographic lines. Setting the letter against fixed baseline, x-height, cap height, and ascender lines gives the viewer a stable reference, so each shift in weight, contrast, and roundness reads as a measurable change. The letter d transforms from Dixi Regular into its contrasted form, then shifts to the Round Contrast variant. From here, the lowercase letter transforms into the uppercase D, which then shifts from Round Contrast to Round and finally back to the Regular variant. The animation ends with the transition from the capital D to the full word Dixi with the slogan these time in English written underneath. The animation can be viewed by scanning the QR code in Figure 14.

» **Figure 14:** *QR code for the animation of the letter d*

Two further animations present a group of letters as they switch through the variants. First, a group of the opening letters of the alphabet was chosen (A, b, c); this animation can be viewed by scanning the QR code in Figure 15. Next, a group of letters b, d, q, and p was chosen, as these often mirror each other and are among the most frequently confused by dyslexic readers (Rawson, 1986; Snowling, 1998). This animation, which can be viewed by scanning the QR code in Figure 16, demonstrates how visually similar letters become well differentiated across the instances. The animation of the and the typeface slogan were added in the end. In the a,b,c animation (figure 15) the slogan is presented in Slovenian while in animation d, q, p b (figure 16) the English slogan was used.

» **Figure 15:** *QR code for the animation of letters A, b, c*

» **Figure 16:** *QR code for the animation of letters b, q, p, d*

Finally, a four-part post displaying all characters of each instance was created. Each card carries one variant, showing its name, a large "Aa", and the full character set. The backgrounds alternate between black and white, placing the contrasted variants on white and the base variants on black. Swiping through the cards one at a time presents every character in a viewer-friendly way. These posts serve as a showcase of the typeface, just as the specimen poster does in physical form. A sample of one card showcasing Dixi Round is shown in Figure 17.

4. Conclusions

This study set out to develop and promote a variable typeface family that improves legibility for individuals with dyslexia while remaining aesthetically appropriate and adaptable for a wider readership. Dixi demonstrates that these objectives are not mutually exclusive, as dyslexia-friendly characteristics and broad everyday usability can be successfully integrated within a single, coherent typographic system.



» **Figure 17:** *One card from the four-part carousel, showing the Dixi Round variant*

The design outcome is a family of four instances: Dixi Regular, Dixi Round, Dixi Regular Contrast, and Dixi Round Contrast. These are built on a shared system of vertical proportions, spacing, and letterform architecture, and linked through two interpolation axes. Maintaining contour compatibility across masters made it possible to define a continuous, two-dimensional design space, rather than a fixed set of styles, in which roundness and bottom-weight contrast can be adjusted independently. This variability is the central contribution of the work and allows the typeface to be tuned to the individual needs of readers. The reading tests (Stevanovski, Medved & Možina, 2026) support the design rationale.

By positioning Dixi as a typeface for everyone, the accompanying promotional material, including a logo, specimen poster, social media posts, and supporting animations, communicates the accessibility features without framing the typeface as a disability tool. Through its slogan and social media-based promotion, it avoids the stigma that has limited the acceptance of earlier dyslexia-oriented typefaces. Taken together, the design, testing, and promotional material show how legibility, aesthetics, and personalisation can be integrated within a contemporary variable typeface.

The present study will be continued. Legibility testing should be conducted on a large and representative sample. Comparative testing with participants without dyslexia would help establish which effects are specific to dyslexic reading. On the basis of these findings, and the feedback gathered through the promotional materials, the Dixi typeface family will be further refined.

5. References

Beier, S. and Larson, K. (2010) 'Design improvements for frequently misrecognized letters', *Information Design Journal*, 18(2), pp. 118–137. DOI: 10.1075/idj.18.2.03bei

Boer, C. (2008) *Dyslexie [typeface]. Dyslexie Font*. Available from: https://www.dyslexiefont.com [Accessed 10 March 2026].

British Dyslexia Association. (2003) *Dyslexia style guide*. Available from: https://www.bumc.bu.edu/jmedday/files/2025/05/Dyslexia-Style-Guide-2023-BDA-Style-Guide-2023.pdf [Accessed 10 March 2026].

Cheng, K. (2020) *Designing type*. London: Laurence King Publishing.

Gonzalez, A. (2011) *OpenDyslexic – About*. Available from: https://opendyslexic.org/about [Accessed 10 March 2026].

Krivec, T., Košak Babuder, M., Godec, P., Weingerl, P. and Stanković Elesini, U. (2020) 'Impact of digital text variables on legibility for persons with dyslexia', *Dyslexia*, 26(1), pp. 87–103. DOI: 10.1002/dys.1646

Kuster, S. M., van Weerdenburg, M., Gompel, M. and Bosman, A. M. T. (2018) 'Dyslexie font does not benefit reading in children with or without dyslexia', *Annals of Dyslexia*, 68(1), pp. 25–42. DOI: 10.1007/s11881-017-0154-6

de Leeuw, R. (2010) *Special font for dyslexia?* Master's thesis. University of Twente.

Luthfiasari, A., Fadillah, C. and Gunawan, F. (2023) 'Fluid geometric: an experimentation of designing flexible multi-style typeface using variable font'. In: *2023 IEEE 9th International Conference on Computing, Engineering and Design (ICCED)*, Kuala Lumpur, Malaysia, 2023, pp. 1–6. DOI: 10.1109/ICCED60214.2023.10425659

Lyon, G. R., Shaywitz, S. E. and Shaywitz, B. A. (2003) 'A definition of dyslexia', *Annals of Dyslexia*, 53(1), pp. 1–14. DOI: 10.1007/s11881-003-0001-9

Možina, K. (2023) *Tipografska kunšt: upodobitev informacij*. Ljubljana: Univerza v Ljubljani, Naravoslovnotehniška fakulteta.

Moura, O., Pereira, M., Moreno, J. and Simões, M. R. (2020) 'Investigating the double-deficit hypothesis of developmental dyslexia in an orthography of intermediate depth', *Annals of Dyslexia*, 70, pp. 43–61. DOI: 10.1007/s11881-020-00190-1

Rawson, M. B. (1986) 'The many faces of dyslexia', *Annals of Dyslexia*, 36(1), pp. 177–191. DOI: 10.1007/BF02648028

Rello, L. and Baeza-Yates, R. (2013) 'Good fonts for dyslexia'. In: *Proceedings of the 15th International ACM SIGACCESS Conference on Computers and Accessibility (ASSETS '13)*, 21–23 October 2013, Bellevue, Washington. New York: Association for Computing Machinery, Article no. 14, pp. 1–8. DOI: 10.1145/2513383.2513447

Snowling, M. (1998) 'Dyslexia as a phonological deficit: evidence and implications', *Child Psychology and Psychiatry Review*, 3(1), pp. 4–11. DOI: 10.1111/1475-3588.00201

Somai, M. S., Peiris, R. L. and Tigwell, G. W. (2025) 'A review of text accessibility standards, guidelines, and font tool limitations'. In: *Proceedings of the 27th International ACM SIGACCESS Conference on Computers and Accessibility (ASSETS '25)*, pp. 1–7. DOI: 10.1145/3663547.3759692

Stein, J. (2023) 'Theories about developmental dyslexia', *Brain Sciences*, 13(2), article 208. DOI: 10.3390/brainsci13020208

Stevanovski, A., Medved, T. and Možina, K. (2026) 'Designing a variable typeface for dyslexia-friendly reading', *Acta Graphica*, 34(2), pp. 39–51.

Wery, J. J. and Diliberto, J. A. (2017) 'The effect of a specialized dyslexia font, OpenDyslexic', *Annals of Dyslexia*, 67(2), pp. 114–127. DOI: 10.1007/s11881-016-0127-1

Yoliando, F. T. (2020) 'A comparative study of dyslexia style guides in improving readability for people with dyslexia'. In: *Proceedings of the International Conference of Innovation in Media and Visual Design (IMDES 2020)*. DOI: 10.2991/assehr.k.201202.050

Zorzi, M., Barbiero, C., Facoetti, A., Lonciari, I., Carrozzi, M., Montico, M., Bravar, L., George, F., Pech-Georgel, C. and Ziegler, J. C. (2012) 'Extra-large letter spacing improves reading in dyslexia', *Proceedings of the National Academy of Sciences*, 109(28), pp. 11455–11459. DOI: 10.1073/pnas.1205566109



© 2026 Authors. Published by the University of Novi Sad, Faculty of Technical Sciences, Department of Graphic Engineering and Design. This article is an open access article distributed under the terms and conditions of the Creative Commons Attribution license 4.0 Serbia (https://creativecommons.org/licenses/by/4.0/deed.en).

Original Scientific Paper https://doi.org/10.24867/GRID-2026-p42

The Impact of Typography on Legibility for People with Dyslexia

Eva Jankulovska
Klementina Možina

University of Ljubljana,
Faculty of Natural Sciences and Engineering, Department of Textiles, Graphic Arts and Design,
Ljubljana, Slovenia

ABSTRACT

More than five per cent of the world's population are estimated to experience difficulties associated with dyslexia. This disorder affects communication abilities, particularly reading and writing. This study examined the impact of different typefaces on reading speed, text comprehension, and short-term memory in individuals with dyslexia. We tested two typefaces specifically designed for people with dyslexia (OpenDyslexic and Sylexiad Sans Spaced Med) and two commonly used typefaces (Arial and Comic Sans MS) that were not designed for this purpose. Four short texts were prepared, each written in a different typeface. Special care was taken to ensure that the texts were of approximately equal length and that they used the same type size and line spacing, thereby providing equal conditions for all participants. For each text, two questions were prepared: one to assess reading comprehension and another to evaluate short-term memory. After reading the texts and answering the questions, participants were also asked to share their subjective impressions and experiences regarding reading in the different typefaces. The study involved 20 participants with dyslexia, aged between 18 and 28 years. After calculating the average reading time for each typeface, the results showed that the text written in Arial, a general-purpose and non-specialised typeface, was read the fastest. In contrast, the text written in Sylexiad Sans Spaced Med required the longest reading time. The text with the highest percentage of correct answers was the one written in Comic Sans MS, whereas the text written in Sylexiad Sans Spaced Med achieved the poorest results. Most participants reported that the texts written in Comic Sans MS and Arial were the easiest to read. To generalise these findings, further research with a larger sample size and a broader age range of participants is required.

KEY WORDS
Dyslexia, comprehension, legibility, reading time, short-term memory, typography

1. Introduction

Dyslexia is a neurodevelopmental disorder that affects an individual's ability to read accurately and fluently despite normal intelligence and adequate educational opportunities (Lyon et al., 2003; González-Valenzuela et al., 2021; Łuniewska et al., 2021). Genetic factors play a significant role, as dyslexia frequently occurs within families (González-Valenzuela et al., 2021). It is one of the most common learning disorders, affecting more than 5% of the global population (Lyon, 2003; Dorwart, 2026). Individuals with dyslexia often experience visual crowding, a phenomenon in which closely spaced letters reduce text legibility. Increasing inter-letter spacing has been identified as an effective typographic intervention for improving reading performance (Evett et al., 2005; Beier et al., 2010; Łuniewska et al., 2021).

One of the most common difficulties associated with dyslexia is the confusion of visually similar letters, such as b and d or p and q. This difficulty is attributed to impaired visual discrimination, making it more challenging to distinguish between similar letterforms (Beier et al., 2010; Rello et al., 2013; Marinus et al., 2016; Mayo Clinic, 2026). Individuals with dyslexia frequently experience difficulties with spatial orientation while

reading, which affects their ability to track lines of text and recognise words efficiently. Consequently, they may lose their place on the page, skip lines, or reread the same words multiple times (Cleveland Clinic, 2026).

Because of deficits in linguistic information processing, reading is typically slower and less fluent for individuals with dyslexia. Additional time is required for word recognition and semantic processing, often resulting in increased cognitive effort, fatigue, and frustration (Dorwart, 2026).

A range of typographic interventions has been proposed to improve legibility for readers with dyslexia. Enlarged counters enhance the recognisability of letterforms, while extended ascenders and descenders improve the discrimination of visually similar characters (Wery, 2017). A slight letter slant may further facilitate the differentiation of similar letterforms (González-Valenzuela et al., 2021). In addition, increased spacing between letters, words, and lines reduces visual crowding and enhances overall legibility (Williams, 2020).

According to the study (Evett et al., 2005), the British Dyslexia Association (BDA) emphasises the importance of selecting simple letterforms and sans-serif typefaces. The BDA recommends typefaces such as Arial, Helvetica, Verdana, and Comic Sans (British Dyslexia Association, 2003).

Arial is a sans serif typeface characterised by uniformly weighted strokes and relatively large counters, which improve letter recognition (Možina, 2023). It is also one of the most widely used typefaces in the Microsoft Windows operating system.

Comic Sans MS was originally developed for comic-style text and younger computer users (Beaumont-Thomas et al., 2017). It features irregular stroke widths and rounded stroke terminals. To improve the distinction between visually similar characters, such as the uppercase I and the lowercase l, the capital I incorporates serifs (Možina, 2023).

Typefaces specifically designed for readers with dyslexia incorporate distinctive typographic features intended to enhance legibility (Rello et al., 2013; Marinus et al., 2016; Wery, 2017). Their primary objective is to maximise the visual distinction between similar letterforms while improving overall legibility (Bohm, 2019). Studies have shown that readers with dyslexia benefit from typefaces with pronounced ascenders and descenders, clearly distinguishable letterforms, and consistent stroke weight (Hillier, 2006; Marinus et al., 2016).

To improve the reading experience of individuals with dyslexia, several specialised typefaces have been developed, including OpenDyslexic, Sylexiad, and Dyslexie. These typefaces incorporate design features intended to enhance legibility and facilitate letter recognition (Hillier, 2006; Marinus et al., 2016; Wery, 2017; Laddusaw et al., 2019).

OpenDyslexic is characterised by heavier strokes at the bottom of each letter. This distinctive weighting is intended to reduce the perception that letters move or rotate during reading, thereby helping readers distinguish individual letters more effectively and reducing reading errors (Wery, 2017; Laddusaw et al., 2019).

Sylexiad is available in two versions: Serif Sylexiad and Sylexiad Sans. Both versions feature simple, rounded letterforms with long, light, uniformly weighted strokes (Hillier, 2006).

This study investigated the effects of different typefaces on reading speed, reading comprehension, and short-term memory in individuals with dyslexia. To address these objectives, the following hypotheses were formulated:

H1: Individuals with dyslexia will read texts presented in typefaces specifically designed for readers with dyslexia (OpenDyslexic and Sylexiad Sans Spaced Med) significantly faster than texts presented in conventional typefaces (Arial and Comic Sans MS).

H2: Participants will achieve higher scores on reading comprehension and short-term memory tasks when reading texts presented in dyslexia-oriented typefaces than when reading texts presented in conventional typefaces.

H3: Participants aged over 20 years will, on average, require less time to read the experimental texts than younger participants.

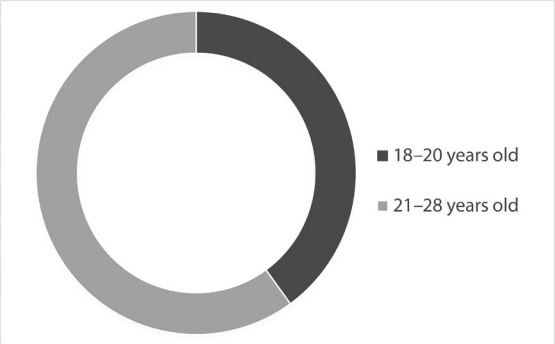
2. Experimental part

This study on the effects of different typefaces on reading speed, reading comprehension, and short-term memory in individuals with dyslexia was conducted at the offices of the Einstein Dyslexia Association in Skopje (Republic of North Macedonia).

The experiment took place in a controlled environment with five participants tested simultaneously. Although all participants were seated in the same room, each completed the tasks individually. The reading passages and accompanying questions were presented sequentially, one at a time.

The study included individuals with a prior clinical diagnosis of dyslexia. A total of 20 participants, aged between 18 and 28 years, took part. Thirteen participants (65%)

were female and seven (35%) were male. For a more detailed analysis of the results, participants were divided into two age groups. The first group consisted of eight participants aged 18–20 years, and the second included 12 participants aged 21–28 years (Figure 1). All participants reported normal or corrected-to-normal vision.



» **Figure 1:** *Age groups of the participants*

To evaluate legibility, we used four different texts selected from the magazine Fokus. The texts covered world news topics. They were slightly adapted so that, excluding spaces, they contained an average of 565 characters. Including spaces, the texts averaged 652 characters.

Each text was set in a different typeface. Two texts were presented in typefaces designed specifically for readers with dyslexia: OpenDyslexic (B) and Sylexiad Sans Spaced Med (C), a variant of the Sylexiad Sans typeface. The remaining two texts were presented in the standard typefaces Arial (D) and Comic Sans MS (A). OpenDyslexic and Sylexiad Sans Spaced Med were chosen because they were specifically designed for readers with dyslexia, whereas Arial and Comic Sans MS were selected because they are widely used online and are generally considered highly legible.

All four texts were set in a 10 pt with line spacing (i.e. leading) of 120% of the type size (i.e. 12 pt). The maximum number of characters per line was 57 for OpenDyslexic (B), 65 for Sylexiad Sans Spaced Med (C), 63 for Comic Sans MS (A), and 66 for Arial (D). Owing to its heavier letterforms and larger internal spacing, which require more horizontal space, the OpenDyslexic text accommodated fewer characters per line. All texts were left-aligned. Figures 2–5 present examples of the texts in the four typefaces. To ensure comparability across texts, all measurements were normalised to 650 characters.

After reading each text, participants answered two multiple-choice questions related to its content. The first question assessed reading comprehension and the second assessed short-term memory.Each question offered three response options, only one of which was correct.

At the end of the testing session, each participant took part in a brief interview to reflect on their overall experience. In particular, participants were asked which of the four typefaces they found easiest and most difficult to read, and to explain the reasons for their preferences.

Naučnicite identifikuvaa gen za koj velat deka može da se povrze so drevnoto poteklo na govorot, koj bil od klučno značenje za opstanokot na čovekot. Rezultatite od ova istražuvanje bea objaveni vo naučnoto spisanie "Natur Communications". Imeno, otkrieno e deka samo lugjeto imaat protein što, možebi, im pomognal da komuniciraat na nov način. Liza Finestek od Univerzitetot „Minesota", koja ne bila vklučena vo istražuvanjeto, reče deka ova e prviot čekor vo započnuvanjeto so proučuvanje na specifični geni što može da vlijaat na razvojot na govorot i na jazikot. Možebi, i naučnicite kje uspeat da im pomognat na onie so govorni mani.

» **Figure 2:** *Text set in Comic Sans MS (A)*

Minatata godina beše vtora posledovatelna godina na rekordna prodažba vo "Volvo", so isporačani 763.389 avtomobili, što e osumprocentno zgolemuvanje vo odnos na prethodnata godina. I pokraj ovoj soliden rezultat, brendot vo sopstvenost na "Geely" tvrdi deka se podgotvuva za „turbulentna 2025 godina poradi predizvikuvačkite pazarni uslovi". Za da ostane konkurentno, "Volvo" ja kompletira ažuriranata ponuda, vklučuvajkji osveženi proizvodi i novi dodatoci vo svojata paleta. Sepak, nema da se fokusira isključivo na električnite vozila. Tie vekje se otkažaa od planovite da bidat celosno električni do 2030 godina.

» **Figure 3:** *Text set in OpenDyslexic (B)*

Koga se počituvaat legendite, dostignuvanjeto dobiva pogolemo značenje. Najdobrite alpski skijački na site vreminja ne ostanaa ramnodušni vo poslednata nedela vo fevruari koga Mikaela Šifrin stana prvata vo istorijata koja ja postigna 100-tata pobeda vo Svetskiot kup. Ovoj unikaten podvig Amerikankata vo Sestriere go postigna malku neočekuvano, bidejkji po dvomesečno otsustvo od igrite poradi pad od Kilington, barem na neodamnešnoto Svetsko prvenstvo vo Zalbach-Hinterglemm, ne se pretstavi najubedlivo. Dvaeset i devetgodishnata skijačka dokaža deka šampionite nikogas ne se otpisuvaat i deka možat da bidat najdobri duri i koga, barem na hartija, ne se vo centarot na vnimanieto.

» **Figure 4:** *Text set in Sylexiad Sans Spaced Med (C)*

Estonija se izdvojuva kako edna od najmalku naselenite zemji vo Evropa, so prosečna gustina na naselenie od samo 30 žiteli na kvadraten kilometar. Ovaa niska naselenost ovozmožuva začuvuvanje na golemi zeleni površini i šumi, koi pokrivaat okolu 50 otsto od teritorijata. Šumite igraat klučna uloga vo pročistuvanjeto na vozduhot, apsorbirajkji jagledor dioksid i osloboduvajkji kislorod. Dopolnitelno, Estonija vložuva značitelni resursi vo koristenjeto na obnovlivi izvori na energija. Iako vo minatoto, golem del od električnata energija se dobivaše od nafteni škrilci, vo poslednite godini, zemjata značitelno ja namali upotrebata na fosilni goriva i se nasoči kon čisti izvori, kako veternici i biomasa.

» **Figure 5:** *Text set in Arial (D)*

3. Ressults and Discussion

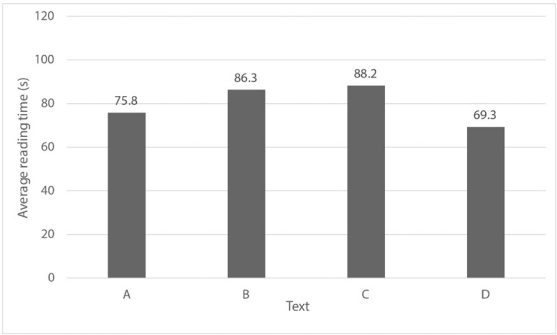
3.1. Reading time

The average time participants required to read the standardised texts was 79.9 seconds. This means that, on average, participants needed almost 80 seconds to read texts of equal length (650 characters).

A more detailed analysis of the standardised data revealed that participants required the least time to read Text D, which was presented in the Arial typeface. The average reading time for this text was 69.3 seconds, representing the fastest reading time recorded among all standardised texts. This finding further supports the conclusion that the Arial typeface is particularly suitable for fast reading, even among individuals with dyslexia. Its simple, clean design, straightforward letterforms, and consistent spacing between characters may contribute to improved legibility and reduced cognitive effort during reading, thereby facilitating text processing.

In contrast, participants required the most time to read Text C (i.e. Sylexiad Sans Spaced Med), with an average reading time of 88.3 seconds. This suggests that Text C was the most demanding and least efficient for rapid reading. A very similar result was observed for Text B (i.e. OpenDyslexic), which had an average reading time of 86.3 seconds. These findings indicate that certain typefaces, although specifically designed for individuals with dyslexia, do not necessarily lead to improved reading performance. After standardisation to a length of 650 characters, Text A (i.e. Comic Sans MS) was read in an average of 75.8 seconds, placing it among the more efficient texts, although it was not the fastest.

The results indicate that selecting a specialised typeface designed to assist individuals with dyslexia does not necessarily guarantee faster reading. Reading speed depends on multiple factors, including the visual clarity of the typeface, the reader's familiarity with a particular typographic style, and the subjective acceptability of the letterforms (Beier et al., 2011). In some cases, widely used typefaces, such as Arial, may enable faster and more fluent reading (Beier et al., 2013) than typefaces specifically developed for individuals with dyslexia.



» **Figure 6:** *Average standardised reading time for each text: (A) Comic Sans MS, (B) OpenDyslexic, (C) Sylexiad Sans Spaced Med, and (D) Arial*

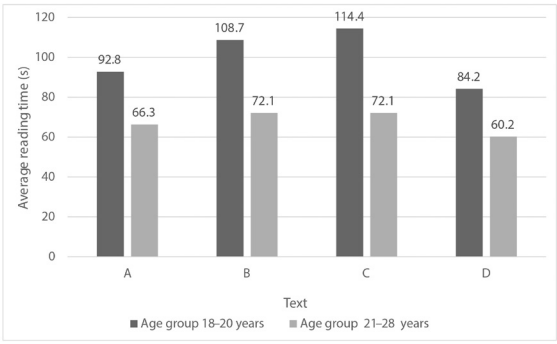
3.1.1. Reading time across different age groups

We were interested in whether individuals develop specific strategies over time that help them cope more effectively with the challenges associated with dyslexia, or whether prolonged exposure to reading and written materials influences reading speed and performance. We hypothesised (H3) that individuals who have lived with dyslexia for many years may gradually learn to adapt to their limitations, develop effective strategies for comprehending and processing texts and, consequently, improve their overall reading skills.

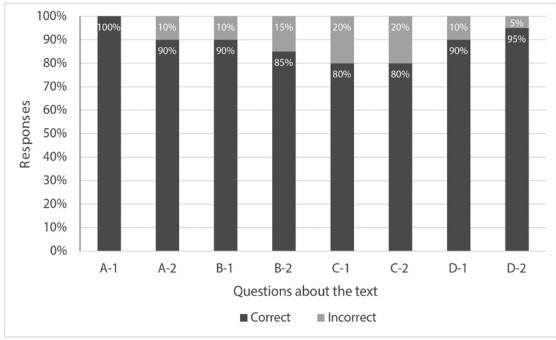
Participants were divided into two age groups: a younger group comprising individuals aged 18–20 years and an older group comprising participants aged 21–28 years (Figure 7). The results revealed clear differences in the time required to read the different texts. All reported values represent standardised data, meaning that the reading times were adjusted to an equivalent text length of 650 characters (including spaces) to ensure greater comparability.

The younger age group (18–20 years) required considerably more time, on average, to read all of the presented texts. The average reading times were 92.82 seconds for Text A (Comic Sans MS), 108.74 seconds for Text B (OpenDyslexic), 114.35 seconds for Text C (Sylexiad Sans Spaced Med), which represented the highest average reading time recorded within this age group, and 84.2 seconds for Text D (Arial). These findings suggest that younger participants may still be developing essential reading skills or may have had less exposure to different typefaces and typographic styles, which could influence their reading efficiency.

In contrast, the older participants (21–28 years) achieved substantially better results. Their standardised average reading times were significantly shorter: 66.34 seconds for Text A (Comic Sans MS), 72.13 seconds for Text B (OpenDyslexic), 72.10 seconds for Text C (Sylexiad Sans Spaced Med) and 60.20 seconds for Text D (Arial). This group therefore read both faster and more efficiently, supporting the assumption that prolonged experience with dyslexia enables individuals to develop strategies that improve reading performance. It appears that, over time, the older participants developed personal techniques such as visualisation, active prediction of meaning, the use of inner speech or filtering out irrelevant information, which allowed them to read more fluently and efficiently.



» **Figure 7:** *Average standardised reading time for participants aged 18–20 and 21–28 years: (A) Comic Sans MS, (B) OpenDyslexic, (C) Sylexiad Sans Spaced Med, and (D) Arial*



» **Figure 8:** *Percentage of correct and incorrect responses for texts presented in (A) Comic Sans MS, (B) OpenDyslexic, (C) Sylexiad Sans Spaced Med, and (D) Arial*

Based on these findings, it can be concluded that age, or more specifically long-term experience with dyslexia, has a significant influence on reading ability. Although dyslexia is a lifelong condition, individuals appear to develop increasingly effective coping strategies over time, contributing to faster reading speeds and improved overall performance in processing written material (Carioti et al., 2021; Basma et al., 2024).

3.2. Reading comprehension and short-term memory

Analysis of the collected data (Figure 8) revealed a high proportion of correct responses, indicating that the participants generally demonstrated a good understanding of the texts they had read. Six of the twenty participants answered all the questions correctly. The remaining participants made, on average, only one or two errors, suggesting a high level of reading comprehension and an effective ability to retrieve information from short-term memory.

Text A, presented in the Comic Sans MS typeface, yielded the highest level of accuracy. All 20 participants (100%) correctly answered the first question assessing text comprehension (A-1). The second question, which evaluated recall of the text (A-2), was answered correctly by 18 participants (90%). Consequently, the overall accuracy for the questions related to Text A was 95%.

The results for Text B, presented in the OpenDyslexic typeface, were slightly lower. The first question assessing comprehension (B-1) was answered correctly by 18 participants (90%), while the second question assessing recall (B-2) was answered correctly by 17 participants (85%). The overall accuracy for Text B was therefore 87.5%, representing a good level of performance, although slightly lower than that observed for Text A.

The lowest level of performance was observed for Text C, which was presented in the Sylexiad Sans Spaced Med typeface. Both questions associated with this text yielded identical results, with 16 of the 20 participants answering correctly, corresponding to an accuracy rate of 80%. Consequently, the overall accuracy for Text C remained at 80%, suggesting that this text was the most challenging in terms of both comprehension (C-1) and recall (C-2). Alternatively, its content or typographic presentation may have been somewhat less accessible to readers.

The final passage, Text D, presented in the Arial typeface, again produced a high level of response accuracy. The first question assessing comprehension (D-1) was answered correctly by 18 participants (90%), while the second question assessing recall (D-2) was answered correctly by 19 participants (95%), resulting in an overall accuracy of 92.5%. These findings indicate that Text D was among the easiest texts to comprehend, remember, and read within the study.

Overall, the findings suggest that differences in typeface had no substantial effect on either text comprehension or the ability to recall information. This is consistent with the findings reported by Beier et al. (2013). The participants successfully answered the majority of the questions regardless of the typeface used, indicating that they adapted well to different typographic presentations. The only notable exception was Text C, presented in the Sylexiad Sans Spaced Med typeface, which produced a slightly lower proportion of correct responses. This may indicate that the text was more demanding, either because of its content or its typographic design. Nevertheless, the overall results support the conclusion that individuals with reading difficulties, such as dyslexia, are able to comprehend written texts successfully.

3.3. Subjective reading experience

Most participants reported that Texts A (Comic Sans MS) and D (Arial) were the easiest to read. Although they did not identify the specific typographic features that contributed to the legibility of these typefaces, their positive evaluations may have been influenced by their

familiarity with them. As these typefaces are commonly used in everyday printed and digital materials, frequent exposure may have made them appear more familiar and, consequently, easier to read (Beier et al., 2013).

In contrast, opinions regarding the typefaces specifically designed for individuals with dyslexia were considerably more divided. Some participants appreciated the increased spacing between letters and lines, as well as the distinctive, playful letterforms of the OpenDyslexic typeface (Text B), reporting that these features helped them maintain focus and follow the text more easily. Others, however, expressed the opposite view, stating that such typefaces made reading more difficult because they perceived them as unusual, hard to read, or even distracting due to their unconventional letterforms and visual rhythm.

The most negative feedback was associated with Text C, which was presented in the Sylexiad Sans Spaced Med typeface and was generally considered the least suitable for reading. Participants frequently commented that the typeface appeared too small and that the letters and lines were spaced too closely, reducing the overall clarity of the text. As a result, they reported having to invest greater effort in identifying individual words and maintaining their place, which negatively affected their overall reading experience.

In addition, several participants noted that typefaces with softer, more rounded letterforms made reading easier, as they were perceived to be visually more comfortable and less tiring for the eyes (Medved et al., 2025).

4. Conclusions

The findings of this study did not support the expectation that typefaces specifically designed for individuals with dyslexia would facilitate faster or more efficient reading than conventional typefaces. Although reading times differed across the four typefaces, the pattern observed did not align with the initial hypothesis. The shortest average reading time was recorded for Arial, followed by Comic Sans MS, while the dyslexia-specific typefaces, OpenDyslexic and Sylexiad Sans Spaced Med, resulted in noticeably longer reading times. These findings suggest that specialised typefaces do not necessarily improve reading performance for all individuals with dyslexia. One possible explanation is participants' greater familiarity with conventional typefaces, which are encountered more frequently in everyday reading materials. In contrast, the distinctive design of OpenDyslexic, for example, may initially appear unfamiliar and therefore demand greater reading effort.

The analysis of comprehension accuracy showed that most participants answered the questions correctly, indicating a generally good understanding of the texts regardless of the typeface used. The highest level of accuracy was achieved for the text presented in Comic Sans MS (95%), whereas the lowest was observed for Sylexiad Sans Spaced Med (80%). This difference may reflect the influence of the typeface on legibility, although variations in text difficulty cannot be ruled out.

An additional finding was the difference between age groups. Participants aged 21–28 years read the texts faster, on average, than those aged 18–20 years. This may be explained by greater reading experience, more developed reading strategies, and improved adaptation to dyslexia over time.

Overall, the results indicate that the first hypothesis (H1), predicting faster reading with dyslexia-specific typefaces, was not supported. The second hypothesis (H2), which predicted better comprehension for texts presented in these typefaces, was only partially supported, as comprehension remained high for OpenDyslexic but was lower for Sylexiad Sans Spaced Med. The third hypothesis (H3), predicting faster reading among older participants, was supported.

Several limitations should be acknowledged. The study involved a relatively small sample, reflecting the practical challenges of recruiting participants with dyslexia. Future research should include larger and more diverse samples representing a broader range of age groups. In particular, further studies should investigate younger readers and older adults, who may have different typographic needs, including a preference for larger type sizes. Such research would contribute to a more comprehensive understanding of the relationship between typography and reading performance in individuals with dyslexia.

5. References

Basma, B., Savage, R. and Bertone, A. (2024) 'The N400 in readers with dyslexia: A systematic review and meta-analysis', *International Journal of Psychophysiology*, 196, 112283, pp. 1–14. DOI: 10.1016/j.ijpsycho.2023.112283

Beaumont-Thomas, B., Connare, V. and Stephens, T. (2017) 'How we made the typeface Comic Sans', *The Guardian*, 28 March 2017. Available from: https://www.theguardian.com/artanddesign/2017/mar/28/how-we-made-font-comic-sans-typography [Accessed 8 June 2026].

Beier, S. and Larson, K. (2010) 'Design improvements for frequently misrecognized letters', *Information Design Journal*, 18(2), pp. 118–137. DOI: 10.1075/idj.18.2.03bei

Beier, S. and Larson, K. (2013) 'How does typeface familiarity affect reading performance and reader preference?', *Information Design Journal*, 20(1), pp. 16–31. DOI: 10.1075/idj.20.1.02bei

Bohm, T. (2019) 'Letter and symbol misrecognition in highly legible typefaces for general, children, dyslexic, visually impaired and ageing readers', *TypographyGuru*. Available from: https://typography.guru/journal/letters-symbols-misrecognition/ [Accessed 8 June 2026].

British Dyslexia Association. (2003) *Dyslexia style guide*. Available from: https://www.bumc.bu.edu/jmedday/files/2025/05/Dyslexia-Style-Guide-2023-BDA-Style-Guide-2023.pdf [Accessed 5 March 2026].

Carioti, D., Masia, M.F., Travellini, S. and Berlingeri, M. (2021) 'Orthographic depth and developmental dyslexia: A meta-analytic study', *Annals of Dyslexia*, 71(3), pp. 399–438. DOI: 10.1007/s11881-021-00226-0

Cleveland Clinic. (2026) Dyslexia: *Finding a Way to Overcome Reading Difficulties*. Available from: https://my.clevelandclinic.org/health/diseases/6005-dyslexia [Accessed 7 February 2026].

Dorwart, L. (2026) 'The Types of Dyslexia'. Available from: https://www.verywellhealth.com/types-of-dyslexia-5214423 [Accessed 10 March 2026].

Evett, L. and Brown, D.J. (2005) 'Text formats and web design for visually impaired and dyslexic readers – Clear Text for All', *Interacting with Computers*, 17(4), pp. 453–472. DOI: 10.1016/j.intcom.2005.04.001

González-Valenzuela, M.-J. and Martín-Ruiz, I. (2021) 'Neuropsychological Perspective on Dyslexia'. In: Misciagna, S. (ed.) *Learning Disabilities – Neurobiology, Assessment, Clinical Features and Treatments*. London: IntechOpen, pp. 1–30. DOI: 10.5772/intechopen.99386

Hillier, R.A. (2006) *A typeface for the adult dyslexic reader.* PhD thesis. Anglia Ruskin University.

Laddusaw, S. and Brett, J. (2019) 'Dyslexia-friendly fonts: Using OpenDyslexic to increase exhibit access', *College & Research Libraries News*, 80(1), pp. 33–36.

Lyon, G.R., Shaywitz, S.E. and Shaywitz, B.A. (2003) 'A definition of dyslexia', *Annals of Dyslexia*, 53(1), pp. 1–14. DOI: 10.1007/s11881-003-0001-9

Łuniewska, M., Wójcik, M. and Jednoróg, K. (2022) 'The effect of inter-letter spacing on reading performance and eye movements in typically reading and dyslexic children', *Learning and Instruction*, 80, 101576. DOI: 10.1016/j.learninstruc.2021.101576

Marinus, E., Mostard, M., Segers, E., Schubert, T.M., Madelaine, A. and Wheldall, K.A. (2016) 'Special Font for People with Dyslexia: Does it Work and, if so, why?', *Dyslexia*, 22(3), pp. 233–244. DOI: 10.1002/dys.1527

Mayo Clinic. (2026) *Dyslexia – Symptoms and causes*. Available from: https://www.mayoclinic.org/diseases-conditions/dyslexia/symptoms-causes/syc-20353552 [Accessed 8 June 2026].

Medved, T., Podlesek, A. and Možina, K. (2025) 'Eye-tracking study on reading fluency in relation to typeface pleasantness influenced by cross-modal correspondence between taste and shape', *Applied Sciences*, 15(1), 326, pp. 1–16. DOI: 10.3390/app15010326

Možina, K. (2023) *Tipografska kunšt: upodobitev informacij*. Ljubljana: Univerza v Ljubljani, Naravoslovnotehniška fakulteta.

Rello, L. and Baeza-Yates, R. (2013) 'Good fonts for dyslexia'. In: *Proceedings of the 15th International ACM SIGACCESS Conference on Computers and Accessibility (ASSETS '13)*, 21–23 October 2013, Bellevue, Washington. New York: Association for Computing Machinery, Article no. 14, pp. 1–8. DOI: 10.1145/2513383.2513447

Wery, J.J. and Diliberto, J.A. (2017) 'The effect of a specialized dyslexia font, OpenDyslexic', *Annals of Dyslexia*, 67(2), pp. 114–127. DOI: 10.1007/s11881-016-0127-1

Williams, G.F. (2020) 'A guide to understanding what makes a typeface accessible', *Medium*. Available from: https://medium.com/the-readability-group/a-guide-to-understanding-what-makes-a-typeface-accessible-and-how-to-make-informed-decisions-9e5c0b9040a0 [Accessed 8 June 2026].



© 2026 Authors. Published by the University of Novi Sad, Faculty of Technical Sciences, Department of Graphic Engineering and Design. This article is an open access article distributed under the terms and conditions of the Creative Commons Attribution license 4.0 Serbia (https://creativecommons.org/licenses/by/4.0/deed.en).

Professional Paper https://doi.org/10.24867/GRID-2026-p43

Partisan Graphic Art and the Contemporary Construction of Collective Memory

ABSTRACT

Paper examines partisan printmaking as one of the most important forms of communication, artistic expression, and propaganda in Slovenia during the Second World War, and its influence on contemporary graphic design. Effective visual communication requires messages that are clear, accessible, and quickly understood by the public. These principles were already present in early propaganda practices following the First World War and reached their peak in partisan graphic production during the national liberation struggle. Partisan print encompassed posters, leaflets, newspapers, brochures, illustrations, caricatures, book design, partisan currency, and other printed materials. Despite severe material and technical limitations, it served as a powerful tool for the dissemination of information, political mobilisation, and the strengthening of national identity. Its visual language relied on direct communication, strong symbolism, expressive figuration, reduced visual elements, and purposeful typography. Beyond supporting the armed resistance, partisan print became an integral part of a broader cultural movement that connected the visual arts, literature, music, and theatre. Building on this legacy, a design-research project marking the 80th anniversary of the end of the Second World War was carried out within the course Visual Analysis of Graphic Products. Through posters, illustrations, photography, digital collages, and animation, students explored contemporary meanings of war, peace, and freedom while establishing a dialogue between partisan visual heritage and present-day social realities. The study demonstrates that partisan print remains a relevant model of visual communication and a valuable cultural heritage that continues to inspire contemporary design through its immediacy, symbolic power, and social engagement.

Boris Beja

University of Ljubljana, Faculty of Natural Sciences and Engineering, Department of Textiles, Graphic Arts and Design, Ljubljana, Slovenia

KEY WORDS
Partisan propaganda, poster, visual communication, collective memory

1. Introduction

In 2025, we commemorated peace and victory over the occupying forces that shaped the lives of countless people across Europe during the Second World War. These celebrations sought to revive the sense of relief, hope and joy that spread throughout Europe after the war had ended. The year also marked several important Slovenian anniversaries connected to the post-war period. We celebrated 80 years of *Mladinska knjiga* and commemorated the 80th anniversary of the *United Nations*. Numerous institutions founded in 1945 also reached significant milestones, including *Cankarjeva založba, DZS, Elan, Fructal, NK Olimpija,* the *RTV Slovenia Big Band,* the *Academy of Fine Arts,* and the *Academy of Theatre*. The newspapers *Večer* and *Primorske novice* were established that same year, as was *Ciciban*, the children's magazine that became an important part of Slovenian cultural life (Vurnik, 2025).

The course *Artistic Analysis of Graphic Products 2* explores the spaces and graphic artefacts that have

shaped visual culture in Slovenia over the past century. Although space itself is limitless, graphic design traditionally confines it to a rectangular format through which visual messages are communicated and interpreted. This reminds us that neither space nor peace should be taken for granted. Both are values that societies continually define, shape and strive to preserve.

1.1. Slovenian Propaganda

Twentieth-century Slovenian graphic design was shaped by four significant historical turning points that profoundly influenced its visual language, appearance, and theoretical understanding. Through bold artistic and formal solutions, designers and artists contributed to the development of graphic production and, through propagandistic methods of communication, also influenced wider social structures. The origins of propaganda in the Slovenian context can be traced back to the First World War, when new methods of informing and mobilising the public began to emerge. Its development continued during the Second World War and, in many respects, persists in contemporary society, where propaganda continues to evolve and seek new ways of achieving its objectives. The poster is a visual message that serves economic, political, or cultural interests. It functions as a medium of communication and is created through the collaboration between a client and a designer. As a communicative form, it combines photography, drawing, painting, and text into a unified visual statement (Požar, 2015).

The first propaganda turning point was the design of plebiscite leaflets for the Slovenian side, designed and illustrated by Maksim Gaspari. In 1918, the artist became an enthusiastic propagandist in Carinthia, creating a series of postcards, posters, and leaflets for General Maister (Mikuž, 1977). The second turning point was Partisan printing, which, in addition to leaflets, posters, occasional publications and periodical press, also produced artistic graphic portfolios. The visual language of Partisan printing was highly diverse. It occasionally adopted new traditions whenever it was possible to follow them. Drawing upon the tradition of pre-war realism, it also engaged with modernism. The artistic and typographic organisation of texts continued and transmitted the experience of modern graphic design, which itself found its models in the revolutionary stylistic expressions of the pre-war and interwar periods. As a temporary art form, it achieved remarkable artistic results in various environments and under spatially impossible conditions (Požar, 2015).

1.2. Partisan Art and Women

Until the Second World War, women occupied a subordinate position in Slovenian visual art, appearing either as portrait subjects or as the artist's muse. Only with the national liberation struggle, when many women took on and performed demanding work in industry and agriculture outside the battlefields, did Slovenian women become equal members of society. These developments were reflected in visual motifs printed on magazine covers, leaflets, and posters. Female and male fighters were consistently depicted with enthusiasm, in a fighting spirit, and in dynamic poses (Figure 1). The iconography is characterized by hostages, wounded people, burned villages, the aggressor, the occupier, flags, broken chains, clenched fists, and similar motifs. All of these elements symbolized the strong resistance of the people, in which women also participated.

This is evident in the work of Nikolaj Pirnat, titled *Partisan Woman in the Assault (Partizanka v jurišu)*, where one of the first depictions of a woman wearing trousers in Slovenian visual art can be observed. The partisan woman clearly points in the direction of resistance with her left hand. She is depicted as the largest figure in the central foreground, while competing visually with the tricolour flag bearing the red five-pointed star. Equal to the male soldiers, she carries a weapon in her right hand (Mikuž, 1977).



» **Figure 1:** *Nikolaj Pirnat, Female Partisan in an Assault, 1944*

The depiction of women became equal to that of men during the National Liberation Struggle. Unlike in the First World War, during the Second World War women actively participated on the battlefields and were also part of the resistance in the liberated territories, where culture and art were being established. They took part in dance and theatre performances as well as in visual art. Visual representations in Partisan art were accompanied by titles that emphasized the role of women and already foreshadowed their active inclusion in social structures after the war, when women were also granted the right to vote. A telling example is the work of Ivo Šubic, who, fol-

lowing the model of Ivan Vavpotič's *The Shackled One (Verigar)*, created the poster *Slovenian Woman, You Are Free and You Will Vote for the First Time* (1944). With clenched fists, the woman has freed herself from her chains, which flutter torn apart in the background, like her hair. The naturalistic depiction of the woman, executed in a classical graphic style with clear drawing and two colours, emphasizes the full plasticity of the body and, ultimately, the arrival of a new era, post-war reconstruction, modernization, and progress (Komelj, 2026).

2. Methods

2.1. Accompanying Exhibition of Student Responses to the Theme of the Second World War

Reflection on Partisan art was explored through contemporary forms of artistic expression and interpretation developed by students. Drawing inspiration from the graphic solutions and visual language of the past, an accompanying exhibition was conceived in collaboration with the Museum and Galleries of the City of Ljubljana. The exhibition was presented alongside Blaž Vurnik's exhibition *1495 Days: Ljubljana During the Second World War*, creating a dialogue between historical visual culture and contemporary artistic responses to the legacy of the Second World War.

2.2. Pedagogical Context and Instructions

The course *Artistic Analysis of Graphic Products 2* is, in its content, continuously based on space. Space, which is limitless, has in graphic production been confined in most cases to a rectangular format within which various artistic operations take place, and these continue and are subjectively interpreted by the recipient in public space. From this, it follows that space should not be taken for granted, and that humanity has deliberately limited it to four walls, within which the individual seeks to find peace. Even this, in contemporary times, and perhaps never, should not be taken for granted. With the second assignment, we created artistic solutions celebrating the 80th anniversary of the end of the Second World War. The visual statements, in the form of posters, were intended to interpret war and peace through metaphorical meanings, without the use of white doves, crosses, or memorial candles. Our intention was to celebrate rather than commemorate the past. The students were not limited in their approach and could address the theme and its interpretation through various fields of graphic creativity, including typography, illustration, 3D modelling, collage, photography, and abstract visual composition. The key aspect was the message and the visual appeal created either digitally or through traditional artistic media. The aim of the assignment was to encourage reflection not only on the visual message but also on the slogans that could be incorporated into the composition of the graphic work. Each work was also required to have its own title. The best works were publicly exhibited at the City Museum of Ljubljana.

2.3. How to Think about the Anniversary of the Second World War?

The artistic statements in the form of posters interpret war and peace. They also commemorate the 80th anniversary of the end of the Second World War. The statements of young people are not limited; although seemingly confined within a rectangular format, they build a dialogue between recent history and the present day. Through diverse media expressions, ranging from typographic solutions, digital illustration, photography and photomontage to traditional collages and those created with contemporary 3D graphic software, we have drawn upon the protagonists of graphic design in Slovenia.

The graphic solutions, or statements, also include slogans that further enhance the visual expression and message. Among them are: *A World That Promised Peace Again Burns in the Flames of Conflict, Inflated in Peace, The Wire Has Fallen, We Have Been Floating on the Wings of Freedom for 80 Years,* and *For 80 Years We Have Looked upon a Peaceful Sky*. Through these captions, we have presented the graphic concepts to the viewers of our posters without moralizing, but rather as a warning that, despite the appearance of peace, we can still hear the rumbling of weapons in our surroundings. And graphic art has always been a weapon. This was well understood by all totalitarian systems, which used propaganda print to construct new forms and relationships within society. Therefore, this project is also, in its own way, a tribute to Partisan art, which under impossible conditions provided information and, not least, visually interpreted messages that were printed in forests or in clandestine printing houses within urban environments.

3. Results

3.1. Manca Baša: Sredi zvezd, noč in dan

The illustration (Figure 2), created by Manca Baša, a master's student of Graphic and Interactive Communications, stems from a reflection on the image of the soldier, which in the collective consciousness is often marked by violence and fear. Soldiers are frequently perceived as anonymous actors of wartime slaughter, while overlooking the fact that beneath the uniforms are individuals.



» **Figure 2:** *Manca Baša: Sredi zvezd, noč in dan*

The author reinterpreted the image of the uniformed figure and expanded it through an accompanying soundscape, thereby evoking a sense of hope while simultaneously referencing the Allied forces whose D-Day operation heralded the eventual end of the Second World War. The depicted soldier does not carry a weapon but a musical instrument, replacing the destruction of war with the harmony of music and the promise of progress, of which graphic design also became a part in the post-war period. The watercolour transitions of blue tones in the sky surrounding the soldier-musician are complemented by a typographic slogan borrowed from the lyrics of a well-known Slovenian popular song. Zemlja pleše ("The Earth Dances") was first performed at the inaugural Slovenian Popular Music Festival in 1962. The music was composed by Mojmir Sepe, while the lyrics were written by Gregor Strniša. In the artwork, the word earth was replaced with war, drawing attention to the fact that, despite celebrating peace and victory over the occupiers, our planet continues to dance to the rhythm of wars, destruction, and human suffering.

The soldier portrayed in the illustration holds a musical instrument rather than a weapon. In this way, the work also commemorates the founding of the Dance Orchestra of Radio Ljubljana in 1945, today known as the RTV Slovenia Big Band. The element of destruction and intimidation is replaced by the melody of music, which symbolizes a quiet longing for peace, freedom, and a world beyond violence. The visual concept was further transformed from a poster into an animation in which the soldier flees from war and seeks to replace the sounds of weapons with music and marching with dance. Music and movement become a space of connection, where the rhythm of life is no longer dictated by violence but by peace. The musical score for the animated artwork was composed by Julijan Andrejaš and Timotej Duvnjak, adding a new experiential dimension for the viewer and further enhancing both the visual message and its perception.

3.2. Alen Fuks: Dance Brings Joy

The digital photomontage by Alen Fuks depicts a soldier in a cheerful pose wearing two different uniforms. This duality arises from the dialogue between a German military uniform and the uniform worn by the Partisans. During the cold winters, the Partisan army was grateful for the contributions and donations knitted for the soldiers by mothers and wives in different communities. A special issue of Mladina from the beginning of August concluded with the appeal: *Equip Our Army! Give all shoes, all clothes, everything to the fighters!*

The cut-up photograph, placed within an expanded composition, represents a dialogue between two soldiers in the contemporary era, where, dressed in different uniforms, we create alliances and fight together under the umbrella of NATO. The photograph, created in the costume collection of Viba Film, establishes a strong conceptual contrast, even though the soldier's smile remains the same in both uniforms (Figure 3). In doing so, the work offers the viewer a question and a reflection: whom? The literary work of Drago Jančar was further developed through a typographic intervention and experimentation in the form of packaging, where the author depicted the pet of the protagonist Ksenija Hribar and placed it, in the form of a preserving jar, within the context of supermarket shelves. In this way, peace and freedom were presented as values that had been preserved and canned for future generations.



» **Figure 3:** *Alen Fuks: Dance Brings Joy*

3.3. Eva Gašperič: Whose Star Is This?

The central motif of the star was adopted from a Slavic symbol of death, which, among other places, appeared on one of the sides of a cradle. By drawing the star, parents warded off evil forces from the newborn and ensured its safety. The central artistic object, which swings and is positioned on the surface of a mobile, is accompanied by the calligraphic inscription: *"Aja tu taja, peace is leaving us."*

Within this piece, we created a pattern to which a three-year-old child contributed with his drawing, while the flowers in the background of the pattern were painted by a right-handed artist using her left hand. The floral background symbolizes peace, which is being eroded by darkness in the form of a brown ground (Figure 4).



» **Figure 4:** *Eva Gašperič, Whose Star Is This?, 2026*

The motif of the star was developed through an intergenerational collaboration that included a retired woman, who hand-embroidered an enhanced version of the symbol from antique furniture using red thread. Through this gesture, we wished to draw attention to the major artistic event organized by the Partisans in Bela Krajina in 1945. Partisan art, or the art created during the period of resistance, is characterized by achievements that remain impressive even today and continue to enrich our cultural and artistic heritage. This heritage extends from visual and performing arts to literature and music. Using the tradition of Bela Krajina embroidery, we wove a new pattern around the star, complemented by an empty space that metaphorically represents an unfinished Bela Krajina circle dance.

Through this gesture, we invite viewers into a dialogue and participation, encouraging them to continue our celestial vault, which is presented frontally in the form of silkscreen stencils on textile (Figure 5), and to dance with us.



» **Figure 5:** *Screen Printing on Textile Applied to the Monumental Sculpture by Stojan Batič in Dražgoše, 2025.*

4. Discussion

4.1. Alen Fuks: That Night I Heard Him

The authorial project by Alen Fuks, which also served as the exhibition poster for the exhibition at the City Museum, was subsequently expanded into an independent exhibition. The exhibition *Tonight I Heard Him* presents a multimedia artistic exploration situated at the intersection of photography, the artist's book, the poster, and the object (Figure 6). Alen Fuks's works do not remain within the boundaries of a single medium; rather, they establish an open field of narrative in which historical memory, personal identity, and the materiality of the photographic image, together with other materials, intertwine, connect with one another, and complement each other conceptually.



» **Figure 6:** *Tonight I Heard Him Exhibition, 2026.*

The title of the exhibition refers to the novel *I Saw Her That Night* by Drago Jančar, one of the most important literary reflections within the Slovenian context on war, loss, and the fragmentary nature of memory.

In the present exhibition, photography does not function as a document of the past, nor as an attempt to imitate it, but rather as a medium of interpretation in which personal and collective memory are continuously reshaped and exchanged, becoming an opportunity for choice or rejection. At the centre of the project is the artist's book (Figure 7), which combines elements of fashion photography, archival imagery, and performative intervention into the photographic image. Images of a model dressed in historical uniforms borrowed from Viba Film establish a tense relationship between the present and the past, between individual identity and the social roles defined by political systems and historical circumstances. The uniform, which usually signifies belonging and discipline, here becomes a space for questioning the fragility of the individual, loss, and responsibility.



» **Figure 7:** *Knjiga umentika na razstavi To noč sem ga slišal.*

One of the key elements of the exhibition is the motif of the stitch. The photographs are not merely carriers of images, but material objects into which the author intervenes through cutting, stitching, and reconstructing the surface. The stitch, executed by Pia Wallner, functions simultaneously as an active line, a drawing, a scar, and a bond. It signifies interruption, damage to the photograph, and the possibility of reconnection. In this way, it becomes a metaphor for memory, which is never complete but is always composed of fragments, gaps, and subsequent reconstructions.

A special role is occupied by the motif of the crocodile, which appears in various segments of the exhibition. It refers to records from the life of Veronika Zarnik, while at the same time assuming the role of a visual symbol that connects the historical narrative with the logic of the contemporary image and its reproduction. In the series of ready-mades presented in packaging, the crocodile enters the field of mass culture and reproducibility, establishing a dialogue between the unique work of art and everyday, serially produced objects. *Tonight I Heard Him* is not merely a question of whom we hear in the echoes of the past, but above all of how we listen to ourselves.

The work explores the relationship between memory and image, between absence and presence, between personal experience and collective memory, as well as the relationship between mentor and student, and between comradeship and patience. In a world where photographs are often understood as evidence, Fuks points out that they can also be spaces of doubt, false projections, and places of silent dialogue with those who are no longer here. Within this dialogue, the image does not merely preserve the position of memory of the past, but becomes an active space in which history and the present continually meet.

5. Conclusions

The poster exhibition, developed during the academic years 2024/2025 and 2025/2026, was presented in five different exhibition venues. It began at the PeF Gallery in Ljubljana (March 2025), after which it continued in Kočevje, where it was exhibited at Šeškov House of the Regional Museum Kočevje (May 2025). There, we symbolically explored the themes of statehood and freedom and reflected upon the First Assembly of Delegates of the Slovenian Nation (1943). In November 2025, a selection of posters was presented to the public in Maribor at the exhibition space of the Museum of National Liberation Maribor. Maribor was chosen in part because Slovenian propaganda material for the Carinthian Plebiscite had been printed there under the leadership of General Maister at the St. Cyril Printing House. The themes of the Peasant Revolt (1573) and the victory of the National Liberation Front were addressed at the Cultural Centre in Krško (December 2025). We also continue to evaluate our findings at the City Museum of Ljubljana (MGML), where the students' visual statements, both in content and form, relate to Dr. Blaž Vurnik's exhibition *1495 Days: Ljubljana During the Second World War*.

Through a variety of media expressions, including typographic solutions, digitally created drawings and illustrations, photography and photomontage, as well as both traditional and digitally produced 3D collages, the students drew inspiration from key figures in Slovenian graphic design. The project concluded with a printed catalogue designed by the student Živa Juvančič. For a young creator whose artistic practice is still developing, it is essential to engage with public presentation, even when this occurs through a "static" visual artwork. On the one hand, collaboration with the City Museum of Ljubljana provided an opportunity for more ambitious artistic production; on the other, it brought a greater sense of responsibility through which

we reflected on the anniversary of the end of the Second World War and the exhibition *1495 Days: Ljubljana During the Second World War*. Equally important was the opportunity to transfer visual concepts from the digital environment to a variety of physical media.

Through the exhibition installation, a dialogue emerged between different authorial approaches and diverse interpretations of the assigned theme.

6. References

Komelj, M. (2026) *Kako misliti partizansko umetnost?* Ljubljana: Založba /*cf.

Mikuž, S. (1977) *Maksim Gaspari: monografija.* Ljubljana: Mladinska knjiga.

Požar, C. (2015) *Stoletje plakata: plakat 20. stoletja na Slovenskem.* Ljubljana: Muzej za arhitekturo in oblikovanje (MAO), Studia humanitatis.

Požar, C. (2025) *The century of the poster: Slovenian poster design in the 20th century.* Zagreb: Museum of Architecture and Design, Kerschoffset.

Vurnik, B. (2025) *1495 dni: Ljubljana med 2. svetovno vojno*. Ljubljana: Muzej in galerije mesta Ljubljane, Mestni muzej Ljubljana.



© 2026 Authors. Published by the University of Novi Sad, Faculty of Technical Sciences, Department of Graphic Engineering and Design. This article is an open access article distributed under the terms and conditions of the Creative Commons Attribution license 4.0 Serbia (http://creativecommons.org/licenses/by/4.0/rs/).

Original Scientific Paper https://doi.org/10.24867/GRID-2026-p44

Artistic and Material Analysis of Dinar, Tolar and Euro

ABSTRACT

Printed money in Slovenia represents an important part of the country's graphic, artistic, and technological heritage, as thirteen different currencies and means of payment have circulated within Slovenian territory since 1820. This paper examines the relationship between the visual design of banknotes and their material and structural properties. The aim of the study was to determine how age, wear, and developments in graphic production technologies affect the quality of the paper substrate and its physical characteristics. Three banknote samples were included in the study: a Yugoslav 100-dinar banknote (V1), a Slovenian 10-tolar banknote (V2), and a 5-euro banknote (V3). In addition to a visual and formal analysis, we examined the basic, surface, structural, and optical properties of the paper, as well as its microscopic characteristics using optical microscopy. Although all analysed samples were manufactured from cotton fibres, they were produced under different historical, economic, and technological conditions. The results indicate that the contemporary euro banknote exhibits the highest degree of material homogeneity, density, and structural compactness, reflecting advances in manufacturing processes and quality control. The older samples, particularly the Slovenian tolar, showed more pronounced signs of mechanical wear, fibre deformation, and changes in surface structure. The findings confirm that prolonged circulation and use significantly contribute to the degradation of banknote paper. At the same time, the study demonstrates that modern banknote production technologies provide a more effective balance between durability, security, and resistance to wear.

Tinkara Stanonik
Boris Beja

University of Ljubljana, Faculty of Natural Sciences and Engineering, Department of Textiles, Graphic Arts and Design, Ljubljana, Slovenia

KEY WORDS
Banknotes, paper, graphic design, paper properties, microscopic analysis

1. Introduction

Printed money represents an important segment of cultural, design, and technological heritage, as it reflects the political, economic, and social transformations of a particular period. Since the beginning of the nineteenth century, several different currencies have circulated within Slovenian territory, and their banknotes bear witness not only to monetary history but also to the development of graphic art, printing technologies, and security systems. Although banknotes are increasingly being replaced by bank cards and digital payment methods in contemporary society, they remain an important carrier of national identity, visual communication, and technological innovation. Due to their everyday use, banknotes are continuously exposed to mechanical stresses such as folding, abrasion, compression, and machine counting, all of which affect their material and structural properties. Their durability is therefore directly related to the selection of raw materials, the development of manufacturing processes, and the introduction of new security and graphic technologies. At the same time, the visual design of banknotes combines aesthetic, functional, and security requirements, making them an important subject of research at the intersection of graphic technology, materials science, and design.

This paper examines the relationship between the visual design of banknotes and their material properties through a comparative analysis of three historically distinct means of payment: a Yugoslav 100-dinar banknote, a Slovenian 10-tolar banknote, and a 5-euro banknote.

The aim of the study is to determine how the development of graphic technologies, different production conditions, and prolonged circulation influence the physical, structural, and optical properties of the paper substrate. By comparing banknotes produced in different economic and technological environments, the research contributes to a better understanding of the impact of technological progress on the durability, quality, and resistance of modern security printing products.

1.1. Samples

This study investigates the properties of banknote paper materials, which, due to their specific nature and everyday use, are continuously exposed to mechanical stresses such as folding, rubbing, and machine counting.

The aim of the research was to compare the properties of banknotes from different historical periods and produced using different graphic production technologies.

Three samples were selected for analysis: Sample 1 (V1), a Yugoslav 100-dinar banknote, Sample 2 (V2), a Slovenian 10-tolar banknote and Sample 3 (V3), a 5-euro banknote. Although all three samples were based on cotton fibres, they were produced under different economic conditions.

The measurements were performed on circulated banknotes. During sample selection, special attention was paid to choosing banknotes that exhibited a comparable degree of material wear in order to ensure the validity of the comparative analysis. Yugoslav dinars and Slovenian tolars were printed in large quantities and under considerable time pressure during periods of high inflation, raising concerns about their long-term quality and durability when compared with the modern, strictly controlled production of euro banknotes.

1.1.1. Dinar (1945-1991)

Following the end of the Second World War, the monetary system was centralized under the National Bank of Yugoslavia, which operated through republican branches, including the National Bank of Slovenia. During the 1950s, banking activities recovered, although frequent monetary instability often increased the importance of foreign convertible currencies in everyday life.

Throughout its existence, the Yugoslav dinar underwent several design changes that reflected the political and ideological identity of socialist Yugoslavia (Figure 1). Banknotes commonly featured partisans, workers, farmers, fishermen, and female figures, while the reverse sides often depicted cities, landscapes, or national landmarks. Portraits of prominent Yugoslav figures, ornamental elements, and revolutionary monuments were also frequently included.



» **Figure 1:** *Sample 1 (V1), the Yugoslav 100-dinar banknote, which was in circulation between 1945 and 1991*

The visual language of the dinar emphasized the working individual in factories and rural environments, highlighting the connection between industrial development and agricultural prosperity. Artistic and cultural heritage also appeared on banknotes, including representations of monumental sculptures such as the memorial by Miodrag Živković in the Sutjeska National Park, one of the most recognizable memorials of the Yugoslav period.

1.1.2. Tolar (1991-2007)

Following Slovenia's declaration of independence in 1991, preparations began for the introduction of a new national currency. After a design competition organized by the Bank of Slovenia, the first regular issue of the Slovenian tolar entered circulation on 30 September 1992. The banknotes were designed by Miljenko Licul, Zvone Kosovelj, Rudolf Španzel, and Janez Boljka (Čelik, 2011).

The visual composition of the tolar was divided vertically. The obverse featured a portrait of a prominent Slovenian figure alongside the denomination, while the reverse presented attributes, artistic works, or achievements associated with the depicted individual. For example, the banknote featuring France Prešeren included references to Zdravljica, while the Jože Plečnik banknote depicted the façade and floor plan of the National and University Library (Banka Slovenije, 2021). In addition to sophisticated graphic design, the banknotes incorporated tactile relief elements to assist visually impaired users and differed in size according to denomination. Typography was based on the Friz Quadrata typeface (Figure 2).

The tolar served as Slovenia's national currency and legal tender from 1992 until the adoption of the euro in 2007. The selected portraits represented some of the most important figures in Slovenian cultural and scientific history, including Primož Trubar, Janez Vajkard Valvasor, Jakob Gallus, Jurij Vega, France Prešeren, Rihard Jakopič, Ivana Kobilca, Jože Plečnik, and later Ivan Cankar. Together, these motifs empha-

sized the cultural, artistic, and intellectual identity of the Slovenian nation (Banka Slovenije, 2025).



» **Figure 2:** *Sample V2, Slovenian 10-tolar banknote, issued during the period when the tolar served as the national currency of Slovenia (1991–2007)*

1.1.3. EURO (2007 -)

On 1 May 2004, the Republic of Slovenia joined the European Union and expressed its intention to become part of the euro area. On 1 January 2007, the euro was introduced in Slovenia, replacing the Slovenian tolar. With the adoption of the common European currency, monetary policy became integrated into the European Central Bank (ECB) system, while the Bank of Slovenia became part of the Eurosystem. The national side of the Slovenian euro coins was designed by Miljenko Licul.

The euro is the official currency of Slovenia and has been in use since 1 January 2007. Before its introduction, Slovenia was required to meet the convergence criteria established for membership in the Economic and Monetary Union. The first series of euro banknotes was designed by Robert Kalina of the Austrian National Bank, who won the European design competition in 1996. Each denomination represents a characteristic architectural style from European history.

The €5 banknote (Figure 3) symbolizes Classical Antiquity, €10 Romanesque architecture, €20 Gothic architecture, €50 the Renaissance, €100 Baroque and Rococo styles, and €200 the iron and glass architecture of the nineteenth century. The front side depicts windows and gateways as symbols of openness and cooperation among European nations, while the reverse side features bridges representing communication and connection within Europe and beyond. The twelve stars of the European Union symbolize harmony and unity. Banknotes differ in size and colour and incorporate numerous security features, including microprinting, infrared elements, and features visible under ultraviolet light (European Central Bank, 2023).



» **Figure 3:** *Sample V3, 5-euro banknote, circulating in Slovenia since the adoption of the euro in 2007*

The second series of euro banknotes, entitled Europa, takes its name from the portrait of Europa, a figure from Greek mythology. While retaining the architectural concept of the first series, it introduces a refreshed visual identity. Designed by Reinhold Gerstetter, the series employs stronger colours, softer forms, and three-dimensional bridge designs, making it easier to distinguish from the first generation of banknotes. In addition to aesthetic improvements, the Europa series incorporates more advanced security features that significantly increase protection against counterfeiting (European Central Bank, 2023). The national side of Slovenian euro coins features important personalities, cultural symbols, and elements of Slovenia's natural and historical heritage. The €2 coin depicts the poet France Prešeren together with the inscription “May all nations live”, while the €1 coin features Primož Trubar and his famous motto “To stand and withstand”. Other motifs include Mount Triglav, Lipizzaner horses, Plečnik’s Cathedral of Freedom, the Sower, the Prince’s Stone, and a stork. Designed by Miljenko Licul in collaboration with Maja Licul and Janez Boljka, these motifs collectively express Slovenia’s national identity, history, and cultural heritage.

2. Methods

2.1. Objectives

The main objective of this research was to investigate how technological advancement, mass production, and the degree of actual wear are reflected in the properties of banknote paper. We aimed to determine whether modern production standards, represented by sample V3, have resulted in a significant improvement in material homogeneity compared with older banknotes (V1 and V2), which circulated during periods of economic pressure. Standard methods were employed to determine the basic, surface, structural, and optical properties of the paper. An optical microscope was used for image analysis, providing a deeper insight into the obtained measurements.

2.2. Hypotheses

Based on the visual inspection, tactile assessment, and historical background of the samples, the following hypotheses were formulated and subsequently evaluated in the conclusion:

1. **Hypothesis 1:** Sample V3 will exhibit the best physical properties, as it represents the highest level of modern papermaking technology.
2. **Hypothesis 2:** Sample V2 will show the weakest performance, as it already appears the most fragile during initial handling, indicating significant mechanical fibre degradation and loss of structural strength.
3. **Hypothesis 3:** Due to rapid mass production and the influence of inflationary periods, samples V1 and V2 will exhibit greater variability and non-uniformity in the measured properties than sample V3.

2.3. Challenges and Methodology of the Research Process

During the research, we encountered several challenges related to data interpretation. Due to the lack of official technical data, which are treated as confidential information, a direct comparison of absolute values (e.g., grammage values) was not possible. Therefore, the analysis was based on relative comparisons between the individual samples. An additional challenge was the influence of banknote wear. When interpreting the results, it was necessary to distinguish between the intrinsic quality of the paper and changes in its properties caused by use and material ageing. Another important aspect of the study was the selection of an appropriate methodology.

Because legal regulations prohibit damaging currency and because the integrity of the samples had to be preserved, only non-destructive measurement methods were employed. The chosen methods enabled a comparative analysis using different approaches, ranging from macroscopic measurements to microscopic fibre imaging and analysis. The experimental work was carried out in several stages. The first stage involved the determination of the basic properties of the samples, the second focused on surface properties, the third on structural properties, and the fourth on optical properties. During the measurements, particular attention was paid to an adequate number of test specimens and to the correct identification of the upper (A) and lower (B).

2.3.1. Description of Testing Methods

For the three selected samples, the following properties were determined in accordance with standard testing methods. Basic properties: grammage, thickness, density, and specific volume, Surface properties: Bendtsen roughness and Bendtsen porosity. Structural properties: sound pulse propagation velocity; Optical properties: opacity.

3. Results and discussion

3.1. Basic Properties

The analysed banknote samples differed in their basic properties (Table 1). Since official banknote grammage data are not publicly available and are considered confidential, it was not possible to calculate the exact deviations from the specified values.

Nevertheless, the measurements provided important insight into the actual grammage values of the analysed samples. Sample V1 exhibited a grammage of 89.0 g/m² with the lowest coefficient of variation. Sample V2 reached a grammage of 91.5 g/m² and showed the highest coefficient of variation (CV = 3.24%), which may be attributed to mechanical wear and the uneven distribution of fibres within the paper structure. Sample V3 achieved the highest grammage, namely 100.8 g/m².

Table 1
Results of grammage, thickness, density, and specific volume measurements

G [g/m²]			d [mm]	r [kg/m³]	n [m/kg³]
V1	1.	90,23	0,102	884,6	0,00113
	2.	87,84	0,115	763,8	0,00131
	S_x	89,0	0,109	824	0,00122
	$\bar{x}$	1,7	0,009	85	0,00013
	CV	1,90	8,47	10,36	10,43
V2	1.	89,41	0,108	827,9	0,00121
	2.	93,6	0,127	737	0,00136
	S_x	91,5	0,118	782	0,00129
	$\bar{x}$	3,0	0,013	64	0,00011
	CV	3,24	11,43	8,21	8,25
V3	1.	98,79	0,114	866,6	0,00115
	2.	102,79	0,112	917,8	0,00109
	S_x	100,8	0,113	892	0,00112
	$\bar{x}$	2,8	0,001	36	0,00004
	CV	2,81	1,25	4,06	3,79

Although no substantial differences in thickness were observed among the investigated samples, V2 was the thickest sample and also exhibited the highest coefficient of variation (11.43%). Variations in thickness result from the internal structure of the paper and the degree of mechanical wear, both of which directly influence the thickness of individual specimens.

Sample V1 was the thinnest, although it also displayed considerable variability. The best results were obtained for sample V3, where the coefficient of variation was only 1.25%.

The highest density was measured for sample V3 (892 kg/m³), reflecting its high compactness and increased fibre content. At the same time, this sample was the most homogeneous and consistent, achieving the lowest coefficient of variation (4.06%), which indicates greater material uniformity. In contrast, sample V2 exhibited the lowest density (782 kg/m³). Combined with its greater thickness and higher coefficient of variation (8.21%), this confirms that the fibres in this paper are less tightly bonded.

The highest specific volume was recorded for sample V2 (0.00129 m³/kg), which is a consequence of its lower density and uneven thickness resulting from the paper structure itself. The lowest specific volume was measured for sample V3 (0.00112 m³/kg), indicating that the material contains the fewest air voids between fibres and is therefore the densest and most compact of the analysed samples.

3.2. Surface Properties

3.2.1. Roughness

As shown in Table 2, a two-sidedness of the material can be observed in samples V1 and V3. In sample V1, the difference between sides A and B amounted to 5.19%, while in V3 it was 3.33%. Despite these differences, both samples still reflect a relatively homogeneous paper structure.

The roughest and most uniform profile was exhibited by sample V2, where the roughness values on both sides were identical (2175 ml/min). The complete absence of two-sidedness in this sample indicates a high degree of mechanical wear. In contrast, sample V3 exhibited the smoothest surface, with roughness values ranging between 1500 and 1550 ml/min. Sample V1 showed the highest standard deviation on side A (126 ml/min) and side B (150 ml/min), further confirming the uneven distribution of fibres and the effects of mechanical paper wear.

3.2.2. Porosity

The porosity of the paper, presented in Table 2, depends on the degree to which the paper structure is filled with fibres, sizing agents, and fillers (Rutar, 2002). All of these parameters significantly influence the physical properties and usability of the banknote.

The lowest level of porosity was determined for sample V3 (9 ml/min), confirming that the sample is dense, compact, and contains a minimal proportion of air voids between fibres (Table 2). In contrast, sample V2 exhibited the highest porosity (55 ml/min), indicating the presence of larger pores that allow air and liquids to pass more easily through the material.

As a result, such paper is somewhat softer to the touch, while higher porosity may negatively affect the visibility and durability of security features, such as watermarks (Rutar, 2002).

Table 2

Results of Roughness and Porosity Measurements

		H_B [ml/min]		P_B [ml/min]	
		A	B	A	B
V1	1.	2000	1700	15	20
	2.	2200	2000	10	10
	3.	1900	2000	20	10
	4.	2000	2000	15	10
	S_x	2025	1925	15	13
	$\bar{x}$	126	150	4	5
	CV	6,21	7,79	27,22	40,00
V2	1.	2300	2400	30	90
	2.	2000	2100	25	70
	3.	2100	2200	60	30
	4.	2300	2000	65	30
	S_x	2175	2175	45	55
	$\bar{x}$	150	171	20	30
	CV	6,90	7,85	45,36	54,55
V3	1.	1400	1500	5	10
	2.	1600	1700	7	15
	3.	1700	1400	10	5
	4.	1500	1400	10	5
	S_x	1550	1500	8	9
	$\bar{x}$	129	141	2	5
	CV	8,33	9,43	30,62	54,71

3.3. Structural Properties

3.3.1. Sound Propagation Velocity

Anisotropy plays a significant role in determining the physical and mechanical properties of the investigated material. As shown in Table 3, the machine direction (MD) is considerably more pronounced than the cross direction (CD) in all analysed samples, confirming the oriented structure of the material. This indicates that the fibres are predominantly aligned in the machine direction, providing the material with greater tensile strength and mechanical stability along that axis. Sound propagation velocities measured in the MD ranged from 0.49 to 0.55 km/s, whereas significantly lower values were recorded in the CD, approximately 0.35 km/s.

Such pronounced yet balanced anisotropy in the machine direction (MD) is particularly important for the service life of banknotes, as they are continuously

exposed to various mechanical stresses during circulation, including folding, rubbing, and handling, as well as numerous environmental influences such as moisture, temperature fluctuations, and contact with liquids. The oriented fibre structure provides increased resistance to mechanical damage and contributes to maintaining the structural integrity of banknotes throughout their period of use.

It was found that the anisotropy values of all analysed samples, despite originating from different periods of banknote production, were comparable and consistent. Based on these results, it can be concluded that the banknotes examined were produced in accordance with strict and uniform manufacturing standards throughout the different historical periods. This confirms that banknote paper production has been technologically well controlled over time and adapted to meet the requirements for high mechanical durability, tensile strength, structural stability, and long-term circulation performance.

Table 3

Results of Sound Wave Propagation Velocity Measurements

		C [km/s]
V1	MD	0,49
	CD	0,35
V2	MD	0,54
	CD	0,34
V3	MD	0,55
	CD	0,35

3.3.2. Opacity

As shown in Table 4, sample V2 exhibited the highest opacity on side A (99.17%), followed by sample V1 on side B (97.40%). In sample V1, a larger difference between sides A and B was observed (3.25%), whereas sample V3 transmitted the greatest amount of light. At the same time, V3 exhibited the lowest coefficient of variation, indicating exceptional material homogeneity.

The slightly lower opacity of sample V3 may be the result of a deliberate technological solution intended to improve the visibility of security features, such as watermarks.

However, additional measurements on a larger number of samples would be required to confirm this hypothesis conclusively. Nevertheless, the opacity of all analysed samples was sufficiently high (Table 4) to prevent unwanted show-through of printing from the opposite side. This ensures a clear visual separation of graphic elements and is essential for high-quality double-sided printing (Rutar, 2002).

Table 4

Results of Opacity Measurements

OP [%]			
		A	B
V1	x_{min}	86,97	90,27
	x_{max}	98,24	100,48
	S_x	94,15	97,40
	$\bar{x}$	4,44	4,14
	CV	4,72	4,25
V2	x_{min}	97,40	90,40
	x_{max}	103,47	99,06
	S_x	99,17	96,17
	$\bar{x}$	2,58	3,49
	CV	2,61	3,63
V3	x_{min}	94,19	94,28
	x_{max}	96,99	95,82
	S_x	95,35	94,90
	$\bar{x}$	1,24	0,73
	CV	1,30	0,77

3.3.3. Optical Microscopy

In sample V1, the microscopic image (Figure 4) reveals a loosened fibre network with noticeable voids or pores. The fibres are distributed rather randomly, and signs of paper ageing are visible, with individual fibres being less interconnected, which explains the higher roughness of the material.



» **Figure 4:** *Optical Microscopy (V1)*

In sample V2, the structure is uneven, and the effects of mechanical wear are clearly visible in Figure 5.



» **Figure 5:** *Optical Microscopy (V2)*

Figure 6 of sample V3 reveals an exceptionally dense, tightly interwoven, and homogeneous cotton fibre structure. Voids between fibres are almost imperceptible, confirming the low porosity (9 ml/min) and high density of the material. The surface is smooth and compact, resulting from the advanced calendering and finishing processes used in modern banknote production.



» **Figure 6:** *Optical Microscopy (V3)*

4. Discussion

Based on the measurements performed, significant differences among the selected banknotes were identified, and all proposed hypotheses were confirmed.

Sample V3 exhibited the best overall properties across all measured parameters. With the highest density, lowest porosity, and exceptional homogeneity, it represents the highest-quality and most technologically advanced material included in the study, providing maximum durability and high resistance to environmental influences. Sample V2 displayed the weakest material properties. Its high roughness, low density, and microscopically visible fibre loosening are direct consequences of extensive mechanical wear.

Compared with V3, samples V1 and V2 showed greater variability in the measured values. This may be attributed to the effects of mass production during periods of inflation and to uneven material wear. However, additional measurements on a larger number of samples would be required to confirm this assumption conclusively. The study demonstrated that material quality, long-term use, and mechanical stress significantly alter the structure of banknotes.

While sample V1 occupies an intermediate position with relatively good dimensional stability, the modern production standards represented by sample V3 provide an optimal balance between opacity, necessary for the visibility of security features, and stiffness required for reliable machine processing.

5. Conclusions

This study examined the relationship between the visual design and material properties of three historically distinct banknotes: the Yugoslav dinar, the Slovenian tolar, and the euro. Although all analysed samples were produced from cotton fibres, significant differences were identified in their physical, structural, surface, and optical characteristics.

The results confirmed all three research hypotheses. The contemporary euro banknote (V3) achieved the highest density, the lowest porosity, and the greatest material homogeneity, demonstrating the advantages of modern papermaking technologies, stricter quality-control procedures, and advanced security-printing standards. In contrast, the Slovenian tolar (V2) exhibited the most pronounced signs of mechanical degradation, including increased roughness, lower density, and a more open fibre structure. The Yugoslav dinar (V1) occupied an intermediate position, showing evidence of ageing while maintaining relatively stable structural properties. Microscopic analysis supported the quantitative measurements and revealed a clear relationship between material compactness, wear resistance, and long-term circulation performance. The study demonstrated that prolonged use, environmental exposure, and mechanical stress significantly influence the physical condition of banknotes, regardless of their original production quality.

Beyond their monetary function, banknotes also represent important artefacts of visual culture. The analysed currencies reflect three different political, cultural, and economic contexts: the socialist identity of Yugoslavia, the nation-building period of independent Slovenia, and the supranational visual identity of the European Union. Their designs illustrate how graphic communication, symbolism, and security requirements have evolved alongside technological innovation. The findings further suggest that the future development of euro banknotes will continue to be shaped by the balance between visual communication, security, sustainability, and durability.

The forthcoming new generation of euro banknotes, currently being developed by the European Central Bank, indicates that banknote design remains an active field of innovation despite the increasing importance of digital payment systems. Future issues are expected to introduce new visual themes, improved security features, and environmentally conscious production processes, while continuing to fulfil their role as both secure payment instruments and carriers of European cultural identity. The research confirms that the evolution of banknotes is not merely a history of money but also a history of graphic design, materials engineering, and technological progress. As such, banknotes remain valuable objects for interdisciplinary research at the intersection of design, culture, and material science.

6. Acknowledgments

Associate Professor dr. Klemen Možina.

7. References

Banka Slovenije. (2021) *Zgodba o tolarju: Razstava ob 30. obletnici Banke Slovenije*. Available from: https://www.bsi.si/sl/podpiramo-umetnost/program-mgbs/razstava/zgodba-o-tolarju [Accessed 27 September 2026].

Banka Slovenije. (2025) *Zgodba o tolarju*. Available from: https://www.bsi.si/sl/gotovina/zgodba-o-tolarju [Accessed 27 September 2026].

Čelik, M. (ed.) (2011) *Oblikovanje republike: Arhitektura, oblikovanje in fotografija v Sloveniji 1991–2011*. Ljubljana: Muzej za arhitekturo in oblikovanje (MAO).

European Central Bank. (2023) *Europa Series Banknotes*. Available from: https://www.ecb.europa.eu/euro/banknotes/current/denominations/html/index.en.html [Accessed 18 December 2023].

Rutar, V. (2002) *Nekatere preizkusne metode karakterizacije papirja in kartona: materiali za tisk in dodelavo: vaje za študente 1. letnika*. Ljubljana: Univerza v Ljubljani, Naravoslovnotehniška fakulteta, Oddelek za tekstilstvo.

Štrucelj, A. (2024) *Papirnate vrečke iz vlaknin enoletnih rastlin*. Diplomsko delo, pp. 20–33. Available from: https://repozitorij.uni-lj.si/IzpisGradiva.php?lang=slv&id=156410 [Accessed 29 December 2025].

© 2026 Authors. Published by the University of Novi Sad, Faculty of Technical Sciences, Department of Graphic Engineering and Design. This article is an open access article distributed under the terms and conditions of the Creative Commons Attribution license 4.0 Serbia (http://creativecommons.org/licenses/by/4.0/rs/).

Review Paper https://doi.org/10.24867/GRID-2026-p45

From Signage to Civic Identity: a Theoretical Framework for Visual Communication in Post-Conflict Urban Space

ABSTRACT

Environmental graphic design is often approached through orientation, legibility, and the organization of spatial information. However, in post-conflict urban contexts, everyday visual communication may carry meanings beyond functional wayfinding: it may communicate memory, authority, belonging, exclusion, care, or neglect. This paper aims to develop a theoretical framework for understanding environmental graphic design and everyday visual communication as functional, symbolic, material, and civic layers of urban space, with particular reference to Bosnia and Herzegovina. The paper uses a critical literature review and conceptual synthesis, connecting environmental graphic design, wayfinding, semiotics, place identity, civic design, and post-conflict urban studies. Six analytical lenses are proposed: functional legibility, graphic and material coherence, semiotic meaning, place identity and affective experience, post-conflict fragmentation, and civic care. These lenses position signs, street names, memorial plaques, commercial graphics, informal markings, scripts, typographic systems, and material conditions as part of the broader public realm. The paper argues that visual communication in post-conflict urban space should be understood not only as a navigational or graphic-design issue, but as something concerning architectural and urban design, and which is equally connected to identity, dignity, memory, belonging, and civic experience.

Laila Mušić

International Burch University
Faculty of Engineering, Natural, and Medical Sciences, Sarajevo, Bosnia and Herzegovina

KEY WORDS
Environmental graphic design, wayfinding, civic identity, post-conflict urban space, visual communication

1. Introduction

Environmental graphic design (EGD) is conventionally approached through orientation, legibility, and the organization of spatial information (Gibson, 2009; Bigat, 2024). Signage systems, maps, and wayfinding hierarchies are typically treated as technical solutions to the problem of helping users move efficiently through built environments. In post-conflict urban contexts, however, everyday visual communication may carry meanings that exceed this functional register. Signs, street names, memorial plaques, commercial graphics, and even informal or unauthorized markings can communicate memory, authority, belonging, exclusion, care, or neglect (Rossi, 1984; D'Avanzo & Zingale, 2023). This is particularly evident in Bosnia and Herzegovina, a country whose urban space continues to bear the visible and symbolic traces of the 1992–1995 war, of earlier socialist-era urban development, and of a fragmented post-Dayton institutional structure (Walasek & Carlton, 2015; Aulić & Kalinić, 2016; Hadžić, 2021).

This paper develops a theoretical framework for understanding environmental graphic design and everyday visual communication as functional, symbolic, material, and civic layers of urban space, with particular refer-

ence to Bosnia and Herzegovina. Rather than treating wayfinding and signage as isolated technical or aesthetic concerns, the paper positions them within a broader disciplinary conversation that includes environmental graphic design, wayfinding theory, semiotics, place identity, civic design, and post-conflict urban studies.

The premise underlying this framework is that urban space is not a neutral physical setting but a layered system of meaning. Aldo Rossi's (1984) reading of the city as a locus of collective memory positions buildings, monuments, and recognizable urban elements as carriers of historical and social significance beyond their immediate function. Harold Proshansky's (1978) concept of place identity complements this by locating that significance in the individual's psychological relationship to the physical environment. More recent scholarship on urban identity (Umar, Winarso & Kustiwan, 2024; Ziyaee, 2018) clarifies that identity in this sense is neither purely material nor purely subjective, but emerges from the interaction of physical form, cultural meaning, social practice, and perception. Writing from a regional design perspective, Ognjeka Finci (2009) extends this argument to the scale of everyday urban elements (e.g. signage, street furniture, and visual communication) arguing that their condition and coherence contribute directly to the humanization, or dehumanization, of urban space.

If urban space carries memory, shapes identity, and communicates social value at this scale, then the visual elements embedded within it (e.g. signs, typography, plaques, materials, commercial graphics, informal markings) cannot be treated as merely practical or decorative additions to the city. This is the starting premise for the theoretical framework developed here

1.1. Problem and Research Gap

Existing literature addresses parts of this relationship without adequately connecting them. Wayfinding and EGD literature offers robust tools for analyzing legibility, hierarchy, and orientation (Gibson, 2009; Bigat, 2024), but typically frames users as navigators moving efficiently between points, without accounting for why visual coherence might matter emotionally, symbolically, or civically. Literature on place identity and environmental psychology (Proshansky, 1978; Ziyaee, 2018) explains how people form emotional and identity-based relationships with the built environment, but does not typically address how everyday graphic elements, as distinct from architecture, participate in that process. Semiotic literature interprets visual communication as a system of meaning, but is rarely brought into contact with the wayfinding literature's technical vocabulary of legibility and hierarchy. Post-conflict and post-socialist urban studies on Bosnia and Herzegovina (Walasek & Carlton, 2015; Aulić & Kalinić, 2016; Hadžić, 2021; Djurasović & Knieling, 2015; Aceska, 2013; Vučetić, 2004) document institutional fragmentation, contested memory, and weak shared civic identity in considerable detail, but the role of everyday visual communication within this condition remains largely unaddressed. Civic design literature (Kaasa, Bingham-Hall & Pietrostefani, 2016; de Kreek et al., 2024; Srinivas & Staszowski, 2018) raises important cautions about the political limits of design intervention, but is rarely brought into dialogue with EGD or wayfinding theory at all.

The gap this paper addresses, then, is not an absence of literature in any one of these fields, but their limited interconnection. Everyday visual communication elements in post-conflict Bosnian cities remain under-theorized as an intersection of symbolic meaning, material condition, and civic experience. Individual elements (e.g. signage, typography, script choice, the physical condition of a plaque or sign) are often treated as secondary design details, despite their potential to shape how public space is read, experienced, and emotionally interpreted.

1.2. Aim

This paper aims to develop an integrated theoretical framework, structured around six analytical lenses that positions visual communication as a functional, symbolic, material, and civic layer of post-conflict urban space:

- functional legibility
- graphic and material coherence
- semiotic meaning
- place identity and affective experience
- post-conflict fragmentation
- civic care

The framework is conceptual and interpretive in nature: it identifies the dimensions along which visual communication in post-conflict urban space should be read, rather than specifying measurable design parameters.

2. Methodology

This paper adopts a critical literature review and conceptual synthesis methodology, rather than an empirical or case-study design. This choice follows from the nature of the research problem: before visual communication in a specific post-conflict urban setting can be productively analyzed empirically, the conceptual vocabulary for doing so needs to be assembled from fields that do not customarily address one another.

The review draws on international and regional literature across five interconnected bodies of work: (1) environmental graphic design and wayfinding theory; (2) semiotics and typography as applied to public space; (3) place identity and environmental psychology; (4) post-conflict and post-socialist urban studies specific to Bosnia and Herzegovina; and (5) civic design theory and its critiques.

Sources include peer-reviewed journal articles, academic books, and conference proceedings, selected for their direct relevance to the relationship between visual communication, urban space, and civic experience.

The synthesis method is thematic rather than statistical: literature from each field is read against the others to identify where arguments converge, diverge, or leave gaps unaddressed. The output is not a dataset but an integrated theoretical framework: six analytical lenses treated not as separate categories but as interdependent tools. This framework is intended as the theoretical foundation for a subsequent empirical case-study application, rather than as a finding to be tested within this paper itself.

It should be stated explicitly that the framework developed in this paper is conceptual and interpretive rather than operational. Its purpose is to identify and organize the dimensions along which visual communication in post-conflict urban space should be read (functional, material, semiotic, affective, political, and civic), not to specify measurable design parameters such as legibility distances, typographic scale, color or contrast specifications, or material standards.

3. Theoretical Foundations

3.1. Functional Legibility

Wayfinding and EGD literature provides the technical starting point for analyzing visual communication as a coordinated system rather than a collection of isolated graphic elements. Finci (2009) argues that visual communication systems should be coordinated, readable, and integrated with their surrounding urban environment rather than treated as secondary additions; her critique of visual clutter and insufficient public information is directly applicable to cities where formal, informal, and commercial signage overlap without coordination, a condition common across urban Bosnia and Herzegovina. Bigat (2024) frames guidance and signing systems as a form of informational design, emphasizing coherent, user-oriented systems organized around key decision points rather than ad-hoc additions. Gibson's (2009) practical wayfinding framework specifies measurable criteria: hierarchy, typographic legibility, visibility, color contrast, mapping, sign placement, and integration with surrounding architecture, offering a vocabulary for evaluating the functional legibility of visual communication systems.

Ganoti and Laskari (2023) extend this beyond pure technical orientation, arguing that EGD contributes to the aesthetic and psychological experience of the city, not only to functional navigation. Even so, conventional wayfinding literature retains a significant limitation for the purposes of this framework: it tends to portray users primarily as navigators moving efficiently between points, which does not explain why visual coherence might matter in an emotional, symbolic, or civic register. D'Avanzo and Zingale (2023) address this directly by reframing "wayfinding" as "placefinding": orientation understood not merely as the efficient delivery of spatial information, but as a process through which people recognize their position within a larger urban narrative involving place, alterity, and identity. This reframing is the conceptual bridge that allows functional legibility to be read alongside the more symbolic and affective lenses developed below.

3.2. Graphic and Material Coherence

Where functional legibility concerns whether a system helps users navigate, graphic and material coherence concerns the physical and formal qualities of that system: typography, color, scale, placement, materiality, physical condition, durability, and relationship to architecture. Finci's (2009) typology of urban visual communication is useful here: she distinguishes three functional groups (traffic, information, advertising) and two formal types (standardized/conventional versus creative communication). This typology allows overlapping systems (such as official traffic and information signage, commercial advertising, tourist information, murals, and memorial plaques) to be read as distinct but co-present layers within the same urban visual field, rather than as a single undifferentiated mass of signage.

Material condition carries particular weight in post-conflict and post-socialist urban settings, where inconsistent maintenance, overlapping institutional authority, and uneven investment produce visibly uneven coherence across a city's visual communication systems. A faded, damaged, or improvised sign communicates something different about maintenance, authority, and care than a coordinated and well-maintained one, independent of the information each conveys. This lens therefore treats the material condition of graphic elements as itself communicative, not merely as a matter of aesthetics or upkeep.

3.3. Semiotic Meaning

Semiotics provides the interpretive tool for reading a city's visual communication as a system of signs through which meaning is produced, circulated, and contested, rather than as a neutral information layer. Rossi's (1984) understanding of the city as a carrier of collective memory extends naturally to everyday graphic elements (street signs, shop signs, plaques, and typographic systems) which, though minor in comparison to architecture, participate in the ongoing production of place narratives. Read alongside D'Avanzo and Zingale's (2023) placefinding concept, the city's

graphic layer must be understood both functionally and semiotically: it organizes movement while simultaneously functioning as a cultural and civic text.

Typography occupies a particularly important position within this lens because it is functional and expressive simultaneously. Beyond conveying information, typographic choices convey tone, institutional authority, informality, commercial pressure, local character, and cultural specificity; the condition, scale, material, and placement of lettering can suggest whether a system is coordinated or improvised, maintained or neglected, inclusive or exclusive. This is heightened in multilingual and multiscript contexts: in Bosnia and Herzegovina, where Latin and Cyrillic scripts and the Bosnian, Croatian, and Serbian languages carry official recognition, script and language choice in public space can exceed communicative function and become a marker of cultural affiliation or symbolic and political meaning. Finci's (2009) typology, introduced above, further supports this lens by allowing standardized, commercial, civic, and creative communication systems to be distinguished and read against one another within the same urban field.

3.4. Place Identity and Affective Experience

Place-identity theory supplies the psychological register through which the preceding lenses connect to lived experience. Proshansky (1978) argues that the physical environment forms part of self-identity, since people develop emotional and cognitive relationships with the places they inhabit. Read alongside Umar, Winarso and Kustiwan's (2024) distinction between the identity of, in, and for urban space, this allows urban identity to be understood as operating simultaneously at the level of a city's visible character and at the level of residents' lived attachment to, or distance from, that same environment. Ziyaee's (2018) matrix for assessing urban identity through cultural landscapes offers a methodological bridge from these theoretical positions toward the visible and material: it validates visual mapping, typological analysis, and semiotic interpretation as legitimate techniques for investigating civic experience, without claiming that visual communication alone produces civic identity.

Finci's (2009) discussion of urban furniture and visual communication as contributing to a city's "aroma" (i.e. the collective usability, intimacy, recognizability, and human character of a place) supports the claim that affective urban experience is shaped as much by ordinary, small-scale elements as by architectural or planning decisions at a larger scale. Whether a public space reads as cared for, neglected, coherent, fragmented, welcoming, or indifferent is communicated substantially through these ordinary elements, which residents encounter daily and which the preceding two lenses (functional legibility and graphic/material coherence) describe in more technical terms.

3.5. Post-Conflict Fragmentation

Bosnia and Herzegovina's urban space cannot be read independently of its post-conflict and post-socialist condition. Walasek and Carlton's (2015) account of the deliberate destruction of cultural heritage during the 1992–1995 war demonstrates that the built environment and its symbolic markers were direct targets precisely because architecture, monuments, and cultural landscapes carried meanings of identity and coexistence. What is preserved, destroyed, rebuilt, marked, or left neglected in the years since continues to determine which histories and identities remain visible in public space.

This symbolic instability is reinforced institutionally. Aulić and Kalinić (2016) show how the post-Dayton consociational political structure (in which power is formally shared among constituent peoples) produces fragmented governance and weak accountability across administrative levels. Hadžić (2021) characterizes the resulting post-war condition as one of weak shared civic nationalism, low social capital, and the absence of a common civic project. For visual communication specifically, this matters because coherent signage and wayfinding depend on coordination, maintenance, regulation, and shared civic intention; where authority is fragmented, graphic systems tend to fragment correspondingly, through inconsistent signage, uneven maintenance, overlapping institutional messages, and competing symbolic narratives.

Urban regeneration literature on Bosnian cities complicates any purely negative reading of this fragmentation. Djurasović and Knieling (2015) show that post-war urban development in Bosnia and Herzegovina has been shaped less by a consistently integrated planning vision than by post-socialist transformation, wartime division, and project-based intervention, helping explain visual disorder as the visible result of broader planning discontinuity rather than an isolated design failure. At the same time, Martinović and Ifko's (2018) study of industrial heritage regeneration in Mostar demonstrates that some urban sites can be reframed as shared civic resources, particularly where regeneration is pursued through inclusive narratives attentive to the social dimension of sustainability. Together, these accounts suggest that fragmentation and the potential for renewed shared meaning coexist within the same urban condition.

This fragmentation is also social rather than purely institutional or infrastructural. For example, Aceska's (2013) study of "us and them" distinctions in post-war Mostar shows that everyday urban space is read through social and symbolic divisions that exceed official ethno-national categories: distinctions between long-term residents and newcomers, competing claims to local belonging, and locally specific forms of attachment. Vučetić (2004) similarly shows that identity boundaries in Bosnia are reproduced through ordinary cultural practices, not only through formal politics. Signs, let-

tering, informal graphics, commercial displays, and memorial markers are plausible sites for this same kind of everyday boundary-making, recognition, or shared belonging, even though this specific connection remains underexplored in the literature reviewed here.

3.6. Civic Care and the Limits of Design Intervention

The final lens addresses how design intervention relates to civic identity, and cautions against overstating what design can achieve. Kaasa, Bingham-Hall and Pietrostefani (2016) argue that design is never politically neutral, since it shapes whose interests and needs become materialized in public systems; signage and wayfinding, from this perspective, are design decisions capable of influencing visibility, access, recognition, and the symbolic character of urban space, not neutral technical improvements. De Kreek et al. (2024) extend this by arguing that meaningful civic design depends on collaboration, sustained institutional relationships, and continuity with local communities, rather than the production of discrete objects or services — implying that graphic coherence alone is insufficient; effective visual communication also depends on maintenance, governance, and institutional accountability.

More critical perspectives caution that design intervention can be redirected toward unintended ends. Srinivas and Staszowski (2018) argue that because civic design operates within political and institutional processes, it is neither neutral nor automatically emancipatory: its outcomes can be co-opted or subverted regardless of original intent. Pupavac (2006), writing specifically on post-conflict cultural reconstruction in Bosnia, cautions against treating culture as a fixed object to be externally managed or repaired. Together, these sources raise pointed questions for any proposed visual-communication framework: who controls the system, whose identity is represented, which forms of public expression are legitimized, and whether "care," once formalized, risks becoming a form of branding or regulatory control.

Finci (2009) and Boer (2023) add a further caution from the opposite direction: excessive standardization carries its own risks. Finci argues that modern urbanization and globalization can produce a homogenous visual language that weakens local distinctiveness, while Boer's concept of the "smooth city" describes an extreme version of this outcome, in which public space becomes increasingly regulated, visually controlled, and optimized in ways that erase informality, friction, and non-normative uses of the city. Taken together, these perspectives establish a productive tension for the framework proposed here: visual communication needs sufficient coherence to support orientation and dignity, but should not be standardized to the point of erasing informal and locally specific expressions of place. This tension positions any design implications of the framework as speculative and analytical rather than corrective: i.e. a way of making civic care more visible and legible, not a claim that improved signage can resolve institutional fragmentation or contested memory.

4. Toward and Integrated Theoretical Framework

Each of the six lenses developed above addresses part of the relationship between visual communication, urban space, and civic experience, but no single lens accounts for it adequately alone. Wayfinding and EGD literature is strongest when visual communication is treated as a practical navigational system, but does not explain its emotional or civic significance. Place-identity literature explains how residents form identity-based relationships with the physical environment, but does not typically address how everyday graphic elements participate in that process. Semiotics enables the interpretation of visual communication as meaning-bearing, while post-conflict and post-socialist urban studies explain how memory, institutional fragmentation, and contested narratives shape the urban environment within which that meaning is produced. Civic design literature complicates the picture further by insisting that design cannot be read as politically neutral, nor as a substitute for structural or institutional change.

The framework proposed here connects these fields around a central claim: everyday visual communication in post-conflict Bosnian urban space should be analyzed as a functional, symbolic, material, and civic layer of that space simultaneously, rather than as belonging to any one of these registers exclusively. It is functional because signs, wayfinding systems, and typographic systems shape orientation and legibility (3.1). It is material because scale, condition, placement, and durability shape the city's visible character independently of informational content (3.2). It is symbolic because these same elements communicate memory, identity, authority, inclusion, and neglect (3.3), a meaning further shaped by place attachment (3.4) and by the specific post-conflict conditions of fragmented memory and institutional authority in Bosnia and Herzegovina (3.5). And it is civic because the presence, coordination, and maintenance of visual communication participates in how residents may experience public space as cared for, fragmented, dignified, indifferent, or hostile, while remaining subject to the political limits on design intervention identified in 3.6.

These six lenses (functional legibility, graphic and material coherence, semiotic meaning, place identity and affective experience, post-conflict fragmentation, and civic care) are proposed not as independent analytical categories to be applied separately, but as interdependent tools. Applied together, they allow a single visual

element, such as a street sign, a memorial plaque, a commercial façade, to be read simultaneously as a navigational aid, a material object in a particular state of repair, a sign within a semiotic system, a contributor to place attachment, a symptom of institutional fragmentation, and a potential site of civic care or neglect. As a conceptual rather than operational framework, these lenses provide categories of interpretation, not measurable design criteria; specifying such criteria for a given urban site is left to future empirical work.

5. Discussion: Contribution to Graphic Design and Visual Communication

Within architecture and urban design, frameworks for reading the public realm typically privilege large-scale spatial and planning decisions. The framework proposed here contributes a complementary position specific to the concerns of graphic engineering and design: it argues that the graphic layer of the city (signage, typography, lettering, commercial graphics, informal markings, and their material condition) is not a secondary or purely aesthetic layer of urban space, but a primary site through which civic identity, dignity, and belonging are materialized and experienced.

For EGD and wayfinding practice specifically, this framework carries several implications. First, decisions conventionally treated as purely technical, e.g. typeface selection, material specification, sign placement, maintenance scheduling, carry civic and symbolic weight, particularly in multiscript and multilingual public space, where such decisions can signal inclusion, neutrality, or exclusion regardless of design intent. Second, graphic and material coherence should be pursued critically rather than as an end in itself: the "smooth city" caution (Boer, 2023) implies that a fully standardized, homogenized visual communication system may achieve legibility while eroding the local specificity and informal expression that also contribute to place attachment. Third, and most directly relevant to designers working in post-conflict contexts, the framework positions design intervention as necessarily partial: visual communication can make civic care, memory, and coherence more visible, but cannot resolve the institutional fragmentation or contested memory that produced their absence in the first place. This framing is intended to support a more self-aware and modest practice of environmental graphic design in divided or post-conflict societies, distinct from approaches that treat signage improvement as a solution to deeper civic or political conditions.

This paper's contribution is deliberately confined to the theoretical framework itself. Testing these six lenses against a specific urban site (mapping how functional legibility, material coherence, semiotic meaning, place identity, post-conflict fragmentation, and civic care interact within a particular Bosnian city's visual landscape) is the task of a subsequent empirical study. The present paper establishes the conceptual foundation that such a study requires, and makes that foundation available to the wider GRID community working at the intersection of graphic design, environmental graphic design, and the public realm.

6. Conclusion

This paper has argued that visual communication in post-conflict urban space (and in Bosnia and Herzegovina specifically) should be understood not only as a navigational or graphic-design concern, but as a functional, symbolic, material, and civic layer of the built environment, connected to identity, dignity, memory, belonging, and civic experience. The research gap addressed here is not an absence of relevant literature, but the limited interconnection between fields that each address part of this relationship: wayfinding and EGD, semiotics, place identity and environmental psychology, post-conflict and post-socialist urban studies, and civic design theory.

The six analytical lenses proposed (i.e. functional legibility, graphic and material coherence, semiotic meaning, place identity and affective experience, post-conflict fragmentation, and civic care) are offered as interdependent tools rather than separate categories, forming an integrated theoretical framework through which everyday visual communication elements can be read simultaneously across these registers. For the discipline of graphic engineering and design, this framework repositions signage, typography, and everyday visual communication as constitutive of the public realm rather than secondary to it, with particular relevance for designers working in divided or post-conflict societies. Because the framework is conceptual rather than operational, it does not itself supply design parameters; translating its six lenses into measurable criteria, and testing them against specific urban sites and visual landscapes in Bosnia and Herzegovina, remains the task of future research.

7. References

Aceska, A. (2013) '"Us" and "Them" in post-war Mostar, Bosnia-Herzegovina'. In: Spasić, I. and Cvetičanin, P. (eds.) Us and Them: *Symbolic Divisions in Western Balkan Societies*. Niš/Belgrade: Centre for Empirical Cultural Studies of South-East Europe and Institute for Philosophy and Social Theory, University of Belgrade, pp. 105–118.

Aulić, Lj. and Kalinić, Z. (2016) 'Institutional design in Bosnia and Herzegovina', *Slovak Journal of Political Sciences*, 16(4), pp. 409–429. DOI: 10.1515/sjps-2016-0020

Bigat, E.Ç. (2024) 'Exploring guidance and signing systems in environmental graphic design as informational design: A study using graphic design examples'. In: *Proceedings of the 12th International Symposium on Graphic Engineering and Design*, Novi Sad, Serbia, 14–16 November 2024. Novi Sad: University of Novi Sad, Faculty of Technical Sciences, Department of Graphic Engineering and Design. DOI: 10.24867/GRID-2024-p66

Boer, R. (2023) *Smooth City: Against Urban Perfection, Towards Collective Alternatives*. Amsterdam: Valiz.

D'Avanzo, D. and Zingale, S. (2023) 'From wayfinding to placefinding: Orientation and alterity in urban spaces', *diid – Disegno Industriale Industrial Design*, DSI No. 1, pp. 258–267. DOI: 10.30682/diiddsi23t2e

de Kreek, M., van de Mosselaer, F., Newell, K., de Waal, M., Gordon, E., Hamm, A., Jaskiewicz, T., Vlachokyriakos, V., Ferri, G., Smeenk, W. and Choi, J.H. (2024) 'What is next for civic design?'. In: Gray, C., Hekkert, P., Forlano, L. and Ciuccarelli, P. (eds.) *DRS2024: Boston*. Boston, USA, 23–28 June 2024. Design Research Society, pp. 1–18. DOI: 10.21606/drs.2024.1577

Djurasović, A. and Knieling, J. (2015) 'Urban transition and sustainability: The case of the city of Mostar, Bosnia and Herzegovina', *Eastern Journal of European Studies*, 6(1), pp. 5–29.

Finci, O. (2009) *Dizajn sistema urbanog mobilijara i vizuelnih komunikacija*. Belgrade: Građevinska knjiga.

Ganoti, R. and Laskari, I. (2023) 'The importance of environmental graphic design in urban spaces', *E3S Web of Conferences*, 436, 12013. DOI: 10.1051/e3sconf/202343612013

Gibson, D. (2009) *The Wayfinding Handbook: Information Design for Public Places*. New York: Princeton Architectural Press.

Hadžić, F. (2021) 'Destructive peace: Absenteeism of mutual civic nationalism and social capital in Bosnia and Herzegovina', *Journal of Social, Humanities and Administrative Sciences*, 7(46), pp. 2158–2167. DOI: 10.31589/JOSHAS.798

Kaasa, A., Bingham-Hall, J. and Pietrostefani, E. (eds.) (2016) *Designing Politics: The Limits of Design*. London: Theatrum Mundi.

Martinović, A. and Ifko, S. (2018) 'Industrial heritage as a catalyst for urban regeneration in post-conflict cities: Case study Mostar, Bosnia and Herzegovina', *Cities*, 74, pp. 259–268. DOI: 10.1016/j.cities.2017.12.013

Proshansky, H.M. (1978) 'The city and self-identity', *Environment and Behavior*, 10(2), pp. 147–169. DOI: 10.1177/0013916578102002

Pupavac, V. (2006) 'Reconstructing post-conflict cultures: A case study of Bosnia'. In: Demaria, C. and Wright, C. (eds.) *Post-Conflict Cultures: Rituals of Representation*. London: Zoilus Press, pp. 133–150.

Rossi, A. (1984) *The Architecture of the City*. Cambridge, MA: The MIT Press.

Srinivas, N. and Staszowski, E. (2018) 'Trickery in civic design: Co-optation, subversion and politics'. In: Fisher, T. and Gamman, L. (eds.) *Tricky Design: The Ethics of Things*. London: Bloomsbury Visual Arts, pp. 59–68. DOI: 10.5040/9781474277211.ch-004

Umar, F., Winarso, H. and Kustiwan, I. (2024) 'Urban identity and planning: Conceptual study on identity of urban, identity in urban, and identity for urban', *Spatium*, 51, pp. 11–20. DOI: 10.2298/SPAT230828002U

Vučetić, S. (2004) 'Identity is a joking matter: Intergroup humor in Bosnia', *Spaces of Identity*, 4(1), pp. 1–28. DOI: 10.25071/1496-6778.8011

Walasek, H. and Carlton, R. (2015) *Bosnia and the Destruction of Cultural Heritage*. Abingdon: Routledge.

Ziyaee, M. (2018) 'Assessment of urban identity through a matrix of cultural landscapes', *Cities*, 74, pp. 21–31. DOI: 10.1016/j.cities.2017.10.021



© 2026 Authors. Published by the University of Novi Sad, Faculty of Technical Sciences, Department of Graphic Engineering and Design. This article is an open access article distributed under the terms and conditions of the Creative Commons Attribution license 4.0 Serbia (http://creativecommons.org/licenses/by/4.0/rs/).

https://doi.org/10.24867/GRID-2026-p46

Reinterpretation of the Artwork Atelje by Gabrijel Stupica into Didactic and Tactile Products

ABSTRACT

Visual artworks are usually experienced through sight, which can limit meaningful engagement for children and for blind and partially sighted (BPS) users. This practice-based study examines how Gabrijel Stupica's Atelje (Studio, 1979–1985) can be reinterpreted as a coordinated set of didactic, interactive and tactile products while retaining a recognisable relationship with the original painting. The developed set comprised a 20-piece and a 154-piece jigsaw puzzle with dedicated packaging, an insert puzzle with removable figures, and two tactile three-dimensional (3D) face reliefs. Production combined image processing, vector drawing, laser cutting, ultraviolet (UV) inkjet printing, 3D modelling and fused deposition modelling (FDM) 3D printing in polylactic acid (PLA). Prototype development examined cutting accuracy, piece fit, material stability, edge finishing, tactile clarity and visual contrast. A formative session with nine children aged 6–13 years, most partially sighted and one with very limited residual vision, was used to identify practical issues in the insert puzzle and to compare the two tactile face versions. Repeated jigsaw-piece geometries were redesigned after they allowed incorrect assembly; manual edge finishing improved the insert puzzle; and the simplified facial relief supported clearer tactile recognition than the more source-derived version, which preserved more of the irregular visual character of the painting but required slower exploration. The findings indicate that accessible reinterpretation depends on selective translation rather than direct reproduction: material, geometry and post-processing must be aligned with the intended perceptual task. The study demonstrates a feasible workflow for developing related didactic and tactile products from one complex artwork and identifies directions for further co-design and structured user testing.

Hana Muck [1]
Raša Urbas [2]

[1] University of Ljubljana, Faculty of Natural Sciences and Engineering, Department of Textiles, Graphic Arts and Design, Ljubljana, Slovenia
[2] University of Ljubljana, Faculty of Natural Sciences and Engineering, Department of Textiles, Graphic Arts and Design, Chair of Information and Graphic Arts Technology, Ljubljana, Slovenia

KEY WORDS
Artwork reinterpretation, tactile reproduction, inclusive design, didactic products, 3D printing, UV printing

1. Introduction

Museums and galleries increasingly treat access as part of interpretation rather than as an additional service. This is especially relevant to visual art, where colour, pictorial detail and the protected surface often carry most of the information. For children, museum learning is strengthened by hands-on activity, play and opportunities to construct meaning through interaction (Andre, Durksen & Volman, 2017; Falk & Dierking, 2018).

Jigsaw puzzle play is also associated with spatial transformation skills because children repeatedly compare, rotate and fit visual forms (Levine et al., 2012). For BPS users, the visual emphasis can create a more fundamental barrier when an artwork cannot be touched or when important information has no non-visual equivalent. Multisensory museum practice therefore treats touch as an interpretative mode in its own right, not simply as a substitute for sight (Axel & Levent, 2003; Levent & Pascual-Leone, 2014; Pye, 2007).

Tactile access, however, does not result from converting every visible detail into relief. Touch gathers information locally and sequentially, so recognisability depends on clear contours, sufficient feature separation, an appropriate scale, and a manageable amount of information.

Studies of tactile graphics, 3D printed cultural objects and multimodal museum interfaces consistently show that direct visual fidelity can conflict with tactile legibility (Avni et al., 2025; Bruns et al., 2023; Cavazos Quero, Iranzo Bartolomé & Cho, 2021; Karaduman, Alan & Yiğit, 2023; Wu et al., 2022). The design task is therefore interpretative: features that are visually subtle may need to be enlarged or emphasised, while dense or redundant detail may need to be removed.

A comparable issue arises when art is adapted for children. Simplification is helpful only when it offers a clearer route into the artwork rather than simply reducing its complexity. Reviews of children's museum learning emphasise interaction, scaffolding and hands-on exploration as key elements of meaningful engagement (Andre, Durksen & Volman, 2017).

A complex painting may therefore benefit from several complementary forms of access: visual assembly can support close looking, removable components can reveal spatial relationships, and tactile relief can make a selected motif available through touch. Using more than one product also avoids treating a single adaptation as universally suitable for every user or task.

Digital graphic prepress and contemporary fabrication technologies make such parallel reinterpretations practical. Raster processing and vector drawing allow selected elements to be isolated, reformatted or simplified; laser cutting translates vector contours into physical components; UV inkjet printing reproduces colour on rigid substrates; and FDM 3D printing can turn linework into raised relief. Yet each transfer from image to object changes the information available to the user. Material behaviour, cutting tolerances, surface finish and relief geometry therefore become part of the communication design rather than secondary production details (Dizon et al., 2021; Montusiewicz, Barszcz & Korga, 2022; Urbas, Pivar & Stanković Elesini, 2016).

The study addresses these questions through Gabrijel Stupica's *Atelje* (Studio, 1979–1985), a large, visually layered painting built around repeated human figures, subdued colour fields, collage-like interventions and irregular contours (Figure 1). Instead of producing a single simplified copy, the project developed a family of related products from the same source image: two jigsaw puzzles of different levels of difficulty, packaging that extends their didactic function, an insert puzzle with removable figures, and two tactile face reliefs that deliberately differ in graphic complexity.

Three questions guided the work: how can the visual identity of one complex artwork be retained across products intended for different modes of perception; how do graphic prepress, material choice and manufacturing constraints influence the resulting interaction; and what can an initial evaluation with BPS children reveal about tactile simplification, edge quality and recognisability? The study is practice-based and prototype-oriented. The user session described below was formative rather than a controlled usability experiment, so its observations are used to refine design decisions rather than to support claims about general accessibility performance.



» **Figure 1:** *Gabrijel Stupica, Atelje (Studio, 1979–1985), the shared visual source for all developed products. Tempera and collage on canvas, 285 × 415 cm, Galerija Božidar Jakac, Kostanjevica na Krki*

2. Materials and methods

2.1. Artwork source and reinterpretation strategy

The experimental work grew out of the interdisciplinary project *Popotovanje papirnatih figuric* (*Journey of Paper Figures*), in which *Atelje* served as a shared source for products designed for different users and modes of engagement. The artwork itself was not altered as the subject; instead, its visual information was reorganised through format, material and interaction. The product family was structured around three modes: visual assembly through jigsaw puzzles, combined visual and tactile exploration through an insert puzzle, and tactile interpretation through 3D facial reliefs. Packaging for the two jigsaw puzzles was designed as part of the didactic experience rather than as storage alone.

A consistent design principle was applied across the prototypes: preserve a recognisable relationship with *Atelje*, but do not transfer complexity mechanically when it would reduce usability. The jigsaw puzzles retained the complete composition, the insert puzzle

separated individual figures from the pictorial field, and the tactile reliefs reduced a selected face to its contour and key internal features. In products oriented towards BPS users, shape, edge definition, relief, size and contrast were treated as functional information.

This approach follows tactile-design research, in which selective simplification and the organisation of salient features are more important than reproducing every visual detail (Cavazos Quero, Iranzo Bartolomé & Cho, 2021; Wu et al., 2022). The design logic of the five product groups is summarised in Table 1.

Table 1

Product groups, intended users, materials and main production processes

Product	Primary user group	Main material	Digital prepress	Production
Small jigsaw puzzle (20 pieces)	Younger sighted children	White acrylic glass, 3 mm	Image prepress; vector puzzle geometry	Laser cutting; UV inkjet printing
Large jigsaw puzzle (154 pieces)	Older / more experienced sighted children	Cardboard, 1.5 mm	Image prepress; denser vector puzzle geometry	Laser cutting; UV inkjet printing
Insert puzzle	Sighted and BPS children	Acrylic glass, 3 mm + foamed PVC, 5 mm	Figure isolation; vectorisation	Laser cutting; UV inkjet printing; bonding; hand finishing
Tactile face reliefs	BPS children	White PLA	Vector drawing; 3D modelling in Blender	FDM 3D printing; sanding; colour accents
Puzzle packaging	Puzzle users	Corrugated board, 1.5 mm	Dieline adaptation; graphic design	Digital printing; lamination; CNC cutting and creasing

2.2. Jigsaw puzzles and packaging

The small jigsaw puzzle was designed in A4 format with 20 pieces and produced from 3 mm white acrylic glass. The large puzzle used an A3 format with 154 pieces. Acrylic sheets of different thicknesses and levels of transparency were trialled for the larger version, but 1.5 mm cardboard was selected for the final prototype because it was lighter, easier to handle and closer to the material behaviour of a conventional jigsaw puzzle. Adobe Photoshop and Adobe Illustrator were used to prepare the artwork, define the formats and draw the cutting geometry. A regular grid provided the initial structure, but the tabs and sockets of individual pieces were then altered manually so that neighbouring pieces did not repeat the same geometry.

Laser cutting was performed on a HyperCUT PRO-6090 system, and the image was printed using an Apex MT-FP6090 UV inkjet printer. A generative image-extension tool was used solely to extend the peripheral areas of the image required for print bleed; the central pictorial content used for recognition remained unchanged.

After cutting, the rigid substrates were cleaned and carefully aligned for printing to ensure accurate registration between the printed image and the puzzle piece geometry. Packaging was developed as part of the product rather than as a neutral container. Dielines were adapted in Pacdora and refined in Adobe Illustrator. The small box measured approximately 200 × 100 × 40 mm and the large box approximately 260 × 150 × 50 mm. Both were made from 1.5 mm corrugated board laminated with printed self-adhesive sheets, then cut and creased on an Esko Kongsberg X20 computer numerical control (CNC) system. The larger box included internal dividers for sorting pieces by colour or form; the smaller box incorporated a simple creative activity based on the human figure motif. In this way, the packaging continued the interpretive logic of the products after the puzzle itself had been stored.

2.3. Insert puzzle

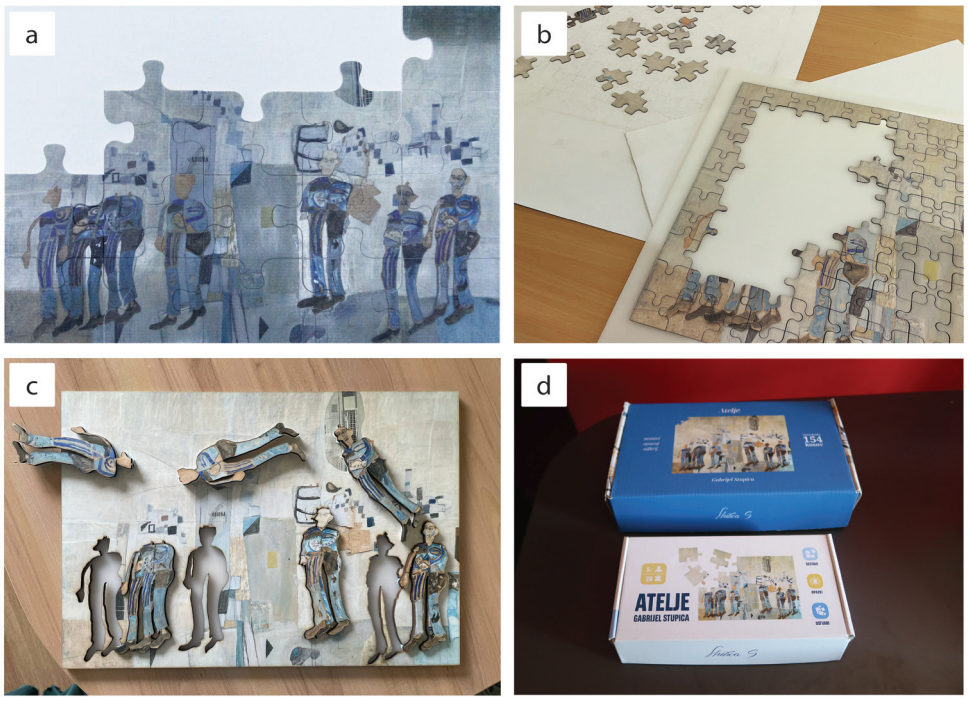
The insert puzzle translated the painting into a removable figure-ground system. Human figures were isolated from the artwork in Adobe Photoshop and redrawn as vector contours in Adobe Illustrator. Three technical files were prepared: one for the removable figures, one for the corresponding openings in the upper layer and one for the supporting base. The bottom layer was cut from 3 mm acrylic glass and the upper layer from 5 mm foamed PVC. The materials also worked as tactile cues, because the acrylic base is relatively smooth while the foamed PVC surface is more textured.

The image was printed onto the foamed PVC using UV inkjet printing, and the layers were bonded after cutting. Because several figures in *Atelje* have thin limbs and partly abstract contours, the vectorisation had to balance a recognisable silhouette with mechanical durability. The intended interaction was simple: a user could remove a figure, explore it as an independent shape, and then locate the corresponding recess within the full composition.

2.4. Tactile face reliefs

A facial detail from *Atelje* was selected for the tactile products and translated into two relief versions. The first, source-derived version followed the visible contours of the painting more closely. Key facial lines were manually traced in Adobe Illustrator and exported as scalable vector graphics (SVG). In Blender, the curves were converted to editable geometry, extruded and joined to a rectangular base so that the raised lines formed a single printable object. A second version intentionally reduced irregularities and internal detail. A generative image tool was used to create an initial symmetrical reference, which was then manually edited and redrawn before the same vector-to-3D workflow was repeated. The generated image therefore served as an intermediate design aid rather than as final printable geometry.

Both reliefs were manufactured on an ELEGOO Neptune 4 Plus using FDM with white PLA filament. Printed edges and selected surfaces were sanded, and the raised facial lines were emphasised in black to increase contrast for users with residual vision. UV inkjet printing was also trialled on the relief surface, but the height difference between the base and raised lines made accurate colour registration more difficult than on a flat substrate. The two versions were produced at a comparable overall size so that the principal difference during tactile exploration was graphic complexity rather than scale. The resulting product set is shown in Figure 2.



» **Figure 2:** *Final didactic products derived from Atelje: (a) small 20-piece jigsaw puzzle, (b) large 154-piece jigsaw puzzle, (c) insert puzzle with removable figures and (d) packaging for the two jigsaw puzzles*

2.5. Formative user evaluation

A formative prototype session was conducted in cooperation with Centre IRIS for education, rehabilitation, inclusion and counselling of BPS people. Nine children aged 6–13 years participated, five boys and four girls. Most were partially sighted, and one participant had very limited residual vision. The session was designed as an initial prototype evaluation rather than a controlled user study.

Observations, spontaneous comments and a short discussion after use were therefore treated as qualitative design feedback, and no inferential statistical analysis was performed. The children explored the insert puzzle and both tactile face versions individually. For the insert puzzle, the observer noted how the figures were handled, whether their positions could be found and whether edges or material transitions interfered with use. For the tactile faces, the source-derived version was presented first and the simplified version second. Exploration strategy, orientation on the surface and recognition of basic facial features were observed, and exploration time was noted during development.

Because the presentation order was fixed and the sample small, time was not analysed as a quantitative outcome. An earlier workshop with children from Kindergarten Trnovo also informed the redesign of the small jigsaw puzzle after repeated piece geometry allowed physically plausible but visually incorrect assembly.

3. Results

3.1. Jigsaw puzzles and packaging

The first small jigsaw puzzle prototype revealed a design problem that was not apparent in the digital cutting file. Repeated tab-and-socket geometry allowed several pieces to connect in positions where the printed motif did not belong.

This became particularly clear during a workshop with children from Kindergarten Trnovo: *Atelje* contains repeated figures and subdued coloured areas, so the image did not always provide an immediate visual correction. Manually varying the piece geometry reduced this ambiguity and produced a more reliable final assembly. The 3 mm white acrylic substrate also provided a stable base for UV printing and gave the printed image a visually clean background.

Material trials for the large jigsaw puzzle revealed a different set of constraints. Transparent acrylic reduced colour density unless additional printed layers or an opaque underprint were used. Thicker acrylic was mechanically stable but required repeated laser passes, which caused local melting and slight deformation at some edges, reducing piece fit. The 1.5 mm cardboard used for the final version avoided these problems and produced a lighter object with handling characteristics closer to a conventional puzzle.

The packaging prototypes added educational functions but also revealed a tolerance issue. The large box used internal dividers that allowed pieces to be sorted, while the small box included space for a child to create an additional figure. Both boxes closed correctly before lamination; after printed self-adhesive sheets were applied to both sides of the board, the added thickness made closure less smooth. The result is a useful reminder that graphic finishing and structural packaging design cannot be separated. A revised dieline should allow for laminated thickness in flap and slot tolerances from the outset.

3.2. Insert puzzle

The insert puzzle was successfully produced as a layered object, and the removable figures could be matched with their corresponding recesses. Material contrast and the 3D edges supported exploration of the composition as a set of separate forms rather than a single image. However, several thin arms and legs inherited from the painted figures were mechanically vulnerable. Small differences in how acrylic glass and foamed PVC responded to laser cutting also produced minor contour mismatches, which required additional care during bonding and alignment. Formative use showed that surface finishing was a functional requirement, not a cosmetic one.

The children understood the basic principle of removing and replacing the figures, but some edges felt too sharp during tactile exploration. Light hand sanding improved comfort without changing the overall contour. Participants also suggested a black outline around the figures to strengthen visual separation for users with residual vision. Accurate cutting alone was therefore insufficient: edge quality, contrast and robustness were equally important to the usefulness of the object.

3.3. Tactile face reliefs

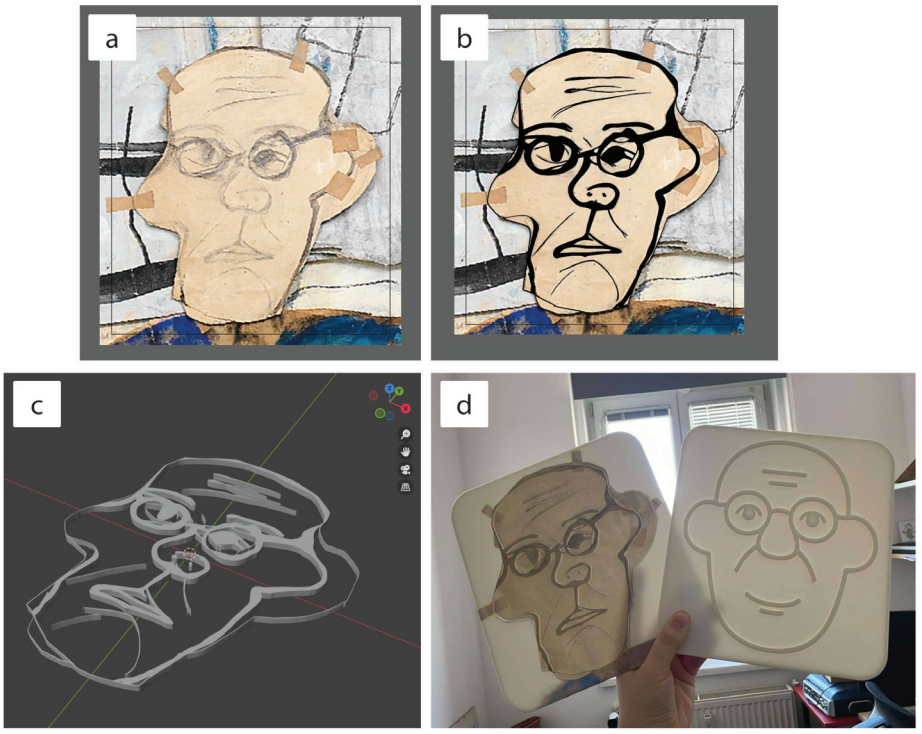
The tactile-face workflow required several iterations. SVG paths that were not fully connected produced fragmented geometry after import into Blender, and the source-derived face generated a relatively dense mesh because of its irregular lines and fine details. In an early print, the relief and base had not been joined into one solid model, so the raised layer separated locally from the backing surface. The geometry was corrected, and the relief was subsequently printed as a single, integrated object.

Post-processing further affected the final result. Sanding reduced small FDM irregularities and improved edge comfort, but it also showed that the part needed sufficient internal support to withstand abrasion without breaking the surface. Colour application by UV inkjet was less predictable on the relief than on the flat puzzle materials: the distance between the print head and the raised features produced slight registration errors and local colour spread. Manually applied black accents therefore provided more controlled visual contrast on the final prototypes. Post-processing should consequently be considered part of tactile design, particularly where roughness or finishing can change how a relief is explored (Dizon et al., 2021).

The clearest qualitative difference was between the two graphic versions of the face. The source-derived relief preserved more of the irregular line structure of the artwork, but it required slower, more focused exploration. The simplified version reduced competing contours and made the head outline, eyes, nose and mouth easier to follow in sequence. The two objects remained recognisably related to the same motif, yet they offered different levels of tactile complexity. The development workflow and the final tactile face reliefs are shown in Figure 3.

3.4. Formative user observations and exhibition deployment

During the Centre IRIS session, the children engaged with both product types. The insert puzzle was generally understandable once the task had been introduced, and the children relied on contour and shape to locate the removable elements. The most consistent criticism concerned edge comfort rather than the basic interaction.

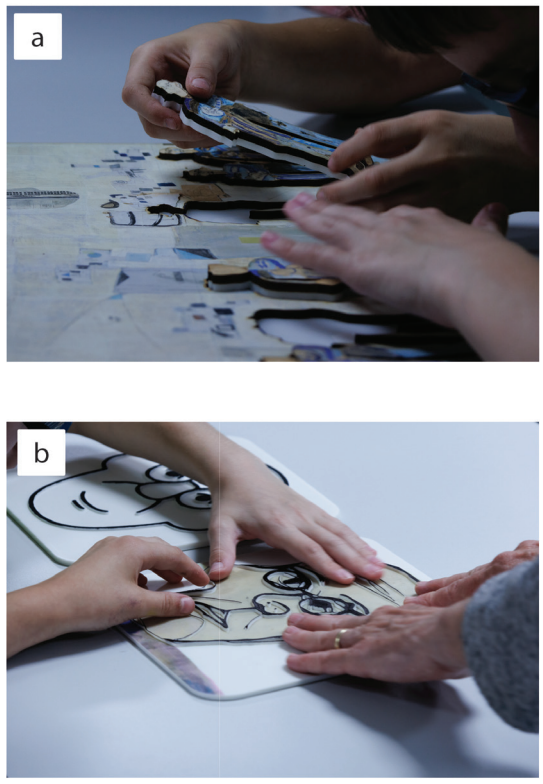


» **Figure 3:** *Development of the tactile face reliefs: (a) selected motif, (b) vector interpretation of the source-derived face, (c) 3D relief modelling in Blender, and (d) final source-derived, simplified tactile versions*

For the tactile faces, the simplified version supported clearer recognition of basic features, while the source-derived version required more time and attention. The relief height and overall object size were considered adequate for exploration. The children also responded positively to having both versions available, as the simplified face supported orientation while the more detailed relief maintained a closer connection with the artwork.

These observations are formative design evidence rather than a general measure of accessibility. The group was small, the age range broad, and the participants had different amounts of residual vision. No standardised questionnaire or quantitative recognition task was used, and the face versions were always presented in the same order. The value of the session lies instead in the concrete issues it exposed: sharp laser-cut edges, fragile contours, the burden of excessive line detail and the usefulness of stronger visual contrast.

The completed products were subsequently presented in the exhibition *Popotovanje papirnatih figuric* at Finžgarjeva galerija (Finžgar Gallery) from 27 May to 2 June 2025. Their installation showed that a single artwork can support several parallel forms of engagement, from conventional visual assembly to removable spatial elements and tactile relief. Exhibition deployment, however, should not be mistaken for validated accessibility; the prototypes remain a basis for further iterative testing. Examples of the formative evaluation are shown in Figure 4.



» **Figure 4:** *Formative evaluation with children from Centre IRIS: (a) exploration of the insert puzzle and (b) comparative tactile exploration of the facial reliefs*

4. Discussion

Across the product family, reinterpretation is a more accurate description of the design process than reproduction. Every prototype began with the same painting, yet the information that mattered shifted with the mode of interaction. The jigsaw puzzles relied on the relationship between piece geometry and the complete image; the insert puzzle relied on silhouette, edge quality and spatial matching; and the tactile faces relied on a hierarchy of raised lines that could be followed by touch. Treating all of these outputs as scaled copies would have ignored both perceptual and manufacturing requirements.

This distinction is especially important for tactile work. Vision can shift quickly between a whole composition and a small detail, whereas touch builds understanding through local, sequential contact. Dense line work that remains coherent to the eye can therefore become ambiguous under the fingers. The clearer response to the simplified face is consistent with research showing that tactile graphics benefit from reduced non-essential detail, adequate feature separation and a deliberate spatial hierarchy (Cavazos Quero, Iranzo Bartolomé & Cho, 2021; Wu et al., 2022). More broadly, 3D printed cultural objects are most effective when scale, material, and surface characteristics are designed for tactile use rather than inherited uncritically from the visual source (Bruns et al., 2023; Montusiewicz, Barszcz & Korga, 2022).

Simplification, however, is not automatically an improvement. The source-derived face retained more of Stupica's irregular visual character, and the children found value in comparing both versions. This points to a useful approach to art interpretation: a clear representation can establish orientation, while a second, richer version preserves complexity for further exploration.

Parallel representations therefore need not compete; they can offer different levels of access to the same motif, in line with multisensory museum approaches that combine complementary channels and degrees of detail (Avni et al., 2025; Levent & Pascual-Leone, 2014).

The insert puzzle illustrates a related shift from looking at an image to reconstructing it through action. Removing a figure, exploring its shape and returning it to the composition makes spatial relationships explicit in a way that the flat painting does not. This type of hands-on engagement is consistent with research on children's museum learning, which identifies interaction with objects and the environment as an important route to meaning-making (Andre, Durksen & Volman, 2017). The jigsaw puzzles operate differently but similarly require repeated comparison of shape, orientation and image information; puzzle play has been associated with children's spatial transformation skills (Levine et al., 2012).

Production decisions had direct consequences for use. Acrylic glass worked well for the small jigsaw puzzle but became less suitable as transparency or thickness increased. Cardboard produced a lighter large jigsaw puzzle; the layered insert puzzle gained useful material contrast but required careful registration; and the 3D reliefs showed that print geometry, infill, sanding and colour application cannot be considered separately. These observations support earlier work showing that manufacturing process, material and finishing influence the perceptual quality of tactile cultural heritage objects (Bruns et al., 2023; Montusiewicz, Barszcz & Korga, 2022).

Colour also played different roles across the prototypes. In the jigsaw puzzles it was the primary carrier of the painting's visual identity. In the BPS oriented products it was deliberately secondary: black accents on the tactile faces and the proposed outline around insert-puzzle figures were intended to support residual vision, while shape, contour and relief remained accessible through touch. This is consistent with multisensory approaches in which colour information is reinforced rather than left as the sole information channel (Cho, 2021).

One further point emerged from developing the products as a set. Inclusive interpretation does not have to mean producing a conventional object alongside a separate "special" version. Sighted children can use the insert puzzle and tactile reliefs, just as BPS children can engage with the same artwork narrative through non-visual information. Designing a family of related objects creates opportunities for shared use while still allowing different perceptual entry points. This principle is consistent with museum accessibility research that embeds inclusion within the main interpretative design rather than adding it afterwards (Avni et al., 2025; Avni, Danial-Saad & Kuflik, 2026).

The limitations of the evaluation remain important. Nine children cannot represent the range of BPS users, the age span was wide, and differences in residual vision were substantial. The fixed order of the facial relief presentation may have introduced a familiarity effect, and exploration time was not analysed under controlled conditions. The long-term durability of the materials, adhesives, paint and relief surfaces was also outside the scope of the work.

The next phase should therefore use iterative co-design, counterbalanced comparisons and task-based measures of recognition, placement, and comfort. It should also compare relief height, line width, surface texture, and more durable or lower-impact materials. A recent systematic review of museum accessibility similarly identifies structured stakeholder involvement and mixed-method evaluation as priorities for moving from promising prototypes to dependable inclusive experiences (Avni, Danial-Saad & Kuflik, 2026).

5. Conclusions

This study developed a coordinated set of didactic, interactive and tactile products from Gabrijel Stupica's *Atelje* using graphic prepress, laser cutting, UV inkjet printing, 3D modelling and FDM 3D printing. The main contribution lies not in any single technology, but in the way the same visual source was translated differently according to task and mode of perception.

The full painting could be retained where visual assembly was useful, figures could be separated where spatial placement mattered, and a selected face could be simplified where dense pictorial detail interfered with tactile recognition.

The production process showed that usability is shaped by seemingly small technical decisions. Repeated jigsaw-piece geometry allowed incorrect assembly, thick acrylic reduced cutting accuracy, laminated packaging altered closing tolerances, layered materials required careful registration, laser-cut edges needed manual finishing, and raised 3D geometry complicated colour application. Accessible products therefore depend on graphic translation, manufacturability and post-processing as much as on visual similarity to the source (Montusiewicz, Barszcz & Korga, 2022; Wu et al., 2022).

The formative session with BPS children was highly informative for comparing the two tactile face versions. The simplified relief was easier to interpret, while the source-derived version retained more of the visual irregularity of the painting. Rather than identifying one representation as universally preferable, the results support a layered approach in which different versions can serve orientation, comparison and deeper exploration. Further co-design and structured user testing are required before the prototypes can be treated as validated accessible products, in line with current evidence that stakeholder involvement and rigorous evaluation are central to effective tactile and multimodal museum design (Avni et al., 2025; Avni, Danial-Saad & Kuflik, 2026).

6. Acknowledgments

The authors thank Centre IRIS and the participating children and professionals for their contribution to the formative prototype evaluation, as well as Hana Stupica, David Tavčar and the collaborators of the *Popotovanje papirnatih figuric* project. They are also grateful to Tamara Trček Pečak, co-supervisor of the diploma thesis, for her guidance and support during its development, and to Jon Brce for technical assistance with UV printing. The authors further acknowledge Pečenko d.o.o. (Ljubljana, Slovenia), a company specialising in acrylic-glass processing, for donating the acrylic offcuts used during prototyping.

7. References

Andre, L., Durksen, T. and Volman, M.L. (2017) 'Museums as avenues of learning for children: A decade of research', *Learning Environments Research*, 20(1), pp. 47–76. DOI: 10.1007/s10984-016-9222-9

Avni, Y., Danial-Saad, A., Sheidin, J. and Kuflik, T. (2025) 'Enhancing museum accessibility for blind and low vision visitors through interactive multimodal tangible interfaces', *International Journal of Human-Computer Studies*, 198, 103469. DOI: 10.1016/j.ijhcs.2025.103469

Avni, Y., Danial-Saad, A. and Kuflik, T. (2026) 'Design for inclusion: A systematic review of technologies and frameworks for enhancing the museum experience of blind and low-vision visitors', *International Journal of Human-Computer Interaction*. DOI: 10.1080/10447318.2026.2623227

Axel, E.S. and Levent, N.S. (eds.) (2003) *Art Beyond Sight: A Resource Guide to Art, Creativity, and Visual Impairment*. New York: Art Education for the Blind and AFB Press.

Bruns, A., Spiesberger, A.A., Triantafyllopoulos, A., Müller, P. and Schuller, B.W. (2023) '"Do touch!" – 3D scanning and printing technologies for the haptic representation of cultural assets: A study with blind target users'. In: Gouet-Brunet, V., Kosti, R. and Weng, L. (eds.) *SUMAC '23: Proceedings of the 5th Workshop on the analySis, Understanding and proMotion of heritAge Contents, 2 November 2023, Ottawa, Canada*. New York: Association for Computing Machinery, pp. 21–28. DOI: 10.1145/3607542.3617351

Cavazos Quero, L., Iranzo Bartolomé, J. and Cho, J. (2021) 'Accessible visual artworks for blind and visually impaired people: Comparing a multimodal approach with tactile graphics', *Electronics*, 10(3), 297. DOI: 10.3390/electronics10030297

Cho, J.D. (2021) 'A study of multi-sensory experience and color recognition in visual arts appreciation of people with visual impairment', *Electronics*, 10(4), 470. DOI: 10.3390/electronics10040470

Dizon, J.R.C., Gache, C.C.L., Cascolan, H.M.S., Cancino, L.T. and Advincula, R.C. (2021) 'Post-processing of 3D-printed polymers', *Technologies*, 9(3), 61. DOI: 10.3390/technologies9030061

Falk, J.H. and Dierking, L.D. (2018) *Learning from Museums*. 2nd ed. Lanham, MD: Rowman & Littlefield.

Karaduman, H., Alan, Ü. and Yiğit, E.Ö. (2023) 'Beyond "do not touch": The experience of a three-dimensional printed artifacts museum as an alternative to traditional museums for visitors who are blind and partially sighted', *Universal Access in the Information Society*, 22(3), pp. 811–824. DOI: 10.1007/s10209-022-00880-0

Levent, N. and Pascual-Leone, A. (eds.) (2014) *The Multisensory Museum: Cross-Disciplinary Perspectives on Touch, Sound, Smell, Memory, and Space*. Lanham, MD: Rowman & Littlefield.

Levine, S.C., Ratliff, K.R., Huttenlocher, J. and Cannon, J. (2012) 'Early puzzle play: A predictor of preschoolers' spatial transformation skill', *Developmental Psychology*, 48(2), pp. 530–542. DOI: 10.1037/a0025913

Montusiewicz, J., Barszcz, M. and Korga, S. (2022) 'Preparation of 3D models of cultural heritage objects to be recognised by touch by the blind – case studies', *Applied Sciences*, 12(23), 11910. DOI: 10.3390/app122311910

Pye, E. (ed.) (2007) *The Power of Touch: Handling Objects in Museum and Heritage Contexts*. Walnut Creek, CA: Left Coast Press.

Urbas, R., Pivar, M. and Stanković Elesini, U. (2016) 'Development of tactile floor plan for the blind and the visually impaired by 3D printing technique', *Journal of Graphic Engineering and Design*, 7(1), pp. 19–26. DOI: 10.24867/JGED-2016-1-019

Wu, C.-F., Wu, H.-P., Tu, Y.-H., Yeh, I.-T. and Chang, C.-T. (2022) 'A study on the design procedure of three-dimensional printable tactile graphics for individuals with visual impairments', *Journal of Visual Impairment & Blindness*, 116(4), pp. 507–516. DOI: 10.1177/0145482X221122754



© 2026 Authors. Published by the University of Novi Sad, Faculty of Technical Sciences, Department of Graphic Engineering and Design. This article is an open access article distributed under the terms and conditions of the Creative Commons Attribution license 4.0 Serbia (http://creativecommons.org/licenses/by/4.0/rs/).

Review Paper https://doi.org/10.24867/GRID-2026-p47

Human by Design: Graphic Design and Design Thinking in the Age of AI

ABSTRACT

This paper examines the intersection of graphic design, human-centered design thinking, and generative AI technologies. It highlights how AI can accelerate tasks such as ideation, prototyping, image generation, typography exploration, and brand experimentation while simultaneously raising important questions about originality, ethics, authorship, and visual culture. Drawing on existing research, this paper demonstrates how designers can use generative AI as a collaborative tool rather than viewing it solely as a replacement for human creativity.Central to the discussion is the argument that design thinking becomes even more valuable in an AI-driven world. While AI excels at producing rapid outputs and identifying patterns, human designers remain essential for empathy, storytelling, critical judgment, cultural understanding, and meaningful communication. The paper emphasizes that the future of graphic design will depend not only on mastering new technologies but also on preserving the human qualities that make design impactful and socially relevant. Ultimately, this paper invites audiences to reconsider the evolving identity of the designer and to envision a future in which creativity, strategy, and technology coexist within a more intentional and collaborative design ecosystem.

Charles T. Weiss

Graphic Communications,
Clemson University, Clemson, USA

KEY WORDS
Graphic design, design thinking, artificial intelligence, generative AI, human-centered design

1. Introduction

Generative artificial intelligence (AI) is transforming the world of graphic design, but this transformation is only the latest major change in the field. Graphic design has always been centered on human interaction, but generative AI threatens to remove the human element from the graphic design process. Fortunately, the human elements that make design more impactful and socially relevant will continue to play a major role in graphic design. Generative AI will simply be another technological change that not only changes the graphic design process but also makes it even more important for humans to remain part of that process. This human-centered approach can be seen in the use of design thinking, which can strengthen the graphic design process while allowing designers to benefit from generative artificial intelligence.

2. History of graphic design

Graphic design is not new. It can be traced to the beginnings of modern civilization. The cave paintings found in the caves at Lascaux, France, provide one example of very early graphic design dating to approximately 10,000 BCE (Meggs, 2025). These paintings are some of the oldest known graphic artifacts, and they demonstrate the ability to tell stories through graphics and the early development of visual communication. A major subsequent stage in graphic design occurred when writing, paper, and printing transformed the written and graphic world. This period culminated in the invention of movable type by Johannes Gutenberg in Germany around 1450 (Meggs, 2025). Movable type transformed the world in many ways because books and documents could be reproduced by machine rather than written by a scribe one letter at a time. Following Gutenberg, design continued to flourish, and the beginnings of modern typography can be seen in the ways books and

documents were reproduced. The Industrial Revolution brought further advancements, including steam-powered printing presses, the ability to create decorative type, the invention of the Linotype press in 1886—the first keyboard typesetting machine—and Eastman Kodak's widely available photographic technology.

The early 1900s were marked by major design shifts and the founding of the Bauhaus in 1919. By the mid-1900s, the Polaroid camera had been invented, and the first Xerox copying machine was introduced. In the 1950s, the first computers were developed, and designers continued to create new visual trends, including Andy Warhol's Campbell's Soup Cans in 1962. Graphic designers continued to push the boundaries of visual communication, and the world experienced a vast array of modern visual design elements.

In 1976, the Apple computer was first introduced and made computers available to more people. This household computer helped create the conditions that led to the development of Photoshop in 1990, one of the first software applications that allowed users to manipulate and edit digital images directly on a computer. In 1993, the first web browser, Mosaic, was launched, and by 1994, 33% of U.S. households had computers. The Internet continued to grow, and by 2005 there were more than 800 million Internet users globally, including 200 million in the United States. Apple also introduced the iPhone in 2007 and the iPad in 2010. In 2015, OpenAI was founded as an artificial intelligence research organization.

All of these changes have had a direct effect on the creation of new graphic design themes and movements. These changes caught many people off guard, but great graphic designers took advantage of new technology and ushered in a new world of graphic design. In many ways, this is the world of graphic design today. Generative AI has brought a new chapter to graphic design, but, as in the past, this chapter will be led by humans with the help of computers and digital processors. If designers do not figure out how to take advantage of AI tools in their workflows, they may be left behind.

3. Human-centered design thinking and graphic design

At the core of the historical transitions in graphic design is the idea that the best designs will continue to be human-centered. For instance, when the printing press was first invented, human graphic designers were still essential to producing worthwhile designs. When the first Apple computer made it possible to create designs at home, a human was still driving the process. Printing presses and computers changed graphic design processes, but humans remained responsible for the outcomes. Traditional graphic designers work with clients to solve design problems. This will continue to be the case as generative AI becomes more readily available, but human designers will still be needed to develop worthwhile solutions that work for clients. Generative AI will become another valuable tool in the graphic designer's toolbox.

One way to examine this transition to generative AI is to consider how design thinking continues to change the way problems are addressed and solved. Design thinking is not a new concept, but it is well suited to combining human-centered thinking with artificial intelligence. Design thinking is also a problem-solving method that emphasizes the user. Through a problem-solving process, designers discover appropriate solutions to the challenges brought before them (Patria et al., 2024).

The idea of design thinking is based on several processes that are carried out in an iterative and flexible manner rather than through a strictly linear process. One definition of design thinking describes it as a discipline that uses the methods and sensibilities of the designer to match the needs of people with technologically feasible and viable business strategies that can be converted into customer value and clear market opportunities (Martin, 2009). While this definition of design thinking was created before the advent of generative AI, it still holds true today. A good designer uses their skills to create what the client wants, even when using generative AI.

Design thinking is a technique that can be adopted by anyone. It is a problem-solving method that can be applied to small or large problems, including graphic design problems. Design has a purpose and intent: to solve a problem. Design thinking provides a framework for designers to solve problems more effectively. This framework is built on five phases: empathy, definition, ideation, prototyping, and testing. Each phase builds upon the others and allows crossover and interaction among the phases. The framework is also centered on people. Design thinking should be used to solve a problem by truly understanding the needs of the people who need a solution, whether the problem involves graphic design or a service. People should remain the focus of the entire process. This approach allows for continual feedback and reflection between phases and gives designers the chance to revisit earlier phases as they move forward. The final solution should be people-centered (Stackowiak & Kelly, 2020).

Creativity is often seen as a core element of design thinking. Designers need to be creative when finding solutions, and design thinking provides a framework for solving problems creatively. Design thinking can also be compared to a toolbox. Each phase is part of the solution, but designers must be familiar with the tools and knowledgeable about how to use them efficiently and properly (Johansson-Sköldberg, Woodilla & Çetinkaya, 2013).

Artificial intelligence and design thinking can also work together to produce more unique and innovative solutions. By proactively incorporating AI, design thinking can transform the design process, stimulate creativity, improve user experience, and benefit society (Sreenivasan & Suresh, 2024).

4. Generative artificial intelligence

Artificial intelligence refers to the ability of machines to perform tasks in ways that mimic aspects of human intelligence (Chang & Tsai, 2024). AI has quickly spread to almost every aspect of life and will continue to grow in ways that have yet to be seen. AI can be encountered when opening a web browser, reading an email, conducting an online search, or playing a game. Artificial intelligence has become a constant presence in everyday life and will continue to expand.

Generative AI is a branch of artificial intelligence focused on generating pixels, text, and ideas. It can quickly generate many possible concepts from a short written prompt. These concepts can include initial ideation, prototyping, image generation, image editing, typography, layout, and branding. The quality of these creations can vary greatly, and the best AI-generated elements are generally produced through well-thought-out and carefully constructed prompts from human users (Kaplan, 2024).

In the world of graphic design, generative AI can create high-quality text, imagery, and other content based on the data and instructions provided to it. The input may consist of user prompts or visual examples that the system uses to create new elements. Generative AI holds enormous potential to create new design opportunities, but its use must be considered within the constraints of intellectual property law, privacy, and copyright (Martineau, 2023).

The various AI tools available, including ChatGPT, DALL-E, Figma, Stable Diffusion, Midjourney, Firefly, and Claude, have been used for visual image generation, iteration, and refinement. They can also facilitate creativity and support decision-making while reducing the time required for design processes. Although these tools have been widely adopted, their role in design is still evolving, and their long-term impact remains to be determined (Choudhury, Eisenbart & Kuys, 2025).

The use of generative AI is also transforming the way graphic design is taught in higher education. Design educators are now being tasked with preparing students to use generative AI as part of the design process. Educators must guide students in understanding the appropriate use of generative AI within the classroom, studio, and professional practice. Generative AI can be seen as a change agent, but graphic design students must still possess strong design skills and creative problem-solving abilities while developing new skills, such as the use of AI. Design students must also cultivate a critical eye to question the authenticity of AI-generated material and view AI as a collaborative tool rather than as a manufacturing system for final products (Fleischmann, 2024).

5. How generative artificial intelligence is changing graphic design

The use of artificial intelligence in graphic design (AIGD) reveals two distinct phases in the evolution of AI and graphic design. The early phase focused on decomposing design tasks into individual components, such as typography generation, layout optimization, and color-palette recommendations. The second phase has expanded these applications into generative models capable of producing typography, images, vector shapes, layouts, and colors. This phase also includes the ability of AI to create holistic systems that bridge human instruction and final artwork. Generative tasks are now a significant part of contemporary design practice. AI can create design elements with transparent backgrounds and can also create vector shapes (Zou, Zhang & Zhao, 2025).

Because of these changes, Generative AI continues to change graphic design in a multitude of ways. These include speed and efficiency in creating ideas, expanding the exploration boundaries, improved communication between designers and clients, greater accessibility to designers who may not have a strong background in graphic design, and providing more time for designers to focus on strategic work like research, storytelling, and strategic decision making.

As an example, generative AI allows designers to quickly develop a multitude of ideas. Just as designers once used pencil and paper to draw thumbnails, generative AI can now be used to produce initial ideas rapidly. This changes the ideation stage to take advantage of AI tools without removing humans from the process. The creation of mood boards is an especially powerful application of AI because it allows designers to explore alternative solutions and move quickly past creative roadblocks. This expedited approach to initial ideation allows designers to spend more time focusing on their solutions (Chen et al., 2025).

AI can also create prototypes quickly and efficiently. These rough initial versions can be used to show potential layouts, package mock-ups, website mock-ups, and social media posts to clients. AI can also shorten the time it takes designers to move from an

abstract idea to something that can be shown to a client and discussed (Furtado, Soares & Furtado, 2024).

Designers can also use generative AI to create backgrounds and illustrations, produce photographs based on prompts, remove or replace objects, expand images to include additional elements, create alternate versions, and quickly test differing visual styles, (Huang et al., 2025).

Typography is another area in which generative AI can assist designers. AI can quickly suggest type pairings, letter styles, color systems, grid layouts, and typographic styles. Unfortunately, typography remains challenging for AI because lettering requires precision, consistency, readability, and cultural awareness (Bosheah & Bilicki, 2025).

Branding concepts are also a useful application of generative AI because various concepts can be created quickly, including alternate imagery, different logos, product visualizations, color combinations, and layout variations. When using generative AI for branding concepts, it is important to remember that a brand is more than a logo, design, or color. For this reason, human-centered judgment in the use of generative AI is more important than ever (Gual-Ortí et al., 2025).

6. The continuing importance of human-centered design

AI can produce patterns and outputs, but human designers provide prompts, experience, and emotion. Humans inherently work with empathy and emotions, whereas AI operates through computational models and user-provided prompts. From a human standpoint, empathy can be developed through interviews, observation, personal experience, and emotional responses.

AI can identify patterns and produce outputs, but human designers study people's experiences and emotions. This human interaction can include one-on-one or group interviews, observation, testing, emotional responses, and lived experiences. These are activities to which generative AI has limited direct access. Generative AI can learn from information derived from human interaction, but it does not process that information in the same embodied and experiential way that humans do. Designers have the human ability to connect visual elements into narratives that create the basis for a story. Humans can interpret what a design and its message communicate, respond emotionally to a design, and relate it to a larger cultural story. These experiences are human-based and cannot be reduced solely to AI (Zhu & Luo, 2024).

Humans can also exercise critical judgment when evaluating a design. For instance, they can assess whether a design is appropriate, accurate, ethical, culturally appropriate, or aligned with a client's goals. AI can produce many options, but it cannot reliably determine which option is appropriate without human-defined criteria and contextual oversight.

Generative AI can also struggle to understand cultural context. AI-generated outputs may fail to account for the background of certain symbols, historical references in designs, cultural and societal representation, stereotypes, regional differences, power relationships, and inclusivity.

Human designers can also better connect a design with its intended message. This includes understanding who the audience is, what message the audience may perceive, how the message will be shared, the context and purpose of the message, and its tone. Generative AI can produce many of these elements, but it may not reliably connect the design to the intended message.

7. How the designer's role is changing

As in past technological innovations, graphic designers must learn to use the tools available to them. The invention of the computer and the Internet transformed graphic design, and designers who did not adopt these technologies were left behind. Generative AI provides even more opportunities to help designers, but designers must learn to use these tools appropriately. Graphic designers may not need to draw countless thumbnails anymore, but they must still be able to generate creative solutions quickly, and generative AI can help with that.

The integration of generative AI into graphic design can be seen as more than a revolution; it can be viewed as an era-defining transformational wave that is changing how creative work is produced. Generative AI provides designers with the ability to automate repetitive tasks while also allowing them to discover new possibilities. AI can significantly boost creativity. Designers who incorporate AI as an aid to their work can take on new roles as the industry moves into uncharted territory. AI does not mean that graphic designers are no longer needed; rather, it offers designers new ways to flourish and grow (Alkahteeb et al., 2025).

In a review by Kumar, Tu and Zallio (2025), the findings indicated that the use of generative AI is undergoing rapid transition. While the use of generative AI in user-experience design is expanding, its implementation remains uneven across design-process stages and practitioner communities. The review found that most applications of generative AI remain exploratory and are limited by the constraints of commercially available tools. Generative AI has found a place

in mid- and late-stage design activities but remains underused in the early stages of design. The integration of generative AI into user experience and design represents a paradigm shift that is continuing to evolve.

8. Responsible use of generative ai

Responsible use of AI and generative AI requires treating the AI component as a collaborative tool rather than a replacement for human-centered design. Designers must remain involved in the process, including evaluating outputs, addressing cultural and ethical concerns, protecting authorship and copyright, and ensuring that generative AI visuals support the intended communication goals. AI can enhance production but may lack intentionality and cultural awareness (Chen & He, 2026).

Through a comprehensive review of 33 papers, a 2024 study identified four paradigms for the use of AI in graphic design: artificial intelligence-driven design automation and generation (AIDAG), artificial intelligence-assisted graphic design and image processing (AGDIP), artificial intelligence in art and creative design processes (AACDP), and artificial intelligence-enhanced visual attention and emotional response modeling (AVERM). These paradigms illustrate the multidimensional role of AI in design, ranging from automation to emotional interaction. The findings suggest that AI serves both as a design tool and as a medium for innovation. AI can enhance the automation and efficiency of the design process while also fostering designers' creative thinking and understanding of users' emotional needs (Li et al., 2024).

Graphic designers must understand both the benefits and the limitations of generative AI. AI should be treated as a tool in the designer's toolbox, but designers will need to determine the most responsible ways to use these tools and learn how to apply AI intentionally in service of a design's purpose and intent.

9. Conclusion

Generative AI will continue to change the world of graphic design. This may scare some designers while exciting others. Designers who embrace generative AI as another tool in their toolbox will continue to grow and build on their design skills, while those who do not embrace it may face a more difficult professional environment as generative AI continues to affect the field.

The tools provided by generative AI should be seen as collaborators rather than final solutions. Human-centered design remains necessary for creating effective graphic design because AI is not yet able to reliably act in the ways humans do. The world of generative AI is still built around human commands and prompts. The power of AI continues to grow rapidly, but generative AI must be used intentionally and within the boundaries of cultural and societal norms.

Graphic design has faced many major changes throughout its history. AI and generative AI are simply another major shift in the field. Just as the printing press and the computer revolutionized graphic design, AI will also transform it. As humans, we can choose to collaborate with AI and continue to grow, or we can fail to adapt to changes in the field. The choice is ours.

10. References

Alkahteeb, S.S., Almomani, I.G., Zoubi, M.K., Issa, M.M., Al Smadi, M.A., Jaradat, H.A. and Abualhumos, T.M. (2025) 'Artificial intelligence in graphic design processes: The impact analysis and challenges', *Mutah Journal of Humanities and Social Sciences*, 40(1), pp. 35–52. DOI: 10.35682/mjhss.v40i1.1084

Bosheah, Z. and Bilicki, V. (2025) 'Challenges in generating accurate text in images: A benchmark for text-to-image models on specialized content', *Applied Sciences*, 15(5), 2274.

Chang, Y. and Tsai, M. (2024) 'Effects of design thinking on artificial intelligence learning and creativity', *Educational Studies*, 50(5), pp. 763–780. DOI: 10.1080/03055698.2021.1999213

Chen, L., Song, Y., Guo, J., Sun, L., Childs, P. and Yin, Y. (2025) 'How generative AI supports human in conceptual design', *Design Science*, 11.

Chen, Z. and He, Y. (2026) 'Ethical dilemmas in artificial intelligence-generated art: Authorship, ownership, and the blurring of creative boundaries', *Digital Scholarship in the Humanities*, 41(2), pp. 647–661.

Choudhury, M.M., Eisenbart, B. and Kuys, B. (2025) 'Artificial intelligence (AI) in the design process – a review and analysis on generative AI perspectives', *Proceedings of the Design Society*, 5, pp. 631–640.

Fleischmann, K. (2024) 'Generative Artificial Intelligence in Graphic Design Education: A Student Perspective', *Canadian Journal of Learning and Technology*, 50(1), pp. 1–17.

Furtado, L.S., Soares, J.B. and Furtado, V. (2024) 'A task-oriented framework for generative AI in design', *Journal of Creativity*, 34(2), 100086.

Gual-Ortí, J., Martínez Moya, J.A., Amat, J. and Felip Miralles, F. (2025) 'The future of logo design: Considering generative AI-assisted designs', *International Journal of Visual Design*, 19(1), pp. 109–123.

Huang, Y., Huang, J., Liu, Y., Yan, M., Lv, J., Liu, J., Xiong, W., Zhang, H., Cao, L. and Chen, S. (2025) 'Diffusion model-based image editing: A survey', *IEEE Transactions on Pattern Analysis and Machine Intelligence*, 47(6), pp. 4409–4437.

Johansson-Sköldberg, U., Woodilla, J. and Çetinkaya, M. (2013) 'Design thinking: Past, present and possible futures', *Creativity and Innovation Management*, 22(2), pp. 121–146.
Kaplan, J. (2024) *Generative Artificial Intelligence*. 1st ed. New York, NY: Oxford University Press.
Kumar, T., Tu, X. and Zallio, M. (2025) 'How generative AI is reshaping UI/UX design workflows: A systematic review'. In: *AHFE International*.
Li, H., Xue, T., Zhang, A., Luo, X., Kong, L. and Huang, G. (2024) 'The application and impact of artificial intelligence technology in graphic design: A critical interpretive synthesis', *Heliyon*, 10(21), e40037.
Martin, R.L. (2009) *The Design of Business*. Boston, MA: Harvard Business Press.
Martineau, K. (2023) *What is Generative AI?*. IBM Research.
Meggs, P.B. (2025) *Meggs' History of Graphic Design*. 7th ed. Newark: John Wiley & Sons Ltd.
Patria, A.S., Ekohariadi, E., Sutiadiningsih, A., Kristiana, N. and Prihadi, K.D. (2024) 'Instrument development of design thinking test for graphic design students', *IJORER: International Journal of Recent Educational Research*, 5(4), pp. 796–807.
Sreenivasan, A. and Suresh, M. (2024) 'Design thinking and artificial intelligence: A systematic literature review exploring synergies', *International Journal of Innovation Studies*, 8(3), pp. 297–312.
Stackowiak, R. and Kelly, T. (2020) *Design Thinking in Software and AI Projects: Proving Ideas Through Rapid Prototyping*. 1st ed. Berkeley, CA: Apress.
Zhu, Q. and Luo, J. (2024) 'Toward artificial empathy for human-centered design', *Journal of Mechanical Design*, 146(6).
Zou, X., Zhang, W. and Zhao, N. (2025) 'From fragment to one piece: A review on AI-driven graphic design', *Journal of Imaging*, 11(9), 289.



© 2026 Authors. Published by the University of Novi Sad, Faculty of Technical Sciences, Department of Graphic Engineering and Design. This article is an open access article distributed under the terms and conditions of the Creative Commons Attribution license 4.0 Serbia (https://creativecommons.org/licenses/by/4.0/deed.en).

Review Paper https://doi.org/10.24867/GRID-2026-p48

The Role and Future Potential of Books and Book Printing in the European Knowledge Economy

ABSTRACT

The authors—who have been working in the world of printed books for decades—sought to identify the challenges and trends that will shape Europeans' future relationship with printed books by analysing recently published academic papers, conference presentations, and expert reports. The report details the driving forces that will have the greatest impact on the European book printing market in the future, as follows. End-user preferences are changing the demand for printed books and other formats. Changes in physical book production methods are driving significant market shifts. Optimizing book production locations will become necessary as supply chains evolve, publishing business models transform, and print-on-demand becomes more widespread. A focus on sustainability - reducing waste during production and throughout the supply chain - is of paramount importance. The availability and cost of paper will be critical following the closures of paper-making machines and mills. The authors also seek to determine what role printed books might play in the development of the European knowledge economy, amid the spread of digitalization. They highlight the strengths of printed books, particularly their proven benefits for reading comprehension and learning. Alternative channels and social media can give printed books a boost. Viral marketing can boost sales of titles. BookTok, a sub-community on TikTok focused on books and literature, has become increasingly popular. Members of this sub-community (known as BookTokers) create videos in which they review, discuss, and joke about the books they've read. The printed book has a unique dual nature: it is both a cultural and a technical product. In this regard, its physical appearance is also important. The authors present the results of a joint research program conducted by Óbuda University and Alföldi Nyomda PLC. - Hungary's leading book printer - which aimed to create modern, attractive visual designs for books and implement them technologically, as well as to develop connections and integrations with digital devices.

Gábor Tóth [1]
Kornél Remete [2]
Csaba Horváth [3]
László Koltai [3]

[1] Technical Association of Paper and Printing Industry, Hungary
[2] Alföldi Nyomda Printing House Plc, Debrecen, Hungary
[3] Óbuda University, Institute of Media Technology and Light Industry, Hungary

KEY WORDS
Book publishing, trends and driving of book printing, new methods of book sales, impact of reading

1. Introduction

The book is a "fantastic product" with a unique dual nature. It is both a cultural and a technical product. For printers, a book may simply mean paper, ink, and manufacturing processes. For publishers, however, it embodies culture, ideas, and intellectual exchange. Both dimensions are indispensable and inseparable. Without technical excellence, there can be no physical book. And without cultural value, printing has no meaning.

Printed books are expected to continue playing an important role in European societies in the future, particularly considering their proven benefits in the areas of reading comprehension and learning (INTERGRAF, FEP & CEPI, 2023).

Óbuda University and Alföldi Printing House—an iconic institution in Hungary with a history spanning more than 460 years—are conducting a joint research program aimed at exploring the expectations of the younger generation of book users regarding print communication. How should the design and production of books be adapted to meet these expectations?

As part of this research program, the authors summarize and analyze the trends expected in the world of books, which will also be the main drivers of the book market and book production in the aftermath of the COVID-19 pandemic. What are the typical changes in lifestyle and habits? How are sustainability issues evolving? What are the consequences of the rise in digital printing and the increasingly widespread use of electronic end-user products? How are these developments being influenced by the explosive growth in production costs?

2. Research methods

The authors—who have been working in the world of printed books for decades—examine recently published scholarly articles, conference presentations, and expert reports to identify the challenges and trends that will shape European societies' future relationship with printed books.

The data presented in this article—regarding book publishing and printing—covers both Western and Eastern Europe, including all 27 EU member states, as well as the United Kingdom, Norway, and Switzerland.

Books include black-and-white and color hardcover books; paperback and flip-through books; educational and religious books; works of fiction and non-fiction; children's books; travel books; general-interest books; art books; and reference books. This category also includes privately published works but excludes photo albums and yearbooks.

Value data have been converted to euros in 2024 constant prices and exchange rates to reflect actual changes in demand, considering the effects of inflation (measured by the consumer price index) and exchange rate fluctuations. Data on print volume is expressed in A4-equivalent pages.

3. An overview of the European book publishing and printing market

In their analysis, the authors drew on the presentations given at the "Shaping the Future with Books 2026" conference held in Brussels in February 2026, as well as on the facts and data published in the "INTERGRAF Book Market Report 2026"—a joint publication by INTEGRAF and SMITHERS (Smithers, 2021) related to the conference— supplemented by conclusions drawn from other academic publications and their own research findings within the scope of this article.

3.1. Book publishing overview

According to the Federation of European Publishers (FEP) the European book market reached its highest ever nominal turnover in 2024, at €24.9 billion. This FEP data covers most major European publishers, but not all. The 2024 figure is nominally ahead of the previous 2007 peak but when adjusted for inflation the turnover is down to €15.5 billion, compared to €22.2 billion in 2007. Partly this is because book prices have risen 38.3% over the past 20 years, far below general inflation (64.1%), putting sustained pressure on publisher margins. The FEP report on the European book market also highlighted a worrying trend in reading engagement identifying 47.2% of Europeans aged 16 and over as non-readers (source: Eurostat). The main reason is lack of interest, not affordability.

Printed books still dominate accounting for 82.9% of the total, but audiobooks are the fastest-growing segment, reaching 4.2% of sales in 2024.

It is difficult to accurately track data on audiobooks due to various subscription models and players such as Spotify, which have the potential to disrupt the status quo (and make tracking more difficult). Europe is a net importer of books; UN Comtrade data show a net deficit of $1.04 billion in 2024. The data in Table 1 show the value of books at the publisher level, not the value of book printing.

Table 1

2024 European book publishing export and import trade ($ million) (UN Comtrade)

	2020	2021	2022	2023	2024
Import	7 737	8 388	7 325	6 968	6 862
Export	6 584	7 289	6 629	6 161	5 827

The Commodity Trade Statistics Database of United Nations Statistics Division is the source for Table 2. Printing children's books shows a significant net import balance (especially from China), reflecting the complex binding and finishing involved in many pop-up books requiring high levels of manual processing.

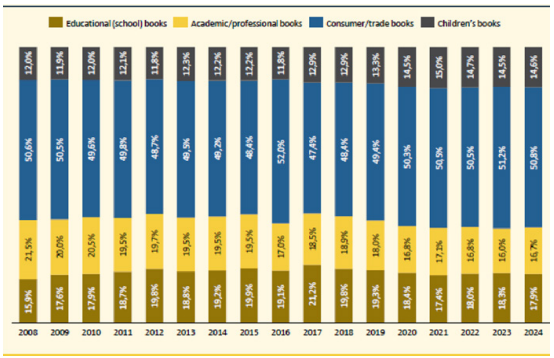
The aggregate revenue data for European publishers is shown in Figure 1, with percentages listed by category.

Biggest segment is consumer/trade books where publishers make money on the best sellers. Popular books don't change and are not time sensitive, so often mass produced and warehoused.

Table 2

2024 European book printing export and import trade ($ thousand)

Commodity	Export value (US$)	Import value (US$)
Maps and hydrographic or similar charts; printed in book form, including atlases, topographical plans and similar	26 432	12 321
Printed matter; children's picture, drawing or coloring books	306 465	653 235
Printed matter; dictionaries, encyclopedias and serial		
instalments thereof	60 261	33 464
Printed matter; books, brochures, leaflets and similar		
printed matter	7 277 091	6 141 257



» **Figure 1:** *European Publisher sales by category 2008-2024 (Smithers, 2021)*

3.2. The market for book printing in Europe

The value of the European book printing market was 7.8 billion euros in 2025; it has been growing at an average CAGR of 1.5% in constant terms since 2020, although that year saw a sharp decline compared to 2019 due to the COVID-19 pandemic. Tables 3 and 4 present the aggregate European and Hungarian book printing industry revenue and nominal output, including projected trends for the next five years.

The European book printing market was valued at 7.8 billion euros in 2025; since 2020, the average compound annual growth rate (CAGR) has not increased; in fact, it has declined slightly (0.1%). In 2020, a sharp decline was observed compared to 2019 due to the COVID-19 pandemic. However, significant growth is projected for the next five years

The pandemic also caused a significant drop in revenue in the Hungarian book printing industry, but performance subsequently improved dramatically. Its outlook for the future follows the European trend.

The situation is different, however, when it comes to printing output. European printing companies are producing fewer books overall, and this trend is expected to intensify in the future. The exceptional volume figures achieved in Hungary in 2024 and 2025 will not be repeated.

Figure 2 clearly illustrates the trends outlined above.

Table 3

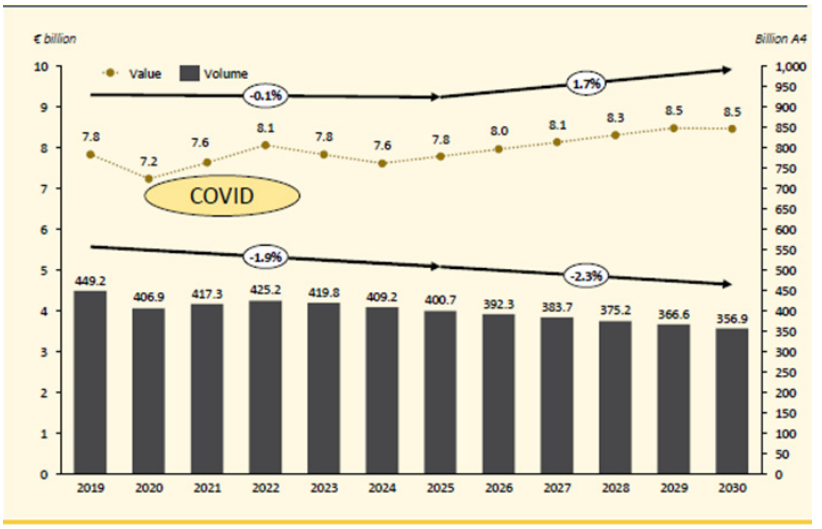
European and Hungarian book printing market by print process 2019-2030 (€ million, constant 2024 values)

	2019	2020	2024	2025	CAGR (%), 2020-25	2026	2030	CAGR (%), 2026-30
All Europe	7,836.2	7,237.4	7,613.9	7,784.4	- 0.1	7,960.0	8,462.7	1.7
Hungary	47.9	45.1	59.1	60.0	5.9	60.7	64.6	1.5

Table 4

European and Hungarian book printing market by print process 2019-2030 (A4 million prints or equivalent)

	2019	2020	2024	2025	CAGR (%), 2020-25	2026	2030	CAGR (%), 2026-30
All Europe	449,212	406,903	409,208	400,671	-1.9	392,270	356,922	-2.3
Hungary	3,609	3,182	3,822	3,811	1.7	3,780	3,663	-0.8



» **Figure 2:** *European book printing output, 2019-2030 ($ billion, billion A4 equivalent) (Smithers, 2021)*

4. Trends and drivers shaping book manufacture in Europe

The key drivers having the greatest influence on the book printing market across Europe going forward are listed below:

- Changing physical book manufacturing methods.
- Changing book manufacture location as supply chains develop and publisher business models change, the rise of print-on-demand.
- Sustainability – reducing waste in manufacture and across supply chains.
- Availability and cost of paper following paper machine and mill closures, the potential impact of Eu Regulation on Deforestation-free Products (EUDR) (although currently books are outside the scope of the regulation).
- End-user preferences change demand for printed books and other formats.

4.1. Book production … is a changing world

During the period under study, significant changes have occurred and continue to occur in book printing technologies and methods. The share of digital printing has been steadily increasing throughout this period. In 2020 digital print- electrophotography and inkjet- accounted for 38.4% of the value of book printing and this will grow to 67.3% by 2030 as more on-demand book manufacturing is used. The value is greatly ahead of print volume, and in 2030 digital will account for 29.0% of output volume. For print suppliers the value of digital book printing is a major opportunity as the services provided to publishers help them serve the book buyers over the useful lifecycle for their title, keeping more titles in print and extending the long tail.

High levels of automation and efficient job changeover make offset litho an efficient technology relative to other analogue printing processes; however, sheetfed offset litho lacks the versatility of digital printing and the technology is not well suited for print on demand.

The use of webfed offset printing for book production remains important, especially for long run production but is declining and both coldset and heatset volumes and values fall throughout the review period. Coldset web litho is used to print diaries, religious, educational and trade publications as well as trade fiction and graphic novels in both hardback and softback format. Heatset offset litho and, to a minor extent, gravure is used for long run color printing. Some book presses have heatset dryers that are typically used for color printing and can be switched off when not required, for example when printing single color work. The market for new web offset book presses has stalled, and at the time of writing it is believed that there are no manufacturers of these presses left, although the existing installed base is kept running with spares and service often supplied by third parties (Moreau & Wells, 2018).

Inkjet printing is taking share of all other print processes including electrophotography. Although electrophotography is being replaced by inkjet, it remains an important part of the business and is widely used for covers, illustrations, some text and picture books.

Table 5 illustrates the changing role of printing technologies in book production. Digital printing takes more value as it can offer faster turnaround, short runs more efficiently keeping more books in print (important for publisher author contract relationships).

Table 5
Trends and outlooks of book sector by process

Book Sector by Process	Print trend	Outlook
Web Offset (heatset) + Gravure	Medium to long run color books – education, coffee table/hobby interest titles	Decline will continue as average runs fall. Commercial presses may generate high levels of trim waste. Inkjet is increasingly competitive at medium to high runs
Coldset Web	Medium to long run mono books – education, hobby interest titles	Decline will continue as presses wear out and skilled litho press minders are difficult to recruit and retain
Sheetfed Litho	Color for softback covers, hardback jackets, color plates	Declining for text sections, still used for covers but fewer specialist mono sheetfed perfecting presses in use as digital machines that can deliver paginated blocks
Inkjet (Webfed)	520-1.4m width, perfecting presses either full color or mono (some 2-colour). No cut off restrictions to minimize trim waste, no section imbalance, any pagination	Integrated and near-line automated finishing. Single-pass book block production with no end-papers or section imbalance waste. New presses e.g. HP T500M filling gaps in coldset machinery
Inkjet (Sheetfed)	Short runs, covers	Growing as inkjet sheetfed installed base grows, B3 as well as B1/B2 where take up has been patchy.
Electrophotography	Mono continuously declining/dead, mono cut sheet for short runs. Color cut sheet for covers/jackets and short run.	Still used in covers and short run color books, use reducing in

The growth of inkjet is due to its ability to enable fast, efficient and cost-effective production of book blocks or folded sections and the technology is the driving force behind print on demand publication. Inkjet and toner printing is used by Amazon who own several book printing facilities in the US, Europe and Asia. These are used for fulfilment of online book ordering through Amazon's marketplace as well as for producing print on demand publications for independent authors through the Amazon KDP (Kindle Direct Publishing) programmed that allows self-publishing in both physical and e-book format. Other providers offer similar self-publishing portals with in-house and bought in print capacity.

Over the past fifteen years there have been significant developments in digital print technology, combining

print with web finishing and binding to manufacture books effectively in a single pass, enabling the economic production of single copies if needed.

4.2. Localized and regional printing models … print isn't necessarily at the printer anymore

E-commerce and changing consumer behavior have transformed books into immediate-demand products. Readers increasingly expected next-day, or even same-day delivery. As a result, printers and publishers had been forced to adopt faster replenishment cycles, shorter production times, and tighter inventory management. This expectation of immediacy was unlikely to disappear and that the industry must evolve accordingly.

In addition to technology, printers should focus on supply chain management and total cost of ownership. Publishers, too, must look beyond per-unit printing costs and consider warehousing, obsolescence, tied-up capital, and environmental impacts. Managing the total cost of the supply chain has become critical to survival.

Subscription-based models and premium editions have transformed books into collector's items, thereby reducing dependence on significant retail discounts.

Printing no longer necessarily must take place at a printing plant. Production can take place wherever it best serves the efficiency of the supply chain. CPI (one of Europe's leading book manufacturers) operates distributed printing networks in the United Kingdom and Germany, with partners in North America, India, Australia, and Singapore. Approximately 20% of on-demand print orders are not produced locally but are routed to international partners, demonstrating a flexible, file-driven production model that minimizes shipping costs and carbon emissions while improving cash flow.

Localized, digital, and on-demand printing models offer both economic and environmental opportunities. Although these models may to some extent displace traditional high-volume printing, they provide flexibility in a market defined by speed, cost pressure, and

sustainability requirements. Digital printing technologies are essential to these models, as they enable scalable production starting from a single copy.

4.3. Sustainability … is not a trend anymore, it is real business

Climate change is one of the biggest topics in the modern era with a huge emphasis being put on environmentally friendly actions for people, companies, and countries. This topic is at the forefront for many consumers and will often influence their feelings towards a company and its products. This mind-set from the public has put pressure on, governments and unions, as well as businesses, to promote sustainable practices (Gladysz et al., 2021).

Sustainability is growing in importance for print suppliers and their publishing customers. The promise of electronic and audio alternatives to physical books included boasts about being more sustainable, but only if the impact of requirement for an electronic reader and power is not included. The consumer demands are making most reputable publishers use sustainably sourced paper and board, with FSC and other certifications widely used. The forthcoming EU deforestation regulations (EUDR) made publishers obtain detailed full-chain traceability information from paper mills, pulp suppliers and printing partners to prove their credentials. EUDR may affect book supply chains in future but in December 2025 the European Parliament plenary vote in favor of the provisional agreement reached with the Council on the EUDR-amending Regulation. This means printed books, newspapers, pictures and other products of the printing industry, manuscripts, typescripts and plans, of paper' have been exempted from the EUDR. Despite this many print providers are offering independently certified and traceable sources of materials used in book manufacturing.

Printers must increasingly prove their credentials by providing clear emissions data about their products. Intergraf recommendation on CO2 emissions calculation in the printing industry', was published in 2013. This recommendation was the only international graphic standard for carbon calculation in the world, designed to ensure that everyone who uses it calculates on the same basis (International Organization for Standardization, 2013).

4.4. Consumer trends … social media is stealing time from consumers to read books

Reading is a very environmentally-friendly activity – be it in the physical or digital world. Retail is not physical vs. online, it is omnichannel. „Print has a strong value proposition for consumers", with price not even in the top five selection criteria of where and why one buys a book. This led to the conclusion that "a beautifully printed book remains important even in an omnichannel market". (Andre Breedt, Nielsen Book)

4.4.1. How do 15-year-olds read in today's world?

37% of students rarely or never read books; 36% read books more often in paper format; 15% read books more often in digital format; and 12% read books equally often in paper or digital format (OECD, 2023)

When comparing between different kinds of readers, the OECD found that "in high-performing education systems more students tend to read books more often in paper format", while "in low-performing education systems more students tend to read books more often using digital devices".

4.4.2. Consumer behavior perspective

Demand for books is ultimately determined by the preferences of readers (or boards of education in the case of school and university text and workbooks). As technology develops there is more choices with titles available as physical books (with associated supply chains) or digitally like e-books and audio books. In education there are many alternatives to traditional printed textbooks including teacher guides, etc. The threat of e-books replacing physical books has not come to pass, with audio books the fastest growing segment (Horvath, Loós & Remete, 2023)

The alternative channels and social media can provide a boost to physical books. Viral marketing can boost titles. BookTok is a subcommunity of TikTok that focuses on books and literature, emerging in 2019 as TikTok became more popular. Members of this subcommunity, (BookTokers), make videos reviewing, discussing, and joking about the books they read. Publishing houses are increasingly collaborating with BookTokers, elevating them to editors in the hope of finding the philosopher's stone, to unearth the next bestseller among the thousands of new releases (Capitani, 2025).

One publisher interviewed noted the impact of this group, citing one example a book on royal dress making taking off when "Megan Markle happened" leading to orders of 50,000 copies as the title took off. Sweden is a case study in the rethink of screen-heavy education and the return of printed books to the classroom.

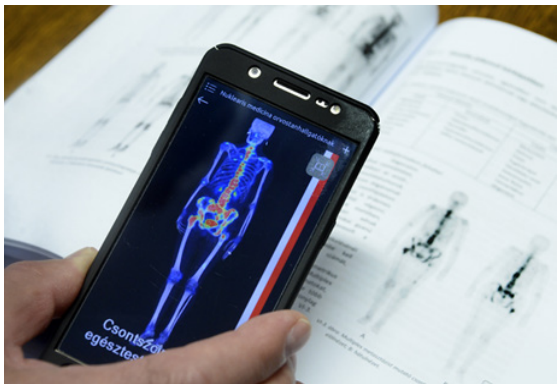
In 2009, Sweden adopted a policy of favoring digital tools such as tablets and computers in the classroom at the expense of printed textbooks with the aim of preparing students for a digitized world. But credible studies showed a decline in educational standards. A global assessment of reading levels, the Progress in International Reading Literacy Study (PIRLS) showed a decline among Sweden's children between 2016

and 2021. In 2023, Sweden's Education Minister Lotta Edholm attributed the decline in academic standards partly to an overreliance on digital devices, saying: "Sweden's students need more textbooks, physical books are important for student learning". To combat this decline, the Swedish government announced an investment worth kr685m in book purchases for schools, with another kr500m investment in 2024 and 2025 to speed up the return of printed educational books.

4.4.3. Books connected to the digital world

The future is digital, in more ways than one, from the production of books to the methods of purchasing and consuming products. The following is an example of the use of augmented reality (AR) in the world of printed books. The purpose of the LibrAR mobile application developed by Alföldi Nyomda is to extend and expand the information that appears in the book.

The camera of the mobile phone or tablet is pointed at the page of the book, and something else appears in the place of the image, e.g.: another image, an image gallery, animation, a 3D model that can be walked around virtually, a video, an audio file starts, but it is also possible, to launch the phone's navigation program and navigate to a specific geographic location, but we can even discover hidden content in a book through it. The special feature of the application is that there is no need to spoil the overall image of the book, for example by placing a QR code, only a well-recognizable image and a so-called marker are needed. Most images and graphics can be used as markers. All that is needed is that it contains sharp, contrasting angles. And the librAR corner mark printed on the corner of the image is just to inform the reader: this image is more than meets the eye. The application of AR therefore opens new dimensions in the world of books and enables readers to have a much more interactive and enjoyable experience (Horvath et al., 2020).



» **Figure 3:** *LibrAR application in use*

4.4.4. The hottest trend in publishing … books you can judge by their cover

Elaborately designed books with patterned edges and other effects started as a trend in romance and have now spread throughout the publishing industry. Printing enables publishers to create even greater value from their existing content.

Paradoxically, the book acquires physicality to be easily communicable digitally: to use a neologism, we could say that it must be "Instagrammable". Translated into concrete terms, to use the American expression: "bold colors, big typography, and a visual hook", i.e. large, bold lettering, splashed across the cover in bright colors to capture the attention of users on social media, where images should stand out quickly to stop the scrolling (Capitani, 2025).

Beyond graphics, in response to the growing attention to book aesthetics, many publishers have introduced tactile elements and special details throughout the volume. Features such as colored or decorated edges (sprayed edges), which are so fashionable today, as well as embossing and special finishes, have become commonplace, transforming books into collectables.



» **Figure 4:** *Books with metallic gilded edge*

Metallic gilded edge – this effect used to be created by painting or dipping the book into a solution but now can be inkjet printed.

Red Tower Books produced 2 million copies of the deluxe edition of ONYX STORM and 500,000 copies of the regular version. The deluxe version was a collectible hardcover with sprayed edges, stenciled artwork and other special design features.

1. Conclusions

The Entire Book Publishing Eco-system is rapidly evolving due to fast changing consumer preferences, increasing volumes of data and drive to eliminate waste.

- Printed Books are highly resilient in the Digital Age because consumers want a tactile, emotional experience
- Books are more than just carriers of information – they can be luxury objects, collectible items or status symbols.
- Publishers are experimenting with different formats – often blending the digital and the physical.
- Better forecasting is leading to fewer unsold copies, reducing publisher's risk – as a result printing is becoming more efficient and generating less waste.
- Digital printing is growing – big opportunities in inkjet in print on demand.
- The workflow of book production is changing- digital print enables more efficient book manufacturing (not just small quantities)
- There are many opportunities for printers to capture more value of the book production process.

Book printers are no longer just printers; they provide publishing supply chain support!

2. Acknowledgments

The authors would like to thank the speakers of "Shaping the Future with Books 2026" and INTERGRAF for providing us with the material of their presentations, as well as the "INTERGRAF Book Market Report 2026" compiled together with Smithers.

3. References

Capitani, L. (2025) *The shape of the book*. PRINTlovers, 25 September. Available from: https://www.printlovers.net/the-shape-of-the-book/ [Accessed 25 September 2025].

Gladysz, B., Krystosiak, K., Ejsmont, K., Kluczek, A. and Buczacki, A. (2021) 'Sustainable Printing 4.0—Insights from a Polish Survey', *Sustainability*, 13(19), 10916. DOI: 10.3390/su131910916

Horvath, C., Koltai, L., Lorincz, I. and Teleki, P. (2020) 'Definition and Measurement of Lay-flat Degree for Books'. In: *Proceedings of Annual Technical Conference of Technical Association of the Graphic Arts*, pp. 153–160.

Horvath, C., Loós, T. and Remete, K. (2023) 'Shaping the European Future with Books (Facts and thoughts regarding a conference)', *Innovations in Publishing, Printing and Multimedia Technologies*, pp. 48–58. DOI: 10.59476/ilpmt2023.48-58

International Organization for Standardization (2013). *ISO 16759:2013 Graphic technology — Quantification and communication for calculating the carbon footprint of print media products*. Geneva: International Organization for Standardization.

OECD (2023) *New PISA results: strengthening education systems in the wake of the pandemic*. PISA in Focus, No. 123. Paris: OECD Publishing. DOI: 10.1787/62fc50a3-en

INTERGRAF, FEP and CEPI (2023) *Books Drive Europe's Knowledge Economy*. Available from: https://www.intergraf.eu/communications/publications/item/426-joint-statement-books-drive-europe-s-knowledge-economy [Accessed 2 October 2026].

Moreau, B. and Wells, N. (2018) *Print Business Trends*. Paris: IDEP France and International Centre for Manufacture by Printing (icmPrint).

Smithers (ed. Thomas Poetz) (2021) *European Book Market Report 2021*. Brussels: Smithers and INTERGRAF.



© 2026 Authors. Published by the University of Novi Sad, Faculty of Technical Sciences, Department of Graphic Engineering and Design. This article is an open access article distributed under the terms and conditions of the Creative Commons Attribution license 4.0 Serbia (https://creativecommons.org/licenses/by/4.0/deed.en).

https://doi.org/10.24867/GRID-2026-p49

Adaptation of Museum Exhibits for Blind and Visually Impaired Visitors

ABSTRACT

Museum collections remain predominantly visual, which restricts access to cultural heritage for blind and visually impaired (BVI) visitors when original objects cannot be touched or visual information cannot be perceived directly. This practice-based study investigates how archival photographic material can be translated into tactile museum objects through digital reconstruction, three-dimensional (3D) modelling, additive manufacturing and multimodal interpretation. Two cases from the National Liberation Museum Maribor were examined: an architectural fragment of the Maribor court prison complex with an adjoining courtyard well, and an identification badge associated with Dachau. Because the available source material consisted of photographs rather than measured drawings or scans, the reconstructions required interpretation of relative proportions, repetition, graphic structure and tactile salience. The architectural model therefore preserves relational rather than absolute scale, while the well was enlarged and produced separately because its perspective did not permit reliable spatial placement. The badge was enlarged, its typography was redrawn in Glyphs, visual distinctions were translated into differentiated relief, and the prominent letter J was produced as a removable element. Models were prepared in Blender and OrcaSlicer and manufactured by fused deposition modelling (FDM) 3D printing using polylactic acid (PLA). 3D animations and audio descriptions were linked to the tactile objects through quick responsive (QR) codes. The results demonstrate a technically feasible workflow that can be implemented in a museum setting to transform incomplete two-dimensional (2D) records into tactile interpretations while making uncertainty explicit. As systematic testing with BVI participants was not completed before exhibition deployment, the findings concern design feasibility, manufacturability and interpretive potential rather than measured accessibility performance.

Raša Urbas
Žiga Ceglar
Boris Beja

University of Ljubljana, Faculty of Natural Sciences and Engineering, Department of Textiles, Graphic Arts and Design, Chair of Information and Graphic Arts Technology, Ljubljana, Slovenia

KEY WORDS
3D modelling, 3D printing, tactile reproduction, museum accessibility, inclusive design, cultural heritage

1. Introduction

Museums increasingly seek to operate as visitor-centred and inclusive cultural environments, yet the interpretation of collections still depends heavily on vision. Objects are commonly protected behind showcases, architectural information is communicated through photographs and drawings, and labels frequently assume visual access. For BVI visitors, this can turn the conservation principle of “do not touch” into a barrier to understanding form, scale and spatial relationships. Museum studies have therefore argued for multisensory interpretation in which touch contributes directly to meaning-making rather than serving only as an auxiliary channel (Pye, 2007; Levent & Pascual-Leone, 2014). Studies involving blind and partially sighted museum users likewise show that access to 3D printed objects can support a more active and positive museum experience when tactile exploration is treated as a legitimate form of engagement (Karaduman, Alan & Yiğit, 2023; Bruns et al., 2023). Digital fabrication has expanded the practical possibilities for such access. Tactile maps, architectural models and replicas can be

produced by additive manufacturing, modified digitally and reproduced without subjecting fragile originals to repeated handling or transport (Urbas, Pivar & Stankovič Elesini, 2016; Montusiewicz, Barszcz & Korga, 2022; Kantaros, Soulis & Alysandratou, 2023). Recent work also emphasises the value of combining tangible models with audio or other digital information, particularly where the physical object alone cannot communicate context or complex spatial relations (Rossetti et al., 2018; Reinhardt et al., 2024; Avni et al., 2025). In this sense, a 3D printed reproduction is not only a copy: it can become an interpretative interface between the protected museum object, the exhibition narrative and the visitor.

Designing a tactile representation requires more than geometric fidelity. Tactile exploration is sequential and local, and recognition depends on clear boundaries, sufficient feature separation, manageable information density and stable elements that can withstand repeated handling (Millar, 1994; Wu et al., 2022). Features that are visually subtle may need to be enlarged or raised, while dense visual detail may need to be simplified. Research on tactile graphics and 3D printed cultural heritage models therefore stresses selective translation rather than indiscriminate reproduction (Wu et al., 2022; Montusiewicz, Barszcz & Korga, 2022). User-centred studies further show that material, scale, interaction method and the structure of audio information all influence the usefulness of tactile museum systems (Bruns et al., 2023; Avni et al., 2025).

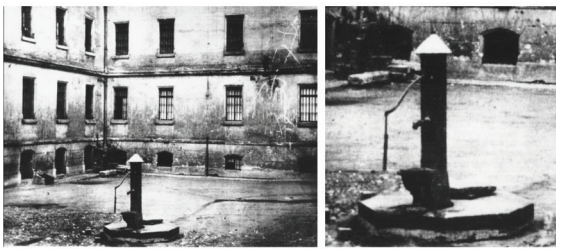
Many documented heritage workflows begin with a physical artefact that can be scanned, photographed from multiple viewpoints or otherwise captured as 3D data (Bruns et al., 2023; Kantaros, Soulis & Alysandratou, 2023; Reinhardt et al., 2024). The present study addresses a different and less straightforward condition: the source objects and architectural context had to be interpreted from archival photographs alone. A single photograph provides evidence of contour, repetition and relative position, but it does not justify hidden geometry, absolute dimensions or perspective-corrected placement. The research was therefore framed as a design-led translation from 2D documentary evidence into a 3D tactile representation, with an explicit distinction between what was visible in the source and what had to be inferred during modelling.

Three questions guided the work: which relationships should be preserved when historical scale cannot be established; how architectural rhythm, typography and colour-based distinctions can be translated into a clear tactile hierarchy; and how tactile objects can be complemented by digital information without making access dependent on vision. The resulting workflow combines 3D modelling, custom typographic reconstruction, FDM 3D printing, mechanical and colour finishing, and QR-linked animation with audio description. The study reports the design, fabrication and exhibition deployment of the resulting objects. It does not treat successful fabrication as equivalent to proven accessibility, because contemporary research consistently identifies the involvement of BVI users and structured evaluation as essential to reliable inclusive design (Avni et al., 2025; Avni, Danial-Saad & Kuflik, 2026).

2. Materials and methods

2.1. Source material and interpretive design strategy

The experimental work was carried out in cooperation with the National Liberation Museum Maribor and began with two archival photographs. The first was a black-and-white image of a courtyard bounded by two adjoining façades, later identified as part of the Maribor court prison complex, with a well visible in the foreground. The second photograph showed an identification badge associated with Dachau, bearing the inscription “Dachau”, the number “136919”, and a large calligraphic letter “J”. Figure 1 shows the architectural source and the well detail. The photographs were treated as documentary references rather than metric drawings. No architectural plans, dimensional data, calibrated scale reference or lens information were available; consequently, no defensible historical scale could be assigned to the reconstructed architecture. All dimensions reported below refer to the designed tactile objects.



» **Figure 1:** *Archival source material used for the architectural interpretation: the Maribor court-prison courtyard (left) and a detail of the courtyard well (right) (Source: National Liberation Museum Maribor)*

The design strategy therefore prioritised relational fidelity over unsupported metric precision. The façade was interpreted through recurring modules: the sequence of openings, storey organisation, window proportions and the distinction between upper rectangular openings and lower arched openings were preserved as a coherent rhythm. Repetition was used deliberately because a regular sequence can be followed progressively by touch and communicates the modular structure of the façade. At the same time, tactile salience was introduced through controlled recesses, projecting sills and simplified bars.

This approach is consistent with tactile-design research, which shows that recognisable structure depends on the selection and organisation of salient features rather than on reproducing every visual detail (Urbas, Pivar & Stankovič Elesini, 2016; Wu et al., 2022). When the photographic evidence did not support a reliable spatial conclusion, uncertainty was retained rather than concealed by speculative geometry. The main constraints of the source material and the corresponding tactile translation strategies are summarised in Table 1.

Table 1
Design logic applied to the tactile reproductions

Object	Constraint in the source material	Tactile translation	Production outcome
Architectural fragment	Single oblique black-and-white photograph; no plans, metric data or defensible absolute scale	Relative proportions; repeated window modules; differentiated recess depths; simplified bars and projecting sills	Large FDM model requiring supports; principal structure stable, but the finest bars proved mechanically vulnerable
Courtyard well	Perspective prevented reliable placement and scale within the courtyard	Detached from the architectural fragment, enlarged and presented as an independent tactile object	Independently manipulable model; supports required for the main print; improved stability and tactile access
Dachau identification badge	Small graphic artefact in which typography, geometric segmentation and colour carry most of the visual information	Enlargement; custom vectorised lettering; raised typography; differentiated relief; removable letter "J"; polychrome finish	Three support-free FDM components; sanding and painting improved surface finish and visual contrast

2.2. Reconstruction of the architectural fragment and courtyard well

The architectural fragment was modelled in Blender from basic polygonal geometry. Two adjoining walls and a floor plane formed the main structure. Rather than deriving a nominal scale from the image, repeated openings were constructed as modules and adjusted until their proportions matched the visible façade. In the final tactile model, the window openings measure approximately 19 × 40 mm and are recessed by 4 mm. Window sills project by approximately 1.5 mm, while the lower arched openings are recessed by approximately 8 mm so that the two opening types create clearly different tactile levels. A slightly raised pavement of approximately 1.6 mm introduces another perceptible transition across the courtyard plane. The bars were simplified into repeated vertical and horizontal members, balancing the visual rhythm of the reference with the mechanical limits of FDM printing.

The courtyard well required a different interpretative strategy. Its apparent dimensions and location are strongly affected by perspective because it is positioned much closer to the camera than the surrounding architecture. Embedding it in the courtyard at an assumed position and scale would therefore have turned photographic ambiguity into seemingly factual spatial information. Instead, the well was enlarged and reconstructed as an independent tactile object. This decision both avoided false precision and increased the opportunity for active manual exploration. The main cylindrical element is approximately 20 mm in diameter and 104 mm high, with a conical cap approximately 32 mm in diameter and 17.5 mm high. The object stands on an octagonal base of approximately 164 × 164 × 12 mm. Curved details, including the handle and spout, were constructed with Bézier curves, rotational modifiers and limited sculpting, while local geometry was simplified to avoid sharp, fragile or confusing transitions.

2.3. Enlarged tactile reconstruction of the Dachau identification badge

The badge presented a different translation problem because its identity is carried primarily by small-scale typography, geometric segmentation and colour. The tactile reproduction was therefore enlarged to an overall width of approximately 196 mm. The upper section was modelled as a shallow rectangular prism and the lower section as a triangular prism. The visual separation between the two fields was supported by differences in relief so that the basic structure could be understood through touch without relying solely on colour.

Typography was reconstructed separately because no existing typeface reproduced the irregular letterforms visible in the source photograph. The image was imported into Glyphs, where the word "Dachau", the number "136919", and the letter "J" were manually redrawn as vector outlines. The resulting OpenType font was imported into Blender and converted into 3D geometry. The inscription was raised by approximately 3.5 mm above the supporting surface, making the typographic information a spatial component of the object rather than

a purely printed graphic layer. The large letter “J” was designed as a removable insert. A recess approximately 5 mm deep was formed in the triangular component, while the separate letter was extruded to approximately 7 mm. It can therefore be removed, rotated, explored independently and returned to the corresponding recess. The original visual identity – dominated by white, red and black – was retained in the final polychrome treatment, but colour was not used as the only information carrier. Structural and graphic distinctions were also translated into level, shape, and raised typography. More general tactile colour vocabularies can use textures or raised pictograms (Cho et al., 2021); here, an object-specific solution was preferred because the goal was to preserve the internal organisation of a single historical artefact.

2.4. 3D printing and post-processing

Completed models were exported as STL files and checked in OrcaSlicer for manifold geometry, open edges, duplicated surfaces and required support structures. Errors that could not be resolved automatically were corrected in Blender. The architectural model and badge components were printed on a Creality K1 Max, while the well was printed on an Original Prusa i3 MK3S. Both printers used material-extrusion/FDM technology, a 0.4 mm nozzle and white PLA filament. Orientation was chosen to reduce supports where possible and to protect the main tactile surfaces. Support structures were required for the architectural fragment and the well, whereas the badge components could be printed without them.

Post-processing was treated as part of tactile design rather than as a purely cosmetic stage. Supports were removed manually, with particular care around projecting sills, bars and curved details. The badge was sanded with P100 and then P400 abrasive paper to reduce pronounced layer lines and local surface irregularities. The inscription and removable letter “J” were painted black and the triangular field red with acrylic paint, while the remaining field was left white. Mechanical smoothing and coating are established post-processing strategies for polymer prints, but they must be controlled so that the intended relief is not rounded off or lost (Dizon et al., 2021).

2.5. 3D animation, audio description and QR-linked interpretation

The same Blender models were reused for short 3D animations. Each object was placed in a virtual scene and animated with keyframes. The architectural fragment was rotated by about 45° because its most informative relationships are on the interior façades; the well was rotated through a full revolution, and the badge through about three revolutions. Studio-style lighting and material shading were used without additional textures, so the form and surface remained visually clear. Spoken descriptions were recorded in concise, easy-to-follow language, focusing on the objects’ form, spatial relationships and key identifying features. The animations were edited in the free edition of DaVinci Resolve, together with the source photographs, narration and closing credits.

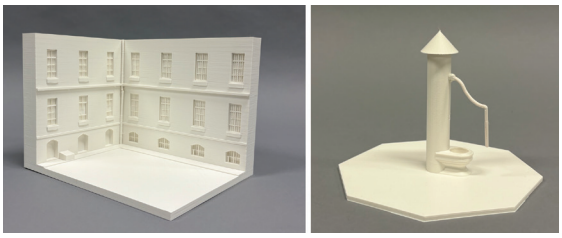
Two videos were produced: one combined the architectural fragment and the well, while the other presented the badge. The videos were hosted online as unlisted content and linked to QR codes positioned with the physical exhibits. The resulting layer did not replace the tactile object; it supplemented it with spoken explanation and moving visualisation. This multimodal logic is consistent with recent museum-accessibility research, which shows that tangible models can be strengthened by structured audio and complementary digital information, provided that interaction remains understandable and under the user’s control (Cavazos Quero, Iranzo Bartolomé & Cho, 2021; Rossetti et al., 2018; Reinhardt et al., 2024; Avni et al., 2025).

3. Results

3.1. Architectural tactile reconstruction

The architectural workflow produced a tactile fragment of the Maribor court prison complex and a separate well. The architectural fragment required approximately 30 h 8 min of printing. Large planes and repeated window modules were reproduced consistently, and the differing recess depths created a clear geometric hierarchy between upper windows, lower openings and the courtyard plane. The main manufacturing weakness occurred in the finest bars: several members were vulnerable during support removal and could deform or break. The result indicates that literal miniature detail is not always compatible with the mechanical requirements of a tactile exhibit intended for repeated handling.

The well printed successfully as an independent element. The main print required approximately 3 h 33 min, while the handle and spout were produced separately. Detaching the well from the courtyard resolved two design problems at once: it prevented an uncertain perspective-derived position from becoming fixed in the architectural representation, and it allowed the object to be enlarged enough for independent exploration. The final architectural reproductions are shown in Figure 2. Their dimensions should therefore be read as interpretive design dimensions, not as measurements or scale-model data for the historical architecture.



» **Figure 2:** *Final FDM-printed tactile interpretations: an architectural fragment of the Maribor court prison complex (left) and an enlarged courtyard well (right)*

3.2. Tactile and typographic reconstruction of the badge

The enlarged badge was produced as three physical components: an upper rectangular part, a lower triangular part, and the removable letter "J". The components could be printed without support structures, which protected the raised lettering and reduced the risk of damaging the principal tactile surface during finishing. After sanding, the inscription remained clearly separated from the base, while the letter could be lifted, turned, and compared with its matching recess. The custom vectorisation retained the distinctive proportions and irregularities of the photographed lettering instead of replacing it with a generic typeface.

Polychrome finishing reintroduced the white, red, and black visual relationships of the source and increased contrast for visitors with residual vision. At the same time, geometry and relief allowed the main segmentation to be explored without colour. A design inconsistency became evident in the finished object: the lower triangular component contains two base relief heights where a single level would provide a clearer tactile field. A revised version should therefore regularise this surface before adding the raised auxiliary stroke and removable "J". Figure 3 shows the reconstructed lettering and the final polychrome tactile badge.



» **Figure 3:** *Development of the tactile identification badge: custom vectorised lettering reconstructed from the archival photograph (left), and final enlarged, polychrome 3D-printed object with removable letter "J" (right)*

3.3. Exhibition deployment and multimodal content

The physical models were installed in the exhibition environment and presented as handling objects alongside protected museum material, including within the exhibition *Z uporom iz teme*. The animations and audio descriptions were made available through QR codes at the display. During development, the initially selected QR service proved unreliable, as the generated link later ceased to function; the codes were therefore recreated using a service that ensured direct access to the hosted videos. This practical issue showed that the durability of an accessible exhibit depends not only on the physical model but also on the persistence and maintenance of its digital layer.

Figure 4 shows the architectural model and badge in the exhibition setting. Their installation confirms that the objects can be manufactured, handled and deployed in a real museum context. It should not, however, be interpreted as a formal usability result. Systematic testing with BVI participants was not completed before the exhibition timetable; consequently, tactile legibility, comprehension, preferred exploration sequence and the value of the removable component were not measured with the intended user group.



» **Figure 4:** *Tactile reconstructions in the exhibition environment: architectural fragment and well (left), and enlarged identification badge displayed alongside protected museum objects (right)*

4. Discussion

The combined cases show that converting a historical photograph into a tactile museum object is better described as interpretive translation than as geometric reconstruction. This distinction is crucial when source data are sparse. A single photograph can support statements about visible contour, repetition, relative position and graphic structure, but it cannot justify hidden geometry, absolute dimensions or a perspective-corrected 3D layout. In the architectural model, relational fidelity was therefore prioritised: façade rhythm, storey organisation, recess hierarchy and the relationship between adjoining walls were preserved, while historical scale was deliberately left undefined. This is consistent with

research showing that tactile recognition depends on the careful selection and organisation of salient features rather than on an unfiltered transfer of visual detail (Wu et al., 2022; Montusiewicz, Barszcz & Korga, 2022).

The separate well is a particularly clear example of a design approach that explicitly acknowledges uncertainty. Because the photograph did not permit reliable placement of the well within the courtyard, an apparently complete reconstruction would have required an arbitrary spatial decision. Presenting the well as an enlarged associated object made that uncertainty visible in the design logic instead of hiding it.

At the same time, the decision improved stability and tactile readability. In heritage interpretation, such explicit treatment of uncertainty is preferable to false precision, especially when a tactile user cannot independently inspect or geometrically interpret the source photograph.

The badge required an inverse strategy: rather than reducing a large spatial environment, the design enlarged a small graphic artefact whose meaning is concentrated in typography, geometry and colour. Enlargement alone, however, would not have made the graphic hierarchy tactile. The custom Glyphs workflow retained the characteristic inscription, while raised lettering, differences in base level and the removable "J" converted visual organisation into spatial organisation. Colour was retained as an additional visual layer for partially sighted and sighted visitors but was not allowed to carry meaning independently.

Research on tactile colour coding similarly shows that information conventionally conveyed by colour can be translated into raised patterns and other tactile distinctions (Cho et al., 2021).

The removable "J" adds a simple form of tangible interaction. Typography is no longer just a relief to be traced on a surface; the character becomes an object that can be removed, explored and reinserted. This principle relates to broader work on smart and multimodal museum exhibits, where tactile replicas are combined with user-controlled channels for additional information (Pistofidis et al., 2021; Pistofidis et al., 2023; Avni et al., 2025). The present solution is intentionally kept low-tech and easily replaceable. Its advantages are simplicity and direct manipulation; its limitations are the risk of losing the separate component and the current lack of evidence that removal improves recognition for blind users.

The physical-digital relationship is equally important. Audio can explain spatial relationships that may be difficult to infer from an unfamiliar object without guidance, while animation can support partially sighted and sighted visitors and provide a shared interpretive layer around the same model. Previous studies of cultural-heritage models have shown the value of pairing tactile objects with structured audio and multimodal information (Rossetti et al., 2018; Reinhardt et al., 2024). In the present project, QR-linked content provided a low-cost, updateable solution, but it also introduced a dependency on a compatible smartphone, an accessible scanning workflow and stable online hosting. User studies of interactive tangible museum interfaces show that autonomy, discoverability and control over audio playback are significant design considerations (Avni et al., 2025). Future versions should therefore consider a directly discoverable tactile trigger in addition to the QR link.

Digital models also have value beyond the immediate exhibition. Once an interpretation has been developed, replicas can be produced for handling sessions, travelling exhibitions or partner institutions without repeatedly transporting or exposing fragile originals. Cultural heritage research has identified this capacity for reproducibility as beneficial for both access and conservation (Montusiewicz, Barszcz & Korga, 2022; Kantaros, Soulis & Alysandratou, 2023; Reinhardt et al., 2024). Nevertheless, reproducibility increases the responsibility to identify the output accurately. Where the source record does not support metric reconstruction, the object should be described as a tactile interpretation or a reconstruction from photographic evidence rather than as an exact replica.

The fabrication process revealed a related technical lesson: tactile design and manufacturing design cannot be separated. FDM is well suited to relatively large and robust forms, but fine bars, overhangs, support scars and layer lines can undermine both mechanical durability and perceptual clarity. The damaged window bars demonstrate that critical details should be adapted to the printing process before fabrication, for example by reducing their number and increasing their section. Post-processing can improve comfort and surface quality, yet excessive sanding can soften the intended relief (Dizon et al., 2021). Trial prints of representative details, alternative orientations and systematic comparison of layer height, infill, nozzle diameter and filament would therefore strengthen a subsequent iteration.

The main limitation of the present work is the lack of systematic evaluation with BVI participants. The objects were designed according to established tactile principles, successfully manufactured and installed in an exhibition, but these achievements do not show how efficiently intended users identify the forms, understand the spatial relationships or interpret the removable component. Studies in which blind users directly evaluate 3D printed cultural assets show that user preference can depend on material, print process, scale and interaction design (Karaduman, Alan & Yiğit, 2023; Bruns et al., 2023; Avni et al., 2025). A recent systematic review similarly identifies structured stakeholder involvement and rigorous, mixed-method evaluation as

central requirements for advancing museum accessibility (Avni, Danial-Saad & Kuflik, 2026). Future work should therefore involve BVI participants in co-design and iterative testing, record tactile exploration strategies and comprehension, and compare alternative relief heights, feature spacing, textures, scales and audio structures.

5. Conclusions

This study presents a reproducible workflow for translating sparse 2D museum records into physical tactile interpretations through 3D modelling, typographic reconstruction, FDM 3D printing, post-processing and multimodal digital content. Its main contribution lies not in a particular software package or printer, but in the design decisions required when the source itself is incomplete: preserving documented relationships rather than inventing absolute scale, using repetition and relief to establish tactile hierarchy, enlarging features when their original size would prevent meaningful exploration, and separating elements when photographic perspective makes their original spatial position uncertain.

The two case studies required complementary translation strategies. In the architectural fragment, repeated window modules and differentiated recesses communicated façade rhythm, while the well was detached and enlarged to avoid implying unsupported spatial precision. In the badge, graphic organisation was translated into spatial organisation through enlargement, custom raised typography, differentiated base levels and a removable typographic component, with colour retained as an additional visual layer. These choices align with the wider literature showing that successful tactile representations depend on selective simplification, perceptually clear feature separation and iterative refinement, rather than on visual fidelity alone (Wu et al., 2022; Montusiewicz, Barszcz & Korga, 2022).

The project also demonstrates the practical museum value of digital replicas. Tactile reproductions can expand opportunities for handling and multisensory interpretation while reducing direct contact with protected originals, and they also allow the same digital model to be reproduced in other institutional contexts (Kantaros, Soulis & Alysandratou, 2023; Reinhardt et al., 2024). At the same time, technical success must not be equated with proven accessibility. The next research stage should systematically involve BVI users in testing and redesign, in line with current evidence emphasising user participation, autonomy and contextual evaluation (Avni et al., 2025; Avni, Danial-Saad & Kuflik, 2026). Such work is necessary if tactile reconstructions are to function not only as technically successful objects but as genuinely understandable and inclusive museum interfaces.

6. Acknowledgments

The authors thank the National Liberation Museum Maribor for providing archival photographic material and for enabling the development and implementation of tactile reconstructions within the museum exhibition context.

7. References

Avni, Y., Danial-Saad, A., Sheidin, J. and Kuflik, T. (2025) 'Enhancing museum accessibility for blind and low vision visitors through interactive multimodal tangible interfaces', *International Journal of Human-Computer Studies*, 198, 103469. DOI: 10.1016/j.ijhcs.2025.103469

Avni, Y., Danial-Saad, A. and Kuflik, T. (2026) 'Design for inclusion: a systematic review of technologies and frameworks for enhancing the museum experience of blind and low-vision visitors', *International Journal of Human-Computer Interaction*, 42(20), pp. 16861–16891. DOI: 10.1080/10447318.2026.2623227

Bruns, A., Spiesberger, A.A., Triantafyllopoulos, A., Müller, P. and Schuller, B.W. (2023) ''Do touch!' – 3D scanning and printing technologies for the haptic representation of cultural assets: a study with blind target users'. In: *Proceedings of the 5th Workshop on analySis, Understanding and proMotion of heritAge Contents, SUMAC '23, 2 November 2023, Ottawa, Canada*. New York: Association for Computing Machinery, pp. 21–28. DOI: 10.1145/3607542.3617351

Cavazos Quero, L., Iranzo Bartolomé, J. and Cho, J. (2021) 'Accessible visual artworks for blind and visually impaired people: comparing a multimodal approach with tactile graphics', *Electronics*, 10(3), 297. DOI: 10.3390/electronics10030297

Cho, J.D., Cavazos Quero, L., Iranzo Bartolomé, J., Lee, D.W., Oh, U. and Lee, I. (2021) 'Tactile colour pictogram to improve artwork appreciation of people with visual impairments', *Color Research & Application*, 46(1), pp. 103–116. DOI: 10.1002/col.22567

Dizon, J.R.C., Gache, C.C.L., Cascolan, H.M.S., Cancino, L.T. and Advincula, R.C. (2021) 'Post-processing of 3D-printed polymers', *Technologies*, 9(3), 61. DOI: 10.3390/technologies9030061

Kantaros, A., Soulis, E. and Alysandratou, E. (2023) 'Digitization of ancient artefacts and fabrication of sustainable 3D-printed replicas for intended use by visitors with disabilities: the case of Piraeus Archaeological Museum', *Sustainability*, 15(17), 12689. DOI: 10.3390/su151712689

Karaduman, H., Alan, Ü. and Yiğit, E.Ö. (2023) 'Beyond ''do not touch'': the experience of a three-dimensional printed artifacts museum as an alternative to traditional museums for visitors who are blind and partially sighted', *Universal Access in the Information Society*, 22(3), pp. 811–824. DOI: 10.1007/s10209-022-00880-0

Levent, N. and Pascual-Leone, A. (eds.) (2014) *The Multisensory Museum: Cross-Disciplinary Perspectives on Touch, Sound, Smell, Memory, and Space*. Lanham: Rowman & Littlefield.

Millar, S. (1994) *Understanding and Representing Space: Theory and Evidence from Studies with Blind and Sighted Children*. Oxford: Clarendon Press.

Montusiewicz, J., Barszcz, M. and Korga, S. (2022) 'Preparation of 3D models of cultural heritage objects to be recognised by touch by the blind – case studies', *Applied Sciences*, 12(23), 11910. DOI: 10.3390/app122311910

Pistofidis, P., Ioannakis, G., Arnaoutoglou, F., Michailidou, N., Karta, M., Kiourt, C., Pavlidis, G., Mouroutsos, S.G., Tsiafaki, D. and Koutsoudis, A. (2021) 'Composing smart museum exhibit specifications for the visually impaired', *Journal of Cultural Heritage*, 52, pp. 1–10. DOI: 10.1016/j.culher.2021.08.013

Pistofidis, P., Arnaoutoglou, F., Ioannakis, G., Michailidou, N., Karta, M., Kiourt, C., Pavlidis, G., Mouroutsos, S.G., Tsiafaki, D. and Koutsoudis, A. (2023) 'Design and evaluation of smart-exhibit systems that enrich cultural heritage experiences for the visually impaired', *Journal of Cultural Heritage*, 60, pp. 1–11. DOI: 10.1016/j.culher.2023.01.004

Pye, E. (ed.) (2007) *The Power of Touch: Handling Objects in Museum and Heritage Contexts*. Walnut Creek: Left Coast Press.

Reinhardt, D., Holloway, L., Thogersen, J., Guerry, E., Corvalan Diaz, C.A., Havellas, W. and Poronnik, P. (2024) 'The Museum of Touch: tangible models for blind and low vision audiences in museums'. In: Lee, J.H., Ostwald, M.J. and Kim, M.J. (eds.) *Multimodality in Architecture: Collaboration, Technology and Education*. Cham: Springer, pp. 135–155. DOI: 10.1007/978-3-031-49511-3_8

Rossetti, V., Furfari, F., Leporini, B., Pelagatti, S. and Quarta, A. (2018) 'Enabling access to cultural heritage for the visually impaired: an interactive 3D model of a cultural site', *Procedia Computer Science*, 130, pp. 383–391. DOI: 10.1016/j.procs.2018.04.057

Urbas, R., Pivar, M. and Stankovič Elesini, U. (2016) 'Development of tactile floor plan for the blind and the visually impaired by 3D printing technique', *Journal of Graphic Engineering and Design*, 7(1), pp. 19–26. DOI: 10.24867/JGED-2016-1-019

Wu, C.-F., Wu, H.-P., Tu, Y.-H., Yeh, I.-T. and Chang, C.-T. (2022) 'A study on the design procedure of three-dimensional printable tactile graphics for individuals with visual impairments', *Journal of Visual Impairment & Blindness*, 116(4), pp. 507–516. DOI: 10.1177/0145482X221122754



© 2026 Authors. Published by the University of Novi Sad, Faculty of Technical Sciences, Department of Graphic Engineering and Design. This article is an open access article distributed under the terms and conditions of the Creative Commons Attribution license 4.0 Serbia (http://creativecommons.org/licenses/by/4.0/rs/).

Professional Paper https://doi.org/10.24867/GRID-2026-p50

Pop-Up Mechanisms as a Means of Visual Expression in Card Design

ABSTRACT

A pop-up card combines graphics with a three-dimensional and interactive form, enriching the way content is presented. The purpose of this article is to analyze the use of moving mechanisms as a means of visual expression in card design. The research material consists of 28 cards designed and made by students of the Department of Printing Technologies at the Warsaw University of Technology. The analysis focused on the relationships between the mechanisms used, the graphic elements, and the visual effect achieved when the card is opened. Multiple layers mechanism appeared most frequently, in 25 cards. Spirals were used in 18 cards, V-folds in 14, and flaps in 4. The most common combination was multiple layers and spirals, used together in 15 cards. The results indicate that these mechanisms serve functions that go beyond mere construction: multiple layer mechanisms create depth and organize the compositional planes, V-folds bring selected elements forward toward the viewer, and spirals introduce a sense of movement and dynamism.

Ewa Kołodziejuk
Joanna Izdebska-Podsiadły

Department of Printing Technology, Institute of Mechanics and Printing, Faculty of Mechanical and Industrial Engineering, Warsaw University of Technology, Warsaw, Poland

KEY WORDS
Pop-up cards, moving mechanisms, paper engineering, visual expression, graphic design

1. Introduction

The history of pop-up mechanisms dates back to the Middle Ages, when scientific manuscripts used movable elements to visualize astronomical or medical data (Smithsonian Institution Libraries, n.d.). Rotating discs were already in use as early as the 13th century by the English monk Matthew Peris (The Ancient Origin of Pop-Up Books, 2023). Although Lothar Meggendorfer is considered the true pioneer of moving mechanisms, having popularized their use in the 19th century (Ptaszek, n.d.; Krahé, 1980). Today, pop-up mechanisms are most commonly associated with children's books and greeting cards, but they can also be applied in other design forms: packaging, advertising materials, or foldable structures, such as architectural models. Moving mechanisms not only serve a structural function but also shape the composition, direct the viewer's attention, and enhance the visual message through movement, depth, and the element of surprise.

A pop-up card combines traditional graphic design with a three-dimensional structure that is revealed when the card is opened. The pop-up mechanisms in these cards are not only an attractive decorative element but also an interactive tool that stimulates the imagination and enhances the message. The recipient activates the mechanism, causing the visual message to unfold from a flat surface into a three-dimensional form. The way the elements appear and move becomes part of the narrative and the design experience. Based on how three-dimensional elements are displayed, two types of pop-up cards can be distinguished: 90-degree and 180-degree (Iizuka et al., 2011). The second type is generally considered more difficult to design, although this largely depends on the number of elements comprising the moving mechanism. Problems often arise during their design and prototyping, such as collisions between elements and parts of the structure sticking out after the card is folded (Okamura & Igarashi, 2009).

Designing pop-up cards requires combining appropriate structural solutions and graphic elements to achieve the desired visual effect. The mechanisms must allow the card to be opened and closed repeatedly and at the same time create a cohesive composition with

the graphic layer. Additionally, it is necessary to take into account the structural limitations of the mechanisms. Three-dimensional elements must not stick out beyond the dimensions of the closed card, and when combining multiple mechanisms, care must be taken to ensure that the elements do not interfere with one another, which could lead to damage to the structure or malfunction. Equally important are the proper selection of the substrate and the size of the bonding surfaces. A bonding area that is too small may cause the elements to come apart, and improperly selected paper may delaminate as a result of the stresses generated when opening and closing the card.

The aim of this article is to analyze the ways in which pop-up mechanisms are used as a means of visual expression in card design. The research material consists of a series of cards created by students. The analysis focuses on the relationship between the mechanism used, the graphic elements, and the effect achieved when the card is opened.

2. Characteristics of Basic Pop-Up Mechanisms

Among the many different pop-up mechanisms, three can be identified as the foundation for building more advanced and complex solutions. These include: multiple layers, V-folds, and spirals, which, when combined, create more advanced and visually striking solutions (Sánchez & Rodríguez, 2014).

The multiple layer mechanism uses paper elements with parallel folds that can be glued to the card base or cut directly from it. The three-dimensional effect is created when the card is opened and closed, and at a 90° angle between its parts, the individual layers form planes parallel to one of the card's base panels. The gluing points should be parallel to the card's center fold. When cutting elements out of the base card, it is recommended to reinforce it with an additional layer of paper, which increases the structure's rigidity and creates a color contrast between the base and the cut-out elements. The multiple layer mechanism allows you to create a sense of depth and build multi-plan compositions, such as landscapes, castles and other buildings, multi-level scenes, or three-dimensional lettering.

The V-fold mechanism gets its name from the shape of the elements attached to the base card, which can form the letter V or its inverted version. The angles on both sides of the card's central fold can be set to any value, maintaining symmetry or creating an asymmetrical arrangement. A three-dimensional effect is created when the card is opened to 180°, and this effect is particularly pronounced with elements of significant height. Three-dimensional elements can be glued to the base card or cut directly from it. The V-fold mechanism allows for the creation of objects positioned perpendicular to the base card, such as castles and other structures, pyramids, tents, facial features, or animal jaws. Combining two V-folds creates a zigzag mechanism, enabling the construction of more complex forms, such as figures with raised hands or birds with outstretched wings. A modification of the V-fold is the moving arms mechanism, which uses four articulated triangles forming a parallelogram. This allows the arm attached to one of the triangles to move in an arc as the card is opened and closed.

The spiral mechanism is a simple yet visually appealing solution. It is created by cutting out a spiral of any shape, starting from its outer edge and ending at the center. Both ends of the spiral are attached to the inner sides of the base card so that when closed, the card lies flat, and when opened, a three-dimensional effect is created. The spiral can take on various shapes, such as a circle, square, heart, or hexagon. Combining it with appropriately selected graphics enhances the visual effect — for example, by depicting a flower, a coiled snake, or a hexagonal honeycomb near a beehive.

All three pop-up mechanisms described earlier can be combined, e.g., multiple layers with a spiral, a V-fold with a spiral, or several V-folds. A greater challenge is combining a V-fold with a multiple layer mechanism, because the three-dimensional effect is achieved in the first case when the page is opened to 180°, and in the second case at a 90° angle. These differences must be taken into account during the design process to ensure that the complete structure functions properly.

3. Research Methodology and Project Implementation

3.1. Card Projects

The pop-up cards were designed by third-year students in the Paper and Printing Technology program as part of the course 'Computer-Aided Packaging Design', taught by Ewa Kołodziejuk, M.Sc. (Eng.). The assignment involved designing and creating a prototype card on any theme, using at least one of the three proposed mechanisms: multiple layers, a V-fold, and a spiral; a combination of several mechanisms; or other additional solutions used independently.

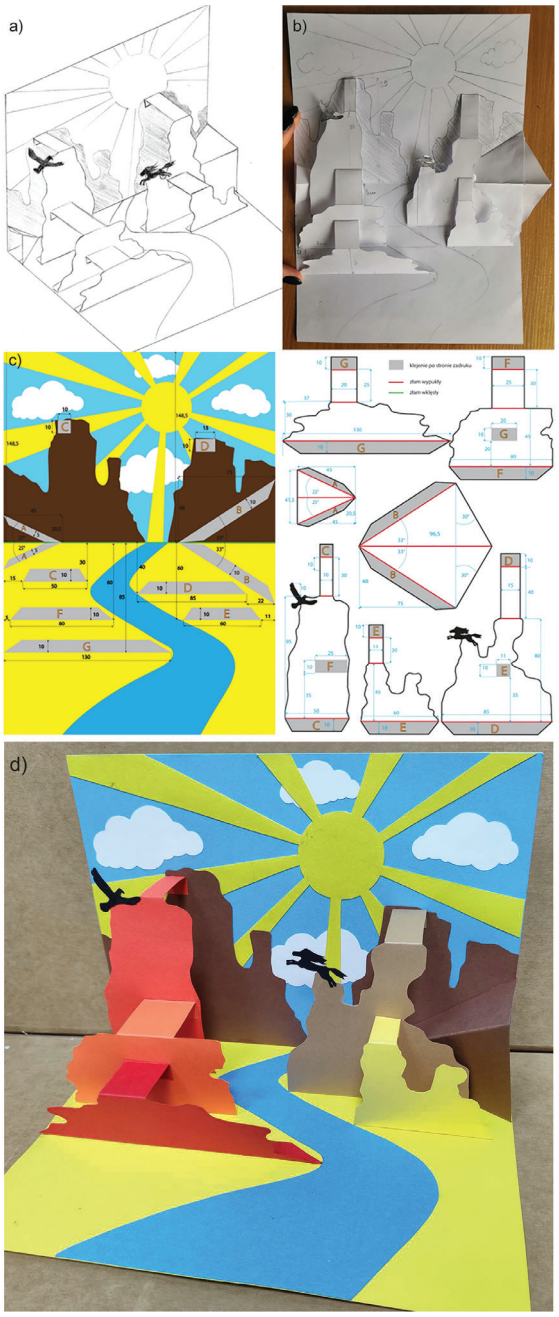
The design and manufacturing process consisted of the following stages:

a) developing a concept in the form of a sketch (Fig. 1a) that took into account the arrangement and shape of the 3D elements as well as the mechanisms used; planning the graphic layer using graphics or shapes cut out of dyed paper;

b) constructing a prototype from white paper and correcting design errors (Fig. 1b);

c) developing a 1:1 scale construction grid (Fig. 1c), either in a vector graphics program or by hand, with dimensions and markings for cut lines, folds, and glue joints;

d) creating a 3D model of the card using cardboard with a basis weight of 160–230 g/m² (Fig. 1d), including cutting out, folding, and gluing the components.



» **Figure 1:** *Stages of card design and manufacturing: a) conceptual sketch, b) white prototype, c) structural grid, d) finished 3D card model*

The students created a total of 28 pop-up cards. A video showcasing the pop-up card prototypes can be downloaded from: https://www.facebook.com/share/v/14uZbqUutwz/ or via the QR code (Fig. 2). The video was edited and the soundtrack was created by third-year student Mateusz Staśkiewicz.

» **Figure 2:** *QR code*

3.2. Analysis of Research Data

The study analyzed the use of pop-up mechanisms in student designs for 3D cards, with particular emphasis on their visual and compositional functions. The analysis is descriptive and comparative in nature and covers 28 cards. Based on video documentation, each card was described, identifying the mechanisms and defining their visual and compositional functions. The classification identified the dominant mechanism—the one that most significantly shapes the card's spatial composition—as well as additional mechanisms that complement its layout, deepen the scene, or introduce further moving elements. The use of different construction principles within a single card was considered a combination of several mechanisms. The repetition of several elements based on the same principle was treated as the use of a single type of mechanism, rather than several different solutions.

4. Results and Discussion

Table 1 describes all the cards, identifying the mechanisms they contain and specifying the functions they perform. Selected examples of the cards are shown in Fig. 3.

Table 1
Characteristics of Pop-Up Cards

No.	Card description	Number and types of pop-up mechanisms used	Visual and compositional function
1	GPS Map	1) multiple layers, 2) V-fold, 3) flap	Creates a three-dimensional scene and enhances the sense of depth.
2	Castle at Night	1) multiple layers, 2) spiral	Builds depth and combines a graphic motif with a three-dimensional form.
3	Nighttime City Panorama	1) multiple layers, 2) spiral	Varies the heights of the buildings and creates an urban perspective.
4	Card with Egyptian Symbols	1) multiple layers, 2) spiral	Brings the main theme (the pyramid) to the foreground.
5	Pink Castle with Green Bushes	1) multiple layers, 2) flap with V-fold	Highlights the castle and creates a fairy-tale-like, multi-layered scene.
6	A stronghold with flying dragons	1) multiple layers, 2) spiral	Highlights the architecture and suggests movement within the scene.
7	Red-and-yellow buildings	1) multiple layers, 2) V-fold	Gives the building a three-dimensional form and creates spatial scenery.
8	A Real Madrid fan card	1) multiple layers, 2) flap with V-fold	Enhances the typographic message and reveals additional content.
9	A soccer fan at the stadium	1-2) combination of multiple layers and V-fold, 3) spiral	Creates a central, prominent accent and contrasts it with a flat background.
10	Birds in a tree	1) multiple layers, 2) spiral	Introduces depth and places the birds on different planes.
11	A birdhouse	1) multiple layers, 2) V-fold (x2)	Places the birdhouse in the foreground, creating a three-dimensional scene.
12	Pink multi-tiered birthday cake	1) multiple layers, 2) spiral	Builds a central motif (the cake) and reinforces the impression of height.
13	Pink and red cake	1-2) combination of multiple layers and V-folds	Focuses attention on the cake and emphasizes its celebratory nature.
14	Card with a bouquet and hearts	1) V-fold, 2) spiral	Brings the bouquet to the foreground and reinforces the celebratory theme.
15	Valentine's Day card with a teddy bear and the words 'I love you'	1) multiple layers, 2) spiral	Combines the text message with the three-dimensional teddy bear.
16	Tulips in a wooden box	1) multiple layers, 2) V-fold (hidden under multiple layer)	Highlights the box and the flowers.
17	'LOVE' card with a heart	1) multiple layers, 2) spiral	Creates a multi-layered composition — combining letters and a heart symbol.
18	A piano with musical notes	1) multiple layers, 2) spiral	Gives the instrument a three-dimensional quality and evokes associations with the music scene.
19	A coffin with a zombie inside	1) multiple layers, 2) flap (combination with steering bar)	Highlights the central object and creates a sense of interior space.

No.	Card description	Number and types of pop-up mechanisms used	Visual and compositional function
20	A cemetery at night	1) multiple layers, 2) spiral	Establishes a foreground and enhances the scene's atmosphere.
21	A multicolored face with geometric patterns	1) V-folds (x3), 2) spiral	Create a sense of volume and draw attention with color and form.
22	A blue dragon	1) V-folds (x2), 2) spirals (x2)	Highlight the figure and suggest movement, creating a unique energy in the scene.
23	An anniversary card for the Volunteer Fire Department (OSP)	1) multiple layers, 2) spiral	Establish an appropriate hierarchy.
24	Café: a teapot, a cup, and croissants	1) multiple layers (x2), 2) flap with spiral, 3) flaps with V-fold (x2)	Organize the composition, bring objects to the foreground, and create a unique atmosphere.
25	A sailboat on the waves	1) multiple layers, 2) spiral	Builds a maritime scene and creates a sense of movement.
26	A landscape with a dam on a river	1) multiple layers, 2) spiral	Establishes multiple planes and guides the viewer's gaze along the river.
27	A capybara	1) multiple layers, 2) V-fold	Combines text and illustration, establishing a clear hierarchy between the title and the character.
28	A dog and a butterfly	1) multiple layers, 2) combination of V-folds (moving arms) 3) pulling tab	Creates a sense of depth, hides part of the illustration behind the foreground, and allows movement.

In the case of cards nos. 1, 11, 21, 27, and 28, it is difficult to identify a dominant mechanism; all the solutions used should be considered equivalent.

Based on an analysis of the mechanisms used, it was found that 24 cards (approximately 86%) utilized two types of mechanisms, while 4 (approximately 14%) combined more than two. In the analyzed set, multiple-layer layouts were used most frequently, appearing in 25 cards (89.3% of the set). Spirals were noted in 18 cards (64.3%), and V-type folds in 14 (50.0%). Flaps appear in 4 designs (14.3%) and were used primarily to combine, within a single design, a multi-layer mechanism—which requires opening the card at a 90° angle—with a V-fold mechanism, which requires the card to be laid flat (180°). One design featured an additional pulling tab mechanism (3.6%). The most common combinations are multi-layer layouts and spirals, which co-occur in 15 cards. Multi-layer layouts combined with V-fold mechanisms were found in 11 designs, and V-fold mechanisms combined with spirals in 5.

Multilayered layouts are the most commonly used solution and, in many projects, form the spatial foundation of the composition. V-folds, spirals, and flaps serve as elements that contribute to the layout: they highlight selected elements, introduce additional planes, or provide the composition with a more dynamic quality. The compilation also notes specific solutions: a flap connected to a control strip, movable arms created using double V-folds, and a pulling tab in the guide. However, these are features of individual designs.

An analysis of the designed cards confirms that the mechanisms used fulfill their intended functions: multilayered layouts create depth and organize the compositional planes; V-fold designs bring selected elements forward toward the viewer, giving them spatial clarity, and spirals create a sense of movement and lightness while directing attention to key elements of the scene.

The cards analyzed (Fig. 3) demonstrate a variety of ways to use pop-up mechanisms. The 'GPS Map' card features a three-dimensional layout of the route and navigational markers. The raised blue line guides the viewer's gaze along the route, while the elements that pop up further capture the viewer's attention. Similarly, in the 'Stadium' design, the central element—a fan wearing a scarf—protrudes toward the viewer, drawing the observer's attention and clearly dominating the composition. The 'Blue Dragon' card also utilizes a three-dimensional figure and additional elements that emphasize the scene's dynamism and expressiveness. In the artwork 'Café', the varying heights of the objects create the impression of a small, three-dimensional scene, highlighting the relationships between the depicted items. Additionally, the flaps reveal croissants served with coffee. The 'Sailboat' card combines layered waves with the three-dimensional form of a boat, creating depth and highlighting the main element of the composition.



» **Figure 3:** *Examples of pop-up cards: a) GPS Map, b) Stadium, c) Blue Dragon, d) Café, e) Sailboat, f) Dog and Butterfly*

In turn, the 'Dog and Butterfly' card uses overlapping layers of plants to create an effect of hiding and revealing the creatures, engaging the viewer in observing the scene. Additionally, the pulling tab engages the viewer and animated the pet, further enhancing its charm.

These examples show that pop-up mechanisms are not only used to create a three-dimensional effect, but also to organize space, direct the viewer's attention, and aid in the interpretation of the depicted subject.

5. Conclusions

An analysis of the presented designs indicates that the pop-up mechanism can serve both a structural function and as a means of visual expression. It influences the way the composition is organized, how depth is created, and how the viewer's attention is directed. The most frequently chosen and dominant mechanism is the multiple layer arrangement. V-fold, spiral, and flap mechanisms appear as elements that contribute to the overall composition. Furthermore, among the analyzed designs, the most common combination is that of multiple layers and spirals, found in 15 cards. Multiple layer mechanisms create a sense of space and depth; V-folds bring an element forward toward the viewer; and spirals introduce movement and dynamism into the composition. Selecting these mechanisms and combining them with other solutions makes it possible to adapt the spatial form to the theme and intended message of the card. The results of the observations indicate that designing a pop-up card requires treating the mechanism as an integral part of the visual concept, rather than merely as a technical means of achieving three-dimensionality.

6. References

Iizuka, S., Endo, Y., Mitani, J., Kanamori, Y. and Fukui, Y. (2011) ‚An interactive design system for pop-up cards with a physical simulation', *The Visual Computer*, 27(6–8), pp. 605–612. DOI: 10.1007/s00371-011-0564-0

Krahé, H. (1980) *Lothar Meggendorfers lebende Bilderbücher.* München: Puppentheatermuseum.

Okamura, S. and Igarashi, T. (2009) ‚An interface for assisting the design and production of pop-up card'. In Butz, A., Fisher, B., Christie, M., Krüger, A., Olivier, P. and Therón, R. (eds.) *Smart Graphics. SG 2009. Lecture Notes in Computer Science*, vol. 5531, pp. 68–78. Berlin, Heidelberg: Springer. DOI: 10.1007/978-3-642-02115-2_6

Ptaszek, I. (n.d.) *Pop-up Books.* Available from: https://liniaprosta.com/pop-up-books/ [Accessed 1 October 2026].

Sánchez, M.S. and Rodríguez, C.H. (2014) ‚Paper engineering in children's literature: Design of paper mechanisms'. In: *Tradition, Transition, Trajectories: Major or Minor Influences? Proceedings of the 9th Conference of the International Committee for Design History and Design Studies (ICDHS 2014)*, pp. 651–656. São Paulo: Blucher. DOI: 10.5151/despro-icdhs2014-0095

Smithsonian Institution Libraries (n.d.) *Paper Engineering: Fold, Pull, Pop & Turn.* Available from: https://www.sil.si.edu/pdf/FPPT_brochure.pdf [Accessed 10 September 2026].

The Ancient Origin of Pop-Up Books (2023) *The Ancient Origin of Pop-Up Books.* Available from: https://pl.joyfulprinting.net/info/the-ancient-origin-of-pop-up-books-85756712.html [Accessed 1 October 2026].



© 2026 Authors. Published by the University of Novi Sad, Faculty of Technical Sciences, Department of Graphic Engineering and Design. This article is an open access article distributed under the terms and conditions of the Creative Commons Attribution license 4.0 Serbia (http://creativecommons.org/licenses/by/4.0/rs/).

Digital media and user experience

05

Original Scientific Paper https://doi.org/10.24867/GRID-2026-p51

Heatmap-Based Area Analysis of Frontal Face Images Using an Eye-Tracking System

ABSTRACT

Facial images are a ubiquitous component of modern web platforms and mobile applications. The widespread use of eye-tracking technology has substantially increased research interest in facial perception and memory. A fundamental question is how facial recognition performance is influenced by observation time and by attention directed towards specific facial features. Memory experiments generally consist of two phases: an observation phase and a recognition phase. To investigate the effect of observation time on recognition accuracy, four image presentation durations were defined during the observation phase: 1 s, 2 s, 4 s, and 8 s. The results showed that correct recognition improved and incorrect recognition decreased as observation time increased. However, a plateau was observed at 4 s, as recognition accuracy in the 8 s condition was nearly identical to that in the 4 s condition, suggesting a threshold beyond which additional observation time provides limited benefit. To validate these findings, heatmap-based analysis was employed. This analysis confirmed the existence of the 4 s threshold and provided evidence for the observed trend. Both the area and perimeter of gaze regions increased with observation time up to 4 s and remained virtually unchanged thereafter. Similarly, the circularity of gaze regions decreased up to the 4 s condition and then stabilised, exhibiting comparable values in both the 4 s and 8 s conditions. These findings demonstrate the utility of heatmap analysis for investigating face observation and recognition processes and support the existence of a critical observation period of approximately 4 s for effective facial memorisation and recognition.

Andrej Iskra
Helena Gabrijelčič Tomc

University of Ljubljana, Faculty of Natural Sciences and Engineering, Department of Textiles, Graphic Arts and Design, Chair of Information and Graphic Art Technology, Ljubljana, Slovenia

KEY WORDS
Frontal facial images, eye tracking, face observation, face recognition success, heatmap analysis.

1. Introduction

Face memory and recognition under real-world conditions are influenced by a variety of factors. Among the most important are:

- face observation time,
- viewing distance,
- viewing angle,
- facial emotional expression.

Research on face memory and recognition can be conducted using facial images as experimental stimuli. Numerous facial image databases have been developed for this purpose. By combining different facial images with controlled experimental conditions, these databases make it possible to investigate the effects of the parameters listed above. Face observation time can be manipulated by varying the duration for which facial images are presented on a display device, most commonly a computer monitor. Similarly, different viewing distances encountered in real-world situations can be simulated by varying the displayed size of the facial images. Fur-

thermore, facial images can be acquired from different viewing angles and with different emotional expressions.

In the present study, we focused specifically on frontal facial images with neutral expressions, presented under conditions designed to approximate natural face observation at a real-world viewing distance of one meter. The main experimental variable was the presentation duration of the facial images, with particular emphasis on determining how presentation time affects subsequent face memory and recognition performance.

A considerable number of studies have previously investigated face memory and recognition (Goldinger et al., 2009, Leyk et al., 2008, Reynolds & Przdek, 1992). In most cases, recognition performance has been quantified using the measure of recognition success A′. Previous studies have also frequently examined recognition performance using an internal facial features approach in which the relative amount of visual attention directed toward the internal facial features is analysed. These regions primarily include the eyes, nose, and mouth, collectively referred to as internal facial features.

In the present study, we introduce a new heatmap-based area analysis method based on heatmaps generated from eye-tracking data. Relatively little research has been conducted on the quantitative analysis of heatmaps (Fux et al., 2024, Jia et al., 2024). The newly developed method was used to provide an additional means of evaluating and validating recognition-performance results. By analysing the spatial distribution of visual attention across facial regions, the proposed approach confirms conventional measures of face recognition performance and feature-based eye-tracking analysis.

Accordingly, the overall study was divided into two experiments, each designed to investigate a specific aspect of the relationship between facial image presentation time, recognition success A′ and heatmap analysis.

2. Methods

2.1. Participants

Participants were recruited from the student population of the Faculty of Natural Sciences and Engineering, University of Ljubljana (Ljubljana, Slovenia). A total of 42 participants took part in the study and were divided into three experimental groups (A, B, and C), with 14 participants in each group. All participants had normal or corrected-to-normal vision and were between 19 and 22 years of age. Participation was voluntary, and participants received a small amount of additional credit toward their laboratory course grade as compensation for their involvement.

2.2. Apparatus

Our research was performed eye tracking system. We used stand-alone eye tracking system Tobii X120. Analysis was done in Tobii Studio 3.4.5 software (User's Manual Tobii Studio, 2016). It is stand-alone eye tracking unit designed for eye tracking studies of real-world flat surfaces.

2.3. Stimuli

For the experiment, we used the publicly available Minear and Park (Minear & Park, 2000) face image database, developed in 2003 at the University of Michigan, Center for Vital Longevity Face Database. The database contains facial images depicting both neutral and emotional expressions, presented from two different viewpoints: frontal and profile views. For the purposes of the present study, only frontal-view facial images with neutral expressions were selected. The images had a resolution of 1280 × 960 pixels. Only facial images of individuals aged 18–29 years were included, ensuring that the age range of the depicted individuals was comparable to that of the study participants.

2.4. Procedure

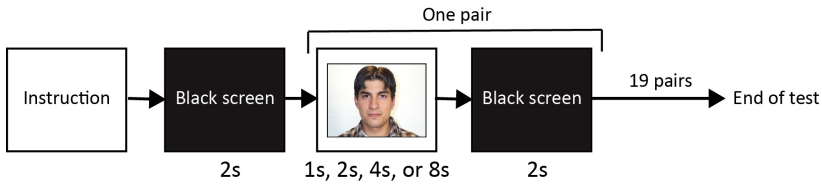
The experiment consisted of two phases: an observation phase and a recognition phase. Four stimulus presentation durations were used: 1, 2, 4, and 8 s, corresponding to four experimental conditions (Test1s, Test2s, Test4s, and Test8s). Each test comprised 20 randomly presented facial images, with an equal number of male and female faces (10 each).

The experimental procedure was based on previously well-known YES/NO recognition memory tasks. Following the initial instructions, a blank black screen was displayed for 2 s before the first facial stimulus appeared. Each subsequent facial image was preceded by a 2-s black screen, which served as a neutral interstimulus interval. The facial images were presented for the predefined duration corresponding to the respective experimental condition (1, 2, 4, or 8 s).

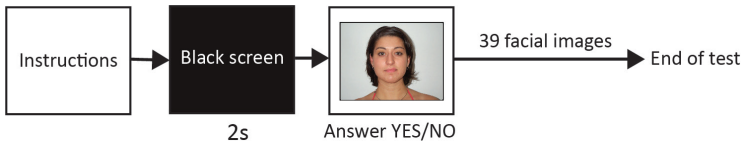
Stimulus presentation was fully automated, and participants had no control over the timing or sequence of the stimuli. The observation phase procedure is illustrated in Figure 1.

The recognition phase comprised 40 facial images: 20 previously presented during the observation phase (old stimuli) and 20 previously unseen images (new stimuli). Following the instructions and an initial 2-s black screen, facial images were presented individually.

For each image, participants indicated whether they had seen the face during the preceding observation



» **Figure 1:** Procedure of the observation phase



» **Figure 2:** Procedure of the recognition phase

phase by providing a yes/no recognition response. After responding, participants advanced to the next image by clicking the mouse button. Unlike the observation phase, the recognition phase was self-paced and had no imposed time limit. The recognition phase procedure is illustrated in Figure 2.

Participants' responses were recorded manually by the experimenter and subsequently transferred to an electronic spreadsheet for further analysis.

2.5. Experiment 1

As previously described, the first experiment examined face recognition performance as a function of stimulus presentation duration. Recognition performance was quantified using the discrimination index (Stanislaw & Todorov, 1999), calculated according to the following equation 1:

$$A' = 0{,}5 + \frac{(CR-FA)(1+CR-FA)}{4CR(1-FA)} \quad (1)$$

where:

- CR represents the proportion of correctly recognized previously presented faces, that is, faces presented during the observation phase and subsequently correctly identified as previously seen during the recognition phase.
- FA represents the proportion of false recognitions, that is, faces not presented during the observation phase but incorrectly identified as previously seen during the recognition phase.

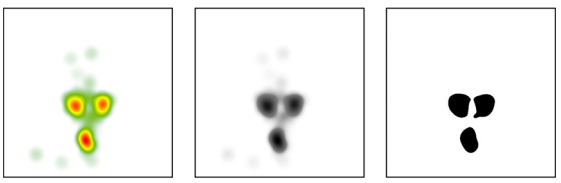
We hypothesized that recognition performance would increase with stimulus presentation duration following a logarithmic relationship, with larger improvements in recognition performance occurring at shorter presentation durations and progressively smaller improvements as presentation duration increased.

2.6. Experiment 2

To further evaluate the results obtained in Experiments 1, a new heatmap-based area analysis was performed using eye-tracking heatmaps. Heatmaps were generated in Tobii Studio based on the recorded gaze data. The principal parameter affecting heatmap generation was the size of the gaze representation, which could be adjusted incrementally. A value of 105 pixels was selected as the optimal setting as it provided sufficiently localized gaze regions while preserving differences associated with the different facial stimulus presentation durations.

Although heatmaps are conventionally represented using a colour scale ranging from red through yellow to green, they were converted to grayscale directly in Tobii Studio. Consequently, gaze regions were represented by different grayscale intensity levels, ranging from black and dark grey to light grey.

The resulting grayscale heatmap images were subsequently imported into ImageJ for quantitative image analysis. The primary parameters of interest were the area, perimeter, and circularity of the gaze regions. Prior to measurement, the grayscale heatmaps were converted into binary (black-and-white) images, allowing the gaze regions to be segmented from the background and analysed as discrete regions. An example of the original colour heatmap, the corresponding grayscale image, and the resulting binary image is shown in Figure 3.



» **Figure 3:** Colour, grayscale, and binary heatmap image

The area, perimeter, and circularity of the resulting binary gaze regions were subsequently analysed. Area and

perimeter were measured in pixels. Circularity, a dimensionless parameter, was used to characterize the spatial dispersion of gaze across the facial image. Circularity was calculated according to Equation 2, where A represents the area and P the perimeter of the gaze region:

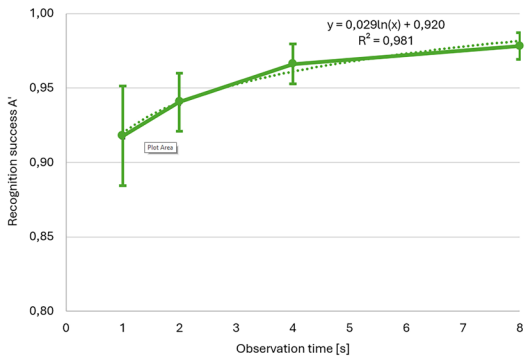
$$Circularity = \frac{4\pi A}{P^2} \quad (2)$$

Higher circularity values indicate more compact and circular gaze regions, whereas lower values indicate more irregular or spatially dispersed gaze patterns.

3. Results

3.1. Experiment 1

Figure 4 shows recognition performance for four different image presentation durations in the observation tests.



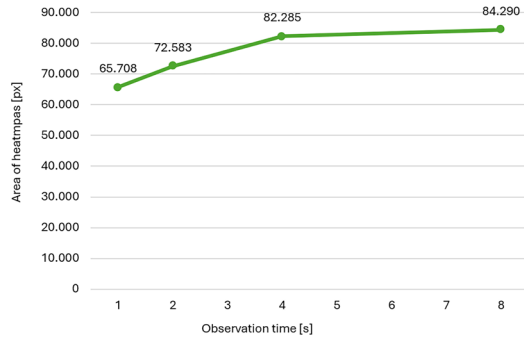
» **Figure 4:** *Results of recognition success*

It can be seen from the figure that the measured results fit the logarithmic curve very well, as indicated by the high R^2 value of 0.981.

The standard deviation decreases with increasing facial image observation time during the observation test, suggesting that longer viewing durations lead to greater similarity in the observation patterns adopted by individual participants. Conversely, shorter facial image presentation times appear to promote a wider range of observation strategies, resulting in greater inter-individual variability in recognition performance. Consequently, recognition performance shows greater dispersion, as indicated by a higher standard deviation (SD).

3.2. Experiment 2

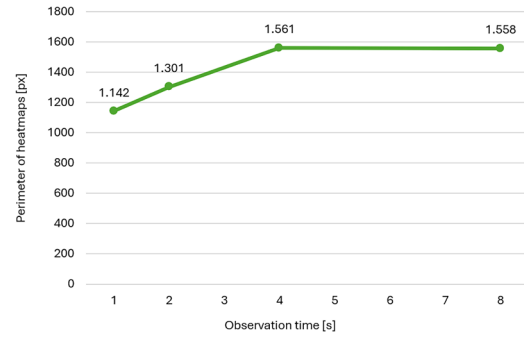
In this experiment, we focused on the analysis of heatmaps and their three parameters: area, perimeter, and circularity. The results for the area of heatmaps as a function of the observation time of facial images are presented in Figure 5.



» **Figure 5:** *Results of area of heatmaps*

The results indicate that the area of heatmaps increases as the observation time of facial images increases, up to approximately 4 seconds. Beyond this point, further increases in observation time produce little additional increase the area of heatmaps.

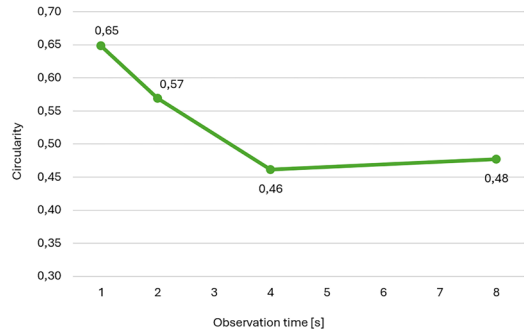
The relationship of perimeter of heatmaps and the observation time of facial images is shown in figure 6.



» **Figure 6:** *Results of perimeter of heatmaps*

Similar to the area, the perimeter of the heatmaps reaches a plateau at an observation time of 4 seconds. Interestingly, at an observation time of 8 seconds, the perimeter is slightly smaller than that measured in the 4-second test.

Figure 7 shows the circularity of the viewing regions as a function of the observation time of facial images.



» **Figure 7:** *Results of circularity of heatmaps*

A similar pattern can be observed in the circularity of heatmaps, with a distinct transition occurring at an observation time of 4 seconds.

4. Discussion

4.1. Experiment 1

The results of the first experiment show a logarithmic relationship between recognition success and the presentation time of facial images in the observation test. The recognition success graph also reveals the most pronounced change and the largest deviation from the fitted logarithmic curve at an observation time of 4 seconds.

These results suggest that an observation time of approximately 4 seconds represents a potential threshold or transition point.

4.2. Experiment 2

Using the newly introduced method for analysing heatmaps, the results for the area and perimeter of these regions showed that both measures increased with increasing observation time of the facial images. This is an expected result, as longer observation times allowed the participants to visually explore a larger area of the face.

However, this increase was observed only up to an observation time of 4 s. Beyond this point, the area of the observed regions remained practically unchanged despite the longer presentation time of the facial images. In our case, area for the 8 s test were almost identical to those obtained for the 4 s test.

The perimeter, however, was slightly smaller at 8 s. In some cases, regions that had previously been separated into distinct areas associated with the eyes and the nose and mouth merged into a single region during the 8 s condition. As a result, the overall area increased slightly, whereas the perimeter of the resulting merged region was smaller than the combined perimeter of the two previously separate regions. An example of this phenomenon is shown in Figure 8.

A similar pattern was observed for circularity, which decreased with increasing observation time up to 4 s and then showed a slight increase at 8 s. This behaviour can also be explained based on the circularity equation presented in the previous section.



» **Figure 8:** *Heatmaps of 4 seconds and 8 seconds test*

5. Conclusions

In this study, we investigated the effect of facial image presentation time on face memorization. The results showed that memorization improved by increasing presentation time, reaching a turning point at approximately 4 seconds. Under the conditions of the present experiment, this duration appeared to be sufficient for participants to memorize the presented faces and achieve a reliable level of recognition performance. Extending the presentation time beyond 4 seconds did not result in further improvements in memorization or recognition performance.

The findings were also supported by the newly developed heatmap-based area method used to analyse heatmaps of viewing areas. All three parameters, area, perimeter, and circularity, showed a clear turning point at 4 seconds. Up to this presentation time, area and perimeter increased, while circularity decreased. However, the values obtained at 8 seconds presentation time were very similar to those observed at 4 seconds, indicating that the spatial characteristics of the viewing areas remained largely unchanged with additional viewing time. This pattern is consistent with the recognition success results, further suggesting that extending viewing time beyond 4 seconds provides little additional benefit for face recognition.

In future studies, this heatmap-based area method could also be applied to investigate the recognition of facial expressions of emotion. Although different theoretical frameworks propose somewhat different classifications of basic emotions, commonly investigated facial expressions include happiness, anger, sadness, fear, and surprise. Future research will therefore focus on how different facial expressions influence users' visual attention and face-recognition performance.

6. References

Fux, M., Monshi, J., Jang, H., Lahey, C. H., Arslan, S. S., Dixon III, W. V., Groth, M. and Sinha, P. (2024) 'Comparing Human Eye-Tracking Heatmaps with DNN Saliency Maps for Faces at Different Spatial Frequencies', *Journal of Vision*, 24(10), 1329. DOI: https://doi.org/10.1167/jov.24.10.1329

Goldinger, S. D., He, Y. and Papesh, M. H. (2009) 'Deficits in cross-race face learning: insights from eye movements and pupillometry', *Journal of Experimental Psychology: Learning, Memory, and Cognition*, 35(5), pp. 1105–1122. DOI: https://doi.org/10.1037/a0016548

Jia, J., Zhao, T., Yang, J. and Wang, Q. (2024) 'Intelligent Evaluation Method for Design Education and Comparison Research between Visualizing Heat-Maps of Class Activation and Eye-Movement', *Journal of Eye Movement Research*, 17(2). DOI: https://doi.org/10.16910/jemr.17.2.1

Leyk, D., Sievert, A., Heiss, A., Gorges, W., Ridder, D., Alexander, T., Wunderlich, M. and Ruter, T. (2008) 'Validation of a short-term memory test for the recognition of people and faces', *Ergonomics*, 51(8), pp. 1125–1136. DOI: 10.1080/00140130802094371

Minear, M. and Park, D. (2004) 'A lifespan database of adult facial stimuli', *Behavior Research Methods, Instruments & Computers*, 36(4), pp. 630–633. DOI: 10.3758/bf03206543

Reynolds, J. K. and Przdek, K. (1992) 'Face recognition memory: the effects of exposure duration and encoding instruction', *Applied Cognitive Psychology*, 6, pp. 279–292. DOI: https://doi.org/10.1002/acp.2350060402

Stanislaw, H. and Todorov, N. (1999) 'Calculation of signal detection theory measures', *Behavior Research Methods, Instruments, & Computers*, 31, pp. 137–149. DOI: https://doi.org/10.3758/BF03207704

Tobii Connect (2016) *User's Manual Tobii Studio version 3.4.5*. Danderyd: Tobii Technology.



© 2026 Authors. Published by the University of Novi Sad, Faculty of Technical Sciences, Department of Graphic Engineering and Design. This article is an open access article distributed under the terms and conditions of the Creative Commons Attribution license 4.0 Serbia (https://creativecommons.org/licenses/by/4.0/deed.en).

Original Scientific Paper https://doi.org/10.24867/GRID-2026-p52

Comprehension of Medication Dosage Instructions: A Comparison of Four Instruction Formats

ABSTRACT

Medication errors resulting from the misinterpretation of dosing instructions remain an important medication safety concern. Visually supported medication instructions may improve the clarity and comprehension of dosing information. This study compared four medication dosage instruction formats displayed on the packaging of a fictitious medicinal product: a conventional handwritten instruction, an action-oriented pictogram, a symbol-oriented dosing instruction, and an action-oriented pictogram accompanied by explanatory text. Sixty participants were randomly assigned to one of the four formats. Comprehension was assessed through response accuracy and confidence, while visual attention was recorded using eye-tracking. Response accuracy differed significantly between the instruction formats, with V3 and V4 achieving the highest accuracy (86.7%) and significantly greater odds of correct interpretation than the conventional handwritten format (46.7%). Eye-tracking measures also differed between formats, with V3 showing a lower proportion of fixation duration within the instruction area than V1. Overall, the findings indicate that the visual representation of medication dosage instructions can influence both comprehension and visual attention and support the potential use of appropriately designed visual and textual elements to improve medication instruction comprehension.

Josip Bota
Nina Hasukić
Rea Franković

University of Zagreb, Faculty of Graphic Arts, Zagreb, Croatia

KEY WORDS
Pictograms, dosage instructions, medication instructions, patient comprehension, medication safety

1. Introduction

Medicine packaging serves as the primary source of information required for the safe and appropriate use of the medicinal product. According to Article 54 of Directive 2001/83/EC, the outer packaging must include the name of the medicinal product, its strength and pharmaceutical form, the active substance, and the method and route of administration. It must also provide a designated space for recording the prescribed dosage. In addition, the packaging is required to display a special warning stating that the medicinal product must be kept out of the sight and reach of children, the expiry date, any special storage precautions, the name and address of the marketing authorization holder, the marketing authorization number, and the manufacturer's batch number (European Parliament and Council of the European Union, 2001). Clearly presented information facilitates the correct identification of the medicinal product, reduces the risk of medication errors, and contributes to the safety of both patients and healthcare professionals.

Medication dosing instructions are not standardized worldwide and vary considerably across countries and healthcare systems. One approach to improving the communication of medication-related information to patients with limited health literacy is the use of visual representations and pictograms on medicine labels and in the package leaflet (Dowse & Ehlers, 2005). The potential benefit of pictorial medication instructions can also be explained by the multimedia principle, according to which information presented through complementary

verbal and visual representations can facilitate comprehension compared with verbal information alone (Mayer, 2021). In medication communication, pictograms may therefore complement textual instructions by providing an additional visual representation of the required action or dosing schedule. Two of the best-known standardized pharmaceutical pictogram systems are the USP Pictogram Library, developed by the United States Pharmacopeia (USP), and PictoRx, developed by the International Pharmaceutical Federation (FIP). Both systems comprise validated pictograms designed to facilitate the communication of medication-related information, including dosage instructions, precautions, storage conditions, and safety warnings. Their primary objective is to improve patient comprehension but are not legally mandated and have not been universally adopted across healthcare system. In the Republic of Croatia like most of Europe, medication use instructions are commonly handwritten by pharmacists on the medicine packaging, a practice that may reduce their readability and hinder patient comprehension.

However, the presence of a pictogram alone does not guarantee correct interpretation. Previous research has shown that pictogram comprehension can depend on factors such as familiarity, design characteristics, cultural context, and health literacy (Dowse et al., 2023; Katz, Kripalani & Weiss, 2006; Menon et al., 2021). Nevertheless, a considerable body of research has examined the potential of pictorial representations to improve the comprehension of medication-related information, with recent evidence indicating that appropriately designed pharmaceutical pictograms can enhance the comprehension of textual medication instructions (Abdu-Aguye et al., 2023; Ferreira-Alfaya, Cura & Zarzuelo-Romero, 2025; Ferreira-Alfaya, Zarzuelo-Romero & Cura, 2024; Reijnen et al., 2022; Sharko et al., 2022). However, no published studies were found that evaluated users' comprehension of the medication instruction and labelling practices currently used in Europe and comparison within different instruction formats. The aim of this study was therefore to investigate how different visual representations of medication dosage instructions affect their comprehension and the allocation of visual attention. Four instruction formats were compared in terms of response accuracy, confidence, and eye-tracking measures, with the conventional handwritten instruction serving as the reference format.

2. Methods

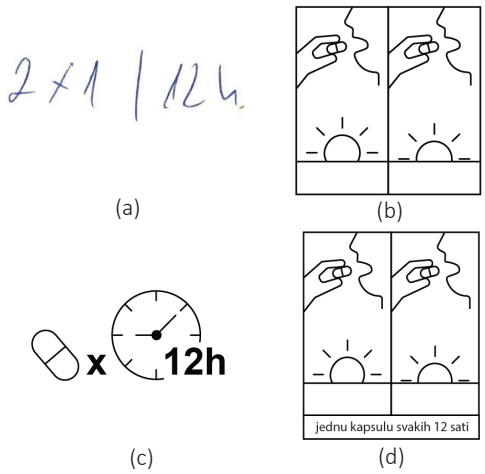
2.1. Samples

A packaging prototype of a medication was developed specifically for the purposes of this study. To minimize the potential influence of prior product or brand familiarity, the designs did not contain any identifiable brand names or commercial product references (Fig. 1). All textual information was presented in Croatian, thereby reflecting the language context of packaging encountered by the target population.



» **Figure 1:** *Packaging prototype*

Together with the conventional handwritten instruction, three alternative visual coding formats were developed, as illustrated in Fig. 2. All four formats were intended to communicate the same dosing instruction: “Take one pill every twelve hours.” The instruction was presented as a handwritten dosing instruction, representing the conventional format commonly used in Croatia and neighboring countries (Fig. 2a); an action-oriented pictogram depicting the intake of one pill in the morning and one in the evening (Fig. 2b); a symbol-oriented dosing instruction combining a pill symbol with a clock symbol and a 12-hour interval (Fig. 2c); and the action-oriented pictogram supplemented with explanatory text (Fig. 2d).



» **Figure 2:** *Four experimental instruction formats: a) Handwritten instructions (V1); b) Action-oriented pictogram (V2); c) Symbol-oriented dosing instruction (V3); d) Action-oriented pictogram and text (V4)*

2.2. Apparatus

The visual stimuli were displayed on a 17.3-inch IPS screen (1920 × 1080 px) of an Acer Nitro 5 laptop, with a maximum luminance of 300 cd/m² and a refresh rate

of 144 Hz. A constant viewing distance of 60 ± 1 cm was maintained throughout the experiment. Before data collection, display color characteristics were calibrated with a Datacolor SpyderX2 Ultra colorimeter to maintain consistent visual presentation across all participants. Eye-tracking data were acquired using a Tobii Pro Fusion system at a sampling frequency of 120 Hz. Stimulus presentation and eye-tracking data acquisition were managed in Tobii Pro Lab (version 26.10).

2.3. Experiment

Prior to the experiment, demographic data was collected and participants were introduced to the experimental procedure. Before presenting one of the four samples each participant was instructed to examine the packaging and the medication instructions displayed on the screen. Viewing time was unrestricted, allowing participants to proceed once they had formed their interpretation. After the stimulus was removed, participants verbally reported their interpretation, which was classified by the researcher as either correct or incorrect. If the initial response was incomplete, a neutral follow-up question was used to clarify the participant's interpretation without suggesting the correct answer. They subsequently rated their confidence in the response on a 10-point scale (1 = not confident at all; 10 = completely confident). Each participant was exposed to only one of the four experimental variants, thereby avoiding potential learning effects between different representations of the same information.

3. Results and discussion

A total of 61 participants were recruited for the study. One participant was excluded after failing the Ishihara color vision test, resulting in a final sample of 60 participants (14 male and 46 female), of whom 24 used vision correction (glasses or contact lenses) during the experiment. Regarding age distribution, 49 participants were aged 18–29 years, 7 were aged 30–45 years, 3 were aged 46–61 years, and 1 participant was aged 62–80 years.

3.1. Eyetracking

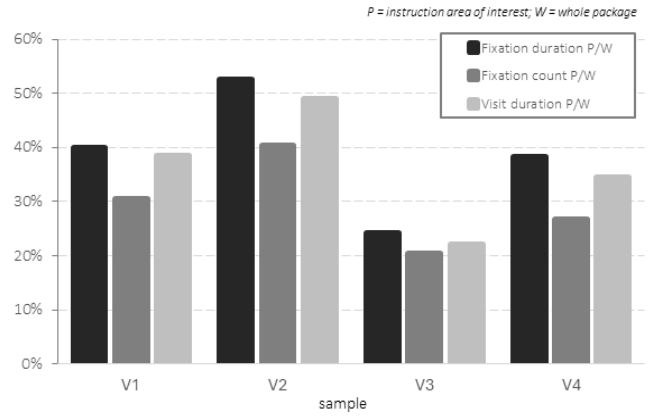
Eye-tracking data were analyzed to examine whether the different instruction formats affected participants' visual attention during information processing. The analysis focused on fixation- and visit-based measures within the instruction area of interest (P). In addition to the absolute eye-tracking measures, the proportion of visual attention allocated to the instruction area relative to the whole package (P/W) was calculated. This normalization was used to indicate how much of the overall visual attention directed toward the package was specifically allocated to the medication instruction. Differences among the four instruction formats were evaluated using the Kruskal–Wallis test. The results are presented in Table 1.

As shown, the instruction format significantly affected several measures of visual attention within the instruction AOI. Significant differences among V1–V4 were found for fixation duration, $H(3) = 9.89$, $p = .020$, $\varepsilon^2 = .123$, fixation count, $H(3) = 8.21$, $p = .042$, $\varepsilon^2 = .093$,

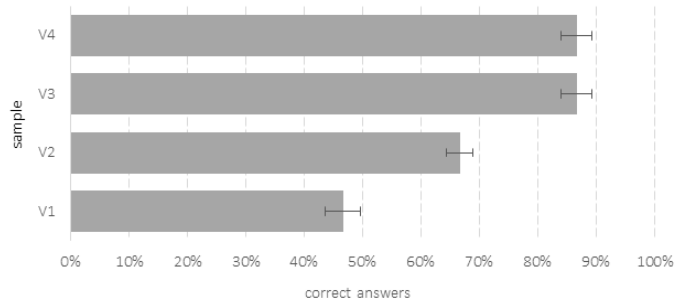
Table 1:
Eye-tracking measures across the four instruction formats

	V1 Median [Q1–Q3]	V2 Median [Q1–Q3]	V3 Median [Q1–Q3]	V4 Median [Q1–Q3]	H(3)	p	ε^2
Fixation duration – P	4.650 [2.532–6.717]	6.442 [5.464–7.648]	3.667 [2.642–4.824]	5.145 [3.838–6.325]	9.89	0.020	0.123
Fixation count – P	14 [7.0–15.0]	17 [15.5–21.0]	12 [9.5–15.0]	14 [11.5–17.0]	8.21	0.042	0.093
Time to first fixation (TTFF) – P	2.795 [1.855–3.675]	2.131 [1.572–3.565]	3.102 [1.688–4.598]	2.798 [1.911–3.846]	1.79	0.617	0.000
Visit duration – P	4.792 [2.970–7.001]	6.733 [5.768–8.367]	4.022 [2.912–5.257]	5.810 [4.288–6.838]	10.14	0.017	0.127
Visit count – P	4 [2.5–5.5]	4 [3.0–5.0]	5 [4.0–7.5]	4 [3.0–5.0]	3.16	0.367	0.003
Proportion of fixation duration (P/W)	0.400 [0.306–0.590]	0.525 [0.419–0.596]	0.242 [0.188–0.316]	0.383 [0.246–0.570]	13.86	0.003	0.194
Proportion of fixation count (P/W)	0.304 [0.260–0.382]	0.405 [0.317–0.461]	0.205 [0.178–0.290]	0.268 [0.190–0.414]	10.55	0.014	0.135
Proportion of visit duration (P/W)	0.384 [0.282–0.527]	0.490 [0.392–0.557]	0.220 [0.181–0.300]	0.346 [0.216–0.518]	14.35	0.002	0.203

P = instruction area of interest; W = whole package ($p < .05$)



» **Figure 3:** *Relative visual attention to the instruction area across the four instruction formats*



» **Figure 4:** *Percentage of correct responses across the four instruction instruction formats (n = 15 per group, N = 60)*

and visit duration, H(3) = 10.14, p = .017, ε^2 = .127. In contrast, no statistically significant differences were observed for time to first fixation or visit count (p > .05).

Differences between the instruction formats became more pronounced when visual attention to the instruction was considered relative to overall package viewing. Significant differences were found for the proportion of fixation duration, H(3) = 13.86, p = .003, ε^2 = .194, fixation count, H(3) = 10.55, p = .014, ε^2 = .135, and visit duration, H(3) = 14.35, p = .002, ε^2 = .203. V2 consistently showed the highest median proportion of visual attention directed toward the instruction area, whereas V3 showed the lowest values across all three measures.

Post hoc comparisons further showed that V2 had a significantly greater proportion of fixation duration than V3 (p = .002), while V1 also showed a greater proportion than V3 (p = .049). Compared with V3, V2 also resulted in a significantly greater proportion of fixation count (p = .008) and visit duration (p = .001).

The relative distribution of visual attention across the four instruction formats was calculated as P/W × 100 and expressed as a percentage of the corresponding eye-tracking measure and is illustrated in Fig. 3. V2 showed the highest proportion of attention directed toward the instruction area across all three measures, whereas V3 consistently showed the lowest values. The median proportion of fixation duration was 0.525 for V2 compared with 0.242 for V3, while the corresponding proportions for fixation count were 0.405 and 0.205, and for visit duration 0.490 and 0.220, respectively. These differences were statistically significant for fixation duration (p = .003), fixation count (p = .014), and visit duration (p = .002).

3.2. Accuracy of responses and confidence results

Four different instruction formats of the same medication instructions (V1–V4) were evaluated. Each instruction format was assessed by a separate group of 15 participants. Comprehension was evaluated based on response accuracy (correct/incorrect) and participants' self-reported confidence in their response, rated on a scale from 1 to 10. The proportion of correct responses differed across the four instruction formats. For V1, 7 of 15 participants (46.7%) provided a correct response. This increased to 10 of 15 participants (66.7%) for V2 and to 13 of 15 participants (86.7%) for both V3 and V4 (Fig. 4).

Pearson's chi-square test indicated a statistically significant association between the instruction format and response accuracy, $\chi^2(3) = 8.13$, p = .043. Cramér's V was 0.368, indicating a moderate association between instruction format and correct interpretation of the instructions.

Differences between individual instruction formats were further examined using odds ratios (OR), with V1 used as the reference condition. Compared with V1, participants presented with V3 had significantly greater odds of correctly interpreting the instructions, OR = 7.43, 95% CI [1.23, 45.01], p = .029. The same result was obtained for V4 compared with V1, OR = 7.43, 95% CI [1.23, 45.01], p = .029. Thus, the odds of a correct response were approximately 7.4 times higher for V3 and V4 than for V1. In contrast, the increase in the odds of a correct response for V2 compared with V1 was not statistically significant. Therefore, the results provide evidence of a difference between V1 and V3 and between V1 and V4, but not between V1 and V2. The results indicate that the way medication instructions are visually represented can substantially influence their comprehension. Compared with the conventional handwritten instruction (V1), both V3 (symbol, pictogram, and text) and V4 (pictogram and text) resulted in significantly higher odds of correct interpretation. The high comprehension accuracy observed for V3 (symbol, pictogram, and text) and V4 (pictogram and text) supports previous findings that combining visual and verbal information can facilitate comprehension (Ferreira-Alfaya, Zarzuelo-Romero & Cura, 2024; Mayer, 2021).

In addition to objective response accuracy, participants' subjective confidence in their responses was evaluated. The median confidence scores were 8 for V1, 9 for V2, 9 for V3, and 10 for V4. Although the descriptive results suggest an increase in confidence across the instruction formats, the Kruskal–Wallis test showed no statistically significant difference in confidence between the four groups, H(3) = 2.18, p = .535. However, when participants were grouped according to whether their response was correct or incorrect, a significant difference in confidence was observed. Participants who provided correct responses reported significantly higher confidence than those who provided incorrect responses (Mann–Whitney U = 143.5, p < .001). Furthermore, response confidence was positively associated with response accuracy (Spearman's ρ = .499, p < .001), which is in accordance with other research (Jin, Verhaeghen & Rahnev, 2022).

When considered together with the eye-tracking results, V3 showed a particularly notable pattern. Compared with V1, V3 combined higher comprehension accuracy (86.7% vs. 46.7%) with a lower proportion of fixation duration within the instruction AOI (24.2% vs. 40.0%), with both comparisons reaching statistical significance. V4 likewise showed significantly higher comprehension accuracy than V1 (86.7% vs. 46.7%), while no significant increase in relative visual attention was observed. In contrast, V2 showed a numerical increase in accuracy (66.7% vs. 46.7%), but this improvement was not statistically significant.

At the individual participant level, the amount of visual attention allocated to the instruction area was not significantly associated with response accuracy after correction for multiple comparisons. Thus, greater fixation duration or fixation count should not be interpreted as directly corresponding to better comprehension. Rather, the combined results indicate that high comprehension accuracy can be achieved without a corresponding increase in visual attention to the instruction area.

Longer visual attention should not necessarily be interpreted as an indication of better instruction performance, as increased fixation duration and fixation count may also reflect greater processing demands. In this context, the results for V3 are particularly noteworthy. Despite receiving a lower proportion of visual attention, V3 achieved a high level of comprehension accuracy. This combination may indicate that the instruction could be extracted with less visual processing, suggesting a potentially more efficient presentation of the instruction. Although ocular metrics have been widely investigated in relation to cognitive load, there is still insufficient understanding of how these measures change with task difficulty (Ekin, Krejtz & Krejtz, 2025). Therefore, fixation-based measures alone cannot determine cognitive processing difficulty, which was not measured directly in the present study, and the interpretation of these findings should be considered with caution.

Although no eye-tracking measure remained significantly associated with comprehension accuracy after correction for multiple comparisons, visit count showed a potentially relevant pattern. Participants who correctly interpreted the instruction tended to revisit the instruction area less frequently. The observed lower number of revisits to the instruction area may indicate that participants were able to integrate the textual and pictorial information more efficiently during the initial inspection, reducing the need for subsequent verification. Eye-tracking research in educational settings has shown that successful learners typically exhibit more goal-directed visual attention patterns and fewer unnecessary transitions between information sources (Jarodzka, Holmqvist & Gruber, 2017). Similarly, van Gog and Scheiter argue that eye movements reflect cognitive and metacognitive processes during learning, with repeated shifts between information sources often indicating ongoing integration or verification of information. Holmqvist et al. (2011) further note that a higher number of visits to an area of interest generally reflects repeated consultation of that information, which may occur because the information is important or because it requires additional processing (Holmqvist et al., 2011). Therefore, the reduced revisit frequency observed in the present study may suggest more efficient processing of the instructional material rather than a need for repeated consultation.

4. Conclusions

This study demonstrated that the instruction format of medication dosage instructions can significantly influence their comprehension. The symbol-oriented instruction (V3) and the pictogram accompanied by explanatory text (V4) resulted in the highest comprehension accuracy, with significantly greater odds of correct interpretation compared with the conventional handwritten instruction (V1). V3 showed a particularly favorable overall pattern, combining high comprehension accuracy with a lower proportion of visual attention directed toward the instruction area. However, eye-tracking measures alone were not associated with comprehension accuracy at the individual level, indicating that visual attention and comprehension should be considered together when evaluating medication instructions.

Overall, the findings support the use of appropriately designed visual elements combined with textual information as an alternative to conventional handwritten dosing instructions.

The findings of this study provide a basis for further investigation of visually supported instructions. Future research could extend the present approach by including larger and more age-diverse participant samples and by evaluating a broader range of dosing instructions and packaging designs. Testing the instruction formats on physical packaging and in more realistic use conditions could further establish their applicability in everyday medication use.

5. Acknowledgments

The research was funded by the Next-Generation EU project- EKKA.

6. References

Abdu-Aguye, S. N., Sadiq, A. M., Shehu, A. and Mohammed, E. N. A. (2023) 'Guessability of standard pharmaceutical pictograms in members of the Nigerian public', *Exploratory Research in Clinical and Social Pharmacy*, 9, 100240. DOI: 10.1016/j.rcsop.2023.100240

Dowse, R. and Ehlers, M. (2005) 'Medicine labels incorporating pictograms: Do they influence understanding and adherence?', *Patient Education and Counseling*, 58(1), pp. 63–70. DOI: 10.1016/j.pec.2004.06.012

Dowse, R., Okeyo, S., Sikhondze, S. and Khumalo, N. (2023) 'Pharmaceutical indication pictograms for low literacy viewers: Health literacy and comprehension', *Health SA Gesondheid*, 28, a2192. DOI: 10.4102/hsag.v28i0.2192

Ekin, M., Krejtz, K. and Krejtz, I. (2025) 'Cognitive Load and Oculometrics in the Educational Scenarios: A Systematic Review and Meta-Analysis', Proceedings of the ACM on Human-Computer Interaction, 9(3), pp. 1–19. DOI: 10.1145/3725832

European Parliament and Council of the European Union (2001) *Directive 2001/83/EC of the European Parliament and of the Council of 6 November 2001 on the Community code relating to medicinal products for human use*. Official Journal of the European Communities, L 311, 28 November 2001, p. 67. Available from: EUR-Lex [Accessed 2 October 2026].

Ferreira-Alfaya, F. J., Cura, Y. and Zarzuelo-Romero, M. J. (2025) 'Effect of pharmaceutical pictograms on the textual comprehension of Prescription Medication Leaflets: A randomized controlled trial', Research in Social and Administrative Pharmacy, 21(4), pp. 245–252. DOI: 10.1016/j.sapharm.2025.01.004

Ferreira-Alfaya, F.J., Zarzuelo-Romero, M.J. and Cura, Y. (2024) 'Pharmaceutical pictograms to improve textual comprehension: A systematic review', *Research in Social and Administrative Pharmacy*, 20(2), pp. 75–85. DOI: 10.1016/j.sapharm.2023.11.007

Holmqvist, K., Nyström, M., Andersson, R., Dewhurst, R., Jarodzka, H. and van de Weijer, J. (2011) *Eye Tracking: A Comprehensive Guide to Methods and Measures*. Oxford: Oxford University Press.

Jarodzka, H., Holmqvist, K. and Gruber, H. (2017) 'Eye tracking in Educational Science: Theoretical frameworks and research agendas', *Journal of Eye Movement Research*, 10(1), pp. 1–18. DOI: 10.16910/jemr.10.1.3

Jin, S., Verhaeghen, P. and Rahnev, D. (2022) 'Across-subject correlation between confidence and accuracy: A meta-analysis of the Confidence Database', *Psychonomic Bulletin & Review*, 29(4), pp. 1405–1413. DOI: 10.3758/s13423-022-02063-7

Katz, M.G., Kripalani, S. and Weiss, B.D. (2006) 'Use of pictorial aids in medication instructions: A review of the literature', *American Journal of Health-System Pharmacy*, 63(23), pp. 2391–2397. DOI: 10.2146/ajhp060162

Mayer, R.E. (2021) 'The Multimedia Principle'. In: Mayer, R.E. and Fiorella, L. (eds.) *The Cambridge Handbook of Multimedia Learning*. Cambridge: Cambridge University Press, pp. 145–157. DOI: 10.1017/9781108894333.015

Menon, D.D., Joy, J.M., Paul, A., Reddy, S.A., Raj, E.A., Krishnan, J.B. and Vilakkathala, R. (2021) 'Effectiveness of pictograms in patients or caregivers in healthcare settings: A systematic review', *Journal of Pharmaceutical Health Services Research*, 12(4), pp. 607–614. DOI: 10.1093/jphsr/rmab049

Reijnen, E., Laasner Vogt, L., Fiechter, J.P., Kühne, S.J., Meister, N., Venzin, C. and Aebersold, R. (2022) 'Well-designed medical pictograms accelerate search', *Applied Ergonomics*, 103, 103799. DOI: 10.1016/j.apergo.2022.103799

Sharko, M., Sharma, M.M., Benda, N.C., Chan, M., Wilsterman, E., Liu, L.G., Demetres, M., Delgado, D. and Ancker, J.S. (2022) 'Strategies to optimize comprehension of numerical medication instructions: A systematic review and concept map', *Patient Education and Counseling*, 105(7), pp. 1888–1903. DOI: 10.1016/j.pec.2022.01.018



© 2026 Authors. Published by the University of Novi Sad, Faculty of Technical Sciences, Department of Graphic Engineering and Design. This article is an open access article distributed under the terms and conditions of the Creative Commons Attribution license 4.0 Serbia (https://creativecommons.org/licenses/by/4.0/deed.en).

Professional Paper https://doi.org/10.24867/GRID-2026-53

Distributed Audiovisual Production and the Evolution of Communication Methodologies for Large-Scale Cultural Events: A Case Study of the Festa Dos Tabuleiros

ABSTRACT

This paper examines how distributed audiovisual production can support the communication of large-scale cultural events through the case of the Festa dos Tabuleiros in Tomar, Portugal. It reconstructs the 2019 operation, which grew from a public-screen service into complete online coverage and signal sharing with local media. The study follows an exploratory qualitative single-case design and draws on planning records, public recordings, a control-room time-lapse, participant observation and YouTube analytics. The operation showed that an academic and institutional team could coordinate distributed acquisition and central production without relying on a conventional outside-broadcast structure. It also exposed a critical communication weakness: a short interruption ended the original streaming sessions, changed the audience entry points and left three unattended public screens outside editorial control. Replacement sessions attracted smaller audiences, although the late stage of the procession prevents that difference from being attributed solely to link discovery. From these observations, the paper proposes a 2027 model based on a non-public clean feed, independently produced partner programmes, an optional official programme and a dedicated silent, graphics-led service for public screens. The case suggests that distributed production should be treated not only as an engineering workflow, but as a communication process involving editorial alignment, audience continuity, platform choice, public information and preservation of audiovisual memory.

Júlio Silva [1]
Paulo Coelho [2]
Ana do Carmo [1]

[1] Polytechnic University of Tomar, TECHN&ART, Technology, Restoration and Arts Enhancement Center, Tomar, Portugal
[2] Polytechnic University of Tomar, Ci2, Smart Cities Research Center, Tomar, Portugal

KEY WORDS
Audiovisual communication, distributed audiovisual production, cultural heritage, media convergence, case study

1. Introduction

Large cultural events communicate shared history, identity and practice as well as bringing people together. Professional live coverage traditionally depended on broadcasters controlling equipment, editorial choices and distribution (Briggs, Burke & Ytreberg, 2020). Although this can provide national visibility, cultural organisations remain dependent on external decisions about availability, news value and programme time.

Digital convergence, networked media and mediatisation now allow live content to be produced and distributed across platforms (Jenkins, 2006; Castells, 2010; Couldry & Hepp, 2017).

Distributed audiovisual production links acquisition, production and distribution resources in different locations within one workflow (Calverley, 2018). Its engineering foundations are established, but its implications for cultural-event communication require closer attention.

Here, communication methodology covers how audiovisual coverage is planned, produced, distributed and accessed, including the decisions that determine what audiences can find, see and understand.

1.1. The Festa dos Tabuleiros communication context

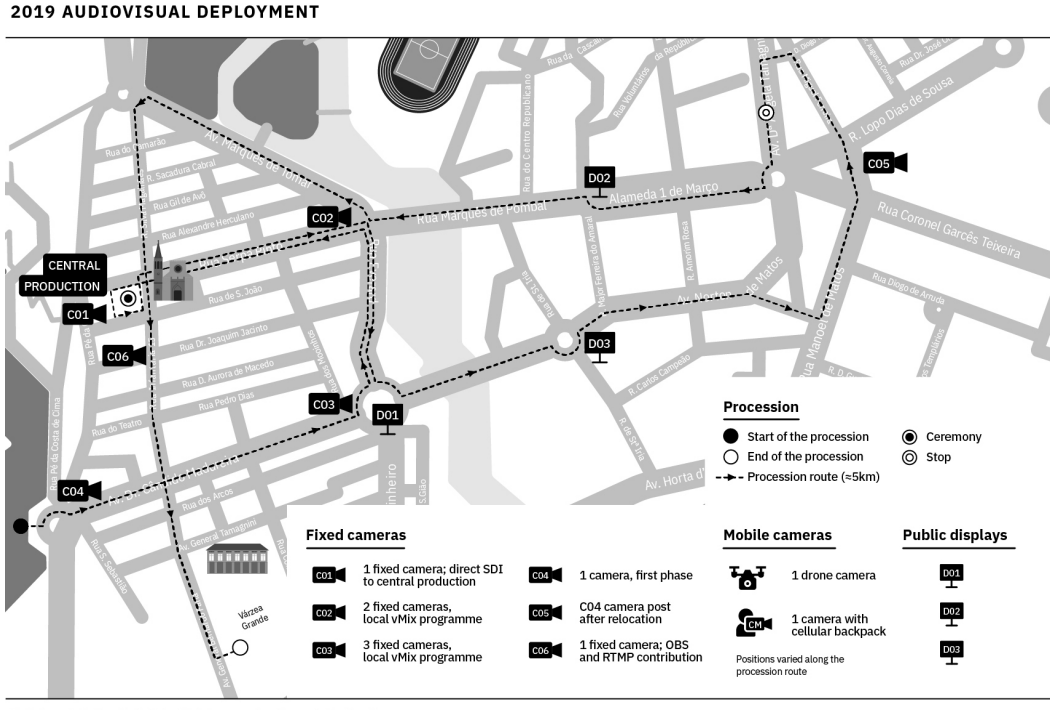
The Festa dos Tabuleiros is a major cultural and religious celebration held every four years in Tomar, Portugal. Its principal public moment is the Cortejo dos Tabuleiros, or Grande Cortejo, in which hundreds of decorated ceremonial structures known locally as *tabuleiros* are carried through the city (Municipality of Tomar, n.d.; RTP/Lusa, 2019). Its scale, duration and symbolic importance make audiovisual coverage both a complex production operation and a form of cultural mediation.

In 2019, approximately 750 *tabuleiros* followed a route of about five kilometres (RTP/Lusa, 2019). No spectator could observe the whole procession from one position. Coverage therefore served distant viewers while helping people in Tomar understand what was happening elsewhere along the route.

Dedicated coverage can prioritise the Festa, widen access and preserve an audiovisual record without imitating a national television programme. Figure 1 illustrates the spatial challenge and Figure 2 illustrates the Grande Cortejo route.



» **Figure 1:** *Spatial extension, participant density and public occupation along the route of the Grande Cortejo of the Festa dos Tabuleiros in 2023. Photographs: Luis Ribeiro (www.luis-ribeiro.pt; Instagram: @lluisrribeiro.fotografia). Reproduced with permission.*



» **Figure 2:** *Spatial reconstruction of the 2019 audiovisual operation, showing the Grande Cortejo route, three public displays (D01–D03), fixed cameras (C01–C06), mobile cameras and central production. C04 and C05 identify the same camera post before and after relocation. Route and locations are schematic; not to scale.*

1.2. Audiovisual communication for cultural heritage and distribution

Communicating living heritage involves more than visibility. UNESCO encourages specialised audiovisual programmes that communicate intangible heritage to the communities concerned rather than present it only as entertainment (UNESCO, 2024). Dedicated coverage should therefore keep the Festa, its people and cultural meaning at the centre.

Audiovisual heritage research connects production, documentation, dissemination and long-term access (Dimoulas et al., 2014; Rossi, 2024), while social-media research relates cultural content to audience understanding (Zhang & Xu, 2024). Institutional coordination, metadata, legal conditions and usable access remain essential (Hauttekeete et al., 2011; Ongena, Huizer & Van de Wijngaert, 2012).

It is also useful to distinguish how the signal travels. In professional terminology, contribution carries audiovisual material to a production centre for further processing, whereas distribution carries a finished programme to viewers (ITU-T, 2022).

This difference is central to the model proposed here. The clean feed is a contribution source from which authorised organisations can build their own programmes; it is not intended as a public stream. The public screens are a separate distribution service because people view them without sound, in shared outdoor spaces and under conditions that require a purpose-built visual output.

1.3. Platform dependence and situated visual communication

Online platforms simplify distribution while shifting control over infrastructure, governance, data and visibility (Nieborg, Duffy & Poell, 2020; Siciliano, 2022; Idiz & Poell, 2025). The 2019 case demonstrates a narrower operational dependence: one public YouTube session served both as audience entry point and source for unattended displays. When it ended, viewers needed a new URL and the display computers could not be redirected because no operators were present; unrelated platform content was later found on the screens. YouTube remains a practical outlet for a final online programme, but it should not carry the dedicated public-screen service. The proposed model separates the two distribution paths.

Table 1

Focused mapping of research strands relevant to the proposed communication model

Reference	Main research object	Technology and operations	Communication and audience	Limitation relative to this study
Calverley (2018)	Time-compensated remote production over IP	Primary	Not central	Does not address cultural-event communication or distinct public outputs.
Kawamoto et al. (2021)	Network configuration and delay in remote professional production	Primary	Not central	Evaluates production performance rather than audience access or editorial control.
Oh, Kim & Lee (2024)	Cloud-based live-media production platform	Primary	Limited	Demonstrates a production platform without an event-centred communication model.
Dimoulas et al. (2014)	Production, archiving and cross-media publication for folkloric heritage	Secondary	Primary	Connects media production and heritage but not live multi-output public-screen delivery.
Zhang & Xu (2024)	Cultural-heritage communication through social media	Not central	Primary	Addresses online meaning and audience understanding rather than live production architecture.
Nieborg, Duffy & Poell (2020)	Platforms and cultural production	Secondary	Primary	Explains platform dependence without specifying an event-distribution workflow.
Ducros et al. (2024)	Event-centric public displays	Secondary	Primary	Addresses situated displays without integrating a live contribution and programme ecosystem.

Note: The authors coded each source from its stated aims, abstract and reported contribution. 'Primary' identifies a principal object of the source; 'Secondary' indicates substantive but non-primary treatment; 'Limited' indicates brief or partial treatment; and 'Not central' means that the dimension falls outside the source's main analytical focus.

Large outdoor LED screens are situated media, not domestic television receivers. Public-space broadcasting links media, place and collective viewing (McQuire, 2010); event-centred displays connect content, event, interaction and display (Ducros et al., 2024); and experiential graphic design integrates information, spatial context and user experience (Petković, Pasanec Preprotić & Kozjan Cindrić, 2025). Display blindness makes immediate relevance essential (Müller et al., 2009). Pixel pitch affects minimum viewing distance (Motlagh & Hashemi, 2010), while standard metrology addresses luminance, uniformity, viewing angle and ambient contrast (ICDM, 2025). These findings support a dedicated silent output designed for rapid comprehension under actual viewing conditions.

2. Research Gap, Aim and Research Question

Relevant research is divided among remote production, cultural media, and platform or public-display studies (Dimoulas et al., 2014; Calverley, 2018; Nieborg, Duffy & Poell, 2020; Kawamoto et al., 2021; Oh, Kim & Lee, 2024; Zhang & Xu, 2024; Ducros et al., 2024). Table 1 maps seven representative works purposively selected from the broader review. It clarifies the intersection addressed here but does not claim systematic coverage. The gap lies at their intersection: none of the mapped sources derives from a documented large cultural procession a model combining a common contribution signal, independent public programmes and a dedicated silent screen service.

We ask: how can the lessons from the 2019 audiovisual operation inform a 2027 model that widens access to the Festa dos Tabuleiros and improves viewing online and on public screens? The objective is to translate documented gaps into collaborative production and distinct public outputs. A parallel engineering study evaluates acquisition, transport and continuity; this paper defines the communication model and functional requirements without prescribing final protocols.

3. Methodology

We use an exploratory qualitative single-case study (Yin, 2018) to examine the 2019 audiovisual operation and develop requirements for a future communication model. The case is treated as a bounded production and distribution system involving image capture, signal transport, online publication, partner-channel use and public-screen display.

3.1. Retrospective case reconstruction

The 2019 project addressed an immediate need and was not a controlled experiment: no comparison, audience survey or indicators were defined in advance. The retrospective reconstruction supports future requirements but cannot establish audience causality or superiority over another model.

The first author helped design and operate the system, providing first-hand knowledge but creating retrospective-bias risk.

Table 2
Evidence categories and limits used in the retrospective case reconstruction

Evidence	Use in this paper	Limit
Contemporaneous project and master's research records	Architecture, operational context and original requirements	Internal documentation is not publicly accessible and lacks several measurements required for retrospective analysis
Unpublished internal technical report Solução de Transmissão da Festa dos Tabuleiros 2019 [Festa dos Tabuleiros 2019 Transmission Solution], prepared from project components subsequently presented in the Multimedia Authoring curricular unit at the School of Technology of Abrantes (ESTA), Polytechnic Institute of Tomar (July 2019)	Contemporary description of workflow and operational incidents	Not publicly available and not a formal system log
Broadcast recordings and control-room time-lapse	Visual sequence, outputs and observable disruption	Do not establish root cause
YouTube pages and analytics exports	Cumulative reach and concurrent-viewer patterns	Incomplete across all channels
Participant account	Intent, decisions, timing and recovery actions	Retrospective and potentially affected by recall

Recollections were checked, where possible, against archived streams, analytics, the July 2019 student report and retained technical material. Uncorroborated claims remain identified as recollections or interpretations.

3.2. Evidence and claim classification

Table 2 distinguishes documented evidence, participant knowledge and future proposals. Claims are classified as verified, observed, inferred or proposed according to their evidential support.

3.3. Analytical procedure

The reconstruction described the 2019 workflow, identified incidents and communication gaps, examined audience exports from both YouTube channels, and translated the findings into 2027 requirements.

Each documented limitation was linked to a communication consequence and future requirement. The result is a prospective framework, not a validated model; metrics and success criteria must be defined before deployment.

The public-screen component is conceptual. It was co-developed from the case and relevant design research, with the communication-design coauthor shaping its information structure and graphic logic. Design review and field testing must assess hierarchy, typography, contrast, timing, cross-screen consistency and outdoor legibility.

The unit of analysis is the complete communication service: acquisition, production, platform session, audience entry point, partner reuse and public screens. Production, session, audience-access and public-presentation continuity are analysed separately because signal recovery does not necessarily restore the viewer service.

4. Results and Discussion

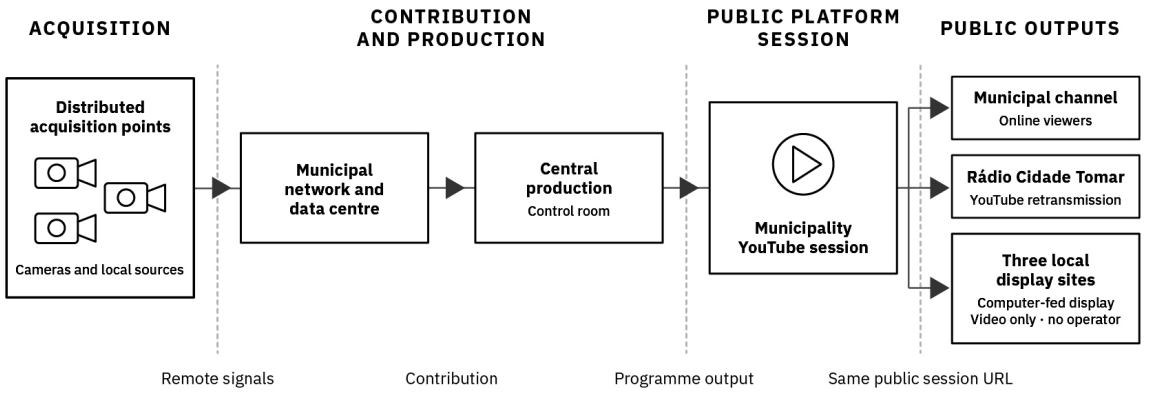
The 2019 operation demonstrates the feasibility of an academic–municipal distributed production using shared equipment and a largely pro bono team. Without a predefined benchmark, its quality and reach cannot be compared with another model.

It also exposed weaknesses in platform dependence, session continuity, screen control and advance communication that shaped the 2027 requirements.

4.1. The 2019 implementation

The project began with a limited aim: carrying live video to public screens placed around the city. About one month before the event, the plan expanded to include complete live coverage of the procession, a new municipal YouTube presence and access to the programme signal for local media. Rádio Cidade de Tomar used that signal. It was also offered to Rádio Hertz, although the records available for this study do not confirm that Rádio Hertz retransmitted it.

There was no dedicated production budget. Institutional partners supplied equipment and infrastructure, while lecturers and students contributed pro bono. The extracurricular team involved Informatics and Multimedia Technologies and TV Direction and Production students from the School of Technology of Abrantes (ESTA), and Multimedia Design and Graphic Arts Technologies students from the School of Technology of Tomar (ESTT), both then part of the Polytechnic Institute of Tomar. These constraints shaped pragmatic decisions; low cost is not the main contribution. Because the procession crossed much of the city, the programme used a distributed multicamera workflow.



» **Figure 3:** *Functional architecture of the 2019 operation, connecting distributed acquisition points, the municipal network and data centre, central production, the Municipality YouTube session, the municipal channel, the Rádio Cidade de Tomar retransmission and the three unattended local display sites.*

Figure 3 summarises its acquisition points, municipal network and data centre, central production, Municipality YouTube session, municipal channel, Rádio Cidade de Tomar retransmission and three display sites. Equipment specifications are outside this paper's scope.

4.2. Distribution and available audience evidence

Table 3 reports YouTube exports to 7 September 2026 for two municipal sessions and two corresponding Rádio Cidade de Tomar retransmissions. Views combine live and later access, are not unique spectators and may overlap across sessions or channels.

On the event date, replacement-session views were 14.7% of the first municipal session and 15.0% of the first Rádio Cidade session. The similar pattern across independent outlets is not a causal estimate of loss: the interruption occurred late, after the main ceremonial moments, leaving less programme and potentially less interest.

The recordings continued circulating after 2019. Listed foreign-country views were at least 605 across twelve countries for the first municipal session, 60 across three for its replacement, 816 across ten for the first Rádio Cidade session and 45 across two for its replacement. These are lower bounds, and country of access does not establish nationality, residence or diaspora membership.

Table 4 and Figure 4 show partial audience rebuilding on Rádio Cidade de Tomar: the replacement began with 17 concurrent viewers (8.3% of the previous session's final 206), reached 52 after five minutes and peaked at 81. These are not individual-retention data, and the late timing prevents attribution solely to the new link.

Table 3

YouTube audience indicators for the four public sessions (publication to 7 September 2026)

Channel and session	Views	Watch time	Average view duration	Views on event date
Municipality – first	9,020	2,203.76 h	14 min 39 s	7,331
Municipality – replacement	1,964	169.03 h	5 min 09 s	1,074
Rádio Cidade – first	10,837	1,573.36 h	8 min 42 s	4,373
Rádio Cidade – replacement	1,709	91.81 h	3 min 13 s	657

Note: Views combine live and on-demand consumption and are not unique-viewer counts. One person may have accessed more than one session or channel. Source: YouTube Analytics exports supplied by the respective channel owners

Table 4

Rádio Cidade de Tomar concurrent-audience indicators from minute-sampled YouTube Analytics exports

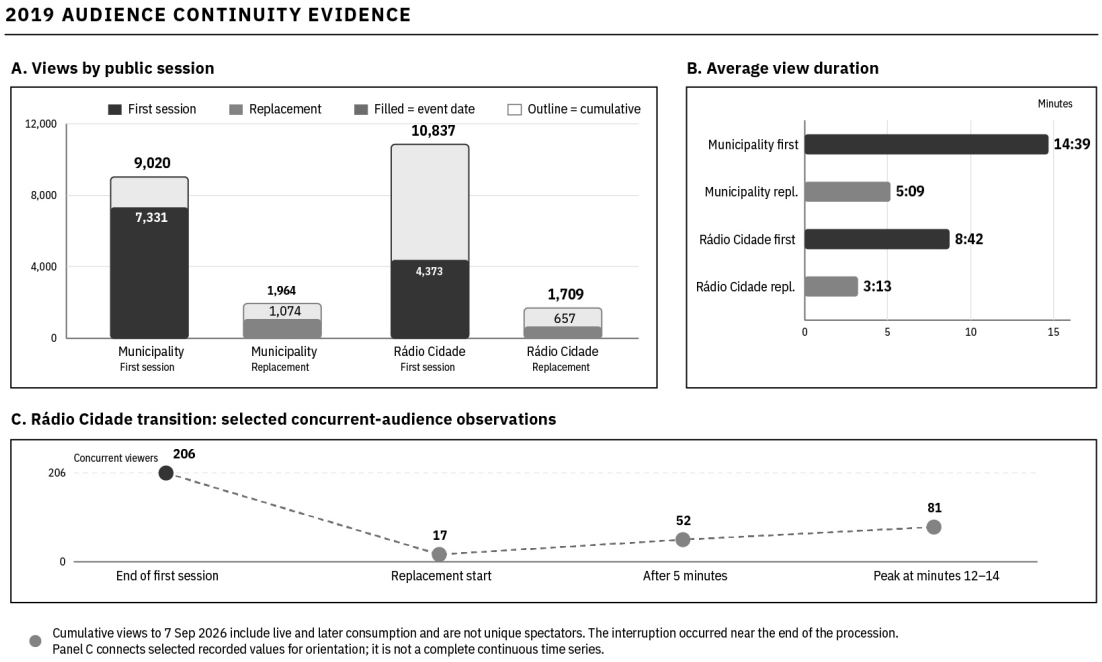
Rádio Cidade de Tomar indicator	First session	Replacement session
Recorded duration	3 h 16 min	27 min
Peak concurrent viewers	387	81
Final recorded audience	206	60
Initial recorded audience	0 before activity	17
Simple mean of minute samples	239.2	62.1
Chat messages	47	1

Note: The simple mean describes the available minute samples and is not a time-weighted audience estimate. Concurrent-viewer data were available only for the Rádio Cidade de Tomar sessions. Source: YouTube Analytics exports supplied by Rádio Cidade de Tomar.

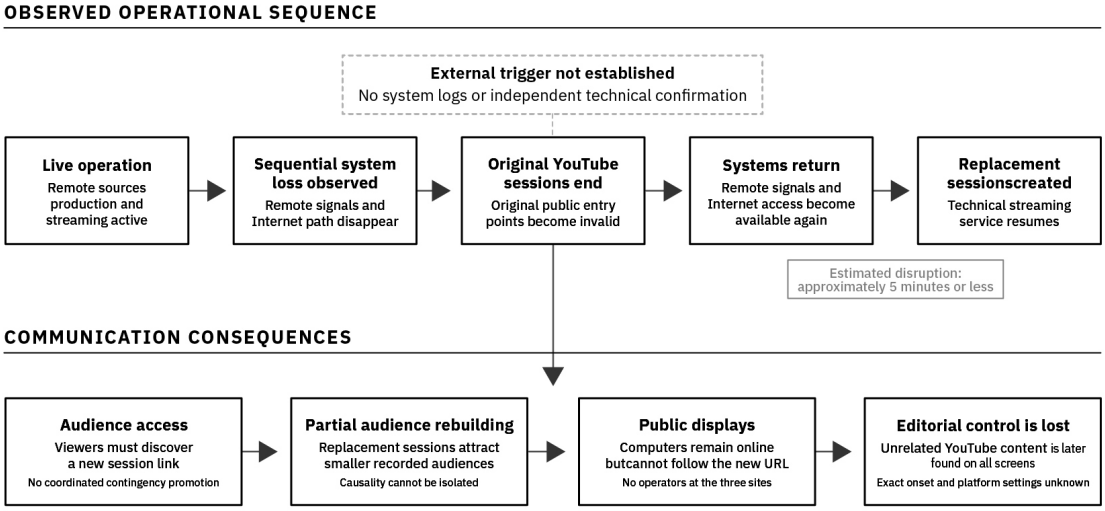
4.3. Interruption and recovery

The team observed municipal data-centre systems become unavailable in sequence, followed by the contribution signals and Internet path; these later returned. Without logs or independent confirmation, the external trigger is unknown. The established production failure was the absence of redundant contribution and distribution paths, for which the production team accepts responsibility. The team created a replacement YouTube session.

The operator estimated recovery in five minutes or less; the control-room time-lapse indicates about four minutes and forty seconds if the remembered 15-second capture interval is correct. This supports an approximate, not certified, five-minute disruption. Production resumed through a new, unannounced public link near the end of the procession. Production, session and audience recovery therefore differed; audience recovery also depended on the limited event time and editorial value remaining. Figure 5 separates the unknown trigger from the observed consequences and the missing redundancy.



» **Figure 4:** *Audience evidence associated with the 2019 session interruption. Views and average view duration cover the four public sessions; concurrent-audience observations are available only for the Rádio Cidade de Tomar transition.*



» **Figure 5:** *Observed interruption and communication consequences in 2019. The external trigger is unknown; missing redundancy is identified as a production-design failure.*

4.4. Consequences for the public screens

The public displays were installed at three locations selected because they were expected to concentrate large numbers of spectators: Rotunda Grande, opposite Casa dos Cubos; the end of Alameda 1 de Março, opposite the Parish Council of Santa Maria dos Olivais; and the existing public screen near the Tomar fire station, as shown in Figure 2. Each location used an independent computer with wired Internet access provided locally by Casa dos Cubos, the Parish Council or the fire station. The computer reproduced the YouTube session and delivered video to the processor of the corresponding display. The displays received no audio. The screens arrived two days before the procession, within a one-month preparation period and without budget or local operators. Relaying YouTube was then workable, but every screen depended on one public URL and manual redirection.

The display computers remained online but did not follow the replacement session; changing the URL required an unavailable local operator. All three screens later showed unrelated YouTube material. Recommendation or autoplay is plausible, but the settings and onset cannot be verified.

The incident demonstrates operational platform dependence: connectivity remained, but editorial control and service continuity did not.

YouTube can distribute the online programme, but should not be the control path for unattended displays.

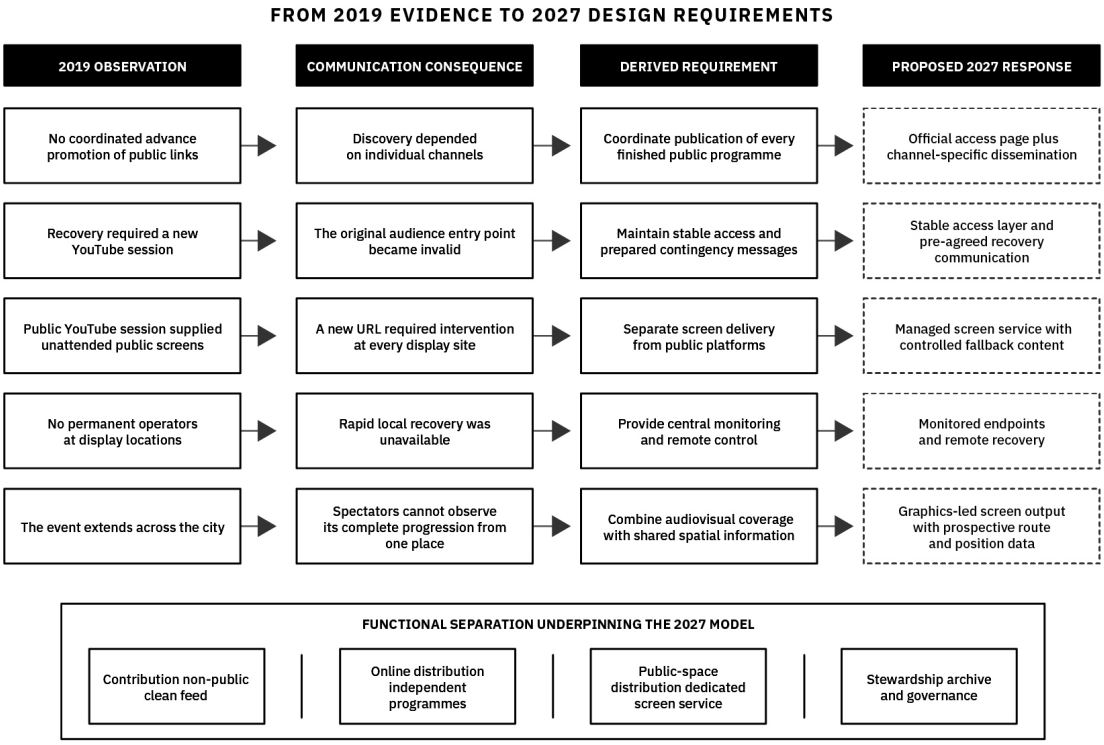
4.5. Communication lessons from the case

Table 5 translates the documented limitations into communication consequences, future requirements and indicators. Figure 6 connects the evidence-based observations and consequences to prospective, unvalidated 2027 responses.

Table 5

Communication requirements derived from documented observations of the 2019 operation

2019 observation	Communication consequence	2027 requirement	Prospective indicator
The public link was not promoted through a coordinated advance strategy	Audience discovery depended on individual channels	Plan and coordinate publication of every final programme link	Reach by channel and access source
Recovery required a new YouTube session	The original audience entry point became invalid	Use a stable public access layer and pre-agreed recovery communication	Time to restore a valid public entry point
Screens reproduced the public YouTube session	A new URL required intervention at every site	Use a managed public-screen service independent of public-platform URLs, with controlled fallback content	Screen-service availability
No permanent screen operators were available	Local recovery could not be performed rapidly	Provide monitored endpoints, central supervision and remote recovery	Detection and remote-recovery time
The event extends across the city	Audiences cannot observe its complete progression from one place	Combine audiovisual coverage with shared spatial information	Location-data latency and accuracy



» **Figure 6:** *Evidence-to-design synthesis linking documented 2019 limitations and communication consequences to derived requirements and proposed components of the 2027 model. Dashed boxes represent prospective responses, not validated outcomes.*

4.6. Proposed communication model for 2027

Figure 7 separates a continuous clean feed, partner and optional official programmes, dedicated screen production, public channels and a shared display service. This paper defines their communication functions rather than selecting cameras, codecs or transport protocols. A parallel engineering study will compare links by latency, resilience, bandwidth, monitoring, interoperability and recovery; remote-production research supports system-level evaluation rather than inference from protocol labels (Kawamoto et al., 2021).

4.6.1. The clean feed as a professional contribution signal

A central team would produce a continuous clean feed of the full procession, combining selected images with ambient sound as a professional contribution source, not a public stream.

The feed still requires editorial choices that preserve spatial continuity and principal moments, but excludes channel-specific commentary, branding, advertising and studio material, which recipients may add independently.

4.6.2. Independent programmes and editorial responsibility

Authorised media organisations could combine the feed with presenters, interviews, reports or commentary while retaining responsibility for their editorial decisions and public links.

The Municipality or Festa Commission could similarly produce an official programme centred on the Festa and Tomar. YouTube is the most feasible current outlet; cable distribution would require a partnership.

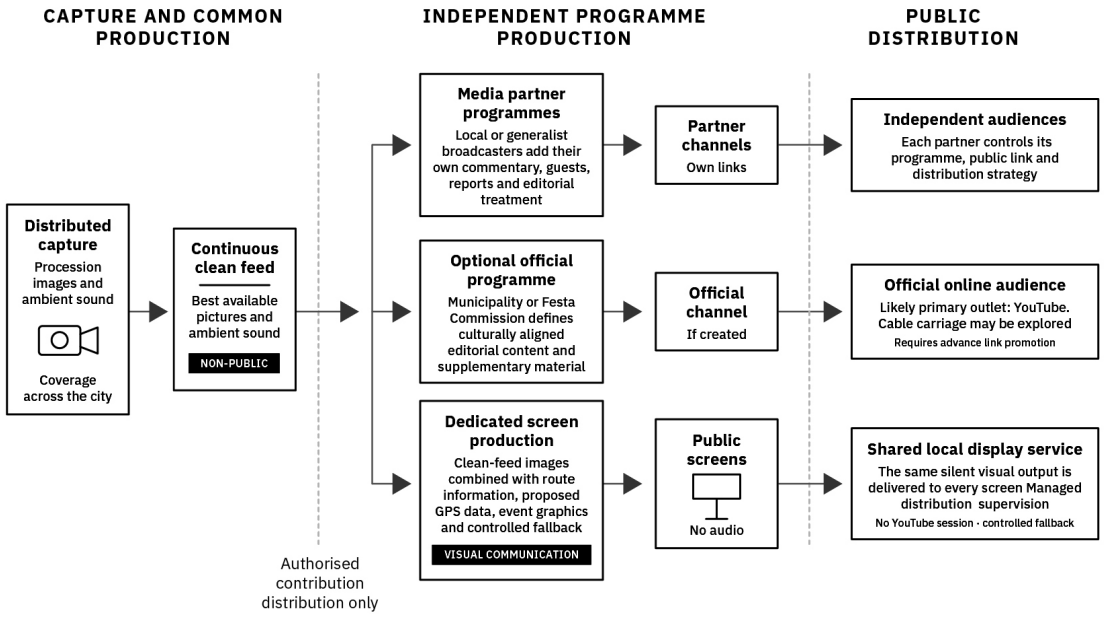
4.6.3. A dedicated visual programme for public screens

Outdoor LED screens require dedicated production, not simple reproduction of the clean feed. Because they have no sound, essential information must work visually at the installed size, distance and conditions.

Figure 8 organises the screen model into information inputs, editorial control, graphic composition, managed delivery and public screens, consistent with event-centred display research (Ducros et al., 2024).

Inputs include the clean feed, route, messages and prospective GPS procession-position data. Editorial control prioritises immediate utility; composition combines live video, identity, orientation and operational information. Brief attention and display blindness require few competing elements (Müller et al., 2009; Ducros et al., 2024). Managed delivery supplies one monitored output and fallback state. This unvalidated design must be tested at the intended sites.

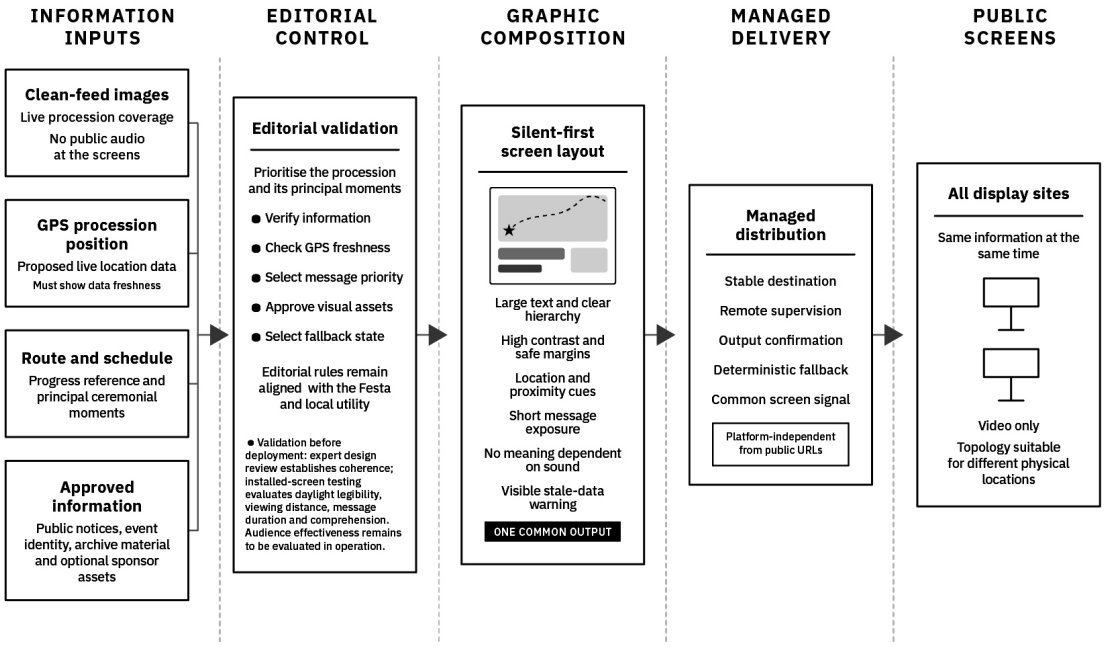
The shared display service would provide consistent content while allowing scheduling within a common information structure (Taniguchi, 2018). Live images remain dominant; persistent elements are limited to event identity, transmission status and procession progress, with safety messages taking priority.



» **Figure 7:** *Proposed 2027 multi-output communication model. A non-public continuous clean feed supports media-partner programmes, an optional official programme and dedicated screen production delivered through a shared local display service.*

Separating screen delivery from YouTube restores control over a silent, glanceable service. Sunlight and reflections reduce contrast, while luminance and tone mapping can improve readability (Qian et al., 2024); procurement must therefore consider measured ambient-light performance, not only resolution or dark-room contrast (ICDM, 2025). Table 6 proposes preliminary requirements. Its 5,000 cd/m² daytime value is an author-defined starting specification, not a universal or validated threshold.

Supplier documentation, site survey and acceptance tests must confirm these prospective requirements using the final graphics and recorded viewing conditions. A proposed GPS marker would indicate a predefined reference element within the procession, not the camera or subject currently shown. Coordinates would be matched to the route, with no assumed correspondence to the selected shot. This unimplemented capability requires tests of reference choice, update interval, latency, accuracy, stale-data indication and fallback.



» **Figure 8:** *Conceptual information and graphics model for public screens, separating information inputs, editorial validation, silent-first graphic composition, managed delivery and common display output*

Table 6

Preliminary minimum procurement or rental requirements for the 2027 public LED screens

Characteristic	Preliminary minimum requirement	Status or verification
Display and deployment	Direct-view LED equipment specified and certified for temporary outdoor use.	Confirms suitability for public-space operation.
Daytime luminance	At least 5,000 cd/m² sustained nominal luminance for screens exposed to direct daylight.	Provisional author specification; verify after installation.
Brightness control	Manual adjustment and preferably automatic control using ambient-light sensing.	Maintains visibility without unnecessary brightness in shade or lower light.
Ambient-light performance	Measure luminance, uniformity, surface reflection and ambient contrast under representative sun and shade.	Use established display-metrology procedures (ICDM, 2025).
Pixel pitch	Select from the minimum and maximum intended viewing distances at each site.	No single pitch is prescribed before the site survey (Motlagh & Hashemi, 2010).
Viewing validation	Test the final graphics at the intended distances and horizontal and vertical viewing angles.	Confirms that essential information remains legible in its actual context.
Continuity and control	Remote status monitoring, controlled fallback content and delivery independent of a public platform URL.	Prevents uncontrolled content and supports recovery without a permanent local operator.
Environmental protection	Supplier-certified protection appropriate to rain, dust, wind and the expected temperature range.	Final ratings depend on the installation and local risk assessment.

4.6.4. Link dissemination and contingency communication

Promotion should concern finished public programmes, not the clean feed. Each channel maintains its link and strategy, while the Municipality or Festa Commission provides a coordinated page of authorised outputs.

Audiences include distant viewers, residents monitoring progress before approaching the route, and spectators seeking events elsewhere in the city. Online and screen programmes may share data and assets, but serve different viewing situations and audio conditions.

4.6.5. Governance, partnerships and archive

The organising bodies would decide clean-feed access case by case through funding, sponsorship or agreed promotion. Ownership and archival rights remain with the Festa Commission or Municipality, as agreed between them.

Before procurement, the Festa Commission and Municipality should assign ownership, finance, operation, partner access, publication, monitoring, recovery and archival delivery. The provider should retain no exploitation rights, while each receiving channel remains editorially responsible. These are prospective governance requirements; the case supports neither a cost estimate nor contractual wording.

After testing, the infrastructure could cover the shorter *Cortejo dos Rapazes and Cortejo do Bodo*, supporting operational validation and the archive. Children's events require all applicable legal, consent and safeguarding measures.

4.6.6. Prospective evaluation framework

Evaluation must cover the complete service: technical continuity, discoverability, comprehension and the ability to follow the procession across outputs.

This end-to-end approach follows ITU-T guidance on user-centred quality and multi-point service monitoring (ITU-T, 2008a; ITU-T, 2008b), without importing managed-IPTV numerical targets.

Post-event content analysis should verify coverage of principal moments, procession prominence and the relevance of supplementary segments. Before deployment, documented design review should assess hierarchy, legibility, consistency, accessibility, contextual relevance, separation of advertising and performance under representative outdoor conditions.

Audience effectiveness requires representative-user tests across distances, angles and light levels. Measures should include task completion, comprehension, reading time, perceived clarity and essential-information visibility, alongside luminance, ambient illuminance and viewing position.

These prospective indicators are not 2019 results. Defining them before implementation creates a baseline for later assessment and publication.

4.7. Communication methodology and engineering relevance

The engineering relevance lies in separating contribution, editorial production, public distribution, screen delivery and archiving, which were coupled in 2019. Cloud architectures can centralize monitoring and switching (Oh, Kim & Lee, 2024), but cloud deployment remains a possible direction rather than a selection made here.

Communication remains central: the service must preserve culturally attentive coverage, practical information, discoverability, independent programmes and the institutional archive.

The parallel engineering study will test how these requirements can be delivered under event conditions; communication defines the required capabilities, and engineering validates their implementation.

5. Conclusions

The case demonstrates that a local cultural organisation and academic partner could produce and share distributed live coverage without a conventional outside-broadcast production.

It establishes feasibility in this context, not technical superiority, equivalent quality or comparative cost. As an exploratory single case involving the first author, it supports analytical rather than statistical generalisation.

The interruption showed that signal recovery alone does not restore audience access or screen control. Replacement sessions attracted smaller audiences, but the late timing prevents causal attribution solely to link discovery. Production, session, audience and public-presentation continuity must therefore be planned as connected but distinct problems.

For 2027, the proposed clean feed, independent programmes, silent screen service, coordinated links and institutional archive remain unvalidated. The model converts the 2019 lessons into a transferable pre-implementation process and baseline against which a later technical system and its communication outcomes can be evaluated.

6. Data availability

The four public recordings were available on the Municipality of Tomar and Rádio Cidade de Tomar YouTube channels at analysis: municipal first (https://www.youtube.com/watch?v=mFyE7eld2M4) and replacement (https://www.youtube.com/watch?v=b448RhMkgjg), and Rádio Cidade first (https://www.youtube.com/watch?v=ckPtf8nRQ68) and replacement (https://www.youtube.com/watch?v=dEwHIKzB5lw). Channel owners supplied aggregated analytics reproduced in Tables 3 and 4. Project records and the internal technical report are not public and are not the sole support for audience results or the interruption sequence.

7. References

Briggs, A., Burke, P. and Ytreberg, E. (2020) *A social history of the media: From Gutenberg to Facebook*. 4th edition. Cambridge: Polity Press.

Calverley, E. (2018) 'Time-compensated remote production over IP', *SMPTE Motion Imaging Journal*, 127(5), pp. 51–57. DOI: 10.5594/JMI.2018.2813199

Castells, M. (2010) *The rise of the network society*. 2nd edition. Chichester: Wiley-Blackwell.

Couldry, N. and Hepp, A. (2017) *The mediated construction of reality*. Cambridge: Polity Press.

Dimoulas, C.A., Kalliris, G.M., Chatzara, E.G., Tsipas, N.K. and Papanikolaou, G.V. (2014) 'Audiovisual production, restoration-archiving and content management methods to preserve local tradition and folkloric heritage', *Journal of Cultural Heritage*, 15(3), pp. 234–241. DOI: 10.1016/j.culher.2013.05.003

Ducros, A., Tabard, A., Dalsgaard, P., Bats, R. and Eriksson, E. (2024) 'A design space for event-centric displays in public libraries', *Frontiers in Computer Science*, 6, 1250861. DOI: 10.3389/fcomp.2024.1250861

Hauttekeete, L., Evens, T., De Moor, K., Schuurman, D., Mannens, E. and Van de Walle, R. (2011) 'Archives in motion: Concrete steps towards the digital disclosure of audiovisual content', *Journal of Cultural Heritage*, 12(4), pp. 459–465. DOI: 10.1016/j.culher.2011.04.004

ICDM. (2025) Information Display Measurements Standard, version 1.3. International Committee for Display Metrology, Society for Information Display. DOI: 10.55410/HHXO3592

Idiz, D.R. and Poell, T. (2025) 'Dependence in the online screen industry', *Media, Culture & Society*, 47(2), pp. 375–393. DOI: 10.1177/01634437241286725

ITU-T. (2008a) ITU-T G.1080. Quality of experience requirements for IPTV services. Geneva: International Telecommunication Union.

ITU-T. (2008b) ITU-T G.1081. Performance monitoring points for IPTV. Geneva: International Telecommunication Union.

ITU-T. (2022) *Question 1/9: Transmission and delivery control of television and sound programme signal for contribution, primary distribution and secondary distribution*. Available from: https://www.itu.int/en/ITU-T/studygroups/2022-2024/09/Documents/qtext/q1_9-en.pdf [Accessed 11 September 2026].

Jenkins, H. (2006) *Convergence culture: Where old and new media collide*. New York: New York University Press.

Kawamoto, J., Shirato, R., Nakatogawa, T. and Kurakake, T. (2021) 'Remote professional media production: Evaluation of network configuration that satisfies delay requirements', *IEEE Access*, 9, pp. 100339–100351. DOI: 10.1109/ACCESS.2021.3096649

McQuire, S. (2010) 'Rethinking media events: Large screens, public space broadcasting and beyond', *New Media & Society*, 12(4), pp. 567–582. DOI: 10.1177/1461444809342764

Motlagh, A.A.N. and Hashemi, B.M.R. (2010) 'Minimal viewing distance calculation in LED display panels', *Journal of Display Technology*, 6(12), pp. 620–624. DOI: 10.1109/JDT.2010.2072982

Müller, J., Wilmsmann, D., Exeler, J., Buzeck, M., Schmidt, A., Jay, T. and Krüger, A. (2009) 'Display blindness: The effect of expectations on attention towards digital signage'. In: Tokuda, H., Beigl, M., Friday, A., Brush, A.J.B. and Tobe, Y. (eds.) *Pervasive Computing*, 11–14 May 2009, Nara, Japan. Berlin: Springer, pp. 1–8. DOI: 10.1007/978-3-642-01516-8_1

Municipality of Tomar. (n.d.) *Festa dos Tabuleiros*. Available from: https://www.cm-tomar.pt/index.php/visitar/festas-e-romarias/festa-dos-tabuleiros [Accessed 23 September 2026].

Nieborg, D.B., Duffy, B.E. and Poell, T. (2020) 'Studying platforms and cultural production: Methods, institutions, and practices', *Social Media + Society*, 6(3), pp. 1–7. DOI: 10.1177/2056305120943273

Oh, H., Kim, S. and Lee, J.-Y. (2024) Implementation of a live media production platform for cloud-based broadcast workflows. *Proceedings of the International Conference on Information and Communication Technology Convergence,* ICTC 2024, 16–18 October 2024, Jeju Island, Republic of Korea. IEEE, pp. 1727–1729. DOI: 10.1109/ICTC62082.2024.10827686

Ongena, G., Huizer, E. and Van de Wijngaert, L. (2012) 'Threats and opportunities for new audiovisual cultural heritage archive services: The Dutch case', *Telematics and Informatics*, 29(2), pp. 156–165. DOI: 10.1016/j.tele.2011.05.005

Petković, G., Pasanec Preprotić, S. and Kozjan Cindrić, A. (2025) 'Experiential graphic design: Informing, inspiring, and integrating people in physical spaces—A review', *Buildings*, 15(11), 1862. DOI: 10.3390/buildings15111862

Qian, Y., Chen, S.-C., Hsiang, E.-L., Akimoto, H., Lin, C.-L. and Wu, S.-T. (2024) 'Enhancing a display's sunlight readability with tone mapping', *Photonics*, 11(6), 578. DOI: 10.3390/photonics11060578

Rossi, E. (2024) 'Beyond the flow, from tape to digital: Insights from Mediaset's archives', *VIEW Journal of European Television History and Culture*, 13(26), pp. 77–86. DOI: 10.18146/view.354

RTP/Lusa. (2019) *Marcelo elogia tradição e juventude da Festa dos Tabuleiros, em Tomar*. Available from: https://www.rtp.pt/noticias/cultura/marcelo-elogia-tradicao-e-juventude-da-festa-dos-tabuleiros-em-tomar_n1158927 [Accessed 12 September 2026].

Siciliano, M.L. (2022) 'How gatekeeping became digital: Infrastructural barriers to participation in conventional and platformized cultural production', *International Journal of Cultural Policy*, 28(7), pp. 888–904. DOI: 10.1080/10286632.2022.2137154

Taniguchi, Y. (2018) 'Content scheduling and adaptation for networked and context-aware digital signage: A literature survey', *ITE Transactions on Media Technology and Applications*, 6(1), pp. 18–29. DOI: 10.3169/mta.6.18

UNESCO. (2024) *Operational directives for the implementation of the Convention for the Safeguarding of the Intangible Cultural Heritage*. Available from: https://ich.unesco.org/en/directives [Accessed 10 September 2026].

Yin, R.K. (2018) *Case study research and applications: Design and methods*. 6th edition. Los Angeles: Sage Publications.

Zhang, J. and Xu, C. (2024) 'A grounded theory-based model of information communication in cultural heritage digital reading on the social media from the perspective of the embodied theory', *Heritage Science*, 12, 208. DOI: 10.1186/s40494-024-01313-2



© 2026 Authors. Published by the University of Novi Sad, Faculty of Technical Sciences, Department of Graphic Engineering and Design. This article is an open access article distributed under the terms and conditions of the Creative Commons Attribution license 4.0 Serbia (http://creativecommons.org/licenses/by/4.0/rs/).

Original Scientific Paper https://doi.org/10.24867/GRID-2026-54

Evaluating the Impact of Generative Artificial Intelligence on Photographic Workflow

ABSTRACT

Recent advances in generative artificial intelligence (GenAI) have significantly transformed photographic post-production by introducing intelligent editing, retouching and image synthesis tools. Although these technologies substantially improve productivity, their influence on image quality, workflow efficiency and user perception remains insufficiently investigated. This study presents an experimental comparison between conventional manual post-production and AI-assisted workflows using Adobe Firefly, ChatGPT and Gemini. Multiple photographic motifs representing different shooting conditions were processed using both conventional and AI-assisted approaches. Workflow efficiency was evaluated through processing time and editing complexity, while image quality was assessed through a user perception study. Additionally, semi-structured interviews with professional photographers were conducted to compare expert opinions with user preferences. The results demonstrate that AI-assisted workflows considerably reduce editing time and simplify several stages of photographic post-production. However, manual editing remains advantageous when precise local adjustments and complete creative control are required. User perception indicates a consistent preference for manually edited photographs, particularly among professional photographers. The findings contribute to a better understanding of the current capabilities and limitations of generative AI within professional photographic production and support informed integration of AI technologies into contemporary photographic practice.

Klara Manca Čanžek
Jure Ahtik

University of Ljubljana, Faculty of Natural Sciences and Engineering, Department of Textiles, Graphic Arts and Design, Ljubljana, Slovenia

KEY WORDS
Generative artificial intelligence, photography, image processing, post-production, visual perception

1. Introduction

Post-production is an important part of the photographic workflow because it combines technical correction with aesthetic interpretation (Davis, 2022; Williamson, 2024; Adobe, 2026a; Adobe, 2026b; Adobe, 2026c; Adobe, 2026d; Adobe, 2026e). Conventional workflows rely on the photographer's knowledge and manual control over exposure, white balance, colour, contrast, local adjustments, retouching, sharpening, cropping and export. This approach offers precise control but can be time-consuming, especially when images require detailed local corrections or skin retouching.

Generative artificial intelligence is changing this workflow by allowing image modifications to be initiated through natural-language instructions and automated image synthesis (Tang, 2023; Ryazadzhiyan, 2024; Arvaj, Šubic & Ahtik, 2025; Ekart & Ahtik, 2026). Contemporary systems can remove distracting objects, alter backgrounds, extend images, modify lighting and colour, retouch details, and generate new visual content. This shifts part of the photographer's work from direct manipulation of individual parameters towards describing, selecting and evaluating generated results.

The aim of this study was to evaluate how generative AI affects photographic post-production in terms of processing time, workflow complexity and perceived visual quality. Manual post-production was compared with AI-assisted editing in Adobe Firefly, ChatGPT and Gemini across several photographic motifs and shooting conditions. The study also examined whether visual preferences differ between general users and professional photographers.

The research addressed four propositions:

1. generative AI shortens post-production time compared with manual editing;
2. manually edited photographs may retain an advantage in perceived quality when precision and naturalness are important;
3. professional photographers may evaluate manual edits differently from non-professional viewers; and
4. AI can simplify individual post-production steps but does not replace the photographer as the source of creative and contextual decisions.

2. Methods

2.1. Photographic material and experimental design

The experiment used 16 source photographs covering four motif groups: portraits, group photographs, fashion/artistic figures and products. The material included photographs taken in studio and outdoor conditions so that the workflows could be tested under different lighting and scene characteristics (Figure 1). All reference photographs were saved in a raw file format.

Three approaches were later compared. In the first, the source photographs were edited manually using a conventional Adobe-based workflow.

In the second, the same photographs were edited with generative AI using Adobe Firefly (Image Model 5), ChatGPT (model GPT-5.4) and Gemini (model Gemini 3.1).

In the third, photographs were generated from detailed text descriptions (prompts) without providing the original image as a reference. This third condition was used to evaluate how closely text-to-image systems could reproduce the intended composition, lighting, colour palette, background and overall aesthetic characteristics of a reference photograph.

2.2. Manual post-production workflow

Manual editing was performed through a sequence of global and local corrections aligned with established digital post-production workflows (Davis, 2022; Alessi, 2025; Cambridge in Colour, 2026).

The workflow comprised opening the image in Adobe Camera Raw, correcting white balance and exposure, adjusting texture and skin, performing local retouching with healing and cloning tools, applying dodge and burn where required, carrying out colour correction in Adobe Lightroom, and exporting the final file. The exact number of operations depended on the motif and the condition of the image.

Portrait and group photographs generally required more detailed retouching, while product photographs more often required global corrections to brightness, contrast, and colour (Figure 2).



» **Figure 1:** *References photographs used in the experiment*



» **Figure 2:** *Photographs with manual postproduction*

2.3. AI-assisted post-production

For AI-assisted post-production, each of the 16 reference photographs was processed using Adobe Firefly (Image Model 5), ChatGPT (model GPT-5.4) and Gemini (model Gemini 3.1), resulting in a total of 48 AI-assisted edits (Figures 3–5).

Generative AI tools enable image content to be modified, removed or added while attempting to integrate the generated elements with the existing visual information (Adobe, 2026a; Adobe, 2026b; Adobe, 2026c; Adobe, 2026d; Adobe, 2026e).



» **Figure 3:** *Photographs with postproduction done using ChatGPT*



» **Figure 4:** *Photographs with postproduction done using Gemini*



» **Figure 5:** *Photographs with postproduction done using Firefly*

The editing process was guided by text prompts describing the intended post-production adjustments. These included exposure and white balance correction, colour adjustment, skin retouching, background clean-up, texture enhancement, sharpening, cropping and colour grading. As far as the individual interfaces and capabilities of the three systems allowed, equivalent instructions and editing objectives were used to ensure comparability between the resulting images.

Processing time was recorded for each tool and photograph. The measurement included preparing and entering the prompt, AI processing and generation of the edited result, and completing the image for export. This enabled the efficiency of the three AI-assisted workflows to be compared with conventional manual post-production.

2.4. AI-based image generation

A separate experiment was conducted to evaluate text-to-image generation. Unlike AI-assisted post-production, the original photographs were not provided to the AI systems as visual references. Instead, ChatGPT, Gemini and Adobe Firefly were instructed to generate new images solely from detailed textual descriptions of the original photographs (Figures 6–8). The prompts described the principal visual characteristics of each reference image, including the subject and composition, pose, facial expression, lighting conditions, colour palette, background and overall visual style. The objective was to determine how effectively each system could interpret a textual description and recreate the intended visual characteristics without direct access to the source photograph.



» **Figure 6:** *Images created using ChatGPT*



» **Figure 7:** *Images created using Gemini*



» **Figure 8:** *Images created using Firefly*

Generation time was measured from the preparation and submission of the prompt to the completion of the generated image.

The resulting images were then included in the user evaluation alongside the manually processed photographs, enabling comparison between conventional photographic post-production and fully AI-generated visual content.

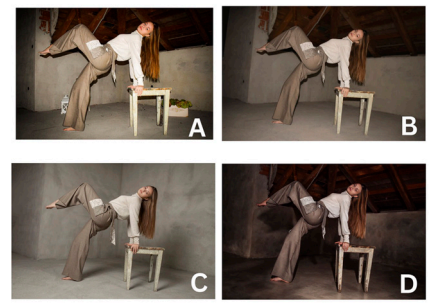
2.5. User survey and professional interviews

A visual preference survey was conducted using FreeOnlineSurveys, with a total of 150 respondents. The survey contained 32 four-image collages. In the first group (Figure 9a), option A was the manually edited reference, and options B, C and D were images generated by ChatGPT, Gemini and Adobe Firefly, respectively. In the second group (Figure 9b), option A again represented the manual edit, while B, C and D represented AI-assisted edits produced by the same three systems.

Participants were not informed which images were manual or AI-based and answered the same question for each collage: which image they preferred.



(a)



(b)

» **Figure 9:** *One example of survey collage: (a) manual postproduction compared to AI generated images, (b) manual postproduction compared to AI postproduction*

Respondents also reported their age, gender, photographic experience and previous use of AI for image creation or editing. The sample consisted of 71% women and 29% men; 58% were aged 18–25. Sixty-six percent did not practise photography, 32% identified as amateur photographers and 2% as professional photographers. Sixty-three percent had previously used AI for image creation or editing.

To complement the survey, semi-structured interviews were conducted with two professional photographers working in event, portrait and product photography. The interviews addressed image selection, post-production practices, time requirements, software use, AI-assisted functions and perceived limitations of AI in professional work.

3. Results

3.1. Processing time

Manual post-production required approximately 17 minutes per photograph on average, with substantial variation by motif. Group photographs were the most time-consuming, averaging about 22 minutes, followed by fashion and artistic figures (18 minutes), portraits (17 minutes) and products (13 minutes). The number of manual processing steps followed the same general pattern, ranging from an average of 9 steps for product photographs to 16 for group photographs (Table 1).

Table 1
Manual post-production time and average number of steps by photographic motif

Motif	Average time	Minimum	Maximum	Average steps
Portrait	17:00	12:41	23:23	11
Group photograph	22:00	20:25	23:54	16
Fashion/ artistic figure	18:00	10:08	22:52	10
Product	13:00	11:26	16:37	9

AI-assisted editing was markedly faster. Average processing times were 5:05 for ChatGPT, 5:12 for Gemini, and 5:03 for Adobe Firefly. ChatGPT showed the narrowest observed range (4:33–5:53), Gemini ranged from 4:22 to 6:30, while Adobe Firefly varied more substantially (1:55–7:39). The differences between tools were small in average terms, but the variability indicates that task complexity and prompt interpretation affected individual processing times (Table 2).

Table 2
Processing time for AI-assisted post-production

Tool	Minimum	Maximum	Average steps
ChatGPT	4:33	5:53	5:05
Gemini	4:22	6:30	5:12
Adobe Firefly	1:55	7:39	5:03

3.2. Visual characteristics of AI-assisted results

AI-assisted tools were effective for broad corrections and rapid stylistic changes, but their limitations became evident in tasks requiring precise local control. This balance between automation and creative control is also emphasised in discussions of contemporary photographic post-processing (Ryazadzhiyan, 2024; Williamson, 2024).

Portrait retouching was particularly sensitive: the systems sometimes altered skin texture, facial proportions, or identity-related details. Automatic cropping could also change the original composition or reduce surrounding space. These effects were less problematic in product photography, where clearly specified materials, textures, lighting, and background characteristics produced more convincing results.

In the text-to-image condition, the systems generally translated detailed descriptions into visually polished images. However, generated portraits presented new interpretations rather than reproductions of the person in the reference photograph. This limits the method in applications where identity must be preserved. Product imagery was more suitable for generative approaches because the desired object, surface, lighting, and studio appearance could be described more directly.

3.3. Survey results

In the first survey block, which compared the manual reference with fully generated alternatives, the mean share of selections was 21.25% for the manual image, 38.38% for ChatGPT, 24.56% for Gemini, and 24.50% for Adobe Firefly. ChatGPT received the highest share in 8 of the 16 comparisons. Adobe Firefly produced the strongest single result in this block, receiving 73% of selections in one collage, but its performance was less consistent across examples (Table 3).

In the second block, which compared manual editing with AI-assisted editing of the source photographs, mean selection shares were 22.21% for the manual edit, 29.94% for ChatGPT, 21.00% for Gemini, and 26.69% for Adobe Firefly. ChatGPT was the most frequently preferred option in 7 of 16 comparisons.

These results indicate that the general survey sample often responded positively to the immediate visual impact of AI-based outputs (Table 3).

Table 3
Mean preference shares in the two survey blocks

Survey block	Manual (A)	ChatGPT (B)	Gemini (C)	Firefly (D)
Generated images	21.25%	38.38%	24.56%	24.50%
AI-assisted edits	22.21%	29.94%	21.00%	26.69%

3.4. Professional versus non-professional perception

The professional subgroup showed a different pattern of preferences. Across the analysed comparisons, professional photographers selected the manually edited option in 59.38% of cases, compared with 15.63% for ChatGPT, 9.38% for Gemini and 15.63% for Adobe Firefly. During evaluation, professionals paid closer attention to facial characteristics, natural skin appearance, expression, background distractions, exposure and colour balance. Non-professional viewers tended to decide more quickly and relied more heavily on the overall visual impression. Because only three respondents in the survey identified as professional photographers, this comparison should be interpreted as exploratory rather than as a population-level estimate.

4. Discussion

The results support the proposition that generative AI can substantially reduce the time required for photographic post-production, consistent with the broader shift towards automated and AI-supported image-processing workflows described in the literature (Intihar, 2023a; Intihar, 2023b; Tang, 2023; Ryazadzhiyan, 2024). In this experiment, AI-assisted editing took approximately five minutes per image, compared with an average of approximately 17 minutes for manual editing. The largest efficiency gains are therefore likely to occur in repetitive or broadly defined tasks such as exposure balancing, colour adjustment, background clean-up and the removal of distracting elements.

Efficiency, however, did not imply complete equivalence between workflows. Conventional post-production remains closely connected to deliberate, photographer-controlled adjustments and creative decision-making (Williamson, 2024; Alessi, 2025). Manual editing retained an advantage where the desired outcome depended on precise local corrections, preservation of facial identity, natural skin texture, controlled composition and repeatable creative decisions. AI systems could produce visually attractive results rapidly, but they also introduced unpredictable changes. This distinction is especially relevant in professional contexts, where technical consistency and fidelity to the photographed subject can be more important than immediate visual impact.

The survey demonstrates that perceived quality depends on the observer and the evaluation criterion. The overall sample frequently preferred AI-generated or AI-edited variants, while the very small professional subgroup showed a stronger preference for manual edits. This suggests a difference between rapid aesthetic appeal and professional evaluation based on technical detail, naturalness and control. The finding should not be generalised beyond the present sample, particularly because the professional subgroup consisted of only three respondents.

The interviews reinforce this interpretation. Existing AI-enabled photography tools likewise position automation around selected tasks such as culling, generative fill, detail enhancement and image correction rather than around the complete replacement of photographic decision-making (Aftershoot, 2025; Adobe, 2026a; Adobe, 2026b; Adobe, 2026c; Adobe, 2026d; Adobe, 2026e; Topaz Labs, 2026). Both professional photographers described AI primarily as a supporting tool for selected tasks rather than a replacement for the complete photographic workflow. Their current use focused on functions such as object removal, generative fill and basic corrections, while image selection, contextual judgement and final aesthetic decisions remained human-led. The interviews also highlighted that professional workflow efficiency depends strongly on good capture practice and on the volume and type of assignment.

The study has several limitations. It used a limited set of photographs and three AI systems, and the visual survey sample consisted mainly of young, non-professional respondents. The professional comparison drew on only three survey participants, supplemented by two interviews. In addition, generative AI systems develop rapidly, so performance observed during the experiment may change as models and interfaces are updated.

Future work should therefore involve larger and more balanced expert samples, additional photographic genres and tools, controlled image-quality criteria, and repeated testing across model versions.

5. Conclusions

Generative AI can significantly accelerate photographic post-production and streamline several routine editing stages. Across the tested tools, AI-assisted editing required roughly five minutes per image, compared with approximately 17 minutes for conventional manual editing.

The technology was particularly effective for global corrections, background modifications and rapid visual enhancement.

At the same time, manual post-production remained more controllable for demanding local adjustments, facial retouching, identity preservation and deliberate composition. The survey showed that AI outputs can be highly appealing to general viewers, whereas the professional subgroup more frequently selected manual edits and evaluated details more critically. Taken together, the results support a hybrid workflow in which generative AI is used to accelerate suitable operations, while the photographer retains responsibility for selection, creative direction, quality control and the final image.

6. Acknowledgments

The authors acknowledge the survey participants and the professional photographers who contributed their time and experience to the study.

7. References

Adobe (2026a) *Adobe Bridge*. Available from: https://www.adobe.com/products/bridge.html [Accessed 1 October 2026].

Adobe (2026b) *Adobe Lightroom*. Available from: https://www.adobe.com/products/photoshop-lightroom.html [Accessed 1 October 2026].

Adobe (2026c) *Adobe Photoshop: Generative Fill*. Available from: https://www.adobe.com/si/products/photoshop/generative-fill.html [Accessed 1 October 2026].

Adobe (2026d) *Adobe Photoshop: Photoshop features*. Available from: https://www.adobe.com/si/products/photoshop.html [Accessed 1 October 2026].

Adobe (2026e) *Post-production: a beginner's guide*. Available from: https://www.adobe.com/be_en/creativecloud/video/discover/post-production.html [Accessed 1 October 2026].

Aftershoot (2025) *What is culling in photography?* Available from: https://aftershoot.com/blog/understanding-culling-in-photography/ [Accessed 1 October 2026].

Alessi, M.S. (2025) *What is post processing in photography?* Boris FX. Available from: https://borisfx.com/blog/what-is-post-processing-in-photography/ [Accessed 1 October 2026].

Arvaj, L.B., Šubic, T. and Ahtik, J. (2025) 'Analysis of relevance and appeal of visual presentation of meat products generated using artificial intelligence', *Applied Sciences*, 15(15), 8328. DOI: 10.3390/app15158328

Cambridge in Colour (2026) *Digital photo editing workflow*. Available from: https://www.cambridgeincolour.com/tutorials/digital-photo-editing-workflow.htm [Accessed 1 October 2026].

Davis, J. (2022) *Photography post-production in 6 steps*. Jeremy Davis Photography. Available from: https://jeremydavisphotography.com/photoblog/photography-post-production-in-6-steps/ [Accessed 1 October 2026].

Ekart, B. and Ahtik, J. (2026) 'Authorship disclosure and consumer perception of AI-generated graphic design', *Journal of Graphic Engineering and Design*, 17(2), pp. 23–32. DOI: 10.24867/jged-2026-2-023

Intihar, M. (2023a) *Umetna inteligenca (AI) v fotografiji I. del*. e-Fotografija.si. Available from: https://www.e-fotografija.si/umetna-inteligenca-(ai)-v-fotografiji,2317.html [Accessed 1 October 2026].

Intihar, M. (2023b) *Umetna inteligenca (AI) - že desetletja v naših kamerah III. del*. e-Fotografija.si. Available from: https://www.e-fotografija.si/umetna-inteligenca-(ai)-ze-desetletja-v-nasih-kamerah-iii-del,2325.html [Accessed 1 October 2026].

Ryazadzhiyan, H. (2024) 'The transformation of photography by artificial intelligence generative AI technology', *Journal of Artificial Intelligence Practice*, 6(1), pp. 27–31.

Tang, Z. (2023) 'The transformation of photography by artificial intelligence generative AI technology', *Journal of Artificial Intelligence Practice*, 6(8), pp. 57–62. DOI: 10.23977/jaip.2023.060809

Topaz Labs (2026) *Professional-grade photo and video editing powered by AI*. Available from: https://www.topazlabs.com/ [Accessed 1 October 2026].

Williamson, S. (2024) *Post-processing photography: how to balance efficiency and creativity*. Imagely. Available from: https://www.imagely.com/post-processing/ [Accessed 1 October 2026].

© 2026 Authors. Published by the University of Novi Sad, Faculty of Technical Sciences, Department of Graphic Engineering and Design. This article is an open access article distributed under the terms and conditions of the Creative Commons Attribution license 4.0 Serbia (http://creativecommons.org/licenses/by/4.0/rs/).

Original Scientific Paper https://doi.org/10.24867/GRID-2026-p55

Designing Mental Well-Being Mobile Applications: Insights into User Preferences for User Interface Design

ABSTRACT

User interface design can influence how users perceive and evaluate mental well-being mobile applications. However, empirical evidence regarding users' preferences for specific visual interface characteristics remains limited. This paper presents an experimental evaluation of user preferences for alternative interface designs of a mental well-being mobile application prototype. The study focused on four visual characteristics: interface colour, colour palette, interface theme, and graphical elements. An A/B testing approach was used to compare alternative design solutions, with data collected through a questionnaire completed by 35 participants. Five interface colours were examined (blue, green, purple, red, and orange) together with contrasting and monochromatic palettes, light and dark themes, and illustrations versus photographs. The results showed the highest perceived attractiveness for blue and green interfaces, an overall preference for light themes, and a consistent preference for illustrations over photographs. A statistically significant association was also found between interface colour and preferred colour palette ($\chi^2(4) = 40.112$, $p < 0.001$, Cramer's $V = 0.239$). The findings provide practical insights into users' visual preferences for mental well-being mobile applications.

Gala Golubović
Saša Petrović
Sanja Cvetojević
Iva Juretić
Stefan Đurđević

University of Novi Sad, Faculty of Technical Sciences, Department of Graphic Engineering and Design, Novi Sad, Serbia

KEY WORDS
User interface design, mHealth, mental well-being, mobile applications

1. Introduction

The increasing use of mobile applications in the field of health and well-being has emphasized the importance of designing interfaces that are not only functional, but also visually appropriate, accessible, and supportive of a positive user experience. User interface design can influence users' perception, emotional responses, interaction with content and overall evaluation of an application. Among visual elements, colour plays an important role, affecting readability, visual hierarchy, navigation, emotional perception, and the perceived credibility of presented information (Garrett, 2011; Elliot & Maier, 2014; Park & Kang, 2017). Research has also shown that colour can have a particularly strong influence on users compared with other visual elements, while appropriate colour combinations can contribute to a more pleasant and comprehensible user experience (Pelet & Papadopoulou, 2012). These aspects are particularly important in mobile applications designed to support mental well-being, where users may interact with the application in emotionally sensitive situations. Colour associations can influence the perceived atmosphere of an interface, with blue and green commonly associated with safety, stability, and calmness, while cooler colours may support relaxation and introspection (Valdez & Mehrabian, 1994; Labrecque & Milne, 2012; Swasty & Adriyanto, 2017; Bargas-Avila & Hornbæk, 2011). At the same time, the design of health-related applications needs to account for accessibility, sufficient contrast, consistency, and the use of additional visual cues rather than relying exclusively on colour (Wiklund, Kendler & Strochlic, 2016; W3C, 2018). Cultural differences should also be considered, as the meanings and emotional associations of colours may vary across cultural contexts (Cyr, Head & Larios, 2010; Kondratova & Goldfarb, 2007).

Understanding users' preferences for UI design elements is therefore important when developing mental well-being mobile applications that are both usable and emotionally appropriate. Previous research emphasizes the importance of combining psychological, functional, cultural, and accessibility considerations when selecting visual characteristics for health-related interfaces (Nielsen & Budiu, 2013; Sutcliffe, 2022). Therefore, this study investigates user preferences regarding selected user interface characteristics of mental well-being mobile applications to identify visual design solutions that better reflect users' preferences and expectations.

2. Methods

2.1. Research Design

The study investigated users' preferences regarding selected user interface characteristics of a mental well-being mobile application. Based on the literature review, particular attention was given to colour, colour palettes, interface themes, and graphical content, as these visual characteristics can influence users' perception and overall impression of health-related mobile applications.

An A/B testing approach was employed to examine users' preferences by presenting pairs of alternative interface designs and recording their choices. Data were collected using a questionnaire consisting of 58 questions. In the A/B comparisons, participants evaluated the presented design alternatives for each of the five selected colours.

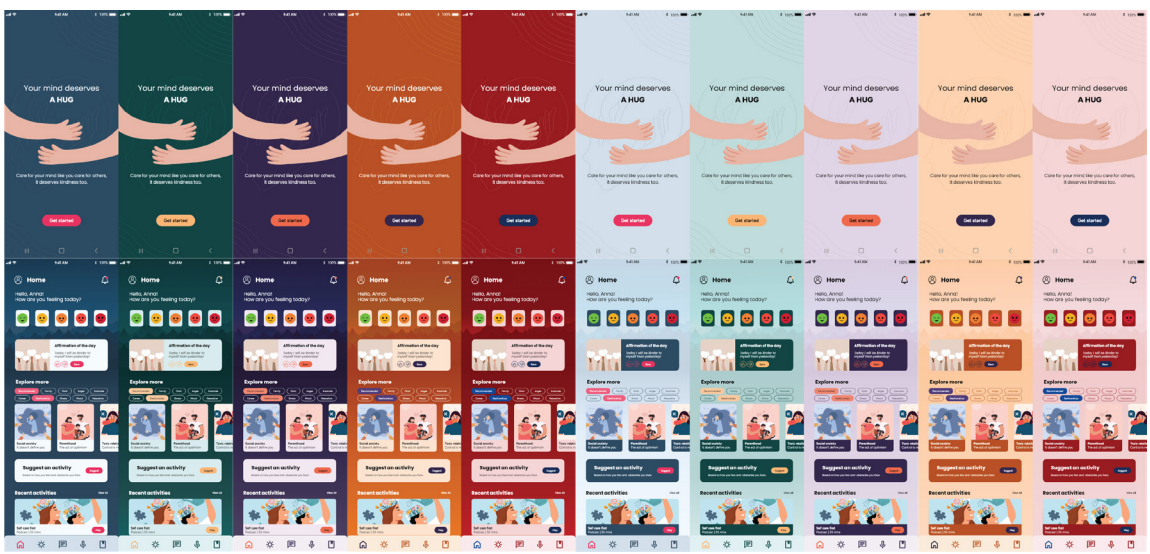
In addition to A/B comparisons, the questionnaire included questions concerning participants' gender and age, perceived attractiveness of the presented interfaces, and the extent to which the application was associated with the mental well-being domain.

2.2. Stimuli

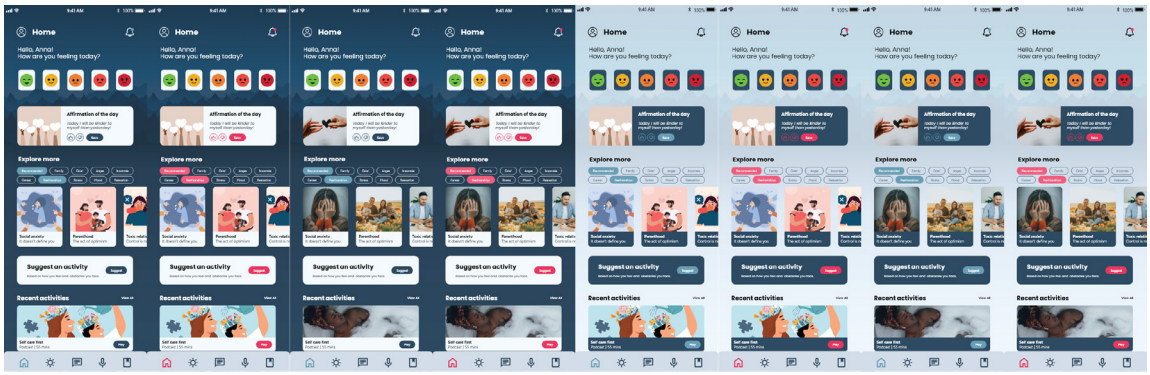
The stimuli were developed to examine preferences for five interface colours: green, blue, purple, red, and orange. The colours were selected based on recommendations for the use of colour in health-related mobile applications, with green and blue representing the most recommended colours, purple a neutral option, and red and orange the least recommended options. Accessibility considerations were also incorporated into the stimulus design, particularly regarding colour combinations that may be problematic for individuals with colour vision deficiencies. Adequate contrast between background and text was maintained throughout the designs.

Two types of application screens were designed: an onboarding screen and a home screen (Figure 1). Each screen was developed using all five selected colours in both light and dark themes.

To investigate preferences for colour palettes, each stimulus was additionally presented in contrasting and monochromatic variants in both light and dark themes. Since previous findings indicated that graphical content can affect users' overall impression of an application, an additional comparison examined preferences for illustrations versus photographs. These stimuli were likewise presented across both themes and colour palette variants (Figure 2).



» **Figure 1:** *Onboarding and home screen stimuli*



» **Figure 2:** *Variations of the blue-colour stimuli used in the study*

3. Results and discussion

A total of 35 participants were part of the study, including 20 female (57%) and 15 male (43%) participants. The largest age group was participants aged 26–35, accounting for 54% of the sample.

3.1. Perceived attractiveness of interface colours

To examine the general preference for interface colours, participants evaluated five onboarding screen stimuli presented in the dark theme with a contrasting colour palette. The stimuli were rated individually on a five-point Likert scale, ranging from 1 (completely unattractive) to 5 (completely attractive).

The blue interface received the highest mean attractiveness rating (M = 4.11), followed closely by the green interface (M = 4.06). Purple received a mean rating of 3.71, while red and orange were rated lower, with mean scores of 3.51 and 3.31, respectively.

The higher attractiveness ratings of blue and green are consistent with previous research associating these colours with safety, stability, calmness, and trust, particularly in health-related contexts (Valdez & Mehrabian, 1994; Labrecque & Milne, 2012; Swasty & Adriyanto, 2017).

3.2. Preferences for colour palettes

The A/B tests examined participants' preferences between monochromatic and contrasting colour palettes, considering both light and dark themes and both onboarding and home screens. For each of the five colours, four stimulus pairs were compared, resulting in 20 A/B comparisons for each participant. The results presented below are the combined responses from all participants for the five colours.

When all five colours were considered together, the dark-theme onboarding screen showed a slight overall preference for the contrasting palette, with 91 selections compared with 84 for the monochromatic palette. At the individual colour level, contrasting palettes were preferred for blue and green, whereas monochromatic palettes were preferred for purple, orange, and red.

A similar, although weaker, tendency was observed for the light-theme onboarding screen, where the contrasting palette received 88 preferences compared with 87 for the monochromatic palette. At the individual level, blue was the only colour for which the contrasting palette was preferred.

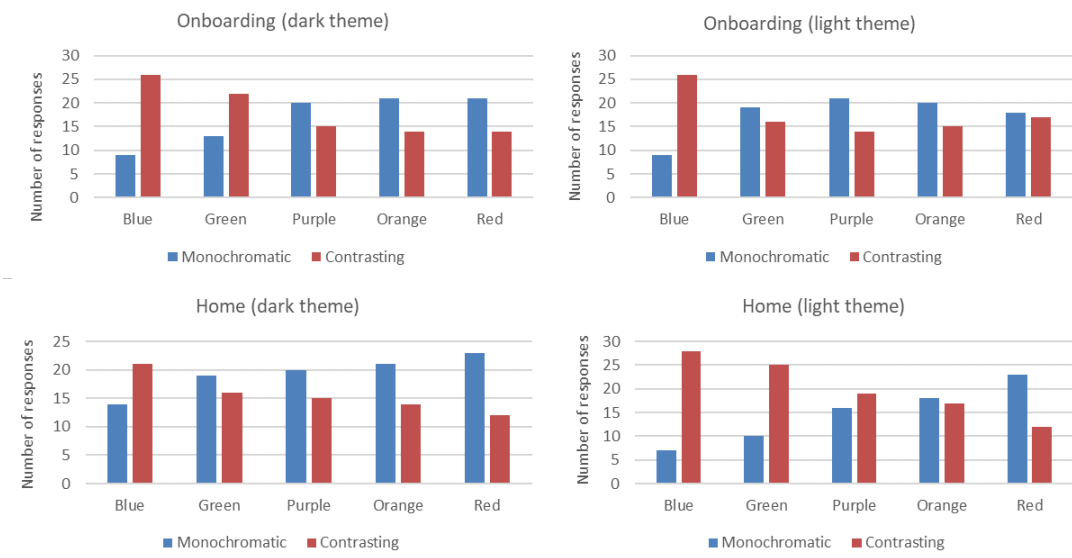
For the dark-theme home screen, the overall preference was reversed: participants selected the monochromatic palette 97 times compared with 78 selections for the contrasting palette. Blue was the only colour that deviated from this overall pattern.

In contrast, the light-theme home screen showed a clear preference for the contrasting palette, with 101 selections compared with 74 for the monochromatic palette. Contrasting palettes were preferred for blue, green, and purple at the individual colour level.

Overall, the results indicate that preference for monochromatic versus contrasting palettes was not uniform, but varied according to the interface screen, theme, and base colour (Figure 3).

These results suggest that colour preference depends partly on how colours are combined within the interface. The significant association between interface colour and preferred palette supports this finding.

This is consistent with previous research on the importance of colour combinations and contrast for users' perception and overall experience (Pelet & Papadopoulou, 2012).



» **Figure 3:** *Preferences for monochromatic and contrasting colour palettes across interface themes and screens*

3.3. Preferences for interface theme

Participants also compared light and dark versions of the onboarding and home screens. For the onboarding screen, 96 responses indicated a preference for the light theme, compared with 79 for the dark theme. The preference for the light theme was particularly evident for the blue, orange, and red stimuli.

A comparable pattern was observed for the home screen, where the light theme received 93 preferences compared with 82 for the dark theme. At the individual colour level, the light theme was preferred for blue, red, and orange stimuli.

These findings indicate an overall preference for light interfaces across both types of screens (Figure 4).

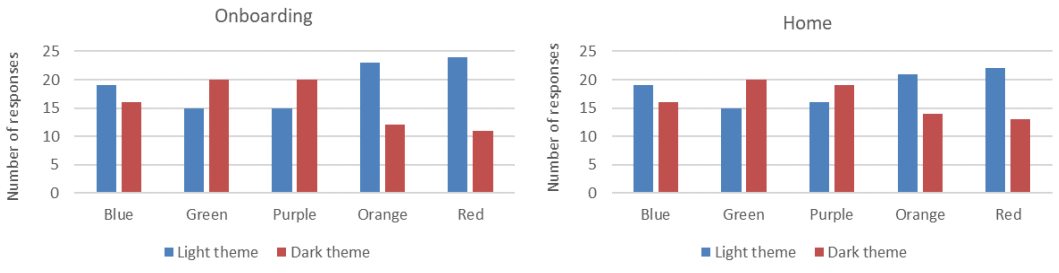
The preference for light interfaces is consistent with previous findings on the use of lighter background colours in interface design (Pelet & Papadopoulou, 2012). However, the absence of a statistically significant association between colour and theme suggests that the preference for light themes was not strongly dependent on the selected interface colour.

3.4. Preferences for graphical elements

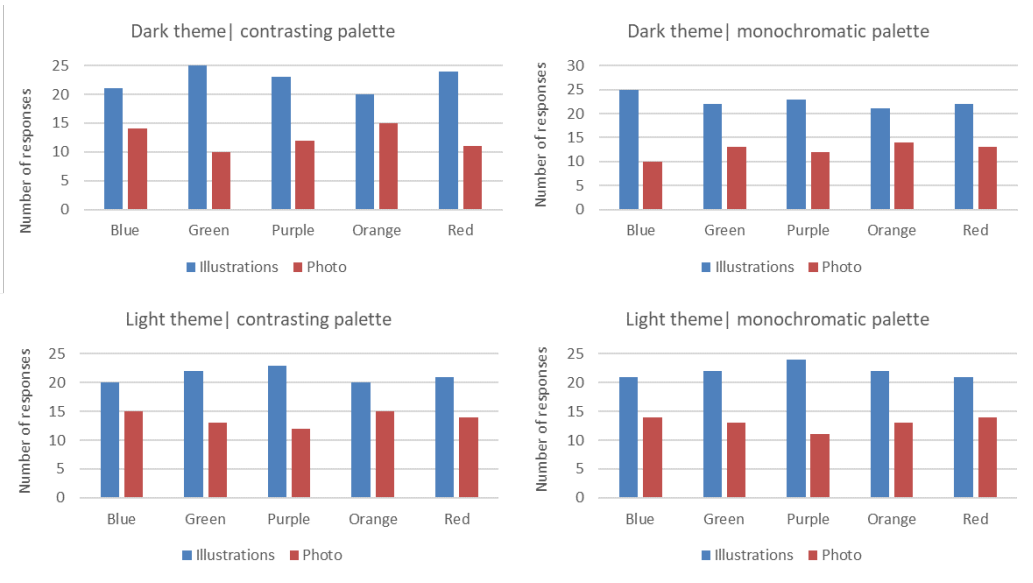
The final A/B comparison examined participants' preferences for illustrations versus photographs on the home screen. The comparison was performed separately for each colour, theme, and colour palette, resulting in 20 stimulus pairs.

The results showed a consistent preference for illustrations over photographs across all tested conditions (Figure 5). The same pattern was observed across the different colours, interface themes, and colour palettes. This indicates a consistent preference for illustrations in the tested application.

The consistency of this preference across all tested conditions is notable, as it suggests that the preference for illustrative content was relatively robust to changes in colour, theme, and palette. This suggests that graphical style may be an important UI characteristic alongside colour and theme.



» **Figure 4:** *Preferences for light and dark interface themes*

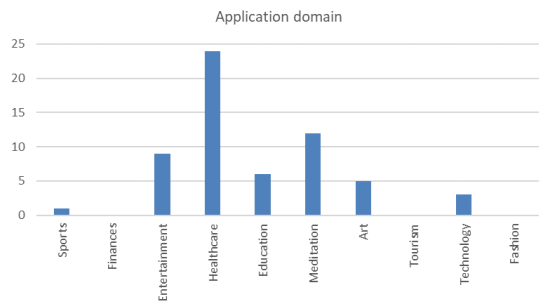


» **Figure 5:** *Preferences for illustrations and photographs across interface conditions*

3.5. Perceived application domain

Following the A/B comparisons, participants were asked to indicate which application domain they associated with the presented interface designs. They could select one or more predefined domains, including sport, finance, entertainment, healthcare, education, meditation, and art, as well as tourism, technology, and fashion.

Healthcare was the most frequently selected domain, with 24 responses, followed by meditation, with 12 responses (Figure 6). These results suggest that the visual characteristics of the stimuli were predominantly interpreted as belonging to the health-related domain, while the relatively high association with meditation further supports their relevance to the mental well-being context.



» **Figure 6:** *Participants' associations with the application domain*

3.6. Associations between interface characteristics

To further examine the relationships between the investigated interface characteristics, Pearson's chi-square tests of independence were conducted. The analyses examined associations between interface colour and colour palette, interface colour and theme, screen type and colour palette, screen type and interface theme, as well as colour palette and interface theme (Table 1).

A statistically significant association was found between interface colour and preferred colour palette, $\chi^2(4) = 40.112$, $p < 0.001$, with a Cramer's V of 0.239. Participants more frequently preferred contrasting palettes for blue and green interfaces, whereas monochromatic palettes were more frequently preferred for purple, orange, and red interfaces.

No statistically significant association was found between interface colour and preferred theme for either the home screen, $\chi^2(4) = 4.268$, $p = 0.371$, or the onboarding screen, $\chi^2(4) = 1.830$, $p = 0.767$. Similarly, no significant association was found between screen type and colour palette, $\chi^2(1) = 0.000$, $p = 1.000$, or between screen type and interface theme, $\chi^2(1) = 0.104$, $p = 0.748$.

Finally, the analyses conducted separately for each colour showed no statistically significant association between colour palette and interface theme (all $p > 0.05$). These findings indicate that, while colour was significantly associated with the preferred type of colour palette, preferences for interface theme were generally independent of the selected colour, colour palette, and screen type. In contrast, preferences for interface theme appeared relatively stable across colours and screen types.

Table 1
Associations between interface characteristics

Interface characteristic	χ^2	df	p
Colour × palette	40.112	4	<0.001
Colour × theme – Home	4.268	4	0.371
Colour × theme – Onboarding	1.830	4	0.767
Screen type × palette	0.000	1	1.000
Screen type × theme	0.104	1	0.748

4. Conclusions

This study investigated user preferences regarding selected user interface characteristics of mobile applications designed to support mental well-being, with particular emphasis on colour, colour palettes, interface themes, and graphical elements. Using an A/B testing approach, the study provided insights into how different visual solutions are perceived and preferred by users.

The results showed a clear preference for blue and green as the primary interface colours, which received the highest attractiveness ratings among the colours tested. This is consistent with previous research linking these colours with calmness, safety, stability, and health. The results further indicated that preferences for colour palettes varied according to the interface colour. A statistically significant association was found between interface colour and preferred colour palette ($\chi^2(4) = 40.112$, $p < 0.001$, Cramer's $V = 0.239$), with contrasting palettes more frequently preferred for blue and green, and monochromatic palettes more frequently preferred for purple, orange, and red. These findings suggest that colour and palette selection should be considered together when designing mental well-being mobile interfaces.

Participants also showed an overall preference for the light theme over the dark theme for both onboarding and home screens. In addition, the results demonstrated a consistent preference for illustrations over photographs, regardless of the colour, theme, or palette used. This suggests that graphical style should also be considered when designing mental well-being applications.

The findings suggest that the visual design of mental well-being applications should go beyond aesthetic considerations and account for users' preferences, accessibility, and the context in which the application is used. Based on the results, cooler colours, carefully selected contrasting elements, light interface themes, and coherent illustrative graphics can represent promising design directions for this type of application. At the same time, colour should be used consistently and in combination with other visual cues to ensure clarity and accessibility.

Overall, the study demonstrates that UI design choices can play an important role in shaping users' initial perceptions and preferences for mental well-being applications. The identified preferences can serve as practical guidelines for designers when developing interfaces intended to create a clear, accessible, visually appealing, and supportive user experience. The findings provide empirical support for considering colour and palette selection as interconnected aspects of UI design rather than independent design decisions. Future research could further investigate how these visual preferences relate to users' emotional responses, usability, engagement, and long-term acceptance of mental well-being applications.

5. Acknowledgments

This research has been supported by the Ministry of Science, Technological Development and Innovation (Contract No. 451-03-34/2026-03/200156) and the Faculty of Technical Sciences, University of Novi Sad through project "Scientific and Artistic Research Work of Researchers in Teaching and Associate Positions at the Faculty of Technical Sciences, University of Novi Sad 2026" (No. 01-3609/1).

6. References

Bargas-Avila, J.A. and Hornbæk, K. (2011) 'Old wine in new bottles or novel challenges: A critical analysis of empirical studies of user experience'. *In: Proceedings of the SIGCHI Conference on Human Factors in Computing Systems*, pp. 2689–2698. DOI: 10.1145/1978942.1979336

Cyr, D., Head, M. and Larios, H. (2010) 'Colour appeal in website design within and across cultures: A multi-method evaluation', *International Journal of Human-Computer Studies*, 68(1–2), pp. 1–21. DOI: 10.1016/j.ijhcs.2009.08.005

Elliot, A.J. and Maier, M.A. (2014) 'Color psychology: Effects of perceiving color on psychological functioning in humans', *Annual Review of Psychology*, 65, pp. 95–120. DOI: 10.1146/annurev-psych-010213-115035

Garrett, J.J. (2011) *The Elements of User Experience: User-Centered Design for the Web and Beyond. Berkeley*, CA: New Riders.

Kondratova, I. and Goldfarb, I. (2007) 'Color Your Website: Use of Colors on the Web'. In: Aykin, N. (ed.) *Usability and Internationalization. Global and Local User Interfaces*. DOI: 10.1007/978-3-540-73289-1_16

Labrecque, L.I. and Milne, G.R. (2012) 'Exciting red and competent blue: The importance of color in marketing', *Journal of the Academy of Marketing Science*, 40(5), pp. 711–727. DOI: 10.1007/s11747-010-0245-y

Nielsen, J. and Budiu, R. (2013) *Mobile Usability*. Berkeley, CA: New Riders.

Park, H. and Kang, S. (2017) 'Color as design elements for healthcare websites'. In: *Proceedings of AIC 2017 Jeju*, pp. 36–39.

Pelet, J. and Papadopoulou, P. (2012) 'The effect of colors of e-commerce websites on consumer mood, memorization and buying intention', *European Journal of Information Systems*. DOI: 10.1057/ejis.2012.17

Sutcliffe, A. (2022) *Designing for User Engagement: Aesthetic and Attractive User Interfaces*. Cham: Springer Nature.

Swasty, W. and Adriyanto, A.R. (2017) 'Does color matter on web user interface design', *CommIT (Communication and Information Technology) Journal*, 11(1), pp. 17–24. DOI: 10.21512/commit.v11i1.2088

Valdez, P. and Mehrabian, A. (1994) 'Effects of color on emotions', *Journal of Experimental Psychology: General*, 123(4), pp. 394–409. DOI: 10.1037/0096-3445.123.4.394

Wiklund, M.E., Kendler, J. and Strochlic, A.Y. (2016) *Usability Testing of Medical Devices*. Boca Raton: CRC Press.



© 2026 Authors. Published by the University of Novi Sad, Faculty of Technical Sciences, Department of Graphic Engineering and Design. This article is an open access article distributed under the terms and conditions of the Creative Commons Attribution license 4.0 Serbia (http://creativecommons.org/licenses/by/4.0/rs/).

Original Scientific Paper https://doi.org/10.24867/GRID-2026-p56

A Study of the Impact of JPEG Compression on Visual and Digital Image Degradation

ABSTRACT

A key feature of the JPEG standard is the ability to control the degree of compression, and, consequently, the extent of information loss that occurs during image encoding. Modern image-editing environments, including professional software suites such as Adobe Photoshop, allow users to select the desired compression level. However, the software documentation rarely contains a comprehensive analysis of the precise relationship between the intensity of compression and the resulting deterioration in image quality. This study analysed the impact of different JPEG compression levels on perceived image quality and selected digital image characteristics. Following analysis of the results, a set of practical recommendations has been formulated.

Leszek Markowski

Warsaw University of Technology, Institute of Mechanics and Printing, Poland

KEY WORDS
JPEG, lossy compression, block artefacts, Adobe Photoshop

1. Introduction

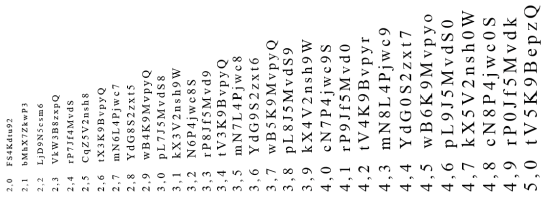
JPEG encoding facilitates high-ratio image compression, with ratios as high as 20:1, though this result in some loss of detail. The compression process takes place in several stages. First, the image stored in the RGB colour space is converted to the YCbCr colour space, where Y represents luminance and Cb and Cr are the chrominance components. As the human eye is less sensitive to changes in colour than to changes in luminance, it is possible to reduce the file size without any noticeable loss of quality. In the process of chroma subsampling, the resolution of the Cb and Cr channels is reduced, usually by half both horizontally and vertically. This means that several neighbouring pixels share colour information, which significantly reduces the amount of data. The image is then divided into 8 × 8 pixels blocks, on which further operations are performed. The algorithm applies a discrete cosine transform (DCT) to each block, which transforms the image data into frequency coefficients. The next stage is the quantisation of the coefficients, which is the main source of quality loss. At this stage, the compression level (image quality) is determined. The stronger the compression, the more coefficients are set to zero. This results in a smaller file size, but characteristic distortions, known as JPEG artefacts, appear. (Karwowski, 2019).

A key benefit of the JPEG algorithm is its capacity to adjust the compression level, enabling users to customise it for specific images to achieve the smallest possible file size while maintaining acceptable quality. The popular image-processing programme Adobe Photoshop also offers such a tool; however, there is no clear information on how it works (Adobe Help Center, 2023). This project was undertaken due to the lack of detailed documentation on the criteria for using this function.

2. Methods

To determine the optimal level of JPEG compression for various source images, a series of visual assessments were conducted. For the purposes of this study, a new test image was created based primarily on a selection of high-quality photographs and graphics, as well as the results of a review of the sensitivity of different tests used in previous studies on JPEG compression artefacts (Markowski & Jeliński, 2011; Żurek, 2021). Fifteen groups of elements were arranged on an A4 sheet (Fig. 2). Each group was used to assess the reproduction of different

aspects: text legibility, microline resolution, tonal continuity, colour uniformity and detail recognisability. The groups, numbered from 1 to 15, comprise: 1) an alphanumeric scale with 31 sizes of randomly generated characters, in positive and negative variants and on backgrounds of varying shade and contrast (Fig. 1); 2) a microline scale with line widths ranging from 0.05 to 0.25 mm; 3) a continuous greyscale range of 0–100%; 4) colour gradients; 5) an ordered colour chart; 6) a randomly arranged colour chart; 7) a map; 8) a woodcut; 9) textures; 10) a steel engraving; 11) an offset print reproduction; 12) a photograph lacking fine detail; 13) a photograph with typical detail; 14) a photograph with high detail; 15) a miniature group photograph. Vector objects were created for text, line art and colour fields. The original reproduction sources were saved in the lossless TIFF format. The entire test was created using Adobe Illustrator and then rasterised to PNG format using the 'optimised composition without interlacing' option and a base resolution of 300 ppi, which is standard in print reproduction. The PNG file was used as the source material for preparing all the test samples in Photoshop, which were saved in JPEG format at the thirteen available quality levels (0–12).



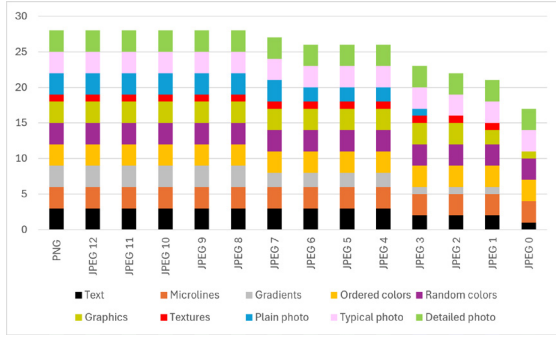
» **Figure 1:** *A test for assessing the recognisability of alphanumeric characters, shown at a magnification of 2:1. Each of the 31 size levels features a random combination of 10 characters; successive levels differ by 0.1 points. The characters are set in Times New Roman*

The visual assessment of the test images was carried out under diffused lighting, using the method of alternating comparison of samples displayed in the same position on the monitor screen. The samples were analysed from 25 cm, which is considered the standard minimum distance for good vision. The study utilised an Eizo ColorEdge CS2740 monitor with an IPS panel and a resolution of 3840 × 2160 pixels (164 ppi). The images were viewed at actual size (A4 format) and at a 2:1 magnification factor to assess fine details more accurately. All JPEG samples were compared with the original in PNG format. The following rating scale was used: 0 – poor quality, 1 – adequate, 2 – good, 3 – identical to the original.

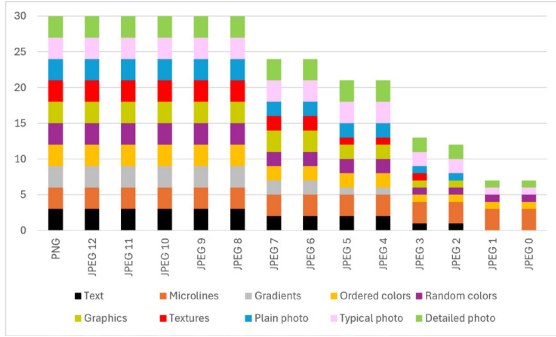
3. Results

3.1. Visual evaluation of test images

The ten most representative elements were selected for evaluation. Figures 3 and 4 present the results of the visual analysis of test elements subjected to lossy compression. At a 1:1 magnification, the first drop in quality is observed at level 7, and subsequent drops occur gradually at levels 3–0. The most significant adverse changes affect gradients, text, graphic reproduction, and photographs with large areas of similar tonality, such as clouds against the sky. The textures used are so fine that they cannot be distinguished at a 1:1 scale. At a 2:1 magnification, compression artifacts are more visible, which is why the overall ratings are lower than when viewed at a 1:1 scale. The first decline in the quality of alphanumeric characters, gradients, and textures occurs at level 7, with subsequent declines—gradually—at levels 5, 3, and 1. At levels 1–0, half of the test elements were completely degraded.



» **Figure 3:** *Cumulative results of visual evaluations of test images viewed at 1:1 magnification after JPEG compression at levels 12–0. The first drop in quality occurs at level 7, and subsequent drops occur gradually at levels 3–0*



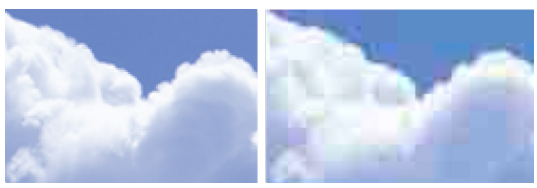
» **Figure 4:** *Cumulative results of visual evaluations of test images viewed at a 2:1 magnification after JPEG compression at levels 12–0. As in Fig. 3, the first noticeable drop in quality occurs at level 7, followed by gradual declines at levels 5, 3, and 1. At levels 1–0, half of the test elements were completely degraded*



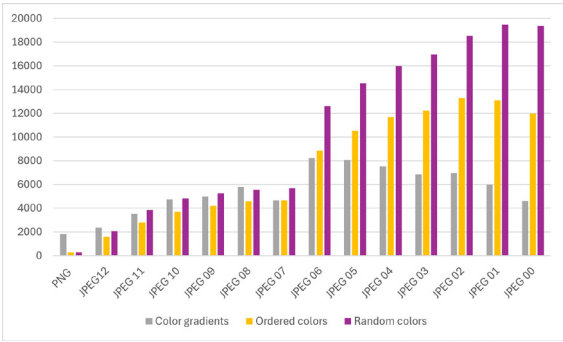
» **Figure 2:** *Test image developed for the visual assessment of image degradation after JPEG compression (scale 1:2)*
Sources of originals: 7 – Butler, S., The Atlas of Ancient and Classical Geography. E-book: 21.11.2005;
8 – Digital National Museum. Women carrying a jug, vertical woodcut;
10 – stamp for the Iceland Post designed by Czesław Słania (steel engraving based on a drawing by August Mayer);
11 – stamp for the Polish Post designed by Jan Rutka; stamp for the Lithuanian Post designed by Balakauskaite;
12, 13, 14 – photographs by Leszek Markowski;
15 – photomontage created by AI

3.2. The effect of JPEG compression on the number of colors

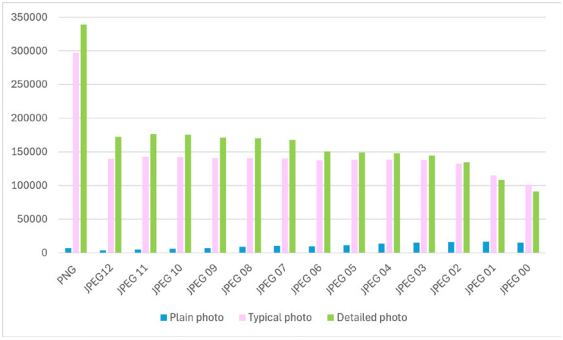
One of the key factors in determining the effectiveness of the JPEG algorithm is the change in the number of unique colours in an image. To investigate this effect at various compression levels, the Image Color Counter tool available on the Novaboard platform (Image Color Counter, 2026) was used. The results are presented in Figures 6 and 7. Figure 6 shows changes in the number of colours in gradients (Test 4) and colour charts (Tests 5 and 6), while Figure 7 shows changes in photographic images (Tests 12, 13, and 14). In images containing vectorgenerated gradients and test patterns, an unexpected relationship was observed: at successive compression levels, the number of colours increases rather than decreases. This effect is the result of the operation of the JPEG algorithm and the recalculation of pixel values in 8 × 8 blocks. As a result of the conversion process from PNG to JPEG 12, the number of unique colours is reduced by 50%. At higher compression levels, there is only a minimal reduction in the number of unique colours. However, there is an exception to this rule, which applies to photographs of clouds with a limited tonal range. In this case, the number of colours increases at subsequent quantisation levels (see Fig. 5). Color changes in compressed images are visible as tonal jumps and local discolouration. These changes only become apparent at compression levels lower than 5. It was determined that desaturation effects were not evident at any compression level.



» **Figure:** *5: A magnified section of a PNG image (left) and the same image after lossy JPEG compression at level 0 (right). The PNG image shows only pixelation. In the JPEG image, in addition to pixelation, there is a blocky effect caused by lossy compression. Within individual blocks, many pixels appear discoloured, and colours not present in the original — navy blue, purple, turquoise, and yellow — are visible*



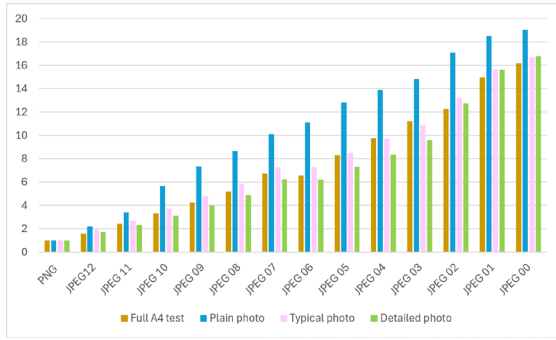
» **Figure 6:** *Number of unique colours before and after JPEG compression (levels 12–0) in selected images containing colour gradients, ordered colour arrays and randomly arranged colour arrays. Tests with solid-colours fields do not fully demonstrate the specific characteristics of JPEG compression — after stronger compression, the number of colours increases rather than decreases*



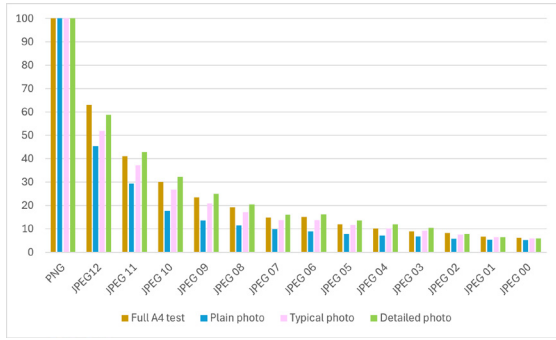
» **Figure 7:** *The number of unique colours in selected photographs before and after JPEG compression (levels 12–0): plain photo with large areas of similar tone, typical photo with a moderate amount of detail, and detailed photo with a high amount of detail*

3.3. JPEG compression levels in adobe photoshop and compression ratio

To compare the effectiveness of compression at different JPEG settings, the degree of compression was calculated. This is defined as the ratio of the data size before compression to the size after compression. This calculation was performed on selected original photographs. Figure 8 shows that the compression ratio depends on the image content. Images with little tonal variation and few details (plain photo) are most susceptible to compression. Each successive compression level reduces the file size, but this relationship is not linear. The diagrams in Figure 9 illustrate this phenomenon more clearly, showing the JPEG file size as a percentage of the original PNG size. At level 8, for examle, files range from 12% to 20% of the original size, depending on the image content. At level 4, it is approximately 7–12%. This means that at level 8, files are 5 to 8 times smaller. However, increasing the compression to level 4 only reduces their size by about half, which causes a significantly higher risk of artefacts appearing.



» **Figure 8:** *A comparison of the ratio compression for selected image files at each JPEG level from 12 to 0 (PNG/JPEG)*



» **Figure 9:** *A comparison of the compression efficiency of selected image files at JPEG levels 12–0, expressed as a percentage of the original file size. (JPEG × 100) / PNG*

3.4. Sensitivity of test images



» **Figure 10:** *Examples of alphanumeric test patterns in PNG (left) and JPEG 0 (right) formats, with two contrast variants: ΔL = 60 and ΔL = 40. Artifacts along the edges blur the shapes of the characters; this degradation is more pronounced for objects with lower contrast. Magnification: 2:1*

Alphanumeric test (Fig. 10): Alphanumeric characters are among the most objective elements of a visual assessment, as they provide a relatively unambiguous evaluation criterion in the form of a recognition threshold. For the test to be sufficiently sensitive, it must include very small characters, which are difficult to read. In this study, evaluation at a magnification of 2:1 was found to be more reliable than evaluation at a scale of 1:1.

Line test (Fig. 11): Rasterisation of the line test converts a vector line into a pixel image at a specified resolution (300 ppi). The pixels making up the image take on intermediate values and merge with one another, which prevents the lines from being reproduced correctly. The resolution of the input file (300 ppi) and the monitor resolution (164 ppi) set a practical limit on the reproduction of lines with a width of approximately 0.17 mm. An additional issue with similar line tests (e.g. Siemens Star) is the occurrence of interference phenomena, which makes reliable assessment difficult. This limits the effectiveness of such tests for evaluating images on a monitor.



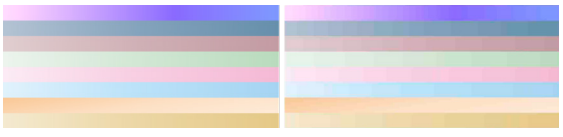
» **Figure 11:** *Enlarged images of test lines, displayed on a monitor with a resolution of 164 ppi, after rasterisation to a resolution of 300 ppi and saving in PNG format. The original line widths are shown below the examples. Lines narrower than 0.17 mm become blurred because of rasterisation. This effect is so pronounced that it masks the artefacts caused by lossy compression. Magnification: 3:1*

Textures: Test image containing textures enables an objective assessment of quality based on the recognisability of the material's texture. Some textures are so fine that they must be analysed under magnification.



» **Figure 12:** *Images of the textures of various fabrics at 2:1 magnification: the original PNG on the left and the image after JPEG compression at level 0 on the right. Compression causes degradation of the actual fabric structure*

Gradients: Continuous tonal scales proved to be the most sensitive element of the entire test. Artifacts in the form of tonal jumps appear at compression level 7 and are visible on the screen without magnification.

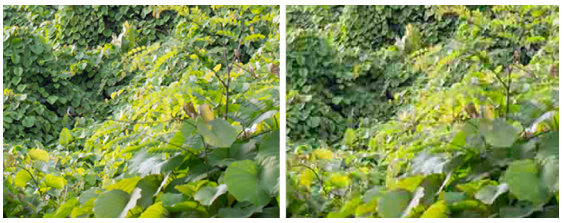


» **Figure 13:** *Colour gradients on a 1:1 scale: the PNG image on the left and JPEG-compressed at level 0 on the right*

Original photographs: A photograph of clouds against a plain sky (plain photo), characterised by little tonal variation, proved to be the most susceptible to lossy compression artefacts. A photograph of a butterfly with typical levels of detail (typical photo) and a photograph of ivy with a high level of detail (detailed photo) showed significantly greater resistance to artefacts. Distortions in these images only became visible at a 2:1 magnification, when saved as JPEGs at compression levels lower than 4.



» **Figure 14:** *A section of the PNG image on the left and the image after JPEG compression at level 0 on the right. Undesirable posterisation and colour distortion are visible*



» **Figure 15:** *A magnified section of a PNG image (left) and a JPEG image compressed at level 0 (right). Although the compressed image is less sharp and blurred in places, the high level of detail largely masks artefacts such as posterisation, colour shifts and block artefacts*

4. Conclusions

Based on a visual assessment of the test images, practical conclusions were drawn regarding the compression of image files in Adobe Photoshop.

- Evaluating test samples at a magnification of 2:1 enables more accurate and the detection of more rendering errors. Consequently, the overall ratings of the test images at various compression levels were more varied at a 2:1 magnification (range 30–7) than at a 1:1 scale (range 28–17).
- As the compression level increases, adverse changes appear most rapidly in gradients and photographs containing large, tonally uniform areas. Minor tonal discontinuities begin to become visible from quality level 7. At level 3, very distinct tonal jumps appear in gradients.

- Images without plain, uniform colours or gradients that are intended for viewing on a screen at a scale of 1:1 can be safely compressed in Photoshop, even at level 4–6. A significant loss of quality in text and photographs containing large uniform areas was observed at compression levels 3–0.
- For highly detailed photographs that are often viewed at high magnification, a compression level of 8–10 is optimal, in line with professional photography recommendations (Mansurov, 2018). Below level 8, artefacts appear in text, gradients and textures. This makes characters difficult to read, causes tonal jumps and blurring of textures, which may prevent them from being correctly identified.
- When comparing the quality of the output images with the size of the compressed files, a compression level of 8 can be considered optimal. For a typical photograph, a file saved at this level was approximately six times smaller than the original. Using a compression level of 4 can reduce the file size by a further twofold, but there is a high risk of artefacts occurring.
- In typical photographic images, the JPEG format always reduces the number of unique colours, regardless of the selected compression level. At higher compression levels, this reduction in the number of colours is only slightly greater and depends on the nature of the image. Visually, this does not manifest as desaturation. Local colour shifts resulting from the division of the image into blocks and the averaging of pixel values within them have a greater impact on colour reproduction. JPEG encoding can generate additional colours in images with little tonal variation, which may cause colour shifts.
- Reducing the resolution of a PNG image from 300 ppi to 250 ppi results in a loss of detail comparable to that caused by compression JPEG at level 4. Reducing it to 200 ppi results in a loss comparable to compression level 2. Therefore, high resolution is the most important factor in preserving image quality. Even reducing the resolution by as little as 20 per cent can result in a greater loss of image information than heavy JPEG compression.

5. References

Adobe Help Center (2023) *Zapisywanie plików w formatach graficznych.* Available from: https://helpx.adobe.com/pl/photoshop/using/saving-files-graphics-formats.html [accessed 20 august 2026].

Image Color Counter (2026) *Novaboard*. Available from: https://novaboard.app/tools/image-color-counter/ [accessed 20 august 2026].

Karwowski, D. (2019) Zrozumieć kompresję obrazu. Podstawy Technik kodowania stratnego oraz bezstratnego obrazów. 1st ed., version 1.3. Poznań.

Mansurov, N. (2018) *JPEG compression levels in photoshop and lightroom*. Photography life. Available from: https://photographylife.com/jpeg-compression-levels-in-photoshop-and-lightroom [accessed 20 september 2026].

Markowski, l. and Jeliński, p. (2011) 'Wyznaczanie progów wizualnej bezstratności przy kompresji oryginałów cyfrowych', *Przegląd papierniczy*, pp. 229–234.

Żurek, K. (2021) *Wpływ kompresji stratnej na jakość obrazów w formacie jpeg.* Praca przejściowa na kierunku papiernictwo i poligrafia w specjalności grafika komputerowa i technologie cyfrowe w poligrafii. Politechnika warszawska.



© 2026 Authors. Published by the University of Novi Sad, Faculty of Technical Sciences, Department of Graphic Engineering and Design. This article is an open access article distributed under the terms and conditions of the Creative Commons Attribution license 4.0 Serbia (http://creativecommons.org/licenses/by/4.0/rs/).

Original Scientific Paper https://doi.org/10.24867/GRID-2026-p57

Evaluation of Visual Aesthetics and Communication Effectiveness in Digital Advertising

ABSTRACT

Digital advertising requires visual content that simultaneously attracts users and effectively communicates information. While aesthetic quality is commonly regarded as an essential component of graphic design, its relationship with communication effectiveness has not yet been sufficiently investigated through empirical user studies. This research experimentally compares two contrasting design strategies: a design-oriented approach emphasizing visual aesthetics and an advertising-oriented approach prioritizing communication efficiency. Following an analysis of contemporary design practices, twenty advertisements covering ten thematic categories were created according to both approaches. User perception was evaluated through a structured survey measuring both message comprehension and visual attractiveness. The experimental results reveal that advertisements designed according to advertising principles consistently achieve higher communication effectiveness. Unexpectedly, these advertisements also receive higher aesthetic ratings than those designed primarily according to visual refinement. The findings indicate that communication clarity has a stronger influence on users' overall evaluation than aesthetic sophistication alone. The study contributes to a better understanding of visual communication in digital media and provides practical recommendations for balancing aesthetics and communication performance when designing digital advertising content.

Rina Petričević
Jure Ahtik

University of Ljubljana, Faculty of Natural Sciences and Engineering, Department of Textiles, Graphic Arts and Design, Ljubljana, Slovenia

KEY WORDS
Graphic design, digital advertising, visual communication, user experience, visual perception

1. Introduction

Digital media combine technological platforms with visual, textual and audiovisual content and enable interactive, two-way communication. Their accessibility and cost-efficiency have made them central to contemporary communication and marketing (Price, 2025). As digital communication has expanded, graphic design has become more than an aesthetic addition: it functions as a strategic means of organising information, building brand identity and supporting user interaction (Bočaj & Ahtik, 2023; Interaction Design Foundation, 2025; Galvan, 2026). Visual content is particularly important in digital advertising because images, typography, colour, composition and other graphic elements must attract attention while also communicating a message clearly. Effective digital content therefore depends on understanding the target audience, selecting appropriate graphic elements, maintaining brand consistency, adapting content to platforms and aligning visual decisions with communication and conversion goals (British Academy of Graphic Design, 2026; Dot iT, 2024).

Graphic design and advertising can nevertheless emphasise different priorities. A design-oriented approach may place visual quality, aesthetic refinement, innovation and user experience at the centre, whereas an advertising-oriented approach prioritises message clarity, user response, direct communication and campaign effectiveness.

In practice, successful digital communication requires a balance between these objectives.

The aim of this study was to examine how these two approaches affect message comprehension and visual preference. Three hypotheses were evaluated:

- H1, that an analysis of existing design examples can be used to establish criteria for quality-oriented and effectiveness-oriented advertising design;
- H2, that advertisements designed for communication effectiveness transmit their message more successfully than advertisements designed primarily for visual quality;
- H3, that visually refined advertisements are preferred by users over effectiveness-oriented advertisements.

2. Methods

2.1. Design approaches and stimulus development

Before producing the experimental material, examples of good practice in graphic design and advertising were analysed. These examples were divided into two groups: design-oriented examples focusing on visual attractiveness, aesthetics and quality, and advertising-oriented examples focusing on usability, effectiveness, functionality and successful communication. The analysis included contemporary identities, information design and advertising campaigns, including award-winning work (Marketing Magazin, 2022; Velkavrh, 2024; Hilder, 2025; Coggan & Wilson, 2025).

Based on the analysis of good-practice examples, the two approaches were operationalised through distinct sets of design priorities. The design-oriented approach primarily emphasised visual quality, aesthetic refinement and originality. In this condition, graphic elements such as colour, typography, composition, imagery, negative space and visual hierarchy were treated as central components of the advertisement. Greater emphasis was placed on creating a visually coherent and distinctive composition, while the communication of the advertising message could be more subtle or indirect. The visual solution was therefore not necessarily structured around the immediate recognition of the advertised product or service. Instead, the approach allowed greater freedom for experimentation, interpretation and innovative visual expression. Success was understood primarily in terms of the overall aesthetic quality, originality and visual impact of the final design.

In contrast, the advertising-oriented approach prioritised communication effectiveness and the ability of the advertisement to convey its intended message quickly and clearly. Visual elements were selected and organised primarily according to their contribution to message comprehension rather than their independent aesthetic value. Particular attention was therefore given to clear visual hierarchy, easily identifiable products or services, concise textual information and direct communication with the target audience. Where appropriate, advertisements also incorporated a clearly visible call to action (CTA) to guide users towards the intended response. Compared with the design-oriented condition, the relationship between imagery, typography and other graphic elements was consequently more functional: each element was expected to support the central message and reduce ambiguity. Success in this condition was associated with the clarity of the message, ease of interpretation, ability to attract and direct attention and the overall effectiveness of the advertisement in communicating its intended purpose.

The distinction between the two conditions did not imply that design-oriented advertisements were intended to be ineffective or that advertising-oriented advertisements disregarded aesthetics. Rather, the experimental distinction concerned the relative priority assigned to aesthetic expression and communication performance during the design process. This made it possible to examine whether advertisements developed primarily around visual quality would differ from those developed primarily around communication effectiveness in terms of both message comprehension and users' aesthetic preferences.

Twenty advertisements were created across ten thematic categories, with two advertisements per theme: one following design-oriented criteria and one following advertising-oriented criteria. Adobe Photoshop 2025 and Adobe Illustrator 2025 were used to create the advertisements. The experimental setup is shown in Figures 1–2.



» **Figure 1:** *Designed advertisements following design-oriented criteria*



» **Figure 2:** *Designed advertisements following advertising-oriented criteria*

2.2. Survey procedure

Two survey versions, A and B, were prepared. Survey A tested advertisements created according to design-oriented principles, while Survey B tested advertisements created according to advertising-oriented principles. Both surveys consisted of two parts. The first part evaluated message comprehension for the corresponding design approach. The second part was identical in both survey versions and directly compared aesthetic preferences for the design-oriented and advertising-oriented advertisements within each theme. Screenshots of the survey interface and evaluation questions are presented in Figures 3–5.



» **Figure 3:** *Steps of the first part of Survey A*



» **Figure 4:** *Steps of the first part of Survey B*



» **Figure 5:** *Steps of the second part of both surveys*

The surveys were conducted in person. The advertisements were projected on a large screen in a slightly darkened room, while respondents recorded their answers on printed questionnaires. During the comprehension task, each advertisement was displayed for four seconds before respondents answered what the advertisement promoted. During the preference task, paired advertisements remained visible without a fixed time limit so that participants could compare them before selecting the version they preferred.

A total of 94 respondents participated, with 47 assigned to Survey A and 47 to Survey B. Across the full sample, 52% were women and 48% men. Thirty per cent were aged 18–25, 18% were 26–35, 20% were 36–50 and 32% were over 50. Seventy-eight per cent used social media daily and 65% reported noticing online advertisements very often. Most respondents (79%) did not work in media or media design, 10% did and 11% reported partial involvement. Responses were entered and analysed in Microsoft Excel.

3. Results

3.1. Message comprehension

Both design approaches produced predominantly correct responses, but the advertising-oriented condition achieved a higher overall comprehension rate. In Survey A, 89% of responses to design-oriented advertisements were correct, compared with 93% in Survey B for advertising-oriented advertisements. This result supported H2: advertisements structured around communication effectiveness conveyed their messages more successfully.

Table 1

Overall message-comprehension results for the two design approaches

Condition	Participants	Correct responses	Incorrect responses
Design-oriented (Survey A)	47	89%	11%
Advertising-oriented (Survey B)	47	93%	7%

Gender differences were small. In Survey A, women answered correctly in 90% of cases and men in 88%; in Survey B, the corresponding values were 92% and 94%. The study therefore did not identify a meaningful gender-related difference in advertisement comprehension.

Some differences emerged when respondents were grouped according to their involvement with media and design.

In Survey A, respondents identified as designers achieved 96% correct answers, compared with 85% among lay respondents. In Survey B, both lay respondents and designers achieved 93% correct answers. Consequently, the advertising-oriented approach performed better among lay respondents and those partially involved with media, whereas designers achieved their highest comprehension scores with the design-oriented advertisements.

3.2. Aesthetic preference

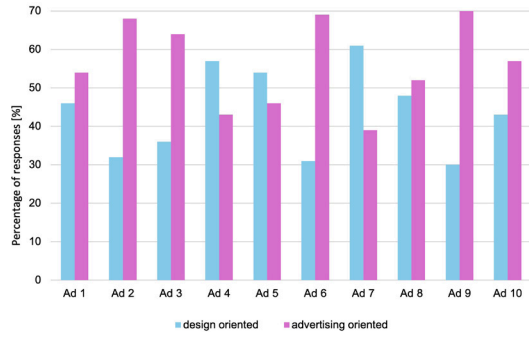
The second part of the survey directly compared paired advertisements from the two approaches. Advertising-oriented advertisements were preferred in seven of the ten thematic comparisons (advertisements 1, 2, 3, 6, 8, 9 and 10), while design-oriented advertisements were preferred in three comparisons (advertisements 4, 5 and 7). Across all comparisons, 56% of selections favoured the advertising-oriented version and 44% favoured the design-oriented version.

Table 2

Preference for design-oriented and advertising-oriented advertisements

Group	Design-oriented	Advertising-oriented
All respondents	44%	56%
Men	42%	58%
Women	45%	55%
Lay respondents	44%	56%
Designers	46%	54%

The same general preference was observed among men, women, lay respondents and designers. Men selected the advertising-oriented advertisements in 58% of comparisons and women in 55%; lay respondents selected them in 56%, and designers in 54%. These results contradicted H3, which predicted that visually quality-oriented advertisements would be preferred. The survey results comparing users' preferences for design-oriented and advertising-oriented advertisements are shown in Figure 6.



» **Figure 6:** *Preference for Design-Oriented and Advertising-Oriented Advertisements*

4. Discussion

The results indicate that communication clarity and visual appeal should not be treated as opposing objectives. Although the design-oriented condition was developed to emphasise visual quality, the advertising-oriented advertisements achieved both a higher comprehension rate and a higher overall preference score. This suggests that respondents' aesthetic evaluations were influenced not only by formal visual refinement but also by how immediately and clearly the advertisement communicated its purpose.

This interpretation is consistent with established principles of digital content creation, where visual elements are expected to support a clear goal, target audience and desired action rather than function independently of the communication task (Dot iT, 2024; British Academy of Graphic Design, 2026). Graphic design for user experience similarly requires a balance between aesthetics and usability, with typography, colour and layout adapted to users' needs and information structure (Interaction Design Foundation, 2025).

The difference in comprehension between the two conditions was relatively small—89% versus 93%—and both approaches performed well overall. The subgroup comparison also suggests that expertise may influence how visual information is interpreted: designers achieved 96% correct responses for the design-oriented advertisements, whereas lay respondents benefited more from the directness of the advertising-oriented approach. These observations support the value of designing for a defined audience rather than assuming that a single visual strategy will perform equally well for all users.

The findings should be interpreted in light of several limitations. The advertisements were created by one designer, so subjective design decisions may have affected individual comparisons. The sample of 94 participants limits generalisation, and the four-second exposure used for the comprehension task does not fully reproduce real-world digital media use. The operational distinction between 'quality-oriented' and 'effectiveness-oriented' design also depends on the criteria established from the selected good-practice examples. A broader analysis of reference material and a larger experimental sample could strengthen future studies. Despite these limitations, the study demonstrates the practical importance of integrating aesthetic and communication objectives. Contemporary digital environments require designers to respond to changing platforms, user expectations and communication goals while maintaining visual coherence and brand identity (Keyline Digital Design College, 2023; Kushwaha, 2023). The results suggest that clear hierarchy, direct messaging and functional visual choices can contribute not only to comprehension but also to perceived attractiveness.

5. Conclusions

This study compared design-oriented and advertising-oriented approaches to digital advertising, using twenty advertisements across ten themes, together with an in-person survey of 94 participants. The advertising-oriented advertisements produced a higher overall rate of correct message comprehension (93% versus 89%) and were more frequently preferred in direct aesthetic comparisons (56% versus 44%).

H1 was supported because the analysis of good-practice examples enabled the formulation of distinct criteria for the two approaches. H2 was supported because advertising-oriented advertisements communicated their message more successfully on average. H3 was rejected because respondents more often preferred the advertising-oriented advertisements rather than the visually quality-oriented alternatives.

The findings indicate that effective digital advertising depends on a balance between aesthetics and communication performance. Visual attractiveness remains important for gaining attention, but clear messaging, functional organisation and alignment with the communication objective also shape users' aesthetic evaluation. Digital content should therefore be designed so that visual quality supports, rather than competes with, the intended message.

6. Acknowledgments

The authors acknowledge all participants who took part in the user study.

7. References

British Academy of Graphic Design. (2026) *How to create effective graphic designs for social media: a guide.* Available from: https://www.graphicdesignacademy.uk/blog/how-to-create-effective-graphic-designs-for-social-media--a-guide [Accessed 21 January 2026].

Bočaj, N. and Ahtik, J. (2023) 'Effects of visual complexity of banner ads on website users' perceptions', *Applied Sciences.* 13(24), 13317. DOI: 10.3390/app132413317

Coggan, G. and Wilson, A. (2025) *30 inspiring infographics.* Available from: https://www.creativebloq.com/graphic-design-tips/information-graphics-1232836 [Accessed 10 March 2026].

Dot iT. (2024) *Exploring the essence of visual content.* Available from: https://dotit.org/exploring-the-essence-of-visual-content/ [Accessed 21 January 2026].

Galvan, M. (2026) *The history of graphic design.* Available from: https://www.flux-academy.com/blog/the-history-of-graphic-design [Accessed 20 January 2026].

Hilder, R. (2025) *These are the 13 projects that caught my eye at D&AD New Blood.* Available from: https://www.creativebloq.com/professional-development/creative-careers/new-blood-top-picks [Accessed 10 March 2026].
Interaction Design Foundation. (2025) *What is graphic design?* Available from: https://www.interaction-design.org/literature/topics/graphic-design [Accessed 16 January 2026].
Keyline Digital Design College. (2023) *Navigating the creative challenges of a graphic designer.* Available from: https://keyline.co.za/blog/navigating-the-creative-challenges-of-a-graphic-designer/ [Accessed 19 January 2026].
Kushwaha, S. (2023) *Top graphic design challenges and how to overcome them.* Available from: https://www.visualbest.co/blogs/graphic-design-challenges/ [Accessed 20 January 2026].
Marketing Magazin. (2022) *Triglav komplet.* Available from: https://www.marketingmagazin.si/opazeno/triglav-komplet [Accessed 17 March 2026].
Price, K. (2025) *What is digital media?* Available from: https://www.sessions.edu/notes-on-design/what-is-digital-media/ [Accessed 16 January 2026].
Velkavrh, Z. (2024) *Velika nagrada Brumen – celostna grafična podoba Centra Rog.* Available from: https://brumen.org/blog/velika-nagrada-brumen-celostna-graficna-podoba-centra-rog/ [Accessed 8 May 2026].

© 2026 Authors. Published by the University of Novi Sad, Faculty of Technical Sciences, Department of Graphic Engineering and Design. This article is an open access article distributed under the terms and conditions of the Creative Commons Attribution license 4.0 Serbia (http://creativecommons.org/licenses/by/4.0/rs/).

Original Scientific Paper https://doi.org/10.24867/GRID-2026-p58

Comparison of Various Least Significant Bit Modifying Methods Used for Image Data Hiding

Patricija Nakić
Aleš Hladnik

Faculty of Natural Sciences and Engineering, Department of Textiles, Graphic Arts and Design
University of Ljubljana, Slovenia

ABSTRACT

Digital communication has increased the need for techniques that protect information not only by securing its content, but also by concealing the existence of the message itself. This paper focuses on image steganography, with particular emphasis on Least Significant Bit (LSB) methods, which hide data in digital images by modifying the least significant bits of pixel values. The aim of the study is to compare selected LSB based approaches for data hiding in images and to assess their performance under different image processing conditions. The main hypothesis of this paper is that LSB based steganographic methods enable reliable extraction of hidden data from unchanged Portable Network Graphics (PNG) images, while their extraction efficiency decreases significantly when the images are exposed to processing operations that alter pixel values or image structure. At the same time, it is assumed that the use of Reed-Solomon coding can improve the resistance of hidden message when the number of errors remains limited. To test this hypothesis, three methods were examined: 1-bit LSB substitution, 2-bit LSB substitution, and an LSB method combined with Reed-Solomon error correcting coding. The comparison is performed on five selected images in the PNG format, and the stego-images are evaluated before and after different image processing operations, including Gaussian noise, blurring, image downscaling, image copying, and format conversion. The results show that all three methods provide successful extraction of the hidden message when the carrier images remain unchanged. However, the reliability of extraction is reduced after operations that modify the LSB plane or change the structure of the image. Gaussian noise negatively affects all methods, although the Reed-Solomon based approach demonstrates better resistance in cases with limited number of errors. Blurring and downscaling have the most destructive effect, while image copying and format conversion don't significantly influence extraction reliability when the pixel values remain preserved. These findings confirm that LSB steganography is suitable mainly for unchanged or losslessly preserved images, whereas its main limitation is low robustness against subsequent image processing operations..

KEY WORDS
Least significant bit, steganography, image data hiding, image processing, Reed-Solomon codes

1. Introduction

The rapid growth of digital communication has considerably increased the amount of private, sensitive and/or confidential information exchanged through digital media. Consequently, methods for protecting said information have become increasingly more important. While cryptography protects content of the information

shared by transforming it into an unreadable form, steganography aims to conceal the very existence of said information by embedding it into an apparently ordinary carrier such as an image, audio file or video (Cox et al., 2008; Fridrich, 2012). Digital images are particularly suitable carriers because of their widespread use, relatively large amount of data and inherent redundancy.

1.1. Least Significant Bit image steganography

One of the simplest approaches to image steganography is the Least Significant Bit (LSB) substitution technique. A digital pixel value can be represented as a sequence of binary digits, with the LSB having the smallest contribution to the numerical value of the pixel. Replacing this bit therefore changes an 8-bit pixel value by at most one intensity level. Such changes are usually difficult to perceive visually, making the LSB-plane suitable for hiding additional information (Altaay et al., 2012).

The method of the basic 1-bit LSB approach is computationally simple and provides relatively high embedding capacity, while also producing only minor visual changes. The capacity can be further increased by modifying two LSB instead of one. However, increasing the number of modified bits also increases the modification of the carrier data and can therefore affect both image quality and statistical detectability.

The main limitation of spatial domain LSB techniques is their relatively low robustness. Because hidden information is stored directly in the pixel values, operations such as filtering, addition of noise, image resizing and lossy compression can modify or even destroy the embedded bit stream. An efficient steganographic method represents a compromise between embedding capacity, visual invisibility and robustness against subsequent image processing procedures (Fridrich, 2012).

1.2. Increasing robustness by error-correcting codes

One possible approach to improving the robustness of LSB steganography is the introduction of error-correcting codes. Reed-Solomon (RS) codes add redundant symbols to the original data before embedding and allow a limited number of errors introduced during transmission or image processing, which is then corrected during decoding. Combining RS coding with conventional LSB embedding therefore preserves the simplicity of spatial domain techniques while providing additional protection against isolated errors in the hidden data (Fontaine & Galand, 2009).

The aim of the study was to compare three LSB-based image steganography methods, which are 1-bit LSB substitution, 2-bit LSB substitution and 1-bit LSB substitution combined with RS error correction. In addition to extraction from unchanged stego-images, robustness was examined after the addition of random noise, blurring, image downscaling, file copying and image format conversion from PNG to BMP as explained in the Methods section. The comparison focuses on successful reconstruction of the hidden message, preservation of the embedded bits and bit error rate (BER).

2. Methods

2.1. Test images and data preparation

Five standard images from the USC-SIPI Image Database (USC-SIPI Image Database, n.d.) were selected to represent different image dimensions and levels of visual complexity. Images Airplane (labeled as A), Peppers (B) and Mandrill (C) were originally 512 x 512 pixel, 24-bit TIFF images. Airplane contains comparatively large smooth regions, Peppers represents an intermediate level of edges and colour transitions, whereas Mandrill contains a large amount of fine texture and local variation. In addition, the 1024 x 1024 pixel, 8-bit grayscale Airport image (D) and the 256 x 256 pixel, 24-bit Tree image (E) were used.

Before embedding, the images were converted to the Portable Network Graphics (PNG) format in order to avoid changes of pixel values caused by lossy compression. The images were standardized to 8 bits per channel using Adobe Photoshop. During program execution, the carrier images were additionally converted to RGB mode, resulting in three 8-bit colour channel values for each pixel used by the embedding algorithms.

The same secret message: “To je skrivna informacija.” (en. “This is the secret information.”) was used for all experiments. The text was encoded using UTF-8 before converting it into its binary representation. For the conventional 1-bit and 2-bit LSB methods, a 32-bit header containing the length of the message and a 32-bit CRC32 checksum were added to the data. The header allowed the extraction algorithm to determine the required number of bits, whereas CRC32 was used to verify the integrity of the reconstructed message.

2.2. Implementation of the LSB methods

All embedding and extraction algorithms were implemented in Python (version 3.13) and executed in its IDLE environment. The Pillow library was used for image handling, NumPy for array manipulation and bitwise operations and the Python zlib module for CRC32 calculation. RS coding was implemented using the reedsolo package.

For 1-bit LSB substitution, the RGB image was converted into a NumPy array and flattened into a one-dimensional sequence of colour channel values. The header, that is the CRC32 value and UTF-8 message were converted into binary form and joined into a single payload. The least significant bit of each successive channel value was cleared using a bitwise & (and) operation and replaced by the corresponding payload bit using bitwise | (or) operation. So one message bit was stored in each colour channel value. For 2-bit LSB substitution the general procedure remained unchanged, but the payload was divided into two bit symbols. The 32 bit header and CRC32 checksum were retained, while twice as many payload bits could be stored in each image channel value.

For the RS LSB method the UTF-8 encoded message was first protected using RS coding before 1-bit LSB embedding. 16 RS correction symbols were added using RSCodec(16). A 32-bit header containing the length of the RS coded message was placed before the encoded payload, after which the complete bit stream was embedded into the least significant bits of the image channel values. During extraction the header was first recovered, followed by the specified number of encoded bits. The extracted binary data was converted back to bytes and passed to the RS decoder, which attempted to correct errors before reconstructing the original message

2.3. Performance indicators

Performance of the three steganographic methods was evaluated using several complementary indicators (metrics) describing the correctness and robustness of message extraction. The primary quantitative metric was BER (Bit Error Rate) (Malathi & Gireesh Kumar, 2025). BER is calculated as

$$BER = \frac{N_{error}}{N_{total}} \quad (1)$$

where N_error is the number of incorrectly recovered message bits and N_total is the total number of bits in the original message. A BER of 0 corresponds to error free recovery, while increasing BER values indicates a progressively larger proportion of incorrectly extracted bits.

The percentage of preserved bits was derived from BER according to:

$$P_{preserved} = (1 - BER) \times 100\% \quad (2)$$

100% preserved bits corresponds to BER = 0, while lower percentages indicate increasing degradation of the embedded message.
Extraction was additionally evaluated according to the message matching, classified as complete, partial or absent. For the 1-bit and 2-bit LSB methods, the validity of the extracted header and the result of the CRC32 integrity check were also recorded. The header stored information required for determining the length of the embedded message and managed to enable the extraction algorithm to identify the relevant part of the bit stream.

The integrity of the extracted message was verified using CRC32. The CRC32 value was stored together with the hidden data and subsequently compared with the value calculated from the extracted message. The use of a CRC field as part of the data structure is consistent with the CRC32 mechanism described in the GZIP file-format specification (Deutsch, 1996).

In the present implementation, CRC32 calculation was performed using functionality provided by the Python zlib library (Python documentation, 2026). CRC32 was used solely as an integrity check and did not provide error correction. Therefore, failure of the CRC32 check was treated as evidence that the extracted data or the stored checksum had been altered.

For the RS-LSB method, RS decoding was included as an additional performance indicator. The combination of LSB image steganography and RS coding has been specifically proposed as a means of increasing the robustness of hidden-data recovery (Raiyan & Kabir, 2025).

RS coding was used because its additional redundancy can improve steganographic schemes by allowing corrupted encoded data to be reconstructed under suitable error conditions (Fontaine & Galand, 2009).

The correction capability is nevertheless limited. RS decoding can recover the encoded information only when the number and distribution of errors or erasures remain within the correction capability of the applied code (Jing et al., 2022). In the implemented procedure, the extracted bit stream was converted into RS coded bytes and passed to the decoder, which attempted to correct errors before reconstructing the original message.

For this reason, successful final message recovery was evaluated separately from the raw BER in the RS-LSB method. A nonzero BER in the encoded data does not necessarily imply unsuccessful extraction, since the RS decoder may still reconstruct the original message if the introduced errors are correctable. Conversely, failure of RS decoding was treated as unsuccessful extraction.

When the extraction algorithm could not retrieve enough bits from the modified image, extraction was classified as unsuccessful and BER and the percentage of preserved bits were not reported.

3. Results

3.1. Visual comparison of original and stego-images

No visually noticeable differences were observed between the original images and the corresponding stego-images after message embedding with any of the three methods. Across all five test images, the embedded data did not produce visible changes that could be identified by direct visual inspection.

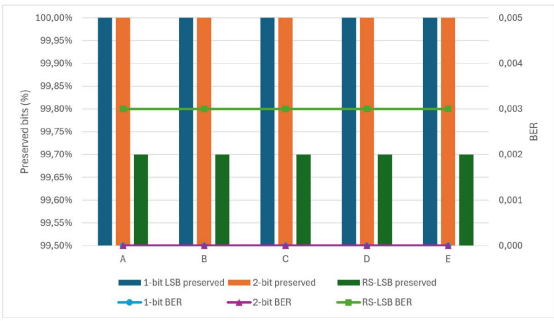
3.2. Extraction from unmodified stego-images

For the unmodified stego-images, all three methods achieved complete message recovery for all five test images. For the 1-bit and 2-bit LSB methods, the extracted headers were correct, and CRC32 verification was successful in every case. For the RS-LSB method, RS decoding was successful for all five images.

The percentage of preserved message bits was 100% and BER was 0.0 for all images and all three methods. Complete agreement between the extracted and original message was therefore obtained for all images that were not subject to an image processing operation.

3.3. Effect of noise

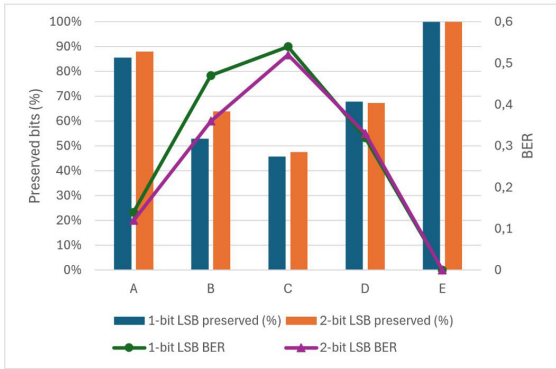
After Gaussian noise with a value of 0.005 was applied, all three methods succeeded in recovering the complete hidden message from all five images. The percentage of preserved bits remained 100%, and BER was 0.0 for every combination of image and method. For both the 1-bit and 2-bit LSB methods, the extracted header was correct, and CRC32 verification was successful for all five images. RS decoding was also successful for every image processed using the RS-LSB method. Thus, under this low noise level no differences in final message recovery were detected among the three methods studied.
At a higher Gaussian noise level of 0.01, complete message matching was again obtained for all five images and all three methods (Fig. 1). However, differences were observed for the individual performance indicators. For the 1-bit and 2-bit LSB methods, the extracted header remained correct for all images. The preserved bit percentage was 100% and BER remained 0.0. CRC32 verification, however, failed in all five cases for both methods. For the RS-LSB method, RS decoding was successful for all five images. The percentage of preserved bits was 99.7%, corresponding to a BER of 0.003. Despite this non-zero BER value, the final decoded message completely matched the original message in all cases.



» **Figure 1:** *Percentage of preserved bits after adding Gaussian noise (noise 0.01)*

3.4. Effect of blurring

Blurring with a radius of 0.4 produced a wide range of extraction results for the 1-bit and 2-bit LSB methods (Fig. 2). For images A-D, no method was able to achieve complete message recovery.

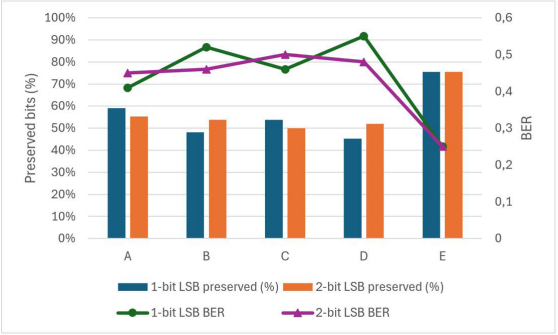


» **Figure 2:** *Percentage of preserved bits after image blurring (blur 0.4)*

For the 1-bit LSB method, the preserved bit percentage ranged from 45.7% to 85.6% for images A-D. The corresponding BER values ranged from 0.14 to 0.54. For the 2-bit LSB method, the preserved bit percentage for images A-D ranged from 47.6% to 88.0%, while BER ranged from 0.12 to 0.52. Image E differed from the other four images. For both the 1-bit and 2-bit LSB methods, the extracted header was incorrect, but complete message matching was obtained when the known message length was used during evaluation. The preserved-bit percentage was 100% and BER was 0.0 with both methods. For the RS-LSB method, extraction could not be performed for any of the five blurred images. The program returned an error indicating that the image did not contain enough bits for message extraction.

3.5. Effect of image downscaling

After image downscaling by a factor of 0.95, complete message recovery was not achieved for any of the three methods. For both 1-bit and 2-bit LSB methods, the extracted headers were incorrect for all five images and CRC32 verification failed in every case.



» **Figure 3:** *Percentage of preserved bits after image downscaling (downscale 0.95)*

For the 1-bit LSB method, the percentage of preserved bits ranged from 45.2% to 75.5%. The corresponding BER values ranged from 0.25 to 0.55. For the 2-bit LSB method, preserved-bit percentages ranged from 50.0% to 75.5%, with BER values between 0.25 and 0.5. For the RS-LSB method, extraction could not be completed for any of the five downscaled images.

3.6. Effect of image copying

After image copying, identical extraction results were obtained for all five test images and all three methods. The complete message was recovered in every case, the preserved-bit percentage was 100%, and BER was 0.0. For the 1-bit and 2-bit LSB methods, the extracted headers were correct, and CRC32 verification was successful for all images. For the RS-LSB method, RS decoding was successful in all five cases.

3.7. Effect of image format conversion

After conversion from PNG to BMP, complete message recovery was obtained for all five test images and all three methods. The preserved bit percentage remained 100% and BER was 0.0 in every case. For both the 1-bit and 2-bit LSB methods, the extracted headers were correct, and CRC32 verification was successful for all five images. For RS-LSB, RS decoding was successful in every case.

The measured extraction results after PNG to BMP conversion were therefore identical to those obtained for the unmodified stego-images as well as for copied images.

4. Discussion

The results demonstrate that the investigated LSB approaches are highly reliable as long as the pixel values and their ordering remain unchanged. The perfect extraction obtained from unmodified images, copied images, and images converted from PNG to BMP is consistent with the spatial nature of LSB embedding: when the underlying RGB values are preserved, the embedded least significant bits remain available to the extraction algorithm. Importantly, the format conversion result applies specifically to the lossless PNG to BMP conversion tested here and should not be generalized to lossy formats such as JPEG.

Noise produced a different type of disturbance. At the lower tested level, no measurable message errors occurred. At a Gaussian noise level of 0.01, the distinction between data integrity and final message recovery became more apparent. In the 1-bit and 2-bit methods, the message bits themselves remained unchanged, as reflected by BER = 0, although CRC32 verification failed. This combination is consistent with corruption of the separately embedded CRC32 value rather than the message payload itself. Consequently, CRC32 should not be used as the sole measure of extraction performance but should be interpreted together with BER and direct message matching.

The RS-LSB method behaved differently at the same noise level. Although a small number of bit errors was detected (BER = 0.003), RS decoding recovered the original message perfectly. Here we can see the clearest advantage of RS-LSB observed in the experiment: error correcting redundancy can compensate for a limited number of bit errors. The advantage is therefore not necessarily reflected in a lower BER, but in the ability to reconstruct the correct final information despite those errors.

Blurring and downscaling represented much more severe disturbances. Unlike isolated bit modifications, both operations alter pixel values systematically and, in the case of downscaling, also change the spatial organization and number of pixels. Since the investigated methods depend on reading specific least significant bits in the expected sequence, these transformations disrupt the structure required for extraction.
This also explains why RS coding provided no practical benefit under these conditions. Error correction is useful when the encoded bit stream can still be retrieved and the number of errors remains within the correction capability of the code, but it cannot recover information when the bit stream structure itself can no longer be read correctly.

The apparently successful recovery from blurred image E requires particular caution. Although the message was recovered with BER = 0, its header was incorrect. During evaluation, the actual message length was known in advance, allowing the correct section of the extracted bit stream to be selected independently of the corrupted header. Under normal extraction conditions, in which the message length is unknown, such recovery would not be reliable. The result for image E should therefore not be interpreted as evidence of genuine robustness to blurring.

No clear robustness advantage of the 2-bit LSB method over the 1-bit method was observed. Its primary advantage is increased embedding capacity rather than improved resistance to image processing. RS-LSB provided an advantage specifically when the disturbance produced a limited number of correctable errors, but it retained the fundamental vulnerability of spatial LSB embedding to transformations that modify pixel values or their arrangement. Overall, the results are related to two types of post-processing: operations that preserve the pixel data, for which all three methods remained reliable, and operations that modify the pixel structure, for which extraction became unreliable.

5. Conclusions

All three investigated LSB methods provided reliable message extraction when the carrier image remained unchanged or underwent operations that preserved its pixel values. Under these conditions, the 1-bit LSB, 2-bit LSB and RS-LSB methods all achieved error-free message recovery.

RS coding improved robustness when a limited number of bit errors was introduced, as demonstrated under the higher tested noise level, where the original message was fully recovered despite a nonzero BER. However, this protection was ineffective against blurring and downscaling because these operations disrupted the pixel values and/or spatial organization required for correct reconstruction of the embedded bit stream.

Accordingly, none of the three methods can be regarded as universally superior. The 1-bit LSB method offers the simplest implementation, the 2-bit method provides greater embedding capacity, and RS-LSB adds tolerance to a limited number of bit errors. The appropriate choice therefore depends primarily on the expected post-processing of the carrier image and on the required balance between embedding capacity and robustness. The findings further emphasize that the demonstrated resistance to format conversion applies only to the tested lossless PNG to BMP conversion and cannot be extended to lossy image formats without additional testing.

6. References

Altaay, A.A.J., Sahib, S.B. and Zamani, M. (2012) 'An Introduction to Image Steganography Techniques'. In: *Proceedings of the International Conference on Advanced Computer Science Applications and Technologies*, ACSAT 2012, 26–28 November 2012, Kuala Lumpur, Malaysia. IEEE Computer Society, pp. 122–126.

Cox, I.J., Miller, M.L., Bloom, J.A., Fridrich, J. and Kalker, T. (2008) *Digital Watermarking and Steganography*. 2nd edition. Burlington: Elsevier Inc.

Deutsch, P. (1996) GZIP file format specification version 4.3. IETF Datatracker. Available from: https://datatracker.ietf.org/doc/html/rfc1952 [Accessed 23 April 2026].

Fontaine, C. and Galand, F. (2009) 'How Reed-Solomon Codes Can Improve Steganographic Schemes', *EURASIP Journal on Information Security*, 2009(2), pp. 1–10. DOI: 10.1155/2009/274845

Fridrich, J. (2012) *Steganography in Digital Media: Principles, Algorithms and Applications*. 1st edition. Cambridge: Cambridge University Press.

Jing, Z., Choi, H. and Song, H.Y. (2022) 'Decoding Process of RS Codes with Errors and Erasures: An Overview', *The Journal of Korean Institute of Communications and Information Sciences*, 47(11), pp. 1747–1754. DOI: 10.7840/kics.2022.47.11.1747

Malathi, P. and Gireesh Kumar, T. (2025) 'Deep Steganographic Approach for Reliable Data Hiding Using Convolutional Neural Networks and Adaptive Loss Optimization', *Scientific Reports*, 15(1). DOI: 10.1038/s41598-025-26867-4

Python Software Foundation. (no date) *Python documentation – zlib — Compression compatible with gzip*. Available from: https://docs.python.org/3/library/zlib.html [Accessed 24 April 2026]

Raiyan, S.R. and Kabir, M.H. (2025) 'SCreedSolo: A Secure and Robust LSB Image Steganography Framework with Randomized Symmetric Encryption and Reed Solomon Coding', *Pattern Recognition and Computer Vision*, ACPR. DOI: 10.48550/arXiv.2503.12368

University of Southern California, Signal and Image Processing Institute. (no date) *USC-SIPI Image Database*: Volume 3: Miscellaneous. Available from: https://sipi.usc.edu/database/database.php?volume=misc [Accessed 23 April 2026]



© 2026 Authors. Published by the University of Novi Sad, Faculty of Technical Sciences, Department of Graphic Engineering and Design. This article is an open access article distributed under the terms and conditions of the Creative Commons Attribution license 4.0 Serbia (https://creativecommons.org/licenses/by/4.0/deed.en).

Original Scientific Paper https://doi.org/10.24867/GRID-2026-p59

The Effect of Avatar Realism on Character Resemblance, Enjoyment, and Data-Safety Concern in Self-Avatar Video Games

ABSTRACT

This paper investigates whether the degree of visual realism of a player's self-avatar affects user experience in video games, building on a 2024 pilot study (Kerac et al., 2024). While the original study used a third-person runner game with lower-fidelity avatars generated through Ready Player Me, the present study applies the same experimental paradigm to a third-person shooter game using Avaturn, a newer and more realistic avatar-creation platform. Responses from two temporally separated samples (2024, n = 17; 2026, n = 36) were compared on perceived character resemblance, enjoyment of the character-creation process, attitudes toward applying this approach to other media, and privacy concerns, alongside gaming skill level as a control measure. Data were analyzed using the Mann-Whitney U test due to violations of normality. No statistically significant differences were found between groups on any of the measured variables, including character resemblance (p = .724), enjoyment of the creation process (p = .571), attitudes toward other media (p = .761), or privacy concern (p = .165), and the two samples were comparable in gaming skill level (p = .163). These findings suggest that, at least within this sample, increased avatar realism alone does not produce a measurably different user perception.

Jelena Kerac
Tamara Ilić
Neda Milić Keresteš
Sandra Dedijer
Bojan Banjanin

University of Novi Sad, Faculty of Technical Sciences, Department of Graphic Engineering and Design, Novi Sad, Serbia

KEY WORDS
Digital avatars, avatar realism, identification, user experience, data privacy

1. Introduction

Digital avatars have become an integral part of contemporary interactive media, from video games and virtual reality to social platforms and online shopping. With the development of digital technologies that aid in creating three-dimensional models based on user photographs, as well as generative models with the same practical use, it can be observed that the degree of virtual realism of avatars is increasing.

This rapid growth over that past half a decade raises the question of how this change affects user experience and importantly for this particular paper, player's sense of identification with their own digital representative.

Existing research indicates that avatars are not purely aesthetic elements, but significantly influence users' attention, engagement and behaviour (Kao & Harrell, 2015), and that the process of identification with an avatar is dynamic and dependent on a range of factors, including the authenticity of the experience, the narrative description of the character as well as the interactivity of gameplay. However, researchers in the field have not reached a consensus on whether, and to what extent, a given type of avatar affects the experience in digital environments.

This paper builds on a pilot study conducted in 2024 (Kerac et al., 2024), which used an experimental third-person-perspective (3PP) runner-type game featuring

avatars of a lower degree of realism, created via the Ready Player Me platform. In this paper, the same experimental paradigm, adapted to the shooter genre (3PP shooter), is applied using a newer, more realistic avatar-creation platform, Avaturn ("Avaturn | Realistic 3D avatar creator," n.d.). By comparing the responses of participants from two temporally separated data-collection cycles (2024 and 2026), the paper aims to examine whether and how the degree of avatar realism together with a simultaneous change in game genre, story depth, environmental realism, and the way players are onboarded into the game affects the perception of character-player resemblance, enjoyment of the character-creation process itself, attitudes toward extending this approach to other media, and concern for privacy.

In this paper besides introduction and conclusion, there are four other sections. In section two, the relevant literature is displayed, in section three the experiment design and setup, together with the participants' data is showcased. Section four serves as the results showcase, while section five displays discussion of the results together with the limitations.

2. Background

As with other products, user experience in games has no single definition that everyone agrees with. The experience of playing a game can be viewed as a subjective relationship between the player and the game, one that goes beyond the technical-technological implementation of the game (Bernhaupt, 2015). Since this relationship is subjective, it is almost impossible to define (Popper, 1994; Bernhaupt, 2015).

Unlike other interactive products, a game alongside its user interface has one more dimension, which occupies a significantly different space in user-experience research compared to other products that are focused on the user interface and data architecture.

2.1. The Concept of a Video Game

(Bergonse, 2017) managed to reduce the definition of a video game to five points. First, a game enables interaction between a computer, a player, and in some cases multiple players; then, this interaction takes place in a fictional context formed in the player's mind through interaction and the recognition of visual patterns on the screen, as well as the relationship between input via some of the computer's peripheral devices and the actions produced by that input. These patterns are defined by a collection of instructions in the form of computer code or hardware. "Interaction is sustained through the player's emotional attachment and the outcomes of their actions within this functional context" (Bergonse, 2017).

If we look at the user experience according to (Klimmt et al., 2008; Klimmt et al., 2009), it could be studied through player enjoyment and is based on three factors:

5. the experience of the game's feedback,
6. recurring feelings of relief and tension, and
7. fascination stemming from being drawn into a fictional or new world.

Thus, control, tension and relief (which for the sake of this this paper be viewed through flow) and immersion are, according to (Csikszentmihalyi, 1990; Murray, 1998; Brown, 2004; Ermi & Mäyrä 2005; Klimmt et al., 2008; Klimmt et al., 2009; Calleja, 2012), among the basic pillars of user, i.e., player, experience in video games.

2.2. Identification and Its Effects as an Element of User Experience

Avatars and digital characters do not have a purely aesthetic role; they significantly affect users' attention, engagement and thinking, both in interactive media and video games and in educational settings (Kao & Harrell, 2015).

This influence largely stems from the fact that users tend to identify with digital characters. Identification represents an imaginative process through which an audience member or player adopts the identity, goals and perspective of a given character, and it is clearly distinct from simply rooting for or liking a character (Cohen, 2001).

In video games, identification with an avatar is not constant, rather, it becomes dynamic and depends on the player's current state. Factors that promote and reinforce this process include, among others, the authenticity of the experience during play (Christoph et al., 2009), the narrative definition of the character, which increases the implicit association between the character and the player's self-concept (Klimmt et al., 2010), interactive gameplay (Hefner et al., 2007), and the flow effect (Chen & Koek 2020).

Although a player can identify with several different elements during play, such as the game itself, the group of players, or the avatar, the focus of this process remains on the connection between the user and their digital representative. A high level of identification with the avatar can reliably predict deeper immersion in the game, adopting the role of the character, escapism, but also the occurrence of specific psychological effects (Van Looy et al., 2010).

Besides its effect on engagement with the game, identification also carries certain effects with it, such as stereotype threat, the Proteus effect, social presence, and the psychological sense of salience in the mind or memory.

The effect of salience in the mind or memory (Avatar Identity Salience, AIS) strengthens the association of avatar traits, i.e., it plays a part in using remembered examples to understand and create the categories to which the avatar belongs (Harrell, 2009). Social presence is understood as the influence of social and para-social interactions occurring over the internet in the situations for learning and performing in a digital environment (Kreijns et al., 2022). The Proteus effect is an effect that occurs at the personal level and can lead to a change in an individual's behaviour so that it comes to match the avatar's presentation (Yee & Bailenson, 2007), for example, if a player in a game plays as an avatar that appears to do good deeds, the players themselves will also start doing good deeds (Happ et al., 2013).

Stereotype threat is an effect that, unlike the Proteus effect, is external, that is, if a player has the feeling that other players hold a negative image of them, they themselves will start to behave in accordance with that image. For example, a person performs worse when playing with an avatar belonging to the same stereotyped group as themselves (for instance, it is thought that women are bad at shooting games, so a woman playing with a female character may, because of this, get a worse result) (Kaye et al., 2018). Fraser et al. (2024) examined whether users within a virtual environment prefer more or less realistic characters. They concluded that there is no statistically significant difference between stylized and more realistic characters. (Mull et al., 2015) concluded that people would rather interact with avatars they find attractive, and that such avatars receive a higher level of trust. Imangi et al. (2025) reached a similar conclusion, finding that participants trusted attractive avatars more, perceiving them as likeable and conveying a sense of authority.

2.3. Choice of Game Perspective in the Context of Player-Resembling Characters

In order to better understand whether there is a preferred point of view for the player in digital and virtual environments (VE), this section reviews literature dealing with computer games and other computer-based interactive multimedia, as well as literature examining the player perspective in virtual reality (VR).

Won & Zhou (2024) investigated whether playing in first-person perspective (1PP) increases player movement in virtual reality, and whether 1PP offers an advantage in promoting the mimicking of a digital avatar's movement. Moreover, they also examined the influence of a lookalike avatar on users' movement and mimicking. They found no significant difference in movement or mimicking between the use of a lookalike avatar and a non-lookalike avatar. Another interesting question for research in digital and virtual environments is whether first-person perspective or third-person perspective (3PP) offers superior spatial understanding and more intuitive movement for participants with varying levels of gaming experience. According to Wang et al. (2025), 3PP helped increase spatial awareness and cooperation in larger-scale, complex tasks in VR. They also found that 3PP allowed for higher social presence. Regarding the feeling of ownership over the digital avatar, Gorisse et al. (2019) found that the first-person perspective is the more favourable one. However, they note that ownership scores remained notably high in the third-person perspective as well. Dufresne et al. (2026) conducted a comparative study of avatar embodiment and identification in 1PP VR and a 3PP mobile game. Of particular significance for this paper, they found that while 1PP VR grants higher embodiment along with embodiment-related identification, owing to higher avatar ownership, embodiment in 3PP on mobile was achieved through similarity identification, and possibly wishful identification. These findings suggest that when researching avatar identification through similarity or lookalike avatars, a 3PP non-VR experience represents a valid methodological approach.

2.4. Sense of Security in the Context of Data Protection

Users' privacy concerns can be directed toward two "addresses": the first is toward other users of the platform (for example, whether another social-network user will misuse published data), and the second is toward the platform itself (Waldman, 2016). The second "address" is the one of interest in this paper, since the platform used in both studies is not a social-networking platform.

However, users were still required to take a photograph of themselves and upload it to the platform in order to generate their in-game character. Madden (2014) reports that a large majority (91%) of respondents (based in the US) agree that users have lost control over how companies collect their personal data, while 80% of them are concerned about how businesses and advertising companies use that data. On the other hand, over 50% of respondents in Madden's study are willing to share their personal data with such companies if it means they can use their services for free.

2.5. Research Questions and Hypothesis

Following the literature review, the following research questions were formulated:

- RQ1: Do respondents who used the newer, more realistic avatar-creation system judge their character to resemble them more, compared to respondents who used the older, less realistic system?
- RQ2: Does the degree of enjoyment of the character-creation process itself differ between the two versions of the system?

- RQ3: Does the attitude that other media should also adopt this way of creating characters differ between the two versions?
- RQ4: Does the degree of privacy concern differ between the two versions of the system?
- RQ5: Are the two samples comparable in terms of demographic characteristics and gaming experience (gender, gaming habits, skill level), so that any differences in attitudes can be attributed to the avatar system rather than to differences in sample composition?

Following the literature, specifically building on to the knowledge of (Fraser et al., 2024) the following hypothesis is set:

- H1: The level of realism in digital avatars in video games should not impact the preference of players when it comes to the adaption of technology as long as players do not report high worry towards data safety.

The research questions were formulated with the intent of examining whether the different level of realism of the characters the players played with, and the different game design, affects how much players identify with the character, how much they like the way the character is made, and whether it affects concern for security/privacy.

3. Experiments and design

This chapter addresses the design of the experiment, both the stimulus, i.e., the game used in the experiment, and the setup of the environment in which the experiment took place.

The purpose of this paper is to compare players' self-avatar characters when using the Avaturn platform, which produces more realistic characters, versus the Ready Player Me platform, which produced less realistic characters. The experiment that used the Ready Player Me platform was published two years ago, and the game design, methodology, and participant information can be found in (Kerac et al., 2024).

This video game was purpose-built as a software tool for conducting empirical research in the field of user experience and for measuring neurophysiological responses during interaction with digital avatars.

The 2026 experiment used a third-person shooter set in a dark, post-processed environment designed to evoke an abandoned, post-apocalyptic arena. Onboarding was handled diegetically rather than breaking immersion with external menus, instructions were integrated into the world via a wall-mounted board, which also directed players to create their avatar on the Avaturn platform. Pictograms on the board distinguished hostile non-playable characters, NPCs (red smoke, "KILL") from friendly ones (blue smoke, "FRIEND").

Gameplay was structured into rounds and waves, with enemy timing randomized on each playthrough. Entities were split into a red (enemy) and blue (friendly) team, spawning in fixed zones and advancing toward the player along a central path until clicked on by player ("shoot") or until it crossed a red line. Central to the experiment was avatar integration for NPCs: each player's Avaturn-generated 3D model was stripped of its controls and colliders by a custom script, turning it into a visual "shell" used for enemy and ally NPCs. Non-functional decorative elements (furniture, plants, terrain features) were added purely to help players suspend disbelief in an otherwise absurd premise of occasionally being "attacked" by NPCs wearing their own face.

Player flow was roughly the same for each experiment participant. The game followed these steps:

Terms of participation → Avaturn privacy terms → select/create avatar → QR-code photo capture → body/skin selection customization → hair customization → clothing choices → glasses → shoes → return to game (Next) → preview clone (C key) → start game (R key).

For the first 5 minutes, NPCs are faceless, distinguished only by team-colored smoke. After 340 seconds, player-modeled entities begin appearing sporadically (red team roughly twice as often as blue).

The experiment took place in the measurement laboratory of the Department of Graphic Engineering and Design, Faculty of Technical Sciences, University of Novi Sad, using: one computer, two laptops, keyboard, mouse, monitor, mbt EEG smart headsets, and a Pupil Labs eye tracker. The room was air-conditioned and dimly lit, with comfort checked with each participant. Participants received water and a snack, and signed a consent form (with an optional photo-consent clause) before beginning. Compensation was either course credit or payment equivalent to half an hour's wage; participation was voluntary and withdrawal possible at any time, including opting out of any piece of equipment.

3.1. Participants

A total of 36 participants took part in the study. The majority of participants were female (N = 29, 80.6%), while male participants made up a smaller part of the sample (N = 7, 19.4%).

In terms of age structure, the sample predominantly consisted of a younger population. The largest number of participants belonged to the 18 – 24 age group

(N = 32, 88.9%). A smaller number of participants were aged 25 – 30 (N = 3), while only one participant belonged to the 50 – 65 age group. In line with the age structure, the participants' educational profile indicates that they are primarily students. 32 participants (88.9%) reported that they were currently studying. Two participants hold a master's degree, one holds a doctorate, and one has completed secondary school.

In addition to demographic characteristics, data on participants' gaming habits were also collected. The largest group of participants (N = 13, 36.1%) stated that they played computer games when they were younger but no longer play them. On the other hand, a quarter of the sample (N = 9, 25%) are regular players who play video games several times a week. The remaining participants play games less often than once a month (N = 5), at least once every two weeks (N = 4), at least once a month (N = 2), or at least once a week (N = 1). Two participants stated that they never play, nor have ever played, computer games.

On a five-point scale assessing their own video-game playing ability (skill), where 1 is the lowest and 5 the highest rating, the average rating was 3.17 (SD = 1.01). The largest number of participants rated their skill with an average score of 3 (N = 14).

Finally, participants answered questions about their experience of their in-game avatar using a five-point scale (0 = not at all, 4 = completely). On the statement that the in-game character resembled them, participants gave an average rating of 2.97 (SD = 1.11), indicating moderate to fairly strong agreement. In addition, participants largely enjoyed the way the character was created, reflected in a high average rating of 3.33 (SD = 0.96) for this item.

4. Results

Participants' responses were placed into two groups. The Old group consists of responses recorded in 2024, while the New group consists of responses collected in 2026.

Data were analysed using Jamovi. Prior to the primary analysis, the assumptions for parametric tests were checked. The Shapiro-Wilk normality test showed that the response distributions significantly deviated from a normal distribution for all examined variables (SkillLevel: $W = 0.95$, $p = .035$; Q1_Resemblance: $W = 0.85$, $p < .001$; Q2_Like: $W = 0.76$, $p < .001$; Q3_OtherMedia: $W = 0.83$, $p < .001$; Q4_Privacy: $W = 0.88$, $p < .001$), which was expected given the ordinal nature of the scale (0 – 4) and the pronounced clustering of responses at higher scale values. Levene's test of homogeneity of variances did not show significant deviations for any variable (all $p > .09$), meaning the assumption of homogeneity of variance was not violated.

Because the normality assumption was violated, the Mann-Whitney U test was used as the primary test of between-group differences.

Descriptive statistics show that participants from both groups gave, on average, similar responses. For the New group, the median rating of character resemblance (Q1) was 3 ($M = 2.97$, $SD = 1.11$), while for the Old group ($n = 17$) the median was also 3 ($M = 3.12$, $SD = 0.99$). Similarly, enjoyment of the character-creation system (Q2) had a similar median in both groups (New: $M = 3.33$, $SD = 0.96$; Old: $M = 3.53$, $SD = 0.72$), as did the attitude toward applying such a system in other media (Q3), where the median was also 3 in both groups (New: $M = 3.03$, $SD = 1.06$; Old: $M = 3.12$, $SD = 1.05$). The only difference in medians was recorded for privacy concern (Q4), where the New group had a median of 1 ($M = 1.33$, $SD = 1.15$) and the Old group a median of 0 ($M = 1.00$, $SD = 1.41$). Gaming skill level (SkillLevel) was likewise comparable between groups (New: Mdn = 3, $M = 3.17$, $SD = 1.01$; Old: Mdn = 3, $M = 2.71$, $SD = 1.40$).

The Mann-Whitney U test did not show statistically significant differences between the groups for any of the examined variables. For character-resemblance rating (Q1_Resemblance), the difference was not significant, $U = 288.00$, $p = .724$, rank-biserial correlation $r = .06$. For enjoyment of the character-creation system (Q2_Like), the difference was also not significant, $U = 279.50$, $p = .571$, $r = .09$. For the attitude toward applying the system in other media (Q3_OtherMedia), no significant difference was found, $U = 290.50$, $p = .761$, $r = .05$. For privacy concern (Q4_Privacy), the difference did not reach statistical significance, although it showed a somewhat larger, small-to-moderate effect, $U = 235.50$, $p = .165$, $r = -.23$. Finally, gaming skill level (SkillLevel) did not differ significantly between groups, $U = 228.00$, $p = .163$, $r = -.23$, confirming that the samples are comparable on this characteristic.

5. Discussion and limitations

The results of this study provide no evidence that the perceived resemblance of the character, enjoyment of the avatar-creation process, attitude toward applying this approach in other media, or privacy concern differ statistically significantly between participants who used the older, less realistic avatar system and those who used the newer, more realistic system. These findings suggest that, at least based on this sample, increased avatar realism by itself does not lead to a measurably different user perception along the dimensions examined.

RQ1 (character resemblance): No, respondents who used the newer, more realistic system (Avaturn) did not judge their character to resemble them more than those who used the older system.

Median resemblance ratings were identical across groups (Mdn = 3 for both), and the Mann-Whitney test found no significant difference, U = 288.00, p = .724, r = .06.

RQ2 (enjoyment of the creation process): No, enjoyment of character creation did not differ significantly between versions, U = 279.50, p = .571, r = .09. Both groups rated this highly, which likely reflects a ceiling effect, the creation process was well-liked regardless of which platform was used, leaving little room for a realism-driven difference to emerge.

RQ3 (attitude toward extending the approach to other media): No significant difference was found, U = 290.50, p = .761, r = .05. Both groups showed similarly favorable attitudes (median of 3 in both), indicating that enthusiasm for seeing this style of avatar creation adopted elsewhere is not contingent on how realistic the specific system experienced was.

RQ4 (privacy concern): Privacy concern did not differ significantly between versions, U = 235.50, p = .165, though this produced the largest effect size in the study (r = −.23, small-to-moderate), with the New (more realistic) group trending toward slightly higher concern (Mdn = 1, M = 1.33) than the Old group (Mdn = 0, M = 1.00). This result is a possible signal, while it did not reach significance, possibly due to the unequal and modest sample sizes (n = 36 vs. n = 17), it should motivate for future research in the field of data gathering. It is unclear in this experiment if the change is due to the avatar realism, or general lack of trust in digital companies collecting such personal data that has been occurring in the past two years globally.

RQ5 (sample comparability): The samples were comparable in terms of gaming skill level, indicating that differences in participants' gaming experience likely did not act as a hidden factor that could explain the absence of differences in the attitudes examined. Similarly they are comparable in terms of education and somewhat in age.

The results lend support to H1. Neither the enjoyment of the character-creation process (Q2) nor the attitude toward extending this kind of avatar system to other media (Q3) differed significantly between the Old (less realistic) and New (more realistic) groups, U = 279.50, p = .571 and U = 290.50, p = .761 respectively. Following Q2 and Q3 results, avatar realism, on its own, did not shift how favorably participants viewed the system or their willingness to see it applied elsewhere.

Privacy concern (Q4) was low in both groups (medians of 0 – 1 on a 0 – 4 scale) and did not differ significantly between them, U = 235.50, p = .165, even though it produced the largest effect size of any variable (r = –23, small-to-moderate). In other words, the condition specified in H1 was satisfied for this sample: nobody reported high privacy worry.

Several methodological limitations must be taken into account when interpreting these results. First, and most importantly, the groups differ in the game genre (runner versus shooter) and in the two-year time gap between data-collection periods.

Because of this, even if significant differences had been found, it would not be possible to confidently attribute them solely to avatar realism rather than to game genre or some other factor.

Second, the sample sizes were unequal (n = 36 versus n = 17), which reduced the statistical power of the tests, particularly for the Old group. This is especially relevant to the result for privacy concern, where a small-to-moderate effect was recorded (r = –.23) that did not reach significance at this sample size, but the possibility that this difference would prove statistically reliable with a larger and more balanced sample should not be ruled out.

6. Conclusions

This paper compared two self-avatar games that were made with different levels of detail, different genres, and different approaches to onboarding players into the game. Through the literature, the topics of usability, functionality and aesthetics as elements of user experience were covered, along with user experience in games, identification and the effect of identification, together with character likeability. The paper also covered the choice of game perspective and the sense of security in the context of data protection.

The research questions and the hypothesis examined whether the level of avatar realism affects the level of avatar-player similarity, whether there was a change in the degree of enjoyment of this way of creating characters, and whether there was a change in opinion regarding whether people would like to see this way of creating characters used in other media as well. One question also compared attitudes toward data protection in the context of these two games, and, finally, whether these two samples are at all comparable in terms of demographic characteristics and gaming experience.

The results of this study provide no evidence that the perceived resemblance of the character, enjoyment of the avatar-creation process, attitude toward applying this approach in other media, or privacy concern differ statistically significantly between participants who used the older, less realistic avatar system and those who used the newer, more realistic system.

These findings suggest that, at least based on this sample, increased avatar realism by itself does not lead to a measurably different user perception along the dimensions examined.

7. Acknowledgments

This research has been supported by the Ministry of Science, Technological Development and Innovation (Contract No. 451-03-137/2025-03/200156) and the Faculty of Technical Sciences, University of Novi Sad through project "Scientific and Artistic Research Work of Researchers in Teaching and Associate Positions at the Faculty of Technical Sciences, University of Novi Sad 2025" (No. 01-50/295).

8. References

Avaturn | Realistic 3D avatar creator. (no date) *Avaturn*. Available from: https://avaturn.me/ [Accessed 27 May 2026].

Bergonse, R. (2017) 'Fifty Years on, What Exactly is a Videogame? An Essentialistic Definitional Approach', *The Computer Games Journal*, 6(4), pp. 239–255. DOI: 10.1007/s40869-017-0045-4

Bernhaupt, R. (ed.) (2015) *Game User Experience Evaluation*. Cham: Springer International Publishing. DOI: 10.1007/978-3-319-15985-0

Brown, E. and Cairns, P. (2004) 'A grounded investigation of game immersion'. In: *CHI '04 Extended Abstracts on Human Factors in Computing Systems*. New York: ACM, pp. 1297–1300. DOI: 10.1145/985921.986048

Calleja, G. (2012) 'In-game: from immersion to incorporation', *Choice Reviews Online*, 49(05), pp. 49–2483. DOI: 10.5860/CHOICE.49-2483

Chen, V.H.H. and Koek, W.J.D. (2020) 'Understanding Flow, Identification with Game Characters and Players' Attitudes'. In: Yannakakis, G.-N., Liapis, A., Kyburz, P., Volz, V., Khosmood, F. and Lopes, P. (eds.) *Proceedings of the International Conference on the Foundations of Digital Games (FDG '20)*, Bugibba, Malta. New York: ACM, pp. 1–4. DOI: 10.1145/3402942.3409784

Csikszentmihalyi, M. (1990) *Flow: The Psychology of Optimal Experience*. New York: Harper & Row.

Dufresne, F., Gorisse, G. and Christmann, O. (2026) 'Characterizing Device Transitions and Their Impact on Presence, Embodiment and Avatar Identification in Cross-Platform Virtual Environments', *IEEE Transactions on Visualization and Computer Graphics*, pp. 1–14. DOI: 10.1109/TVCG.2026.3668931

Ermi, L. and Mäyrä, F. (2005) 'Fundamental Components of the Gameplay Experience: Analysing Immersion'. In: Jenson, J. (ed.) *Changing Views: Worlds in Play – Selected Papers of the 2005 Digital Games Research Association's Second International Conference*, Vancouver: Digital Games Research Association and Simon Fraser University, pp. 15–27. DOI: 10.26503/dl.v2005i1.119

Fraser, A.D., Branson, I., Hollet, C.R., Speelman, C.P. and Rogers, S.L. (2024) 'Do realistic avatars make virtual reality better? Examining human-like avatars for VR social interactions', *Computers in Human Behavior: Artificial Humans*, 2(2), 100082. DOI: 10.1016/j.chbah.2024.100082

Gorisse, G., Christmann, O., Houzangbe, S. and Richir, S. (2019) 'From Robot to Virtual Doppelganger: Impact of Visual Fidelity of Avatars Controlled in Third-Person Perspective on Embodiment and Behavior in Immersive Virtual Environments', *Frontiers in Robotics and AI*, 6, 8. DOI: 10.3389/frobt.2019.00008

Happ, C., Melzer, A. and Steffgen, G. (2013) 'Superman vs. BAD Man? The Effects of Empathy and Game Character in Violent Video Games', *Cyberpsychology, Behavior, and Social Networking*, 16(10), pp. 774–778. DOI: 10.1089/cyber.2012.0695

Harrell, D.F. (2009) 'Avatar art: transformative outcomes of the Advanced Identity Representation Project'. In: *Proceedings of the 15th International Symposium on Electronic Art (ISEA2009)*, Belfast, Ireland.

Hefner, D., Klimmt, C. and Vorderer, P. (2007) 'Identification with the Player Character as Determinant of Video Game Enjoyment'. In: Ma, L., Rauterberg, M. and Nakatsu, R. (eds.) *Entertainment Computing – ICEC 2007*. Berlin, Heidelberg: Springer, pp. 39–48. DOI: 10.1007/978-3-540-74873-1_6

Imangi, I., Lakshan, S., De Silva, S.M., Arachchi, H.A.D.M. and Samarasinghe, G.D. (2025) '3D- AI Avatar Attributes Impacting on Bank Customers' Perceived Experience'. In: *2025 5th International Conference on Advanced Research in Computing (ICARC)*, pp. 1–6. DOI: 10.1109/ICARC64760.2025.10963179

Kao, D. and Harrell, D.F. (2015) 'Toward avatar models to enhance performance and engagement in educational games'. In: *2015 IEEE Conference on Computational Intelligence and Games (CIG)*, Tainan, Taiwan: IEEE, pp. 246–253. DOI: 10.1109/CIG.2015.7317959

Kaye, L.K., Pennington, C.R. and McCann, J.J. (2018) 'Do casual gaming environments evoke stereotype threat? Examining the effects of explicit priming and avatar gender', *Computers in Human Behavior*, 78, pp. 142–150. DOI: 10.1016/j.chb.2017.09.031

Kerac, J., Milić Keresteš, N., Golubović, G. and Ilić, T. (2024) 'Exploring The Impact Of Stereotype Threat And Identification On Gaming Performance: A Pilot Study Using Custom Avatars'. In: *Proceedings of the Twelfth International Symposium on Graphic Engineering and Design – GRID 2024*, Novi Sad: University of Novi Sad, Faculty of Technical Sciences, pp. 281–290. DOI: 10.24867/GRID-2024-p29

Klimmt, C., Rizzo, A., Vorderer, P., Koch, J. and Fischer, T. (2009) 'Experimental evidence for suspense as determinant of video game enjoyment', *CyberPsychology & Behavior*, 12(1), pp. 29–31. DOI: 10.1089/cpb.2008.0060

Klimmt, C., Hefner, D., Vorderer, P., Roth, C. and Blake, C. (2010) 'Identification With Video Game Characters as Automatic Shift of Self-Perceptions', *Media Psychology*, 13(4), pp. 323–338. DOI: 10.1080/15213269.2010.524911

Klimmt, C., Hartmann, T. and Frey, A. (2007) 'Effectance and Control as Determinants of Video Game Enjoyment', *CyberPsychology & Behavior*, 10(6), pp. 845–848. DOI: 10.1089/cpb.2007.9942

Klimmt, C., Hefner, D. and Vorderer, P. (2009) 'The Video Game Experience as "True" Identification: A Theory of Enjoyable Alterations of Players' Self-Perception', *Communication Theory*, 19(4), pp. 351–373. DOI: 10.1111/j.1468-2885.2009.01347.x

Kreijns, K., Xu, K. and Weidlich, J. (2022) 'Social Presence: Conceptualization and Measurement', *Educational Psychology Review*, 34(1), pp. 139–170. DOI: 10.1007/s10648-021-09623-8

Madden, M. (2014) 'Public Perceptions of Privacy and Security in the Post-Snowden Era'. *Pew Research Center*, 12 November. Available from: https://www.pewresearch.org/internet/2014/11/12/public-privacy-perceptions/ [Accessed 29 June 2025].

Mull, I., Wyss, J., Moon, E. and Lee, S.-E. (2015) 'An exploratory study of using 3D avatars as online salespeople: The effect of avatar type on credibility, homophily, attractiveness and intention to interact', *Journal of Fashion Marketing and Management*, 19(2), pp. 154–168. DOI: 10.1108/JFMM-05-2014-0033

Murray, J. (1998) *Hamlet on the Holodeck: The Future of Narrative in Cyberspace*. Cambridge, MA: The MIT Press.

Popper, K.R. (1994) *Knowledge and the Body-Mind Problem: In Defence of Interaction*. London: Routledge.

Van Looy, J., Courtois, C. and De Vocht, M. (2010) 'Player identification in online games: validation of a scale for measuring identification in MMORPGs'. In: *Proceedings of the 3rd International Conference on Fun and Games (Fun and Games '10)*, New York: ACM, pp. 126–134. DOI: 10.1145/1823818.1823832

Waldman, A.E. (2016) 'Privacy, Sharing, and Trust: The Facebook Study', *Case Western Reserve Law Review*, 67(1).

Wang, Z., Li, X., Huang, J., Jin, Y., Chen, Y. and Zhang, D. (2025) 'Effects of Avatar Visibility and Perspective on Social Presence and Performance in Dynamic VR Collaboration Tasks', *IEEE Transactions on Visualization and Computer Graphics*, 31(10), pp. 9179–9194. DOI: 10.1109/TVCG.2025.3591830

Won, A.S. and Zhou, S. (2024) 'Effects of first vs. third-person perspective and self- versus other-avatars on user movements in virtual reality', *International Journal of Human-Computer Studies*, 187, 103259. DOI: 10.1016/j.ijhcs.2024.103259

Yee, N. and Bailenson, J. (2007) 'The Proteus Effect: The Effect of Transformed Self-Representation on Behavior', *Human Communication Research*, 33(3), pp. 271–290. DOI: 10.1111/j.1468-2958.2007.00299.x



© 2026 Authors. Published by the University of Novi Sad, Faculty of Technical Sciences, Department of Graphic Engineering and Design. This article is an open access article distributed under the terms and conditions of the Creative Commons Attribution license 4.0 Serbia (http://creativecommons.org/licenses/by/4.0/rs/).

Professional Paper https://doi.org/10.24867/GRID-2026-p60

Animated Presentation of the Story of The Nevlje Mammoth

ABSTRACT

In today's globalised world, rapidly evolving digital technologies increasingly shape our daily lives. Their continual development brings both challenges and opportunities, including new ways to preserve cultural and natural heritage Animation – with its many styles and subgenres – has become an essential part of modern media and everyday communication. Although originally created for entertainment, it is now widely used in marketing, advertising, and especially education. Animated storytelling can vividly bring the past to life, presenting traditions, heritage, and artefacts in ways that capture attention and help preserve knowledge for future generations. It is particularly valuable for presenting artefacts that, although well known, lack accessible professional or scientific material. One such example is the nearly complete skeleton of the Nevlje mammoth, one of Slovenia's most important palaeontological discoveries, dating back roughly 20,000 years. Public information about the find remains limited, especially in terms of visual material and reconstructions of the mammoth's life and the circumstances of its death. Existing presentations are further weakened by outdated interpretations that no longer align with current scientific understanding. A 2D animated presentation offers an engaging new way to explore this discovery. It is suitable for all generations and can be made accessible to visually and hearing-impaired audiences through sound design and subtitles. By introducing animation as an additional medium, we can enrich the scarce existing material and broaden public understanding of the mammoth's story.

Brita Mandelj
Tanja Nuša Kočevar
Andrej Iskra

Faculty of Natural Sciences and Engineering, Ljubljana, Slovenia

KEY WORDS
2D animation, Nevlje mammoth, palaeontology, natural heritage, cultural heritage

1. Introduction

In today's globally oriented world, rapidly evolving digital technologies increasingly affect our daily lives. Alongside negative effects, this constant development also brings positive opportunities that open up new methods and approaches for preserving both cultural and natural heritage. By introducing more engaging and appealing forms of heritage presentation, museum visitor numbers rise and interest in heritage itself grows, which in turn supports its preservation. 2D animation, as an example,once very time-consuming, is now much faster and easier. This allows animation to be used in areas where it was previously impossible or uneconomical, thereby not only enriching them visually but also giving them greater visibility and broader social recognition. With the help of animation, we can bring past stories, traditions, heritage and artefacts back to life in a way that attracts the attention of the masses and, consequently, they can be preserved for future generations (Connolly, 2025). We can particularly shed light on fields that, despite significant recognition, have only a small number of publicly accessible materials. An example of this is the Nevlje mammoth, which is one of the most important palaeontological discoveries in Slovenia, an almost fully preserved 20,000-year-old woolly mammoth skeleton (Bezek, 2015). The goal of the project was to create an educational 2D animation with original illustrations and audio narration telling the story of the Nevlje mammoth, to be posted on a local museum's website to educate people about this important piece of heritage. By highlighting these kinds of examples and presenting them

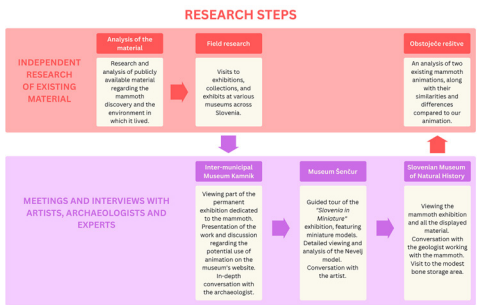
in a way that is appealing and educational, learning about heritage becomes fun and engaging for all audiences and keeps its cultural memory very much alive.

2. Methods

2.1. Research

The aim of the research was to obtain as much information as possible about the life of the Nevlje mammoth, the causes of its death, and the unexpected discovery of its skeleton. We wanted to find out what the environment of Nevlje was like during the last ice age and who the individuals were who played a key role in the story of this important palaeontological find. The research included visits to museums and exhibitions, documentation of material, interviews with archaeologists, experts and artists, as well as visits to locations related to the story of the mammoth in the Kamnik region. The information and expert guidance obtained had a key impact on the design of the storyboard content and contributed to the scientific basis of the project, which was continually upgraded in cooperation with institutions and individuals.

The research steps we undertook are graphically represented in the diagram in Figure 1.



» **Figure 1:** *Research steps*

2.1.1. Research on the discovery of the mammoth skeleton

Less than a kilometre from Kamnik towards the Tuhinjska Valley lies the town of Nevlje, through which the Nevljica River flows. Due to floods and subsidence of the banks, regulation works began in the winter of 1938 and ended with the construction of a reinforced concrete bridge over the Nevljica riverbed, which still bears the name for which it became famous – the Mammoth Bridge (Bezek, 2013, 2015).

On 14 March 1938, while digging the foundations for the bridge support, the workers encountered an unexpected obstacle in the form of a "stump", which they reported to Mayor Ferdinand Novak. He recognised it as a fossilised bone, stopped the work and asked the veterinary inspector of Kamnik, Josip Nikolaj Sadnikar, for advice. Sadnikar confirmed the mayor's assumption that they had come across the remains of a woolly mammoth. Once it was clear that this was more than just an isolated find, after Sadnikar's son uncovered a rib and tibia, as shown in Figure 2, they informed the Mining Administration in Ljubljana about the discovery (Bezek & Bezek, 1998; Bezek, 2013, 2015; Čebašek, 2018; Vulikić, 2005).



» **Figure 2:** *Discovery of the mammoth skeleton (Bezek, 2015)*

On 16 March 1938, at the initiative of the Mining Administration, the naturalist and zoologist Dr Fran Kos and the taxidermist Viktor Herfort, from the Natural History Department of the National Museum in Ljubljana, came to Nevlje. Dr Kos carried out his excavations with precision, systematically and in an organised manner. He filled the shafts where the first bones were discovered and protected them from decay caused by exposure to air. He systematically excavated along stratigraphic layers to a depth of 250 cm (Bezek, 2015; Jeršek & Križnar, 2001; Kos, 1939a, 1939b; Križnar, 2021). Due to a lack of financial resources, the forecast of bad weather and disputes with the locals, the bones were transported to Ljubljana on 4 May 1938 by several carriages to the Natural History Department of the National Museum (Bezek, 2015; Jeršek & Križnar, 2001; Kos, 1939b).

Archival documents of the Museum of Natural History show that, due to various problems, including financial ones, the procedures for preserving the bones and assembling the mammoth skeleton did not begin until April 1939, followed by the conservation of the ox in May 1940 (Križnar, 2014). Researchers established that the remains belonged to a male mammoth of extraordinary size, measuring 574 cm in length and 361 cm in height, who died at about 40 years of age and lived around 20,000 years ago. So far, science has not identified the cause of his death, nor has it been able to prove that a human was directly involved in it (Bezek, 2015; Jamnik and Križnar, 2024; Železnikar, 2008).

The preparation of the skeleton was carried out in accordance with the methods of the time. The skeleton was attached to a metal structure that supported it and, at the same time, indicated the missing parts. The complete reconstruction of the mammoth skeleton was first presented to the public at the end of 1941, during World War II. Because of the war, the bones were dismantled and stored in crates, and after the end of the war they were reassembled. Since then, the mammoth has been the central exhibit of the Natural History Museum of Slovenia. Today visitors can view the replica on display, shown in Figure 3, as the original bones have been conserved because of degradation (Bezek, 2015; Jeršek & Križnar, 2001; Križnar, 2014).



» **Figure 3:** *The replica on display*

The first memorial in the Kamnik region, dedicated to the mammoth, is the bridge over the regulated riverbed of the Nevljica River, which was named the Mammoth Bridge when it was opened in 1938 The most recent commemoration was erected to mark the 85th anniversary of the discovery: a life-size bronze sculpture of a mammoth by sculptor Miha Kač, installed in Kamnik in the immediate vicinity of the confluence of the Nevljica and Kamniška Bistrica rivers and shown in Figure 4 (Občina kamnik, n.d.).



» **Figure 4:** *Life-size bronze sculpture of the mammoth by sculptor Miha Kač*

2.1.2. Field research

The first institution we visited after defining the project topic was the Inter-Municipal Museum Kamnik, where we viewed the permanent exhibition dedicated to the mammoth. During the visit, we met the director of the museum, Mrs Zora Torkar, and the archaeologist, Mrs Janja Železnikar. They expressed interest in and openness to including animation in the museum's online content and in its possible use to supplement the exhibition. This was followed by an expert meeting with Mrs Janja Železnikar, at which we presented the then current version of the storyboard and asked her for further guidance. Drawing on the scientific findings of paleobotanist Ana Budnar-Lipoglavšek, we also talked with the archaeologist about a possible visual reconstruction of the Ice Age environment around Nevlje. She suggested that we visit the exhibition Slovenia in Miniature at the Museum of the Municipality of Šenčur, where the artist Igor Grabnar was exhibiting a model presenting his interpretation of the environment of that time.

In the Museum of the Municipality of Šenčur, we visited an exhibition called Slovenia in Miniature, which is partly still in progress. The exhibition consists of models through which the artist Igor Grabnar presents key events in Slovenia and important milestones in the history of the Republic of Slovenia. After the tour, we met the artist, who said that he created the model of the Ice Age Nevlje on the basis of consultations with experts, including archaeologist Janja Železnikar. He presented in detail a model that illustrates his interpretation of the environment of Nevlje in the last Ice Age with mammoths. Information about the depicted environment is summarised on the information board next to the model, which he prepared in cooperation with Mr Matija Križnar from the Natural History Museum in Ljubljana. Mr Grabnar told us that he is in contact with the Šporar family, who keep part of the photographic archive from the excavations of the mammoth in 1938. With his consent, we obtained contacts from both sources for further research.

This was followed by a meeting with geologist Mr Matija Križnar from the Natural History Museum of Slovenia, the author of several scientific papers in the field of palaeontology, which were an important source in the development and production of this project. The visit also included a behind-the-scenes tour of the museum, including a modest depot with some mammoth bone fragments. We provided him with an updated version of the mammoth storyboard, which he found pleasant. In order to illustrate the animal background, he recommended the inclusion of species such as reindeer, elk, wolverine, arctic fox, and wolves. While these species are typical of this environment, we also possess fossilized remains of these species from the surrounding area. He graciously provided us with access to the photographic archive, which encompasses the Nevlje mammoth

excavations in 1938 and the subsequent time of bone protection and skeletal assembly in the museum. This was followed by a study of the exhibition featuring the mammoth skeleton in the Natural History Museum and an analysis of the accompanying material.

2.1.3. Existing solutions

During the research, only two similar existing solutions in the form of animation were identified. In the first case, the subject is a 3D animation of the Nevlje mammoth, which is located in the mammoth room of the Natural History Museum in Ljubljana. The visual element is presented in a continuous loop on a large monitor. The background of the animation is constituted by a live video projection from a camera positioned in the corner of the room. The digital 3D model of the mammoth skeleton is being gradually upgraded by the addition of muscles and hair, until the complete image of the animal as it existed during the Ice Age is revealed. The depiction of the room, which has been employed as the background of the presentation, is then transformed into a three-dimensional model of a snowy landscape. The depiction of the mammoth in its natural environment is static. In comparison to our own depiction, the 3D mammoth model is characterised by a significantly squatter posture and greater rigidity. Its movement is confined to the head and neck region. The image of the monitor with the animation described is shown in Figure 5.



» **Figure 5:** *The image of the monitor with the animation*

Another example of the use of animation as a tool to display professional content related to natural heritage was also found in the mammoth room of the Natural History Museum, only on a second, smaller monitor. It is a 3D animation that is more stylized, and it features more characters and scenes. Similar to our animation, it begins with a map showing Europe today and during the last glaciation. The story then focuses on the depiction of Nevlje in the Ice Age, where a herd of mammoths moves across a snowy steppe. The next scene shows the Paleolithic people and their hunt for a mammoth. The movement of the characters is rigid and slow, while the movements of the "camera" are faster and smoother. The emphasis in depicting the landscape is on the steppe and not on the swamp. The Paleolithic people are implicated in the mammoth's death in the animation, which modern science has not been able to confirm.

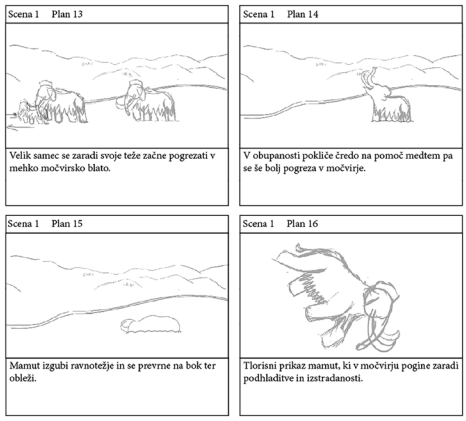
2.2. Animation pre-production

2.2.1. Synopsis

The animation begins with Europe as we know it today, and then we spin time 23,000 years back in time to the time of the last ice age. The Northern Glacier covers the whole of northern Europe. The frame focuses on the territory of Slovenia, which is partially covered by the Alpine Glacier. The frame then zooms in on the surface, which shows a swampy world where reindeer and elk graze, with snow-capped mountains in the background. A mammoth steps into the foreground, which at first we see only halfway through. We focus on its features: hair, tusks and trunks. As the frame expands, we see a herd of mammoths moving across the wetland. The largest of them begins to sink into the soft mud as the herd leaves it. It lets out one last dramatic cry before it topples over and dies. From a bird's eye view, we see his corpse decomposing until only the bones covered with snow remain. Sediment is deposited on the bones in summer, and in winter they are covered with snow. After numerous deposits, they are covered with grass. After the last winter, we can follow the construction work along the regulation of the Nevljica riverbed. We see two workers who have found something and inform the mayor about it, who is passing by. He recognizes a fossilized bone in the obstacle. In the next scene, he holds the bone in his hand while Josip Nikolaj Sadnikar looks at it with a monocle, indicating to him that it is a mammoth. A hand holds a newspaper that reports on the finding of a mammoth. When the hand releases the newspaper, the façade of the National Museum of Slovenia is displayed. This is followed by a demonstration of excavations at the Nevlje site, led by Dr. Fran Kos, followed by a demonstration of the assembly of the mammoth skeleton in the museum, followed by the final museum installation of the skeleton on an iron frame. This frame represents the transition from monochromatic to chromatic style. The last one is a bronze statue of a mammoth, erected on the occasion of the 85th anniversary of the find, which is then photographed by someone. The last shot of the animation is a realistic photograph of this statue.

2.2.2. Storyboard

The synopsis is followed by a storyboard that visually presents the plot. The animation is illustrated scene by scene in a series of rectangles, with a description beneath each one explaining what is happening in that particular shot. Figure 6 shows an excerpt from the animation, while Appendix 1 contains the complete storyboard.



» **Figure 6:** *Excerpt from the storyboard of the Nevlje mammoth animation*

2.2.3. Defining styles

Given the structure of the animation, which spans three distinct time periods, the Palaeolithic era, 1938, and the present day, we decided to assign a unique and recognisable visual style to each of them. This approach enables viewers to clearly distinguish between the three periods without the need for narration or subtitles. The animation begins in the Palaeolithic era, specifically 23,000 years ago, in the area where the town of Nevlje stands today. This period is depicted in a style inspired by Palaeolithic illustrations commonly found in books. Characteristic features of these illustrations include desaturated colours, earthy brown and green tones, soft forms, subtle shadows, and textured surfaces.

The next visual style represents the year 1938, when the skeleton was discovered. This period is portrayed using a combination of monochromatic and chromatic rendering. Black-and-white photographs taken at the excavation site in 1938, for which we obtained permission to use, form the background, while the main figures and bones are rendered in colour. This allows for a realistic depiction of the scene while simultaneously using colour to emphasise the most significant events and key figures. The present day is depicted in a colourful, semi-realistic style inspired by our own photographs. Appropriately, the final shot of the animation features an actual photograph of the mammoth statue, unveiled in 2023 to mark the 85th anniversary of the discovery. This further reinforces the significance of the find and highlights its importance as a real-world cultural heritage asset that should be preserved.

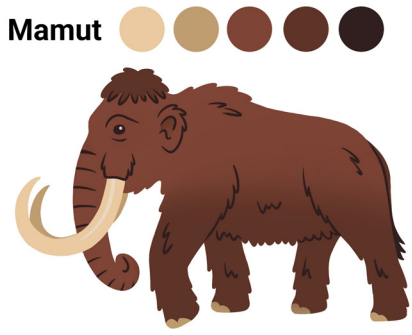
2.2.4. The script

We devoted considerable time to developing the script for several reasons. The primary objective was to present accurate and verifiable information about the life, death, and discovery of the Nevlje mammoth. The second major challenge was to convey this information in a clear, engaging, and concise manner, which proved to be a demanding task. As a result, the script underwent numerous revisions and reductions before we were satisfied with its content and structure. Once we considered it complete, we submitted it to Mrs. Janja Železnikar and Mr. Matija Križnar for review. They provided valuable feedback and suggested several corrections, which we carefully incorporated into the final version of the script.

2.3. Animation production

2.3.1. Analysis and drawing of characters

Character design was a lengthy process that required extensive analysis and planning, as our goal was to create characters that were both recognisable and stylised. All characters were designed and illustrated using the IbisPaint X drawing software. The mammoth, as the main character, presented a particular challenge. On the one hand, we wanted it to remain as faithful as possible to scientifically accurate depictions of woolly mammoths; on the other, it needed to be simplified and stylised to fit the visual language of the animation. To support this process, we created an inspiration collage containing a variety of realistic and stylised mammoth depictions gathered during our research. Alongside these references, we compiled a list of key woolly mammoth characteristics that had to be considered during the design process. The initial sketch was based on the shape of the skeleton exhibited in the Natural History Museum and on the mammoth statue created by Miha Kač. We then developed a full illustration of the mammoth and established its colour palette. The final character design and colour palette are presented in Figure 7.



» **Figure 7:** *The final drawing of the mammoth figure and the color palette that was used*

The animation also features human characters, which are divided into primary and secondary roles. Their design was likewise informed by detailed research, including archival photographic material, the aesthetics of contemporary fashion trends, and the visual style of the animation itself. The primary characters are the only human figures depicted in colourful clothing,

using the basic colours blue (Nande Novak, Mayor), green (Josip Nikolaj Sadnikar, Veterinary Inspector), and red (Dr. Fran Kos, Zoologist). As shown in Figure 8, their designs are based on real black-and-white photographs. All secondary characters wear clothing in shades of brown, reflecting the most common colour of men's attire in Slovenia during the 1930s.



» **Figure 8:** *Final drawing of the main human characters with color palettes*

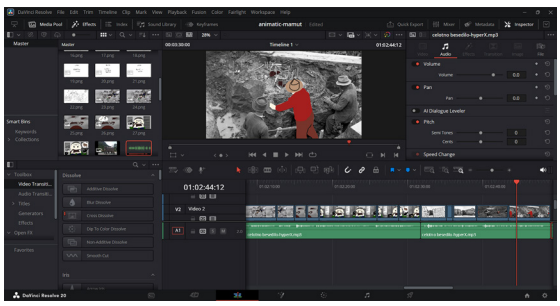
2.3.2. Recording narration audio

We recorded the narration in the visual evaluation laboratory at the faculty. We selected this location because of its relatively small size and infrequent use, which provided easier access and a more controlled recording environment. The recording was carried out using a Blue Yeti microphone connected via USB to an HP laptop, with Adobe Audition 2025 used for audio capture. The script was recorded in several sections, and the quality of each recording was checked immediately afterwards. Whenever a recording did not meet the required standard, it was repeated.

2.3.3. Making an animatic

The animatic was created in DaVinci Resolve 19. We imported all key frames from the storyboard, along with several additional in-between frames, and synchronised them with the recorded narration. All visual and audio elements were arranged chronologically according to the script.

The video was produced in a resolution of 1920 × 1080 pixels, the standard format for Full High Definition (Full HD) video. The frame rate was set to 24 frames per second (fps). Finally, we added opening and closing credits containing all relevant information. Figure 9 shows a screenshot of the animatic production process.



» **Figure 9:** *Screenshot of the animatic in DaVinci Resolve*

2.3.4. Backgrounds

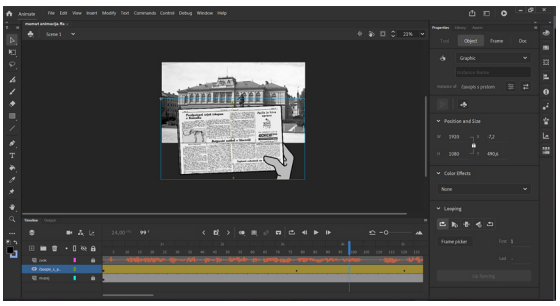
The various visual styles used throughout the animation are accompanied by distinct backgrounds that differ not only in colour schemes but also in the media from which they are created. Some scenes feature fully hand-illustrated backgrounds, such as the maps of Europe and Slovenia, while others use authentic photographs, including scenes from the twentieth century and images of the mammoth statue. In several instances, illustration and photography are combined, blending seamlessly into one another, as seen in the depiction of the Ice Age landscape of Nevlje. The illustrated backgrounds were created in the IbisPaint X drawing software, while the photographs were edited in Adobe Photoshop. Only minor adjustments were made to the photographs, primarily involving brightness correction and the removal of small visual imperfections that could interfere with the animation process. These corrections were carried out using the Spot Healing Brush tool. We intentionally limited the extent of the edits in order to preserve the authenticity of the photographs, as they represent the most reliable visual evidence of historical events in Nevlje. Permission to use the photographs was obtained either directly from their owners, such as the photographs provided by Mr. Naglič, or the materials were sourced from the public domain, including newspaper articles. The image that underwent the most extensive editing was the Ice Age landscape of Nevlje. As a base, we used a satellite image from Google Maps showing Nevlje during the summer season, with the Kamnik-Savinja Alps visible in the background. Because we wanted the landscape to appear snow-covered, we made use of Neural Filters, one of the newer features available in Adobe Photoshop. This AI-powered tool transformed the summer landscape into a winter scene. We then selectively applied the effect to the mountains and hills using a brush, ensuring that only the desired areas were affected. Additional adjustments were made using adjustment layers to achieve a less saturated and more earthy colour palette that better matched the atmosphere of the scene. Once the photographic background had been finalised, it was transferred to IbisPaint X, where we illustrated the swamp and prehistoric animals in the foreground.

2.3.5. Animation and video editing

We used Adobe Animate and DaVinci Resolve to create the animation. The project was produced in the standard Full High Definition (Full HD) format of 1920 × 1080 pixels, with a frame rate of 24 frames per second (fps). These settings ensured a high-quality visual output while maintaining smooth character movement and seamless transitions between individual frames. Based on the animatic, we defined the individual scenes and imported the corresponding audio, backgrounds, and character assets. Two different animation techniques were used throughout the project. All human and animal charac-

ters were animated using traditional frame-by-frame animation, in which each frame is drawn by hand. An exception is the scene featuring Josip Nikolaj Sadnikar, where certain movements were created using computer-generated animation to improve clarity and achieve smoother motion. This technique was also applied to the scenes involving the newspaper and the camera, as these objects required only limited movement, primarily entering and exiting the frame, while containing numerous small details that would have been highly time-consuming to animate entirely by hand. Nevertheless, traditional animation was still employed in these scenes for the movement of the characters' fingers. A screenshot of the animation process is shown in Figure 10. After completion, each scene was exported separately in MP4 format.

The completed animated sequences, together with scenes that did not require manual animation, were imported into DaVinci Resolve as PNG and MP4 files. There, we assembled the entire animation, added the narration and sound effects on separate audio tracks where necessary, and synchronised all visual and audio elements into a cohesive final composition.



» **Figure 10:** *Screenshot of the animating process in Adobe Animate*

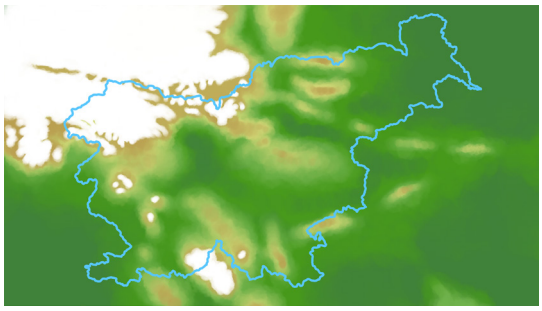
To ensure smooth transitions between scenes, we incorporated various effects available within the software. The transition used most frequently was Cross Dissolve, which provided subtle, non-distracting transitions and allowed the animation to flow naturally from one scene to the next.

3. Results

The result of our project is a 2D animation, which aims to educate and will be uploaded to a museum's website. The animation tells the story of the Nevlje mammoth's life and death and the discovery of its skeleton, taking us on a journey through different styles and using real photographs as the basis for its visuals.

3.1. Animation description

The first part is characterised by topographic depictions of Europe and Slovenia, drawn and illustrated according to real maps and not strongly stylised. The alternation of brown and green colours shows differences in altitude – mountains and lowlands – as in actual topographic maps. At the beginning of the animation there is an image of the map of Europe as we see it today. Then we go back 23,000 years into the past, when most of northern Europe was covered by an ice sheet. After this reveal, the image enlarges and focuses on the territory of present-day Slovenia, shown in Figure 11, where the northern part was covered by glaciers, including the Kamnik-Savinja Alps.



» **Figure 11:** *The territory of present-day Slovenia*

The frame is then enlarged to reveal a depiction of the Ice Age environment at the site where the town of Nevlje stands today. The upper half of the scene is a real satellite image, edited in Adobe Photoshop to make it appear as though the mountains are covered in snow. The lower part of the scene is illustrated and shows a swampy world, where we can see moose in the central plane. The animation style in this section is inspired by artistic depictions from the Palaeolithic found in literature and online sources, characterised by unsaturated, earthy shades of colour. The appearance of the environment represents a personal visual interpretation, based on all the information obtained during the research.

In the next frame, a mammoth steps in front of the camera. The scene highlights its size and mass compared with the other animals in the scene. The animation then follows the narrative of the mammoth's individual characteristics. The camera then zooms out and expands to a wider frame that shows an entire herd of mammoths travelling across the swamp. Meanwhile, the largest and heaviest mammoth begins to sink into the soft swamp mud. As the herd moves away and leaves the scene, the trapped mammoth lets out a dramatic cry for help, as shown in Figure 12, then rolls onto its side and lies down in the middle of the swamp, symbolising its death.



» **Figure 12:** *The trapped mammoth lets out a dramatic cry for help*

Subsequently, the carcass of a mammoth undergoes various stages of decomposition until only the bones remain. The passage of time is shown in the animation by the changing seasons. The animal's carcass is first covered in snow, followed by summer, when the swamp is half drained and only the bones are visible. This is followed by a depiction of winter, which marks a milestone between the style of the second and third parts of the animation – the transition from the Palaeolithic to the year of the find, 1938.

The third part begins with a black-and-white photograph of the construction site for the regulation of the Nevljica stream. The main human characters, such as the mayor in blue, are presented in colour in the story, while the background consists of real photographs from the skeleton site, which we got permitted to use. With this style, we emphasise the main characters while preserving and sharing the existing documentation of the event. This allows the viewer to imagine the events more easily and at the same time pick out the most important characters and content.

Figure 13 shows the moment when the mayor of Kamnik brought a fragment of bone found by workers at the construction site to the veterinary inspector Josip Nikolaj Sadnikar. In the next frame, Mr Sadnikar confirms that the remains of a woolly mammoth have been found. The picture shows that the background behind the figure is blurred, creating the effect of depth in the room.



» **Figure 13:** *Josip Nikolai Sadnikar, who carefully examines the bone brought by the mayor*

The next frame shows a hand holding a newspaper with an article about the discovery of a mammoth skeleton. The hand then descends from the scene, revealing a photograph of the National Museum in the background.

The next frame, depicts an excavation led by Dr Fran Kos, dressed in red. The assembly of the mammoth skeleton is shown in the following frame, after it has already been transported to what was then the National Museum, today the Slovenian Natural History Museum. The next frame shows the assembled mammoth skeleton, which shifts from a monochromatic display to a colourful image, i.e. the fourth and final style of animation, which represents modern day. The last frames of the animation first show the illustration presented in Figure 14, followed by a life-size photograph of the hairy mammoth statue, the work of sculptor Miha Kač. The transition between illustration and animation is created by a camera with which a tourist photographs the statue using a flash. With this approach, we aim to present the mammoth legacy in the Kamnik region.



» **Figure 14:** *Illustration of the mammoth sculpture in Kamnik*

3.1.1. Intended use and audience

The final product is used for educational purposes and is intended for a broad audience, i.e. it does not have a specific target group. It is aimed at anyone who would like to learn more about this exceptional palaeontological find from the Kamnik region.

4. Discussion

The creation of the 2D animation demonstrated that animation can be an effective tool for presenting scientific and cultural heritage content to a wider audience. By combining factual information with visual storytelling, the project transformed the story of the Nevlje mammoth into an engaging and accessible educational experience.

One of the main challenges was balancing scientific accuracy with a concise and visually appealing narrative. This was addressed through extensive research, multiple revisions of the script, and consultations with experts,

ensuring that the information remained both reliable and understandable. The use of three distinct visual styles for the Palaeolithic era, 1938, and the present day proved particularly effective in helping viewers distinguish between different historical periods. In addition, the combination of traditional frame-by-frame animation and digital techniques allowed for a visually rich result while maintaining an efficient production workflow.

The integration of archival photographs and historically accurate references further strengthened the credibility of the animation and connected the audience with real events surrounding the discovery of the mammoth skeleton. At the same time, the project highlighted the potential of animation as a medium for communicating local heritage and raising awareness of important historical and scientific discoveries. Although the animation's short duration limited the amount of information that could be included, the final product successfully presents the key aspects of the Nevlje mammoth's story in an engaging and accessible way.

The creation of the 2D animation demonstrated that animation can be an effective tool for presenting scientific and cultural heritage content to a wider audience. By combining factual information with visual storytelling, the project transformed the story of the Nevlje mammoth into an engaging and accessible educational experience. One of the main challenges was balancing scientific accuracy with a concise and visually appealing narrative. This was addressed through extensive research, multiple revisions of the script, and consultations with experts, ensuring that the information remained both reliable and understandable. The use of three distinct visual styles for the Palaeolithic era, 1938, and the present day proved particularly effective in helping viewers distinguish between different historical periods. In addition, the combination of traditional frame-by-frame animation and digital techniques allowed for a visually rich result while maintaining an efficient production workflow.

The integration of archival photographs and historically accurate references further strengthened the credibility of the animation and connected the audience with real events surrounding the discovery of the mammoth skeleton. At the same time, the project highlighted the potential of animation as a medium for communicating local heritage and raising awareness of important historical and scientific discoveries. Although the animation's short duration limited the amount of information that could be included, the final product successfully presents the key aspects of the Nevlje mammoth's story in an engaging and accessible way.

5. Conclusions

The 2D animation about the Nevlje mammoth represents an important contribution to raising awareness of our palaeontological heritage and the need for its preservation. Through an engaging and contemporary visual approach, the animation presents the discovery of the fossilised mammoth skeleton in 1938, bringing this remarkable extinct animal closer to both younger and older audiences and helping to ensure that its story remains in their memory.

The result of this project is a three-minute 2D animation that tells the complete story of the Nevlje mammoth and presents it in a fresh and visually engaging way. One of the main motivations behind the creation of the animation was an early fascination with the mammoth skeleton displayed at the Natural History Museum in Ljubljana, which deepened upon learning that it had been discovered near the author's hometown. Despite the significance of this find, relatively little written and visual material has been published about it, even though it is still regarded as one of the best-preserved fossilised mammoth skeletons in Central Europe. We are proud of the completed animation, which presents the mammoth's story and the discovery of its remains in a simple and visually appealing manner, while educating audiences of all ages about this exceptional palaeontological find.

The animation will be published on the website of the Kamnik Inter-Municipal Museum, where it will be freely accessible to all visitors. As animation is a relatively simple, engaging, and accessible medium for presenting historical and scientific discoveries, it could also be used to communicate other stories related to important finds or notable achievements within the local environment. In doing so, it could help raise awareness of valuable yet lesser-known aspects of local heritage that often remain overlooked and underappreciated.

6. Acknowledgments

I would like to express my sincere gratitude to my co-authors, Tanja Nuša Kočevar and Andrej Iskra, for their trust, guidance, valuable advice, and constructive feedback throughout the creation of this work.

I would also like to thank Zori Torkar, Director of the Kamnik Inter-Municipal Museum, and Janja Železnikar from the Department of Archaeology, for their interest in the project and their support for including its final product, the 2D animation, in the museum’s online content. I am particularly grateful to Janja Železnikar for her continuous guidance, encouragement, and assistance throughout the development of this work. My special thanks also go to Matija Križnar from the Slovenian Museum of Natural

History for his professional expertise, helpful advice, and support during the preparation of this project.

Finally, I would like to thank Ivan Grabnar from Museum Šenčur for his valuable suggestions and Matjaž Šporar for granting permission to use the photographic material.

7. References

Bezek, B. and Bezek, D. (1998) Po sledeh neveljskega mamuta. Kamnik: Osnovna šola Frana Albrehta.

Bezek, D. (2013) 'Po sledeh neveljskega mamuta', *Proteus*, 75, pp. 462–467.

Bezek, D. (2015) Mamut v naših krajih. 1st ed. Ljubljana: Viharnik, pp. 3–38.

Čebašek, I. (2018) Okostje orjaškega mamuta izkopano v Nevljici pri Kamniku. Kamnik.info. Available from: https://www.kamnik.info/okostje-orjaskega-mamuta-izkopano-v-nevljici-pri-kamniku/ [Accessed 1 May 2025].

Connolly, M. (2025) Cultural Heritage Animation Projects: Your 101 Full Guide!. Available from: https://educationalvoice.co.uk/cultural-heritage-animation-projects/ [Accessed 5 September 2025].

Jamnik, P. and Križnar, M. (2024) 'Nove kamenodobne najdbe nad najdiščem mamuta v Nevljah', *Kamniški zbornik*, 27, pp. 89–99.

Jeršek, M. and Križnar, M. (2001) 'Kustodiat za geologijo- razkrivanje geološke dediščine Slovenije', *SCOPOLIA*, pp. 18–20.

Kos, F. (1939a) 'Paleolitske najdbe ob Nevljici', *Etnolog*, 11, pp. 417–419.

Kos, F. (1939b) 'Neveljski paleolitik', *Glasnik muzejskega društva za Slovenijo*, 20, pp. 25–65.

Križnar, M. (2014) 'Neveljski mamut v nekaterih arhivskih zapisih', *ARGO*, 57, pp. 63–67.

Križnar, M. (2021) 'Zgodovina in razvoj muzejskega naravoslovja do osamosvojitve Prirodoslovnega muzeja leta 1944', *SCOPOLIA*, pp. 91–97.

Občina Kamnik (n.d.) Občina Kamnik praznuje: Odprtje trga in odkritje skulpture mamuta v naravni velikosti. Available from: https://www.kamnik.si/post/738950 [Accessed 1 April 2025].

Vulikić, V. (2005) Kamniški kulturnik in mecen Josip Nikolaj Sadnikar. Znameniti Kamničani. Kamnik: Agencija za razvoj turizma in podjetništva v občini Kamnik.

Železnikar, J. (2008) Mamut po mamutu. Kamnik: Medobčinski muzej, pp. 1–16.



© 2026 Authors. Published by the University of Novi Sad, Faculty of Technical Sciences, Department of Graphic Engineering and Design. This article is an open access article distributed under the terms and conditions of the Creative Commons Attribution license 4.0 Serbia (http://creativecommons.org/licenses/by/4.0/rs/).

https://doi.org/10.24867/GRID-2026-p61

User-Centered UX/UI Design of a Mobile Flight Search Application

ABSTRACT

The growing adoption of mobile applications has transformed access to travel-related services, increasing the demand for intuitive and clearly structured digital products. This paper presents a user-centered UX/UI design process for a mobile flight search application prototype. The research combined an analysis of existing flight search platforms with two surveys conducted at different stages of the design process. The first survey comprised 24 questions and involved 50 respondents. It examined travel habits, expectations of flight search services and preferences regarding the presentation of information, informing functional requirements and a low-fidelity prototype. The second survey comprised 20 questions and involved 35 respondents. It examined preferences for navigation, interface components, colour palettes and typography, guiding the high-fidelity prototype developed in Figma. In the first survey, 48 of 50 respondents rated information clarity as important or very important, and 46 assigned these ratings to the visibility of additional costs. In the second survey, 28 of 35 respondents preferred bottom navigation and 24 preferred colour changes as button feedback. The resulting prototype combines persistent navigation, structured flight information, card-based results and consistent visual components across search, booking and ticket management screens. The findings support an emphasis on clear information architecture and restrained visual complexity within the surveyed samples. They provide a traceable rationale for interface decisions, while improvements in task performance, satisfaction and cognitive load remain to be established through task-based usability testing. The case study illustrates how staged preference research can inform the design of travel-related mobile applications.

Stefan Đurđević
Gala Golubović
Dragana Žilić

University of Novi Sad, Faculty of Technical Sciences, Department of Graphic Engineering and Design, Novi Sad, Serbia

KEY WORDS
User experience, user interface, mobile application, flight search, user-centered design

1. Introduction

Flight search interfaces must communicate several interdependent choices within a small display: origin and destination, travel dates, connections, schedules, fares and optional services. A visually simple screen is insufficient if users cannot identify the information needed to compare offers or understand the consequences of a booking decision. The design problem therefore concerns both the organisation of the search process and the visual presentation of its individual steps.

Human-centred design provides a framework for considering users throughout the development of interactive systems (International Organization for Standardization, 2019). For flight search, this raises a practical question: how can reported user needs and interface preferences be translated into a coherent mobile prototype? The present paper addresses this question through a mobile flight search application prototype, connecting two stages of survey research to the resulting information architecture and visual design.

2. Methods

2.1. Study design and research context

The process comprised an examination of existing services, a first user survey, the definition of user needs and a representative persona, low-fidelity prototyping, a second survey of interface preferences, and high-fidelity prototyping. Wizz Air, eSky, Kiwi and Skyscanner were examined as reference services. Their interfaces informed the exploration of search, booking and information presentation. This examination supplied design context rather than a controlled benchmark or a ranking of current commercial products.

2.2. Survey instruments and respondents

The first questionnaire contained 24 questions organised into three parts: demographics; travel habits and experience with flight search services; and ratings of existing website displays. It included categorical choices, five-point ratings and an open question about sources of dissatisfaction. The second questionnaire contained 20 questions. Five concerned demographics and mobile use, while 15 examined preferences for navigation, feedback, content organisation, visual emphasis, notifications, colour, typography and icons.

Table 1 summarises the samples. The first survey included 50 respondents and the second 35. Recruitment procedures and respondent overlap between stages were not documented sufficiently to support a longitudinal analysis. Consequently, the surveys are treated as separate descriptive datasets, and their sample sizes are not added to infer a number of unique participants.

Table 1
Sample characteristics and questionnaire scope

Characteristic	Survey 1	Survey 2
Number of respondents	50	35
Number of questions	24	20
Women, n (%)	40 (80.0)	26 (74.3)
Men, n (%)	10 (20.0)	9 (25.7)
Aged 18–25, n (%)	43 (86.0)	33 (94.3)
Aged 26–45, n (%)	6 (12.0)	1 (2.9)
Aged 46–65, n (%)	1 (2.0)	1 (2.9)

2.3. Analysis and prototyping

Responses were analysed descriptively using reported frequencies and percentages. Percentages in the tables are recalculated from documented counts and rounded to one decimal place; totals may differ slightly from 100% due to rounding. For selected five-point importance items, ratings of 4 and 5 are combined explicitly.

The first survey guided the functional structure and low-fidelity screens. The second informed visual and interaction choices in the high-fidelity Figma prototype. The logo was created in Adobe Illustrator. No controlled task experiment, performance baseline or standardised post-use usability score was made. The output is therefore an interactive design prototype, without demonstrated airline inventory, payment or check-in system integration.

3. Results

3.1. Flight search needs and information priorities

The first survey identified information visibility and control over bookings as prominent concerns. On the five-point scale, where 1 indicated “not important at all” and 5 “very important”, 42 respondents selected 5 and 6 selected 4 for information clarity. For clearly displayed additional costs, 34 selected 5 and 12 selected 4. For a cancellation option, the corresponding counts were 26 and 14. Table 2 reports these combined ratings alongside selected categorical responses.

Table 2
Selected requirements from Survey 1 (n = 50)

Requirement or preference	Response criterion	n	%
Clear presentation of information	Rating 4 or 5	48	96.0
Visible information on additional costs	Rating 4 or 5	46	92.0
Option to cancel a booking	Rating 4 or 5	40	80.0
Availability on multiple platforms	Selected preference	37	74.0
Availability in Serbian and English	Selected preference	36	72.0
Notifications of flight price changes	Positive response	44	88.0
Discounts for regular users	Positive response	45	90.0

These responses support treating essential information as a primary design requirement. In particular, clarity should include the visibility of costs that may alter the apparent attractiveness of a fare. Cancellation is a related control requirement: users need

to find the relevant action and understand its conditions. The data establish the importance respondents attached to these features, rather than the effectiveness of any particular implementation.

When asked which listed flight search service they used most frequently, 27 respondents selected Wizz Air (54.0%), ten Skyscanner (20.0%), two eSky (4.0%) and two Kiwi (4.0%); nine selected non-use (18.0%). These figures describe the sample's choices among the offered categories. They do not estimate market shares. The inclusion of non-users also means that expectations of flight search should not be interpreted as evaluations based uniformly on extensive experience.

Open responses described problems with organisation and the visibility of relevant information. Among the requested improvements were clearer cancellation options and a calendar that makes prices easier to inspect. These comments were used as qualitative design input; no formal coding scheme or theme frequency analysis was documented. In the flight-choice importance item, 25 respondents assigned the highest rating to the number of connections, providing a reason to make connection information easy to locate during comparison.

3.2. From requirements to a low-fidelity structure

The requirements were translated into a sequence covering search, comparison, flight details, booking and subsequent ticket management. A representative persona and a user journey were constructed to support design decisions. The persona was a design aid rather than a statistically established user segment. Low-fidelity screens then defined the placement of controls and the links between screens before colour and typography were finalised.

The structure included entry and account screens, a home screen, flight search and results, flight details, booking steps, e-tickets, notifications and account settings. Ancillary choices such as insurance, baggage and seats were represented as successive booking steps, with access to further information. This creates an opportunity to explain optional services in context, although comprehension of those explanations requires subsequent observation of users completing booking tasks.

3.3. Interface preferences in the second survey

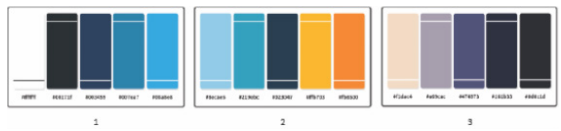
The second survey provided more specific input for navigation and visual components. Bottom navigation was selected by 28 of 35 respondents (80.0%), compared with seven who selected a side menu. Colour change was the preferred form of button feedback for 24 respondents (68.6%); seven selected a shadow and four selected a size or shape change. These responses guided the persistent bottom navigation and interactive button variants in the prototype.

Table 3

Selected interface preferences from Survey 2 (n = 35)

Interface decision	Preferred option	n	%
Primary navigation	Bottom navigation	28	88.0
Button feedback	Colour change	24	68.6
Content presentation	Cards with detailed information	19	54.3
Colour scheme	Palette 2	21	60.0
Body typeface	San Francisco	21	60.0
Emphasis typeface	Poppins	16	45.7
Icon style	Filled icons	19	54.3

For content presentation, 19 respondents preferred cards with detailed information, ten preferred an image-based presentation with minimal text, and six preferred a tabular presentation. Cards therefore received a narrow majority, rather than a unanimous preference. The layout adopted cards to group the attributes of each offer, while retaining textual details needed for comparison. The preference for clear separation of content sections further informed the organisation of the screens. Figure 1 shows the offered color palettes.



» **Figure 1:** *Color Palettes 1, 2 and 3*

Palette 2 was selected by 21 respondents (60.0%), compared with nine selecting Palette 1 and five selecting Palette 3. For body text, San Francisco received 21 selections, ahead of both Inter and Open Sans. For emphasis text, Poppins received 16 selections (45.7%), Inter 11 and Montserrat eight. Poppins was therefore the most frequently chosen option, but did not obtain an absolute majority. This distinction matters when describing the strength of the design rationale.

The difference between icon preferences was also small: 19 respondents selected filled icons and 16 selected outline icons. Filled icons were incorporated into the design, but this result does not justify a general claim that they are superior. Their interpretation still depends on the task, accompanying labels and the familiarity of individual symbols. A visual preference provides a starting point for design, not a substitute for checking whether users recognise a control.

3.4. Translating preferences into a visual system

Mobile flight search application prototype identity combined a cloud and aircraft symbol with a Montserrat wordmark. The application palette used blue tones as primary colours and yellow and orange as secondary accents, with black and white used for text and backgrounds. San Francisco was used for body text and Poppins for emphasis. Rounded buttons, grouped content and filled icons supplied a consistent set of visual elements across the main screens.

This translation was selective. Stronger preferences, such as bottom navigation, shaped the main interaction structure, while weaker differences, such as the filled-icon result, informed a provisional style choice. The design rationale is thus traceable without treating every selected option as an independently validated usability improvement. Consistency across screens is a design objective; its effects on learning and error rates were not measured in this study.

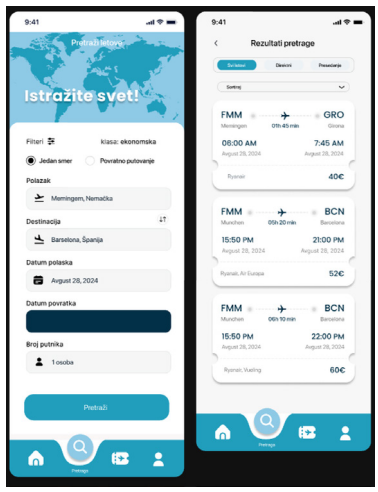
3.5. High-fidelity search and comparison screens

The high-fidelity prototype implemented the screen structure and visual choices in Figma. Its bottom navigation connects the home screen, flight search, e-tickets and profile. Secondary functions are available through additional menus and settings. The home screen contains destination and flight suggestions in card sections, and a notification entry provides access to updates. The presence of suggestions supports exploration, while the dedicated search section provides a direct route for users with a specific journey in mind.

Figure 2 shows the original search and results screens. The search form collects the journey type, origin, destination, dates and passenger information. The results screen groups flight attributes within cards and provides options for changing the presentation of results. In this arrangement, each offer has a recognisable visual boundary, supporting the intended comparison of route, time and price information. Screen content, dates and prices are illustrative prototype data.

The results screen operationalises the preference for cards, while the search form separates input choices from the comparison stage. This separation reduces the amount of content that must be presented at one time, but it also requires users to move between stages when revising a query. The design therefore creates a testable question: can users modify their travel criteria and compare alternatives without losing their place or overlooking a relevant fare condition?

The prototype retains a visually prominent header and destination imagery. Its interpretation of simplicity is therefore based mainly on grouping and hierarchy, rather than the complete removal of decorative content. Whether those elements help orientation or occupy space better used for fare information remains an issue for usability evaluation on mobile devices.



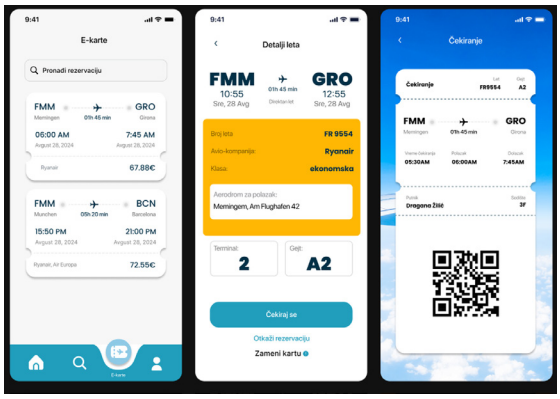
» **Figure 2:** *Search and results screens with the original Serbian interface*

3.6. Booking and ticket management

Selecting a flight opens its details and a route into booking. The represented sequence covers insurance, baggage and seat selection, passenger information, payment selection and confirmation. Supplementary information is accessible during relevant booking steps. These screens express the intended interaction flow; the prototype does not demonstrate real financial transactions or a live reservation service.

Figure 3 shows e-ticket access, flight details and the check-in representation. The e-ticket section presents booked flights and a search option. A selected flight leads to details with check-in, cancellation and ticket-change actions, followed by a screen containing a QR code. This sequence connects the search and purchase concept with later travel tasks. The QR code is part of the prototype visualisation and is not evidence of an operational boarding credential.

The notification and profile screens represent additional requirements from the first survey. Notifications provide a place for price and travel updates, while the profile includes collected points and available discounts. Such functions were motivated by stated interest in alerts and loyalty benefits. Their inclusion does not establish that respondents would enable notifications, return more often or complete more bookings in actual use.



» **Figure 3:** *E-ticket and check-in screens with illustrative booking data*

3.7. Interaction behaviour and implementation scope

Figma components and variants were used to define navigation states and button feedback. The bottom navigation remains fixed during scrolling and changes its active state between sections. Buttons change colour on interaction, while selection controls use a coloured outline. Centred overlays represent supplementary messages and can be dismissed by clicking outside them. The design also specifies transitions between screens, with 300 ms timing.

The implemented component behaviour makes the prototype suitable for examining screen-to-screen navigation. However, interface simulation does not establish the reliability of a deployed application. Price monitoring, multilingual content, cross-platform delivery, cancellation rules and payment processing would require further implementation and validation. The case study's result is the documented design and its interactive representation, rather than a production flight booking system.

4. Discussion

The main contribution is the explicit connection between two types of evidence and two levels of design. Survey 1 identified what respondents wanted to find or control, including prices, additional costs and booking changes. Survey 2 informed how the interface could present those functions, including navigation position, feedback and typographic choices. Treating these stages separately helps prevent a preferred visual treatment from being mistaken for a functional requirement.

The resulting emphasis on grouping, consistent components and visible feedback is compatible with established usability heuristics (Nielsen, 1994). In this case, however, that compatibility is an interpretation of the design, not the result of a formal heuristic evaluation. Similarly, participants' preference for an interface element cannot establish its effect on task performance. Nielsen (2001) stresses the importance of observing actual use when evaluating interfaces; this is the necessary next step for a mobile flight search application.

Several limitations restrict generalisation. Both samples were small and concentrated among respondents aged 18–25, with women forming the majority. Self-reported preferences may differ from behaviour during time-sensitive travel tasks. The study does not support inferential comparisons between demographic groups or an estimate of preferences among the wider travelling population.

A subsequent evaluation should observe participants searching for a specified route, comparing total costs, changing baggage choices and finding cancellation conditions. Completion rates, time, errors and post-task assessments could then be compared across design alternatives. Recruitment should include less frequent travellers and a wider age range. Accessibility checks should address text legibility, contrast, touch targets, motion and assistive technology support. Such work would test the expected benefits without assuming them from preference data.

5. Conclusions

Mobile flight search application prototype case demonstrates a structured way to translate flight search needs and interface preferences into an interactive mobile design. The first survey highlighted information clarity, visible additional costs and booking control; the second informed bottom navigation, button feedback, cards, colour and typography. The resulting prototype connects search, comparison, booking and ticket management through a consistent visual structure. These findings support the design rationale within the surveyed samples. Claims of improved usability, lower cognitive load or greater satisfaction require direct evaluation of the completed interaction flow.

6. Acknowledgment

This research has been supported by the Ministry of Science, Technological Development and Innovation (Contract No. 451-03-34/2026-03/200156) and the Faculty of Technical Sciences, University of Novi Sad through project "Scientific and Artistic Research Work of Researchers in Teaching and Associate Positions at the Faculty of Technical Sciences, University of Novi Sad 2026" (No. 01-3609/1).his research did not receive any specific grant from funding agencies in the public, commercial, or not-for-profit sectors.

7. References

International Organization for Standardization. (2019) ISO 9241-210:2019. *Ergonomics of human-system interaction — Part 210: Human-centred design for interactive systems*. Geneva, ISO.

Nielsen, J. (1994) *10 usability heuristics for user interface design*. Available from: https://www.nngroup.com/articles/ten-usability-heuristics/ [Accessed 13 June 2026].

Nielsen, J. (2001) *First rule of usability? Don't listen to users*. Available from: https://www.nngroup.com/articles/first-rule-of-usability-dont-listen-to-users/ [Accessed 13 June 2026].



© 2026 Authors. Published by the University of Novi Sad, Faculty of Technical Sciences, Department of Graphic Engineering and Design. This article is an open access article distributed under the terms and conditions of the Creative Commons Attribution license 4.0 Serbia (http://creativecommons.org/licenses/by/4.0/rs/).

Original Scientific Paper https://doi.org/10.24867/GRID-2026-p62

Decoding Brand Experience in AR Vs. Web Interfaces via Gaussian Graphical Models

ABSTRACT

In the saturated digital marketplace, Augmented Reality (AR) has shifted from a novelty to a critical interface tool, directly overcoming the physical limitations of product evaluation. This paper investigates the structure of conditional dependencies within brand experience indicators across two distinct digital environments: traditional static web interfaces and interactive AR virtual try-on tools. Utilizing a field experiment design with a global cosmetics brand (Garnier) as the stimulus, data were gathered through a single-phase protocol focusing solely on AR (Study A) and a sequential within-subjects protocol comparing Web and AR platforms (Study B). To capture the dynamic, interconnected nature of consumer perceptions, a network approach using Gaussian Graphical Models (GGM) was deployed to map and compare the conditional networks of brand experience items across both mediums. The structural analysis reveals moderately dense networks in both contexts, empirically demonstrating that brand experience operates as a highly integrated, holistic system rather than a set of independent dimensions. Ultimately, the findings highlight how immersive technologies reconfigure consumer touchpoints, offering fresh methodological insights for digital interface design and visual marketing analytics.

Jelena Spajić [1]
Ksenija Mićić [2]
Bojana Milić [1]

[1] Faculty of Technical Sciences, Department of Industrial Engineering and Management, Novi Sad, Serbia
[2] L'Oréal Balkan, Belgrade, Serbia

KEY WORDS
Augmented reality (AR), virtual try-on, brand experience, Gaussian Graphical Model (GGM), network analysis

1. Introduction

The rapid evolution of digital commerce has compelled brands to transition from static online touchpoints to highly immersive visual interfaces. In this context, brand experience emerges primarily as a psychological and symbolic construct concerned with meaning and emotion rather than simple transaction ease (e.g. Mićić, 2026). It is specifically evoked by brand-identified stimuli, such as visual identity, interactive elements, and ambient design. Grounding this concept, Brakus et al. (2009) define brand experience as subjective, internal consumer responses (sensations, feelings, and cognitions) and behavioral responses elicited by brand-related stimuli across the entire customer journey. Empirically validated as a direct operationalization of Schmitt's (1999) strategic experiential modules, the four-dimensional framework by Brakus et al. (2009) captures four distinct facets:

- Sensory Experience: Aesthetic impressions and direct stimulation of the human perceptual apparatus (sight, sound, touch, taste, smell) that leave a memorable perceptual trace.
- Affective Experience: Emotional responses ranging from subtle moods to deep affective resonance, transforming transactional interactions into emotionally charged relationships.
- Intellectual Experience: The stimulation of complex mental activity, convergent/divergent thinking, imagination, and problem-solving curiosity.
- Behavioral Experience: Bodily actions, physical engagement, and lifestyle changes resulting from interactive motor activities.

While Schmitt (1999) originally formulated experiential modules from a managerial perspective, Brakus et al. (2009) refined the framework into a consumer-centric scale optimized for quantitative measurement, omitting the relational dimension due to its empirical overlap with affective and behavioral dimensions.

In existing literature, brand experience dimensions are almost exclusively treated as independent latent variables acting in parallel. However, the immersive nature of AR forces the simultaneous activation of multiple sensory and cognitive channels. Interactive real-time features imply that immediate visual cues spill over into emotional states or trigger intellectual curiosity. Recent empirical work confirms that AR-induced psychological states create cross-dimensional cognitive offloading and unique predictive pathways unobserved in static digital formats (Hilken et al., 2017; Yim et al., 2017; Heller et al., 2019; Rauschnabel et al., 2022; Kim et al., 2023; Mitrović et al., 2024; Mićić, 2026). To address this structural shift, it is essential to move beyond traditional latent factor models and examine how these dimensions interact network-wise. Consequently, this study poses the following research question: What are the structural characteristics and conditional interdependencies of brand experience dimensions within an augmented reality environment compared to traditional web interfaces?

2. Methods

2.1. Experimental design and context

A multi-stage quantitative experimental field experiment was conducted to maintain ecological validity. Hair color products from Garnier were selected as the experimental stimulus, as Garnier represents a highly familiar global brand with a mature, globally deployed virtual try-on platform. Hair coloring represents a high-involvement purchasing decision characterized by strong visual evaluation requirements and an inherent inability to conduct physical pre-purchase trials. The methodology encompasses two independent experimental protocols:

- Study A (Single-phase AR Protocol): Participants interacted exclusively with the AR virtual try-on tool prior to completing the evaluation instrument (N=142).
- Study B (Sequential Within-Subjects Protocol): A separate cohort evaluated the product line first on the official static web interface (Phase 1) and subsequently engaged with the AR virtual try-on tool (Phase 2), completing evaluations after each stage (N=126).

2.2. Sample and procedure

Data collection was conducted in Serbia in October and November 2025 using a structured online questionnaire distributed via purposive and virtual snowball sampling (Baltar & Brunet, 2012). From an initial pool of 324 responses, 56 were excluded following quality control procedures, yielding a final validated sample of 268 real consumers (NstudyA=142; NstudyB=126). In line with the target population for hair color products, both cohorts were overwhelmingly female (Study A: 99.3%; Study B: 94.4%) with broad age representation across 18 to over 55 years, centered around the 25–34 age bracket (~33%). Approximately two-thirds of respondents in both samples actively use hair dye products (~68%), ensuring high category involvement, while roughly 27% had prior experience with AR try-on tools. Participation was voluntary, anonymous, and conducted in accordance with digital ethics guidelines.

2.3. Measures and questionnaire development

Data was collected via structured electronic questionnaires. The four core dimensions defined by Brakus et al. (2009): Sensory (SBE), Affective (ABE), Behavioral (BBE), and Intellectual (IBE) brand experience, were operationalized on 7-point Likert scales. Reverse-coded items (SBE3R, ABE2R, BBE3R, IBE2R) were retained specifically as diagnostic indicators of experiential disengagement and friction. The complete operationalization of the four brand experience dimensions, adapted for the digital virtual try-on context based on Brakus et al. (2009), along with the corresponding item codes and adapted items, is provided in Table 1.

Table 1 (part 1)

Brand Experience Measurement Scale and Item Operationalization (adapted from Brakus et al., 2009)

Code	Dimension	Adapted Items
SBE1	Sensory	Virtual try-on of Garnier hair colors is visually appealing.
SBE2	Sensory	Virtual try-on of Garnier hair colors is visually and sensorially interesting.
SBE3R	Sensory (Reverse)	Virtual try-on of Garnier hair colors is not appealing to my senses.
ABE1	Affective	Virtual try-on of Garnier hair colors induces certain feelings in me (mood, excitement, trust...).

Table 1 (part 2)
Brand Experience Measurement Scale and Item Operationalization (adapted from Brakus et al., 2009)

Code	Dimension	Adapted Items
ABE2R	Affective (Reverse)	I do not feel strong emotions toward the Garnier brand while using the virtual hair color try-on tool.
ABE3	Affective	While using the Garnier virtual hair color try-on tool, I feel pleasure and emotional satisfaction.
BBE1	Behavioral	Virtual try-on of Garnier hair colors encourages me to take concrete actions regarding the product (exploring options, comparing shades...).
BBE2	Behavioral	Virtual try-on of Garnier hair colors influences my behavior (browsing products, planning a purchase...).
BBE3R	Behavioral (Reverse)	Virtual try-on of Garnier hair colors is not action oriented.
IBE1	Intellectual	Virtual try-on of Garnier hair colors makes me think about the products.
IBE2R	Intellectual (Reverse)	Virtual try-on of Garnier hair colors does not make me think.
IBE3	Intellectual	Virtual try-on of Garnier hair colors stimulates my curiosity and motivates me to explore further.

2.4. Gaussian graphical models (GGM)

Unlike traditional latent factor models, Gaussian Graphical Models (GGMs) treat brand experience as a dynamic system of directly interconnected indicators, a property particularly suited for immersive AR environments where sensory, cognitive, and emotional responses co-activate (Epskamp et al., 2018). Nodes represent survey items, while edges reflect conditional partial correlations after controlling for all other variables.

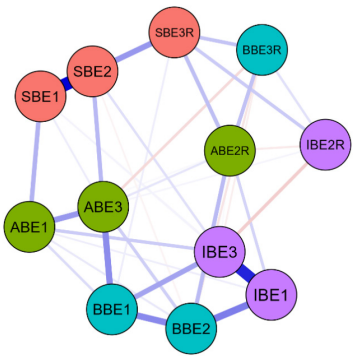
To prevent overfitting and eliminate spurious connections in sample-level estimates, regularization was applied via the EBICglasso (Least Absolute Shrinkage and Selection Operator) algorithm in JASP, yielding a sparse, parsimonious network retaining only strong empirical signals (Epskamp et al., 2018). Network topology was evaluated using edge weights, sparsity indices, Node Strength, and Expected Influence (EI), a key centrality metric that accounts for both positive and negative associations (Robinaugh et al., 2016). Traditional closeness and betweenness metrics were excluded due to known instability under LASSO penalization.

Network stability and parameter replicability were verified via 1,000 non-parametric bootstrap iterations and case-dropping bootstrap procedures (Epskamp et al., 2018). Consequently, structural inferences focus exclusively on robust, high-stability patterns.

3. Results

3.1. Study A: standalone AR network structure

The estimated GGM for Study A revealed a dense network with 39 non-zero edges out of 66 possible pairs (sparsity index = 0.409). Under pure AR exposure, brand experience functions as an integrated, co-activating network.



» **Figure 1:** *Network analysis using GGM for the four-dimensional brand experience framework: Study A*

Key partial correlations reflect immediate cross-dimensional spillover:

8. Sensory Coherence: The strongest positive edge occurred between SBE1 ↔ SBE2 (rpartial=0.636), demonstrating that AR provides a highly unified perceptual anchor.

9. Cognitive-Behavioral Coupling: High internal cognitive alignment (IBE1 ↔ IBE3, 0.548) actively coupled with behavioral exploration (BBE2 ↔ IBE1, 0.325).
10. Affective Activation and Action Linkage: Emotional stimulation connected directly to motor/behavioral action (ABE3 ↔ BBE1, 0.283). Furthermore, the strong edge between BBE1 ↔ BBE2 (0.294) confirms the internal coherence of the behavioral dimension, suggesting that in an augmented reality context, affective activation is not isolated but directly feeds into behavioral action and user engagement.

Centrality indices revealed that sensory aspects are the core drivers of the network. Specifically, visual appeal (SBE1: Expected Influence = 0.778) and sensory interest (SBE2: Strength = 1.252, EI = 1.135) emerged as central network hubs, indicating that the initial sensory impression activates and propagates through the rest of the brand experience dimensions. Conversely, reverse-coded non-engagement items (e.g., IBE2R: EI =-2.138) remained at the network periphery, showing minimal integration with the core positive experience nodes.

3.2. Study B: comparative network analysis (AR vs. Web)

The comparative structural analysis of the estimated networks (Figure 2) reveals fundamental insights into how brand experience operates across traditional and immersive digital channels. The AR network displays 39 non-zero edges out of 66 potential connections (sparsity index = 0.409), whereas the Web network exhibits 41 non-zero edges (sparsity index = 0.379).

Both empirical structures reflect moderately dense, highly interconnected networks. From a theoretical standpoint, this pattern reinforces a core premise: brand experience does not function as a set of isolated, independent dimensions. Instead, regardless of the digital medium deployed, brand experience operates as a highly integrated system of mutually reinforcing perceptual, affective, cognitive, and behavioral nodes. However, as illustrated in Figure 2, comparing Study A (AR experience) and Study B (Web vs. AR) reveals clear structural shifts in how information is processed across channels.

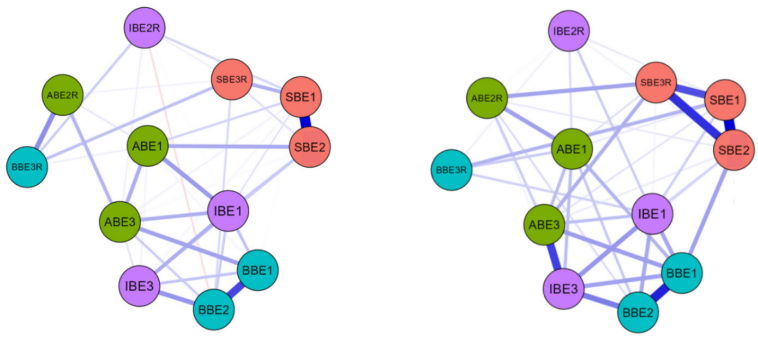
Centrality shifts across media are detailed in Table 2. While sensory visual interest (SBE2) maintains high centrality across both interfaces (AR: Strength = 1.083, EI = 1.101; Web: Strength = 1.011, EI = 1.011), comparing the baseline Web environment to the subsequent AR exposure reveals clear structural shifts. In the Web condition, user experience is predominantly driven by pragmatic, goal-oriented behavior (BBE1: EI = 0.922) and information-seeking curiosity (IBE3: EI = 0.685).

Upon transition to the AR interface, centrality sharply shifts toward sensory immersion and direct cognitive engagement. Specifically, sensory appeal (SBE1) increases in expected influence from 0.685 in Web to 1.040 in AR, while cognitive thinking (IBE1) jumps from 0.197 to 0.865. Conversely, pragmatic behavioral searching (BBE1: EI = 0.517) and informational curiosity (IBE3: EI =-0.039) recede in importance under AR conditions. Across both interfaces, reverse-coded items (except for SBE3R in the Web condition) consistently remain at the network periphery, confirming the structural stability of the underlying brand experience network.

Table 2

Standardized Centrality Metrics for AR and Web Interfaces (Study B)

Item	AR Strength	AR Expected Influence	Web Strength	Web Expected Influence
SBE1	1.018	1.040	0.685	0.685
SBE2	1.083	1.101	1.011	1.011
SBE3R	-1.036	-0.900	0.532	0.532
ABE1	0.141	0.212	-0.063	-0.063
ABE2R	-1.157	-1.014	-1.029	-1.029
ABE3	0.708	0.747	0.514	0.514
BBE1	0.465	0.517	0.922	0.922
BBE2	0.859	0.419	0.145	0.145
BBE3R	-1.007	-0.872	-1.667	-1.667
IBE1	0.833	0.865	0.197	0.197
IB2R	-1.783	-2.076	-1.934	-1.934
IBE3	-0.124	-0.039	0.685	0.685



» **Figure 2:** *Gaussian Graphical Models for Augmented Reality (left) and Website (right): Study B*

4. Discussion

Addressing the research question, the empirical network structures demonstrate that brand experience in AR is not merely an amplified version of web browsing, but an architectural reconfiguration of consumer perceptions:

1. Simultaneous multi-sensory activation in AR: In line with Heller et al. (2019) and Rauschnabel et al. (2022), AR interfaces anchor consumer experience in sensory co-activation (SBE1, SBE2). Real-time visual feedback reduces cognitive strain, enabling direct transfers between sensory perception, curiosity (IBE1), and emotional engagement (ABE3).
2. Task-oriented processing in static web: Static web interfaces require active cognitive processing and manual search behaviors (BBE1, IBE3). Consumers must mentally bridge the gap between static product images and real-life application, shifting centrality toward behavioral search actions.
3. Rejection of unidimensional latency: Network connectivity metrics affirm that brand dimensions (Brakus et al., 2009) act as mutually reinforcing components within an interactive system, validating GGM network analysis as a superior diagnostic tool for immersive UX environments.

5. Conclusions

This study advances digital marketing literature by demonstrating that AR virtual try-on technology fundamentally reconfigures the internal structure of brand experience. By treating sensory, affective, behavioral, and intellectual dimensions as connected network nodes rather than isolated latent variables, we show that AR serves as a powerful sensory-cognitive engine. For UX strategists, AR deployment should be treated not as a secondary promotional feature, but as a primary perceptual anchor designed to streamline decision-making and deepen brand engagement.

This paper represents part of a broader PhD thesis research exploring the mechanisms of augmented reality and brand equity in digital environments (Mićić, 2026). To build upon these empirical findings, future research should embrace larger, cross-cultural samples to enhance the generalizability of the network structures across diverse consumer segments. Furthermore, expanding this methodology to other product categories and industries (such as fashion apparel, eyewear, home furnishings, and interactive automobile configurators) will test the structural boundary conditions of immersive brand networks. Future studies could also deploy longitudinal experimental designs to track how network dependencies evolve over repeated AR exposure, as well as combine psychometric network modeling with objective physiological measures (e.g., eye-tracking and facial coding) to map the exact cognitive and sensory pathways of immersive consumer interfaces.

6. References

Baltar, F. and Brunet, I. (2012) 'Social research 2.0: Virtual snowball sampling method using Facebook', *Internet Research*, 22(1), pp. 57–74. DOI: 10.1108/10662241211199960

Brakus, J.J., Schmitt, B.H. and Zarantonello, L. (2009) 'Brand experience: What is it? How is it measured? Does it affect loyalty?', *Journal of Marketing*, 73(3), pp. 52–68. DOI: 10.1509/jmkg.73.3.052

Epskamp, S., Borsboom, D. and Fried, E.I. (2018) 'Estimating psychological networks and their accuracy: A tutorial paper', *Behavior Research Methods*, 50(1), pp. 195–212. DOI: 10.3758/s13428-017-0862-1

Heller, J., Chylinski, M., de Ruyter, K., Mahr, D. and Keeling, D.I. (2019) 'Let me imagine that for you: Transforming the retail frontline through augmenting customer mental imagery ability', *Journal of Retailing*, 95(2), pp. 94–114. DOI: 10.1016/j.jretai.2019.03.005

5. Hilken, T., de Ruyter, K., Chylinski, M., Mahr, D. and Keeling, D.I. (2017) 'Augmenting the eye of the beholder: Exploring the strategic potential of augmented reality to enhance online service experiences', *Journal of the Academy of Marketing Science*, 45(6), pp. 884–905. DOI: 10.1007/s11747-017-0541-x

Kim, J.-H., Kim, M., Park, M. and Yoo, J. (2023) 'Immersive interactive technologies and virtual shopping experiences: Differences in consumer perceptions between augmented reality (AR) and virtual reality (VR)', *Telematics and Informatics*, 77, article 101936. DOI: 10.1016/j.tele.2022.101936

Mićić, K. (2026) *The impact of augmented reality technology on brand experience and brand equity.* PhD thesis. Faculty of Technical Sciences, University of Novi Sad.

Mitrović, K., Spajić, J., Milić, B., Bošković, D. and Lalić, D. (2024) 'Rebranded reality: How AR brand experience impacts brand equity', *Tehnički vjesnik – Technical Gazette*, 31(5), pp. 1438–1447. DOI: 10.17559/TV-20240209001321

Rauschnabel, P.A., Babin, B.J., tom Dieck, M.C., Krey, N. and Jung, T. (2022) 'What is augmented reality marketing? Its definition, complexity, and future', *Journal of Business Research*, 142, pp. 1140–1150. DOI: 10.1016/j.jbusres.2021.12.084

Robinaugh, D.J., Millner, A.J. and McNally, R.J. (2016) 'Identifying highly influential nodes in the complicated grief network', *Journal of Abnormal Psychology*, 125(6), pp. 747–757. DOI: 10.1037/abn0000181

Schmitt, B.H. (1999) *Experiential marketing: How to get customers to sense, feel, think, act, and relate to your company and brands*. New York: Free Press.

Yim, M.Y.-C., Chu, S.-C. and Sauer, P.L. (2017) 'Is augmented reality technology an effective tool for e-commerce? An interactivity and vividness perspective', *Journal of Interactive Marketing*, 39, pp. 89–103. DOI: 10.1016/j.intmar.2017.04.001



© 2026 Authors. Published by the University of Novi Sad, Faculty of Technical Sciences, Department of Graphic Engineering and Design. This article is an open access article distributed under the terms and conditions of the Creative Commons Attribution license 4.0 Serbia (http://creativecommons.org/licenses/by/4.0/rs/).

Review Paper https://doi.org/10.24867/GRID-2026-p63

Artificial Intelligence for Enhancement of Low-Light Photographs

ABSTRACT

Photographs captured under low-light conditions are often characterized by reduced contrast, pronounced noise, loss of detail, and color reproduction deviations, which can significantly reduce their visual quality. Traditional image enhancement methods can partially alleviate these problems, but their effectiveness often depends on parameter selection and the characteristics of a particular scene. The development of artificial intelligence and deep learning has enabled the use of more advanced models in which image enhancement is learned directly from data. This paper reviews contemporary methods for enhancing photographs captured under low-light conditions, with particular emphasis on CNN- and Retinex-based models, GAN and zero-reference approaches, Transformer architectures, and diffusion models. Their basic principles, training strategies, datasets, and quality assessment metrics are analyzed. A comparative review of selected studies shows a shift toward models that improve perceptual quality and generalization and reduce dependence on paired training data, while computational efficiency remains an important challenge.

Iva Juretić
Ivana Jurič
Saša Petrović
Sanja Cvetojević

University of Novi Sad, Faculty of Technical Sciences, Department of Graphic Engineering and Design, Novi Sad, Serbia

KEY WORDS
Artificial intelligence, low-light image enhancement, deep learning, Retinex, Transformer, diffusion models

1. Introduction

Low-light photography remains a challenging task because only a limited amount of light reaches the camera sensor during image acquisition. As a result, low-light photographs are often affected by reduced contrast, pronounced noise, color distortion, and loss of visible detail (Guo et al., 2023). These problems become particularly severe under extremely low illumination, where the small number of captured photons leads to a low signal-to-noise ratio. Extending the exposure time can increase the amount of captured light, but it also increases the risk of motion blur caused by camera shake or movement within the scene (Chen et al., 2018).

A wide range of methods has been developed to address these degradations, from gray-level transformations, histogram equalization, and Retinex-based techniques to more recent deep learning approaches. Traditional enhancement methods can improve image brightness and contrast, but they may also amplify noise, suppress fine details, introduce halo artifacts, or produce color distortions. Their performance may also depend strongly on parameter selection and the characteristics of the input image (Zhan, Goh & Sunar, 2024). With the development of neural networks, low-light image enhancement has increasingly shifted toward data-driven methods that learn image representations directly from training data and are able to address several degradation types within a single framework.

Recent studies cover a broad range of architectures and learning strategies, including convolutional neural networks, Retinex-based deep models, generative adversarial networks, zero-reference methods, Transformer-based architectures, and diffusion models (Liu & Fan, 2025). These approaches differ not only in their enhancement mechanisms, but also in their dependence on paired training data, generalization ability, computational requirements, and evaluation strategies. In mobile photography, low-light enhancement can also be based on multi-frame or burst processing, where several consecutive images are combined to obtain a higher-quality result.

Google Night Sight is one example of this approach, using multiple captured frames for photography under very low-light conditions (Liba et al., 2019). These multi-frame methods are not considered in detail in this review, which focuses on single-image enhancement.

This paper reviews and compares recent artificial intelligence-based methods for low-light photograph enhancement, with particular emphasis on their underlying principles, datasets, evaluation procedures, advantages, and limitations. The review also considers commonly used datasets and image quality assessment metrics, while selected studies are compared to highlight the main directions in the development of this research field.

2. Characteristics and degradations of low-light photographs

Photographs captured under low-light conditions are commonly affected by reduced contrast, color reproduction errors, and image noise, all of which negatively influence their visual quality (Guo et al., 2023). Unfavorable imaging conditions may include insufficient or uneven illumination, backlighting, and other lighting situations that reduce image quality and lead to loss of visual information (Tian et al., 2023).

One of the main challenges of photography under extremely low illumination is a low signal-to-noise ratio, which is associated with the small number of photons captured by the sensor. Images acquired with short exposure times may contain substantial noise, whereas longer exposures increase the risk of motion blur caused by camera shake or movement of objects within the scene (Chen et al., 2018).

Increasing the ISO sensitivity can make an image appear brighter, but it also amplifies the noise already present in the captured signal. Subsequent image processing, such as pixel-value scaling or histogram stretching, cannot compensate for the inherently low signal-to-noise ratio (Chen et al., 2018).

Severe color distortions may also occur under extremely low-light conditions. Chen et al. (2018) describe an example in which, despite the use of a very high ISO setting, the captured image remained dark and exhibited pronounced noise and noticeable color shifts. Zheng et al. (2026) further note that low-light photographs may exhibit low brightness, poor scene visibility, high noise levels, and loss of detail. These degradations can become even more pronounced in non-uniformly illuminated scenes, where illumination varies spatially and very dark and very bright regions may occur simultaneously within the same image.

3. Low-light image enhancement methods

A variety of approaches have been developed for low-light image enhancement, ranging from traditional image processing techniques to modern methods based on artificial intelligence and deep learning. The development of this field reflects a gradual shift from predefined algorithmic procedures toward data-driven approaches (Zhan, Goh & Sunar, 2024).

3.1. Traditional enhancement methods

Traditional methods for enhancing low-light photographs include a range of mathematical and algorithmic techniques, among which gray-level transformations, histogram equalization, and Retinex-based methods are commonly used (Zhan, Goh & Sunar, 2024). These approaches can also be classified according to whether they operate in the spatial or frequency domain. Spatial-domain methods directly modify pixel values, whereas frequency-domain methods first transform the image and then apply appropriate filtering operations in the transformed domain (Liu & Fan, 2025).

Gray-level transformations are used to adjust image brightness, contrast, and dynamic range by modifying individual pixel values. This group includes linear, logarithmic, piecewise linear, and gamma transformations (Zhan, Goh & Sunar, 2024).

However, these methods may not adequately handle a wide range of illumination levels, which can result in detail loss in overexposed or underexposed regions (Zhan, Goh & Sunar, 2024).

Histogram equalization modifies the distribution of gray levels in order to increase image contrast and expand the dynamic range. Global histogram equalization is applied to the entire image, whereas adaptive histogram equalization divides the image into smaller regions that are processed independently (Zhan, Goh & Sunar, 2024). A limitation of adaptive histogram equalization is that it may excessively increase local contrast and amplify noise. Contrast Limited Adaptive Histogram Equalization (CLAHE) addresses this problem by restricting the amount of contrast enhancement, thereby reducing excessive noise amplification (Zhan, Goh & Sunar, 2024).

Retinex-based approaches rely on decomposing an image into illumination and reflectance components. These methods can improve contrast, brightness, and dynamic range while helping preserve color appearance. The development of Retinex-based enhancement has led to methods such as Single-Scale Retinex (SSR), Multi-Scale Retinex (MSR), and Multi-Scale Retinex with Color Restoration (MSRCR) (Zhan, Goh & Sunar, 2024).

Nevertheless, Retinex methods may introduce halo artifacts and color distortions, while parameter selection can be challenging because a single parameter configuration does not necessarily produce satisfactory results across different images (Zhan, Goh & Sunar, 2024).

A representative example of a traditional Retinex-based approach is LIME (Low-light Image Enhancement via Illumination Map Estimation), proposed Guo, Li and Ling (2017). Unlike methods that separately estimate both reflectance and illumination, LIME estimates only the illumination map, thereby reducing the complexity of the problem. An initial illumination map is obtained from the maximum value among the RGB channels at each pixel and is subsequently refined using a structure prior to preserve image structure.

The authors experimentally compared LIME with several traditional enhancement techniques, including HE, AHE, gamma correction, and other Retinex-based and variational methods. On the HDR dataset, LIME achieved the lowest average LOE value among the compared methods, indicating better preservation of the natural lightness order in the enhanced images (Guo, Li & Ling, 2017).

Frequency-domain methods, such as homomorphic filtering and wavelet transforms, process different frequency components of an image and may preserve image details more effectively than spatial-domain approaches. However, they are generally more sensitive to parameter selection, while both spatial- and frequency-domain techniques may amplify noise and show limited effectiveness under challenging low-light conditions (Liu & Fan, 2025).

Because traditional methods have a limited ability to model complex patterns and relationships within image data and to adapt to varying image characteristics, increasing attention has been directed toward data-driven enhancement approaches (Zhan, Goh & Sunar, 2024).

3.2. Artificial intelligence-based methods

Traditional low-light image enhancement methods often rely on physical models, predefined assumptions, and manual parameter adjustment, which can limit their adaptability to different imaging conditions (Ye, Qiu & Zhang, 2024). Learning-based methods instead use data to learn how low-light images should be enhanced.

Recent methods use different learning strategies, including supervised, unsupervised, zero-shot, and fusion-based learning (Liu & Fan, 2025). The main difference between these approaches lies in the type of training data and supervision they use. The terms zero-reference and zero-shot are not used consistently across the literature.

In this paper, zero-reference refers to methods such as Zero-DCE, which are trained without paired or unpaired reference images and use non-reference loss functions during training (Guo et al., 2020). The main distinction is that zero-reference methods may still involve model training, but without reference images, whereas zero-shot methods do not rely on prior training on an external dataset. ExCNet, for example, trains a small CNN at test time using only the input image (L. Zhang et al., 2019).

The following section presents representative CNN, Retinex-based, GAN, unsupervised and zero-reference, Transformer, and diffusion-based methods.

4. Modern AI-based approaches to low-light image enhancement

Modern artificial intelligence-based approaches to low-light image enhancement employ a variety of architectures and learning strategies. These include convolutional neural networks, Retinex-based approaches, generative adversarial networks, unsupervised and zero-reference methods, Transformer architectures, and more recent diffusion models (Liu & Fan, 2025).

4.1. Early deep learning approaches and CNN architectures

One of the early deep learning approaches to low-light image enhancement was LLNet, introduced by Lore, Akintayo and Sarkar (2017). The method is based on a deep autoencoder designed to improve contrast and reduce noise within a single framework. During training, images were artificially darkened and corrupted with Gaussian noise in order to simulate different low-light conditions.

The authors also proposed S-LLNet, a variant in which contrast enhancement and denoising are handled by two successive modules. Both models were tested on synthetically degraded images and naturally captured low-light photographs using PSNR and SSIM. On dark images with added synthetic noise, LLNet and S-LLNet performed better than the traditional methods used for comparison, with S-LLNet achieving the highest PSNR and SSIM values in several cases (Lore, Akintayo & Sarkar, 2017).

A different CNN-based strategy was introduced with MBLLEN (Multi-Branch Low-Light Enhancement Network) by Lv et al. (2018). The network follows a fully convolutional design and includes modules for feature extraction, enhancement, and fusion. Features obtained at different depths of the network are processed separately and then combined to produce the final enhanced image. This multi-branch structure allows the method to address several common low-light degradations, including insufficient brightness, reduced contrast, noise, and artifacts.

The model was trained on a synthetic dataset generated from VOC images and evaluated using several measures, including PSNR and SSIM. On synthetic low-light images without additional noise, MBLLEN reached a PSNR of 26.56 dB and an SSIM of 0.89, outperforming all methods included in the comparison (Lv et al., 2018). Similar performance gains were reported for images affected by Poisson noise, and the method was also tested on real low-light photographs.

Ren et al. (2019) approached the problem using a Deep Hybrid Network with two complementary processing streams. An encoder–decoder branch reconstructs the global scene content, while a second branch focuses on edges and structural information through a spatially varying recurrent neural network. Along with the MSE loss, perceptual and adversarial losses were used during training to improve the visual quality of the output. The contribution of the edge-processing branch was confirmed experimentally: the average PSNR and SSIM increased from 27.67 dB and 0.9156 without this branch to 28.43 dB and 0.9662 when it was included (Ren et al., 2019).

MIRNet, developed by Zamir et al. (2020), is a general image restoration and enhancement architecture rather than a model designed exclusively for low-light enhancement. Its multi-scale design uses parallel streams at different spatial resolutions, allowing information to be exchanged across scales while preserving high-resolution details. The architecture also incorporates spatial and channel attention mechanisms. For image enhancement, MIRNet was evaluated on the LOL and MIT-Adobe FiveK datasets. It achieved a PSNR of 24.14 dB and an SSIM of 0.83 on LOL, and a PSNR of 23.73 dB and an SSIM of 0.925 on MIT-Adobe FiveK, outperforming the methods included in the corresponding comparisons (Zamir et al., 2020).

4.2. Deep learning-based Retinex approaches

The development of deep learning has made it possible to combine the basic Retinex principle, in which an image is decomposed into reflectance and illumination components, with models that learn the required representations and constraints directly from data. This reduces the dependence on hand-crafted priors and careful parameter tuning that is typical of traditional Retinex methods (Wei et al., 2018). One of the early representative methods in this group is Retinex-Net, proposed by Wei et al. (2018). The model consists of two subnetworks: Decom-Net, which separates the input image into reflectance and illumination components, and Enhance-Net, which adjusts the illumination component. The enhancement process includes decomposition, illumination adjustment, and reconstruction, while additional denoising is applied to the reflectance component. For training, the authors introduced the LOL (LOw-Light) dataset containing 500 pairs of images of the same scenes captured under low- and normal-light conditions. Of these, 485 pairs were used for training and 15 for evaluation. Retinex-Net was also tested on the LIME, MEF, and DICM datasets and compared with traditional methods including LIME, SRIE, NPE, and DeHz. According to the authors, the method was able to brighten dark regions without causing severe overexposure and preserved image details more effectively when enhancement and denoising were performed jointly (Wei et al., 2018).

A further development of this idea is KinD (Kindling the Darkness), introduced by Y. Zhang, J. Zhang and Guo (2019). The method also follows the Retinex formulation by separating an image into illumination and reflectance components. The illumination component is used for brightness adjustment, while the reflectance component is processed to remove degradations such as noise and color distortion. The network is trained using pairs of images captured at different exposure levels and does not require ground-truth reflectance or illumination maps (Y. Zhang, J. Zhang & Guo, 2019). A total of 450 pairs from the LOL dataset were used for training, while evaluation was carried out on the LOL, LIME, NPE, and MEF datasets using PSNR, SSIM, LOE, and NIQE. On the LOL dataset, KinD achieved a PSNR of 20.87 dB and an SSIM of 0.802, outperforming the other methods included in the comparison. It also obtained the lowest NIQE value among the compared methods on the same dataset (Y. Zhang, J. Zhang & Guo, 2019).

URetinex-Net, proposed by Wu et al. (2022), introduces a different strategy based on deep unfolding. Instead of treating Retinex decomposition as a fixed optimization procedure, the individual optimization steps are unfolded into learnable network modules that infer implicit priors from data. The architecture includes modules for initialization, iterative optimization, and illumination adjustment, with the aim of suppressing noise while preserving details in both reflectance and illumination components. The model was trained and tested on the LOL dataset, while its generalization ability was further examined on the SICE dataset without retraining or additional adaptation. On LOL, URetinex-Net achieved a PSNR of 21.33 dB and an SSIM of 0.835 and outperformed the compared methods in terms of PSNR, SSIM, and LPIPS. It also showed strong performance on the SICE dataset across most of the evaluated metrics (Wu et al., 2022).

4.3. GAN, unsupervised, and zero-reference approaches

The need for large numbers of paired low-light and normal-light images is one of the main limitations of supervised methods. This has motivated the development of approaches that can be trained without paired reference images, or even without corresponding normal-light examples.

One representative unsupervised method is EnlightenGAN, proposed by Jiang et al. (2021). The model is based on a generative adversarial network and is trained using unpaired low-light and normal-light images. Its architecture includes both global and local discriminators, together with an attention mechanism guided by illumination information from the input image.

This allows different regions of the image to be enhanced according to their local lighting conditions. The training set contained 914 low-light and 1,016 normal-light images collected from several datasets, without one-to-one pairing between them. EnlightenGAN was evaluated on the MEF, NPE, LIME, VV, and DICM datasets, where it achieved the best average NIQE score among the compared methods. In a subjective evaluation involving 23 images, it also obtained the best average rank of 1.78 (Jiang et al., 2021).

A different strategy is used by Zero-DCE (Zero-Reference Deep Curve Estimation), proposed by Guo et al. (2020). The method formulates low-light enhancement as an image-specific curve estimation problem. Its DCE-Net predicts high-order curves that adjust pixel values and the dynamic range of the input image. Zero-DCE does not require paired or unpaired reference images during training. Instead, the network is optimized using non-reference loss functions related to spatial consistency, exposure control, color constancy, and illumination smoothness (Guo et al., 2020).

A later extended version introduced Zero-DCE++, a lightweight model with approximately 10,000 parameters and substantially lower computational requirements (Li, Guo & Loy, 2022). In a subjective evaluation conducted on 199 images from five datasets, Zero-DCE received the highest average score among the compared methods, while Zero-DCE++ achieved the second-best result (Li, Guo & Loy, 2022).

SCI (Self-Calibrated Illumination), developed by Ma et al. (2022), is another lightweight unsupervised approach. The method uses a cascaded illumination learning process with shared weights and a self-calibration module. This additional calibration process is required during training, whereas inference relies only on the basic network block, which keeps the computational cost low. An unsupervised loss is used to improve the model's ability to adapt to different scenes. SCI was evaluated on the MIT and LSRW datasets and compared with traditional, supervised, and unsupervised methods.

On the MIT dataset, it achieved a PSNR of 20.45 dB and an SSIM of 0.893, while the experiments also showed that the model requires relatively low computational resources. The authors further examined its use as a preprocessing method for low-light face detection and nighttime semantic segmentation (Ma et al., 2022).

4.4. Transformer-based approaches

Transformer architectures can model relationships between spatially distant regions of an image. This is particularly useful under very low-light conditions, where local information may not be sufficient for reliable reconstruction. Recent methods therefore combine attention mechanisms with information about illumination, noise, or local image characteristics.

Xu et al. (2022) proposed SNR-Aware Low-light Image Enhancement, which combines Transformer and convolutional operations. Their contribution is adjusted according to the signal-to-noise ratio in different image regions. Transformer-based long-range processing is used more strongly in areas with very low SNR, while local convolutional operations are emphasized in regions with higher SNR.

An SNR map is also used to guide the attention mechanism and feature fusion. The model was evaluated on seven datasets, including LOL-v1, LOL-v2, SID, SMID, and SDSD. On LOL-v1, it achieved a PSNR of 24.61 dB and an SSIM of 0.842, while on LOL-v2-real it reached a PSNR of 21.48 dB and an SSIM of 0.849, outperforming the methods included in the comparison (Xu et al., 2022).

Wang et al. (2023) developed LLFormer, a Transformer model intended for the enhancement of ultra-high-resolution images. The authors also introduced the UHD-LOL dataset with 4K and 8K images in order to test how well low-light enhancement methods perform at substantially higher resolutions than those typically used in existing datasets. LLFormer uses axis-based multi-head self-attention and cross-layer feature fusion to reduce the computational cost of processing large images. The model achieved the best results among the compared methods on UHD-LOL4K and UHD-LOL8K. Additional evaluation on LOL and MIT-Adobe FiveK showed that LLFormer also performs competitively on standard datasets. On MIT-Adobe FiveK, it achieved a PSNR of 25.75 dB and an SSIM of 0.923 (Wang et al., 2023).

Cai et al. (2023) proposed Retinexformer, which combines the Retinex principle with a Transformer architecture in a one-stage framework. The model first estimates illumination information to improve image visibility and then restores degradations that are hidden in dark regions or introduced during the light-up process. Its Illumination-Guided Transformer uses illumination information to guide the modeling of non-local interactions between regions with different lighting conditions. Retinexformer was evaluated on thirteen datasets, including LOL, SID, SMID, SDSD, and MIT-Adobe FiveK. On LOL-v1, it achieved a PSNR of 25.16 dB and an SSIM of 0.845, while on MIT-Adobe FiveK it reached a PSNR of 24.94 dB, outperforming the methods included in the corresponding comparisons (Cai et al., 2023).

4.5. Diffusion models

Diffusion models represent a more recent direction in low-light image enhancement and use a generative process to reconstruct higher-quality images. Although they can produce strong perceptual results, they often require substantial computational resources and relatively long inference times. For this reason, recent work has also focused on improving their efficiency.

Jiang et al. (2023) proposed DiffLL, which combines a diffusion model with wavelet transformation. The input image is first transformed into the wavelet domain, where components representing global information and high-frequency image details are separated.

The diffusion process is then applied to a component with reduced spatial resolution, while high-frequency details are reconstructed using a dedicated High-Frequency Restoration Module (HFRM). This reduces the computational cost of the diffusion process while preserving image details.

DiffLL was evaluated on the LOL-v1, LOL-v2-real, and LSRW datasets, as well as on several real-world datasets without reference images. On LOL-v1, it achieved a PSNR of 26.34 dB and an SSIM of 0.845, while on LOL-v2-real it reached a PSNR of 28.86 dB and an SSIM of 0.876, outperforming the methods included in the comparison. The authors also report that the proposed method is at least 70 times faster than the previously compared diffusion-based image restoration approaches (Jiang et al., 2023).

A more recent method is Diff-Retinex++, introduced by Yi et al. (2025). The model combines the generative capability of diffusion models with physically motivated Retinex principles. Its architecture includes a Denoising Diffusion Model (DDM) and a Retinex-Driven Mixture of Experts (RMoE), while Retinex information is incorporated through a dedicated attention module that guides the enhancement process.

The Mixture-of-Experts design allows the model to activate different components depending on the characteristics of the input image. Diff-Retinex++ was evaluated on LOL-v1, LOL-v2-real, LOL-v2-synthetic, and LSRW, together with additional real-world scenes captured under different illumination levels. On LOL-v1, it achieved the best results among the compared methods in terms of PSNR, SSIM, FID, and MAE, while it also obtained the best overall performance on LOL-v2-real.

Experiments on extremely dark real-world scenes further showed that the model was able to preserve image details, color reproduction, and structural content (Yi et al., 2025).

5. Datasets and image quality assessment metrics

5.1. Datasets

Evaluation of low-light image enhancement methods relies on a range of datasets that include paired low-light and well-exposed images, as well as real-world datasets without reference images.

One of the most widely used datasets is LOL (LOw-Light), which contains pairs of the same scenes captured under low- and normal-light conditions. The original LOL dataset consists of 485 image pairs for training and 15 pairs for testing (Wei et al., 2018). Its later version, LOL-v2, includes real and synthetic subsets (Yang et al., 2021).

For extremely low-light conditions, the See-in-the-Dark (SID) dataset introduced by Chen et al. (2018) is particularly relevant.

SID contains 5,094 short-exposure RAW images with corresponding long-exposure reference images captured using Sony α7S II and Fujifilm X-T2 cameras.

The dataset includes both indoor and outdoor scenes recorded under very low illumination, with the reference images acquired using exposure times 100 to 300 times longer than those of the corresponding input images.

MIT-Adobe FiveK is also used in several studies considered in this review, although it was not originally developed specifically as a low-light image dataset. It is a broader photographic image enhancement dataset containing 5,000 photographs covering a wide range of scenes and lighting conditions.

Each image was independently retouched by five trained photographers (Bychkovsky et al., 2011). In MIRNet, the images produced by Expert C were used as reference images, with 4,500 images used for training and 500 for testing (Zamir et al., 2020).

To evaluate low-light enhancement methods on ultra-high-resolution images, Wang et al. (2023) introduced UHD-LOL, which consists of the UHD-LOL4K and UHD-LOL8K subsets. UHD-LOL4K contains 8,099 pairs of 4K images, while UHD-LOL8K contains 2,966 pairs of 8K images.

These datasets make it possible to assess how well enhancement models handle image resolutions substantially higher than those used in earlier low-light datasets.

The main characteristics of the datasets discussed above are summarized in Table 1.

Table 1
Summary of datasets used in the reviewed studies

Dataset	Size	Resolution	Data type	Pairing	Image format / domain
LOL-v1 (Wei et al., 2018)	500 low-/normal-light image pairs	400 × 600	Real scenes	Paired	PNG (converted from RAW)
LOL-v2-real (Yang et al., 2021)	789 pairs (689 training, 100 testing)	Not specified	Real	Paired	Not specified
LOL-v2-synthetic (Yang et al., 2021)	1,000 samples (900 training, 100 testing)	Not specified	Synthetic	Not explicitly stated	Not specified
SID (Chen et al., 2018)	5,094 short-exposure images; 424 long-exposure references	4240 × 2832 (Sony); 6000 × 4000 (Fujifilm)	Real	Paired	RAW
MIT-Adobe FiveK (Bychkovsky et al., 2011)	5,000 photographs; five retouched versions per image	Not specified	Real photographs	Input-output pairs	RAW input; retouched output versions
UHD-LOL4K (Wang et al., 2023)	8,099 low-light/normal-light image pairs	4K	Synthetic	Paired	Not specified
UHD-LOL8K (Wang et al., 2023)	2,966 low-light/normal-light image pairs	8K	Synthetic	Paired	Not specified

Note: Only characteristics explicitly reported in the cited studies are included. "Not specified" means that the cited source used for the table does not state that characteristic; no value was inferred.

5.2. Image quality assessment metrics

PSNR (Peak Signal-to-Noise Ratio) and SSIM (Structural Similarity Index Measure) are among the most commonly used metrics for quantitative evaluation of enhanced images. PSNR is based on the difference between pixel values in the reference and processed images, with higher values indicating lower reconstruction error. Wang et al. (2004) noted that measures based only on pixel-wise error do not necessarily correspond well to human perception of image quality, which motivated the development of SSIM as a structure-based measure. SSIM compares luminance, contrast, and structural information between two images, with higher values indicating greater similarity to the reference image (Wang et al., 2004).

Perceptual similarity is also evaluated using metrics such as LPIPS (Learned Perceptual Image Patch Similarity). LPIPS measures the difference between images using features extracted from deep neural networks.

R. Zhang et al. (2018) showed that deep features can correspond more closely to human judgments of perceptual similarity than traditional measures such as PSNR and SSIM. For LPIPS, lower values indicate a smaller perceptual distance between the compared images.

When a suitable reference image is not available, NIQE (Natural Image Quality Evaluator) can be used. NIQE does not require a reference image or prior training on subjectively rated distorted images. Instead, image quality is estimated from the deviation between the statistical characteristics of the evaluated image and a model built from natural, undistorted images (Mittal, Soundararajan & Bovik, 2013). Lower NIQE values indicate that the image statistics are closer to those of natural images.

FID (Fréchet Inception Distance), introduced by Heusel et al. (2017), is also commonly used for generative approaches. FID compares the distributions of real and generated images by using the means and covariance matrices of their feature representations in the Inception feature space. Lower FID values indicate greater similarity between the two distributions, while stronger degradation generally results in higher FID values (Heusel et al., 2017).

Because these metrics capture different aspects of image quality, low-light image enhancement studies often use several of them together to assess both numerical fidelity and perceptual quality.

6. Comparative analysis of selected studies

The studies included in Table 2 were selected as representative examples of the main approaches discussed in this review. Selection was based on their relevance to a distinct methodological approach, the availability of quantitative evaluation on commonly used low-light datasets, and, where available, publicly accessible implementations.

Table 2 (part 1)

Comparative overview of selected studies on low-light image enhancement

Dataset	Size	Resolution	Pairing	Image format / domain
Lore, Akintayo and Sarkar (2017) LLNet / S-LLNet	Deep auto-encoder	Synthetically degraded and real low-light images; PSNR↑, SSIM↑	On dark images with added noise, LLNet and S-LLNet achieved better PSNR and SSIM results than the traditional methods used for comparison.	Joint contrast enhancement and denoising; trained on artificially darkened images with added Gaussian noise.
Wei et al. (2018) Retinex-Net	Retinex + deep learning	LOL, LIME, MEF, DICM; qualitative evaluation and comparison	The model brightened dark regions without severe overexposure and preserved details more effectively when enhancement and denoising were performed jointly.	Decom-Net + Enhance-Net; the study introduced the LOL dataset containing 500 image pairs.
Zamir et al. (2020) MIRNet	Multi-scale CNN	LOL, MIT-Adobe FiveK; PSNR↑, SSIM↑	MIRNet outperformed the compared methods on the LOL and MIT-Adobe FiveK datasets in terms of PSNR and SSIM.	Parallel streams at different resolutions and attention mechanisms; preservation of high-resolution details.
Jiang et al. (2021) EnlightenGAN	GAN, unsupervised learning	MEF, NPE, LIME, VV, DICM; NIQE↓, subjective evaluation	Achieved the best average NIQE score among the compared methods and the best average rank in the subjective evaluation.	Does not require paired low-light/normal-light images; uses global and local discriminators together with attention.
Guo et al. (2020); Li, Guo & Loy (2022) Zero-DCE / Zero-DCE++	Zero-reference	NPE, LIME, MEF, DICM, VV, etc.; subjective evaluation, PI↓, PSNR↑, SSIM↑, MAE↓	Zero-DCE received the highest average subjective score on 199 images, while Zero-DCE++ achieved the second-best result.	Training without paired or unpaired reference data; Zero-DCE++ contains approximately 10,000 parameters.
Wu et al. (2022) URetinex-Net	Retinex + deep unfolding	LOL, SICE; MAE↓, PSNR↑, SSIM↑, LPIPS↓	Outperformed most of the compared methods in terms of PSNR, SSIM, and LPIPS on LOL and showed good generalization to SICE without additional training.	Retinex optimization steps are unfolded into a learnable network; evaluated on SICE without retraining.
Xu et al. (2022) SNR-Aware	CNN + Transformer	LOL-v1, LOL-v2, SID, SMID, SDSD; PSNR↑, SSIM↑	Achieved better PSNR and SSIM results than the methods included in the comparison on LOL-v1, LOL-v2-real, and LOL-v2-synthetic.	An SNR map controls the balance between local convolutional processing and long-range Transformer processing.
Wang et al. (2023) LLFormer	Transformer	UHD-LOL4K, UHD-LOL8K, LOL, MIT-Adobe FiveK; PSNR↑, SSIM↑, LPIPS↓, MAE↓	Achieved the best results among the compared methods on UHD-LOL4K and UHD-LOL8K and also performed well on LOL and MIT-Adobe FiveK.	Designed for 4K/8K images; axis-based self-attention reduces computational complexity.
Cai et al. (2023) Retinexformer	Retinex + Transformer	LOL-v1/v2, SID, SMID, SDSD, FiveK, etc.; PSNR↑, SSIM↑	Outperformed the compared methods on several low-light datasets, with particularly strong improvements on images affected by noise and other degradations.	One-stage Retinex framework with an Illumination-Guided Transformer; evaluated on a large number of datasets.

Table 2 (part 2)
Comparative overview of selected studies on low-light image enhancement

Dataset	Size	Resolution	Pairing	Image format / domain
Jiang et al. (2023) DiffLL	Diffusion model + wavelet	LOL-v1, LOL-v2-real, LSRW and real-world unpaired datasets; PSNR↑, SSIM↑, LPIPS↓, FID↓, NIQE↓, BRISQUE↓, PI↓	Achieved the best quantitative results among the compared methods on LOL-v1, LOL-v2-real, and LSRW, together with improvements in perceptual metrics.	Diffusion is performed in a lower-resolution wavelet domain; the authors report at least 70× faster processing than the compared diffusion-based approaches.
Yi et al. (2025) Diff-Retinex++	Retinex + diffusion model	LOL-v1, LOL-v2-real/synthetic, LSRW, A-LLIE; PSNR↑, SSIM↑, LPIPS↓, FID↓, MAE↓	On LOL-v1, it achieved the best PSNR, SSIM, FID, and MAE results among the compared methods; on LOL-v2-real, it achieved the best overall performance.	Combines generative diffusion with Retinex information and a Mixture-of-Experts architecture.

Note: Numerical results from different studies should not be directly ranked when different datasets and experimental conditions are used.
Note: ↑ indicates that a higher value represents better performance, while ↓ indicates that a lower value represents better performance.

Since the reported results were obtained using different datasets, training settings, implementations, and experimental conditions, numerical values from different studies should not be treated as a single performance ranking.

A review of the selected studies shows a gradual expansion in the capabilities of low-light image enhancement methods. Early approaches such as LLNet were mainly focused on contrast enhancement and noise reduction, while Retinex-Net and later Retinex-based models introduced an explicit separation of illumination and reflectance within neural network architectures.

MIRNet highlighted the importance of multi-scale processing and attention mechanisms, whereas EnlightenGAN and Zero-DCE reduced the dependence on paired training data through unsupervised and zero-reference learning.

More recent Transformer-based approaches extend the ability to model long-range spatial dependencies and handle more complex degradation patterns. SNR-Aware uses local signal-to-noise ratio estimates to guide the enhancement process, LLFormer is specifically designed for ultra-high-resolution images, while Retinexformer combines a Transformer architecture with the Retinex principle.

Diffusion models represent an even more recent direction. DiffLL aims to reduce their computational cost through wavelet transformation, whereas Diff-Retinex++ combines generative diffusion with physically motivated Retinex information.

7. Conclusion

The reviewed studies show a gradual shift from earlier deep learning models, which mainly focused on contrast enhancement and noise reduction, toward more complex architectures that address illumination, noise, color, and structural details at the same time. Deep learning-based Retinex methods introduced an explicit separation of reflectance and illumination, while more recent models such as URetinex-Net and Retinexformer aim to overcome some of the limitations of classical Retinex approaches by learning implicit priors and modeling long-range dependencies between different image regions (Wu et al., 2022; Cai et al., 2023).

Another important direction is the reduced dependence on paired training data. Collecting low-light and normal-light images of the same scene can be difficult, especially under real-world conditions. EnlightenGAN addresses this issue by using unpaired data, while Zero-DCE does not require either paired or unpaired reference images during training (Jiang et al., 2021; Guo et al., 2020). Such approaches can make low-light enhancement more practical in cases where suitable reference datasets are difficult to obtain.

Transformer architectures improve the ability to model relationships between spatially distant image regions, but they can also increase computational complexity, particularly when processing high-resolution images. Recent models therefore use specialized attention mechanisms, hybrid CNN–Transformer structures, and architectures designed for large images (Xu et al., 2022; Wang et al., 2023; Cai et al., 2023).

A similar limitation is present in diffusion models because of their iterative processing. DiffLL shows that wavelet transformation can reduce processing time and memory requirements, although the authors note that the method is still not efficient enough for direct real-time video processing (Jiang et al., 2023).

The reviewed results also show that the quality of an enhanced image cannot be fully described by a single metric. PSNR and SSIM provide reference-based measures of reconstruction quality, while LPIPS, NIQE, and FID provide additional information related to perceptual quality. For this reason, quantitative evaluation is often supported by visual comparison and subjective assessment. At the same time, numerical results reported in different studies should be interpreted within the context of their datasets and experimental conditions rather than treated as a direct ranking of methods.

Overall, the choice of method depends on the application and available data. Supervised methods are suitable when paired low- and normal-light images are available, while unsupervised and zero-reference approaches are more practical when such data are difficult to obtain. Lightweight models are better suited to applications with limited computational resources, whereas Transformer-based models can be useful for high-resolution images. Diffusion models can provide strong enhancement results, but their higher computational cost may limit their use in real-time applications.

8. Acknowledgments

This research has been supported by the Ministry of Science, Technological Development and Innovation (Contract No. 451-03-34/2026-03/200156) and the Faculty of Technical Sciences, University of Novi Sad through project “Scientific and Artistic Research Work of Researchers in Teaching and Associate Positions at the Faculty of Technical Sciences, University of Novi Sad 2026” (No. 01-3609/1).

9. References

Bychkovsky, V., Paris, S., Chan, E. and Durand, F. (2011) 'Learning Photographic Global Tonal Adjustment with a Database of Input/Output Image Pairs'. In: *Proceedings of the IEEE Conference on Computer Vision and Pattern Recognition (CVPR)*, pp. 97–104. DOI: 10.1109/CVPR.2011.5995332

Cai, Y., Bian, H., Lin, J., Wang, H., Timofte, R. and Zhang, Y. (2023) 'Retinexformer: One-stage Retinex-based Transformer for low-light image enhancement'. In: *Proceedings of the IEEE/CVF International Conference on Computer Vision (ICCV)*, pp. 12470–12479. DOI: 10.1109/ICCV51070.2023.01149

Chen, C., Chen, Q., Xu, J. and Koltun, V. (2018) 'Learning to See in the Dark'. In: *Proceedings of the IEEE Conference on Computer Vision and Pattern Recognition (CVPR)*, pp. 3291–3300.

Guo, C., Li, C., Guo, J., Loy, C.C., Hou, J., Kwong, S. and Cong, R. (2020) 'Zero-Reference Deep Curve Estimation for Low-Light Image Enhancement'. In: *Proceedings of the IEEE/CVF Conference on Computer Vision and Pattern Recognition (CVPR)*, pp. 1780–1789. DOI: 10.1109/CVPR42600.2020.00185

Guo, J., Ma, J., García-Fernández, Á.F., Zhang, Y. and Liang, H. (2023) 'A survey on image enhancement for low-light images', *Heliyon*, 9(4), e14558. DOI: 10.1016/j.heliyon.2023.e14558

Guo, X., Li, Y. and Ling, H. (2017) 'LIME: Low-Light Image Enhancement via Illumination Map Estimation', *IEEE Transactions on Image Processing*, 26(2), pp. 982–993. DOI: 10.1109/TIP.2016.2639450

Heusel, M., Ramsauer, H., Unterthiner, T., Nessler, B. and Hochreiter, S. (2017) 'GANs Trained by a Two Time-Scale Update Rule Converge to a Local Nash Equilibrium'. In: *Advances in Neural Information Processing Systems*, 30, pp. 6626–6637.

Jiang, H., Luo, A., Han, S., Fan, H. and Liu, S. (2023) 'Low-Light Image Enhancement with Wavelet-based Diffusion Models', *ACM Transactions on Graphics*, 42(6), Article 238, pp. 1–14. DOI: 10.1145/3618373

Jiang, Y., Gong, X., Liu, D., Cheng, Y., Fang, C., Shen, X., Yang, J., Zhou, P. and Wang, Z. (2021) 'EnlightenGAN: Deep Light Enhancement Without Paired Supervision', *IEEE Transactions on Image Processing*, 30, pp. 2340–2349. DOI: 10.1109/TIP.2021.3051462

Li, C., Guo, C. and Loy, C.C. (2022) 'Learning to Enhance Low-Light Image via Zero-Reference Deep Curve Estimation', *IEEE Transactions on Pattern Analysis and Machine Intelligence*, 44(8), pp. 4225–4238. DOI: 10.1109/TPAMI.2021.3063604

Liba, O., Murthy, K., Tsai, Y.-T., Brooks, T., Xue, T., Karnad, N., He, Q., Barron, J.T., Sharlet, D., Geiss, R., Hasinoff, S.W., Pritch, Y. and Levoy, M. (2019) 'Handheld Mobile Photography in Very Low Light', *ACM Transactions on Graphics*, 38(6), Article 164, pp. 1–16. DOI: 10.1145/3355089.3356508.

Liu, F. and Fan, L. (2025) 'A review of advancements in low-light image enhancement using deep learning', *Neurocomputing*, 652, 131052. DOI: 10.1016/j.neucom.2025.131052

Lore, K.G., Akintayo, A. and Sarkar, S. (2017) 'LLNet: A deep autoencoder approach to natural low-light image enhancement', *Pattern Recognition*, 61, pp. 650–662. DOI: 10.1016/j.patcog.2016.06.008

Lv, F., Lu, F., Wu, J. and Lim, C. (2018) 'MBLLEN: Low-Light Image/Video Enhancement Using CNNs'. In: *Proceedings of the British Machine Vision Conference (BMVC)*, paper 220.

Ma, L., Ma, T., Liu, R., Fan, X. and Luo, Z. (2022) 'Toward Fast, Flexible, and Robust Low-Light Image Enhancement'. In: *Proceedings of the IEEE/CVF Conference on*

Computer Vision and Pattern Recognition (CVPR), pp. 5637–5646. DOI: 10.1109/CVPR52688.2022.00555

Mittal, A., Soundararajan, R. and Bovik, A.C. (2013) 'Making a "Completely Blind" Image Quality Analyzer', *IEEE Signal Processing Letters*, 20(3), pp. 209–212. DOI: 10.1109/LSP.2012.2227726

Ren, W., Liu, S., Ma, L., Xu, Q., Xu, X., Cao, X., Du, J. and Yang, M.-H. (2019) 'Low-Light Image Enhancement via a Deep Hybrid Network', *IEEE Transactions on Image Processing*, 28(9), pp. 4364–4375. DOI: 10.1109/TIP.2019.2910412

Tian, Z., Qu, P., Li, J., Sun, Y., Li, G., Liang, Z. and Zhang, W. (2023) 'A Survey of Deep Learning-Based Low-Light Image Enhancement', *Sensors*, 23(18), 7763. DOI: 10.3390/s23187763

Wang, T., Zhang, K., Shen, T., Luo, W., Stenger, B. and Lu, T. (2023) 'Ultra-High-Definition Low-Light Image Enhancement: A Benchmark and Transformer-Based Method'. In: *Proceedings of the AAAI Conference on Artificial Intelligence*, 37(3), pp. 2654–2662. DOI: 10.1609/aaai.v37i3.25364

Wang, Z., Bovik, A.C., Sheikh, H.R. and Simoncelli, E.P. (2004) 'Image quality assessment: From error visibility to structural similarity', *IEEE Transactions on Image Processing*, 13(4), pp. 600–612. DOI: 10.1109/TIP.2003.819861

Wei, C., Wang, W., Yang, W. and Liu, J. (2018) 'Deep Retinex Decomposition for Low-Light Enhancement'. In: *Proceedings of the British Machine Vision Conference (BMVC)*, paper 155.

Wu, W., Weng, J., Zhang, P., Wang, X., Yang, W. and Jiang, J. (2022) 'URetinex-Net: Retinex-Based Deep Unfolding Network for Low-Light Image Enhancement'. In: *Proceedings of the IEEE/CVF Conference on Computer Vision and Pattern Recognition (CVPR)*, pp. 5901–5910. DOI: 10.1109/CVPR52688.2022.00581

Xu, X., Wang, R., Fu, C.-W. and Jia, J. (2022) 'SNR-Aware Low-Light Image Enhancement'. In: *Proceedings of the IEEE/CVF Conference on Computer Vision and Pattern Recognition (CVPR)*, pp. 17714–17724.

Yang, W., Wang, W., Huang, H., Wang, S. and Liu, J. (2021) 'Sparse Gradient Regularized Deep Retinex Network for Robust Low-Light Image Enhancement', *IEEE Transactions on Image Processing*, 30, pp. 2072–2086. DOI: 10.1109/TIP.2021.3050850

Ye, J., Qiu, C. and Zhang, Z. (2024) 'A survey on learning-based low-light image and video enhancement', *Displays*, 81, 102614. DOI: 10.1016/j.displa.2023.102614

Yi, X., Xu, H., Zhang, H., Tang, L. and Ma, J. (2025) 'Diff-Retinex++: Retinex-Driven Reinforced Diffusion Model for Low-Light Image Enhancement', *IEEE Transactions on Pattern Analysis and Machine Intelligence*, 47(8), pp. 6823–6841. DOI: 10.1109/TPAMI.2025.3563612

Zamir, S.W., Arora, A., Khan, S., Hayat, M., Khan, F.S., Yang, M.-H. and Shao, L. (2020) 'Learning Enriched Features for Real Image Restoration and Enhancement'. In: Vedaldi, A., Bischof, H., Brox, T. and Frahm, J.-M. (eds.) *Computer Vision – ECCV 2020*, Lecture Notes in Computer Science, vol. 12370, pp. 492–511. DOI: 10.1007/978-3-030-58595-2_30

Zhan, J., Goh, E.S. and Sunar, M.S. (2024) 'Low-light image enhancement: A comprehensive review on methods, datasets and evaluation metrics', *Journal of King Saud University – Computer and Information Sciences*, 36(10), 102234. DOI: 10.1016/j.jksuci.2024.102234

Zhang, L., Zhang, L., Liu, X., Shen, Y., Zhang, S. and Zhao, S. (2019) 'Zero-Shot Restoration of Back-lit Images Using Deep Internal Learning'. In: *Proceedings of the 27th ACM International Conference on Multimedia*, pp. 1623–1631. DOI: 10.1145/3343031.3351069

Zhang, R., Isola, P., Efros, A.A., Shechtman, E. and Wang, O. (2018) 'The Unreasonable Effectiveness of Deep Features as a Perceptual Metric'. In: *Proceedings of the IEEE Conference on Computer Vision and Pattern Recognition (CVPR)*, pp. 586–595. DOI: 10.1109/CVPR.2018.00068

Zhang, Y., Zhang, J. and Guo, X. (2019) 'Kindling the Darkness: A Practical Low-Light Image Enhancer'. In: *Proceedings of the 27th ACM International Conference on Multimedia*, pp. 1632–1640.

Zheng, Y., Zhou, L., Jin, K., Jin, S., Liang, Z., Zhao, W. and Zhang, W. (2026) 'A comprehensive review of low-light image enhancement methods', *Signal Processing: Image Communication*, 140, 117435. DOI: 10.1016/j.image.2025.117435



© 2026 Authors. Published by the University of Novi Sad, Faculty of Technical Sciences, Department of Graphic Engineering and Design. This article is an open access article distributed under the terms and conditions of the Creative Commons Attribution license 4.0 Serbia (http://creativecommons.org/licenses/by/4.0/rs/).

Original Scientific Paper https://doi.org/10.24867/GRID-2026-p64

Personal vs. Promotional Influencer Content on Instagram and TikTok: Engagement and Disclosure Practices

ABSTRACT

Influencer marketing combines personal communication with commercial content, making audience engagement and promotional disclosure important aspects of influencer–brand communication. This study examines engagement with personal and promotional influencer content on Instagram and TikTok, as well as differences in the use of official platform disclosure labels. The analysis included 795 publicly available Reel/video posts from 20 local and regional influencers active on both platforms. Engagement rates were compared across content types and platforms, while promotional posts were additionally analysed according to disclosure practices. No significant overall effect of content type, platform, or their interaction was found. Personal content showed higher engagement than promotional content on Instagram, while no significant difference was observed on TikTok. The use of official platform disclosure labels differed significantly between the two platforms, with higher use on TikTok. The findings indicate that engagement patterns are not determined by platform or promotional content alone and that disclosure practices may vary across platform environments.

Rastko Milošević
Selena Nikolić
Savka Adamović
Ivana Tomić

University of Novi Sad, Faculty of Technical Sciences, Department of Graphic Engineering and Design, Novi Sad, Serbia

KEY WORDS
Influencer marketing, Instagram, TikTok, engagement rate, promotional content, disclosure transparency

1. Introduction

Social media influencers have become important intermediaries between brands and consumers because they combine content creation, audience interaction, and commercial communication within the same social media presence. Unlike conventional advertising, influencer marketing embeds brand-related messages into the ongoing communication between creators and their followers, drawing on relationships characterized by trust, perceived authenticity, similarity, and psychological attachment (Campbell & Farrell, 2020; Ki et al., 2020; Kim & Kim, 2021).

Audience engagement represents an important indicator of how users actively respond to social media content. However, engagement with influencer content may depend on numerous factors, including the characteristics of the influencer, audience size, content strategy, commercial nature of the post, and the platform on which the content is published (Tafesse & Wood, 2021). Consequently, evaluating influencer marketing effectiveness requires considering both the distinction between personal and promotional communication and the platform-specific context in which these messages appear.

Previous research has examined influencer marketing from multiple perspectives, including influencer characteristics, audience engagement, authenticity, and influencer–brand collaboration dynamics (Tafesse & Wood, 2021; Campbell & Farrell, 2020; Milošević et al., 2022; Milošević et al., 2024).

2. Theoretical backgrounds and hypotheses

2.1. Personal and promotional influencer content

A distinctive feature of influencer marketing is the coexistence of personal and commercial content within the same social media profile. Personal content is generally unrelated to direct brand or product promotion, whereas promotional content results from a commercial relationship between an influencer and a brand. Because both types of posts appear as part of the influencer's continuous communication with followers, commercial messages enter an already established influencer–audience relationship.

Commercial collaborations may challenge perceptions of influencer authenticity, as followers often value intrinsic motivation and non-commercial orientation (Audrezet et al., 2020). At the same time, characteristics such as informational value, influencer trustworthiness, attractiveness, and perceived similarity can strengthen trust in branded content (Lou & Yuan, 2019). However, promotional content should not automatically be expected to generate lower audience engagement. Gross and von Wangenheim (2022), in an analysis of 64,438 Instagram posts, found that sponsored posts could generate higher engagement than non-sponsored posts, depending on influencer and message characteristics. These findings suggest that the relationship between promotional content and audience engagement is not straightforward, and that the commercial nature of a post alone does not provide a sufficient basis for predicting the direction of audience response.

Engagement is additionally associated with broader characteristics of influencer strategy. Tafesse and Wood (2021) found that follower count and content volume were negatively associated with follower engagement on Instagram, whereas followee count was positively associated with engagement, and these relationships varied according to influencers' domains of interest. Taken together, previous findings suggest that engagement is shaped by multiple interrelated factors rather than simply by whether a post is promotional.

Accordingly, the following hypotheses are proposed:

H1: Engagement rate differs between personal and promotional influencer content.

H1a: Engagement rate differs between personal and promotional content on Instagram.

H1b: Engagement rate differs between personal and promotional content on TikTok.

2.2. Platform-specific engagement

Instagram and TikTok both represent visually oriented platforms widely used by influencers, but their content ecosystems and patterns of use differ. Platform characteristics can shape how users encounter, consume, and respond to influencer content. Research on TikTok, for example, has shown that platform-specific characteristics of influencer communication are relevant to follower responses. Barta et al. (2023) found that originality and perceived opinion leadership contributed to influencer effectiveness on TikTok and that humor enhanced message effectiveness through followers' hedonic experience.

These findings, together with evidence that influencer engagement depends on content and profile characteristics (Tafesse & Wood, 2021), indicate that engagement patterns observed on one social media platform cannot necessarily be assumed to apply identically to another. Previous findings therefore provide no clear expectation regarding engagement differences between Instagram and TikTok or whether personal and promotional content perform differently across the two platforms. Based on this, the following hypotheses were proposed:

H2: Engagement rate differs between Instagram and TikTok.

H3: The effect of content type on engagement rate depends on the platform.

2.3. Promotional disclosure

Because influencer advertising is integrated into content that may visually and stylistically resemble non-commercial posts, users may not always immediately recognize the commercial relationship behind a message. Disclosure mechanisms therefore represent an important component of transparency in influencer marketing.

Standardized platform disclosure labels provide a particularly explicit way of signalling commercial relationships. Boerman (2020) experimentally demonstrated that Instagram's standardized "Paid partnership with [brand]" disclosure increased recognition of influencer content as advertising. The disclosure also indirectly increased brand recall and intention to engage with the post through advertising recognition, while no negative effect on parasocial interaction with the influencer was observed.

Commercial relationships may also be communicated through hashtags, textual descriptions, brand tags, collaboration functions, coupon codes, and other indicators. However, these mechanisms differ in their standardization and visibility. Moreover, Instagram and TikTok differ in their technical affordances, content formats, and communication conventions, which provides a

basis for examining whether creators use platform-native disclosure mechanisms equally frequently across the two environments. The present study therefore focuses specifically on the official platform disclosure label as a standardized and directly comparable indicator, rather than treating it as equivalent to the broader concept of overall promotional transparency.

Accordingly, we proposed the following hypothesis:

H4: The rate of official platform disclosure-label use for promotional content differs between Instagram and TikTok.

3. Methodology

3.1. Sample and content selection

The study included 20 local and regional social media influencers (17 women and 3 men), primarily active within the Serbian and broader regional social media environment, who were active on both Instagram and TikTok. For descriptive purposes, accounts were classified separately on each platform as nano (<10,000 followers), micro (10,000–99,999), macro (100,000–999,999), or mega influencers (≥1,000,000). The Instagram sample included 4 nano, 5 micro, 9 macro, and 2 mega accounts, while the TikTok sample included 3 nano, 4 micro, 10 macro, and 3 mega accounts.

Only Reel/video posts published within the 12 months preceding data collection, conducted in May 2026, were eligible. Posts were classified as personal or promotional, and up to 10 eligible posts per influencer, platform, and content type were randomly selected. Giveaway and pinned posts were excluded because of their potentially atypical engagement and visibility. For both platforms, the engagement rate (ER) for each post was calculated as:

$$Engagement\ rate = \frac{\text{Likes} + \text{Comments} + \text{Shares}}{\text{Number of followers}} \times 100\% \quad (1)$$

For inferential analyses, post-level ER values were averaged within each influencer for the four platform × content-type conditions (Instagram–personal, Instagram–promotional, TikTok–personal, and TikTok–promotional), with the influencer retained as the unit of analysis.

Promotional posts were also coded by disclosure method (official platform disclosure, Instagram Collaboration, tag in the post description, hashtag, coupon code, QR code, and no recorded disclosure), while the official platform disclosure label was used as the directly comparable indicator for the inferential comparison between Instagram and TikTok.

3.2. Statistical Analysis

Data were prepared and summarized in Microsoft Excel, while inferential analyses were conducted in jamovi 2.7 (The jamovi project, 2025), following standard statistical procedures described by Navarro and Foxcroft (2025). The analyses were performed within the R-based statistical environment, with relevant procedures supported by the afex and emmeans packages (R Core Team, 2025; Singmann, 2024; Lenth, 2025).

Raw engagement rates were summarized using means, medians, standard deviations, minima, and maxima. Because the distributions were positively skewed and included several extreme values, engagement rates were transformed using ln(ER + 1) for inferential analysis.

A 2 × 2 repeated-measures ANOVA was used to examine the effects of platform (Instagram vs. TikTok), content type (personal vs. promotional), and their interaction. Additional within-platform comparisons were performed using paired-samples tests, with Wilcoxon signed-rank tests used where appropriate. The difference in official disclosure-label use between platforms was also tested using a paired Wilcoxon signed-rank test.

4. Results

4.1. Descriptive engagement patterns

As previously mentioned in 3.2. Statistical Analysis, a substantial variability was observed in the raw engagement rates data. Across all four conditions, means exceeded medians, indicating positively skewed distributions and the influence of several high-engagement observations (Table 1).

Table 1
Descriptive statistics of raw engagement rates by platform and content type

Condition	M (%)	Md (%)	SD	Min	Max
Instagram – Personal	10.66	5.16	14.50	0.82	64.50
Instagram – Promotional	11.45	3.82	23.10	0.55	99.50
TikTok – Personal	11.49	4.38	18.20	1.57	75.90
TikTok – Promotional	8.25	3.89	13.60	1.03	61.70

The largest discrepancy between the mean and median occurred for promotional Instagram content, where the mean engagement rate was 11.45% but the median was only 3.82%. Log transformation reduced the impact

of extreme values and produced more balanced distributions. On the transformed scale, mean engagement rates were 2.01 (SD = 0.89) for personal Instagram content, 1.76 (SD = 1.07) for promotional Instagram content, 1.99 (SD = 0.93) for personal TikTok content, and 1.76 (SD = 0.84) for promotional TikTok content.

4.2. Effects of platform and content type

The repeated-measures ANOVA results (Table 2) showed that the main effect of content type did not reach the conventional threshold for statistical significance, $F(1, 19) = 3.90$, $p = .063$, $\eta^2p = .170$. Personal content nevertheless showed a descriptively higher transformed engagement rate than promotional content across the two platforms.

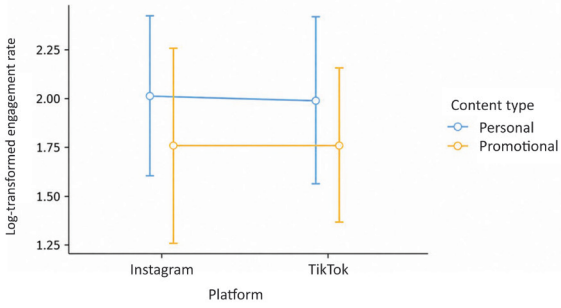
There was no significant main effect of platform, $F(1, 19) = 0.01$, $p = .934$, $\eta^2p < .001$. Overall engagement rates were therefore highly similar between Instagram and TikTok.

The platform × content-type interaction was also not significant, $F(1, 19) = 0.02$, $p = .902$, $\eta^2p = .001$. Thus, there was no statistical evidence that the relationship between personal and promotional content differed systematically between Instagram and TikTok.

Table 2
Repeated-measures ANOVA results for log-transformed engagement rates

Effect	F(1,19)	p	η^2p
Content type	3.90	.063	.170
Platform	0.01	.934	<.001
Platform × Content type	0.02	.902	.001

The corresponding estimated marginal means and 95% confidence intervals are shown in Figure 1. Accordingly, the hypotheses predicting an overall difference between personal and promotional content (H1), a difference between Instagram and TikTok (H2), and a platform-dependent effect of content type (H3) were not supported.



» **Figure 1:** *Estimated marginal means of log-transformed engagement rates by platform and content type, with 95% confidence intervals*

4.3. Within-Platform Comparisons

Additional analyses examined personal and promotional content separately within each platform (Table 3). On Instagram, personal content showed significantly higher engagement rate than promotional content, W = 169,

p = .015, $r_{rb} = .610$, supporting H1a. On TikTok, the difference between personal and promotional content was not statistically significant, $t(19) = 1.63$, $p = .120$, $d = .364$; therefore, H1b was not supported. However, the significant Instagram comparison and non-significant TikTok comparison do not themselves indicate a platform-dependent content-type effect, as the platform × content-type interaction was found to be not significant.

Table 3
Within-platform comparisons of personal and promotional content engagement rates

Platform	Test	Statistic	p	Effect size
Instagram	Wilcoxon	W = 169	.015	$r_{rb} = .610$
TikTok	Paired t-test	t(19) = 1.63	.120	d = .364

**Note. The Wilcoxon signed-rank test was used for Instagram due to non-normal paired differences, whereas the paired-samples t-test was used for TikTok.*

4.4. Disclosure of Promotional Content

A total of 199 Instagram and 196 TikTok promotional posts were included in the disclosure of promotional content analysis. The most common disclosure method on both platforms was a tag in the post description, accounting for 55.28% of promotional Instagram posts and 59.69% of promotional TikTok posts. The distribution of disclosure methods across the two platforms is presented in Table 4.

On Instagram, the Collaboration feature was observed in 34.17% of promotional posts, whereas the official platform disclosure label was not recorded in any analyzed promotional post. On TikTok, the official platform label

Table 4
Distribution of promotional disclosure methods on Instagram and TikTok

Disclosure method	Instagram n (%)	TikTok n (%)
Official platform label	0 (0.00)	27 (13.78)
Collaboration	68 (34.17)	N/A
Tag in description	110 (55.28)	117 (59.69)
Hashtag	16 (8.04)	34 (17.35)
Coupon code	3 (1.51)	5 (2.55)
QR code	0 (0.00)	0 (0.00)
No recorded disclosure	2 (1.01)	13 (6.63)

was present in 27 posts (13.78%). Hashtags were used in 8.04% of Instagram and 17.35% of TikTok promotional posts. Posts with no recorded disclosure represented 1.01% of Instagram and 6.63% of TikTok promotional content. At the influencer level, the mean official disclosure-label rate was 0.00% on Instagram (Md = 0.00%) and 13.50% on TikTok (Md = 5.00%). The Wilcoxon signed-rank test indicated a statistically significant platform difference, W = 0, **p = .005**, r_{rb} = –1.00. Ten influencers had identical disclosure rates on both platforms (0%), while all remaining ten influencers showed higher official disclosure-label use on TikTok. Thus, H4 was supported. It is also notable that promotional posts without any disclosure were more than six times as common on TikTok (6.63%) as on Instagram (1.01%), indicating platform differences in disclosure practices beyond the use of official platform labels.

5. Conclusions

The results indicate that audience engagement cannot be attributed simply to content type or platform. No statistically significant overall effects of content type or platform, or their interaction, were found. Personal content nevertheless showed statistically significant higher engagement rate than promotional content on Instagram, whereas no statistically significant difference was observed on TikTok. This supports previous research suggesting that influencer engagement is shaped by multiple factors rather than by promotional content alone (Tafesse & Wood, 2021; Gross & von Wangenheim, 2022).

A clearer platform difference emerged in promotional disclosure, where official platform disclosure labels were significantly more frequently used on TikTok, while tags in post descriptions were the most common disclosure method on both platforms. Overall, the findings highlight the importance of considering both content characteristics and platform-specific disclosure practices when planning influencer collaborations.

The findings should be interpreted in light of the relatively small, non-probability sample of 20 local and regional influencers and the observational design of the study. Other factors that may influence engagement, such as account size, content niche, and posting characteristics, were not controlled. Future research could examine these relationships using larger and more diverse samples.

6. Acknowledgment

This research has been supported by the Ministry of Science, Technological Development and Innovation (Contract No. 451-03-34/2026-03/200156) and the Faculty of Technical Sciences, University of Novi Sad through project “Scientific and Artistic Research Work of Researchers in Teaching and Associate Positions at the Faculty of Technical Sciences, University of Novi Sad 2026” (No. 01-3609/1).

7. References

Audrezet, A., de Kerviler, G. and Moulard, J.G. (2020) 'Authenticity under threat: When social media influencers need to go beyond self-presentation', *Journal of Business Research*, 117, pp. 557–569. DOI: 10.1016/j.jbusres.2018.07.008

Barta, S., Belanche, D., Fernández, A. and Flavián, M. (2023) 'Influencer marketing on TikTok: The effectiveness of humor and followers’ hedonic experience', *Journal of Retailing and Consumer Services*, 70, 103149. DOI: 10.1016/j.jretconser.2022.103149

Boerman, S.C. (2020) 'The effects of the standardized Instagram disclosure for micro- and meso-influencers', *Computers in Human Behavior*, 103, pp. 199–207. DOI: 10.1016/j.chb.2019.09.015

Campbell, C. and Farrell, J.R. (2020) 'More than meets the eye: The functional components underlying influencer marketing', *Business Horizons*, 63(4), pp. 469–479. DOI: 10.1016/j.bushor.2020.03.003

Gross, J. and von Wangenheim, F. (2022) 'Influencer marketing on Instagram: Empirical research on social media engagement with sponsored posts', *Journal of Interactive Advertising*, 22(3), pp. 289–310. DOI: 10.1080/15252019.2022.2123724

Ki, C.W.C., Cuevas, L.M., Chong, S.M. and Lim, H. (2020) 'Influencer marketing: Social media influencers as human brands attaching to followers and yielding positive marketing results by fulfilling needs', *Journal of Retailing and Consumer Services*, 55, 102133. DOI: 10.1016/j.jretconser.2020.102133

Kim, D.Y. and Kim, H.Y. (2021) 'Trust me, trust me not: A nuanced view of influencer marketing on social media', *Journal of Business Research*, 134, pp. 223–232. DOI: 10.1016/j.jbusres.2021.05.024

Lenth, R.V. (2025) emmeans: Estimated Marginal Means, aka Least-Squares Means. R package. Available from: https://cran.r-project.org/package=emmeans.

Lou, C. and Yuan, S. (2019) 'Influencer marketing: How message value and credibility affect consumer trust of branded content on social media', *Journal of Interactive Advertising*, 19(1), pp. 58–73. DOI: 10.1080/15252019.2018.1533501

Milošević, R., Komlenić, A., Kašiković, N., Banjanin, B. and Menzildžić, D. (2022) 'Instagram influencers’ responsiveness to a small business collaboration outreach'. In: Vladić (ed.) Proceedings - *The Eleventh International Symposium GRID 2022, 3–5 November 2022, Novi Sad, Serbia*. Novi Sad: University of Novi Sad, Faculty of Technical Sciences, Department of Graphic Engineering and Design, pp. 237–243.

Milošević, R., Adamović, S., Komlenić, A., Menzildžić, D., Dimovski, V. and Vasilić, P. (2024) 'The impact of reciprocity on Instagram pet influencer posting response times'. In: Pál (ed.) Proceedings - *The Twelfth International Symposium GRID 2024, 14–16 November 2024, Novi Sad, Serbia*. Novi Sad: University of Novi Sad, Faculty of Technical Sciences, Department of Graphic Engineering and Design, pp. 317–322.

Navarro, D.J. and Foxcroft, D.R. (2025) *Learning Statistics with jamovi: A Tutorial for Beginners in Statistical Analysis*. Cambridge: Open Book Publishers. DOI: 10.11647/OBP.0333

R Core Team (2025) R: *A Language and Environment for Statistical Computing*, Version 4.5. Vienna: R Foundation for Statistical Computing. Available from: https://www.r-project.org.

Singmann, H. (2024) *afex: Analysis of Factorial Experiments. R package*. Available from: https://cran.r-project.org/package=afex.

Tafesse, W. and Wood, B.P. (2021) 'Followers' engagement with Instagram influencers: The role of influencers' content and engagement strategy', *Journal of Retailing and Consumer Services*, 58, 102303. DOI: 10.1016/j.jretconser.2020.102303

The jamovi project (2025) *jamovi*, Version 2.7 [Computer software]. Available from: https://www.jamovi.org.



© 2026 Authors. Published by the University of Novi Sad, Faculty of Technical Sciences, Department of Graphic Engineering and Design. This article is an open access article distributed under the terms and conditions of the Creative Commons Attribution license 4.0 Serbia (https://creativecommons.org/licenses/by/4.0/deed.en).

Ecology and sustainable materials

06

Original Scientific Paper https://doi.org/10.24867/GRID-2026-p65

Optimization of Fenton-like Oxidation for Cyan Printing Dye Removal in the Presence of Polyethylene Terephthalate Microplastics

ABSTRACT

The simultaneous presence of synthetic dyes and microplastics in industrial wastewaters represents an emerging environmental challenge that may significantly influence the performance of advanced oxidation processes. In this study, the efficiency of Fenton-like oxidation for the removal of Cyan printing dye in the presence of polyethylene terephthalate (PET) microplastics was investigated. Process optimization was performed using a three-level Definitive Screening Design (DSD) by evaluating the effects of five operating parameters, namely initial dye concentration, green-synthesized nano zero-valent iron (nZVI) dosage, PET concentration, solution pH and hydrogen peroxide concentration. The developed statistical model exhibited excellent predictive capability with a coefficient of determination (R^2) of 0.977 and an adjusted coefficient of determination (R^2adj) of 0.967. Analysis of variance confirmed the statistical significance of the model ($p < 0.0001$). Statistical analysis revealed that solution pH was the most influential factor affecting Cyan dye removal, followed by nZVI dosage, while H_2O_2 concentration, initial dye concentration and PET microplastic concentration also showed statisticaly significant effects. In addition, a significant interaction between nZVI dosage and H_2O_2 concentration confirmed the importance of their balanced ratio, wheras increasing PET concentration slightly reduced decolorization efficiency. The maximum experimental decolorization efficiency reached 85%, while model optimization predicted a maximum efficiency of 96% under the following operating conditions: 108.9 mgL^{-1} initial dye concentration, 48.7 $mgFeL^{-1}$ nZVI dose, 5.3 gL^{-1} PET concentration, pH of 5.82 and 4.78 mM hydrogen peroxide. The obtained results demonstrate that efficient treatment of Cyan printing wastewater in the presence of PET microplastics requires simultaneous optimization of all process variables and provide valuable insight into the combined effects of adsorption and oxidation occurring during the Fenton process.

Vesna Gvoić [1]
Aleksandra Tubić [2]
Maja Vujić [2]
Jasmina Agbaba [2]
Dejan Krčmar [2]
Živko Pavlović [1]
Miljana Prica [1]

[1] University of Novi Sad, Faculty of Technical Sciences, Department of Graphic Engineering and Design, Novi Sad, Serbia
[2] University of Novi Sad, Faculty of Sciences, Department of Chemistry, Biochemistry and Environmental Protection, Novi Sad, Serbia

KEY WORDS
Fenton oxidation, PET microplastics, cyan printing dye, advanced oxidation processes, wastewater treatment, process optimization, definitive screening design

1. Introduction

Industrial wastewater containing synthetic dyes represents one of the most challenging environmental issues due to its high color intensity, complex chemical composition, and resistance to conventional biological treatment. Large volumes of dye-containing effluents are generated by numerous industrial sectors, including textile, paper, leather, food, cosmetic, and printing industries. Even at low concentrations, synthetic dyes impart

intense coloration to receiving water bodies, reduce light penetration, inhibit photosynthetic activity, and may produce toxic, mutagenic, or carcinogenic degradation products, thereby posing significant risks to aquatic ecosystems and human health. Recent estimates indicate that a substantial fraction of industrial dye-containing wastewaters is still discharged without adequate treatment, emphasizing the need for more efficient remediation technologies (Song et al., 2024; Rathi et al., 2021).

Among printing dyes, Cyan pigments based on copper phthalocyanine derivatives exhibit exceptional chemical, thermal, and photochemical stability owing to their highly conjugated aromatic structure. These characteristics provide excellent printing performance but simultaneously make their removal from wastewater particularly difficult. Conventional physicochemical and biological treatment technologies often fail to achieve satisfactory degradation because of the low biodegradability and structural stability of phthalocyanine compounds. Consequently, the development of efficient treatment strategies for Cyan printing wastewater remains an important environmental challenge (Xiao et al., 2024; Rathi et al., 2021).

Besides dissolved organic contaminants, industrial effluents increasingly contain microplastic particles originating from polymer processing, packaging materials, synthetic coatings, printing substrates, and equipment cleaning operations. Plastic production has increased continuously over recent decades, resulting in the extensive accumulation of plastic waste in terrestrial and aquatic environments (Tumwesigye et al., 2023; Fu et al., 2021; Chamas et al., 2020).

Among the different polymer types, polyethylene terephthalate (PET) is one of the most extensively manufactured engineering plastics owing to its excellent mechanical properties, chemical resistance, and widespread application in food packaging, beverage bottles, and industrial materials. Mechanical abrasion, weathering, and fragmentation generate PET microplastics that are now frequently detected in industrial and municipal wastewaters. Their occurrence has been reported in freshwater systems, marine environments, sediments, soils, atmospheric deposition, drinking water, and living organisms, highlighting their global environmental significance (Du et al., 2021; Chamas et al., 2020).

Among the available treatment technologies, Advanced Oxidation Processes (AOPs) have emerged as one of the most promising approaches for the degradation of refractory organic pollutants. Their effectiveness relies on the in-situ generation of highly reactive oxygen species, particularly hydroxyl radicals (•OH), which possess extremely high oxidation potential and react non-selectively with a wide range of organic compounds. Hydroxyl radicals promote cleavage of chromophoric groups, aromatic rings, and other recalcitrant molecular structures, leading to discoloration, oxidation, and in favourable cases complete mineralization into carbon dioxide and water (Ma et al., 2021; Nidheesh et al., 2018). Owing to these characteristics, AOPs have been successfully applied for the treatment of wastewaters containing dyes, pharmaceuticals, pesticides, antibiotics, and other persistent contaminants (Xiao et al., 2024; Lai et al., 2021; Miklos et al., 2018).

Among AOPs, the Fenton process remains one of the most extensively investigated oxidation technologies because of its operational simplicity, relatively low cost, and high oxidation efficiency. The process is based on catalytic decomposition of hydrogen peroxide in the presence of ferrous ions, producing hydroxyl radicals capable of rapidly degrading complex organic molecules. Numerous studies have demonstrated that Fenton and Fenton-like oxidation processes can achieve decolorization efficiencies frequently exceeding 90% for azo, anthraquinone, triphenylmethane, and phthalocyanine dyes under optimized reaction conditions, confirming their applicability for the treatment of highly colored industrial wastewaters (Heryanto & Tahir, 2025; Xiao et al., 2024; Deng & Brillas, 2023). However, process performance strongly depends on operational parameters such as pH, hydrogen peroxide dosage, iron concentration, reaction time, and wastewater composition (Song et al., 2024).

Despite extensive research on Fenton oxidation of synthetic dyes, considerably less attention has been devoted to complex wastewater systems containing suspended microplastics (Xiao et al., 2024). PET particles may adsorb dye molecules before oxidation, compete for reactive oxygen species, or undergo oxidative surface modifications that alter their adsorption behaviour during treatment (Kovačić et al., 2024). Consequently, the apparent dye removal efficiency may represent the combined contribution of adsorption onto PET surfaces and oxidative degradation by hydroxyl radicals.

Despite the increasing interest in the interaction between advanced oxidation processes and microplastics, systematic investigations on the Fenton oxidation of phthalocyanine-based printing dyes in the presence of PET microplastics remain scarce (Song et al., 2024). Therefore, this study aimed to evaluate the efficiency of the Fenton process for the removal of Cyan printing dye in the presence of PET microplastics.
Process optimization was performed using the Definitive Screening Design (DSD) methodology by systematically evaluating the effects of five key operational parameters: initial dye concentration, nZVI dosage - iron concentration, solution pH, PET concentration and hydrogen peroxide concentration. Optimization was initially conducted in a model aqueous system to establish the optimal operating conditions prior to their application to real printing wastewater.

2. Materials and Methods

2.1. Materials and chemicals

Cyan water-based printing dye (Flint Group, Germany) was selected as the target pollutant in this study. The dye belongs to the phthalocyanine class (Color Index PB15:3; CAS No. 147-14-8) and has a molecular formula of $C_{32}H_{16}CuN_8$ with a molar mass of 576.07 g mol^{-1}. The maximum absorption wavelength (λmax) of the dye was determined at 636 nm and was used for spectrophotometric monitoring throughout the experiments.

Commercial polyethylene terephthalate (PET) microplastic particles (Sigma-Aldrich, USA) were used as representative microplastics because of their widespread occurrence in industrial wastewaters and their environmental relevance.

Hydrogen peroxide (30%, NRK Engineering, Serbia), sodium hydroxide (>98.8%, POCH, Poland), sulfuric acid (>96%, J.T. Baker, USA), and iron(III) chloride hexahydrate (Centrohem, Serbia) were of analytical grade and used without further purification. All aqueous solutions were prepared using deionized water.

Nano zero-valent iron (nZVI) particles were synthesized using a green synthesis procedure based on green tea (Camellia sinensis) leaf extract, following the method originally proposed by Machado et al. (2013) and subsequently applied in our previous study (Prica et al., 2020).

2.2. Fenton oxidation experiments

Fenton oxidation experiments were conducted in batch mode using a six-position jar-test apparatus (FC6S, Velp Scientifica, Italy). The experiments were performed in 500 mL glass beakers containing 250 mL of aqueous Cyan printing dye solution. The initial dye concentration was varied between 20 and 180 mgL^{-1} according to the experimental design. PET microplastic particles were added at concentrations ranging from 1 to 10 gL^{-1}, while the concentration of green-synthesized nZVI catalyst varied between 0.75 and 60 $mgFeL^{-1}$. The initial pH of the reaction mixture was adjusted within the range of 2–10 using 0.1 M H_2SO_4 or 0.1 M NaOH solutions. Subsequently, hydrogen peroxide was added at concentrations between 1 and 11 mM to initiate the Fenton oxidation process. All experiments were carried out at room temperature (23 ± 1 °C) under continuous stirring at 120 rpm for 60 min.

Following the reaction, the residual concentration of Cyan dye was determined spectrophotometrically by measuring the absorbance at its maximum absorption wavelength (636 nm) using a UV–Vis spectrophotometer (Genesys 10S, Thermo Scientific, USA). The decolorization efficiency (E, %) was calculated according to Eq. (1):

$$E\ (\%) = \frac{A_0 - A_t}{A_0} * 100 \quad (1)$$

where: A_0 is the initial dye absorbance of Cyan dye aqueous solution; A_t is absorbance of Cyan dye aqueous solution after Fenton-like process.

2.3. Statistical analysis

The experimental matrix was established using a three-level Definitive Screening Design (DSD) to optimize the Fenton oxidation process. Five operating parameters were selected as independent variables: initial Cyan dye concentration (20–180 mgL^{-1}), nZVI dosage (0.75–60 $mgFeL^{-1}$), PET microplastic concentration (1–10 gL^{-1}), solution pH (2–10), and hydrogen peroxide concentration (1–11 mM). Each parameter was evaluated at three levels (–1, 0, and +1), representing the lower, central, and upper experimental values (Prica et al., 2020). Experimental design generation, regression analysis, and process optimization were carried out using JMP® 13 software (SAS Institute Inc., Cary, NC, USA). The DSD methodology was selected because it enables efficient screening of significant factors while minimizing the number of experimental runs and allowing independent estimation of the main effects without confounding with second-order interactions (Pereira et al., 2018).

3. Results and Discussions

3.1. Fenton oxidation process efficiency

The efficiency of the Fenton oxidation process for the removal of Cyan printing dye in the presence of PET microplastics was evaluated using a Definitive Screening Design (DSD). The experimental matrix comprised 28 experimental runs in which five operating variables were simultaneously investigated. The corresponding decolorization efficiencies obtained under different operating conditions are summarized in Table 1.
The obtained results revealed a pronounced dependence of the Fenton oxidation efficiency on the selected operating conditions. Dye removal efficiencies ranged from only 2.0% to 85%, confirming that the process performance was strongly governed by the interaction of the investigated variables.

The lowest removal efficiencies were generally observed under alkaline conditions combined with low catalyst dosage, whereas considerably higher decolorization efficiencies were achieved under acidic conditions and increased nZVI concentrations. The highest experimental removal efficiency (85%) was obtained under intermediate operating conditions, indicating that simultaneous optimization of all process variables is required to maximize the oxidation performance.

The broad variation in removal efficiency demonstrates the complexity of the investigated system, in which dye oxidation and adsorption onto PET microplastics may occur simultaneously. Unlike conventional aqueous systems, the presence of PET particles introduces additional interactions that may influence hydroxyl radical availability as well as the apparent decolorization efficiency. Consequently, optimization based on statistical experimental design represents an appropriate approach for identifying the combined effects of multiple operating variables.

3.2. Statistical evaluation of the developed model

The adequacy of the developed DSD model was evaluated using regression analysis and analysis of variance (ANOVA). As presented in Table 2, the proposed model exhibited an excellent agreement with the experimental data, with a coefficient of determination (R^2 = 0.98) and an adjusted coefficient of determination (R^2adj = 0.97), indicating that approximately 98% of the variability in Cyan dye removal could be explained by the selected operating variables.
Furthermore, the relatively low root mean square error (RMSE = 5.16) confirms the satisfactory predictive capability of the developed model.

The ANOVA results further confirmed the statistical significance of the regression model. As shown in Table 3, the calculated F-value of 101.136 with a probability value below 0.0001 indicates that the model adequately describes the relationship between the investigated variables and the response. Therefore, the developed statistical model can be considered reliable for both interpretation of individual process parameters and optimization of the Fenton oxidation process.

Table 1

Decolorization efficiency (%) of the Fenton process for a synthetic Cyan printing dye solution

Number	Dye concentration (mgL^{-1})	nZVI dosage (mgL^{-1})	PET concentration (mgL^{-1})	pH	H_2O_2 concentration (mM)	Fenton process efficiency (%)
1	100	60	10	10	11	45.15
2	100	0.75	1	2	1	58.63
3	180	30.4	1	10	11	21.66
4	20	30.4	10	2	1	47.72
5	180	0.75	5.5	2	11	72.16
6	20	60	5.5	10	1	74.28
7	180	60	1	6	1	82.95
8	20	0.75	10	6	11	12.6
9	180	60	10	2	6	69.44
10	20	0.75	1	10	6	2.01
11	180	0.75	10	10	1	2.75
12	20	60	1	2	11	62.94
13	100	30.4	5.5	6	6	79.71
14	100	60	10	10	11	40.41
15	100	0.75	1	2	1	60.31
16	180	30.4	1	10	11	15.36
17	20	30.4	10	2	1	65.99
18	180	0.75	5.5	2	11	71.21
19	20	60	5.5	10	1	72.55
20	180	60	1	6	1	70.75
21	20	0.75	10	6	11	10.14
22	180	60	10	2	6	65.63
23	20	0.75	1	10	6	6.53
24	180	0.75	10	10	1	6.86
25	20	60	1	2	11	58.88
26	100	30.4	5.5	6	6	84.98
27	100	30.4	5.5	6	6	81.69
28	100	30.4	5.5	6	6	76.15

Table 2
Summary of fit

Source	Value
R2	0.98
R2 Adj	0.97
Root Mean Square Error	5.16

Table 3
ANOVA results for the proposed model

Source	Degrees of freedom	Sum of Squares	Mean Square	F parameter
Model	8	21533.035	2691.630	101.136
Error	19	505.665	26.610	Prob>F
C. Total	27	22038.700	-	<0.0001

The estimated regression coefficients are presented in Table 4. Among the investigated factors, solution pH exhibited the greatest influence on the process efficiency, followed by nZVI dosage. This observation is consistent with the well-established mechanism of the Fenton reaction, which is known to achieve maximum efficiency under acidic conditions. At low pH values, iron remains predominantly in its soluble form, enabling continuous catalytic decomposition of hydrogen peroxide and efficient generation of hydroxyl radicals.
As the pH increases, ferric hydroxides are progressively formed, reducing the concentration of catalytically active iron species and consequently decreasing the oxidation efficiency. Similar behaviour has been widely reported for homogeneous and heterogeneous Fenton systems treating dye-containing wastewaters (Xiao et al., 2024; Nidheesh et al., 2018).

Furthermore, increasing the catalyst concentration enhanced hydroxyl radical production by providing a greater number of active iron sites available for hydrogen peroxide activation. Consequently, higher nZVI dosages promoted faster degradation of the chromophoric structure of the phthalocyanine dye. However, excessively high iron concentrations may also lead to non-productive radical consumption through scavenging reactions, indicating that an optimum catalyst dosage is required to maximize process performance.

Table 4
Parameter estimates sorted by statistical significance

Term	Estimate	Std Error	t ratio	Prob >|t|
pH	-17.268	1.154	-14.970	<0.0001*
nZVI dosage	16.989	1.154	14.730	<0.0001*
H_2O_2 concentration	-6.614	1.154	-5.730	<0.0001*
PET concentration	-3.667	1.154	-3.180	0.0049*
nZVI dosage * H_2O_2 conc.	-5.626	1.824	-3080	0.0061*
Dye concentration	3.257	1.154	2.820	0.0109*

Hydrogen peroxide concentration and PET concentration also significantly affected dye removal, although to a lesser extent. In addition, the interaction between nZVI dosage and H_2O_2 concentration was found to be statistically significant ($p = 0.0061$), suggesting that the oxidation efficiency depends not only on the individual reagent concentrations but also on their mutual balance during hydroxyl radical generation. Initial dye concentration showed a statistically significant positive effect, indicating that the selected concentration range was suitable for efficient oxidation under optimized operating conditions.

Although hydrogen peroxide is the primary source of hydroxyl radicals, its excessive addition may reduce oxidation efficiency because H_2O_2 competes with dye molecules for hydroxyl radicals, producing less reactive hydroperoxyl radicals ($HO_2\bullet$). This phenomenon has been frequently reported in Fenton-based oxidation processes and explains why increasing the oxidant concentration beyond the optimum value does not necessarily improve pollutant removal (Deng & Brillas, 2023).

PET microplastic concentration was likewise identified as a statistically significant factor. Increasing the concentration of PET particles resulted in a slight decrease in the overall Fenton oxidation efficiency. This behaviour may be attributed to the dual role of PET microplastics within the reaction system. On one hand, PET particles can adsorb Cyan dye molecules onto their surface, thereby reducing the dissolved dye concentration. On the other hand, adsorption may limit the accessibility of dye molecules to hydroxyl radicals, while PET surfaces may additionally interfere with radical reactions occurring in the aqueous phase. Consequently, the experimentally observed decolorization efficiency represents the combined outcome of adsorption and oxidative degradation, rather than oxidation alone (Song et al., 2024).

Overall, these findings demonstrate that the efficiency of the Fenton oxidation process is governed by a combination of operational parameters rather than by a single factor, highlighting the importance of multivariable optimization for complex wastewater systems containing both dissolved dyes and suspended PET microplastics.

3.3. Optimization of the Fenton oxidation process

The optimal operating conditions for the Fenton oxidation process were determined using the prediction profiler generated by the Definitive Screening Design (DSD) model (Figure 1). The profiler simultaneously illustrates

the influence of each process variable on the predicted decolorization efficiency while maintaining the remaining variables at their optimum levels. This approach enables visualization of both the direction and magnitude of individual factor effects and provides a practical tool for selecting the most favorable operating conditions.

According to the developed model, the maximum predicted decolorization efficiency of 96% was achieved at an initial Cyan dye concentration of approximately 108.9 mgL^{-1}, with 48.7 mgL^{-1} of nZVI, 5.3 gL^{-1} of PET microplastics, a pH of 5.82 and 4.78 mM hydrogen peroxide. These results demonstrate that complete optimization of the process does not necessarily correspond to the highest or lowest values of all investigated variables, but rather to an optimal balance between catalyst dosage, oxidant concentration, solution pH, and PET content.

The prediction profiler clearly indicates that the concentration of nZVI exerts a positive effect on the process efficiency within the investigated range, whereas increasing PET concentration beyond its optimal value leads to a gradual decrease in dye removal. The latter observation is consistent with the well-known scavenging effect of excess hydrogen peroxide, which consumes hydroxyl radicals and decreases their availability for oxidation of the target pollutant. Similarly, increasing PET concentration may reduce the apparent oxidation efficiency due to enhanced adsorption of dye molecules onto the polymer surface, thereby altering the balance between adsorption and oxidative degradation.

The optimum pH predicted by the statistical model was approximately 5.8, which is higher than the optimum commonly reported for conventional homogeneous Fenton systems. This behavior may be attributed to the use of green-synthesized nZVI as a heterogeneous iron source, whose catalytic activity can be maintained over a wider pH range compared with dissolved ferrous ions. Furthermore, thesimultaneous presence of PET microplastics may modify the reaction environment through adsorption phenomena occurring at the solid–liquid interface, resulting in a shift of the optimum operating conditions.

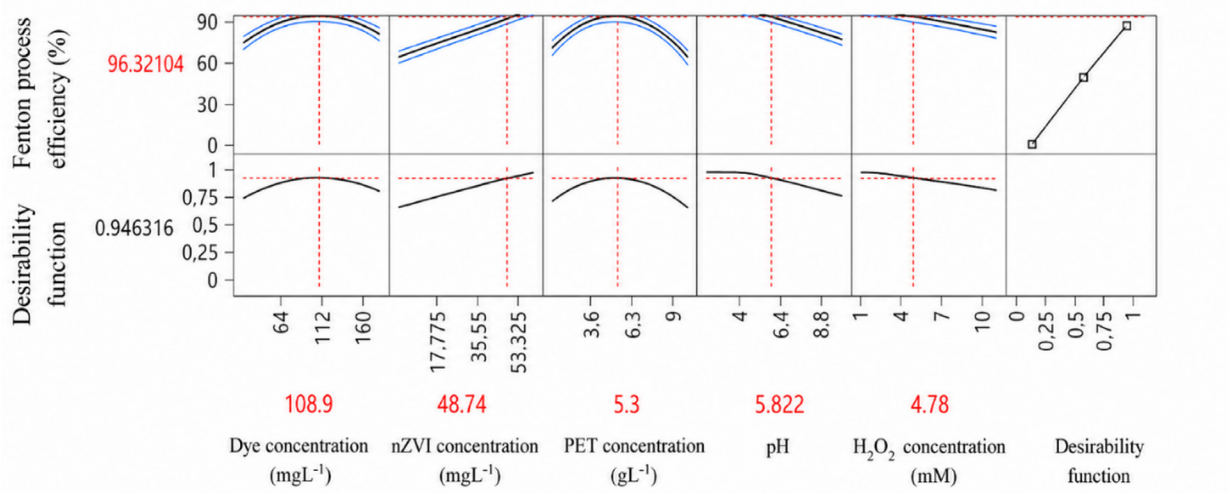
Overall, the prediction profiler confirms that efficient removal of Cyan printing dye can be achieved only through simultaneous optimization of all investigated process variables. The developed DSD model therefore represents a reliable tool for predicting process performance and defining operating conditions suitable for subsequent application to real printing wastewater.

4. Conclusion

The present study demonstrated that the efficiency of Fenton oxidation for the removal of Cyan printing dye is strongly influenced by the simultaneous presence of PET microplastics and by the operating conditions of the oxidation process. Application of the Definitive Screening Design enabled efficient evaluation of five process variables while substantially reducing the number of required experiments.

The developed statistical model showed excellent predictive performance (R^2 = 0.98), confirming the suitability of the DSD approach for optimization of complex oxidation systems. Among the investigated variables, solution pH and nZVI dosage were identified as the dominant factors governing dye removal, whereas excessive PET concentrations negatively affected the process efficiency. The interaction between nZVI dosage and hydrogen peroxide concentration was also found to be statistically significant, emphasizing the importance of maintaining an appropriate catalyst-to-oxidant ratio.

The optimized operating conditions predicted a decolorization efficiency of approximately 96%, demonstrating the high potential of the investigated process for



» **Figure 1:** *Optimization diagram of Fenton oxidation process*

treating Cyan printing wastewater. Furthermore, the results indicate that PET microplastics not only represent an additional contaminant but may also influence the overall treatment efficiency through simultaneous adsorption of dye molecules and modification of oxidation processes occurring in the reaction system.

Overall, the findings contribute to a better understanding of Fenton oxidation in complex wastewater matrices containing both synthetic dyes and microplastics and provide a basis for the future application of optimized Fenton-based technologies for the treatment of real printing industry effluents.

5. Acknowledgements

We gratefully acknowledge the financial support of the Ministry of Science, Technological Development, and Innovation of the Republic of Serbia (Grants No. 451-03-33/2026-03/200125, 451-03-34/2026-03/200125, and 451-03-34/2026-03/200156) and the University of Novi Sad, Faculty of Technical Sciences through the project "Scientific and Artistic Research Work of Researchers in Teaching and Associate Positions at the Faculty of Technical Sciences, University of Novi Sad 2026" (No. 01-3609/1).

6. References

Chamas, A., Moon, H., Zheng, J., Qiu, Y., Tabassum, T., Jang, J.H., Abu-Omar, M., Scott, S.L. and Suh, S. (2020) 'Degradation rates of plastics in the environment', *ACS Sustainable Chemistry and Engineering*, 8(9), pp. 3494–3511. DOI: 10.1021/acssuschemeng.9b06635

Deng, F. and Brillas, E. (2023) 'Advances in the decontamination of wastewaters with synthetic organic dyes by electrochemical Fenton-based processes', *Separation and Purification Technology*, 316, 123764. DOI: 10.1016/j.seppur.2023.123764

Du, S., Zhu, R., Cai, Y., Xu, N., Yap, P., Zhang, Y., He, Y. and Zhang, Y.Z. (2021) 'Environmental fate and impacts of microplastics in aquatic ecosystems: A review', *RSC Advances*, 11(26), pp. 15762–15784. DOI: 10.1039/d1ra00880c

Fu, L., Li, J., Wang, G., Luan, Y. and Dai, W. (2021) 'Adsorption behavior of organic pollutants onto microplastics: A review', *Ecotoxicology and Environmental Safety*, 217, 112207. DOI: 10.1016/j.ecoenv.2021.112207

Heryanto, H. and Tahir, D. (2025) 'Trends, mechanisms, and the role of advanced oxidation processes in mitigating azo, triarylmethane, and anthraquinone dye pollution: A bibliometric analysis', *Inorganic Chemistry Communications*, 175, 114104. DOI: 10.1016/j.inoche.2025.114104

Kovačić, M., Tomić, A., Tonković, S., Pulitika, A., Zjaćić, J.P., Katančić, Z., Genorio, B., Kušić, H. and Božić, A.L. (2024) 'Pristine and UV-Weathered PET Microplastics as Water Contaminants: Appraising the Potential of the Fenton Process for Effective Remediation', *Processes*, 12(4), 844. DOI: 10.3390/pr12040844

Ma, D., Yi, H., Lai, C., Liu, X., Huo, X., An, Z., Li, L., Fu, Y., Li, B., Zhang, M., Qin, L., Liu, S. and Yang, L. (2021) 'Critical review of advanced oxidation processes in organic wastewater treatment', *Chemosphere*, 287, 130104. DOI: 10.1016/j.chemosphere.2021.130104

Machado, S., Pinto, S., Grosso, J., Nouws, H., Albergaria, J. and Delerue-Matos, C. (2013) 'Green production of zero-valent iron nanoparticles using tree leaf extracts', *Science of the Total Environment*, 445–446, pp. 1–8. DOI: 10.1016/j.scitotenv.2012.12.033

Miklos, D.B., Remy, C., Jekel, M., Linden, K.G., Drewes, J.E. and Hübner, U. (2018) 'Evaluation of advanced oxidation processes for water and wastewater treatment – A critical review', *Water Research*, 139, pp. 118–131. DOI: 10.1016/j.watres.2018.03.042

Nidheesh, P.V., Zhou, M. and Oturan, M.A. (2018) 'An overview on the removal of synthetic dyes by advanced oxidation processes', *Chemosphere*, 287, pp. 132–150. DOI: 10.1016/j.chemosphere.2017.12.195

Pereira, A., Reis, M., Leca, J., Rodrigues, P. and Marques, J. (2018) 'Definitive Screening Designs and latent variable modelling for the optimization of solid phase microextraction (SPME): Case study- Quantification of volatile fatty acids in wines', *Chemometrics and Intelligent Laboratory Systems*, 179, pp. 73–81. DOI: 10.1016/j.chemolab.2018.06.010

Prica, M., Tubić, A., Lončarski, M., Gvoić, V., Vasiljević, S., Pavlović, Ž. and Agbaba, J. (2020) 'Application of advanced oxidation process for the removal of synthetic water-based printing dye and microplastics from aqueous solution'. In: *Proceedings of 10th International Symposium on Graphic Engineering and Design, GRID 2020, 12–14 November 2020, Novi Sad, Serbia*. Novi Sad: University of Novi Sad, Faculty of Technical Sciences, Department of Graphic Engineering and Design, pp. 243–250. DOI: 10.24867/GRID-2020-p26

Rathi, B.S., Kumar, P.S. and Show, P.L. (2021) 'A review on effective removal of emerging contaminants from aquatic systems using advanced oxidation processes', *Chemosphere*, 287, 131911. DOI: 10.1016/j.jhazmat.2020.124413

Song, J., Zhu, L., Yu, S., Li, G. and Wang, D. (2024) 'The synergistic effect of adsorption and Fenton oxidation for organic pollutants in water remediation: An overview', *RSC Advances*, 14(45), pp. 33489–33511. DOI: 10.1039/D4RA03050H

Tumwesigye, E., Nnadozie, C.F., Akamagwuna, F.C., Noundou, X.S., Nyakairu, G.W. and Odume, O.N. (2023) 'Microplastics as vectors of chemical contaminants and biological agents in freshwater ecosystems: Current knowledge status and future perspectives', *Environmental Pollution*, 330, 121829. DOI: 10.1016/j.envpol.2023.121829

Xiao, J., Guo, S., Wang, D. and An, Q. (2024) 'Fenton-like reaction: Recent advances and new trends', *Chemistry – A European Journal*, 30, e202304337. DOI: 10.1002/chem.202304337

© 2026 Authors. Published by the University of Novi Sad, Faculty of Technical Sciences, Department of Graphic Engineering and Design. This article is an open access article distributed under the terms and conditions of the Creative Commons Attribution license 4.0 Serbia (https://creativecommons.org/licenses/by/4.0/deed.en).

Original Scientific Paper https://doi.org/10.24867/GRID-2026-p66

Development and Characterization of a Functional UV-Photopolymerized PEGDA/PETMP/BMEP Hydrogel Adsorbent for Methylene Blue Removal from Aqueous Media

Betul Eymur Donmez [1,2]
Aslı Beyler Cigil [3]

[1] Gazi University, Graduate School of Natural and Applied Sciences, Department of Advanced Technologies, Ankara, Türkiye
[2] Middle East Technical University, Central Laboratory, Ankara, Türkiye
[3] Gazi University, Vocational School of Technical Sciences, Department of Chemistry and Chemical Processing Technologies, Ankara, Türkiye

ABSTRACT

Highly colored effluents from printing and related industries are an environmental concern because many colorants persist in aqueous environments and resist conventional biological treatment. In this study, a phosphate-functional hydrogel was prepared via UV photopolymerization and evaluated as an adsorbent for methylene blue (MB), a model cationic dye. The network was formed by UV-induced thiol–(meth)acrylate reactions of poly(ethylene glycol) diacrylate (PEGDA), the tetrafunctional thiol pentaerythritol tetrakis(3-mercaptopropionate) (PETMP), and the phosphate-containing comonomer bis[2-(methacryloyloxy)ethyl] phosphate (BMEP; about 10 wt% of the monomers), which was intended to introduce ionizable sites for interaction with MB. A BMEP-free PEGDA/PETMP hydrogel with the same PEGDA-to-solvent ratio and thiol:(meth)acrylate molar ratio (0.78:1) served as a control. Both hydrogels were characterized by Fourier-transform infrared spectroscopy (FTIR), thermogravimetric analysis (TGA), and swelling measurements, while dried Hfunc was also examined by scanning electron microscopy (SEM). MB removal from 10 mg L^{-1} solutions was followed by UV–Vis spectrophotometry as a function of contact time. FTIR spectra showed differences in the C-H and fingerprint regions, consistent with compositional differences between the formulations. After 24 h in deionized water, the swelling ratio was 55.5% for the control and 65.1% for the BMEP-containing hydrogel. After 24 h in 50 mL of 10 mg L^{-1} MB, removal reached 80.8% for the BMEP-containing hydrogel and 27.0% for the control. Under the conditions examined, the BMEP-containing formulation showed substantially greater MB removal than the BMEP-free control. These results indicate the potential of UV-curable phosphate-functional hydrogels as adsorbents for cationic dyes, with possible relevance to colored aqueous streams from printing and related processes.

KEY WORDS
UV photopolymerization, thiol–acrylate hydrogel, PEGDA, PETMP, BMEP, phosphate-functional hydrogel, methylene blue, adsorption

1. Introduction

The discharge of intensely colored industrial effluents is an environmental concern because many synthetic colorants persist in aqueous environments and are difficult to remove by conventional treatment processes. Printing operations are one such source: water-based inks may remain dispersed or dissolved in process water, particularly during equipment cleaning and color-change procedures, producing strongly col-

ored effluents with complex organic content. Recent work on printing wastewater has emphasized the need for efficient color-removal strategies, including adsorption-based approaches (Kara et al., 2026).

Adsorption is widely investigated for removing dyes and other colored contaminants because of its operational simplicity and its applicability to compounds that are not readily biodegradable. Hydrogels are particularly attractive adsorbents: their three-dimensional crosslinked networks absorb substantial amounts of water while retaining structural integrity, and their composition, crosslink density, swelling behavior, and functional groups can be tailored to control interactions with dissolved contaminants (Yang et al., 2022). Hydrogel-based materials have accordingly been studied for the adsorption of organic dyes and other colorants from aqueous media (Pereira et al., 2021; Kara et al., 2026).

Methylene blue (MB) is a water-soluble cationic dye widely used as a model contaminant for evaluating adsorbent performance. Its strong visible absorption enables quantitative monitoring by UV-Vis spectrophotometry, and its cationic character makes it well-suited to probe interactions with negatively charged or ionizable groups (Yang et al., 2022). Depending on the adsorbent, MB uptake may involve electrostatic attraction, hydrogen bonding, or both. MB has also been discussed in the context of effluents from paper, printing, and dyeing industries (Rafatullah et al., 2010). In the present work, however, MB is used as a model cationic dye rather than as a representative printing pigment, so that the behavior of the developed hydrogel can be evaluated under controlled conditions.

Poly(ethylene glycol) (PEG)-based acrylate and methacrylate monomers provide a versatile platform for hydrophilic crosslinked networks, and multifunctional thiols can participate in UV-induced thiol-ene/thiol-acrylate network formation with (meth)acrylate groups (Cramer & Bowman, 2001; Hoyle & Bowman, 2010). Pentaerythritol tetrakis(3-mercaptopropionate) (PETMP), which contains four thiol groups, can therefore act as a multifunctional crosslinker in PEG-based networks. Burke et al. (2019) photopolymerized PEG dimethacrylate with a series of thiols under UV irradiation and found that PETMP formed hydrogels, whereas mercaptoacetate-based thiols did not copolymerize; incorporating PETMP also reduced the swelling ratio and stiffness relative to PEG dimethacrylate alone. These results indicate that thiol structure and functionality govern both network formation and the properties of the resulting hydrogel. UV photopolymerization is attractive for hydrogel preparation because it enables rapid network formation under comparatively mild conditions, and it allows functional comonomers to be incorporated to tailor the chemical environment of the network.

Introducing ionizable groups provides an additional means of tuning hydrogel–adsorbate interactions. Anionic functionalities such as carboxylate (–COO–) and sulfonate (–SO3–) groups are commonly incorporated into hydrogel networks to enhance the adsorption of cationic dyes through electrostatic attraction and ion-exchange interactions (Nasser, Thamer & Altaleb, 2025), and phosphorus-containing groups offer an alternative ionizable functionality (Nayl et al., 2026). Bis[2-(methacryloyloxy)ethyl] phosphate (BMEP) combines two polymerizable methacrylate groups with a phosphate moiety bearing an acidic P–OH group. BMEP was employed as a crosslinker in poly(vinylphosphonic acid) (PVPA) hydrogels developed for the adsorption of cationic MB, in which the acidic phosphorus-containing groups promoted interactions with MB, and the adsorption data followed pseudo-second-order kinetics and Langmuir-type behavior (Anil et al., 2020).

Previous work has thus examined, separately, PEG-based networks crosslinked with multifunctional thiols such as PETMP (Burke et al., 2019) and BMEP-containing phosphate-functional networks for MB adsorption (Anil et al., 2020). These systems differ in an important respect. In PVPA–BMEP hydrogels, BMEP crosslinks a polymer that already carries a high density of phosphonic acid groups, whereas in a PEG-based network, the ionizable phosphate functionality is introduced by BMEP into an otherwise non-ionic matrix. Whether BMEP-derived phosphate functionality can promote MB uptake within a UV-curable PEG–thiol network has not been addressed in the studies cited above.

Accordingly, the present study investigates a UV-photopolymerized poly(ethylene glycol) diacrylate (PEGDA)/PETMP/BMEP hydrogel as a functional adsorbent for the removal of MB from aqueous media. PEGDA serves as the PEG-based network-forming component, PETMP as a tetrafunctional thiol crosslinker, and BMEP as a reactive phosphate-containing comonomer. We hypothesized that the acidic P–OH groups of BMEP, which can ionize in aqueous media, would provide anionic sites for electrostatic interaction with MB^+. To compare the phosphate-containing formulation with a BMEP-free network, the BMEP-containing hydrogel was compared with a BMEP-free PEGDA/PETMP control that had the same PEGDA-to-solvent ratio and thiol:(meth)acrylate molar ratio and was prepared under the same processing and UV-curing conditions. Both hydrogels were characterized by Fourier-transform infrared (FTIR) spectroscopy, thermogravimetric analysis (TGA), and swelling measurements; dried Hfunc was also examined by scanning electron microscopy (SEM). MB removal was evaluated by monitoring the residual concentration by UV-Vis spectrophotometry as a function of contact time. This approach aims to establish a simple UV-curable phosphate-functional hydrogel platform

with potential relevance to colored aqueous streams associated with printing and related processes.

2. Methods

2.1. Materials

Poly(ethylene glycol) diacrylate (PEGDA, Mn ≈ 700 g mol^{-1}), pentaerythritol tetrakis(3-mercaptopropionate) (PETMP), bis[2-(methacryloyloxy)ethyl] phosphate (BMEP), and 2-hydroxy-2-methylpropiophenone (HMPP, photoinitiator) were used for hydrogel preparation. Methylene blue (MB) was used as a model cationic dye. Deionized water and ethanol were used as solvents. All reagents were purchased from Sigma-Aldrich and Merck.

2.2. Hydrogel preparation

Precursor solutions were prepared in water/ethanol (5:1, v/v) with the amounts given in Table 1. Deionized water and ethanol were mixed first, followed by PEGDA and BMEP (for the BMEP-containing formulation only), HMPP, and, finally, PETMP. The mixtures were homogenized, cast into the same Teflon mold, and irradiated with UV light for 5 min using a Luzchem Expo exposure panel equipped with six 8-W T5 LZC-UVA-367 lamps (λmax ≈ 367 nm) at a sample-to-lamp distance of 15 cm. After photopolymerization, the hydrogels were removed from the mold, washed thoroughly with deionized water to remove soluble residual species, and dried in an oven at 40 °C for 4 h. Specimens of similar geometry and dry mass were cut from the resulting hydrogels for the swelling and adsorption experiments. The BMEP-containing and the BMEP-free hydrogels are referred to as H_{func} and $H_{control}$, respectively.

Table 1

Composition of the precursor solutions of H_{func} and $H_{control}$

Component	$H_{control}$ (BMEP-free)	H_{func} (BMEP-containing)
PEGDA (g)	2.4	7.2
PETMP (g)	0.656	2.64
BMEP (g)	-	1.128
HMPP (g)	0.112	0.336
Deionized water (mL)	4	12
Ethanol (mL)	0.8	2.4

Both formulations have the same PEGDA-to-solvent ratio (0.5 g per mL of solvent) and the same HMPP content relative to PEGDA (4.7 wt%). The molar ratio of thiol to (meth)acrylate groups is also the same in both (0.78:1, calculated with PEGDA Mn = 700 g mol^{-1}, PETMP 488.66 g mol^{-1}, and BMEP 322.25 g mol^{-1}). BMEP corresponds to 10.3 wt% of the monomers (PEGDA, PETMP, and BMEP). The PETMP amount was increased in H_{func} to account for the additional methacrylate groups supplied by BMEP and maintain the same thiol:(meth)acrylate molar ratio. This does not establish an identical network architecture or crosslink density.

2.3. Characterization

FTIR spectra of the dried hydrogels were recorded on a Shimadzu IRSpirit-X series spectrometer in attenuated total reflection (ATR) mode over 4000–600 cm^{-1} and are presented as transmittance. The fracture surfaces of dried H_{func} were sputter-coated with a 3 nm Au/Pd layer and examined with a QUANTA 400F field emission scanning electron microscope using an ETD detector at 30 kV. Thermogravimetric analysis (TGA) of the hydrogels was performed using a PerkinElmer TGA 4000 (USA). Samples were heated from 30 °C to 750 °C at a heating rate of 40 °C min^{-1} under a nitrogen flow of 20 mL min^{-1}. The derivative thermogravimetry (DTG) curve is the instrument derivative of the thermogravimetric (TG) curve, smoothed with a Savitzky–Golay filter (cubic polynomial, 10.5 °C window). $T_{10\%}$ and $T_{50\%}$ are the temperatures at which the mass fell to 90% and 50% of the initial mass, and the residue was taken at 740 °C.

2.4. Swelling measurements

The swelling behavior was determined gravimetrically. Prior to the measurements, the hydrogels were dried in an oven at 40 °C for 4 h and weighed (Wd). Each specimen was placed in a separate beaker containing 20 mL of deionized water. After 15 min, 30 min, 60 min, 4 h, and 24 h, the specimen was removed, the surface water was gently blotted with filter paper, and the swollen specimen was weighed (Wt) and returned to the same water. The swelling ratio was calculated as:

$$SR\ (\%) = (W_t - W_d) / W_d \times 100 \quad (1)$$

One specimen of each hydrogel is reported in Table 2 ($H_{control}$, 0.6294 g dry; H_{func}, 0.63 g dry) without standard deviations; $H_{control}$ was not weighed at 4 h.

2.5. MB adsorption experiments

A dry hydrogel specimen (0.6291 g for H_{func} and 0.6253 g for $H_{control}$) was placed in 50 mL of a 10 mg L^{-1} MB solution at room temperature without stirring. The pH of the solution was neither measured nor adjusted. At 5, 10, 20, 30, 60, and 120 min and at 24 h, a 3–4 mL aliquot was withdrawn while the hydrogel remained in the beaker throughout the experiment, and its absorbance was measured; the aliquots were not returned to the beaker. Filtration or centrifugation was not used because the hydrogel material remained in the beaker during sampling. An adsorbent-free control containing the same 10 mg L^{-1} MB solution was maintained for 24 h under the same light, temperature, and agitation conditions as

the hydrogel-containing samples; both were kept without stirring. Its color and absorbance at 664 nm were compared with those of the initial solution. Absorbance was measured using a Thermo Scientific GENESYS 150 UV–Vis spectrophotometer with a 1 cm quartz cuvette.

The MB concentration was determined from the absorbance at 664 nm, using deionized water as the blank. The calibration curve was prepared from standard solutions of 2, 4, 6, 8, and 10 mg L^{-1}. The 8 and 10 mg L^{-1} standards were measured after five-fold dilution (1 mL of solution + 4 mL of deionized water), so the concentrations in the cuvette were 1.6 and 2.0 mg L^{-1}; the 10 mg L^{-1} solution was also measured without dilution (A = 2.225), which is exactly five times its diluted reading (A = 0.445). The absorbance was proportional to the concentration over 1.6–10 mg L^{-1} (Figure 1), and the calibration line was forced through the origin:

$$A = a\, C_{cuv} \quad (2)$$

with a = 0.219 L mg^{-1} and R^2 = 0.997. The MB concentration in a sample was calculated as:

$$C_t = DF\, A_t / a \quad (3)$$

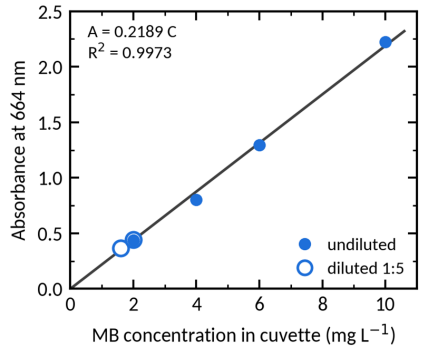
where A_t is the absorbance at 664 nm and DF is the dilution factor, $DF = (V_{sample} + V_{water}) / V_{sample}$; DF = 1 for undiluted samples and DF = 5 for 1 mL of sample + 4 mL of water. The initial concentration C0 was the value measured for the initial solution by the same procedure on the day of the experiment (10.2 mg L^{-1}, from the 10 mg L^{-1} solution measured without dilution; A = 2.225). MB removal and the amount adsorbed per gram of dry hydrogel (q_t) were calculated as:

$$R\,(\%) = (C_0 - C_t) / C_0 \times 100 \quad (4)$$

$$q_t = [C_0 V_0 - C_t V_t - \Sigma_{j<t}\, C_j V_{s,j}] / m_{gel} \quad (5)$$

$$V_t = V_0 - \Sigma_{j<t}\, V_{s,j} \quad (6)$$

where V_0 (L) is the solution volume when the hydrogel was added, $V_{s,j}$ (L) is the volume withdrawn at the j-th sampling, V_t (L) is the volume in the beaker before the t-th sampling, and m_{gel} (g) is the dry hydrogel mass. Because the withdrawn aliquots were not returned to the beaker, the MB removed with them is subtracted in Equation (5). R is a ratio of concentrations and does not depend on the withdrawn volume. Because individual aliquot volumes are specified only as a 3-4 mL range, the reported q_t values are approximate estimates based on 3.5 mL per aliquot. The removal percentages do not require this volume assumption.

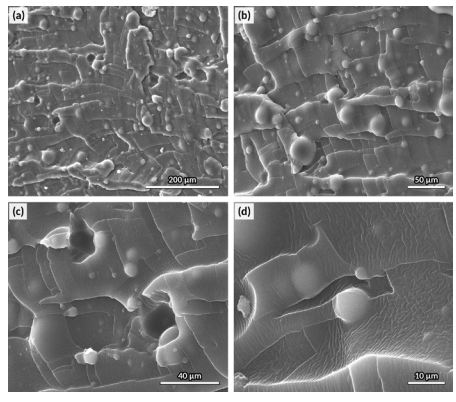


» **Figure 1:** *Calibration curve of MB at 664 nm. Open symbols: standards diluted 1:5 before measurement (8 and 10 mg L^{-1}); the 10 mg L^{-1} solution was also measured without dilution. Concentrations are those in the cuvette. Line: A = 0.219 C (R^2 = 0.997)*

3. Results

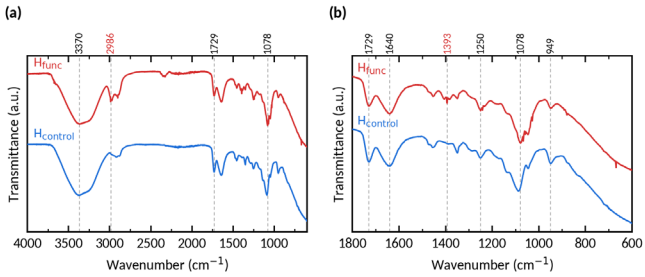
3.1. Morphology and chemical structure

SEM images of the fracture surface of the dried Hfunc at increasing magnification are shown in Figure 2. The surface is dense and continuous, with stepped fracture patterns consistent with fracture in a crosslinked network and scattered spherical features ranging from a few to a few tens of micrometers (Figure 2a,b). At higher magnification, cavities with smooth walls, spheres lying in or at the edge of the cavities, and a fine wrinkled texture on the fracture facets are visible (Figure 2c,d). No open, interconnected pores were observed in the dry state.



» **Figure 2:** *SEM images of the fracture surface of dried H_{func} at (a) 500×, (b) 1000×, (c) 2000×, and (d) 5000×*

The FTIR spectra of $H_{control}$ and H_{func} are shown in Figure 3. Both spectra were dominated by the bands of the PEGDA/PETMP network: a broad O–H stretching band cen-



» **Figure 3:** *FTIR spectra of $H_{control}$ and H_{func}: (a) 4000–600 cm⁻¹ and (b) 1800–600 cm⁻¹. The spectra are offset vertically for clarity*

tered at about 3370 cm⁻¹, C-H stretching bands between 3000 and 2850 cm⁻¹, the ester C=O stretching band at 1729 cm⁻¹, a band at 1640 cm⁻¹, ester C-O-C stretching near 1250 cm⁻¹ and an intense C-O-C stretching band of the PEG backbone at about 1085 cm⁻¹. Compared with $H_{control}$, the spectrum of H_{func} showed additional absorption near 2986 cm⁻¹, a distinct band at about 1393 cm⁻¹, a stronger band at 1250 cm⁻¹, and a broader and stronger C-O-C envelope whose maximum shifted from 1087 to 1078 cm⁻¹. The band at 1640 cm⁻¹ overlaps the bending vibration of water, and the S-H band of PETMP (about 2570 cm⁻¹) and the $=CH_2$ band of the acrylate groups (about 810 cm⁻¹) were not distinguishable from the baseline in either spectrum, so no conclusion on the conversion of the thiol and (meth)acrylate groups can be drawn. Phosphate-related vibrations may overlap the ester and ether bands in the fingerprint region, and ATR intensities depend on sample contact; the spectral differences are therefore treated as qualitative evidence rather than a quantitative measure of phosphate incorporation.

3.2. Thermal behavior

The TG and DTG curves of $H_{control}$ and H_{func} are presented in Figure 4. Both hydrogels exhibited only limited mass loss below 150 °C (1.6% for $H_{control}$ and 2.2% for H_{func}), followed by the principal degradation process at higher temperatures. H_{func} showed an earlier thermal degradation than the BMEP-free $H_{control}$, with T10% values of 337.3 and 375.1 °C and T50% values of 396.9 and 410.1 °C, respectively. The DTG minimum was less intense for H_{func} (−43.9 % min⁻¹) than for $H_{control}$ (−61.2 % min⁻¹), whereas the temperatures of maximum degradation rate were close (396 and 405 °C). The most pronounced difference between the two networks was observed at high temperature: H_{func} retained 7.12% of its initial mass at 740 °C, whereas $H_{control}$ left only 0.25% residue (Figure 4a, inset).

3.3. Swelling behavior

The swelling ratios of $H_{control}$ and H_{func} are given in Table 2 and Figure 5b (the swelling of H_{func} is illustrated by the photographs in Figure 5a). During the first hour, H_{func} showed substantially faster water uptake than $H_{control}$, reaching 34.9%, 44.4%, and 49.2% at 15, 30, and 60 min, respectively, compared with 3.6%, 4.5%, and 11.5% for $H_{control}$. H_{func} reached 54.0% at 4 h. After 24 h, the swelling ratios reached 65.1% for H_{func} and 55.5% for $H_{control}$. Thus, the largest difference between the formulations was observed during the early stage of hydration. These results are based on a single specimen of each hydrogel and should be confirmed by replicate measurements.

Table 2

Swelling ratio (%) of one specimen of each hydrogel in deionized water (20 mL per specimen); – = not measured

Specimen	W_d (g)	15 min	30 min	60 min	4h	24h
$H_{control}$	0.6294	3.6	4.5	11.5	-	55.5
H_{func}	0.63	34.9	44.4	49.2	54.0	65.1

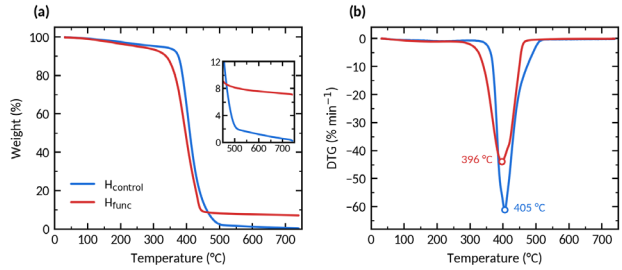
Table 3

Swelling ratio after 24 h in deionized water (one specimen of each hydrogel) and MB removal and estimated amount adsorbed (q) after 24 h. The q estimates assume 3.5 mL per withdrawn aliquot

Hydrogel	Swelling ratio at 24 h (%)	MB removal (%)	q at 24h (mg g⁻¹)
$H_{control}$	55.5	27.0	0.17
H_{func}	65.1	80.8	0.47

3.4. Methylene blue adsorption

Based on the calibration, MB removal by H_{func} increased from 13.3% at 5 min to 54.0% at 120 min and 80.8% at 24 h, whereas $H_{control}$ increased from 9.1% at 5 min to 16.5% at 120 min and 27.0% at 24 h (Figure 6b; Table 3). After correction for the decreasing solution volume and for MB removed in earlier aliquots, the estimated amounts adsorbed at 24 h, assuming 3.5 mL per withdrawn aliquot, were approximately 0.47 mg g⁻¹ for H_{func} and 0.17 mg g⁻¹ for $H_{control}$ (Figure 6c). After 24 h, the solution in contact with Hfunc was visibly lighter than that in contact with $H_{control}$, and the H_{func} hydrogel was intensely stained by the dye (Figure 6a). These values describe adsorption



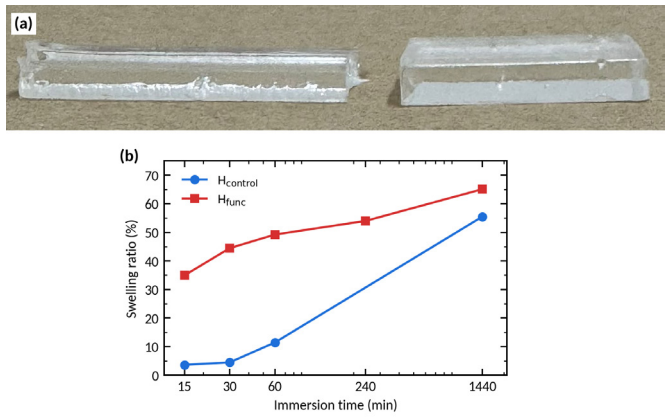
» **Figure 4:** *(a) TG and (b) DTG curves of $H_{control}$ and H_{func}; inset in (a): residue region.*

under the present experimental conditions and should not be interpreted as maximum adsorption capacities because only about 0.5 mg of MB was initially available in 50 mL of solution. All sample readings were within the 1.6–10 mg L^{-1} calibration range. The substantially greater MB removal observed for H_{func} relative to $H_{control}$ should be interpreted in light of the swelling behavior and the compositional differences between the two formulations. The adsorbent-free MB control showed no visible change in color, and its absorbance at 664 nm after 24 h under the same conditions was 2.198, compared with 2.225 for the initial solution (a decrease of about 1.2%); this change is much smaller than the decreases observed with the hydrogels, supporting the association of the concentration decrease with hydrogel presence; the removal values reported here were not corrected for it.

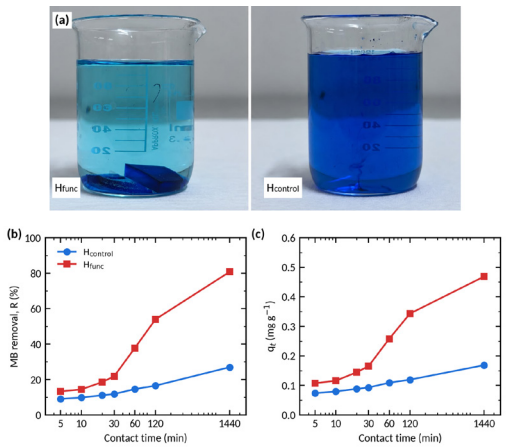
4. Discussion

The principal finding is the greater MB removal by the BMEP-containing formulation under the conditions examined: Hfunc removed 80.8% after 24 h, compared with 27.0% for $H_{control}$. The specimens were cut from hydrogels prepared in the same Teflon mold and had similar geometry and dry masses, reducing differences associated with initial specimen shape and adsorbent dose. The adsorbent-free MB control showed no visible color change, and its absorbance after 24 h was about 1.2% lower than the initial value, much smaller than the decreases observed with the hydrogels, supporting the association of the concentration decrease with the presence of hydrogels; the removal values were not corrected for this blank change. A possible contribution to the higher removal by H_{func} is electrostatic interaction between ionized BMEP-derived phosphate sites and cationic MB, as proposed for other phosphorus-containing hydrogels (Anil et al., 2020; Nayl et al., 2026). However, the pH and phosphate ionization were not determined, so the present results do not establish this mechanism. $H_{control}$ also showed MB uptake, indicating that phosphate functionality is not the sole possible contributor to dye retention in these networks.

The greater PETMP amount in Hfunc was required to maintain the same thiol:(meth)acrylate ratio after adding the methacrylate groups supplied by BMEP. Although this ratio and the PEGDA-to-solvent ratio were matched, the formulations differed in the PETMP-to-PEGDA mass ratio (0.37 versus 0.27 g g^{-1}) and total monomer content. Equal functional-group ratios do not establish equal crosslink densities or network structures (Cramer & Bowman, 2001). Consequently, the comparison demonstrates a formulation-level difference rather



» **Figure 5:** *(a) Photographs illustrating the swelling of Hfunc in a preliminary test: a dry piece (left; dried in an oven at 40 °C for 4 h) and a piece cut from the same specimen after 24 h in deionized water (right); (b) swelling ratios of $H_{control}$ and H_{func} (one specimen of each) in deionized water as a function of immersion time; lines connect the measured points*



» **Figure 6:** *(a) Photographs of the MB solutions after 24 h of contact with H_{func} (left) and $H_{control}$ (right) in a preliminary test (10 mg L^{-1} MB, ≈0.63 g of dry hydrogel); (b) MB removal and (c) estimated amount of MB adsorbed, q_t, by $H_{control}$ and H_{func} as a function of contact time (50 mL of 10 mg L^{-1} MB solution; 0.6253 g and 0.6291 g of dry hydrogel, respectively). The q_t values assume 3.5 mL per withdrawn aliquot*

than isolating the effect of phosphate groups. Burke et al. (2019) reported changes in swelling and stiffness upon incorporating PETMP into PEG dimethacrylate hydrogels, illustrating the relevance of thiol-containing network composition, although their system differs from the present PEGDA-based formulations.

H_{func} exhibited faster early hydration and a higher 24 h swelling ratio than $H_{control}$ (65.1% versus 55.5%). The swelling and removal values did not increase proportionally across the formulations, and no direct quantitative relationship can be inferred because swelling was measured in deionized water, and dye uptake in the MB solution. H_{func} continued to remove MB between 2 and 24 h, with MB removal increasing from 54.0% to 80.8%, despite substantial water uptake during the first hour in the separate swelling experiment. This is consistent with dye uptake extending beyond the early hydration period, without establishing a diffusion-controlled mechanism or an equilibrium endpoint.

The dense appearance of the dried H_{func} surface does not contradict its ability to absorb water. Dry-state SEM describes the observed fracture surface rather than the hydrated network, and neither SEM nor the bulk swelling ratio determines the wet-state mesh size or pore connectivity. The spherical features and cavities may reflect trapped air or heterogeneity formed during photopolymerization, but their origin cannot be resolved from these images. They should not be interpreted as evidence of an interconnected porous structure. Because SEM was performed only for H_{func}, the effect of formulation on morphology cannot be assessed by comparison with $H_{control}$.

The BMEP-containing formulation showed earlier thermal degradation and a greater residual mass at 740 °C. Related phosphate-containing UV-cured acrylate systems (Liang & Shi, 2004; Chen et al., 2008a; Chen et al., 2008b; Chen, Song & Hu, 2010) have shown degradation pathways involving phosphate decomposition and condensed-phase char formation (Liang & Shi, 2004; Chen et al., 2008a; Chen et al., 2008b). These coating systems offer a possible interpretation of the residual mass difference rather than evidence that the same mechanism occurred in the present hydrogels. Together, the FTIR and TGA results support physicochemical differences between the formulations, but do not independently establish covalent incorporation of BMEP, phosphorus content, or residue composition. TGA is used here as a complementary characterization method; high-temperature degradation behavior does not establish stability or resistance to leaching under aqueous adsorption conditions.

The removal percentages were obtained at an initial dry hydrogel dose of approximately 12.6 g L^{-1} and should be interpreted in that context. Only about 0.5 mg of MB was initially present, so the estimated 24 h uptake values of 0.47 and 0.17 mg g^{-1} do not represent maximum adsorption capacities. Repeated withdrawal of aliquots increased the hydrogel-to-solution ratio; the mass-balance calculation corrects for sampled dye and declining volume, while uncertainty in individual aliquot volumes limits the precision of qt. One adsorption time series and one swelling specimen per formulation are reported. Replicate measurements, controlled-pH experiments, and a range of initial concentrations are needed to distinguish chemical affinity from network effects and assess capacity. The printing-related relevance is therefore a motivation for future testing with actual wastewater and pigment-containing streams; the present experiments establish comparative removal of a model cationic dye in solution.

5. Conclusions

A UV-photopolymerized PEGDA/PETMP/BMEP hydrogel was prepared and evaluated for the removal of the model cationic dye methylene blue. With specimens of similar geometry and dry mass, H_{func} showed 80.8% removal after 24 h compared with 27.0% for the BMEP-free $H_{control}$; the adsorbent-free MB solution showed no visible change in color, and its absorbance decreased by only about 1.2% under the same conditions. H_{func} also showed faster initial hydration and a higher 24 h swelling ratio, while FTIR and TGA provided complementary evidence of physicochemical differences between the formulations. These findings support further study of UV-curable phosphate-containing networks for cationic-dye removal, while the specific role of phosphate groups, adsorption capacity, and performance in printing wastewater require further investigation.

6. References

Anil, I., Gunday, S.T., Bozkurt, A. and Alagha, O. (2020) 'Design of crosslinked hydrogels comprising poly(vinylphosphonic acid) and bis[2-(methacryloyloxy)ethyl] phosphate as an efficient adsorbent for wastewater dye removal', *Nanomaterials*, 10(1), 131. DOI: 10.3390/nano10010131

Burke, G., Cao, Z., Devine, D.M. and Major, I. (2019) 'Preparation of biodegradable polyethylene glycol dimethacrylate hydrogels via thiol-ene chemistry', *Polymers*, 11(8), 1339. DOI: 10.3390/polym11081339

Chen, X., Hu, Y., Song, L. and Xing, W. (2008a) 'Combustion and thermal behavior of polyurethane acrylate modified with a phosphorus monomer', *Journal of Fire Sciences*, 26(2), pp. 93–108. DOI: 10.1177/0734904107083863

Chen, X., Hu, Y., Song, L. and Xing, W. (2008b) 'Thermal properties and combustion behaviors of UV-cured phosphate triacrylate/star poly(urethane acrylate) oligomer blends', *Polymers for Advanced Technologies*, 19(5), pp. 393–398. DOI: 10.1002/pat.1022

Chen, X., Song, L. and Hu, Y. (2010) 'Flammability and thermal degradation of epoxy acrylate modified with phosphorus-containing compounds', *Journal of Applied Polymer Science*, 115(6), pp. 3332–3338. DOI: 10.1002/app.30477

Cramer, N.B. and Bowman, C.N. (2001) 'Kinetics of thiol–ene and thiol–acrylate photopolymerizations with real-time Fourier transform infrared', *Journal of Polymer Science Part A: Polymer Chemistry*, 39(19), pp. 3311–3319. DOI: 10.1002/pola.1314

Hoyle, C.E. and Bowman, C.N. (2010) 'Thiol–ene click chemistry', *Angewandte Chemie International Edition*, 49(9), pp. 1540–1573. DOI: 10.1002/anie.200903924

Kara, F., Birtane, H., Kandirmaz, E.A. and Cigil, A.B. (2026) 'A sustainable approach to ink colorant removal using modified cellulose from waste-paper', *Polymer Engineering & Science*, 66(6), pp. 4738–4752. DOI: 10.1002/pen.70537

Liang, H. and Shi, W. (2004) 'Thermal behaviour and degradation mechanism of phosphate di/triacrylate used for UV curable flame-retardant coatings', *Polymer Degradation and Stability*, 84(3), pp. 525–532. DOI: 10.1016/j.polymdegradstab.2003.11.006

Nasser, A.M., Thamer, B.M. and Altaleb, H.A. (2025) 'Chitosan-g-poly (styrene sulfonate) hydrogel with crosslinked polymeric for the efficient remediation of cationic dyeing wastewater', *Journal of King Saud University – Science*, 37(6), 7382025. DOI: 10.25259/JKSUS_738_2025

Nayl, A.A., Ahmed, I.M., Alsahli, S.A., Arafa, W.A.A., AlShammari, K.L., Gomha, S.M., Alanazi, M.D., Doma, A.S., AlHazmi, A.F.A., Bräse, S. and Abd-Elhamid, A.I. (2026) 'Highly selective removal of cationic dye using a novel synthesized polyacrylic polyacrylamide phosphate (PAA@PAm@P) hydrogel', *Scientific Reports*, 16(1), 19564. DOI: 10.1038/s41598-026-56160-x

Pereira, A.G.B., Rodrigues, F.H.A., Paulino, A.T., Martins, A.F. and Fajardo, A.R. (2021) 'Recent advances on composite hydrogels designed for the remediation of dye-contaminated water and wastewater: a review', *Journal of Cleaner Production*, 284, 124703. DOI: 10.1016/j.jclepro.2020.124703

Rafatullah, M., Sulaiman, O., Hashim, R. and Ahmad, A. (2010) 'Adsorption of methylene blue on low-cost adsorbents: a review', *Journal of Hazardous Materials*, 177(1–3), pp. 70–80. DOI: 10.1016/j.jhazmat.2009.12.047

Yang, Y., Zhu, Q., Peng, X., Sun, J., Li, C., Zhang, X., Zhang, H., Chen, J., Zhou, X., Zeng, H. and Zhang, Y. (2022) 'Hydrogels for the removal of the methylene blue dye from wastewater: a review', *Environmental Chemistry Letters*, 20(4), pp. 2665–2685. DOI: 10.1007/s10311-022-01414-z

© 2026 Authors. Published by the University of Novi Sad, Faculty of Technical Sciences, Department of Graphic Engineering and Design. This article is an open access article distributed under the terms and conditions of the Creative Commons Attribution license 4.0 Serbia (http://creativecommons.org/licenses/by/4.0/rs/).

Review Paper https://doi.org/10.24867/GRID-2026-p67

Adsorption of Pollutants from Complex Offset Printing Wastewaters: Mechanisms, Mass Transport and Kinetic Models

ABSTRACT

This paper presents an overview of the theoretical basis of liquid–solid adsorption, with an emphasis on physical and chemical adsorption, the main stages of mass transport and the most frequently applied kinetic models. Particular attention is paid to the limitations of interpreting kinetic data and to the distinction between mathematical fitting and the actual adsorption mechanism. The overview indicates that reliable interpretation of adsorption processes must consider both surface interactions and mass-transfer resistances in the boundary layer and in adsorbent pores. In the context of printing engineering, these theoretical considerations are particularly relevant for the treatment of offset printing effluents such as waste developer and waste fountain solution, where adsorption is used as a polishing step following electrocoagulation/flotation as the primary treatment stage.

KEY WORDS
Adsorption, mass transport, adsorption kinetics, offset printing effluents

Savka Adamović [1]
Rastko Milošević [1]
Aleksandra Mihailović [2]
Selena Samardžić Cvijanović [2]
Robert Lakatoš [2]

[1] University of Novi Sad, Faculty of Technical Sciences, Department of Graphic Engineering and Design, Novi Sad, Serbia
[2] University of Novi Sad, Faculty of Technical Sciences, Department of Fundamental Sciences, Novi Sad, Serbia

1. Introduction

Industrial development is inevitably accompanied by the generation of wastewaters of complex composition containing organic and inorganic pollutants of different origins and reactivities. The selection of an appropriate treatment method depends on the effluent composition, pollutant concentration, process requirements and economic constraints. Among the available treatment methods, adsorption occupies a prominent place because of its ease of implementation, chemical stability of adsorbents, high affinity towards dissolved substances and high removal efficiency at low pollutant concentrations (Deryło-Marczewska et al., 2010; Sen Gupta & Bhattacharyya, 2011). These characteristics make adsorption particularly suitable for polishing stages in complex printing wastewater treatment trains, where stringent discharge limits must be met despite variable effluent composition.

The importance of adsorption is especially pronounced in complex industrial wastewaters, where a high total organic load is accompanied by competitive effects of different dissolved species. In such systems, successful application of adsorption treatment depends not only on adsorption capacity, but also on the adsorption mechanism and process kinetics. Therefore, understanding mass transport and the proper interpretation of kinetic models are essential for the design and optimisation of adsorption systems and for minimising operating costs in industrial practice (Qiu et al., 2009; Ponnusami et al., 2010; Sen Gupta & Bhattacharyya, 2011).

Within the context of wastewater management in the printing industry, this issue is particularly important for offset printing effluents, since waste offset developer and waste fountain solution contain complex mixtures of dissolved organic substances and require carefully selected treatment sequences. Theoretical understanding of adsorption therefore has direct practical value for the design of combined electrocoagulation/flotation and adsorption treatment systems in printing practice.

2. Mechanisms of adsorption and mass transport

Adsorption is defined as a change in the concentration of a component at the interface between two phases, and in a liquid–solid system the adsorbate is transferred from the solution and bound to the surface of a solid adsorbent. Depending on the nature of the bonds established between the adsorbent and the adsorbate, two limiting forms of adsorption are distinguished: physical adsorption and chemical adsorption, which represent two extremes of a continuum of possible interaction mechanisms (Adamović, 2016).

Physical adsorption is based on van der Waals forces, London forces and dipole–dipole interactions, is generally reversible and occurs with lower adsorption enthalpies. In contrast, chemical adsorption involves stronger ionic, covalent, coordinate covalent or hydrogen bonds, is usually irreversible and is associated with higher adsorption enthalpies. Physical adsorption often results in multilayer adsorption, whereas chemical adsorption is usually associated with monolayer formation at active sites on the adsorbent surface (Tričković, 2009; Kostić, 2014).

In real systems, physical and chemical adsorption need not be strictly separated and may occur simultaneously or successively. Therefore, the adsorption mechanism cannot be interpreted solely on the basis of assumed bond type, but must be linked to process kinetics and transport limitations within the system (Qiu et al., 2009; Sen Gupta & Bhattacharyya, 2011).

Mass transport of dissolved adsorbate species from the bulk solution to the active sites of the adsorbent is an integral part of every adsorption process. When the adsorbent is porous, the transport mechanism may be described through four stages: bulk diffusion through the solution, film diffusion through the hydrodynamic boundary layer, intraparticle diffusion through the pores of the adsorbent and, finally, adsorption by binding of adsorbate molecules to active sites inside the pores (Kuo et al., 2008; Wang et al., 2008; Doğan et al., 2009; Çeçen & Aktaş, 2011).

Some authors describe liquid–solid adsorption through three basic steps: transport of the adsorbate from the liquid phase to the external surface of the adsorbent, transport through the liquid film attached to the adsorbent surface and interaction of the adsorbate with active sites on the adsorbent surface leading to physical or chemical adsorption (Hameed & El-Khaiary, 2008; Plazinski et al., 2009; Valderrama et al., 2010; Sen Gupta & Bhattacharyya, 2011). Regardless of whether a three-step or four-step representation is used, the essential point remains the same: the slowest step determines the overall process rate.

If the slowest step is transport through the solution or the boundary layer, adsorption can be regarded as transport-controlled. When intraparticle diffusion is the slowest step, pore structure and particle size become decisive factors. Only when the interaction of the adsorbate with active sites is the slowest stage can adsorption be considered chemically controlled. Transport-controlled adsorption is more common at low mixing intensity and low adsorbate concentration, whereas under intensive mixing, higher adsorbate concentration and with porous adsorbents of small particle size, intraparticle diffusion may become dominant (Wang et al., 2008; Plazinski et al., 2009; Ahmaruzzaman, 2010; Sen Gupta & Bhattacharyya, 2011).

For offset printing effluents, such distinctions are important because the composition of treated developer or fountain solution may include a broad spectrum of organic compounds with different diffusivities and affinities for activated carbon or carbon nanomaterials. Consequently, the same adsorbent may exhibit different apparent kinetic behaviour depending on the wastewater matrix and pretreatment stage. As a result, appropriate kinetic modelling becomes essential for quantifying mass-transport limitations and identifying the dominant adsorption mechanism in such complex systems.

3. Adsorption kinetic models

In the design of adsorption treatment, the most important parameters for characterizing adsorbents are adsorption capacity and adsorption kinetics. Kinetic analysis provides information on the rate of attainment of equilibrium, the possible adsorption mechanism, the transition states within the system and the suitability of a given adsorbent for technological and environmental applications, including printing wastewater treatment (Deryło-Marczewska et al., 2010; Sen Gupta & Bhattacharyya, 2011). Mathematical models used for the analysis of adsorption data may generally be divided into reaction models and diffusion models. Reaction models describe the change of adsorption capacity with time without explicit consideration of mass transport, whereas diffusion models attempt to represent the

actual course of adsorption through film diffusion, intraparticle diffusion and mass transfer to active sites in the adsorbent (Qiu et al., 2009; Ponnusami et al., 2010).

3.1. Lagergren's pseudo-first-order model

Lagergren's pseudo-first-order model is among the oldest and most frequently used models for the description of adsorption kinetics in liquid–solid systems. It assumes that the adsorption rate is proportional to the difference between the equilibrium adsorption capacity and the capacity at a given time (Wang et al., 2008; Qiu et al., 2009).

The applicability of this model strongly depends on the reliable determination of the equilibrium adsorption capacity. In practice, the pseudo-first-order model is often suitable only for the initial period of adsorption, whereas at longer contact times significant deviations may appear between experimental and theoretically calculated values. Therefore, its interpretation must be approached with caution, especially when the aim is to infer the nature of the adsorption mechanism from mathematical fitting alone (Aly et al., 2014).

3.2. Pseudo-second-order model

The pseudo-second-order model assumes that the adsorption rate depends on the number of unoccupied active sites and is frequently associated with chemical interaction between the adsorbate and the adsorbent. In a large number of adsorption systems, this model shows very good agreement with experimental data, especially for the adsorption of organic and inorganic pollutants on carbonaceous adsorbents (Hameed, 2008; Sen Gupta & Bhattacharyya, 2011; Aly & Luca, 2013; Plazinski, 2013).

However, good agreement with the pseudo-second-order model does not necessarily mean that the process is exclusively chemically controlled. The literature indicates that the same model may also be successfully applied to systems where physical adsorption and diffusion resistances play an important role. Therefore, the pseudo-second-order model may be regarded as a useful mathematical description of adsorption kinetics, but not as sufficient proof for the unequivocal definition of the adsorption mechanism (Plazinski et al., 2009; Qiu et al., 2009).

3.3. Elovich model

The Elovich model was developed for chemisorption processes on energetically heterogeneous surfaces. Its basic assumption is that the adsorption rate decreases exponentially with the increasing amount adsorbed, while desorption and interactions between adsorbed species do not have a dominant effect at low surface coverage (Plazinski et al., 2009; Sen Gupta & Bhattacharyya, 2011).

This model is applied to describe the adsorption of various pollutants, including phosphates, cadmium, chromium, copper, phenols, and nitroaromatic compounds. Its advantage lies in accounting for the energetic heterogeneity of the adsorbent surface, but even good agreement with the Elovich model is not sufficient for an independent interpretation of the overall adsorption mechanism without complementary mass-transfer analysis (Qiu et al., 2009; Shen et al., 2009; Sheng et al., 2010).

3.4. Diffusion models

Unlike reaction models, diffusion models aim to describe the actual course of adsorption through successive mass-transport steps. In practice, the Weber–Morris intraparticle diffusion model and the Dumwald–Wagner model are most commonly used. The Weber–Morris model is based on the dependence of the adsorbed amount on the square root of time and is used to estimate the contribution of intraparticle diffusion to the overall adsorption kinetics. If the linear portion of the plot passes through the origin, intraparticle diffusion may be considered the sole rate-controlling step over the corresponding adsorption stage. Deviation from the origin indicates the presence of additional resistances, most often film diffusion (Alkan et al., 2007; Hameed, 2008; Doğan et al., 2009; Valderrama et al., 2010).

The Dumwald–Wagner model is also used to analyse internal diffusion and to assess whether intraparticle transport is the determining step of the adsorption process. The advantage of diffusion models is that they offer a more realistic insight into the adsorption pathway than reaction models, especially in systems with porous adsorbents and pronounced transport resistances. Therefore, their use should be an integral part of any serious kinetic analysis of adsorption systems (Cheng et al., 2008; Qiu et al., 2009; Hai et al., 2012; Tang et al., 2012).

A practical implication for wastewater treatment in the printing industry is that reactor design based only on pseudo-second-order fitting may lead to suboptimal contact times and adsorbent doses. For real offset printing effluents, diffusion analysis is needed in order to distinguish between surface interaction effects and matrix-dependent transport limitations and to avoid misleading mechanistic conclusions based solely on reaction-model fitting.

4. Discussion

The literature overview shows that pseudo-first-order and pseudo-second-order models are very frequently used in adsorption studies, whereas diffusion models are

usually applied as complementary tools for mechanism interpretation. However, reaction models alone cannot represent the real adsorption pathway because they do not explicitly include mass transport stages. As a result, they often provide a good mathematical fit to experimental data, but without sufficient basis for an unambiguous conclusion about the dominant mechanism of the process (Qiu et al., 2009; Ponnusami et al., 2010).

Proper interpretation of adsorption kinetics requires simultaneous consideration of the properties of the adsorbent and adsorbate, mixing conditions, adsorbate concentration, particle size and porosity of the adsorbent, as well as the results obtained from both reaction and diffusion models. Only such an approach allows a more reliable distinction between transport-controlled and chemically controlled adsorption. In this sense, kinetic analysis should not be regarded as a formal approximation of experimental data, but rather as an important tool for the rational design of adsorption treatments for complex industrial wastewaters (Ahmaruzzaman, 2010; Sen Gupta & Bhattacharyya, 2011).

The relevance of this theoretical framework lies in its direct applicability to the optimisation of wastewater treatment in offset printing production systems. Adsorption can serve as a polishing stage after electrocoagulation/flotation treatment of offset printing effluents, while the correct interpretation of kinetic models helps prevent oversimplified conclusions during process scale-up and practical implementation.

5. Conclusion

Adsorption is an efficient and flexible method for the removal of organic matter from complex industrial wastewaters. The apparent adsorption rate and the observed kinetic behaviour are determined by the combined influence of adsorbate–adsorbent surface interactions and mass-transfer resistances, with the slowest stage controlling the overall process kinetics. Lagergren's pseudo-first-order model, the pseudo-second-order model and the Elovich model are useful for the mathematical description of kinetics, whereas diffusion models allow a more realistic assessment of the adsorption pathway and identification of the dominant transport limitations. Therefore, reliable interpretation of adsorption mechanisms can only be achieved through the combined use of reaction and diffusion models together with critical consideration of the experimental conditions (Qiu et al., 2009; Sen Gupta & Bhattacharyya, 2011).

In addition, for wastewater streams generated in offset printing, the combination of adsorption theory with application-specific knowledge can support the development of more efficient and better-supported treatment strategies for waste offset developer and waste fountain solution in combined electrocoagulation/flotation–adsorption treatment trains. The conceptual framework discussed in this paper is also relevant for the treatment of effluents from other printing techniques and, more broadly, for adsorption-based polishing stages in wastewater management across the printing industry.

6. Acknowledgments

This research has been supported by the Ministry of Science, Technological Development and Innovation (Contract No. 451-03-34/2026-03/200156) and the Faculty of Technical Sciences, University of Novi Sad through project "Scientific and Artistic Research Work of Researchers in Teaching and Associate Positions at the Faculty of Technical Sciences, University of Novi Sad 2026" (No. 01-3609/1).

7. References

Adamović, S. (2016) *Elektrokoagulacioni i adsorpcioni tretmani efluenata u grafičkim procesima ofset štampe*. PhD thesis. University of Novi Sad, Faculty of Technical Sciences.

Ahmaruzzaman, M. (2010) 'A review on the utilization of fly ash', *Progress in Energy and Combustion Science*, 36(3), pp. 327–363. DOI: 10.1016/j.pecs.2009.11.003

Alkan, M., Demirbaş, Ö. and Doğan, M. (2007) 'Adsorption kinetics and thermodynamics of an anionic dye onto sepiolite', *Microporous and Mesoporous Materials*, 101(3), pp. 388–396. DOI: 10.1016/j.micromeso.2006.12.007

Aly, Z. and Luca, V. (2013) 'Uranium extraction from aqueous solution using dried and pyrolyzed tea and coffee wastes', *Journal of Radioanalytical and Nuclear Chemistry*, 295(2), pp. 889–900. DOI: 10.1007/s10967-012-1851-6

Aly, Z., Graulet, A., Scales, N. and Hanley, T. (2014) 'Removal of aluminium from aqueous solutions using PAN-based adsorbents: characterisation, kinetics, equilibrium and thermodynamic studies', *Environmental Science and Pollution Research*, 21(6), pp. 3972–3986. DOI: 10.1007/s11356-013-2305-6

Çeçen, F. and Aktaş, Ö. (2011) *Activated Carbon for Water and Wastewater Treatment: Integration of Adsorption and Biological Treatment*. Weinheim: Wiley-VCH.

Cheng, W., Wang, S.G., Lu, L., Gong, W.X., Liu, X.W., Gao, B.Y. and Zhang, H.Y. (2008) 'Removal of malachite green (MG) from aqueous solutions by native and heat-treated anaerobic granular sludge', *Biochemical Engineering Journal*, 39(3), pp. 538–546. DOI: 10.1016/j.bej.2007.10.016

Deryło-Marczewska, A., Marczewski, A.W., Winter, S. and Sternik, D. (2010) 'Studies of adsorption equilibria and kinetics in the systems: Aqueous solution of dyes–mesoporous carbons', *Applied Surface Science*, 256(17), pp. 5164–5170. DOI: 10.1016/j.apsusc.2009.12.085

Doğan, M., Abak, H. and Alkan, M. (2009) 'Adsorption of methylene blue onto hazelnut shell: Kinetics, mechanism and activation parameters', *Journal of Hazardous Materials*, 164(1), pp. 172–181. DOI: 10.1016/j.jhazmat.2008.07.155

Hameed, B.H. (2008) 'Equilibrium and kinetic studies of methyl violet sorption by agricultural waste', *Journal of Hazardous Materials*, 154(1–3), pp. 204–212. DOI: 10.1016/j.jhazmat.2007.10.010

Hameed, B.H. and El-Khaiary, M.I. (2008) 'Sorption kinetics and isotherm studies of a cationic dye using agricultural waste: Broad bean peels', *Journal of Hazardous Materials*, 154(1–3), pp. 639–648. DOI: 10.1016/j.jhazmat.2007.10.081

Hai, T., Gui-Zhong, L., You-Bin, Y. and Jian-Long, G. (2012) 'Enhancement of removal of organic pollutants from coking wastewater through adsorption by modified coal fly ash', *Environment Protection Engineering*, 38(3), pp. 79–95. DOI: 10.5277/EPE120308

Kostić, M.M. (2014) *Sinteza i karakterizacija ksantovanih biosorbenata i njihova primena za uklanjanje katjonskih polutanata iz vodenih rastvora*. PhD thesis. University of Niš, Faculty of Sciences and Mathematics.

Kuo, C.Y., Wu, C.H. and Wu, J.Y. (2008) 'Adsorption of direct dyes from aqueous solutions by carbon nanotubes: Determination of equilibrium, kinetics and thermodynamics parameters', *Journal of Colloid and Interface Science*, 327(2), pp. 308–315. DOI: 10.1016/j.jcis.2008.08.038

Plazinski, W. (2013) 'Binding of heavy metals by algal biosorbents: Theoretical models of kinetics, equilibria and thermodynamics', *Advances in Colloid and Interface Science*, 197–198, pp. 58–67. DOI: 10.1016/j.cis.2013.04.002

Plazinski, W., Rudzinski, W. and Plazinska, A. (2009) 'Theoretical models of sorption kinetics including a surface reaction mechanism: A review', *Advances in Colloid and Interface Science*, 152(1–2), pp. 2–13. DOI: 10.1016/j.cis.2009.07.009

Ponnusami, V., Rajan, K.S. and Srivastava, S.N. (2010) 'Application of film-pore diffusion model for methylene blue adsorption onto plant leaf powders', *Chemical Engineering Journal*, 163(3), pp. 236–242. DOI: 10.1016/j.cej.2010.07.052

Qiu, H., Lv, L., Pan, B.C., Zhang, Q.J., Zhang, W.M. and Zhang, Q.X. (2009) 'Critical review in adsorption kinetic models', *Journal of Zhejiang University – Science A*, 10(5), pp. 716–724. DOI: 10.1631/jzus.A0820524

Sen Gupta, S. and Bhattacharyya, K.G. (2011) 'Kinetics of adsorption of metal ions on inorganic materials: A review', *Advances in Colloid and Interface Science*, 162(1–2), pp. 39–58. DOI: 10.1016/j.cis.2010.12.004

Shen, X.E., Shan, X.Q., Dong, D.M., Hua, X.Y. and Owens, G. (2009) 'Kinetics and thermodynamics of sorption of nitroaromatic compounds to as-grown and oxidized multiwalled carbon nanotubes', *Journal of Colloid and Interface Science*, 330(1), pp. 1–8. DOI: 10.1016/j.jcis.2008.10.023

Sheng, G.D., Shao, D.D., Ren, X.M., Wang, X.Q., Li, J.X., Chen, Y.X. and Wang, X.K. (2010) 'Kinetics and thermodynamics of adsorption of ionizable aromatic compounds from aqueous solutions by as-prepared and oxidized multiwalled carbon nanotubes', *Journal of Hazardous Materials*, 178(1–3), pp. 505–516. DOI: 10.1016/j.jhazmat.2010.01.110

Tang, B., Lin, Y., Yu, P. and Luo, Y. (2012) 'Study of aniline/ε-caprolactam mixture adsorption from aqueous solution onto granular activated carbon: Kinetics and equilibrium', *Chemical Engineering Journal*, 187, pp. 69–78. DOI: 10.1016/j.cej.2012.01.088

Tričković, J. (2009) *Primena sorpcionih parametara odabranih hidrofobnih organskih polutanata na organskoj materiji sedimenta za procenu njihove dostupnosti u sistemima sediment–voda*. PhD thesis. University of Novi Sad, Faculty of Sciences.

Valderrama, C., Barrios, J.I., Caetano, M., Farran, A. and Cortina, J.L. (2010) 'Kinetic evaluation of phenol/aniline mixtures adsorption from aqueous solutions onto activated carbon and hypercrosslinked polymeric resin (MN200)', *Reactive and Functional Polymers*, 70(3), pp. 142–150. DOI: 10.1016/j.reactfunctpolym.2009.11.003

Wang, X.S., Zhou, Y.Z., Jiang, Y. and Sun, C. (2008) 'The removal of basic dyes from aqueous solutions using agricultural by-products', *Journal of Hazardous Materials*, 157(2–3), pp. 374–385. DOI: 10.1016/j.jhazmat.2008.01.004

© 2026 Authors. Published by the University of Novi Sad, Faculty of Technical Sciences, Department of Graphic Engineering and Design. This article is an open access article distributed under the terms and conditions of the Creative Commons Attribution license 4.0 Serbia (http://creativecommons.org/licenses/by/4.0/rs/).

Original Scientific Paper https://doi.org/10.24867/GRID-2026-p68

Photo-Assisted Green Synthesis with LED(590nm) of Silver Nanoparticles and Evaluation of Their Antibacterial Activity in Specific Water Based Coatings

ABSTRACT

This study investigates a light-driven green synthesis strategy with light emitting diodes at 590 nm for the production of silver nanoparticles using Mentha spicata extract as a bioactive reducing and capping agent. Unlike conventional sunlight-assisted approaches, a controlled LED irradiation system was employed to promote nanoparticle formation under reproducible conditions. The influence of the plant-derived compounds on the nucleation and stabilization of silver nanoparticles was evaluated through UV–Vis spectroscopy and Transmission Electron Microscopy (TEM). The obtained silver nanoparticles were subsequently incorporated into a specific water-based varnish matrix designed for paperboard packaging coating applications. The antimicrobial performance of the developed nanocomposite coatings was assessed against Escherichia coli K12 and Bacillus subtilis 3562, demonstrating effective antibacterial activity after nanoparticle incorporation. The results highlight the potential of LED-assisted biosynthesis as a controllable and sustainable route for the preparation of silver nanoparticle-based coatings with antimicrobial functionality, offering promising perspectives for advanced packaging applications in the food and pharmaceutical sectors.

KEY WORDS
LED (590nm) photo-assisted green synthesis of silver nanoparticles, silver nanoparticles coatings, antibacterial coatings, packaging

Iskren Spiridonov [1]
Katya Pashova [2]
Rumyana Boeva [1]
Nevena Lazarova-Zdravkova [3]

[1] University of Chemical Technology and Metallurgy, Department of Pulp, Paper and Printing Arts, Sofia, Bulgaria
[2] University of Chemical Technology and Metallurgy, Department of Chemical Engineering, Sofia, Bulgaria
[3] University of Chemical Technology and Metallurgy, Department of Biotechnology, Sofia, Bulgaria

1. Introduction

Among the most extensively studied nanomaterials are silver nanoparticles (AgNPs), which have attracted considerable attention because of their diverse physicochemical and biological characteristics. In particular, AgNPs exhibit notable antimicrobial and antioxidant activity, as well as distinctive electrical and optical properties, making them valuable for a wide range of technological and biomedical applications.

In recent years, increasing attention has been directed toward environmentally sustainable approaches for the synthesis of AgNPs. Green synthesis methods have emerged as promising alternatives to conventional chemical and physical techniques because they can reduce the use of hazardous reagents and energy-intensive processes. Depending on the biological source and reaction conditions, these approaches can facilitate the formation of nanoparticles with controlled physicochemical characteristics, good colloidal stability, and significant biological activity. Consequently, green-synthesized AgNPs have become an important area of research for applications where both nanoparticle performance and environmental compatibility are important considerations (Fahim et al., 2024; Zehra et al., 2025).

A considerable number of recent studies have focused on biological approaches for the synthesis of nanoparticles, primarily because these methods offer an environmentally sustainable alternative to conventional synthesis techniques. Although traditional physical and chemical

approaches can provide effective nanoparticle production, they may require substantial energy and material inputs and can involve chemical reagents with potential environmental and toxicological concerns. These limitations have contributed to the increasing interest in greener and more sustainable synthesis strategies. Plant-derived extracts represent one of the most widely investigated biological systems for the synthesis of silver nanoparticles (AgNPs). Extracts obtained from different plant parts, including leaves, stems, bark, flowers, fruits, roots, and seeds, contain a diverse range of biologically active compounds. These include polyphenols, flavonoids, alkaloids, quinones, terpenoids, enzymes, essential oils, and other secondary metabolites. Such phytochemicals can participate in the reduction of silver ions (Ag^{+}) to elemental silver (Ag^{0}) and can also contribute to the stabilization of the newly formed nanoparticles. The adsorption of these compounds onto the nanoparticle surface can reduce particle aggregation and consequently improve the stability of the resulting colloidal system. Numerous plant species have been investigated as biological sources for the production of AgNPs, with successful examples including Aloe vera (Anju et al., 2021), Lawsonia inermis (Alhomaidi et al., 2022), and Magnolia alba (De Mel et al., 2025). These studies demonstrate the potential of plant-mediated synthesis as an environmentally compatible approach for producing silver nanoparticles while utilizing naturally occurring compounds as reducing and stabilizing agents. Nevertheless, the properties of the synthesized AgNPs can vary considerably depending on the plant species, the composition and concentration of the extract, and the specific physicochemical conditions employed during synthesis.

In recent years, increasing scientific attention has been directed toward the use of LED-assisted green photochemical synthesis as an external physical factor for regulating the formation of silver nanoparticles (Anjum et al., 2022). LED sources offer several advantages, including relatively low energy consumption, precise control over the emitted wavelength, and broad technological accessibility. The application of LED irradiation can influence the kinetics of nanoparticle formation and may also affect important physicochemical characteristics, such as particle size and morphology, as well as their resulting functional properties. The selection of an appropriate wavelength or spectral range can therefore provide an additional means of controlling the synthesis process and tailoring the properties of the obtained AgNPs. Previous studies have demonstrated that light-assisted synthesis can contribute to the production of silver nanostructures with enhanced catalytic and antimicrobial performance (Anh et al., 2020; Gurung et al., 2024; Mai-Ngoc et al., 2025).

Coatings are applied to printed products and packaging to enhance their optical, physical, mechanical, barrier and antibacterial properties (Bozhkova et al., 2015; Bozhkova et al., 2017; Spiridonov et al., 2024). In the present study, a single type of water-based coating was selected. This coating is formulated for in-line application on printing presses using anilox cylinders with different transfer volumes, selected according to the specific processing conditions, substrate characteristics, and quality requirements. The experimental work aimed to enhance the antibacterial performance of the coating while also improving its optical, mechanical and barrier properties.

2. Methods

2.1. Silver Nanoparticles Synthesis and incorporation in water-based coating

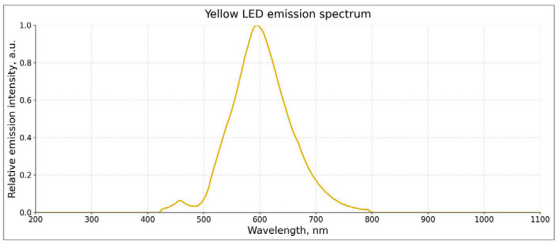
Aqueous extracts of Mentha spicata were prepared by mixing 5 g of dried plant material with 200 mL of distilled water. The suspension was placed on a heated magnetic stirrer and maintained at 500 rpm. When the temperature of the mixture reached approximately 70 °C, stirring was continued for a further 10 min to facilitate the extraction of water-soluble phytochemicals. The resulting extract was subsequently allowed to cool to room temperature and was clarified by vacuum filtration. Silver nitrate solutions with accurately defined concentrations were prepared by dissolving $AgNO_3$ (purity >99.8%, Sigma-Aldrich) in distilled water. The solutions were mixed vigorously at room temperature using a magnetic stirrer (Boeco MMS-3000, Germany). The concentrations used for the four $AgNO_3$ samples are presented in Table 1.

For the nanoparticle synthesis, 500 µL of the prepared Mentha spicata extract was introduced dropwise into 20 mL of the respective aqueous $AgNO_3$ solution under continuous vigorous stirring. The photo of light-emitting-diode-assisted configuration for silver nanoparticle synthesis is shown on Figure 1.

Figure 2 shows the relative emission intensity of used in this experiment yellow light emitting diodes with peak



» **Figure 1:** *Light-emitting-diode assisted configuration for silver nanoparticle synthesis*



» **Figure 2:** *Relative emission intensity of used in this experiment yellow light emitting diodes*

at 590nm. The reaction mixture was simultaneously irradiated with yellow LED light, and stirring was maintained for 3 min. Following synthesis, the silver nanoparticles were evaluated using a UV–Vis spectrophotometer (T60, PG Instruments Ltd., U.K.).

The AgNP dispersions obtained from all four $AgNO_3$ concentrations were subsequently incorporated into DRUCKFARBEN NAB109L0000Fvarnish at a concentration of 30% (v/v). For each formulation, the final mixture volume was adjusted to 40 mL. Following the addition of the nanoparticle dispersion, each formulation was thoroughly homogenized under continuous stirring to ensure uniform distribution of the AgNPs throughout the varnish matrix.

Table 1
$AgNO_3$ concentration

Name	$AgNO_3$ concentration, (mmol/L)
Sample 1	5
Sample 2	7
Sample 3	10
Sample 4	20

2.2. Antibacterial experiments

The antibacterial activity of the samples was assessed using the agar disc diffusion method against facultatively anaerobic Gram-negative *Escherichia coli* K12 NBIMCC 407 and aerobic Gram-positive *Bacillus subtilis* NBIMCC 3562. Both strains were obtained from the Bulgarian National Bank of Industrial Microorganisms and Cell Culture. Liquid and solid cultivation media were prepared using Luria–Bertani (LB) medium for *E. coli* and Nutrient Broth (NB) and Nutrient Agar (NA) for *B. subtilis*. All media were supplied by HiMedia Laboratories. The strains were cultivated, subcultured, and maintained on their respective media, with stock cultures stored at 4 °C. Culture incubation was performed in an ES-20/60 shaker.

For each experiment, a single colony of each strain was inoculated into 50 mL of the corresponding broth: LB for *E. coli* K12 and NB for *B. subtilis* NBIMCC 3562. The cultures were incubated for 24 h at 37 °C and 30 °C, respectively, with agitation at 220 rpm. Subsequently, 100 µL aliquots of bacterial suspensions adjusted to a turbidity of 0.5 McFarland, corresponding to approximately 1.5×10^8 CFU/mL, were distributed uniformly over the surfaces of the respective agar plates. Sterile filter paper discs supplied by HiMedia Laboratories, each measuring 6 mm in diameter, were impregnated with 6 µL of the test sample and placed on the agar surface.

Varnish formulations containing different concentrations of silver nanoparticles were examined to determine the antibacterial activity of the resulting nanocomposites. Varnish without silver nanoparticles served as a matrix control, allowing assessment of the intrinsic antibacterial activity of the varnish itself. A disc impregnated with an equivalent volume of distilled water was included as a negative control. The formation of a clear zone of inhibited bacterial growth surrounding a disc was interpreted as evidence of antibacterial activity.

Following overnight incubation at the temperature appropriate for each strain, inhibition zone diameters were measured from edge to edge through the centre of the disc in accordance with the Kirby–Bauer Disk Diffusion Susceptibility Test Protocol (Hudzicki, 2009). All experiments were conducted in triplicate, and mean inhibition zone diameters were calculated.

3. Results

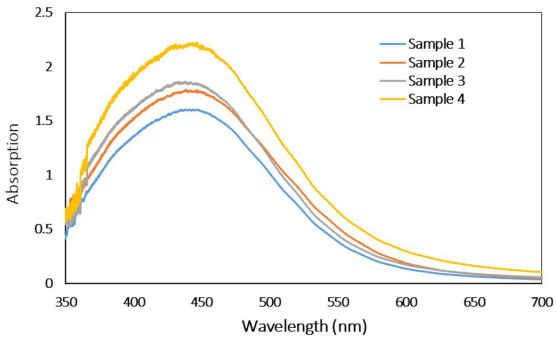
Following the addition of the Mentha spicata extract to the aqueous $AgNO_3$ solutions, the reaction mixtures were subjected to continuous yellow LED irradiation for 3 min under vigorous stirring. The formation of silver nanoparticles was accompanied by a visible change in the appearance of the reaction mixtures, indicating the reduction of Ag^+ ions and the formation of metallic silver nanoparticles. The synthesized AgNPs were subsequently characterized by UV–Vis spectroscopy, and the corresponding absorption spectra are presented in Figure 3. A clear dependence of the absorption intensity on the initial $AgNO_3$ concentration was observed. In general, increasing the concentration of silver nitrate resulted in a higher UV–Vis absorbance, which can be associated with a greater amount of silver nanoparticles formed in the reaction medium. The observed peaks, with maxima in interval of 443-447 nm, correspond to the characteristic surface plasmon resonance of spherical silver nanoparticles.

Several samples were prepared by incorporating different volumes of the AgNP suspension into the paper varnish, according to Table 1. The antibacterial activity was evaluated against B. subtilis 3562 and E. coli K12 using the disk diffusion method. No inhibition zones were observed for the varnish samples without silver nanoparticles or for the negative control. The antibacterial activity of the varnish formulations (Figure 4)

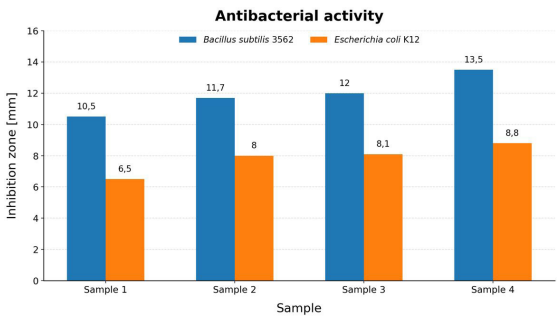
increased with increasing volume of the AgNP suspension incorporated into the varnish, with B. subtilis 3562 exhibiting greater susceptibility than E. coli K12, consistent with our previous findings (Spiridonov et al., 2024).

Differences in susceptibility between Gram-positive and Gram-negative bacteria may be related to differences in cell envelope structure and composition. In particular, the outer membrane of Gram-negative bacteria, containing lipopolysaccharides, represents an additional permeability barrier that can influence interactions with antimicrobial agents (Delcour, 2009; Silhavy et al., 2010; Sun et al., 2022).

The higher susceptibility of B. subtilis 3562 observed in the present study is also consistent with the assay-dependent differences reported for AgNPs by Kim et al. (2011), who showed that the relative responses of E. coli and B. subtilis varied depending on the experimental method. In addition, Hsueh et al. (2015) demonstrated that Ag^+ ions released from AgNPs play an important role in their antibacterial activity against B. subtilis. Based on these findings, the enhanced inhibition observed for B. subtilis 3562 may be related to differences in bacterial cell envelope characteristics and susceptibility to AgNP-mediated



» **Figure 2:** *UV-Vis spectra of silver nanoparticles synthesized with 5, 7, 10, 20 mmol/l aqueous solution of silver nitrate and extract from Mentha spicata for 3 minutes under direct sunlight*



» **Figure 3:** *Antibacterial activity of silver nanoparticle-containing varnish formulations against B. subtilis 3562 and E. coli K12, determined by the disk diffusion method*

antibacterial effects. As the antibacterial activity was assessed using the disk diffusion method, the observed inhibition zones may also be influenced by the potential release of Ag^+ ions from the incorporated AgNPs and their subsequent diffusion through the agar (Hsueh et al., 2015), as well as by matrix–nanoparticle interactions and assay-dependent effects. Overall, the AgNP-containing varnish formulations demonstrated antibacterial activity against both tested strains, with a more pronounced inhibitory effect observed against B. subtilis 3562.

4. Conclusions

The developed LED-assisted method represents a rapid, energy-efficient, and environmentally compatible approach for nanoparticle synthesis, used for incorporation in water-based coatings. The combination of renewable plant-derived resources with low-energy LED irradiation enables nanoparticle formation under relatively mild conditions, while reducing reliance on harsh chemical reagents and energy-intensive processing. The possibility of controlling the irradiation wavelength and exposure conditions offers an important advantage for the systematic optimization of nanoparticle formation. The LED-assisted synthesis represents a promising development of the previously established by authors plant-mediated approach, providing greater control over the photochemical conditions while retaining the advantages of simple, energy-efficient and sustainable synthesis strategy. These features highlight the potential of LED-assisted synthesis as a sustainable alternative to conventional nanoparticle production methods and contribute to the development of more resource-efficient and environmentally responsible synthesis strategies implemented in water-based coatings, used in printing and packaging industry. Further studies could focus on optimizing the LED-assisted synthesis by investigation different LED configurations and irradiation wavelengths, irradiation conditions, as well as varying silver nitrate concentration.

This study leads to establishing reproducible LED-assisted protocols for the controlled production of silver nanoparticles with tailored characteristics and improved suitability for applications and implementation in water-based coatings with antibacterial characteristics.

The study provides a experiment for evaluating the antibacterial contribution of the LED assisted synthesis of silver nanoparticles (AgNPs) in the widely used in packaging and printing industry water based coating matrix. In addition to the negative control, a varnish formulation without AgNPs was included, allowing the intrinsic antibacterial activity of the varnish matrix to be distinguished from the effect of the incorporated nanoparticles. Furthermore, several formulations containing increasing amounts of AgNP suspension were evaluated, revealing a consistent increase in inhibition

zones for both B. subtilis 3562 and E. coli K12 (from 10.5 to 13.5 mm and from 6.5 to 8.8 mm, respectively). Thus, provides evidence for a concentration-dependent relationship between AgNP incorporation and antibacterial activity and offers a more systematic basis for optimizing the composition of the antibacterial varnish. The discussion also provides a comprehensive interpretation of the results by considering bacterial cell-envelope differences, Ag^+ ion release, diffusion through the agar, and matrix–nanoparticle interactions.

The obtained results clearly demonstrate significant antibacterial activity of the water-based coating with incorporated LED assisted synthesized AgNP, which intensifies with increasing nano particle concentration. The results could be directly applicable in practice and industry.

5. Acknowledgment

This study is funded by the financial support, provided by the Scientific Research Centre at University of Chemical Technology and Metallurgy, Sofia, under Contract No. 59-33.

6. References

Alhomaidi, E., Jasim, S.A., Amin, H.I.M., Lima Nobre, M.A., Khatami, M., Jalil, A.T. and Hussain Dilfy, S. (2022) 'Biosynthesis of silver nanoparticles using Lawsonia inermis and their biomedical application', *IET Nanobiotechnology*, 16, pp. 284–294. DOI: 10.1049/nbt2.12096

Anh, M.N.T., Nguyen, D.T.D., Thanh, N.V.K., Phong, N.T.P., Nguyen, D.H. and Nguyen-Le, M.-T. (2020) 'Photochemical Synthesis of Silver Nanodecahedrons under Blue LED Irradiation and Their SERS Activity', *Processes*, 8(3), 292. DOI: 10.3390/pr8030292

Anju, T.R., Parvathy, S., Valiya Veettil, M., Rosemary, J., Ansalna, T.H., Shahzabanu, M.M. and Devika, S. (2021) 'Green synthesis of silver nanoparticles from Aloe vera leaf extract and its antimicrobial activity', *Materials Today: Proceedings*, 43, pp. 3956–3960. DOI: 10.1016/j.matpr.2021.02.665

Anjum, S., Chaudhary, R., Khan, A.K., Hashim, M., Anjum, I., Hano, C. and Abbasi, B.H. (2022) 'Light-Emitting Diode (LED)-Directed Green Synthesis of Silver Nanoparticles and Evaluation of Their Multifaceted Clinical and Biological Activities', *RSC Advances*, 12, 22266. DOI: 10.1039/D2RA03503K

Bozhkova, T.Ts., Boeva, R.K., Spridonov, I.T., Sapkota, J., Nedelchev, Y.V., Kašiković, N., Dedijer, S. and Pal, M. (2017) 'Improvement of physical-mechanical and optical properties of the packaging production through coating with aqueous polymer dispersions in accordance with the environmental protection requirements', *Bulgarian Chemical Communications*, 49, Special Issue L, pp. 169–173.

Bozhkova, T.Ts., Spridonov, I.T., Nedelchev, Y., Boeva, R.K. and Ganchev, A. (2015) 'Improvement of the physical-mechanical and optical properties of printing production with biodegradable overprint varnishes', *Bulgarian Chemical Communications*, 47, Special Issue A, pp. 60–63.

De Mel, S., Gruenler, J., Khoury, L., Heynes, A., Fazekas, J., Damaske, K., Galbadage, T., Gunasekera, R.S. and Anderson, R.S. (2025) 'Green synthesis of silver nanoparticles using Magnolia alba leaf extracts and evaluating their antimicrobial, anticancer, antioxidant, and photocatalytic properties', *Scientific Reports*, 15, 23709. DOI: 10.1038/s41598-025-08468-3

Delcour, A.H. (2009) 'Outer membrane permeability and antibiotic resistance', *Biochimica et Biophysica Acta (BBA) – Proteins and Proteomics*, 1794(5), pp. 808–816. DOI: 10.1016/j.bbapap.2008.11.005

Fahim, M., Shahzaib, A., Nishat, N., Jahan, A., Bhat, T.A. and Inam, A. (2024) 'Green Synthesis of Silver Nanoparticles: A Comprehensive Review of Methods, Influencing Factors, and Applications', *JCIS Open*, 16, 100125. DOI: 10.1016/j.jciso.2024.100125

Gurung, S., Sarmin, M. and Hoda, M. (2024) 'Implications of White Light-Emitting Diode-Based Photoirradiation on Green Synthesis of Silver Nanoparticles by Methanol- and Aqueous-Based Extracts of Bergenia ciliata Leaves', *Nanomaterials*, 14(7), 1327. DOI: 10.3390/nano14161327

Hsueh, Y.-H., Lin, K.-S., Ke, W.-J., Hsieh, C.-T., Chiang, C.-L., Tzou, D.-Y. and Liu, S.-T. (2015) 'The antimicrobial properties of silver nanoparticles in Bacillus subtilis are mediated by released Ag^+ ions', *PLoS ONE*, 10(12), e0144306. DOI: 10.1371/journal.pone.0144306

Hudzicki, J. (2009) Kirby-Bauer disk diffusion susceptibility test protocol. American Society for Microbiology. Available from: https://asm.org/protocols/kirby-bauer-disk-diffusion-susceptibility-test-pro [Accessed 10 June 2026].

Kim, S.W., Baek, Y.-W. and An, Y.-J. (2011) 'Assay-dependent effect of silver nanoparticles to Escherichia coli and Bacillus subtilis', *Applied Microbiology and Biotechnology*, 92(5), pp. 1045–1052. DOI: 10.1007/s00253-011-3611-x

Mai-Ngoc, T.A., Vo, N.K., Nguyen, C.D., Nguyen, T.K.X. and Do Beilstein, T.S. (2025) 'Photochemical Synthesis of Silver Nanoprisms via Green LED Irradiation and Evaluation of SERS Activity', *Beilstein Journal of Nanotechnology*, 16, pp. 1417–1427. DOI: 10.3762/bjnano.16.103

Silhavy, T.J., Kahne, D. and Walker, S. (2010) 'The bacterial cell envelope', *Cold Spring Harbor Perspectives in Biology*, 2(5), a000414. DOI: 10.1101/cshperspect.a000414

Spiridonov, I.T., Pashova, K., Boeva, R.K., Hinkov, I. and Lazarova-Zdravkova, N. (2024) Study of effect of silver nanoparticles synthesized using extract from Sideritis scardica, incorporated into water-based and UV coatings. *Proceedings of 12th International Symposium on Graphic Engineering and Design*, GRID 2024, 14–16 November 2024, Novi Sad, Serbia, pp. 479–483. DOI: 10.24867/GRID-2024-p52

Sun, J., Rutherford, S.T., Silhavy, T.J. and Huang, K.C. (2022) 'Physical properties of the bacterial outer membrane', *Nature Reviews Microbiology*, 20, pp. 236–248. DOI: 10.1038/s41579-021-00638-0

Zehra, S.H., Ramzan, K., Viskelis, J., Viskelis, P. and Balciunaitiene, A. (2025) 'Advancements in Green Synthesis of Silver-Based Nanostructures for Biomedical Applications', *Nanomaterials*, 15(4), 252. DOI: 10.3390/nano15040252



© 2026 Authors. Published by the University of Novi Sad, Faculty of Technical Sciences, Department of Graphic Engineering and Design. This article is an open access article distributed under the terms and conditions of the Creative Commons Attribution license 4.0 Serbia (https://creativecommons.org/licenses/by/4.0/deed.en).

Review Paper https://doi.org/10.24867/GRID-2026-p69

Bio-Based, Biodegradable and Hybrid Coatings for Paper-Based Packaging: Functional Performance and End-of-Life Considerations

ABSTRACT

The growing demand for recyclable and high-performance paper-based packaging has intensified research on biopolymer coatings as alternatives to conventional petroleum-derived barrier layers. This review examines peer-reviewed studies published primarily between 2017 and 2026, focusing on chitosan, cellulose and nanocellulose, starch and other polysaccharides, proteins, lignin, bio-based and biodegradable polyester systems. Representative studies were selected to cover major material classes, modification strategies, coating methods, functional properties, processing aspects, and end-of-life performance. Particular attention is given to crosslinking, polymer blending, hydrophobic modification, nanocomposite reinforcement, and multilayer coating design. Relationships between coating composition, morphology, continuity, filler dispersion, coating weight, and processing conditions are discussed in relation to water resistance, water-vapor and oxygen barrier performance, grease resistance, mechanical properties, surface characteristics, and printability. Because experimental and testing conditions differ among studies, the results are compared primarily in terms of general trends and improvements relative to control samples rather than by direct numerical ranking. The reviewed literature shows that no single material class provides optimal performance across all functional requirements. Recent developments increasingly focus on low-coat-weight and scalable coating systems, waste-derived and fully bio-based raw materials, multifunctional coatings, end-of-life criteria such as biodegradability, laboratory-scale repulpability, fiber recovery, and potential compatibility with paper recycling. Future progress will depend on balancing functional performance, processability, resource efficiency, safety, and potential compatibility with existing paper-recycling streams, to be confirmed under industrial conditions.

Milena Ristić
Vesna Gvoić
Živko Pavlović
Miljana Prica

University of Novi Sad, Faculty of Technical Sciences, Department of Graphic Engineering and Design, Novi Sad, Serbia

KEY WORDS
Bio-based coatings, biodegradable coatings, paper-based packaging, barrier properties, repulpability

1. Introduction

Paper and paperboard are widely used packaging materials due to their favorable printability, availability, relatively low cost, and potential recyclability and biodegradability (Mujtaba et al., 2022; Jahangiri, Mohanty & Misra, 2024). However, their cellulose-based structure is both hygroscopic and porous, which results in limited barrier properties of untreated paper against water and water vapor, gases, aromas, oils, and fats (Li et al., 2019; Mujtaba et al., 2022). These limitations are particularly important in food packaging, where the control of moisture, oxygen, and fatty components, as well as the preservation of mechanical stability under humid con-

ditions, is of critical importance (Mujtaba et al., 2022; Jahangiri, Mohanty & Misra, 2024). One of the most common approaches to improving the functionality of paper is the application of a surface coating that fills the pores, reduces the free volume between cellulose fibers, and forms a continuous protective layer (Li et al., 2019; Jin et al., 2021). Traditionally, synthetic polymers such as polyethylene, poly(ethylene terephthalate), synthetic latexes, poly(vinyl alcohol), and fluoropolymer-based systems have been used for this purpose. Although these materials can provide good barrier and mechanical properties, their use may hinder paper recycling and increase dependence on fossil-based raw materials (Mujtaba et al., 2022; Jahangiri, Mohanty & Misra, 2024). Consequently, increasing attention is being directed toward biopolymer and bio-based coatings based on chitosan, starch, cellulose and nanocellulose, alginate, proteins, polylactic acid (PLA), and polyhydroxyalkanoates (PHA) (Mujtaba et al., 2022; Shorey & Mekonnen, 2022; Jahangiri, Mohanty & Misra, 2024).

The increasing environmental concerns associated with the long-term persistence of petrochemical plastics, the difficulties in managing multilayer packaging systems, and the dependence on non-renewable resources have encouraged the development of renewable and potentially biodegradable materials, subject to application-specific safety assessment, for improving the functional properties of paper-based packaging. In this context, biopolymers represent a particularly important group of materials, as they can originate from plant, animal, microbial, and biomass-derived industrial sources, while certain classes also exhibit good film-forming ability, favorable gas barrier properties, biocompatibility, and the possibility of chemical modification.

This review covers natural biopolymers, bio-based synthetic polymers, biodegradable polymers that may be fossil-derived, and hybrid systems combining biopolymers with synthetic polymers or inorganic nanomaterials. Accordingly, bio-based origin, biodegradability, and biopolymer content are treated as distinct material characteristics (Mujtaba et al., 2022; Jahangiri, Mohanty & Misra, 2024).

Among the materials that have attracted the greatest attention for paper and paperboard coatings are chitosan, cellulose and nanocellulose, starch, alginate, lignin, proteins, and biodegradable polyesters, while more recent research has increasingly focused on their blends, nanocomposites, and multilayer systems (Mujtaba et al., 2022; Eslami & Mekonnen, 2023; Poulose et al., 2024; Adak & Teramoto, 2025). Different classes of biopolymers provide different advantages when used as paper coatings. Polysaccharides, such as chitosan, cellulose, nanocellulose, starch, and alginate, generally exhibit good film-forming ability and can form relatively uniform and compact layers on the paper surface (Mathew & Oksman, 2017; Herrera, Jin et al., 2021; Mujtaba et al., 2022). Natural polyphenols, such as tannins and certain lignin-derived components, can absorb UV radiation and exhibit antioxidant activity (Mujtaba et al., 2022; Zhu et al., 2023). Biodegradable polyesters, such as polylactic acid (PLA), poly(3-hydroxybutyrate) (PHB), and poly(3-hydroxybutyrate-co-3-hydroxyvalerate) (PHBV), are generally more hydrophobic than many polysaccharides. Their lower affinity for water can therefore contribute to improved protection of paper against moisture and direct contact with water (Shorey & Mekonnen, 2022; Calosi et al., 2024; Pieters & Mekonnen, 2024). However, biodegradability does not imply rapid degradation in every environment. The degradation of these polyesters depends on their composition and crystallinity, coating thickness, temperature, moisture, microbial activity, and the conditions of the applied test (Eslami & Mekonnen, 2023; Lors, Leleux & Park, 2025).

At the same time, the natural or bio-based origin of a polymer does not automatically ensure optimal coating performance. Its application may be limited by hydrophilicity, brittleness, insufficient thermal and mechanical stability, aggregation, and poor compatibility between different components (Mujtaba et al., 2022; Jahangiri, Mohanty & Misra, 2024). In polysaccharides such as chitosan and cellulose-based materials, polar functional groups contribute to good film-forming ability, but at the same time increase their affinity for water (Mujtaba et al., 2022; Dodangeh et al., 2026).

This paper presents a review of peer-reviewed studies published primarily between 2017 and 2026. The literature search focused primarily on peer-reviewed publications indexed in major scientific databases (Web of Science and Scopus). Search terms included combinations of “paper coating”, “paper-based packaging”, “bio-based coating”, “biopolymer coating”, “biodegradable coating”, “barrier coating”, “repulpability”, and “recyclability”. Studies were selected to provide representative examples of major material classes, modification strategies, coating methods, functional properties, and end-of-life considerations.

2. Functional requirements of paper-based coatings

Biopolymer coatings can significantly modify the properties of paper and broaden its application in packaging systems. Their performance depends on the type of biopolymer, the composition and structure of the coating, as well as the coating and processing methods. In addition to improving resistance to water, gases, oils, and fats, the coating can also affect the mechanical, surface, and printing properties of paper and provide additional active functions. The homogeneity and continuity of the formed

layer are particularly important, since the presence of pores, cracks, or an uneven distribution of components can reduce the barrier and mechanical performance of the coating (Shorey & Mekonnen, 2022; Mujtaba et al., 2022). Therefore, the performance of biopolymer coatings should be evaluated based on the overall combination of properties rather than on individual test results.

Current developments are increasingly focused on multicomponent and multifunctional systems in which different properties can be simultaneously tailored to meet the requirements of specific packaging applications (Eslami & Mekonnen, 2023; Zhu et al., 2023; Peng et al., 2024).

2.1. Water and moisture barrier properties

The hydrophilic and porous nature of paper limits its application in packaging systems with more demanding product-protection requirements. Interfiber pores facilitate liquid penetration and water vapor transport, while the hydroxyl groups of cellulose exhibit a strong affinity for water. Surface coating can therefore serve two main functions (Mujtaba et al., 2022; Shorey & Mekonnen, 2022): reducing direct contact between cellulose fibers and water, and sealing or narrowing the pores through which moisture transport occurs.

In the reviewed literature, water resistance is most commonly evaluated using the water contact angle (WCA) and Cobb test, whereas water vapor transport is expressed as the water vapor transmission rate (WVTR) or water vapor permeability (WVP). These parameters describe different aspects of material performance: WCA primarily characterizes surface wettability, the Cobb test quantifies the amount of liquid water absorbed by paper, while WVTR and WVP describe water vapor transport through the entire coated system (Shankar & Rhim, 2018; Adak & Teramoto, 2025).

The distinction between surface wettability and actual water absorption is particularly important for hydrophobic polyester coatings. Adak & Teramoto (2025) showed that contact angle values do not necessarily correlate directly with water absorption, while the optimized PBAT/hectorite nanocomposite coating exhibited an exceptionally low Cobb value. In more hydrophilic polysaccharide-based systems, the relationship between coating structure and moisture-barrier performance is more complex. Nanocellulose can form a dense and uniform network that reduces water penetration; however, the addition of a hydrophilic plasticizer may increase moisture uptake. Herrera, Mathew & Oksman (2017) demonstrated that the application of a nanocellulose coating significantly reduced moisture absorption, whereas the addition of sorbitol increased it due to its hydrophilic nature.

Current strategies for improving moisture-barrier properties therefore include hydrophobic modification, chemical crosslinking, combination with more hydrophobic components, and nanocomposite reinforcement (Herrera, Mathew & Oksman, 2017; Shorey & Mekonnen, 2022; Fang et al., 2025; Adak & Teramoto, 2025).

2.2. Oxygen and gas barrier properties

Excessive oxygen transport through packaging materials can promote oxidative processes and reduce product stability. Therefore, coating performance is commonly evaluated by measuring the oxygen transmission rate (OTR), oxygen permeability (OP), or resistance to air permeation (Mujtaba et al., 2022; Shorey & Mekonnen, 2022). Effective gas-barrier performance is generally achieved by forming a dense and continuous layer that restricts gas transport through the material. Nanocellulose is particularly attractive in this respect because of its ability to form compact networks of nanofibrils. Herrera, Mathew & Oksman (2017) showed that nanocellulose-based coatings significantly improve oxygen-barrier properties compared with the uncoated porous substrate, with particularly effective protection achieved using a thin plasticized nanocellulose coating. Another important mechanism involves the formation of a tortuous diffusion path. When platelet-shaped nanofillers are well dispersed within a polymer matrix, gas molecules are forced to diffuse around the impermeable particles, thereby increasing the effective path length through the coating. In PBAT/hectorite nanocomposites, the good dispersion of nanoclay at an optimal concentration resulted in a significant reduction in both oxygen and water-vapor transport (Adak & Teramoto, 2025).

Very high gas-barrier performance can also be achieved with protein-based and biopolyelectrolyte systems. Fisher et al. (2026) developed a fully bio-based coating composed of fish gelatin and DNA, both derived from fish-processing by-products. Under appropriate conditions, gelatin and DNA interact to form a polymer-rich phase known as a complex coacervate. This polymer-rich phase was subsequently applied as a coating to kraft paper, reducing the oxygen transmission rate by approximately 70% compared with uncoated paper. A subsequent thermal treatment at 150 °C induced structural rearrangement and strengthened intermolecular interactions within the coating, resulting in an OTR reduction of approximately 99%. These findings indicate that the formation of a compact polymeric structure followed by thermal stabilization can provide highly effective oxygen-barrier properties without the use of a conventional synthetic polymer matrix.

2.3. Oil and grease resistance

Resistance to oils and fats is particularly important for paper-based packaging intended for products with a high

lipid content. Due to its open fibrous structure, uncoated paper allows relatively rapid penetration of nonpolar liquids. Therefore, a functional coating should reduce the available transport pathways and form a sufficiently homogeneous and continuous surface layer (Shankar & Rhim, 2018; Shorey & Mekonnen, 2022). In the reviewed studies, resistance to oils and fats is most commonly evaluated using the Kit test, while oil-based Cobb tests, oil contact angle measurements, and longer-term penetration tests are also applied. The findings indicate that, in addition to chemical composition, coating morphology plays an important role in determining grease-barrier performance. Shorey & Mekonnen (2022) showed that esterified lignin provides better resistance to oils and fats than the unmodified system, which was associated with improved lignin dispersion and a more homogeneous PBAT/lignin coating structure. The optimized PBAT/hectorite nanocomposite system achieved the maximum Kit rating of 12 (Adak & Teramoto, 2025), while a crosslinked chitosan/tannin system combined high oil and grease resistance with barrier properties against gases and moisture, as well as UV protection (Zhu et al., 2023). High resistance to oils and fats can therefore be achieved through several approaches, including the use of hydrophobic polymers, the incorporation of nanomaterials, and the formation of crosslinked biopolymer networks.

2.4. Mechanical properties

In addition to improving barrier performance, a functional coating should preserve or enhance the mechanical properties of paper. The most commonly evaluated parameters include tensile strength, elongation at break, tear resistance, burst strength, and wet tensile strength. Improvements in these properties may result from stronger bonding between surface fibers, the filling of surface irregularities, and the formation of a more compact polymeric or nanocomposite layer (Herrera, Mathew & Oksman, 2017; Shorey & Mekonnen, 2022). An increase in strength does not necessarily imply better overall mechanical performance. Plasticization can improve flexibility but may also increase sensitivity to water, while a higher degree of crosslinking can enhance structural stability but reduce material elongation. Therefore, an appropriate balance between strength and flexibility is essential in the design of functional coatings (Herrera, Mathew & Oksman, 2017; Dodangeh et al., 2026). The importance of coating structure and crosslinking for mechanical performance was clearly demonstrated by Yu et al. (2022), who developed a multilayer coating based on chitosan and dopamine-modified carboxymethyl cellulose using a layer-by-layer assembly approach followed by oxidative crosslinking. Increasing the number of layers and applying subsequent crosslinking improved the mechanical properties of the paper by promoting stronger fiber bonding and enhanced interlayer interactions. These findings indicate that mechanical reinforcement depends not only on coating composition, but also on coating architecture and the crosslinking strategy. For packaging applications, maintaining mechanical stability in the presence of water is particularly important. Shorey & Mekonnen (2022) showed that esterified lignin incorporated into a PBAT matrix significantly improved the wet tensile properties of paper compared with uncoated paper and systems with poorer lignin dispersion. This improvement was associated with the hydrophobic nature of the coating, more effective fiber coverage, and reduced water penetration into the paper substrate.

2.5. Surface properties and printability

Surface properties of coatings are particularly important in graphic and packaging applications, as coating microstructure, surface roughness, porosity, and binder distribution directly influence ink absorption and the uniformity of the printed surface. Du et al. (2018) demonstrated that the partial replacement of synthetic latex with starch-based bio-latex alters the microstructure of pigment coatings. In contrast to synthetic styrene-butadiene (SB) latex, whose particles deform more readily during drying and form a more continuous film, bio-latex particles tend to retain a more spherical morphology. Increasing the bio-latex content resulted in changes in pore structure, a slight increase in surface roughness, and a reduction in coating gloss. These changes can affect ink absorption and transfer and, consequently, print quality.

Therefore, the replacement of petrochemical binders with renewable alternatives should be evaluated not only from the perspective of sustainability, but also in terms of the relationship between coating microstructure and print-related properties. A more direct relationship between the structure of bio-based coatings and printability was reported by Liu et al. (2023), who developed a starch-based bio-latex modified with cationic cellulose nanocrystals (CCNC). The incorporation of CCNC promoted the formation of a more compact coating structure and simultaneously resulted in higher print optical density, improved surface pick resistance, and lower tone value increase compared with the control systems. These findings highlight the importance of tailoring the microstructure of bio-based coatings in order to achieve both improved sustainability and satisfactory printing performance.

2.6. Additional functionality

Modern biopolymer coatings are increasingly being developed as multifunctional systems that, in addition to basic barrier and mechanical properties, can provide antimicrobial and antioxidant activity, UV protection, reduced migration of selected substances, and improved end-of-life performance (Shankar & Rhim, 2018; Mujtaba et al., 2022; Zhu et al., 2023). A coating based on alginate, carboxymethyl cellulose (CMC), and carrageenan, supplemented with grapefruit seed extract, represents

an example of an active system that combines barrier and antibacterial functions. The coated paper exhibited strong antibacterial activity against Listeria monocytogenes and Escherichia coli under the applied test conditions, demonstrating that the coating can provide an active function in addition to acting as a physical barrier (Shankar & Rhim, 2018). A broader example of multifunctionality is provided by a crosslinked chitosan/tannin system that combines oil and grease resistance, barrier properties against gases and moisture, UV protection, biodegradability, and paper repulpability. Such a combination of properties demonstrates that coating functionality can extend beyond product protection during use to include requirements related to the material's end-of-life behavior (Zhu et al., 2023).

In addition to incorporating active components, multifunctional coatings can be developed by combining materials with complementary properties in multicomponent and multilayer structures. Eslami & Mekonnen (2023) developed a multilayer structure consisting of paper, thermoplastic starch (TPS), and an outer layer of PLA, PBAT, PHBV, or PVOH. TPS primarily contributed to oxygen-barrier performance, whereas the outer polymer layer improved resistance to water, water vapor, and oil. The most favorable overall barrier performance was achieved with the TPS/PHBV system, indicating that distributing complementary functions among individual layers may be more effective than relying on a single material. Although all of the investigated systems contained a bio-based TPS layer, they were not necessarily fully bio-based: PVOH is a synthetic polymer that is not typically bio-based, whereas commercial PBAT is generally produced predominantly from fossil-derived feedstocks despite being biodegradable.

A similar multilayer concept was applied by Yi et al. (2022) using a hybrid nanocellulose–PDMS coating. The first cellulose nanofibril (CNF) layer filled pores within the paper structure and contributed to improved oil and barrier resistance, while the outer layer containing polydimethylsiloxane (PDMS) and CNF microparticles provided pronounced hydrophobicity. Multifunctionality can also include properties associated with the behavior of the material after use. Peng et al. (2024) developed a bio-based coating composed of chitosan, glutinous rice starch, and PLA using an emulsion stabilized by cellulose nanocrystals (CNC). Chitosan and starch formed a continuous polymer matrix, while PLA microspheres contributed to hydrophobicity and the formation of a rougher surface structure. An important advantage of this system is that, in addition to water and oil resistance and self-cleaning properties, it retains biodegradability and the ability to recover paper fibers through repulping, thereby improving its end-of-life sustainability.

For food-packaging applications, functional performance must be considered together with material safety and compliance with food-contact requirements. The natural, bio-based, or biodegradable origin of a coating component does not by itself guarantee its suitability for direct contact with food. Potential migration of residual crosslinking agents, plasticizers, photoinitiators, solvents, nanoparticles, and unreacted coating components should therefore be evaluated under conditions that reflect the intended food type, contact time, and temperature. Active compounds may also affect the sensory properties of packaged products or migrate at concentrations exceeding their intended technological function.

Consequently, the development of biopolymer-based and hybrid coatings for food packaging should include overall and specific migration testing, toxicological assessment where required, and verification of compliance with applicable food-contact legislation, in addition to conventional barrier, mechanical, and end-of-life evaluation (Mujtaba et al., 2022; Jahangiri, Mohanty & Misra, 2024). However, food-contact safety, migration behavior, and toxicological performance are not systematically evaluated in most of the reviewed studies, which represents an important limitation of the available literature. Consequently, these aspects were not included in the detailed comparative analysis presented in this review and should be addressed more systematically in future research.

2.7. End-of-life considerations

The end-of-life performance of coated paper cannot be described using a single criterion. Bio-based origin, biodegradability, compostability, repulpability, fiber recovery, and recyclability represent distinct characteristics and should therefore be evaluated separately. A coating may be derived from renewable resources without being readily biodegradable, while a biodegradable polymer may require specific temperature, moisture, microbial, or industrial-composting conditions for effective degradation. Similarly, laboratory-scale repulpability indicates that the coated paper can be disintegrated and that fibers may be recovered under the applied test conditions, but it does not by itself demonstrate compatibility with industrial paper-recycling processes.

Among the reviewed systems, Zhu et al. (2023) reported both biodegradability and laboratory-scale repulpability for a crosslinked chitosan/tannin coating. Peng et al. (2024) also evaluated biodegradation and paper-fiber recovery for a chitosan, glutinous-rice-starch, and PLA coating. Haider, Wang and Li (2026) investigated the influence of PLA coating weight on barrier performance and laboratory-scale repulpability. Their results showed that coating weight affected both functional performance and the recovery of the paper substrate, demonstrating that end-of-life behavior depends not only on polymer type but also on the amount and structure of the applied coating.

These results indicate potential compatibility with paper recycling, but they should not be interpreted as proof of full recyclability under industrial conditions. Industrial recycling performance also depends on coating detachment, fiber yield and quality, screening losses, adhesive or reject formation, process-water contamination, and the operating conditions of the recycling mill. Therefore, future studies should report the applied repulping procedure, coating weight, fiber-recovery yield, reject content, and the quality of the recovered fibers. Claims of biodegradability or compostability should likewise specify the applied test method, environmental conditions, duration, and degree of degradation or disintegration. Until such assessments are performed under relevant pilot- or industrial-scale conditions, the terms laboratory-scale repulpability, fiber recovery, and recyclability should not be used interchangeably.

The multifunctionality of coatings can therefore be achieved through the incorporation of natural active components, crosslinking, the combination of materials with different properties, and the formation of multilayer structures. Their effectiveness depends not only on composition but also on coating structure, homogeneity, and interactions between individual components. Consequently, current research is increasingly focused on coatings capable of meeting several functional requirements simultaneously, both during use and after disposal (Shankar & Rhim, 2018; Eslami & Mekonnen, 2023; Zhu et al., 2023; Peng et al., 2024). The functional performance of bio-based, biodegradable, and hybrid coated paper should therefore be evaluated using multiple criteria, including resistance to water, gases, oils, and fats, mechanical, surface, and printing properties, additional active functions, and clearly defined end-of-life characteristics. The main functional requirements, evaluation parameters, representative studies, and improvement mechanisms are summarized in Table 1.

As shown in Table 1, no single modification strategy provides optimal performance across all categories simultaneously. Improvement in one property may be accompanied by changes in others; therefore, the development of functional coatings requires a careful balance between barrier, mechanical, surface, and other properties according to the requirements of the intended application.

Table 1 (part 1)

Functional requirements, evaluation parameters, and improvement mechanisms of bio-based, biodegradable, and hybrid coatings for paper-based materials

Functional requirement	Evaluation parameter/test	Evaluated property	Representative studies	Main improvement mechanisms
Water resistance	WCA, Cobb60	Surface wettability and liquid water absorption	Shorey & Mekonnen, 2022; Yi et al., 2022; Peng et al., 2024; Fang et al., 2025; Adak & Teramoto, 2025;	Hydrophobic modification, pore sealing, formation of a continuous coating, and increased roughness of the hydrophobic surface.
Moisture barrier	WVTR, WVP	Water-vapor transport through coated material	Herrera, Mathew & Oksman, 2017; Zhu et al., 2023; Peng et al., 2024; Fisher et al., 2026	Dense polymer network formation, crosslinking, hydrophobic modification, and extension of the diffusion pathway.
Oxygen/ gas barrier	OTR, OP, and resistance to air permeation	Oxygen/gas transport through coated material	Herrera, Mathew & Oksman, 2017; Eslami & Mekonnen, 2023; Ruberto et al., 2024; Adak & Teramoto, 2025; Fisher et al., 2026;	Dense polymeric/nanofibrillar network, pore sealing, reduction of free volume, and multilayer structure
Oil/grease resistance	Kit test, oil Cobb test, and oil contact angle	Resistance to penetration of oils and fats	Shorey & Mekonnen, 2022; Yi et al., 2022; Zhu et al., 2023; Peng et al., 2024; Adak & Teramoto, 2025;	Continuous film formation, pore sealing, hydrophobic modification, and combination of complementary components
Mechanical performance	Tensile strength, elongation at break, tear/ burst resistance, and wet tensile strength	Strength, flexibility and mechanical integrity	Herrera, Mathew & Oksman, 2017; Jin et al., 2021; Shorey & Mekonnen, 2022; Peng et al., 2024;	Intermolecular interactions, crosslinking, fiber bonding, and nanoreinforcement

Table 1 (part 2)

Functional requirements, evaluation parameters, and improvement mechanisms of bio-based, biodegradable, and hybrid coatings for paper-based materials

Functional requirement	Evaluation parameter/test	Evaluated property	Representative studies	Main improvement mechanisms
Surface properties and printability	Surface roughness, gloss, porosity, wettability, optical density, and tone value increase	Surface quality and suitability for printing	Du et al., 2018, Jin et al., 2021; Liu et al., 2023	Control of coating porosity and morphology, binder distribution, and formation of a more compact structure
Active functionality	Antimicrobial and antioxidant activity, UV protection, and self-cleaning properties	Additional protective/active functions	Shankar & Rhim, 2018; Zhu et al., 2023; Peng et al., 2024	Natural extracts, polyphenols, functional additives, and controlled surface morphology
End-of-life performance	Biodegradation under specified conditions; compostability according to applicable standards; laboratory repulpability and fiber-recovery tests; recyclability assessment in relevant paper-recycling systems	Biodegradation behavior, compliance with compostability requirements, recoverability of paper fibers, and compatibility with paper-recycling processes	Zhu et al., 2023; Peng et al., 2024; Haider, Wang & Li, 2026	Selection of materials and coating architectures that facilitate degradation under defined conditions, fiber separation during repulping, or compatibility with established paper-recycling operations

3. Comparative analysis of functional performance

The functional properties of bio-based, biodegradable, and hybrid coating systems depend on the type of polymer, the structure of the formed layer, the modification method, coating weight, and processing conditions (Mujtaba et al., 2022; Ruberto et al., 2024; Gómez et al., 2024). A homogeneous and continuous coating with fewer defects generally contributes to improved functional performance, whereas cracks, pores, or uneven distribution of coating components may reduce barrier efficiency (Ruberto et al., 2024; Gómez et al., 2024). Coating weight is also an important parameter; however, increasing the amount of applied material does not necessarily lead to a proportional improvement in performance. At higher coating weights, changes in formulation viscosity and film formation may impair leveling and promote non-uniform deposition or localized defects (Haider, Wang & Li, 2026).

The dispersion and concentration of functional additives can further influence coating morphology and performance. For example, well-dispersed hectorite nanoclay improved the barrier properties of PBAT-based coatings, whereas excessive nanoclay loading promoted aggregation and reduced coating efficiency (Adak & Teramoto, 2025).

Therefore, when comparing different coating systems, it is more appropriate to consider overall trends and improvements relative to control samples rather than individual numerical values, since differences in polymer composition, coating weight, application method, drying conditions, and testing procedures may affect the reported results (Mujtaba et al., 2022; Gómez et al., 2024).

Table 2 presents a comparative overview of selected representative studies. The studies were chosen to illustrate different coating-material classes, modification strategies, application methods, and functional properties rather than to provide an exhaustive account of all coating systems reported in the literature.

Table 2 (part 1)

Overview of selected studies on bio-based, biodegradable, and hybrid coatings for paper-based packaging

Study	Coating material/ system	Modification	Coating method	Coating weight (g/m^2)	Water / moisture barrier	O_2 / gas barrier	Grease/ oil	Mechanical, additional, and end-of-life properties
Vrabič Brodnjak (2017)	Curdlan/ chitosan	Polymer blending	Blade coating	5*	Improved water barrier	—	—	5:5 curdlan/ chitosan ratio showed favorable mechanical performance
Battisti et al. (2017)	Gelatin	Transglutaminase + glycerol + citric acid	Spray coating	NR	Significant reduction in WVP	—	—	Antimicrobial/antioxidant activity; no improvement in mechanical properties
Shankar & Rhim (2018)	Alginate/ CMC/carrageenan + GSE	Ternary blend + active agent	Wire-bar coating	4.5 ± 0.4; 7.6 ± 1.0; 8.8 ± 1.1	Reduced water absorption and WVP; increased hydrophobicity	—	Improved oil resistance	Improved tensile properties; strong antimicrobial activity
Bhardwaj, Bhardwaj & Negi (2021)	Chitosan with different degrees of acetylation (DA)	Degree of acetylation/ deacetylation	Surface coating	1.6 ± 0.2; 2.3 ± 0.3	Improved water-barrier properties	Increased resistance to air permeance	—	burst index, tensile energy absorption, stretch, stiffness, and folding properties
Wang et al. (2020)	Cellulose stearoyl ester	Long-chain esterification	Bar coating	0.5–23.6	Water-vapor barrier ratio up to 90%; WCA ≈ 99–109°	—	—	Smooth and continuous coating; complete surface coverage achieved at 5.2 g/m^2
Chi, Wang & Catchmark (2020)	Starch polyelectrolyte complexes	Ionic complexation	Dip coating	≈10	WVP reduced by up to ~40%	—	Kit 12; low oil penetration	Tensile strength ↑ ~18%; Young's modulus ↑ ~21%; dense and defect-free structure
Jeong & Yoo (2020)	WPC/ beeswax/ sucrose	Protein–lipid blending	Brush coating	NR	Strong improvement in water and water-vapor barrier with increasing beeswax content	—	WPC provided oil barrier; high beeswax content increased oil penetration	Clear moisture–oil barrier trade-off
Shorey & Mekonnen (2022)	Esterified lignin/PBAT	Lignin esterification + blending	Doctor blade	12.07–14.81 (20 µm coatings)	Strong water resistance; barrier further improved at higher coating thickness	Improved O_2 barrier; up to 55.2% reduction in oxygen permeability for esterified lignin/PBAT	Improved oil and grease resistance	Esterification improved lignin dispersion and compatibility with PBAT; thicker coatings provided better overall barrier performance

Table 2 (part 2)

Overview of selected studies on bio-based, biodegradable, and hybrid coatings for paper-based packaging

Study	Coating material/ system	Modification	Coating method	Coating weight (g/m²)	Water / moisture barrier	O_2 / gas barrier	Grease/ oil	Mechanical, additional, and end-of-life properties
Zhu et al. (2023)	Chitosan/ tannin-derived epoxy system	Crosslinking	Rod coating	4.05 ± 0.84	WVTR 1252.9 → 298.6 g/m²·d; WCA 102.51°; Cobb60 15.31 g/m²	OP 597.1 → 136.2 cm³/(m²·d·0.1 MPa)	Kit 12	UV shielding; improved mechanical properties; biodegradable and repulpable coating
Ruberto et al. (2024)	CNC/ chitosan bilayer	Multicomponent/ bilayer coating	Slot-die coating + NIR drying	CNC: 22–33; Cht: 3–4	WVP 0.23–0.28 g·mm/(m²·d·Pa) for bilayer systems	Air permeability: 4.2–1.5 nm/(Pa·s); O_2 permeability: 2.7–1.1 cm³·mm/(m²·d·kPa)	—	Scalable deposition; coating homogeneity controlled by suspension viscosity and process parameters
Poulose et al. (2024)	PFJ/PHB multilayer	Multilayer architecture	Rod coating + extrusion coating	PHB: 20 or 30; PFJ: NR*	Specific WVTR reduced by ~95% for two-layer and ~90–91% for three-layer systems	Three-layer structure showed better O_2 barrier than two-layer systems, although OP remained relatively high	Improved grease resistance in three-layer systems	PFJ increased bonding strength; three-layer coatings showed moderate adhesion and improved creasing performance
Adak & Teramoto (2025)	PBAT/ hectorite nanoclay	Nanocomposite reinforcement	Bar coating	22 ± 1; 32 ± 1	WVTR ↓ up to 48.5% relative to neat PBAT coating; lowest Cobb60 = 0.3 g/m²	OTR ↓ up to 58.3% relative to neat PBAT coating	Kit 12; no oil penetration for extended periods	5 wt% nanoclay provided optimum performance; higher loading promoted aggregation
Fang et al. (2025)	Hydrophobically modified chitosan (CHI-g-OA_2)	Hydrophobic grafting + crosslinking	Linear coating machine	4.25 ± 0.81	WCA 121.0 ± 3.0°; Cobb60 8.33 ± 1.2 g/m²; reduced WVTR	Gas-barrier function retained	Kit 10.3 ± 0.6/12; improved oil repellency	Dense crosslinked structure; improved tensile strength and thermal stability
Dodangeh et al. (2026)	Regenerated cellulose/ chitosan/ citric-acid coating systems	Chitosan incorporation + citric-acid crosslinking	Casting-knife coating	NR	WVP as low as (11.0 ± 0.32) × 10^{-5} g/(m·d·Pa) in citric-acid-crosslinked samples	—	—	TS reached 14.20 ± 0.29 MPa for CA20%-RC; combined RC:CH90:10-CA10% system showed TS of 12.30 ± 0.43 MPa

Table 2 (part 3)

Overview of selected studies on bio-based, biodegradable, and hybrid coatings for paper-based packaging

Study	Coating material/ system	Modification	Coating method	Coating weight (g/m^2)	Water / moisture barrier	O_2 / gas barrier	Grease/oil	Mechanical, additional, and end-of-life properties
Cao et al. (2026)	PLA/PHA	Polymer blending + hot pressing	Spray coating + hot pressing	NR	Increased surface hydrophobicity; higher PHA content generally increased WCA	Lowest OTR, 15.15 ± 1.25 $cm^3/(m^2 \cdot 24\ h)$, obtained for the 50:50 PLA/PHA blend	—	Hot pressing improved coating uniformity; 50:50 blend provided the most favorable balance of barrier and mechanical properties
Fisher et al. (2026)	Fish gelatin/DNA	Complex coacervation + thermal curing	Wire-wound rod coating	26	WVTR ↓ ~83% after curing at 150 °C	OTR ↓ ~99% after curing at 150 °C	Coating improved grease resistance before curing (Kit 9.2); grease resistance decreased with increasing curing temperature (Kit 4.4 at 150 °C)	Fully bio-based system; thermal curing strongly enhanced water-vapor and oxygen-barrier performance
Haider, Wang & Li (2026)	PLA + citric acid	Coat-weight optimization + plasticization	Bar coating	2.00 ± 0.50; 4.50 ± 1.10; 6.68 ± 0.72; 9.98 ± 2.26	Minimum WVTR 83.97 $g/(m^2 \cdot day)$; Cobb60 reduced from ~20 to ~3 g/m^2	—	Maximum Kit 11.2 ± 0.40	Repulpable across the investigated coating weights; 6.68 ± 0.72 g/m^2 provided the best balance between barrier performance and laboratory-scale repulpability.

Note: '—' indicates that the corresponding property was not evaluated or reported in the cited study, whereas NR indicates that the dry coating weight was not reported. Numerical values from different studies should not be directly ranked because coating formulations, application conditions, coating weights, substrate properties, drying conditions, and testing procedures differ among studies. In addition, the reported OTR, OP, WVTR, and WVP values were obtained under different temperature and relative-humidity conditions and using paper substrates with different compositions, grammages, thicknesses, and surface characteristics. These parameters strongly influence the measured barrier performance; therefore, the numerical values should be interpreted only within the experimental conditions of the corresponding study. Where reported, laboratory-scale repulpability, fiber recovery, biodegradability, or other end-of-life characteristics are included in the final column. These terms describe distinct properties and should not be interpreted as evidence of full industrial recyclability.

* For Vrabič Brodnjak (2017), 5 g/m^2 of coating solution was applied; this value represents the applied solution amount rather than a measured dry coating weight.

* For Poulose et al. (2024), the PHB coating weight was reported as 20 or 30 g/m², whereas the PFJ layers were reported by thickness rather than coating weight.

4. Future directions in bio-based, biodegradable and hybrid coatings for paper and packaging

Future research on biopolymer coatings for paper is increasingly shifting from the improvement of individual barrier properties toward integrated systems that combine high functional performance with renewable raw materials, more sustainable processing, and compatibility with paper recycling. Particular attention is being directed toward coatings capable of meeting several requirements simultaneously, including barrier, mechanical, surface, and end-of-life performance.

One important development pathway is the use of industrial and agro-industrial by-products as sources of functional coating components. Kraft lignin, rice straw, sugar beet pulp, potato processing by-products, waste fatty acids, tannin-rich biomass, and fish-processing residues have all been investigated as sources of polymers, proteins, polyphenols, or nanocellulose. These studies demonstrate that secondary raw materials can contribute to functional barrier and mechanical performance and may reduce the use of virgin or fossil-derived resources, although many reported coating systems still contain synthetic or fossil-derived components (Shorey & Mekonnen, 2022; Saini et al., 2022; Fadel et al., 2022; Poulose et al., 2024; Zhang et al., 2024; Fisher et al., 2026). An important future challenge will be to increase the proportion of renewable and secondary raw materials while maintaining simple processing, functional performance, repulpability, and recyclability of coated paper.

Another major direction is the development of multifunctional coatings that provide additional functions beyond conventional moisture, gas, and grease barriers. Depending on their composition, biopolymer-based systems may exhibit antimicrobial activity, antioxidant properties, UV protection, or self-cleaning behavior. For example, polysaccharide coatings containing grapefruit seed extract have shown antibacterial activity, while chitosan/tannin systems provide both barrier performance and UV protection. Pickering-emulsion-based coatings containing chitosan, starch, and PLA have further demonstrated the possibility of combining hydrophobic, oil-resistant, self-cleaning, biodegradable, and repulpable characteristics within a single system (Shankar & Rhim, 2018; Zhu et al., 2023; Peng et al., 2024). The design of nanocomposite and multilayer structures offers an additional route for tailoring coating performance. Well-dispersed nanomaterials can improve barrier properties at relatively low filler contents, whereas excessive concentrations may promote aggregation and reduce coating efficiency. Multilayer systems provide greater flexibility because individual layers can be designed to perform complementary functions. Combinations of thermoplastic starch with biodegradable polyesters, as well as protein-based layers combined with PHB, illustrate how gas, moisture, oil, and mechanical performance can be distributed across different layers rather than being provided by a single material (Eslami & Mekonnen, 2023; Poulose et al., 2024; Adak & Teramoto, 2025).

Future progress will also depend on the environmental impact of the coating process itself. For this reason, increasing attention is being paid to waterborne formulations, solvent-free systems, lower-energy processing, and alternative curing methods. Photocrosslinking is particularly promising because it can form stable polymer networks without prolonged thermal treatment. Kuo, Chuang & Liao (2026) for example, developed a bio-based photocurable coating based on acrylated epoxidized soybean oil and curcumin as a natural photoinitiator, demonstrating the potential of combining renewable components with rapid curing and good water resistance. However, future applications, particularly in food packaging, should also consider the safety of photoinitiators and possible residual unreacted components.

Overall, future progress is likely to depend less on identifying a single optimal polymer and more on designing complete coating systems in which raw-material selection, modification strategy, coating architecture, processing conditions, functional performance, and end-of-life considerations are evaluated together. Promising systems should achieve the required performance at low coating weights, be compatible with efficient processing, and demonstrate potential compatibility with paper-recycling processes. However, their performance, processability, and recyclability must be confirmed under relevant pilot- and industrial-scale conditions.

5. Conclusions

The reviewed studies demonstrate that a broad range of coating materials and systems can improve the functional performance of paper-based packaging. These include natural biopolymers, bio-based synthetic polymers, biodegradable polymers that may be fossil-derived, and hybrid systems combining biopolymers with synthetic polymers or inorganic nanomaterials. Improvements have been reported in resistance to water, water vapor, oxygen, oils and grease, as well as in mechanical and surface properties. However, bio-based origin, biodegradability, compostability, repulpability, and recyclability are distinct characteristics and should not be treated as equivalent. Moreover, no single material or modification strategy provides optimal performance for all packaging requirements.

Coating performance depends not only on material composition but also on coating continuity and morphology, pore sealing, polymer-network density, filler dispersion, coating weight, layer architecture, and application and drying conditions. The most appropriate strategy—such as crosslinking, hydrophobic modification, polymer blending, nanocomposite reinforcement, or multilayer design—therefore depends on the required function, intended conditions of use, coating weight, and processing method. Particular attention should be given to systems that achieve the required barrier performance at low coating weights and are compatible with continuous coating processes. For applications in the graphic and packaging industries, preservation of suitable surface properties and printability should also be considered alongside barrier and mechanical performance. Nevertheless, industrial scalability must be confirmed under relevant processing conditions, including coating speed, formulation rheology and stability, foaming, drying requirements, and energy consumption.

Future development should focus on multifunctional coating systems that balance functional performance, material safety, responsible raw-material selection, resource-efficient processing, and appropriate end-of-life performance. The renewable or waste-derived origin of coating components, the environmental impact of coating production, biodegradation or compostability under specified conditions, and compatibility with paper-recycling processes should be evaluated separately but as complementary sustainability criteria. Since most of the reviewed systems have been investigated at laboratory or pilot scale, further validation under industrial processing and recycling conditions is required before their practical environmental advantages and suitability for large-scale paper-based packaging applications can be confirmed.

6. Acknowledgment

This research has been supported by the Ministry of Science, Technological Development and Innovation (Contract No. 451-03-34/2026-03/200156) and the Faculty of Technical Sciences, University of Novi Sad through project “Scientific and Artistic Research Work of Researchers in Teaching and Associate Positions at the Faculty of Technical Sciences, University of Novi Sad 2026” (No. 01-3609/1).his research did not receive any specific grant from funding agencies in the public, commercial, or not-for-profit sectors.

7. References

Adak, B. and Teramoto, Y. (2025) 'Poly(butylene adipate-co-terephthalate)/synthetic hectorite clay nanocomposite coated paper-based sustainable barrier materials for packaging application', *Progress in Organic Coatings*, 209, 109549. DOI: 10.1016/j.porgcoat.2025.109549

Battisti, R., Fronza, N., Vargas Júnior, Á., Silveira, S.M. and Damas, M.S.P. (2017) 'Gelatin-coated paper with antimicrobial and antioxidant effect for beef packaging', *Food Packaging and Shelf Life*, 11, pp. 115–124. DOI: 10.1016/j.fpsl.2017.01.009

Bhardwaj, S., Bhardwaj, N.K. and Negi, Y.S. (2021) 'Surface coating of chitosan of different degree of acetylation on non surface sized writing and printing grade paper', *Carbohydrate Polymers*, 269, 117674. DOI: 10.1016/j.carbpol.2021.117674

Calosi, M., D’Iorio, A., Buratti, E., Cortesi, R., Franco, S., Angelini, R. and Bertoldo, M. (2024) 'Preparation of high-solid PLA waterborne dispersions with PEG-PLA-PEG block copolymer as surfactant and their use as hydrophobic coating on paper', *Progress in Organic Coatings*, 193, 108541. DOI: 10.1016/j.porgcoat.2024.108541

Cao, C., Ahn, K., Hong, S.J., Kim, Y.-T., He, Z., Huang, H., Wang, Z., Lee, E. and Shim, Y. (2026) 'Spray-coated polylactic acid/polyhydroxyalkanoate biodegradable bioplastic films on paper: A sustainable strategy for enhancing barrier and mechanical properties', *Progress in Organic Coatings*, 210, 109685. DOI: 10.1016/j.porgcoat.2025.109685

Chi, K., Wang, H. and Catchmark, J.M. (2020) 'Sustainable starch-based barrier coatings for packaging applications', *Food Hydrocolloids*, 103, 105696. DOI: 10.1016/j.foodhyd.2020.105696

Dodangeh, F., Pontillo, A.R.N., Chen, S., Welton, T., Xu, C.C. and Rohani, S. (2026) 'Ionic liquid-regenerated cellulose–chitosan coatings: A bio-based coating for enhancing paper packaging performance', *Surfaces and Interfaces*, 80, 108342. DOI: 10.1016/j.surfin.2025.108342

Du, Y., Liu, J., Wang, B., Li, H. and Su, Y. (2018) 'The influence of starch-based bio-latex on microstructure and surface properties of paper coating', *Progress in Organic Coatings*, 116, pp. 51–56. DOI: 10.1016/j.porgcoat.2017.12.009

Eslami, H. and Mekonnen, T.H. (2023) 'Flexible and green multilayer paper coating for barrier enhancement of paper packaging', *Sustainable Materials and Technologies*, 37, e00694. DOI: 10.1016/j.susmat.2023.e00694

Fadel, S.M., Abou-Elseoud, W.S., Hassan, E.A., Ibrahim, S. and Hassan, M.L. (2022) 'Use of sugar beet cellulose nanofibers for paper coating', *Industrial Crops and Products*, 180, 114787. DOI: 10.1016/j.indcrop.2022.114787

Fang, J., Wang, J., Han, Y., Qi, D. and Chen, T. (2025) 'Bio-based waterproof and oil-repellent coatings for paper packaging: Synergistic effect of oleyl alcohol and chitosan on performance enhancement', *Progress in Organic Coatings*, 208, 109526. DOI: 10.1016/j.porgcoat.2025.109526

Fisher, S.G., Buck, Z., Karim, M.J. and Grunlan, J.C. (2026) 'Fish-based biopolymer complex coacervate coating for improved paper oxygen and water barrier', *Biomacromolecules*, 27(1), pp. 795–804. DOI: 10.1021/acs.biomac.5c02091

Gómez, N., Vergara, P., Fillat, Ú. and Villar, J.C. (2024) 'Effect of metering systems and drying methods on the barrier properties of paper coated with multiple layers of cellulose nanofibres', *Progress in Organic Coatings*, 189, 108323. DOI: 10.1016/j.porgcoat.2024.108323

Haider, Q., Wang, Y. and Li, K. (2026) 'Effect of coating weight on barrier performance and recyclability of solvent based PLA coated paper', *Progress in Organic Coatings*, 220, 110437. DOI: 10.1016/j.porgcoat.2026.110437

Herrera, M.A., Mathew, A.P. and Oksman, K. (2017) 'Barrier and mechanical properties of plasticized and cross-linked nanocellulose coatings for paper packaging applications', *Cellulose*, 24(9), pp. 3969–3980. DOI: 10.1007/s10570-017-1405-8

Jahangiri, F., Mohanty, A.K. and Misra, M. (2024) 'Sustainable biodegradable coatings for food packaging: Challenges and opportunities', *Green Chemistry*, 26(9), pp. 4934–4974. DOI: 10.1039/D3GC02647G

Jeong, S. and Yoo, S. (2020) 'Whey protein concentrate-beeswax-sucrose suspension-coated paperboard with enhanced water vapor and oil-barrier efficiency', *Food Packaging and Shelf Life*, 25, 100530. DOI: 10.1016/j.fpsl.2020.100530

Jin, K., Tang, Y., Liu, J., Wang, J. and Ye, C. (2021) 'Nanofibrillated cellulose as coating agent for food packaging paper', *International Journal of Biological Macromolecules*, 168, pp. 331–338. DOI: 10.1016/j.ijbiomac.2020.12.066

Kuo, C.-T., Chuang, T.-Y. and Liao, Y.-C. (2026) 'Bio-derived photocurable resin for water resistant coatings', *Progress in Organic Coatings*, 212, 109882. DOI: 10.1016/j.porgcoat.2025.109882

Li, H., Qi, Y., Zhao, Y., Chi, J. and Cheng, S. (2019) 'Starch and its derivatives for paper coatings: A review', *Progress in Organic Coatings*, 135, pp. 213–227. DOI: 10.1016/j.porgcoat.2019.05.015

Liu, L., An, X., Zhang, X., Cheng, Z., Guo, J., Nie, S., Cao, H., Liu, H. and Ni, Y. (2023) 'Understanding the versatile roles of cellulose nanocrystals in α-amylase immobilization, starch hydrolysis, colloidal stability and printability towards advanced starch based bio-latex performance', *Chemical Engineering Journal*, 460, 141808. DOI: 10.1016/j.cej.2023.141808

Lors, C., Leleux, P. and Park, C.H. (2025) 'State of the art on biodegradability of bio-based plastics containing polylactic acid', *Frontiers in Materials*, 11, 1476484. DOI: 10.3389/fmats.2024.1476484

Mujtaba, M., Lipponen, J., Ojanen, M., Puttonen, S. and Vaittinen, H. (2022) 'Trends and challenges in the development of bio-based barrier coating materials for paper/cardboard food packaging: A review', *Science of the Total Environment*, 851, 158328. DOI: 10.1016/j.scitotenv.2022.158328

Peng, Y., Guo, J., Gao, Y., Li, X., Ni, M., Shen, X., Chu, Z., Yang, Z. and Hu, Y. (2024) 'Facile preparation of Pickering emulsion-based coatings for hydrophobic, oil-resistant, biodegradable green paper-based packaging', *Food Hydrocolloids*, 149, 109624. DOI: 10.1016/j.foodhyd.2023.109624

Pieters, K. and Mekonnen, T.H. (2024) 'Stable aqueous dispersions of poly(3-hydroxybutyrate-co-3-hydroxyvalerate) (PHBV) polymer for barrier paper coating', *Progress in Organic Coatings*, 187, 108101. DOI: 10.1016/j.porgcoat.2023.108101

Poulose, S., Jönkkäri, I., Hedenqvist, M.S. and Kuusipalo, J. (2024) 'Potato fruit juice – Poly(3-hydroxybutyrate) multi-layer coated paperboards for bio-based packaging', *Progress in Organic Coatings*, 194, 108594. DOI: 10.1016/j.porgcoat.2024.108594

Ruberto, Y., Vivod, V., Juhant Grkman, J., Lavrič, G., Graiff, C. and Kokol, V. (2024) 'Slot-die coating of cellulose nanocrystals and chitosan for improved barrier properties of paper', *Cellulose*, 31(6), pp. 3589–3606. DOI: 10.1007/s10570-024-05847-3

Saini, S., Kardam, S.K., Kadam, A.A., Kumar, V. and Gaikwad, K.K. (2022) 'Green and energy-efficient extraction of cellulose nano-fibrils from rice straw and its coating to improve functional properties of rice straw paperboard made via refiner mechanical pulping', *Progress in Organic Coatings*, 165, 106747. DOI: 10.1016/j.porgcoat.2022.106747

Shankar, S. and Rhim, J.-W. (2018) 'Antimicrobial wrapping paper coated with a ternary blend of carbohydrates (alginate, carboxymethyl cellulose, carrageenan) and grapefruit seed extract', *Carbohydrate Polymers*, 196, pp. 92–101. DOI: 10.1016/j.carbpol.2018.04.128

Shorey, R. and Mekonnen, T.H. (2022) 'High-performance compostable paper coatings from esterified lignin and poly(butylene adipate-co-terephthalate) (PBAT) biocomposites for replacing plastic in packaging applications', *International Journal of Biological Macromolecules*, 209, pp. 472–484. DOI: 10.1016/j.ijbiomac.2022.04.037

Vrabič Brodnjak, U. (2017) 'Experimental investigation of novel curdlan/chitosan coatings on packaging paper', *Progress in Organic Coatings*, 112, pp. 86–92. DOI: 10.1016/j.porgcoat.2017.06.030

Wang, W., Qin, C., Li, W., Ge, J. and Feng, C. (2020) 'Improving moisture barrier properties of paper sheets by cellulose stearoyl ester-based coatings', *Carbohydrate Polymers*, 235, 115924. DOI: 10.1016/j.carbpol.2020.115924

Yi, K., Fu, S., Zhang, H., Zhang, H., Wang, Y. and Huang, Y. (2022) 'Cellulose nanofibrils/polydimethylsiloxane double-layer coating for fabrication of high barrier and excellent water- and oil-resistance paper', *Progress in Organic Coatings*, 172, 107123. DOI: 10.1016/j.porgcoat.2022.107123

Yu, F., Shi, H., Wang, K., Li, H. and Peng, L. (2022) 'Preparation of robust and fully bio-based modified paper via mussel-inspired layer-by-layer assembly of chitosan and carboxymethyl cellulose for food packaging', *International Journal of Biological Macromolecules*, 222, pp. 1238–1249. DOI: 10.1016/j.ijbiomac.2022.09.243

Zhang, R., Tan, J., Ma, T., Xu, M., Chen, W., Zhu, F. and Cao, Y. (2024) 'Developing waste fatty acid-grafted-silicone oil as repulpable, enhanced gas- and water-resistant coating for the paper industry', *ACS Applied Polymer Materials*, 6(19), pp. 11964–11973. DOI: 10.1021/acsapm.4c02086

Zhu, Q., Tan, J., Li, D., Zhang, T., Liu, Z. and Cao, Y. (2023) 'Cross-linked chitosan/tannin extract as a biodegradable and repulpable coating for paper with excellent oil-resistance, gas barrier and UV-shielding', *Progress in Organic Coatings*, 176, 107399. DOI: 10.1016/j.porgcoat.2022.107399



© 2026 Authors. Published by the University of Novi Sad, Faculty of Technical Sciences, Department of Graphic Engineering and Design. This article is an open access article distributed under the terms and conditions of the Creative Commons Attribution license 4.0 Serbia (http://creativecommons.org/licenses/by/4.0/rs/).

Original Scientific Paper https://doi.org/10.24867/GRID-2026-p70

Development and Characterization of PLA/PBAT/Chitosan-Based Biodegradable Films for Active Strawberry Packaging Applications

ABSTRACT

The increasing environmental concerns associated with conventional petroleum-based plastics have accelerated the development of sustainable and biodegradable packaging materials for food preservation applications. In this study, biodegradable films based on poly(lactic acid) (PLA), poly(butylene adipate-co-terephthalate) (PBAT), and chitosan were developed and evaluated as active packaging materials for extending the shelf life of strawberries. Six different film formulations were prepared, including neat PLA, PLA/chitosan, neat PBAT, PBAT/chitosan, PLA/PBAT blend, and PLA/PBAT/chitosan composite films. Chitosan was incorporated for its biodegradability, film-forming ability, UV-blocking properties, and antimicrobial properties, while PLA and PBAT were selected to combine the rigidity of PLA with the flexibility of PBAT. The structural, thermal, and optical properties of the prepared films were characterized using Fourier Transform Infrared Spectroscopy (FTIR), Thermogravimetric Analysis (TGA), and UV–Visible spectroscopy. FTIR analysis was employed to investigate intermolecular interactions among the polymeric components, whereas TGA was used to evaluate the thermal stability and degradation behavior of the films. UV–Vis measurements were conducted to determine the light barrier properties, which are critical for reducing photooxidative deterioration of fresh produce. The color and gloss properties of the obtained films were measured using an X-Rite eXact spectrophotometer. To evaluate the printability performance of the films, flexographic printing trials were conducted using an IGT F1 laboratory printing tester under controlled conditions. Following printing, the colorimetric and gloss characteristics of the printed films were re-evaluated to determine the influence of the film formulations on print quality. The practical applicability of the developed films was assessed through strawberry storage experiments. Changes in weight loss, visual appearance, color retention, firmness, and overall quality parameters were monitored during storage. It is anticipated that incorporating chitosan into PLA/PBAT-based systems will improve barrier properties and enhance strawberry preservation by reducing moisture loss and delaying spoilage. The findings of this study are expected to provide valuable insights into the design of environmentally friendly active packaging materials and demonstrate the potential of PLA/PBAT/chitosan composite films as sustainable alternatives to conventional food packaging systems.

KEY WORDS

Biodegradable packaging, chitosan, strawberry preservation, active food packaging

Hatice Birtane

Marmara University, Department of Chemistry, Faculty of Science, Istanbul, Türkiye

1. Introduction

The widespread use of conventional petroleum-based plastics has created serious environmental concerns, particularly because of their persistence in the environment and dependence on non-renewable fossil resources (Javed et al., 2026). The extensive use of plastics in food packaging has therefore increased the interest in sustainable and biodegradable alternatives. Although the primary function of food packaging is to protect food products from external factors and minimize quality losses during storage, current research has increasingly focused on active packaging systems that can provide additional protective functions (Hussain, Akhter & Maktedar, 2024). Incorporating properties such as antimicrobial activity, reduced ultraviolet (UV) transmission, and controlled moisture and gas transfer into packaging materials can be particularly beneficial for fresh fruits and vegetables with a short shelf life (Kontominas, 2026; Cazón, Mateus & Silva, 2025).

Poly(lactic acid) (PLA) is one of the most extensively studied biodegradable polymers for food packaging applications due to its potential production from renewable resources, biodegradability, good mechanical properties, transparency, and compatibility with conventional thermoplastic processing techniques (Hasoon & Panicker, 2026; Jayaseelan, 2024). Its relatively rigid structure and mechanical strength are advantageous for packaging applications.

However, its limited flexibility and relatively brittle nature can restrict its use in applications where greater toughness and deformability are required. The moisture barrier performance of PLA may also need further improvement depending on the intended application. For these reasons, considerable research has focused on blending PLA with other biodegradable polymers and incorporating functional components to tailor its properties for specific packaging requirements (Olonisakin et al., 2025; Ramli, 2026).

Poly(butylene adipate-co-terephthalate) (PBAT) is an aliphatic–aromatic copolyester that has attracted considerable attention as a flexible biodegradable polymer for packaging applications. Compared with PLA, PBAT generally exhibits higher flexibility, elongation at break, and toughness, which makes it suitable for packaging materials exposed to bending or mechanical deformation. On the other hand, its relatively low stiffness may limit its performance when used alone in applications requiring greater dimensional stability. Combining PLA and PBAT can therefore provide a practical approach for balancing the rigidity and mechanical strength of PLA with the flexibility and toughness of PBAT. The resulting properties of PLA/PBAT blends are strongly influenced by the composition, phase morphology, and interactions between the polymer components.

The incorporation of a natural functional component into such blends may provide an additional means of improving their performance and broadening their potential use in food packaging (Roy et al., 2024; Adeebpasha et al., 2026).

Chitosan is a natural polysaccharide mainly obtained through the deacetylation of chitin and has been widely investigated for food packaging because of its biodegradability, biocompatibility, film-forming ability, and inherent antimicrobial activity. The amino and hydroxyl groups present along its molecular structure can participate in interactions with other polymeric components, allowing the development of films with tailored properties. In particular, the antimicrobial activity of chitosan has made it an attractive component for packaging systems intended to slow microbial growth and extend the shelf life of fresh and processed foods.

Chitosan-containing films may also reduce light transmission and thus provide an additional protective function. However, the hydrophilic nature of chitosan can increase its sensitivity to moisture, which may affect the performance of the resulting films under humid conditions. Incorporating chitosan into more hydrophobic biodegradable polyester matrices such as PLA and PBAT may therefore offer a way to combine the functional characteristics of chitosan with the mechanical and processing advantages of biodegradable polyesters (Kartik, Shelly & Madurai, 2026).

Strawberries are among the fresh fruits that undergo rapid quality deterioration after harvest due to their high respiration rate, susceptibility to microbial growth, moisture loss, softening, and color changes. Their relatively short shelf life makes appropriate packaging particularly important during postharvest handling and storage (Aykanat et al., 2025). Moisture loss can lead to reductions in fruit weight and changes in texture, while microbial growth can accelerate spoilage. Exposure to oxygen and light may further contribute to oxidative deterioration and undesirable color changes. Consequently, packaging films designed for strawberry preservation should ideally provide more than mechanical protection. Control of moisture and gas transfer, reduced light transmission, and antimicrobial activity are desirable characteristics for maintaining strawberry quality during storage. Bringing these functions together in a biodegradable packaging material represents an important approach toward the development of active packaging systems for highly perishable produce (Lin & Jung, 2026).

In addition to food preservation performance, the optical and printing characteristics of packaging films are important from a practical and commercial perspective. Packaging materials not only protect food products but also serve as a surface for product identification, branding, and visual communication with consumers.

Film color, gloss, transparency, and printability can therefore influence the overall applicability of biodegradable packaging materials. Flexographic printing is widely used for flexible packaging because of its suitability for polymeric substrates and its potential for high-speed printing. However, differences in polymer composition and surface characteristics can influence ink transfer as well as the resulting color and gloss of printed films (Kumar et al., 2025). For this reason, evaluating the printing behavior of biodegradable films together with their structural, thermal, and optical properties can provide a more comprehensive assessment of their suitability for practical food packaging applications.

In the present study, six different biodegradable film formulations were developed with the aim of producing sustainable and active packaging materials for strawberry preservation. The formulations consisted of neat PLA, PLA/chitosan, neat PBAT, PBAT/chitosan, PLA/PBAT, and PLA/PBAT/chitosan films. The PLA/PBAT combinations were designed to obtain a more balanced combination of rigidity and flexibility, while the incorporation of chitosan was intended to introduce additional functional characteristics, particularly antimicrobial and light-barrier effects. The chemical structures of the films were investigated by Fourier Transform Infrared Spectroscopy (FTIR), while their thermal stability was evaluated using Thermogravimetric Analysis (TGA). UV–Visible spectroscopy was employed to assess their optical and light-barrier characteristics.

The color and gloss properties of the films were determined using an X-Rite eXact spectrophotometer, and their printability was examined through flexographic printing trials performed with an IGT F1 laboratory printing tester. The color and gloss properties were subsequently re-evaluated after printing to determine the effect of film composition on print quality. Finally, strawberry storage experiments were conducted to assess the practical performance of the developed films under food packaging conditions. Weight loss, visual appearance, color, firmness, and overall quality were monitored throughout storage. In this way, the study aimed to evaluate PLA-, PBAT-, and chitosan-based biodegradable films not only in terms of their material characteristics but also with respect to their printing performance and ability to maintain the quality of a real food product.

2. Methods

Polylactic acid (Mw ~60,000) used as a matrix was supplied from Sigma-Aldrich. Polybutylene adipate terephthalate and chitosan were purchased from Sigma-Aldrich. All solvents used in the experiments were of high purity and were obtained from Sigma Aldrich. Strawberries were obtained from the local agricultural center in Türkiye.

2.1. The preparation of the active packaging films

PLA, PBAT, and PLA/PBAT-based packaging films with and without chitosan were prepared by the solvent casting method. Prior to film preparation, PLA and PBAT pellets were dried under vacuum at 80 °C for 8 h to remove residual moisture.

Six different film formulations were prepared: neat PLA, PLA/chitosan, neat PBAT, PBAT/chitosan, PLA/PBAT, and PLA/PBAT/chitosan.

For the preparation of the PLA films, PLA pellets were dissolved in chloroform under continuous stirring at room temperature until a homogeneous polymer solution was obtained. For the PLA/chitosan formulation, a predetermined amount of chitosan powder was directly added to the PLA solution without prior dissolution.

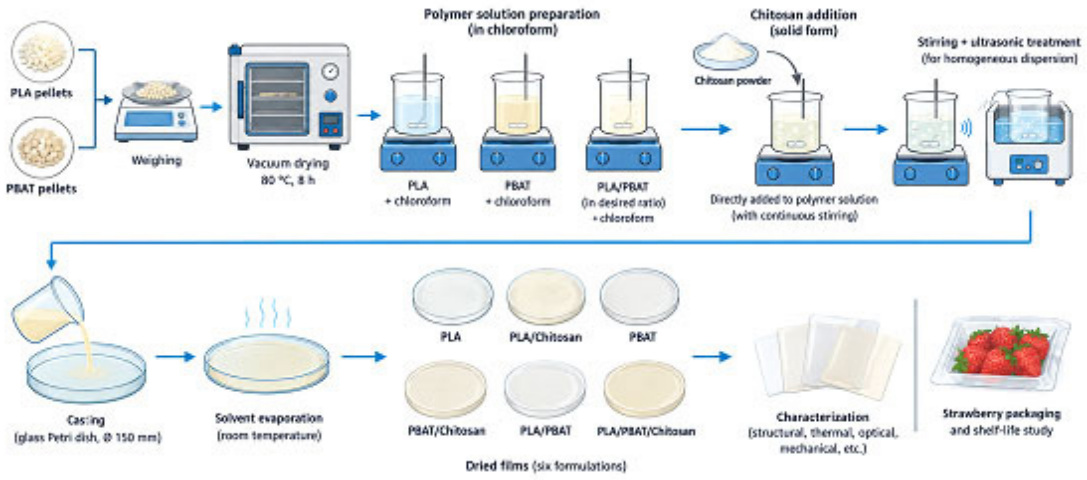
The mixture was continuously stirred to promote the homogeneous dispersion of chitosan within the polymer solution. Similarly, PBAT films were prepared by dissolving PBAT in chloroform, while the PBAT/chitosan formulation was obtained by directly incorporating chitosan powder into the PBAT solution under continuous stirring.

For the PLA/PBAT blend films, predetermined amounts of PLA and PBAT were dissolved in chloroform and mixed thoroughly to obtain a homogeneous polymer blend. For the PLA/PBAT/chitosan formulation, chitosan powder was directly added to the PLA/PBAT solution and dispersed under continuous stirring. In all chitosan-containing formulations, chitosan was incorporated in its solid form and was not subjected to a separate dissolution step.

The resulting film-forming formulations were subjected to ultrasonic treatment to improve the dispersion of chitosan and reduce the formation of visible aggregates.

Subsequently, the formulations were cast onto glass Petri dishes (diameter: 150 mm) and allowed to dry under room conditions until complete solvent evaporation. The dried films were carefully removed from the Petri dishes and stored in a desiccator until further characterization and packaging experiments.

The films were coded according to their compositions as PLA, PLA/Chitosan, PBAT, PBAT/Chitosan, PLA/PBAT, and PLA/PBAT/Chitosan. The neat PLA and PBAT films and the PLA/PBAT blend were used as reference formulations, while the corresponding chitosan-containing films were prepared to investigate the effect of chitosan incorporation on the physicochemical, thermal, optical, and packaging properties of the films. A schematic representation of the film preparation procedure is presented in Figure 1.



» **Figure 1:** *A schematic representation of the film preparation procedure*

2.2. Characterization

Fourier-Transform Infrared Spectroscopy (FTIR) analysis was conducted using a Bruker IFS 66/S spectrometer equipped with ATR capability. Thermal gravimetric analysis (TGA) was performed with a Perkin Elmer STA6000 instrument, with measurements carried out in the temperature range of 30°C to 750°C under a nitrogen atmosphere at a heating rate of 10°C/min. The colors of the obtained nanocomposite packaging films were measured by X-Rite eXact portable spectrophotometer according to the ISO 13655:2017 standard. The measurement conditions of the spectrophotometer were determined as a polarization filter with 0/45° geometry with a 2° observer angle and a D50 light source in the range of 400-700 nm. Color differences were calculated using the CIELab (2000) technique (Equation 1). ISO 11664-6:2014.

Calculations were performed by calculating the average of five measurements. ΔL*, Δa*, and Δb*: Difference in L*, a*, and b* values between the specimen and target colors, respectively. The lightness is represented by the L* axis, which ranges from white to black. The red area is connected to green by the a* axis, whereas the b* axis runs from yellow to blue. (1) Where ΔL*, ΔC*, and ΔH* are the CIEL*a*b* metric lightness, chroma, and hue differences, respectively, calculated between the standard and sample in a pair, and ΔR is the interaction term between the chroma and hue differences. SL, SC, and SH are the weighting functions for lightness, chroma, and hue components. The values calculated for these functions vary according to the positions of the sample pair considered in the CIEL*a*b* color space. The kL, kC, and kH values are the parametric factors to be adjusted according to different viewing parameters, such as textures, backgrounds, and separations, for the lightness, chroma, and hue components. The gloss measurements of all nanocomposite packaging films were carried out with the BYK Gardner GmbH micro gloss 75° geometry by ISO 8254-1:2009.

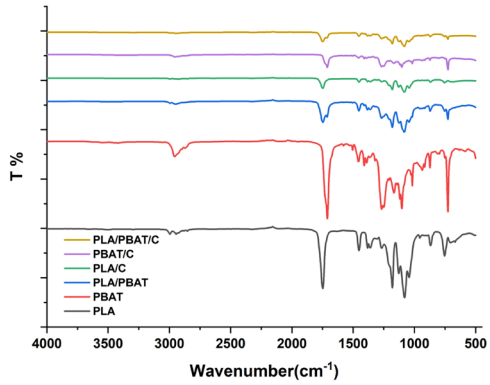
The contact angles of nanocomposite packaging films were found on Pocket Goniometer Model PG-X, version 3.4 (FIBRO Systems AB, Sweden). Surface-free energy was calculated according to the ASTM D5946 standard test method, depending on the water contact angle. The images of droplets were then recorded by using a CCD video camera. The transparency of the nanocomposite packaging films was examined visually. Gravure prints were made on the obtained films with SEIGWERK ethyl alcohol solvent blue 20 seconds viscosity ink at 1m/s printing speed with RK printing proofer, and the color properties of the obtained prints were determined by X-Rite eXact portable spectrophotometer according to the ISO 13655:2017 standard. To examine the storage of fresh strawberry using nanocomposite packaging films, strawberry were obtained from the local agricultural center in Türkiye. Fresh strawberry were characterized by a red color (80 % ripening stage), where unblemished, rot-free, well-formed strawberry were selected. Three selected strawberries of the same maturity were placed in the middle of the dried nanocomposite packaging film with three different contents. The strawberries were tightly wrapped with nanocomposite packaging films. All specimens were stored at room temperature and the same relative humidity and were examined both visually and tactilely daily.

3. Results

3.1. Structural characterization of the packaging films

FTIR spectroscopy was used to investigate the chemical structures and possible molecular interactions among PLA, PBAT, and chitosan in the biodegradable packaging films. Figure 2 presents the FTIR spectra of neat PLA, PLA/chitosan, neat PBAT, PBAT/chitosan, PLA/PBAT, and PLA/PBAT/chitosan films.

The characteristic absorption bands of the individual polymers were observed in the spectra of the corresponding films, confirming the presence of their main functional groups.



» **Figure 2:** *FTIR spectra of neat PLA, PLA/chitosan, neat PBAT, PBAT/chitosan, PLA/PBAT, and PLA/PBAT/chitosan films*

The FTIR spectrum of the neat PLA film showed the characteristic absorption bands associated with its ester groups and aliphatic carbon chains. The bands observed in the region of approximately 2995–2945 cm^{-1} can be assigned to the asymmetric and symmetric stretching vibrations of C–H groups, respectively. The strong absorption band around 1750–1760 cm^{-1} corresponds to the stretching vibration of the ester carbonyl (C=O) groups, which is characteristic of PLA.

The absorption bands observed in the region of approximately 1450–1360 cm^{-1} can be attributed mainly to C–H bending vibrations. In addition, the bands in the range of approximately 1300–1000 cm^{-1} are associated with C–O and C–O–C stretching vibrations of the ester groups in the PLA backbone. These characteristic bands confirm the polyester structure of the PLA film (Alpdoğan et al., 2025).

The spectrum of the neat PBAT film exhibited the characteristic absorption bands associated with its aliphatic and aromatic ester structure. The strong band observed around 1710–1720 cm^{-1} can be attributed to the stretching vibration of the ester carbonyl (C=O) groups. The bands in the region of approximately 2950–2850 cm^{-1} are related to the C–H stretching vibrations of the aliphatic segments. The absorption bands observed in the lower wavenumber region, particularly between approximately 1300 and 1000 cm^{-1}, can be associated with C–O and C–O–C stretching vibrations of the ester groups. In addition, bands related to the aromatic terephthalate units can be observed in the region of approximately 1600–1450 cm^{-1}. The presence of these characteristic absorptions is consistent with the chemical structure of PBAT.

The incorporation of chitosan resulted in additional absorption bands associated with its polysaccharide structure. In the FTIR spectra of the PLA/chitosan, PBAT/chitosan, and PLA/PBAT/chitosan films, the broad band appearing in the region of approximately 3200–3500 cm^{-1} can be assigned to the overlapping O–H and N–H stretching vibrations of chitosan. The bands around 2920–2870 cm^{-1} are associated with C–H stretching vibrations. The characteristic absorption bands of chitosan in the region of approximately 1650–1550 cm^{-1} can be related to the amide I and amide II groups, respectively. Furthermore, the absorption bands observed in the region of approximately 1150–1000 cm^{-1} are mainly associated with C–O–C and C–O stretching vibrations of the polysaccharide backbone. The appearance or increased intensity of these bands in the chitosan-containing films provides evidence for the incorporation of chitosan into the polymeric film matrix.

For the PLA/chitosan films, the characteristic carbonyl band of PLA remained clearly visible, while the broad O–H/N–H absorption associated with chitosan became more pronounced compared with the neat PLA film. Any changes in the position, width, or intensity of these bands may indicate interactions between the hydroxyl and amino groups of chitosan and the ester groups of PLA. Such interactions can occur through hydrogen bonding between the polar functional groups of the two components. However, the absence of a new, distinct absorption band suggests that the incorporation of chitosan does not result in the formation of a completely new chemical structure, but rather promotes intermolecular interactions within the composite film.

A similar behavior was observed for the PBAT/chitosan films. The characteristic carbonyl absorption of PBAT remained detectable after the addition of chitosan, while the broad O–H/N–H stretching region became more prominent. The coexistence of the characteristic bands of PBAT and chitosan indicates that both components were retained in the resulting film structure. Changes in the intensity and/or position of the carbonyl and hydroxyl/amino-related bands can be associated with intermolecular interactions between the polyester matrix and chitosan. These interactions may influence the morphology, mechanical behavior, and barrier characteristics of the resulting films (Alpdoğan et al., 2025).

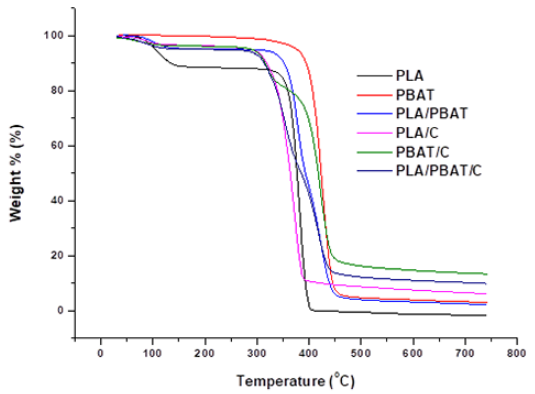
The FTIR spectrum of the PLA/PBAT blend film contained the characteristic absorption bands of both polyesters. In particular, the strong carbonyl absorption associated with the ester groups and the bands attributed to C–H and C–O–C stretching vibrations were maintained after blending. The presence of the characteristic bands of both polymers without the appearance of an entirely new dominant absorption band suggests that the blending process primarily resulted in physical mixing and intermolecular interactions rather than

the formation of new covalent bonds. Nevertheless, changes in peak intensity, broadening, or slight shifts in the characteristic bands may reflect interactions between the PLA and PBAT chains and changes in the local chemical environment within the blend.

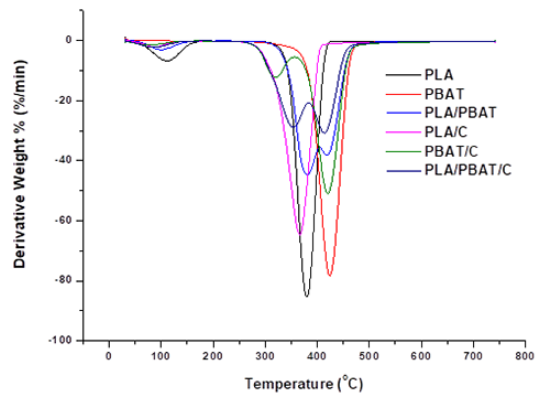
The PLA/PBAT/chitosan film exhibited the characteristic absorption bands of all three components. The ester carbonyl and C–O–C bands originating from PLA and PBAT were observed together with the broad O–H/N–H stretching band and other characteristic absorptions associated with chitosan.

The simultaneous presence of these bands confirms the successful incorporation of PLA, PBAT, and chitosan into the composite film. Compared with the corresponding binary systems, changes in the relative intensity and position of some characteristic bands may indicate increased intermolecular interactions among the three components.

In particular, hydrogen bonding involving the hydroxyl and amino groups of chitosan and the carbonyl groups of PLA and PBAT may contribute to the observed spectral changes.



(a)



(b)

» **Figure 3:** *a) TGA curves of the packaging films, b) DTG curves of the packaging films*

3.2. Thermal characterization of the packaging films

Figure 3 presents the TGA curves of the biodegradable packaging films, while the corresponding thermal analysis results are given in Table 1. All films exhibited a distinct mass loss with increasing temperature, and their thermal degradation behavior varied depending on the film composition.

The main degradation observed for the neat PLA and PBAT films can be attributed to the decomposition of the polyester chains and ester groups. For the PLA/chitosan and PBAT/chitosan films, the degradation of the polysaccharide structure of chitosan occurred together with the degradation of the polyester component. This resulted in changes in the TGA profiles and maximum degradation temperatures of the chitosan-containing films.

The thermal behavior of the PLA/PBAT film reflects the combined degradation characteristics of both polyesters, whereas the PLA/PBAT/chitosan film is influenced by the contribution of all three components. Possible hydrogen bonding between the hydroxyl and amino groups of chitosan and the carbonyl groups of the polyesters may affect the intermolecular interactions within the films and, consequently, their thermal degradation behavior.

The higher residue content at elevated temperatures observed for the chitosan-containing films can be associated with the carbonization tendency of the chitosan structure. Overall, the TGA results indicate that the film formulation has a significant effect on both the thermal degradation temperature and the residual mass at high temperatures (Alpdoğan et al., 2025).

Table 1

TGA results of the packaging films

Formulations	T_5 (°C)	T_{max} (°C)	Char %
PLA	109.71	381.64	0
PBAT	376.65	426.07	3.1
PLA/PBAT	133.99	376.69	2.1
PLA/C	234.42	371.35	6.1
PBAT/C	292.76	423.33	11
PLA/PBAT/C	148.9	348.39	10

3.3. Color properties of the packaging film

The initial visual appearance and post-printing CIE L* a* b* color coordinates of the developed films are presented in Table 2. The neat PLA and PBAT films were visually transparent, whereas the PLA/PBAT film exhibited a white appearance. The incorporation of chitosan changed the visual appearance of the films to a yellowish-white color.

This change indicates that chitosan addition affected the optical characteristics of the polymer matrices and is consistent with the ability of chitosan-containing systems to modify the surface and bulk properties of PLA-based materials (Aydemir, Altay & Akyol, 2021; Gartner, Li & Almenar, 2015).

A particularly important observation was obtained for the chitosan-containing films. Although PLA/chitosan, PBAT/chitosan and PLA/PBAT/chitosan films exhibited a similar yellowish-white appearance before printing, they did not show the same printing behaviour. While PBAT/chitosan could be successfully printed, effective ink transfer was not achieved on PLA/chitosan and PLA/PBAT/chitosan under the applied printing conditions. This finding indicates that the poor printability observed in the latter films cannot be attributed solely to the presence of chitosan. Rather, the effect of chitosan appears to be dependent on the polymer matrix (Izdebska-Podsiadły, 2021).

Ink transfer and adhesion on polymeric substrates are strongly governed by surface chemistry, wettability, surface energy and the compatibility between the ink and substrate. Aydemir, Altay and Akyol (2021) reported that the interaction between inks and polymer substrates is determined by the balance between polar and dispersive interactions, and that compatibility between the surface characteristics of the substrate and the ink is essential for effective wetting and adhesion. Similarly, previous research on flexographic printing of compostable PLA/PBAT films demonstrated that these films may exhibit limitations in ink adhesion, highlighting the importance of substrate surface characteristics in printability (Hansuebsai & Nawakitwong, 2020).

The different behaviors observed among the chitosan-containing films may therefore be related to changes in the surface characteristics generated by the interaction between chitosan and the polyester matrix. Chitosan contains hydroxyl and amino functional groups and can modify the wettability and interfacial characteristics of PLA-based systems. Gartner, Li and Almenar (2015) demonstrated that the incorporation of chitosan into PLA-based structures can substantially affect wettability and interfacial adhesion, while changes in intermolecular interactions can further modify the adhesion behavior. Thus, the presence and distribution of chitosan at the film surface may alter the interaction between the substrate and the solvent-based printing ink.

The successful printing of PBAT/chitosan, despite its yellowish-white initial appearance, is particularly significant. It demonstrates that the initial color of the substrate and the presence of chitosan alone are not sufficient to predict printability. Instead, the final printing response appears to depend on the specific surface characteristics generated by the interaction between the polyester matrix and chitosan.

This matrix-dependent behavior is also consistent with previous studies showing that changes in the surface properties of biodegradable polymer films can significantly influence ink wetting, ink-layer formation and print quality (Aydemir, Altay & Akyol, 2021; Izdebska-Podsiadły, 2021).

Table 2

Visual appearance and CIELAB color coordinates of the films after printing

Film sample	Initial visual appearance	L*	a*	b*	Printing result
PLA	Transparent	17	19	–53	Successful ink transfer
PBAT	Transparent	14	16	–47	Successful ink transfer
PLA/PBAT	White	17	14	–47	Successful ink transfer
PLA/Chitosan	Yellowish-white	78	–1	+10	No effective ink transfer
PBAT/Chitosan	Yellowish-white	27	5	–53	Successful ink transfer
PLA/PBAT/Chitosan	Yellowish-white	80	–2	+8	No effective ink transfer

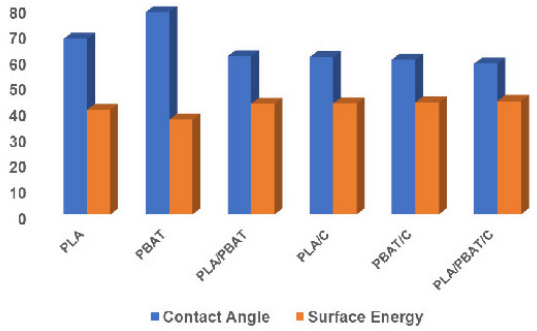
Overall, the colorimetric results clearly distinguish between successful and unsuccessful ink transfer. Successfully printed films exhibited a pronounced color shift towards the blue region, whereas PLA/chitosan and PLA/PBAT/chitosan retained their initial yellowish-white appearance.

These findings demonstrate that CIELAB measurements can provide objective support for the visual assessment of print transfer. More importantly, the contrasting behavior of PBAT/chitosan and PLA/chitosan-based films indicates that the effect of chitosan on printability is matrix-dependent rather than simply related to its presence in the formulation. Therefore, optimization of biodegradable polyester/chitosan films for printing applications should consider not only the bulk formulation but also the surface chemistry, wettability and ink–substrate compatibility.

3.4. Surface properties of the packaging film

The contact angles and surface energy values of the prepared packaging films were investigated, and the results are presented in Figure 4. The contact angle of the neat PBAT film was measured as 78.4°, indicating a relatively hydrophobic surface. In comparison, the neat PLA film exhibited a lower contact angle of 68.0°. The lower contact angle of PLA suggests a relatively higher surface polarity, which is also consistent with its higher surface energy (40.5 mN/m) compared with PBAT (36.7 mN/m).

The incorporation of chitosan resulted in a noticeable decrease in the contact angle of both PLA and PBAT films. The contact angle decreased from 68.0° for neat PLA to 61.0° for PLA/chitosan, while the corresponding surface energy increased from 40.5 to 43.0 mN/m. Similarly, the contact angle of PBAT decreased from 78.4° to 60.0° after the incorporation of chitosan, accompanied by an increase in surface energy from 36.7 to 43.4 mN/m. This behavior can be attributed to the hydrophilic hydroxyl and amino groups present in the chitosan structure, which increase the polarity of the film surface and promote stronger interactions with water.

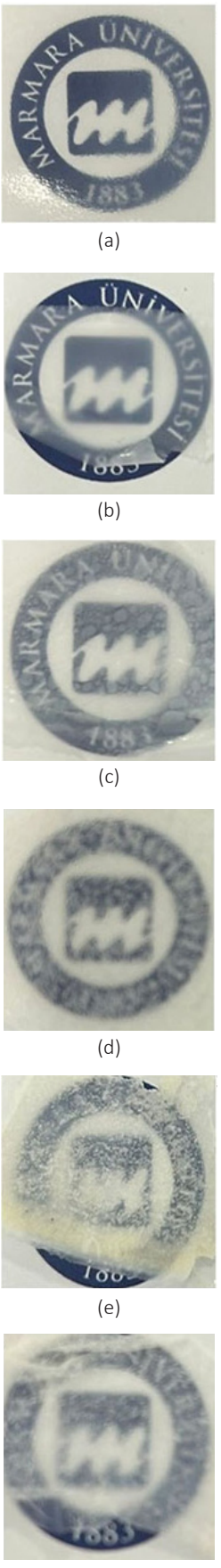


» **Figure 4:** *Contact angles and surface energies of the nanocomposite packaging films*

The PLA/PBAT blend exhibited a contact angle of 61.3° and a surface energy of 42.9 mN/m, indicating that blending the two polyesters substantially increased the surface polarity compared with neat PBAT. The lowest contact angle was observed for the PLA/PBAT/chitosan film (58.4°), which also showed the highest surface energy (43.9 mN/m).

This result indicates that the combined presence of PLA, PBAT, and chitosan produced the most hydrophilic surface among the investigated films. Overall, the decrease in contact angle and the corresponding increase in surface energy following chitosan incorporation suggest that chitosan plays an important role in modifying the surface characteristics of the packaging films. These changes may also influence the wettability, adhesion, and printability of the films, which are important properties for packaging applications.

As illustrated in Figure 5, flexible and translucent packaging films were successfully prepared by the solvent casting method. Among the investigated films, neat PLA exhibited the highest transparency, followed by PBAT and PLA/PBAT films. The relatively high transparency of PLA can be associated with its homogeneous film structure and good optical uniformity. PBAT also showed a relatively transparent appearance, whereas the PLA/PBAT blend exhibited a moderate decrease in transparency, which may be related to differences in the optical properties and phase structure of the two polymers.



» **Figure 5:** *Images of a) PLA, b) PBAT, c) PLA/PBAT, d) PLA/C, e) PBAT/C, and f) PLA/PBAT/C packaging films*

The incorporation of chitosan resulted in a noticeable decrease in the transparency of the films. This effect was observed for both the individual polymers and the PLA/PBAT blend. The reduction in transparency may be attributed to the heterogeneous distribution of chitosan within the polymer matrix and the resulting increase in light scattering at the polymer–chitosan interfaces. In addition, possible intermolecular interactions between chitosan and the polyester matrices may affect the microstructure of the films and contribute to their opaquer appearance. Overall, the results indicate that the optical properties of the prepared films are strongly influenced by both polymer composition and chitosan incorporation, with neat PLA providing the most transparent film among the formulations investigated.

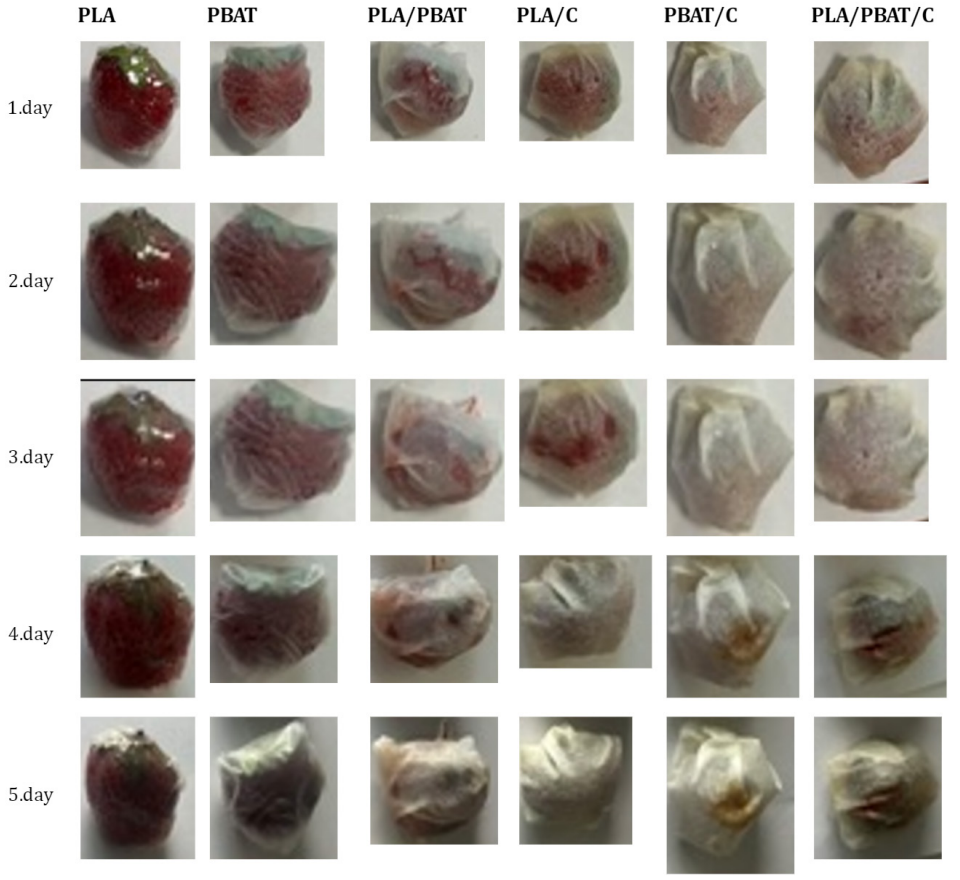
Strawberries are highly perishable fruits with a short postharvest shelf life due to their high moisture content, respiration rate, and susceptibility to microbial deterioration. Therefore, the effect of the prepared packaging films on the preservation of fresh strawberries was evaluated during storage by monitoring changes in their visual appearance, color, weight loss, and overall quality. Figure 6 presents photographs of the strawberries packaged with the prepared films during the storage period. Noticeable differences in the appearance of the strawberries were observed depending on the film composition.

3.5. Storage studies of the nanocomposite packaging film

The strawberries packaged with neat PLA, PBAT, and PLA/PBAT films showed changes in appearance during storage, while the incorporation of chitosan generally helped maintain a better visual appearance.

In particular, the PLA/PBAT/chitosan film provided a more favorable preservation effect, with the strawberries maintaining their fresh appearance for a longer period compared with those packaged with the corresponding polyester films without chitosan. The improved preservation performance of the chitosan-containing films may be associated with the antimicrobial properties of chitosan and its contribution to the barrier characteristics of the packaging system. In addition, the combination of PLA and PBAT may provide a more balanced film structure by combining the rigidity of PLA with the flexibility of PBAT.

Overall, the photographic observations indicate that film composition plays an important role in maintaining strawberry quality during storage. Among the formulations investigated, the PLA/PBAT/chitosan film showed promising potential for extending the visual quality and freshness of strawberries, suggesting that the combination of PLA, PBAT, and chitosan can be advantageous for biodegradable active food packaging applications.



» **Figure 6:** *Photographs of the strawberries packaged with the prepared films during the storage period*

4. Conclusions

In this study, biodegradable PLA, PBAT, and PLA/PBAT-based packaging films containing chitosan were developed by the solvent casting method and evaluated as potential packaging materials for fresh strawberries. The effects of polymer composition and chitosan incorporation on the structural, thermal, surface, optical, and printing properties of the films were investigated, together with their performance during strawberry storage.

The FTIR results confirmed the characteristic functional groups of PLA, PBAT, and chitosan in the corresponding films, while the observed spectral changes suggested intermolecular interactions between the film components. TGA analysis showed that the thermal degradation behavior of the films was affected by their composition, with chitosan incorporation contributing to changes in the degradation profiles and residual mass. Surface characterization revealed that the incorporation of chitosan decreased the contact angle and increased the surface energy of both PLA- and PBAT-based films, indicating an increase in surface polarity. Among the prepared films, neat PLA exhibited the highest transparency, followed by PBAT and PLA/PBAT, whereas the addition of chitosan reduced the transparency of the films.

The prepared films also showed suitable characteristics for printing applications, while their optical and surface properties were influenced by the polymer composition and the presence of chitosan. During strawberry storage, the chitosan-containing films generally provided better preservation of the visual appearance and freshness of the fruit. In particular, the PLA/PBAT/chitosan film showed promising performance in maintaining strawberry quality compared with the corresponding films without chitosan. This behavior can be associated with the antimicrobial character of chitosan and the complementary properties of PLA and PBAT.

Overall, the results demonstrate that the combination of PLA, PBAT, and chitosan can provide biodegradable packaging films with tunable surface, optical, thermal, and functional properties. Among the formulations investigated, PLA/PBAT/chitosan showed considerable potential for fresh strawberry packaging and may represent a promising alternative to conventional petroleum-based packaging materials.

5. References

Adeebpasha, A., Hemavathi, A.B., Hebbar, H.U., Babu, A. and Bindya, S. (2026) 'Development and characterization of PBS and PBAT blend based sustainable films for food packaging applications', *Discover Polymers*, 3. DOI: 10.1007/s44347-026-00061-9

Alpdogan, C., Birtane, H., Cagrı Mehmetoglu, A., Kaya, Y., Beyler Cigil, A. and Sahinbaskan, T. (2025) 'Sustainable active packaging films from PLA and PBAT with thyme oil: Extending the shelf life of cherry tomatoes', *Journal of Applied Polymer Science*, 142. DOI: 10.1002/app.57583

Aydemir, C., Altay, B.N. and Akyol, M. (2021) 'Surface analysis of polymer films for wettability and ink adhesion', *Color Research & Application*, 46, pp. 489–499. DOI: 10.1002/col.22579

Aykanat, B., Genovese, F., Admane, N., Verrastro, V., Sanzani, S.M., Cavalluzzi, M.M. and Matera, A. (2025) 'Effect of different postharvest pre-treatments on the overall quality of organic strawberries during cold storage', *Journal of Agricultural Engineering*, 56. DOI: 10.4081/jae.2025.1752

Cazón, P., Mateus, A.R. and Silva, A.S. (2025) 'Advances in active packaging using natural biopolymers and fruit by-products for enhanced food preservation', *Food Research International*, 213, 116439. DOI: 10.1016/j.foodres.2025.116439

Gartner, H., Li, Y. and Almenar, E. (2015) 'Improved wettability and adhesion of polylactic acid/chitosan coating for bio-based multilayer film development', *Applied Surface Science*, 332, pp. 488–493. DOI: 10.1016/j.apsusc.2015.01.157

Hansuebsai, A. and Nawakitwong, S. (2020) 'Printability analysis of compostable films by flexographic water based ink', *Key Engineering Materials*, 843, pp. 26–32. DOI: 10.4028/www.scientific.net/kem.843.26

Hasoon K.T., N. and Panicker, U.G. (2026) 'Beyond fossil plastics: Next-generation PLA-based bio-packaging for industrial applications – advances, challenges, and data-driven insights', *RSC Advances*, 16, pp. 15095–15118. DOI: 10.1039/d5ra08379f

Hussain, S., Akhter, R. and Maktedar, S.S. (2024) 'Advancements in sustainable food packaging: From eco-friendly materials to innovative technologies', *Sustainable Food Technology*, 2, pp. 1297–1364. DOI: 10.1039/d4fb00084

Izdebska-Podsiadły, J. (2021) 'Effect of plasma surface modification on print quality of biodegradable PLA films', *Applied Sciences*, 11, 8245. DOI: 10.3390/app11178245

Javed, A., Mehmood, W., Bhatnagar, A. and Dessbesell, L. (2026) 'Bio-based plastics in food packaging: Performance, environmental impact, end-of-life, technology readiness level and market trends', *Applied Food Research*, 6, 102219. DOI: 10.1016/j.afres.2026.102219

Jayaseelan, M. (2024) Application of polylactic acid (PLA) in food packaging. In: *Biopolymers in Pharmaceutical and Food Applications*, pp. 79–93. DOI: 10.1002/9783527848133.ch4

Kartik, R., Shelly, K. and Madurai, S.L. (2026) Chitosan-based food packaging materials: A review of fabrication strategies from casting to foaming. In: *Handbook of Bio-based Packaging for Agri-food Applications*, pp. 103–125. DOI: 10.1039/9781839168154-00103

Kehinde Olonisakin, Mohanty, A.K., Mahendra Thimmanagari and Misra, M. (2025) 'Recent advances in biodegradable polymer blends and their biocomposites: A comprehensive review', *Green Chemistry*. DOI: 10.1039/d5gc01294e

Kontominas, M.G. (2026) 'Recent advances in polymeric food packaging materials: Application of biodegradable materials in active and intelligent packaging systems', *Sustainable Food Technology*. DOI: 10.1039/d6fb00206d

Kumar, A., Kumar, A., Wei, S., Chopra, S., Rudra, S.G. and Rabbani, A. (2025) 'Biodegradable and smart packaging films for food quality and safety: A review', *Applied Food Research*, 5, 101491. DOI: 10.1016/j.afres.2025.101491

Lin, C.-Y. and Jung, J. (2026) 'Lignoholocellulose-based biopads from upcycled agri-food byproducts for sustainable clamshell packaging and enhanced strawberry preservation', *Carbohydrate Polymer Technologies and Applications*, 15, 101176. DOI: 10.1016/j.carpta.2026.101176

Ramli, R.A. (2026) 'A critical review of biodegradable polymers for food packaging: Enhancing functionality and environmental sustainability', *Food Research International*, 229, 118497. DOI: 10.1016/j.foodres.2026.118497

Roy, S., Ghosh, T., Zhang, W. and Rhim, J.-W. (2024) 'Recent progress in PBAT-based films and food packaging applications: A mini-review', *Food Chemistry*, 437, 137822. DOI: 10.1016/j.foodchem.2023.137822



© 2026 Authors. Published by the University of Novi Sad, Faculty of Technical Sciences, Department of Graphic Engineering and Design. This article is an open access article distributed under the terms and conditions of the Creative Commons Attribution license 4.0 Serbia (http://creativecommons.org/licenses/by/4.0/rs/).

Review Paper https://doi.org/10.24867/GRID-2026-p71

Ecological Aspects of the Production of Molded Paper Pulp Packaging: Generation and Treatment of Industrial Wastewater

ABSTRACT

The production of packaging from molded paper pulp represents one of the most promising solutions for improving the sustainability of the packaging and graphics industry thanks to the possibility of using recycled fibers, reducing the use of primary raw materials, and contributing to the principles of the circular economy. However, the process of production and recycling of paper pulp is characterized by intensive water consumption and the generation of significant amounts of industrial wastewater containing suspended matter, organic pollutants, lignin residues, chemicals from the processing process, and other contaminants. This review systematizes the available knowledge about the technological stages of production of molded paper pulp packaging, the sources of wastewater, and their potential impact on the environment. Special attention is paid to the role of recycling of paper materials, the application of circular economy principles in the graphic industry, as well as the importance of rational management of water resources during the production process. The basic characteristics of industrial wastewater from the pulp and paper sector are presented, along with an overview of mechanical, chemical, and biological methods of their treatment, with an emphasis on their possibilities, limitations, and contribution to reducing the burden on the environment. Also, modern trends in the development of more environmentally friendly technologies for the production and purification of wastewater are considered, including the reduction of water consumption, the closing of process water cycles, and the application of sustainable technological solutions. Analysis of the available literature indicates that the integration of efficient wastewater treatment systems with sustainable resource management is one of the key prerequisites for reducing the ecological footprint of the graphic and paper industry and the successful implementation of the principles of sustainable development.

Teodora Gvoka
Savka Adamović
Gojko Vladić
Katarina Maričić Picajkić
Gordana Bošnjaković
Gala Golubović

University of Novi Sad, Faculty of Technical Sciences, Department of Graphic Engineering and Design, Novi Sad, Serbia

KEY WORDS
Packaging, industrial wastewater, wastewater treatment, circular economy, sustainable development

1. Introduction

The modern development of the graphic and packaging industry is aimed at finding materials and production processes that, in addition to meeting functional and economic requirements, enable reducing the negative impact on the environment. Special attention is paid to materials based on cellulose fibers, among which packaging made of molded paper pulp represents a significant alternative to conventional packaging materials. Its application is based on the possibility of using recycled paper fibers, a relatively simple shap-

ing process, the possibility of recycling and biodegradability, which opens up space for more efficient inclusion of paper waste in new production cycles (Su et al., 2018; Dey et al., 2020; Semple et al., 2022).

Paper and cardboard packaging occupies an important place in the modern packaging sector, thanks to a wide range of applications, convenience for printing, recyclability, and availability of raw materials. Materials based on cellulose fibers can be shaped into different geometries and adapted to the requirements of protection, transportation, and product presentation. At the same time, the use of recycled fibers allows extending the life cycle of paper materials and reducing the need to use primary raw materials (Kirwan, 2005; Hogarth, 2005; Riley, 2012). The historical development of molded fiber packaging shows that this technology is not new, but its importance is growing in recent years due to the increased need for more sustainable packaging solutions (Wever & Twede, 2007; Didone et al., 2017).

Molded paper pulp is a fibrous suspension that, after preparation and processing of the raw material, is shaped into a suitable product using a mold. Depending on the origin of the fibers, primary or secondary raw materials can be used, whereby recycled paper represents a significant raw material basis for the production of new paper and packaging products. The process of recycling paper includes a series of procedures that remove unwanted components, including residual graphic inks, adhesives, coatings, and other materials, after which the fibers are prepared for reuse (Biermann, 1996; Sixtra et al., 2006; Kirwan, 2011).

The characteristics of molded fibrous materials depend on the properties of the initial raw material, the length and morphology of the fibers, the way they are processed, the conditions of shaping and finishing. Recycled fibers may lose some of their original strength, swelling degree, and other functional characteristics during repeated processing cycles. However, modern processing procedures enable the improvement of material properties and their application in various areas of the packaging industry (Gurav et al., 2003; Vishtal & Retulainen, 2012; Debnath et al., 2022).

Molded paper pulp is of particular importance in the production of protective packaging, transport liners, trays, containers and other shaped packaging elements. The possibility of adjusting the geometry of the product to the requirements of the packaged product, as well as the possibility of combining mechanical protection with a relatively small packaging mass, represents significant advantages of this material. At the same time, the development of new molding technologies, including modern approaches to mold making, further expands the application possibilities of molded fibrous materials in industrial production (Martínez et al., 2016; Didone et al., 2017).

However, the environmental acceptability of molded fiber packaging cannot be viewed only on the basis of the properties of the final product. To assess the overall impact, it is necessary to consider the entire life cycle of the material- from the selection of raw materials and the preparation of fibers, through the production and design of packaging, to its use, recycling, and final disposal. In this context, the secondary flows created during production play a significant role, among which are solid residues and wastewater (Verghese et al., 2011; Silva & Pålsson, 2022).

2. Packaging made of molded paper pulp and recycled fibers

The process of manufacturing molded fiber products can be seen as part of a wider system of cellulose raw materials processing. In the case of primary fibers, the process includes raw material preparation, pulp production, cleaning, possibly bleaching, refining, and preparation for product formation. With recycled paper materials, the process is additionally focused on removing components that are not desirable in the new production cycle. This includes the removal of foreign materials, coating residues, adhesives, ink, and other impurities (Kirwan, 2005; Koch, 2006; Sixtra et al., 2006). Recycling of paper materials allows fibers to be re-introduced into the production system after use, thus reducing the need to use primary raw materials. However, this process simultaneously requires a certain amount of water and energy, and certain phases can lead to the creation of waste streams with an increased content of suspended and dissolved substances. Therefore, the sustainability of recycling should not only be viewed through the amount of reused material, but also through the efficiency of using water, energy, and auxiliary chemicals (Su et al., 2018; Haile et al., 2021).

The composition of the raw material is of particular importance for the quality of the obtained pulp. Different types of paper waste can contain different amounts of ink, coatings, adhesives, and other additives, which is why the proper separation of waste paper is one of the important prerequisites for obtaining high-quality recycled fibers. In addition, the choice of fiber source affects their physical and mechanical characteristics, and therefore the properties of the final packaging (Dey et al., 2020; Semple et al., 2022). The use of recycled cellulose fibers in packaging is related to the concept of replacing materials based on fossil resources with materials from renewable or secondary sources. Cellulosic materials can represent a potential alternative to certain plastic packaging solutions, especially in cases where the required properties of the product can be achieved without the application of complex barrier systems. However, applications requiring increased resistance to moisture,

oil, grease, or gases may require additional coatings or functional layers, thus changing the overall material composition and complexity of the recycling process (Su et al., 2018; Schenker et al., 2021; Semple et al., 2022).

Therefore, modern research is increasingly directed towards the development of cellulosic materials with improved barrier properties, as well as towards the use of alternative fibrous raw materials. In addition to wood fibers, various non-wood plant raw materials and agro-industrial residues are examined, which further expands the potential of circular biomass use in paper and packaging production (Kamoga et al., 2013; Karlovits et al., 2020).

3. Waste generation in the graphic and packaging industry

The graphic industry includes a large number of interconnected processes, from the production of paper and cardboard to printing, finishing, and production of finished graphic and packaging products. During these processes, different types of waste are created, which, according to their origin and characteristics, can be classified into material remains, technological and chemical waste, as well as emissions into the air (Figure 1). Material residues include waste paper and cardboard, scraps and defective products, while technological-chemical waste includes residues of inks, solvents, cleaning agents and various filtrates (Magrini et al., 2020; El Salam, 2023). A special problem is the flows that occur in paper recycling processes. Their composition depends on the origin of waste paper, previous graphic processes, and applied chemical agents. Inks, coatings, and adhesives can reach the water phase during defibering and cleaning, which is why wastewater with a complex composition is formed. In addition to suspended fibers, such waters may contain organic matter and other components originating from the raw material and the technological process (Wen et al., 2016; Hubbe et al., 2016).

Waste management in the graphic industry therefore requires an integrated approach that encompasses all material flows. Prevention of waste generation, rational use of raw materials and water, reuse of materials, and efficient purification of waste streams are interrelated activities. Their goal is not only to reduce the amount of waste, but also to preserve the material and energy value of the resources found in the production system (Tencati et al., 2016; Megale Coelho et al., 2020).

In this sense, the problem of wastewater cannot be separated from the overall industrial waste management system. Water used during production can become a carrier of fibers, ink, adhesives, and other components, so its uncontrolled discharge can represent an additional burden on aquatic ecosystems. The impact of pulp and paper industry wastewater on aquatic ecosystems has been the subject of many years of research, with particular consideration being given to organic load, suspended matter, and the presence of various difficult-to-degrade compounds (Poole et al., 1978; Lindholm-Lehto et al., 2015; Singh et al., 2022).

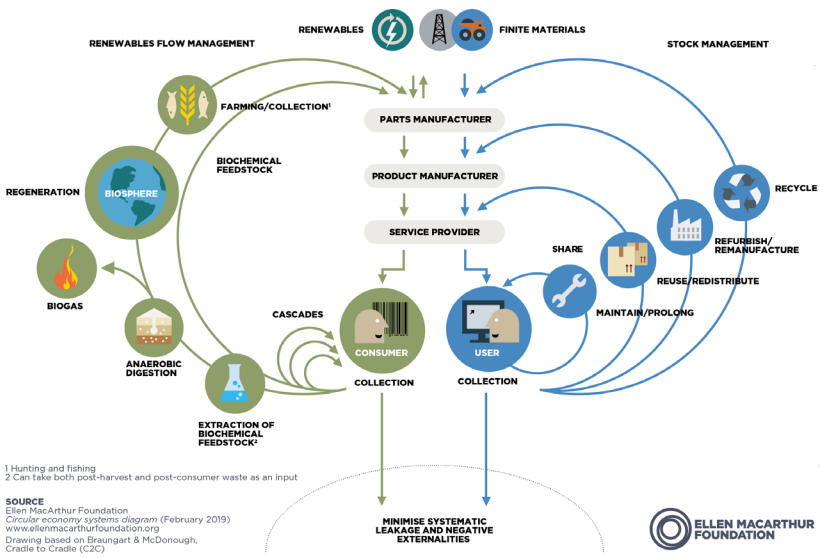
3.1. Circular economy as a framework for materials and waste management

The traditional linear production model is based on the principle of taking natural resources, processing them into products, using them, and finally discarding them. Such a system implies a continuous flow of primary raw materials and the generation of waste after the end of the product's life cycle. In contrast, the circular economy (Figure 2) seeks to keep materials and products in use as long as possible and to reduce the loss of their material value (Geissdoerfer et al., 2017; Korhonen et al., 2018). The concept of circular economy was developed through different approaches to resource management, and in modern literature it is associated with the principles of reducing resource consumption, reuse, recycling, and re-inclusion of materials in production flows (Winans et al., 2017; Popović & Radivojević, 2022). Unlike the linear model, in the circular system waste is not viewed exclusively as the end product of the process, but as a potential secondary raw material whose value can be preserved by appropriate technological procedures.



(a) (b) (c) (d)

» **Figure 1:** *Overview of the different types of waste generated by the graphic industry: a) Material remains (Lundberg Tech, 2026), b) Chemical waste (GMG EnviroSafe, 2026), c) Gas emissions (Future US, 2021), d) Wastewater (EDG Ltd., 2026)*



» **Figure 2:** *Circular economy systems diagram (Ellen MacArthur Foundation, 2019)*

In the graphic industry, the principles of the circular economy can be applied to different levels of the production system. At the level of raw materials, this means increasing the use of recycled fibers and other secondary materials. At the production level, it includes the rationalization of water and energy consumption, the reduction of waste generation, and the optimization of technological processes. At the product level, it involves designing packaging that can be reused, recycled, or otherwise returned to the material cycle (Kirchherr et al., 2017; Silva & Pålsson, 2022). The closure of water courses is of particular importance. In the production of paper and molded fibrous materials, water is an important process resource, which is why the reduction of its consumption and the possibility of reuse after appropriate treatment can contribute to greater system efficiency. Thus, the relationship between packaging production and wastewater treatment is viewed as part of a wider resource management system, rather than as two separate processes. However, the circular economy involves more than just increasing the recycling rate. According to Korhonen et al. (2018), the concept has certain limitations related to the physical limits of material cycles, energy requirements, and the possibility of material quality loss during repeated cycles. Therefore, it is necessary to simultaneously consider the technological, economic, and environmental justification of the proposed solutions (Neves & Marques, 2022).

For the paper and packaging industry, this approach is particularly important, as it enables the connection of paper recycling, fiber reuse, rational water management, and treatment of the generated waste streams into a single system. In this way, the production of molded fiber packaging can be seen as part of a wider strategy of closing material flows.

4. Industrial wastewater

Wastewater is water whose physical, chemical, or biological parameters have changed due to its use in a specific production or other process. Industrial wastewater can have a very complex composition, which depends on the type of industry, the raw materials used, the technological process, and the chemical agents used. Their treatment represents an important segment of environmental protection, especially when the water after use is discharged into a natural recipient or public sewage system (Povrenović & Knežević, 2013).

The characterization of wastewater is the basis for choosing the appropriate treatment procedure. Physical characteristics include, among other things, the content of suspended and dissolved substances, while chemical characteristics refer to the presence of various organic and inorganic components. Chemical oxygen demand (COD) and biochemical oxygen demand (BOD) are especially used to assess the organic load, while the pH value is one of the basic parameters that affects the course and efficiency of numerous treatment processes (Povrenović & Knežević, 2013).

Wastewater from the pulp and paper industry can contain different groups of pollutants. Their composition depends on the production process and the raw materials used, but may include suspended matter, dissolved organic matter, ink, lignin components, and various hard-to-degrade compounds. The complexity of the composition determines the need to combine different purification procedures (Badar & Farooqi, 2012; Hubbe et al., 2016). Therefore, the choice of treatment must be adapted to the characteristics of the specific waste stream. Depending on the degree of pollution, mechanical, physical-chemical, chemical, biological, and advanced oxidation processes can be applied. Com-

bining several procedures enables the achievement of an appropriate degree of purification and can contribute to a more efficient use of water in the production process (Hermosilla et al., 2015; Hubbe et al., 2016).

4.1. Wastewater treatment procedures from the graphic industry

The treatment of industrial wastewater is most often organized as a multi-stage system in which different groups of pollutants are removed by appropriate processes. Mechanical treatments represent one of the initial stages and aim to remove large particles, fibers, and suspended matter. These processes include sieving, filtration, sedimentation, and flotation. Their application can reduce the load on the subsequent stages of treatment and enable more efficient removal of smaller particles and dissolved components (Badar & Farooqi, 2012; Hubbe et al., 2016).

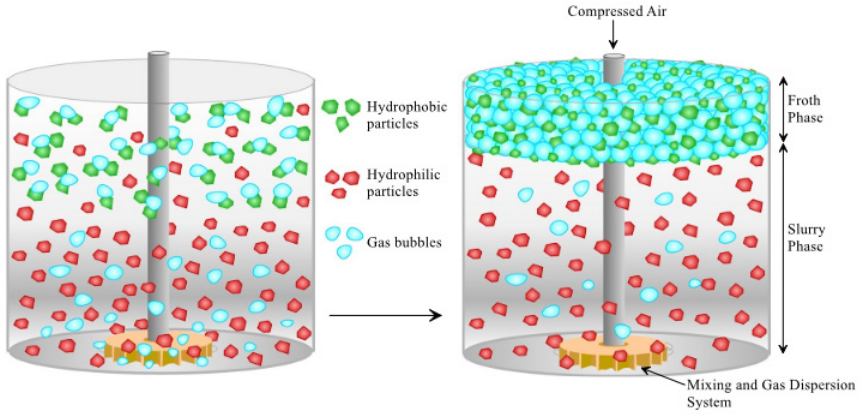
Flotation (Figure 3) is based on the separation of particles that, due to differences in density and interaction with gas bubbles, can be separated on the surface of the water. In systems where light fibrous particles, pigments, or certain organic components are present, flotation can be an effective way to separate them. The application of this procedure is particularly important when it is necessary to reduce the concentration of suspended substances before the next stages of processing.

Coagulation and flocculation belong to physico-chemical procedures that have a significant application in the treatment of industrial wastewater. Coagulation involves the destabilization of colloidal and suspended particles by the addition of a suitable coagulant, while flocculation enables their mutual connection and the formation of larger aggregates, flocs. The resulting flocs can then be separated by settling or flotation (Hubbe et al., 2016; Vasiljević et al., 2023).

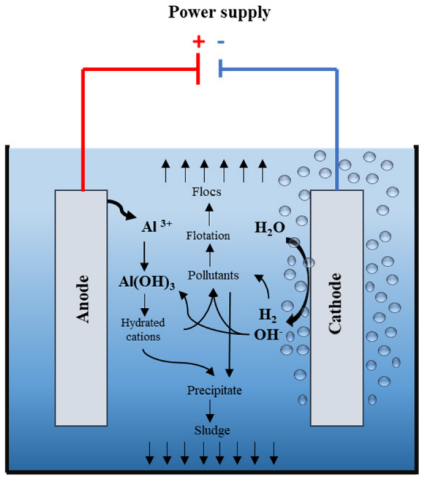
Coagulation processes can be realized using various compounds based on aluminum or iron. The effectiveness of coagulation depends on a number of factors, among which are the characteristics of wastewater, pH value, concentration of pollutants, type and dose of coagulant, as well as time and intensity of mixing. Therefore, the optimal process conditions are most often determined experimentally, using standardized laboratory procedures such as the JAR test (Vasiljević et al., 2023). Polyaluminum chloride is one of the groups of coagulation agents used to remove suspended and colloidal substances from different types of wastewater. Its action is related to the neutralization of particle charges and the formation of hydroxide species that enable the removal of pollutants from the aqueous phase. The influence of pH and coagulant concentration on the efficiency of this process has been confirmed by research on various industrial wastewaters (Zhang et al., 2023). Coagulation can be combined with flocculation and flotation, which enables a more efficient separation of the formed aggregates. Adding a polymeric flocculant can contribute to the creation of larger and more stable flocs, which are more easily separated from the aqueous phase. This combined approach is particularly important in waters with a high content of suspended and organic matter (Vasiljević et al., 2023).

In addition to classical chemical coagulation, electrochemical procedures are also being investigated. Electrocoagulation (Figure 4) enables the creation of coagulation species on site, using electrodes based on aluminum or iron. This procedure is being investigated as a possibility for the treatment of wastewater from the pulp and paper industry, especially due to the potential for the simultaneous removal of suspended and organic matter (Katal & Pahlavanzadeh, 2011; Bassyouni et al., 2023).

Biological treatments represent another important group of processes, especially when wastewater contains biodegradable organic matter. Their effectiveness depends on the biodegradability of the compounds present and the conditions in which the microorganisms perform their function. In the case of pulp and paper industry wastewater, biological processes can be part of combined systems in which previous physicochemical processes reduce the water load (Hubbe et al., 2016; Toritsegbone et al., 2024).



» **Figure 3:** *Schematic diagram of flotation (Pawlik, 2022)*



» **Figure 4:** *Schematic diagram of electrocoagulation (Almukdad et al., 2021)*

Advanced oxidation processes represent an additional possibility for the removal of hard-to-degrade organic compounds. Their application is based on the generation of highly reactive oxidation species that can decompose complex organic molecules. In the pulp and paper industry, the application of various advanced oxidation technologies has been investigated, especially for streams containing resistant organic components (Hermosilla et al., 2015).

The modern approach to the treatment of industrial wastewater increasingly involves combining different methods. Mechanical processes may precede chemical ones, while chemical or physicochemical treatments may be followed by biological treatment or advanced oxidation processes. The choice of combination depends on the initial composition of the water, the required quality after treatment, the possibility of reusing the water, and the requirements for its final disposal (Badar & Farooqi, 2012; Hubbe et al., 2016).

4.2. Wastewater produced in the production of molded fiber packaging

In the context of the production of packaging from recycled paper pulp, the problem of wastewater is particularly related to the fact that the pulping and preparation process takes place in the presence of a significant amount of water. During the process, paper fibers, ink, adhesives, coatings, and other components present in the secondary raw material can pass into the water phase. In this way, the water used in the production process becomes a technological waste stream whose composition depends on the type of input paper and process conditions. Such water represents a characteristic example of the connection of material and water flow in a circular system. On the one hand, paper recycling enables the reuse of cellulose fibers and the extension of their life cycle. On the other hand, the recycling process itself generates wastewater that needs to be treated in order to prevent the transfer of pollutants into the environment. A sustainable system therefore requires simultaneous management of both solid and liquid waste streams.

This is precisely why the treatment of wastewater generated in the production of molded fibrous materials is an important segment of the overall sustainability of this packaging solution. Effective treatment enables the reduction of the concentration of suspended and organic substances, while the possibility of reusing the treated water additionally contributes to the rationalization of the consumption of water resources. At the same time, the resulting sediment and separated fibrous matter can represent a potential secondary material, provided that their composition and quality allow for safe reuse. A review of the available literature shows that the treatment of pulp and paper industry wastewater is increasingly being considered within an integrated resource management system. In addition to the removal of pollutants, the possibility of water regeneration, the use of separated materials, and the reduction of the total consumption of resources are of increasing importance (Hubbe et al., 2016; Haile et al., 2021). Such an approach is in accordance with the basic principles of the circular economy, according to which the goal is to reduce the loss of materials and energy and retain resources in the production system as long as possible.

5. Conclusions

Molded paper pulp packaging represents a material solution that enables the use of recycled cellulose fibers and their re-inclusion in the production cycle. Its characteristics, wide application potential, and recyclability contribute to its importance in the modern development of sustainable packaging. However, the sustainability of this solution cannot be assessed only on the basis of the origin and properties of the final product, but requires consideration of the complete production system, including the consumption of water, energy, auxiliaries and the generation of waste streams.

The production of pulp from recycled paper is associated with the generation of wastewater that may contain fibers, suspended matter, organic components, remnants of ink, adhesives and other pollutants. Therefore, the treatment of these waters represents an important element of managing the impact of the graphic and packaging industry on the environment. Mechanical, physico-chemical, chemical, biological and advanced oxidation processes represent different possibilities, the application of which can be combined depending on the characteristics of the specific waste stream. Coagulation and flocculation are of particular importance, because they enable the destabilization and separation of suspended and colloidal substances,

while combining with flotation can further improve the separation of formed aggregates. The selection of the appropriate coagulant, its dosage, and process conditions is an important part of treatment optimization. At the same time, the possibility of reusing treated water and using separated material opens up additional possibilities for closing material and water flows.

Based on the reviewed literature, it can be concluded that sustainable wastewater management in the production of molded fiber packaging cannot be viewed in isolation from the broader concept of circular economy. Connecting the recycling of paper materials, rational water consumption, appropriate wastewater treatment, and reuse of separated materials is the basis for the development of a more efficient and sustainable production system. In this context, research and optimization of physico-chemical wastewater treatment procedures are important not only from the aspect of achieving the required water quality, but also from the aspect of improving the overall material and ecological efficiency of production.

6. Acknowledgments

This research has been supported by the Ministry of Science, Technological Development and Innovation (Contract No. 451-03-34/2026-03/200156) and the Faculty of Technical Sciences, University of Novi Sad through project “Scientific and Artistic Research Work of Researchers in Teaching and Associate Positions at the Faculty of Technical Sciences, University of Novi Sad 2026” (No. 01-3609/1).

7. References

Badar, S. and Farooqi, I.H. (2012) 'Pulp and paper industry—Manufacturing process, wastewater generation and treatment'. In: Malik, A. and Grohmann, E. (eds.) *Environmental Protection Strategies for Sustainable Development*. Berlin: Springer, pp. 397–436. DOI: 10.1007/978-94-007-1591-2_13

Bassyouni, D., Ali, S., Abdel-Aziz, M.H. and Elashtoukhy, E. (2023) 'Electrocoagulation technique and statistical analysis for treatment of real effluent from the pulp and paper industry', *International Journal of Electrochemical Science*, 18, 100389. DOI: 10.1016/j.ijoes.2023.100389

Biermann, C.J. (1996) *Handbook of Pulping and Papermaking*. 2nd ed. New York: Academic Press. DOI: 10.1016/B978-0-12-097362-0.X5000-6

Debnath, M., Sarder, R., Pal, L. and Hubbe, M.A. (2022) 'Molded pulp products for sustainable packaging: Production rate challenges and product opportunities', *BioResources*, 17(2), pp. 3810–3870. DOI: 10.15376/biores.17.2.Debnath

Dey, A., Sengupta, P., Pramanik, N.K. and Alam, T. (2020) 'Paper and other pulp based eco-friendly moulded materials for food packaging applications: A review', *Journal of Postharvest Technology*, 8(3), pp. 1–21.

Didone, M., Saxena, P., Meijer, E.B., Tosello, G., Bissacco, G., McAloone, T.C., Pigosso, D.C.A. and Howard, T.J. (2017) 'Moulded pulp manufacturing: Overview and prospects for the process technology', *Packaging Technology and Science*, 30(6), pp. 231–249. DOI: 10.1002/pts.2289

El Salam, S.H.A. (2023) 'The impact of the sustainability development on graphic design', *Journal of Heritage and Design*, 3(16), pp. 429–445. DOI: 10.21608/jsos.2022.139798.1249

Geissdoerfer, M., Savaget, P., Bocken, N.M.P. and Hultink, E.J. (2017) 'The circular economy—A new sustainability paradigm?', *Journal of Cleaner Production*, 143, pp. 757–768. DOI: 10.1016/j.jclepro.2016.12.048

Gurav, S.P., Bereznitski, A., Heidweiller, A. and Kandachar, P.V. (2003) 'Mechanical properties of paper-pulp packaging', *Composites Science and Technology*, 63(9), pp. 1325–1334. DOI: 10.1016/S0266-3538(03)00104-0

Haile, A., Gelebo, G.G., Tesfaye, T., Mengie, W., Mebrate, M.A., Abuhay, A. and Limeneh, D.Y. (2021) 'Pulp and paper mill wastes: Utilizations and prospects for high value-added biomaterials', *Bioresources and Bioprocessing*, 8, 35. DOI: 10.1186/s40643-021-00385-3

Hermosilla, D., Merayo, N., Gascó, A. and Blanco, Á. (2015) 'The application of advanced oxidation technologies to the treatment of effluents from the pulp and paper industry: A review', *Environmental Science and Pollution Research*, 22(1), pp. 168–191. DOI: 10.1007/s11356-014-3516-1

Hogarth, C. (2005) 'Moulded pulp packaging'. In: Kirwan, M.J. (ed.) *Paper and Paperboard Packaging Technology*. Oxford: Blackwell Publishing, pp. 414–422.

Hubbe, M.A., Metts, J.R., Hermosilla, D., Blanco, M.A., Yerushalmi, L., Haghighat, F., Lindholm-Lehto, P., Khodaparast, Z., Kamali, M. and Elliott, A. (2016) 'Wastewater treatment and reclamation: A review of pulp and paper industry practices and opportunities', *BioResources*, 11(3), pp. 7953–8091. DOI: 10.15376/biores.11.3.Hubbe

Kamoga, O.L.M., Byaruhanga, J.K. and Kirabira, J.B. (2013) 'A review on pulp manufacture from non wood plant materials', *International Journal of Chemical Engineering and Applications*, 4(3), pp. 144–148. DOI: 10.7763/IJCEA.2013.V4.281

Karlovits, I., Kavčič, U., Lavrič, G., Šinkovec, A. and Zorić, V. (2020) 'Digital printability of papers made from invasive plants and agro-industrial residues', *Cellulose Chemistry and Technology*, 54(5–6), pp. 523–529. DOI: https://doi.org/10.35812/CelluloseChemTechnol.2020.54.53

Katal, R. and Pahlavanzadeh, H. (2011) 'Influence of different combinations of aluminum and iron electrode on electrocoagulation efficiency: Application to the treatment of paper mill wastewater', *Desalination*, 265, pp. 199–205. DOI: 10.1016/j.desal.2010.07.052

Kirchherr, J., Reike, D. and Hekkert, M. (2017) 'Conceptualizing the circular economy: An analysis of 114 definitions', *Resources, Conservation and Recycling*, 127, pp. 221–232. DOI: https://doi.org/10.1016/j.resconrec.2017.09.005

Kirwan, M.J. (2005) 'Paper and paperboard—Raw materials, processing and properties'. In: Kirwan, M.J. (ed.) *Paper and Paperboard Packaging Technology*. Oxford: Blackwell Publishing, pp. 1–49.

Kirwan, M.J. (2011) 'Paper and paperboard packaging'. In: Coles, R. and Kirwan, M.J. (eds.) *Food and Beverage Packaging Technology*. Oxford: Blackwell Publishing, pp. 213–251.

Koch, G. (2006) 'Raw material for pulp'. In: Sixta, H. (ed.) *Handbook of Pulp*. Weinheim: Wiley-VCH, pp. 21–61.

Korhonen, J., Honkasalo, A. and Seppälä, J. (2018) 'Circular economy: The concept and its limitations', *Ecological Economics*, 143, pp. 37–46.

Lindholm-Lehto, P.C., Knuutinen, J.S., Ahkola, H.S.J. and Herve, S.H. (2015) 'Refractory organic pollutants and toxicity in pulp and paper mill wastewaters', *Environmental Science and Pollution Research*, 22(9), pp. 6473–6499. DOI: 10.1007/s11356-015-4163-x

Magrini, C., D'Addato, F. and Bonoli, A. (2020) 'Municipal solid waste prevention: A review of market-based instruments in six European Union countries', *Waste Management & Research*, 38, pp. 1–20. DOI: 10.1177/0734242X19894622

Martínez, K.Y.P., Toso, E.A.V. and Morabito, R. (2016) 'Production planning in the molded pulp packaging industry', *Computers & Industrial Engineering*, 98, pp. 554–566. DOI: 10.1016/j.cie.2016.05.024

Megale Coelho, P., Corona, B., ten Klooster, R. and Worrell, E. (2020) 'Sustainability of reusable packaging—Current situation and trends', *Resources, Conservation & Recycling: X*, 6, 100037. DOI: 10.1016/j.rcrx.2020.100037

Poole, N.J., Wildish, D.J., Kristmanson, D.D. and Waldichuk, M. (1978) 'The effects of the pulp and paper industry on the aquatic environment', *CRC Critical Reviews in Environmental Control*, 8(1–4), pp. 153–195. DOI: 10.1080/10643387709381661

Popović, A. and Radivojević, V. (2022) 'The circular economy—Principles, strategies and goals', *Economics of Sustainable Development*, 6(1), pp. 45–56. DOI: 10.5937/ESD2201045P

Povrenović, D. and Knežević, M. (2013) *Osnove tehnologije prečišćavanja otpadnih voda*. Beograd: Tehnološko-metalurški fakultet.

Riley, A. (2012) 'Paper and paperboard packaging'. In: Emblem, A. and Emblem, H. (eds.) *Packaging Technology—Fundamentals, Materials and Processes*. Oxford: Woodhead Publishing, pp. 178–239.

Schenker, U., Chardot, J., Missoum, K., Vishtal, A. and Bras, J. (2021) 'Short communication on the role of cellulosic fiber-based packaging in reduction of climate change impacts', *Carbohydrate Polymers*, 254, 117248. DOI: 10.1016/j.carbpol.2020.117248

Semple, K.E., Zhou, C., Rojas, O.J., Nkeuwa, W.N. and Dai, C. (2022) 'Moulded pulp fibers for disposable food packaging: A state-of-the-art review', *Food Packaging and Shelf Life*, 33, 100908. DOI: 10.1016/j.fpsl.2022.100908

Silva, N. and Pålsson, H. (2022) 'Industrial packaging and its impact on sustainability and circular economy: A systematic literature review', *Journal of Cleaner Production*, 333, 130165. DOI: 10.1016/j.jclepro.2021.130165

Singh, A.K., Kumar, A. and Chandra, R. (2022) 'Environmental pollutants of paper industry wastewater and their toxic effects on human health and ecosystem', *Bioresource Technology Reports*, 20, 101250. DOI: 10.1016/j.biteb.2022.101250

Sixtra, H., Potthast, A. and Krotschek, A.W. (2006) 'Chemical pulping processes'. In: Sixta, H. (ed.) *Handbook of Pulp*. Weinheim: Wiley-VCH, pp. 109–475.

Su, Y., Yang, B., Liu, J., Sun, B., Cao, C., Zou, X., Lutes, R. and He, Z. (2018) 'Prospects of replacement of some plastics in packaging with lignocellulose materials: A brief review', *BioResources*, 13(2), pp. 4550–4576. DOI: 10.15376/biores.13.2.Su

Tencati, A., Pogutz, S., Moda, B., Brambilla, M. and Cacia, C. (2016) 'Prevention policies addressing packaging and packaging waste: Some emerging trends', *Waste Management*, 56, pp. 35–45. DOI: 10.1016/j.wasman.2016.06.025

Toritsegbone, E.T., Peterson, T.N. and Thobeka, P.M. (2024) 'Exploration of free and immobilized biocatalysts for the treatment of paper industry effluents', *Separation & Purification Reviews*, 54(4), pp. 258–275. DOI: 10.1080/15422119.2024.2382313

Vasiljević, S., Vujić, M., Agbaba, J., Federici, S., Ducoli, S., Tomić, R. and Tubić, A. (2023) 'Efficiency of coagulation/flocculation for the removal of complex mixture of textile fibers from water', *Processes*, 11(3), 820. DOI: 10.3390/pr11030820

Verghese, K., Crossin, E. and Jollands, M. (2011) 'Packaging materials'. In: Verghese, K., Lewis, H. and Fitzpatrick, L. (eds.) *Packaging for Sustainability*. London: Springer, pp. 211–250.

Vishtal, A. and Retulainen, E. (2012) 'Deep-drawing of paper and paperboard: The role of material properties', *BioResources*, 7(3), pp. 4424–4450. DOI: 10.15376/biores.7.3.4424-4450

Wever, R. and Twede, D. (2007) 'The history of molded fiber packaging: A 20th century pulp story'. In: *Proceedings of the 23rd IAPRI Symposium on Packaging*, Windsor, UK, 3–5 September 2007.

Wen, Z., Di, J. and Zhang, X. (2016) 'Uncertainty analysis of primary water pollutant control in China's pulp and paper industry', *Journal of Environmental Management*, 169, pp. 67–77. DOI: 10.1016/j.jenvman.2015.11.061

Winans, K., Kendall, A. and Deng, H. (2017) 'The history and current applications of the circular economy concept', *Renewable and Sustainable Energy Reviews*, 68, pp. 825–833. DOI: https://doi.org/10.1016/j.rser.2016.09.123

Zhang, L., Liu, X., Zhang, M., Wang, T., Tang, H. and Jia, Y. (2023) 'The effect of pH/PAC on the coagulation of anionic surfactant wastewater generated in the cosmetic production', *Journal of Environmental Chemical Engineering*, 11(2), 109312. DOI: 10.1016/j.jece.2023.109312

© 2026 Authors. Published by the University of Novi Sad, Faculty of Technical Sciences, Department of Graphic Engineering and Design. This article is an open access article distributed under the terms and conditions of the Creative Commons Attribution license 4.0 Serbia (https://creativecommons.org/licenses/by/4.0/deed.en).

Original Scientific Paper https://doi.org/10.24867/GRID-2026-p72

Recyclability Assessment of Pressure-Sensitive Labels Made from Agro-Industrial By-Products

ABSTRACT

The growing demand for sustainable packaging materials has increased the use of agro-industrial by-products as alternative fibre sources in packaging production. However, the recyclability of such materials remains an important factor for their successful integration into circular economy systems. This study investigates the recyclability of pressure-sensitive labels (PSLs) containing citrus, barley, and grape agro-industrial fibres. All label materials were printed under identical conditions using conventional offset printing ink. Recycling was performed according to the INGEDE Method 11 under laboratory conditions. For each label type, laboratory sheets were produced from pulp obtained before and after the deinking flotation process. Recycling efficiency was evaluated through measurements of optical properties, including ISO brightness, CIE Lab colour coordinates and opacity. Citrus fibre-based labels exhibited the highest recycling efficiency, showing the greatest increase in brightness and the most effective removal of ink particles. Barley fibre-based labels showed moderate improvements, whereas grape fibre-based labels exhibited the lowest deinking efficiency, with a larger amount of residual ink remaining after flotation. The findings confirm that pressure-sensitive labels manufactured from agro-industrial by-products can be successfully recycled using conventional deinking technology. Nevertheless, the recycling performance is strongly influenced by the type of agro-industrial fibres incorporated into the paper structure, highlighting the importance of considering recyclability during the design of sustainable label materials.*

Marina Vukoje Bezjak
Nika Krajačić
Rahela Kulčar
Katarina Itrić Ivanda

University of Zagreb Faculty of Graphic Arts, Zagreb, Croatia

KEY WORDS
Pressure-sensitive labels, agro-industrial by-products, recycling, circular economy

1. Introduction

The transition from a linear to a circular economy has become one of the key strategies for achieving sustainable development and reducing the environmental impacts associated with industrial production. Unlike the traditional linear model of "take–make–dispose", the circular economy aims to maintain the value of materials and products through reuse, repair, remanufacturing and recycling while minimizing waste generation and the consumption of virgin resources (Meherishi et al., 2019) . Within this framework, packaging plays a crucial role because of its short service life and the large quantities of waste generated after use. Consequently, packaging materials are increasingly being designed according to eco-design principles, taking into account not only their functionality but also their recyclability and compatibility with existing waste management systems (Liu et al., 2023; Meherishi et al., 2019). Paper-based packaging is considered one of the most sustainable packaging materials due to its renewable origin, high recycling rates and well-established collection infrastructure. Approximately 40% of all packaging materials are paper or paperboard, and paper packaging exhibits one of the highest recycling rates among packaging materials.

Nevertheless, successful recycling depends on numerous factors, including fibre composition, printing inks, coatings, adhesives and multilayer structures that may reduce fibre recovery efficiency and deteriorate the quality of recycled pulp (Runte et al., 2015). Therefore, recyclability has become an essential criterion during the design phase of paper-based packaging products. The growing demand for renewable raw materials has stimulated considerable interest in the utilization of agro-industrial by-products as alternative lignocellulosic fibre sources for paper production (Abd El-Sayed et al., 2020). Every year, the agricultural and food industries generate enormous quantities of residues, including grape, banana, coconut, corn, citrus peels and other lignocellulosic wastes that are often disposed of by landfilling or incineration, creating additional environmental burdens. Since these residues contain significant amounts of cellulose and hemicellulose, they represent valuable secondary raw materials that can replace a portion of virgin wood fibres in paper production while simultaneously contributing to waste valorisation and resource efficiency (Alzate Acevedo et al., 2021; Jeetah & Jaffur, 2021; Vallejo et al., 2021). The incorporation of agro-industrial fibres into paper products therefore supports circular economy principles by extending the value chain of agricultural biomass and reducing dependence on forest resources.

Among paper-based packaging products, pressure-sensitive labels (PSLs) represent an important application because they are extensively used in the food, beverage, pharmaceutical and logistics sectors. A pressure-sensitive label typically consists of three functional layers: a facestock, an adhesive layer and a release liner (Kirwan, 2011; Marošević Dolovski, 2016). Although these multilayer structures provide excellent functionality during product use, they also complicate recycling processes (Runte et al., 2015). Adhesives, printing inks and other non-fibrous components may interfere with repulping and deinking, reduce pulp quality and generate contaminants that adversely affect recycled paper production. Consequently, newly developed sustainable label materials should be evaluated not only regarding their functional performance but also with respect to their recyclability.

Recent studies have demonstrated that pressure-sensitive labels manufactured from agro-industrial by-products exhibit promising optical and functional properties while contributing to a reduced environmental footprint. Furthermore, paper products containing agricultural residues have shown potential as sustainable alternatives to conventional wood-based materials (Karlovits et al., 2020; Pogačar & Gregor-Svetec, 2025). However, despite increasing interest in alternative fibre sources, relatively few studies have investigated how these materials behave during recycling processes (Pogačar et al., 2023; Vukoje et al., 2021). Since recyclability is one of the fundamental requirements of circular packaging systems, comprehensive evaluation of recycling performance is necessary before these materials can be widely adopted by industry.

The quality of recycled paper is commonly assessed through laboratory deinking procedures, with flotation representing the most widely applied industrial method for removing hydrophobic ink particles from waste paper (Vukoje & Rožić, 2018). The efficiency of flotation is generally evaluated using optical properties such as ISO brightness, colour coordinates (CIE L*a*b*), opacity and Effective Residual Ink Concentration (ERIC), together with image analysis of residual ink particles. These parameters provide valuable information regarding ink removal efficiency, fibre cleanliness and the overall quality of recycled pulp.

Therefore, the aim of this study was to evaluate the recyclability of pressure-sensitive labels containing agro-industrial by-products originating from citrus grape, and barley residues. Recycling was performed according to the INGEDE Method 11, and the influence of flotation deinking on recycling efficiency was assessed through optical characterization and image analysis of recycled laboratory sheets. The results provide new insights into the suitability of agro-industrial fibre-based pressure-sensitive labels for integration into existing paper recycling systems and contribute to the development of more sustainable packaging materials.

2. Materials and methods

2.1. Pressure-sensitive label materials

Three commercially available paper-based pressure-sensitive labels (PSLs) containing agro-industrial by-products were used in this study. The investigated facestock materials were produced from citrus (C), grape (G) and barley (B) residues. According to the manufacturer's specifications, the facestock consisted of 15% agro-industrial by-products, 40% post-consumer recycled fibres and 45% virgin wood pulp. The citrus fibres originated from residues remaining after juice production, grape fibres from wine production residues, and barley fibres from brewing industry by-products. All label materials were supplied with a glassine release liner (70 g m^{-2}; 61 µm) certified by the Forest Stewardship Council (FSC). The citrus and barley labels were coated with a permanent acrylic emulsion adhesive (S2030), while the grape labels contained a permanent rubber-based hot-melt adhesive (S2047N) (Avery Dennison, Europe). Each label was applied to a cardboard substrate to simulate real packaging conditions, as labels typically enter the recycling stream attached to paper or paperboard packaging.

2.2. Printing procedure

Test samples were printed using a commercial dry-offset printing press designed for pressure-sensitive label production under industrial conditions. A UV-curable warm red offset ink was printed as a full-tone solid on all three label materials. Printing conditions, substrate preparation and curing parameters were maintained constant throughout the experiment to eliminate process-related variability.

2.3. Laboratory recycling

Laboratory recycling was performed according to ISO 21993:2020 standard procedure intended for evaluating the deinkability of printed paper products (ISO, 2020). For each label material, printed samples were manually shredded into small pieces and disintegrated in for 20 min using laboratory disintegrator Enrico Toniolo. Following disintegration, the pulp suspension was homogenized, after which two sets of laboratory sheets were prepared. The first set was produced directly from the pulp suspension without flotation (BF), while the second set was prepared after flotation deinking (F). Flotation was performed in a laboratory flotation cell by introducing air into the suspension, allowing hydrophobic ink particles to attach to air bubbles and be removed as froth. Following flotation, the pulp was homogenized again before sheet formation. Laboratory handsheets with a target grammage of 45 g m^{-2} were prepared using a standard Rapid-Köthen sheet former (ISO 5269- 2, 2004).

2.4. Optical characterization

The recycling efficiency was evaluated by measuring the optical properties of the laboratory sheets obtained from pulp before and after flotation. Measurements were performed using a Technidyne Colour Touch 2 spectrophotometer. ISO brightness (R457) was determined according to ISO 2470 (ISO, 2016), while CIE L*ab** colour coordinates, CIE whiteness were determined according to ISO 11475 and Effective Residual Ink Concentration (ERIC) were determined according to (ISO, 2008) Ten measurements were performed for each sample and the results are reported as the mean value ± standard deviation.

3. Results and discussion

Figure 1 presents representative laboratory handsheets prepared from undeinked (UP) and deinked pulp (DP). Visual examination revealed distinct differences in the morphology of the recycled handsheets. The Citrus samples exhibited uniformly distributed coloured fibres originating from the citrus agro-industrial residues incorporated into the facestock material (Figures 1a and 1b). In contrast, the Barley (Figures 1c and 1d) and Grape samples (Figures 1e and 1f) contained numerous coloured agglomerates that are most likely associated with adhesive-related stickies formed during repulping and insufficiently removed during flotation. These agglomerates were particularly pronounced in the Grape samples, which contained a rubber-based hot-melt adhesive, whereas the Citrus samples showed no comparable adhesive deposits. The observed differences are consistent with the adhesive systems used in the investigated labels. While Citrus and Barley employed the same acrylic emulsion adhesive, Grape contained a rubber-based hot-melt adhesive, which is generally more prone to the formation of larger hydrophobic agglomerates during recycling.



(a)



(b)

» **Figure 1 (part 1):** *Representative handsheets prepared from undeinked and deinked pulps obtained from pressure-sensitive label materials: (a) Citrus – UP; (b) Citrus –DP; (c) Barley – UP; (d) Barley – DP; (e) Grape – UP; (f) Grape – DP*



(c)



(d)



(e)



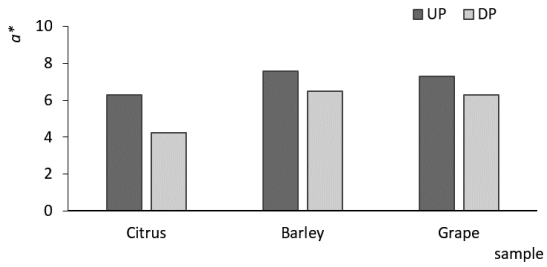
(f)

» **Figure 1 (part 2):** *Representative handsheets prepared from undeinked and deinked pulps obtained from pressure-sensitive label materials: (a) Citrus – UP; (b) Citrus –DP; (c) Barley – UP; (d) Barley – DP; (e) Grape – UP; (f) Grape – DP*

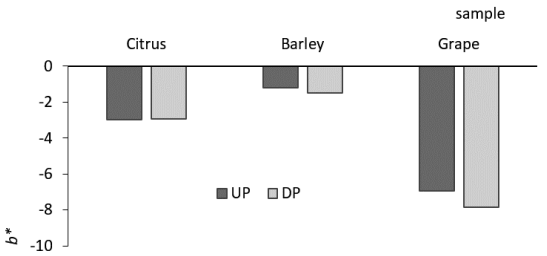
The *a** colorimetric parameter values of the samples produced from undeinked pulp (UP) and deinked pulp (DP) are presented in Figure 2. The positive a values obtained for all samples indicate the presence of a red colour component in the recycled handsheets. Following flotation, the a values decreased for all investigated materials, with the largest reduction observed for citrus. Because the printing ink used in this study was water-based, the decrease in a* should not be interpreted exclusively as the removal of discrete ink particles. During repulping, soluble or finely dispersed colourants may migrate into the fibre network, resulting in partial staining of the cellulose fibres. Consequently, the remaining positive *a** values reflect both residual colourants associated with the fibres and visible coloured contaminants (Vukoje et al., 2021b).

The negative *b** values (Figure 3) indicate a shift toward the blue region of the CIELAB color space. Since the investigated samples were printed with red printing ink and visual assessment confirmed that the papers exhibited a reddish appearance, the observed blue component cannot be attributed to either the printing ink or the inherent color of the paper. Instead, it is most likely associated with the presence of optical brightening agents (OBAs) incorporated into the paper. This interpretation is consistent with our previous study, which demonstrated that the Grape base PSL contained the highest amount of OBAs, followed by Citrus and Barley (Vukoje et al., 2021a). Accordingly, the Grape samples exhibited the most negative *b** values, whereas the Barley samples showed values closest to zero. The agree-

ment between the present and previous findings further supports the contribution of OBAs to the *b** colorimetric parameter and is consistent with the persistence of OBAs in the recycled paper after the deinking process. *The negligible changes in b* after flotation indicate that the optical brightening agents remained associated with the fibre network throughout recycling, as expected for compounds incorporated within the paper structure.

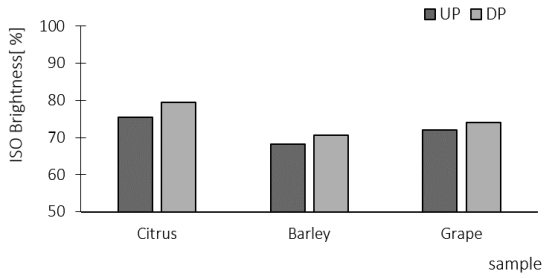


» **Figure 2:** *a* colorimetric parameter of samples obtained from undeinked (UP) and deinked (DP) pulp*



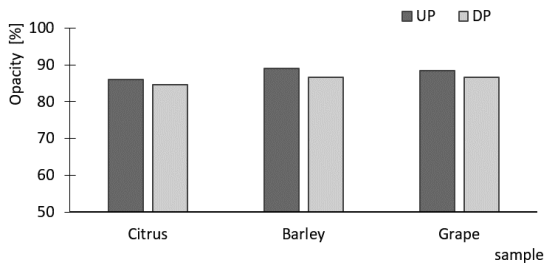
» **Figure 3:** *b* colorimetric parameter of samples obtained from undeinked (UP) and deinked (DP) pulp*

The ISO brightness values (Figure 4) increased for all samples after the deinking process, indicating an improvement in the optical properties of the recycled papers. The increase in ISO brightness is attributed to the removal of the red printing ink during flotation, resulting in higher reflectance at 457 nm. The largest increase was observed for the Citrus sample, which is consistent with the greatest reduction in the **a*** value, suggesting the most effective removal of the red color component. Smaller increases were observed for the Barley and Grape samples, indicating a lower degree of improvement in brightness after deinking. Although ISO brightness increased for all samples after flotation, this increase does not necessarily indicate complete removal of the printing ink. Since water-based colourants may partially stain the fibres, the increase in brightness should rather be interpreted as an overall improvement in optical cleanliness resulting from the removal of coloured contaminants and a reduction in the red colour component.



» **Figure 4:** *ISO Brightness of samples obtained from undeinked (UP) and deinked (DP) pulp*

The opacity values of the papers before and after deinking are presented in Figure 5. A slight decrease in opacity was observed for all samples following the deinking process. The reduction was relatively small, ranging from approximately 1 to 2 percentage points. The decrease in opacity is most likely associated with the loss of mineral fillers during the flotation process. Since fillers contribute significantly to light scattering within the paper structure, their partial removal reduces the opacity of the recycled sheets. Among the investigated samples, Barley exhibited the highest opacity values both before and after deinking, whereas Citrus showed the lowest opacity. The relatively small decrease in opacity indicates that flotation removed only a limited fraction of mineral fillers while preserving the integrity of the fibre network.



» **Figure 5:** *Opacity of samples obtained from undeinked (UP) and deinked (DP) pulp*

To complement the optical measurements, flotation yield was calculated to estimate the amount of material removed during flotation. The flotation yield values are presented in Table 1. The flotation yield was calculated based on the mass of the sample used in the recycling process and the mass of the foam collected as a filter cake on a Büchner funnel. The flotation yield of the samples was calculated using Equation (1):

$$\text{Flotation yield} = \left(1 - \frac{m_p}{m_u}\right) * 100 \qquad (1)$$

Where:

- m_p = mass of the foam, i.e., the filter cake
- m_u = mass of the sample introduced into the recycling process

Table 1
Flotation yield

	C	B	G
m_u, g	100	100	100
m_p, g	25.16	34.20	22.47
Flotation yield, %	74.84	65.80	77.53

Barley exhibited the lowest flotation yield, indicating that the largest amount of material was transferred into the froth fraction. Nevertheless, this was not accompanied by the largest decrease in either the a parameter or ERIC. This suggests that the removed material consisted predominantly of adhesive-derived contaminants, fillers and fines rather than colour-forming components originating from the water-based printing ink. Conversely, Grape exhibited the highest flotation yield but retained the largest number of visible adhesive agglomerates after flotation, indicating that flotation yield alone cannot be used as an indicator of deinking efficiency.

The combined results demonstrate that the recycling behaviour of the investigated labels was governed not only by the printing ink but also by the structural characteristics of the facestock and the adhesive system. The Citrus based PSL material differed fundamentally from the Barley based and Grape based PSL material because the coloured features observed in the recycled handsheets originated predominantly from naturally coloured citrus fibres rather than adhesive-derived contaminants. In contrast, the Barley and Grape based PSL samples contained numerous adhesive-related agglomerates (stickies), indicating that adhesive behaviour during repulping had a greater influence on the visual quality of the recycled sheets than the printing ink itself. These findings demonstrate that visual assessment alone cannot be interpreted as an indicator of residual ink content, since the observed coloured structures originate from different components depending on the investigated label material. Therefore, a comprehensive assessment of recyclability requires the combined interpretation of optical properties, flotation yield and visual examination.

4. Conclusions

The investigated pressure-sensitive labels containing agro-industrial by-products proved compatible with conventional paper recycling by flotation. However, the results demonstrated that the visual appearance of the recycled handsheets was governed by different mechanisms depending on the label material. In Citrus-based labels, the visible coloured structures originated primarily from naturally coloured citrus fibres incorporated into the facestock, whereas the Barley and Grape materials exhibited adhesive-related agglomerates (stickies) remaining after flotation. Furthermore, the water-based printing ink partially coloured the fibre network during repulping, indicating that colourimetric changes cannot be attributed solely to the removal of discrete ink particles. Consequently, the recyclability of agro-industrial pressure-sensitive labels should be evaluated using a combination of optical measurements, flotation yield and visual assessment, while considering the individual contributions of fibres, adhesives and printing ink to the final appearance of the recycled paper.

5. Acknowledgments

This research was supported by the Croatian Science Foundation under project IP-2022-10-3864, CirEiD.

6. References

Abd El-Sayed, E. S., El-Sakhawy, M. and El-Sakhawy, M. A. M. (2020) 'Non-wood fibers as raw material for pulp and paper industry', *Nordic Pulp & Paper Research Journal*, 35, pp. 215–230. DOI: 10.1515/npprj-2019-0064

Alzate Acevedo, S., Díaz Carrillo, Á. J., Flórez-López, E. and Grande-Tovar, C. D. (2021) 'Recovery of Banana Waste-Loss from Production and Processing: A Contribution to a Circular Economy', *Molecules*, 26, 5282. DOI: 10.3390/molecules26175282

ISO (2020) *ISO 21993:2020 Paper and pulp — Deinkability test for printed paper products*. Geneva: International Organization for Standardization.

Jeetah, P. and Jaffur, N. (2021) 'Coconut Husk, a Lignocellulosic Biomass, as a Promising Engineering Material for Non-wood Paper Production', *Journal of Natural Fibers*, 00, pp. 1–15. DOI: 10.1080/15440478.2021.1889428

Karlovits, I., Kavčič, U., Lavrič, G., Šinkovec, A. and Zorić, V. (2020) 'Digital printability of papers made from invasive plants and agro-industrial residues', *Cellulose Chemistry and Technology*, 54, pp. 523–529. DOI: 10.35812/CelluloseChemTechnol.2020.54.53

Kirwan, M. J. (2011) 'Paper and Paperboard Packaging'. In: *Food and Beverage Packaging Technology: Second Edition*. pp. 213–250. DOI: 10.1002/9781444392180.ch8

Liu, W., Zhu, Z. and Ye, S. (2023) 'A Framework Towards Design for Circular Packaging (DfCP): Design Knowledge, Challenges and Opportunities', *Circular Economy and Sustainability*. DOI: 10.1007/s43615-023-00264-3

Marošević Dolovski, A. (2016) 'Etikete i etiketiranje', *Print Magazin*, 4.
Meherishi, L., Narayana, S. A. and Ranjani, K. S. (2019) 'Sustainable packaging for supply chain management in the circular economy: A review', *Journal of Cleaner Production*, 237, 117582. DOI: 10.1016/j.jclepro.2019.07.057
Pogačar, A., Bolanča-Mirković, I. and Gregor-Svetec, D. (2023) 'Print Durability and Recyclability of Label Paper Equipped with Printed RFID Antenna', *Sustainability*, 16, 129. DOI: 10.3390/su16010129
Pogačar, A. and Gregor-Svetec, D. (2025) 'Eco-Friendly Design for Sustainable Gift Packaging', *Applied Sciences*, 15. DOI: 10.3390/app15062973
Runte, S., Putz, H.-J., Bussini, D., Limongi, L. and Elegir, G. (2015) 'Recyclability criteria for paper based packaging products', *Cellulose Chemistry and Technology*, 49, pp. 667–676.
Vallejo, M., Cordeiro, R., Dias, P. A. N., Moura, C., Henriques, M., Seabra, I. J., Malça, C. M. and Morouço, P. (2021) 'Recovery and evaluation of cellulose from agroindustrial residues of corn, grape, pomegranate, strawberry-tree fruit and fava', *Bioresources and Bioprocessing*, 8. DOI: 10.1186/s40643-021-00377-3
Vukoje, M., Bolanča Mirković, I., Babić, A. and Majnarić, I. (2021a) 'The influence of labels on paper recycling'. In: Ćorić, D., Šolić, S. and Ivušić, F. (eds.) *Matrib 2021 - Materials, Tribology and Recycling*. Zagreb: Hrvatsko društvo za materijale i tribologiju (HDMT), pp. 487–498.
Vukoje, M., Itrić Ivanda, K., Kulčar, R. and Marošević Dolovski, A. (2021b) 'Spectroscopic Stability Studies of Pressure Sensitive Labels Facestock Made from Recycled Post-Consumer Waste and Agro-Industrial By-Products', *Forests*, 12(12), 1703. DOI: 10.3390/f12121703
Vukoje, M. and Rožić, M. (2018) 'Various valorisation routes of paper intended for recycling – A Review', *Cellulose Chemistry and Technology*, 52, pp. 515–541.

© 2026 Authors. Published by the University of Novi Sad, Faculty of Technical Sciences, Department of Graphic Engineering and Design. This article is an open access article distributed under the terms and conditions of the Creative Commons Attribution license 4.0 Serbia (http://creativecommons.org/licenses/by/4.0/rs/).

Review Paper https://doi.org/10.24867/GRID-2026-p73

The Role of the Graphic Industry in Extending Garment Lifespan

ABSTRACT

The overconsumption of fast fashion products and hyper-production cycles are considered as significant causes of the increasing amount of textile-related municipal solid waste (MSW). The textile industry is recognized as a substantial contributor to global greenhouse gas emissions, with varying contribution estimates (up to 10%). Systemic solutions and circularity are predominantly proposed, acknowledging that long-term regulations often lead to large-scale implementation of circular economy. This paper aims to explore the contribution of the graphic industry to textile reuse. With that in mind, the 45 studies were chosen for the review based on their emphasis on reusability, in order to gain insight into the possibilities for a person involved in the graphic industry to aim for sustainability regarding textile consumption. Furthermore, this summarization of knowledge may contribute to raising awareness among students and young people through potential workshops focused on the creative reuse of textiles, in order to encourage them to incorporate the principles of reusability into their future projects and workplaces. In the textile industry, reuse is advised as a preferable solution compared to textile recycling and is presented in literature as an extension of the garment's longevity, mainly through collaborative consumption and sharing systems (bartering and lending). The European Union is marked as the leader in terms of textile reuse, with the percentage of textiles reused of around 18%. Serbia, on the other hand, generates roughly 90 000 tons of textile waste per year, and about 81 000 eventually end up in landfill. These findings served as the motivation for conducting this study, with the aim of exploring the potential contribution of the graphic industry to prolonging garment lifespan and promoting textile reuse.

Tamara Ilić
Bojan Banjanin
Jelena Kerac

University of Novi Sad, Faculty of Technical Sciences, Department of Graphic Engineering and Design, Novi Sad, Serbia

KEY WORDS
Sustainability, textile reuse, upcycling, circular economy, graphic industry

1. Introduction

In 2024 in a joint report, ZSL (Zoological Society of London) and WWF (The World Wide Fund for Nature) warned that what we do in the next 5 years (until the year 2029) will determine the future of all life on planet Earth (WWF, 2024). They pointed out that “we” have 5 years to redirect the world towards sustainability before the impact on the environment and climate change lead to irreversible consequences that they consider nearly unimaginable. It may be implied that by “we”, they are not relying on their organizations only, so in this paper we consider ways for us to contribute as well, dominantly in the field of the graphic industry. The WWF suggested that all countries should develop and set in motion nation-wide plans that would include reducing excessive energy usage and greenhouse gas emissions. Investments in the public and private sector are recommended so that the chosen policies would be enacted in the largest possible scope.

Furthermore, certain efforts are being made in order to raise awareness and to educate people about recycling and reduced energy consumption. Although the interest of the general public for recycling has grown, it is considered that in the absence of decisive policies,

it would probably be impossible to avoid a scenario of increased prices of energy, water, raw materials and manufacturing costs. Additionally, approaches established in the 20th century are considered not sustainable enough to satisfy the necessities of the 21st century. Because of that, it is believed that the concept of sustainable growth is the fundamental part of the economic and environmental policies (Chavan, 2014).

In order to understand excessive consumer needs and necessities, the concept of consumerism will be discussed. Consumerism is believed to have its roots in the 18th century but it has reached its current potential in the past few decades, during which both the consumption and discarding of products have increased, to the extent that pleasure and social acceptance is evaluated through consuming (Assadourian et al., 2010). The authors state that:

> *Like a tsunami, consumerism has engulfed human cultures and Earth's ecosystems. Left unaddressed, we risk global disaster. But if we channel this wave, intentionally transforming our cultures to center on sustainability, we will not only prevent catastrophe but may usher in an era of sustainability - one that allows all people to thrive while protecting, even restoring, Earth.*

In their book, Assadourian and associates do not treat enjoyment and engagement as distinct concepts and by using the verb "thrive" they do not focus on any particular dimension of human flourishing, whether financial, ecological, political, or otherwise, instead choosing to leave the phrase open to interpretation by distinguished value systems. Moreover, consumption represents the intermediary, middle-men between identity and values (Ekström & Salomonson, 2014). In their book "Work, Consumerism and the New Poor", author Zygmunt Bauman points out that consumption has replaced labour as the main determinator of social status (Bauman, 2005).

Clothing, apparel and other textile products are marked as elements of symbolic consumption, where people are often under the influence of others while also wishing to consequently be perceived as authentic individuals. In addition, negative aspects of consumption are pointed out, mainly regarding products that are mass produced and purchased in unnecessary quantities (Paço et al., 2020). When making clothing purchasing decisions, consumers rarely take into consideration the impact their actions have on the environment (Hiller Connell, 2010).

Nevertheless, we shouldn't overlook those who adopted different kinds of environmentally responsible behaviours when shopping for clothes.

One should consider whether this behaviour is a privilege for them and whether or not they are renouncing other things in life because of their beliefs. It should also be considered whether they are motivated by internal or external factors. An important aspect of consumer culture regarding textile is the throwaway spirit which can be attributed to a range of factors, including practical ones such as inappropriate clothing size or a lack of storage space, as well as changes in taste or in current clothing trends and the lack of information regarding recycling (Domina & Koch, 2002).

The clothing disposal behaviour bears a significant importance, considering that consumers usually have the autonomy in deciding whether, when and how they dispose of their unwanted clothing, which impacts the amount of created textile waste, the lifespan of the clothing, and the possibility of its reuse and recycling (Laitala, 2014). Additionally, the insufficient storage space and the need to buy new clothing items are recognized as the main motives for certain consumer behaviours (Ha-Brookshire & Hodges, 2009). The fast fashion tendency relying on throwing clothes away after a short period causes impacts to the environment, public health and the economy (Shirvanimoghaddam et al., 2020). Even after embracing the throwaway spirit, consumers can still choose to get rid of their unwanted garments altruistically, by donating them to charity organizations or members of the community in need.

Unlike the linear clothing consumerist model which usually ends in throwing garments away, the circular model is designed to ensure the continuous circulation of resources through repeated cycles with the aim of maximizing their potential for reuse (Bukhari, Carrasco-Gallego & Ponce-Cueto, 2018). Circular economies are not only focused on the amount of waste that ends up in landfills, but also towards establishing a system of deeper synchronicity with natural cycles (Dubey et al., 2019). Furthermore, a circular economy can contribute to community well-being by creating job opportunities and improving existing working conditions, but also by promoting equality and transparency (Ramírez-Escamilla et al., 2024). The importance of including consumers into the whole process by explaining the value of their old clothing that still has usage potential, thus raising collective awareness and nurturing responsible behaviour in consumption are also proclaimed.

The growing awareness of sustainability is reflected in the way consumption and production are approached. Moreover, an increased interest for collaborative consumption among consumers is noticed and among companies as well, as some of them raise awareness on the need for the production of environmentally friendly products (Wagner & Heinzel, 2020). It is concluded that consumer attitudes towards products made in-line with the guiding principles of a circular economy are mostly positive.

Regarding this, one might hypothesize a scenario (Paço et al., 2020) in which all new clothing would be made almost entirely using existing textiles, since the materials such as cotton and polyester can be recycled multiple times and for multiple purposes (Juanga-Labayen, Labayen & Yuan, 2022). Companies have recognized the need to reduce textile waste followed by rising consumer awareness. It is believed that consumers have a significant part in encouraging awareness, which is confirmed by the EU Textile Strategy, in which consumers are recognized as the 4th most important of the "12 core aspects of textile circularity" (EURATEX, 2020):

> *Consumers shall choose what is best for them and the environment. We need educated responsible consumers matching consciousness when purchasing.*

Apart from consumers and companies, governments also share a significant part of the responsibility (Paço et al., 2020). With the goal of reshaping behaviour patterns of textile overconsumption and reducing textile waste, environmentally and financially sustainable long-lasting country-wide programs are recommended (Ekström & Salomonson, 2014). The United Nations have adopted 17 goals and 169 targets in order to encourage countries to prioritise environmental protection and sustainable development and for clothing companies to promote sustainable production models and social responsibility (Abbate et al., 2024). Additionally, the European Commission has announced in 2015 that a circular economy is one of the most important political directions of the EU and that state subsidies should be redirected towards reducing the initial costs of investment into circular business models (Jia et al., 2020).

The French government is questioning the producer responsibility through their Extended Producer Responsibility system (EPR) which requires contribution of textile producers to the management of textile products, including collection, sorting, reuse and recycling (Sandin & Peters, 2018). The French model can be considered as an example for other countries (Bukhari, Carrasco-Gallego & Ponce-Cueto, 2018). Moreover, they have introduced eco taxes, which producers or vendors pay to non-profit organizations like ReFashion for managing textile collection, although they also have been directly fined for not meeting certain goals and targets (Bueno, 2026). As a reason for not meeting their goals, among others, they pointed to the oversaturation of African markets with textiles exported from Western European and Asian countries.

Consumers generally express an interest in environmentally friendly and sustainable consumption, yet their intentions may be hindered by practical challenges, such as higher prices and less comfortable materials. This discrepancy contributes to the gap between consumers' environmental aspirations and their actual consumption practices.

Study participants (Janigo & Wu, 2015) have pointed out the positive experiences in redesigning clothing and design planning. Additionally, they have emphasized the comfort regarding second-hand clothing. On the other hand, it has been partially confirmed that practicality is their main concern, even when participants stated that they prefer second-hand clothing over newer ones.

In other words, even among participants with a high level of environmental awareness, their willingness to invest time and effort in something that does not offer immediate benefits remains uncertain. Furthermore, the connection between the need for instant gratification and the fear of missing out (Noor & Fatihat, 2025) regarding textile reuse and recycling requires further research.

The aim of this paper is to explore the environmental impact of the textile industry and waste and concepts of textile reuse and upcycling, and investigate how knowledge and practices from the graphic industry can contribute to extending the garment lifespan. To address these aims, 45 studies were analysed as part of a mini review examining textile reuse and the potential contribution of the graphic industry.

2. Methods

To address these previously mentioned objectives, the existing literature was reviewed with particular attention given to studies examining the environmental aspects of the textile industry and textile waste, as well as their connections to the graphic industry. The methodology employed in this review involved identifying relevant literature through searches conducted in Scopus and Google Scholar, screening the retrieved studies and selecting those that were subsequently analysed and taken into consideration. These databases were selected with the aim of primarily identifying peer-reviewed publications.

However, the fact that the study was peer-reviewed or not wasn't an excluding factor. The inclusion criteria focused on publications available in the English language, however, studies from any geographical scope were considered. Reports published by prominent organisations were also included, while theses and dissertations mostly weren't included as they were recognized as more relevant to the future workshops.

Furthermore, studies focusing primarily on chemical and mechanical textile recycling were excluded, as the paper primarily focuses on textile reuse and upcycling. Studies revolving around artistic practices or garment tailoring were also excluded.

Additionally, relevant studies identified while screening the reference lists of other publications were included. The literature search employed Boolean search strings, following methodological approaches and key phrases similar to those used by Sandin and Peters (2018), with additional search terms related to the graphic industry, including printing, dyeing, digital technologies, artificial intelligence, and other relevant processes or technologies.

3. Results

A total of 45 studies were selected for the review and attention was given to a state-of-the-art overview of the field, with an emphasis on recent research and emerging technologies. Accordingly, 32 of the selected studies (71.11%) were published between 2020 and 2026, indicating that the majority of the literature reflects relatively recent points of view. In terms of publication type, journal articles constitute the largest share, accounting for 82.22% of the total number of publications. The remaining publications include books, reports and conference papers (2), thesis and web page article (1). The majority of the selected publications were published by publishers including Elsevier, Taylor & Francis, SageJournals, MDPI, Wiley and Springer. From a geographical perspective, publications originating from European countries are particularly relevant due to the geographical and cultural proximity of these countries to the authors' country. The distribution of the selected publications by type is presented in Table 1. The distribution of studies by year is presented in Table 2, which shows the number of publications published each year and their proportion of the total literature. The selected literature can be divided into two thematic areas. The first group of studies focuses primarily on the environmental aspects of the textile industry, textile waste, reuse, and circular economy principles. The second group includes studies addressing the relationship between the textile and graphic industries, either directly or indirectly, including the application of graphic technologies, printing, dyeing and related digital technologies.

Table 1

The distribution of the selected studies by type

Type	Number of studies	Percentage of total studies
Journal Article	37	82.22
Book	2	4.44
Report	2	4.44
Conference Paper	2	4.44
Thesis	1	2.22
Web Page Article	1	2.22
Total	45	100

Table 2

The distribution of the selected studies by year

Year	Number of studies	Percentage of total studies
2002	1	2.22
2005	1	2.22
2009	1	2.22
2010	2	4.44
2014	3	6.66
2015	1	2.22
2018	2	4.44
2019	2	4.44
2020	6	13.32
2021	1	2.22
2022	4	8.88
2023	1	2.22
2024	5	11.10
2025	7	15.54
2026	8	17.76
Total	45	100

4. Discussion

In further discussion, the motives and benefits of mutual engagement and the contributions of the graphics industry, mostly through textile printing and contributions of digital technologies towards sustainability will be considered. A person's intent to behave in a certain way is heavily influenced by cognitive, social, and personal factors. Social factors are considered the most important when analyzing behaviour that can be described as environmentally aware and it is pointed out how extremely difficult and unlikely it is for a person to live excluded from social currents (Wu et al., 2023). Furthermore, environmentally and socially oriented initiatives find their way to individuals who are likely to be interested in them through social media and individuals who feel a strong emotional connection to their community are over time more likely to develop environmental awareness. It has been shown that people are more willing to embrace environmentally aware behaviours when those activities elicit additional satisfaction or a positive emotional outcome. This feeling might be initiated via social media by showing people different ways their donated textile is used. Social media marketers use the platform to promote a certain product, yet not every purchase has to include purchasing a new clothing piece (Mahmood & Khan, 2026).

In the paper "Crafting Wellbeing: Exploring the Link Between Textile Craft and Wellbeing", it is shown that positive emotions can be triggered by designing textiles.

Sewing, knitting and stitching are mentioned as contributing to the transformation of community members for the better and improving general community well-being. Moreover, the program's accessibility and the potential to serve as a creative, artistic outlet which does not require any specific previous formal education are pointed out (McCabe & Maguire, 2026). On the other hand, the subject's frustrations while working with textiles was noticed, for example the fear of failure, stress caused by making mistakes or the difficulty of working with certain materials that are harder to manipulate. However, these frustrations have been shown to contribute to the development of sequential problem solving skills.

The importance of introducing different integrated approaches and interdisciplinarity to the students was considered in order to deepen their understanding of topics such as circularity and sustainability, both in their artistic endeavors and their professional work. Thorough research on the potentials of the curriculum integration was recommended (Mansour et al., 2020).

The contribution of textile and fashion designers was emphasized in the upcycling practice that is considered as one of the most effective ways for people with limited engineering knowledge or skills to contribute (Jiu & Sethi, 2025). Nevertheless, questions remain regarding the consumer acceptance of this type of product in the current market. Posters with recycled clothing were designed (Yin, 2024).

Artistic practices that include reusing textile waste in order to create art pieces were also mentioned, followed by warnings of certain dangers that can arise from inadequate handling of textile waste (Tusaasiirwe, Kwesiga & Njeru, 2025). However, the findings suggest a link between environmental awareness and both the interest in learning about upcycling practices and the willingness to purchase upcycled garments (Bhatt, Silverman & Dickson, 2019). The process of mutual clothing upcycling was explored, as study participants pointed out that previously used or second-hand garments did not cause them any discomfort and were mostly satisfied with the results, stating that they would gladly wear their upcycled products for at least two more years (Janigo & Wu, 2015). Around 52% study participants believe that the process should be promoted as a social experience.

The upcycling process was labeled as a practice that includes different kinds of engagement compared to a tailor's corrections. The acceptance rate of upcycled products by the consumers and the market for them was previously mentioned. Apart from that, quality control becomes significantly more difficult, as quality control systems are generally designed to minimize unexpected outcomes. It is advised that the criterion for quality control should subsequently be redefined when applied to upcycling products (Senevirathne & Kinkini, 2026).

Furthermore, the future clients and consumers expectations influence the market needs along with the specifications and production standards. The reuse and upcycling practices may complicate the production process instead of simplifying it at first. The success of innovative approaches is closely tied to the consumers' perception of a product and the quality of a product is often equated with uniformity (Senevirathne & Kinkini, 2026).

The discovery of mauveine in the 1860s by Henry Perkin marks the rise of synthetic dyes that surpassed the natural ones that dominated the textile industry up until the 19th century, due to their lower price, repeatability and higher affinities towards textiles (Mansour et al., 2020).

The estimated amount of 70 million tons of synthetic dyes are produced each year, with 280.000 tons being released into wastewater, while the textile industry itself utilizes around 10.000 tons every year. Most of the synthetic dyes contain mercury, cadmium, lead and arsenic.

Interest in the use of natural dyes is emerging due to the rising awareness and strict policies (Lara, Cabral & Cunha, 2022). The materials gathered for natural dye extraction are the peelings of beet, Indian fig and ficus leaves as representatives of red, yellow and green pigment, respectively. Optimal conditions for performing the extraction and separation are required, followed by utilization of the appropriate solvent for leaching the pigments out of the plants. To determine the optimal conditions, researchers varied the concentrations, temperatures, pH values and time intervals, in order to achieve consistent and repeatable fabric colouring.

The textile dyeing process is considered a significant water-pollution contributor, accounting for 17-20% of the total water pollution caused by the textile industry. Utilizing pigments extracted from microorganisms, bacteria and fungi, and the production of indigo pigments using Escherichia coli in fermentation reservoirs was considered, resulting in production benefits such as variety of hues and low costs due to the bacteria proliferation (Lara, Cabral & Cunha, 2022).

Researchers have attempted extracting a black pigment from post-consumer textile and plant waste for the purpose of dyeing cotton and their outcomes were compared to those of a conventional black pigment (Iftikhar, Mohsin & Khan, 2026). Pomegranate crust, walnut leaves, coffee sediment and Aleppo pine bark were utilized in a creative process that resulted in the clothing collection called "Hamadryad" inspired by Greek mythology (Gencal Öztürk & Sünter Eroğlu, 2026).

Additionally, around 15-25% of custom mixed screen printing inks remain unused, mostly due to the overestimation and limited possibilities of its reuse, followed by the disposal of garments with unintended printing results.

Abandoning the norm that revolves around rejecting the product due to irregularities or inconsistencies is recommended as a part of a larger paradigm shift that praises designer's creativity in finding ways to transform those irregularities into authentic features. Screen printing is presented as a significant textile waste producer and considered as environmentally challenging, which are the main reasons why digital printing is being advocated for as a potential substitute in the long run (Kulkarni & Dedhia, 2021). However, several reasons for retaining it emerge, smaller initial investments in screen printing have the potential to mobilize unemployed individuals and students, its principles are relatively easily understood and the DIY approach can serve as a playground for textile reuse and upcycling practices.

Digital printing serves as an introduction to other digital technologies and their contribution to textile reuse. Visual prototyping and textile material mock-ups are mentioned as ways of avoiding unnecessary sample production and replacing them with virtual ones for digital evaluation. It is estimated that this approach could reduce waste produced in the prototyping phase by 70% (Cui et al., 2026).

Sorting textile materials and products has been labeled as one of the most demanding contributing processes of textile reuse and recycling since it requires identifying the textile material and sorting it into a specific category depending on certain criteria such as material type, dyeing and/or printing, the presence of buttons, zippers, previously upcycled materials… During textile identification, the morphological differences of fibers might not be distinctive enough, especially when distinguishing synthetic fibers (Baloyi et al., 2024). However, the technique of near-infrared (NIR) spectroscopy is achieving an accuracy higher than 90% when identifying cotton fiber and around 100% for polyester, polyamide, acrylic textile, silk and wool.

When it comes to communities working towards a common goal, crowdfunding practices has emerged a means of collective project financing that usually relies on internet platforms designed by UI/UX designers, developers and copywriters (Pei et al., 2022). The significance of the information and the way they are presented to potential donors and sponsors, along with visual symbols and interactivity has an impact on the success of gathering funds.

When it comes to textile reuse, digital technologies impact the forming connections between individuals who wish to throw their garment away and those who wish to gather them, via digital products such as online second-hand shops. In that case, designers and copyright workers are the ones who partially enable that connection (Nilsson et al., 2025). Additionally, utilizing online platforms and digital tools resulted in a positive effect on consumers towards previously used clothing. It is shown that 42% of study participants declared that they shop for used clothing online while up to 60% of younger participants (age group 18 to 24) displayed the same behaviour (Charnley et al., 2022). Participants pointed out the practicality of the online shopping approach and reported feeling less anxiety about personal hygiene.

Moreover, online platforms offer a clothing collection service, allowing donors to have their used garments collected directly from their addresses which solves the clothing donation impracticality problem revolving around the location of donation containers. However, the problem of trust persists as 55% of study participants (Charnley et al., 2022) point out the lack of trust towards the salesperson in-person, while only 8% place trust in both online and in-person shopping. One of the applications developed to connect sellers and buyers is "Thread Link", which is presented as using a transparent and technologically advanced donation management system relying on the concept of gamification of the process, and including the local community towards responsible clothing donation and sustainable fashion (Chiranjeevi et al., 2025).

The possibilities that tools relying on artificial intelligence bring are mostly considered in the domain of automated quality control and condition assessment of a clothing piece, textile sorting systems and textile waste reduction. However, emerging problems are insufficient datasets and the lack of trained models for these specific fields (Nisa et al., 2025).

The most prominent contributions to the automatisation of quality control, fault detection and sorting processes are deep learning and computer vision methods. Sorting is considered the phase that poses the greatest challenges for automation, considering that it is still predominantly performed manually. Manual sorting is often based on a subjective judgement, consequently resulting in mistakes (Nisa et al., 2025).

Utilizing tools that rely on artificial intelligence finds its niche in market analysis and design optimization in order to explore product longevity, user experience and waste management (Dong, Liang & Suh, 2026). We share the opinion that manual and repeating tasks are the ones that should be delegated or outsourced, not the creative aspects of a job.

The challenges regarding the integration of AI-based tools are mentioned in a form of the availability of datasets which have to be specially designed for the task at hand ensuring a balanced representation of the different classes in the training dataset (Nisa et al., 2025). Precise labeling and listing of details on the given material or fabric gathered for model training is required, as the difficulties in identification and sorting are present, especially for highly reflective textile materials.

Additionally, the challenges are manifested through the process of implementation of complex hybrid systems in small recycling chains. High costs of purchasing machinery and software, the challenges of integrating new technologies and a noticeable resistance to change by the employees and their fears over losing their jobs were noticed (Glogar, Petrak & Mahnić Naglić, 2025).

5. Conclusions

The concept of reuse implies an extension of the clothing lifespan and usually finding a new owner to prolong it. This partially explains the massive garment exports from the global North to the global South. Although the underlying idea of donating surplus clothing from more affluent societies to those in need may seem beneficial, the needs of the countries and communities selected as recipients should be carefully assessed to ensure that such donations are appropriate and genuinely beneficial. With that in mind, the upcycling fashion collection "Return to Sender" by the Ugandan brand "BUZIGAHILL" emerged as a response to mass textile importing, as a way of offering the chance to purchase clothing upcycled as a result of their creativity and resourcefulness.

On the other hand, the aspect of upcycling practices that raises concerns is the subsequent complexity of the upcycled clothing pieces in a form of presence of attached stitches, patches, zippers, buckles, rivets and many more elements which potentially do more harm than good when sorting for potential recycling. The problem of mixed materials is pointed out in the literature and the importance of research on mutually compatible materials which can be processed together in order to strive towards efficiency regarding separation and recycling has emerged.

In the long run, the possibility of installing containers with sorting departments on the University of Novi Sad campus for the purpose of textile donation by students and citizens should be considered. This approach could eventually lead to exploring mechanisms and approaches to textile sorting on the campus, which has repeatedly been marked as the most challenging phase of textile reuse and recycling, further establishing the network of volunteers.

Initial assessment and eventual decision whether the piece is adequate for selling online, donated to charity or used in upcycling workshops would be entrusted to trained volunteers. The approach requires estimation whether it is worth the effort and can it truly make a difference.

A holistic approach to textile recycling and reuse should be considered, having in mind that such an approach is difficult to implement fully from the get go.

The transition towards more circular practices is a time consuming process that involves adaptation and development of new habits. In its initial stages, sorting, reuse and upcycling may have limited impact and even seem counterproductive. However, developing these practices over time is very beneficial for establishing sustainability and circularity in the long run. For this reason, it is particularly important to determine the level of interest in such practices among students, young people and citizens of Novi Sad, Serbia. Understanding their attitudes and perception towards second-hand and donated clothing and their willingness to engage in sorting and donation practices can provide valuable insight into the potential for developing a more circular approach. Equally important is identifying the degree of distrust or reluctance towards such practices, including the barriers that may prevent people from adopting them in the first place.

To achieve that, the people who already practice circularity and awareness should be identified in order to find out about their habits and occupations and how to approach them, to find out whether these ideas could receive support from the local government and if there is any possible financial aid for this type of project. It is also important to find out how many citizens might be interested in buying garments that have been renewed by upcycling practices. The interest of the members of the graphic industry in contributing and finding volunteers who would contribute in their own creative ways should be assessed.

Potential buyers of upcycled clothing should be surveyed in order to find out how they would perceive the potential modifications and be aware of students' opinions on reused clothing. Appropriate methods for approaching those in need should be considered, along with how social media might help the visibility of such projects. Additionally, ways of gaining trust and support of our community and subsequent guidance towards donating or even actively participating should be considered.

The challenges associated with work allocation and logistics in volunteer-based initiatives should be assessed, along with the potential for textile industry companies to offer incentives to individuals who donate their clothing. In light of modern trends, the act of donating and participating in workshops might be gamified in order to maintain both individual and collective engagement, particularly among younger people.

The need to answer some of these questions is the need to abandon the paradigm which centers on optimization and automatization exclusively, and replace it with an approach that explores the values of our fellow citizens, students, donors, volunteers, workshop members, graphic and fashion designers, local news agencies, and all of the values that shape our production processes and artistic practices.

"This year's State of the World report is a cultural mindbomb exploding with devastating force. I hope it wakes a few people up."
Kalle Lasn

6. Acknowledgments

This research has been supported by the Ministry of Science, Technological Development and Innovation (Contract No. 451-03-34/2026-03/200156) and the Faculty of Technical Sciences, University of Novi Sad through project "Scientific and Artistic Research Work of Researchers in Teaching and Associate Positions at the Faculty of Technical Sciences, University of Novi Sad 2026" (No. 01-3609/1).

7. References

Abbate, S., Centobelli, P., Cerchione, R., Nadeem, S.P. and Riccio, E. (2024) 'Sustainability trends and gaps in the textile, apparel and fashion industries', *Environment, Development and Sustainability*, 26, pp. 2837–2864. DOI: 10.1007/s10668-022-02887-2

Assadourian, E., Amodeo, M., Andersen, R., Anderson, R., Andrews, C., Aubel, J., Bates, A., Bortz, W., Costanza, R., Cullinan, C., Dawson, J., de Graaf, J., Engelman, R., Farley, J., Finkelpearl, S., Ganly, K., Gardner, G., Han, A., Hartzfeld, J., Hemenway, T., Kaga, Y., Kubiszewski, I., Linn, S., Mair, J., Maniates, M., Miller, P., Morgan, K., Newman, P., Orr, D.W., Renner, M., Sachs, J., Samuelsson, I., Schor, J., Shuman, M.H., Sonnino, R., Urbanska, W., Starke, L. and Mastny, L. (2010) *State of the World 2010: Transforming Cultures From Consumerism to Sustainability*. Princeton: Princeton University Press.

Baloyi, R.B., Gbadeyan, O.J., Sithole, B. and Chunilall, V. (2024) 'Recent advances in recycling technologies for waste textile fabrics: a review', *Textile Research Journal*, 94(3-4), pp. 508–529. DOI: 10.1177/00405175231210239

Bauman, Z. (2005) *Work, Consumerism and the New Poor*. 2nd ed. Maidenhead: McGraw-Hill Education.

Bhatt, D., Silverman, J. and Dickson, M.A. (2019) 'Consumer interest in upcycling techniques and purchasing upcycled clothing as an approach to reducing textile waste', *International Journal of Fashion Design, Technology and Education*, 12(1), pp. 118–128. DOI: 10.1080/17543266.2018.1534001

Bukhari, M.A., Carrasco-Gallego, R. and Ponce-Cueto, E. (2018) 'Developing a national programme for textiles and clothing recovery', *Waste Management & Research: The Journal for a Sustainable Circular Economy*, 36(4), pp. 321–331. DOI: 10.1177/0734242X18759190

Bueno, P. (2026) *French Authorities Impose €170,000 Fine on Refashion for Waste Management Breaches*. Modaes, The Global Fashion Business Journal. Available from: https://www.modaes.com/global/companies/france-fines-refashion-170000-euros-for-textile-waste-collection-failures [Accessed 30 August 2026].

Charnley, F., Knecht, F., Muenkel, H., Pletosu, D., Rickard, V., Sambonet, C., Schneider, M. and Zhang, C. (2022) 'Can Digital Technologies Increase Consumer Acceptance of Circular Business Models? The Case of Second Hand Fashion', *Sustainability*, 14(8), 4589. DOI: 10.3390/su14084589

Chavan, R.B. (2014) 'Environmental Sustainability through Textile Recycling', *Journal of Textile Science & Engineering*, S2, 007. DOI: 10.4172/2165-8064.S2-007

Mondikathi, C., Lohitha, C.V., Roshni, S., Ganesh, G., Naga Anjaneyulu, B. and Gopinadh, K. (2025) 'Thread Link: An IoT-enabled smart cloth donation system with GSM-based SMS notifications', *International Journal of Advanced Research*, 13(11), pp. 176–184. DOI: 10.21474/IJAR01/22221

Cui, P., Liu, C., Jin, S., Liu, Q., Luo, J. and Xue, Y. (2026) 'Minimizing textile waste through virtual prototyping: A digital color and texture simulation framework for chenille fabrics', *Cleaner Engineering and Technology*, 33, 101261. DOI: 10.1016/j.clet.2026.101261

Domina, T. and Koch, K. (2002) 'Convenience and Frequency of Recycling: Implications for Including Textiles in Curbside Recycling Programs', *Environment and Behavior*, 34(2), pp. 216–238. DOI: 10.1177/0013916502342004

Dong, W., Liang, J. and Suh, S. (2026) 'Effectiveness of AI Technologies in Reducing Textile Waste in the Fashion Industry', *Textile Research Journal*, 96(3-4), pp. 428–451. DOI: 10.1177/00405175251357582

Dubey, R., Gunasekaran, A., Childe, S.J., Papadopoulos, T. and Helo, P. (2019) 'Supplier relationship management for circular economy: Influence of external pressures and top management commitment', *Management Decision*, 57(4), pp. 767–790. DOI: 10.1108/MD-04-2018-0396

Ekström, K.M. and Salomonson, N. (2014) 'Reuse and Recycling of Clothing and Textiles—A Network Approach', *Journal of Macromarketing*, 34(3), pp. 383–399. DOI: 10.1177/0276146714529658

EURATEX. (2020) *12 Specific Points to Make the EU Textile Circular Economy Happen*. Brussels: EURATEX. Available from: EURATEX – 12 Specific Points to Make the EU Textile Circular Economy Happen [Accessed 24 August 2026].

Gencal Öztürk, R.Z. and Sünter Eroğlu, N. (2026) 'Utilization of Natural Dyes for the Development of Screen-Printing Sustainable *Textiles*', Textiles, 6(3), 80. DOI: 10.3390/textiles6030080

Glogar, M., Petrak, S. and Mahnić Naglić, M. (2025) 'Digital Technologies in the Sustainable Design and Development of Textiles and Clothing—A Literature Review', *Sustainability*, 17(4), 1371. DOI: 10.3390/su17041371

Ha-Brookshire, J.E. and Hodges, N.N. (2009) 'Socially Responsible Consumer Behavior?: Exploring Used Clothing Donation Behavior', *Clothing and Textiles Research Journal*, 27(3), pp. 179–196. DOI: 10.1177/0887302X08327199

Hiller Connell, K.Y. (2010) 'Internal and external barriers to eco-conscious apparel acquisition', *International Journal of Consumer Studies*, 34, pp. 279–286. DOI: 10.1111/j.1470-6431.2010.00865.x

Iftikhar, K., Mohsin, M. and Khan, A. (2026) 'Development and performance improvement of bio-based black pigment for textile printing by upcycling of textile and plant waste', *Pigment & Resin Technology*, pp. 1–9. DOI: 10.1108/PRT-05-2025-0057

Janigo, K.A. and Wu, J. (2015) 'Collaborative Redesign of Used Clothes as a Sustainable Fashion Solution and Potential Business Opportunity', *Fashion Practice*, 7(1), pp. 75–97. DOI: 10.2752/175693815X14182200335736

Jia, F., Yin, S., Chen, L. and Chen, X. (2020) 'The circular economy in the textile and apparel industry: A systematic literature review', *Journal of Cleaner Production*, 259, 120728. DOI: 10.1016/j.jclepro.2020.120728

Jiu, Z. and Sethi, M.H. (2025) 'Is Upcycling the Best Approach for Designers to Contribute to Sustainable Textile Industry?', *TEXTILE*, 23(2), pp. 276–288. DOI: 10.1080/14759756.2025.2465167

Juanga-Labayen, J.P., Labayen, I.V. and Yuan, Q. (2022) 'A Review on Textile *Recycling* Practices and Challenges', Textiles, 2(1), pp. 174–188. DOI: 10.3390/textiles2010010

Kulkarni, A.N. and Dedhia, E.M. (2021) 'Management of Digital Printing Ink Waste with Cotton Fabric using Screen Printing Method', *Journal of Scientific Research*, 65(4), pp. 186–189. DOI: 10.37398/JSR.2021.650430

Laitala, K. (2014) 'Consumers' clothing disposal behaviour – a synthesis of research results', *International Journal of Consumer Studies*, 38, pp. 444–457. DOI: 10.1111/ijcs.12088

Lara, L., Cabral, I. and Cunha, J. (2022) 'Ecological Approaches to Textile Dyeing: A Review', *Sustainability*, 14(14), 8353. DOI: 10.3390/su14148353

Mahmood, S.M.F. and Khan, A.R. (2026) 'From Waste to Value: Second-Hand Retail as a Catalyst for Sustainable Consumption in the Finnish Circular Economy', *Circular Economy and Sustainability*, 6, 257. DOI: 10.1007/s43615-026-00977-1

Mansour, H., Hilal, N., Alhajri, S., Al-Yahyai, F. and Al-Amri, M. (2020) 'The education of art culture at Sultanate of Oman through the multidisciplinary integration between graphic design and eco-friendly textile printing. Part 1: Standardization of extraction and dyeing with natural wastes products', *Energy Reports*, 6, pp. 933–939. DOI: 10.1016/j.egyr.2019.12.020

McCabe, M. and Maguire, H. (2026) 'Crafting Well-being: Exploring the Link Between Textile Craft and Wellbeing', *TEXTILE*, 24(3), pp. 624–639. DOI: 10.1080/14759756.2026.2629438

Nilsson, K., Becker Frahm, L., Rexfelt, O., Strömberg, H. and Nhu Laursen, L. (2025) 'Turning Trash into Treasure is Hard Work! How The Activities of Consumers and Reuse Enablers Extend Product Lifetimes'. In: *Proceedings of the 6th Product Lifetimes and the Environment Conference (PLATE 2025), Aalborg, Denmark*, 2–4 July 2025. Aalborg: Aalborg University Open Publishing. DOI: 10.54337/plate2025-10343

Nisa, H., Van Amber, R., English, J., Islam, S., McCorkill, G. and Alavi, A. (2025) 'A Systematic Review of Reimagining Fashion and Textiles Sustainability with AI: A Circular Economy Approach', *Applied Sciences*, 15(10), 5691. DOI: 10.3390/app15105691

Noor, S.S.N. and Fatihat, G.G. (2025) 'The Influence of FOMO (Fear of Missing Out), Instant Gratification, and Financial Literacy on Buy Now Pay Later (BNPL) Usage among Generation Z University Students in Indonesia'. In: *Proceedings of the International Student Conference on Business, Education, Economics, Accounting, and Management (ISC-BEAM 2025)*.

Paço, A., Leal Filho, W., Ávila, L.V. and Dennis, K. (2020) 'Fostering sustainable consumer behavior regarding clothing: Assessing trends on purchases, recycling and disposal', *Textile Research Journal*, 91(3-4), pp. 373–384. DOI: 10.1177/0040517520944524

Pei, X., Huang, Z., Yang, Y. and Bestoon, O. (2022) 'Research on user donation and information sharing in textile crowdfunding', *Industria Textila*, 73(6), pp. 671–679. DOI: 10.35530/IT.073.06.202195

Ramírez-Escamilla, H.G., Martínez-Rodríguez, M.C., Padilla-Rivera, A., Domínguez-Solís, D. and Campos-Villegas, L.E. (2024) 'Advancing Toward *Sustainability*: A Systematic Review of Circular Economy Strategies in the Textile Industry', *Recycling*, 9(5), 95. DOI: 10.3390/recycling9050095

Sandin, G. and Peters, G.M. (2018) 'Environmental impact of textile reuse and recycling – A review', *Journal of Cleaner Production*, 184, pp. 353–365. DOI: 10.1016/j.jclepro.2018.02.266

Senevirathne, B.M.L.S. and Kinkini, A.C.I. (2026) 'Integrating Wabi-Sabi and Mottainai into Sustainable Screen Printing: A Practice-Led Study', *International Journal of Research and Innovation in Social Science*, 10(4), pp. 8713–8731. DOI: 10.47772/IJRISS.2026.100400609

Shirvanimoghaddam, K., Motamed, B., Ramakrishna, S. and Naebe, M. (2020) 'Death by waste: Fashion and textile circular economy case', *Science of The Total Environment*, 718, 137317. DOI: 10.1016/j.scitotenv.2020.137317

Tusaasiirwe, P., Kwesiga, P. and Njeru, S.N. (2025) 'Upcycled Art Production from Post-Consumer Textile Waste to Foster Environmental *Sustainability* Awareness', *TEXTILE*, 23(3–4), pp. 617–637. DOI: 10.1080/14759756.2025.2515746

Wagner, M.M. and Heinzel, T. (2020) 'Human Perceptions of Recycled Textiles and Circular Fashion: A Systematic Literature Review', *Sustainability*, 12(24), 10599. DOI: 10.3390/su122410599

WWF. (2024) *Living Planet Report 2024: A System in Peril*. Gland, Switzerland: WWF. Available from: https://www.wwf.org.uk/sites/default/files/2024-10/living-planet-report-2024.pdf [Accessed 24 August 2026].

Wu, M., Al Mamun, A., Yang, Q., Gao, J., Rahman, M.K. and Al Shami, S.S.A. (2023) 'Modeling the intention and donation of second-hand clothing in the context of an emerging economy', *Scientific Reports*, 13, 15106. DOI: 10.1038/s41598-023-42437-y

Yin, Z. (2024) *Development of a modern Chinese social poster design on the theme of old clothing recycling*. Master's thesis. Kyiv National University of Technologies and Design.



© 2026 Authors. Published by the University of Novi Sad, Faculty of Technical Sciences, Department of Graphic Engineering and Design. This article is an open access article distributed under the terms and conditions of the Creative Commons Attribution license 4.0 Serbia (http://creativecommons.org/licenses/by/4.0/rs/).

Original Scientific Paper https://doi.org/10.24867/GRID-2026-p74

Development of Green-Synthesized Silver Nanoparticle-Containing PCL Coatings for Paper Packaging Materials

Filiz Kara

Baskent University, Faculty of Engineering, Department of Industrial Engineering, Ankara, Türkiye

ABSTRACT

Growing environmental concerns and the increasing demand for sustainable packaging materials have accelerated the development of biodegradable and functional paper-based packaging systems. Although paper is widely preferred for its excellent printability, low cost, and recyclability, its inherently poor barrier properties limit its use, particularly in food packaging. Surface coating with biodegradable polymers and antimicrobial nanomaterials has emerged as an effective strategy to overcome these limitations while preserving the desirable characteristics of paper. Among antimicrobial nanomaterials, silver nanoparticles (AgNPs) have attracted considerable attention owing to their broad-spectrum antibacterial activity. Green synthesis approaches further enhance their sustainability by eliminating the need for hazardous reducing agents, with hydroxyethly cellulose (HEC) serving as both a reducing and stabilizing agent. In this study, AgNPs synthesized via an HEC-mediated, autoclave-assisted one-pot green synthesis method were incorporated into a polycaprolactone (PCL) matrix and applied onto paper substrates to improve their functional performance. UV–Vis spectroscopy showed a characteristic absorption band at approximately 430 nm, while DLS analysis revealed an average hydrodynamic particle size of 240 nm with a PDI of 0.303. PCL coating formulations containing different amounts of AgNP were applied onto coarse filter paper surfaces in two layers using a glass rod. The structural, thermal, and surface properties of the coated papers were evaluated by ATR-FTIR spectroscopy, thermogravimetric analysis (TGA), water contact angle, and surface free energy measurements. The printability of the coated papers was evaluated using an IGT C1 laboratory printing tester at a printing pressure of 350 N and a printing speed of 1 m min^{-1} using Toyo Process Cyan ink. The color properties of the papers before and after printing were determined using an X-Rite eXact spectrophotometer, while surface gloss was measured using a BYK-Gardner gloss meter. The developed PCL-AgNP coating system successfully combines biodegradability, antimicrobial functionality, and printability while addressing the intrinsic barrier limitations of paper. This environmentally friendly surface modification strategy demonstrates significant potential for developing next-generation active paper-based food packaging materials with enhanced functionality and industrial applicability.

KEY WORDS

Silver nanoparticles, green synthesis, polycaprolactone, paper packaging, antibacterial coating

1. Introduction

Paper-based materials are increasingly considered for packaging applications because they are renewable, recyclable, and biodegradable. However, the porous and hydrophilic nature of cellulose-based paper limits its resistance to moisture, oils, and gases, making uncoated paper unsuitable for many applications that require effective barrier properties. Surface coating is commonly used to overcome these limitations. Although petroleum-based polymers such as polyethylene provide effective protection, their use can reduce the biodegradability and recyclability of paper. This has increased interest in biodegradable polymers as more sustainable coating materials for paper-based packaging (Adak et al., 2025).

Polycaprolactone (PCL) is a biodegradable aliphatic polyester with good film-forming ability and relatively hydrophobic character. These properties make PCL suitable for coating cellulose-based substrates. PCL can also serve as a polymer matrix for incorporating functional agents, making it suitable for the development of active coatings (Lo Faro et al., 2023). The properties of biodegradable polymer coatings can be further modified through the incorporation of nanomaterials. In particular, metal-based nanoparticles can improve the functional performance of these coatings and provide antimicrobial activity, extending their potential use in active packaging systems (Vukoje & Bota, 2025).

Silver nanoparticles (AgNPs) have attracted considerable interest in food packaging due to their strong antimicrobial activity against a broad range of microorganisms. Their high surface-area-to-volume ratio and effectiveness at relatively low concentrations make them suitable for active packaging applications aimed at reducing microbial contamination and extending food shelf life.

AgNPs can be incorporated into polymer matrices, biodegradable films, and surface coatings, making them suitable for the development of functional packaging materials. In addition to providing antimicrobial activity, their incorporation may influence the barrier, thermal, mechanical, and optical properties of the resulting material. For paper-based packaging, AgNP-containing polymer coatings therefore provide a useful approach for combining the advantages of cellulose-based substrates with additional functionality (Okur et al., 2025).

The synthesis method of AgNPs is also important for the development of sustainable functional materials. Conventional chemical synthesis generally requires reducing and stabilizing agents, whereas green synthesis methods aim to simplify nanoparticle production and reduce the use of potentially harmful chemicals. Natural polymers and cellulose derivatives can be useful in this respect because their functional groups can interact with silver ions and with the surface of the resulting nanoparticles.

Hydroxyethyl cellulose (HEC) is a water-soluble, non-ionic cellulose derivative containing abundant hydroxyl groups. HEC has previously been used as a polymeric medium in the preparation of AgNPs and can contribute to nanoparticle formation and stabilization (El-Sheikh et al., 2013) . Its use is therefore suitable for preparing AgNP dispersions that can subsequently be incorporated into polymer-based coating formulations.

Most studies on AgNP-containing papers have focused primarily on antimicrobial or barrier properties. However, adding nanoparticles to a coating can also change the surface and optical characteristics of paper. These changes are important when the coated material is intended to be printed, since color and gloss contribute directly to the appearance of the final product. The amount and distribution of nanoparticles within the coating may affect the original color of the paper as well as its appearance after printing (Todorova et al., 2024; Jung et al., 2018). Evaluating these properties together with wettability and thermal behavior can therefore provide a more complete assessment of AgNP-containing paper coatings.

In this study, AgNPs were prepared by an HEC-mediated, autoclave-assisted one-pot method and subsequently incorporated into PCL coatings applied to coarse filter paper. Three different amounts of the AgNP were used to examine their effect on the coated paper.

The resulting materials were evaluated in terms of chemical structure, thermal behavior, water contact angle, surface free energy, color, and gloss. Color and gloss were also measured after printing with cyan ink to determine how AgNP incorporation affected the appearance of the printed surface.

2. Methods

2.1. Materials

Hydroxyethyl cellulose, polycaprolactone (Sigma-Aldrich), and silver nitrate ($AgNO_3$; ISOLAB Chemicals) were used as raw materials. All solvents and other chemicals used in the experiments were of analytical grade and were used as received without further purification.

2.2. Green Synthesis and Characterization of AgNPs

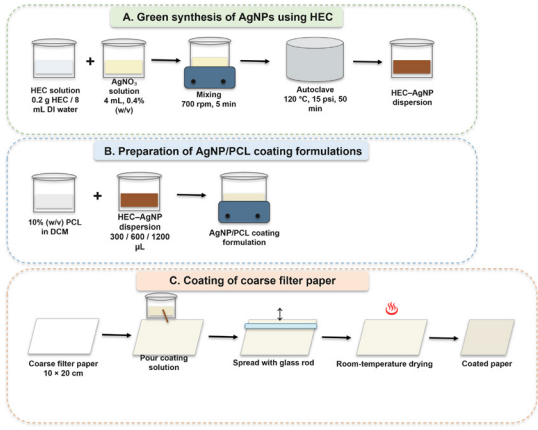
AgNPs were synthesized through a green, one-pot autoclave-assisted method using HEC, without the addition of conventional reducing agents or other toxic chemicals. In this approach, HEC served as the polymeric medium for AgNPs formation under autoclave conditions. First, 0.2 g of HEC was dissolved in 8 mL of deionized water with magnetic stirring.

After complete dissolution, 4 mL of 0.4% (w/v) $AgNO_3$ solution was added slowly, and the mixture was stirred at 700 rpm for 5 min. The solution was then placed in an autoclave (NÜVE NC 90M) and heated at 120 °C and 15 psi for 50 min. A clear change in the color of the solution was observed after autoclaving, providing an initial indication of AgNP formation through the reduction of silver ions (Ag^+) (Figure 1) (Venkatesham et al., 2014). AgNPs formation was examined by UV–Vis spectroscopy over the wavelength range of 200–800 nm using a Hitachi U-1800 spectrophotometer (Digilab, Tokyo, Japan). The hydrodynamic particle size distribution was determined by dynamic light scattering (DLS) using a Zetasizer Nano ZS90 (Malvern Instruments, UK).

2.3. Preparation and Characterization of P-PCL and AgNPs-Loaded Papers

A 10% (w/v) PCL solution was prepared in 10 mL of dichloromethane (DCM) under magnetic stirring. A few drops of Tween 80 were added to facilitate homogeneous dispersion. HEC-AgNP dispersion was then added separately to the PCL solution at volumes of 300, 600, and 1200 µL, and each mixture was thoroughly mixed using a magnetic stirrer. A PCL solution without HEC-AgNPs was prepared in the same manner as the control coating solution. Coarse filter paper (P) (ISOLAB, 60 g/m²) was cut into 10 × 20 cm pieces. The prepared coating solutions were poured onto the paper surfaces and spread uniformly over the entire area. The papers were dried at room temperature, and the coating procedure was repeated to obtain a second layer. After the second application, the coated papers were completely dried at room temperature. The paper coated with PCL alone was designated as P-PCL, whereas the papers coated with PCL containing 300, 600, and 1200 µL of HEC-AgNP dispersion were designated as P-PCL-AgNP1, P-PCL-AgNP2, and P-PCL-AgNP3, respectively (Figure 1).

The chemical structure of the uncoated and coated papers was analyzed by ATR-FTIR spectroscopy using a Thermo Nicolet iS10 spectrometer (Thermo Fisher Scientific, USA). The spectra were recorded over the range of 4000–600 cm^{-1} with 32 scans at a resolution of 4 cm^{-1}. The thermal behavior of the coated papers was evaluated using a TGA 4000 thermogravimetric analyzer (PerkinElmer, USA). The samples were heated from 30 to 750 °C at a heating rate of 10 °C/min under a nitrogen atmosphere. The water contact angles of the coated paper samples were measured using a Pocket Goniometer PG-X, Version 3.4 (FIBRO Systems AB, Sweden). A droplet of deionized water was placed on the coated paper surface, and the droplet profile was recorded using a CCD video camera. The water contact angle was determined from the recorded droplet images. The surface free energy of the coated paper was subsequently calculated based on the measured water contact angle in accordance with ASTM D5946.



» **Figure 1:** *Schematic representation of AgNP synthesis, preparation of coating formulations, and coating of coarse filter paper*

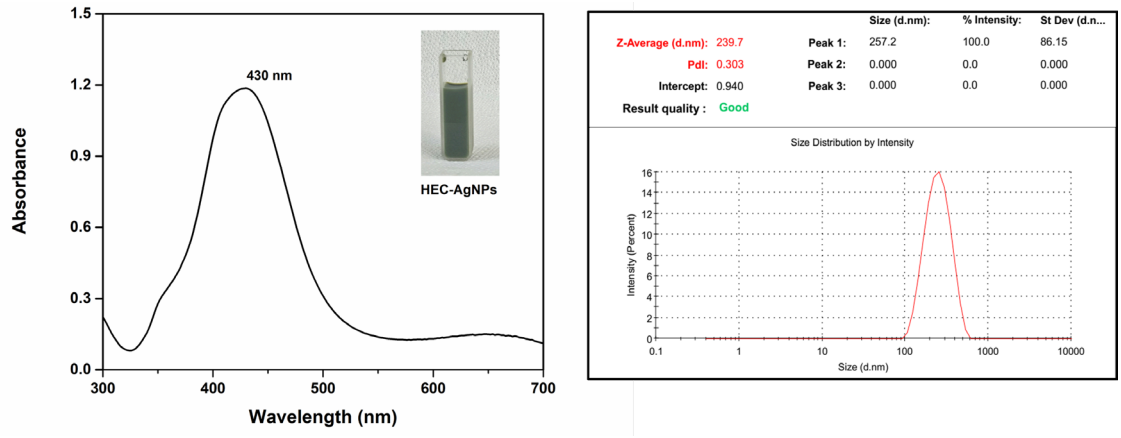
2.4. Printability, Color, and Gloss Measurements

The printability of the coated paper samples was evaluated using an IGTC1 laboratory printing tester. Test prints were produced using Toyo Process Cyan ink under controlled printing conditions. The printing speed was set at 1 m/min, while the applied printing pressure was 350 N. The same printing conditions were used for all coated paper samples to ensure a consistent comparison of their printing performance. The colors of the coated papers before and after printing were measured using an X-Rite eXact portable spectrophotometer in accordance with ISO 13655:2017. Color measurements were performed using a 0°/45° geometry, a 2° standard observer, and a D50 illuminant over the wavelength range of 400–700 nm. The color coordinates were expressed in the CIELAB color space as L*, a*, and b*, where L* represents lightness, a* represents the red–green chromatic coordinate, and b* represents the yellow–blue chromatic coordinate. The gloss of the coated paper surfaces before and after printing was measured using a BYK-Gardner gloss meter according to ISO 8254-1:2009. Gloss measurements were reported in gloss units (GU) using the specified measurement geometry.

3. Results

3.1. UV–Vis and DLS Analysis

The formation of AgNPs was evaluated by UV–Vis spectroscopy. The initially colorless HEC solution changed to dark brown after the reaction, and the corresponding UV–Vis spectrum showed a distinct absorption band centered at approximately 430 nm. DLS measurements showed an average hydrodynamic particle size of 239.7 nm with a PDI value of 0.303 (Figure 2).



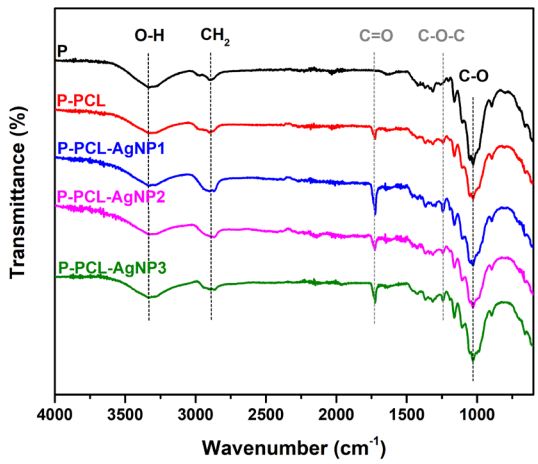
(a) (b)

» **Figure 2:** *(a) UV–Vis absorption spectrum and (b) DLS particle size distribution of HEC-AgNPs*

3.2. ATR-FTIR Analysis

The ATR-FTIR spectra of the uncoated paper (P), PCL-coated paper (P-PCL), and AgNP-containing coated papers (P-PCL-AgNP1, P-PCL-AgNP2, and P-PCL-AgNP3) are shown in Figure 3. The spectrum of P showed a broad band at 3338 cm^{-1} and a C–H stretching band at 2902 cm^{-1}. A weak band was observed at 1647 cm^{-1}. Several bands were also present at 1421, 1371, and 1313 cm^{-1}. Strong absorption bands were observed at 1161 and 1028 cm^{-1}, together with a band at 896 cm^{-1}.

After PCL coating, a new carbonyl band appeared at 1723 cm^{-1} and a band was observed at 1242 cm^{-1}. The carbonyl band was also present in the AgNP-containing samples at 1723, 1728, and 1725 cm^{-1} for P-PCL-AgNP1, P-PCL-AgNP2, and P-PCL-AgNP3, respectively. The band around 1240 cm^{-1} was observed at 1243 cm^{-1} for P-PCL-AgNP1 and 1244 cm^{-1} for P-PCL-AgNP2 and P-PCL-AgNP3. The cellulose bands at around 1161–1163, 1028–1031, and 895–896 cm^{-1} were retained in all coated samples. No new bands or consistent shifts in the main band positions were observed after the addition of HEC-AgNPs.



» **Figure 3:** *FTIR spectra of uncoated and coated papers*

3.3. TGA-DTG Analysis

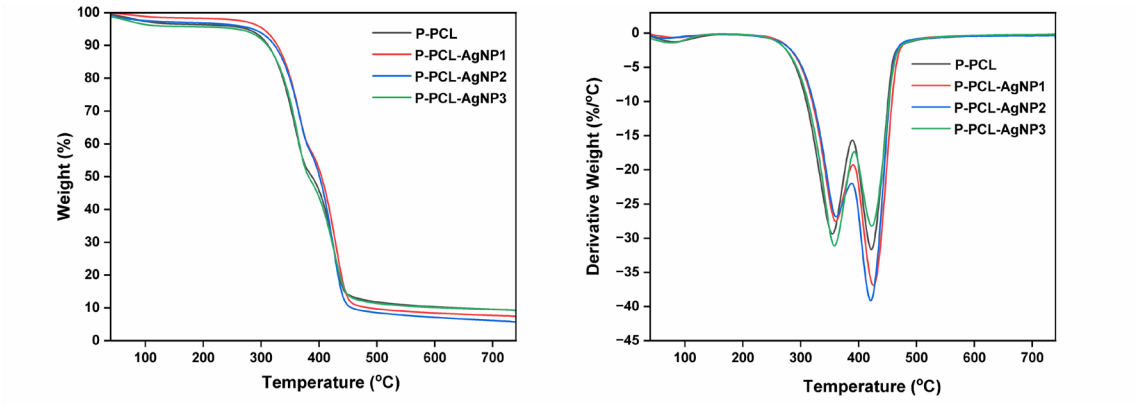
The thermal behavior of P-PCL and AgNP-containing coated papers prepared using AgNPs synthesized in the presence of HEC (P-PCL-AgNP1, P-PCL-AgNP2, and P-PCL-AgNP3) was investigated by TGA and DTG (Figure 4a and 4b). The mass loss below 150 °C was 3.4% for P-PCL, 1.6% for P-PCL-AgNP1, 2.9% for P-PCL-AgNP2, and 4.2% for P-PCL-AgNP3. The main mass loss occurred between approximately 250 and 500 °C.

In this region, two partially overlapping peaks were observed in the DTG curves. The first DTG peak was recorded at 354.7 °C for P-PCL, 360.6 °C for P-PCL-AgNP1, 361.2 °C for P-PCL-AgNP2, and 357.9 °C for P-PCL-AgNP3. The second DTG peak occurred at 421.7, 425.7, 420.7, and 422.8 °C, respectively. The second DTG peak was more pronounced for P-PCL-AgNP1 and P-PCL-AgNP2 than for P-PCL and P-PCL-AgNP3. At 740 °C, the remaining residues were 9.2% for P-PCL, 7.4% for P-PCL-AgNP1, 5.6% for P-PCL-AgNP2, and 9.3% for P-PCL-AgNP3.

3.4. Hydrophilicity and Surface Free Energy

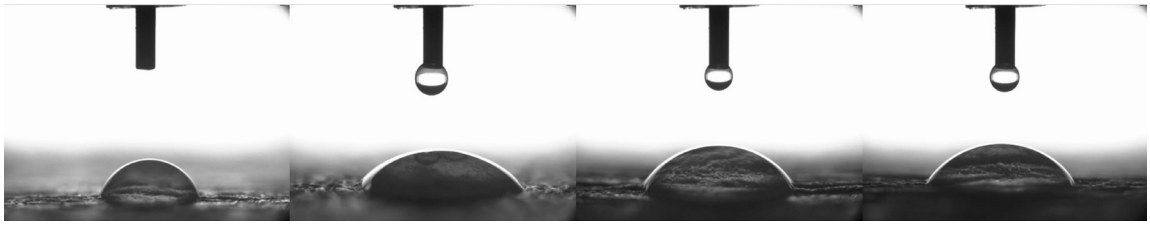
Representative water droplet images of the coated paper samples are shown in Figure 5, while the water contact angle and surface free energy values of all samples, including the uncoated paper, are presented in Table 1. The uncoated paper (P) had a water contact angle of 18.0°, which increased to 72.0° after PCL coating. The addition of AgNPs decreased the contact angle to 49.5°, 48.4°, and 47.9° for P-PCL-AgNP1, P-PCL-AgNP2, and P-PCL-AgNP3, respectively.

The surface free energy showed an opposite trend. The value decreased from 58.6 mJ/m^2 for P to 39.0 mJ/m^2 for P-PCL and then increased to 47.2–47.7 mJ/m^2 after AgNP incorporation. Only small differences were observed among the AgNP-containing samples.



(a) (b)

» **Figure 4:** *TGA (a) and DTG (b) curves of coated papers*



(a) (b) (c) (d)

» **Figure 5:** *Representative water droplet images of (a) P-PCL, (b) P-PCL-AgNP1, (c) P-PCL-AgNP2, and (d) P-PCL-AgNP3*

Table 1
Water contact angle and surface free energy of uncoated and coated papers

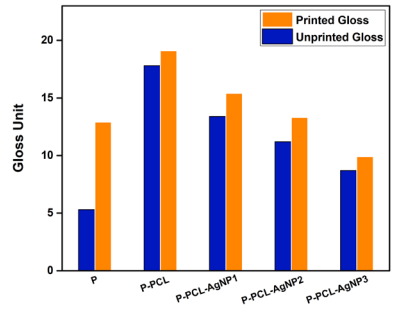
Sample	Water contact angle (°)	Surface free energy (mJ/m²)
P	18.0	58.6
P-PCL	72.0	39.0
P-PCL-AgNP1	49.5	47.2
P-PCL-AgNP2	48.4	47.6
P-PCL-AgNP3	47.9	47.7

3.5. Color and Gloss Measurements

The CIELAB color coordinates of the unprinted and printed paper samples are presented in Table 2. Before printing, P showed L*, a*, and b* values of 89.43, 1.04, and 4.03, respectively. After PCL coating, these values were 91.52, 0.05, and 3.42, respectively. AgNP incorporation resulted in L* values of 89.28, 88.02, and 79.86 for P-PCL-AgNP1, P-PCL-AgNP2, and P-PCL-AgNP3, respectively. The corresponding a* values remained close to zero (0.03, 0.41, and −0.67), whereas the b* values increased progressively from 13.35 to 14.39 and 16.65. After printing with cyan ink, the L* values were 35.41 for P and 31.84 for P-PCL, while values of 38.01, 29.35, and 35.91 were obtained for P-PCL-AgNP1, P-PCL-AgNP2, and P-PCL-AgNP3, respectively.

All printed samples showed negative a* and b* values. The b* value of P-PCL was −50.83 and became progressively less negative with AgNP incorporation, reaching −41.23, −38.72, and −31.07 for P-PCL-AgNP1, P-PCL-AgNP2, and P-PCL-AgNP3, respectively.

The gloss values of the unprinted and printed paper samples are shown in Figure 6. Before printing, the gloss value increased from 5.3 GU for P to 17.8 GU for P-PCL. The AgNP-containing samples showed gloss values of 13.4, 11.2, and 8.7 GU for P-PCL-AgNP1, P-PCL-AgNP2, and P-PCL-AgNP3, respectively. After printing, the gloss value of P-PCL was 19.1 GU, while values of 15.4, 13.3, and 9.9 GU were obtained for P-PCL-AgNP1, P-PCL-AgNP2, and P-PCL-AgNP3, respectively. The decreasing trend in gloss with increasing AgNP addition was maintained after printing.



» **Figure 6:** *Gloss values of the unprinted and printed paper samples*

Table 2
CIELAB color coordinates of the unprinted and printed paper samples

Sample	Before printing L*	a*	b*	After printing L*	a*	b*
P	89.43	1.04	4.03	35.41	–11.64	–49.20
P-PCL	91.52	0.05	3.42	31.84	–7.85	–50.83
P-PCL-AgNP1	89.28	0.03	13.35	38.01	–13.05	–41.23
P-PCL-AgNP2	88.02	0.41	14.39	29.35	–12.81	–38.72
P-PCL-AgNP3	79.86	–0.67	16.65	35.91	–11.48	–31.07

4. Discussion

The color change from colorless to dark brown and the appearance of an absorption band at approximately 430 nm indicate the formation of AgNPs. The absorption band is attributed to the surface plasmon resonance (SPR) of AgNPs, which is generally observed in the 400–500 nm region and is associated with the reduction of Ag^+ ions and formation of metallic silver nanoparticles (Ashraf et al., 2016). SPR bands within approximately 410–450 nm has also been commonly reported for spherical AgNPs (Zaheer & Rafiuddin, 2012). DLS analysis showed an average hydrodynamic particle size of 239.7 nm with a PDI of 0.303. Since DLS measures the hydrodynamic diameter of particles in dispersion, the measured size includes the nanoparticle together with its associated surface layer and surrounding solvated components. The PDI value indicates a moderately polydisperse particle population rather than a highly uniform size distribution (Wang & Wei, 2022).

The FTIR spectrum of the uncoated paper showed the characteristic bands of cellulose (Figure 3). The broad band at 3338 cm^{-1} is assigned to O–H stretching, while the band at 2902 cm^{-1} is related to C–H stretching. The weak band at 1647 cm^{-1} can be associated with adsorbed water in the cellulose structure. The bands at 1421 and 1371 cm^{-1} are related to CH_2 scissoring and C–H bending vibrations, respectively. The band at 1161 cm^{-1} is assigned to asymmetric C–O–C stretching of the glycosidic linkage, while the band at 1028 cm^{-1} is related to C–O stretching of the pyranose ring. The band at 896 cm^{-1} is characteristic of the β-glycosidic linkages of cellulose (Oh et al., 2005).

The main change after PCL coating was the appearance of a strong band at 1723 cm^{-1}, assigned to ester C=O stretching of PCL, together with a band at 1242 cm^{-1} associated with asymmetric ester C–O–C stretching (Elzein et al., 2004). These bands were also observed in all AgNP-containing samples, indicating the presence of PCL in the coated papers. The cellulose bands around 1160, 1030, and 896 cm^{-1} remained visible after coating. HEC is a cellulose ether, and its main FTIR bands overlap with those of the cellulose-based paper (Refaat et al., 2023). Therefore, HEC cannot be clearly distinguished from the paper substrate in the spectra.

The addition of HEC-AgNPs did not produce new bands or consistent shifts in the main PCL and cellulose bands. Small differences were observed mainly in band intensities at 1723 cm^{-1}. These differences may be related to variations in the amount and distribution of the coating within the analyzed area. Overall, the FTIR results showed that the characteristic PCL and cellulose bands were retained after HEC-AgNP incorporation.

The TGA/DTG profiles of all samples showed a similar multi-step degradation pattern, which can be related to the presence of the cellulose-based paper substrate together with HEC and PCL. AgNP incorporation did not substantially alter the overall shape of the degradation profile, although some differences were observed in the degradation temperatures and DTG peak intensities. The mass loss below 150 °C can mainly be attributed to the removal of adsorbed and hydrogen-bonded water.

The hydrophilic hydroxyl groups of cellulose ethers contribute to water retention within the structure, and a similar low-temperature mass loss associated with retained moisture has been observed in HEC-based materials (Zor et al., 2024) . The lower mass loss of P-PCL-AgNP1 and P-PCL-AgNP2 compared with P-PCL may be related to interactions between AgNPs and hydroxyl groups in the polymer chains, which can affect water retention within the structure (Orsuwan, 2023).

In contrast, P-PCL-AgNP3 showed a higher mass loss in this region. This difference may be associated with variations in sample composition and the number of hydrophilic groups available for interaction with water. The first DTG peak appeared between 355 and 361 °C, which falls within the main thermal degradation range of cellulosic materials. Cellulose degradation generally occurs between approximately 315 and 400 °C and involves cleavage of glycosidic bonds and breakdown of the polymer chains (Yang et al., 2007). Therefore, the first DTG peak can be mainly associated with the degradation of the cellulose-based paper substrate and HEC. Compared with P-PCL, which showed this peak at 355 °C, the peak shifted to 361 °C for both P-PCL-AgNP1 and P-PCL-AgNP2 and to 358 °C for P-PCL-AgNP3. These small shifts to higher temperatures may result from interactions between AgNPs and the surrounding polymeric structure.

The effect of AgNPs on thermal degradation can vary depending on the polymer matrix and nanoparticle–polymer interactions, and changes in degradation temperature (Ramos et al., 2014; Orsuwan, 2023). The second DTG peak, observed between 421 and 426 °C, can be mainly associated with PCL degradation. The thermal degradation of PCL involves random chain scission followed by successive depolymerization from the chain ends, with ε-caprolactone formed during the degradation process (Persenaire et al., 2001).

The second peak occurred at 422 °C for P-PCL and at 426, 421, and 423 °C for P-PCL-AgNP1, P-PCL-AgNP2, and P-PCL-AgNP3, respectively. Since the peak temperature did not show a consistent increase after AgNP incorporation, AgNPs had no clear systematic effect on the degradation temperature of PCL. The more pronounced second DTG peak for P-PCL-AgNP1 and P-PCL-AgNP2 indicates a higher degradation rate in this temperature region. This difference may be related to the coating composition and the distribution of AgNPs within the polymer matrix. The residue remaining at 740 °C ranged from approximately 6% to 9% and did not show a consistent change with AgNPs incorporation. The final residue may include carbonaceous products formed during the degradation of the cellulose-based components together with thermally stable silver-containing material (Ramos et al., 2014).

The differences among the samples may therefore result from both the coating composition and the amount of carbonaceous residue formed during thermal degradation. Overall, AgNP incorporation did not change the main multi-step degradation profile of the coated papers. The first DTG peak shifted slightly toward higher temperatures, whereas no consistent change was observed in the second peak associated mainly with PCL degradation. These results suggest that AgNP incorporation caused only minor changes in the thermal degradation behavior of the coated papers without markedly affecting their overall thermal profile.

The uncoated paper (P) showed a low water contact angle (18.0°), which can be related to the hydrophilic hydroxyl groups of cellulose and the porous structure of the paper. After PCL coating, the contact angle increased to 72.0° for P-PCL, showing the lower wettability of the PCL-coated surface. This increase is consistent with the relatively hydrophobic character of PCL. However, the contact angle remained below 90°, which is generally associated with hydrophilic wetting behavior (Law, 2014). AgNP incorporation decreased the water contact angle to 49.5°, 48.4°, and 47.9° for P-PCL-AgNP1, P-PCL-AgNP2, and P-PCL-AgNP3, respectively. The lower contact angles indicate improved wettability of the AgNP-containing coated surfaces compared with P-PCL. This change may be associated with the modification of the surface characteristics after AgNP incorporation.

Since the AgNPs were incorporated as an HEC-based dispersion, the hydroxyl-rich structure of HEC may also contribute to the increased interaction of the coated surface with water (Bellen et al., 2023). Only small differences in contact angle were observed among the three AgNP-containing samples. The surface free energy results followed the opposite trend to the water contact angle. PCL coating decreased the surface free energy from 58.6 mJ/m² for P to 39.0 mJ/m² for P-PCL. After AgNP incorporation, the values increased to 47.2, 47.6, and 47.7 mJ/m² for P-PCL-AgNP1, P-PCL-AgNP2, and P-PCL-AgNP3, respectively. The increase in surface free energy, together with the decrease in water contact angle, indicates improved wettability of the AgNP-containing coated papers.

The incorporation of AgNPs affected the optical appearance of the PCL-coated paper. While the uncoated paper exhibited a relatively neutral appearance, AgNP incorporation resulted in a progressive increase in positive b* values, indicating a gradual shift toward yellowish tones (P-PCL-AgNP3, b* = 16.65). This concentration-dependent optical change can be associated with the presence of AgNPs within the coating layer. The incorporation of AgNPs can affect the optical characteristics of coated paper, and the resulting changes may depend on the amount and distribution of nanoparticles within the coating (Todorova et al., 2024; Jung et al., 2018). The increase in yellowness was accompanied by a decrease in L* at the highest AgNP addition (P-PCL-AgNP3, L* = 79.86). Thus, the highest AgNP formulation produced the most pronounced yellowish and darker appearance among the investigated coatings. This behavior can be attributed to the optical contribution of the AgNP-containing layer. However, AgNP concentration alone may not determine the final color, since particle size, aggregation state, dispersion, and coating structure can also influence the optical response of nanoparticle-containing films and coatings.

Therefore, the observed color changes can be interpreted as a concentration-dependent optical response of the PCL–AgNP coating. The effect of AgNP incorporation was also evident in the surface gloss. PCL application increased the gloss compared with the uncoated paper (17.8 vs. 5.3 GU). However, increasing AgNP addition progressively reduced the gloss, with the lowest value obtained for P-PCL-AgNP3 (8.7 GU). The gloss of nanoparticle-coated paper surfaces is closely related to surface topography, as changes in the coating structure can influence specular reflection (Samyn et al., 2016). Accordingly, the reduction in gloss with increasing AgNP addition may be associated with changes in the surface structure and light-scattering characteristics of the PCL coating. The same concentration-dependent tendency was retained after printing. Although the cyan printing ink dominated the absolute color coordinates, the progressive increase in b* from P-PCL (−50.83) to P-PCL-AgNP1 (−41.23), P-PCL-AgNP2 (−38.72), and P-PCL-AgNP3

(−31.07) indicates that increasing AgNP addition shifted the printed surface toward less negative b* values. In other words, the printed samples became progressively less blue as the AgNP addition increased. This indicates that the optical characteristics of the underlying functional coating were still reflected in the final printed appearance, despite the strong contribution of the cyan ink. The post-print gloss values showed a similar trend. P-PCL exhibited the highest gloss value (19.1 GU), whereas the gloss decreased with increasing AgNP addition, reaching the lowest value for P-PCL-AgNP3 (9.9 GU).

The retention of the same decreasing tendency after printing suggests that the reduction in surface gloss originated primarily from the coated substrate rather than from the printing step itself. Differences in the surface structure and optical roughness of nanoparticle-containing paper coatings can influence their gloss characteristics (Samyn et al., 2011). Overall, the results demonstrate a concentration-dependent effect of AgNP incorporation on both color and gloss. Increasing AgNP addition produced progressively more yellowish coating surfaces while reducing gloss. After printing, the cyan ink became the dominant contributor to the measured color coordinates; nevertheless, the systematic shift toward less negative b* values with increasing AgNP addition indicates that the underlying functional coating continued to influence the final printed appearance. These findings are particularly relevant for active packaging papers, where AgNP addition should be considered not only in relation to functional performance but also to the optical characteristics and print appearance of the final substrate.

5. Conclusions

HEC-mediated AgNPs were successfully incorporated into PCL coatings and applied to coarse filter paper. The addition of AgNPs did not alter the main chemical structure or thermal degradation profile of the PCL-coated papers, but it affected their surface and optical properties. Compared with PCL alone, the AgNP-containing coatings showed lower water contact angles and higher surface free energy, indicating improved surface wettability. Increasing AgNP addition also resulted in a more yellowish appearance and a gradual decrease in surface gloss.

The effect of the coating composition remained visible after printing. Although cyan ink dominated the color of the printed samples, differences associated with AgNP addition were still observed, particularly in the b* values and gloss. Overall, the results show that AgNPs can be incorporated into PCL-coated paper while maintaining the main structural and thermal characteristics of the coating. At the same time, the changes in wettability, color, and gloss indicate that the amount of AgNPs should be considered when such coatings are intended for printed paper-based applications.

6. Acknowledgments

The author thanks Assoc. Prof. Dr. Emine Arman Kandırmaz for her assistance with the color and gloss measurements.

7. References

Adak, B., Baidya, S. and Teramoto, Y. (2025) 'Biopolymers and their nanocomposites coated paper-based high barrier and sustainable food packaging materials', *Carbohydrate Polymers*, 367, 123966. DOI: 10.1016/j.carbpol.2025.123966

Ashraf, J.M., Ansari, M.A., Khan, H.M., Alzohairy, M.A. and Choi, I. (2016) 'Green synthesis of silver nanoparticles and characterization of their inhibitory effects on AGEs formation using biophysical techniques', *Scientific Reports*, 6, 20414. DOI: 10.1038/srep20414

Bellen, F., Carbone, E., Baatsen, P., Jones, E.A.V., Kabirian, F. and Heying, R. (2023) 'Improvement of endothelial cell-polycaprolactone interaction through surface modification via aminolysis, hydrolysis, and a combined approach', *Journal of Tissue Engineering and Regenerative Medicine*, 2023, 5590725. DOI: 10.1155/2023/5590725

El-Sheikh, M.A., El-Rafie, S.M., Abdel-Halim, E.S. and El-Rafie, M.H. (2013) 'Green synthesis of hydroxyethyl cellulose-stabilized silver nanoparticles', *Journal of Polymers*, 2013, 650837. DOI: 10.1155/2013/650837

Elzein, T., Nasser-Eddine, M., Delaite, C., Bistac, S. and Dumas, P. (2004) 'FTIR study of polycaprolactone chain organization at interfaces', *Journal of Colloid and Interface Science*, 273(2), pp. 381–387. DOI: 10.1016/j.jcis.2004.02.001

Jung, J., Raghavendra, G.M., Kim, D. and Seo, J. (2018) 'One-step synthesis of starch-silver nanoparticle solution and its application to antibacterial paper coating', *International Journal of Biological Macromolecules*, 107, pp. 2285–2290. DOI: 10.1016/j.ijbiomac.2017.10.108

Law, K.Y. (2014) 'Definitions for hydrophilicity, hydrophobicity, and superhydrophobicity: Getting the basics right', *The Journal of Physical Chemistry Letters*, 5(4), pp. 686–688. DOI: 10.1021/jz402762h

Lo Faro, E., Bonofiglio, A., Barbi, S., Montorsi, M. and Fava, P. (2023) 'Polycaprolactone/starch/agar coatings for food-packaging paper: Statistical correlation of the formulations' effect on diffusion, grease resistance, and mechanical properties', *Polymers*, 15(19), 3921. DOI: 10.3390/polym15193921

Oh, S.Y., Yoo, D.I., Shin, Y., Kim, H.C., Kim, Y.H., Chung, Y.S., Park, W.H. and Youk, J.H. (2005) 'Crystalline structure analysis of cellulose treated with sodium hydroxide and carbon dioxide by means of X-ray diffraction and FTIR spectroscopy', *Carbohydrate Research*, 340(15), pp. 2376–2391. DOI: 10.1016/j.carres.2005.08.007

Okur, E.E., Eker, F., Akdaşçi, E., Bechelany, M. and Karav, S. (2025) 'Comprehensive review of silver nanoparticles in food packaging applications', *International Journal of Molecular Sciences*, 26(20), 9842. DOI: 10.3390/ijms26209842

Orsuwan, A. (2023) 'Effect of cellulose nanocrystals and green synthesized silver nanoparticles on mechanical properties and antimicrobial activity of banana flour/agar composite films', *Heliyon*, 9(4), e15102. DOI: 10.1016/j.heliyon.2023.e15102

Persenaire, O., Alexandre, M., Degée, P. and Dubois, P. (2001) 'Mechanisms and kinetics of thermal degradation of poly(ε-caprolactone)', *Biomacromolecules*, 2(1), pp. 288–294. DOI: 10.1021/bm0056310

Ramos, M., Fortunati, E., Peltzer, M., Dominici, F., Jiménez, A., Garrigós, M.C. and Kenny, J.M. (2014) 'Influence of thymol and silver nanoparticles on the degradation of poly(lactic acid) based nanocomposites: Thermal and morphological properties', *Polymer Degradation and Stability*, 108, pp. 158–165. DOI: 10.1016/j.polymdegradstab.2014.02.011

Refaat, A., Elhaes, H. and Ibrahim, M.A. (2023) 'Effect of alkali metals on physical and spectroscopic properties of cellulose', *Scientific Reports*, 13, 21649. DOI: 10.1038/s41598-023-48850-7

Samyn, P., Van Erps, J., Thienpont, H. and Schoukens, G. (2011) 'Paper coatings with multi-scale roughness evaluated at different sampling sizes', *Applied Surface Science*, 257(13), pp. 5613–5625. DOI: 10.1016/j.apsusc.2011.01.059

Todorova, D., Yavorov, N. and Vrabič-Brodnjak, U. (2024) 'Impact of silver nanoparticle treatment and chitosan on packaging paper's barrier effectiveness', *Polymers*, 16(15), 2127. DOI: 10.3390/polym16152127

Venkatesham, M., Ayodhya, D., Madhusudhan, A., Babu, N.V. and Veerabhadram, G. (2014) 'A novel green one-step synthesis of silver nanoparticles using chitosan: Catalytic activity and antimicrobial studies', *Applied Nanoscience*, 4(1), pp. 113–119. DOI: 10.1007/s13204-012-0180-y

Vukoje, M. and Bota, J. (2025) 'Effect of PCL nanocomposite coatings on the recyclability of paperboard packaging', *Recycling*, 10(2), 53. DOI: 10.3390/recycling10020053

Wang, Y. and Wei, S. (2022) 'Green fabrication of bioactive silver nanoparticles using Mentha pulegium extract under alkaline: An enhanced anticancer activity', *ACS Omega*, 7(1), pp. 1494–1504. DOI: 10.1021/acsomega.1c06267

Yang, H., Yan, R., Chen, H., Lee, D.H. and Zheng, C. (2007) 'Characteristics of hemicellulose, cellulose and lignin pyrolysis', *Fuel*, 86(12–13), pp. 1781–1788. DOI: 10.1016/j.fuel.2006.12.013

Zaheer, Z. and Rafiuddin (2012) 'Silver nanoparticles to self-assembled films: Green synthesis and characterization', *Colloids and Surfaces B: Biointerfaces*, 90, pp. 48–52. DOI: 10.1016/j.colsurfb.2011.09.037

Zor, M., Yazici, H., Şen, F., Eroğlu, E., Candan, Z., Rodrigue, D. and Wang, X. (2024) 'Preparation and characterization of hydroxyethyl cellulose/nanolignin composite films', *BioResources*, 19(4), pp. 7354–7365. DOI: 10.15376/biores.19.4.7354-7365

© 2026 Authors. Published by the University of Novi Sad, Faculty of Technical Sciences, Department of Graphic Engineering and Design. This article is an open access article distributed under the terms and conditions of the Creative Commons Attribution license 4.0 Serbia (http://creativecommons.org/licenses/by/4.0/rs/).

Original Scientific Paper https://doi.org/10.24867/GRID-2026-p75

Improving the Printability of PLA-Based Active Packaging Films Using Exopolysaccharide Obtained by *Ligilactobacillus Salivarius* KC66L

Aslı Beyler Çiğil [1]
Berat Çınar Acar [2]
Zehranur Yüksekdağ [2]
Hatice Birtane [3]

[1] Gazi University, Department of Chemistry and Chemical Process Technology, Ankara, Türkiye
[2] Gazi University, Department of Biology, Gazi University, Ankara, Türkiye
[3] Marmara University, Department of Chemistry, Istanbul, Türkiye

ABSTRACT

Polylactic acid (PLA) has been identified as a promising bio-based polymer for sustainable food packaging applications. Nevertheless, its limited functionality and surface characteristics may constrain its performance in advanced packaging and printing applications. In this study, exopolysaccharide produced by Ligilactobacillus salivarius KC66L (EPS-KC66L) was incorporated into PLA films at 1, 2.5, and 5 wt% to investigate its effects on the chemical, thermal, optical, surface, printability, and antibacterial properties of the resulting films. The PLA/EPS films were prepared via solvent casting and characterized by ATR-FTIR, thermogravimetric analysis, UV–Vis spectroscopy, contact angle and instrument-derived surface energy measurements, colour and gloss analysis, and printing tests. The analysis of ATR-FTIR spectra indicated that the physical incorporation of EPS into the PLA matrix did not result in significant alterations to the characteristic structure of the PLA. The study found that there was no adverse effect of EPS incorporation on thermal stability, and that the maximum degradation temperature increased slightly, from 384.5 °C for neat PLA to 387.4 °C for PLA/5-EPS. The incorporation of EPS resulted in a modification of the optical and surface characteristics of the films. The 5 wt% formulation exhibited reduced visible transparency, a lower water contact angle (61.2°) and a higher instrument-derived surface energy (42.9 mJ m^{-2}). Following the printing process, PLA/5-EPS demonstrated the lowest color difference (ΔE_{00} = 1.82) in relation to the printed reference sample. This finding suggests that PLA/5-EPS exhibits enhanced color reproduction capabilities when compared with unprinted PLA (ΔE_{00} = 4.71). However, no detectable inhibition zones against Escherichia coli or Staphylococcus aureus were observed in the agar diffusion assay. The investigation established that EPS-KC66L modified the surface and printing-related properties of PLA films without compromising their thermal stability. Of the formulations examined, the 5 wt% formulation demonstrated the most favourable surface wettability and print colour reproduction. These findings demonstrate the potential of microbial EPS as a functional modifier for the development of sustainable and printable PLA-based packaging materials.

KEY WORDS
PLA, Exopolysaccharide (EPS), Printability, Surface free energy, Ligilactobacillus salivarius

1. Introduction

Packaging plays a critical role in maintaining the quality and safety of food products throughout the supply chain, from production to consumption, while also extending shelf life and reducing food losses. However, a substantial proportion of conventional food packaging materials are derived from petroleum-based polymers that are resistant to biodegradation, contributing to the accumulation of plastic waste and posing significant challenges to environmental sustainability. The packaging sector represents one of the major areas of plastic consumption, and the widespread use of single-use packaging has further intensified the need for more sustainable alternatives. Consequently, in recent years, increasing research attention has been directed toward the development and application of biodegradable polymers derived from renewable resources, which offer lower environmental impact and considerable potential for sustainable food packaging (Hassan, 2026).

Polylactic acid (PLA) has emerged as a promising alternative to conventional petroleum-based polymers due to its bio-based origin, biocompatibility, processability, and favorable physicochemical properties for packaging applications. Despite the significant potential of neat PLA in the packaging sector, it possesses only limited intrinsic biological functionality. This restricts its ability to provide active protection beyond the conventional barrier and containment functions of packaging. This limitation is particularly relevant to the development of next-generation active food packaging systems designed to directly contribute to food preservation and shelf-life extension. Consequently, there has been significant research interest in enhancing the functional performance of PLA through incorporation of natural or biologically derived active components. Recent studies have demonstrated that the integration of antimicrobial and other functional agents into PLA-based materials can impart additional bioactive properties. This represents a promising strategy for the development of active, more sustainable food packaging systems (Zeng et al., 2026).

It is evident that microbial biopolymers have attracted increased attention among the functional components incorporated into active packaging systems. This is due to their potential to combine sustainability with the desired functional properties. Exopolysaccharides (EPS) are a prominent class of microbial biopolymers, defined as high-molecular-weight polysaccharides secreted extracellularly by microorganisms. In addition to their biocompatibility, low toxicity, and film-forming ability, certain EPS have been reported to exhibit antioxidant and antimicrobial activities, making them promising candidates for food packaging applications. A notable increase in research interest has been observed focusing on EPS produced by lactic acid bacteria and their potential utilization as structural or functional components in food packaging materials. Recent studies have demonstrated that EPS derived from various microorganisms, including species of the *Lactobacillus* and *Ligilactobacillus* genera, may exhibit favorable film-forming and rheological characteristics, along with biological activities that could be exploited in the development of functional and active food packaging systems (Mazumder et al., 2025). *L. salivarius* is a promising probiotic bacterium capable of producing a variety of biologically active metabolites (Yuksekdag et al., 2025). Moreover, microbial postbiotics comprise a diverse range of bioactive molecules, including exopolysaccharides, which may contribute to their functional properties (Çelik et al., 2024; Yuksekdag et al., 2025). The incorporation of EPS into a polymer matrix has been demonstrated to have the potential to impart biological functionality to the resulting material. Furthermore, molecular and interfacial interactions between the polymer chains and EPS result in modification of the material's structural and surface characteristics. Such interactions have the capacity to influence several key properties of the resulting films, including surface morphology, hydrophilicity, surface free energy, and barrier performance. Indeed, a recent study demonstrated that incorporating exopolysaccharides (EPS) from *Bacillus licheniformis* into alginate-based films resulted in strong hydrogen-bonding interactions between the polymer matrix and the EPS. As a result, significant changes in the films' morphology, mechanical properties, and barrier properties were observed (Bayrak & Omeroglu, 2026). In a biopolymer-based packaging system, it is essential to establish relationships between additive-polymer interfacial interactions, additive dispersion and aggregation behaviour, and the resulting measurable surface and barrier properties, in order to understand the practical performance of the developed materials (Hassan, 2026).

However, the industrial applicability of food packaging materials is not determined solely by their biological activity, mechanical performance, or barrier properties. The packaging surface must also provide a suitable substrate for the printing of product information, branding elements, traceability data, and other graphical content. Therefore, printability represents an important technological requirement that should be considered alongside the functional performance of sustainable packaging materials. This aspect is particularly important for non-absorbent polymeric substrates such as PLA, where adequate wetting of the surface by the printing ink and strong adhesion after drying are critical for achieving satisfactory print quality. Previous studies on PLA films have demonstrated that modifications to surface characteristics can significantly influence wettability and ink adhesion, so directly affecting printing performance (Izdebska-Podsiadły, 2021).

Surface free energy (SFE) is one of the key parameters leading the interactions between a polymeric substrate and printing ink. The ability of an ink to wet and spread

over the substrate and then form a stable and uniform ink layer largely depends on the relationship between the surface free energy of the solid substrate and the surface tension of the ink. However, printing performance is not governed by surface energy alone; surface polarity and topography (roughness) also play important roles in determining ink wetting, spreading, and adhesion. In PLA-based systems, changes in both the polar and dispersive components of surface free energy have been shown to influence ink-substrate interactions and, consequently, overall printing performance (Izdebska-Podsiadły, 2021).

The importance of these relationships has become increasingly evident as research interest in sustainable printed packaging grows. For instance, studies on PLA/PCL/SiO2-based biopolymer films have demonstrated that variations in film composition can significantly alter surface morphology, contact angle, and surface free energy. These factors are closely associated with ink adhesion and overall print quality. These findings indicate that incorporating functional components into a biopolymer matrix can influence not only the structural and physicochemical characteristics of the resulting material but also its surface-ink interactions and, consequently, its printability (Poljaček et al., 2026). Therefore, when evaluating the effects of functional components incorporated into active packaging systems, it is important to consider not only conventional mechanical and barrier properties but also the relationship between preprint surface characteristics and post-printing performance.

Recent studies have increasingly focused on the potential of microbial exopolysaccharides (EPS) in sustainable and active food packaging systems, with research primarily concentrating on their film-forming capacity and the impact on the barrier, mechanical, and biological properties of packaging materials (Mazumder et al., 2025). On the other hand, several studies have investigated the relationships among surface free energy, wettability, and ink adhesion in PLA-based packaging materials (Poljaček et al., 2026). However, studies directly linking the surface modifications induced by incorporating microbial-derived EPS as a functional additive into PLA-based active packaging films to their printability characteristics remain limited. A thorough evaluation of the effects of EPS incorporation on the physicochemical properties of PLA surfaces and its influence on printing performance is therefore essential to comprehending the practical and industrial applicability of sustainable active packaging materials.

Accordingly, in the present study, EPS derived from *Ligilactobacillus salivarius* KC66L (EPS-KC66L) was incorporated into PLA films at different concentrations. The effects of EPS incorporation on the chemical structure, thermal stability, optical properties, surface wettability, surface energy, and printing performance of the resulting films were systematically investigated. Particular emphasis was placed on establishing the relationship between EPS-induced changes in surface characteristics and the color reproduction and gloss properties of the printed films. In addition, the antibacterial activity of the films against Escherichia coli and Staphylococcus aureus was evaluated.

2. Methods

2.1. Materials

Polylactic acid (PLA, Mw ≈ 60,000 g mol^{-1}) was purchased from Sigma-Aldrich and used as the polymer matrix. Trichloroacetic acid (TCA) and Tween 80 were also obtained from Sigma-Aldrich. All solvents and other chemicals used in the experiments were of analytical grade and were used as received without further purification.

2.2. Isolation of Exopolysaccharide (EPS)

EPS was isolated from *Ligilactobacillus salivarius* KC66L using a modified procedure based on previously reported methods (Kanmani et al., 2011; Shi et al., 2014). The activated bacterial culture, adjusted to a McFarland standard of 0.5, was inoculated into de Man, Rogosa, and Sharpe (MRS) medium at 2% (v/v) and incubated at 37 °C for 24 h. The resulting active culture was subsequently inoculated into 800 mL of MRS medium at 2% (v/v) and incubated at 37 °C for an additional 48 h.

Following incubation, the culture was heat-treated at 95 °C for 10 min and allowed to cool to room temperature. An 80% (v/v) TCA solution was added, and the mixture was stirred for 2 h. The culture was then centrifuged at 9000 rpm for 15 min at 4 °C, and the resulting supernatant was mixed with three volumes of cold 96% ethanol (1:3, v/v) to precipitate the EPS. After incubation at 4 °C for 24 h, the precipitated EPS was recovered by centrifugation at 9000 rpm for 15 min. The recovered EPS was dissolved in sterile distilled water, lyophilized, and stored at 4 °C until further use.

2.3. Preparation of PLA/EPS Packaging Films

In the present study, PLA-based composite packaging films were prepared using a solvent casting approach. This approach has been widely employed in the fabrication of biopolymer and exopolysaccharide-based films. However, the present study introduces several modifications based on previously reported methods (Ferreira et al., 2014; Guerrero et al., 2024). Polylactic acid (PLA) was used as the primary film-forming polymer, while the previously isolated EPS-KC66L was incorporated into the film formulations as a func-

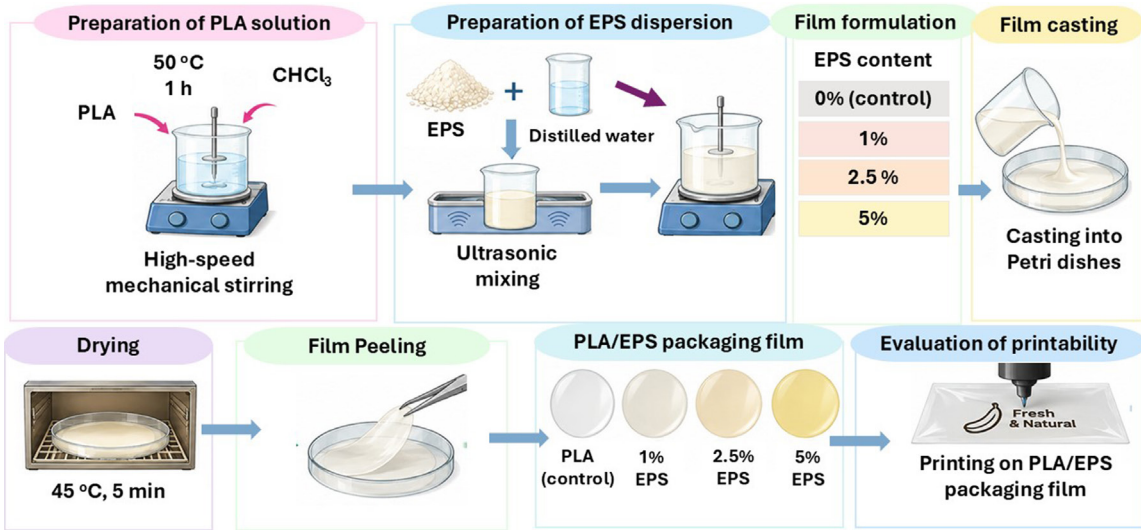
tional additive. Chloroform was used as the solvent, and Tween 80 was employed as a surfactant.

A 10% (w/v) PLA solution was prepared in chloroform and mechanically stirred at high speed at 50 °C for 1 h to obtain a homogeneous polymer solution. Subsequently, Tween 80 was added at a concentration of 3%. To prepare the EPS-KC66L phase, 0.5 g of EPS-KC66L was dissolved in 5 mL of distilled water. The resulting EPS-KC66L dispersion was incorporated into the PLA/Tween 80 solution to obtain films containing 1, 2.5, and 5 wt% EPS-KC66L relative to the PLA content. To promote homogeneous dispersion of EPS-KC66L within the PLA matrix, the resulting mixtures were ultrasonicated for 4 min. The film-forming mixtures were then poured into Petri dishes and cast using the solvent-casting method. The films were dried at 45 °C for 5 min to facilitate solvent removal and film formation. After drying, the films were carefully peeled from the Petri dishes and subsequently used for further characterization. A PLA/Tween 80 film without EPS-KC66L (0% EPS-KC66L) was prepared under the same conditions and used as the control. A schematic representation of the preparation procedure for the PLA/EPS packaging films is presented in Figure 1.

heated from 30 to 750 °C under a nitrogen atmosphere at a heating rate of 10 °C min^{-1}. The thermogravimetric profiles were analyzed to determine the temperatures corresponding to 5% and 10% mass loss (T_5 and T_{10}, respectively) and the maximum degradation temperature (T_{max}), and to evaluate the effect of EPS incorporation on the thermal stability and degradation behavior of the PLA-based films.

The optical properties of the films were evaluated using a Shimadzu UV-2450 UV–Vis spectrophotometer (Kyoto, Japan). Light transmittance measurements were performed to evaluate the optical transparency of the films. In addition, the visual appearance and transparency of the prepared films were documented photographically as they were placed in Petri dishes.

The surface wettability of the films prior to printing was evaluated using a Pocket Goniometer PG-X, version 3.4 (FIBRO System AB, Sweden). Water contact angles were measured using the integrated CCD camera and determined by the instrument software. Surface energy values were obtained directly from the PG-X software using the measured contact angle data and its built-in calculation procedure. Measurements were performed



» **Figure 1:** *Schematic representation of the preparation and printing of PLA/EPS packaging films*

2.4. Characterization

The chemical structures of the prepared packaging films were characterized by attenuated total reflectance Fourier-transform infrared (ATR-FTIR) spectroscopy using a Bruker IFS 66/S spectrometer. The spectra were recorded over the wavenumber range of 400–4000 cm^{-1} using 32 scans to identify the characteristic functional groups of PLA and EPS and to investigate possible interactions between the film components.

Thermogravimetric analysis (TGA) was performed using a PerkinElmer STA6000 instrument. The samples were

in triplicate, and the results are expressed as mean ± standard deviation. The contact angle and instrument-derived surface energy values were used to comparatively evaluate changes in the surface characteristics of the PLA/EPS films resulting from EPS incorporation.

The color characteristics of the packaging films were measured using an X-Rite eXact portable spectrophotometer in accordance with ISO 13655:2017. Measurements were performed using 0°/45° geometry with a polarization filter, a 2° standard observer, and D50 illumination over the wavelength range of 400-700 nm. Five measurements were performed for each sample, and the mean values were used for further

analysis. Color values were expressed in the CIELAB color space as L*, a*, and b*, where L* represents lightness from black to white, a* represents the green (-a*) to red (+a*) axis, and b* represents the blue (-b*) to yellow (+b*) axis. Color differences (ΔE_{00}) were calculated according to the CIEΔE_{2000} color-difference formula in accordance with ISO 11664-6:2014.

$$\Delta E_{00} = \sqrt{\left(\frac{\Delta L'}{k_L S_L}\right)^2 + \left(\frac{\Delta C'}{k_C S_C}\right)^2 + \left(\frac{\Delta H'}{k_H S_H}\right)^2 + R_T \frac{\Delta C'}{k_C S_C}\frac{\Delta H'}{k_H S_H}} \quad (1)$$

where $\Delta L'$, $\Delta C'$, and $\Delta H'$ represent the differences in lightness, chroma, and hue between the reference and sample, respectively. S_L, S_C, and S_H are the weighting functions for the lightness, chroma, and hue components, respectively, while k_L, k_C, and k_H are parametric factors accounting for variations in experimental and viewing conditions. R_T is the rotation term that accounts for the interaction between chroma and hue differences in the blue region of the CIEL*a*b* color space.

2.5. Printing of PLA/EPS Packaging Films

The prepared packaging films were printed using a red solvent-based printing ink supplied by Siegwerk. Printing trials were performed using an IGT F1 printability tester at a printing speed of 1 m min^{-1} and a printing pressure of 300 N. Identical printing conditions were applied to all film formulations to enable direct comparison of their printing performance. The adhesion of the printed ink layer to the film surface was evaluated using a cross-cut tape test with transparent tesa® 4124 PVC tape. Following the formation of the cross-cut pattern, the tape was firmly applied to the printed surface and subsequently peeled off at an angle of 180°. The degree of ink adhesion was evaluated using a five-point visual scale. The scale ranged from 1, representing very poor adhesion with substantial ink removal, to 5, representing very good adhesion with no ink visible upon removal.

2.6. Antibacterial Activity of PLA/EPS Packaging Films

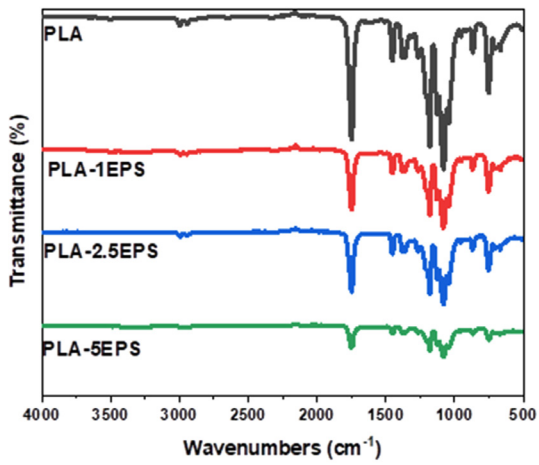
The antibacterial activity of the PLA/EPS films was qualitatively evaluated against *Escherichia coli* ATCC 11229 and *Staphylococcus aureus* ATCC 25923 using a film agar diffusion assay adapted from Ozdemir et al. (2023). Fresh bacterial colonies were transferred into Mueller-Hinton (MH) broth and incubated at 37 °C for 1-2 h. The turbidity of the bacterial suspensions was adjusted to 0.5 McFarland standard (~1.5×10^8 CFU mL^{-1}), and the suspensions were uniformly inoculated onto Mueller-Hinton agar plates using a sterile swab. Film samples corresponding to control PLA and PLA films containing 1, 2.5, and 5 wt% EPS-KC66L were aseptically placed directly onto the inoculated agar surface using sterile forceps. The plates were incubated at 35-37 °C for 24 h. Following incubation, antibacterial activity was qualitatively evaluated based on the presence or absence of a visible inhibition zone around the film samples. The PLA film without EPS was used as the negative control.

3. Results and discussion

3.1. Structural Characterization of PLA/EPS Packaging Films

ATR-FTIR analysis was performed to investigate the chemical structure of the PLA/EPS packaging films (Figure 2) and possible interactions between PLA and EPS-KC66L. Neat PLA exhibited its characteristic absorption bands at 2995 and 2945 cm^{-1}, corresponding to C-H stretching vibrations, together with a strong ester carbonyl (C=O) stretching band at 1749 cm^{-1}. The bands detected at approximately 1452 and 1382 cm^{-1} were attributed to CH_3 bending vibrations, while the bands at 1181, 1128, 1081, and 1043 cm^{-1} were associated with C-O-C and C-O stretching vibrations of the PLA ester backbone (Enumo et al., 2020).

It was demonstrated that the incorporation of EPS-KC66L resulted in no alteration to the characteristic absorption bands of PLA in the composite films. The carbonyl band remained unchanged at 1748-1749 cm^{-1}, while the major C-O/C-O-C bands were observed at approximately 1180-1181, 1127-1128, and 1080-1081 cm^{-1}. No distinct new absorption bands or substantial shifts in the major PLA bands were observed as EPS content increased. These findings indicate that the incorporation of EPS-KC66L did not substantially alter the chemical structure of the PLA matrix and provide no evidence for the formation of new covalent bonds between the components (Wang et al., 2020). Overall, the spectral results suggest that EPS-KC66L was physically incorporated into the PLA matrix without evidence of substantial chemical modification of the PLA structure.



» **Figure 2:** *FTIR spectra of PLA/EPS packaging films*

3.2. Thermal Characterization of PLA/EPS Packaging Films

Thermogravimetric analysis revealed a low-temperature mass-loss region followed by the thermal degradation of the PLA-rich matrix. The TGA results are summarized in Table 1. A noticeable mass loss occurred below approximately 160 °C in all formulations, including the PLA control (Figure 3). Therefore, this event was not attributed exclusively to EPS-KC66L incorporation and may instead be associated with the removal of absorbed moisture and/or low-molecular-weight or volatile constituents present in the film formulations. The extent of this initial mass loss did not show a systematic dependence on EPS-KC66L concentration, with the PLA/2.5-EPS film exhibiting a comparatively greater mass loss in this region.

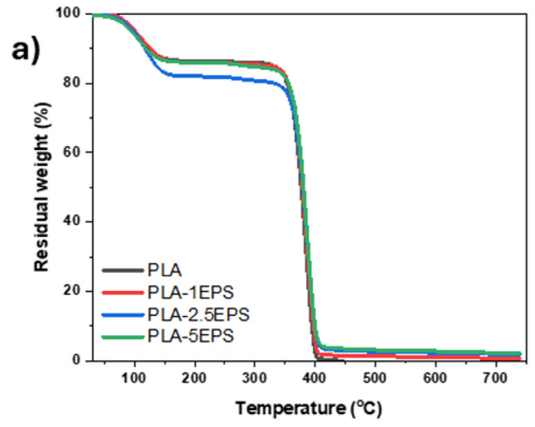
The degradation stage occurred at substantially higher temperatures and was dominated by PLA matrix degradation. The maximum degradation temperature (T_{max}) was approximately 384.5 °C for the PLA control film and 384.9, 387.0, and 387.4 °C for the PLA/1-EPS, PLA/2.5-EPS, and PLA/5-EPS films, respectively. Thus, incorporation of 1 wt% EPS-KC66L had little influence on the degradation temperature, whereas increasing the EPS-KC66L content to 2.5 and 5 wt% resulted in a modest shift of T_{max} toward higher temperatures. These results indicate that EPS-KC66L incorporation did not compromise the thermal stability of the PLA-rich matrix, while the 2.5 and 5 wt% formulations exhibited a slight increase in T_{max}. Overall, the preservation of the characteristic main degradation profile of PLA, together with the relatively small changes in T_{max}, suggests that EPS-KC66L incorporation did not substantially alter the overall thermal degradation behavior of the PLA-rich matrix. This observation is also consistent with the ATR-FTIR results, which showed preservation of the characteristic PLA absorption bands without the appearance of prominent new bands following EPS-KC66L incorporation.

Table 1

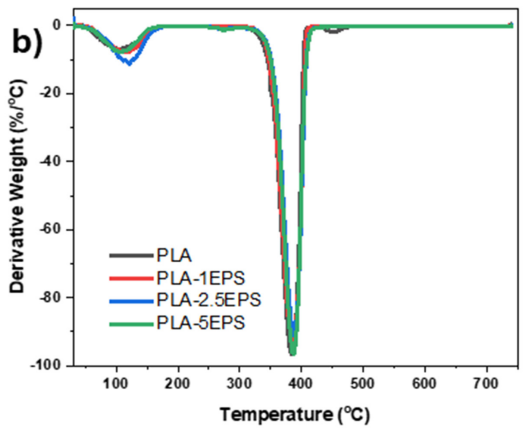
TGA results of PLA/EPS packaging films

	T_5 (°C)*	T_{10} (°C)*	T_{max} (°C)
PLA	95.8	123.3	384.5
PLA/1-EPS	101.6	126.8	384.9
PLA/2.5-EPS	98.6	117.8	387
PLA/5-EPS	94.5	119.4	387.4

*T_5 and T_{10} correspond to temperatures at 5 and 10% total mass loss, respectively, and include the low-temperature loss of moisture and/or volatile constituents.



(a)



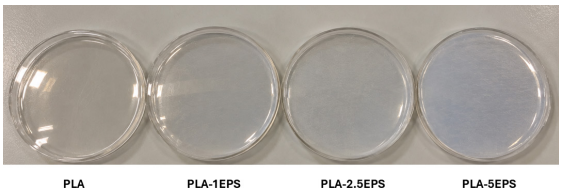
(b)

» **Figure 3:** *a) TGA curves of PLA/EPS packaging films, b) DTG curves of PLA/EPS packaging films*

3.3. Optical Properties of PLA/EPS Packaging Films

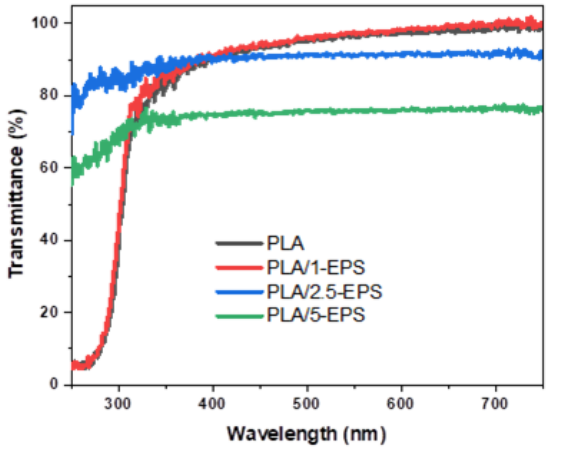
The visual appearance and optical properties of the PLA/EPS packaging films are shown in Figure 4. Control PLA and PLA/1-EPS films appeared transparent and relatively uniform. As the EPS content increased, the films gradually became whiter and more opaque. This change was noticeable in PLA/2.5-EPS and became more pronounced in PLA/5-EPS. Similar decreases in transparency with increasing additive content have been reported for PLA-based composite films and have been attributed to increased light scattering caused by the presence of different phases within the polymer matrix (Sanchez-Garcia et al., 2008; Machado et al., 2021). The whitening observed at higher EPS contents may therefore be related to the distribution of EPS within the PLA matrix.

The UV-Vis transmittance spectra (Figure 5) were consistent with the visual appearance of the films. PLA showed high transmittance in the visible region, as commonly reported for PLA-based packaging films (Boarino et al., 2022; Liu et al., 2024). The addition of



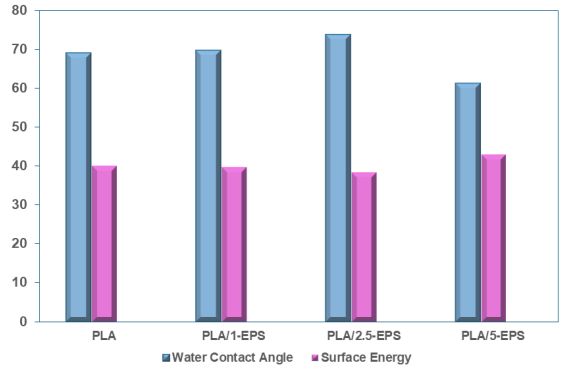
» **Figure 4:** *Visual appearance and transparency of PLA and PLA/EPS packaging films*

1% EPS-KC66L had little effect on the overall transmittance profile, while PLA/2.5-EPS retained a transmittance of around 90% across most of the visible region. A clearer decrease was observed at the highest EPS content, with PLA/5-EPS showing transmittance values of approximately 75-77%. This reduction also agrees with the more opaque appearance of the PLA/5-EPS film observed visually. The differences among the films did not follow a clear trend with increasing EPS-KC66L content, particularly in the UV region. This suggests that the changes in UV transmittance cannot be explained by EPS concentration alone. The optical behavior of the films may also depend on how EPS-KC66L is distributed within the PLA matrix. Previous studies on PLA-based composites have shown that the dispersion and aggregation of the incorporated phase can have a strong influence on light transmission (Boarino et al., 2022). Overall, EPS-KC66L affected the optical properties of the PLA films without causing a complete loss of transparency. The largest change was observed for PLA/5-EPS, which showed the greatest reduction in optical clarity.



» **Figure 5:** *UV-Vis transmittance spectra of PLA and PLA/EPS packaging films*

3.4. Surface Wettability and Surface Energy of PLA/EPS Packaging Films



» **Figure 6:** *Contact Angle and Surface Energy of Produced Films*

The water contact angle and surface energy values of the PLA/EPS films are given in Table 2. PLA showed a water contact angle of 69.0° ± 0.6 and a surface energy of 40.1 ± 0.7 mJ m^{-2}. The contact angle was close to the 70-75° range previously reported for untreated PLA films (Abdulkareem et al., 2021; Muñoz-Shugulí et al., 2023), indicating that the PLA surface was moderately wettable rather than highly hydrophobic. The surface energy was also within the range reported for untreated PLA (33–40 mJ m^{-2}), although these values can vary with film preparation and the method used for surface characterization (Izdebska-Podsiadły & Dörsam, 2017).

Table 2

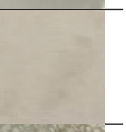
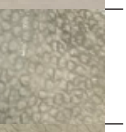
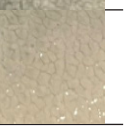
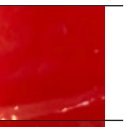
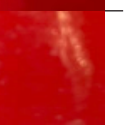
The water contact angle and surface energy of the PLA/EPS films

	WCA (°)	SE (mJ m^{-2})
PLA	69.0±0.6	40.1±0.7
PLA/1-EPS	69.7±0.4	39.8±0.4
PLA/2.5-EPS	73.6±0.3	38.4±0.3
PLA/5-EPS	61.2±0.5	42.9±0.6

The addition of 1% EPS-KC66L had little effect on the surface properties of PLA. The contact angle increased slightly from 69.0° to 69.7° ± 0.4, while the surface energy decreased from 40.1 to 39.8 ± 0.4 mJ m^{-2}. These small differences suggest that 1% EPS-KC66L did not markedly change the film surface. At 2.5% EPS-KC66L, the contact angle increased to 73.6° ± 0.3 and the surface energy decreased to 38.4 ± 0.3 mJ m^{-2}, indicating a modest decrease in surface wettability. Similar changes in wettability have been observed in modified and composite PLA films, where the composition and morphology of the surface can affect its interaction with water (Muñoz-Shugulí et al., 2023).

A different trend was observed for PLA/5-EPS. The water contact angle decreased to 61.2° ± 0.5, while

Table 3
Optical properties of printed and unprinted PLA/EPS packaging films

	L^*	a^*	b^*	DE_{00}	Gloss (GU)	Image
Ref. Base Paper	91.85	2.12	-12.81	Ref	6.7	
Unprinted PLA	81.33	2.68	-11.42	7.00	21.5	
Unprinted PLA/1-EPS	83.29	4.38	-10.83	6.62	20.4	
Unprinted PLA/2.5-EPS	81.28	4.10	-6.14	9.26	19.8	
Unprinted PLA/5-EPS	82.96	1.77	-5.28	7.92	18.3	
Ref. Printed Paper	42.35	63.20	24.76	REF	8.9	
Printed PLA	47.55	70.11	28.09	4.71	22.1	
Printed PLA/1-EPS	45.58	67.38	27.25	2.71	20.8	
Printed PLA/2.5-EPS	44.29	66.72	36.03	4.95	19.9	
Printed PLA/5-EPS	42.17	61.78	27.72	1.82	18.7	

the surface energy increased to 42.9 ± 0.6 mJ m^{-2}. The lower contact angle indicates that the film surface became more wettable at the highest EPS-KC66L content. This agrees with the increase in surface energy, as higher surface energy in PLA has been associated with lower water contact angles and improved wettability (Jordá-Vilaplana et al., 2014). The marked change at 5% EPS-KC66L suggests that a higher EPS content had a stronger effect on the film surface.

From a printing perspective, the changes observed for PLA/5-EPS are particularly important. Surface energy and wettability influence how liquid inks spread and interact with polymer surfaces. In general, a higher surface energy promotes better wetting and contact between the ink and the substrate, although ink adhesion also depends on factors such as ink composition, drying conditions, and interfacial interactions (Jordá-Vilaplana et al., 2014). The higher surface energy measured for PLA/5-EPS may therefore be beneficial for subsequent printing.

3.5. Printability Properties of PLA/EPS Packaging Films

The CIELAB color parameters of the unprinted PLA/EPS films are presented in Table 3. The L* values remained within a relatively narrow range, showing that the addition of EPS-KC66L had little effect on the overall lightness of the films. All PLA-based films had lower L* values than the reference paper, which is expected given the different optical characteristics of polymer films and paper substrates. Previous studies have also shown that the L* values of PLA films can vary depending on film composition, processing conditions, thickness, and measurement conditions (Iglesias Montes et al., 2019; Wang & Rhim, 2016).

The clearest change with increasing EPS-KC66L content was observed in the b* values. Starting from a more negative value for neat PLA, b* gradually shifted toward less negative values as the EPS content increased, particularly at 2.5% and 5%. This shift indicates a decrease

in the blue component and a movement toward the yellow region of the CIELAB color space. In contrast, the a* values did not follow a clear trend, increasing at 1% and 2.5% EPS-KC66L and then decreasing at 5%. Overall, EPS-KC66L affected the film color mainly along the blue-yellow axis, while its effect on lightness and the red–green coordinate was less systematic. Similar changes in CIELAB parameters have been reported for PLA-based composite films following the incorporation of dispersed components (Iglesias Montes et al., 2019; Wang & Rhim, 2016). The changes observed at higher EPS-KC66L contents are also in line with the visual appearance of the films, where more noticeable whitish regions were observed at 2.5% and 5% EPS-KC66L.

The ΔE_{00} values, calculated using the reference base paper, represent the overall color difference between the films and the paper substrate. Among the formulations, PLA/2.5-EPS showed the largest color difference from the base paper. However, the ΔE_{00} values do not directly represent the color change caused by EPS-KC66L, since the base paper rather than neat PLA was used as the reference. Therefore, the ΔE00 values are interpreted as the color difference between each film and the base paper (Luo et al., 2001).

The CIELAB color parameters of the printed PLA/EPS films are presented in Table 3. Printed neat PLA had higher L*, a*, and b* values than the printed reference paper, showing that the color of the printed film differed from that of the paper substrate. The addition of EPS-KC66L mainly affected the a* and b* values. The b* value increased noticeably at 2.5% EPS-KC66L, corresponding to a shift toward yellow. At 5% EPS-KC66L, b* decreased again and was closer to the value measured for neat PLA. A similar concentration-dependent pattern was not observed for the other color coordinates. Thus, the color differences after printing varied with EPS-KC66L content, but did not increase consistently as the EPS concentration increased.

A notable difference was observed in the ΔE00 values of the printed films. The value decreased from 4.71 for neat PLA to 2.71 for PLA/1-EPS and further to 1.82 for PLA/5-EPS. In contrast, PLA/2.5-EPS showed a slightly higher ΔE_{00} value of 4.95. The effect of EPS-KC66L was therefore not concentration-dependent. Among the PLA-based films, PLA/5-EPS showed the smallest color difference from the printed reference paper. The lower ΔE_{00} value of PLA/5-EPS may be related to the surface properties of this film. As discussed above, PLA/5-EPS had the lowest water contact angle and the highest surface energy among the tested formulations, indicating greater surface wettability. Surface wettability and surface energy are known to influence the interaction of printing inks with polymer substrates and can affect ink spreading and the appearance of the printed layer (Aydemir et al., 2021; Poljaček et al., 2026). The improved color match observed for PLA/5-EPS may therefore be associated with its different surface characteristics.

The differences observed after printing may also be linked to the presence of EPS-KC66L at the film surface. Changes in EPS content and its distribution within the PLA matrix can affect surface wettability and, in turn, the interaction of the film with printing ink. This may partly explain why PLA/5-EPS showed a lower ΔE_{00} value than neat PLA. However, ΔE_{00} alone is not sufficient to demonstrate improved ink-film interaction. What can be clearly stated is that PLA/5-EPS showed the closest color match to the printed reference paper, together with the highest surface wettability among the tested films.

The gloss values decreased with increasing EPS-KC66L content in both unprinted and printed films. Before printing, gloss decreased from 21.5 GU for neat PLA to 18.3 GU for PLA/5-EPS. A similar decrease was observed after printing, from 22.1 to 18.7 GU. Changes were also seen in the CIELAB color parameters, particularly in the b* values at higher EPS-KC66L contents. These findings indicate that EPS-KC66L affected both the color and surface gloss of the PLA films.

Gloss gradually decreased as the EPS-KC66L content increased. Similar effects have been reported for biopolymer coatings and polymer films, where surface heterogeneity was found to influence specular gloss (Trezza & Krochta, 2001; Wittmann et al., 2021). The PLA-based films were also noticeably glossier than the reference paper, which is reasonable considering the different surface characteristics of polymer films and paper. Substrate properties have previously been shown to affect gloss, color, and print quality in PLA films (Izdebska-Podsiadły, 2021). PLA/5-EPS is particularly interesting in this respect. It had the lowest gloss after printing, but at the same time showed the lowest ΔE_{00}. In other words, this formulation gave the closest color match to the printed reference paper despite having a less glossy surface.

3.6. Ink Adhesion Behavior of PLA/EPS Packaging Films

The reference paper, neat PLA, and PLA/1-EPS received a score of 5, indicating very good ink adhesion. For PLA/2.5-EPS and PLA/5-EPS, the score decreased slightly to 4, with small amounts of ink observed on the tape after peeling. Despite this decrease, ink adhesion remained good for all PLA/EPS films. The slightly lower scores at 2.5% and 5% EPS-KC66L may be related to changes in the film surface. Ink adhesion to polymer substrates depends on several factors, including surface energy, wettability, and the interactions between the ink and the substrate (Aydemir et al., 2021). Since EPS-KC66L also affected the surface properties of the PLA films, these changes may have influenced their inter-

action with the printing ink. However, the difference was small, and even at the highest EPS-KC66L content, the films maintained good overall ink adhesion.

Adding a second component to PLA does not always have the same effect on ink adhesion. Studies on PLA-based blends have reported different adhesion behavior depending on the type and distribution of the added material and the resulting changes in surface wettability (Poljaček et al., 2026). In our films, the small decrease in adhesion at 2.5% and 5% EPS-KC66L appears to follow the changes observed in the surface properties. Still, the decrease was minor, and good ink adhesion was retained even at the highest EPS-KC66L content.

The frictional behavior of the films was evaluated according to ISO 8295. The reference paper had the lowest COF (0.30), compared with 0.40 for neat PLA. As the EPS-KC66L content increased, the COF rose to 0.41, 0.47, and 0.49 for PLA/1-EPS, PLA/2.5-EPS, and PLA/5-EPS, respectively. The steady increase in COF indicates greater resistance to sliding after the addition of EPS-KC66L.

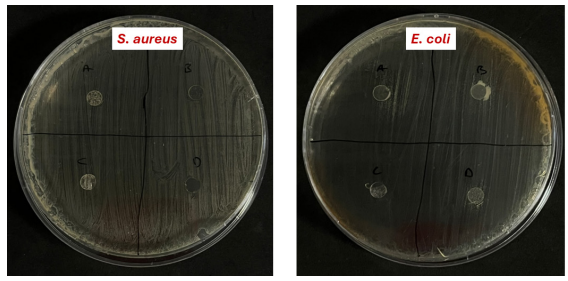
Friction is particularly relevant during film handling and converting, where contact with rollers and other machine surfaces affects web transport (Budinski, 2001). A higher COF can help limit slippage, although too much friction may also make film transport more difficult. In the present films, the increase was gradual, with the highest value measured for PLA/5-EPS.

It is also worth noting that COF, wettability, and ink adhesion did not change in the same way. COF increased steadily with EPS-KC66L content, whereas the contact angle first increased and then dropped at 5% EPS-KC66L. Ink adhesion showed only a small decrease at 2.5% and 5%. These differences are not unexpected, since ink–film interactions depend on several surface properties rather than on a single parameter (Aydemir et al., 2021; Izdebska-Podsiadły, 2021). Despite these changes, all PLA/EPS films retained good-to-very-good ink adhesion.

3.7. Antibacterial Activity of PLA/EPS Packaging Films

The antibacterial activity of the PLA/EPS films against Escherichia coli and Staphylococcus aureus was examined using an agar diffusion assay (Figure 7). No clear inhibition zone was observed around neat PLA (A) or any of the EPS-containing films (B-D). Increasing the EPS-KC66L content did not change this result.

The absence of an inhibition zone alone does not necessarily indicate a lack of antibacterial activity. In agar diffusion tests, the observed response depends on the release and diffusion of antimicrobial components from the material into the surrounding agar. If the active component remains within the polymer matrix



» **Figure 7:** *Agar diffusion assay of PLA/EPS films against E. coli and S. aureus. A: PLA control; B: PLA/1-EPS; C: PLA/2.5-EPS; D: PLA/5-EPS*

or is released only to a limited extent, a clear inhibition zone may not develop even when antibacterial activity occurs through direct contact. In this study, no clear inhibition zone was observed around the films, but no visible bacterial growth was seen on the film surfaces either. Based on this observation, the film surface may have limited bacterial growth to some extent.

4. Conclusions

Microbial EPS from *Ligilactobacillus salivarius* KC66L was successfully incorporated into PLA films without major changes in the chemical structure or thermal behavior of PLA. ATR-FTIR results were consistent with physical incorporation of EPS-KC66L, and only small changes were observed in the main thermal degradation region. The main differences appeared in the optical and surface properties of the films, and they did not always follow the EPS-KC66L concentration. The 5 wt% film was less transparent than neat PLA but had a lower water contact angle and higher surface energy. It also showed the closest color match to the printed reference paper, with ΔE_{00} decreasing from 4.71 for neat PLA to 1.82 for PLA/5-EPS. Increasing the EPS-KC66L content also reduced gloss and increased the coefficient of friction. Ink adhesion, however, remained good to very good for all formulations. No clear inhibition zones were observed against E. coli or S. aureus in the agar diffusion test. At the same time, no visible bacterial growth was seen on the film surfaces. Since this method relies on the release and diffusion of active components from the film, the absence of an inhibition zone does not exclude a possible contact-dependent effect. Of the formulations tested, PLA/5-EPS gave the best combination of surface wettability and color matching after printing, although its optical clarity was lower. Overall, the findings suggest that EPS-KC66L is a promising modifier for adjusting the surface and printing properties of PLA films. Its use in packaging will require a balance between the improved surface characteristics and the loss of transparency at higher EPS contents.

5. Acknowledgments

The authors gratefully acknowledge the Gazi University Scientific Research Projects Coordination Unit for financial support (Project No. **FGA-2025-9893**).

6. References

Abdulkareem, A., Kasak, P., Nassr, M. G., Mahmoud, A. A., Al-Ruweidi, M. K. A., Mohamoud, K. J., Hussein, M. K. and Popelka, A. (2021) 'Surface modification of poly(lactic acid) film via cold plasma assisted grafting of fumaric and ascorbic acid', *Polymers*, 13(21), 3717. DOI: 10.3390/polym13213717

Aydemir, C., Altay, B. N. and Akyol, M. (2021) 'Surface analysis of polymer films for wettability and ink adhesion', *Color Research & Application*, 46(2), pp. 489–499. DOI: 10.1002/col.22579

Bayrak, S. and Omeroglu, M. A. (2026) 'Development and characterization of EPS-modified alginate films with improved barrier, antioxidant, antimicrobial, and antibrowning capabilities', *Food Chemistry*, 513, 149017. DOI: 10.1016/j.foodchem.2026.149017

Boarino, A., Schreier, A., Leterrier, Y. and Klok, H.-A. (2022) 'Uniformly dispersed poly(lactic acid)-grafted lignin nanoparticles enhance antioxidant activity and UV-barrier properties of poly(lactic acid) packaging films', *ACS Applied Polymer Materials*, 4(7), pp. 4808–4817. DOI: 10.1021/acsapm.2c00420

Budinski, K. G. (2001) 'Friction of plastic webs', *Tribology International*, 34(9), pp. 625–633. DOI: 10.1016/S0301-679X(01)00055-X

Çelik, K., Yüksekdağ, Z., Çınar Acar, B. and Kara, F. (2024) 'Determination of antioxidant and antimicrobial activities of cell-free supernatant (CFSKC27L) and exopolysaccharide (EPSKC27L) obtained from Ligilactobacillus salivarius KC27L', *Journal of Tekirdag Agricultural Faculty*, 21(4). DOI: 10.33462/jotaf.1370839

Enumo, A., Gross, I. P., Saatkamp, R. H., Pires, A. T. N. and Parize, A. L. (2020) 'Evaluation of mechanical, thermal and morphological properties of PLA films plasticized with maleic acid and its propyl ester derivatives', *Polymer Testing*, 88, 106552. DOI: 10.1016/j.polymertesting.2020.106552

Ferreira, A. R. V., Torres, C. A. V., Freitas, F., Reis, M. A. M., Alves, V. D. and Coelhoso, I. M. (2014) 'Biodegradable films produced from the bacterial polysaccharide FucoPol', *International Journal of Biological Macromolecules*, 71, pp. 111–116. DOI: 10.1016/j.ijbiomac.2014.04.022

Guerrero, G. B., Santos, K. L., Kamimura, E. S. and de Oliveira, C. A. F. (2024) 'Application of microbial exopolysaccharides in packaging films for the food industry: A review', *International Journal of Food Science & Technology*, 59(1), pp. 17–29. DOI: 10.1111/ijfs.16789

Hassan, D. (2026) 'Chitosan, starch, cellulose, and alginate-based biodegradable nanocomposite food coatings: Interfacial modifications, quality metrics, and lifecycle perspectives: A review', *Carbohydrate Polymer Technologies and Applications*, 16, 101224. DOI: 10.1016/j.carpta.2026.101224

Iglesias Montes, M. L., Luzi, F., Dominici, F., Torre, L., Cyras, V. P., Manfredi, L. B. and Puglia, D. (2019) 'Design and characterization of PLA bilayer films containing lignin and cellulose nanostructures in combination with umbelliferone as active ingredient', *Frontiers in Chemistry*, 7, 157. DOI: 10.3389/fchem.2019.00157

Izdebska-Podsiadły, J. (2021) 'Effect of plasma surface modification on print quality of biodegradable PLA films', *Applied Sciences*, 11(17), 8245. DOI: 10.3390/app11178245

Izdebska-Podsiadły, J. and Dörsam, E. (2017) 'Effects of argon low temperature plasma on PLA film surface and aging behaviors', *Vacuum*, 145, pp. 278–284. DOI: 10.1016/j.vacuum.2017.09.001

Jordá-Vilaplana, A., Fombuena, V., García-García, D., Samper, M. D. and Sánchez-Nácher, L. (2014) 'Surface modification of polylactic acid (PLA) by air atmospheric plasma treatment', *European Polymer Journal*, 58, pp. 23–33. DOI: 10.1016/j.eurpolymj.2014.06.002

Kanmani, P., Kumar, S. R., Yuvaraj, N., Paari, K. A., Pattukumar, V. and Arul, V. (2011) 'Production and purification of a novel exopolysaccharide from lactic acid bacterium Streptococcus phocae PI80 and its functional characteristics activity in vitro', *Bioresource Technology*, 102(7), pp. 4827–4833. DOI: 10.1016/j.biortech.2010.12.118

Liu, L., Wu, Y., Yun, X., Wang, X., Li, J., Chen, L., Lin, F., Wang, S., Dong, T. and Song, L. (2024) 'UV-barrier poly(lactic acid) film with light-stabilized Eu complexes as filler', *International Journal of Biological Macromolecules*, 271(2), 132529. DOI: 10.1016/j.ijbiomac.2024.132529

Luo, M. R., Cui, G. and Rigg, B. (2001) 'The development of the CIE 2000 colour-difference formula: CIEDE2000', *Color Research and Application*, 26(5), pp. 340–350. DOI: 10.1002/col.1049

Machado, N. M. P., Melo, G. C., Camargo, M. F., Feijó, G. G., Putton, B. M. S., Steffens, C., Cansian, R. L., Pessan, L. A. and Moreira, F. K. V. (2021) 'Melt extrusion of environmentally friendly poly(L-lactic acid)/sodium metabisulfite films for antimicrobial packaging applications', *Journal of Renewable Materials*, 9(2), pp. 337–349. DOI: 10.32604/jrm.2021.011081

Mazumder, S., Bhattacharya, D., Lahiri, D. and Nag, M. (2025) 'Microbial-mediated biopolymers (exopolysaccharides) in food packaging: A current time approach in food safety', *ACS Food Science & Technology*, 5(11), pp. 3996–4010. DOI: 10.1021/acsfoodscitech.5c00639

Muñoz-Shugulí, C., Rodríguez-Mercado, F., Benbettaieb, N., Guarda, A., Galotto, M. J. and Debeaufort, F. (2023) 'Development and evaluation of the properties of active films for high-fat fruit and vegetable packaging', *Molecules*, 28(7), 3045. DOI: 10.3390/molecules28073045

Ozdemir, Y., Birtane, H. and Beyler-Çigil, A. (2023) 'An evaluation of antibacterial properties and cytotoxicity of UV-curable biocompatible films containing hydroxyethyl cellulose and silver nanoparticles', *International Journal of Biological Macromolecules*, 245, 125516. DOI: 10.1016/j.ijbiomac.2023.125516

Poljaček, S. M., Tomašegović, T. and Priselac, D. (2026) 'Toward sustainable printed packaging: Surface properties and ink adhesion behavior of PLA/PCL/nanosilica biopolymer blends', *Polymers*, 18(3), 422. DOI: 10.3390/polym18030422

Sanchez-Garcia, M. D., Gimenez, E. and Lagaron, J. M. (2008) 'Morphology and barrier properties of solvent cast composites of thermoplastic biopolymers and purified cellulose fibers', *Carbohydrate Polymers*, 71(2), pp. 235–244. DOI: 10.1016/j.carbpol.2007.05.041

Shen, J., Ramírez-Gómez, Á., Wang, J. and Zhang, F. (2025) 'Autonomous sewing technology and system: A new strategy by integrating soft fingers and machine vision technology', *Textiles*, 5(4), 45. DOI: 10.3390/textiles5040045

Shi, T., Aryantini, N. P. D., Uchida, K., Urashima, T. and Fukuda, K. (2014) 'Enhancement of exopolysaccharide production of Lactobacillus fermentum TDS030603 by modifying culture conditions', *Bioscience of Microbiota, Food and Health*, 33(2), pp. 85–90. DOI: 10.12938/bmfh.33.85

Trezza, T. A. and Krochta, J. M. (2001) 'Specular reflection, gloss, roughness, and surface heterogeneity of biopolymer coatings', *Journal of Applied Polymer Science*, 79(12), pp. 2221–2229. DOI: 10.1002/1097-4628(20010321)79:12<2221::AID-APP1029>3.0.CO;2-F

Wang, L. F. and Rhim, J. W. (2016) 'Grapefruit seed extract incorporated antimicrobial LDPE and PLA films: Effect of type of polymer matrix', *LWT - Food Science and Technology*, 74, pp. 338–345. DOI: 10.1016/j.lwt.2016.07.066

Wang, Q., Ji, C., Sun, J., Zhu, Q. and Liu, J. (2020) 'Structure and properties of polylactic acid biocomposite films reinforced with cellulose nanofibrils', *Molecules*, 25, 3306. DOI: 10.3390/molecules25143306

Wittmann, B., Montmitonnet, P., Burr, A., Gauthier, C., Agassant, J. F. and Casoli, A. (2021) 'BRDF and gloss computation of polyurethane coatings from roughness measurements: modelling and experimental validation', *Progress in Organic Coatings*, 156, 106247. DOI: 10.1016/j.porgcoat.2021.106247

Yuksekdag, Z., Kilickaya, R., Kara, F. and Cinar Acar, B. (2025) 'Biogenic-synthesized silver nanoparticles using the Ligilactobacillus salivarius KC27L postbiotic: Antimicrobial, anti-biofilm, and antioxidant activity and cytotoxic effects', *Probiotics and Antimicrobial Proteins*, 17, pp. 3685–3699. DOI: 10.1007/s12602-025-10481-x

Zeng, Y., Li, Y. and Qiu, C. (2026) 'Plasma-assisted electrospinning of PLA/PVA/ε-polylysine bilayer antibacterial films for active food packaging', *Polymer Engineering and Science*, 66(8), pp. 6071–6079. DOI: 10.1002/pen.70645



© 2026 Authors. Published by the University of Novi Sad, Faculty of Technical Sciences, Department of Graphic Engineering and Design. This article is an open access article distributed under the terms and conditions of the Creative Commons Attribution license 4.0 Serbia (http://creativecommons.org/licenses/by/4.0/rs/).

Graphic materials and substrates

07

Original Scientific Paper https://doi.org/10.24867/GRID-2026-p76

Bio-Based Antibacterial Paper Coatings Enabled by Surface-Modified Silver Nanoparticles

Emine Arman Kandirmaz
Arif Ozcan

Marmara University,
Faculty of Applied Sciences,
Printing Technologies,
Istanbul, Turkey

ABSTRACT

The increasing demand for safer food products and the growing concern over microbial contamination have accelerated the development of sustainable active packaging materials capable of extending shelf life and improving food safety. In this study, bio-based antibacterial paper coatings were developed using a starch matrix reinforced with surface-modified silver nanoparticles (m-AgNPs). The coating formulations were prepared with varying nanoparticle loadings (0, 1, 2.5, and 5 wt%) to investigate the influence of m-AgNP concentration on antibacterial performance and coating functionality. Prior to application, the rheological behavior of the coating dispersions was evaluated to ensure their suitability for coating processes. The formulations were subsequently applied onto paper substrates using an automatic laboratory-scale film applicator under controlled conditions. After drying, the coated papers were characterized in terms of coating deposition and antibacterial activity. The antimicrobial performance of the developed coatings was assessed against the Gram-negative bacterium Escherichia coli and the Gram-positive bacterium Staphylococcus aureus using the disk diffusion method. The results demonstrated that the incorporation of surface-modified silver nanoparticles significantly enhanced the antibacterial performance of the starch-based coatings. Increasing nanoparticle concentration resulted in progressively larger inhibition zones, indicating a concentration-dependent antimicrobial effect. Among the investigated formulations, the coating containing 5 wt% m-AgNP exhibited the highest antibacterial activity against both bacterial strains. The surface modification of silver nanoparticles improved their dispersion stability within the starch matrix, promoting more effective nanoparticle–polymer interactions and contributing to the formation of highly functional antimicrobial surfaces. The findings highlight the potential of starch/m-AgNP composite coatings as environmentally friendly and high-value alternatives to conventional petroleum-based active packaging materials. The developed system provides an effective strategy for integrating renewable biopolymers and nanotechnology to produce next-generation antibacterial paper packaging with enhanced food protection capabilities.

KEY WORDS
Active food packaging, starch coating, surface-modified silver nanoparticles, antibacterial paper, sustainable packaging, bio-based materials, nanotechnology

1. Introduction

Packaging protects the product it contains from unwanted effects, moisture loss or spoilage, damage that may occur due to external factors, and biological degradation. However, these basic functions are becoming insufficient to meet the new needs of today's increasingly consumption-oriented lifestyle and the habits that accompany it.

Consumers now want access to both fresh, high-quality, and safe food (Upadhyay et al., 2024). At this point, the selection, design, and facilitation of packaging materials suitable for the structural characteristics of the food product are extremely important for the preservation and maintenance of quality (Yue et al., 2024).

Various chemical substances can be added to paper during production to give it different properties depending on its intended end use. Paper has a rough surface and does not exhibit the same properties at every point. Therefore, certain chemical substances are added to the paper to fill the voids and create a smoother structure. Surface coating makes the paper physically and chemically more resistant (Ozcan et al., 2021). Some of the substances used in paper surface coating are fillers, binders, optical brighteners, anti-foaming agents, pH balancers, and preservatives. Some existing chemical substances used in paper surface coating or pulp may have negative effects on the environment and human health. This is of serious importance in the production of papers to be used in food packaging (Kunam et al., 2024).

Applications involving coating the surfaces of packaging products, which fall into the active packaging category, with antioxidant natural biopolymer materials to make them suitable for food contact are gaining increasing importance. Environmentally friendly, renewable, and biodegradable natural pigments and dyes are being developed to replace the synthetic pigments currently used to coat food-contact packaging papers. Recent studies have shown that coating paper surfaces with natural dyes and pigments known for their antibacterial and antioxidant properties can provide protection against external factors when in contact with food (Aloui et al., 2011; Rudra et al., 2013).

Antimicrobial agents are defined as substances that inhibit or limit the growth of microorganisms such as bacteria, fungi, and single-celled organisms. Antimicrobial chemicals are essentially divided into two categories: antimicrobial products used industrially to control microorganisms, and chemicals designed to inhibit the growth of pathogens in the environment and on external surfaces. Antimicrobials used in the control of microorganisms are chemicals used in food, textile and paper products, cooling towers, and ventilation systems. Chemicals designed to inhibit pathogens on external surfaces include sterilizers, disinfectants, sanitizing products, and antiseptics (Fahmy et al., 2020).

Due to its strong antibacterial effect and non-toxicity, silver and silver compounds are frequently used in daily life by coating the surfaces of many materials (textiles, ceramics, metals, plastics, glass, paints, etc.) where various microorganisms are frequently found during or after production. Materials containing silver are durable and retain silver ions on their surfaces for a long time (Kawashita et al., 2000). Today, we can see the use of nanotechnology in many fields. It is possible to encounter nano properties even in many ordinary products we use in daily life. Nanotechnological studies are being conducted to control individual atoms or molecules in order to design or create new products (Mohammad et al., 2012; Cerqueira et al., 2018). This technology has a wide range of applications in the food industry in different areas such as increasing product safety, nutrition, reducing agricultural inputs, and new manufacturing methods. For many years, most of the food products we consume have contained nano-components in their structure (Sekhon, 2010; Schnettler et al., 2014; del Rosario Herrera-Rivera et al., 2024).

In this study, bio-based antibacterial paper coatings were developed using a starch matrix reinforced with surface-modified silver nanoparticles (m-AgNPs). The coating formulations were prepared with varying nanoparticle loadings (0, 1, 2.5, and 5 wt%) to investigate the influence of m-AgNP concentration on antibacterial performance and coating functionality. The antimicrobial performance of the developed coatings was assessed against the Escherichia coli and Staphylococcus aureus using the disk diffusion method.

2. Materials and methods

2.1. Materials

In this study, natural starch was used as the coating matrix. Silver nitrate (AgNO3, ≥99.9% purity), sodium borohydride (NaBH4, ≥98% purity), polyvinylpyrrolidone (PVP, mean molecular weight ≈40,000 g/mol), nitric acid (HNO3, 65% w/w), and glycerol were obtained from Sigma-Aldrich and used without any further purification. Deionized water was used in the preparation of all solutions. 80 g/m2 UPM commercial paper was preferred as the coating substrate.

2.2. Methods

2.2.1. Synthesis and surface modification of silver nanoparticles

Surface-modified silver nanoparticles (m-AgNP) were synthesized under laboratory conditions using a chemical reduction method. For this purpose, 0.01 M NaBH4 and 0.01 M PVP solutions were mixed in a 1:1 volume ratio and homogenized on a magnetic stirrer at 1000 rpm for 1 hour. Then, a reduction reaction was carried out by adding a 0.1 M AgNO3 solution dropwise to the reaction medium. The change in the color of the solution from colorless to light yellow during the reaction was considered the first visual indication of the formation of silver nanoparticles (El Hotaby et al.,

2017). After the reaction was completed, the synthesized nanoparticles were filtered, washed with deionized water, and dried under controlled conditions.

The obtained silver nanoparticles were surface modified with nitric acid (65%, w/w) to improve their surface properties and increase their dispersion stability within the polymer matrix (Lestari et al., 2025). For this purpose, the dried nanoparticles were re-dispersed in deionized water, and surface activation was performed by adding a certain amount of HNO3. The prepared suspension was treated in an ultrasonic bath for 6 hours to reduce particle agglomeration and ensure homogeneous surface modification. Following the modification process, the nanoparticles were washed several times with deionized water to remove acid and reaction byproducts, then dried and stored for use in characterization and preparation of coating formulations.

2.2.2. Preparation and application of starch-based antibacterial coating formulations

Coating formulations were prepared using a 10% by weight (w/v) starch solution. For this purpose, the required amount of starch was dispersed in deionized water and heated to 97 °C under continuous magnetic stirring to ensure complete gelatinization. After obtaining a homogeneous dispersion, the system was cooled to room temperature (25 ± 2 °C). Glycerol was added to the cooled starch dispersion as a plasticizer at a ratio of 1.5 mL/100 mL and magnetic stirring was applied for 15 minutes (El-Lakany et al., 2026). Then, silver nanoparticles, synthesized in the laboratory and surface-modified, were added to the dispersion at ratios of 1%, 2.5%, and 5% by weight, based on the amount of dry starch. The formulations were mechanically mixed to ensure homogeneous distribution of the nanoparticles within the starch matrix. A starch dispersion without nanoparticles was also prepared using the same steps and used as a control group. Before coating application, the flow behavior of all prepared formulations was evaluated by rheological analysis.

The prepared coating dispersions were applied to 80 g/m2 base paper surfaces using an automated laboratory-type coating device with a No. 4 K-bar (Mayer rod). The coating process was carried out under constant application conditions to obtain a homogeneous wet film thickness in all samples. The coated samples were dried under controlled laboratory conditions and conditioned before analysis (Kansal et al., 2020).

The coating amount was determined gravimetrically based on the mass difference per unit area of the papers before and after coating, and the results were expressed in g/m2. All measurements were performed in triplicate.

2.2.3. Characterization

Changes in the chemical structure of synthesized and surface-modified silver nanoparticles were investigated using Fourier Transform Infrared Spectroscopy (ATR-FTIR). Analyses were performed using a PerkinElmer Spectrum 100 ATR-FTIR spectrophotometer (PerkinElmer Inc., Waltham, MA, USA) in the wavenumber range of 400–4000 cm^{-1} and with a spectral resolution of 2 cm^{-1}. The obtained spectra were evaluated to determine the changes occurring in the functional groups after surface modification.

The morphology and particle sizes of the synthesized silver nanoparticles were examined using scanning electron microscopy (SEM). SEM analyzes were carried out with a Philips XL30 SEM device. Before analysis, dried nanoparticle samples were placed on the SEM carrier and coated with a thin layer of platinum to increase electron conductivity. Using the obtained micrographs, the morphology, particle size and possible agglomeration state of the nanoparticles were evaluated.

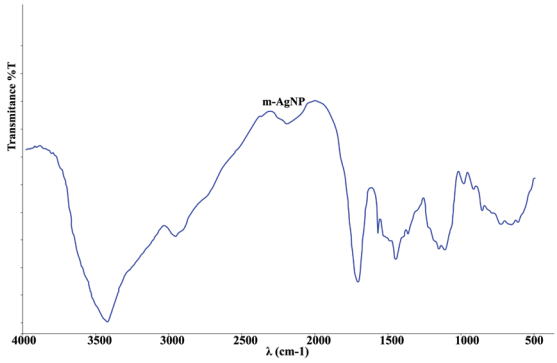
Hydrodynamic particle size, polydispersity index (PDI) and zeta potential values of nanoparticles were determined using the Malvern Zetasizer Nano ZS90 (Malvern Instruments Ltd., Worcestershire, United Kingdom) device, which works on the dynamic light scattering (DLS) principle. The obtained data were used to evaluate the colloidal stability of the synthesized nanoparticles and the effect of surface modification on their dispersion properties.

The antibacterial efficacy of the prepared coating formulations was evaluated using the disk diffusion method. Gram-negative and Gram-positive were selected as test microorganisms. Bacterial cultures were activated by incubating them in Tryptic Soy Broth (TSB) medium at 37 °C for 24 hours prior to the experiment. After the activated cultures were spread homogeneously on the surface of solid medium under sterile conditions, 6 mm diameter disks prepared from uncoated base paper, paper coated only with starch, and coated paper containing different concentrations of surface-modified silver nanoparticles were aseptically placed on the medium. After incubating the Petri dishes at 37 °C for 24 hours, the diameters of the inhibition zones formed around the samples were measured using a digital caliper and evaluated as an indicator of antibacterial activity. All experiments were performed in triplicate, and the results are reported as mean ± standard deviation.

3. Results and discussion

The ATR-FTIR spectra of surface-modified silver nanoparticles are given in Figure 1. The characteristic bands observed in the spectra allowed for the evaluation of

the surface chemistry of the synthesized nanoparticles and the functional group changes that occurred after the modification process. The absorption band determined in the range of 1695–1615 cm^{-1} in pure AgNP samples was associated with the stretching vibrations of amide carbonyl (C=O) in the PVP structure. Similarly, the bands observed at 1462 cm^{-1} and 1423 cm^{-1} originated from the vibrations of the tertiary nitrogen groups in the PVP chains, while the bands at 2953 cm^{-1} and 2874 cm^{-1} corresponded to the asymmetric and symmetric stretching vibrations of the aliphatic –CH2 groups, respectively. The broad absorption band observed at approximately 3447 cm^{-1} was associated with the stretching vibrations of the hydroxyl groups (–OH) and the water molecules adsorbed on the surface. These characteristic bands demonstrate that PVP successfully functions as a coating and stabilizing agent on the synthesized silver nanoparticles. This results in line with literature (Pasieczna-Patkowska, Cichy & Flieger, 2025).

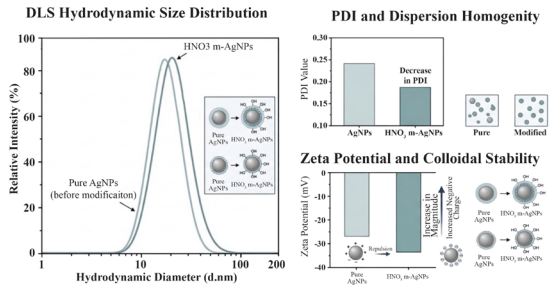


» **Figure 1:** *ATR-FTIR spectrum of m-AgNPs*

Significant changes were observed in the ATR-FTIR spectrum after surface modification with HNO3 (65%, w/w) followed by a 6-hour ultrasonic dispersion treatment. In particular, the intensity of the broad –OH stretching band in the 3420–3455 cm^{-1} range increased by approximately 35–40% compared to pure AgNP samples. In addition, the band associated with hydroxyl groups and adsorbed water molecules on the surface became more prominent around 1630 cm^{-1}, indicating an increase in oxygen-containing functional groups on the surface. These changes reveal that nitric acid treatment increased hydroxylation on the nanoparticle surface and resulted in a more hydrophilic surface structure (Mohammadi, Ishak & Sultan, 2024).

The literature reports that surface activation with nitric acid promotes the formation of oxygen-containing functional groups on metal nanoparticles, thereby increasing the strength of hydroxyl bands. Furthermore, this chemical transformation on the surface is said to increase the colloidal stability of the nanoparticles, reduce agglomeration, and ensure more homogeneous distribution within polymer matrices. The ATR-FTIR results obtained in this study are consistent with these findings, confirming that the applied surface modification was successful and that hydrophilic functional groups capable of enhancing interaction with the starch matrix were effectively formed on the nanoparticle surface. (Li & Li, 2019; Huang et al., 2019).

The hydrodynamic dimensions, polydispersity index (PDI), and zeta potential values of pure and surface-modified silver nanoparticles are given in Figure 2. Dynamic light scattering (DLS) analyses revealed that the average hydrodynamic diameter of AgNPs before modification was in the range of 35.5–49.3 nm. In contrast, after surface modification with HNO_3, the hydrodynamic dimension was observed to increase to the range of 37.8–51.5 nm. This limited increase in size can be attributed to the hydration layer and changes in surface chemistry due to the formation of hydroxyl-rich functional groups on the nanoparticle surface. Considering that the DLS technique determines the hydrodynamic diameter in the dispersion medium, not the dry particle diameter, the observed increase is considered a natural consequence of surface modification.



» **Figure 2:** *DLS and Zeta potential of AgNPs and m-AgNPs*

While the polydispersity index was measured in the range of 0.25–0.29 in AgNPs before modification, it decreased to the range of 0.18–0.22 after surface modification. This decrease in PDI values indicates that the nanoparticles have a narrower size distribution and the dispersion homogeneity increases. In general, PDI values < 0.30 are considered to be indicative of acceptable monodispersity and good dispersion properties in nanoparticle dispersions. Therefore, the results obtained reveal that the surface modification performed with HNO_3 not only changes the surface chemistry but also improves the dispersion behavior of the particles (Badawy et al., 2010).

Zeta potential, a key indicator of colloidal stability, was determined to be −27.10 mV in AgNPs before modification, while it increased to −33.80 mV after surface modification. An absolute value exceeding 30 mV indicates an increase in electrostatic repulsive forces between nanoparticles, resulting in a significant reduction in

agglomeration tendency. This finding supports the idea that oxygen-containing surface functional groups, identified in ATR-FTIR analyses, create additional negative charges on the nanoparticle surface, enhancing dispersion stability. Similarly, the literature reports that acid-activated silver nanoparticles exhibit higher absolute zeta potential values, supporting the formation of more stable colloidal systems. (Gontijo et al., 2020)

When the effect of surface modification on the dispersion behavior within the starch matrix was evaluated, heterogeneous dispersion regions and an initial tendency towards agglomeration were observed in systems containing unmodified AgNPs. This can be attributed to the limited interfacial interactions between the nanoparticle surface and the hydrophilic starch matrix. In contrast, formulations using m-AgNPs showed a more homogeneous dispersion at all nanoparticle concentrations. The hydrophilic functional groups formed as a result of HNO3 modification strengthened hydrogen bonding and other secondary interactions with the starch chains, enabling more effective dispersion of nanoparticles within the polymer matrix. Furthermore, the high viscosity and steric hindrance of the starch matrix limited particle mobility, suppressing re-agglomeration and contributing to the maintenance of dispersion stability. The observed limited local heterogeneities are considered to be due to the natural structural organization of the starch chains rather than nanoparticle aggregation (Abreu et al., 2015; Srikhao et al., 2023).

When all the obtained results are evaluated together, it is concluded that surface modification with HNO_3 not only changes the surface chemistry of the nanoparticles but also increases colloidal stability, improves particle size distribution, and strengthens interface compatibility with the starch matrix, thus significantly contributing to the achievement of more homogeneous composite coatings.

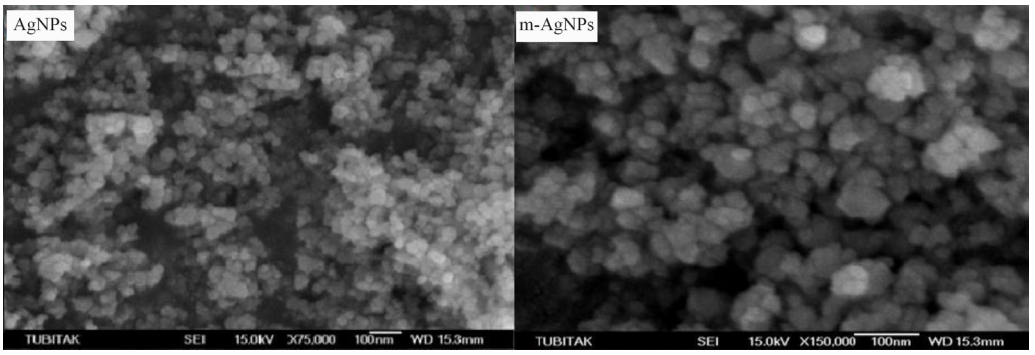
Figure 3 presents SEM images of synthesized pure AgNPs and surface-modified AgNPs. SEM analyses allowed for the evaluation of the morphology, size distribution, and agglomeration tendency of the nanoparticles. In both samples, it was determined that the particles generally exhibited a homogeneous distribution and no significant agglomeration formation was observed.

SEM micrographs of pure AgNPs show that the nanoparticles have a largely spherical morphology and their particle sizes range from approximately 35–48 nm. The narrow size distribution indicates that the nucleation and growth steps occur in a controlled manner during chemical reduction. This can be explained by the rapid reduction capacity of NaBH4, which is due to the controlled particle growth and the limitation of secondary agglomeration (Polte et al., 2012).

It was determined that the morphological integrity of the nanoparticles was preserved after surface modification, but the particle size increased slightly to the range of 38–53 nm. However, it was observed that the m-AgNPs exhibited a more regular size distribution and the distance between particles was more homogeneous. The limited increase in size is thought to be related to the oxygen-containing functional groups formed on the nanoparticle surface after HNO3 treatment and the resulting surface hydration. Nevertheless, the preservation of particle morphology indicates that the applied surface modification did not compromise the structural integrity of the nanoparticles.

SEM results were found to be consistent with DLS and zeta potential analyses. The limited increase in hydrodynamic diameter and decrease in PDI values in the m-AgNPs in DLS analyses support the more homogeneous particle distribution observed in the SEM images. Similarly, the increase in zeta potential from −27.10 mV to −33.80 mV reveals an increase in electrostatic repulsive forces between particles and a decrease in agglomeration tendency. Considering these findings together, it is concluded that surface modification with HNO3 not only alters the surface chemistry but also improves the morphological homogeneity and colloidal stability of the nanoparticles (Danaei et al., 2018).

The obtained results are consistent with the spherical morphology and particle sizes in the range of 20–60 nm reported in the literature for silver nanoparticles synthe-

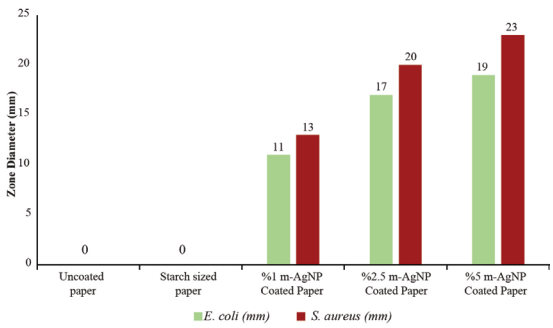


» **Figure 3:** *SEM images of AgNPs and m-AgNPs*

sized by chemical reduction methods. Furthermore, they support the literature findings that surface activation with acid improves dispersion quality and provides a more homogeneous distribution within polymer matrices without significantly altering the morphology of the nanoparticles (Agnihotri, Mukherji & Mukherji, 2013).

All four different coating formulations (control, 1% m-AgNP, 2.5% m-AgNP, and 5% m-AgNP) were successfully obtained without any visible phase separation or precipitation. A slight increase in the viscosity of the dispersions was observed with increasing nanoparticle concentration, and in the formulation containing 5% m-AgNP, it was necessary to extend the mixing time compared to the other formulations to ensure that the nanoparticles were completely homogeneously distributed within the starch matrix. However, it was determined that after additional mixing, the dispersion acquired a homogeneous appearance and maintained suitable flow properties for coating application.

All prepared formulations were successfully applied to the base paper surfaces using a No. 4 K-bar (Mayer rod) in a laboratory-type automated coating device. During the coating process, no streaking, irregular film formation, flow, or coating defects were observed on the surface; a continuous and homogeneous coating layer was obtained in all samples. As a result of gravimetric analyses, the average coating weight was determined as 8.0 g/m2 in all formulations, and no statistically significant difference was found between the samples ($p > 0.05$). This indicates that the change in nanoparticle concentration did not affect the amount of coating applied and that all samples were prepared under comparable coating conditions.



» **Figure 4:** *Antibacterial activity of coatings against E. coli and S. aureus*

The antibacterial activity of starch-based coatings containing varying concentrations of surface-modified silver nanoparticles (m-AgNP) was evaluated against Escherichia coli and Staphylococcus aureus bacteria using the disk diffusion method, and the results are presented in Figure 4. It was determined that no inhibition zones were formed against either bacterial species in the uncoated base paper and control samples coated only with starch. This finding reveals that starch alone does not exhibit antibacterial activity and that the observed antimicrobial activity is entirely due to the surface-modified silver nanoparticles added to the coating formulation (Boukraâ & Amara, 2008).

Significant inhibition zones were formed in all coating formulations containing m-AgNP, and it was observed that antibacterial activity increased steadily with increasing nanoparticle concentration. In coatings containing 1% m-AgNP, inhibition zones of 11 mm and 13 mm were obtained for E. coli and S. aureus, respectively, while these values increased to 17 mm and 20 mm with an increase in nanoparticle concentration to 2.5%. The highest antibacterial activity was determined in coatings containing 5% m-AgNP, with inhibition zones of 19 mm for E. coli and 23 mm for S. aureus. The results demonstrate a significant dose-response relationship between the concentration of surface-modified silver nanoparticles and antibacterial performance (De Plano et al., 2025).

In all formulations, the inhibition zones obtained against S. aureus were found to be higher than those obtained against E. coli. This difference stems from fundamental differences in the cell wall structures of Gram-positive and Gram-negative bacteria. Gram-negative bacteria have an outer membrane containing lipopolysaccharide (LPS) in addition to a thin peptidoglycan layer, which can partially restrict the diffusion of nanoparticles and Ag^+ ions into the cell. In contrast, Gram-positive bacteria lack an outer membrane, and their thick peptidoglycan layer allows for direct interaction with silver nanoparticles. The higher S. aureus inhibition observed in our study suggests that the surface chemistry and dispersion properties of the m-AgNPs used interact more effectively with the Gram-positive cell surface (Tripathi & Goshisht, 2022).

The increase in antibacterial performance is consistent with previous characterization results. ATR-FTIR analyses revealed an increase in surface hydroxyl groups after HNO_3 modification, while DLS analyses showed lower PDI values and higher absolute zeta potential. These findings indicate that the m-AgNPs are more homogeneously distributed within the starch matrix and exhibit a reduced tendency towards agglomeration. Homogeneous distribution increased the active nanoparticle surface area, enhancing the likelihood of contact with microorganisms and thus contributing to improved antibacterial efficacy.

The antimicrobial effect of silver nanoparticles is explained by complementary mechanisms such as disruption of cell membrane permeability, triggering of reactive oxygen species (ROS) formation, inactivation of intracellular proteins and enzymes, suppression of DNA replication, and controlled release of Ag^+ ions. Increasing the nanoparticle concentration increased the

active contact surface area and the amount of released Ag^+ ions, promoting the growth of inhibition zones.

The results obtained are consistent with the concentration-dependent antibacterial behavior reported in the literature for silver nanoparticles used in starch and other polysaccharide matrices. Previous studies have also reported that surface-functionalized AgNPs, in particular, enhance antibacterial efficacy by providing higher colloidal stability and more homogeneous dispersion compared to unmodified nanoparticles. The starch/m-AgNP coating system developed in this study demonstrated effective antibacterial activity even at low nanoparticle loadings, and the formulation containing 5% m-AgNP exhibited the highest performance against both bacterial species, revealing it as a promising alternative for environmentally friendly active coating systems that can be used in food packaging (Yoksan & Chirachanchai, 2010; Rhim, Park & Ha, 2013).

4. Conclusions

In this study, starch-based antibacterial coatings enhanced with surface-modified silver nanoparticles were successfully developed and homogeneously applied to paper-based packaging surfaces. Surface modification significantly increased antibacterial efficacy by improving the colloidal stability and dispersion of nanoparticles within the starch matrix. In particular, the coating containing 5% m-AgNP showed the highest inhibition performance against both Escherichia coli and Staphylococcus aureus. The findings demonstrate that the developed bio-based coating system is a promising alternative for active food packaging due to its potential to reduce microbial contamination. With its simple production method, use of renewable raw materials, and scalable structure, this approach offers a significant alternative that can contribute to the development of sustainable and high-performance next-generation active packaging technologies.

5. Acknowledgments

This study was supported by Marmara University, Commission of Scientific Research Project (M.U. BAPKO) under project FBA-2025-11702.

6. References

Abreu, A.S., Oliveira, M., de Sá, A., Rodrigues, R.M., Cerqueira, M.A., Vicente, A.A. and Machado, A.V. (2015) 'Antimicrobial nanostructured starch based films for packaging', *Carbohydrate Polymers*, 129, pp. 127–134. DOI: 10.1016/j.carbpol.2015.04.021

Agnihotri, S., Mukherji, S. and Mukherji, S. (2013) 'Size-controlled silver nanoparticles synthesized over the range 5–100 nm using the same protocol and their antibacterial efficacy', *RSC Advances*, 4(8), pp. 3974–3983. DOI: 10.1039/c3ra44507k

Aloui, H., Khwaldia, K., Slama, M.B. and Hamdi, M. (2011) 'Effect of glycerol and coating weight on functional properties of biopolymer-coated paper', *Carbohydrate Polymers*, 86(2), pp. 1063–1072. DOI: 10.1016/j.carbpol.2011.06.026

Badawy, A.M.E., Luxton, T.P., Silva, R.G., Scheckel, K.G., Suidan, M.T. and Tolaymat, T.M. (2010) 'Impact of environmental conditions (pH, ionic strength, and electrolyte type) on the surface charge and aggregation of silver nanoparticles suspensions', *Environmental Science & Technology*, 44(4), pp. 1260–1266. DOI: 10.1021/es902240k

Boukraâ, L. and Amara, K. (2008) 'Synergistic effect of starch on the antibacterial activity of honey', *Journal of Medicinal Food*, 11(1), pp. 195–198. DOI: 10.1089/jmf.2007.502

Cerqueira, M.A., Vicente, A.A. and Pastrana, L.M. (2018) 'Nanotechnology in food packaging: opportunities and challenges', *Nanomaterials for Food Packaging*, pp. 1–11. DOI: 10.1016/B978-0-323-51271-8.00001-2

Danaei, M., Dehghankhold, M., Ataei, S., Hasanzadeh Davarani, F., Javanmard, R., Dokhani, A., Khorasani, S. and Mozafari, M.R. (2018) 'Impact of particle size and polydispersity index on the clinical applications of lipidic nanocarrier systems', *Pharmaceutics*, 10(2), 57. DOI: 10.3390/pharmaceutics10020057

De Plano, L.M., Morganti, D., Nicotra, G., Calorenni, P., Sciuto, E.L., Oddo, S. and Conoci, S. (2025) 'Engineered phage-silver nanoparticle complexes as a new tool for targeted therapies', *Scientific Reports*, 15(1), 36135. DOI: 10.1038/s41598-025-05069-y

del Rosario Herrera-Rivera, M., Torres-Arellanes, S.P., Cortés-Martínez, C.I., Navarro-Ibarra, D.C., Hernández-Sánchez, L., Solis-Pomar, F., Pérez-Tijerina, E. and Román-Doval, R. (2024) '*Nanotechnology in food packaging materials: role and application of nanoparticles*', RSC Advances, 14(30), pp. 21832–21858. DOI: 10.1039/D4RA03711A

El Hotaby, W., Sherif, H., Hemdan, B., Khalil, W. and Khalil, S. (2017) 'Assessment of in situ-prepared polyvinylpyrrolidone-silver nanocomposite for antimicrobial applications', *Acta Physica Polonica A*, 131(6), pp. 1554–1560. DOI: 10.12693/APhysPolA.131.1554

El-Lakany, S.A., Elgindy, N.A., Kamoun, E.A., Masanga, P.M., El-Moslamy, S.H., Abu-Serie, M., Aly, R.G. and Abo Aasy, N.K. (2026) 'Phyto-assisted synthesized CuO NPs embedded in crosslinked zein/alginate composite films for hastening wound healing and tissue regeneration in rats bio-template', *Drug Delivery and Translational Research*, 16(5), pp. 1388–1405. DOI: 10.1007/s13346-025-01948-z

Fahmy, H.M., Salah Eldin, R.E., Abu Serea, E.S., Gomaa, N.M., AboElmagd, G.M., Salem, S.A., Elsayed, Z.A., Edrees, A., Shams-Eldin, E. and Shalan, A.E. (2020) '*Advances in nanotechnology and antibacterial properties of biodegradable food packaging materials*', RSC Advances, 10(35), pp. 20467–20484. DOI: 10.1039/D0RA02922J

Gontijo, L.A.P., Raphael, E., Ferrari, D.P.S., Ferrari, J.L., Lyon, J.P. and Schiavon, M.A. (2020) 'pH effect on the synthesis of different size silver nanoparticles evaluated by DLS and their size-dependent antimicrobial activity', *Matéria (Rio de Janeiro)*, 25(04), e-12845. DOI: 10.1590/S1517-707620200004.1145

Huang, B., Liu, G., Wang, P., Zhao, X. and Xu, H. (2019) 'Effect of nitric acid modification on characteristics and adsorption properties of lignite', *Processes*, 7(3), 167. DOI: 10.3390/pr7030167

Kansal, D., Hamdani, S.S., Ping, R., Sirinakbumrung, N. and Rabnawaz, M. (2020) 'Food-safe chitosan–zein dual-layer coating for water-and oil-repellent paper substrates', *ACS Sustainable Chemistry & Engineering*, 8(17), pp. 6887–6897. DOI: 10.1021/acssuschemeng.0c02216

Kawashita, M., Tsuneyama, S., Miyaji, F., Kokubo, T., Kozuka, H. and Yamamoto, K. (2000) 'Antibacterial silver-containing silica glass prepared by sol–gel method', *Biomaterials*, 21(4), pp. 393–398. DOI: 10.1016/S0142-9612(99)00201-X

Kunam, P.K., Ramakanth, D., Akhila, K. and Gaikwad, K.K. (2024) 'Bio-based materials for barrier coatings on paper packaging', *Biomass Conversion and Biorefinery*, 14(12), pp. 12637–12652. DOI: 10.1007/s13399-022-03241-2

Lestari, D.Y., Syoufian, A., Hariani, P.L., Saviola, A.J., Oh, W.-C., Amin, A.K., Pratika, R.A. and Wijaya, K. (2025) 'Facile green synthesis of silver nanoparticles decorated on sulfonated graphene oxide by rambutan (Nephelium lappaceum) leaf extract and application as a catalyst for converting benzene into nitrobenzene', *Results in Engineering*, 25, 104321. DOI: 10.1016/j.rineng.2025.104321

Li, B. and Li, K. (2019) 'Effect of nitric acid pre-oxidation concentration on pore structure and nitrogen/oxygen active decoration sites of ethylenediamine-modified biochar for mercury (II) adsorption and the possible mechanism', *Chemosphere*, 220, pp. 28–39. DOI: 10.1016/j.chemosphere.2018.12.099

Mohammad, A.W., Lau, C.H., Zaharim, A. and Omar, M.Z. (2012) 'Elements of nanotechnology education in engineering curriculum worldwide', *Procedia-Social and Behavioral Sciences*, 60, pp. 405–412. DOI: 10.1016/j.sbspro.2012.09.398

Mohammadi, M., Ishak, M.R. and Sultan, M.T.H. (2024) 'Exploring chemical and physical advancements in surface modification techniques of natural fiber reinforced composite: a comprehensive review', *Journal of Natural Fibers*, 21(1), 2408633. DOI: 10.1080/15440478.2024.2408633

Ozcan, A., Tozluoglu, A., Arman Kandirmaz, E., Tutus, A. and Fidan, H. (2021) 'Printability of variative nanocellulose derived papers', *Cellulose*, 28(8), pp. 5019–5031. DOI: 10.1007/s10570-021-03861-3

Pasieczna-Patkowska, S., Cichy, M. and Flieger, J. (2025) 'Application of Fourier transform infrared (FTIR) spectroscopy in characterization of green synthesized nanoparticles', *Molecules*, 30(3), 684. DOI: 10.3390/molecules30030684

Polte, J., Tuaev, X., Wuithschick, M., Fischer, A., Thuenemann, A.F., Rademann, K., Kraehnert, R. and Emmerling, F. (2012) 'Formation mechanism of colloidal silver nanoparticles: analogies and differences to the growth of gold nanoparticles', *ACS Nano*, 6(7), pp. 5791–5802. DOI: 10.1021/nn301724z

Rhim, J.W., Park, H.M. and Ha, C.S. (2013) 'Bio-nanocomposites for food packaging applications', *Progress in Polymer Science*, 38(10–11), pp. 1629–1652. DOI: 10.1016/j.progpolymsci.2013.05.008

Rudra, S.G., Singh, V., Jyoti, S.D. and Shivhare, U.S. (2013) 'Mechanical properties and antimicrobial efficacy of active wrapping paper for primary packaging of fruits', *Food Bioscience*, 3, pp. 49–58. DOI: 10.1016/j.fbio.2013.07.002

Schnettler, B., Crisóstomo, G., Mora, M., Lobos, G., Miranda, H. and Grunert, K.G. (2014) 'Acceptance of nanotechnology applications and satisfaction with food-related life in southern Chile', *Food Science and Technology*, 34, pp. 157–163. DOI: 10.1590/S0101-20612014005000001

Sekhon, B.S. (2010) 'Food nanotechnology–an overview', *Nanotechnology, Science and Applications*, pp. 1–15. DOI: 10.2147/nsa.s12187498

Srikhao, N., Ounkaew, A., Srichiangsa, N., Phanthanawiboon, S., Boonmars, T., Artchayasawat, A., Theerakulpisut, S., Okhawilai, M. and Kasemsiri, P. (2023) 'Green-synthesized silver nanoparticle coating on paper for antibacterial and antiviral applications', *Polymer Bulletin*, 80(9), pp. 9651–9668. DOI: 10.1007/s00289-022-04530-6

Tripathi, N. and Goshisht, M.K. (2022) 'Recent advances and mechanistic insights into antibacterial activity, antibiofilm activity, and cytotoxicity of silver nanoparticles', *ACS Applied Bio Materials*, 5(4), pp. 1391–1463. DOI: 10.1021/acsabm.2c00014

Upadhyay, A., Agbesi, P., Arafat, K.M.Y., Urdaneta, F., Dey, M., Basak, M., Hong, S., Umeileka, C. and Argyropoulos, D. (2024) 'Bio-based smart packaging: Fundamentals and functions in sustainable food systems', *Trends in Food Science & Technology*, 145, 104369. DOI: 10.1016/j.tifs.2024.104369

Yoksan, R. and Chirachanchai, S. (2010) 'Silver nanoparticle-loaded chitosan–starch based films: Fabrication and evaluation of tensile, barrier and antimicrobial properties', *Materials Science and Engineering: C*, 30(6), pp. 891–897. DOI: 10.1016/j.msec.2010.04.004

Yue, C., Wang, M., Zhou, Z., You, Y., Wang, G. and Wu, D. (2024) 'Cellulose-based intelligent packaging films with antibacterial, UV-blocking, and biodegradable properties for shrimp freshness monitoring', *Chemical Engineering Journal*, 488, 150975. DOI: 10.1016/j.cej.2024.150975



© 2026 Authors. Published by the University of Novi Sad, Faculty of Technical Sciences, Department of Graphic Engineering and Design. This article is an open access article distributed under the terms and conditions of the Creative Commons Attribution license 4.0 Serbia (http://creativecommons.org/licenses/by/4.0/rs/).

Original Scientific Paper https://doi.org/10.24867/GRID-2026-p77

ph-Responsive Starch Films Incorporating Purple Sweet Potato Anthocyanins and Bacterial Nanocellulose

Sanja Mahović Poljaček
Tamara Tomašegović
Davor Donevski

University of Zagreb,
Faculty of Graphic Arts,
Zagreb, Croatia

ABSTRACT

This study investigated the development and colorimetric properties of pH-sensitive indicators by incorporating anthocyanins extracted from purple sweet potato into a starch matrix. The ability of pH-sensitive indicators to change color with variations in food conditions enables their application in real-time freshness and safety monitoring of food products. The assumption that purple sweet potato anthocyanins act as pH-sensitive indicators is based on well-established anthocyanin chemistry and experimentally observed color transitions under varying pH. In this study, anthocyanins were extracted from different purple sweet potato sources – fresh flesh, fresh peel, and dried peel – to evaluate their behavior. The aim was to determine which part of the purple sweet potato provides the greatest source of anthocyanins. The obtained extracts were incorporated into starch matrices based on maize and wheat starch. Bacterial nanocellulose was added to each matrix to enhance the functional performance of the produced films. The results of the research showed that fresh flesh extract provided the highest anthocyanin content (296.07 mg/100 g), followed by fresh peel (206.65 mg/100 g) and dried peel (115.72 mg/100 g). The colorimetric and optical differences between the produced films were observed for dry films and after their immersion in buffer solutions with pH values ranging from 3.0 to 10.0. All prepared films exhibited distinct pH-dependent color changes throughout the investigated pH range, with transitions from reddish-pink under acidic conditions through purple near neutral pH to green, blue, and teal shades under alkaline conditions. The fresh flesh extract generally produced the most pronounced color response, while the incorporation of bacterial nanocellulose preserved the pH-responsive behavior and modified the optical and colorimetric properties of the films, with more consistent color trajectories observed for some formulations, especially films with fresh peel extract and 30% bacterial nanocellulose. The findings demonstrate the potential for producing starch-based pH-sensitive films by incorporating anthocyanins extracted from purple sweet potato and bacterial nanocellulose. The developed bio-based films show potential for use as natural visual pH indicators in intelligent food-packaging applications.

KEY WORDS
Smart packaging, pH indicators, anthocyanins, purple sweet potato, BNC, starch matrix

1. Introduction

Smart packaging has emerged as an advanced approach in food packaging technology, providing functions that go beyond the primary roles of conventional packaging, such as product protection, containment, and communication. Unlike traditional packaging systems, smart packaging incorporates indicators, sensors, or other func-

tional components that can provide information about the condition, quality, or safety of the packaged product and its surrounding environment. Among the different types of smart packaging, visual indicators that respond to changes in pH have attracted considerable attention because of their potential to provide a simple, non-destructive means of monitoring food quality and freshness (D'Almeida & de Albuquerque, 2024). Such systems can be particularly useful for detecting changes associated with food deterioration, including the formation of volatile basic compounds and shifts in acidity during microbial growth (Ludwicka, Kaczmarek & Białkowska, 2020).

Natural pigments have gained increasing interest as active components for the development of pH-responsive colorimetric indicators, particularly due to the growing demand for sustainable, safer materials for food packaging applications. Among naturally occurring pigments, anthocyanins are especially promising because they are water-soluble compounds belonging to the flavonoid family and exhibit distinct color changes in response to pH. Their colorimetric response is associated with structural transformations between different molecular forms, resulting in a range of visible colors under acidic, neutral, and alkaline conditions (Qin et al., 2021). In addition to their pH sensitivity, anthocyanins are widely available in nature and can be obtained from various plant sources, including red cabbage, purple sweet potato, black carrot, berries, grapes, and other fruits, vegetables, and agricultural by-products (Chen et al., 2020; Faisal et al., 2023; Xiao et al., 2023). The use of such sources also supports the valorization of agro-industrial residues and contributes to the development of more sustainable functional materials.

To develop pH-responsive films with anthocyanins as natural pigments, they can be incorporated into a variety of natural and synthetic matrices, including starch, cellulose and cellulose derivatives, chitosan, gelatin, alginate, pectin, polyvinyl alcohol, and other biodegradable polymer systems (Koshy et al., 2021; Qin et al., 2021). These matrices provide structural support for the pigments while enabling the fabrication of films, coatings, and indicator labels. Among biopolymeric materials, starch is particularly attractive because of its abundance, low cost, biodegradability, renewability, and film-forming ability. Starch-based films can therefore serve as suitable matrices for incorporating natural pH-sensitive pigments, offering the possibility of developing environmentally friendly indicator materials for smart packaging applications. Recent studies have demonstrated the successful development of starch-based anthocyanin films for monitoring the freshness of products such as pork, shrimp, and other perishable foods (Bao et al., 2022; Faisal et al., 2023; Koshy et al., 2021). The performance of these films may depend on the type and structure of the starch matrix, with the amylose content also influencing the functionality and stability of anthocyanin-based pH indicators (Faisal et al., 2023). Nevertheless, the mechanical and barrier properties of starch films may be limited, which has encouraged the incorporation of reinforcing materials and nanostructured components. Bacterial nanocellulose (BNC) is a promising biobased material for improving the functional properties of polymeric films. Due to its nanoscale fibrillar network, high specific surface area, mechanical strength, and ability to form interconnected structures, BNC can contribute to the reinforcement of biopolymer-based matrices. Its combination with starch may therefore provide a suitable platform for developing films with improved structural properties while maintaining the advantages of renewable and biodegradable materials (Ludwicka, Kaczmarek & Białkowska, 2020; Mahović Poljaček et al., 2024). Furthermore, the incorporation of anthocyanins into starch/BNC-based systems may enable the development of multifunctional films that combine structural performance with pH-responsive colorimetric functionality. Recent research has demonstrated the potential of starch-based films containing BNC and natural anthocyanins extracted from red cabbage as pH-responsive materials for smart packaging applications (Lee, Durst & Wrolstad, 2005; Mahović Poljaček et al., 2024).

Overall, the development of pH-responsive starch films incorporating natural anthocyanins and bacterial nanocellulose represents a promising approach for the design of sustainable smart packaging materials. In this study, purple sweet potato anthocyanins were incorporated into starch-based films containing bacterial nanocellulose to develop pH-responsive materials with potential application as colorimetric indicators for food smart packaging. The resulting films were evaluated in terms of their visual response to different pH conditions, with the aim of assessing their potential for use as indicator labels for monitoring changes in food quality and freshness.

2. Materials and methods

In this study, purple sweet potato (Ipomoea batatas L.) has been used as a source of anthocyanins. Purple sweet potato anthocyanins are characterized by relatively high stability compared with some other natural anthocyanin sources and exhibit pronounced color changes under different pH conditions. These properties make them attractive for the development of natural colorimetric indicators for food quality monitoring. To determine the most suitable source of anthocyanins from sweet potato (SWP), pigments were extracted from three different sources: fresh peel, fresh flesh, and dried, ground peel. Ethanol, distilled water, and hydrochloric acid were used as the extraction solvent. A solvent mixture was prepared by combining 189 mL of ethanol, 2 mL of HCl, and 50 mL of water. For each extraction, 25 g of SWP material, either fresh peel, fresh flesh, or dried and ground peel, was added to the solvent. The mixture was stirred at 60

°C for 30 min to facilitate pigment extraction. Subsequently, the mixture was cooled to 4 °C and kept at this temperature for 24 h. The extracts were then vacuum-filtered through filter paper to remove solid residues and collect the anthocyanin-containing solution. All extracts were stored in glass bottles at 4 °C until further analysis.

After extraction, the anthocyanin solutions were incorporated into maize- and wheat-starch-based film-forming solutions at concentrations of 14% (v/v) and 12% (v/v), respectively. The film-forming solutions were prepared by dissolving starch in distilled water. Glacial acetic acid (CAS No. 64-19-7) was first diluted to a 1% (v/v) solution and then added to the film-forming solutions at 3% (v/v) for the maize starch (MS)-based solutions and 5% (v/v) for the wheat starch (WS)-based solutions. Glycerol (99.5% purity, CAS No. 56-81-5) was added at concentrations of 15% (v/v) for MS and 20% (v/v) for WS.

Additionally, a set of samples containing bacterial nanocellulose (BNC) was prepared in this study. Our previously published research demonstrated that the incorporation of BNC into starch-based films positively influenced their colorimetric properties, resulting in more vibrant and stable colorimetric responses (Mahović Poljaček, Tomašegović & Donevski, 2026; Mahović Poljaček et al., 2024). In the present study, BNC was added to the film-forming solutions at concentration of 30% (v/v), based on the volume of the BNC suspension, which contained 0.15% dry matter. Bacterial nanocellulose (BNC) was produced from the cellulose-rich biofilm generated during the acetic fermentation of apple juice, following the method described by Lavrič, Medvešček and Skočaj (2020).

The mixtures containing predetermined amounts of dissolved starch, glycerol and acetic acid, with and without BNC, were heated on a temperature-controlled hotplate (Tehtnica, Rotamix 550 MMH, Slovenia) and continuously stirred using a DLS Digital Overhead Stirrer (Velp Scientifica Srl, Italy). After approximately 30 min of mixing, equal volumes of the film-forming solutions were poured into Petri dishes to obtain films of uniform thickness. The poured solutions were then dried and stored in a ventilated environmental chamber at 25 °C and 50% relative humidity (RH) for 10 days.

The produced films were labelled according to the starch matrix, anthocyanin source, and BNC content. “MS” and “WS” denote maize starch and wheat starch films, respectively, while “SWP FP”, “SWP FF”, and “SWP DP” refer to extracts obtained from fresh purple sweet potato peel, fresh flesh and dried peel, respectively. Films without BNC were designated as “0BNC”, while films containing 30% (v/v) of BNC suspension were designated as “30BNC”.

To determine the concentration of anthocyanin pigments extracted from the different SWP sources, the total monomeric anthocyanin content was determined using the pH differential method described by Lee, Durst and Wrolstad (2005). A Shimadzu UV-1900i UV–Vis spectrophotometer (Shimadzu Scientific Instruments, Kyoto, Japan) was used for the measurements. The method is based on the difference in anthocyanin absorbance at pH 1.0 and pH 4.5, measured at a wavelength of 520 nm. This difference in absorbance results from structural transformations of anthocyanins between the two pH conditions. The absorbance spectra of the samples were recorded over the wavelength range of 250–750 nm. The anthocyanin pigment concentration, expressed as cyanidin-3-glucoside equivalents, was calculated using Equation (1), according to Lee, Durst and Wrolstad (2005).

$$\text{Anthocyanin pigment (cyanidin-3-glucoside equivalents,mg/L)} = (A \times MW \times DF \times 1000)/(\varepsilon \times l) \quad (1)$$

where $A = (A_{520\ nm} - A_{700\ nm})_{at\ pH\ 1.0} - (A_{520\ nm} - A_{700\ nm})_{at\ pH\ 4.5}$; MW = 449.2 g moL^{-1} for cyanidin-3-glucoside; DF = dilution factor, l = path-length (cm), ε = 26.900 molar extinction coefficient, in L/mol cm for cyanidin-3-glucoside and 10^3 = factor for conversion from g to mg.

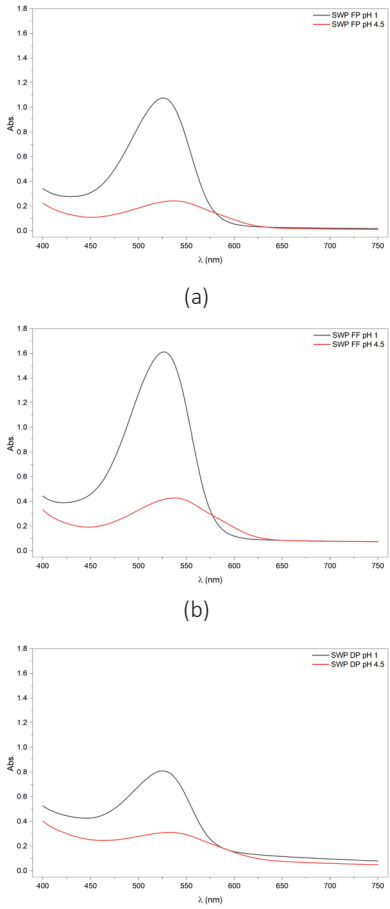
The colorimetric properties of the pH indicators were measured for the dried films and after immersion for 15 min in buffer solutions in buffer solutions ranging from pH 3.0 to pH 10.0. A Techkon SpectroDens spectrophotometer (TECHKON GmbH, Königstein, Germany) was used for the measurements. The spectral reflectance of the films was measured relative to a calibrated white reference, and the CIE L*a*b* color coordinates were calculated from the reflectance data. The results are expressed as lightness (L*) and chromatic coordinates (a* and b*) in the CIE L*a*b* color space (Fairchild, 2013). All measurements were performed using a D50 illuminant and a 2° standard observer with an M1 filter. Each sample was measured at ten different points, and the results are reported as mean values. To evaluate the pH-dependent color changes of the indicator films, the mean total color difference (ΔE^*_{ab}) was also calculated.

3. Results and discussion

3.1. Determination of the total monomeric anthocyanin pigment content

The UV–Vis absorption spectra of anthocyanin extracts obtained from different SWP sources at pH 1.0 and 4.5 are shown in Figure 1. Figure 1.a presents the absorption spectra of the anthocyanin extract obtained from fresh peel, Figure 1.b shows the spectra of the extract obtained from fresh flesh, and Figure 1.c presents the spectra of

the extract obtained from dried peel. Table 1. presents the absorbance values of the extracts at 520 and 700 nm. According to the calculations based on Equation (1), the anthocyanin concentrations in the extracts from fresh peel, fresh flesh, and dried peel, expressed as mg of cyanidin-3-glucoside equivalents per 100 g, were 206.65, 296.07, and 115.72 mg/100 g, respectively.



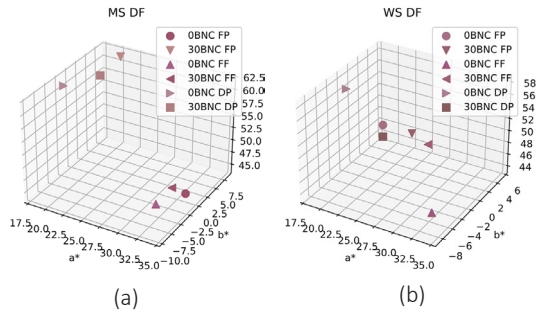
» **Figure 1:** *UV-Vis absorption spectra of SWP anthocyanin extracts, a) fresh peel, b) fresh flesh and c) dried peel*

Table 1
Absorbance values of extracts at 520 and 700 nm at pH values of 1.0 and 4.5

Absorbance	SWP fresh peel		SWP fresh flesh		SWP dried peel	
	pH 1.0	pH 4.5	pH 1.0	pH 4.5	pH 1.0	pH 4.5
A_{520}	1.061	0.228	1.585	0.402	0.802	0.305
A_{700}	0.022	0.014	0.078	0.077	0.096	0.061

3.2. Properties of produced starch-based films

Figure 2 presents the CIE L*a*b* values of the dry films (DF) prepared from different starch types and compositions. Figure 2a presents the results for samples without and with BNC based on maize starch (MS), while Figure 2b presents the corresponding results for samples based on wheat starch (WS). The films exhibited colors ranging between the red and yellow regions of the CIE L*a*b* color space. In Figure 2a, the results are distributed into two distinct regions. The 0BNC DP, 30BNC DP and 30BNC FP samples form a high-lightness and low-redness cluster. In contrast, the 0BNC FP, 0BNC FF and 30BNC FF formulations are grouped at lower lightness and significantly higher redness values. The introduction of BNC (30BNC vs. 0BNC) resulted in changes in redness, with the most pronounced differences observed for the 30BNC FP and 30BNC DP samples. Figure 2b shows that the samples based on wheat starch exhibited greater dispersion in terms of both lightness and the yellow–blue coordinate compared with the maize starch-based films. The 0BNC DP sample remained an outlier, characterized by high lightness and low redness. In contrast, 0BNC FF exhibited the lowest lightness and b* value, indicating a shift toward the blue region. The remaining samples (30BNC DP, 0BNC FP, 30BNC FP, and 30BNC FF) formed a central cluster with intermediate lightness and higher b* values in comparison to other samples. This grouping suggested a similar balance between the chromatic contribution of the anthocyanin extracts and the optical properties of the film matrix. In the BNC-containing films, the formation of the nanocellulose network likely enhanced light scattering and reduced the relative dominance of the anthocyanin coloration, resulting in a shift toward intermediate lightness and higher b* values. This effect was particularly evident for the DP extract, which had the lowest anthocyanin concentration (Figure 1.c). The similar position of the 0% BNC FP samples indicated that a comparable optical response can also be obtained without BNC when the contribution of the FP anthocyanins is balanced by the optical characteristics of the starch matrix.



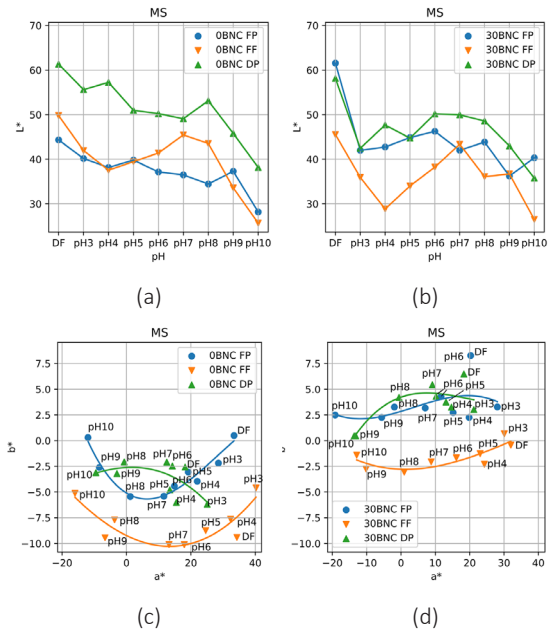
» **Figure 2:** *CIE L*a*b* values of starch-based films: (a) maize starch and (b) wheat starch*

The comparable CIE L*a*b* values obtained for the 0% BNC films containing SWP DP extract, irrespective of the starch type, suggest that the color of these films was primarily determined by the relatively low pigment contribution of the dried-peel extract and the optical characteristics of the starch matrix, while the differences between maize and wheat starch had a comparatively minor effect on the overall color. Similarly, the 0% BNC films containing SWP FF extract exhibited comparable CIE L*a*b* values for both starch types. In this case, the relatively high anthocyanin content of the fresh-flesh extract likely contributed strongly to the overall film color, reducing the relative influence of differences in the starch matrix. The similar color coordinates may therefore indicate that, in the absence of BNC, both starch matrices provided comparable optical environments for the incorporated anthocyanins.

3.3. Colorimetric properties of maize-based films

Absolute CIE L*a*b* values measured for the maize starch-based films after immersion in buffer solutions (pH 3.0–10.0) are presented in Figure 3, where DF on the horizontal axis denotes dry film. Figures 3a and 3b show the lightness (L*) values for films without and with BNC, respectively. The 0BNC samples showed distinct differences in lightness, with the DP (dried peel) sample exhibiting the highest values, while FF (fresh flesh) and FP (fresh peel) showed lower and more variable responses across the pH range. Among the 30BNC films, DP and FF also showed considerable changes in lightness, whereas FP remained relatively stable from pH 3.0 to 9.0. Overall, the 0BNC films exhibited higher maximum lightness values than the 30BNC films. The DP samples consistently showed the highest lightness within both groups, while highly alkaline conditions (pH 10.0) caused a sharp decrease in lightness for almost all samples, except for 30BNC FP, which remained relatively high.

The higher lightness (L*) observed for the 0BNC films compared with the 30BNC films may be related to differences in the optical properties and interactions between the starch matrix and the BNC network. The consistently higher lightness observed for the DP samples in both groups may be associated with the drying of the SWP peel, which may have altered the pigment composition and reduced the concentration of extractable anthocyanins. In contrast, the higher anthocyanin concentrations measured in the FF and FP extracts may be associated with their lower baseline lightness. These observations are consistent with the calculated anthocyanin concentrations presented in Section 4.1, where the lowest anthocyanin concentration was measured in the SWP DP extract and the highest in the SWP FF extract. The pronounced variations observed for SWP FF may be related to the pH-dependent structural changes of anthocyanin compounds (Sohany et al., 2021). Under highly alkaline conditions (pH 9–10), the lower lightness observed for the 0BNC films may be associated with changes in the starch matrix and degradation of anthocyanin compounds. The presence of BNC may have contributed to maintaining the structural integrity of the film matrix and may have limited pigment degradation under alkaline conditions (Abdelkader, Hamed & Gomaa, 2024).



» **Figure 3:** *CIE L*a*b* values of maize-based films: a), c) without BNC and b),d) with BNC*

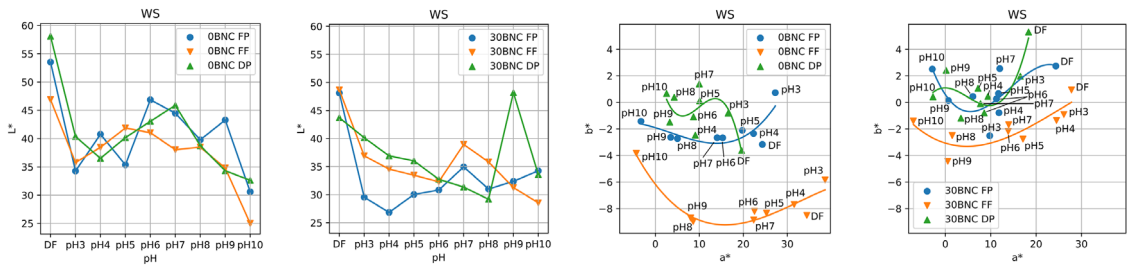
Figures 3c and 3d show chromaticity diagrams illustrating the color changes across pH values from 3 to 10 along the a* (green-red) and b* (blue-yellow) axes for the maize starch-based indicator films. The DF label denotes dry films. Across all samples, increasing pH shifted the a* values from positive (red) toward negative (green) values, reflecting pH-induced changes in the structure and equilibrium of anthocyanin chromophores. Across both formulations, the extracts exhibited a clear pH-responsive chromatic shift: acidic conditions (pH 3.0-5.0) were associated with red to purple hues and higher positive a* values, neutral conditions (pH 6.0-8.0) represented an intermediate transition region, while alkaline conditions (pH 9.0-10.0) resulted in a pronounced shift toward green hues and negative a* values. These color changes are consistent with the known pH-dependent structural transformations of anthocyanins, including changes in the relative proportions of flavylium, quinoidal, and other structural forms, followed by degradation under strongly alkaline conditions (Mahović Poljaček, Tomašegović & Donevski, 2026). Among the pigment sources, FF (fresh flesh) exhibited the most pronounced red coloration at pH 3.0, whereas DP (dried peel) showed an arched trajectory toward higher b* values around pH 6.0-7.0. The incorporation of 30% BNC

resulted in shifts in the color trajectories, particularly along the b* axis, which may be related to changes in the optical properties and light-scattering behavior of the nanocellulose-containing matrix. Similar effects of BNC incorporation on the colorimetric response of starch-based anthocyanin films have been reported, with changes in the a* and b* coordinates depending on BNC concentration and pH (Ghadiri Alamdari et al., 2022). Furthermore, the 30BNC films showed more consistent color trajectories compared with the 0BNC samples, with 30BNC FP (fresh peel) exhibiting a relatively smooth transition along the a* axis while maintaining positive b* values. This behavior indicates a relatively consistent color response of the 30BNC FP formulation over the investigated pH range and highlights its potential for application as a pH-responsive indicator film.

3.4. Colorimetric properties of wheat-based films

Absolute CIE L*a*b* values measured for the wheat starch-based films after immersion in buffer solutions (pH 3.0–10.0) are presented in Figure 4. The CIE L* (lightness) results revealed clear differences between the control (0BNC) and nanocellulose-reinforced (30BNC) wheat starch formulations across the tested pH range. For the 0BNC samples, lightness values remained relatively high, ranging primarily between 35 and 47, with the highest values observed under near-neutral conditions at pH 6.0-7.0. However, all 0BNC samples exhibited a pronounced decrease in lightness under strongly alkaline conditions, reaching their minimum values at pH 10.0, particularly for 0BNC FF. In contrast, the addition of 30% BNC generally decreased the baseline lightness across most of the investigated pH range. The relatively high lightness measured for the 30BNC DP sample at pH 9 represents an exception to the trend observed for the other samples. This deviation may have resulted from variability occurring after immersion in buffer solutions and swelling. Despite the low baseline, BNC incorporation altered the pH-dependent lightness response. The 30BNC FP sample showed a gradual increase in lightness from pH 4.0 to pH 10.0, without the pronounced decrease observed for the corresponding 0BNC sample. Overall, the analysis of the lightness results indicated that incorporating 30% BNC into the wheat starch matrix generally resulted in lower lightness compared with the 0BNC samples. This difference may be related to changes in the optical properties and light-scattering behavior associated with the denser BNC-containing network. Similar effects of the film matrix on the colorimetric response of anthocyanin-based starch films have been reported, indicating that interactions between anthocyanins and the polymer matrix can influence the observed CIE L*a*b* values and pH-dependent color changes (Choi et al., 2017; Koshy et al., 2021). For the 0BNC samples, the relatively high lightness observed at pH 6.0–7.0, followed by a pronounced decrease at pH 10.0, may be associated with pH-induced changes in the starch matrix and structural transformations and degradation of anthocyanin compounds under strongly alkaline conditions, which may alter the optical properties of the films. Purple sweet potato anthocyanins are known to undergo pH-dependent structural transformations, resulting in substantial changes in color and colorimetric parameters, with degradation becoming more pronounced under strongly alkaline conditions (Ke et al., 2024; Koshy et al., 2021; Sohany et al., 2021). In contrast, the presence of BNC may have contributed to maintaining the structural integrity of the film matrix under alkaline conditions, resulting in a more stable lightness response, particularly for the 30BNC FP formulation. This interpretation is consistent with previous studies showing that the polymer matrix can influence the stability and pH-responsive behavior of anthocyanin-containing films.

Results of the chromatic coordinates (Figures 4c-d) of wheat starch-based films demonstrated distinct pH-responsive trajectories from pH 3 to pH 10, varying significantly by extract source. Fresh flesh (FF) formulations consistently maintained lower b* values compared to fresh peel (FP) and dried peel (DP) extracts, which exhibited lower redness (a*) and higher yellowness (b*) under acidic conditions. The addition of bacterial nanocellulose (30BNC) narrowed the chromatic range of the pH-sensitive films while maintaining the overall direction of the pH-dependent colur transition. The shift toward the yellow direction (positive b* values) may be associated with changes in the optical properties of the film matrix caused by the incorporation of the BNC network. This observation is consistent with the results obtained for



(a) (b) (c) (d)

» **Figure 4:** *CIE L*a*b* values of wheat-based films: a), c) without BNC and b), d) with BNC*

the maize-starch-based films, although the effect was slightly more pronounced for the wheat-starch films, suggesting that interactions between BNC and the starch matrix may contribute to the observed color response.

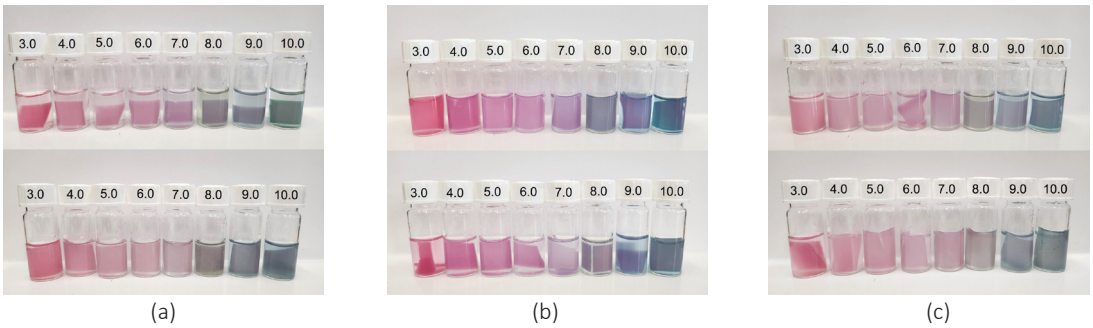
3.5. Visual analysis of starch-based films in varied-pH environment

Visual color changes of the pH-responsive MS-based and WS-based films after 15 min of immersion in buffer solutions (pH 3-10) are presented in Figures 5 and 6. Figures 5a-c show the immersed maize starch films containing SWP anthocyanin extracts from fresh peel, fresh flesh, and dried peel, respectively. The upper images show films without BNC, whereas the lower images show films containing 30% BNC. The MS-based indicator films exhibited a distinct pH-dependent color transition, progressing from pink/red under acidic conditions (pH 3.0-6.0) through purple at near-neutral conditions (pH 7.0-8.0) to green-blue under alkaline conditions (pH 9.0-10.0). These color changes are consistent with the pH-dependent structural transformations of anthocyanins, in which the flavylium cation predominates under acidic conditions, while quinoidal and other deprotonated forms become increasingly important as pH increases, followed by degradation under strongly alkaline conditions (Ke et al., 2024; Koshy et al., 2021). Similar pH-dependent color transitions have also been reported for starch-based films containing BNC and anthocyanins (Mahović Poljaček, Tomašegović & Donevski, 2026). Among the pigment sources, the FF (fresh flesh) extract produced the most visually pronounced color response, followed by FP (fresh peel), whereas DP (dried peel) exhibited darker and more muted tones. The latter may be related to changes in pigment composition or stability during the drying process. The incorporation of 30% BNC slightly reduced the apparent lightness of the films, which may be associated with the optical properties and light-scattering behavior of the nanocellulose network, while the overall pH-dependent color transitions remained clearly distinguishable (Mahović Poljaček, Tomašegović & Donevski, 2026)

The results presented in Figure 6 demonstrate that wheat starch-based film formulations containing SWP fresh peel (FP), fresh flesh (FF), and dried peel (DP) extracts exhibited clear and distinct pH-dependent color transitions across the tested pH range of 3.0-10.0.

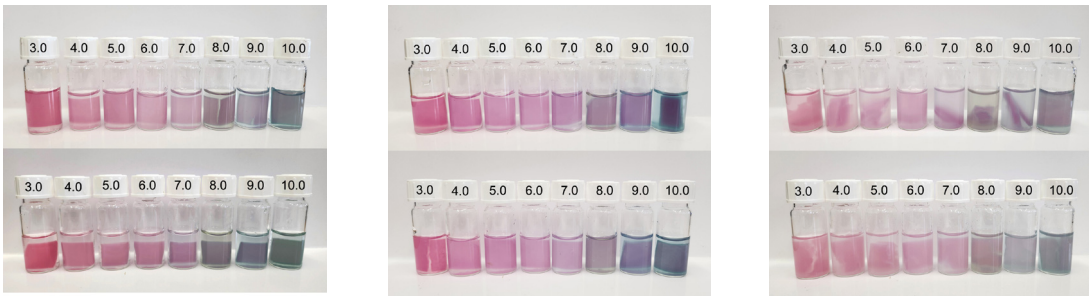
Under acidic conditions (pH 3.0-6.0), the films maintained reddish-pink hues characteristic of anthocyanin-based indicators. These hues gradually changed to light purple near neutral pH (pH 7.0), followed by transitions to dark purple, blue, and deep teal/grey under increasingly alkaline conditions (pH 8.0-10.0). These changes are consistent with the well-known pH-dependent structural transformations of anthocyanins, including the conversion of flavylium cations into quinonoidal and other deprotonated forms at higher pH values (Castañeda-Ovando et al., 2009). The more intense coloration observed for the films containing the SWP FF extract can be attributed, at least in part, to its higher anthocyanin content compared with the FP and DP extracts. The higher concentration of anthocyanins provides a greater amount of pH-sensitive chromophores, resulting in more pronounced and visually distinguishable color changes. In contrast, although fresh peel is also rich in anthocyanins, peel extracts may contain other co-extracted compounds, including phenolic compounds and other constituents, which can influence the resulting color through copigmentation and light-scattering effects (Castañeda-Ovando et al., 2009). The weaker coloration and less pronounced color transitions observed for the DP extract may be related to its lower anthocyanin content, which may have resulted from the drying process. Anthocyanins are susceptible to degradation during drying, particularly under elevated temperatures and in the presence of oxygen, which can lead to the formation of less intensely colored or colorless degradation products (Patras et al., 2010). Consequently, the lower anthocyanin content of the DP extract resulted in lower initial color intensity and less pronounced visual changes across the investigated pH range.

The results presented in Figure 6 demonstrate that wheat starch-based film formulations containing SWP fresh peel (FP), fresh flesh (FF), and dried peel (DP) extracts exhibited clear and distinct pH-dependent color transitions across the tested pH range of 3.0-10.0.



(a) (b) (c)

» **Figure 5:** *Visual color changes of maize starch-based films at different pH values (3.0–10.0): a) fresh peel extract, b) fresh flesh extract, and c) dried peel extract; upper images: 0BNC, lower images: 30BNC*



(a) (b) (c)

» **Figure 6:** *Visual color changes of wheat starch-based films at different pH values (3.0–10.0): a) fresh peel extract, b) fresh flesh extract, and c) dried peel extract; upper images: 0BNC, lower images: 30BNC*

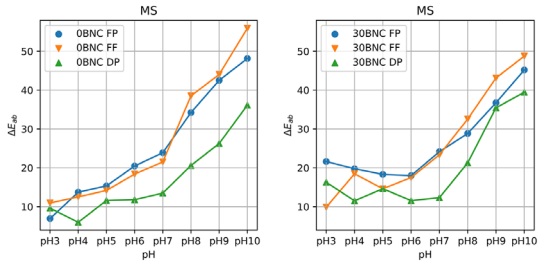
Under acidic conditions (pH 3.0-6.0), the films maintained reddish-pink hues characteristic of anthocyanin-based indicators. These hues gradually changed to light purple near neutral pH (pH 7.0), followed by transitions to dark purple, blue, and deep teal/grey under increasingly alkaline conditions (pH 8.0-10.0). These changes are consistent with the well-known pH-dependent structural transformations of anthocyanins, including the conversion of flavylium cations into quinonoidal and other deprotonated forms at higher pH values (Castañeda-Ovando et al., 2009). The more intense coloration observed for the films containing the SWP FF extract can be attributed, at least in part, to its higher anthocyanin content compared with the FP and DP extracts. The higher concentration of anthocyanins provides a greater amount of pH-sensitive chromophores, resulting in more pronounced and visually distinguishable color changes. In contrast, although fresh peel is also rich in anthocyanins, peel extracts may contain other co-extracted compounds, including phenolic compounds and other constituents, which can influence the resulting color through copigmentation and light-scattering effects (Castañeda-Ovando et al., 2009). The weaker coloration and less pronounced color transitions observed for the DP extract may be related to its lower anthocyanin content, which may have resulted from the drying process. Anthocyanins are susceptible to degradation during drying, particularly under elevated temperatures and in the presence of oxygen, which can lead to the formation of less intensely colored or colorless degradation products (Patras et al., 2010). Consequently, the lower anthocyanin content of the DP extract resulted in lower initial color intensity and less pronounced visual changes across the investigated pH range.

Furthermore, comparison of the upper rows (0BNC) and lower rows (30BNC) indicates that the incorporation of bacterial nanocellulose (BNC) preserved the pH-responsive color-changing behavior of the films while maintaining visually distinguishable color differences. These results demonstrate the potential of the developed starch/BNC films containing SWP anthocyanins as visual pH indicators for intelligent food-packaging applications.

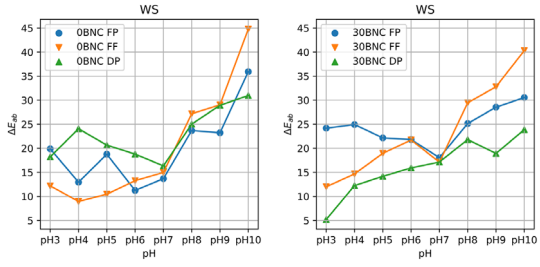
3.6. Color differences of starch-based films in varied-pH environment

Figures 7 and 8 show the total color difference (ΔE^*_{ab}) of the maize and wheat starch-based pH indicator films calculated after immersion in buffer solutions at different pH values (pH 3.0-10.0). Each point represents the ΔE^*_{ab} difference between the means of ten CIE L*a*b* measurements taken on dry film and immersed samples. A ΔE^*_{ab} value of approximately 1 corresponds to a just noticeable color difference, while values of approximately 3 and 5 indicate moderate and highly noticeable color differences, respectively. Figure 7a shows the colorimetric differences for the maize starch without BNC. Colorimetric differences between the immersed films and the corresponding dry films increase with pH. For all three anthocyanin sources (FP, FF and DP) the slope is noticeably steeper from pH 7.0, for the alkaline pH levels. The DP sourced films show smaller colorimetric differences compared to FP and FF which are more similar in that regard. In other cases, displayed in Figure 7b and Figure 8a and 8b, the acidity of solutions appears to have no or very little effect on colorimetric difference. While the colorimetric differences of films immersed in acidic solutions from the dry films are quite large, they are similar for different acidic pH levels. Furthermore, it can be noted that curves become steep for the alkaline pH levels. At alkaline pH levels, the addition of BNC appears to reduce the colorimetric differences in MS films to some extent, although the observed differences remain very noticeable. In all cases, at alkaline pH levels, the largest colorimetric differences are visible on FF films. The MS FP films, Figure 7a and 7b, show colorimetric differences close to those of FF films. For WS films, Figure 8a and 8b, the differences between FF and FP are somewhat larger, but FP still exhibits very large colorimetric differences. It can also be noted that colorimetric differences of FP films do not increase monotonically along the alkaline

pH range for the WS films without BNC, but they do increase monotonically for the WS films with BNC.



» **Figure 7:** *Total color difference (CIE ΔE*ab) of maize starch-based pH indicator films at different pH values: a) without BNC and b) with BNC*



» **Figure 8:** *Total color difference (CIE ΔE*ab) of wheat starch-based pH indicator films at different pH values: a) without BNC and b) with BNC*

4. Conclusions

In this research, purple sweet potato anthocyanins sourced from fresh peel (FP), fresh flesh (FF), and dry peel (DP) were successfully incorporated into maize- and wheat-starch-based films to obtain pH-responsive colorimetric indicators. Among the investigated anthocyanin sources, the fresh flesh extract exhibited the highest total monomeric anthocyanin content (296.07 mg/100 g), followed by the fresh peel (206.65 mg/100 g), while the dried peel extract showed the lowest content (115.72 mg/100 g). Bacterial nanocellulose (BNC) incorporation influenced the colorimetric properties of the produced dry films (before their immersion in buffer solutions), with the effect depending on starch type and anthocyanin source. In BNC-free films, maize and wheat starch exhibited comparable color responses, indicating a relatively minor influence of starch type on the overall film color. All produced starch-based films exhibited distinct pH-dependent color changes over the investigated pH range from 3.0 to 10.0 after immersion in buffer solutions. The films changed from reddish-pink hue under acidic conditions, through purple shades near neutral pH, to green, blue, and teal tones under alkaline conditions, confirming their potential as visual pH indicators. The films with FF generally produced the most intense and visually pronounced color response, consistent with the higher anthocyanin content. For maize-starch-based films, the incorporation of 30% BNC altered the color trajectories, particularly along the b* axis, while providing a more consistent color response across the investigated pH range, and specifically highlighting the potential of the 30BNC FP formulation as a pH-responsive indicator film. Furthermore, the incorporation of 30% BNC narrowed the chromatic range of the wheat-starch-based films while preserving the overall pH-dependent color transition, but with a general shift towards positive b* values- suggesting that BNC-starch interactions influence the optical and colorimetric response of the films. Overall, the results of this research demonstrated that purple sweet potato anthocyanins combined with starch and bacterial nanocellulose can provide visually distinguishable pH-responsive films. The produced materials therefore show promising potential for use as natural colorimetric indicators in intelligent food packaging applications, particularly for visual monitoring of changes associated with food quality and spoilage.

5. Funding

This research was supported by the NextGenerationEU project NPOO MAHOVIĆ POLJAČEK 2025/2029 2025106.

6. References

Abdelkader, R. M. M., Hamed, D. A. and Gomaa, O. M. (2024) 'Red cabbage extract immobilized in bacterial cellulose film as an eco-friendly sensor to monitor microbial contamination and gamma irradiation of stored cucumbers', *World Journal of Microbiology and Biotechnology*, 40(9), 258. DOI: 10.1007/s11274-024-04047-2

Bao, Y., Cui, H., Tian, J., Ding, Y., Tian, Q., Zhang, W., Wang, M., Zang, Z., Sun, X., Li, D., Si, X. and Li, B. (2022) 'Novel pH sensitivity and colorimetry-enhanced anthocyanin indicator films by chondroitin sulfate co-pigmentation for shrimp freshness monitoring', *Food Control*, 131, 108441. DOI: 10.1016/j.foodcont.2021.108441

Castañeda-Ovando, A., Pacheco-Hernández, M. d. L., Páez-Hernández, M. E., Rodríguez, J. A. and Galán-Vidal, C. A. (2009) 'Chemical studies of anthocyanins: A review', *Food Chemistry*, 113(4), pp. 859–871. DOI: 10.1016/j.foodchem.2008.09.001

Chen, S., Wu, M., Lu, P., Gao, L., Yan, S. and Wang, S. (2020) 'Development of pH indicator and antimicrobial cellulose nanofibre packaging film based on purple sweet potato anthocyanin and oregano essential oil', *International Journal of Biological Macromolecules*, 149, pp. 271–280. DOI: 10.1016/j.ijbiomac.2020.01.231

Choi, I., Lee, J. Y., Lacroix, M. and Han, J. (2017) 'Intelligent pH indicator film composed of agar/potato starch and anthocyanin extracts from purple sweet potato', *Food Chemistry*, 218, pp. 122–128. DOI: 10.1016/j.foodchem.2016.09.050

D'Almeida, A. P. and de Albuquerque, T. L. (2024) 'Innovations in food packaging: From bio-based materials to smart packaging systems', *Processes*, 12(10), 2085. DOI: 10.3390/pr12102085

Fairchild, M. D. (2013) *Color Appearance Models*. 3rd edn. Chichester: Wiley.

Faisal, M., Bevilacqua, M., Bro, R., Bordallo, H. N., Kirkensgaard, J. J. K., Hebelstrup, K. H. and Blennow, A. (2023) 'Colorimetric pH indicators based on well-defined amylose and amylopectin matrices enriched with anthocyanins from red cabbage', *International Journal of Biological Macromolecules*, 250, 126250. DOI: 10.1016/j.ijbiomac.2023.126250

Ghadiri Alamdari, N., Forghani, S., Salmasi, S., Almasi, H., Moradi, M. and Molaei, R. (2022) 'Ixiolirion tataricum anthocyanins-loaded biocellulose label: Characterization and application for food freshness monitoring', *International Journal of Biological Macromolecules*, 200, pp. 87–98. DOI: 10.1016/j.ijbiomac.2021.12.188

Ke, F., Liu, D., Qin, J. and Yang, M. (2024) 'Functional pH-sensitive film containing purple sweet potato anthocyanins for pork freshness monitoring and cherry preservation', *Foods*, 13(5), 736. DOI: 10.3390/foods13050736

Koshy, R. R., Koshy, J. T., Mary, S. K., Sadanandan, S., Jisha, S. and Pothan, L. A. (2021) 'Preparation of pH sensitive film based on starch/carbon nano dots incorporating anthocyanin for monitoring spoilage of pork', *Food Control*, 126, 108039. DOI: 10.1016/j.foodcont.2021.108039

Lavrič, G., Medvešček, D. and Skočaj, M. (2020) 'Papermaking properties of bacterial nanocellulose produced from mother of vinegar, a waste product after classical vinegar production', *TAPPI Journal*, 19(4), pp. 197–203. DOI: 10.32964/TJ19.4.197

Lee, J., Durst, R. W. and Wrolstad, R. E. (2005) 'Determination of total monomeric anthocyanin pigment content of fruit juices, beverages, natural colorants, and wines by the pH differential method: Collaborative study', *Journal of AOAC International*, 88(5), pp. 1269–1278. DOI: 10.1093/jaoac/88.5.1269

Ludwicka, K., Kaczmarek, M. and Białkowska, A. (2020) 'Bacterial nanocellulose—A biobased polymer for active and intelligent food packaging applications: Recent advances and developments', *Polymers*, 12(10), 2209. DOI: 10.3390/polym12102209

Mahović Poljaček, S., Tomašegović, T., Strižić Jakovljević, M., Jamnicki Hanzer, S., Murković Steinberg, I., Žuvić, I., Leskovac, M., Lavrič, G., Kavčič, U. and Karlovits, I. (2024) 'Starch-based functional films enhanced with bacterial nanocellulose for smart packaging: Physicochemical properties, pH sensitivity and colorimetric response', *Polymers*, 16(16), 2259. DOI: 10.3390/polym16162259

Mahović Poljaček, S., Tomašegović, T. and Donevski, D. (2026) 'Structural, interfacial, and pH-responsive colorimetric characterization of starch–nanocellulose–anthocyanin indicators developed for biodegradable PLA/PCL food packaging', *Journal of Food Measurement and Characterization*, 20(6), pp. 12465–12486. DOI: 10.1007/s11694-026-04495-4

Patras, A., Brunton, N. P., O'Donnell, C. and Tiwari, B. K. (2010) 'Effect of thermal processing on anthocyanin stability in foods; mechanisms and kinetics of degradation', *Trends in Food Science & Technology*, 21(1), pp. 3–11. DOI: 10.1016/j.tifs.2009.07.004

Qin, Y., Yun, D., Xu, F., Chen, D., Kan, J. and Liu, J. (2021) 'Smart packaging films based on starch/polyvinyl alcohol and Lycium ruthenicum anthocyanins-loaded nano-complexes: Functionality, stability and application', *Food Hydrocolloids*, 119, 106850. DOI: 10.1016/j.foodhyd.2021.106850

Sohany, M., Tawakkal, I. S. M. A., Ariffin, S. H., Shah, N. N. A. K. and Yusof, Y. A. (2021) 'Characterization of anthocyanin associated purple sweet potato starch and peel-based pH indicator films', *Foods*, 10(9), 2005. DOI: 10.3390/foods10092005

Xiao, Z., Han, L., Gu, M., Zhu, Y., Zhang, Y., Li, Z., Xie, T. and Lu, F. (2023) 'Performance comparison of anthocyanin-based smart indicator films', *Food Packaging and Shelf Life*, 40, 101187. DOI: 10.1016/j.fpsl.2023.101187



© 2026 Authors. Published by the University of Novi Sad, Faculty of Technical Sciences, Department of Graphic Engineering and Design. This article is an open access article distributed under the terms and conditions of the Creative Commons Attribution license 4.0 Serbia (http://creativecommons.org/licenses/by/4.0/rs/).

Original Scientific Paper https://doi.org/10.24867/GRID-2026-p78

Surface Free Energy of Polyethylene After Corona Treatment and its Stability at Different Storage Temperatures

ABSTRACT

Polymeric materials, especially polyethylene, are among the most widely used materials due to their mechanical properties, low price, and chemical resistance. However, its low surface free energy and poor wettability represent a major problem in cases where good adhesion of inks, adhesives, or coatings is necessary. The surface free energy of polymeric materials can be increased, for example, by corona, plasma, or flame treatment. This work focuses on monitoring the changes in the surface free energy of polyethylene film after corona treatment. The stability of this treatment was evaluated over time at different storage temperatures of the treated polyethylene film (10 °C, room temperature, and 40 °C). The surface free energy was evaluated by the sessile drop method based on the evaluation of the contact angles of four liquids (water, ethylene glycol, formamide and diiodomethane) on the OCA 50 device. The results show a significant decrease in the free surface energy during first day after corona treatment.

Bohumil Jašúrek
Veronika Holeňová
Jan Vališ

University of Pardubice, Faculty of chemical technology, Department of Graphic Arts and Photophysics, Pardubice, Czech Republic

KEY WORDS
Surface free energy, polyethylene, contact angle, corona, temperature influence

1. Introduction

Polymeric materials are currently among the most widely used materials worldwide, used in various sectors (packaging industry, construction and building industry, textile industry, agriculture, automotive industry, etc.). The most widely used polymer materials include polyethylene (PE), polypropylene (PP), polyethylene terephthalate (PET), polystyrene (PS), and polyvinyl chloride (PVC). The advantages of polymer materials are their good mechanical properties, chemical resistance, and low price. A significant part of the produced polymer materials must be further processed by printing (packaging of various products, textile materials, floor coverings, electronics, etc.). A general problem with printing on most polymer materials is their low free surface energy and wettability, which represents a fundamental problem in cases where it is necessary to ensure good adhesion and spreading of inks, adhesives, or coatings. The surface free energy of some polymers is summarised in Table 1. In order for a liquid, such as printing ink, to wet the printed surface, its surface tension must be lower than the free surface energy of the printed material. The surface tension of inks depends on the type and composition of inks (for example, inkjet inks 22–45 mN/m, offset inks ~37 mN/m, water based flexographic inks 34–38 mN/m) (Izdebska, 2016). Polar liquids such as water have a higher surface tension and nonpolar one has a lower surface tension.

Table 1
Surface free energy of chosen polymeric films (Izdebska, 2016)

Polymeric film	PP	PE	PVC	PS	PET
Surface free energy (mJ/m^2)	29–30	31–36	36–39	43–44	43–47

The surface free energy of polymeric materials and its wettability can be increased by various methods (corona discharge in air, application of low-temperature plasma, flame activation, chemical effect of acid solution,

application of reactive gases – chlorination, fluorination, etc.). In printing, corona discharge treatment is often used to treat the surfaces of polymer printed materials. However, the increasing of the surface free energy and hydrophilic character of treated surfaces is not permanent and there is a noticeable decrease of these parameters in time, and it is called hydrophobic recovery (Guimond & Wertheimer, 2004; Pascual et al., 2008).

Evaluation of the surface free energy of polymers can be done by various methods developed by Berthelot, Anthonow, Girifalco and Good, Fowkes, Owens and Wendt, Wu, Zisman, etc. (Izdebska, 2016). In this paper, the Owens-Wendt method (Owens & Wendt, 1969) was used. This method uses two liquids (one polar and one non-polar) with known surface tensions. According to this method, the polar and dispersive components of the surface free energy (γ) can be estimated (Equation 1),

$$\frac{\gamma_l \cdot (1+\cos(\theta))}{2 \cdot (\gamma_l^d)^{0.5}} = (\gamma_s^p)^{0.5} \cdot \left[\frac{(\gamma_l^p)^{0.5}}{(\gamma_l^d)^{0.5}}\right] + (\gamma_s^d)^{0.5} \quad (1)$$

where ϑ is the contact angle, γ_l is the surface tension of the liquid and γ_s is the surface tension of the solid or the surface free energy. The terms with subscripts *p* and *d* refer to the polar or dispersive component, respectively. Equation 1 is linear equation ($y = ax + b$), where $(\gamma_s^p)^{0.5}$ is the slope of the line and $(\gamma_s^d)^{0.5}$ is the intercept of this line on the *y* axis. The total surface free energy of solid (γ_s) is the sum of polar (γ_s^p) and dispersive (γ_s^d) components $(\gamma_s = \gamma_s^p + \gamma_s^d)$.

This article evaluates changes in the surface free energy of polyethylene film after corona treatment at different storage temperatures (10 °C, room temperature and 40 °C) using the Owens-Wendt method.

2. Experimentals

2.1. Materials

The polyethylene film tested in this paper was from the Czech company GRANITOL and is supplied under the trade name GRANIL O. It is a single-layer non-shrinkable LDPE (low-density polyethylene) film with 60 µm thickness, thermal resistance −50 °C to +85 °C and can be printed with inks.

Four liquids were used for measurements of contact angles on LDPE film. These liquids were distilled water, ethylene glycol (purity > 99.8 %), formamide (> 99.5 %) and diiodomethane (> 99 %). All liquids, except distilled water, were supplied by MERCK.

2.2. Equipment

The Lab Treator ASL 400 TUM from Ahlbrandt (Germany) was used for corona treatment of LDPE film. The device is equipped with a corona unit with two ceramic electrodes, and its speed of movement over the treated material can be changed. The samples were attached to an aluminium table base that serves as a counter electrode. In this work, the speed of movement of the corona unit was 10 m/min at a power 800 W. Corona treatment of the samples under these conditions was always performed twice (immediately after each other). Measurements were carried out at a room temperature.

Goniometer OCA 50EC from DataPhysics (Germany) was used for measuring of contact angles (sessile drop method) of four liquids. For each measurement (before corona treatment, after corona treatment and subsequent measurements over time), 4 samples were prepared and the contact angles of 3 drops of each liquid were measured on each sample. The contact angles of the drops were measured using SCA20 software. Each drop was scanned for 10 seconds (frequency 1 frame per second). The average contact angle values were used to calculate the free surface energy of LDPE using the Owens-Wendt method. The standard deviation was determined for all sample measurements. After corona treatment, contact angles were measured and subsequently the samples were stored under different temperature conditions (10 °C – refrigerator, room temperature – laboratory and 40 °C – oven). Contact angle measurements were performed 2 and 4 hours after corona treatment and next after 1 day, 7 days, 14 days etc. in a period more than two months (see Tables 3, 4, a 5).

3. Results and discussion

First, the surface free energy of the untreated LDPE was measured. Untreated LDPE was measured three times over a five-month period to evaluate stability and repeatability of measurements. The results are presented in Table 2. The results indicate that the surface free energy of untreated LDPE is stable and that the measurement repeatability is very good. The differences between measurements are within the standard deviation. The surface free energy of untreated LDPE was around 26 mJ/cm² and its polar component around 2 mJ/m².

Table 2

Surface free energy (γ_s) of untreated LDPE with polar (γ_s^p) and dispersive (γ_s^d) components. The values in brackets are standard deviations

Measurements	γ_s^p (mJ/m²)	γ_s^d (mJ/m²)	γ_s (mJ/m²)
1	2.0 (0.7)	23.5 (1.5)	25.5 (0.9)
2	2.2 (0.7)	24.0 (0.9)	26.2 (0.7)
3	1.7 (0.4)	24.4 (0.5)	26.1 (0.6)

Tables 3, 4 and 5 summarise the changes in the surface free energy of corona discharge treated LDPE and its decrease over a period of more than two months at room temperature, lower temperature 10 °C (refrigerator) and elevated temperature 40 °C (oven). After corona discharge treatment of LDPE, a significant increase in surface free energy (39–42 mJ/m²) is observed in all measurements, driven by an increase in its polar component (from ~2 mJ/m² to ~12 mJ/m²). The most pronounced decrease in surface free energy is observed for all tested samples during the first day after corona treatment (31.7 mJ/cm² for room temperature, 32.7 mJ/cm² for 10 °C, 31.9 mJ/cm² for 40 °C) and significant changes can be observed as early as 4 hours after treatment. This also corresponds to a significant drop in the polar component, whereas changes in the dispersive component are minor. After more than two months of samples aging, the greatest decrease in surface free energy was observed for samples stored at 40 °C. At the end of this period, the average free surface energy of these samples was 27.8 mJ/cm² (untreated samples ~26 mJ/cm²). The samples stored at room temperature had an average surface free energy 31.6 mJ/cm² and at lower temperature 29.7 mJ/cm². Furthermore, for samples aged at elevated temperatures, a more rapid decrease in free surface energy to values below 30 mJ/cm² can be observed. These values were reached only one week after corona treatment.

The standard deviation of the total free surface energy (γ_s) was low for all measurements (mainly in the range 0.2–0.8 mJ/cm²), indicating good repeatability of the measurements. For each temperature, the standard deviation was calculated based on four evaluated samples.

Table 3

Surface free energy (γ_s) of corona discharge treated LDPE film with polar (γ_s^p) and dispersive (γ_s^d) components in terms of the storage time aged in air at room temperature. The values in brackets are standard deviations

Aging time	γ_s^p (mJ/m²)	γ_s^d (mJ/m²)	γ_s (mJ/m²)
0 hours	12.5 (0.8)	28.5 (0.9)	42.0 (0.4)
2 hours	12.4 (0.4)	29.8 (0.9)	42.2 (0.6)
4 hours	6.8 (2.9)	30.4 (2.7)	37.2 (0.6)
1 day	2.9 (0.2)	28.8 (0.2)	31.7 (0.3)
7 days	2.8 (0.2)	29.5 (0.2)	32.3 (0.2)
21 days	1.9 (0.2)	28.2 (1.1)	30.1 (0.9)
31 days	3.2 (0.5)	28.7 (0.3)	31.9 (0.2)
71 days	3.2 (0.5)	28.4 (0.9)	31.6 (0.4)

Table 4

Surface free energy (γ_s) of corona discharge treated LDPE film with polar (γ_s^p) and dispersive (γ_s^d) components in terms of the storage time aged in air at lower temperature (10 °C). The values in brackets are standard deviations

Aging time	γ_s^p (mJ/m²)	γ_s^d (mJ/m²)	γ_s (mJ/m²)
0 hours	10.9 (2.2)	30.0 (1.9)	40.9 (0.6)
2 hours	5.4 (1.0)	32.6 (1.7)	38.0 (1.0)
4 hours	2.0 (0.3)	31.3 (0.9)	33.3 (0.6)
1 day	2.2 (0.4)	30.5 (1.1)	32.7 (0.7)
7 days	2.3 (0.4)	30.2 (0.8)	32.5 (0.7)
14 days	3.1 (1.5)	28.9 (1.5)	32.0 (0.3)
47 days	3.3 (1.1)	26.2 (1.0)	29.5 (0.4)
69 days	3.5 (1.1)	26.21.0)	29.7 (0.8)

Table 5

Surface free energy (γ_s) of corona discharge treated LDPE film with polar (γ_s^p) and dispersive (γ_s^d) components in terms of the storage time aged in air at elevated temperature (40 °C). The values in brackets are standard deviations

Aging time	γ_s^p (mJ/m²)	γ_s^d (mJ/m²)	γ_s (mJ/m²)
0 hours	12.2 (1.0)	26.8 (0.3)	39.0 (0.8)
2 hours	9.8 (0.5)	28.0 (0.4)	37.8 (0.8)
4 hours	8.0 (0.6)	27.8 (0.3)	35.8 (0.5)
1 day	2.6 (0.5)	29.3 (0.8)	31.9 (0.4)
7 days	2.6 (0.5)	27.3 (0.9)	29.9 (0.6)
14 days	2.2 (0.1)	26.2 (0.3)	28.4 (0.2)
28 days	2.4 (0.3)	26.3 (0.3)	28.7 (0.3)
76 days	2.2 (0.4)	25.5 (0.7)	27.8 (0.6)

4. Conclusions

Increasing the surface free energy and wettability of polymer materials by corona discharge treatment is a commonly used method, for instance, in the printing industry. However, this increase in surface free energy of polymer films is unstable; in the case of non-polar polymers such as polyethylene and polypropylene, the surface free energy decreases relatively quickly, and the hydrophobic surface is restored. This study investigated the effect of temperature and aging time on changes in the surface free energy of LDPE film after corona treatment. Measurements demonstrated a significant decrease in surface free energy within a few hours after corona treatment. In general, the most pronounced changes occurred during the first day after treatment, while the subsequent decrease in the following weeks was slow and gradual. The storage temperature (10°C, room temperature and 40°C) had little impact on the reduction of surface free energy during the first day after corona treatment. However, elevated storage temperatures resulted in a more rapid decrease in surface free energy over the

long term; values below 30 mJ/cm² were reached just one week after corona treatment. These rapid changes in the surface free energy of polymer materials must be taken into account during the processing of polymer films (e.g. printing, lamination, gluing), because the aging time after corona treatment significantly changes the surface properties of the treated materials.

5. References

Guimond, S. and Wertheimer, M.R. (2004) ‚Surface degradation and hydrophobic recovery of polyolefins treated by air corona and nitrogen atmospheric pressure glow discharge', *Journal of Applied Polymer Science*, 94(3), pp. 1291–1303. DOI: 10.1002/app.21134

Izdebska, J. (2016) ‚Printing on Polymers: Theory and Practice'. In: Izdebska, J. and Thomas, S. (eds.) *Printing on Polymers: Fundamentals and Applications*. Oxford: Elsevier, pp. 1–20. DOI: 10.1016/B978-0-323-37468-2.00001-4

Owens, D.K. and Wendt, R.C. (1969) ‚Estimation of the surface free energy of polymers', *Journal of Applied Polymer Science*, 13(8), pp. 1741–1747. DOI: 10.1002/app.1969.070130815

Pascual, M., Balart, R., Sanchez, L., Fenollar, O. and Calvo, O. (2008) ‚Study of the aging process of corona discharge plasma effects on low density polyethylene film surface', *Journal of Materials Science*, 43(14), pp. 4901–4909. DOI: 10.1007/s10853-008-2712-0



© 2026 Authors. Published by the University of Novi Sad, Faculty of Technical Sciences, Department of Graphic Engineering and Design. This article is an open access article distributed under the terms and conditions of the Creative Commons Attribution license 4.0 Serbia (http://creativecommons.org/licenses/by/4.0/rs/).

Original Scientific Paper https://doi.org/10.24867/GRID-2026-p79

The Influence of Paper Substrate and Coating Formulation on Barrier Properties of Packaging Papers

Urška Kavčič
Patricija Pevec

Pulp and Paper Institute, Ljubljana, Slovenia

ABSTRACT

Strict EU PPWR and REACH regulations are pushing the packaging industry towards more sustainable and recyclable packaging materials. Although paper is an excellent sustainable and recyclable substrate, demanding packaging applications (e.g. barrier packaging papers) require functional coatings to provide appropriate barriers against moisture and grease and at the same time meet food contact safety requirements. Based on this demand, the presented study investigates the development of bio-based barrier coatings and their application on two different paper substrates (varying in grammage, surface and structural properties). Base papers were characterized for grammage, thickness, porosity (penetration dynamic analysis) and surface morphology (scanning electron microscopy). Following, four different bio-based coating solutions with different additives ((1) starch, (2) starch + bark-based CNF, (3) starch + bark-based CNF + AKD, (4) starch + bark-based CNF + PVA)) were developed and applied on the selected base papers using the rod coating technique.

The assessment of the coated paper samples regarding water vapour, oil and grease barrier properties was carried out. WVTR (at 50% and 85% RH), Cobb Unger, and KIT tests were evaluated and the results demonstrate how the selected paper base properties and coating formulation (with different additives) influence the barrier properties and provide solutions for over 95% bio-based barrier coating packaging paper.

The results of the study showed that the greatest influence on the barrier properties had the base paper grammage and starch coating, while the additives provided fine-tuning of the final barrier performance.

1. Introduction

Fibre-based packaging is more and more popular due to its high recyclability rate; however, its porous, hydrophilic, and moisture-sensitive nature does not fulfil the requirements for food packaging. To enhance the functional properties of the substrate, the paper must be coated to impart barrier properties against gases, water vapor, oils, and greases. The final performance of the developed coated paper material depends on both the base paper characteristics and the coating formulation.

The characteristics such as porosity, roughness, and density of the uncoated base paper significantly influence the barrier properties attainable by coatings. A smooth, dense substrate enables flawless, consistent coating, which is crucial for attaining low permeability; in contrast, porous or uneven substrates may induce coating imperfections that serve as pathways for gas

and moisture ingress even after coating (Järnström et al., 2026; Marinelli et al., 2023; Rovera et al., 2020).

Besides base paper properties, coating and its functional additives are important for achieving barrier properties. Due to its natural origin, biodegradability, low cost, and excellent film-forming ability, starch is a promising material for developing sustainable barrier coatings for paper and paperboard (Li et al., 2019). When properly formulated and applied, starch-based coatings substantially improve barrier properties; however, the barrier performance is often limited by its sensitivity to moisture and humidity. Further enhancement can be achieved through the incorporation of functional additives that have to be selected carefully to improve barrier performance without compromising the recyclability of the coated paper (Bakker et al., 2022; Chi et al., 2023). Nanocellulose (CNF) as a reinforcing and tortuosity-building filler can improve barrier properties, particularly gas barrier; however, its hydrophilicity can limit performance when exposed to higher relative humidities (Afra, Mohammadnejad & Saraeyan, 2016; Chi et al., 2023; Lengowski et al., 2023; Wang et al., 2017). It can be obtained from different raw materials, one of them being the use of discarded bark biomass to produce bark-based CNF (Borrega et al., 2026). To overcome its hydrophilicity, alkyl ketene dimer (AKD) can serve as a sizing agent and hydrophobic modifier and polyvinyl alcohol (PVA) as a water-dispersible binder with favourable barrier characteristics (Christophliemk et al., 2017; Huang et al., 2023). AKD is a classic internal sizing agent that reacts with cellulose hydroxyl groups to impart hydrophobicity, thereby reducing water uptake and improving oil resistance. It forms covalent linkages with the cellulose surface, contributing to moisture barrier improvements that are particularly relevant when starch-based coatings are hydrophilic and prone to water uptake (Roberts, 1997). On the other hand, PVA is widely used as a water-soluble, non-toxic binder in starch-based coatings due to its film-forming ability and compatibility with CNF. PVA contribute to barrier performance through its dense film-forming capability and its potential to improve continuity and reduce defects that act as diffusion pathways. In starch-based systems, PVA often acts in synergy with other additives (CNF and AKD) to achieve balanced barrier properties without drastically increasing coat (Huang et al., 2023). When these components are combined in well-designed formulations, the coating can synergistically reduce water vapour transmission rate (WVTR) and enhance grease/oil resistance, while supporting recyclability of the cellulose substrate.

The influence of PVA and AKD additives in coatings on the barrier properties of packaging paper was investigated by Shen et al. (2021). The results showed that PVA coating reduced the WVTR by forming a continuous film that sealed the pores of the surface. The incorporation of AKD improved the water resistance further, resulting in lower Cobb values. They demonstrated that combining a film-forming polymer with a hydrophobic agent can improve the barrier properties of the paper.

Despite the high interest in barrier coatings for paper packaging, a clear gap exists in terms of studies concentrating on the evaluation of the impact of each individual component on the obtained barrier performance. Besides, research specifically investigating the application of bark-derived cellulose nanofibrils (CNF) in such coatings remains limited. Thus, the present work aims to fill this research gap by analysing the effects of the coating formulation (including bark-based CNF) and its individual components on the barrier properties of coated paper. The study investigates the effect of two different base papers (with different properties) and four coating formulations with different functional additives (bark-based CNF, AKD, PVA) on the resulting barrier properties of coated paper. This approach offers a thorough understanding of the interactions between the substrate and coating formulation and their contribution to the barrier performance of the developed coated paper materials to water vapour, oils and greases.

2. Matherials and Methods

In the presented research, two different base papers (Paper 1 and Paper 2) produced by Goričane papermill (Slovenia) were used for coating application. The base papers were firstly characterized regarding basic and surface properties. Grammage (ISO 536), thickness (ISO 534), smoothness (ISO 8791-2), porosity (ISO 5636-3) and filler content at 500°C (ISO 1762) were determined. Additionally, the surface morphology and cross-section of the base papers were characterised using a scanning electron microscope (SEM; JEOL JSM-6060 LV, Japan).

Additionally, the samples were characterised with a penetration dynamics analyser Emtec PDA.C 02 (Emtec, Germany). During this method, a testing sample is placed in contact with a testing liquid. The instrument continuously monitors the drop in the ultrasonic signal due to the penetration (capillary absorption) of 16% isopropyl alcohol (IPA) to determine the porosity of the sample surface.

Following this, four different bio-based coating solutions based on starch (S) A4692 (Avebe, The Netherlands) with different additives to enhance the barrier performance were developed. As additives, unbleached bark-based cellulose nanofibers (CNF) VTT20 produced in the scope of the SuperBark project, alkyl ketene dimer (AKD) and polyvinyl alcohol (PVA) Exceval AQ-4104 (Kuraray, Japan) were used. All final developed coating solutions had a bio-based content of at least 95%.

The developed coating solutions (Table 1) were applied in one layer (10 g/m^2) on the base papers with a laboratory rod coater RK Print Coater. After coating,

the samples were dried in a ventilation oven under controlled conditions at 105°C for one minute.

The prepared coated samples were evaluated regarding barrier properties important for food packaging paper. Water vapour transmission rate (WVTR) was determined in accordance with the gravimetric method (ISO 2528 standard) at 50% as well as 85% relative humidity and 23°C. Oil absorption (Cobb Unger 30 s) was evaluated according to SCAN-P 37:77 and grease resistance (KIT test) according to TAPPI T559 standard procedure. All samples were conditioned under standard conditions in accordance with ISO 187 prior to testing.

Table 1

Developed coating solutions and contents of the components used

	Solid content (wt%)	**The content (%) of each component in the coating formulation**			
Sample		Starch	CNF	AKD	PVA
S	25	100	0	0	0
S+CNF	20	97	3	0	0
S+CNF+AKD	20	92	3	5	0
S+CNF+PVA	20	92	3	0	5

3. Results and Discussion

The evaluation of the selected base papers revealed that Paper 1 and Paper 2 differ considerably in their structural and surface properties as presented in Table 2. Paper 1 had a lower grammage (51.2 g/m²), thickness (57 µm), and filler content (7%) compared to Paper 2 (90 g/m², 90 µm, and 13%, respectively). Due to lower filler content and different surface pre-coating, Paper 1 also exhibited higher Bendtsen smoothness and porosity values (90 mL/min for both), whereas Paper 2 showed values of 50 and 1.5 mL/min. Both papers were sized using a rosin-based sizing agent.

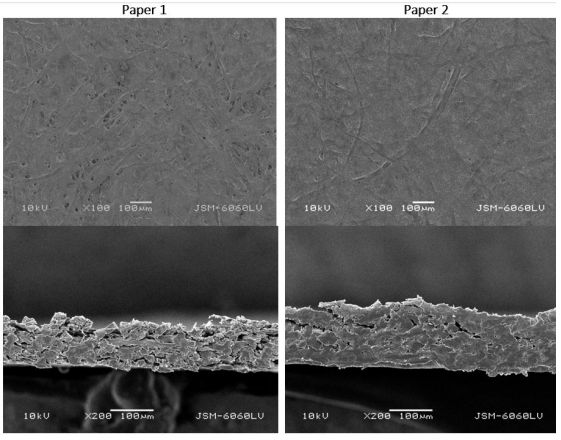
Table 2

Basic properties of the base papers used

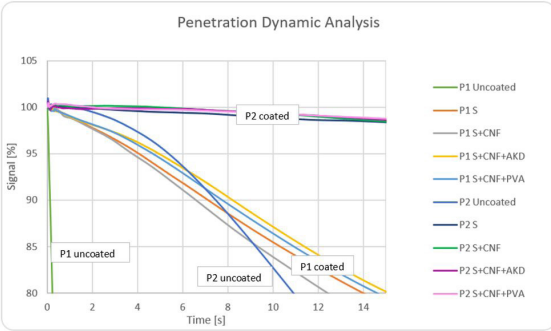
	Paper 1	**Paper 2**
Grammage (g/m²)	51.2	90
Filler at 500°C (%)	7	13
Thickness (µm)	57	90
Smoothness Bendtsen (mL/min)	90	50
Porosity Bendtsen (mL/min)	90	1.5
Type of sizing agent	Rosin sizing agent	Rosin sizing agent

The differences in porosity, thickness, and surface structure between the two paper substrates were also clearly observed in the SEM images (Figure 1). Paper 1 exhibited a more open and heterogeneous surface structure, whereas Paper 2 showed a denser and more compact structure with a smoother surface.

To gain a deeper insight into paper porosity, penetration dynamics analysis of all coated and uncoated samples was performed. For the evaluation of porosity, 16% isopropanol (IPA) was used as it is a very wetting fluid, so penetration is governed mainly by capillary absorption and the natural pore structure of the substrate. The decrease in ultrasonic signal intensity in the first 15 seconds after the sample was in contact with the testing liquid is presented in Figure 2. The penetration dynamics of the two uncoated base paper substrates, Paper 1 (P1) and Paper 2 (P2), show a significant difference. The uncoated Paper 1 shows an extremely rapid drop in the signal, reaching the 95% threshold almost immediately, which indicates a very porous network with fast capillary absorption. In contrast, uncoated Paper 2 shows a considerably lower penetration rate, indicating a significantly denser pore structure of the base. All coated samples on Paper 1 decrease the porosity of the paper (the signal drops to 95% between 4 and 6 seconds), which is good evidence that the coatings are successfully blocking the open surface pores and limiting capillary transport. However, the porosities of coated samples on Paper 1 are very similar to uncoated Paper 2. The coatings on the denser Paper 2 achieve almost complete barrier performance against 16% IPA. The signal intensity of all coated P2 samples is almost the same over the entire 15-second measurement time and is above 98%, with excellent resistance to wetting and penetration. PDA results show that the application of coatings seals the porous network of more porous base papers (Paper 1) efficiently, but the combination of dense base paper (Paper 2) with barrier coatings forms a near-impermeable structure to polar wetting liquids.



» **Figure 1:** *SEM images of the base papers. Surface (top) and cross-section (bottom)*

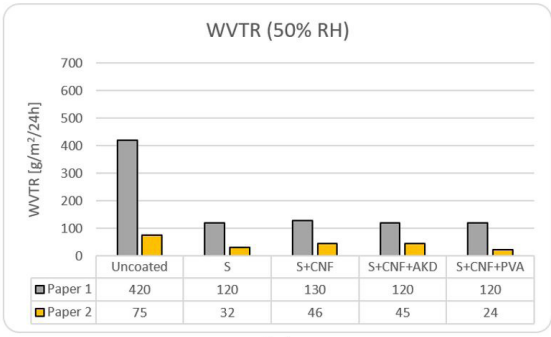


» **Figure 2:** *Penetration dynamic chart with 16% IPA as a testing liquid. P1 presents samples on Paper 1 and P2 presents samples on Paper 2*

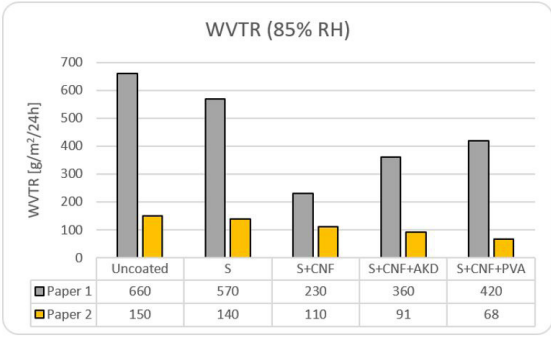
Water vapour transmission rate (WVTR) measurements at 50% and 85% relative humidity (RH) revealed significant differences in barrier performance between the two substrates (Figure 3). Paper 2 outperformed Paper 1 by more than five times when uncoated; however, WVTR at 50% RH is almost halved in comparison to WVTR at 85% RH. Large differences were also evident when both papers were coated with the developed coating formulations, which could be attributed to the thickness and porosity of the base papers. At 50% RH, uncoated Paper 1 exhibited high WVTR (420 g/m^2/24h), which decreased sharply upon applying coating S (120 g/m^2/24h); however, additives in the coating formulations did not further decrease WVTR. WVTR of samples on Paper 2 systematically reduced from 75 g/m^2/24h (uncoated) down to a minimum of 24 g/m^2/24h with the S+CNF+PVA formulation. Higher humidity (85% RH) increased WVTR overall. On Paper 1, the S+CNF formulation provided the strongest barrier enhancement, reducing WVTR to (230 g/m^2/24h), whereas additional AKD or PVA proved counterproductive. Conversely, samples on Paper 2 displayed an improvement with each added component from Uncoated (150 g/m^2/24h) to the sample coated with S+CNF+PVA coating solution (68 g/m^2/24h). Overall, S+CNF is optimal for upgrading the porous Paper 1 at high RH, while S+CNF+PVA yields the best performance among coating solutions on the denser Paper 2 substrate at both relative humidities.

Besides WVTR barrier properties, the prepared coated samples were evaluated also for oil and grease barrier properties.

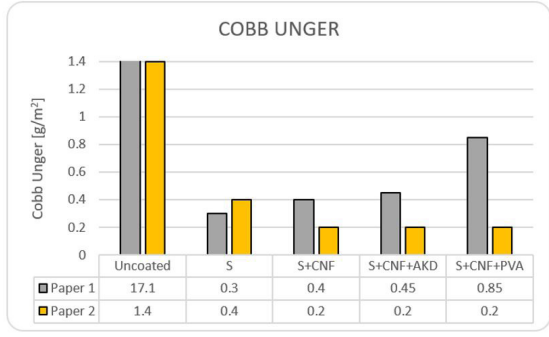
Oil absorbency was evaluated with the Cobb Unger testing method after 30 seconds of sample/oil contact. A lower Cobb Unger value represents lower oil absorption. Grease resistance was evaluated with the KIT test, where the highest value (12) presents superior grease resistance and where the solution applied on the surface of the sample does not stain the surface. As can be seen from Figure 4 a huge difference is evident between uncoated papers, where uncoated Paper 1 showed extremely poor oil barrier with a Cobb Unger value of 17.1 g/m^2 and a KIT value of 0, while uncoated Paper 2 exhibited much lower oil absorbency (1.4 g/m^2) and a KIT value of 1, further



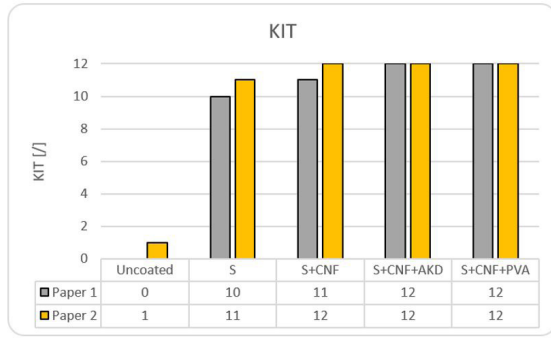
(a)



(b)



(a)



(b)

» **Figure 3:** *WVTR of tested samples at 50% RH (a), and 85% RH (b)*

» **Figure 4:** *Cobb Unger (a) and KIT values (b) for tested samples*

confirming the importance of a denser structure and higher grammage of the base paper. After coating application, both barriers increased significantly. With starch coating (S), oil absorbency dropped to 0.3 and 0.4 g/m^2, while KIT values increased to 10 or 11. The addition of CNF and other additives further improved the Cobb Unger on Paper 2, while on Paper 1 the barrier decreased slightly. However, KIT values increased to the highest value (12) and remained the same for all coating formulations with additives (CNF, AKD or PVA) on Paper 2.

4. Conclusion

In conclusion, the evaluation of water vapour and oil and grease barrier properties emphasises the importance of the choice of the base paper substrate. The denser and less porous structure of Paper 2 consistently outperformed Paper 1 under all testing conditions and thus had the most critical impact on overall barrier efficiency. The primary starch coating (S) is critical in establishing the basic barrier, while the addition of functional additives is mostly a fine-tuning process to adjust specific barrier properties. In particular, the CNF was found to be critical for enhancing WVTR performance on the more porous Paper 1 substrate under high relative humidity (85% RH) conditions. However, the fully formulated S+CNF+PVA coating mixture showed the best overall performance, with the lowest water vapour transmission rates and excellent oil and grease resistance. In particular, no significant differences in the grease and oil barrier properties were observed for Paper 2 with different functional additives (CNF, AKD or PVA) added to the starch base, as all formulation combinations provided excellent grease repellency and low oil absorption.

5. Acknowledgment

The SuperBark project (grant agreement No. 101112447) is supported by the Circular Bio-based Europe Joint Undertaking and its members.

Funded by the European Union. Views and opinions expressed are however, those of the author(s) only and do not necessarily reflect those of the European Union or CBE JU. Neither the European Union nor the CBE JU can be held responsible for them.

6. References

Afra, E., Mohammadnejad, S. and Saraeyan, A. (2016) 'Cellulose nanofibils as coating material and its effects on paper properties', *Progress in Organic Coatings*, 101, pp. 455–460. DOI: 10.1016/j.porgcoat.2016.09.018

Bakker, S., Kloos, J., Metselaar, G.A., Esteves, A.C.C. and Schenning, A.P.H.J. (2022) 'About gas barrier performance and recyclability of waterborne coatings on paperboard', *Coatings*, 12(12), 1841. DOI: 10.3390/coatings12121841

Borrega, M., Lahtinen, P., Spönla, E. and Kalliola, A. (2026) 'Tailoring the polyphenol content of softwood bark residues for cellulose nanofibril barrier films', *Carbohydrate Polymer Technologies and Applications*, 15, 101204. DOI: 10.1016/j.carpta.2026.101204

Chi, K., He, J., Lin, W., Bokhari, S.M.Q. and Catchmark, J.M. (2023) 'Electrostatically complexed natural polysaccharides as aqueous barrier coatings for sustainable and recyclable fiber-based packaging', *ACS Applied Materials & Interfaces*, 15(9), pp. 12248–12260. DOI: 10.1021/acsami.2c17886

Christophliemk, H., Ullsten, H., Johansson, C. and Järnström, L. (2017) 'Starch-poly(vinyl alcohol) barrier coatings for flexible packaging paper and their effects of phase interactions', *Progress in Organic Coatings*, 111, pp. 13–22. DOI: 10.1016/j.porgcoat.2017.04.018

Huang, S., Wang, X., Zhang, Y., Meng, Y., Hua, F. and Xia, X. (2023) 'Water and oil-grease barrier properties of PVA/CNF/MBP/AKD composite coating on paper', *Scientific Reports*, 13(1), 12292. DOI: 10.1038/s41598-023-38941-w

Järnström, L., Christophliemk, H., Bohlin, E., Larsson, J. and Emilsson, P. (2026) 'Multilayer barrier coatings with starch/bentonite for paperboard—the effects of the number of layers and the drying strategy on the barrier properties', *Coatings*, 16(3), 299. DOI: 10.3390/coatings16030299

Lengowski, E.C., Bonfatti Júnior, E.A., Coelho Simon, L., de Muniz, G.I., de Andrade, A., Neves Leite, A. and de Miranda Leite, E.L. (2023) 'Nanocellulose coating on Kraft paper', *Coatings*, 13(10), 1705. DOI: 10.3390/coatings13101705

Li, H., Qi, Y., Zhao, Y., Chi, J. and Cheng, S. (2019) 'Starch and its derivatives for paper coatings: a review', *Progress in Organic Coatings*, 135, pp. 213–227. DOI: 10.1016/j.porgcoat.2019.05.015

Marinelli, A., Lyytikäinen, J., Tanninen, P., Curto, B.D. and Leminen, V. (2023) 'Barrier, converting, and tray-forming properties of paperboard packaging materials coated with waterborne dispersions', *Packaging Technology and Science*, 37(3), pp. 149–165. DOI: 10.1002/pts.2784

Roberts, J.C. (1997) 'A review of advances in internal sizing of paper'. In: Baker, C.F. (ed.) *The Fundamentals of Papermaking Materials, Transactions of the XIth Fundamental Research Symposium, 21–26 September 1997, Cambridge, United Kingdom*. Manchester: Fundamental Research Committee, pp. 209–263. DOI: 10.15376/frc.1997.1.209

Rovera, C., Türe, H., Hedenqvist, M.S. and Farris, S. (2020) 'Water vapor barrier properties of wheat gluten/silica hybrid coatings on paperboard for food packaging applications', *Food Packaging and Shelf Life*, 26, 100561. DOI: 10.1016/j.fpsl.2020.100561

Shen, Z., Rajabi-Abhari, A., Oh, K., Yang, G., Youn, H.J. and Lee, H.L. (2021) 'Improving the barrier properties of packaging paper by polyvinyl alcohol based polymer coating—effect of the base paper and nanoclay', *Polymers*, 13(8), 1334. DOI: 10.3390/polym13081334

Wang, J., Gardner, D.J., Stark, N.M., Bousfield, D.W., Tajvidi, M. and Cai, Z. (2017) 'Moisture and oxygen barrier properties of cellulose nanomaterial-based films', *ACS Sustainable Chemistry & Engineering*, 6(1), pp. 49–70. DOI: 10.1021/acssuschemeng.7b03523



© 2026 Authors. Published by the University of Novi Sad, Faculty of Technical Sciences, Department of Graphic Engineering and Design. This article is an open access article distributed under the terms and conditions of the Creative Commons Attribution license 4.0 Serbia (https://creativecommons.org/licenses/by/4.0/deed.en).

Original Scientific Paper https://doi.org/10.24867/GRID-2026-p80

Silicone Elastomers as Additives in the Paper Manufacturing Process

ABSTRACT

Silicone elastomers can act as effective lubricants in the paper manufacturing process. They reduce friction between paper fibers and processing equipment, such as rollers and presses, thereby helping to prevent paper breakage and improving the overall efficiency of the production line. This research focuses on the formulation and characterization of silicone elastomer-based emulsions that can be used to improve paper properties. In the first part of the investigation, Fourier transform infrared (FTIR) spectroscopy was employed to analyze the structural properties of the initial silicone elastomers. Following the successful emulsification process, a physicochemical characterization of the obtained system was performed. The quality and stability of the emulsion were evaluated through three key aspects. Particle size and the stability of the dispersed phase were investigated by dispersion analysis, which revealed a predominantly nanoscale droplet distribution with a smaller fraction of larger droplets. The oil-in-water emulsion type was accurately identified using conductometric measurements of the system's electrical conductivity. Surface properties and the interaction of the emulsion with a solid substrate were determined through contact angle measurements using an indirect method. The results indicated a low contact angle, which may present challenges for future applications. The obtained findings confirm the successful formulation of the emulsion and provide insight into the correlation between the structure of the initial elastomers and the final emulsion performance, enabling their precise application in improving paper quality.

Nevena Vukić [1]
Darko Manjenčić [2]
Marijana Vasić [2]
Milica Ivanović [2]

[1] University of Kragujevac, Faculty of Technical Sciences Čačak, Serbia
[2] Academy Kruševac, Department of Technical and Technological Studies, Kruševac, Serbia

KEY WORDS
Silicone composites, emulsification, crosslink density, conductometry, dispersion analysis

1. Introduction

Silicone-based materials represent an important class of polymeric materials with a distinctive combination of chemical, thermal, mechanical, and surface properties, which has enabled their application in a wide range of industrial fields (Clarson, 2003). Their versatility has led to the development of numerous silicone-based products and formulations tailored to specific applications, including those in the paper industry. These additives can have positive effects on papermaking processes and the final properties of paper products (Gu, 2022). One of the primary applications of silicone elastomers in the paper manufacturing is surface modification. Silicone elastomers can be used to provide paper with specific surface properties, such as improved smoothness and water repellency. By incorporating silicone-based release agents into paper coatings or sizing agents, manufacturers can create a non-stick surface that prevents the adhesion of adhesives and other substances (Kelar Tučeková, 2020). This is particularly important in applications such as labels, where easy release of labels from the substrate is essential.

In contrast, silicone can be incorporated into paper coatings to improve the release properties of the paper surface (Abenghal & Brouillette, 2024). These elastomers help enhance the adhesion of the silicone coating,

resulting in a more efficient production process and a paper product with excellent release properties.

Silicone elastomers also act as effective lubricants in the papermaking process. They reduce friction between paper fibers and processing equipment, such as rollers and presses, which helps prevent paper breakage and improves the overall efficiency of the production line. Also, silicone lubricants can reduce the accumulation of static electricity on the paper surface, which can cause problems such as dust attraction and paper jamming. In addition to lubrication, silicone elastomers can prevent blocking, i.e., the tendency of paper sheets to adhere to one another during storage or handling. By applying a silicone-based anti-blocking agent to the paper surface, manufacturers can ensure that paper sheets remain separated and easy to handle. Silicone can be formulated to provide both lubricating and anti-blocking properties, making it an effective solution for paper manufacturers.

Water resistance is a crucial property for many paper products, particularly those used in packaging applications (Zhang, 2024). Silicone elastomers can be used to improve the water resistance of paper by forming a hydrophobic barrier on the paper surface (Rajendra et al., 2014). This barrier prevents water from penetrating the paper, thereby helping to protect the contents of the package and maintain the integrity of the paper product. Silicone-based water-repellent agents can be applied to paper using various methods, such as coating, spraying, or dipping. Depending on the formulation and coating conditions, silicone-based coatings can also influence the mechanical and durability properties of paper. (Zhang, 2024).

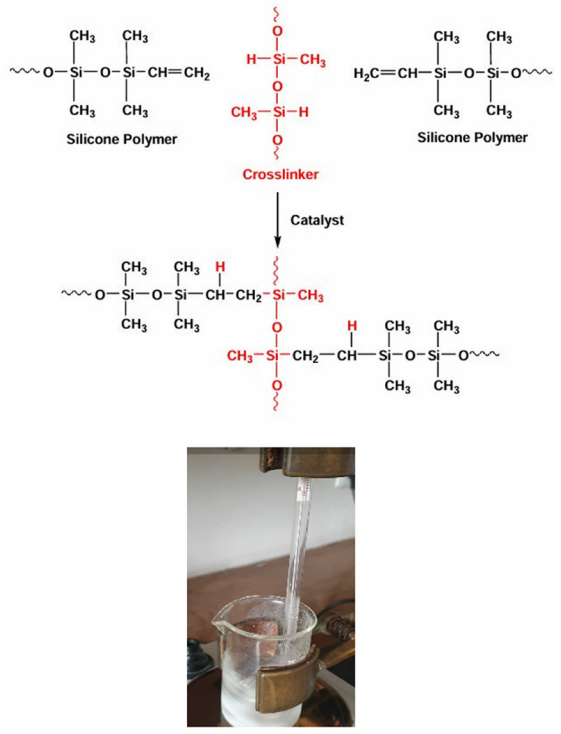
In some paper applications, such as tissues and sanitary products, softness and flexibility are important properties (Pawlak, 2022). Silicone elastomers can be used to enhance these properties by reducing the stiffness of the paper fibers and improving the overall hand feel of the paper. The application of silicone elastomers can therefore produce a paper product that is gentle on the skin and has a pleasant texture.

In this paper, silicone elastomer-based emulsions were formulated and characterized. The investigation comprised the structural characterization of the initial silicone elastomers by Fourier transform infrared (FTIR) spectroscopy. The obtained emulsions were evaluated in terms of dispersed-phase properties, emulsion type, and surface interactions with a solid substrate using dispersion analysis, conductometric measurements, and contact angle measurements, respectively. The results provide a basis for assessing the relationship between the structural properties of the starting silicone elastomers and the properties of the resulting emulsions, which is essential for their further optimization and application.

2. Experimental part

2.1. Materials and Methods

Precursors for the siloxane elastomer were Vinyl-functionalised siloxane with terminal group (SFA 42102, vinyl content 0.15 mmol g^{-1}, Viscosity 1000 mPa s) and Hydrogen siloxane with lateral groups (SFA 11430, hydrogen content 3.3 mmol g^{-1}, Viscosity 1000 mPa s) both provided from CHT GMBH BEZEMA, Germany. As a catalyst in PDMS was used platinum complex containing vinyl groups (KAT-A, GMBH BEZEMA, Germany). Surface modified hydrophilic SiO_2 nanofillers were provided from Evonik Resource Efficiency GmbH, Germany. In the synthesis of silicone composites, active fillers with a high specific surface were used hydrophilic (AEROSIL 300) of 300 m^2 g^{-1}, particle size d50 = 10 nm. Lutensol nonionic surfactant based on C10-rich iso-fatty alcohol ethoxylates. It has a cloud point of approximately 60 °C and density of around 0.98 g cm^{-3} provided from BASF Germany and linear alkylbenzene sulfonic acid (LABSA/DDBSA). The method of preparing the emulsion system is shown in Figure 1.



» **Figure 1:** *Silicone emulsification and chemical structure of siloxanes*

2.2. Emulsification and modification of liquid silicone rubbers

Siloxane elastomers were prepared by a conventional method, with the hydrogen- and vinyl-siloxane ratios 50/50 (wt:wt). Formulation of prepared materials

based on different contents of vinyl siloxane and the composites with SiO_2 nanofillers is shown in Table 1. For syntheses was used 0.1 wt% platinum catalyst (KAT-A, corresponding to approximately 1000 ppm Pt relative to the total siloxane mass). All components were added to a laboratory vacuum mixer and homogenized for 1 h. The high shear made the good mixing of all components in high viscosity material, with good dispersion and distribution of fillers, which was of great importance for samples with a high percentage of nanofillers. The preparation of the emulsion was started by the prior dissolution and incorporation of the emulsifier into the silicone phase to ensure optimal system stability. During the process, the aqueous phase was gradually added to the prepared silicone phase under high-speed propeller mixing. The mixing speed was continuously and proportionally increased from 200 to 4000 rpm as the aqueous phase was added. The alternating increase in rotational speed ensured efficient homogenization and the formation of a fine and stable emulsion. During emulsion preparation, hydrophilic silicon dioxide acted as a highly effective stabilizer through the Pickering stabilization mechanism. Under the influence of strong shear forces generated at mixing speeds of up to 3000 rpm, the particles became preferentially positioned at the silicone-water interface. The hydrophilic silanol groups (Si-OH) present on the particle surfaces established strong interactions with water molecules, thereby forming a protective, rigid layer around the dispersed droplets. Simultaneously, the silicon dioxide particles formed a three-dimensional structure within the system, which further immobilized the droplets and contributed to the long-term stability and homogeneity of the emulsion.

laboratory conductivity meter, InoLab Level 1 (WTW, Germany), equipped with a standard measuring cell with an integrated temperature sensor. The measurement principle is based on recording the electrical current passing through the solution according to Ohm's law, based on which the instrument primarily determines the electrical conductance, expressed in siemens (S). Taking into account the cell constant of the measuring cell, the instrument software converts the measured conductance into specific electrical conductivity, expressed in µS cm-1. The instrument was calibrated using a standard 0.01 mol L^{-1} KCl solution. All measurements were performed with automatic temperature compensation (ATC), with the measured values normalized to the reference temperature of 25 °C.

Dispersion analysis of the silicone emulsion was performed using the dynamic light scattering (DLS) method on a Zetasizer Nano ZS instrument (Malvern Instruments, UK). The method is based on monitoring the Brownian motion of the dispersed-phase droplets as a function of time by analyzing fluctuations in the intensity of laser light scattered at a defined detection angle. A helium-neon laser with a wavelength of λ = 633 nm was used as the light source. All measurements were performed at a constant temperature of 25 °C, following appropriate dilution of the sample with distilled water to avoid multiple-scattering effects and minimize interparticle interactions. The hydrodynamic diameter of the droplets and the estimated polydispersity index (PDI) were determined as the main parameters, with PDI serving as an indicator of the homogeneity of the size distribution within the system.

Table 1

Formulations of prepared materials based on different contents of vinyl siloxane and the composites hydrophilic nanofillers*
- all siloxane ratios contained the same amount of filler

Sample	Siloxane ratio		Content of SiO_2, wt%	Amount of emulsifier
	By weight	By mol	Hydrophilic	3-5% of the silicone phase, depending on the mixing conditions –
Hydrogen-vinyl 50/50	1-1	10-1	1	

2.3. Characterization of synthesized materials

Chemical structure of obtained siloxane materials was analyzed by Fourier-transform infrared FTIR spectrophotometer Thermo-Nicolet Nexus 670 (ThermoFischer Scientific, USA). Attenuated total reflection, ATR, with one reflection on the crystals of germanium was used for the recording. 100 scans were recorded per sample at a resolution of 4 cm^{-1}. As a detector was used deuterated triglycerin sulphate, DTGS. To process the spectra, the Thermo-Nicolet Omnic 6.0 software was used.

The specific electrical conductivity of the aqueous solutions was measured conductometrically using a

The contact angle of the silicone emulsion was determined using an indirect method with a laboratory goniometer. The method is based on analysis of the profile of an emulsion droplet deposited on a standardized solid substrate, with the geometrical parameters of the droplet used for software-based calculation of the contact angle (θ) at the three-phase contact line (solid-liquid-vapor). All measurements were performed under controlled conditions at room temperature. The obtained contact angle values were used as indicators of the surface properties and the hydrophilic-lipophilic balance (HLB) of the investigated emulsion system.

3. Results and discussion

Figure 2 and Table 2 show the results of the FTIR analysis of the synthesized materials molecular structure. Sharp bands at 2961 cm^{-1} and 2905 cm^{-1} originated from the asymmetric and symmetric C-H stretching vibrations of Si-CH3. Also, clearly observed are characteristic peaks of siloxane matrix that originated from the functional groups $Si-CH_3$, Si-O-Si, and Si-C. Hydrophilic silica was attached to the silicone matrix because reactive OH groups react secondary interactions (of the hydrogen bond type) with the silicone chain, and the absence of hydroxyl vibrations (3200-4000 cm^{-1}) was confirmed on FTIR analysis. The ratios of silicone in which vinyl siloxane is present in a smaller proportion show the quantitative reaction of the double bond C=C in vinyl siloxanes, which confirms the absence of peaks at wavelengths greater than 3000 cm^{-1}. The FTIR spectrum of the investigated sample (Figure 2c) shows characteristic bands confirming the structure of silicon dioxide. The intense peak at 1080 cm^{-1} is attributed to the asymmetric stretching vibration of Si-O-Si bonds.

Table 2

Characteristic bands in the FTIR spectrum of obtained materials

Wavelength, cm^{-1}	Functional group
3000 – 2800	CH_3 and CH_2 group
1450	Asymmetric stretching CH_3
~1290	$C-Si-CH_3$
~1250	$(CH_3)_3$, Si
1130 – 1000	Si-O-Si
1155	Si-O
790	$SiCH_3$ twisting

The specific electrical conductivity of the aqueous solutions was measured conductometrically. The final values were recorded after stabilization of the measurement signal using the integrated AutoRead function. Measurements were performed on five emulsion samples.

Note: The samples were diluted with water having an electrical conductivity of 2 µS cm^{-1} to obtain a 5% (v/v) emulsion solution. Electrical conductivity was measured at room temperature (25 °C ± 1).

Table 3

Results of electrical conductivity measurements of the 5% emulsion sample

Measurement No.	1	2	3	Average value
Electrical conductivity (µS cm^{-1})	98.2	98.3	98.2	98.26

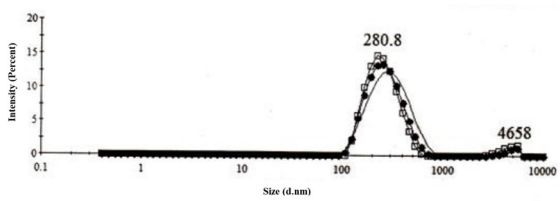
The measured specific electrical conductivity of the diluted sample at room temperature was 98.2 µS cm^{-1}. Since the oil phase acts as an electrical insulator, the ability of the system to conduct electric current depends directly on the nature of the external (continuous) phase. The measured conductivity value, being of a significant magnitude, clearly indicates that the continuous phase consists of water containing mobile ions, thereby identifying the investigated system as an oil-in-water (O/W) emulsion.

Dispersion analysis of the silicone emulsion was performed using the dynamic light scattering (DLS) method on a Zetasizer instrument in three consecutive replicates at a temperature of 25 ± 1 °C, following dilution of the sample with distilled water at a 1:100 (v/v) ratio. Table 4 presents the mean hydrodynamic diameter values of the droplets in the silicone emulsion sample, while Figure 3 illustrates the droplet size distribution within the system.

Table 4

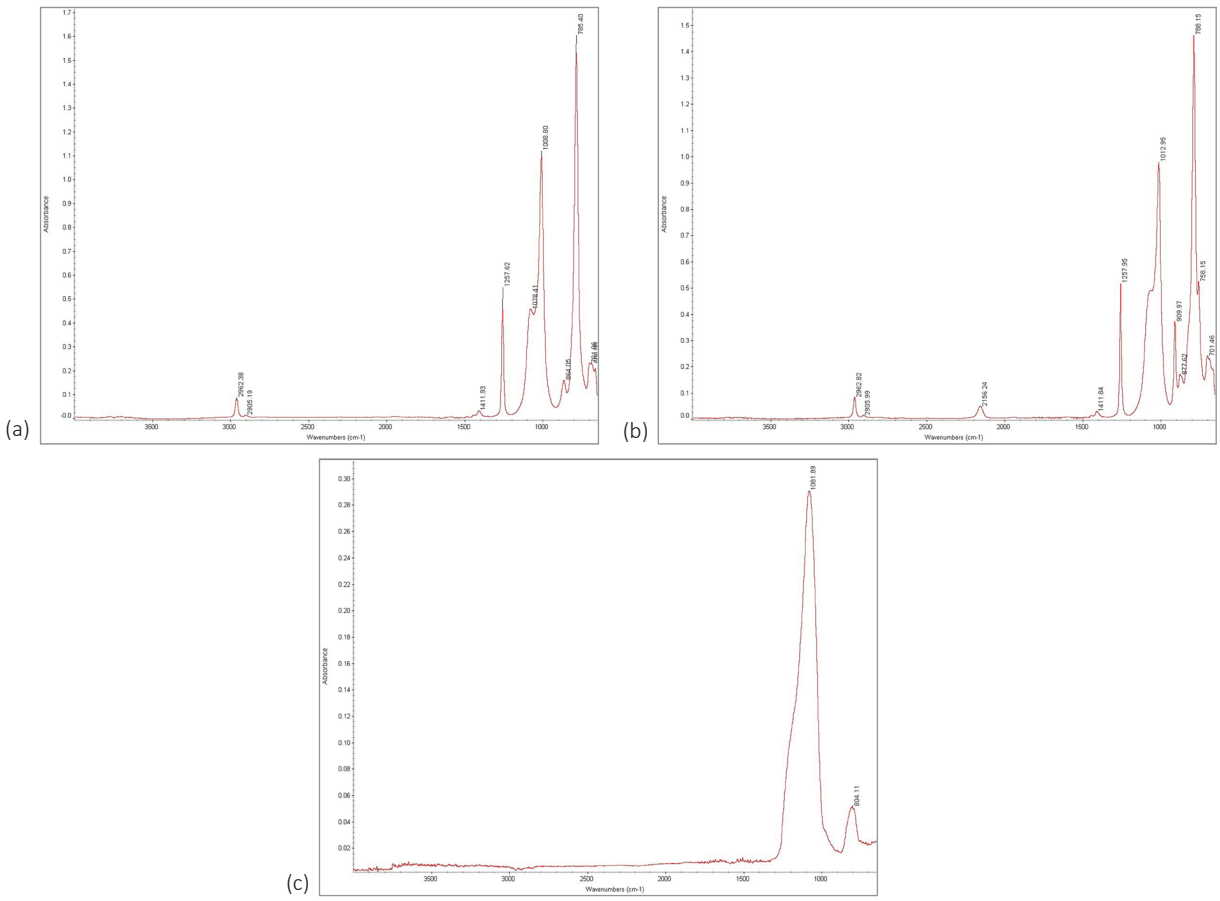
Mean droplet diameter of the silicone emulsion sample

Measurement No.	Peak 1	%	Peak 2	%
1	310.8	100	-	0
2	257.3	94.6	4528	5.4
3	274.3	96.8	4787	3.2
dsr ±σ (nm)	280.8 ± 27.34		4658 ± 183.1	



» **Figure 3:** *Results of the determination of the mean droplet diameter of the emulsion sample*

The results of the dispersion analysis clearly indicate that the investigated system is an emulsion with droplet sizes predominantly in the nanometer range. Analysis of the results presented in Table 3 and Figure 3 indicates a bimodal droplet size distribution, with two distinct maxima being observed. The first maximum occurs at 280.8 ± 27.34 nm and represents the mean diameter of more than 95% of the droplets present in the emulsion sample. The second maximum occurs at 4658.16 ± 116.1 nm and represents the mean diameter of a smaller droplet fraction, accounting for approximately 5% of the total number of droplets present in the emulsion. The presence of two distinct droplet fractions and the resulting bimodal distribution indicates a relatively high polydispersity index (PDI), estimated to be approximately 0.4-0.7. Such a high PDI value indicates pronounced heterogeneity and a broad droplet size distribution, confirming that the system is not monodisperse but consists of two distinct droplet populations.



» **Figure 2:** *FTIR spectra of: a) silicon elastomers vinil, b) silicon elastomers hidrogen and c) hydroplic fillers*

The measured contact angle of the silicone emulsion on the solid paper substrate was θ = 38.08°. A contact angle substantially below 90° indicates high wettability and a pronounced affinity of the liquid system for the investigated solid substrate. The low contact angle may be attributed to the effective reduction of interfacial tension at the liquid-solid interface, which is properties of emulsion systems containing surface-active agents capable of modifying the interactions between the liquid phase and hydrophobic substrates.

4. Conclusions

Considering the potential of silicone-based materials to modify the surface and properties of paper, the development of stable silicone emulsions represents an important theme. In this research a silicone-based oil-in-water (O/W) emulsion was successfully formulated and characterized using FTIR spectroscopy, conductometric measurements, dynamic light scattering (DLS), and contact angle analysis. FTIR analysis confirmed the characteristic structures of the silicone matrix and silicon dioxide, while conductivity measurements confirmed the O/W character of the obtained emulsion. DLS analysis showed a predominantly nanoscale droplet population, with more than 95% of the droplets having a mean hydrodynamic diameter of approximately 280.8 nm. However, the presence of a smaller fraction of larger droplets resulted in a bimodal size distribution and relatively high polydispersity. The measured contact angle of 38.08° indicated good wettability of the emulsion on the investigated paper substrate.

The advantage of the formulated silicone system manifests through the use of a lower catalyst content in combination with a higher-molar-mass vinyl siloxane, providing a basis for the preparation of crosslinked elastomers with improved mechanical properties.
In addition, the obtained silicone elastomers exhibit good homogeneity within the emulsion system, which directly contributes to the stability and quality of the material and, consequently, to the performance of the final products, resulting in improved paper properties.

5. Acknowledgments

This study was supported by the Ministry of Science, Technological Development and Innovation of the Republic of Serbia, and these results are parts of the Grant No. 451-03-33/2026-03/ 200132.

6. References

Abenghal, L. and Brouillette, F. (2024) 'Phosphate Esters: New Coating Materials for a Sustainable Release Paper', ChemistrySelect, 9(19), e202400134. DOI: 10.1002/slct.202400134

Clarson, S.J. (2003) 'Silicones and Silicone-Modified Materials: A Concise Overview'. In: Clarson, S.J., Fitzgerald, J.J., Owen, M.J., Smith, S.D. and Van Dyke, M.E. (eds.) *Synthesis and Properties of Silicones and Silicone-Modified Materials*. Washington, DC: American Chemical Society, pp. 1–10.

Gu, L. (2022) 'Silicone Applications in Pulp and Paper'. In: *2022 PEERS/IBBC Conference*.

Kelar Tučeková, Z., Galmiz, O., Kelar, J., Kováčik, D., Stupavská, M., Šrámková, P., Zemánek, M., Vallade, J. and Černák, M. (2020) 'Adhesive Properties of Silicone-Coated Release Liner Paper Enhanced by Atmospheric Pressure Plasma Pre- and Post-Treatment', *Coatings*, 10(11), 1102. DOI: 10.3390/coatings10111102

Pawlak, J.J., Frazier, R., Vera, R.E., Wang, Y. and Gonzalez, R. (2022) 'Review: The softness of hygiene tissue', *BioResources*, 17(2), pp. 3509–3550. DOI: 10.15376/biores.17.2.Pawlak

Rajendra, V., Sicard, C., Brennan, J.D. and Brook, M.A. (2014) 'Printing silicone-based hydrophobic barriers on paper for microfluidic assays using low-cost ink jet printers', *Analyst*, 139(24), pp. 6361–6365. DOI: 10.1039/c4an01626b

Zhang, R., Tan, J., Ma, T., Xu, M., Chen, W., Zhu, F. and Cao, Y. (2024) 'Developing Waste Fatty Acid-Grafted-Silicone Oil as Repulpable, Enhanced Gas and Water Resistant Coating for the Paper Industry', *ACS Applied Polymer Materials*, 6(19), pp. 11964–11973. DOI: 10.1021/acsapm.4c02086



© 2026 Authors. Published by the University of Novi Sad, Faculty of Technical Sciences, Department of Graphic Engineering and Design. This article is an open access article distributed under the terms and conditions of the Creative Commons Attribution license 4.0 Serbia (http://creativecommons.org/licenses/by/4.0/rs/).

Original Scientific Paper https://doi.org/10.24867/GRID-2026-p81

Effect of Glycerol and Hydrophobic Silica on the Mechanical and Surface Properties of Starch-based Films: A Response Surface Methodology Approach

ABSTRACT

Starch-based films are promising biodegradable alternatives to conventional polymeric materials. However, their poor mechanical properties and high affinity for water limit their practical applications. The combined effects of plasticizer and hydrophobic nanoparticle content on the mechanical and surface properties of starch-based films remain insufficiently understood. In this study, potato starch films containing glycerol and hydrophobic nano-silica were prepared and characterized for their mechanical properties and surface free energy. Response Surface Methodology (RSM) was used to evaluate the effects of film composition and identify a formulation that balances mechanical and surface properties, with potential applications in printing technologies.

KEY WORDS
Starch films, mechanical properties, surface free energy, design of experiment, response surface methodology

Arkadiusz Jeznach [1]
Łucja Dybowska-Sarapuk [1,2]
Zuzanna Żołek-Tryznowska [1]

[1] Faculty of Mechanical and Industrial Engineering, Warsaw University of Technology, Warsaw, Poland
[2] NOVELINKS Sp. z o.o., Warsaw, Poland

1. Introduction

Starch is a readily available, biodegradable, inexpensive, and renewable polysaccharide and can be harvested without destroying the plant (Ray, Narayan Das & Das, 2021; Ojogbo, Ogunsona & Mekonnen, 2020). It is well known that starch exhibits filmogenic properties and, upon processing, can form films that are green, environmentally friendly, and biodegradable alternatives to plastic materials intended for various applications (Colivet & Carvalho, 2017; Freitas, González-Martínez & Chiralt, 2023). Films formed from starch are isotropic, odorless, tasteless, colorless, non-toxic, and biodegradable (A'yun & Bintoro, 2021; Castro et al., 2022).

Among the many disadvantages of these materials, the most significant are their poor mechanical properties and affinity for water. These limitations hinder their widespread commercial application. Therefore, various strategies have been developed to overcome these limitations and improve the overall performance of starch-based materials. For example, modifications to starch can be performed to improve its final properties. For example, UV-B irradiation or cold plasma to modify the properties of corn and potato starches (Kurdziel et al., 2022; da Fonseca de Albuquerque et al., 2022). Another solution is to develop various blends or enhance the properties of starch-based films with nanoparticles, such as micro- or nanocellulose (Żołek-Tryznowska et al., 2023), nanoclays (Muangmala et al., 2026), or metal oxide nanoparticles (Dhiman et al., 2025).

Response surface methodology (RSM) can be successfully applied for the optimization of starch-based materials. Tessema et al. have applied a Box-Behnken experimental design from response surface methodology to optimize the levels of anchote starch, glycerol, and acetic acid for the development of edible films (Tessema, Admassu & Dereje, 2023). The optimum level results in a film with maximum tensile strength (10.076 MPa) and elonga-

tion at break (33.95%) at 3.801% w/v anchote starch, 28.566% w/w glycerol, and 0.1% w/v acetic acid concentration (Tessema, Admassu & Dereje, 2023), which are values comparable to low-density polyethylene (tensile strength ~ 10MPa) (Szlachetka et al., 2021). Furthermore, Gupta et al. combined RSM methodology along with an artificial neural network coupled with a genetic algorithm to predict the effect of the concentration of independent variables on the responses (Gupta, Guha & Srivastav, 2026). However, the tensile strength of taro starch optimized with the combined RSM model was much lower (~2.45 MPa) than that of anchote starch. Tafa et al. used the RSM approach to optimize tef starch films, reporting tensile strength of 17.97–24.25 MPa, elongation at break of 1.21–2.03%, and elastic modulus of 17.58–108.69 MPa (Tafa, Satheesh & Abera, 2023).

In this study, hydrophobic nano-silica was incorporated into starch-based films to simultaneously modify their surface and mechanical properties. The effects of hydrophobic nano-silica content (up to 0.5) and glycerol concentration, used as a plasticizer, on the surface and mechanical properties of the resulting starch/silica composites were systematically investigated. A Design of Experiments (DoE) approach, with some modifications, combined with Response Surface Methodology (RSM), was employed to evaluate the effects and interactions of these formulation variables and to determine the optimal composition of the composite films. The optimized formulation is expected to provide a promising starch-based material with properties suitable for printing applications.

2. Methods

2.1. Materials

Potato starch (CAS 9005-25-8), glycerin (purity ≥ 99%, CAS 56-81-5) as a plasticizer, and diiodomethane (purity ≥ 99%, CAS 75-11-6) for contact angle measurements, and ethanol (purity ≥ 96%, CAS 64-17-5) for silica solubilization were purchased from Sigma-Aldrich. Amorphous, hydrophobic silica, Aerosil R 972 (CAS 68 611-44-9) with a BET specific surface area of 90–130 $m^2 \cdot g^{-1}$, an average particle size of 16 nm, and a carbon content of 0.6–1.2 wt.%, was purchased from Evonik. All reagents were used as received.

2.2. Experiment design

Response surface methodology (RSM) was applied to evaluate the combined effects of glycerol and hydrophobic silica content on the mechanical and surface properties of starch-based films. The experimental design was based on a central composite design (CCD) geometry with two formulation factors. The initial design comprised four factorial and four axial points and was subsequently supplemented with an independently prepared center-point formulation and independent replicates of two axial formulations. The two independent variables were glycerol (28.28–91.72%) and silica (0.25–0.50 g) content, while the thickness, tensile strength, and SFE properties of the composite film were evaluated. The ranges of independent parameters were selected based on our previous results (Żołek-Tryznowska et al., 2024). The experimental dataset comprised the initial eight formulations (Z1–Z8) and three additional independently prepared films, including repeated formulations at 28.28% glycerol/0.375 g SiO_2 and 91.72% glycerol/0.375 g SiO_2, as well as an additional formulation at the design center (60% glycerol/0.375 g SiO_2).

2.3. Film production

The film production description was shown in our previous works (for example, see (Żołek-Tryznowska et al., 2024)).

All reagents (starch, plasticizer, and water) were heated up to 95 °C upon stirring with a mechanical stirrer. The silica was dissolved in 20 mL of ethanol, homogenized, and added to the starch suspension, and mixed. Next, the starch suspension was cast onto the Teflon® plates and dried in the climate room for one week under controlled conditions (23 ± 0.5°C; 50 ± 1% RH). When the samples dried, they were carefully torn off. The mechanical and surface free energy measurements were conducted one week after film preparation to ensure repeatability.

2.4. Film properties

The thickness for the mechanical measurements was measured with a hand-held micrometer with 0.001 mm resolution and an error of ±0.5 mm. The mechanical properties were determined using a Z010 tensiometer (Zwick-Roell, Germany) in accordance with ISO 527-1. The measurements were performed using specimens with dimensions of 15 mm in width and 100 mm in length. The initial grip separation was set to 50 mm, while the stretching rate was maintained at 100 $mm \cdot min^{-1}$. The tensile strength (TS), elongation at break (EaB), and Young's modulus (YM) were determined from the corresponding stress–strain curves.

The surface free energy was determined using the Drop Shape Analysis System (DSA 30E, Krüss, Germany) from the contact angles of formamide and diiodomethane using the Owens-Wendt method (Owens & Wendt, 1969). Due to the hydrophilic properties of the starch film and its affinity for water, we eliminate water contact angle measurements.

2.5. Statistical analysis

The experimental data were analyzed using STATGRAPHICS Centurion 19.1.3. Quadratic models containing linear effects (A, B), interaction (AB), and quadratic terms (A^2, B^2) were initially considered. Model reduction was performed by removing unsupported higher-order terms while maintaining model hierarchy. The final models were selected based on analysis of variance (ANOVA), coefficient significance, model complexity, coefficients of determination (R^2 and adjusted R^2), predicted R^2, prediction error sum of squares (PRESS), and the physical interpretability of the response.

3. Results and discussion

In this work, we apply response surface methodology to investigate the synergistic effect of glycerol and hydrophobic silica content on several parameters of starch-based films. The experimental design was performed using CCD with some modifications. Table 1 presents the experimental design and responses used in modeling. The RSM was used to study the linear, quadratic, and interaction effects of glycerol and silica content on the studied responses.

Table 1

Data values of variables and responses: Young's modulus (YM), tensile strength (TS), elongation at break (EaB), thickness (h), total surface free energy (SFE), and its polar and dispersive components

Entry	Sample	Independent variables		Responses						
		Glycerol (%)	Silica (g)	YM (MPa)	TS (MPa)	EaB (%)	h (µm)	SFE total (mN/m)	SFE polar (mN/m)	SFE dispersive (mN/m)
1	Z1	40.00	0.250	6.16	0.96	40.90	181.00	53.42	22.82	30.61
2	Z2	80.00	0.250	86.79	2.98	48.38	166.75	51.88	10.37	41.51
3	Z3	40.00	0.500	138.83	3.84	46.67	116.22	55.68	21.86	33.82
4	Z4	80.00	0.500	30.30	2.24	36.20	165.70	35.89	1.13	34.76
5	Z5	28.28	0.375	1073.10	18.05	9.43	118.50	53.29	20.46	32.83
6	Z6	91.72	0.375	13.75	1.47	43.10	183.80	46.96	9.15	37.81
7	Z7	60.00	0.250	86.17	3.23	59.10	115.20	53.04	14.73	38.31
8	Z8	60.00	0.500	60.50	2.95	48.00	127.70	56.13	22.32	33.80
9	Z5	28.28	0.375	312.00	6.32	34.00	138.80	52.14	13.29	38.85
10	Z6	91.72	0.375	5.02	0.80	–	198.40	52.31	13.79	38.52
11	Z9	60.00	0.375	14.60	1.50	54.00	202.50	52.59	12.28	40.31

Table 2

Summary of the fitted RSM models for mechanical properties, film thickness, and surface free energy: A – glycerol content; A^2 – quadratic effect of glycerol content; 2FI – two-factor interaction model

Response	Model	p-value	R^2	Adj. R^2	Significant terms
Et	Linear	0.1803	0.3484	0.1855	*p > 0.05*
σM	Linear	0.1713	0.3566	0.1958	*p > 0.05*
εtB	Quadratic	0.0648	0.6757	0.5136	*A^2: p < 0.05*
h	Linear	0.1440	0.3840	0.2300	*p > 0.05*
Total SFE	2FI	0.1192	0.5444	0.3492	*p > 0.05*
Polar SFE	Linear	0.1278	0.4021	0.2526	*A: p < 0.05*
Dispersive SFE	2FI	0.1446	0.5161	0.3087	*p > 0.05*

The adequacy of the fitted response surface models was evaluated using analysis of variance (ANOVA), model p-values, coefficients of determination (R^2 and adjusted R^2), standard error, and the prediction error sum of squares (PRESS). The experimental responses and the statistical parameters of the fitted models are summarized in Table 2. Depending on the response, reduced linear, interaction, or quadratic models were selected after eliminating unsupported higher-order terms while preserving the model hierarchy. R2 ranged from 0.3484 to 0.6757 for the mechanical properties and from 0.4021 to 0.5444 for the surface free energy components. Although the overall models did not reach statistical significance at the 0.05 level (p = 0.0648–0.1803), individual model terms revealed significant formulation effects. In particular, the quadratic effect of glycerol content on elongation at break was significant (A^2, p=0.0293), while glycerol content significantly affected the polar component of SFE (p=0.0495). Therefore, the fitted models were used primarily to describe response trends within the investigated experimental domain and to support multi-response desirability analysis rather than for unrestricted prediction outside the studied factor ranges.

After model reduction, the final regression equations, expressed in terms of the actual factor levels, were obtained to describe the effects of glycerol and silica contents on the mechanical properties, film thickness, and surface free energy components, as shown in Eqs 1–7.:

$$YM = 609.132 - 7.8046A + 67.3467B \quad (1)$$

$$TS = 10.4893 - 0.123139A + 2.48B \quad (2)$$

$$EaB = -30.6074 + 2.88338A - 23.3467B - 0.0224156A^2 \quad (3)$$

$$h = 132.757 + 0.829641A - 71.1067B \quad (4)$$

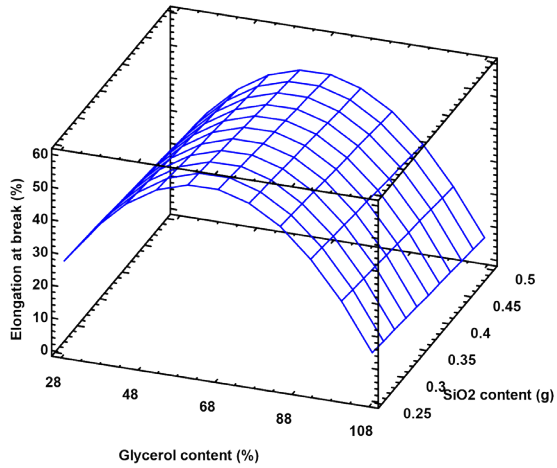
$$SFE_{total} = 22.1044 + 0.5738A + 95.3133B - 1.8250AB \quad (5)$$

$$SFE_{polar} = 26.7871 - 0.1789A - 3.4800B \quad (6)$$

$$SFE_{dispersive} = 13.9819 + 0.4418A + 49.0267B - 0.9960AB \quad (7)$$

where A is glycerol content (%), and B is silica content (g).

The fitted linear model showed a negative relationship between glycerol content and YM and TS, while the effect of silica on YM and TS is positive. However, there is no statistical significance (p < 0.05). Furthermore, the EaB initially increases at lower-to-intermediate glycerol content and then decreases at higher glycerol levels (see Figure 1). This is related to the fact that glycerol exhibited a significant quadratic effect on EaB (A^2, p = 0.0293). In contrast, silica showed a negative but non-significant effect on EaB. This tendency corresponds to the expected plasticizing effect of glycerol, which increases molecular mobility by spreading the starch chains and consequently lowers the stiffness of the polymer matrix. Finally, glycerol and silica have positive and negative effects on film thickness, respectively.



» **Figure 1:** *Response surface plot for EaB*

The glycerol-silica formulation had a markedly greater influence on the SFE components than on the total surface free energy. Increasing glycerol content significantly decreased the polar SFE component (p<0.05). This effect has been observed in other studies and is related to the presence of hydroxyl groups in glycerol. Increasing the hydrophobic silica content up to 0.50 g did not significantly (p>0.05) lower the polar component of the film surface free energy, indicating that the increase in hydrophobicity of the film was not significant. The dispersive component showed opposite trends, increasing with glycerol and decreasing with SiO_2 content, although these effects were not statistically significant (p>0.05).

Numerical optimization was performed to determine the compromise between the mechanical and surface performance. Therefore, Young's modulus, tensile strength, and elongation at break were maximized, while film thickness and the total surface free energy were targeted at 150 µm and 52 mN/m, respectively. Considering the hydrophobic nature of the silica filler, the polar component of surface free energy was minimized, whereas the dispersive component was maximized. The optimum composition was obtained at approximately 52.88% glycerol and 0.3745 g silica, with an overall desirability of ~0.592 (see Table 3). Furthermore, the predicted composition lies within the experimental factor space, close to the central point, increasing its practical relevance as a candidate for formulation for further validation. Unfortunately, the predicted R2 values for individual models were low; the predicted composition should not be treated as a global optimum; and a validation experiment with a film containing approximately 53% glycerol and 0.375 silica should be performed.

Table 3

Multi-response desirability optimization of glycerol and silica contents and predicted properties of the starch-based films.

Response	Optimization goal	Criterion	Predicted value	Individual desirability
YM (MPa)	Maximize	Max. = 300	221.66	0.739
TS (MPa)	Maximize	Max. = 6.5	4.91	0.755
EaB (%)	Maximize	Max. = 60	50.44	0.841
h (µm)	Target	150	150.00	1.000
Total SFE (mN/m)	Target	52	52.00	1.000
Polar SFE (mN/m)	Minimize	—	16.02	0.303
Dispersive SFE (mN/m)	Maximize	—	35.98	0.498

Overall desirability: D = 0.592

4. Conclusions

This study investigated the combined effects of glycerol and hydrophobic nano-silica on the mechanical and surface properties of starch-based films. Glycerol content significantly affected elongation at break and the polar component of surface free energy, whereas the effect of silica was less pronounced within the investigated concentration range. Despite the limited predictive ability of the fitted models, Response Surface Methodology enabled the identification of formulation trends and supported multi-response optimization. A formulation containing approximately 53% glycerol and 0.375 g silica was identified as a promising balance between mechanical and surface properties. Further studies should validate this formulation experimentally and evaluate its printability.

5. Acknowledgments

This work was partially funded by project no. M-ERANET/3/1/BREATHTAKING/2026 co-funded by the National Centre for Research and Development (NCBR) under M-ERA.NET 3 Call 2025.

6. References

A'yun, A.Q. and Bintoro, N. (2021) 'The Effect of Starch Proportion in Coating Materials and Storage Temperatures on The Physical Qualities of Curly Green Chili (Capsicum annuum L)', IOP *Conference Series: Earth and Environmental Science*, 828(1), 012040. DOI: 10.1088/1755-1315/828/1/012040

Castro, J.I., Navia-Porras, D.P., Arbeláez Cortés, J.A., Mina Hernández, J.H. and Grande-Tovar, C.D. (2022) 'Synthesis, Characterization, and Optimization Studies of Starch/Chicken Gelatin Composites for Food-Packaging Applications', *Molecules*, 27(7), 2264. DOI: 10.3390/molecules27072264

Colivet, J. and Carvalho, R.A. (2017) 'Hydrophilicity and physicochemical properties of chemically modified cassava starch films', *Industrial Crops and Products*, 95, pp. 599–607. DOI: 10.1016/J.INDCROP.2016.11.018

da Fonseca de Albuquerque, M.D., Bastos, D.C., Ţălu, Ş., Matos, R.S., Pires, M.A., Salerno, M., da Fonseca Filho, H.D. and Simão, R.A. (2022) 'Vapor Barrier Properties of Cold Plasma Treated Corn Starch Films', *Coatings*, 12(7), 1006. DOI: 10.3390/COATINGS12071006

Dhiman, S., Kumari, A., Kumari, S. and Sharma, R. (2025) 'Advanced biodegradable starch-based nanocomposite films incorporating zinc oxide nanoparticles: Synthesis, characterization, and efficacy in antibacterial food packaging applications', *Journal of Environmental Chemical Engineering*, 13(3), 116296. DOI: 10.1016/J.JECE.2025.116296

Freitas, P.A.V., González-Martínez, C. and Chiralt, A. (2023) 'Antioxidant starch composite films containing rice straw extract and cellulose fibres', *Food Chemistry*, 400, 134073. DOI: 10.1016/J.FOODCHEM.2022.134073

Gupta, R.K., Guha, P. and Srivastav, P.P. (2026) 'Comparative Study on the Optimization and Characterization of Underutilize Taro Starch Based Composite Film using Response Surface Methodology and Artificial Neural Network Coupled with Genetic Algorithm', *Food and Bioprocess Technology*, 19(2), 70. DOI: 10.1007/S11947-025-04149-1

Kurdziel, M., Łabanowska, M., Pietrzyk, S., Pająk, P., Królikowska, K. and Szwengiel, A. (2022) 'The effect of UV-B irradiation on structural and functional properties of corn and potato starches and their components', *Carbohydrate Polymers*, 289, 119439. DOI: 10.1016/J.CARBPOL.2022.119439

Muangmala, W., Roidoung, S., Boonjaed, D. and Namnongor, P. (2026) 'Development and characterization of heat-sealable tapioca starch-nanoclay bionanocomposite film for food packaging applications', *Future Foods*, 14, 101144. DOI: 10.1016/J.FUFO.2026.101144

Ojogbo, E., Ogunsona, E.O. and Mekonnen, T.H. (2020) 'Chemical and physical modifications of starch for renewable polymeric materials', *Materials Today Sustainability*, 7–8, 100028. DOI: 10.1016/J.MTSUST.2019.100028

Owens, D.K. and Wendt, R.C. (1969) 'Estimation of the surface free energy of polymers', *Journal of Applied Polymer Science*, 13(8), pp. 1741–1747. DOI: 10.1002/app.1969.070130815

Ray, R., Narayan Das, S. and Das, A. (2021) 'Mechanical, thermal, moisture absorption and biodegradation behaviour of date palm leaf reinforced PVA/starch hybrid composites', *Materials Today: Proceedings*, 41, pp. 376–381. DOI: 10.1016/J.MATPR.2020.09.564

Szlachetka, O., Witkowska-Dobrev, J., Baryła, A. and Dohojda, M. (2021) 'Low-density polyethylene (LDPE) building films – Tensile properties and surface morphology', *Journal of Building Engineering*, 44, 103386. DOI: 10.1016/J.JOBE.2021.103386

Tafa, K.D., Satheesh, N. and Abera, W. (2023) 'Mechanical properties of tef starch based edible films: Development and process optimization', *Heliyon*, 9(2), e13160. DOI: 10.1016/j.heliyon.2023.e13160

Tessema, A., Admassu, H. and Dereje, B. (2023) 'Development of edible films based on anchote (Coccinia abyssinica) starch: process optimization using response surface methodology (RSM)', *Journal of Food Measurement and Characterization*, 17(1), pp. 430–446. DOI: 10.1007/S11694-022-01632-7

Żołek-Tryznowska, Z., Bednarczyk, E., Tryznowski, M. and Kobiela, T. (2023) 'A Comparative Investigation of the Surface Properties of Corn-Starch-Microfibrillated Cellulose Composite Films', *Materials*, 16(9), 3320. DOI: 10.3390/MA16093320

Żołek-Tryznowska, Z., Jeznach, A., Bednarczyk, E., Murawski, T., Piłczyńska, K., Sikora, S. and Tryznowski, M. (2024) 'Effect of hydrophobic nano-silica content on the surface properties of corn-starch films', *Industrial Crops and Products*, 214, 118582. DOI: 10.1016/J.INDCROP.2024.118582



© 2026 Authors. Published by the University of Novi Sad, Faculty of Technical Sciences, Department of Graphic Engineering and Design. This article is an open access article distributed under the terms and conditions of the Creative Commons Attribution license 4.0 Serbia (http://creativecommons.org/licenses/by/4.0/rs/).

Original Scientific Paper https://doi.org/10.24867/GRID-2026-p82

Formulation-Dependent Properties of Rice Starch-Based Adhesives for Wet-Strength Paper Labels

ABSTRACT

The development of sustainable adhesives from renewable resources represents an important step toward reducing the environmental impact of packaging materials. This study investigated four rice starch-based adhesive formulations (L1–L4), including systems modified with chitosan and alginate, for potential application in paper labels on glass packaging. The physicochemical properties were characterized by measuring pH, apparent viscosity, and non-volatile solids content, while mechanical performance was evaluated using tensile tests on three paper substrates (V1–V3) in the machine direction (MD) and cross-machine direction (CD). The adhesive formulations exhibited pH values between 5 and 7, apparent viscosities ranging from 2,500 to 5,000 mPa·s, and solids contents of 10–20%. L1 (starch–chitosan–alginate) demonstrated the highest viscosity (5,000 mPa·s) despite having the lowest solids content (10%), indicating that rheological behavior was strongly influenced by formulation composition rather than solids concentration alone. Mechanical testing revealed that adhesive with rice starch, chitosan and alginate exhibited the highest average maximum tensile force (3.98 N), whereas rice starch and alginate adhesive achieved the highest average elongation (30.3 mm). The maximum recorded tensile force was 5.1 N, while elongation reached 66.1 mm, demonstrating considerable differences among adhesive formulations, paper substrates, and testing directions. These findings highlight the importance of balancing rheological characteristics, mechanical resistance, and flexibility when designing bio-based adhesives. Overall, rice starch-based formulations showed promising potential for sustainable paper labeling applications. Further investigation of adhesive durability, washing resistance, and industrial processing performance is required to establish their suitability for wet-strength and removable labels on glass packaging.

Urška Klenovšek
Urška Vrabič-Brodnjak

University of Ljubljana, Faculty of Natural Sciences and Engineering, Department of Textiles, Graphic Arts and Design, Ljubljana, Slovenija

KEY WORDS
Rice starch-based adhesives, bio-based adhesives, chitosan, alginate, tensile properties, paper labels, sustainable packaging

1. Introduction

The transition to resource-efficient packaging has stimulated interest in adhesives derived from renewable feedstocks. Adhesives form a small but functionally important component of paper-based packaging: they must wet the substrate, develop sufficient interfacial contact, withstand conversion and distribution stresses, and remain compatible with the intended end-of-life processing. Consequently, replacing a conventional formulation with a bio-based adhesive requires an application-specific assessment of processing rheology, bonding performance and durability rather than an evaluation of renewable content alone (Vrabič-Brodnjak & Vidmar, 2025). Glass-bottle and jar labels represent a particularly demanding case because the adhesive joins a fibrous and often wet-strength-treated paper to a smooth, non-porous glass surface. Labels may encounter condensation, immersion, mechanical handling and cleaning operations. As a conventional technology benchmark,

Márquez, Alarcia and Velasco (2020) developed water-based acrylic pressure-sensitive adhesives for glass-bottle paper labels and assessed their behaviour in cold and wet conditions. Their findings demonstrate that moisture resistance and label adhesion are important practical criteria, although the acrylic chemistry and application process differ from those of starch-based systems. Wash-off behaviour during container cleaning introduces an additional design challenge: resistance during service and ease of removal during recovery may require a controlled balance, which should be verified using defined test criteria. Starch is an attractive candidate for waterborne adhesives because it is widely available, renewable and rich in hydroxyl groups capable of hydrogen bonding with cellulose-rich paper surfaces. Gelatinised starch can provide viscosity and film formation, but its response depends strongly on concentration, processing history and moisture. Such hydrophilic formulations may undergo changes in cohesion and water sensitivity, making the use of other polysaccharides a plausible route to modification. Work on starch–chitosan materials has identified opportunities to tailor intermolecular interactions and physical behaviour through blending, although observations made on standalone films cannot automatically be equated with bond strength at paper–glass interfaces (Wan Yusof, Sabar & Zailani, 2024; Vrabič-Brodnjak & Vidmar, 2025; Klenovšek & Vrabič-Brodnjak, 2026). Chitosan is a polysaccharide containing amino and hydroxyl functionalities and can participate in hydrogen bonding and, depending on pH and protonation, electrostatic interactions. Recent reviews describe starch–chitosan blends as tunable polymer systems for films and coatings, with properties dependent on preparation and component ratios (Wan Yusof, Sabar & Zailani, 2024). For an aqueous adhesive, these interactions may influence dispersion, apparent viscosity, setting behaviour and adhesive-layer integrity. However, any specific advantage for bonded wet-strength paper needs to be substantiated by measurements of peel or shear behaviour, fracture locus and performance following wet exposure; compatibility alone does not establish improved adhesion. Alginate offers a complementary modification strategy through its hydrophilic, carboxylate-bearing chains and pronounced ability to modify aqueous solution rheology. Kiattijiranon, Auras and Sane (2024) reported hydrogen bonding, interfacial adhesion and improved functional performance in sodium-alginate/starch multilayer packaging films. This supports the broader materials rationale for combining these two polysaccharides, but those results relate to films rather than to liquid adhesive deposition and paper-to-glass bonding. In practice, higher viscosity can improve resistance to flow or penetration in some coating operations while making pumping, transfer, levelling or spreading more difficult in others. Thus, viscosity must be considered together with non-volatile solids, coat weight and the specific application equipment.

An additional gap concerns the paper substrate itself. Wet-strength grades are designed to retain integrity under aqueous exposure, but grammage and paper anisotropy can modify deformation and failure in bonded assemblies. Samples taken parallel to the machine direction (MD) and the cross direction (CD) can exhibit different tensile responses owing to fibre orientation. Moreover, a tensile or peel-type loading configuration probes a different stress state from an in-plane shear configuration. Directly comparing several adhesive compositions across paper grades and directions can therefore clarify whether an apparent improvement reflects adhesive properties, substrate deformation or the test geometry. Against this background, the present work compares four rice starch-based formulations: starch–chitosan–alginate (L1), starch–alginate (L2), starch–chitosan (L3) and starch only (L4). Three wet-strength papers with grammages of 65, 80 and 75 g/m² were tested in MD and CD, and the study includes adhesive pH, Brookfield apparent viscosity, non-volatile solids and reported mechanical and washing evaluations. Beyond the primary measurements, we examine the descriptive ratio of viscosity to solids content to highlight formulation-dependent thickening at different concentrations. The objective of our research was to link formulation, processing-relevant physicochemical behaviour and the requirements of paper labels for glass packaging, while distinguishing measured outcomes from mechanisms that remained to be confirmed experimentally.

2. Methods and materials

2.1. Adhesives and paper substrates

Four formulations were designated L1–L4 as summarized in Table 1. The carbonate component reported-CO_3 in the description after was used for pH regulation in L1 and L3. Three wet-strength papers were examined: V1 (65 g/m²), V2 (80 g/m²) and V3 (75 g/m²). Test strips were cut parallel to the machine direction (MD) or cross direction (CD).

Table 1
Materials and formulation design

Sample name	Adhesive formulation	Substrate conditions
L1	Rice starch + chitosan + alginate	V1, V2, V3; MD and CD
L2	Rice starch + alginate	V1, V2, V3; MD and CD
L3	Rice starch + chitosan	V1, V2, V3; MD and CD
L4	Rice starch only	V1, V2, V3; MD and CD

2.2. Physical-chemical analysis

The pH of each formulation was measured with a calibrated pH meter following EN 1245:2011. Samples were equilibrated at 23 ± 2 °C, and measurements were performed in duplicate. Apparent viscosity was measured with a Brookfield rotational viscometer at 23 ± 0.5 °C, using the same spindle and rotational speed for all samples. Because polymer-based adhesives may be shear-dependent, the reported viscosities are compared as apparent values under shared test settings. Non-volatile solids content was determined gravimetrically, using 2 g of formulation dried at 105 ± 2 °C to constant mass; the reported method cites ASTM D1489. Solids content (%) = 100 × (dry residue mass / initial sample mass).

2.3. Mechanical analysis and washing analysis of durability of labels

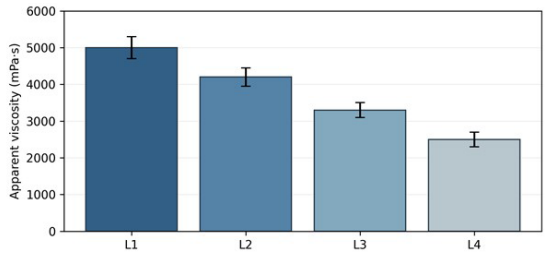
Bonded paper specimens underwent tests designated T-tests on dynamometer Instron tensile testing machine, with comparisons between MD and CD direction. The precise specimen geometry was 10 x 1.5 cm, test speed was 25 mm/min, length between the testing clamps was 10 cm and 10 replicates were made at each sample.

A separate washing challenge exposed bonded labels to a commercial washing-machine cycle for 1 h at 55 °C and drying using commercial, washing tablets.

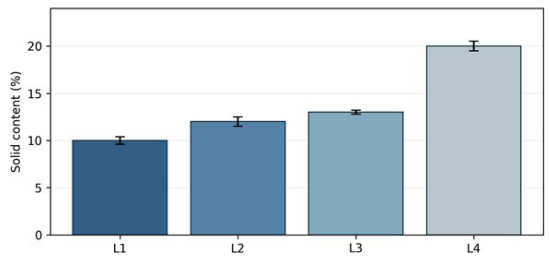
3. Results and discussion

3.1. pH, viscosity and solids content

According to results, pH varied from 5 (L3), 6 (L2) to 7 (L1 and L4). Apparent viscosity decreased in the order L1 > L2 > L3 > L4, whereas non-volatile solids decreased in the opposite order (L4 > L3 > L2 > L1). Thus, the observed processing-relevant viscosity cannot be explained by solids loading alone. Figure 1 presents the measured viscosities and Figure 2 the solid contents. The physicochemical characterization of the four adhesive formulations (L1–L4) revealed notable differences in pH, apparent viscosity, and non-volatile solids content, indicating that adhesive composition strongly influences their processing behavior. The pH values ranged from 5 to 7, with L3 exhibiting the lowest pH (5), followed by L2 (6), while L1 and L4 showed neutral conditions (pH 7). These differences may influence the ionization of functional groups, intermolecular interactions, and the structural organization of the adhesive systems. As shown in Figure 1, apparent viscosity progressively decreased from approximately 5000 mPa·s for L1 to 4200 mPa·s for L2, 3300 mPa·s for L3, and 2500 mPa·s for L4. This represents an overall viscosity reduction of approximately 50% between L1 and L4. Such differences are particularly relevant for industrial adhesive applications, as viscosity directly affects adhesive flow, spreadability, coating uniformity, and application efficiency. From a practical perspective, L4 appears particularly promising for applications requiring relatively high solids content combined with low viscosity. Such a combination may facilitate adhesive application while potentially reducing the amount of water that must be removed during drying. Conversely, the higher viscosity of L1 may be advantageous in applications requiring greater resistance to flow, although it could present challenges during coating or spreading.



» **Figure 1:** *Apparent viscosity of the four adhesives L1-L4; error bars reproduce the supplied ± values*

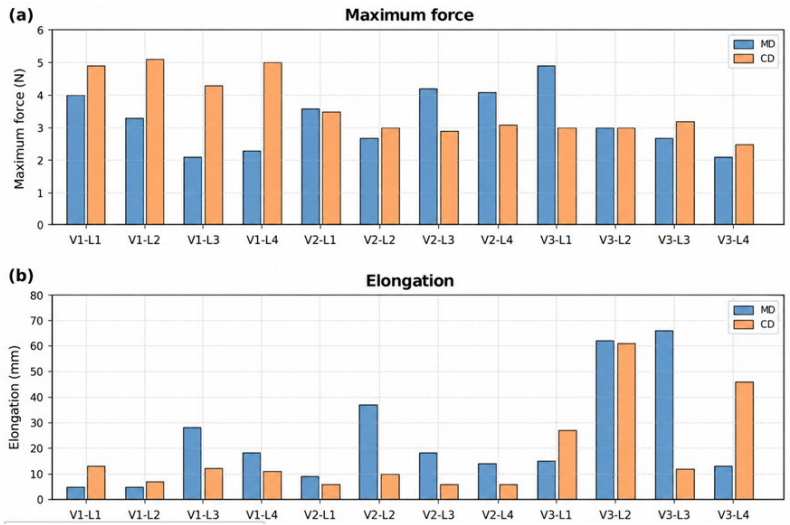


» **Figure 2:** *Non-volatile solids content of the four adhesives L1-L4; error bars reproduce the supplied ± values*

3.2. Mechanical properties

The mechanical properties of the adhesive formulations (L1–L4) were evaluated using tensile tests (T-test) on three paper substrates (V1–V3) in the machine direction (MD) and cross-machine direction (CD). Maximum tensile force and elongation at maximum force are presented in Figure 3a and 3b.

The results revealed differences in mechanical performance depending on adhesive formulation, paper substrate, and testing direction. L1 exhibited the highest average maximum tensile force (3.98 N), followed by L2 (3.35 N), L3 (3.23 N), and L4 (3.18 N). The highest individual force (5.1 N) was recorded for L2 on V1 in the CD direction. In contrast, L2 demonstrated the highest average elongation (30.3 mm), followed by L3 (23.7 mm), L4 (18.0 mm), and L1 (12.5 mm). The highest individual elongation (66.1 mm) was observed for L3 on V3 in the MD direction. Differences between MD



» **Figure 3:** *a) Maximum force and b) elongation at break in MD in CD direction for all 4 adhesives (L1-L4) and 3 paper samples (V1-V3)*

and CD further indicated the influence of paper fiber orientation on mechanical behavior. Nevertheless, L1 provided the highest average tensile-force resistance, whereas L2 and L3 showed greater deformability. These findings suggest that adhesive performance depends on both formulation and substrate characteristics, highlighting the importance of balancing strength and flexibility for paper-based packaging applications.

3.3. Washing resistance and adhesive bond stability

In addition to the mechanical characterization, the adhesive formulations were subjected to a washing challenge at 55 °C for 1 h in the presence of washing tablets. This experiment was designed to evaluate adhesive-bond stability under conditions involving elevated temperature, water exposure, and detergent-induced chemical interactions. Washing resistance is an important characteristic for adhesive applications involving removable labels, reusable packaging systems, and materials that may undergo aqueous cleaning processes. Exposure to warm water may promote swelling and plasticization of hydrophilic adhesive components, particularly polysaccharide-based materials such as alginate and chitosan. Water penetration into the adhesive network can disrupt hydrogen bonding and reduce cohesive or interfacial strength. Furthermore, detergent components may alter the adhesive–substrate interface and facilitate bond weakening or label separation. The pH and viscosity differences observed among the formulations may also influence water penetration and washing behavior.

As shown in Figure 4, all formulations exhibited varying degrees of label detachment and paper degradation. L1 showed extensive label separation, with a large portion of the paper detached from the glass surface, suggesting reduced adhesion under washing conditions. In contrast, L2 demonstrated greater label retention, with most of the paper remaining attached to the glass. L3 exhibited pronounced paper tearing and surface deterioration, while L4 showed partial label detachment and fragmentation. These observations suggest that adhesive composition influences wash-off behavior and the integrity of paper labels during washing. From a reusable glass packaging perspective, easier label removal, as observed for L1, may be advantageous for cleaning and relabeling processes. However, further quantitative evaluation of adhesive residue and detachment efficiency is required to establish the suitability of the formulations for industrial washing applications.



L1 *L2* *L3* *L4*

» **Figure 4:** *Representative photographs of paper labels bonded to glass containers after washing at 55 °C for 1 h using washing tablets: (a) L1, (b) L2, (c) L3, and (d) L4*

3.4. Implications for sustainable packaging

The findings demonstrate the potential of biopolymer-containing adhesive formulations for paper-based packaging applications. The most important observations were the superior overall T-test response of L1, the increased flexibility associated with alginate and/or chitosan incorporation, and the influence of paper orientation on mechanical performance. The opposite trends observed for viscosity and solids content further demonstrate that adhesive processing characteristics cannot be predicted solely from non-volatile solids concentration. These results suggest that formulation-dependent molecular interactions play an important role in determining adhesive behavior and that optimization should account for both processing requirements and the mechanical performance of bonded substrates. Therefore, L1 appears promising where mechanical resistance under the investigated T-test conditions is prioritized, whereas L4 offers potential processing advantages owing to its combination of lower viscosity and higher solids content. The final selection of an adhesive formulation should also consider its mechanical performance across different substrates and its resistance to, or controlled removal during, washing.

4. Conclusions

Four rice starch-based adhesive formulations exhibited pH values of 5–7, apparent viscosities of 2,500–5,000 mPa·s, and solids contents of 10–20%. L1 (starch–chitosan–alginate) demonstrated the highest viscosity despite having the lowest solids content, indicating that adhesive composition and intermolecular interactions strongly influence rheological behavior. Mechanical testing revealed that L1 provided the highest average maximum tensile force (3.98 N), while L2 exhibited the greatest average elongation (30.3 mm). Differences between machine (MD) and cross-machine (CD) directions further highlighted the influence of paper substrate orientation on bonding performance. Overall, the results demonstrate the potential of rice starch-based adhesives as sustainable alternatives for paper labels on glass packaging. Further optimization and washing-resistance evaluation are necessary to establish their suitability for industrial applications, particularly wet-strength and removable labeling systems.

5. Acknowledgments

The authors acknowledge the financial support from the Slovenian Research Agency (research core funding No. P2-0450), Problem-Based Learning of Students in the Working Environment: Economy, Non-Economy and Non-Profit Sector in the Local/Regional Environment 2024–2027 (with collaboration with Papirnica Vevče d.o.o. and dr. Žiga Nose).

6. References

ASTM International (2021) *ASTM D1489-09(2021): Standard Test Method for Nonvolatile Content of Aqueous Adhesives*. West Conshohocken, PA: ASTM International. DOI: 10.1520/D1489-09R21

European Committee for Standardization (CEN) (2011) *EN 1245:2011: Adhesives — Determination of pH*. Brussels: CEN.

Kiattijiranon, P., Auras, R.A. and Sane, A. (2024) 'Enhanced functional properties for packaging applications using sodium alginate/starch bilayer and multilayer films', *ACS Applied Polymer Materials*, 6(8), pp. 4642–4650. DOI: 10.1021/acsapm.4c00224

Klenovšek, U. and Vrabič Brodnjak, U. (2026) 'Lignin-based adhesives for various packaging applications', *Polymers*, 18(15), 1905, pp. 1–28. DOI: 10.3390/polym18151905

Márquez, I., Alarcia, F. and Velasco, J.I. (2020) 'Synthesis and properties of water-based acrylic adhesives with a variable ratio of 2-ethylhexyl acrylate and n-butyl acrylate for application in glass bottle labels', *Polymers*, 12(2), 428. DOI: 10.3390/polym12020428

Vrabič Brodnjak, U. and Vidmar, A. (2025) 'Sustainable adhesive formulation and performance evaluation of bacterial nanocellulose and aloe vera for packaging applications', *Molecules*, 30(15), 3136, pp. 1–18. DOI: 10.3390/molecules30153136

Wan Yusof, W.R., Sabar, S. and Zailani, M.A. (2024) 'Starch–chitosan blends: A comprehensive review on the preparation, physicochemical properties and applications', *Biopolymers*, 115(5), e23602. DOI: 10.1002/bip.23602

© 2026 Authors. Published by the University of Novi Sad, Faculty of Technical Sciences, Department of Graphic Engineering and Design. This article is an open access article distributed under the terms and conditions of the Creative Commons Attribution license 4.0 Serbia (https://creativecommons.org/licenses/by/4.0/deed.en).

Education and learning innovation

08

Original Scientific Paper https://doi.org/10.24867/GRID-2026-p83

Student Preferences in Shaping the Learning Space and Their Impact on the Educational Process

ABSTRACT

The physical environment in which learning takes place has increasingly been recognized as an important factor influencing students' motivation, emotions, and academic performance. Contemporary approaches to the design of educational environments emphasize the need for evidence-based planning that considers students' experiences and learning preferences. The aim of this study was to identify the spatial characteristics that students perceive as contributing most significantly to productive learning and to examine how different design elements influence their perception of educational spaces. The research was conducted through a questionnaire administered to fifty students of the Faculty of Technical Sciences, University of Novi Sad. The survey investigated students' preferences regarding learning methods, spatial organization, environmental comfort, collaborative spaces, and architectural characteristics of learning environments. The collected data were analyzed using descriptive statistical methods and interpretation of students' evaluations. The findings indicate that students consider individual learning to be the most productive learning approach, while learning during lectures received the lowest evaluation. Functional characteristics of learning environments, particularly ergonomic furniture, adequate thermal comfort, and appropriate equipment, were identified as the most influential factors affecting learning productivity. Conversely, decorative elements such as colors and interior aesthetics were found to have a considerably lower impact. Nevertheless, students expressed a clear preference for modern, well-lit, technologically equipped learning environments and recognized the value of dedicated spaces for relaxation and informal interaction as contributors to collaboration, knowledge exchange, and academic motivation. The results suggest that improvements to higher education learning environments should prioritize functionality, comfort, and adaptability rather than purely aesthetic interventions. The study contributes to the growing body of research supporting evidence-based design approaches in educational space design and provides practical guidelines for the planning and renovation of university learning spaces.

Ivan Pinćjer [1]
Nada Miketić [1]
Vladimir Dimovski [2]
Jelica Čupić [1]

[1] University of Novi Sad, Faculty of Technical Sciences, Department of Graphic Engineering and Design, Novi Sad, Serbia
[2] University of Donja Gorica, Faculty of Design and Multimedia, Podgorica, Montenegro

KEY WORDS
Learning environments, higher education, learning productivity, educational space, students' perceptions

1. Introduction

University learning spaces support more than scheduled teaching: they also accommodate individual study, collaborative work, informal exchange and access to learning resources. As educational practices change, the design of these spaces must account for activities and users rather than only visual appearance. Brown (2005) argues that formal and informal spaces should be considered as parts of an integrated learning environment, while Temple (2008) emphasizes their role in the wider university community.

Researchers have examined the relationship between spatial characteristics and learning using several approaches. In his study, Brooks (2011) investigated outcomes in contrasting formal learning environments. Barrett et al. (2015) reported associations between classroom design and academic progress among primary-school pupils; their findings provide a broader environmental-design perspective, although they cannot be transferred directly to university students. Research focused specifically on higher education indicates that learning-space preferences are strongly related to the activity being undertaken and the need for quiet or collaboration (Beckers, van der Voordt & Dewulf, 2016).

This study examines students' evaluations of learning approaches and university spaces at the Faculty of Technical Sciences, University of Novi Sad. It aims to identify the environmental characteristics associated with perceived productivity, evaluate preferences for visual and architectural features, and examine the perceived role of rest and interaction spaces. The objective is to inform design priorities based on student-reported experience, without claiming effects on academic achievement.

2. Materials and methods

A questionnaire survey was conducted among 50 students at the Faculty of Technical Sciences, University of Novi Sad. The questionnaire comprised 30 numbered questions addressing study practices, university facilities, visual and functional characteristics, informal spaces, and potential improvements. This conference paper analyzes a subset of results documented in the broader research, using the complete thesis only to clarify the original instrument and response categories. The original study reports that 26 respondents (52%) were master's students and 16 (32%) were fourth-year students; the remaining eight respondents were from other study years or doctoral studies.

The analyzed questions included five-point scales for perceived productivity of individual study, group study and learning during lectures; ratings of eight environmental factors; and evaluations of five features of an illustrated contemporary interior. Other questions required selection between two illustrated environments or agreement with statements about rest areas and informal interaction. Responses were processed in Microsoft Excel and summarized by counts and percentages. For five-point scales, ratings of 1–2 were additionally classified as negative, 3 as neutral, and 4–5 as positive. Each factor was rated separately by all 50 respondents. The original thesis includes the questionnaire and its visual stimuli. No inferential tests or objective learning-performance measurements were reported. Consequently, all comparisons are descriptive and concern respondents' perceptions, not demonstrated improvements in learning.

3. Results

3.1. Preferences for learning approaches

Individual study received the most favorable ratings: 29 respondents (58%) rated it 5 and seven (14%) rated it 4, yielding 72% positive ratings (4–5). Group learning had a more mixed distribution, with 17 students (34%) choosing the midpoint rating of 3 and 20 (40%) providing positive ratings. Learning during lectures had 13 positive ratings (26%), while 22 students (44%) assigned ratings of 1 or 2. Thus, individual study was the most favorably perceived option, whereas studying during lectures was the least favorably rated of the three approaches.

3.2. Visual preferences and spatial character

For the comparison between a neutral, light-colored interior and a visually dynamic interior, 28 students (56%) selected the neutral option and 22 (44%) the colorful alternative. A separate question contrasted two illustrated learning environments: one with windows, daylight, vegetation and natural ventilation, and another enclosed environment without windows and with artificial lighting (Figure 1). The first was preferred by 43 students (86%), versus seven (14%) for the second (Figure 1). Because several characteristics varied simultaneously, the result cannot isolate the effects of daylight, plants, windows or ventilation individually.



(a)



(b)

» **Figure 1:** *Original visual alternatives from survey: (a) daylit, planted space with windows; (b) enclosed space with artificial lighting*

3.3. Rest, social interaction and recreation

A suitable rest area was perceived as potentially motivating better learning by 41 respondents (82%), while seven were uncertain and two disagreed. Thirty students (60%) agreed that a creative rest area could encourage longer stays on campus. Thirty-seven (74%) considered such areas potentially useful for initiating group work or projects, and 40 (80%) agreed that informal exchange could help solve learning-related problems. For a proposed recreation/play area, 26 students (52%) selected the response that it would make them more active and energetic for learning; 24 (48%) selected the alternative that it would distract them. These are expectations rather than observed behavioral effects.

3.4. Functional and architectural characteristics

When respondents rated eight factors for their influence on perceived learning productivity, furniture comfort received 39 positive scores (78%), room temperature 37 (74%), and availability of learning equipment 33 (66%). These factors were followed by the possibility of cooperating without disturbance (29; 58%) and choosing a seat (26; 52%). Fewer positive scores were given to freedom of movement (16; 32%), room colors/design (15; 30%) and an outdoor view (14; 28%). Table 1 reports the complete positive-score comparison, based on the original frequency table for question 26.

Table 1

Positive ratings (scores 4–5) for environmental factors affecting perceived learning productivity (n = 50)

Factor	Positive (n)	Positive (%)
Furniture comfort	39	78%
Room temperature	37	74%
Equipment and resources	33	66%
Cooperation without disturbance	29	58%
Choice of seating location	26	52%
Freedom of movement	16	32%
Room colors and design	15	30%
Outdoor view	14	28%

In a separate evaluation of an illustrated modern interior (question 27), bright lighting was positively rated by 38 students (76%), high ceilings by 36 (72%), and technological modernity by 37 (74%). Cheerful colors received 31 positive ratings (62%), while classroom transparency received only 18 (36%) and 25 negative ratings (50%). These findings suggest a favorable response to brightness and modernity, alongside reservations about visually open classroom boundaries.

4. Discussion

The preference for individual learning does not negate students' support for shared areas. Respondents associated focused study with comfortable, functional conditions, while also recognizing the potential of rest spaces to support informal exchange and collaboration. Beckers, van der Voordt and Dewulf (2016) similarly found that students' spatial preferences depend on whether activities require concentration or communication. The present results therefore favor a differentiated campus environment offering both quiet areas and places for interaction, rather than a single design solution.

Furniture comfort, temperature and adequate equipment emerged as more important to perceived productivity than decorative characteristics. This functional emphasis is consistent with the broader literature on environmental conditions and learning, although the evidence from Barrett et al. (2015) concerns primary schools rather than higher education. Brooks (2011), by contrast, examined formal learning spaces in a university context and illustrates why future research should combine students' perceptions with measured educational outcomes. The present study cannot establish that changing any physical factor would increase performance.

Visual findings also require careful interpretation. The 86% preference for the daylit, planted environment involved a comparison in which several features changed together; the individual contributions of lighting, greenery and enclosure cannot be separated. Likewise, favorable ratings for modernity and lighting coexist with relatively low ratings for classroom transparency, suggesting that openness may not always be perceived as beneficial. Temple (2008) emphasizes that campus spaces support broader institutional and social functions, while Brown (2005) discusses the value of connecting formal and informal learning environments. Together, these perspectives support balancing privacy, functionality and social opportunity. The study is limited to 50 respondents from one faculty, with a sample concentrated in senior and master's-level students. Its findings are descriptive, self-reported and partly based on illustrated scenarios rather than direct experience in controlled spaces. Broader samples, on-site assessments and before-and-after evaluations would be needed to test the generalizability and practical effects of proposed changes.

5. Conclusions

Among the surveyed students, individual study received the highest perceived-productivity ratings. Furniture comfort, thermal conditions and adequate equipment were more frequently rated as influential than interior color, views or freedom of movement. At the same time, respondents favored a daylit and planted visual alterna-

tive, positively evaluated brightness and technological modernity, and recognized the potential benefits of rest and interaction areas.These findings suggest that university space improvements should prioritize functional comfort and suitable resources while providing a complementary range of quiet and informal environments. Visual interventions should be considered in relation to the activities they support, not solely their aesthetic effect. The results offer practical, institution-specific evidence of student preferences rather than causal proof of improved academic performance.

Considering the results obtained in this study, it is worth examining whether the teaching and learning approaches currently applied at the university could be adapted to better accommodate students' preferences. However, it should be acknowledged that the number of students attending particular courses may represent a limiting factor in the implementation of different learning approaches.

Providing students with greater opportunities for independent learning, which was identified as the preferred approach by the majority of respondents, could contribute to improving the quality of education and facilitating knowledge acquisition. Working with smaller groups is certainly one of the prerequisites for implementing advanced teaching methods, including the flipped classroom approach. This approach involves students independently studying theoretical materials outside scheduled class hours, which aligns with their expressed learning preferences.In such a model, classrooms and scheduled teaching sessions would be adapted to support collaborative activities and the practical application of theoretical knowledge acquired independently before class. Teaching sessions would become more interactive, encouraging discussion, the exchange of opinions, and collaborative problem-solving rather than passive participation in traditional lectures.

The implementation of this approach would also benefit from modifications to the physical learning environment, particularly the spatial configuration of classrooms. Changes in seating arrangements, the positioning of instructors in relation to students, and the possibility of moving freely within the classroom could facilitate the transformation of students from passive observers into active participants in the learning process. Such an environment would encourage the exchange of experiences, critical discussion, and knowledge acquisition through interaction.

These changes would affect not only students but also instructors, whose roles would shift from traditional positions of authority and control toward those of facilitators, moderators, and active participants in discussions. This transition would require instructors to engage with questions, perspectives, and ideas that may not always be anticipated or fully addressed through predefined teaching materials.

6. Acknowledgments

This research has been supported by the Ministry of Science, Technological Development and Innovation (Contract No. 451-03-34/2026-03/200156) and the Faculty of Technical Sciences, University of Novi Sad through project “Scientific and Artistic Research Work of Researchers in Teaching and Associate Positions at the Faculty of Technical Sciences, University of Novi Sad 2026” (No. 01-3609/1).

7. References

Barrett, P., Davies, F., Zhang, Y. and Barrett, L. (2015) 'The impact of classroom design on pupils' learning: Final results of a holistic, multi-level analysis', *Building and Environment*, 89, pp. 118–133. DOI: 10.1016/j.buildenv.2015.02.013

Beckers, R., van der Voordt, T. and Dewulf, G. (2016) 'Learning space preferences of higher education students', *Building and Environment*, 104, pp. 243–252. DOI: 10.1016/j.buildenv.2016.05.013

Brooks, D.C. (2011) 'Space matters: The impact of formal learning environments on student learning', *British Journal of Educational Technology*, 42(5), pp. 719–726. DOI: 10.1111/j.1467-8535.2010.01098.x

Brown, M. (2005) 'Learning spaces'. In: Oblinger, D.G. and Oblinger, J.L. (eds.) *Educating the Net Generation*. Boulder, CO: EDUCAUSE. Available from: https://www.educause.edu/research-and-publications/books/educating-net-generation/learning-spaces

Temple, P. (2008) 'Learning spaces in higher education: An under-researched topic', *London Review of Education*, 6(3), pp. 229–241. DOI: 10.1080/14748460802489363

© 2026 Authors. Published by the University of Novi Sad, Faculty of Technical Sciences, Department of Graphic Engineering and Design. This article is an open access article distributed under the terms and conditions of the Creative Commons Attribution license 4.0 Serbia (http://creativecommons.org/licenses/by/4.0/rs/).

Original Scientific Paper https://doi.org/10.24867/GRID-2026-p84

Analysis of the Use of and Attitudes Towards Generative Artificial Inteligence Among Graphic Art Students

ABSTRACT

The rapid development of generative artificial intelligence (genAI) is reshaping higher education by transforming learning processes, teaching practices, and creative disciplines such as graphic design. Despite the growing adoption of genAI tools, empirical evidence on their use and perceived impact among graphic arts students remains limited. This study examines the frequency and purposes of genAI use, students' perceptions of its benefits and risks, and the relationships between AI literacy, usage patterns, and responsible use in higher education. Data were collected through an anonymous online questionnaire completed by 202 undergraduate and postgraduate graphic arts students at the Faculty of Natural Sciences and Engineering, University of Ljubljana. Descriptive statistics and Spearman's rank correlation analysis were used to examine the data. The findings indicate that most students are familiar with genAI and use it regularly, primarily to explain course content, generate ideas, write academic texts, summarise materials, and search for information. A statistically significant positive correlation was found between self-assessed knowledge of genAI and the frequency of its use, suggesting that greater familiarity with the technology encourages its integration into academic work. However, no statistically significant relationships were identified between self-assessed AI literacy and either the perceived benefits and risks of genAI or students' self-control in using these tools. Participants recognised substantial advantages, including increased efficiency, time savings, and improved access to information, while simultaneously expressing concerns about unreliable outputs, plagiarism, reduced critical thinking, ethical issues, privacy, and dependence on technology. The results show that effective integration of genAI into graphic art education requires not only technical proficiency but also the systematic development of AI literacy, critical evaluation skills, ethical awareness, and clear institutional guidelines for responsible and sustainable use.

Patricija Nakić
Nuša Ceglar
Lara Koštomaj
Jan Simončič
Urška Stanković Elesini

University of Ljubljana, Faculty of Natural Sciences and Engineering, Chair of Information and Graphic Arts Technology, Ljubljana, Slovenia

KEY WORDS
Generative artificial intelligence (genAI), graphic arts students, AI literacy, self-control, technology dependence, ethics

1. Introduction

The field of artificial intelligence (hereafter AI) is developing rapidly. Research by the Statistical Office of the Republic of Slovenia (Mlakar, 2025) indicates that more than half of the population aged 16 to 74 have already heard of AI technologies, with secondary school pupils and university students standing out at 94%. Generative artificial intelligence tools (hereafter genAI), such as ChatGPT, Copilot, Gemini and DALL-E, are used by 21% of Slovenia's population, while this share is again considerably higher among secondary school pupils and university students (70%). AI has moved from research laboratories into all areas of everyday life, and the educational environment is by no means

exempt from this development. AI is transforming the ways in which learning and teaching take place (Cvajdik, 2025), and is used by both students and teachers for a variety of purposes and in a range of ways.

AI serves as a learning aid (Jarc, 2026; Pitts, Marcus & Motamedi, 2025), providing students with immediate support through easier access to information (Cvajdik, 2025; Pitts, Marcus & Motamedi, 2025; Stephenson & Armstrong, 2026), data organisation (Molek, 2023), analysis, and quicker, better understanding of complex subject matter (Adil, 2025; Cvajdik, 2025; Molek, 2023; Stephenson & Armstrong, 2026; Zhang, Jantakoon & Laoha, 2025). In this way, it saves students time (Stephenson & Armstrong, 2026), and allows them to adapt their learning to their own needs. AI also enables the creation of coherent texts and supports research activities (Molek, 2023). Students use AI tools for essay writing, sourcing materials, explaining course content, solving tasks, and creating summaries (Cvajdik, 2025). Several studies confirm that AI contributes to self-evaluation (Tan, Cheng & Ho Ling, 2025) and improves learning outcomes (Adil, 2025) although this effect is weakest among primary school pupils and stronger among secondary school pupils and university students; among different types of AI, chatbots have shown the strongest effect on learning outcomes (Dong, Tang & Wang, 2025). Research further reports that the use of AI is associated with higher levels of student engagement and motivation (Adil, 2025; Sun et al., 2026; Tan, Cheng & Ho Ling, 2025), while AI tools are used more frequently by students with slightly lower levels of creativity (Sun et al., 2026; Tan, Cheng & Ho Ling, 2025).

Despite its many advantages, the use of AI also entails risks and challenges. Jarc (2026) emphasises that AI should not replace independent thinking, while Jaca (2024) points out that AI cannot replace empathy or the personal relationship between teacher and student. AI users must be aware of errors in texts and of incorrect information that AI can spread as misinformation (Mlakar, 2025). AI may generate texts that are cognitively, demographically, ideologically and linguistically biased, or reproduce stereotypes relating to gender, race or social status. It is therefore important for users to evaluate AI-generated information critically (Adil, 2025; Licardo, Puncer & Todorović, 2025; Mlakar, 2025; Molek, 2023).

Accordingly, developing digital literacy and the ability to verify sources is of vital importance. Several authors have raised concerns about the risks of plagiarism (Cvajdik, 2025; Licardo, Puncer & Todorović, 2025; Molek, 2023). AI tools can generate original text that is sometimes difficult to identify as inauthentic; therefore, it is essential to establish clear guidelines for AI use and employ plagiarism detection tools. Licardo, Puncer and Todorović (2025) also highlight the possibility of the anthropomorphisation of AI, where a user attributes human characteristics to the technology, potentially leading to over-reliance or dependency.

Furthermore, several authors urge caution against excessive reliance on technology (Cvajdik, 2025; Mlakar, 2025), since dependency may undermine the development of critical thinking, reduce creativity and originality, and weaken independent problem-solving skills (Jaca, 2024; Licardo, Puncer & Todorović, 2025; Molek, 2023; Pitts, Marcus & Motamedi, 2025; Sun et al., 2026). The use of AI must be responsible (Jarc, 2026; Mlakar, 2025; Molek, 2023) and should support the development of higher-order cognitive skills (Molek, 2023). Moreover, challenges persist regarding technological limitations and unequal access to these technologies.

The use of large-scale data centres can also have significant environmental consequences (Molek, 2023) due to their high energy consumption, as well as social implications arising from an increased digital divide between different social groups (Licardo, Puncer & Todorović, 2025). Furthermore, the application of AI raises questions regarding intellectual property, as it is not always clear who holds the authorship of AI-generated content, or whether copyright-protected data may be used for model training (Licardo, Puncer & Todorović, 2025). Challenges associated with AI also include a lack of transparency and the opacity of algorithms (Adil, 2025; Jarc, 2026; Mlakar, 2025), alongside infrastructure-related issues (Adil, 2025). The implementation of AI must be oriented towards inclusion and equity to ensure equal access to knowledge and emerging technologies (UNESCO, 2025).

When using AI, it is essential to respect academic integrity (Jarc, 2026; Licardo, Puncer & Todorović, 2025; Pitts, Marcus & Motamedi, 2025), as well as privacy and personal data protection (Adil, 2025; Jarc, 2026; Molek, 2023). AI systems frequently collect large amounts of user information, which may pose significant risks of data misuse. European legislation, particularly the GDPR and the Artificial Intelligence Act, sets out rules for protecting personal data and restricts certain high-risk practices, such as social scoring or the mass collection of biometric data (Licardo, Puncer & Todorović, 2025).

The use of AI creates an urgent need for clear ethical guidelines to ensure its fair, secure, and inclusive application in education (Cvajdik, 2025; Jarc, 2026), and to promote the use of technologies in a manner that respects human rights, safety, and dignity (Licardo, Puncer & Todorović, 2025). Within the framework of the Beijing Consensus on Artificial Intelligence and Education, UNESCO has developed guidelines for educational policymakers, as well as competency frameworks for students and teachers. These documents aim to help countries understand the opportunities and risks associated with AI, while supporting the development of the skills necessary for life and work in the AI era (UNESCO,

2025). Consequently, universities are formulating guidelines that specify how and when students may use AI in their studies (Cvajdik, 2025), alongside appropriate legislation and education and training programmes for both teachers and students to ensure the responsible use of AI (Molek, 2023; Pitts, Marcus & Motamedi, 2025). Only through such measures can AI contribute to the enhancement of the learning process while simultaneously mitigating risks to society, individuals, and the environment (Licardo, Puncer & Todorović, 2025).

In a study by Xiaoyu, Zainuddin and Leng (2025), the authors investigated how specific genAI tools, such as ChatGPT, Midjourney, Stable Diffusion and Telegram Bot, influence pedagogical practices. GenAI enables the generation of text, images and audio content, which simplifies the personalisation of teaching, fosters interactive learning and enhances content creation. Likewise, in this study, the authors highlighted that genAI enhances teaching efficiency by enabling the faster production of learning materials, providing instantaneous feedback, and reducing teacher workload. Furthermore, genAI increases student engagement and motivation, facilitates self-paced learning, and reduces stress. It also encourages idea generation and the development of generic skills, such as critical thinking, problem-solving, collaboration and communication.

In her research, Molek (2023) notes that AI cannot replace human cognition, creativity, and critical judgement and must therefore remain a supplement to the pedagogical process. Students must develop critical thinking and their own sense of judgement, while lecturers should establish clear rules for AI use, encourage creative and non-written forms of knowledge presentation, and ensure that the use of technology supports long-term learning objectives. Xiaoyu, Zainuddin and Leng (2025) state that challenges are emerging regarding the accuracy of AI, academic integrity, and its limited effectiveness. To mitigate these risks, the authors advocate a hybrid approach that combines genAI with teacher supervision. While AI in education is a beneficial tool with numerous advantages, its use demands a thoughtful and responsible approach and, above all, appropriate regulation (Jaca, 2024).

AI enables the automation of administrative tasks, such as marking and organising learning activities, allowing teachers to devote more time to lesson preparation and student engagement. It also facilitates data-driven decision-making through the analysis of large amounts of student performance data and supports the improvement of teaching strategies.

Research conducted by the Slovenian Student Organisation (2025), reported by Jarc (2026), concludes that AI is becoming an indispensable part of study at Slovenian universities. It enables students to access information more easily, solve tasks more efficiently, summarise and rephrase texts, and organise their work. Survey results from ŠOS (2025) indicate that 90% of students use AI, with 39% using it daily. The most popular tools are ChatGPT, Google AI, Grammarly, and Copilot, which assist students with information retrieval, learning, assignment writing, idea development, and study organisation. The application of AI varies according to the field of study; however, it generally supports students by summarising and rephrasing text, explaining course material, and generating graphs or analyses. Although AI facilitates the study process, some students have admitted to breaches of academic integrity, highlighting the need for clear ethical guidelines and rules for responsible use. Furthermore, AI can contribute to the development of digital literacy, critical thinking, and creativity. ŠOS (2025) adopted the Resolution on the use of AI in daily studies (ŠOS, 2025) which emphasises that AI should support learning rather than replace human cognition and interaction.

1.1. Applications of genAI in graphic design studies

Fundamental aspects of the graphic design curriculum include UI and UX design, photography, 3D design and animation, corporate identity creation, marketing graphics (such as posters, catalogues and flyers), and prepress-related tasks. Throughout all stages of the creative process, a range of tools and software applications incorporating genAI technology are utilised.

In a study by Fleischmann (2024) involving a small group of 17 students, several advantages of using genAI were identified: improved efficiency in design tasks (76%), enhanced creativity and inspiration (80%), data-driven insights (53%), and the potential for the adaptation and personalisation of designs (35%). Conversely, drawbacks included ethical challenges such as content theft and plagiarism (94%), along with concerns about the loss of human touch and the limited ability of genAI to comprehend emotion and aesthetics (82%). Notably, none of the students regarded genAI as a threat to employability, despite 82% acknowledging that AI will replace certain traditional tasks. Furthermore, 82% of students expressed a desire to deepen their knowledge of genAI, highlighting a strong need for the systematic, project-oriented integration of prompt engineering and ethical reflection into the curriculum.

In his study, Alsswey (2025) examined utilitarian and hedonic benefits, user experience, and learnability. Accordingly, a questionnaire based on several existing studies (Laugwitz, Held & Schrepp, 2008; Silva, 2015; Venkatesh, Thong & Xu, 2012) was developed, refined, and adapted to the specific characteristics of the graphic design field. The research involved 112 graphic design students, divided into an experimental and a control group. The former utilised tools such as Midjourney,

Leonardo, and Adobe Express, while the latter used traditional graphic software, including Adobe Illustrator, Adobe InDesign, and Adobe Photoshop. Students in the experimental group reported that these tools facilitated their workflow, reduced cognitive load, and increased their confidence during creative tasks. They particularly highlighted the ability to quickly generate multiple design iterations, which gave them the freedom to explore potential solutions without the fear of irreversible errors. Participants also identified real-time feedback and intelligent suggestions as key advantages that enhanced learnability and supported a more relaxed user experience. The author concludes that the integration of genAI into graphic design curricula can significantly benefit both the functional and experiential aspects of the learning process.

1.2. Research purpose and hypotheses

The aims of this research are to compare the attitudes of graphic arts students towards genAI and to analyse perceived benefits and risks, ethical concerns, and their understanding of the impact of genAI on the future development of graphic design. We examined how graphic arts students utilise genAI tools within the study process, which advantages and risks they perceive, and which individual factors – particularly AI literacy, self-control, perceived creativity, and study workload – are associated with a more profound, critical, and responsible application of genAI. We formulated the following hypotheses:

H1: Students with a higher level of self-rated knowledge of genAI integrate this technology into their study process more frequently.

H2: A higher level of AI literacy among students leads to a stronger perception of the benefits and risks associated with the use of genAI.

H3: Students with a higher level of AI literacy demonstrate better self-control and a more considered use of artificial intelligence tools.

2. Methodology

The research was conducted in three phases:

4. Literature review and analysis: Domestic and international literature on the use of various genAI tools in graphic arts, education, and creative processes was analysed. Professional articles, scientific studies, and case studies of different genAI tools were reviewed, with particular attention to their impact on the learning process, creativity, and the evolution of graphic arts.
5. Survey design and data collection: Based on the literature review and similar studies, a student survey questionnaire was developed. The survey was conducted anonymously.
6. Data analysis and comparison: The survey results were processed, analysed, and compared with findings from comparable research.

2.1. Research tools

The online survey tool Arnes 1KA, developed by the Centre for Social Informatics at the Faculty of Social Sciences, University of Ljubljana, was used to design and administer the questionnaire. Data obtained from the survey were exported and organised in Microsoft Excel (Microsoft Corp., USA). Statistical analysis of the data was conducted using IBM SPSS Statistics (IBM Corp., USA).

2.2. Survey questionnaire

Source frameworks and structure of the survey questionnaire. The questionnaire was based on the studies cited in the introductory chapter, with its primary objective being to gain insight into students' familiarity with and general attitudes towards generative artificial intelligence tools in the context of their study obligations. The survey algorithm is presented in the appendix.

The survey covered demographic characteristics, the frequency of genAI use, respondents' subjective assessments of their own literacy in this field, and reflections on the impact of these technologies on creativity, academic integrity, and associated risks. The questionnaire consisted of 20 questions and employed a combination of methodological approaches. Most questions were closed-ended. In three questions, respondents were asked to indicate their level of agreement with statements on a five-point Likert scale, allowing precise quantitative analysis of student attitudes. To gain a deeper understanding of specific areas, open-ended questions were included, giving respondents the opportunity to justify their answers in their own words. To ensure the survey was as efficient as possible and tailored to each individual, logical branching was implemented using conditional logic (if statements). This mechanism ensured that students, based on key responses – for instance, whether they use genAI at all – were directed only to the relevant sections of the questionnaire. This approach prevented the completion of unnecessary questions, reduced the time required for participation, and enhanced the reliability of the collected data.

Participants. The survey questionnaire was completed by 202 students, of whom 34.1% were enrolled in the Graphic and Media Technology higher education professional programme (VS GMT), 51.4% in the Graphic and Interactive Communication university programme (UNI GIK), and 14.5% in the Graphic and Interactive

Communication master's programme (MAG GIK). The study included students from the first, second, and third years of their respective programmes, as well as those in their final thesis year. In terms of gender distribution, 77.1% of respondents were female, 18.9% were male, and 4% preferred not to answer.

Statistical analysis. Survey results were organised in Microsoft Excel, and Spearman's rank correlation coefficients were calculated in IBM SPSS Statistics.

Ethical approval. The survey questionnaire was approved by the Research Ethics Committee of the Faculty of Natural Sciences and Engineering, University of Ljubljana (UL NTF), at its session on 15 June 2026.

3. Results

3.1. Familiarity with and Use of genAI Among Graphic Arts Students

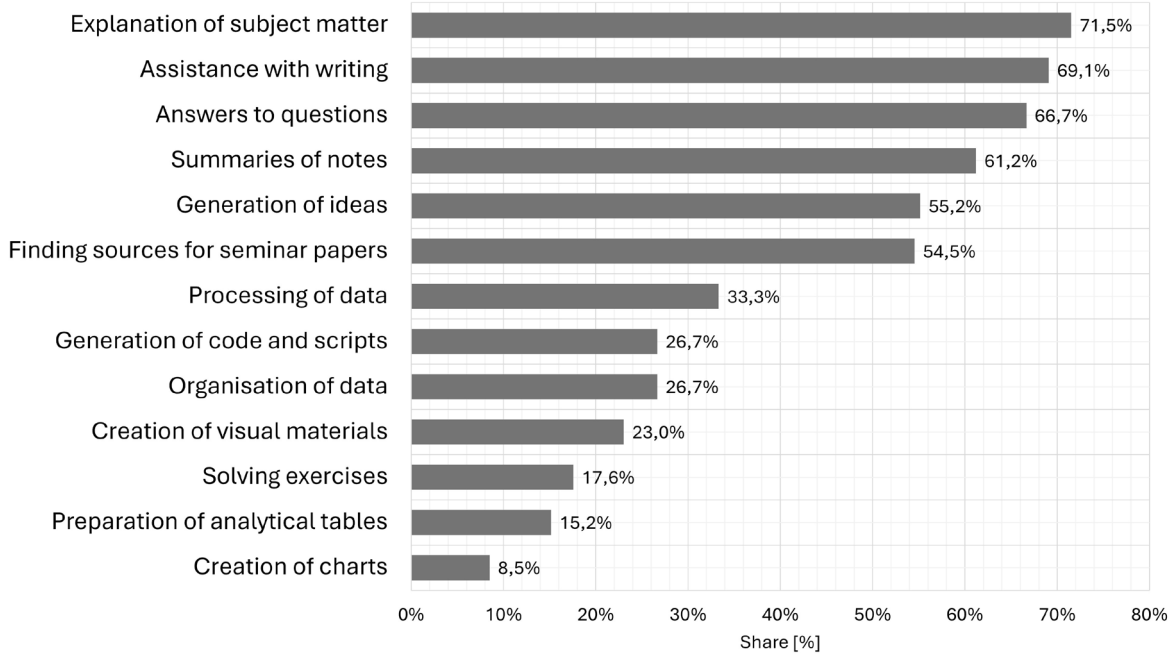
The research findings indicate that only 6.4% of students rate their familiarity with genAI as very good, while the majority (74.2%) assess their knowledge as either good or fair. Furthermore, 12.9% of students rate their familiarity as very poor, while 6.4% report that they are not familiar with genAI at all. The mean score for self-rated familiarity with genAI was $\bar{x} = 2.77$ (SD = 0.98, n = 189). These results align with findings that genAI is widely recognised among pupils and students. Within the Slovenian population aged 16–74, more than half have heard of AI, while among pupils and students this proportion reaches 94% (Mlakar, 2025).

This high level of awareness is also consistent with the results of the ŠOS (2025) study, in which 90% of students stated that they use AI in their studies (Jarc, 2026).

Generative AI is used daily by 10.6% of students and several times a week by 21.2%, while over a third (38.1%) use genAI occasionally. Nearly one-third (39.2%) use genAI rarely or never. The mean score for the frequency of genAI use was $\bar{x} = 3.01$ (SD = 1.15, n = 189). These results partially align with the study by Jarc (2026), which reports less intensive daily use, whereas some reviews highlight growth in regular genAI use among students (Stephenson & Armstrong, 2026).

The results of the Spearman's rank correlation analysis revealed a statistically significant, moderate positive correlation between self-rated familiarity with genAI and the frequency of its use in student work ($\rho s = 0.409$, $p < 0.001$). This indicates that students who are more familiar with genAI tend to integrate the technology into their work more often. Better technical knowledge may reduce uncertainty about its application and enhance the ability to identify opportunities for its integration into the study process. Conversely, more frequent use may also lead to greater familiarity, as students develop additional skills and understanding through practical experience. Since the correlation is moderate, it can be inferred that familiarity with genAI is not the sole factor determining its use. The frequency of use is likely influenced by other factors, such as tool accessibility, the nature of the tasks, digital competencies, perceived usefulness, and potential ethical or security concerns.

As illustrated in Figure 1, students most frequently use genAI for explaining course material, assisting with text



» **Figure 1:** *Purpose of using generative artificial intelligence tools (n = 165)*

writing, answering questions, creating summaries of study notes, generating ideas, and searching for sources for assignments. In contrast, it is used somewhat less often for data processing and for generating code or scripts. The use of genAI among the students in this study aligns with the findings of Cvajdik (2025) and Molek (2023), who observe that students primarily use genAI as a learning support tool for comprehension, summarisation, writing, and research, rather than as a complete substitute for their academic work. These results are also consistent with the observations of Jarc (2026) and Stephenson and Armstrong (2026), who note that students mainly employ AI to support their studies and the preparation of academic assignments.

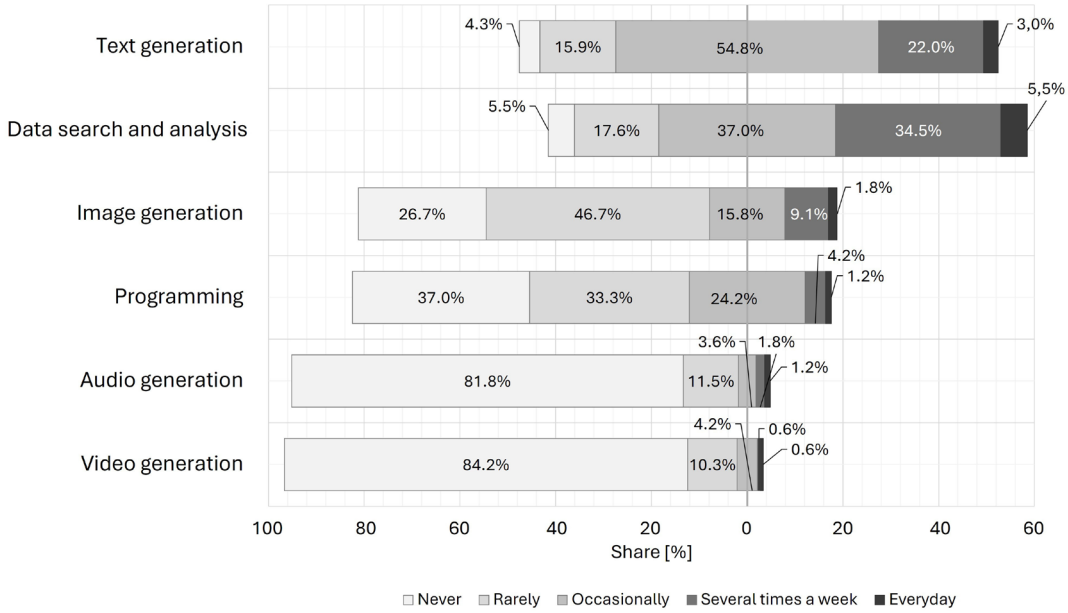
Students use genAI on a daily or several-times-weekly basis primarily for data search and analysis, and for the generation of text and images, whereas it is used considerably less for programming and for the generation of audio and video content (Figure 2). This finding is consistent with studies by Cvajdik (2025) and Molek (2023), which indicate that, in educational contexts, genAI is most commonly used for text generation, explanation, information retrieval and information organisation. The less frequent use of image-generation tools diverges from research in the field of design, which emphasises the importance of such tools in the development of visual ideas (Alsswey, 2025; Xiaoyu, Zainuddin & Leng, 2025).

The most frequently used genAI tools are ChatGPT (94.5%), Gemini (50.3%), Canva AI and Adobe Firefly (both 15.2%), Copilot (13.9%), and NotebookLM (11.5%). Other tools used by fewer than 10% of students include Grok, Claude, Perplexity, Midjourney, DALL-E, DeepSeek, and Stable Diffusion. These results are consistent with the findings of other studies (Jarc, 2026; Mlakar, 2025), although a slight divergence is evident when compared with the studies by Alsswey (2025) and Xiaoyu, Zainuddin and Leng (2025) in the field of graphic design, which report a higher proportion of use of tools such as DALL-E, Midjourney, and Stable Diffusion, all of which are important for the creation and exploration of visual imagery.

3.2. AI literacy and self-regulation in AI use

In this study, we were interested in how students self-assess their AI literacy (e.g. the appropriate selection and use of AI tools according to purpose, the critical evaluation of solutions generated by genAI, and the responsible use of genAI, including issues such as privacy and bias). However, as AI literacy was assessed through self-report, the measure primarily reflects students' confidence in, and perceptions of, their own competences rather than their actual technical knowledge.

The results showed that only 10.3% of students rated their self-assessed AI literacy as very good, while more than half (53.9%) rated it as good. A further 32.1% considered their AI literacy to be moderate, whereas 3.6% rated it as poor. The mean self-assessed AI literacy score was $\bar{x} = 2.29$ (SD = 0.70, n = 165). This finding is consistent with studies indicating that frequent use of genAI does not necessarily imply a high level of critical and ethical AI literacy, as responsible use requires an understanding of its limitations, the ability to verify outputs, and awareness of potential risks (Adil, 2025; Licardo, Puncer & Todorović, 2025).
The results indicate a relatively positive self-perception of AI literacy; however, they also suggest a continuing need for systematic training (Mlakar, 2025).



» **Figure 2:** *Frequency of use of generative artificial intelligence tools by purpose (n = 163)*

A total of 16.8% of students rated their self-regulation in the use of genAI as very good, while 45.3% and 33.5% rated it as good and average, respectively. A further 4.3% of students considered their self-regulation in the use of genAI to be poor; the mean score was $\bar{x}$ = 2.25 (SD = 0.78, n = 161). Self-regulation is an important factor in preventing excessive reliance on genAI and in maintaining active, independent learning (Sun et al., 2026). Strong self-regulation reduces the risk of students using the tool uncritically or as a substitute for their own effort (Licardo, Puncer & Todorović, 2025). The results of our analysis indicate a relatively high level of responsible use of the technology.

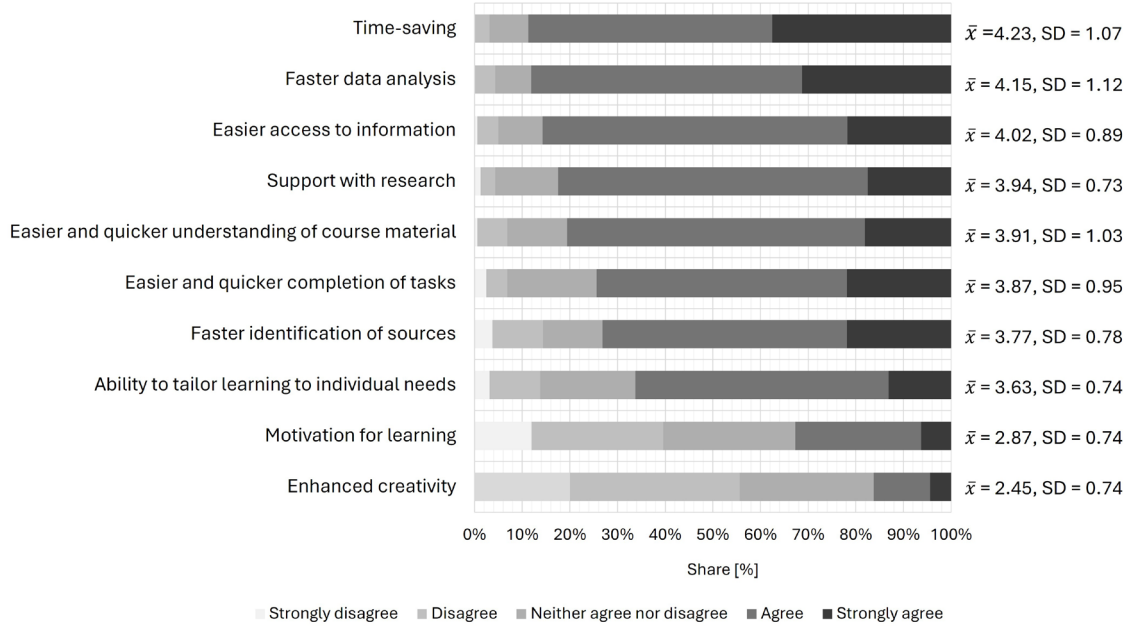
The results of Spearman's rank correlation analysis in our sample did not show a statistically significant association between self-assessed AI literacy and self-regulation in the use of AI (ρ_s = 0.092, p = 0.245). This finding suggests that knowledge of, or literacy in, AI does not necessarily imply more controlled, reflective, or self-regulated use of AI tools. An individual may have a good understanding of the functioning, possibilities, and limitations of artificial intelligence, yet this does not in itself guarantee a higher level of self-control in its use. Self-regulation may be more closely related to other factors, such as personality traits, work habits, digital discipline, the level of dependence on technology, organisational rules, ethical awareness, or perceived risks associated with AI use. Although AI literacy and self-regulation may be conceptually related in the context of AI use, in practice they do not necessarily occur together and should therefore be treated as partially distinct dimensions of digital behaviour. In practical terms, this means that measures aimed at developing AI literacy may not, in themselves, be sufficient to promote responsible and self-regulated use of AI. In addition to education about how AI functions, it would be advisable to include content on critical evaluation, ethical use, setting boundaries for AI use, verifying outputs, preventing excessive reliance on AI tools, and fostering digital self-regulation.

In this study, we examined whether creativity, the ability to solve problems creatively, workload-related pressure, and commitment to completing academic tasks influence the frequency with which students use genAI in their work (Sun et al., 2026; Tan, Cheng & Ho Ling, 2025). Spearman's correlation coefficients did not reveal any statistically significant associations among these variables in our sample.

3.3. Perceived advantages of using genAI and their relationship with self-assessed AI literacy

Students identified the main advantages of using genAI (Figure 3) as saving time, faster data analysis, easier access to information, support for research, easier and quicker understanding of course material, more efficient task completion, faster identification of sources, and the ability to tailor learning to individual needs. These findings are consistent with several studies (Adil, 2025; Cvajdik, 2025; Stephenson & Armstrong, 2026), which indicate that genAI primarily facilitates students' access to information, research activities, explanation of subject matter, and more efficient task completion. By contrast, our students did not regard motivation for learning or enhanced creativity as principal advantages, which partly diverges from the findings of some studies (Sun et al., 2026; Tan, Cheng & Ho Ling, 2025) that highlight the potential of AI to foster creativity.

The influence of students' self-assessed AI literacy level (categorised as very good, good, moderate, or



» **Figure 3:** *Advantages of using genAI (n = 160)*

poor) on their perceptions of the benefits of using genAI tools in the study process was examined. Associations were assessed using Spearman's rank correlation coefficient (ρs), with statistical significance determined based on the p-value (p) (Table 1).

Based on the results presented in Table 1, no statistically significant correlations were found between the level of self-assessed AI literacy and any of the listed benefits (all $p > 0.05$). It can therefore be concluded that students' perceptions of the benefits of genAI are independent of their perceived competence in using these technologies. In most cases, Spearman's coefficients were weak and negative, indicating that a higher level of self-assessed AI literacy was not associated with higher ratings of these benefits.

Regardless of their level of self-assessed AI literacy, students gave the highest ratings to benefits related to efficiency and speed. In particular, time savings received notably high scores ($\bar{x}$ = 4.17–4.28), indicating widespread recognition of genAI as a tool for improving efficiency. The correlation with self-assessed AI literacy was not statistically significant (ρs = −0.042, p = 0.599). Ratings for faster data analysis ranged from $\bar{x}$ = 4.08–4.33, confirming that students perceive the greatest value of genAI in information processing. Students also assigned high ratings to easier access to information ($\bar{x}$ = 3.67–4.09), reflecting the role of genAI as an advanced information retrieval tool.

Cognitive and research-related benefits include support in conducting research, as well as easier and faster comprehension of study material. Although the correlation between research support and self-assessed AI literacy was not statistically significant, the p-value (0.056) was closest to the significance threshold (ρs = −0.152). This finding suggests a slight trend whereby students with lower self-assessed AI literacy may have emphasised this benefit somewhat more than those with the highest levels of literacy ($\bar{x}$ = 4.05 for "good" literacy compared with $\bar{x}$ = 3.81 for "very good" literacy). Ratings for easier and faster comprehension of study material were more stable ($\bar{x} \approx 3.80$), indicating that genAI is perceived as an important cognitive aid regardless of prior knowledge of the technology. An interesting pattern emerges regarding the adaptation of learning to individual needs, with higher ratings reported by students with lower self-assessed AI literacy. This may suggest that students who feel less proficient in using genAI perceive it as a valuable source of support for tailoring their study process to their individual needs. By contrast, more proficient users may approach these benefits more selectively and critically, as they may be more aware of the technology's limitations, particularly in academically demanding tasks. The lowest-rated benefits were motivation for learning and increased creativity. Mean values for these two items remained low across all groups, suggesting that students generally do not perceive genAI as significantly enhancing intrinsic motivation for learning or contributing substantially to the development of originality, but rather as a functional tool for improving productivity.

3.4. Risks associated with the use of generative artificial intelligence and their association with AI literacy

As shown in Figure 4, students rated all challenges and risks relatively highly. They recognised that excessive use of genAI tools may weaken an individual's critical thinking skills. They were particularly aware of issues related to "hallucinations", namely the citation of sources that do not actually exist, and they also perceived risks associated with over-reliance on technology and inaccurate

Table 1

Mean ratings of perceived genAI benefits ($\bar{x}$) according to students' level of self-assessed AI literacy, and the analysis of Spearman's rank correlation coefficients (ρs) (n = 160)

Advantages of using genAI	AI literacy categories ($\bar{x}$)				Spearman's rank correlation coefficient	
	Very good	Good	Moderate	Poor	ρ_s	p
Easier access to information.	3.94	4.09	3.96	3.67	-0.096	0.229
Support with research.	3.81	4.05	3.83	3.83	-0.152	0.056
Faster data analysis.	4.31	4.15	4.08	4.33	-0.057	0.471
Easier and quicker understanding of course material.	3.75	3.99	3.85	3.83	-0.072	0.364
Ability to tailor learning to individual needs.	3.81	3.67	3.42	4.17	-0.115	0.147
Faster identification of sources.	3.38	3.79	3.83	4.00	0.055	0.487
Time-saving.	4.19	4.28	4.17	4.17	-0.042	0.599
Easier and quicker completion of tasks.	3.50	4.05	3.67	4.00	-0.094	0.235
Motivation for learning.	3.06	2.96	2.67	2.83	-0.122	0.124
Enhanced creativity.	2.81	2.49	2.19	3.17	-0.087	0.276

responses ($\bar{x}$ = 4.05), reflecting limited trust in the technical reliability of AI systems. Considerable concern was expressed regarding copyright and intellectual property issues (plagiarism and the inappropriate use of others' ideas), as well as ethical issues and privacy threats. Environmental impacts appear to be an area about which students are either less informed or to which they attach less immediate importance. Although bias and stereotypes are frequent topics of discussion among experts, students rated this risk as the least critical compared with the others, albeit still with a relatively high mean score. For all statements, the mean score ($\bar{x}$) exceeded 3.5, indicating that respondents generally agreed that all listed risks exist. The standard deviation (SD) values were fairly consistent (0.8–1.0), suggesting that students' opinions were relatively similar, with no extreme variability.

These results are consistent with findings from previous studies, which identify "hallucinations", unreliable sources, plagiarism, bias, privacy issues, and over-reliance on technology as key risks associated with genAI (Licardo, Puncer & Todorović, 2025; Mlakar, 2025; Molek, 2023). This strong agreement regarding the potential decline in independent critical thinking is further supported by authors who emphasise that the use of genAI should be pedagogically guided and critically integrated rather than left solely to students' individual discretion (Cvajdik, 2025; Jarc, 2026).

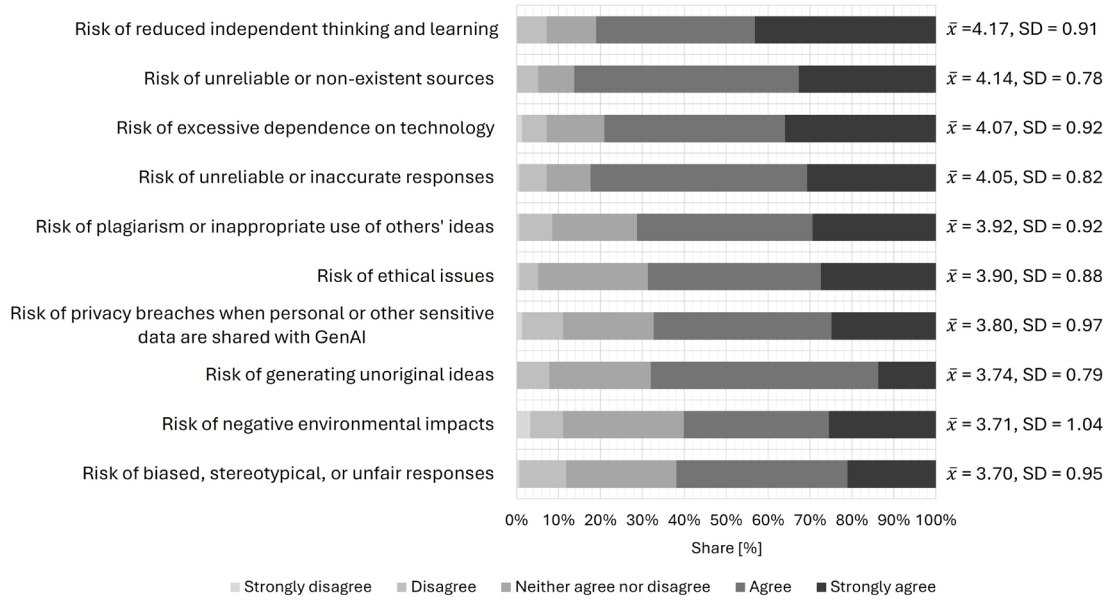
Students' perceptions of the risks associated with the use of genAI were analysed in relation to varying levels of self-assessed AI literacy. Table 2 presents the results of a comparative analysis of self-assessed AI literacy levels and perceived risks associated with genAI use.
The data include mean scores for risks associated with genAI use, categorised according to students' AI literacy levels, together with Spearman's rank correlation coefficients.

The results in Table 2 indicate a generally high level of awareness regarding potential hazards; however, no statistically significant differences were observed between the AI literacy categories.

Perception of technical and academic risks. Students highlighted the unreliability, or even the non-existence, of sources cited by genAI as one of the most prominent risks. This item achieved the highest scores among students with very good self-assessed literacy ($\bar{x}$ = 4.40), suggesting that those with greater knowledge are particularly aware of the phenomenon of so-called AI "hallucinations". The risk of unreliable or inaccurate answers was rated similarly highly, with mean scores ($\bar{x}$) of 4.00 or above across all AI literacy categories.

Academic integrity. Students expressed concern about a decline in independent thinking and learning. Interestingly, this concern was most pronounced among students with a medium level of literacy ($\bar{x}$ = 4.31), whereas students with poor self-assessed AI literacy rated this risk slightly lower ($\bar{x}$ = 3.60).
The issue of plagiarism and the inappropriate use of others' ideas remains constant across all groups, with the highest mean score observed among students with poor self-assessed AI literacy ($\bar{x}$ = 4.20).

Ethical, privacy, and social risks. In the field of ethics, students with poor literacy stand out, having rated ethical issues with an exceptionally high mean score ($\bar{x}$ = 4.80). This may indicate a certain level of mistrust



» **Figure 4:** *Perceived challenges and risks associated with the use of genAI (n = 160)*

Table 2

Mean risk ratings associated with the use of genAI by students' level of self-assessed AI literacy and analysis of Spearman's rank correlation coefficients (n = 153)

Advantages of using genAI	AI literacy categories (x^-)				Spearman's rank correlation coefficient	
	Very good	Good	Moderate	Poor	ρ_s	p
Risk of generating unoriginal ideas.	3.53	3.75	3.80	3.60	-0.062	0.450
Risk of unreliable or non-existent sources.	4.40	4.11	4.12	4.00	0.050	0.541
Risk of unreliable or inaccurate responses.	4.20	4.00	4.10	4.00	-0.013	0.875
Risk of reduced independent thinking and learning.	3.93	4.17	4.31	3.60	0.071	0.380
Risk of plagiarism or inappropriate use of others' ideas.	3.93	3.93	3.86	4.20	-0.044	0.588
Risk of biased, stereotypical, or unfair responses.	3.93	3.67	3.69	3.80	-0.052	0.521
Risk of privacy breaches when personal or other sensitive data are shared with genAI.	3.80	3.75	3.84	4.20	0.037	0.649
Risk of excessive dependence on technology.	3.60	4.06	4.18	4.40	0.103	0.206
Risk of ethical issues.	4.13	3.92	3.71	4.80	-0.073	0.369
Risk of negative environmental impacts.	3.60	3.77	3.67	3.40	-0.011	0.897

towards technology due to a lack of understanding of how it operates. The group with poor literacy is also the most concerned about over-reliance on technology (x^- = 4.40) and threats to privacy (x^- = 4.20), which could be a consequence of limited technical understanding of how data are actually processed and protected.

On the other hand, environmental issues received, on average, the lowest scores among all risks (x^- = 3.40–3.77), suggesting that students currently regard the impact of genAI on the environment as less critical than direct academic or ethical challenges.

Statistical analysis of the correlation between literacy and risk perception. Statistical analysis using Spearman's correlation coefficients (ρs) showed no statistically significant correlations between students' self-assessed AI literacy and their perception of risks. All p-values were substantially higher than the significance threshold ($p > 0.05$). The lowest p-value was associated with the issue of over-reliance on technology ($p = 0.206$), yet it still did not reach statistical significance. It can therefore be concluded that the level of knowledge regarding genAI does not significantly influence how hazardous students perceive the technology to be. Awareness of risks such as information inaccuracy, lack of originality, and ethical dilemmas is evident among all students, regardless of how proficient they feel in using these tools.

3.5. Ethical and moral concerns regarding the use of genAI

A majority of students (56.6%) reported having no ethical or moral concerns when using genAI, while 43.4% reported such concerns. The most frequently cited concerns were copyright infringements involving the use of others' work, environmental impacts, the erosion of creativity and critical thinking, data privacy, plagiarism, and issues concerning the credibility of information. Concerns regarding the use of genAI are discussed by numerous authors (Cvajdik, 2025; Licardo, Puncer & Todorović, 2025; Molek, 2023), who highlight authorship, plagiarism, privacy, bias, information credibility, and the need for clear ethical guidelines. Students' responses further confirm that these concerns relate not only to academic integrity but also to the broader social and environmental consequences of AI use (Jarc, 2026; Mlakar, 2025).

3.6. The future of genAI integration in the study process

An analysis of students' open-ended responses reveals a complex and ambivalent outlook on the future of genAI in the academic environment.

- Inevitability of integration and radical systemic change. The vast majority of students recognise genAI as a technology that has become a constant in the academic environment. They predict that its use will only intensify, necessitating a radical adaptation of the educational system. They place particular emphasis on the need to update curricula, assessment methods, and approaches to coursework, as traditional methods are losing their original value due to AI capabilities.
- The binary nature of use. Students present both constructive and destructive possibilities for genAI use. Constructive use involves genAI as a "tool" or "assistant" for faster resource searching, explaining complex subjects, aiding

idea generation, translation, and summarising. Destructive use frames it as a means of ”easier work”, leading to the passive transcription of answers without actual understanding (“laziness”, “solving tasks instead of the student”).
- Cognitive and pedagogical risks. In their responses, students highlight the atrophy of critical thinking (less independent thought and analysis), a reduction in creativity (generated content is accepted as fact, which stifles personal innovation), and increasingly superficial knowledge (the fear that future generations will graduate with significantly less actual knowledge and critical distance from information).
- Ethical responsibility and regulation. Students emphasise that responsibility for a secure future lies not only with the technology itself but also with users and institutions. They highlight the need for regulations on ethical use (defining where use is permitted and where it is not) and for education focused on critical application (how to verify and evaluate genAI outputs instead of relying on them blindly).

Students perceive genAI as a "double-edged sword". While they welcome increased productivity and greater access to information, they recognise a clear risk of intellectual regression. Consistent with these student views, findings from other research (Cvajdik, 2025; Molek, 2023; UNESCO, 2025) emphasise that genAI will become a permanent part of the educational landscape. However, its value will depend on thoughtful integration, clear rules of use, transparency, the development of critical literacy, and the responsible application of AI in higher education.

4. Conclusion

The study confirmed H1, which posits that students with higher levels of self-assessed AI literacy integrate genAI technology into their study processes more frequently. The results of Spearman’s correlation analysis revealed a statistically significant, moderately positive correlation between self-assessed knowledge of genAI and frequency of use ($\rho s = 0.409$, $p < 0.001$). This suggests that greater familiarity with the technology reduces uncertainty and enables students to identify opportunities for its application more readily.

Hypothesis H2, which proposed that a higher level of AI literacy leads to a stronger perception of the benefits and risks associated with genAI use, was rejected. Statistical analysis showed no significant correlation between the level of AI literacy and the perception of benefits such as time savings or faster data analysis ($p > 0.05$). Similarly, regarding risks, AI literacy does not significantly influence how hazardous students perceive the technology to be. Students perceive the benefits and dangers of genAI independently of how competent they feel in using it.

Finally, the third hypothesis (H3), which proposed that students with higher levels of AI literacy would demonstrate better self-control and more deliberate use of AI tools, was also rejected. The research found no statistically significant correlation between self-assessed AI literacy and self-control during use ($\rho s = 0.092$, $p = 0.245$). This indicates that technical knowledge and AI literacy alone do not necessarily guarantee more controlled or self-regulated use; self-control is likely to be more closely related to an individual’s personality traits and work habits.

GenAI in the academic environment represents a "double-edged sword". The vast majority of students recognise it as an inevitable, permanent tool that will require radical adaptation of the educational system, assessment methods and curricula. Although the technology significantly enhances productivity and access to information, it poses a serious risk of intellectual regression and the atrophy of critical judgement if used uncritically.

The results indicate that educational institutions must not assume that students with superior technical knowledge (higher AI literacy) will automatically be more critical or less concerned about risks. As risks are rated highly across all groups, it is essential to integrate critical judgement and the ethical use of genAI into study programmes for all students, regardless of their prior knowledge. In the specific field of graphic design, while AI automates repetitive tasks and expands creative possibilities, it cannot fully replace human empathy, an authorial approach, or creative depth.

The future of education will therefore be based on a hybrid approach in which genAI serves as a supplement to support the development of higher-order cognitive abilities, while human oversight remains crucial for ensuring academic integrity and upholding ethical standards. Only through thoughtful integration and the promotion of critical literacy can genAI genuinely contribute to improving learning without compromising long-term educational goal.

5. Acknowledgements

The project is supported by the Digital UL Centre as part of the B.I.3 measure (Development of innovative and modern approaches, methods, and forms of work in education), funded under the Development Pillar of Funding at the University of Ljubljana. The measure aims to align education with the needs of the digital age and prepare students for future challenges by providing practical, flexible, and personalised learning experiences.

6. References

Adil, J. J. G. (2025) 'AI in Education: A Systematic Literature Review of Emerging Trends, Benefits, and Challenges', *Seminars in Medical Writing and Education*, 4, 795. DOI: 10.56294/mw2025795

Alsswey, A. (2025) 'Examining students' perspectives on the use of artificial intelligence tools in higher education: A case study on AI tools of graphic design', *Acta Psychologica*, 258, 105190. DOI: 10.1016/j.actpsy.2025.105190

Cvajdik, M. (2025) Kako umetna inteligenca preoblikuje študij in poučevanje v letu 2025. Available from: https://www.fakulteta.doba.si/doba-znanja/kako-umetna-inteligenca-preoblikuje-studij-in-poucevanje-v-letu-2025 [Accessed 3 March 2026].

Dong, L., Tang, X. and Wang, X. (2025) 'Examining the effect of artificial intelligence in relation to students' academic achievement: A meta-analysis', *Computers and Education: Artificial Intelligence*, 8, 100400. DOI: 10.1016/j.caeai.2025.100400

Fleischmann, K. (2024) 'Generative Artificial Intelligence in Graphic Design Education: A Student Perspective', *Canadian Journal of Learning and Technology*, 50(1), pp. 1–17. DOI: 10.21432/cjlt28618

Jaca, C. A. L. (2024) 'Artificial Intelligence in Education: A Threat or a Tool for Teaching'. In: *The Asian Conference on Education & International Development 2024 Official Conference Proceedings, 25–29 March 2024, Tokyo, Japan. Tokyo, IAFOR*, pp. 1007–1017. DOI: 10.22492/issn.2189-101X.2024.81

Jarc, K. (2026) Je UI le klik do znanja? Umetna inteligenca v študiju. Available from: https://www.dostop.si/je-ui-le-klik-do-znanja-umetna-inteligenca-v-studiju/ [Accessed 9 March 2026].

Laugwitz, B., Held, T. and Schrepp, M. (2008) 'Construction and Evaluation of a User Experience Questionnaire'. In: Holzinger, A. (ed.) HCI and Usability for Education and Work. USAB 2008, 20–21 November 2008, Graz, Austria. Berlin/Heidelberg, Springer, pp. 63–76. DOI: 10.1007/978-3-540-89350-9_6

Licardo, M., Puncer, M. and Todorović, T. (2025) 'Izbrani temeljni pojmi, vezani na etično rabo generativne umetne inteligence v izobraževanju'. In: Flogie, A. and Čotar Konrad, S. (eds.) *Izobraževanje v dobi generativne umetne inteligence: mednarodne smernice in raziskave*. Koper, Založba Univerze na Primorskem, pp. 319–342. DOI: 10.26493/978-961-293-431-6.17

Mlakar, T. (2025) Dan varne rabe interneta. Available from: https://www.stat.si/StatWeb/news/Index/13423 [Accessed 9 March 2026].

Molek, N. (2023) Umetna inteligenca v izobraževanju in raziskovanju: Izzivi, etična vprašanja in smernice. Available from: https://www.fos-unm.si/media/pdf/doktorski_kolokviji/Gradivo/Eticne_smernice_Umetna_inteligenca_v_izobrazevanju_in_raziskovanju_v1.pdf [Accessed 15 March 2026]

Pitts, G., Marcus, V. M. and Motamedi, S. (2025) 'Student Perspectives on the Benefits and Risks of AI in Education'. In: *2025 ASEE Annual Conference & Exposition*, 22–25 June 2025, Montreal, Quebec, Canada. DOI: 10.18260/1-2--57693

Silva, P. (2015) 'Davis' Technology Acceptance Model (TAM) (1989)'. In: Al-Suqri, M. N. and Al-Aufi, A. S. (eds.) *Information Seeking Behavior and Technology Adoption: Theories and Trends*. Hershey, PA, IGI Global Scientific Publishing, pp. 205–219. DOI: 10.4018/978-1-4666-8156-9.ch013

Stephenson, R. and Armstrong, C. (2026) Student Generative Artificial Intelligence Survey 2026. HEPI Report 199. Higher Education Policy Institute. Available from: https://www.hepi.ac.uk/reports/student-generative-ai-survey-2026/

Sun, P., Li, J., Chen, X., Cui, M. and Yan, L. (2026) 'The impact of maladaptive perfectionism on AI dependence among college students: The mediating role of self-control and the moderating role of academic engagement', *Acta Psychologica*, 263, 106294. DOI: 10.1016/j.actpsy.2026.106294

Študentska organizacija Slovenije (ŠOS). (2025) Resolucija o umetni inteligenci v visokem šolstvu. Available from: https://www.studentska-org.si/wp-content/uploads/2026/01/2_RESOLUCIJA-O-UMETNI-INTELIGENCI-V-VISOKEM-SOLSTVU-1.pdf [Accessed 9 March 2026].

Tan, X., Cheng, G. and Ho Ling, M. (2025) 'Artificial intelligence in teaching and teacher professional development: A systematic review', *Computers and Education*: Artificial Intelligence, 8, 100355. DOI: 10.1016/j.caeai.2024.100355

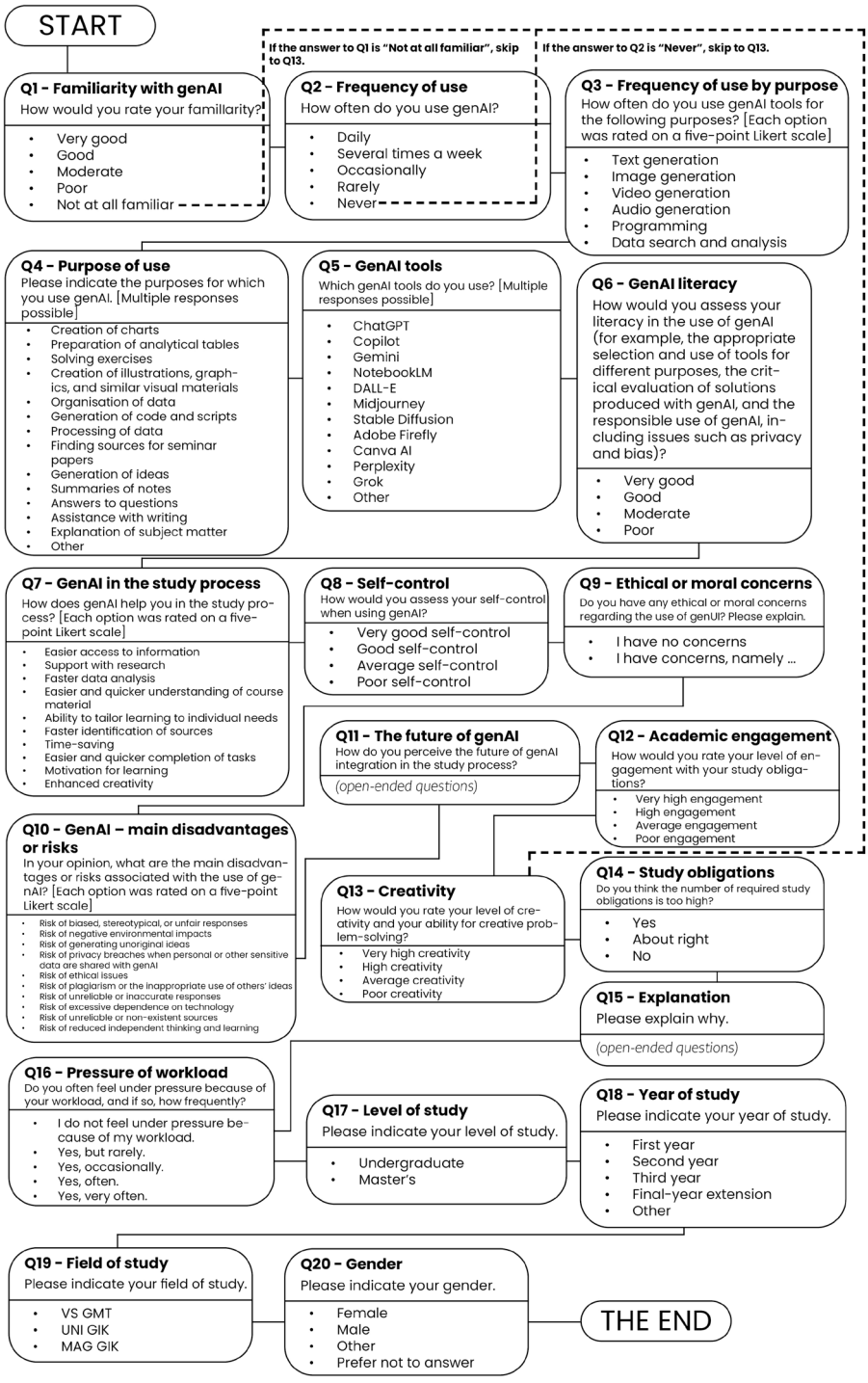
UNESCO. (2025) Artificial intelligence in education. Available from: https://www.unesco.org/en/digital-education/artificial-intelligence [Accessed 1 March 2026].

Venkatesh, V., Thong, J. Y. L. and Xu, X. (2012) 'Consumer Acceptance and Use of Information Technology: Extending the Unified Theory of Acceptance and Use of Technology', *MIS Quarterly*, 36(1), pp. 157–178. DOI: 10.2307/41410412

Xiaoyu, W., Zainuddin, Z. and Leng, C. H. (2025) 'Generative artificial intelligence in pedagogical practices: a systematic review of empirical studies (2022–2024)', *Cogent Education*, 12(1), 2485499. DOI: 10.1080/2331186X.2025.2485499

Zhang, J., Jantakoon, T. and Laoha, R. (2025) 'Artificial intelligence in education: A meta-analysis of empirical studies', *Higher Education Studies*, 15(2), pp. 189–210. DOI: 10.5539/hes.v15n2p189

7. Appendix: Survey questionnaire flowchart



© 2026 Authors. Published by the University of Novi Sad, Faculty of Technical Sciences, Department of Graphic Engineering and Design. This article is an open access article distributed under the terms and conditions of the Creative Commons Attribution license 4.0 Serbia (https://creativecommons.org/licenses/by/4.0/deed.en).

https://doi.org/10.24867/GRID-2026-p85

Artificial Intelligence as a Learning Assistant: Design and Evaluation of the Asking Ai+ Platform for Graphic Engineering Education

ABSTRACT

The increasing use of artificial intelligence (AI) in graphic engineering, design and desktop publishing has created a need for educational environments that combine structured instructional materials with on-demand learner support. This paper presents the second development phase of the ASKING educational platform, referred to as ASKING AI+, in which a dedicated AI chatbot is integrated into the existing multimedia learning environment. The original ASKING platform provides practical lessons for Adobe, Affinity and Microsoft Office applications in text-and-image, video and AI-avatar formats. These instructional modalities have already been examined in two controlled student studies, providing an empirical basis for further platform development. The new ASKING Assistant is configured to answer domain-specific questions, explain practical procedures step by step, support troubleshooting and design decisions, and generate formative quizzes on request. The assistant prioritizes the platform knowledge base and is accessible from the platform homepage and from the end of each lesson, allowing learners to request help at the point of need. The paper describes the development rationale, chatbot configuration, website integration and the relationship between the new conversational layer and findings from the previous evaluations. A dedicated student evaluation of the chatbot-enhanced platform is planned as the next research stage, with particular emphasis on perceived additional learning support, usefulness of question answering and quizzes, clarity, learner control and objective learning outcomes.

Nemanja Kašiković [1]
Dragana Glušac [2]
Velibor Premčevski [2]
Aleksandar S. Anđelković [1]
Nemanja Tasić [1]

[1] University of Novi Sad, Faculty of Technical Sciences, Novi Sad, Serbia
[2] University of Novi Sad, Technical Faculty "Mihajlo Pupin", Zrenjanin, Serbia

KEY WORDS
Artificial intelligence, educational platform, AI chatbot, graphic engineering education, Desktop Publishing, formative assessment, multimedia learning

1. Introduction

Digital transformation has changed both professional workflows and the competencies expected from students in graphic engineering and design. Contemporary graphic technology education extends beyond traditional printing processes and increasingly includes cross-media production, software-intensive workflows, data processing and AI-supported design activities. Consequently, educational programmes need to combine disciplinary knowledge with practical digital skills and flexible learning resources that students can use while solving authentic tasks (Liang, Wang & Wang, 2024; Taneja, 2025). Experience from graphic engineering students also shows that digital environments can provide flexibility, but sustained attention, motivation and meaningful interaction remain important conditions for effective online learning (Tomić et al., 2022).

Generative AI and large language models have introduced a new form of educational interaction. In addition to generating content, conversational systems can

answer learner questions, provide explanations, support problem solving and act as virtual tutors. Reviews of ChatGPT and related large language models identify considerable potential for personalized guidance and immediate feedback, while also emphasizing risks associated with inaccurate information, overreliance, academic integrity and the need for human verification (Kasneci et al., 2023; Lo, 2023). More recent research on educational chatbots indicates that conversational support can contribute to self-regulated learning by helping learners identify resources, select strategies and monitor their progress, although the effects are not uniformly positive across all contexts (Guan et al., 2025).

The introduction of more advanced technology does not, however, guarantee superior learning. The Cognitive Theory of Multimedia Learning emphasizes limited processing capacity, active processing and the importance of instructional design in coordinating verbal and visual information (Mayer, 2024). Similarly, empirical studies of video tutorials indicate that learning effects depend on design, task characteristics and cognitive load rather than on the medium alone (Fan, Bower & Siemon, 2024). This consideration is especially relevant in software learning, where novices need to follow procedures, locate interface elements and immediately apply a sequence of operations in a real working environment.

The ASKING platform was developed in this context as a practical educational environment for learning DTP-related software and the application of AI in contemporary graphic workflows. Its first phase focused on the creation of structured lessons in several presentation modalities. Following the initial development, two student experiments evaluated the underlying instructional formats in Microsoft Excel and Adobe Illustrator (Kašiković et al., 2026a; Zeljković et al., 2026). The results did not support a simple assumption that a more technologically sophisticated format is automatically more effective. Instead, they emphasized structure, pacing, signaling and learner control. These findings directly motivated the second development phase: rather than replacing existing materials, ASKING AI+ adds an optional conversational assistant that learners can activate when they need clarification, troubleshooting or a knowledge check.

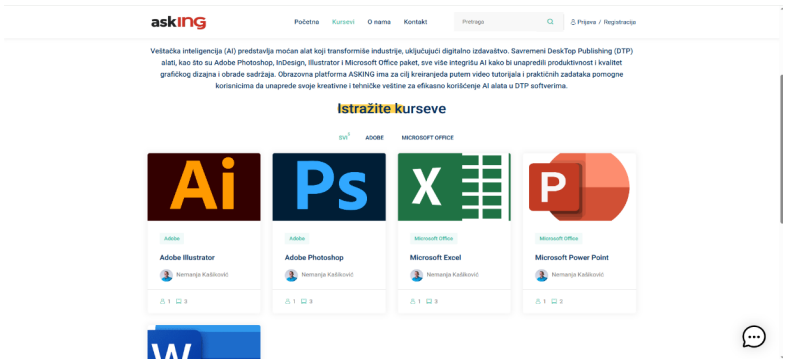
The aim of this paper is therefore to present the design and integration of the ASKING AI+ conversational learning layer, relate its design to the evidence obtained in previous ASKING evaluations, and define a research framework for its dedicated student evaluation. The contribution is not a claim that the new chatbot has already improved learning outcomes. Rather, the paper documents an evidence-informed transition from multimodal content delivery toward learner-initiated, context-sensitive AI support within a specialized graphic engineering education platform.

2. Development and previous evaluation of asking

2.1. Original platform and multimodal lesson structure

The original ASKING platform was designed around practical, modular lessons for nine software applications used in graphic preparation, design and office workflows: Adobe Photoshop, Illustrator and InDesign; Affinity Photo, Designer and Publisher; and Microsoft Word, Excel and PowerPoint. The first development phase organized lesson content in three complementary formats: (1) step-by-step text-and-image instructions, (2) screen-recorded video tutorials with narration, and (3) AI-avatar video tutorials created using Studio D-ID. The intention was to allow the same procedural content to be approached through different media while retaining a practical orientation toward task completion (Kašiković et al., 2025).

Figure 1 presents the course overview from the first phase of the ASKING platform. The interface was developed to make individual software courses directly accessible and to support repeated use of lesson materials outside a conventional classroom setting.



» **Figure 1:** *ASKING platform course overview developed in Phase 1*

Table 1
Previous evaluations of ASKING instructional modalities

Study	Learning task	Conditions and sample	Main result	Design implication for ASKING AI+
Kašiković et al. (2026)	Microsoft Excel procedural functions	Static text-and-image; human-narrated video; AI-avatar video; N = 65	No statistically significant differences in knowledge acquisition, practical task performance or seven-day retention. Some participants perceived the avatar as distracting.	Technological complexity alone should not drive the platform. Keep support optional and focused on the learner's immediate need.
Zeljković et al. (2026)	Introductory Adobe Illustrator / business-card task	Text-and-image instruction; AI-avatar video; N = 81	Text-and-image material produced higher immediate knowledge scores; no significant group differences in practical performance or delayed-test scores.	Preserve learner control, pacing and clear visual/procedural structure; use AI as support rather than compulsory delivery.

2.2. Evidence from student evaluations

The first-stage instructional materials were subsequently evaluated in two controlled studies. The studies addressed different software environments and different comparisons, but together they provide a useful empirical basis for the next platform iteration. Their main characteristics and design implications are summarized in Table 1.

In the Excel study, 65 participants were analyzed across three conditions: static materials, video with human narration and video with an AI-generated avatar. No statistically significant differences were detected in immediate learning, practical performance or retention, and the qualitative responses suggested that the AI avatar was useful for some learners but visually distracting for others (Kašiković et al., 2026a). In the Adobe Illustrator study, 81 first-year students were randomly assigned to text-and-image or AI-avatar video instruction. The text-and-image group performed better on the immediate post-test, whereas practical-task and delayed-retention outcomes did not differ significantly between groups (Zeljković et al., 2026).

These results are important for the design of ASKING AI+ because they shift the development question from "Which medium is the most advanced?" to "When and how should technology support the learner?" The new phase therefore retains the existing lesson formats and adds a learner-controlled assistant that can be called only when needed. This approach is consistent with multimedia-learning principles and with evidence that learner control and well-structured content can be more important than the mere presence of visually rich or AI-generated elements (Mayer, 2024; AlShaikh, Al-Malki & Almasre, 2024).

3. Design and integration of the asking ai+ assistant

3.1. Design requirements and pedagogical role

The ASKING Assistant was configured as a specialized educational chatbot rather than as a general-purpose conversational system. Its primary role is to support practical learning in the same nine software applications covered by the ASKING platform and to connect explanations with the workflows, terminology and tasks used in the educational materials. The assistant is intended to complement, not replace, the written and video lessons.

The main design requirements were defined as follows:

- provide clear, professional and immediately applicable explanations for Adobe, Affinity and Microsoft Office workflows;
- explain the logic and order of a procedure rather than giving only a final answer;
- prioritize the materials uploaded to the ASKING knowledge base before using general knowledge;
- support troubleshooting by identifying likely causes and proposing solutions from simpler to more complex;
- support design and prepress decisions related to composition, typography, readability, color, document dimensions, resolution, bleed, fonts and PDF export;
- generate formative quizzes and mini-checks when the learner requests them; and
- state uncertainty instead of inventing software commands, and use current web information only when version-dependent or time-sensitive information is required.

These constraints are important in software education because a plausible but incorrect menu name, command or sequence can immediately prevent task completion. The configuration therefore explicitly instructs the assistant not to invent tools or interface options and to distinguish stable domain knowledge from information that may change between software versions. This design also reflects the broader recommendation that educational use of large language models requires critical verification and explicit attention to system limitations (Kasneci et al., 2023; Lo, 2023).

3.2. Knowledge-grounded question answering and practical support

The assistant uses the uploaded ASKING learning materials as its first source of domain context. If the required answer is not covered by the knowledge base, it may rely on general knowledge, while web search is reserved for information that can change over time, such as software versions, new AI functions, licensing conditions or current capabilities. In practical questions, the preferred response structure contains the software name, the user's goal, ordered steps, relevant notes and a short self-check. This organization is intended to make the answer directly transferable to work in the target application.

The conversational layer also broadens the function of the platform beyond fixed lesson sequences. A learner can request clarification of a term, ask why a particular step is necessary, compare two software tools, obtain feedback on a workflow, describe an error or ask how an AI function can be incorporated into a DTP process. When an error cannot be diagnosed from the description alone, the assistant is instructed to ask for the software version, intended action and observed outcome, and may suggest that a screenshot be provided. This creates a form of just-in-time learning support that was not available in the first platform phase.

3.3. Formative quizzes and knowledge checks

An additional function is on-demand quiz generation. The chatbot can create a knowledge check for a selected program, topic and level (beginner, intermediate or advanced). If the learner does not define the topic or difficulty, the assistant requests the missing information. Questions can be multiple choice, true/false, short answer, practical scenarios or questions concerning the correct order of procedural steps. The default interaction presents one question at a time, waits for the learner's answer, provides immediate corrective feedback and explanation, and displays a final score with a recommendation on what should be reviewed.

This function is deliberately described as formative and learner-initiated rather than as a fully adaptive assessment engine. The current implementation can tailor the topic and difficulty and can respond to the learner's answers, but it does not yet implement a validated algorithm that automatically models long-term learner performance or dynamically changes the curriculum. Such analytics-based adaptation remains a possible later development. This distinction is important because the pedagogical value of a chatbot should be evaluated on implemented functions rather than on assumed capabilities.

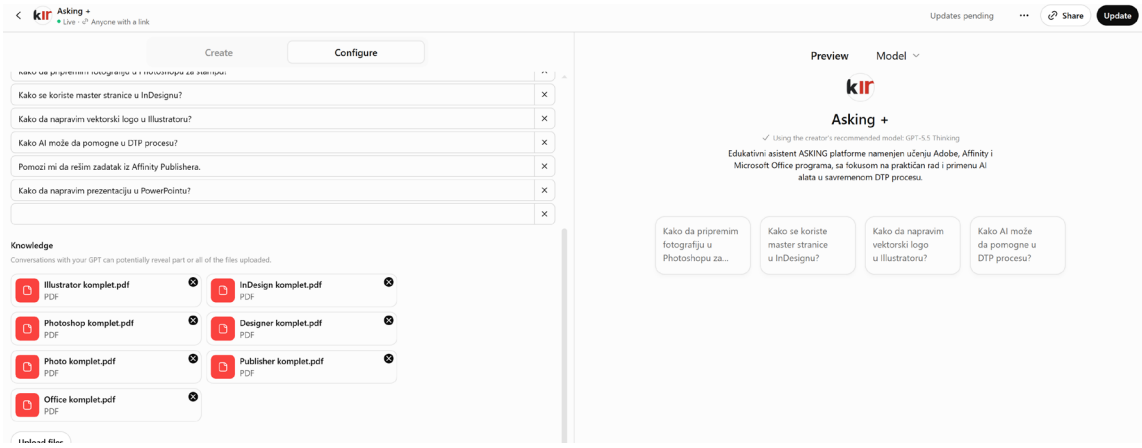
3.4. Website integration and two-phase platform structure

The chatbot was integrated into the ASKING learning workflow at several access points. A direct link to the ASKING GPT Bot was added to the platform homepage. The same access button was also placed at the end of each lesson, enabling students to move from a completed lesson directly to questions, clarification or a quiz without searching for a separate support service. The platform-side integration was configured to connect the educational website with the dedicated

Table 2

ASKING AI+ integration points and intended educational functions

Integration point	Implemented function	Educational purpose
Platform homepage	Direct link to the ASKING Assistant	Make AI support visible and available independently of a specific lesson.
End of each lesson	Repeated access button to the same assistant	Enable immediate questions, troubleshooting or self-check after learning content.
ASKING GPT configuration	Knowledge base, domain instructions, practical response rules and quiz behavior	Keep responses aligned with platform content and DTP learning goals
"About us" page	Project divided into Phase 1 and Phase 2	Make the development trajectory and the new AI-supported layer transparent to users.



» **Figure 2:** *ASKING Assistant configuration with domain knowledge resources and conversation starters*

ASKING GPT Bot, while the “About us” page was reorganized to present the project as two development phases: Phase 1, focused on multimodal lesson creation and validation, and Phase 2, focused on conversational AI support and formative knowledge checking. The public assistant can be accessed at: https://chatgpt.com/g/g-6a43cd1b6c48819198c96ca3e92b9169-asking.

Figure 2 illustrates the configuration environment of the ASKING Assistant, including the uploaded domain knowledge resources and predefined conversation starters. The configuration demonstrates that the chatbot is organized around the same software families as the platform rather than around unrestricted general conversation.

4. Implemented functionality and design rationale

The main development result of Phase 2 is an operational conversational support layer added to a platform whose instructional materials have already undergone empirical evaluation. The relationship between the two phases is therefore cumulative: Phase 1 provides the learning content and evidence concerning presentation modalities, while Phase 2 introduces an interaction mechanism through which the learner can request additional explanation, diagnosis or assessment at a self-selected moment.

This distinction is pedagogically relevant. The AI-avatar videos used in the earlier experiments were pre-authored instructional presentations: the avatar delivered a fixed narration and did not answer questions or adapt its explanation during the experiment. By contrast, ASKING AI+ is learner initiated. A student who understands a lesson does not need to interact with the chatbot, while a student who encounters a problem can request a shorter explanation, a sequence of steps, a comparison, an example or a quiz. Thus, the chatbot is designed to add control rather than another compulsory stream of information. This responds directly to the previous finding that pacing, clear visual signaling and learner control matter in introductory software learning (Zeljković et al., 2026).

The quiz function introduces a second change: the platform can now move from content presentation to immediate formative interaction. Educational chatbots have been associated with support for self-regulated learning processes, particularly resource identification, strategy enactment and monitoring of understanding (Guan et al., 2025). In ASKING AI+, a quiz can be requested immediately after a lesson and can therefore serve as a lightweight self-check before the learner moves to the next task. The assistant’s feedback is intended to explain why an answer is correct or incorrect rather than simply report a score.

The knowledge-priority rule also addresses a central limitation of generative AI in education. General-purpose language models can produce fluent answers that are incorrect or poorly matched to a specific course. By prioritizing uploaded ASKING materials and by instructing the assistant not to invent software commands, the design attempts to narrow the response space and maintain alignment with the course. This does not eliminate the need for verification, particularly for version-dependent software information, but it provides a clearer instructional boundary than unrestricted chatbot use.

The approach is also consistent with current directions in graphic design education. Project-based and authentic learning approaches emphasize practical application and structured guidance (Taneja, 2025), while graphic technology education increasingly requires competence across conventional production, digital media and AI-supported workflows (Liang, Wang & Wang, 2024). AI tools in graphic design can be valuable as supportive media without necessarily outperforming

conventional methods in every task (Ardhianto & Aquirel, 2026). In this sense, ASKING AI+ treats AI as an additional learning instrument rather than as a substitute for software knowledge or instructor expertise.

5. Proposed student evaluation of the chatbot-enhanced platform

The next research stage will evaluate the chatbot itself. This is necessary because the two completed studies examined the instructional modalities of the original platform, not the effect of real-time conversational assistance. The primary future research question is whether students perceive that the ASKING Assistant provides additional help beyond the existing lesson materials, especially because it can answer questions at the point of difficulty and generate quizzes on request.

The planned evaluation will focus on the following research questions:

- RQ1: Do students perceive the chatbot as providing additional support for understanding and completing ASKING lessons?
- RQ2: How useful, clear and actionable are the chatbot's answers to software and DTP-related questions?
- RQ3: Do students consider the on-demand quiz function useful for checking knowledge and identifying topics that require revision?
- RQ4: Does chatbot access affect learner confidence, perceived control, engagement and the need to search for external explanations?
- RQ5: In a controlled extension of the study, do subjective benefits correspond to measurable differences in immediate knowledge, practical performance or retention?

A first evaluation stage can use a post-use questionnaire after students complete a defined set of ASKING lessons with chatbot access. A five-point Likert scale would allow direct comparison with the subjective dimensions already used in previous ASKING research, while open-ended questions would capture examples of useful answers, unclear responses, unsuccessful interactions and suggestions for improvement. The questionnaire should specifically separate the usefulness of question answering from the usefulness of quizzes, because these functions support different learning processes.

A second, controlled stage can compare students using the standard ASKING lesson environment with students using the same lessons plus ASKING AI+. To maintain comparability with the previous studies, the experiment can include a pre-test, immediate post-test, practical task and delayed retention test. If interaction logs are technically available and collected with appropriate consent, they may be used only as supplementary evidence to examine the types of questions students ask and the frequency of quiz use. The central criterion should remain learning value rather than interaction volume.

The planned evaluation is particularly important because positive perception does not automatically

Table 3

Proposed dimensions for the ASKING AI+ student evaluation

Evaluation dimension	Example indicator	Proposed measure
Additional learning support	The chatbot helped me understand content that was unclear in the lesson.	Likert 1–5 + comment
Answer usefulness	The answers were relevant and could be applied directly in the software.	Likert 1–5
Clarity and procedure	The step-by-step explanations were easy to follow.	Likert 1–5
Quiz usefulness	The quiz helped me identify what I understood and what I should review.	Likert 1–5 + quiz usage
Learner control	I could obtain the amount and type of explanation I needed.	Likert 1–5
Trust and verification	I knew when an answer should be checked against the lesson or software version.	Likert 1–5 + comment
Learning outcomes (extended study)	Knowledge acquisition, practical application and retention.	Pre/post test, practical task, delayed test

imply improved performance. Both completed ASKING studies demonstrated that engagement with a technologically novel format and objective learning outcomes can diverge (Kašiković et al., 2026a; Zeljković et al., 2026). The future chatbot study should therefore report subjective evaluations clearly and, where possible, connect them with objective measures instead of treating satisfaction as evidence of effectiveness.

6. Discussion

ASKING AI+ represents a change in the role assigned to AI within the platform. In the first phase, AI was primarily used to produce instructional presentation through a generated avatar. In the second phase, AI becomes an interactive learning assistant. This change is not merely technical: it changes the timing and direction of interaction. The learner decides when support is needed, formulates the question and can request another explanation or a quiz. Such interaction has the potential to support self-regulation and reduce the gap between encountering a problem and receiving guidance, which is a central advantage of conversational systems in education (Guan et al., 2025).

At the same time, the previous ASKING findings argue against assuming that AI interaction will necessarily improve achievement. The Administrative Sciences study found equivalent objective outcomes across static, human-video and AI-avatar modalities, while the Applied Sciences study found an immediate-learning advantage for structured text-and-image material without a corresponding advantage in practical performance or retention (Kašiković et al., 2026a; Zeljković et al., 2026). The appropriate interpretation is therefore not that AI should be removed, but that it should be used where it provides a distinct pedagogical function. In ASKING AI+, that function is on-demand explanation, troubleshooting and formative dialogue.

This principle is consistent with the wider literature. Multimedia learning theory emphasizes the management of limited cognitive resources and the purposeful organization of words and visuals (Mayer, 2024). AI-assisted multimedia systems can be effective when their features are linked to clear instructional functions rather than added as decorative technological complexity (AlShaikh, Al-Malki & Almasre, 2024). Likewise, recent work in graphic design shows that AI tools can provide useful alternatives and references while not consistently producing superior results to conventional approaches (Ardhianto & Aquirel, 2026).

The specialized scope of ASKING AI+ is another important aspect. Generic AI tools can provide broad assistance, but the platform is intended for procedural learning in a defined domain. Graphic engineering education requires attention not only to software commands but also to design quality, prepress preparation, color, typography, file formats and production requirements. A domain-oriented assistant can connect these concepts with specific software tasks. Similar multimedia-supported approaches have also been proposed for process-oriented areas such as textile screen printing, suggesting that the underlying method could be extended to other technical subjects in graphic and textile engineering (Kašiković et al., 2026b).

The current development nevertheless has limitations. First, the dedicated chatbot has not yet been evaluated with students, so its effectiveness remains an empirical question. Second, responses generated by a large language model can vary, and the knowledge base must be maintained as software and platform content evolve. Third, access through a third-party conversational AI environment introduces dependency on changes in that service. Finally, academic integrity, copyright, privacy and the verification of generated information must remain explicit parts of student guidance. These limitations are not reasons to avoid the technology, but they define the conditions under which the next evaluation should be conducted.

7. Conclusions

This paper presented the second development phase of the ASKING educational platform for graphic engineering, design and DTP education. The original platform combined step-by-step written materials, conventional video tutorials and AI-avatar video lessons across Adobe, Affinity and Microsoft Office applications. Two subsequent student studies provided evidence that more technologically complex presentation formats do not automatically produce better learning outcomes and highlighted the importance of structure, pacing and learner control.

ASKING AI+ builds on that evidence by adding a dedicated conversational assistant instead of replacing the established lesson formats. The assistant is configured to prioritize ASKING knowledge materials, provide practical step-by-step explanations, support troubleshooting and design/prepress decisions, and generate formative quizzes on request. Access is integrated through the platform homepage and the end of individual lessons, while the project presentation has been reorganized into Phase 1 and Phase 2 to make the development path explicit.

The next stage is empirical evaluation of the chatbot-enhanced environment. Students will assess whether the assistant provides additional help in learning, whether its answers are useful and actionable, and whether the quiz function contributes to knowledge checking and revision. A subsequent controlled comparison can determine whether these perceived benefits are accompanied by measurable changes in knowledge

acquisition, practical task performance or retention. In this way, ASKING can continue to develop as an evidence-based educational environment in which AI is introduced according to demonstrated learning needs rather than technological novelty alone.

8. Acknowledgments

The initial development of the ASKING educational platform was supported by the Provincial Secretariat for Higher Education and Scientific Research, Autonomous Province of Vojvodina, Republic of Serbia, through the project “ASKING AI+- Intelligent Learning Platform with AI Chatbot Support and Adaptive Learnig” (No. 002341972 2026 09418 002 000 000 001 04 002).

9. References

AlShaikh, R., Al-Malki, N. and Almasre, M. (2024) 'The implementation of the cognitive theory of multimedia learning in the design and evaluation of an AI educational video assistant utilizing large language models', *Heliyon*, 10(3), e25361. DOI: 10.1016/j.heliyon.2024.e25361

Ardhianto, P. and Aquirel, T.F. (2026) 'Integrating AI image generation into the designer's creative process for mascot creation', *Journal of Graphic Engineering and Design*, 17(2), pp. 33–43. DOI: 10.24867/JGED-2026-2-033

Fan, E., Bower, M. and Siemon, J. (2024) 'Video tutorials in the traditional classroom: the effects on different types of cognitive load', *Technology, Knowledge and Learning*, 29(4), pp. 2017–2036. DOI: 10.1007/s10758-024-09754-1

Guan, R., Raković, M., Chen, G. and Gašević, D. (2025) 'How educational chatbots support self-regulated learning? A systematic review of the literature', *Education and Information Technologies*, 30(4), pp. 4493–4518. DOI: 10.1007/s10639-024-12881-y

Kašiković, N., Glušac, D., Premčevski, V., Anđelković, A. and Tasić, N. (2025) 'Using Studio D-ID (Creative Reality Studio) in educational platform Asking'. In: Rakić, S., Medić, N. and Popovic, L. (eds.) *2nd International Conference on Trends and Challenges in Digital Education (DETC 2025): Book of Abstracts, 7–9 November 2025, Novi Sad, Serbia*. Novi Sad: University of Novi Sad, Faculty of Technical Sciences, p. 15. DOI: 10.5281/zenodo.17478797

Kašiković, N., Dedijer, S., Zeljković, Ž., Glušac, D., Premčevski, V., Anđelković, A.S. and Tasić, N. (2026a) 'Evaluating the effectiveness of AI-supported digital training: implications for organizational learning and decision-making', *Administrative Sciences*, 16(6), 246. DOI: 10.3390/admsci16060246

Kašiković, N., Dedijer, S., Vladić, G., Maričić, K. and Zeljković, Ž. (2026b) 'Enhancing textile screen printing education through multimedia learning approaches'. In: *Proceedings of the 9th International Scientific Conference Contemporary Trends and Innovations in the Textile Industry, CT&ITI 2026, 17–18 September 2026, Belgrade, Serbia*. Belgrade: Union of Textile Engineers and Technicians of Serbia, pp. 44–54. DOI: 10.5937/ct_iti26044k

Kasneci, E., Seßler, K., Küchemann, S., Bannert, M., Dementieva, D., Fischer, F., Gasser, U., Groh, G., Günnemann, S., Hüllermeier, E., Krusche, S., Kutyniok, G., Michaeli, T., Nerdel, C., Pfeffer, J., Poquet, O., Sailer, M., Schmidt, A., Seidel, T., Stadler, M., Weller, J., Kuhn, J. and Kasneci, G. (2023) 'ChatGPT for good? On opportunities and challenges of large language models for education', *Learning and Individual Differences*, 103, 102274. DOI: 10.1016/j.lindif.2023.102274

Liang, J., Wang, H. and Wang, X. (2024) 'Modern engineering education in graphic technology at universities'. In: Pál, M. (ed.) *Proceedings - 12th International Symposium on Graphic Engineering and Design, GRID 2024, 14–16 November 2024, Novi Sad, Serbia.* Novi Sad: University of Novi Sad, Faculty of Technical Sciences, Department of Graphic Engineering and Design, pp. 759–764. DOI: 10.24867/GRID-2024-p81

Lo, C.K. (2023) 'What is the impact of ChatGPT on education? A rapid review of the literature', *Education Sciences*, 13(4), 410. DOI: 10.3390/educsci13040410

Mayer, R.E. (2024) 'The past, present, and future of the cognitive theory of multimedia learning', *Educational Psychology Review*, 36(1), 8. DOI: 10.1007/s10648-023-09842-1

Taneja, K. (2025) 'A framework of project-based learning (PBL) pedagogy for graphic design education', *Journal of Graphic Engineering and Design*, 16(4), pp. 25–36. DOI: 10.24867/JGED-2025-4-025

Tomić, I., Pinćjer, I., Dedijer, S. and Adamović, S. (2022) 'Online learning during COVID-19 pandemic as perceived by the students of Graphic engineering and design', *Journal of Graphic Engineering and Design*, 13(2), pp. 15–20. DOI: 10.24867/JGED-2022-2-015

Zeljković, Ž., Kašiković, N., Stefanović, M., Janković Žugić, A., Dedijer, S., Petrović, S. and Jurič, I. (2026) 'Text-and-image materials versus an AI-avatar video for introductory Adobe Illustrator learning: a randomized two-group study', *Applied Sciences*, 16(15), 7735. DOI: 10.3390/app16157735

© 2026 Authors. Published by the University of Novi Sad, Faculty of Technical Sciences, Department of Graphic Engineering and Design. This article is an open access article distributed under the terms and conditions of the Creative Commons Attribution license 4.0 Serbia (http://creativecommons.org/licenses/by/4.0/rs/).

Professional Paper https://doi.org/10.24867/GRID-2026-p86

Industrial Heritage as a Learning Environment: An Exploratory Case Study in Graphic Technologies and Design Education

ABSTRACT

This study explores how industrial graphic heritage can contribute to the contemporary teaching of graphic technologies and design through Project-Based Learning (PBL) and university-industry collaboration. It analyses, as an exploratory case study, the project «Celebrating 140 Years of Tipografia Lousanense», developed by the Polytechnic University of Tomar (Portugal) in collaboration with Gráfica Lousanense. Using PBL as a pedagogical framework, this initiative involved undergraduate students in Design and Graphic Arts Technology in observing production processes, engaging with company specialists and creating communication materials to meet the company's specific needs. The results suggest that industrial graphic heritage can function simultaneously as a cultural resource and a learning context, bringing together technical knowledge, design practice and professional engagement. The project also produced audiovisual content, graphic objects and exhibition materials that help to publicly communicate the history of this printing company. Although centred on a single case, the study highlights the potential of heritage-related educational projects to develop professional skills and support their public appreciation.

Miguel Sanches
Ana do Carmo
Júlio Silva

TECHN&ART, Technology, Restoration and Arts Enhancement Center, Polytechnic University of Tomar, Tomar, Portugal

KEY WORDS
Industrial heritage, graphic technologies education, graphic design education, Project-Based Learning

1. Introduction

1.1. Industrial graphic heritage as an educational opportunity

Industrial graphic heritage occupies a unique position at the intersection of technological innovation, material culture and graphic communication. Some former printing companies preserve machinery, artefacts and documentary collections, but they also embody technical knowledge, production processes and professional cultures that document the evolution of graphic technologies over time. Although their historical and cultural importance is widely recognised, industrial heritage contexts can also provide learning opportunities through direct contact with materials, technologies, production processes and professional practices. In the teaching of graphic technologies and design, these contexts can complement studio and laboratory-based learning, giving students access to authentic industrial environments and different forms of technical and professional knowledge.

This perspective creates an opportunity to bring together industrial heritage, project-based learning and collaboration between universities and industry within a shared educational context. Rather than viewing heritage merely as something to be preserved, this study explores its potential as an authentic learning environment, in which historical research, design practice, technical knowledge and professional interaction can come together.

Throughout this project, students on the bachelor's degree programme in Design and Graphic Arts Technology developed graphic communication materials, audiovisual content and exhibition materials, drawing on their engagement with the archives and industrial observation. The exhibition, organised as part of the project's public dissemination, served both as an educational outcome and as a strategy for interpreting and communicating industrial graphic heritage to wider audiences.

1.2. Research question and objective

The study seeks to answer the following question: How can industrial heritage contribute to the contemporary teaching of graphic technologies and design through project-based learning and university-industry collaboration? The aim is to explore how a heritage enhancement project can provide a meaningful learning environment for students of graphic technologies and design, integrating historical research and design practice in collaboration with an industrial partner.

1.3. Case and contribution

The research adopts an exploratory case study methodology, centred on the project «Celebrating 140 Years of Tipografia Lousanense». Project-Based Learning (PBL) provides the pedagogical framework for the educational experience, enabling students to tackle real-world design challenges within an authentic industrial context. The case study analyses how the collaboration between the Polytechnic University of Tomar (UPTomar) and Gráfica Lousanense fostered learning through historical research, observation of production processes, interaction with company experts, and the development of communication materials that met the institution's specific needs. The analysis of this case study suggests that industrial heritage can function simultaneously as a cultural resource and an educational environment.

2. Industrial graphic heritage, graphic technologies and design education

Industrial graphic heritage represents a field where the history of technology, material culture, design and education converge. Over more than five centuries, the evolution of printing technologies has profoundly transformed the production and circulation of knowledge, influencing communication, education, the economy and the construction of cultural identities. At the same time, the successive introduction of new technologies – from manual typesetting to digital printing – has not eliminated earlier processes but has built up a tangible and intangible legacy that documents the technical and social evolution of graphic production.

In this context, the industrial heritage associated with graphic technologies goes beyond the preservation of historic machinery or buildings. It also encompasses the production processes, specialist knowledge, professional practices and forms of work organisation that enabled the development of the printing industry. Its preservation therefore takes on a technological, cultural and educational dimension, offering unique contexts for understanding the relationship between design, production and innovation.

This framework seeks to establish this relationship through four complementary perspectives: the conceptualisation of industrial heritage as both technological and cultural heritage; the historical evolution of printing as a practice that links production and design; the complementarity between graphic technologies, education and design education; and, finally, the value of authentic industrial environments as spaces for experiential learning and PBL.

2.1. Industrial heritage as technological and cultural heritage

Industrial heritage is currently understood as a collection of tangible and intangible assets that bear witness to the history of productive activities and the technological evolution of industrial societies. According to the *Dublin Principles*, developed jointly by ICOMOS & TICCIH (2011), industrial heritage comprises sites, buildings, structures, machinery, infrastructure, documents, landscapes and knowledge associated with industrial activities, possessing historical, technological, scientific, social and cultural value. This definition significantly broadens the traditional notion of heritage, shifting the focus from purely architectural preservation to an integrated understanding of production systems and the communities that gave rise to them.

The material dimension of the industrial printing heritage includes factories, workshops, equipment, tools, printing plates, movable type, graphic archives, proofs and objects produced during industrial activity. These elements document different stages of technological development, providing an insight into production methods, technical capabilities and the changes brought about by successive innovations.

However, the preservation of these objects loses some of its significance if it is separated from the intangible dimension of heritage. The technical knowledge accumulated by printers, typographers, typesetters, engravers and machine operators constitutes a living heritage, passed on through practice, on-the-job training and experience accumulated over generations. Knowing how to prepare a printing form, fine-tune a letterpress, adjust an offset press or interpret the characteristics

of paper represents a set of skills that can hardly be preserved through written documentation alone.

In the case of the graphic arts, this perspective takes on particular significance. The evolution of printing has been characterised by successive technological changes (manual typesetting, mechanical typesetting, phototypesetting, offset printing and digital printing), which coexisted for extended periods and gave rise to different forms of technical knowledge. Each technology introduced new possibilities for visual communication, new materials and new skills, contributing to the development of contemporary graphic culture.

Industrial graphic heritage thus represents a technological archive of the history of printed communication. Preserving workshops, machinery and processes means preserving evidence of the evolution of information reproduction technologies and the cultural practices associated with editorial, commercial and institutional production. In addition to its historical value, this heritage has significant educational potential, enabling us to understand the evolution of technologies through direct experience of the production processes.

This approach aligns heritage preservation with a philosophy of active enhancement. Rather than preserving equipment merely as static, inert museum objects, it seeks to maintain an understanding of the technological processes involved, thereby facilitating demonstrations, research, training and cultural mediation. In this way, it is possible to transform industrial heritage into technological memory and a resource for new educational practices.

2.2. Printing and graphic design as interconnected practices

The history of printing is the history of the evolution of visual communication systems and the production of knowledge. Since Gutenberg perfected the use of movable-type printing in the 15th century, printing has become one of the main drivers of the dissemination of information, literacy and the cultural transformations that accompanied European modernity.

Briggs and Burke (2002) demonstrate that each innovation in printing technology has profoundly altered the ways in which information is produced, distributed and consumed. The letterpress enabled the large-scale reproduction of texts and images; the mechanisation of printing significantly increased productivity during the Industrial Revolution; lithography and, later, offset printing expanded the possibilities of multicolour printing; while digital printing has enabled personalisation, short-run production and new business models such as print-on-demand.

This technological evolution never took place in isolation. Changes in production processes directly influenced visual language, page layout, typography, illustration and, subsequently, graphic design as an autonomous discipline. Technology shaped formal possibilities, but at the same time it also opened new creative opportunities.

Before the profession of graphic design became established, the printer often played a role in visual design. Jury (2012) demonstrates that, between the 18th and 19th centuries, many printers selected typefaces, defined typographical hierarchies, organised layouts, designed ornamentation and made aesthetic decisions that would today be attributed to a graphic designer. The printer was simultaneously a craftsman, a technician and the creator of the graphic composition.

This historical relationship shows that design and production have always been deeply intertwined. The contemporary separation between design and manufacture stems primarily from the industrialisation of production processes and the professional specialisation that took place during the 20th century. Even so, design decisions remain dependent on the characteristics of materials, printing processes, finishing techniques and the available technological limitations or capabilities.

The history of graphic design is a process of constant interaction between technological innovation and visual culture (Meggs & Purvis, 2009). Each technological transformation has given rise to new graphic languages, new editorial formats and new possibilities for communication. The development of photography, colour printing, photocomposition and desktop publishing has simultaneously altered both working methods and the visual outcomes produced.

This perspective provides an important conceptual foundation for graphic design education, arguing that knowledge of graphic technologies is not a secondary subject but a fundamental component of the ability to design for graphic production.

2.3. Graphic technologies and graphic design education

Graphic technologies education and graphic design education share common objectives relating to the production of visual artefacts but differ in their epistemological focuses and the skills they prioritise. Whilst the former centres on the realisation of these solutions through mastery of materials, processes and graphic production technologies, the latter focuses predominantly on design, visual communication and the resolution of design problems.

Lawson (2005) defines design as an activity involving the resolution of complex problems based on the development of iterative solutions. The design process involves research, the interpretation of contexts, the generation of alternatives, experimentation and continuous evaluation. Designers develop skills to meet communication needs through the synthesis of function, meaning and form. Cross (2011) adds that «designerly ways of knowing» constitute a specific form of knowledge, distinct from scientific or humanistic approaches. Designers produce knowledge through experimentation, modelling and the construction of solutions, combining creativity with technical reasoning. However, the development of graphic solutions also depends on an understanding of production processes. Education in graphic technologies provides this specialist knowledge, enabling an understanding of material properties, ink behaviour, printing systems, colour management, file preparation, finishing, process sustainability and quality control.

The concept of the «reflective practitioner», introduced by Schön (1983), holds that professional knowledge emerges from reflection during action. The project evolves through the interaction between thinking and doing and is continually adjusted considering the results of experimentation. In *Educating the Reflective Practitioner* (1987), Schön applies this perspective to teaching, arguing that professional learning must take place in environments where students face real problems and reflect critically on their decisions.

In this context, education in graphic technologies broadens design education by introducing a dimension of technological literacy. Students learn not only to design a graphic object, but also to anticipate production constraints, optimise processes, select appropriate technologies and make informed decisions regarding production.

Design and graphic production learning benefits significantly from the interaction between academic contexts and authentic industrial environments. Whilst classrooms, laboratories and workshops enable students to develop fundamental skills, much professional knowledge is only truly consolidated when students participate in real-world production situations, where materials, equipment, time constraints, restrictions and decision-making coexist within the same context. This perspective is reflected in PBL approaches.

3. Project-based learning and university-industry collaboration

3.1. Project-Based Learning in design and technology education

Project-Based Learning (PBL) is an active learning approach in which students construct knowledge through inquiry and engagement with real-world problems. Its conceptual roots lie in Dewey's notion of learning by doing and in Kilpatrick's project method, and one of its central principles is the deliberate alignment between academic learning and professional contexts (Franco, 2023). Thomas (2000) identifies five defining criteria: the centrality of the project in the curriculum, a driving question, constructive investigation, student autonomy and realism. Unlike Problem-Based Learning, which centres on the analysis of a problem, PBL culminates in a concrete artefact or outcome.

This requirement is particularly relevant to design and graphic technologies education, where the artefact is both the outcome and the medium of learning. Materialising a proposal – a printed piece, a publication, a video – obliges students to reconcile conceptual intentions with the constraints of materials, printing processes and media. Biggs and Tang (2011) describe this as the development of functioning knowledge: the capacity to put declarative knowledge, such as typography, colour or pre-press, to work in real decisions. Schön's (1983, 1987) reflective practitioner provides the complementary frame: in open-ended design situations, knowledge develops through reflection-in-action, as solutions are tested and adjusted, and reflection-on-action, as process and outcome are critically reviewed.

3.2. University-industry collaboration as an educational context

Ankrah & Al-Tabbaa (2015) define university-industry collaboration as interaction between higher education and industry aimed at exchanging knowledge and technology. Among its forms, their review identifies student involvement in industrial projects, the use of industrial facilities and the participation of professionals in educational activities. Among its benefits, it identifies students' and lecturers' exposure to practical problems and current technologies. The authors also distinguish between collaboration understood as a planned transfer of knowledge and collaboration in which knowledge emerges from sustained interaction between participants.

For programmes such as Design and Graphic Arts Technology, this second perspective is particularly relevant. Learning depends on materials, production processes and contexts of use that are difficult to reproduce fully in the classroom or laboratory. When a project originates in

a real industrial challenge, the partner is not merely the recipient of student work: it helps create the conditions for learning by setting the brief, giving access to facilities and processes, and bringing professional knowledge into the project. Students then work with actual objectives, requirements and constraints, while the project remains framed by pedagogical goals. The project «Celebrating 140 Years: A Creative Partnership between Industry and Higher Education» is an instance of this approach.

4. Methodology

4.1. Research design

This study adopts an exploratory, qualitative case study design to examine how industrial graphic heritage can inform the teaching of graphic technologies and design through PBL and university-industry collaboration. The case study approach allows for the analysis of a contemporary phenomenon within its real-world context, considering the relationships between activities, participants and contextual conditions (Yin, 2017)

The unit of analysis is the educational and collaborative project «Celebrating 140 Years: A Creative Partnership between Industry and Higher Education», developed between UPTomar and Gráfica Lousanense. The case is understood as a process that includes the development of the project within the curriculum, engagement with the company and its heritage, the development and selection of proposals, the discussion of production possibilities, and the public presentation of the results through an exhibition.

The exploratory design allows us to examine the educational opportunities and the relationships between heritage, design, graphic technologies and professional practice offered by this experience, without seeking to establish causal effects or directly measure learning outcomes. PBL provides the pedagogical framework for the experience, whilst the case study constitutes the research design through which the project is analysed.

4.2. Case selection and context

This case study was deliberately selected because it provides a context in which industrial graphic heritage, project-based learning, the teaching of design and graphic technologies, and university-industry collaboration come together in the development of a project with a specific communicative purpose.

The collaboration between UPTomar and Gráfica Lousanense provided students with access to historical documents, equipment, production processes and professional expertise. The selection of this case is therefore based on the relevance of these characteristics to the research question rather than on statistical representativeness (Yin, 2017).

The case was analysed between February 2025 and May 2026, covering the development of the curriculum project in the second semester of the 2024/25 academic year, the subsequent activities involving the selection and preparation of the projects, and their public presentation at the exhibition held in 2026. The historical context, the terms of the collaboration and the different stages of the project are described in Section 5.

4.3. Educational and collaborative setting

The project involved second-year students in the bachelor's degree in Design and Graphic Arts Technology at the Tomar School of Technology, part of UPTomar. It was organised as a transdisciplinary project incorporating three course modules, each supervised by one of the authors of this article:

- the design component was developed as part of the course of Artwork (second author);
- the selection of printing techniques and the graphic production were carried out as part of the Offset component in the course of Printing – Offset II and Pad Printing (first author);
- the narrative structure, editing and post-production of the audiovisual content were carried out as part of the course of Multimedia Design (third author).

The challenge originated with the printing company and was formalised by the lecturers in a written brief. Access was granted to the company's premises, historical resources and staff, and a representative from the company helped to curate the works presented in the exhibition.

The dual role of authors and project coordinators provides in-depth contextual knowledge but may also influence the selection and interpretation of evidence, through prior expectations and familiarity with the project and the students. Retrospective memory was used solely to locate and organise documented materials, and not as independent evidence of activities, decisions or learning.

To minimise this risk, the analysis focuses on materials produced or documented during the project and explicitly distinguishes between documentary evidence, the researchers' interpretations and inferences regarding learning opportunities.

4.4. Sources of evidence

The study draws on multiple sources of evidence to examine the context, development and outcomes of the project (Yin, 2017). These sources include:

- The document setting out the planned learning programme (the objectives, the distribution of tasks across the course modules and the planned timetable) is therefore interpreted as a statement of intent to be compared with the documented activities and outcomes.
- The photographic and video records of the on-site visit, which constitute selective evidence of the industrial context and the activities carried out during the visit. These include images of the spaces, equipment and processes observed by the students, as well as records of information and testimonies gathered from the company representative. These materials are not considered a complete record of the participants' experiences but are used to document the students' engagement with the industrial context and the resources made available by the company.

4.5. Analytical approach

The analysis of the students' work is limited to the pieces selected for public display at the exhibition and documented in the accompanying catalogue. This collection constitutes a defined corpus of the project's outcomes and does not represent the entirety of the students' work.

The choice of this corpus allows for the analysis of artefacts which, within the scope of the project itself, underwent the selection process and were deemed suitable for public presentation. The artefacts are not used as a means of assessing the students nor as direct evidence of the acquisition of skills. They are analysed as material evidence of the design decisions, technical choices and approaches to interpreting heritage developed within the context of the project.

For the graphic designs, the analysis considers the selection and transformation of elements relating to the history and identity of Gráfica Lousanense, the visual and typographical decisions, the relationship between concept, form and content, and the proposed printing and finishing techniques. It also considers the relationship between the graphic solutions and the production possibilities discussed as part of the collaboration with the company.

In the case of audiovisual content, the analysis considers the selection and organisation of the materials collected during the project, the aspects of the company's history and activities that were prioritised, and the choices made regarding narrative structure and editing. Where different students drew on materials from a common source, the differences in the ways in which these materials were selected, organised and interpreted are considered.

The analysis combines a contextual reconstruction of the case with a qualitative analysis of the various materials documenting its development and outcomes (Yin, 2017). The materials were organised by project stage and by type of source. The analysis sought to link planned activities, documented activities, development decisions and the outcomes produced, distinguishing between directly observable evidence and the researchers' interpretations.

Based on the research question and the theoretical framework, six analytical dimensions were defined, which were subsequently refined during the case analysis. These dimensions were operationalised in an analytical matrix that links each dimension to the aspects to be observed and to the main sources of evidence used (Table 1). The matrix was applied to the corpus of artefacts selected for the exhibition and linked to the other documentary sources in the case.

Table 1
Analytical matrix

Dimension	Focus of the analysis	Evidence
Industrial heritage	Presence and use of elements from the company's history, equipment or materials	Historical documentation, on-site visit, artefacts
Design and graphic technologies	The relationship between visual decisions and technical solutions	Proposals, models, specifications, artefacts
University-industry collaboration	Interaction with the company and contributions from its staff	Project records, on-site visit, meetings
Professional practice	Addressing a real-world challenge and taking production requirements into account	Statements, proposals, artefacts
Interpretation of heritage	How a company's history and identity are reflected in contemporary communication	Artefacts, videos, exhibition
Documented learning opportunities	Documented situations in which students were required to draw on their knowledge, make decisions, integrate different subject areas or respond to production conditions.	Set of sources

The analysis of the selected artefacts is integrated within these dimensions and does not constitute a standalone analysis of the objects as design pieces. The works are considered in relation to the context in which they were produced and to the other sources of evidence. Thus, a particular graphic solution can be analysed simultaneously as a design decision, a response to a technical possibility, an interpretation of an element of heritage, and the result of an interaction with the industrial context.

The analysis of the artefacts is carried out in Section 6 using selected examples from the corpus. The study considers works that highlight different relationships between the analytical dimensions, namely the use of elements from the company's history or identity, the relationship between visual concept and production possibilities, the exploration of printing and finishing techniques, and the different ways in which historical and documentary materials are interpreted in audiovisual content.

The analysis seeks first to identify the observable elements in the artefacts and then to relate them to other sources within the case study. This approach enables the results produced by the students to be interpreted within the context of the activities, decisions and interactions that characterised the project.

Schön's concepts (1983, 1987) are used as an interpretative framework for analysing documented relationships between practical situations, design decisions and review processes. Thomas (2000) provides guidance on interpreting the development of responses to an authentic challenge, whilst Ankrah & Al-Tabbaa (2015) contribute to the analysis of collaboration and knowledge relationships between universities and industry.

These dimensions constitute an analytical framework developed for this study and are not a validated assessment tool. The analysis distinguishes between observable outcomes, documented processes and inferred learning opportunities.

Comparing different sources makes it possible to contrast planned activities, documented activities and the results produced. Where different sources do not support a particular interpretation, this limitation is made explicit rather than being resolved through inference.

The scope of the evidence limits the conclusions that can be drawn. The final artefacts, on their own, do not prove that skills have been acquired, and the selective documentation of the project does not provide a complete account of learning or collaboration. The conclusions therefore relate to the educational practices and opportunities documented in this case, rather than to measured individual learning outcomes.

5. The case: celebrating 140 years of Tipografia Lousanense

5.1. Tipografia Lousanense: historical and industrial context

Tipografia Lousanense was founded in 1885 in the town of Lousã, in the district of Coimbra, Portugal, by Aníbal Fernandes Tomás Pipa, who opened the print shop with the release of the newspaper «Jornal da Louzan». As was common in 19th-century Portuguese printing works, the company combined the production of a local newspaper with more general commercial and editorial printing, a dual function that placed the business at the intersection of industrial production and regional public life. Briggs and Burke (2002) describe this convergence between printing technology and the press precisely as constitutive of the emerging modern media landscape in nineteenth-century Europe. The print shop changed owners twice during its first decade and a half of existence: it was acquired in 1893 by Bernardino Lopes Padilha, and was subsequently sold, in 1898, to Júlio Ribeiro dos Santos, a former employee of the firm (Sanches et al., 2026). This transaction marked the beginning of an unbroken family lineage in the management of the company, which has continued through five generations to the present day; this continuity is, in itself, a central defining feature of the company and one of the elements that the programme of events marking its 140th anniversary sought to highlight to the public.

Over the following decades, the company's premises changed location several times, in line with the growth of its business. Each move was accompanied by an expansion of production capacity and a gradual modernisation of equipment and processes, culminating in the operation the company runs today. In the publishing sector, Tipografia Lousanense has built a reputation in the field of book printing, having printed works by authors such as Nobel Prize-winning author José Saramago; this places the company within the broader context of the history of publishing and printing in Portugal, rather than merely within the sphere of local commercial printing.

The company's technological development reflects the broader evolution of printing from manual typesetting to offset and, more recently, digital and hybrid workflows (Briggs & Burke, 2002). This trajectory is further marked by quality and sustainability certifications, the introduction of digital printing, and the implementation of an integrated management system, illustrating the company's transition from artisanal production to contemporary industrial and digital practices.

Alongside its documentary records, the company preserves historic printing equipment, machinery and printed materials accumulated over 140 years of

continuous operation. At the time of the exhibition, these resources were being inventoried as a first step towards their conservation, restoration and possible future museum use. This approach aligns with international principles for industrial heritage conservation, which emphasise documenting and safeguarding both the tangible and intangible traces of historical production, including machinery, materials and technical knowledge (ICOMOS & TICCIH, 2011).

The case of Lousanense is distinctive precisely because it is not a disused industrial site or a site turned into a museum, but a company that remains in continuous commercial operation, and simultaneously a body of industrial heritage. It is this combination of active industrial practice and an emerging awareness of heritage – formalised through the family's own initiative to mark the 140th anniversary – that provided the empirical basis and institutional impetus for the collaborative project analysed in this study, which is discussed in the following sections.

5.2. The university-industry collaboration and the educational project

The collaboration between UPTomar and Gráfica Lousanense took place as part of the celebrations marking the company's 140th anniversary, to be commemorated in 2025. Formalised as a partnership between higher education and the printing industry, the initiative involved the company, lecturers and students. The collaboration was structured around a specific challenge set for the students: to develop graphic designs and multimedia content capable of celebrating the history, identity and activities of Gráfica Lousanense.

The initiative brought together three academic areas of the bachelor's degree (Graphic Design, Graphic Technologies and Multimedia Design), combining conceptual development, graphic production and audiovisual content. The initial brief called for the development of a set of commemorative graphic items, namely posters, postcards and leaflets, complemented by audiovisual content. Students were also required to consider the technical characteristics of the proposed items and explore possibilities for special printing and finishing techniques.

The project began through direct contact between the students and the company. An initial presentation in February 2025, led by a representative from Gráfica Lousanense, provided an insight into the company's history and its professional context (Figure 1a). This activity was followed by an on-site visit to the premises in March 2025, during which the students collected visual records and information, spoke directly with professionals and observed production processes, equipment and working practices (Figure 1b).



(a)



(b)

» **Figure 1:** *Initial contact with the industrial partner: (a) presentation of Gráfica Lousanense at UP Tomar in February 2025; (b) on-site visit to the company's facilities in March 2025. Note: Photographs by the authors*

The development of the proposals required the integration of knowledge from the various curricular areas involved. In the field of Graphic Design, the students developed visual proposals for the commemorative items, incorporating elements relating to the history and evolution of Gráfica Lousanense. In the field of Graphic Technologies, the proposals were analysed in terms of printing processes and possible complementary techniques, including special inks, varnishes, embossing, debossing and die cutting. In Multimedia Design, audiovisual content was developed to complement the printed items and extend the experience through digital media.

Interaction with the industry partner continued beyond the initial briefing and fieldwork. In November 2025, a further meeting was held with the manager of Gráfica Lousanense, at which the students' selected proposals were presented and the possibilities for their production were discussed (Figure 2a). This stage introduced a new dimension to the interaction between the academic proposals and the demands of professional production. The discussion focused particularly on the technical feasibility of the selected solutions and on defining the most appropriate printing and finishing strategies (Figure 2b).

This phase was significant because the projects were no longer regarded solely as academic proposals. Their development now involved considering how visual and conceptual decisions could be realised as physical graphic



(a)



(b)

» **Figure 2:** *Discussion of the selected student proposals with the industrial partner: (a) presentation and discussion of the selected graphic artefacts; (b) detail of the production discussion. Note: Photographs by the authors*



(a)



(b)

» **Figure 3:** *Public presentation of the project: (a) exhibition opening; (b) exhibition view. Note. Photographs by Joana Cordeiro. Reproduced with permission*

objects through specific production processes. The relationship between design and production thus became an integral part of the educational experience, enabling students to weigh up visual and communicational decisions against technical constraints and possibilities.

The project subsequently extended beyond the classroom and the industrial setting, taking on a public dimension through an exhibition.

5.3. Public exhibition and dissemination

The exhibition, held at the Casa dos Cubos – Centre for Photography Studies in Tomar, between 25 February and 17 May 2026, brought together the students' selected projects, including posters, postcards and leaflets, as well as audiovisual works and materials relating to the history of graphic production and Gráfica Lousanense (Figure 3).

The exhibition served both as a platform for the public presentation of the results of the educational project and as an opportunity to share aspects of the company's industrial graphic heritage with a wider audience. The work produced by the students (informed by their engagement with the company, its production processes and the historical materials made available to them) was presented alongside with elements documenting the company's history and graphic heritage.

In this way, the project established a link between the contemporary work produced by the students and the company's historical legacy. The graphic proposals were based on information relating to the history, identity and technological evolution of Tipografia Lousanense, while the historical materials presented in the exhibition helped to contextualise this work. The interplay between the graphic and audiovisual works developed by the students and the company's historical materials thus established a dialogue between past and present, bringing industrial graphic heritage closer to contemporary practices in design and graphic production.

The project therefore unfolded through a series of interlinked experiences: engagement with the industrial partner, an exploration of the company's history and professional context, observation and documentation in the workplace, the development of design proposals and graphic technologies, and a discussion of production possibilities and public presentation through an

exhibition. These stages were not isolated activities, but successive phases of integration between academic learning, professional practice, and the interpretation and communication of the company's graphic heritage.

In this regard, the case provides a concrete context in which design, graphic technologies and multimedia production were brought together around an authentic industrial object and a real commemorative challenge. The university-industry collaboration served not merely as a context external to teaching activities, but as an integral part of the learning process itself.

6. Analysis and discussion

6.1. Industrial graphic heritage as an authentic learning environment

This case demonstrates that industrial graphic heritage can serve not only as a subject of historical research, but also as an authentic learning environment. The educational experience went beyond the conventional context of the classroom and the laboratory through direct contact, within the company, with its equipment, production processes, historical materials and technical knowledge.

The students' first contact with the company provided them with an insight into aspects of graphic production that are difficult to replicate in full within an academic context. The visit to the premises enabled them to observe production spaces and equipment, gather visual records and information, and engage directly with professionals. These experiences were subsequently drawn upon in the development of the graphic and audiovisual proposals. The industrial context thus served not merely as a source of visual references, but as part of the conditions within which the project was conceived and developed.

The industrial environment also provided access to forms of knowledge embedded in practice. The company's history, its equipment, production processes and professional experience constituted a body of knowledge that complemented the academic knowledge acquired at university. This aspect is consistent with the concept of industrial heritage adopted in this study, which encompasses not only material remains, but also processes, technical knowledge and professional practices.

This case thus allows us to distinguish between learning about industrial heritage and learning through industrial heritage. In the former case, the company and its history would primarily be subjects of study. In the latter, which characterises this project, the heritage context also shapes the design process and provides material, historical and professional information that informs the project's development.

This aspect is particularly significant because Gráfica Lousanense maintains an active industrial environment; it is not a heritage site removed from its context. The students encountered a company that continues to operate while preserving and beginning to organise historical equipment and materials. The coexistence of current production and accumulated industrial heritage created a context in which continuity and technological transformation could be observed side by side.

6.2. Learning design through an authentic project

The project also illustrates how a real-life brief can structure the learning process as a sequence of interconnected design activities. Rather than treating research, conceptualisation, development, production and communication as separate exercises, the project organised these activities around a common objective: to celebrate and communicate the company's 140-year history.

The process documented in this case involved contacting the company, gaining an understanding of its history and professional context, conducting on-site observation and documentation, developing graphic and audiovisual proposals, considering production options, selecting and preparing the final outputs, and subsequently presenting them in a public exhibition.

This sequence is consistent with the characteristics of PBL discussed by Thomas (2000), namely the centrality of the project, the presence of an authentic problem or purpose, research, and the production of concrete results. The relevance of PBL in this case lies not only in the fact that the students produced artefacts, but in the way in which these resulted from an open-ended challenge that required research, interpretation and decision-making.

The physical outcomes are particularly significant in this context. The posters, postcards, leaflets and videos were not merely exercises produced for assessment. They were developed as part of a commemorative project and subsequently selected for public display. The exhibition thus extended the project beyond the production of the individual artefacts and added a communicative dimension to the process.

The evidence does not allow us to establish individual learning gains. It does, however, allow us to document situations in which students were asked to investigate, make design decisions, consider technical possibilities, communicate proposals and respond to a real-world project context. These situations constitute documented learning opportunities, which correspond to the level of interpretation supported by the study's exploratory design.

6.3. Learning graphic technologies through industrial practice

The project did not treat graphic technologies as a subsequent stage, separate from the design. The brief asked students to consider printing and finishing options, whilst the development of the proposals involved discussing techniques such as special inks, varnishes, embossing, debossing and die cutting. A subsequent meeting with the company focused specifically on the technical feasibility of the selected proposals and on the most appropriate printing and finishing strategies.

The selected artefacts provide visible evidence of this relationship. The exhibition documentation identifies different combinations of offset printing and finishing techniques used on the posters, postcards and leaflets, including fluorescent ink, scratch-off ink, UV varnish, hot and cold foil stamping, die-cutting and matt lamination. These variations show that the technical aspect was not uniform throughout the project, but rather formed part of the specific development of the different proposals.

The case thus illustrates the role of industrial practice in contextualising technological knowledge. The students were asked to consider how a visual proposal might be transformed into a physical object and how different production processes might contribute to the intended result. This relationship is consistent with the argument developed earlier in the paper, according to which design decisions and technological decisions constitute interlinked dimensions of graphic production.

6.4. Connecting design and graphic technology education

The project was structured around three areas of the bachelor's degree: Graphic Design, Graphic Technologies and Multimedia Design. The graphic proposals were developed in line with the company's identity and history; the technological aspect focused on the possibilities for printing and finishing; and the audiovisual component extended the project into another form of communication.

This approach made it possible to establish links between conceptual decisions, visual communication, technological choices and material outcomes. A poster, for example, was not considered solely in terms of composition or visual identity. The proposed printing process and finishing were also incorporated into the design brief. Similarly, a leaflet involved the organisation of information and editorial structure, while also considering the format, printing and finishing.

This case thus illustrates a form of integration in which design and technology remain distinct fields of knowledge yet operate within a shared design context. This relationship is consistent with the historical perspective outlined in Section 2, according to which design and graphic production are deeply intertwined and the possibilities for visual communication depend, at different times, on the technologies available.

The importance of this integration becomes particularly evident in the transition from design to production. The meeting held with the company directly incorporated the production context into the development process. The proposals had to be discussed in terms of what could be technically achieved, and the printing and finishing techniques were adjusted accordingly.

This project thus created an opportunity for students to experience graphic design not merely as the creation of visual solutions, but as the design of objects that will need to be brought to life. This aspect reinforces the view of graphic technologies as an integral part of design competence, rather than as a separate technical discipline.

6.5. University-industry collaboration as a learning condition

The collaboration with Gráfica Lousanense took place at various stages of the project and was not limited to the initial briefing. Firstly, the company set the challenge and provided information about its history and professional background. Secondly, the students visited the premises, where they were introduced to the equipment, processes and staff. Thirdly, the company took part in the discussion of the selected proposals and their feasibility for production. Finally, the results were presented publicly at an exhibition focusing on collaboration.

This sequence is relevant to understanding the university–industry collaboration proposed by Ankrah and Al-Tabbaa (2015). Their review identifies student involvement in industrial projects, interaction with professionals and access to industrial environments as forms of interaction between universities and industry that can bridge the gap between academic and professional knowledge.

In this case, the company's contribution was not limited to the role of client or recipient. Its involvement helped to shape the conditions under which the project unfolded. The company's history formed the subject of the project; its premises and resources provided the context for the research; its staff contributed contextual and technical knowledge; and the company's production capabilities influenced subsequent design decisions.

This does not mean that the company has replaced the university's educational role. Rather, the collaboration has established a complementary relationship between academic supervision and the professional context. The educational framework has remained an integral part of the university curriculum, whilst the industrial partner

has introduced elements of authenticity that are difficult to replicate in full within a purely academic setting.

Thomas (2000) is equally relevant in this context, as the project combined a real-world problem with research, collaboration and the production of concrete results. The case illustrates how university-industry collaboration can reinforce these characteristics of PBL, providing a real-world context in which the project acquires purpose and constraints.

6.6. From learning about heritage to interpreting heritage through design

The project drew on the company's history, identity, technological development and material resources as sources of information. The students engaged with these materials through a company presentation, a site visit, historical documentation and the observation of equipment and processes. They subsequently transformed selected aspects of this information into contemporary graphic and audiovisual communication.

This transformation is evident in the diversity of approaches represented in the exhibition. Some entries emphasised the company's longevity and continuity since 1885; others highlighted technological developments, its identity, its values or its relationship with printing. The audiovisual content also offered different ways of organising and communicating information about the company. The exhibition placed these contemporary interpretations in dialogue with historical materials and documentation relating to the activities of Tipografia Lousanense.

The audiovisual content added a temporal and auditory dimension to the representation of the industrial context. By recording the machinery in operation, the processes and the sounds of the working press, the students sought to convey the dynamics of the work and the production processes. This representation made it possible to showcase aspects of industrial activity that a static image does not convey in the same way, such as rhythm and sequence.

This process is significant because the interpretation of heritage does not necessarily depend on the literal reproduction of historical materials. Design can serve as a means of selecting, organising and translating information into forms that are accessible to contemporary audiences. In this case, posters, postcards, leaflets and audiovisual content have become both educational outputs and objects of interpretation.

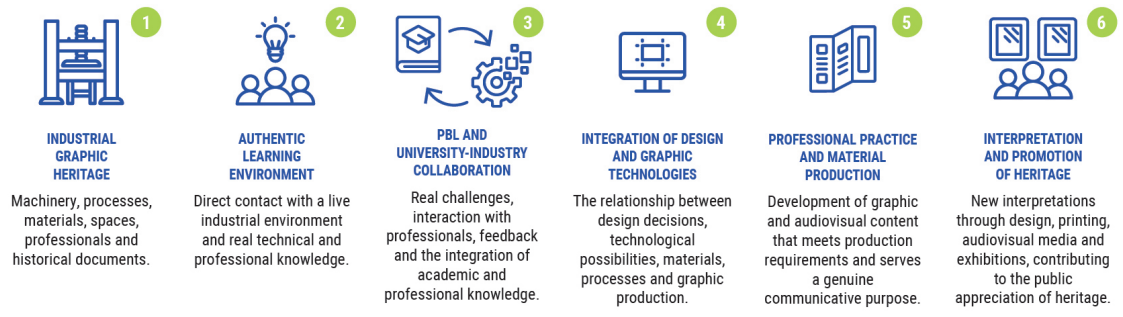
The relationship with industrial heritage is therefore reciprocal in nature. The students had the opportunity to learn through engagement with the company's history and material culture, whilst their work produced new ways of communicating that heritage to the public. The exhibition reinforced this reciprocity by placing the contemporary works in dialogue with historical materials and company documentation.

This interpretation is consistent with the concept of industrial heritage set out in the *Dublin Principles* (ICOMOS & TICCIH, 2011), which encompasses both tangible and intangible dimensions and recognises the importance of documentation, interpretation and engagement with the public. It also draws on the historical relationship between print production, technology and communication discussed by Jury (2012) and Meggs and Purvis (2009).

The case thus suggests that design education can contribute to heritage interpretation without turning students into heritage specialists. Its contribution lies in the application of design and communication skills to historical and industrial materials, producing new forms of interpretation capable of bridging the gap between heritage sites and contemporary audiences.

6.7. Integrative discussion

Taken together, the results reveal a sequence of relationships rather than a set of isolated educational activities. The industrial graphic heritage provided the authentic context; PBL provided the project framework; university-industry collaboration linked the educational process to professional practice; and the integration of design



» **Figure 4:** *Relationship between industrial graphic heritage, authentic context-based learning and the integration of design and graphic technologies*

and graphic technologies enabled students to move from historical information and conceptual proposals to tangible and communicative outcomes. This sequence should not be presented as a validated educational model or as a transferable framework. Rather, it represents the relationships observed in this specific case (Figure 4).

The evidence is more consistent regarding the conditions and opportunities created by the project: the students were exposed to a real-world industrial environment, interacted with professionals, worked with historical and technical information, produced concrete graphic and audiovisual outputs, considered production possibilities and took part in a public exhibition.

The case therefore suggests that industrial graphic heritage can occupy a productive position between cultural heritage and higher education in design and graphic technologies. Its educational value in this context stems not only from its historical importance, but also from its ability to bring together materiality, technology, professional knowledge, design decisions and communication within a real-world project.

7. Conclusions

7.1. Answer to the research question

This study sought to answer the question of how industrial heritage can contribute to the contemporary teaching of graphic technologies and design through PBL and university-industry collaboration. The case study «Celebrating 140 Years: A Creative Partnership between Industry and Higher Education» suggests that industrial graphic heritage can function both as a cultural resource and as an authentic educational context.

The contribution of the heritage context was not limited to providing access to historical content. The company's facilities, equipment, materials, production processes, historical information and professional expertise formed the framework within which the students developed their responses to an authentic project. PBL provided a structure for mobilising these resources in research, design development, technical decision-making and production activities, whilst collaboration with the industry partner brought these activities closer to a real-world professional context.

The study therefore suggests that industrial graphic heritage can support learning when it is approached not only as a subject to be studied, but also as a context through which students can investigate, design, produce and communicate.

7.2. Contributions

This project highlights the educational value of the interplay between design and graphic technologies in the context of a shared project. The development of posters, postcards and leaflets required conceptual and visual decisions to be aligned with formats, printing processes and finishing options. The audiovisual outcomes extended this integration to another form of communication.

The project also provided opportunities to gain experience of professional working conditions, including an external briefing, interaction with a company, production requirements and the public presentation of selected results. These experiences complement the learning that takes place in the classroom and laboratory by applying design and technical knowledge to a specific project.

The study does not establish individual learning gains. Rather, its contribution lies in documenting the conditions and opportunities through which students were able to draw upon and connect different forms of knowledge.

The project also demonstrates a reciprocal relationship between education and heritage interpretation. The students had the opportunity to learn through the company's history, its technological development, its material resources and its professional practices, whilst the graphic and audiovisual outputs created ways of communicating these elements to wider audiences.

The exhibition took on particular significance in this process by placing the students' contemporary work in dialogue with the company's historical materials. The combination of documentation, graphic design, audiovisual content and the exhibition itself contributed to the public's understanding of Gráfica Lousanense's industrial legacy.

7.3. Limitations and future research

Several limitations affect the scope of these findings. Firstly, the study focuses on a single case, involving a specific industrial partner, a specific higher education programme and a specific curricular context. The findings should therefore not be regarded as statistically generalisable. Secondly, the analysis is based on project documentation and selected outcomes, rather than on a longitudinal assessment of individual learning. Thirdly, there is no comparative case study that would allow the educational experience to be assessed by contrast.

These limitations point to several possibilities for future research. Comparative studies could analyse similar collaborations involving other forms of industrial heritage or different educational contexts. Future research could also incorporate interviews with students, reflective accounts or longitudinal assessments,

enabling a more direct investigation into the influence of engagement with industrial heritage on learning.

Overall, this case suggests that industrial graphic heritage can serve as a meeting point between design, production and interpretation. Its educational value lies precisely in the possibility of bringing these dimensions together within an authentic context.

8. Acknowledgments

This work was supported by TECHN&ART, Technology, Restoration and Arts Enhancement Center, Polytechnic University of Tomar (UPTomar), with funding from the Fundação para a Ciência e a Tecnologia, under project UID/05488/2025.

The authors would like to thank Gráfica Lousanense for its collaboration and for providing access to its industrial facilities, historical resources, technical knowledge and professional expertise throughout the project. The authors also acknowledge CEFT – Casa dos Cubos for hosting the exhibition and supporting the public dissemination of the project outcomes. Finally, the authors thank the students involved in the project for their engagement, creative contributions and active participation in the documentation and interpretation of Gráfica Lousanense's graphic heritage.

9. References

Ankrah, S. and AL-Tabbaa, O. (2015) 'Universities–industry collaboration: A systematic review', *Scandinavian Journal of Management*, 31(3), pp. 387–408. DOI: 10.1016/j.scaman.2015.02.003

Biggs, J. and Tang, C. (2011) *Teaching for Quality Learning at University* (4th edition). McGraw-Hill.

Briggs, A. and Burke, P. (2002) *A Social History of the Media: From Gutenberg to the Internet*. Wiley.

Cross, N. (2011) *Design Thinking: Understanding How Designers Think and Work*. Bloomsbury Publishing.

Franco, A. (2023) Aprendizagem Baseada em Projetos. Metodologia de ensino-aprendizagem. Católica Learning Innovation Lab. Available from: https://doi.org/10.34632/9789725409756 [Accessed 15 July 2026].

ICOMOS & TICCIH. (2011) *Dublin Principles. Joint ICOMOS – TICCIH Principles for the Conservation of Industrial Heritage Sites, Structures, Areas and Landscapes*. Available from: https://ticcih.org/about/about-ticcih/dublin-principles/ [Accessed 15 July 2026].

Jury, D. (2012) *Graphic Design Before Graphic Designers: The Printer as Designer and Craftsman 1700-1914*. Thames & Hudson Ltd.

Lawson, B. (2005) *How Designers Think* (Fourth edition). Architectural Press.

Meggs, P. B. and Purvis, A. W. (2009) *História do design gráfico*. Cosac Naify.

Sanches, M., Romão, P. and Torres, A. (2026). *Celebrar 140 Anos: uma parceria criativa entre indústria e ensino superior*. Instituto Politécnico de Tomar.

Schön, D. A. (1983) *The Reflective Practitioner How Professionals Think in Action*. Basic Books.

Schön, D. A. (1987) *Educating the Reflective Practitioner Toward a New Design for Teaching and Learning in the Professions*. Jossey-Bass Inc., Publishers.

Thomas, J. W. (2000) *A Review of Research on Project-Based Learning*. Autodesk Foundation, California.

Yin, R. K. (2017) *Case Study Research and Applications: Design and Methods* (6th Revise). SAGE Publications.

© 2026 Authors. Published by the University of Novi Sad, Faculty of Technical Sciences, Department of Graphic Engineering and Design. This article is an open access article distributed under the terms and conditions of the Creative Commons Attribution license 4.0 Serbia (http://creativecommons.org/licenses/by/4.0/rs/).

Professional Paper https://doi.org/10.24867/GRID-2026-p87

Kis Magyaróra: Learning a Language Through Applied Art

ABSTRACT

This paper presents Kis magyaróra (Little Hungarian Lesson), an artistic research project that explores visualization and drawing as aids in learning the Hungarian language. Building on Rudolf Arnheim's understanding of visual thinking as equal to verbal thinking, the project develops a personal visual system in which linguistic structures, word formation, and other specificities of the language are translated into drawings, expressive typography, and mnemonic images. The theoretical framework connects medieval memory culture, semiotics, the Gestalt principle of closure in comics, and Jacques Rancière's notion of intellectual emancipation. The results are a series of three risograph-printed zines, each accompanied by a poster and a learning card. The project argues that learning can be a creative rather than a merely reproductive process, and that a personal visual system can become readable to others when it relies on shared, collective experience.

Asja Komadina

University of Novi Sad, Faculty of Technical Sciences, Department of Graphic Engineering and Design, Novi Sad, Serbia

KEY WORDS
Drawing, semiotics, visual learning, mnemonic image, visualization, Hungarian language

1. Introduction

This paper explores the possibilities of visualization and artistic interpretation as aids in learning the Hungarian language. Through a series of drawings that illustrate different linguistic structures, ways of word formation, and other specificities of the language, it proposes an approach to learning based on visual communication.

It also contributes to the understanding of how visual approaches can enrich the cognitive processes involved in acquiring knowledge, and opens space for further research into the interaction of art and education in the field of language and communication.

The project is rooted in a combination of curiosity about the Hungarian language and culture and a visual way of learning that the author developed spontaneously, having never adapted well to the conventional educational system and needing to find her own way of remembering material. Hungarian, often considered one of the most demanding languages to learn, is approached here from the perspective of a complete beginner, and its perceived difficulty is questioned by laying visual foundations that anyone can understand.

By presenting the language in a creative and accessible way, the project also aims to lower the initial barrier to learning and to popularize it. The research method is artistic and is not burdened by the need for a strictly scientific or didactic outcome. Visualization is understood here as the process of translating abstract linguistic content into concrete visual form. The process of visualization is not treated as the final result, but as a way of seeing – a method for gaining insight into how one learns and understands. Throughout the paper, the question is raised whether the role of strict rationality in learning is overestimated, and how a more creative approach might be developed. The result is a series of three zines, each with an accompanying poster and learning card. The zine, a small-format printed or digital publication usually focused on a single topic, was chosen as the format for its ease of production and distribution.

2. Theoretical background

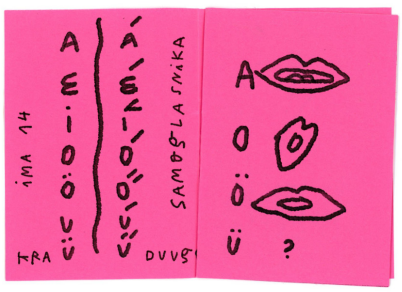
The principle "everything is in everything," formulated by the educator Joseph Jacotot and presented by Rancière, proposes that any knowledge, once truly acquired, is proof of the ability to learn (Rancière, 1991).

Someone who has learned to ride a bicycle has, in essence, demonstrated the capacity to learn to solve complex equations. This idea helped reframe the author's unease with conventional ways of learning: what was needed was simply a way to learn. Part of that way was the visual coding of content , such as grouping, marking categories with small drawings, and connecting things by association.

The idea for the project emerged from such spontaneous drawing during individual Hungarian lessons (Figure 1). Since the language was completely foreign and there was no existing knowledge to connect it to, the material was explained through familiar objects, jokes, imaginary characters, and situations. Two factors proved important: undivided attention during lessons, and the informality of individual lessons, which left freedom to master the material in a personally suitable way. It also became apparent that this kind of visual thinking quickly led to the question of what the essence of a new idea or concept is. The drawing demanded the most concise form of information.



(a)



(b)

» **Figure 1:** *Sketches in a notebook for Hungarian lessons (a) and the original Kis magyaróra zine (b), A. Komadina, 2024*

2.1. Visual thinking

In school, we are encouraged to rely mostly on logic and the linearity of language, yet artists have long understood intuitively that the visual domain constitutes a different kind of memory and learning. In the broadest sense, visual learning refers to the way people understand and remember information presented through images, diagrams, maps, and other visual means. Images are more than representations of words; they are a form of thinking in their own right, deeply connected to the ways we perceive and understand the world.

Rudolf Arnheim treats visual perception as a form of conceptual knowledge that is distinct from, yet closely intertwined with, language-based cognition (Arnheim, 1969). He regards visual thinking as equal to verbal thinking and emphasizes that aesthetic and visual language is present in everyday life, including scientific discourse, where diagrams and tables are responsible for order, clarity, and the relationship between meaning and form. The value of visual design is therefore not in dispute; what is often questioned is the equality of visual and verbal thinking, the latter being generally accepted as dominant.

Arnheim distinguishes intellectual from intuitive cognition. Intellectual cognition is what we usually mean by "thinking": it proceeds analytically, step by step, is most often expressed in language, and builds understanding linearly from the simple to the complex. Intuitive cognition takes place within perception itself, simultaneously and interwovenly, as when looking at a picture: understanding is immediate and whole, while details are discovered gradually. Although intellectual cognition is often regarded as superior, both play their part in thinking. Arnheim illustrated this with an experiment in which participants were asked to represent various concepts through drawing; while describing their drawings, they realized they had come to understand their own relationship to those concepts better. Drawing was not merely an external manifestation of thought but, like writing, a means of exploring and forming it (Arnheim, 1969).

The boundary between the linearity of speech and reading and the spatiality and simultaneity of looking or drawing is not as sharp as it appears. As Saussure observes, regardless of the linearity of speech, words in memory are organized associatively and branch out, mirroring the way visual information is experienced, where associative structure can be immediately visible in space (Saussure, 1959). The two processes naturally build upon each other.

2.2. Medieval memory culture

Memory (Lat. *memoria*) held far greater value in the Middle Ages. With limited opportunities for writing things down, people relied on their inner worlds to store knowledge, and memorization was a fundamentally creative skill involving both deep understanding of the material and ways of recalling it. The idea of mapping knowledge with the help of imagination dates back to ancient Rome: the method of loci, today better known as the memory palace, involved mentally arranging images within an imagined space so that they could be recalled when needed. Systematized in the rhetorical text *Rhetorica ad Herennium*, the method passed into

the education of orators and lawyers and, through the preservation of ancient texts in monasteries, into medieval monastic practice, where authors such as Hugh of Saint Victor adapted it to spiritual contemplation and the memorization of sacred texts (Carruthers, 2008).

Carruthers (2008) describes two key processes: *divisio*, the division of a whole into smaller parts, and *compositio*, the assembly of those parts into a composition to be memorized. The composition gives a broad picture of the relationships between elements, while the elements themselves serve as mnemonic triggers for the story or concept being remembered. Illuminations in manuscripts were not regarded as representations of reality but as material for contemplation and a kind of reading – access points to a wider mental library.

A mnemonic device can be defined as any technique, image, or structure that facilitates memory by linking new content with something already known or easily imagined. Illuminations also had another important function: to teach the reader a model of thinking, a scheme of how one can think visually (Carruthers, 2008).

A notable example is Thomas Murner's *Logica Memorativa*, a system for teaching Aristotelian logic to schoolchildren, published in 1509 and describing a card game for learning (Figure 2). Each card depicts a scene in which the relationships between elements correspond to the logical relationships they illustrate. The cards carry no explanatory text and rely entirely on the analogy between image and logical concept; a detailed description is given only in the book (Campos Benítez, 2019).



» **Figure 2:** *Card depicting a logical concept, Logica Memorativa, Thomas Murner, 1509 (Campos Benítez, 2019)*

Research on imagery mnemonics offers one explanation for why medieval mnemonic imagery was so often strange: the advantage commonly attributed to bizarre images lies less in bizarreness itself than in the uniqueness of the encoding – the more specific an association, the easier it is to recall (Lesgold & Goldman, 1973).
With the spread of books and literacy and the move toward greater rationality in the Enlightenment, the way information was stored changed, and this skill lost its popularity. Images continued to make their own revolutions, as in Diderot's *Encyclopédie*, but they became more realistic and turned toward describing the external world. Today, mnemonic techniques are mostly used with children, most familiarly in alphabet books, where letters are learned in association with familiar objects and creatures. It seems accepted that children learn most easily this way, but it remains unclear why the same approach is considered unsuitable for older learners and adults.

2.3. Personal and collective ways of reading

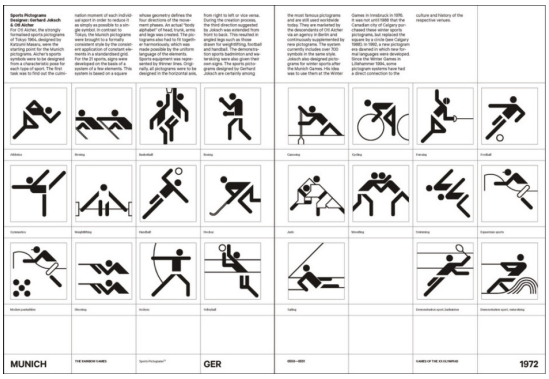
Medieval illuminations remain understandable hundreds of years later, although they were made for a relatively small group of people. One answer to why may lie in the relationship between the personal and the collective. Personal systems of visual communication might seem too idiosyncratically coded to be understood, yet people are shaped by their surroundings – community and culture – which may be the key to reading personal works. Otl Aicher's pictograms for the 1972 Munich Olympics were built on a strictly defined grid, using only certain angles and abstracted depictions of people and objects (Figure 3a). The design philosophy rested on strictly defined rules rather than emotion, and its aim was universality – a sign that communicates regardless of who is looking at it – reflecting the spirit of post-war Germany, which sought to present itself as rational, modern, and international. In the same year, Wolfgang Schmidt began *Lebenszeichen* (*Signs of Life*; Figure 3b).

Although visually refined in a similar way, it had the opposite aim: to describe the personal through visual play, as a systematic visual inventory of the human body, emotions, states, and experiences. Of 893 planned pictograms, Schmidt realized 262, and later applied them to posters, books, installations, and commercial projects.

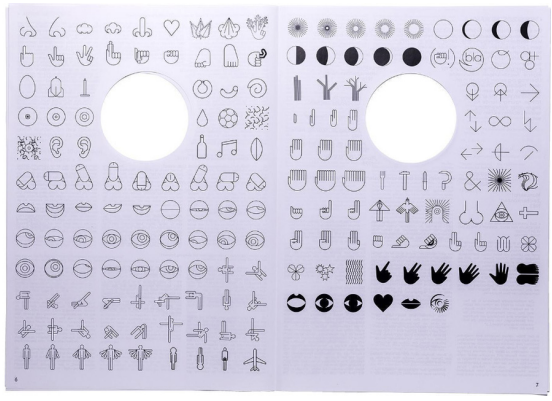
Schmidt's work can be seen as a forerunner of today's emoji, whose role is precisely personal expression and the description of human experience. Unlike Aicher's system, which starts from predefined parameters, Schmidt's developed over time: visual thinking follows the inner logic of the visual thinker, and the system emerges through accumulation. What made *Signs of Life* readable as a game, a system, and a means of expression was the shared, collective experience of corporeality, emotion, and narrative.

This is why the word collective, which implies shared knowledge and values that enable reading through implicit understanding, is used here instead of universal, which implies neutrality and the absence of values.

The same idea can be examined through perhaps the most universal human experience – language. Saussure defines language as a system of signs that express ideas, in which no sign is autonomous: its meaning derives exclusively from its relationships with other signs within the system. Language is a convention, and the nature of the agreed sign makes little difference, which is why Saussure compares language with other sign systems such as traffic signs, military signals, or sign language (Saussure, 1959). It follows that intelligibility arises not from a correspondence between sign and reality but from the internal consistency of the system itself: any set of visual signs that stand in some relationship to one another becomes, in theory, readable.



(a)



(b)

» **Figure 3:** *Pictograms for the Munich Olympic Games, Otl Aicher, 1972 (a; The Olympic Design, n.d.); Signs of Life, Wolfgang Schmidt, 1972 (b; Weirich, n.d.)*

2.4. Comics and visual narratives

Comics are a good illustration of this idea, since their understanding also depends on the relationship between the whole and its parts. Scott McCloud explains how we understand comics as a whole, although they move from panel to panel, through the Gestalt principle of closure – "observing the parts but perceiving the whole" (McCloud, 1993, p. 63) – the way we fill in visual information missing between panels and mentally create a meaningful whole. The principle appears in many historical periods. The Bayeux Tapestry, made in the 11th century, depicts a series of temporally separate events – coronation, negotiations, preparations for invasion, the crossing of the sea, and the Battle of Hastings in 1066 – which read as a clear story, like a comic. In the bands above and below the main scenes, there are parallel narratives, characters, and symbols relying on culturally established knowledge, such as the social and political context, familiarity with Aesop's fables, and the symbolism of the time. McCloud (1993) also describes *non-sequitur* transitions, sequences of seemingly unrelated panels that become a whole simply by being placed in sequence; by the same principle, a collage is perceived as a whole although it combines very different materials. The format, the page, and the series of pages are therefore key to perceiving parts as connected, suggesting that visual understanding is far more elastic than mere enrichment or interpretation of text.

2.5. Who is a good student?

For Rancière (1991), learning is one of the fundamental properties of human intelligence. He compares this natural ability to solving riddles and to connecting what we already know with what we want to learn, citing the mother tongue, which all children master through communication, attempts, failures, and play. Children also learn visual language through drawing: they use it to imagine, describe objects and beings, and recall what interests them, categorizing, deconstructing, and exploring relationships between things without instruction. Most people therefore have experience of visual learning, but this language is forgotten because it is not cultivated.

In school, the learning process becomes alienated, and understanding is turned into absolutes and dichotomies of right and wrong, with interpretation in the hands of an authority who decides whether an understanding is correct. Because understanding is placed in the hands of another, the world begins to divide into two intelligences, inferior and superior – a distinction that finds parallels with Arnheim's intuitive and intellectual cognition. Rancière calls this pattern the circle of powerlessness, and opposes to it intellectual emancipation: the awareness of the equality of intelligences, and the conviction that what makes a person incapable of learning is not a lack of instruction but the belief in the inferiority of one's own intelligence. The most an emancipated person can do for another is to encourage them to become emancipated too (Rancière, 1991), and one way of doing so is to offer one's own model of thinking. One reading of this project is precisely as such an offer.

2.6. Characteristics of the Hungarian language

Before the lessons, Hungarian was almost entirely unfamiliar. It shares some similarities with Serbian, including certain identical or similar words, especially in everyday domains such as food or administration, and both languages have phonetic scripts, so the logic of reading is the same. However, Hungarian has 14 vowels compared with five in Serbian, which initially makes correct reading difficult, especially since a wrong vowel can completely change the meaning of a word. The differences are more numerous still: surnames are written before first names, dates follow the year-month-day format, and the end of a sentence often determines its meaning. Hungarian belongs to the Finno-Ugric family, but shares very few useful similarities with Finnish.

Hungarian is an agglutinative language, meaning that words are formed by adding suffixes and prefixes to a root. From the root *tan*, for example, as many as 16 different terms can be derived, from *tanár* (teacher) to *hangtan* (phonetics). Suffixes express location, possession, position, and movement, while verbal prefixes can change the meaning of a verb entirely (Gyöngyösi & Hetesy, 2014; Lingvopedia, n.d.).

A good example is the sentence *Kimegyek az állatkertből* (I am going out of the zoo): *állat* – animal, *kert* – garden, *-ből* – suffix meaning "out of"; *ki-* – verbal prefix meaning "out," added to *megy* – to go; and *-ek* – ending for the first person singular, present tense. What makes Hungarian particularly interesting for visualization is the combination of strict grammatical rules and vivid compound words, as well as a script in which diacritics, found on nine vowels, give an expressive and playful character.

At the beginning it is important to understand the basic rules and logic of the language, while learning vocabulary leaves ample room for imagination. Two examples that became illustrations in the zines are *bundáskenyér* (French toast), literally "bread in a fur coat" (*bunda* – fur coat, *kenyér* – bread), and *nagynéni* (aunt), literally "big auntie" (*nagy* – big, *néni* – auntie).

3. Methods

The first step took place in the context of Hungarian lessons, as described above. The visualization of the material first happened through sketches, followed by a phase of shaping the sketches into drawings and grouping them into thematic units. After that, the work focused on ways of understanding and navigating the content that would make it easier to read. The final part of the process was the production of the zines, posters, and cards, and attention to the material qualities of the objects, whereby the whole work turns fully toward the reader.

3.1. Understanding and memorizing through visualization

The guiding principle of visualization in learning is simple: connecting the unknown with the known. Vowel harmony, for example – the principle by which the choice of a suffix is determined by the type of vowels in the word – was personified as an opera singer (Figure 4). The character is familiar and clear in memory, and her expressive pose is amusing, which increases the chance that she will be remembered; the whole image serves as a mnemonic trigger for the concept of vowel harmony. Spontaneity is an integral part of the process, since associations arise while focusing on the material rather than on the act of drawing. Through an expressive and free visual language, an imaginary world of Hungarian is built, creating a deeper connection with the language: the thought process does not end with understanding a word but extends into associative mapping and emotional acceptance. This whole process is an act of visual thinking in Arnheim's sense – the drawings are not illustrations of content or literal situations, but a way of thinking and of arriving at the essence of what is being learned.

3.2. Shaping the content

The second part of the process involved building on the basic drawings. The opera singer, for instance, was connected with the relevant material – the two main groups of vowels, high and low. The high vowels are placed at the top of the opposite page and the low vowels at the bottom, so that the whole visual appearance of the spread can be memorized and the material recalled through the arrangement of its elements and the relationships between them (Figure 4). Typography also contributed to memorization in various ways, sometimes because the letterform itself was expressive or contained something that could be connected with the object it names, and sometimes because the nature of the stroke conveyed the feeling of the word: *jeges* (icy) looks as if it is shivering, while *forró* (hot) looks as if it is burning.

The original zine served as a guide to the feeling to be preserved in the work (Figure 5). The visual language partly retains the rawness of sketches, associated with sincerity and immediacy. Three interrelated thematic units emerged from the material: the first covering the basic rules of Hungarian, the second more specific grammatical rules and an introduction to sentence building, and the third the memorization of words. A dominant color was chosen for each, evoking, respectively, accessibility, focus, and fun. The original zine fit on a single A4 sheet and served mainly as a reminder and a curiosity; the aim then was only to shape sketches into drawings and connect them into a whole instead of leaving them scattered across a notebook. The zine format, popular among subcultures that do not necessarily have a wide audience, was retained

for its immediacy, small dimensions, and low production cost, and adapted to the expanded content.



(a)



(b)

» **Figure 4:** *Opera singer drawing and extension of the content, Kis magyaróra I (Serbian-language edition), A. Komadina, 2026*



(a)



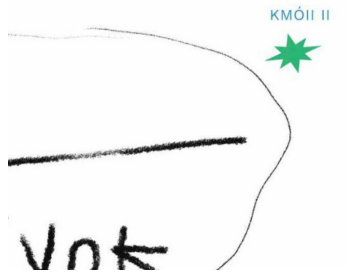
(b)

» **Figure 5:** *Spread from the original Kis magyaróra zine, 2024 (a) and from Kis magyaróra III, 2026 (b), A. Komadina*

3.3. Communicating with the reader

An important motivation for shaping the illustrations into zines was the wish to share a new approach to learning with two groups of readers: people who already learn Hungarian or are interested in Hungarian culture, and others who may have no particular interest in the language but are drawn to the visual language. The last step therefore involved looking at the content from a distance, consciously considering the reader for the first time. The aim was for the content to sit on the border between intelligibility and play, preserving a sense of discovery while offering enough explanation to remain understandable.

Addressing the reader is also visually coded through the Work Sans typeface, which is neutral in relation to the handwriting but round and friendly (Figure 6b). It carries background information – instructions on how to read a page, short grammar rules, or simply the title of a topic. Navigation symbols indicate that the material is easy (Figure 6a), that it builds on something from another zine, or that it is an example of the topic at hand; they are vector-precise and refined, matching the code used for addressing the reader. Reading thus requires a degree of intellectual independence and the will to build understanding rather than receive the material through exhaustive instructions, reflecting Rancière's thesis of intellectual emancipation. The approach relies on the natural human capacity for narrative closure (McCloud, 1993) and on the intuitive understanding of a whole through its parts, which is the logic of language itself (Saussure, 1959).



(a)



(b)

» **Figure 6:** *Star symbol indicating easy material (a) and Work Sans in relation to handwriting (b), Kis magyaróra II, A. Komadina, 2026*

The learning cards and posters have a dual function: they can be used for learning, but also serve as decorative objects. Even in the latter case, they keep their original role, since through constant exposure learning happens unobtrusively. The posters were made on the same principle as the zines, with familiar illustrations extended with new material (Figure 7). The whole series – zines, cards, and posters – functions as a mnemonic map, that is, as mnemonic triggers organized into a whole.



(a)



(b)

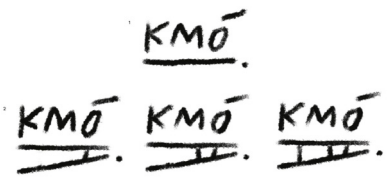
» **Figure 7:** *A6 page from Kis magyaróra III (a) and the related A3 poster (b), A. Komadina, 2026*

In addition to the printed version, the work exists in digital form, which allows easy and relatively inexpensive reproduction and use.



» **Figure 8:** *Zines Kis magyaróra I, II, and III with posters, A. Komadina, 2026*

The production also has a sustainable character. All material was risograph-printed, mostly in a single color, with the exception of details in the zines. Risograph printing has a smaller environmental footprint than laser or inkjet printing, as it uses soy- or rice-bran-based inks instead of inks with toxic solvents and prints without heat, significantly reducing energy consumption. The work is bound with a hand stapler, and most of the printed material was used. The series has a flexible logo that can denote both individual issues and the whole series (Figure 9), leaving the series open to visual continuation without loss of consistency.



» **Figure 9:** *Logo of the Kis magyaróra series, A. Komadina, 2026*

4. Results

The three zines present the basic grammatical rules and some linguistic features of Hungarian. Through a series of visual associations and short written explanations, they show how learning can itself be a creative process and propose a different approach to learning languages and to acquiring new knowledge in general.

The series, titled *Kis magyaróra I, II,* and *III*, consists of zines with accompanying learning cards, bound together with bands containing short usage guidelines, and posters (Figure 8). The zines and cards are A6, while the posters are A3.

5. Discussion

The series can be read in several ways: as an aid to learning, as an introduction to and advocate for learning a new language, and as an object with aesthetic value. The last and broadest reading connects directly to the medieval understanding of visual mnemonic devices as mental models for thinking and remembering.

Just as Schmidt's *Signs of Life* became readable through shared experience, the personal associations in the zines rely on collective knowledge, such as familiar characters, everyday objects, and humor, which allows others to read a system that originated as a private learning tool.

The project has firm conceptual foundations in learning and visualization, as well as a clear visual language, which opens space for further development in several directions. An interpretation in digital space, through a website or an application, would make the content more accessible, add a layer of interactivity and play, and raise the question of the role of movement in memory. Within applied arts, the series could be expanded with additional posters and cards or other functional objects. Since the method is artistic, its effect on other learners has not yet been systematically evaluated, and testing the materials with different groups of learners would be a valuable next step. The most ambitious direction would be to examine the possibilities for an entirely new, more personal and intuitive model of learning and teaching, applied to languages but also to other fields of knowledge.

6. Conclusions

Drawing is a tool for thinking, and it can create a space in which acquiring knowledge is a creative process. This project examined how drawing can translate linguistic structures and create a personal space of meaning. The process shows that visual learning rests not only on the aesthetic dimension of the image but on its capacity to organize, transform, and convey meaning through a system of associations. The visual interpretation of Hungarian lessons demonstrated how the symbolic system of a language can be translated into a visual system with its own logic, in which each illustration functions as part of a mnemonic map and visual patterns are remembered through form and emotional context, not only through rules.

The zine format plays an important role, becoming an object that imitates the thought process: a portable set of mnemonic triggers and a diary of learning, through which visual thinking becomes visible and accessible to others. In the spirit of Rancière's emancipated learner, the reader is offered a model of visual thinking. On a theoretical level, the work supports Arnheim's thesis of the unity of perception and thinking: the visual image is not a reproduction of a concept but its equivalent in thought. Most contemporary educational systems still rely predominantly on linear ways of learning, although memory is by nature associative and tied to emotion. The advantages of a visual, simultaneous, and personal system of learning may be especially important at a time when linear reasoning is increasingly left to machines.

7. Acknowledgments

This paper is based on the author's master's thesis at the Academy of Arts, University of Novi Sad, study program Graphic Communications, completed under the mentorship of Prof. Gabrijela Spasojević.

8. References

Arnheim, R. (1969) *Visual Thinking.* Berkeley: University of California Press.

Campos Benítez, J.M. (2019) 'Analogy and visual content: The Logica memorativa of Thomas Murner', *Philosophies*, 4(1), p. 2. DOI: 10.3390/philosophies4010002

Carruthers, M. (2008) *The Book of Memory: A Study of Memory in Medieval Culture.* 2nd edn. Cambridge: Cambridge University Press.

Gyöngyösi, L. and Hetesy, B. (2014) *Szia! Jó napot! Viszlát!* Novi Sad: Forum Könyvkiadó.

Lesgold, A.M. and Goldman, S.R. (1973) 'Encoding uniqueness and the imagery mnemonic in associative learning', *Journal of Verbal Learning and Verbal Behavior,* 12(2), pp. 193–202.

Lingvopedia. (n.d.) *Hungarian*. Studio GAUS GmbH. Available from: https://lingvo.info/lingvopedia/hungarian [Accessed 25 September 2026].

McCloud, S. (1993) *Understanding Comics: The Invisible Art.* Northampton, MA: Kitchen Sink Press.

Rancière, J. (1991) *The Ignorant Schoolmaster: Five Lessons in Intellectual Emancipation.* Translated by K. Ross. Stanford: Stanford University Press.

Saussure, F. de (1959) *Course in General Linguistics*. Translated by W. Baskin. New York: Philosophical Library.

The Olympic Design. (n.d.) *Munich 1972 pictograms.* Available from: https://www.theolympicdesign.com/olympic-games/pictograms/munich-1972/ [Accessed 25 September 2026].

Weirich, M. (n.d.) *All the Things You Are: The Signs of Life by Wolfgang Schmidt.* Available from: https://www.maximweirich.info/projects/all-the-things-you-are-the-signs-of-life-by-wolfgang-schmidt [Accessed 25 September 2026].

© 2026 Authors. Published by the University of Novi Sad, Faculty of Technical Sciences, Department of Graphic Engineering and Design. This article is an open access article distributed under the terms and conditions of the Creative Commons Attribution license 4.0 Serbia (http://creativecommons.org/licenses/by/4.0/rs/).

Professional Paper https://doi.org/10.24867/GRID-2026-p88

From Studio to Shelf: Integrating Retail Contexts into Packaging Design Education

ABSTRACT

Packaging design projects in the classroom are usually judged in the studio, up close, with full control over lighting, scale, and context. But a real shelf does not offer any of that. This paper looks at three student designed brand systems, Lapinette, Crema Bianca, and PECK, developed in a Fall 2025 undergraduate Package Design course at the American University in Dubai (AUD), and asks a simple question: does packaging that succeeds in a studio critique also succeed on a shelf? Each brand was built from concept to final production and evaluated through instructor and peer critique once completed. What came out of this critique is what this paper calls a translation problem: even the strongest, most carefully researched projects showed gaps once shelf conditions were considered, mainly around legibility at a distance and how clearly color communicated flavor or category. The critique also surfaced a second finding worth separating out, that being noticed on a shelf and being wanted enough to buy are not the same thing. Rather than treating these gaps as mistakes, this paper argues they point to something useful for design education: that the studio and the shelf are simply testing different skills, and that packaging design courses would benefit from treating the shelf itself.

Petra Merhy

Department of Visual Communication, American University in Dubai (AUD), Dubai, United Arab Emirates

KEY WORDS

Packaging design education, shelf visibility, practice-based research, retail context, design pedagogy

1. Introduction

Packaging is one of the only design objects that most people physically pick up, compare, and choose between on a near-daily basis, often without ever recognizing it as a design decision at all. A shopper reaching for cereal, ice cream, or crackers is making dozens of small visual judgments in a matter of seconds, usually without pausing to think about typography, color, or hierarchy in any conscious way. This everyday familiarity can make packaging feel like a simple design task, but it is precisely this speed that makes it one of the more demanding ones. A shopper typically has only a few seconds to notice a product, understand what it is, and decide whether it is worth a second look, all while competing against dozens of other products vying for the same sliver of attention (Klimchuk & Krasovec, 2013). Packaging, in this sense, has been described as functioning like a silent salesman, communicating a brand's identity and value without a person there to explain it (Klimchuk & Krasovec, 2013), and doing so almost entirely within the narrow window of a shopper's glance.

Despite this, packaging design education is often developed and evaluated within the studio, a space that removes many of the pressures of the real shelf. Visual attributes such as color contrast, typography, imagery, and structural form are known to play a critical role in attracting attention and differentiating products under real, crowded retail conditions (Underwood, Klein & Burke, 2001), yet studio-based packaging projects frequently prioritize conceptual development, branding narrative, and aesthetic polish over how a design will actually perform once removed from that controlled setting (Underwood, 2003). Industry-focused literature has similarly emphasized that packaging should be evaluated in relation to its surrounding competitors rather than as an isolated object (Pentawards, 2023), a retail-centered

lens that is often missing from academic critique, where a project is more commonly judged on its own terms, at close range, and without competition. This gap connects to a broader question in design pedagogy about

how students learn to apply their skills under real-world conditions. Experiential learning theory holds that learning is strengthened through direct experience, reflection, and application, rather than through instruction alone (Kolb, 1984), and design disciplines in particular tend to generate knowledge through cycles of making, testing, and reflecting on real practice (Biggs & Büchler, 2008). Assessing design work adds a further layer of difficulty here, since design outcomes are still frequently judged through subjective critique rather than more measurable performance indicators (Davis, 2017), a challenge that becomes especially visible in packaging, where success depends heavily on how quickly and clearly a design communicates to a viewer who was never going to look closely in the first place (Clement, Kristensen & Grønhaug, 2013).

This paper examines that gap through three student-designed brand systems, Lapinette, Crema Bianca, and PECK, developed as part of an undergraduate Package Design course. Each brand was evaluated through instructor and peer critique following completion, with a specific focus on how the packaging was likely to perform under real shelf conditions rather than in studio presentation alone. Rather than treating any shortcomings surfaced through this process as failures, this paper argues that they point to a translation problem: a distinction between the skills that make packaging succeed in a studio setting and the skills that make it succeed on an actual shelf. The following sections outline the methodology used to gather and evaluate this material, present the three case studies in detail, and discuss what their shared patterns suggest about packaging design education more broadly.

2. Methodology

This study follows a practice-based, qualitative case study methodology. The material analyzed is not survey or experimental data, but the actual design work produced by students, alongside the discussion and critique that surrounded it. This approach fits the nature of design research, where knowledge is generated through making, testing, and reflecting on real practice rather than through detached measurement (Biggs & Büchler, 2008).

The data for this paper comes from a Package Design course (VCGD362) taught in Fall 2025, in which twelve students worked individually to build a complete brand identity, from concept to shelf-ready packaging, with a minimum of six products or SKUs per brand. From this cohort of twelve, three projects were purposively selected as case studies for this paper: Lapinette, Crema Bianca, and PECK. These three were not chosen because the entire class performed at the same level, but because these particular students executed the process correctly at every stage, from the initial market research to the final choice of SKUs, typography, and color. This is a deliberate methodological choice: if weaker projects showed gaps between studio design and shelf performance, the finding would be unremarkable. The fact that even carefully executed, well-researched projects still showed these gaps is precisely what makes the case studies useful evidence for this paper's argument, that strong work on a laptop or in a studio presentation does not automatically translate into strong performance on an actual shelf.

2.1. Data Collection: The Course Process (Fall 2025)

The first stage of data collection took place during the course itself. Before any design work began, students were required to visit a supermarket they shop at regularly and identify a product category they wanted to work with. Each student photographed an average of four to six competitor products, a mix of examples they felt worked well and examples they felt did not, whether in terms of visual appeal, clarity, or shelf presence. These photographs were then discussed as a class, allowing students to identify what to aim for and what mistakes to avoid before starting their own designs.

The project brief, communicated to students through the course syllabus and weekly reminders on Blackboard, required a fixed structure for the final submission: an introduction and project brief, brand development (logo, color, typography, brand story), market research and competitor analysis, concept development (mood boards and sketches), structural design, graphic design and flavor differentiation, prototyping, physical documentation of final prototypes, digital mockups and shelf display renders, and a

final reflection. Digital mockups were mandatory specifically as a contingency, so that a project would still be fully presentable even if the physical print quality fell short.

Beyond in-class discussion, students were also instructed to test their work informally with classmates, friends, and family before bringing it to the instructor, treating these informal viewers as stand-in customers whose honest reactions mattered as much as academic feedback. Once packaging was printed, mocked up, and photographed, all twelve projects were presented and critiqued as a group, with the instructor and all students present. Each project received approximately ten minutes, a short presentation followed by open critique. Critique was semi-structured around a consistent set of questions: does this stand out on a shelf, do you like it

and why or why not, what would you normally buy in this category, and would you be interested in buying this new product instead. Several students were notably candid in this stage, stating plainly that they would not personally buy a given product and explaining why, which added a layer of honest, consumer-style feedback beyond academic critique. Feedback during these sessions was captured through instructor field notes; the sessions themselves were not audio or video recorded. Final photographed work and digital mockups were separately documented by students and submitted through Blackboard as part of the final presentation.

2.2. Data Analysis: The Research Process (Summer 2026)

The second stage of this study is distinct from the course itself. Following the completion of the Fall 2025 course, the three selected case studies were revisited as a formal research process during Summer I 2026, structured around a seven-week plan: a literature review situating the project within existing packaging and pedagogy research, a review of the shelf-related critique data already gathered during the course, synthesis of the instructor field notes against the final submitted documentation, comparative analysis between studio-stage design decisions and shelf-related critique findings, and preparation of the findings into this paper. Framing the course and the research as two separate stages, rather than treating the course itself as the study, allows this paper to move beyond a simple project report and to instead analyze the course outcomes with a research lens applied after the fact.

2.3. Limitations

Two limitations of this methodology are acknowledged directly. First, the shelf evaluation conducted in this study did not involve a true side-by-side comparison with physical competitor products on an actual shelf; competitor comparisons instead relied on students recalling and referencing the market research they had conducted earlier in the project. Second, the critique panel was limited to the instructor and peer students within a single class, rather than including other design instructors, external evaluators, or actual consumers. Both limitations are addressed further in the concluding sections of this paper as directions for future coursework and research.

3. Case studies: Three Student Brand Systems

The case studies presented in this paper come from a Package Design course (VCGD362), where senior students were asked to build a complete brand identity from concept to shelf-ready packaging, with a minimum of six products or SKUs. The project ran over roughly 40 days and moved through several stages: market research, concept development, structural and graphic design, prototyping, and final production. What makes this project useful for the present study is not only the final output, but the way shelf awareness was built into the process from the very beginning, and then tested again at the end through public critique.

Before any design work began, students were asked to visit a supermarket they shop at regularly, walk through the aisles, and identify a product category they wanted to work with. They were then asked to photograph examples they liked and examples they felt were not working, whether in terms of visual appeal, clarity, or shelf presence. These photographs became the basis for an in-class discussion comparing strong and weak packaging examples, so that students could identify what to aim for and what mistakes to

avoid before starting their own designs. This early exposure to real shelf conditions, rather than a purely conceptual studio brief, set the tone for the rest of the project.

Once the final packaging was printed, mocked up, and photographed, the projects were exhibited on campus for one week. During this time, students presented their work to the class and to the instructor, discussing their design decisions, the challenges they faced, and how their earlier market research shaped their final outcome. It is important to note that this evaluation was conducted through critique and discussion rather than a controlled side-by-side shelf test with competing commercial products; comparisons to well-known brands were raised by students from memory, drawing on the research they had done at the start of the project. Three brands from this cohort were selected as case studies for this paper: Lapinette, a storybook-inspired baking brand; Crema Bianca, a premium Italian gelato line; and PECK, a food and connection-focused brand built around crackers, spreads, nuts, and cheese.

3.1. Lapinette (designed by Emmanuelle Nafaa)

Lapinette is built around a fictional baker character, Delphine, and applies a soft, pastel, storybook aesthetic across a full line of cake mixes, chocolate bars, sprinkles, candles, and whipping cream. During critique, students responded strongly to how distinct the brand felt on the shelf: the vintage, fairytale mood was something they said they rarely, if ever, see in a real bakery aisle, where most competing products lean on bold colors and straightforward product photography rather than narrative illustration.



» **Figure 1:** *Lapinette, final printed brand system as exhibited on campus. Student work by Emmanuelle Nafaa.*

At the same time, the critique surfaced several concerns that are directly tied to shelf performance rather than studio presentation. On the cake mix boxes, the brand name, flavor name, and the words “Cake Mix” all sit at a similar visual weight, which slows down how quickly a shopper could scan the package and understand what it is. The QR code element, styled as a flat, modern graphic, was also flagged as inconsistent with the painted, illustrated style used everywhere else on the packaging. Finally, because every flavor in the line shares the same frame, ribbon, and bunny motif, differentiating between flavors from shelf distance would be difficult without a stronger color or icon system per variant.



» **Figure 2:** *Lapinette Red Velvet Delight cake mix box, showing the shared frame, ribbon, and bunny motif, and the flat QR code element discussed in critique. Student work by Emmanuelle Nafaa.*

3.2. Crema Bianca (designed by Asma Nowbandi)

Crema Bianca takes a more restrained, minimalist approach, built around a premium Italian gelato concept with a clean color palette and simple line art across tubs, stick boxes, waffle cones, toppings, and whipped cream cans. In critique, students consistently described the line as looking more expensive and higher-end than typical supermarket ice cream, crediting this to its simplicity, in contrast to the more saturated, pattern-heavy packaging common in the freezer aisle.



» **Figure 3:** *Crema Bianca, final printed brand system, including tubs, stick boxes, waffle cones, toppings, and whipped cream cans. Student work by Asma Nowbandi.*

However, that same simplicity introduced some shelf-related risks. The flavor names on the tub lids, set in a script or serif typeface, were noted as elegant but low in contrast against the busy floral or marbled patterns behind them, which would likely be hard to read quickly at freezer-case distance. The color-to-flavor logic was also inconsistent: purple for lavender or green for olive oil reads intuitively, but pink for “Rosa Rosa” or tan for vanilla would be harder for a shopper to decode at a glance, without relying on the text. Additionally, the seamless illustrated pattern that worked cleanly on the flat tub label became visibly distorted when wrapped around the curved paper cups, a challenge the student had already identified in her own reflection on the project.



» **Figure 4:** *Close-up of Crema Bianca cup lids, showing the illustrated pattern distorting around the curved seam and low-contrast flavor names discussed in critique. Student work by Asma Nowbandi.*

3.3. PECK (designed by Maria Semaan)

PECK is built around the idea of shared eating and connection, inspired by the Lebanese mezza tradition, and includes crackers, spreads, nuts, dried fruits, and cheese. During critique, the hand-drawn illustration style used across the packaging was singled out as a strong point of differentiation, standing out clearly against the more conventional, polished look of typical supermarket packaging in the same categories.



» **Figure 5:** *PECK cracker boxes, final printed packaging, showing the hand-drawn wordmark and background line-art pattern discussed in critique. Student work by Maria Semaan.*

Even so, several issues emerged that would affect how well PECK performs on an actual shelf. On smaller formats, such as jar lids and box ends, the hand-drawn "PECK" wordmark began to compete with the busy line-art pattern used as a background texture, making the logo harder to read at a glance. The brand's category color-coding, while generally effective for shelf differentiation, was not fully consistent: it was unclear in places whether a given color represented a product category or a specific flavor variant. Finally, the cheese products, wrapped in wax and cloth with only a small circular sticker for branding, were flagged as losing brand presence almost entirely against their white wrap and dark staging, despite being some of the most premium items in the line.



» **Figure 6:** *PECK Brie, wax and cloth wrap with a small circular branding sticker, illustrating the reduced brand presence noted in critique. Student work by Maria Semaan.*

3.4. Summary of Findings

Across all three brands, the critique process revealed a consistent gap between what works in a controlled studio presentation and what would likely hold up under real shelf conditions. None of the concerns raised in critique were addressed afterward, as the projects were finalized and exhibited as submitted, without a revision stage. Rather than treating this as a shortcoming, this paper treats it as evidence: the students had internalized shelf-awareness early, through their initial market research, but the 40-day project timeline did not allow space to test and revise their designs against that same shelf-thinking once the work was finished. This gap between early awareness and final execution is discussed further in Section 4.

4. Discussion

Taken together, the three case studies point to a broader issue than any single critique note on its own. Lapinette, Crema Bianca, and PECK were selected precisely because their creators had followed the process correctly, from market research through to final production, and had clearly absorbed the lessons of the early studio brief. Yet all three still ran into shelf-related concerns once evaluated through critique. This is best understood not as a shortcoming in any individual project, but as evidence of what could be called a translation problem: the skills that make a package succeed in a controlled studio presentation are related to, but not identical with, the skills that make it succeed on an actual shelf. A student can follow every step of a brief correctly and still produce work that has not yet been fully translated into shelf-ready communication, because the two contexts are simply not testing the same thing. The studio rewards conceptual strength, narrative, and visual craft at close range; the shelf demands all of that plus near instant legibility from a distance, in competition with dozens of other products for a few seconds of attention.

The most consistent issue across all three brands was legibility and hierarchy at a distance. Elements that read clearly in a close-up studio presentation, such as the flavor names on Lapinette's cake mix boxes, the PECK wordmark against its background pattern, or Crema Bianca's script typography, became harder to parse once shelf distance and competing visual noise were factored in. Closely related to this was the question of color-to-flavor logic. In all three brands, color functioned as a differentiation tool, but its logic was not always intuitive: a shopper scanning quickly relies on color as one of the fastest available cues, often faster than reading text, and when that color mapping is not immediately clear, legibility suffers even if the typography itself is technically readable. This suggests that improving color-to-flavor logic is

not a cosmetic fix but a direct lever for improving shelf recognition (Clement, Kristensen & Grønhaug, 2013).

The critique sessions also surfaced a second, distinct layer of shelf performance that is easy to overlook if visibility is treated as the only goal: purchase intent. Several students were candid during critique in stating that they personally would not buy a given product, even in cases where they liked the design itself. This distinction matters. A package can solve the legibility problem and still not translate into a shopper wanting to buy it, because that reaction was not about whether the design was noticed or understood correctly, but about brand and product fit, personal taste, or simply not being the target customer for that particular

flavor or concept. Visibility and purchase intent are therefore best treated as two separate hurdles rather than one. Being seen and read correctly on a shelf is a necessary first step, but it is not the same as being wanted, and design evaluation that stops at legibility risks mistaking the first hurdle for the finish line.

It is worth being clear about what this paper is, and is not, arguing. The issues identified here are not evidence that the students misunderstood the brief or that the process itself was flawed; if anything, the fact that carefully researched, well-executed projects still surfaced these concerns shows how different the conditions of a real shelf are from those of a studio critique, regardless of how thoroughly a designer has prepared. The market itself is simply a harder, less forgiving test than the studio, and this paper treats that as a market reality worth building into design education, rather than as a gap in any single project or process.

This points naturally to a direction for future work. The present study relied on critique and discussion rather than a direct, side-by-side comparison with real competitor products, a limitation already noted in Section 2. A useful next step would be to test student packaging more directly against actual competitor products, either by physically placing them together on a shelf or by building a virtual shelf simulation, to observe more precisely how these designs perform in direct visual competition rather than in critique discussion alone. Doing so would allow the translation problem identified here to be tested, and potentially addressed, under conditions much closer to the real retail environment these designs are ultimately meant for.

5. Conclusions

This paper set out to examine how three well-executed student packaging projects, Lapinette, Crema Bianca, and PECK, held up once evaluated with shelf conditions in mind, rather than through studio presentation alone. Across all three, the same underlying pattern emerged: work that was conceptually strong, well researched, and carefully produced still surfaced legibility and recognition concerns once shelf distance and competition were taken into account. This paper has argued that this is best understood as a translation problem, a distinction between the skills required to succeed within a studio setting and the additional skills required to succeed on an actual retail shelf, rather than as any failure on the part of the students or the process they followed.

The most consistent finding across the three case studies was that legibility and recognition at a distance, closely tied to how intuitively color communicated flavor or category, remained the clearest gap between studio and shelf performance. A second, related finding was that visibility and purchase intent are not the same thing: a package can be noticed and correctly understood and still fail to be wanted, a distinction that matters for how shelf performance is evaluated going forward. Together, these findings suggest that packaging design education would benefit from treating the shelf, and not only the studio critique, as a genuine site of testing and learning.

This study is limited by its reliance on critique and discussion rather than a direct, side-by-side comparison against real competitor products, and by a critique panel limited to the instructor and peer students. Future work building on this paper could address both, either through a physical shelf test placing student packaging alongside real competitor products, or through a virtual shelf simulation that allows for repeatable, more controlled comparison. Such a step would extend the practice-based approach used here, allowing the translation problem identified in this paper to be tested more directly, and would offer a clearer picture of what packaging design education still needs to teach once a project leaves the studio and enters the market it was always meant for.

6. Acknowledgments

The author would like to thank the students of the Fall 2025 Package Design (VCGD362) course at the American University in Dubai, in particular Emmanuelle Nafaa (Lapinette), Maria Semaan (PECK), and Asma Nowbandi (Crema Bianca), whose brand systems form the basis of the case studies in this paper.

7. References

Biggs, M. and Büchler, D. (2008) 'Eight criteria for practice-based research in the creative and cultural industries', *Art, Design & Communication in Higher Education*, 7(1), pp. 5–18.DOI: 10.1386/adch.7.1.5_1

Clement, J., Kristensen, T. and Grønhaug, K. (2013) 'Understanding consumers' in-store visual perception: The influence of package design features on visual attention', *Journal of Retailing and Consumer Services*, 20(2), pp. 234–239. DOI: 10.1016/j.jretconser.2013.01.003

Davis, M. (2017) *Teaching Design: A Guide to Curriculum and Pedagogy for Graphic Designers*. New York: Allworth Press.

Klimchuk, M.R. and Krasovec, S.A. (2013) *Packaging Design: Successful Product Branding from Concept to Shelf*. 2nd ed. Hoboken: Wiley.

Kolb, D.A. (1984) *Experiential Learning: Experience as the Source of Learning and Development*. Englewood Cliffs: Prentice Hall.

Pentawards (2023) The Package Design Book 7. Cologne: Taschen.

Underwood, R.L. (2003) 'The communicative power of product packaging: Creating brand identity via lived and mediated experience', *Journal of Marketing Theory and Practice*, 11(1), pp. 62–76.

Underwood, R.L., Klein, N.M. and Burke, R.R. (2001) 'Packaging communication: Attentional effects of product imagery', *Journal of Product & Brand Management*, 10(7), pp. 403–422. DOI: 10.1108/10610420110410531

© 2026 Authors. Published by the University of Novi Sad, Faculty of Technical Sciences, Department of Graphic Engineering and Design. This article is an open access article distributed under the terms and conditions of the Creative Commons Attribution license 4.0 Serbia (http://creativecommons.org/licenses/by/4.0/rs/).

Review Paper https://doi.org/10.24867/GRID-2026-p89

Crossing the Boundaries of Conventional: Examining Various Approaches in Teaching Video Game Development

ABSTRACT

Working as a teacher, professor, or instructor involves many roles, one of the most important being the conveyance of knowledge to students. Or is it? A shifting and unstable job market, inaccessible equipment, a lack of information, and many other factors represent obstacles that should be addressed in order to update a potentially obsolete curriculum and remain current. In addition, the emerging use of machine learning tools raises questions about the educational system as a whole and the way it conveys knowledge and adapts its programs and curricula to this new environment. The ever-changing job market also influences the way teachers approach designing their classes and how they interact with students. This paper examines the existing literature on different practices for teaching game development in order to better understand contemporary teaching frameworks. It also investigates different methods of teaching video game development to contribute to the scientific community and the existing body of research. As a result of this investigation, a comparison of the reviewed literature, and insights gained from three years of conducting various courses and programs in the field of game development, several suggestions for teaching approaches and possible future directions are proposed in the hope of improving the way game development is taught in schools and universities, and perhaps even help changing how the educational system is perceived in today's rapidly changing world.

Bojan Banjanin
Tamara Ilić
Jelena Kerac
Rastko Milošević

University of Novi Sad, Faculty of Technical Sciences, Department of Graphic Engineering and Design, Novi Sad, Serbia

KEY WORDS
Video game development, education, video game, curriculum development, studio-based learning, project-based learning, teaching frameworks, mentorship

1. Introduction

Games and their development, technology, industry, jobs, and market demands- the whole world is changing rapidly. It surely should not be different for video game development courses, teaching program structure, and curricula in higher education. If education is viewed alongside Industrial Revolutions, then Education 1.0 begins with the First Industrial Revolution in the 18th century. It assumes the lecturer at the centre and learners who have a mostly passive role (Miranda et al., 2021). The Second Industrial Revolution brought Education 2.0, with learners a little bit more engaged in the education process. Education 3.0 characterized computerization where learners were empowered to educate themselves independently from the teaching process. Lastly, in Education 4.0 teaching process characterize technological advancements enabling digitalization, virtualization, datafication and smartification (Ramírez-Montoya et al., 2022; Kowalski et al., 2026). In works of Banjanin and his colleagues (Banjanin et al., 2022; Banjanin et al., 2024), the authors investigated different perspectives on incorporating games into university curriculum. In the first paper, some definitions of games and video games

are discussed, along with the influence of simulations, simulation games, and serious games on learning, as well as advantages of using game-based learning (GBL) in education. The authors concluded that both artistic and technical skills can be and should be developed by using simulation games in the studies of Graphic engineering and design and that further research should be done to propose detailed guidelines and best practices on incorporating game elements in simulation (e.g., of the printing process) and combining knowledge from different branches of engineering and art industry. In the second paper, the authors investigated different approaches to using games in education. The first approach is by using non-educational and educational games (see chapter 2, section 2.1) in the teaching process, and the second one is by implementing constructivist approaches where students learn about certain topics by making games. They also suggested teaching with Community of Inquiry (CoI) in mind, from which they adopted Teaching Presence from the overall educational experience originally introduced by Garrison, Anderson, and Archer (1999).

They implemented all these principles in university lectures and different courses outside of the university curricula which utilized Unreal Engine and Unreal Editor for Fortnite (UEFN) as primary game engines. They analysed the relationship between the number of working hours in one class compared to the total number of hours in the semester. The authors also reported and compared the number of hours spent on traditional follow-along type of teaching (traditional approach), number of working hours in teams, and mentor consultation hours. They discovered a trend where an increased number of working hours on projects, in contrast to the traditional ex cathedra, follow-along approach, can lead to numerous benefits not only for students but also for teachers. Students better understand game design concepts and develop technical skills more independently and with greater understanding of the matter. Teachers, on the other hand, had the opportunity to work on a variety of projects, which led to broadening their knowledge and gave them experience of how to approach similar projects and problems in the future. This approach, combined with the teaching presence adopted from the CoI framework, led to creating open and more enjoyable learning environments. The conclusions were tested in practical settings but were based on qualitative assessment acquired by conversations with the students and backed up by experience from different teaching courses throughout several years of teaching practice.

This paper aims to continue the research discussed in the abovementioned investigations and to build upon them by exploring different approaches found in the recent literature. This is also supported by findings from the recent teaching practice, and the possible framework is suggested according to the examined body of scientific papers.

2. Methods

This study employs a narrative literature synthesis method (Bourhis, 2017) to examine the evolution of educational approaches used in teaching video game development. Narrative synthesis was selected because the field incorporates diverse pedagogical traditions, including research on serious games, game-based learning, constructionist learning, project-based learning, studio-based learning, and professional practice frameworks.

The primary corpus consisted of five influential studies explicitly focused on game-development education, curriculum design, assessment, and professional preparation (Banjanin et al., 2022; Banjanin et al., 2024; Pierce et al., 2025; Hughes & Kavanagh, 2025; Gunnars & Palmquist, 2026).

To strengthen the synthesis, additional systematic reviews related to game-based learning, serious games, project-based learning, and Education 4.0 were incorporated (Huang et al., 2023; Brandl & Schrader, 2024; Mingyu et al., 2024; Khoo et al., 2025; Mushtaq et al., 2025). These sources provided broader contextual understanding regarding emerging trends in higher education and their relevance for contemporary game-development curricula.

The analysed studies were compared according to: (1) Educational objectives, (2) Teaching methodologies, (3) Assessment approaches, (4) Collaboration structures, (5) Industry integration, (6) Learning outcomes, (7) Curriculum recommendations.

The resulting synthesis was used to help identify common themes, developmental patterns, and recurring challenges within the field.

2.1. Serious games and educational applications

The relationship between games and education has attracted considerable scholarly attention over the last three decades. One of the most obvious ways of implementing games into educational practice is by using serious games. Serious games, as defined by Abt (1971) presents fusion of serious thinking and problem-solving with experimental and emotional freedom of gaming. Another definition given by Michael and Chen (2005) defines serious games as games whose main purpose is not entertainment, fun, or pleasure.

Research consistently indicates that serious games provide meaningful opportunities for experiential learning by encouraging active participation rather than passive information consumption (Banjanin et al., 2022; Brandl & Schrader, 2024). The educational value of serious games is closely linked to their ability to create simulated

environments that allow experimentation without real-world consequences. Such characteristics are particularly valuable in disciplines involving expensive equipment, hazardous procedures, or highly complex processes (Banjanin et al., 2022). Brandl and Schrader (2024) suggested that serious games contribute positively to student engagement and motivation but also highlighted the need for more adaptive systems capable of responding to individual learner needs. Importantly, research regarding serious games helped redefine the relationship between technology and education. Rather than treating digital technologies solely as mechanisms for content delivery, researchers increasingly viewed interactive systems as learning environments within which students could construct and test understanding through participation (Banjanin et al., 2022; Brandl & Schrader, 2024).

2.2. Constructionist learning and learning through game creation

While serious-games research focused on the educational use of games, another line of inquiry examined educational value in the process of game creation itself. This perspective draws heavily from constructionist theory, particularly the work of Jean Piaget (1951) and later educational researchers such as Kafai and Burke (2015). Constructionist learning emphasizes the creation of meaningful artifacts through which learners externalize and refine their understanding of concepts and systems. Within this framework, learning emerges through design, experimentation, reflection, and reconstruction. Educational benefits emerge from the process of creating games rather than from interaction with finished products. Works by Gunnars and Palmquist (2026) and Khoo et al. (2025) indicate that such activities contribute to computational thinking, design thinking, systems thinking, creativity, collaboration, and communication skills.

2.3. Project-Based Learning (PBL) in game development education

Project-Based Learning (PBL) has become one of the most influential pedagogical approaches in contemporary game-development education. PBL positions learning within meaningful projects that require students to investigate problems, collaborate with peers, apply theoretical concepts, and produce tangible outcomes. Because professional game development is fundamentally organized around project work, PBL provides a natural alignment between educational practice and industry expectations (Huang Li & Shang, 2023; Gunnars & Palmquist, 2026). A review conducted by Huang and associates found that gamified project-based learning enhances both educational outcomes and learner satisfaction. Their research identified several strategies through which game elements can be integrated into project-based environments, including gamification of project structures, integration of educational games, and game creation activities themselves. Gunnars and Palmquist (2026) identified project-based learning as the internationally dominant educational model within game-development programs. Their findings suggest that projects provide opportunities not only for technical learning but also for professional socialization, interdisciplinary collaboration, and creative experimentation.

2.4. Community of Inquiry, mentorship, and teaching presence

As game-development education increasingly adopts project-based approaches, researchers have devoted greater attention to the role of mentorship and collaborative learning environments. One particularly influential framework is the Community of Inquiry (CoI) (Garrison, Anderson & Archer, 1999), which conceptualizes meaningful educational experiences through the interaction of teaching, social and cognitive presence (Banjanin et al., 2024).

Teaching presence refers to instructional design, facilitation, and guidance; social presence concerns interpersonal interaction and collaboration; and cognitive presence involves knowledge construction through reflection and discourse (Garrison, Anderson, & Archer, 1999). Game-development education provides a particularly suitable environment for the application of this framework because students work collaboratively, engage in continuous dialogue, and participate in iterative development processes (Banjanin et al., 2024). In the work of Banjanin et al. (2024), it was demonstrated that increasing opportunities for project discussions, mentorship, and collaborative work significantly improved educational outcomes. Their findings indicate that students benefit from educational models emphasizing consultation, guidance, and teamwork rather than relying exclusively on instructor demonstrations. Rather than functioning solely as lecturers, educators increasingly assume roles as facilitators, mentors, reviewers, and collaborators. Such developments align closely with both constructionist learning theory and professional practice within creative industries (Banjanin et al., 2024; Pierce et al., 2025).

2.5. Studio-Based Learning and industry simulation

A major development within contemporary game-development education is the adoption of studio-based learning (SBL). Studio pedagogy originates from architecture, industrial design, and fine-arts education and emphasizes learning through creation, critique, revision, and reflective practice throughout involvement in real-life projects (Al-Hammoud, Hussain & Araji, 2025). Unlike lecture-centred instruction, studio environments encourage students to engage directly with problems while receiving continual feedback from peers and instructors (Pierce et al., 2025; Gunnars and Palmquist, 2026).

One of the examples within game-development education is the Game Studio Simulator model developed by Pierce and colleagues (Pierce et al., 2025). Based on more than ten years of curriculum refinement, the model integrates software engineering and game design students into multidisciplinary teams operating within simulated production environments. Students participate in milestone reviews, collaborative planning, project presentations, and iterative development cycles that resemble professional studio workflows. Results suggest improvements in both student satisfaction and learning outcomes.

Studio pedagogy offers several advantages. First, it creates opportunities for authentic collaboration across disciplines. Second, it supports iterative learning through continuous revision and feedback. Third, it develops professional competencies related to communication, teamwork, and project management. Finally, it exposes students to production constraints and organizational structures commonly encountered in professional practice (Pierce et al., 2025; Gunnars & Palmquist, 2026).

Research within university game-development programs likewise demonstrates positive effects of studio-inspired approaches. Educational models allocating substantial time to project work and mentorship consistently produce stronger outcomes than those focused primarily on instructor-led demonstrations. These findings suggest that students benefit from environments where learning occurs through participation and creation rather than observation alone (Banjanin et al., 2024).

In the peer-review synthesis chapter, Güneş et al. (2026) examine international game design programs. They emphasized that successful programs balance technical, artistic, and theoretical competencies. It was also found that studio-based and project-based learning are the most dominant approaches to teaching game design.

In the perspective article, Fauilloux et al. (2025) synthesized evidence on student-led game design. They found that student-created games, which are a combination of game-based learning and design-based learning, promote systems thinking, collaboration, and engagement.

2.6. Limitations

2.6.1. Assessment and collaborative learning

Assessment represents one of the most persistent and complex challenges within contemporary game-development education (Pierce et al., 2025; Gunnars and Palmquist, 2026). While project-based learning and studio pedagogy have become widely accepted as effective educational approaches, institutions continue to face difficulties when evaluating individual student achievement within collaborative production environments.

In their experience, the authors of this paper also experienced this limitation during the implementation of PBL in a university course in game development. Students work in teams of three or two. The main issue arises in determining a quantity of work done by individual members of a team (for example in the case of absence from class during milestone's presentations and during some of the development process in the classroom). So, in some cases, an unequal distribution of the work between team members is noticed, which later appeared as a problem during the assessment.

Students working within multidisciplinary teams contribute in different ways and at different times throughout the production cycle. Students that took a programmer role may produce substantial amounts of code while students with designer role focus on documentation, gameplay systems, and balancing. Students with artistic roles contribute visual assets, user-interface elements, and animations, while students with producer role coordinate schedules, tasks, and communication among team members. These roles were distributed so that one member took various roles in the development process. Because contributions differ in form rather than quantity alone, evaluating individual assessment becomes challenging.

In the work of Hughes and Kavanagh (2025), an innovative solution known as the Trunk and Branch assessment model was proposed. In this approach, students first develop a shared collaborative foundation referred to as the "trunk." Subsequently, each student expands the project through individual work known as a "branch." This structure allows educators to evaluate both collaborative competence and individual achievement while maintaining authenticity within the learning environment. Approximately 72% of participants reported that the approach contributed to their professional development.

2.6.2. Selection of representative research papers

The present study employs a narrative synthesis rather than a formal systematic review or meta-analysis. While the selected corpus includes influential and recent publications, the methodology does not follow strict inclusion and exclusion protocols such as those associated with PRISMA-based review studies (Huang, Li & Shang, 2023; Gunnars & Palmquist, 2026). Consequently, the findings should be interpreted as conceptual and integrative rather than exhaustive representations of the field.

2.6.3. Lack of longitudinal evidence regarding professional outcomes after graduation

Many studies rely heavily on qualitative methodologies, participant feedback, educator observations, and case-study approaches. Although these methods provide valuable insight into educational

practice, they frequently lack longitudinal evidence regarding professional outcomes after graduation. Additional research examining employability, career progression, long-term skill retention, and professional success would strengthen understanding of the effectiveness of different educational models.

3. Results

3.1. Evolution of Educational Thinking in Game Development Education

Analysis of the reviewed literature reveals a progressive evolution of educational thinking regarding video game development. This evolution can be described through four interconnected stages:

1. Stage 1: Games as Educational Tools
2. Stage 2: Learning Through Game Creation
3. Stage 3: Studio-Based Learning
4. Stage 4: Ecosystem-Based Professional Formation

Stage 1: Games as Educational Tools

The earliest educational approaches treated games primarily as instructional media. Educational researchers focused on how serious games and simulations could improve motivation, engagement, and retention of knowledge across diverse academic disciplines. During this period, games were viewed principally as mechanisms for teaching content rather than as objects of study or development (Banjanin et al., 2022; Brandl & Schrader, 2024).

A key contribution of this stage was the demonstration that interactive systems could support experiential learning more effectively than passive instructional methods. Serious games established the legitimacy of interactive learning environments within higher education and contributed significantly to the later development of game-oriented pedagogical approaches (Banjanin et al., 2022; Brandl & Schrader, 2024).

Stage 2: Learning Through Game Creation

The second stage emerged from constructionist theories of learning. Instead of consuming educational games, students were encouraged to create them. Learning occurred through the design and development process itself. Researchers observed that game creation required learners to integrate technical, creative, and organizational knowledge across multiple domains.

As students designed mechanics, built systems, created assets, and evaluated user experiences, they acquired skills extending beyond traditional disciplinary boundaries (Gunnars & Palmquist, 2026; Khoo et al., 2025).

This stage marked a fundamental transition in educational thinking. Educational value no longer originated solely from interaction with finished products but from participation in creation processes.

Stage 3: Studio-Based Learning

The third stage introduced educational models inspired by professional production environments. Programs increasingly adopted multidisciplinary teams, long-term projects, milestone reviews, sprint planning, and collaborative workflows.

Within these environments, students assumed specialized roles resembling industry practice. Learning became situated within authentic contexts, and educational activities mirrored real production pipelines more closely than traditional coursework. Studio pedagogy began replacing isolated assignments with sustained development experiences (Pierce et al., 2025; Banjanin et al., 2024).

Stage 4: Ecosystem-Based Professional Formation

The most recent stage extends beyond project work itself and conceptualizes game-development education as a professional ecosystem. Educational success is no longer measured solely through technical competence but through the development of professional identities, collaborative capabilities, reflective practice, and participation in communities of practice.

Students are viewed as emerging professionals who gradually transition into the industry through mentorship, industry engagement, portfolio development, and authentic production experiences. This ecosystem perspective forms the conceptual foundation of contemporary educational frameworks (Pierce et al., 2025; Gunnars & Palmquist, 2026).

3.2. Proposed game development education framework

The proposed framework synthesizes key findings identified throughout the reviewed literature in the hope of further developing the game education development narrative. This framework can be presented in terms of the six most important aspects (pillars) of contemporary game education approaches (Table 1).

Together, these pillars establish a comprehensive framework for contemporary curriculum development that integrates educational theory, professional practice, and industry requirements and aligns with the reviewed literature.

Table 1
Proposed game development education framework

	Name	Short description
Pillar 1	Project-based learning	Projects function as the primary vehicle for knowledge construction and skill development. Students learn through solving meaningful problems and producing authentic outcomes.
Pillar 2	Multidisciplinary collaboration	Students collaborate across disciplinary boundaries in ways that mirror professional game-production environments.
Pillar 3	Teaching presence and mentorship	Educators guide learning through mentorship, consultation, feedback, and reflective discussion.
Pillar 4	Authentic industry simulation	Educational environments incorporate workflows, methodologies, tools, and practices commonly found within professional studios.
Pillar 5	Hybrid assessment	Assessment balances collaborative achievement with individual accountability through multidimensional evaluation systems.
Pillar 6	Professional identity development	Curricula support the transition from student identity toward professional participation within game-development communities.

3.3. Future research directions

The reviewed literature suggests that future research should move beyond evaluating isolated pedagogical interventions and instead focus on understanding game-development education as a dynamic educational ecosystem (Pierce et al., 2025; Gunnars & Palmquist, 2026).

One of the most significant research priorities concerns longitudinal evaluation of educational outcomes. Most existing studies examine learning outcomes at the conclusion of individual courses, semesters, or academic programs. These investigations frequently report improvements in engagement, project quality, collaboration, and student satisfaction. More research is needed to understand how different educational approaches influence employability, career progression, industry retention, and long-term professional development.

Assessment innovation represents another important area requiring additional investigation. While recent contributions, such as the Trunk and Branch model, provide promising solutions for balancing collaborative and individual evaluation, challenges remain. Future research should explore assessment systems capable of measuring technical competence, creativity, communication skills, leadership, collaboration, and professional development simultaneously.

Generative artificial intelligence is likely to become one of the most influential factors affecting game-development education in the coming years. Tools based on large language models, procedural content generation, machine learning, and AI-assisted programming are already altering professional workflows. The authors of this paper identified, through their work with university students and students across different courses, extensive use of generative AI, primarily Anthropic's Claude and Google Gemini for code generation, issues with workflow, and challenges in finding certain technical solutions during game development. Future studies should investigate the pedagogical implications, ethical considerations, and assessment challenges associated with AI-supported development practices.

4. Discussion and conclusion

The reviewed literature demonstrates a clear transition from content-centred educational models toward ecosystem-oriented professional formation. This transformation reflects broader developments in higher education as well as changing expectations within the game industry.

One of the most significant findings concerns the evolving role of educators. Traditional models positioned instructors as primary knowledge providers. Contemporary approaches increasingly emphasize mentorship, facilitation, consultation, and reflective guidance. Students acquire knowledge through participation in meaningful activities rather than through passive reception of information (Banjanin et al., 2024; Pierce et al., 2025). The convergence between educational theory and professional practice represents another notable trend. Concepts such as project-based learning, constructionism, experiential learning, and reflective practice increasingly align with professional development methodologies including agile production, milestone reviews, iterative design, and collaborative problem-solving (Huang et al., 2023; Pierce et al., 2025; Gunnars & Palmquist, 2026).

Game-development education has evolved substantially beyond its origins in technical instruction. Contemporary programs increasingly emphasize project ownership, multidisciplinary collaboration, mentorship, industry simulation, reflective practice, and professional identity development.

The literature reviewed in this study suggests that four major stages characterize this evolution: games as educational tools, learning through game creation, studio-based learning, and ecosystem-based professional formation. Each stage represents a deeper integration of educational theory and professional practice.

The proposed framework synthesizes these developments into a unified conceptual model. By emphasizing project-based learning, mentorship, collaboration, authentic production, hybrid assessment, and professional identity formation, the framework provides guidance for future curriculum design and educational innovation.

Ultimately, successful game-development education extends beyond teaching students how to build games. It creates ecosystems through which students become game developers.

5. Acknowledgments

This research has been supported by the Ministry of Science, Technological Development and Innovation (Contract No. 451-03-34/2026-03/200156) and the Faculty of Technical Sciences, University of Novi Sad through project "Scientific and Artistic Research Work of Researchers in Teaching and Associate Positions at the Faculty of Technical Sciences, University of Novi Sad 2026" (No. 01-3609/1).

6. References

Abt, C.C. (1971) *Ernste Spiele: Lernen durch gespielte Wirklichkeit*. Kiepenheuer & Witsch.

Al-Hammoud, R., Araji, M. and Hussain, Z. (2025) 'Studio-based learning: fostering integration, creativity and practical skills development', *Proceedings of the Canadian Engineering Education Association (CEEA).* DOI: 10.24908/pceea.2025.19644

Banjanin, B., Kerac, J., Adamović, S. and Milošević, R. (2024) 'Game design studies: Through the educational prism'. In: *Proceedings of the International Symposium on Graphic Engineering and Design (GRID 2024), 14–16 November 2024, Novi Sad, Serbia*. University of Novi Sad, Faculty of Technical Sciences, Department of Graphic Engineering and Design.

Banjanin, B., Milić Keresteš, N., Milošević, R. and Adamović, S. (2022) 'Video games as a learning tool: Potential applications in the graphic engineering and design studies'. In: *Proceedings of the International Symposium on Graphic Engineering and Design (GRID 2022), 3–5 November 2022, Novi Sad, Serbia.* University of Novi Sad, Faculty of Technical Sciences, Department of Graphic Engineering and Design.

Bourhis, J. (2017) 'Narrative literature review'. In: *The SAGE Encyclopedia of Communication Research Methods*, Vol. 4, pp. 1076–1077. SAGE Publications.

Brandl, L.C. and Schrader, A. (2024) 'Serious games in higher education in the transforming process to Education 4.0—Systematized review', *Education Sciences*, 14(3), 281. DOI: 10.3390/educsci14030281

Fouilloux, C.A., Compton, J.S., Naing, N., Anderson, M. and Hite, J.L. (2025) 'Game design as a STEM pedagogy', *Journal of Microbiology & Biology Education*, 27(1). DOI: 10.1128/jmbe.00173-25

Garrison, D.R., Anderson, T. and Archer, W. (1999) 'Critical inquiry in a text-based environment: Computer conferencing in higher education', *The Internet and Higher Education*, 2(2), pp. 87–105. DOI: 10.1016/S1096-7516(00)00016-6

Güneş, F., Ekin, C.Ç. and Aydoğdu, A.G. (2026) *Digital game design education in higher education: Curriculum models, pedagogical approaches and institutional structures*. IntechOpen.

Gunnars, F. and Palmquist, A. (2026) 'Teaching game development at universities: A systematic literature review of educational practices for multidisciplinary industrial demands', *Games and Culture*. DOI: 10.1177/15554120261442965

Huang, W., Li, X. and Shang, J. (2023) 'Gamified project-based learning: A systematic review of the research landscape', *Sustainability*, 15(2), 940. DOI: 10.3390/su15020940

Hughes, E. and Kavanagh, W. (2025) 'Trunk and branch: Fostering autonomous peer supportive learning environments through delivery & assessment'. In: *Proceedings of the 9th Conference on Computing Education Practice (CEP '25)*, pp. 13–16. Association for Computing Machinery.

Kafai, Y.B. and Burke, Q. (2015) 'Constructionist gaming: Understanding the benefits of making games for learning', *Educational Psychologist*, 50(4), pp. 313–334. DOI: 10.1080/00461520.2015.1124022

Khoo, Y.Y., Ramdan, M.R., Abdullah, N.L., Abd Aziz, N.A. and Mahjom, N. (2025) 'The impacts of game-based learning on thinking and learning in higher education context: A scoping review', *International Journal of Education in Mathematics, Science, and Technology*, 13(3), pp. 623–637. DOI: 10.46328/ijemst.4776

Kowalski, M.E., de Vasconcelos Gomes, L.A., Borini, F.M. and Bernardes, R.C. (2026) 'Business-to-business ecosystem smartification for manufacturing: A definition, an integrative framework, and future directions', *Technovation*, 151, 103425. DOI: 10.1016/j.technovation.2025.103425

Michael, D.R. and Chen, S.L. (2005) *Serious games: Games that educate, train, and inform*. Thomson Course Technology.

Mingyu, G., Yunus, M.M. and Rafiq, K.R.M. (2024) 'Educational games and game-based approaches in higher education: A systematic review (2014–2023)', *International Journal of Academic Research in Progressive Education and Development*, 13(1), pp. 899–919. DOI: 10.6007/IJARPED/v13-i1/20555

Miranda, J., Navarrete, C., Noguez, J., Molina-Espinosa, J.M., Ramírez-Montoya, M.S., Navarro-Tuch, S.A., Bustamante-Bello, M.R., Rosas-Fernández, J.B. and Molina, A. (2021) 'The core components of Education 4.0 in higher education: Three case studies in engineering education', *Computers & Electrical Engineering,* 93, 107278. DOI: 10.1016/j.compeleceng.2021.107278

Mushtaq, N., Nazeer, N., Fayaz, I. and Gulzar, F. (2025) 'Next-gen learning: Gamification's impact on higher education', *Education and Information Technologies*, 30, pp. 15691–15717. DOI: 10.1007/s10639-025-13431-w

Piaget, J. (1951) Organization and pathology of thought. Columbia University Press.

Pierce, C., Woodward, C.J., Trevillian, A. and Pham, T. (2025) 'Game studio simulator: Integrating industry practice and formative individual assessment in collaborative game development capstone projects', *ACM Transactions on Computing Education*, 25(4), Article 56. DOI: 10.1145/3764595

Ramírez-Montoya, M.S., Castillo-Martínez, I.M., Sanabria-Z, J. and Miranda, J. (2022) 'Complex thinking in the framework of Education 4.0 and open innovation—A systematic literature review'*, Journal of Open Innovation: Technology, Market, and Complexity,* 8, 4. DOI: 10.3390/joitmc8010004



© 2026 Authors. Published by the University of Novi Sad, Faculty of Technical Sciences, Department of Graphic Engineering and Design. This article is an open access article distributed under the terms and conditions of the Creative Commons Attribution license 4.0 Serbia (http://creativecommons.org/licenses/by/4.0/rs/).

Emerging technologies

09

Professional Paper https://doi.org/10.24867/GRID-2026-p90

Rapid Prototyping and Fabrication of Unmanned Surface Vessels: A 3D Printing Case Study

ABSTRACT

The transition from a computer-aided design (CAD) model to physical fabrication is a critical stage in the development of Unmanned Surface Vessels (USVs). Despite the efficiency of computational approaches for accelerating the design and optimization of complex geometry forms, the physical validation of these digital models remains a key step to ensure their viability. The proposed paper offers a holistic case study on the fabrication of parametrically designed USVs using 3D printing technologies. The primary objective is to evaluate the practical constructability of the algorithmically generated geometries in order to transform them into tangible products. The physical prototypes are evaluated based on the following parameters: printability, structural continuity of segmented hull parts, surface smoothness, and assembly capabilities. Based on the findings, the integration of additive manufacturing into a parametric design workflow can be established within a reliable framework considering manufacturing methods and assembly strategies that the product requires depending on its operational conditions.

George-Robert Reynik
Panagiotis Kyratsis

University of Western Macedonia,
Department of Product and
Systems Design Engineering,
Kila Kozani, Greece

KEY WORDS
Unmanned surface vessels, 3D printing, rapid prototyping, computational design, modular assembly, fabrication

1. Introduction

The design and manufacturing of Unmanned Surface Vessels (USVs) require a methodical approach to ensure that complex hull forms can withstand real-world operational demands. Traditionally, the development cycle of marine vessels has relied on extensive physical modeling and iterative testing.

Recently, this process has been significantly streamlined by computational design tools that automate the generation of hull geometries to achieve rapid prototyping. However, a successful design is not defined solely by its digital representation; it must also account for production limitations and physical constructability. Transforming a digital USV design into a physical prototype introduces several manufacturing challenges, particularly when utilizing additive manufacturing. A holistic product design approach must consider how the vessel will be fabricated, evaluating parameters such as the structural integrity of the printed parts, the continuity of segmented sections, and the overall surface smoothness and curve fairness, which impacts hydrodynamics. The purpose of this paper is to evaluate the transition of algorithmically generated USV geometries into tangible, functional prototypes. Rather than focusing on the computational mechanics of the generative algorithm, this study serves as a practical evaluation of its physical output.

By producing scaled models utilizing 3D printing technologies, the research assesses important fabrication factors: the compatibility of the generated models with 3D printing hardware, the structural continuity of segmented hull parts upon assembly, the resulting surface smoothness, and the overall ease of assembling the modular components. Ultimately, this physical validation aims to confirm that the generated geometries are not merely theoretical concepts, but practical, constructible solutions for rapid marine prototyping.

2. Literature survey

Nowadays, algorithmic and computational design represent a transformative methodology in modern product development, shifting the focus from manual geometric manipulation to parameter-driven processes (Kyratsis et al., 2025b). By establishing a direct relationship between design intent and mathematical parameters (Pektas, 2023), this approach allows for the automated generation of complex forms. The dynamic nature of parametric modeling means that any adjustment to foundational variables automatically updates the entire model (Janssen & Stouffs, 2015), enabling rapid exploration of diverse design iterations without needing to rebuild geometries from scratch. This continuous evolution of shapes based on predefined rules ensures both flexibility and precision.

In recent years, the integration of computational design directly with digital manufacturing technologies has emerged as a cornerstone of Industry 4.0 (Kyratsis et al., 2025a). This alignment optimizes not only the generation of the product's form but also its physical fabrication. Automating the product design phase creates a seamless pipeline that drastically reduces development time and enhances manufacturing efficiency across various industries (Aidinli et al., 2025).

2.1. Prototyping in Marine Design

Historically, marine architecture relied heavily on the systematic testing of scaled physical models to analyze factors like resistance and hydrodynamics (Fonseca et al., 2022). As computational technologies advanced, software-based simulations largely replaced physical models during the preliminary design stages, allowing for automated generation and testing of various hull forms (Park et al., 2022).

However, despite these digital advancements, physical prototyping remains a critical step in the modern design cycle. Computational design systems excel at creating diverse, complex geometries tailored to specific operational requirements. Yet, translating these digital variations into functional marine vessels requires rigorous physical validation to assess practical constructability (Minaoglou et al., 2025). Implementing physical prototyping methodologies alongside computational design ensures that customized algorithms yield products that perform reliably in real-world scenarios.

2.2. Geometry and Constructability

The geometric definition of a vessel's hull is the key attributing factor to its stability, operational efficiency, and structural integrity. Parametric algorithms effectively manage this complexity by utilizing fundamental defining curves, such as the centerline and deckline, to generate the broader hull surfaces (Harries, 1998).

Advanced mathematical representations, particularly Non-Uniform Rational B-Splines (NURBS) (Zhou et al., 2022) and Bézier curves (Khan et al., 2017), provide the necessary flexibility to create smooth, continuous shapes required for marine applications.

What bridges the gap between these mathematical definitions and physical reality is the vessel's constructability. The algorithmic generation of shapes and structures must follow the vessel's physical constraints to ensure the final product is structurally viable and sea-worthy. During the computational phase, design parameters should be managed in a way so that the resulting geometry is not only hydrodynamically sound but also match the limitations of the chosen manufacturing technique.

2.3. 3D Printing Computational Forms

Additive manufacturing has become tightly integrated into parametric design workflows since it allows complex, algorithmically generated geometries to be fabricated directly, without the constraints imposed by traditional tooling (Kourmouki et al., 2025). This creates a direct pathway from the digital concept to the physical object. To prepare a computational hull for 3D printing, the algorithm must carry out a series of geometric modifications. These include scaling techniques to shell the geometry, defining precise wall thicknesses, and executing Boolean operations to ensure the model is solid, watertight and 3D-printable.

How well the digital model translates into a physical object depends largely on the quality of the fabrication process itself. For thin-walled components printed in materials such as PLA or PETG, production parameters such as layer height, print speed and extrusion settings, directly influence whether the final part conforms to the design's geometric and structural requirements. When carefully controlled, these parameters ensure that the algorithmically generated surfaces are translated reliably into the physical prototype, with adequate surface finish and mechanical integrity.

2.4. Assembly and Modularity

Most commercially available 3D printers have a limited build volume, resulting in large computational forms such as Unmanned Surface Vessels being divided into manageable segments for fabrication. Algorithmic systems address this by using automated planar slicing cuts that divide the hull into individual parts that fall within the printer's build parameters. A key concern in segmented 3D printing is ensuring that the individual parts reassemble with structural continuity and hold their original form. To address this, algorithms generate internal connectors and interlocking joints tailored to each sliced surface, providing both alignment and structural coherence.

The physical assembly of the segments serves as a practical test of the algorithm's viability, evaluating the ease of construction, the tightness of the joints, and the overall integrity of the final assembled prototype. By embedding manufacturing and assembly constraints directly into the generative process, the workflow can become an efficient pipeline from digital modeling to the physical object.

3. Design methodology

The transition from a digitally generated geometry to a physical object requires a systematic and structured approach to ensure the result is both functional and constructible. The computational tool used is designed to manage the full design-to-fabrication pipeline, from generating the hull geometry to automating the segmentation, and finally producing the connectors and joints required for assembly. An important aspect of the case-study is the calibration of the fabrication parameters controlling these processes, as finding the appropriate values is essential in producing a result that is geometrically accurate and straightforward to manufacture. To evaluate the practical output of the computational design process, a fabrication methodology was developed around the additive manufacturing of scaled physical prototypes, turning theoretical hull designs into tangible test models.

3.1. Fabrication targets and data

The primary objective of producing 3D-printed models is to empirically verify the practical viability and constructability of the computational designs. Converting these digital USV hulls into physical constructs allows for the examination of several design aspects. The first one being geometric compatibility, ensuring that the generated models can be 3D-printed without extensive manual intervention.

Closely related to this is the question of segmentation continuity. Once the individual sections are assembled, they must maintain both structural and visual coherence, which is essential to the integrity of the scaled prototype.

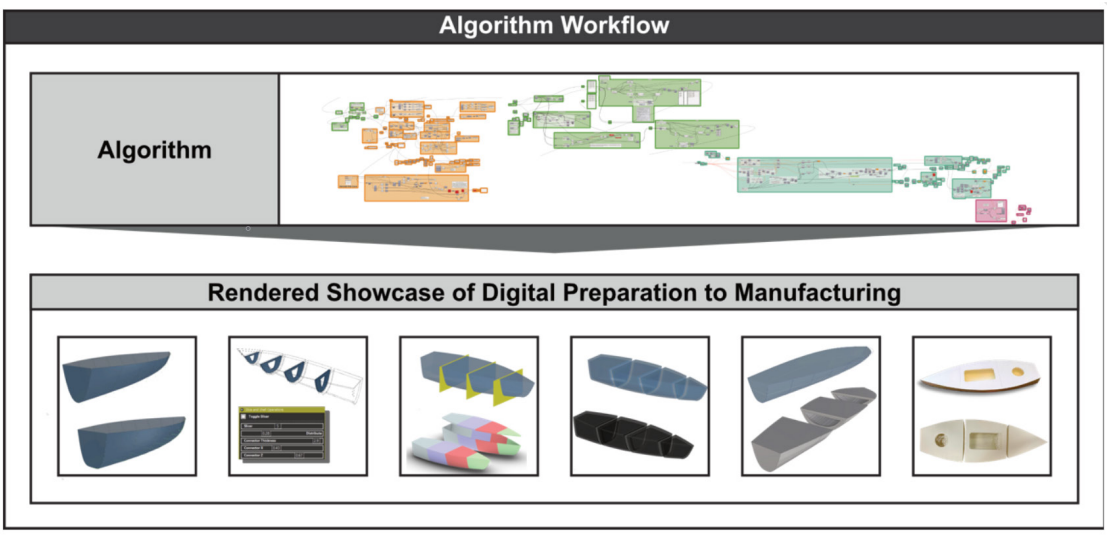
The surface quality of the printed hulls is equally important, as smoothness and curve fairness directly affect the hydrodynamic performance and can be a decisive factor in any transition to full-scale production. Finally, the ease of physical assembly is assessed, since the practicality of assembling the printed segments is a strong indicator of how well the design approach would scale.

3.2. Digital Preparation for Manufacturing

Before physical fabrication can begin, the algorithm automatically processes the generated surface geometry through a series of preparation steps to make it 3D printed-ready (Figure 1). The process begins with shell generation, where a non-uniform scaling technique is applied to the outer hull surfaces to produce a solid geometry with a defined wall thickness. The deck is then extruded to match these thickness parameters, ensuring it integrates flush with the hull and fully encloses the vessel.

Once the base geometry is established, the hull is divided into segments to accommodate the build volume constraints of standard desktop 3D printers. The algorithm generates cutting planes at equal intervals, systematically splitting the hull, deck, and any internal structures into manageable parts. At each cut seam, internal connectors are automatically generated to facilitate structural alignment during assembly.

This is achieved by extracting the cross-sectional profile at each split plane and extruding it inwards, forming precise interlocking joints between adjacent segments.



» **Figure 1:** *Digital Preparation Steps*

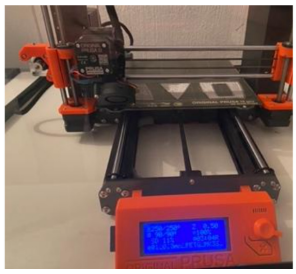
When the segmented hull is complete, rectangular and circular openings are incorporated into the deck geometry to serve a dual purpose: providing physical access to the internal compartments and acting as the interface through which the two hulls are joined.

The hull is then mirrored across a centerline that is calculated based on user-defined parameters and the housing dimensions required to enclose the electronics and propulsion components, producing the full catamaran configuration with a precisely controlled separation between the two hulls.

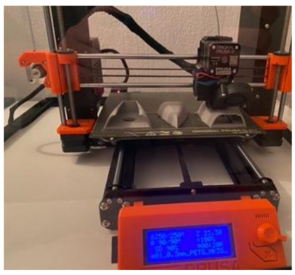
3.3. Fabrication of Test Model 01 (Scale 1:10)

In order to conduct a quick and affordable analysis of the computational design process, a prototype on a 1:10 scale was produced first.

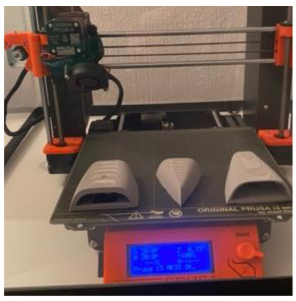
This scale provides sufficient physical volume to inspect design features and print quality while minimizing material usage and print time. Figure 2 depicts the different stages of the 3D printing process completion.



(a)



(b)



(c)

» **Figure 2:** *Printing Stages of Test Model 1*

The model was fabricated using an Original Prusa™ i3 MK3S+ 3D printer, with the print files prepared in PrusaSlicer™ version 2.7.4. Prusament™ PETG was selected as the material for its durability and layer adhesion properties.

The print was performed at a temperature of 250°C, utilizing a 0.30 mm layer height and a 20% infill density, successfully completing without the need for additional support structures (Table 1).

Table 1

Print data of test model 01

Print Data of Test Model 01	
Printing Material	Prusament™ PETG
Printing Temperature	250° C
Layer Height	0.30 mm
Infill Density	20%
Supports	No
Printing Time	3 hours and 30 minutes
Dimensions	209 x 71.5 x 26 mm

3.4. Fabrication of Test Model 02 (Scale 1:3)

Upon the validation of prototype 01, a much larger prototype at a 1:3 scale was printed. The maximum wall thickness of this model equals to 21 mm to save time and reduce material consumption (Figure 3).

This larger prototype was printed on a CreatBotTM D600 Pro industrial printer using PLA EVOTM material.

Manufacturing parameters included a printing temperature of 220 degrees Celsius, a layer height of 0.30 mm, and 0% of infill with necessary supports added. The total time for printing prototype 02 amounted to more than 30 hours (Table 2).

Table 2

Print data of test model 02

Print Data of Test Model 02	
Printing Material	PLA EVO™
Printing Temperature	220° C
Layer Height	0.30 mm
Infill Density	0%
Supports	Yes
Printing Time	30 hours and 30 minutes
Dimensions	696 x 238 x 86 mm



(a)

(b)

(c)

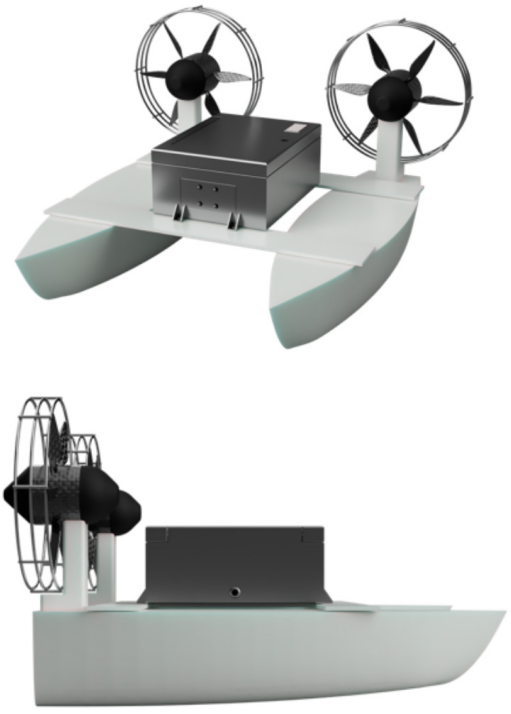
» **Figure 3:** *Printing Parts of Test Model 2*

3.5. Assembly and Physical Evaluation

The physical realization of the USV models allowed for a comprehensive evaluation of the digital-to-physical workflow. The assembly phase served as a direct test of the algorithmically generated internal connectors.

For both Test Model 01 and Test Model 02, the generated joints provided adequate tolerance and structural alignment, confirming the capability to accurately join segmented hull parts. Furthermore, the physical prototypes verified that the surface geometries remained smooth and continuous across the segmented boundaries.

The larger scale of Test Model 02 provided detailed insights into how the printed geometries behave under greater volumetric demands, successfully demonstrating the system's capacity for creating large-scale, modular marine prototypes (Figure 4).



» **Figure 4:** *Final Assembly with Integrated Propulsion Mechanisms*

4. Conclusions

This paper presented a holistic case study on the transition of algorithmically generated Unmanned Surface Vessel (USV) hull geometries from digital models into physical objects through additive manufacturing. By fabricating two scaled prototypes, a 1:10 model in PrusamentTM PETG and a larger 1:3 model in PLA EVOTM, the study evaluated the practical constructability of computationally designed hulls across the key dimensions of printability, structural continuity, surface smoothness, and assembly feasibility.

The results confirmed that the automatically generated internal connectors provided adequate tolerance and structural alignment, allowing the segmented parts to be joined accurately, while preserving smooth, continuous surfaces across the seam boundaries.

The larger-scale model further demonstrated the workflow's capacity to produce modular marine prototypes under greater volumetric and material demands.

Overall, the case study shows that embedding manufacturing and assembly constraints directly into the parametric design process yields a reliable digital-to-physical pipeline, provided that the fabrication and assembly methodologies are calibrated to the material, scale, and operational environment of the vessel. Future work will focus on extending the modular fabrication approach to larger, multi-hull configurations.

5. References

Aidinli, K., Minaoglou, P., Kyratsis, P. and Efkolidis, N. (2025) 'Automating product design and fabrication within the furniture industry', *Designs*, 9(5), 116. DOI: 10.3390/designs9050116

Fonseca, I.A., Gaspar, H.M., de Mello, P.C. and Sasaki, H.A.U. (2022) 'A standards-based digital twin of an experiment with a scale model ship', *Computer-Aided Design*, 145, 103191. DOI: 10.1016/j.cad.2021.103191

Harries, S. (1998) *Parametric Design and Hydrodynamic Optimization of Ship Hull Forms*. Berlin: Mensch-und-Buch-Verlag. ISBN: 978-3-933346-24-7

Janssen, P. and Stouffs, R. (2015) 'Types of parametric modelling'. In: Ikeda, Y., Herr, C.M., Holzer, D., Kajima, S., Kim, M.J. and Schnabel, M.A. (eds.) *Emerging Experience in Past, Present and Future of Digital Architecture: Proceedings of the 20th International Conference of the Association for Computer-Aided Architectural Design Research in Asia (CAADRIA 2015)*. Hong Kong: CAADRIA, pp. 157–166. DOI: 10.52842/conf.caadria.2015.157

Khan, S., Gunpinar, E. and Mert Dogan, K. (2017) 'A novel design framework for generation and parametric modification of yacht hull surfaces', *Ocean Engineering*, 136, pp. 243–259. DOI: 10.1016/j.oceaneng.2017.03.013

Kourmouki, A., Minaoglou, P., Anastasiadis, A., Gudaitiene, R. and Kyratsis, P. (2025) '3D CAD and 3D printing-based product design: Case study of an armchair', *Innovations in Publishing, Printing and Multimedia Technologies*, 1(2), pp. 12–21. DOI: 10.59476/ilpmt2025.v1i2.12-21

Kyratsis, P., Markopoulos, A.P., de Amorim Almeida, H. and Spahiu, T. (2025) 'Design and manufacturing: An Industry 4.0 perspective', *Machines*, 13(10), 927. DOI: 10.3390/machines13100927

Kyratsis, P., Tzotzis, A. and Davim, J.P. (2025) *CAD-based Programming for Design and Manufacturing*. Cham: Springer Nature Switzerland. DOI: 10.1007/978-3-031-78747-8

Minaoglou, P., Kakoulis, K. and Kyratsis, P. (2026) 'Customized helmet design using computational and physical prototyping design principles', *Journal of Graphic Engineering and Design*, 17(1), pp. 53–64. DOI: 10.24867/JGED-2026-1-053

Park, S.W., Kim, S.H., Kim, Y.I. and Lee, I. (2022) 'Hull form optimization study based on multiple parametric modification curves and free surface Reynolds-averaged Navier–Stokes (RANS) solver', *Applied Sciences*, 12(5), 2428. DOI: 10.3390/app12052428

Pektas, S.T. (2023) 'Parametric design as a tool / as a goal: Shifting focus from form to function'. In: Guler, K. (ed.) *Transforming Issues in Housing Design*. Hoboken, NJ: Wiley, pp. 221–232. DOI: 10.1002/9781119857198.ch16

Zhou, H., Feng, B., Liu, Z., Chang, H. and Cheng, X. (2022) 'NURBS-based parametric design for ship hull form', *Journal of Marine Science and Engineering*, 10(5), 686. DOI: 10.3390/jmse10050686



© 2026 Authors. Published by the University of Novi Sad, Faculty of Technical Sciences, Department of Graphic Engineering and Design. This article is an open access article distributed under the terms and conditions of the Creative Commons Attribution license 4.0 Serbia (http://creativecommons.org/licenses/by/4.0/rs/).

https://doi.org/10.24867/GRID-2026-p91

A Case Study in Functionally Graded Lattice Design for a Surfskate Deck: Workflow and Reduced-Scale Prototype

ABSTRACT

Skateboard and surfskate decks are typically built from multi-ply laminates whose stiffness is largely uniform across the board, regardless of how load is distributed in use. This case study explores an alternative: a single deck whose internal lattice varies in strut thickness and cell layout according to a local load-intensity field. Using Grasshopper for Rhinoceros 3D, a parametric deck is generated, the field is thresholded into four bands (rigid core, transition, compliant mid-span, edge), and each band is populated with a strut lattice and meshed volumetrically (OpenVDB) for fused filament fabrication (FFF). In this first prototype the field is an analytic proxy based on distance to the truck mounts, not a finite element result; coupling to Karamba3D shell analysis is the immediate next step. The workflow is demonstrated on a 240 mm reduced-scale PLA deck that follows the longitudinal camber and includes strut-free zones at the truck-mount positions, generated by suppressing struts locally rather than by a post-hoc Boolean cut. Hand loading showed the rigid core held as intended, while the thinnest struts in the compliant and edge bands fractured rather than flexed, indicating PLA is unsuitable for this strut geometry at this scale. The aim is to show, through one concrete example, that load-informed lattice grading is a feasible route to digitally fabricated, single-piece sports equipment, and to document the pipeline and its current simplifications as groundwork for a more general design method.

Panagiota Ligka [1]
Athina Tziarou [1]
Renata Gudaitiene [2]
Panagiotis Kyratsis [1]

[1] Department of Product and Systems Design Engineering, University of Western Macedonia, Koila, Western Macedonia
[2] Kaunas Kolegija, Higher Education Institution, Kaunas, Lithuania

KEY WORDS
Case study, functionally graded lattices, generative design, additive manufacturing, sports equipment design

1. Introduction

Skateboard decks are conventionally made from glued wood plies, and their stiffness is set by ply count, thickness and orientation, and is largely uniform across the surface (Willard & Loferski, 2018). Deck flex is nonetheless a recognised selection criterion among riders: stiffer boards are associated with responsive “pop” and precision, while more compliant boards are associated with comfort, damping and smooth carving. Surfskates, which use pivoting truck systems to emulate surfing-style turns, make carving response a primary design concern. Because a laminate cannot readily place stiffness where it is needed, designers must largely accept one compromise for the whole board. Additive manufacturing relaxes this constraint. Functionally graded lattices allow relative density and cell geometry to change continuously or in steps within a single printed part, and grading driven by load fields builds on established ideas in structural optimisation and cellular solids (Bendsøe & Kikuchi, 1988; Gibson & Ashby, 1997; Li et al., 2020).

This paper describes such a workflow, built in GrasshopperTM for Rhinoceros 3DTM, and a first reduced-scale prototype printed by FFF in PLA, building on a generative design methodology previously applied to different applications (Ligka, Manavis & Kyratsis, 2026; Manavis et al., 2022). The aims are: (i) to define a parametric deck and truck-mount layout; (ii) to convert a load-intensity field into discrete lattice bands; (iii) to

generate a graded lattice for each band suitable for FFF; and (iv) to compare the printed deck's hand-tested flex qualitatively with the grading pattern. The work is intentionally scoped as a proof of pipeline, and its simplifications are stated in Sections 2.2, 2.3 and 4.

2. Methods

2.1. Parametric deck and truck-mount zones

The deck outline is a closed planar curve with rounded nose and tail, defined by length and width sliders, and lofted to a longitudinally cambered surface (centre raised relative to the nose and tail). A signed camber parameter also permits a rocker profile (centre dropped) at negative values; the prototype uses positive camber only. A quad-dominant analysis mesh is generated whose target edge length sets the lattice cell pitch. Two elliptical zones mark the truck mounting areas along the longitudinal axis. Their centres are placed 15% of deck length from each end (a wheelbase of 0.70 L). The layout is symmetric about the deck centre by design, for this proof of pipeline: (i) it removes setback as a free variable, so band behaviour can be attributed to the grading rather than the layout; (ii) with a symmetric outline and camber, the proxy field should yield a near mirror-symmetric band partition, which serves as a built-in sanity check; and (iii) it matches the symmetric (twin-tip) outline used. Asymmetric truck setback is left for later work, together with the asymmetric pop and carve load cases, which will break this symmetry in the final field.

The full-scale deck is 800 mm long. The prototype is a 0.30-scale version (240 mm) to fit the printer's build volume. Outline and camber are scaled uniformly, while cell pitch (4.5 mm) and shell thickness (5 mm) are set independently of scale so that the lattice does not collapse into a solid. A full-scale version of the same definition was also generated and mesh-validated per band (Section 4).

2.2. Load-intensity field and banding

In the present prototype the load-intensity field is an analytic proxy computed per mesh face from a linear decay with distance to the truck zones, combined with a camber falloff term. It is not the output of a finite element solve. The proxy allowed the banding-to-lattice pipeline to be developed and validated independently of the structural solver. The camber falloff term was implemented but not tested independently, so its influence on the band pattern was not evaluated.

The intended field is the per-face envelope (maximum) of principal von Mises stress from two Karamba3D shell load cases: a tail "pop" load and an offset "carve" load with vertical and lateral components, with pinned supports at the truck zones (Preisinger, 2013). A torsional couple is a planned extension (Section 4).

Table 1
Band definitions and lattice parameters (default thresholds)

Band	Normalized intensity	Lattice type	Strut diameter (mm)
Rigid core	> 0.75	Cubic-type edge lattice	2.5
Transition	0.50- 0.75	Same topology, thinner struts	~1.3
Compliant mid-span	0.25- 0.50	Diagonal edge-strut lattice	~1.0
Edge	< 0.25	Diagonal edge-strut lattice, thinnest struts	0.9

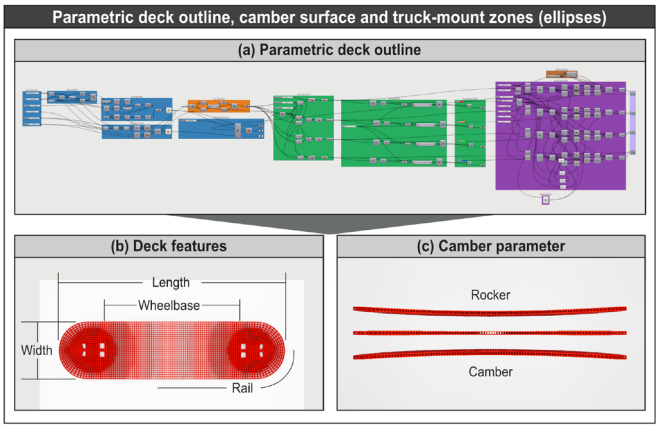
2.3. Lattice generation

Each band mesh is duplicated into a bottom layer and a top layer, offset along the surface normal by the shell thickness (measured between outer faces) and joined by vertical struts at welded vertices. Both layers follow the camber of the deck surface in Section 2.1 rather than a flat reference plane. In the rigid-core and transition bands, struts follow the edges of the analysis mesh to form a cubic-type edge lattice. In the two lower bands, diagonal struts spanning across each quad face are used instead. Cell pitch is absolute (4.5 mm) and scale-independent by construction: the upstream remesh edge length is divided by the scale factor so the final printed cell size stays 4.5 mm regardless of scale.

Struts are converted to volumetric distance fields and meshed per band with the Dendro plugin (an OpenVDB wrapper, version 1.3) (Museth, 2013), which yields watertight iso-surface meshes. The voxel size was 0.3 mm. Dendro requires strut radius to sufficiently exceed the voxel size for reliable iso-surface extraction; for the thinnest struts (0.9 mm diameter, 0.45 mm radius) against a 0.3 mm voxel size, the radius-to-voxel ratio was 1.5.

The four bands are meshed independently and exported as four separate watertight bodies that meet at shared boundary curves, rather than as a single unified shell (~5.2 million total faces across bands, validated in Rhino). Attempts at a mesh Boolean union of the full strut network were unreliable and were abandoned.

The version of Dendro used has no native unit-cell library, so re-entrant auxetic cells could not be generated directly. The two lower bands instead use diagonal struts at low diameter. This is a placeholder



» **Figure 1:** *Parametric deck outline, camber surface and truck-mount zones (ellipses)*

for future re-entrant auxetic cells and is not expected to exhibit a negative Poisson's ratio; no such behaviour is claimed or measured for this prototype.

Eight strut-free zones at the truck-mount positions (four per truck, matching a representative bolt pattern scaled with the deck) are left open in the rigid-core band by suppressing strut generation locally rather than by a subtractive Boolean cut on the finished mesh. This is implemented as a toggleable filter, so the same definition can generate an uninterrupted rigid-core lattice when mounting provision is not required.

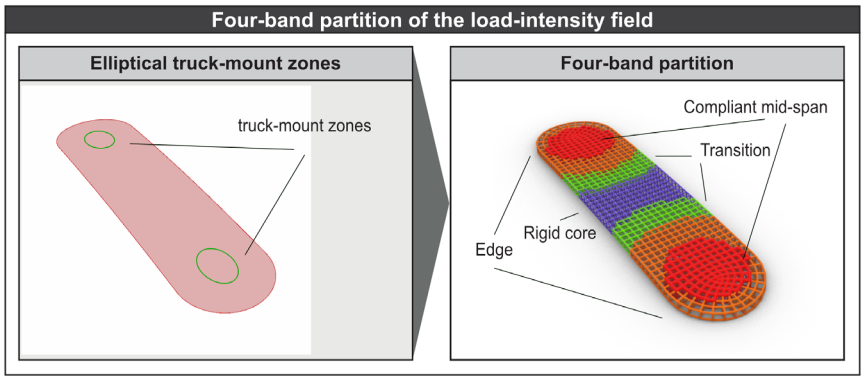
2.4. Fabrication

The deck was printed on a Bambu Lab P2S with a 0.4 mm nozzle in Bambu Basic PLA. Layer height was set to 0.2 mm with 3 outer perimeter walls, a print speed of 60 mm/s, and a nozzle temperature of 215°C using Bambu Studio with standard tree supports. The four band bodies were printed together as a single multi-body job, with boundaries meeting at shared contact curves rather than overlapping. The minimum printable strut diameter was 0.8 mm, twice the nozzle diameter; the thinnest band used (0.9 mm) sits above this floor with margin. PLA was chosen for its low cost and fast, reliable printing, which suited rapid iteration on a proof-of-pipeline prototype. At 0.30 scale the prototype is a demonstrator of the workflow and is not intended for riding.

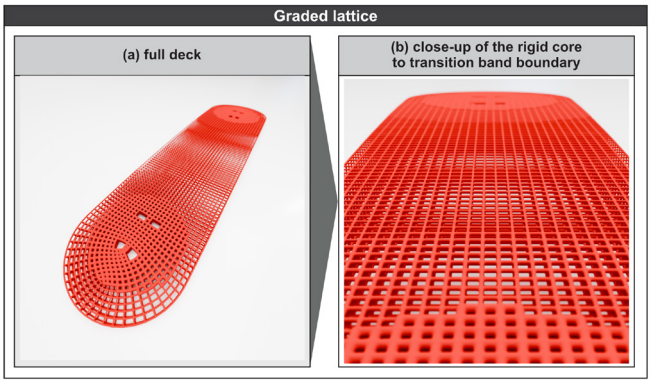
3. Results

3.1. Deck geometry and band partition

Figure 1 shows the parametric deck with its truck-zone ellipses, and Figure 2 the four-band partition of the analysis mesh. The rigid core forms two zones centred on the truck mounts, and the transition band wraps these and extends toward the rails. The compliant mid-span band lies between the two truck zones, and the edge band occupies the nose, tail and rail perimeter. This arrangement follows from the construction of the proxy field, which places the highest intensity around the truck zones, and should not be read as validation of the grading.



» **Figure 2:** *Four-band partition of the load-intensity field (rigid core, transition, compliant mid-span, edge)*



» **Figure 3:** *Graded lattice: (a) full deck; (b) close-up of the rigid core to transition band boundary. Strut diameter decreases from the rigid core to the transition band, though the step is subtle at this render scale and lighting; bands are not colour-coded in this figure (cf. Figure 2)*

3.2. Lattice output

Figure 3 shows the generated lattice, and Table 2 lists the prototype parameters. Each of the four bands was meshed as a separate watertight body, approximately 5.2 million faces in total across all four components, and all four pass mesh validation in Rhino (closed, manifold, no degenerate faces) after the repair step in Section 2.3.

Table 2
Prototype parameters

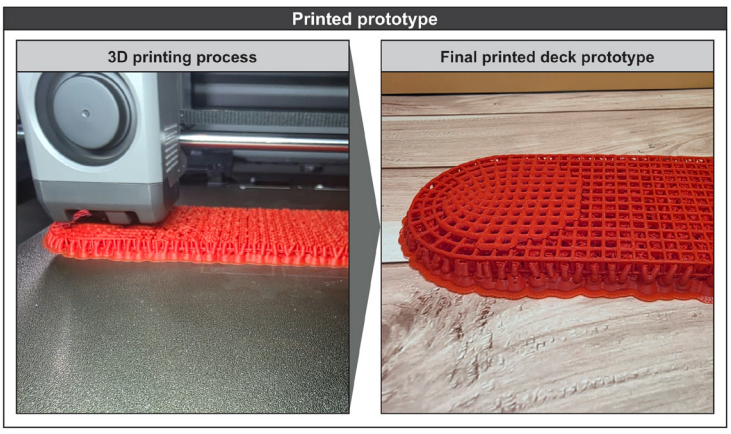
Parameter	Value
Deck length (scaled)	240 mm (0.30 × 800 mm)
Cell pitch	4.5 mm
Shell thickness	5.0 mm
Strut diameter	0.9 mm (minimum) to 2.5 mm (Table 1)
Voxel size	0.3 mm
Band thresholds	0.25, 0.50, 0.75
Material / printer	PLA / Bambu Lab P2S, 0.4 mm nozzle

3.3. Printed prototype and flex behavior

During hand-loading and support removal, several of the thinnest (edge-band, 0.9 mm) struts fractured rather than flexed; PLA's low strain-to-failure made it unsuitable for the sub-1 mm compliant struts, which required elastic bending rather than brittle fracture to behave as intended. This indicates that material choice, not only strut geometry, is a binding constraint on the graded-lattice concept: a flexible printable material (e.g. a TPU) is likely necessary for the compliant and edge bands to function as designed, while a stiffer material such as PLA may remain appropriate for the rigid core.

4. Discussion

The workflow shows that a load-intensity field can be carried through banding, lattice construction and volumetric meshing into a printable, parametric definition. The main value at this stage is the pipeline itself: every dimension, threshold and strut diameter remains a live parameter, so a redesign means regenerating the defini-



» **Figure 4:** *Printed prototype (left: in progress on the build plate; right: completed part before load testing). Several edge-band struts subsequently fractured under hand loading; see Section 3.3*

tion rather than remodelling the deck. The most important findings for later versions were practical: lattice cell pitch must be decoupled from deck scale, struts must be sized against voxel size for reliable meshing, and mesh Boolean operations on the full strut network proved unreliable at this density. A volumetric union of the band fields in Dendro, rather than a mesh-level Boolean, is the route we intend to test for a single unified shell.

The following limitations should be read alongside any result:

- Load field. The banding is driven by an analytic proxy, not FEA, so the pattern is a hypothesis about where stiffness is needed. With supports at the truck zones, the largest bending moment from a rider's weight lies between them, so the compliant mid-span runs against simple beam intuition and needs to be checked against a solved field. The camber falloff term was also not tested independently.
- Banding. Bands are stepped, and the default thresholds (0.25, 0.50, 0.75) were not optimised or compared with alternatives. Continuous grading is planned.
- Loading. Real deep carving involves asymmetric weight transfer and torsion along the long axis. The planned carve load case includes only vertical and lateral components, with a torsional couple as future work.
- Geometry. Two features of real decks are omitted from the base surface: transverse concave (the side-to-side dish across the width, used by riders for foot location and leverage) and nose and tail kicks (the upturned ends, which contribute to pop and control). Longitudinal camber is present and is followed by the lattice shell. The truck layout is also symmetric, and asymmetric setback is left for later work. All of these should be added in later versions.
- No auxetic behaviour. The compliant bands use diagonal struts as a placeholder, not a re-entrant or chiral topology. No claim of negative Poisson's ratio or indentation resistance is made for this prototype. True auxetic cells need a strut-based generator with native re-entrant unit cells, or a custom cell definition, and would require direct mechanical characterisation to confirm (Kolken & Zadpoor, 2017).
- Band assembly. The four lattice bands are exported as separate watertight bodies meeting at shared boundaries rather than as a single unified shell. A mesh Boolean union was attempted but proved unreliable at this strut density and was not pursued further.
- Scale, material and fabrication. The deck is printed at 0.30 scale in PLA, a stiff, brittle polymer with limited elastic recovery; its absolute stiffness, damping and pop are not representative of a conventional laminated deck or a rideable board. The full print job took 9 h 20 min using Bambu Studio's automatic tree supports. Several of the thinnest (0.9 mm) edge-band struts fractured during hand loading and support removal rather than flexing elastically, confirming that PLA's low strain-to-failure is unsuitable for this strut geometry; support strategy and orientation for thin-strut bands also warrant evaluation in future prints. A flexible filament such as TPU is the immediate next material to test for the compliant and edge bands, while a stiffer material such as PLA may remain appropriate for the rigid core. A full-scale (800 mm) version of the same definition was generated and mesh-validated per band, but required multi-part segmentation to fit the build volume and was not fabricated for this paper.
- Testing. Manual deflection testing is qualitative. It had no uniform-lattice control and no measured load or displacement, so it cannot separate the effect of grading from that of geometry and supports. It is no substitute for instrumented stiffness measurements or rider trials.
- Rider relevance. The grading, with stiffness at the truck zones where load is transferred and flex elsewhere, is intended to reflect how riders discuss deck flex. Testing with riders, and comparison with commercial surfskate decks, would be needed to show that the graded layout produces a ride that skaters actually prefer.



» **Figure 5:** *Illustrative concept render (not a functional test) showing the intended in-use context of a full-scale, assembled version of the design*

Figure 5 illustrates the intended full-scale application as a non-functional concept render; the prototype reported here was not ridden.

5. Conclusions

The parametric Grasshopper workflow maps a load-intensity field to four lattice bands and produces an FFF-ready, camber-following graded lattice

deck with toggleable strut-free zones at the truck mounts, demonstrated as a 0.30-scale (240 mm) PLA prototype. Hand loading showed that the rigid core remained stiff as intended, but the thinnest struts in the compliant and edge bands fractured under load rather than flexing, indicating that PLA is not a suitable material for this strut geometry at this scale.

6. Acknowledgments

The authors acknowledge the support of the University of Western Macedonia and Polis University in facilitating this research.

7. References

Bendsøe, M.P. and Kikuchi, N. (1988) 'Generating optimal topologies in structural design using a homogenization method', *Computer Methods in Applied Mechanics and Engineering*, 71(2), pp. 197–224. DOI: 10.1016/0045-7825(88)90086-2

Gibson, L.J. and Ashby, M.F. (1997) *Cellular Solids: Structure and Properties*. 2nd ed. Cambridge: Cambridge University Press. DOI: 10.1017/CBO9781139878326

Kolken, H.M.A. and Zadpoor, A.A. (2017) 'Auxetic mechanical metamaterials', *RSC Advances*, 7(9), pp. 5111–5129. DOI: 10.1039/c6ra27333e

Li, Y., Feng, Z., Hao, L., Huang, L., Xin, C., Wang, Y., Bilotti, E., Essa, K., Zhang, H., Li, Z., Yan, F. and Peijs, T. (2020) 'A Review on Functionally Graded Materials and Structures via Additive Manufacturing: From Multi-Scale Design to Versatile Functional Properties', *Advanced Materials Technologies*, 5. DOI: 10.1002/admt.201900981

Ligka, P., Manavis, A. and Kyratsis, P. (2026) 'Design of a lampshade using generative design methodology', *Computer-Aided Design & Applications*, 24(2), pp. 119–132. DOI: 10.14733/cadaps.2027.119-132

Manavis, A., Firtikiadis, L., Spahiu, T., Efkolidis, N. and Kyratsis, P. (2022) 'Parametric Architectural Design using shapes and structures', *Journal of Graphic Engineering and Design*, 13(4), pp. 13–20. DOI: 10.24867/JGED-2022-4-013

Museth, K. (2013) 'VDB: High-resolution sparse volumes with dynamic topology', *ACM Transactions on Graphics*, 32(3), Article 27. DOI: 10.1145/2487228.2487235

Preisinger, C. (2013) 'Linking structure and parametric geometry', *Architectural Design*, 83(2), pp. 110–113. DOI: 10.1002/ad.1564

Willard, D.T. and Loferski, J.R. (2018) 'Skateboards as a Sustainable Recyclable Material', *Recycling*, 3(4), Article 20. DOI: 10.3390/recycling3020020



© 2026 Authors. Published by the University of Novi Sad, Faculty of Technical Sciences, Department of Graphic Engineering and Design. This article is an open access article distributed under the terms and conditions of the Creative Commons Attribution license 4.0 Serbia (http://creativecommons.org/licenses/by/4.0/rs/).

https://doi.org/10.24867/GRID-2026-p92

A Case Study in Auxetic Structure Design for an Adaptive 3D-Printed Handbag

ABSTRACT

Everyday products such as handbags have fixed geometries that cannot adapt to changing loads. Auxetic lattices, which expand laterally when stretched, offer one route to adaptive form, but they have mainly been explored in engineering and wearable-tech contexts rather than in everyday consumer products. This paper presents a case study applying auxetic design to a 3D-printed handbag. Using Rhino and Grasshopper with the Linketix plugin, we built a parametric tote whose four planar walls carry a rotating-unit auxetic pattern driven by a single deployment parameter. A quadrilateral (rotating-square) configuration was developed into a complete bag, with hinge necks between cells and handle attachment holes and rings located parametrically from the handle geometry so that the handles stay usable at every deployment state. A triangular configuration was generated at lattice level for comparison. A prototype of the bag body, without handles or rings, was printed in a flexible TPU and tested by hand to assess expansion and shape recovery. This case study offers an initial, concrete example of how load-responsive auxetic structures might be applied to adaptive consumer products, and as a starting point for a more general design workflow to be developed in future work.

Athina Tziarou [1]
Panagiota Ligka [1]
Nikolla Vesho [2]
Panagiotis Kyratsis [1]

[1] Department of Product and Systems Design Engineering, University of Western Macedonia, Koila, Western Macedonia
[2] Polis University, Tirana, Albania

KEY WORDS
Auxetic structures, negative Poisson's ratio, 3D printing, TPU, parametric design, Grasshopper, adaptive products, handbag design

1. Introduction

Consumer products such as handbags are designed with static geometries that do not change in response to varying contents or loads. This fixed design can limit comfort, ergonomics, and functional adaptability in daily use. Auxetic metamaterials and structures with a negative Poisson's ratio, which expand laterally when stretched, can offer a pathway to create load-responsive, adaptive forms. While auxetics have been studied extensively in aerospace, biomedical, sports, and textile applications, their use in everyday fashion accessories remains underexplored (Bagewadi et al., 2026).

This paper presents a case study that applies auxetic lattice design to a 3D-printed handbag, exploring how parametric modelling and flexible materials can enable adaptive geometry in a consumer product. The contribution is a practical, documented parametric workflow, including the failure points encountered, and empirical observations on cell-type behaviour in TPU, aiming to inform future adaptive product development (Shirzad et al., 2025).

2. Background and literature review

2.1. Auxetic Structures and Negative Poisson's Ratio

Auxetic materials exhibit a negative Poisson's ratio, meaning they expand in transverse directions when subjected to tensile loading, and contract when compressed (Bagewadi et al., 2026; Johnston & Kazanci, 2021). This behavior contrasts with conventional materials, which thin out when stretched. The phe-

nomenon arises from specific micro-architectures, such as re-entrant, chiral, or rotating unit geometries that reconfigure under load (Bagewadi et al., 2026; Farshbaf et al., 2025; Papadopoulou, Laucks & Tibbit, 2017).

Key mechanical advantages of auxetics include enhanced energy absorption, indentation resistance, fracture toughness, and conformability to complex surfaces (Junio et al., 2023; Sobreira, Ayres & Pagnan, 2024). These properties make them attractive for protective apparel, biomedical devices, sports equipment, and increasingly, wearable and fashion applications (Kabir et al., 2022; Papadopoulou et al., 2017; Sobreira, Ayres & Pagnan, 2024).

2.2. 3D Printing of Auxetic Lattices in Flexible Polymers

Additive manufacturing enables precise realization of complex auxetic geometries that would be difficult or impossible to produce with traditional methods (Bagewadi et al., 2026; Farshbaf et al., 2025). Thermoplastic polyurethane (TPU) is a popular flexible filament for 3D printing auxetic lattices due to its elasticity, durability, and ability to undergo repeated deformation (Farshbaf et al., 2025). Recent studies have investigated the mechanical properties of 3D-printed TPU lattice structures, including the effects of build orientation and loading direction (Beloshenko et al., 2023).

However, the extent to which existing research addresses standardized mechanical testing of flexible lattice structures and their application in consumer fashion products remains unclear.

2.3. Parametric Design with Grasshopper for Lattice Structures

Grasshopper, a visual scripting environment for Rhino 3D, enables the parametric generation and modification of lattice geometries. Parametric modelling is particularly useful for exploring different unit-cell configurations and adjusting geometric parameters, while research on 3D-printed auxetic metamaterials has also examined computational approaches to mechanical analysis (Garg et al., 2025). The parametric model allows rapid iteration between quadrilateral, triangular, and hexagonal cell geometries, supporting the comparison of different lattice configurations.

2.4. Auxetics in Fashion and Consumer Products

Although auxetic textiles and wearable components have been explored for clothing, footwear, and protective equipment, applications in fashion accessories such as handbags remain an area for further development. Existing research highlights the potential of auxetic materials in design and architecture, as well as their broader applications across product categories (Papadopoulou, Laucks & Tibbit, 2017; Sobreira, Ayres & Pagnan, 2024).

Research into auxetic componentry has also considered its potential in human-centred product design, highlighting the relevance of these structures to products that interact directly with users (Urquhart et al., 2024).

This gap motivates the present case study, which bridges auxetic metamaterial design with everyday product form and function.

3. Methods

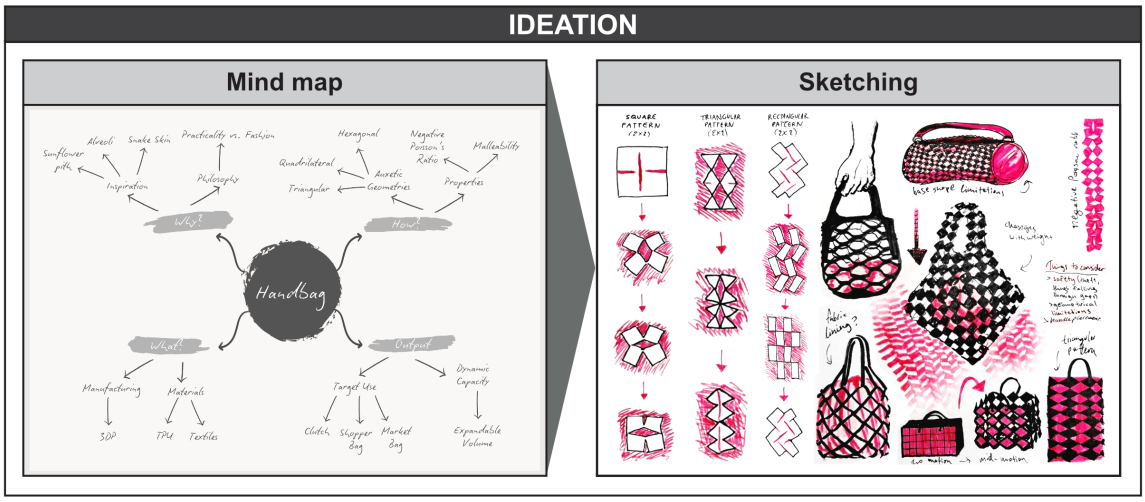
3.1. Workflow overview

The design was implemented parametrically in Rhinoceros 3D version 8 using Grasshopper™ and the Linketix auxetic-mechanism plugin. Custom Grasshopper Python components were written with the assistance of the Raven AI plugin, and the authors verified each stage by inspecting the resulting geometry and measured values. The workflow has six stages: (1) definition of a rectangular tote from four planar walls and a bottom, (2) generation of an auxetic pattern on each wall from a shared deployment parameter (Fig. 1), (3) conversion of the pattern into printable solids, (4) addition of hinge connections between cells, (5) parametric handle attachment, and (6) fabrication in flexible TPU and manual testing.

3.2. Bag form and pattern generation

The bag is a closed rectangular tote. Four vertical walls and a bottom cap are placed in the Grasshopper model with the walls on the XZ and YZ planes. At the current settings the unthickened envelope is *54.9 × 21.96 × 54.9 mm.* No surface mapping was used. Each wall gets its own pattern, generated flat on that wall's plane, which avoids the seam and strut-end problems that occurred when patterns were morphed onto a curved bag surface (Section 3.8).

Patterns were generated with the Linketix Rectangular 1 component. The component takes a plane, a cell length and width, the number of cells in each direction (Extent X and Extent Y) and a Motion value from 0 to 1 that deploys the pattern. Cell size equals the wall dimension divided by the cell count. The front and back walls use *5 × 5* cells (*100* cells each) and the side walls use *2 × 5* cells (*40* each), a total of *280* cells with a side length of *5.49 mm.* The back and right walls are mirrored copies of the front and left walls, and all walls share one Motion control. In the rest state (*Motion = 0*) the pattern is a plain square grid, and the re-entrant gaps open only as Motion increases.



» **Figure 1:** *Conceptual mind map and initial hand-drawn pattern iterations exploring auxetic handbag geometries and cell types*

3.3. Cell types

Linketix offers several auxetic generators. The quadrilateral configuration (Rectangular 1) was carried through to a complete bag. The triangular configuration (Linketix Triangular) was generated for comparison. It has no independent width input, so the cell length *L* was set from the panel width *W* and the number of cells in *X*, n_X:

$$L = \frac{W}{n_X\sqrt{3}} \quad (1)$$

and the number of rows in *Y*, n_Y, was set from the target panel height H and rounded to the nearest integer, because the generator only accepts whole numbers:

$$n_Y = round(\frac{H}{2L}) \quad (2)$$

For the front and back walls (*W = H = 54.9 mm*, n_X = *5*), Eq. (1) gives *L = 6.339 mm* and Eq. (2) gives *4.33,* rounded to n_Y = *4.* This reproduces the *54.9 mm* panel width exactly but gives a height of *2L* n_Y = *50.714 mm, 7.6%* short, because of the integer rounding. The triangular lattice has *224* cells *(32 + 80 + 32 + 80).* A hexagonal configuration was not implemented.

3.4. Solid generation

Each cell outline was converted into a filled planar surface and extruded to a wall thickness of *1.4 mm,* giving *280* closed solids for the quad bag. The bottom is a rigid *1.4 mm* slab sized to the thickened wall footprint. It does not deploy, so the bottom row of cells is locally constrained. This is a deliberate trade-off: the base carries the load, and joining a deploying lattice to a fixed base through a second auxetic panel produces geometric collisions at the seam.

3.5. Hinge necks

At *Motion = 0* neighbouring cells share full edges, so the wall is effectively a solid sheet and the pattern has no hinge mechanism. At *Motion = 0.2* the cells are separated by edge gaps of about *1.6 mm* (digital measurement at edge midpoints) but touch only at zero-width corners, which cannot be printed. To keep the cells connected as a flexible structure, a *1.0 mm* diameter cylindrical neck spanning the wall thickness was added at every shared corner: *492* necks (front *180*, back *180*, left *66*, right *66*). A Python component checked that each neck overlaps both neighbouring cells, and each local cell-neck-cell union was confirmed to be a single closed manifold solid. The bag was therefore designed to be printed at *Motion = 0.2*, not at rest.

3.6. Handle attachment

Two handles were modelled as arcs piped at *1 mm* radius with a *12 mm* rise. To avoid fixing the handles to a lattice that deforms, four attachment cells (two front, two back) are selected parametrically, with no typed coordinates or fixed indices: the top-row cell surfaces of the front and back walls are merged into one list, the four handle endpoints are grafted into separate branches, a Surface Closest Point calculation measures distance from each endpoint to every surface, and a Sort List and List Item (*index 0*) returns the nearest cell for each endpoint. A *1.5 mm* radius hole is cut through each selected cell with a single Boolean difference (one cell at a time), and each result was checked to be a closed manifold solid. A slim ring passes through each hole and is joined to the handle end, so the handle moves freely relative to the lattice at any deployment state (Fig. 2). The handles and rings were designed and checked digitally only. They were not part of the printed prototype (Section 3.7), so their behaviour in use is untested.

3.7. Assembly, boolean limits and export

The complete digital assembly contains about 775 separate closed solids (280 cells, 492 hinge necks, the bottom, and the two handles; the rings add further solids). A single Solid Union of the full set returned an empty result in Grasshopper, even though all inputs were individually valid, so the parts were baked as separate objects and exported as one STL for the slicer to merge.

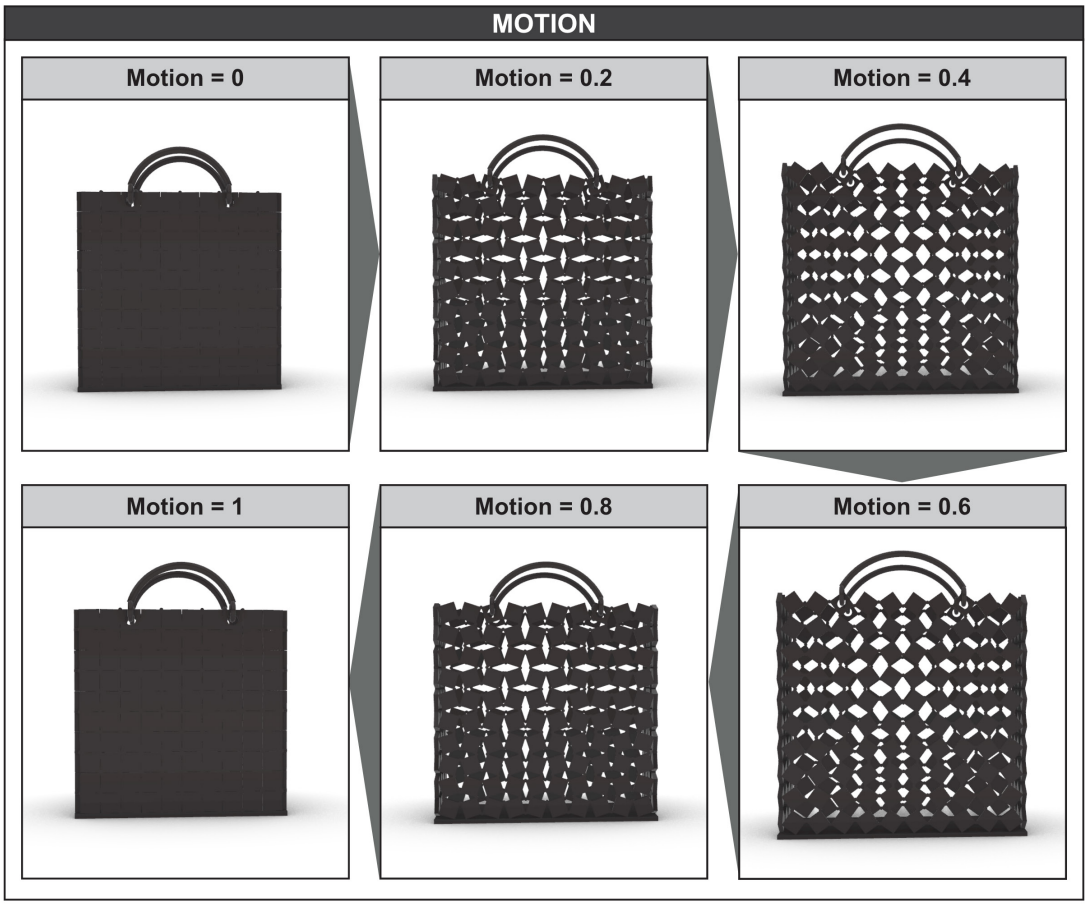
The printed prototype was the bag body only: the cells, hinge necks and bottom, about 773 solids, with the four attachment holes being part of the test print. The handles and rings were left out. The bag body was printed on a direct-drive FDM 3D printer using flexible TPU filament (Shore hardness 95A) with a *0.4 mm* nozzle. Printing parameters were set to a layer height of *0.2 mm*, a print speed of *30 mm/s*, and a nozzle temperature of *210°C.*

3.8. Design iterations and limitations

Several approaches were tried before the final design:

- Surface mapping: Mapping the lattice onto a tapered bag surface produced distorted and twisted loft geometry, so the bag was redesigned as a box with flat walls.
- Cell construction: An early cell definition built from per-panel morphs produced scale errors; a single plane-based generator per wall with cell size computed from the wall dimension replaced it.
- Rest state: Filled-cell walls fuse into a solid sheet at Motion = 0, which led to printing near *Motion = 0.2* and to the hinge necks.
- Handles: Handle geometry attached to fixed coordinates or a rigid band either broke the deformation or failed when Motion changed. Free rings through parametrically located holes replaced both.
- Triangular cells: The hinge-neck logic assumes every shared corner is shared by exactly two cells. Triangular tiling has four-cell junctions, so the hinge, assembly and ring stages were not carried over to the triangular bag.

Remaining limitations: (a) only the quad configuration is a complete printable bag; (b) the hexagonal configuration was not built; (c) Motion is a kinematic parameter, not a force, so the digital results are not loaded-response predictions; (d) the bottom cap does not deploy; (e) no instrumented testing; (f) no Boolean-clean single-solid export; (g) the handles and rings were not printed, so the handle-attachment concept is verified digitally



» **Figure 2:** *Parametric simulation of the quadrilateral handbag model showing continuous lateral expansion across a Motion value range from 0 to 1*

Table 1
Digital deployment of the front/back wall lattice for the two cell types

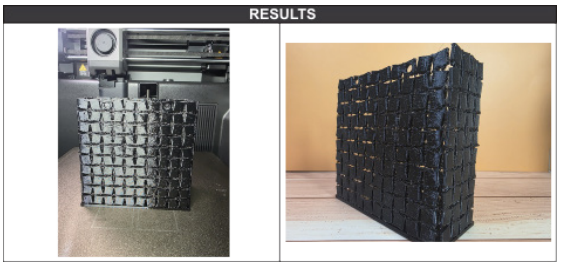
Cell type	Width at Motion 0	Width at Motion 0.3	Width change	Height at Motion 0	Height at Motion 0.3	Height change
Quadrilateral (Rectangular 1)	54.900	63.135	+15.0%	54.900	52.155	-5.0%
Triangular	54.900	59.183	+7.8%	50.714	50.090	–1.2%

only; (h) the single printed prototype experienced thermal sagging and stringing that caused adjacent cells to fuse, preventing physical testing, so the physical behaviour of the lattice is not established by this study.

4. Results

4.1. Digital deformation

The bounding-box width and height of the generated front/back wall lattice were measured in Grasshopper at *Motion = 0* and *Motion = 0.3* (Table 1). The side walls change by the same percentages in the triangular lattice (*+7.8%* width, *–1.23%* height). Similarly, the quadrilateral side walls exhibit a *+15.0%* increase in width and a *-5.0%* decrease in height at

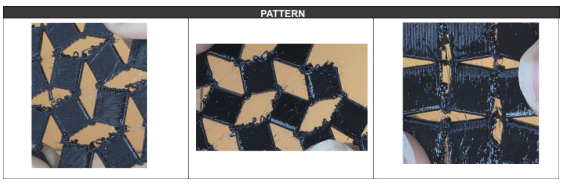


» **Figure 3:** *3D-printed TPU handbag prototype body (quadrilateral configuration) directly on the build bed (left) and standing (right)*

Motion 0.3. These are geometric measurements of the model, not physical expansion under load (Fig. 2).

4.2. Physical behaviour

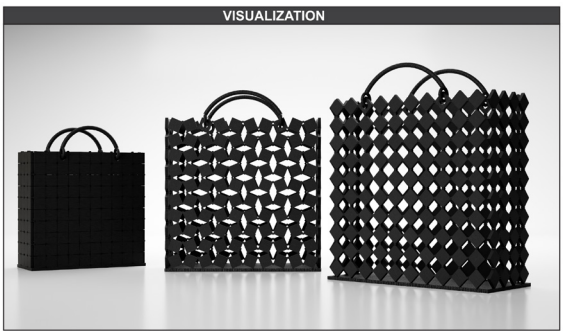
The bag body was printed once in flexible TPU, and at *Motion = 0.2*, as stated previously. Due to the extreme thinness of the *1.0 mm* hinge necks and the flexibility of the material, thermal sagging and stringing occurred during the print, causing adjacent cells to fuse partially together and preventing smooth articulation (Fig. 3, Fig. 4). Because of these localized fusion defects, the physical prototype could not be mechanically tested for live expansion or recovery. Because the print was not entirely successful, this study does not provide physical measurements of expansion or shape recovery, and the digital deployment in Table 1 is the only quantitative evidence of auxetic behaviour



» **Figure 4:** *Macro close-up views of the printed TPU quadrilateral lattice pattern showing cell separation, hinge necks, and stringing/fusion artifacts*

4.3. Handle attachment

The parametric attachment method found the correct cell for each handle endpoint, and all four 1.5 mm holes passed the closed-manifold check (about 9.9 mm³ of material removed per hole). Because the handles connect through free rings instead of being fixed to a cell, they are not tied to a specific deployment state. This is a digital result only: the handles and rings were not printed, so how they work in use remains untested (Fig. 5).



» **Figure 5:** *Final digital visualization of the complete handbag assembly featuring parametric handle integration and free-moving attachment rings across multiple deployment states*

5. Discussion

5.1. What the digital results show

The Motion parameter produces visible lateral opening in the triangular lattice (+7.8% width at Motion 0.3, with a small height loss), confirming auxetic-style deployment in the digital model. While the triangular lattice achieved a measurable +7.8% width expansion at Motion 0.3, the quadrilateral (rotating-square) configuration provides a simpler geometric pathway for future physical iterations, avoiding the complex four-way junction constraints encountered in triangular tiling (Bagewadi et al., 2026; Garg et al., 2025).

5.2. Design implications

The main practical findings are about the design process. Flat-walled forms were far easier to pattern parametrically than a tapered bag, and a lattice of filled cells needs explicit connection geometry (hinge necks) to be a connected structure rather than a solid sheet or a set of loose cells. Whether the 1.0 mm necks are strong and flexible enough in TPU was not established, because the printed prototype experienced thermal sagging and stringing that caused adjacent cells to fuse, preventing meaningful mechanical testing. Handles are best decoupled from a deforming lattice through free rings and holes, and attachment features should be located parametrically so they update as the pattern changes. The triangular lattice shows that hinge strategies developed for rotating-square cells do not carry over to cells with four-way junctions (Papadopoulou, Laucks & Tibbit, 2017; Sobreira, Ayres & Pagnan, 2024).

5.3. Limitations and Future Work

Limitations are listed in Section 3.8. Future work includes: reprinting the bag body with revised settings or neck dimensions, and printing the handles and rings; completing the hexagonal and triangular bags with a hinge approach that handles four-cell junctions; deploying the bottom cap; graded stiffness near the handles (for example attractor-driven cell size or thickness); instrumented force-displacement testing and optical strain analysis; FEM simulation of the cell mechanism; and extension to other products.

Future work should:

- Incorporate instrumented mechanical testing, including force-displacement sensors and optical strain analysis, to obtain more precise measurements of deformation and recovery.
- Explore hybrid materials, such as TPU combined with rigid inserts, to improve structural performance.
- Develop computational simulations, including finite element modeling (FEM), to predict auxetic behavior before printing (Garg et al., 2025).
- Extend the workflow to other product categories, including backpacks, footwear, and protective equipment, building on the wider design applications of auxetic materials (Sobreira, Ayres & Pagnan, 2024; Urquhart et al., 2024).

These directions could help establish a more systematic approach to designing, testing, and optimizing auxetic structures for everyday consumer products.

6. Conclusion

This paper presented a case study applying auxetic lattice design to a 3D-printed handbag. A parametric tote with deploying walls was built in Grasshopper with the Linketix plugin, developed into a complete bag with hinge necks, a rigid base and parametrically located handle attachments, and compared at lattice level with a triangular configuration. The first print of the bag body was unsuccessful due to thermal sagging and stringing that caused adjacent cells to fuse, so physical expansion and recovery remain to be tested in future work, as does the printed performance of the handle attachments. The documented workflow, including the failure points encountered, provides a starting point for adaptive consumer products with auxetic structures.

7. References

Bagewadi, S.S., Hiremath, V.S., Biradar, A.V. and Dhilipkumar, T. (2026) 'State-of-the-art in 3D printing of auxetic structures: Recent progress and perspectives', *Journal of Materials Science: Materials in Engineering*, 21(1), article 89. DOI: 10.1186/s40712-026-00465-2

Beloshenko, V., Beygelzimer, Y., Chishko, V., Savchenko, B., Sova, N., Verbylo, D. and Vozniak, I. (2023) 'Mechanical properties of thermoplastic polyurethane-based three-dimensional-printed lattice structures: Role of build orientation, loading direction, and filler', *3D Printing and Additive Manufacturing*, 10(2), pp. 245–255. DOI: 10.1089/3dp.2021.0031

Farshbaf, S., Dialami, N., Cervera, M., Bakhshan, H. and Chakherlou, T.N. (2025) 'Enhancing the mechanical performance of additively manufactured auxetic structures through design modifications: Experimental and numerical analysis', *Progress in Additive Manufacturing*, 10, pp. 4143–4164. DOI: 10.1007/s40964-025-01062-z

Garg, A., Sharma, A., Zheng, W. and Li, L. (2025) 'A review on artificial intelligence-enabled mechanical analysis of 3D printed and FEM-modelled auxetic metamaterials', *Virtual and Physical Prototyping*, 20(1), e2445712. DOI: 10.1080/17452759.2024.2445712

Johnston, R. and Kazanci, Z. (2021) 'Analysis of additively manufactured (3D printed) dual-material auxetic structures under compression', *Additive Manufacturing*, 38, article 101783. DOI: 10.1016/j.addma.2020.101783

Junio, R.F.P., da Silveira, P.H.P.M., Neuba, L.d.M., Monteiro, S.N. and Nascimento, L.F.C. (2023) 'Development and Applications of 3D Printing-Processed Auxetic Structures for High-Velocity Impact Protection: A Review', *Eng*, 4(1), pp. 903–940. DOI: 10.3390/eng4010054

Kabir, S., Li, Y., Salahuddin, M. and Lee, Y.-A. (2022) 'Drapability of 3D Printed Auxetic Structure Textiles for Wearable Products'. In: *International Textile and Apparel Association Annual Conference Proceedings*, 79(1), 26–29 October 2022, Denver, Colorado, USA. Ames, IA: Iowa State University Digital Press. DOI: 10.31274/itaa.15933

Papadopoulou, A., Laucks, J. and Tibbits, S. (2017) 'Auxetic materials in design and architecture', *Nature Reviews Materials*, 2(12), article 17078. DOI: 10.1038/natrevmats.2017.78

Shirzad, M., Chashmi, M.J., Khakzadkelarijani, S., Kang, J., Bodaghi, M. and Nam, S.Y. (2025) 'Machine-learning-assisted design and optimization of auxetic structures: A bioinspired approach to mimic natural tissues', *Advanced Engineering Materials*, 27(20), article 2500377. DOI: 10.1002/adem.202500377

Sobreira, M.A.S., Ayres, E. and Pagnan, C.S. (2024) 'Auxetic materials in design – applications and possibilities', *Research, Society and Development*, 13(10), e61131046901. DOI: 10.33448/rsd-v13i10.46901

Urquhart, L., Tamburrino, F., Neri, P., Wodehouse, A., Fingland, C. and Razionale, A.V. (2024) 'An examination of auxetic componentry for applications in human-centred biomedical product design settings', *International Journal on Interactive Design and Manufacturing*, 18(8), pp. 5457–5467. DOI: 10.1007/s12008-023-01682-1

© 2026 Authors. Published by the University of Novi Sad, Faculty of Technical Sciences, Department of Graphic Engineering and Design. This article is an open access article distributed under the terms and conditions of the Creative Commons Attribution license 4.0 Serbia (http://creativecommons.org/licenses/by/4.0/rs/).

Professional Paper https://doi.org/10.24867/GRID-2026-p93

FDM 3D Printing of Low-Density Lattice Structures Using Modified Infill Patterns

ABSTRACT

Lattice structures are extremely useful geometric structures that can exhibit a broad range of desired mechanical properties, allowing them to be tailor-made for specific purposes. However, manufacturing of such structures using traditional methods is difficult or even impossible. 3D printing technologies enable vastly easier production of such structures, allowing for easy and fast production of mechanically tuneable materials. While such structures can have any density, low-density variants provide certain properties that can be desirable in a broad spectrum of applications. This paper explores the tuning and production of one such type of lattice structure using desktop FDM 3D printers, with a special emphasis on lowest possible density that can be achieved. Lattice structures are derived from modified selected parametric infill patterns available in the slicer software. Structures are produced using Acrylonitrile Styrene Acrylate with optimised manufacturing parameters that allow for low-density lattice production.

Alan Divjak [1]
Mile Matijević [2]
Krunoslav Hajdek [3]
Marko Morić [3]

[1] Algebra Bernays University, Zagreb, Croatia
[2] University of Zagreb, Faculty of Graphic Arts, Zagreb, Croatia
[3] University North, Koprivnica, Croatia

KEY WORDS
3D printing, lattice, infill, FDM

1. Introduction

Low-density or sparse lattice structures are low-relative-density cellular structures in which a limited amount of material is distributed through a network of interconnected geometric elements (Gibson & Ashby, 1997; Helou & Kara, 2018; Nazir et al., 2019). By placing material only where it contributes to structural or functional performance, these structures can achieve low mass and reduced material consumption while still providing useful stiffness, load-bearing capability, energy absorption or other desired property. Their internal geometry can also be tailored to influence properties such as fluid transport, heat transfer, anisotropy, and deformation behaviour (Panesar et al., 2018).

Additive manufacturing is particularly well suited to the production of sparse lattice structures because it builds components layer by layer, allowing complex internal networks, small repeating cells, and spatially varying geometries to be fabricated without many of the accessibility and tooling constraints associated with conventional manufacturing. It also enables lattice density, cell dimensions, and local geometry to be varied within a single component, making it possible to adapt structural properties to local loading or functional requirements (Ngo et al., 2018; Gibson et al., 2021). These advantages have led to the use of sparse lattice structures in lightweight aerospace and automotive components, impact-absorbing systems, biomedical implants, thermal management devices, sandwich structures, robotic components, and additively manufactured infill.

The lattice structures examined in this paper were designed to gradually absorb kinetic energy of maximum stable-diameter water droplets falling at terminal velocity. The goal of this designed part is to muffle the impact sound through gradual deceleration and breakup of the droplets.

It is important to note that this research paper investigates only the practical capabilities of manufacturing such sparse lattice structures using

additive manufacturing, not the actual acoustic performance of the lattice structure itself.

There are several methods that can produce such low-density lattice structures, but as mentioned, the most convenient one is additive manufacturing (AM), also known as 3D printing. There are two currently available AM technologies that can be thought of as a consumer technology: Stereolithography (SLA) and Fused Deposition Modelling (FDM). While the official technological categories into which these two methods fit are called Vat Photopolymerization and Material Extrusion, the two previously mentioned names have become most widely used, and so SLA and FDM names will be used in this paper (Gibson et al., 2021).

SLA is a very attractive method for lattice structures manufacturing – it has very high resolution and print speed, but the material selection is somewhat limited and using this method can be quite messy in the post-processing steps (Ngo et al., 2018; Gibson et al., 2021).

FDM is also very attractive, but for different reasons – it offers a huge range of materials, many of which are high-performance ones, and models are usable right out of the printer. The downside is limited resolution and slow print speed compared to SLA (Ngo et al., 2018; Gibson et al., 2021).

For the purpose of this research, FDM is the better suited AM method. There are multiple reasons for this. One of the most Important ones is the way that models are prepared for 3D printing. This preparation process is called slicing and it translates a 3D model into instructions that the 3D printer uses to build the actual part (Gibson et al., 2021).

Like all AM technologies, FDM slicing breaks down the 3D model into a series of vertical slices. Since every slice is constructed using material extrusion during printing process, the slices are composed of lines and curves thet represent extrusion paths. This means that a single slice can contain a complex collection of extrusion paths and every one of them can be controlled through slicing settings. This means that the user has an expansive range of options through which he can control material extrusion process.

SLA slicing process is much simpler, as it produces slices that are just images of model's cross-section. Therefore, if a user wanted to create a lattice structure, he would either have to model it by hand or use very limited slicing tools to fill the object with a very simple 3D grid infill.

This is the part where FDM slicing has a huge advantage – infill setting are very rich and customizable, which means that various lattice structures do not have to be modelled – they can be generated during the slicing process (Baich, Manogharan & Marie, 2015; Fernandez-Vicente et al., 2016). This is a huge advantage for FDM method, since the user simply has to model the general shape of the part, and slicer fills the model with the 3D lattice structure of choice. Further, FDM can on average use much stronger high-perfromance materials than SLA, which is important when manufacturing low-density lattices that can be very brittle when made of commonly used SLA materials.

With all this in mind, FDM is the clear choice for manufacturing sparse lattice structures for the outlined application.

2. 3D part design

The 3D model is very simple since it only has to catch water droplets that are falling on the same location. The model is a cuboid with dimensions 30x30x20 mm, with 20 mm being the height. Four vertical edges have a 4 mm fillet applied. Fillet is added to reduce stress on the otherwise sharp edges of the model – ASA is very prone to thermal contraction and warping, even on smaller parts. An easy way to mitigate this is to make sure there are no sharp corners in the horizontal plane. Model was created in Cinema 4D and exported in .stl format, which is the standard exchange format for 3D printing.

Given that 3D printed part quality was inspected visually, an additional part was deigned – a tray with recesses into which models could be neatly arranged for taking photographs. It was made from black Polylactic Acid (PLA) plastic.

3. 3D printing preparation

Next step is model 3D printing preparation or slicing. Model were 3D printed on Bambu Lab X1 Carbon 3D printer and Bambu Studio was used a sn official slicer software for this 3D printer. This printer represents a high-quality, higher-end (albeit by now somewhat old) 3D printer. It was introduced in 2022. at a price of €1,200.

This printer was chosen because of high print quality, ease of use and finely dialled-in printing profiles. Printer was upgraded to 0.4 mm E3D ObXidian hotend for a more stable and precise extrusion. Textured PEI build plate was used, with a thin layer of glue applied to ensure good adhesion.

Appropriate material also has to be selected. While there is a wide selection of materials, Acrylonitrile Styrene Acrylate (ASA) is a good material of choice for 3D printing lattice structures – it is thought, easy to print, low-cost and very resilient to UV light, meaning it can be used outdoors. ASA material was sourced from Bambu Lab.

Model was imported into Bambu Studio V2.7.1.62. ASA material preset was assigned to the model and 0.20 mm Standard printing process was used as the starting point. Although thinner layers can produce more intricate and detailed lattice structure, it also means that the extruded lines are weaker, therefore it was decided to use standard 0.2 mm layer height (Mohamed, Masood & Bhowmik, 2015; Chacón et al., 2017).

Sparse infill pattern was selected next (Baich, Manogharan & Marie, 2015; Fernandez-Vicente et al., 2016). Bambu Studio offers a wealth of infill patterns, 22 in total, and this is the aforementioned advantage that FDM AM has over SLA. Of course, not all pattern can be used successfully for the lattice structures application outlined in this paper.

The infill pattern must have open cells and ability to control the pattern distribution. Open cells are required so that the water can flow through the structure and drain away, while pattern distribution has to be controllable in order to control how the droplets disperse as they travel through the structure. Controllable distribution is key, as many patterns have cells that grow as density decreases. This causes the droplets to interact with very few lattice elements.

However, cell shape in some patterns can be controlled and with careful parameter selection very sparse structures can be created where droplets have many interactions with the lattice structure, even though the density is low. One such pattern of note is the Cross Zag pattern. This pattern is almost identical to classic Rectilinear pattern, meaning that it is an open cell structure composed of layers of spaced lines or struts, with each layer being rotated by 90 degress. The notable distinction is that the layers can be offset. Low density rectilinear pattern is a horizontal matrix of rectangular openings. Offsetting layer by an arbitrary amount shears the opening in a particular direction. If this offset amount is large enough and properly selected, it can lead to a very airy and open structure, exactly the kind that is need for the proposed application. With this in mind, Cross Zag pattern was selected for lattice manufacturing.

Sparse lattices are delicate structures, and high-speed 3D printing is not suited for their production. Slow print speeds produce more predictable extrusion and higher quality results (Mohamed, Masood & Bhowmik, 2015; Chacón et al., 2017). Of course, print time is always a critical factor in 3D printing – one wants to optimize for print speed and quality. Therefore, the first step is to study the impact of print speed on lattice quality. For this purpose, the original model was scaled in Z axis so that it was only 2 mm high – this translates to 10 layers given the selected 0.2 mm layer hight. 10 layers is suitable to establish the print quality and is also few enough layers to enable seeing straight through the lattice, which will be used to detect any lattice defects. Four infill printing speeds were selected: 80, 60, 40 and 20 mm/s. This covers a range from what is generally considered slow to extremely slow printing speed, where it is reasonable to expect that the lattice structures have the best chance of being successfully 3D printed.

Six lattice structure densities were selected for 3D printing, giving a good range of densities to examine the capabilities of the 3D printing process. “Sparse infill density” value determine the density, and the values selected were 10, 8, 6, 4, 2 and 1. It very important to note that density of lattice structures refers to relative density – the ratio between the space filled with material and space not filled with material (Gibson & Ashby, 1997). This does not refer to actual density, e.g. 11.34 g/cm^3 for lead. Realive density is expressed either as a percentage or a fill factor, but both denote the same thing. Selected values determine the theoretical percentage of volume filled with material, therefore these values translate to 90, 92, 94, 96, 98 and 99% empty space in lattice structure. Although there is no set limit to what constitutes “low-density” lattice structures, densities lower than 10% are generally considered the lower limit for such structures.

After the optimal speed was determined, full scale models were produced in the same range of densities. Full models have a heigh of 20 mm or 100 layers.

Both thin and full scale models use the same slicing setting. “Wall loops” setting was set tp 5 In order to give the part structural strength, acting like an outside full density shell inside of which the lattice is held. Parts were printed with no top or bottom layers which exposes the lattice structure on top and bottom side. “Infil/Wall overlap” setting was set to 50 in order to anchor the lattice structure more firmly to the outer wall shell.

While the “Sparse infil density” setting provides the theoretical relative density of the lattice structure, it is expected that there will be deviations from this on account of the very low density of the structures, something that is almost never used in regular 3D printing. To determine the actual relative density, one model with only the wall shell was printed, and it’s weight was measured using a high precision Kern PCB 300-2 scale. Full scale models were weighted after printing, and the weight of the wall shell was subtracted from the weight of each full scale model. That gave the weight of the ASA plastic used for the lattice structure itself. Given the known thickness of the wall shell, a volume for the interior space dedicated to lattice structure was calculated at 25.16 cm^3. ASA material density is defined by Bambu Lab as 1.05 g/cm^3. With volume, weight and density provided, actual relative density was calculated for each full scale model.

4. Parts manufacturing

Models were sliced and saved as .3mf files. 31 models were printed In total: 6 thin models for each of the 4 infill printing speeds, 6 full scale models and one tray model. Each batch of models was printed separately. Printer was allowed too cool down for 30 minutes after printing, which made removing delicate models form the build plate much easier.

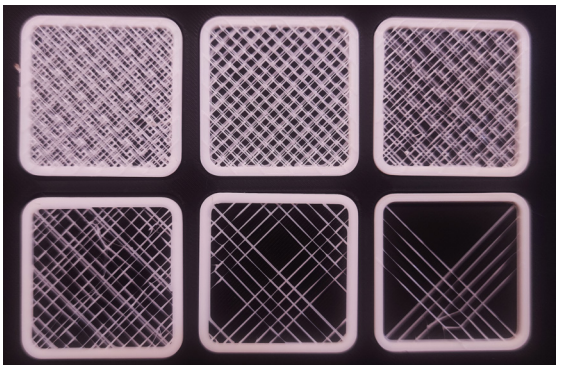
Print time for different batches are noted in Table 1.

Table 1
Batch print time

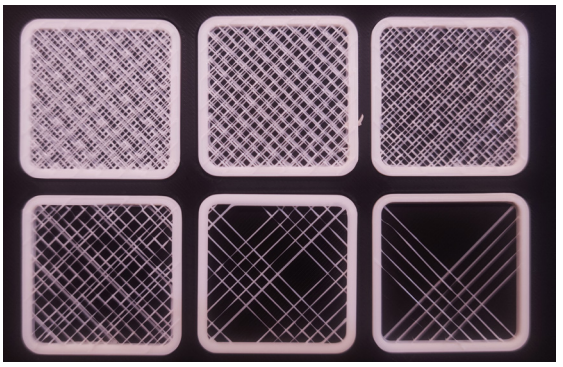
Model batch	Print time
Thin models at 80 mm/s	8m 15s
Thin models at 60 mm/s	9m 3s
Thin models at 40 mm/s	10m 40s
Thin models at 20 mm/s	15m 36s
Full scale models at 20 mm/s	2h 25m

5. Results

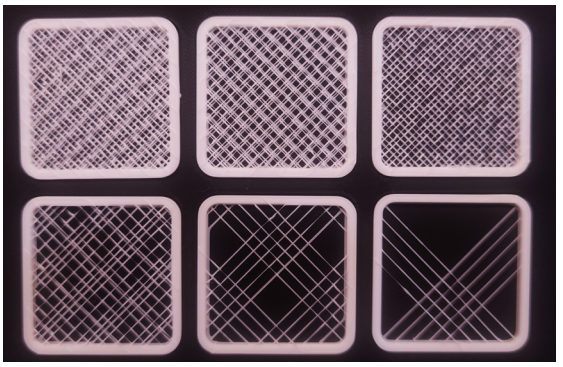
After printing, thin models were placed in a tray and photographed, starting with the 80 mm/s infill printing speed. They were photographed with a Sony A6400 camera, equipped with a Sigma 30mm f/1.4 DC DN Contemporary. Images were cropped to taste. Same was done for full scale models. Results can be seen on Images 1-5. All images show the same model order: top row, left to right: 10, 8 and 6% infill, bottom row, left to right: 4, 2 and 1% infil.



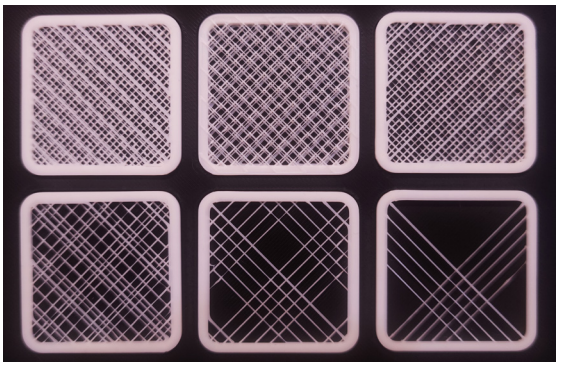
» **Figure 1:** *80 mm/s infill printing speed*



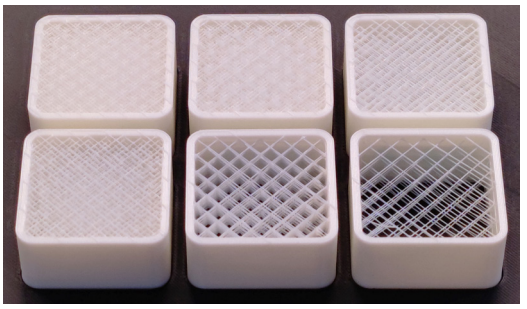
» **Figure 2:** *60 mm/s infill printing speed*



» **Figure 3:** *40 mm/s infill printing speed*



» **Figure 4:** *20 mm/s infill printing speed*



» **Figure 5:** *Full scale parts printed at 20 mm/s infill printing speed*

Wall shell model was weighted, as well as six full scale models. Wall shell model measured weight was 5.82 g. Real relative values were calculated from this. Results are noted in table 2.

Table 2
Full scale model measurements and calculations

Model infil (%)	Model weight (g)	Lattice/infill weight (g)	Real relative density (%)	Difference real/ specified density
10	8.83	3.01	11.39	1.14x
8	8.37	2.55	9.67	1.21x
6	7.64	1.82	6.93	1.16x
4	7.11	1.29	4.92	1.23x
2	6.53	0.71	2.68	1.34x
1	6.19	0.37	1.41	1.41x

6. Discussion

Thin model images show that extrusion quality increases as the speed decreases.

There are numerous extrusion line breaks in 6,4,2 and 1% infills at 80 mm/s. 10 and 8% infills have better quality, since the next layer is always supported by more lines underneath, but the quality is still visibly degraded.

60 mm/s infill are better at 10, 8 and 6%, but 4, 2 and 1% infills are on par with degraded quality from 80 mm/s models.

Quality is significantly better at 40 mm/s speed as there are fewer breaks in 4, 2 and 1% infills. There is still some quality degradation but the extrusion is much more stable.

20 mm/s extrusion speed yields by far the best results. Extrusion is very stabler, and there are only a few line breaks across the entire infill range. Given the large number of lines per layer and number of layer, these rare, sporadic breaks are insignificant.

Full scale models were printed almost flawlessly, with only a few visible extrusion breaks over the entire model range. It is difficult to resolve individual lines in the photographs of the models with higher infills, but close naked-eye and high-resolution image inspection shows that all version have high-quality lattice structures.

Real relative density calculations show that there is on average a 25% volume increase between real and specified relative density and it somewhat increases as the lattice density drops. This means that the printer is over-extruding material compared to what was expected by the slicer. This can be easily fixed since extrusion multiplier can be adjusted to produce the correct amount of plastic. However, this discrepancy does not detract from the fact that very sparse lattice structures were successfully created.

7. Conclusion

Results show that FDM 3D printers can produce remarkably delicate and low-relative-density lattice structures. Even 1% infill density model was printed almost flawlessly, which is impressive given that relative lattice structure densities below 3% are considered extremely low density or ultralight. It is also interesting to note that 1% is the lowest possible value that Bambu Studio allows for infill density. Results are even more impressive if actual, calculated density is considered.

The results demonstrate that FDM 3D printing ia a viable technology for producing very low-density, sparse lattice structures, which can lead to exciting new possibilities for consumer 3D printer applications.

8. References

Baich, L., Manogharan, G. and Marie, H. (2015) 'Study of infill print design on production cost-time of 3D printed ABS parts', *International Journal of Rapid Manufacturing*, 5(3/4), pp. 308–319. DOI: 10.1504/IJRAPIDM.2015.074809

Chacón, J.M., Caminero, M.A., García-Plaza, E. and Núñez, P.J. (2017) 'Additive manufacturing of PLA structures using fused deposition modelling: Effect of process parameters on mechanical properties and their optimal selection', *Materials & Design*, 124, pp. 143–157. DOI: 10.1016/j.matdes.2017.03.065

Fernandez-Vicente, M., Calle, W., Ferrandiz, S. and Conejero, A. (2016) 'Effect of infill parameters on tensile mechanical behavior in desktop 3D printing', *3D Printing and Additive Manufacturing*, 3(3), pp. 183–192. DOI: 10.1089/3dp.2015.0036

Gibson, I., Rosen, D., Stucker, B. and Khorasani, M. (2021) *Additive Manufacturing Technologies*, 3rd edn. Cham: Springer.

Gibson, L.J. and Ashby, M.F. (1997) *Cellular Solids: Structure and Properties*, 2nd edn. Cambridge: Cambridge University Press.

Helou, M. and Kara, S. (2018) 'Design, analysis and manufacturing of lattice structures: an overview', *International Journal of Computer Integrated Manufacturing*, 31(3), pp. 243–261. DOI: 10.1080/0951192X.2017.1407456

Mohamed, O.A., Masood, S.H. and Bhowmik, J.L. (2015) 'Optimization of fused deposition modeling process parameters: a review of current research and future prospects', *Advances in Manufacturing*, 3(1), pp. 42–53. DOI: 10.1007/s40436-014-0097-7

Nazir, A., Abate, K.M., Kumar, A. and Jeng, J.-Y. (2019) 'A state-of-the-art review on types, design, optimization, and additive manufacturing of cellular structures', *International Journal of Advanced Manufacturing Technology*, 104(9–12), pp. 3489–3510. DOI: 10.1007/s00170-019-04085-3

Ngo, T.D., Kashani, A., Imbalzano, G., Nguyen, K.T.Q. and Hui, D. (2018) 'Additive manufacturing (3D printing): A review of materials, methods, applications and challenges', *Composites Part B: Engineering*, 143, pp. 172–196. DOI: 10.1016/j.compositesb.2018.02.012

Panesar, A., Abdi, M., Hickman, D. & Ashcroft, I. (2018) 'Strategies for functionally graded lattice structures derived using topology optimisation for Additive Manufacturing', *Additive Manufacturing*, 19, pp. 81–94. DOI: 10.1016/j.addma.2017.11.008



© 2026 Authors. Published by the University of Novi Sad, Faculty of Technical Sciences, Department of Graphic Engineering and Design. This article is an open access article distributed under the terms and conditions of the Creative Commons Attribution license 4.0 Serbia (https://creativecommons.org/licenses/by/4.0/deed.en).

Original Scientific Paper https://doi.org/10.24867/GRID-2026-p94

Non-Contact 3D Acquisition of Challenging Museum Objects for Cultural Heritage Digitalization

ABSTRACT

The digitalization of cultural heritage represents an important field in contemporary museum object preservation, enabling documentation, research, virtual presentation, and long-term archiving without direct intervention in original artifacts. The aim of this study was to investigate the suitability of various non-contact technologies for acquiring geometric and visual information from museum objects and to create accurate digital twins of these artifacts.The research was conducted in collaboration with the National Museum of Slovenia and focused on selected examples of silver-plated tableware manufactured around 1900. The acquisition of these objects posed significant challenges due to the high reflectivity of metallic surfaces, complex geometries, and the presence of fine reliefs and decorative details. Within the experimental framework, several acquisition technologies were compared, including laser triangulation, structured light scanning, and photogrammetry. Initial test acquisitions were performed using the EinScan HX system, which supports both laser triangulation and structured light scanning. Simultaneously, photogrammetric acquisition was carried out using flash photography and diffuse illumination. Subsequently, a David 3D structured-light system was employed to capture both geometric and color information from the selected objects. Based on the preliminary results, the research focused on optimizing the photogrammetric workflow through the introduction of polarization filters to reduce unwanted reflections. Further improvements included the use of two polarized light sources and the development of a semi-automated background removal procedure, which significantly enhanced the quality of geometric reconstruction. As an additional improvement, the use of the X-Rite ColorChecker Passport color reference target was proposed to ensure greater color accuracy of the captured models. The results demonstrate that appropriately optimized photogrammetry combined with polarized illumination can provide an effective solution for the acquisition of challenging museum objects. The study contributes to the development of cultural heritage digitalization methodologies and provides a foundation for the creation of high-quality digital twins of museum artifacts.

Jure Jarc [1]
Nataša Nemeček [2]
Gašper Oitzl [2]
Andrej Učakar [1]
Deja Muck [1]

[1] University of Ljubljana, Faculty of Natural Sciences and Engineering, Ljubljana, Slovenia
[2] National Museum of Slovenia, Ljubljana, Slovenia

KEY WORDS
Silver plated museum objects, digital twin, photogrammetry, 3D acquisition, structured-light scanning, laser triangulation

1. Introduction

The rapid development of digital technologies has significantly transformed the documentation, preservation, and presentation of cultural heritage. Three-dimensional (3D) digitization has become an indispensable tool for museums, archives, and conservation institutions, enabling accurate documentation, virtual presenta-

tion, scientific analysis, restoration planning, and long-term preservation of valuable artefacts (Mateus et al., 2019; Adamopoulos, Rinaudo & Ardissono, 2021).

Among the various applications of digital heritage, the creation of digital twins has gained increasing importance because it enables the preservation of both geometric and visual information while reducing the need for physical handling of fragile museum collections (Adamopoulos, Rinaudo & Ardissono, 2021).

Despite the rapid development of optical acquisition systems, selecting an appropriate digitization technology remains a challenging task. The quality of 3D acquisition depends not only on the accuracy of the measuring system but also on the optical properties of the object, including surface reflectivity, transparency, texture, colour, geometry and accessibility (Mathys et al., 2015; Iakovaki et al., 2026).

Highly reflective metallic objects belong to the most demanding categories for optical digitization. Specular reflections frequently cause missing data, reconstruction artefacts, geometric inaccuracies and colour distortions regardless of whether laser scanning, structured-light scanning or photogrammetry is employed (Angheluţă & Rădvan, 2020; Melendreras Ruiz, Marín Torres & Sánchez Allegue, 2021).

Several non-contact acquisition technologies are currently used for cultural heritage digitization. Laser triangulation provides high geometric accuracy but is sensitive to reflective materials (Hermary, n.d.). Structured-light scanning generates dense and accurate point clouds; however, its performance decreases when scanning highly reflective surfaces (Eiríksson et al., 2016). Photogrammetry has become one of the most widely adopted techniques because it provides high-quality texture information, requires relatively inexpensive equipment and allows flexible acquisition workflows, although its success strongly depends on controlled illumination conditions and image quality (Guidi, Gonizzi & Micoli, 2014; Iakovaki et al., 2026).

Recent studies indicate that no single acquisition technology is universally suitable for all museum objects. Instead, successful digitization relies on optimized acquisition workflows that combine appropriate hardware, illumination, image preprocessing and reconstruction procedures according to the optical properties of the artefacts (Mathys et al., 2015; Adamopoulos, Rinaudo & Ardissono, 2021).

The present research was conducted in collaboration with the National Museum of Slovenia and focused on silver-plated historical tableware manufactured around 1900. These artefacts represent a particularly demanding case due to their heterogeneous optical properties, ranging from reflective, highly polished areas to partially tarnished and less reflective regions. The acquisition was further complicated by their complex geometry and intricate ornamental details.

Unlike many previous comparative studies, the objective of this research was not only to evaluate three non-contact acquisition technologies (laser triangulation, structured-light scanning and photogrammetry) but also to develop an optimized workflow for digitizing highly reflective museum objects. Particular attention was devoted to minimizing reflections using cross-polarized illumination, improving image preprocessing and optimizing the photogrammetric reconstruction process. The proposed methodology aims to provide practical guidelines for producing accurate digital twins suitable for museum documentation, conservation and future digital presentation.

2. Materials and Methods

2.1. Museum objects

The experimental work was carried out in cooperation with the National Museum of Slovenia. The investigated artefacts consisted of selected silver-plated tableware manufactured around 1900, including a jug and a wine goblet (Figure 1).
These objects were selected because they represent typical silver museum artefacts that combine highly polished, reflective surfaces with partially tarnished or darkened areas, thereby significantly complicating optical 3D acquisition.



» **Figure 1:** *Selected museum objects used in the experimental investigation*

The combination of smooth polished surfaces, curved geometry and fine ornamental details makes such objects particularly demanding for non-contact digitization. These characteristics frequently produce specular reflections, incomplete surface reconstruction and colour inaccuracies when conventional optical acquisition methods are applied.

2.2. Experimental equipment

Three non-contact 3D acquisition technologies were investigated and comparatively evaluated:

- Laser triangulation using the EinScan HX portable hybrid scanner (Shining 3D);
- Structured-light scanning using both the structured-light mode of the EinScan HX and the David 3D structured-light scanning system;
- Image-based photogrammetry using a professional DSLR camera with studio lighting.

The photogrammetric system consisted of a digital camera mounted on a tripod, interchangeable lenses, studio flash units equipped with softboxes, a motorized turntable, linear polarizing filters mounted on the light sources, a circular polarizing filter mounted on the camera lens, and a colour calibration target (X-Rite ColorChecker Passport). Image processing and 3D reconstruction were performed using Agisoft Metashape together with Adobe Photoshop for image preprocessing.

2.3. Experimental workflow

The experimental investigation was designed as a comparative study in which three different acquisition technologies were evaluated under controlled laboratory conditions.

The first phase focused on the comparison of laser triangulation, structured-light scanning and conventional photogrammetry in order to identify the principal limitations of each technique when applied to reflective museum objects.

Laser triangulation was performed after calibration of the EinScan HX system. The scanner operated in Laser Scan mode with a point spacing of 0.2 mm. Since reflective museum artefacts could not be marked directly, positioning targets were attached to externally manufactured 3D-printed dodecahedrons placed around the object. After scanning one side, the object was carefully repositioned to capture all visible surfaces while maintaining the reference targets.

The structured-light mode of the EinScan HX was subsequently evaluated using an identical acquisition procedure. Due to strong reflections from the metallic surfaces, the acquired geometry proved insufficient for reliable reconstruction, and the investigation continued using the David 3D structured-light system, which was specifically designed for high-resolution structured-light acquisition.

In parallel, an initial photogrammetric acquisition was performed using diffuse illumination and studio flash photography. Images were captured from multiple viewing angles while ensuring sufficient overlap between consecutive photographs to support reliable feature matching and camera alignment during reconstruction.

2.4. Workflow optimization

Based on the results obtained during the preliminary acquisitions, the research focused on optimizing the photogrammetric workflow (Figure 2).

The principal improvement consisted of introducing cross-polarized illumination. Linear polarizing filters were mounted on the studio light sources, while a circular polarizing filter was attached to the camera lens. The orientation of the filters was adjusted to minimize specular reflections originating from the metallic surfaces.



» **Figure 2:** *Experimental photogrammetric setup with polarizing filters; the museum object is indicated in red*

In the final acquisition stage, two polarized light sources were employed simultaneously, providing more homogeneous illumination and further reducing residual reflections on the object surface. Multiple object orientations were recorded to ensure complete coverage of complex geometrical features.

2.5. Image preprocessing and 3D reconstruction

Captured photographs were processed prior to photogrammetric reconstruction.
White balance and colour consistency were adjusted using reference images.
A semi-automated background removal procedure was developed in Adobe Photoshop by recording and applying automated processing actions to the complete image dataset. This approach significantly reduced manual intervention while improving segmentation consistency between photographs.

The processed image sets were imported into Agisoft Metashape, where the standard photogrammetric workflow was applied, including image alignment, sparse point cloud generation, dense point cloud reconstruction, polygon mesh generation and texture mapping.

The reconstructed models obtained from all investigated acquisition technologies were subsequently compared with respect to geometric completeness, reconstruction quality, preservation of fine surface details and colour fidelity.

3. Results

3.1. Comparison of the investigated acquisition technologies

The three investigated non-contact acquisition technologies exhibited different performance when applied to highly reflective museum objects. The results demonstrated that the optical properties of silver-plated surfaces significantly influenced the quality of geometric reconstruction and texture acquisition.

Laser triangulation enabled reliable acquisition of larger surface regions and acceptable geometric accuracy for moderately reflective areas.



» **Figure 3:** *Comparison of representative reconstruction results obtained using laser triangulation (A), structured-light scanning (B), and optimized photogrammetry with cross-polarized illumination (C)*

However, highly polished surfaces generated strong reflections that reduced the completeness of the reconstructed geometry. In addition, the absence of colour acquisition limited the suitability of this approach for producing realistic digital twins intended for museum presentation.

The structured-light systems produced dense point clouds with satisfactory geometric detail under favourable conditions. Nevertheless, both investigated systems were sensitive to strong specular reflections originating from the metallic surfaces. Missing surface regions and reconstruction artefacts were observed primarily on highly polished curved areas, requiring extensive post-processing before a complete model could be obtained.

Initial photogrammetric acquisition performed under conventional studio illumination produced high-quality colour information but suffered from numerous reflections visible on the captured images. These reflections negatively affected feature detection during image alignment and reduced the completeness of the reconstructed geometry. Results are summarized in Figure 3.

3.2. Optimization of the photogrammetric workflow

Following the preliminary experiments, the photogrammetric acquisition workflow was progressively optimized to minimize unwanted reflections.

The introduction of cross-polarized illumination significantly reduced specular reflections on the object surface, resulting in improved image quality and more reliable feature detection during photogrammetric processing. The use of two polarized light sources provided more homogeneous illumination and reduced residual reflections in shadowed regions (Figure 4).



» **Figure 4:** *Reduction of specular reflections using a polarizing filter: (left) before adjustment; (right) after adjustment*

An additional improvement was achieved through semi-automated background removal prior to reconstruction. Eliminating unnecessary background information reduced the amount of irrelevant image data processed by the reconstruction software, accelerated model generation and improved segmentation consistency across the complete image dataset.

3.3. Quality of the reconstructed digital twins

The optimized photogrammetric workflow produced the most complete digital twins among the investigated approaches. Fine decorative elements, engraved details and complex free-form surfaces were recon-

structed with high geometric continuity while simultaneously preserving realistic colour information.

Depending on the complexity of the individual artefacts, between 150 and 300 photographs were acquired for each object. The number of photographs and object orientations was adjusted according to the surface geometry, roughness and the presence of movable components. The optimized workflow enabled successful reconstruction of complete digital twins while maintaining efficient computational performance during processing.

The proposed acquisition methodology proved particularly effective for reflective museum artefacts, demonstrating that careful preparation of the acquisition environment is equally important as the selection of the acquisition technology itself. The combination of polarized illumination, optimized image acquisition and semi-automated image preprocessing considerably improved both geometric reconstruction and texture quality (Figure 5).



» **Figure 5:** *Final digital twin of the museum object reconstructed using the optimized photogrammetric workflow with cross-polarized illumination*

4. Discussion

The performed experiments demonstrated that the successful digitization of highly reflective museum objects depends not only on the selected acquisition technology but also on the optimization of the entire acquisition workflow. The comparison of laser triangulation, structured-light scanning and photogrammetry revealed that each technology exhibits specific advantages and limitations when applied to reflective metallic artefacts.

Laser triangulation provided reliable geometric measurements for less reflective surfaces; however, its performance decreased on highly polished regions due to strong specular reflections. Similarly, structured-light scanning produced dense geometric data but proved sensitive to reflective surfaces, resulting in incomplete reconstruction of certain object regions.

Among the investigated approaches, the optimized photogrammetric workflow produced the most complete and visually realistic digital twins for the investigated museum objects. The introduction of cross-polarized illumination substantially reduced specular reflections, improving image quality and increasing the reliability of feature detection during photogrammetric reconstruction. In addition, the semi-automated image preprocessing workflow contributed to more consistent image segmentation and reduced manual processing time.

The results indicate that, for highly reflective museum objects, careful control of illumination conditions is equally important as the selection of the acquisition technology itself. Rather than relying solely on advanced scanning equipment, the proposed workflow demonstrates that a properly optimized photogrammetric approach can produce highly accurate and visually realistic digital twins while requiring relatively accessible hardware.

The developed methodology therefore provides practical recommendations for museums and cultural heritage institutions seeking cost-effective solutions for the digitization of challenging historical artefacts. Furthermore, the proposed workflow can be adapted for other reflective objects with similar optical properties, extending its potential application beyond the investigated case study.

5. Conclusions

This study investigated the applicability of three non-contact acquisition technologies for the digitization of highly

Table 1

Comparison of the investigated non-contact acquisition technologies

Technology	Geometry	Colour	Performance of reflective surfaces	Completeness	Overall suitability for museum digitalization
Laser triangulation	High	No	Moderate	Medium	Medium
Structured light	High	Limited	Low	Medium	Medium
Optimized photogrammetry	High	Excellent	High	High	Excellent

reflective museum objects. Laser triangulation, structured-light scanning and photogrammetry were experimentally evaluated using selected silver-plated historical artefacts from the National Museum of Slovenia.

The comparison demonstrated that all investigated technologies are capable of acquiring three-dimensional data; however, their performance varies considerably when applied to reflective metallic surfaces. While laser triangulation and structured-light scanning encountered limitations caused by specular reflections, the optimized photogrammetric workflow produced the most complete and visually realistic digital twins.

The introduction of cross-polarized illumination, optimized photographic acquisition and semi-automated image preprocessing significantly improved reconstruction quality by reducing reflections and increasing the completeness of the reconstructed geometry. The proposed methodology proved to be an effective and practical and accessible solution for the digitization of challenging museum objects.

The presented workflow contributes to the development of practical methodologies for cultural heritage digitization and provides useful guidelines for museums involved in the creation of accurate digital twins for documentation, conservation and digital presentation.

Future research will focus on further improving colour accuracy through colour-managed acquisition workflows, quantitative accuracy assessment of reconstructed models, and the integration of complementary acquisition technologies for even more demanding museum artefacts.

6. Acknowledgements

The authors gratefully acknowledge the National Museum of Slovenia for providing access to the museum artefacts used in this research and for their professional support throughout the experimental work.

The authors also acknowledge the support of the University of Ljubljana, Faculty of Natural Sciences and Engineering, Department of Textiles, Graphic Arts and Design, where the research was conducted.

7. References

Adamopoulos, E., Rinaudo, F. and Ardissono, L. (2021) 'A critical comparison of 3D digitization techniques for heritage objects', *ISPRS International Journal of Geo-Information*, 10(1), 10. DOI: 10.3390/ijgi10010010

Angheluţă, L.M. and Rădvan, R. (2020) '3D digitization of translucid materials in cultural heritage objects: a comparative study between laser scanning and photogrammetry', *Romanian Journal of Physics*, 65, 906. Available from: https://rjp.nipne.ro/2020_65_7-8/RomJPhys.65.906.pdf [Accessed 3 June 2026].

Eiríksson, E.R., Wilm, J., Pedersen, D.B. and Aanæs, H. (2016) 'Precision and accuracy parameters in structured light 3-D scanning', The International Archives of the Photogrammetry, *Remote Sensing and Spatial Information Sciences*, XL-5/W8, pp. 7–15. DOI: 10.5194/isprs-archives-XL-5-W8-7-2016

Guidi, G., Gonizzi, S. and Micoli, L.L. (2014) 'Image pre-processing for optimizing automated photogrammetry performances', *ISPRS Annals of the Photogrammetry, Remote Sensing and Spatial Information Sciences*, II-5, pp. 145–152. DOI: 10.5194/isprsannals-II-5-145-2014

Hermary, T. (n.d.) Principles of laser triangulation. Hermary. Available from: https://hermary.com/learning/principles-of-laser-triangulation/ [Accessed 4 June 2026].

Iakovaki, E., Konstantakis, M., Giaourtsakis, I., Rentoumi, E., Protopapas, D., Psarras, C. and Koskeridou, E. (2026) 'When reality meets practice: challenges and pitfalls in 3D digitization using structured light scanning and photogrammetry in cultural heritage', *Information*, 17(3), 237. DOI: 10.3390/info17030237

Mateus, L., Fernández, J., Ferreira, V., Oliveira, C., Aguiar, J., Gago, A.S., Pacheco, P. and Pernão, J. (2019) 'Terrestrial laser scanning and digital photogrammetry for heritage conservation: case study of the historical walls of Lagos, Portugal', *The International Archives of the Photogrammetry, Remote Sensing and Spatial Information Sciences*, XLII-2/W11, pp. 843–847. DOI: 10.5194/isprs-archives-XLII-2-W11-843-2019

Mathys, A., Brecko, J., Van den Spiegel, D. and Semal, P. (2015) '3D and challenging materials: guidelines for different 3D digitisation methods for museum collections with varying material optical properties'. In: 2*015 Digital Heritage International Congress, DigitalHeritage 2015, 28 September–2 October 2015, Granada, Spain*. Piscataway: IEEE, pp. 19–26. DOI: 10.1109/DigitalHeritage.2015.7413827

Melendreras Ruiz, R., Marín Torres, M.T. and Sánchez Allegue, P. (2021) 'Comparative analysis between the main 3D scanning techniques: photogrammetry, terrestrial laser scanner, and structured light scanner in religious imagery: the case of The Holy Christ of the Blood', *Journal on Computing and Cultural Heritage*, 15(1), 18. DOI: 10.1145/3469126



© 2026 Authors. Published by the University of Novi Sad, Faculty of Technical Sciences, Department of Graphic Engineering and Design. This article is an open access article distributed under the terms and conditions of the Creative Commons Attribution license 4.0 Serbia (https://creativecommons.org/licenses/by/4.0/deed.en).

Original Scientific Paper https://doi.org/10.24867/GRID-2026-p95

Workflow for Extracting and Structuring Geolinguistic Data from Tesnière's Atlas

ABSTRACT

Tesnière's atlas, published in 1925 and translated into Slovene in 2022, is the first geolinguistic atlas of the Slavic languages as a whole. It represents a form of linguistic heritage that we aim to preserve and pass on to younger generations through digitisation. The atlas is currently available as a printed publication and as a static PDF. Our goal is to transform this static atlas into an interactive web-based resource that enables students and researchers to explore linguistic data dynamically through interactive maps, spatial visualisations, and advanced search. In addition, the digital version will support the integration and reuse of linguistic data across applications and research environments. This article presents the methodology and workflow used to digitise the atlas and prepare its linguistic and geospatial data for the future development of an interactive web atlas. Linguistic reflexes and information about maps and locations were manually transcribed, reviewed, and organised in a multi-sheet Excel workbook. Scanned maps were georeferenced in a GIS environment, and survey locations and linguistic areas were digitised as point and polygon features. The spatial data were exported as GeoJSON files and visually verified in a web environment before being aggregated with the tabular data, transformed, and validated using a custom Python processing pipeline. The resulting four interconnected datasets cover 65 digitised maps and contain 284 locations, 394 linguistic areas, and 6,329 reflexes. These datasets support visualisation, analysis, and reuse across different applications and research environments. Our future work will focus on their use in a fully functional interactive web atlas. However, the workflow presented here is not limited to Tesnière's atlas and can be applied to the digitisation of other historical linguistic atlases and similar cultural heritage collections.

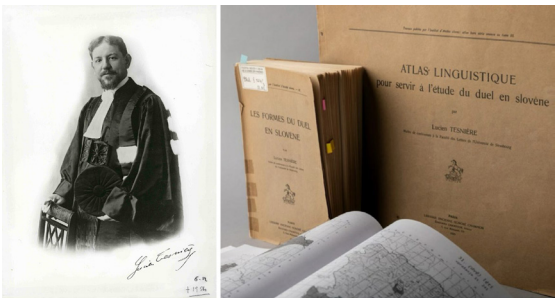
Primož Weingerl [1]
Larisa Kosi [2]
Brina Stankovič Elesini [3]
Svit Bartolj [2]
Urška Stanković Elesini [1]
Sašo Stefanovski [2]

[1] University of Ljubljana, Faculty of Natural Sciences and Engineering, Chair of Information and Graphic Arts Technology, Ljubljana, Slovenia
[2] University of Ljubljana, Faculty of Arts, Department of Geography, Ljubljana, Slovenia
[3] University of Ljubljana, Biotechnical Faculty, Department of Landscape Architecture, Ljubljana, Slovenia

KEY WORDS
Digitisation, linguistic atlas, GIS, georeferencing, cultural heritage

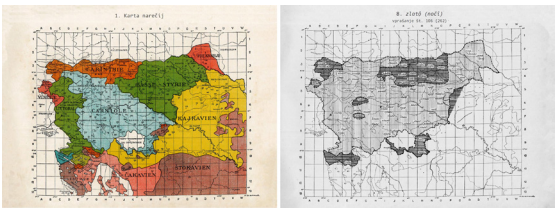
1. Introduction

Lucien Tesnière (1893–1956) was a French linguist who lived in Ljubljana from 1921 to 1924 and worked as a lecturer in French at the newly established University of Ljubljana (Figure 1, left). During this time, under the supervision of professor Antoine Meillet, he prepared his doctoral thesis on the dual in Slovene, which he defended in 1925. His work Les formes du duel en slovène (Tesnière, 1925a) constitutes the principal thesis, while the accompanying thesis was L'Atlas linguistique pour servir à l'étude du duel en slovène (Tesnière, 1925b). This linguistic atlas of the dual was compiled on the basis of a field questionnaire containing 425 questions, which local informants translated into their own dialects; Tesnière then wrote down the responses and entered them on to the maps. The atlas, in which examples of the dual are presented across dialects on individual maps, constitutes the first geolinguistic study of the Slavic languages. It was translated into Slovene only in 2022 (Tesnière, 2022), under the title Lingvistični atlas za študij dvojine v slovenščini (Figure 1, right).



» **Figure 1:** *Lucien Tesnière (left), Les formes du duel en slovène, l'Atlas linguistique pour servir à l'étude du duel en slovène and Lingvistični atlas za študij dvojine v slovenščini (right)*

The linguistic atlas (Tesnière, 1925b; Tesnière, 2022) comprises 70 maps. Each map is divided by meridians and parallels spaced at 10 arc-minute intervals. The rectangles delimited by this grid measure 18.5 km in length and have an average width of 13 km on the ground. These rectangles are numbered 1 to 13 vertically and labelled A to W horizontally. In the atlas, the maps themselves are numbered 1 to 70. The first map, entitled "Map of dialects" (Figure 2, left), shows the geographical division into individual regions, which also broadly indicate the dialect areas. This first map also includes 279 points representing localities – that is, locations where interviews were conducted with 88 speakers, or from which data were taken from existing dialectological literature. The names of these places are listed in two tables in the atlas. The following is a physical map of Slovenia, on the basis of which the other linguistic maps in the atlas were produced. It was prepared in 1921 at the Cartographic Institute in Paris (French: l'Institut cartographique de Paris) (Tesnière, 2022) and includes the names of certain mountain ranges and bays; it also uses the Greenwich prime meridian as its reference.



» **Figure 2:** *Map of dialects (left) and maps with phonetic transcriptions of dialect pronunciations (right)*

In addition to the maps already mentioned, the atlas also contains two stratigraphic cross-sections, while the other maps are two-dimensional and set within Slovene linguistic territory (Figure 2, right). As the author notes, on most maps colours had to be replaced, for typographical and above all financial reasons, by cartographic hatching (hachures), in which the nature and direction of the lines represent different colours, while the density of the hatching indicates different degrees of colour intensity.

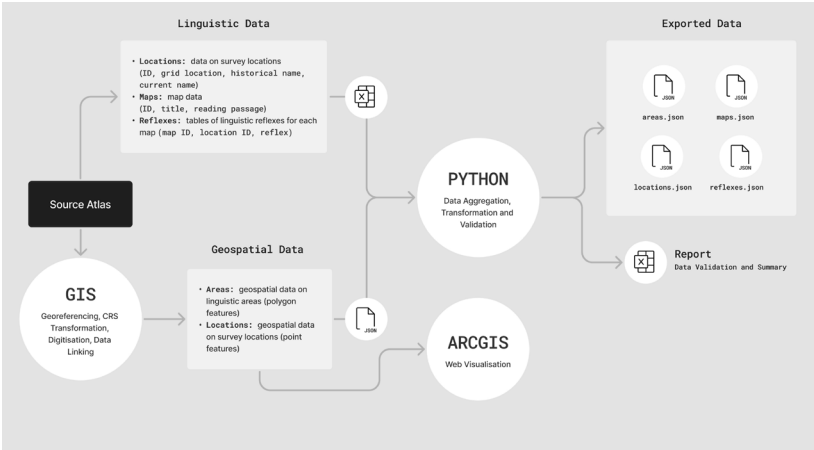
The digitisation of historical linguistic atlases is important not only for preserving their contents but also for making the underlying data more accessible and reusable. In the printed version, linguistic information remains closely tied to individual maps, limiting systematic retrieval, comparison and computational analysis. Converting the atlas into structured digital data helps preserve its information independently of the original physical publication and facilitates its visualisation, analysis, and reuse in linguistic research. Our long-term goal is to develop an interactive web version of Tesnière's linguistic atlas that will enable students and researchers to explore geolinguistic data through interactive maps, spatial visualisations, and advanced search.

The digital version will also enable the atlas to be supplemented with additional materials that could not be included in the printed edition, such as audio recordings. As a first step towards this objective, this article presents the methodology and workflow used to transform the static atlas content into structured geolinguistic data. It describes how information from the printed atlas was transcribed, how locations and linguistic areas were digitised, and how the resulting data were structured, linked, and validated. The prepared datasets provide a basis for their integration and reuse across different applications and for the future implementation of a fully functional interactive atlas.

2. Workflow for extracting and structuring geolinguistic data

The overall workflow is summarised in Figure 3. It consists of two digitisation streams. Linguistic reflexes and information about the corresponding maps and locations were transcribed and organised in tabular form, while survey locations and linguistic areas were digitised in a GIS environment. The resulting tabular and geospatial data are subsequently integrated, transformed, and validated to produce interconnected datasets suitable for web visualisation. The individual stages of this workflow are described in detail in the following subsections.

Of the 70 maps in the atlas, 65 were included in the digitisation process: 64 maps containing linguistic reflexes and map 1, which presents dialect areas. The remaining five contain other types of content: two stratigraphic cross-sections, two physical-geographical maps, and one map showing the extent of Yugoslavia (Tesnière, 2022).



» **Figure 3:** *Overview of the workflow for digitising and structuring geolinguistic data*

2.1. Digitisation of linguistic atlas data

As part of his research on the dual, Tesnière entered the reflexes obtained in interviews (i.e. the phonetic transcriptions of pronunciations) on the individual maps. The reflexes were transcribed with tonemic accentuation. Since the list of individual reflexes is not accessible (the manuscript is kept in the manuscript department of the National and University Library of Strasbourg, and the material is currently being digitised (Sušnik, 2005), it was necessary to transcribe the individual reflexes manually. For the purposes of digitisation, a list of the individual reflexes by locality was required so that they could be re-entered into the network of localities during the digitisation process, as every digitisation project necessarily involves a substantial amount of manual work.

We sought to simplify the transcription process in various ways, including the use of applications and artificial intelligence. However, because the reflexes are often written over the hachures, manual transcription proved more accurate. A further difficulty was the use of special symbols to mark tonemes. On the maps, the meridians and parallels form a degree grid, which made it possible to transcribe the reflexes more systematically.

The work was further facilitated by organising the data in a multi-sheet Excel workbook. The workbook contained two reference worksheets: one with data on locations, including the grid reference, location identifier, historical and current location names, and accompanying notes, and another with data on maps, including the map identifier and title, the relevant questionnaire number, and the associated Slovene text. A separate worksheet, based on a prepared template, was then created for transcribing the linguistic reflexes from each map. Once the map number and location identifier had been entered, the worksheet was partially populated automatically with the relevant data from the reference worksheets. The transcribed reflex and any accompanying notes were then added for each location (Figure 4). Following the initial transcription, the reflexes were reviewed by a second person and compared with the original maps.

An additional challenge was presented by the tonemic transcriptions of the reflexes, which were entered using the special ZRCola font. For this, we used the ZRCola input system provided by ZRC SAZU (ZRCola2, 2019), which enabled basic letter characters to be combined with more complex ones while typing. A further limitation was that the correct display of specialised characters encoded as Unicode Private Use Area code points depended on the availability of the ZRCola font. As described in Section 2.3, these characters were additionally converted into hexadecimal HTML numeric character references to make the underlying code points explicit and to facilitate data transfer and storage.



			Informacije o karti:	41	387–392	Mídva píševa, Mídva svà, Mídva vẹ̑va
ZŠ točke (točka id)	Oznaka kvadrata	Ime kraja (tocka_kraj)	Kraj danes (tocka_kraj_nov)	Št. karte (karta_id)	Številka vprašanja	Slovensko besedilo* (besedilo_tekst)	Refleks
8	B3	Brdo	Brdo	41	387–392	Mídva píševa, Mídva svà, Mídva vẹ̑va	mądsȁ, mídva
11	E3	Malošče	Malošče	41	387–392	Mídva píševa, Mídva svà, Mídva vẹ̑va	mądsȁ
14	F3	Leše (Lesach, Lessach)	Leše	41	387–392	Mídva píševa, Mídva svà, Mídva vẹ̑va	(mídvà)
19	G3	Borovlje	Borovlje	41	387–392	Mídva píševa, Mídva svà, Mídva vẹ̑va	mbá (dva)
64	G4	Slovenski/Slovenji Plajberk	Slovènji Plájberk	41	387–392	Mídva píševa, Mídva svà, Mídva vẹ̑va	mídva
23	I3	Dobrla Ves	Dobrla vàs	41	387–392	Mídva píševa, Mídva svà, Mídva vẹ̑va	nìba, oiba
68	I4	Železna Kápla	Železna Kápla	41	387–392	Mídva píševa, Mídva svà, Mídva vẹ̑va	mədvȁ, vədvȁ
26	K3	Meja Podjunske doline (jaunthal)	Meja med Podjunsko in Mežiško	41	387–392	Mídva píševa, Mídva svà, Mídva vẹ̑va	mẽdva, mídva

» **Figure 4:** *Example of an Excel worksheet used to transcribe linguistic reflexes*

2.2. Georeferencing and spatial data digitisation

In this study, digitisation of geospatial data is used as an umbrella term for the conversion of scanned and later georeferenced cartographic material into vectorised layers with a structured set of attributes (Brennen & Kreiss, 2016). All steps of digitalisation were carried out in ESRI ArcGIS Pro 3.5 (ArcGIS Pro, 2025). The scans of the original maps were not produced within the project but were created for the 2022 translation of the atlas.

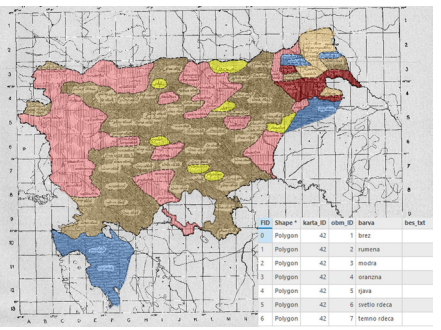
Before the individual maps were processed, two reference feature classes were prepared and used across the whole set of maps. The first was a point feature class containing 53 reference points corresponding to the intersections of the meridians and parallels of the graticule used by Tesnière, which is identical on all maps of the atlas and labelled in degrees and minutes. The points were not digitised from the scans but constructed from the known geographic coordinates of these intersections. The second was a polygon feature class defining the outer limits of the areas to be captured, that is, their maximum extent, together with the area of the German-speaking linguistic enclave of Kočevje (Gottschee), which is likewise identical on all maps. Rather than establishing control points and outer boundaries anew for each map, all operators worked from the same set of reference features. These two reference layers kept the georeferencing uniform across operators and maps, made the individual maps comparable and ensured that recurring areas were vectorised consistently throughout.

The scanned maps were imported as raster layers and georeferenced individually. The original cartographic projection could not be reliably reconstructed from the available material, as the atlas does not include any projection information beyond the graticule itself. The maps were therefore fitted to reference points derived from that graticule, and all work was carried out in the projected coordinate system WGS 84/Pseudo-Mercator (EPSG:3857). For each map, 53 pairs of control points were established, with the first point in each pair marking the position of a graticule intersection on the scanned map and the second the corresponding reference point. The transformation was computed from these pairs as a 2nd order polynomial, which allows a non-linear adjustment of the raster and is therefore suited to older scanned maps exhibiting minor geometric deviations, whether these originate in the initial cartographic production, in deformation of the paper, in uneven scanning, or in subsequent processing. The result of this stage was a georeferenced raster for each map, saved in TIFF format and serving as the basis for subsequent vectorisation (Figure 5).



» **Figure 5:** *Example of a georeferenced map with reference points*

For each map, a new polygon feature class was created to capture the areas of individual dialectal phenomena (Figure 6). The polygons representing the extent of the different dual forms of the word were drawn manually. All maps were vectorised at a uniform scale of 1:50,000, ensuring a comparable degree of generalisation across the set. The reference polygon feature class described above was used throughout as an aid in delimiting the outer boundaries and the Gottschee enclave, so that these recurring areas were captured consistently on every map. In addition to the areas, the locations at which Tesnière recorded his data were captured as a point feature class. The locations were identified from the first map and from the list of locations given in the atlas, yielding a total of 279 points, of which 250 lie within the present-day borders of Slovenia. Each point was placed at the centre of the corresponding present-day settlement. The result of this stage was, for each map included, a polygon feature class of the captured thematic areas together with a point feature class of places.



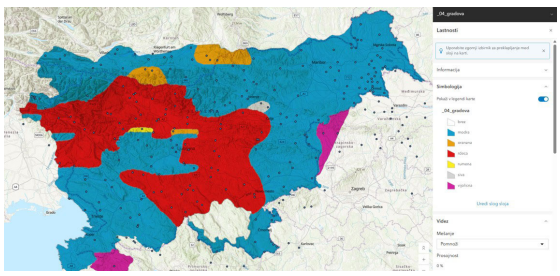
» **Figure 6:** *Digitised map and structured attribute table*

The attributes of the polygon feature classes were edited so that each captured area carried an identifier for the map to which it belonged, an identifier for the area itself, the colour category assigned to it on the original map, together with an empty field reserved for the word form. The point feature class of places was then joined to the polygons by means of a spatial join, which links a point layer to a polygon layer based on the spatial relationship

between them. Each location retained its locality identifier and name. The spatial join added the identifiers of the relevant map and containing area, the corresponding colour category, and an empty field reserved for the later entry of the pronunciation. For each digitised map, this process produced two GeoJSON files: a polygon file containing the geometries and attributes of the linguistic areas, and a point file containing the geometries and attributes of the localities. Point files were distinguished by the suffix _SJ, while the corresponding polygon files used the map filename without this suffix. Both types of files were reprojected to WGS 84 (EPSG:4326) during export, as required by the GeoJSON format specification. GeoJSON was chosen for its simple structure and wide support in web-based geographic information systems, which allows the spatial data to be used outside the software environment in which they were produced.

2.3. Web-based visual verification

After the spatial data had been exported from the GIS environment, the resulting GeoJSON files were visually verified in a web environment before data aggregation. The purpose of this step was to detect potential errors introduced during export and to identify locations or linguistic areas that might have been digitised incorrectly. ArcGIS Online was used for this purpose, and the entire verification was carried out using freely available functionality at no additional cost (Figure 7).



» **Figure 7:** *Example of a digitised map with localities in ArcGIS online web map viewer*

All exported GeoJSON files were imported directly, without any prior adjustment of the files, their attributes or their coordinate system. For each original map, two layers were imported: a point layer of the settlements and a polygon layer of the areas of pronunciation. The layers were assembled into a single web map in Map Viewer. The polygons were symbolised with unique values based on the colour attribute, separately for each map, and the maps were viewed individually by manually switching the visibility of the corresponding pair of layers on and off.

The rendering of the layers and their spatial position were inspected visually, and the attributes and attribute structure were reviewed. The exported locations and linguistic areas were compared with the original maps to verify that they had been transferred correctly and that the spatial features had been digitised accurately. The settlement points were also compared with their associated polygons to verify that each point fell within the area assigned to it. This visual verification made it possible to identify potential export errors, incorrectly positioned locations, and incorrectly drawn area boundaries before the data were aggregated and transformed.

2.4. Data aggregation, transformation and validation

After digitising the linguistic and geospatial data, the resulting datasets were aggregated, transformed, and validated using a custom data-processing pipeline implemented in Python. The pipeline was designed to integrate different types of data: tabular data stored in a multi-sheet Excel workbook and geospatial data exported from the GIS environment as GeoJSON files. During processing, these separate data sources were transformed into a data model suitable for subsequent use in a web environment. The main steps of the data-processing pipeline are summarised in Algorithm 1 and described in detail below. The resulting model is presented in Section 3.1.

Algorithm 1: Data processing pipeline

```
INPUT:
    Tabular data (maps, locations, and reflexes)
    Geospatial point data
    Geospatial area data

IDENTIFY required fields
READ maps, locations, and reflexes
CLEAN values and NORMALISE identifiers
SKIP incomplete location and map records
SKIP duplicate map records

FOR EACH point feature:
    VALIDATE and NORMALISE identifiers
    ASSIGN point geometry to location
    COMPARE with previously assigned geometry
    RECORD geometry conflict, if detected
    IDENTIFY area association, if available

FOR EACH polygon feature:
    VALIDATE and NORMALISE identifiers
    CREATE area with composite identifier
    EXTRACT polygon geometry
    LINK locations to area
    RECORD duplicate area, if detected

CHECK for area associations without polygon geometry
RECORD missing area geometries

FOR EACH reflex record:
    VALIDATE required identifiers
    RECORD invalid row and SKIP it, if necessary
    ASSIGN map and location identifiers
    IDENTIFY associated area, if available
    RECORD missing area association or geometry
    CREATE unique reflex identifier
    ENCODE PUA characters

CHECK for locations without point geometry
AGGREGATE recorded validation results
EXPORT maps, locations, areas, and reflexes
GENERATE report
```

The tabular data input consists of a multi-sheet Excel workbook containing data on locations, maps, and linguistic reflexes, as described in Section 2.1. Because the relevant information is stored in multiple worksheets with varying structures, the required fields are first identified in each worksheet by their column headers. During import, leading and trailing whitespace is removed from textual values, and identifiers are normalised to support

consistent linking between the tabular and geospatial data. Location records are skipped if they lack an identifier or both location names, while map records are skipped if they lack an identifier or both the title and accompanying text. Duplicate map records are also excluded.

The geospatial input consists of point features representing survey locations and polygon features representing linguistic areas. Processing of the geospatial data begins with the point features, which are first validated and normalised. Point geometry is assigned to the relevant location, and the associated area is determined when the necessary identifiers are available. Where the same location occurs in multiple geospatial files, its geometry is compared with the geometry already assigned to that location. If the geometries differ, the previously assigned geometry is retained and the conflict is recorded.

The polygon features are then processed to create the corresponding linguistic area records, with the map and polygon identifiers first validated and normalised. Since polygon identifiers are unique only within an individual map, each area is assigned a composite identifier combining the map identifier and the polygon identifier. For example, polygon 3 on map 4 results in the composite area identifier “4_3”. The polygon geometry is extracted from each feature, and the locations associated with the corresponding composite identifier are linked to the area. Duplicate area identifiers are recorded as soon as they are detected. Once all polygon features have been processed, the pipeline checks whether any area associations derived from the point data lack a corresponding polygon feature and records the affected areas and locations.

The process then iterates through the reflex records. For each record, the required map and location identifiers are first normalised and validated. Records lacking either identifier are classified as invalid, recorded with their worksheet and row number, and excluded from the output. Each valid record is assigned a unique identifier and retains the relevant map and location identifiers from the source data. If the location is associated with an area on the relevant map, the area’s composite identifier is assigned to the reflex record.

Missing area associations and associations without a corresponding polygon feature are also documented. Since reflexes may contain non-standard phonetic characters represented by Unicode Private Use Area (PUA) code points in the ZRCola font, their correct display depends on the availability of this font. To ensure compatibility, PUA characters are also converted to hexadecimal HTML numeric character references. This preserves the original transcription while providing an alternative form suitable for data transfer and storage.

After the point, polygon, and reflex processing stages, the pipeline additionally identifies locations without point geometry and aggregates the recorded validation results. Where available, relevant source information, such as the worksheet and row number or the GeoJSON file, is retained to enable problematic records to be traced back to the source data.

Finally, the processed data are exported as four interconnected datasets representing maps, locations, linguistic areas, and linguistic reflexes. The pipeline also generates a single Excel report containing an overall data summary, processing statistics, source information, and detailed validation results. The summary provides the overall numbers of maps, locations, areas, and reflexes, together with indicators of data completeness and consistency.

3. Results and discussion

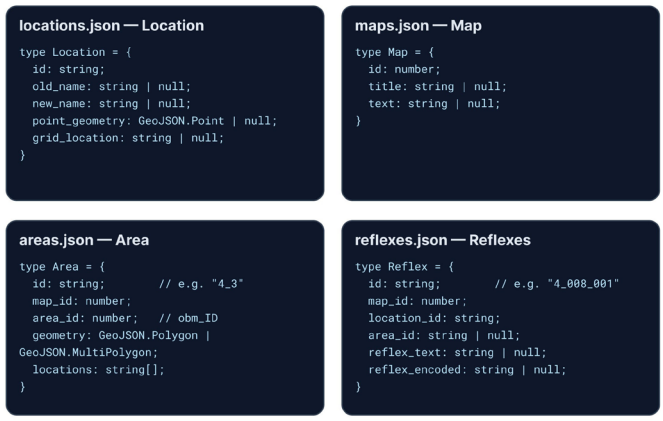
3.1. Data model and dataset structure

The final data model consists of four main entities: maps, locations, linguistic areas, and linguistic reflexes (Figure 8). Maps and locations contain information shared across multiple records, while areas and reflexes are linked to them through the identifiers described in Section 2.4. A map can include multiple areas and reflexes, while the same location can appear on multiple maps. Each reflex is linked to a map and a location, and, where an area association is available, to the relevant linguistic area. This structure reflects the organisation of the original atlas while avoiding the repetition of map and location data in individual reflex records.

Separating the four entities enables independent querying and updating while preserving their relationships. It also supports the intended features of the interactive atlas, including displaying locations and areas, retrieving reflexes for a selected location or map, and comparing linguistic phenomena across maps.

3.2. Dataset overview and validation results

The final datasets cover 65 digitised maps and contain 284 locations, 394 linguistic areas, and 6,329 reflexes. Validation identified no missing point or polygon geometries and no invalid reflex records lacking the required map or location identifiers. However, some linguistic areas had no associated locations despite containing survey points. Inspection in the GIS environment revealed that overlaps between certain polygons had caused locations to be automatically assigned to incorrect areas. These errors were corrected, and the data were re-exported and checked again. This illustrates the



» **Figure 8:** *The final data model*

iterative nature of the workflow, in which results are reviewed and, where necessary, corrected and verified.

The web-based test proved advantageous in several respects, while at the same time revealing the limitations of the environment in which it was carried out. The exported files were imported without any intervention in the data, so that the test also served as a check on the export itself. It was carried out on a web platform, in an environment corresponding to the intended use of the data, where shortcomings in encoding, projection or attribute handling that a desktop environment tolerates become more apparent. Displaying the layers together, moreover, allowed the spatial consistency of the points and polygons to be examined visually, which cannot be judged from the attribute table alone. Several limitations were identified as well. Each layer took a considerable time to load whenever it was made visible, which made moving through the set of maps slow; switching between maps was entirely manual, as the environment provides no mechanism for turning one pair of layers off when another is turned on; the phonetic transcriptions could not be displayed in the custom font that is indispensable here, as the environment does not permit custom fonts to be added. The whole process – loading, symbolising and inspecting each layer in turn – was carried out manually, which, at 130 layers, made the check possible but time-consuming. Taken together, these limitations indicate that a web map of this kind is not suitable for public release, and that the atlas will require a purpose-built solution in which the shortcomings identified here can be overcome.

4. Conclusions

The article outlines the methodology and workflow used to digitise Tesnière's linguistic atlas and prepare its linguistic and geospatial data for further use. Linguistic reflexes and information about maps and locations were transcribed and organised in tabular form, while survey locations and linguistic areas were georeferenced and digitised in a GIS environment. The exported geospatial data were visually verified in a web environment, then aggregated with linguistic data to produce four interconnected datasets. The resulting datasets support visualisation, analysis, and reuse in linguistic research across different environments, independently of the platform, technology, or programming language used.

Our future work will focus on using the resulting datasets to develop a fully functional interactive web atlas that supports displaying locations and areas, retrieving reflexes for a selected location or map, comparing linguistic phenomena across maps, and adding supplementary materials such as audio recordings.

5. Acknowledgments

The project Development of the Interactive Dual Atlas (DVAtlas) is co-funded by the Republic of Slovenia and the European Union from the European Social Fund Plus (ESF+).

6. References

Brennen, J.S. and Kreiss, D. (2016) 'Digitalization'. In: Jensen, K.B., Rothenbuhler, E.W., Pooley, J.D. and Craig, R.T. (eds.) *The International Encyclopedia of Communication Theory and Philosophy. John Wiley & Sons, Ltd*. DOI: 10.1002/9781118766804.wbiect111

Esri. (2025) ArcGIS Pro (Version 3.5.0). Redlands, California, USA: Esri. Available from: https://www.esri.com/en-us/arcgis/products/arcgis-pro/overview [Accessed 15 February 2026].

Sušnik, M. (2005) 'Slovensko narečno gradivo v zapuščini Luciena Tesnièrja', *Jezikovni zapiski*, 31(2), pp. 213–247. DOI: 10.3986/JZ.31.2.11

Tesnière, L. (1925a) *Les formes du duel en slovène*. Paris: Librairie ancienne Honoré Champion.

Tesnière, L. (1925b) *Atlas linguistique pour servir à l'étude du duel en slovène*. Paris: Librairie ancienne Honoré Champion.
Tesnière, L. (2022) *Atlas dvojine v slovenščini*. Translated by Schlamberger Brezar, M. Ljubljana: Znanstvena založba Univerze v Ljubljani.
ZRCola 2 Vnašalni sistem za jezikoslovno rabo. (2019) ZRCola. Available from: https://zrcola.zrc-sazu.si/ [Accessed 3 March 2026].



© 2026 Authors. Published by the University of Novi Sad, Faculty of Technical Sciences, Department of Graphic Engineering and Design. This article is an open access article distributed under the terms and conditions of the Creative Commons Attribution license 4.0 Serbia (http://creativecommons.org/licenses/by/4.0/rs/).

Author index - GRID 2026

A
Adamović, Savka // 549, 573, 611
Adelabu, Oluwafemi S. // 275
Agbaba, Jasmina // 557
Ahtik, Jure // 473, 495
Anđelković, Aleksandar S. // 731
Anvari, Sam // 33
Arman Kandirmaz, Emine // 663

B
Banjanin, Bojan // 507, 629, 769
Bartolj, Svit // 813
Bauk, Stanko // 79
Beja, Boris // 379, 387, 427
Birtane, Hatice // 599, 649
Blaznik, Barbara // 231
Boeva, Rumyana // 157, 579
Bolanča Mirković, Ivana // 79
Borysenko, Olha // 107
Bošnjaković, Gordana // 311, 339, 611
Bota, Josip // 451
Bračko, Sabina // 231
Bratić, Diana // 189

C
Calvo Ivanovic, Ingrid // 19, 243
Čanžek, Klara Manca // 473
Carmo, Ana do // 459, 739
Ceglar, Nuša // 717
Ceglar, Žiga // 427
Cigil, Aslı Beyler // 565, 649
Cigula, Tomislav // 209
Çınar Acar, Berat // 649
Coelho, Paulo // 459
Čupić, Jelica // 713
Cvetojević, Sanja // 481, 537

D
Das, Oisik // 223
Dedijer, Sandra // 63, 145, 507
Dimovski, Vladimir // 713
Divjak, Alan // 799
Donevski, Davor // 673
Dragić, Miroslav // 265
Đurđević, Stefan // 339, 481, 525
Dybowska-Sarapuk, Łucja // 699

E
Efkolidis, Nikolaos // 291
Eriksson, August // 223
Eymur Donmez, Betul // 565

F
Franken, Gregor // 333
Franković, Rea // 451

G
Gabrijelčič Tomc, Helena // 445
Gazibarić, Zoran // 169
Glušac, Dragana // 731
Golubović, Gala // 481, 525, 611
Gómez Robledo, Luis // 255
Grujić, Dragana // 145
Gudaitiene, Renata // 785
Guna, Jože // 237
Gvoić, Vesna // 557, 585
Gvoka, Teodora // 311, 339, 611

H
Hajdek, Krunoslav // 799
Hancock, Gabriella M. // 33
Hasukić, Nina // 451
Havenko, Svitlana // 73
Hernández Andrés, Javier // 255
Hladnik, Aleš // 501
Hoblaj, Rene // 209
Holeňová, Veronika // 683
Holubnyk, Tetyana // 107
Horvat, Irma // 95
Horváth, Csaba // 419
Huertas, Rafael // 255
Huljev, Meri // 79

I
Ilić, Tamara // 507, 629, 769
Iskra, Andrej // 445, 515
Itrić Ivanda, Katarina // 209, 285, 621
Ivanović, Milica // 693
Izdebska-Podsiadły, Joanna // 435

J
Janicki, Piotr // 125
Jankulovska, Eva // 371
Jarc, Jure // 805
Jašúrek, Bohumil // 151, 683
Jeznach, Arkadiusz // 699
Jurečić, Denis // 189
Juretić, Iva // 481, 537
Jurič, Ivana // 179, 199, 537

K
Kalamakidou, Ioanna // 291
Kara, Filiz // 639
Karchakova, Kremena // 157

Karlovits, Igor // 43
Kašiković, Nemanja // 63, 179, 731
Kavčič, Urška // 687
Kerac, Jelena // 507, 629, 769
Kešina, Spomenko // 95
Klenovšek, Urška // 333, 705
Kočevar, Tanja Nuša // 515
Koltai, László // 419
Komadina, Asja // 753
Komarov, Serhii // 125
Kołodziejuk, Ewa // 435
Kosi, Larisa // 813
Koštomaj, Lara // 717
Kovalskyi, Bohdan // 133
Krajačić, Nika // 621
Krčmar, Dejan // 557
Kulčar, Rahela // 209, 285, 621
Kyratsis, Panagiotis // 779, 785, 791
Kyratsis, Vasileios // 291

L
Labetska, Marta // 73
Lakatoš, Robert // 573
Lazarova-Zdravkova, Nevena // 579
Ligka, Panagiota // 785, 791
Liokos, Thomas // 291
Lychridas, Giorgos // 291

M
Mahović Poljaček, Sanja // 87, 673
Majnarić, Igor // 79, 265
Manavis, Athanasios // 291
Mančić, Uroš // 215
Mandelj, Brita // 515
Manjenčić, Darko // 693
Maričić Picajkić, Katarina // 311, 611
Markowski, Leszek // 125, 489
Martínez Domingo, Miguel Ángel // 255
Matijević, Mile // 799
Mattioli, Francesca // 243
Medved, Tanja // 359
Mendeš, Marija Magdalena // 315
Merhy, Petra // 761
Mićić, Ksenija // 531
Mihailović, Aleksandra // 573
Mihaljević, Mila // 315
Miketić, Nada // 199, 297, 713
Milić, Bojana // 531
Milić Keresteš, Neda // 199, 255, 507
Miljković, Petar // 95
Milošević, Rastko // 549, 573, 769
Morić, Marko // 799
Možina, Klementina // 359, 371
Muck, Deja // 805
Muck, Hana // 403
Mušić, Laila // 395
Mustić, Daria // 303
Mylonas, Dimitris // 49

N
Nakić, Patricija // 501, 717
Narić, Bojana // 265
Nasr, Khloud Khaled // 115
Nemeček, Nataša // 805
Nešić, Aleksandra // 179
Nikolić, Selena // 549
Nikolić-Šipek, Alan // 285

O
Oitzl, Gašper // 805
Oladumiye, E. Bankole // 275
Oličkov, Vladimir // 63
Oluyemi, Ayorinde S. // 275
Ozcan, Arif // 663

P
Pál, Magdolna // 179, 199, 297
Pashova, Katya // 579
Pavlović, Živko // 179, 557, 585
Pećanin, Biljana // 145
Petković, Gorana // 189
Petriaszwili, Georgij // 125
Petričević, Rina // 495
Petriv, Yurii // 57
Petrović, Nemanja // 215
Petrović, Nikola // 169
Petrović, Saša // 481, 537
Pevec, Patricija // 687
Pibernik, Jesenka // 315
Pilić, Branka // 179
Pinćjer, David // 339
Pinćjer, Ivan // 199, 297, 713
Pipan, Evelin // 231
Premčevski, Velibor // 731
Preprotić, Suzana Pasanec // 189
Prica, Miljana // 63, 557, 585

R
Ragavaraja, R // 321
Remete, Kornél // 419
Repeta, Vyacheslav // 57
Reynik, George-Robert // 779
Ristić, Milena // 297, 585
Ružičić, Branka // 145
Ryvak, Pavlo // 57

S
Samardžić Cvijanović, Selena // 573
Sanches, Miguel // 739
Šarčević, Iva // 209
Semeniv, Mariia // 133
Semeniv, Vitalii // 133
Silva, Júlio // 459, 739
Simončič, Jan // 717
Škipina, Blanka // 145
Spajić, Jelena // 531
Špiranec, Jana // 87

Spiridonov, Iskren // 157, 579
Sremac, Žanko // 215
Stančić, Mladen // 265
Stankovič Elesini, Brina // 813
Stanković Elesini, Urška // 717, 813
Stanonik, Tinkara // 387
Stefanovski, Sašo // 813
Stevanovski, Ana // 359
Strižić Jakovljević, Maja // 87

T
Tasić, Nemanja // 731
Tomašegović, Tamara // 673
Tomić, Ivana // 255, 549
Tóth, Gábor // 419
Trochoutsos, Chris // 347
Tsigonias, Marios // 347
Tubić, Aleksandra // 557
Tziarou, Athina // 785, 791

U
Učakar, Andrej // 805
Urbas, Raša // 237, 403, 427

V
Valdec, Dean // 95
Valero, Eva M. // 255
Vališ, Jan // 151, 683
Valovyi, Pavlo // 73
Vasić, Marijana // 693
Vesho, Nikolla // 791
Vladić, Gojko // 311, 339, 611
Vonitsanos, Gerasimos // 347
Vrabič-Brodnjak, Urška // 333, 705
Vrbová, Tereza // 151
Vujić, Maja // 557
Vukić, Nevena // 693
Vukoje Bezjak, Marina // 285, 621

W
Weingerl, Primož // 813
Weiss, Charles T. // 413

Y
Yüksekdağ, Zehranur // 649

Z
Zanko, Natalia // 133
Žilić, Dragana // 525
Żołek-Tryznowska, Zuzanna // 699